UNIVERSITY OF STRASBOURG

DOCTORAL SCHOOL OF CHEMICAL SCIENCE

UNIVERSITY OF BELGRADE

FACULTY OF CHEMISTRY

THESIS presented by:

Milan MILOVANOVIĆ

defended on: **28 September 2018**

to obtain the degree of: **Doctor of the University of Strasbourg**

Discipline/Speciality: **Chemistry**

to obtain the degree: **PhD in Chemistry**

Experimental and Theoretical Approaches Coupled with Thermochemistry of Reactions in Solution and the Role of Non-covalent Interactions

THESIS co-supervised by:

Mr DJUKIC Jean-Pierre	Directeur de Recherches au CNRS, Université de Strasbourg, France
Ms MEDAKOVIĆ Vesna	Assistant Professor, University of Belgrade - Faculty of Chemistry, Serbia

REVIEWERS:

Mr BROTHERS Edward	Associate Professor, Texas A & M University at Qatar
Mr AMOURI Hani	Directeur de Recherches au CNRS, Université de Pierre and Marie Curie

OTHER MEMBERS OF THE JURY:

Ms POLOVIĆ Natalija	Associate Professor, University of Belgrade - Faculty of Chemistry, Serbia
Mr ARMSPACH Dominique	Professeur, Université de Strasbourg, France

UNIVERSITÉ DE STRASBOURG

ÉCOLE DOCTORALE DE SCIENCES CHIMIQUES

UNIVERSITÉ DE BELGRADE

FACULTÉ DE CHIMIE

THÈSE présentée par:

Milan MILOVANOVIĆ

soutenue le: **28 septembre 2018**

pour obtenir le grade de: **Docteur de l'Université de Strasbourg**

Discipline/ Spécialité: **Chimie**

pour obtenir le grade: **Doctorat en Chimie**

Les approches Expérimentales et Théoriques combinées à la Thermochimie des réactions "in solutio" et le Rôle des interactions Non-covalentes

THÈSE co-dirigée par:

M DJUKIC Jean-Pierre	Directeur de Recherches au CNRS, Université de Strasbourg, France
Mme MEDAKOVIĆ Vesna	Maître assistant, Université de Belgrade - Faculté de Chimie, Serbie

RAPPORTEURS:

M BROTHERS Edward	Pofesseur agrégé, Université de Texas A & M au Qatar
M AMOURI Hani	Directeur de Recherches au CNRS, Université de Pierre and Marie Curie, France

AUTRES MEMBRES DU JURY:

Mme POLOVIĆ Natalija	Professeur agrégé, Université de Belgrade - Faculté de Chimie, Serbie
M ARMSPACH Dominique	Professeur, Université de Strasbourg, France

УНИВЕРЗИТЕТ У СТРАЗБУРУ

ДОКТОРСКА ШКОЛА ХЕМИЈСКИХ НАУКА

УНИВЕРЗИТЕТ У БЕОГРАДУ

ХЕМИЈСКИ ФАКУЛТЕТ

ДОКТОРСКА ТЕЗА презентује:

Милан МИЛОВАНОВИЋ

датум одбране: **28. септембар 2018.**

за добијање титуле: **Доктор Универзитета у Стразбуру**

Дисциплина/Специјалност: **Хемија**

за добијање титуле: **Доктор наука – хемијске науке**

Експериментални и теоријски приступи комбиновани са термохемијом реакција у раствору и улога нековалентних интеракција

КО-МЕНТОРИ:

Гдин. DJUKIC Jean-Pierre	Directeur de Recherches au CNRS, Université de Strasbourg, France
Гђа. МЕДАКОВИЋ Весна	Доцент, Универзитет у Београду - Хемијски факултет, Србија

ИЗВЕСТИОЦИ:

Гдин. BROTHERS Edward	Associate Professor, Texas A & M University at Qatar
Гдин. AMOURI Hani	Directeur de Recherches au CNRS, Université de Pierre and Marie Curie, France

ОСТАЛИ ЧЛАНОВИ КОМИСИЈЕ:

Гђа. ПОЛОВИЋ Наталија	Ванредни професор, Универзитет у Београду - Хемијски факултет, Србија
Гдин. ARMSPACH Dominique	Professeur, Université de Strasbourg, France

Деки Томиславу (1931-2018)

И свима осталима које волим.

God is smart.

Nature is God's daughter.

We, human beings, are part of nature.

All the time human beings have been trying to find out all secrets of nature.

Perhaps, the best way to achieve that is to be interested in everything,

Physics, chemistry, biology,

All fields in between and beyond.

My main way was, is and, most probably, will be the chemistry.

Nonetheless, I will never leave

Faith,

Hope,

Love.

I sincerely apologize to all of you who have already acknowledged and written these words.

p.s.

God,

Thank You for all things I have seen, felt and learned.

Thank You for keeping me alive.

Acknowledgments

This doctoral dissertation is the result of work on jointly supervised PhD Thesis that has been conducted in parallel at both the Department of General and Inorganic Chemistry, the Faculty of Chemistry, University of Belgrade, Serbia and the Laboratoire Chimie et Systémique Organo-Métalliques (LCSOM), the Institut de Chimie de Strasbourg (UMR 7177), the École doctorale des Sciences Chimiques (EDSC, ED 222), University of Strasbourg, France.

First of all, I would especially like to thank Prof. Dr. Snežana Zarić, for giving me the opportunity to be part of her research group and for being my supervisor during the course of this work. I would like to express my special gratitude to Dr. Jean-Pierre Djukic for accepting to be my supervisor. Many thanks to both of them for guidance, support, many useful advices and discussions during my PhD journey, that helped me a lot to develop myself not only as a chemist but as a person as well. Being part of such collaborative PhD thesis enables me to learn from prominent scientist form all around the world as well as to meet France and many wonderful people. I would also like to thank Dr. Vesna Medaković, for accepting to be my supervisor as well as for all support provided.

I would like to thank Campus France, Fund for young talents – Dositeja that made my stay in France possible as well as the ANR (ANR-DFG project COCOORDCHEM) and the Serbian Ministry of Education, Science and Technological Development (Grant 172065, to SDZ) for their financial support.

Special thankfulness I would like to express to Dr. Hani Amouri and Dr. Edward Brothers for acceptance to revise my doctoral dissertation and to participate in the Thesis Jury, as well as to Dr. Natalija Polović and Dr. Dominique Armspach for acceptance to participate in the Thesis Commission.

Je voudrais remercier le Dr Michel Pfeffer, dont la porte n'a jamais été fermée pour aucune de mes questions, me donnant de bons conseils et explications.

En plus, je voudrais remercier tous mes collègues que j'ai rencontrés dans le groupe du Dr Djukic, en particulier le Dr Mustapha Hamdaoui et Houda Habitta pour m’avoir permis de passer un agréable séjour à Strasbourg ainsi que pour leurs paroles utiles dans les moments difficiles.

Ensuite, je voudrais remercier Mme Geneviève Stoll, Mme Virginie Herbash, Mme Francine Cerni, Mme Isabelle Lapierre et Mme Laurence Barondeau pour toutes les questions administratives résolues qui ont facilité ma vie en France. Aussi, je voudrais remercier tous les gens des services techniques de l'Université de Strasbourg, en particulier Bruno Vincent et Maurice Cope pour toute l'aide fournie.

Искрено бих желео да се захвалим изузетним колегама из студентске службе Хемијског факултета гђи. Зорици Драпшин и гдину. Радомиру Анђелковићу на свој помоћи, увек уз осмех, пружену.

Такође, најлепше се захваљујем колегама који раде у групи проф. др Снежане Зарић: др Ивани Станковић, др Јелени Андрић, Ивани Антонијевић, Дубравки Војислављевић, др Предрагу Петровићу, др Драгану Нинковићу, др Душану Вељковићу и др Душану Маленову на пријатној сарадњи, саветима и разумевању.

Велико хвала и свим искреним и драгим пријатељима на подршци, времену проведеном са мном и вери у мене, како у Србији тако и у Француској. Special thanks are dedicated to Ms Deborah Men for all support given to me.

Захвалио бих се и Јовани Бајић на помоћи око превода дела текста на француски језик, као и Тањи Милутиновић која је прочитала текст докторске дисертације и извршила неопходне техничке корекције.

Мајци Биљани и оцу Рељи неизмерно захваљујем на безусловно пруженој љубави, безрезервној подршци и вери у мене, те на бризи, жртви, и истрајном напору да постанем добар човек. Брату Марку и снаји Јелени захваљујем се на пруженој љубави и подршци. Најлеше хвала и братанцу Матеји на најискренијим осмесима. На послетку, захваљујем се и најдражим рођацима: тетки Мими, течи Милошу, браћи Аци и Кићи на важним саветима, значајној подршци, пажњи и помоћи.

Милан Миловановић

Abstract

This Thesis was guided by the following goals: a) acquiring an extensive thermochemical data library for the achiral organic or organometallic adduct formation with an extension to the organic frustrated Lewis pairs by means of the isothermal titration calorimetry (ITC); b) theoretical modelling of the molecular systems and their thermochemical parameters by the DFT-D methods; c) contribution to the "benchmark" of the computational methods by the constitution of experimental thermochemical base, mentioned earlier.

So far, many aspects of various kinds of chemical bond have well been described in literature, but some of them, especially weak non-covalent interactions, still remain a challenge for the scientific world. The re-emergence of this fundamental subject of the understanding of some unknown aspects of the chemical bond is made possible by new theoretical tools, in particular, the methods known as DFT-D, i.e. DFT corrected for dispersion; they allow to account for the physically relevant way the effects of dispersion at medium and long distances.

London force (named after the physicist Fritz London) or dispersion is ubiquitous in nature. It constitutes an important part of the energy contribution to the stabilization of the tertiary structure of peptides, other natural polymers as well as the spontaneous coalescence of atomic clusters or apolar molecules. The specificity of the London force is that it is related to long distances and is always attractive, thus, it is also effective intra-molecularly and determines in many situations the conformational behavior of organic molecules and organometallics. Combined with electrostatic and orbital interactions, it helps to define the stereochemical course of many reactions; it plays an essential role in the processes of recognition and chiral discrimination.

The heat is one of the rare observables that is accompanied with every (intrinsic) change of the matter and it could be liberated from the matter to its surroundings or reverse (absorbed from the surroundings by the matter). Hence, measuring the heat change of the system of interest is one of the very powerful experimental techniques for monitoring the changes in the studied system. One of the most popular experimental techniques which allows recording of the heat flow within a certain system is calorimetry. According to the thermodynamic lows (Gibbs equations), by knowing the heat changes during a particular process which takes place within a studied system (enthalpy, ΔH) it is possible to know other thermochemical parameters (ΔG, ΔS) of the system.

Acquiring the base of the experimental thermochemical data of huge scope of chemical reactions is being the key for further development of the computational methods.

Hopefully, by having the experimental thermochemical parameters of the system which are in accordance with computationally predicted ones (because of right reasons), the role of non-covalent interactions in the considered system could be rationally elucidated.

In the present Thesis, the isothermal titration calorimetry (ITC) experiments have been used as the main experimental tool. For the purpose of ITC experiments a Nano ITC (*TA Instrument* ®) device was used. As a theoretical tool, the static DFT-D calculations have been performed. Besides those techniques, a search of Cambridge Structural Database (CSD) has been performed as a complementary and helping method to the calculations.

Throughout the Thesis, the research has been focused on the following chemical reactions depicted in Scheme A 1. The reaction systems were selected if: a) they present an important topic in the chemical world or in their course of chemical transformation a step-wise reaction mechanism is assumed/documented (which can be challenging for both experimental and theoretical chemists); b) an influence of non-covalent interactions in the system is significant.

Besides the ITC and theoretical studies, most of the reactions (reactants and reaction products) were fully characterized by standard experimental characterization methods (NMR spectroscopy, Mass spectroscopy, Elemental analysis, X-Ray diffraction, IR spectroscopy). Moreover, the reactions of (F) LPs were monitored by 2D NMR - DOSY experiments.

The ITC journey has covered both kinetic (partial reaction orders, initial rate constants of the reactions, where possible, according to the used reaction conditions) and thermodynamic study (ΔH, ΔG, ΔS) of the reaction systems, while by the DFT-D calculations only the thermochemical parameters (ΔH, ΔG, ΔS) of the reaction systems in gas or/and chlorobenzene phase have been obtained. The CSD search has been performed only in case of the (F) LPs.

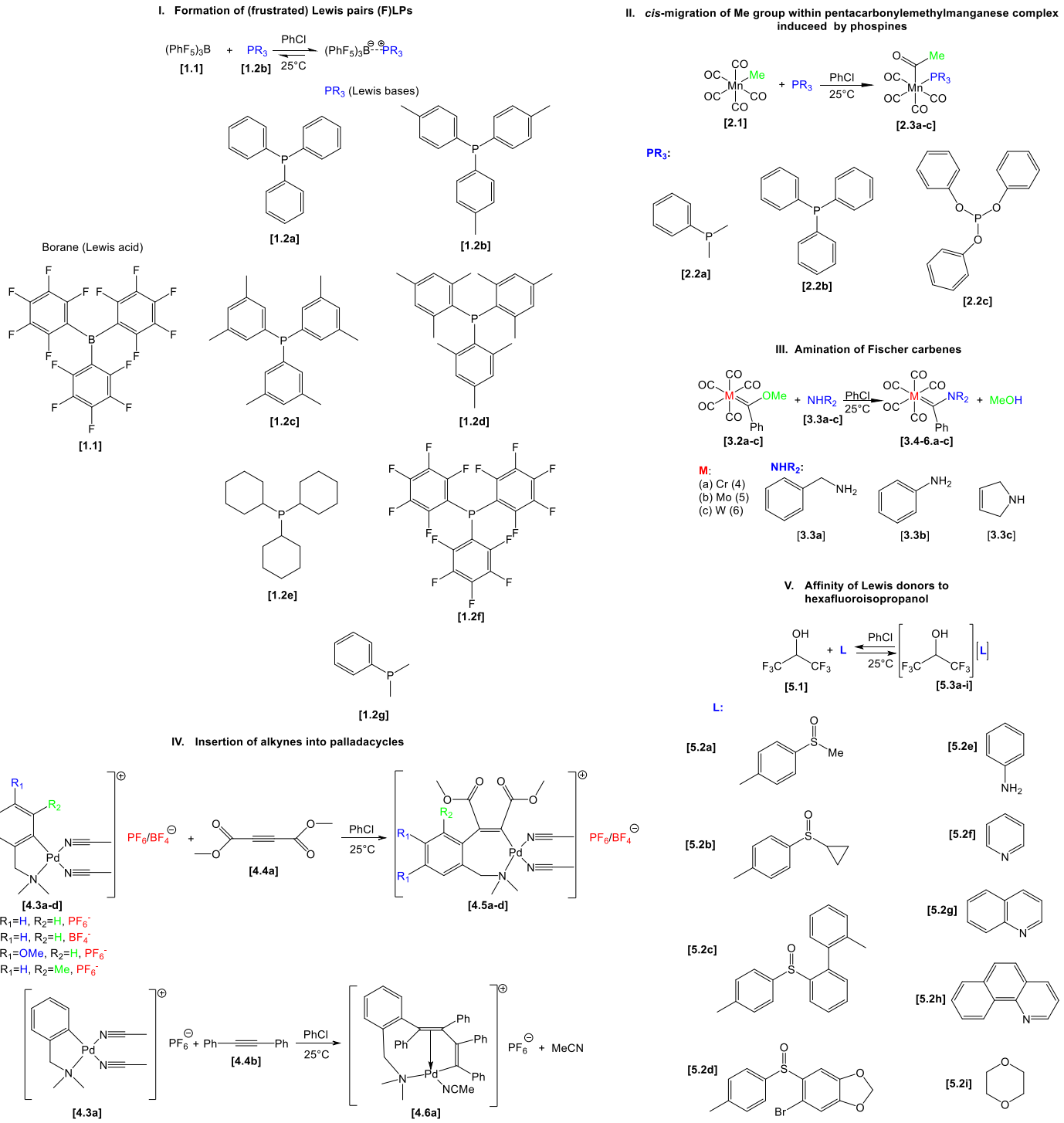

Scheme A1. Schematic representation of the studied reaction systems during the Thesis.

I. Formation of (frustrated) Lewis pairs

The discovery of “frustrated” Lewis acid - base pairs (FLPs), among which tris (pentafluorophenyl) borane with a variety of phosphines are the most studied ones, showed a great influence of the non-covalent interactions in these systems and opened a new field of research in chemistry. The FLP concept, established by Stephan, has found great interest over the past decade. The concept is based on the finding that systems containing Lewis acids and bases, that are prevented from classical donor-acceptor interactions by steric (and electronic) factors, keep their Lewis acidity and basicity and, consequently, are available for interaction with a third molecule. The phosphine-borane pairs, especially “frustrated” ones, have found great use in different domains: from the synthesis and catalysis to the hydrogen storage and materials. Many reports have dealt with calculations on phosphine-borane systems, particularly their interaction energies and related distances between acid and base centers; the influences of the substituents on the boron and phosphorus atoms on their reactivity; the catalytic reaction mechanisms, as well as the importance of non-covalent interactions. In spite of a great number of articles that have dealt with FLPs, some aspects of the chemical behavior of the FLPs are not still fully understood, particularly the actual thermochemistry of the interactions in solution of intermolecular pairs and the actual aggregation mode for such loose “pairs” (FLPs) in solutions.

As mentioned before, the approach, herein used, is mainly based on ITC investigation. The research has revealed quite interesting and, to some instance, surprising results. Namely, **1.1**/**1.2a-c** form cohesive pairs, the system **1.1**/**1.2d** exists within an equilibrium, the system **1.1**/**1.2f** does not show any tendency to forming any stable pair, while the system **1.1**/**1.2e** only with less than 0.2 equivalents of the phosphine form a single reaction product. An assumption of a forming of clusters (most probably consisted of one molecule of the phosphine and, at least, two molecules of the borane), raised up from the ITC thermograms, is confirmed by both 2D DOSY NMR experiments and DFT-D calculations. The ITC Δ*H* results showed that, among all herein studied adduct formations, the highest heat released is obtained during the formation of $mes_3PB(PhF_5)_3$ (**1.1/1.2d**, well-known FLP adduct), suggesting that non-covalent interactions have a huge influence within these systems. The interaction/reaction Δ*H* values (that account for the influence of chlorobenzene explicitly) predicted by theory are in good agreement with the experimental ITC data. Many useful geometrical parameters of classical and frustrated phosphine-borane pairs were obtained by the CSD search. These parameters helped in rationalizing the differences between them considering their mutual orientation and distances.

II. Cis-migration of Me group within the pentacarbonylmethylmanganese complex induced by phosphines

The pentacarbonylmethylmanganese complex has been the first complex containing carbonyl ligands ever synthetized. Since that discovery, the complex has been intensively examined using various experimental techniques available at that time. It has been found that in reaction with nucleophiles a migration of the methyl group to adjacent carbonyl ligand is induced and followed by insertion of the nucleophiles into the complex. Later, the migratory insertion sequence was found to be an important sequence in catalysis. Therefore, many experimental and theoretical researches have been done in order to find its mechanism as well as kinetics of the insertion step of many nucleophilic ligands. The complex has been found to be important in synthesis as a precursor as well as a catalyst. Nevertheless, little has been published on the actual thermochemistry of the insertion-migration reaction of the pentacarbonylmethylmanganese complex with Lewis bases.

The migration-insertion reaction sequence into pentacarbonylmethylmanganese (**2.1**), induced by the series of phosphines (**2.2a-c**, Scheme A 1), has been studied in the sense of experimental kinetic and thermodynamic ITC and theoretical DFT-D investigations.

The reaction tests have suggested that the side reactions (i.e. the isomerization and decarbonylation of the *cis* product) could be avoided at lower reaction temperatures within shorter reaction time periods.

The ITC thermodynamic results (range of ITC raw ΔH_r -9 – -12.5 kcal/mol) have suggested that reasonably stronger interactions could be established through the investigated *cis-migration*-insertion reaction sequence, indicating a difference between the chosen phosphines: their ability to establish non-covalent interactions and nucleophilic affinity. The ITC kinetic results have confirmed partial first reaction order with respect to the complex **2.1**.

Although the static DFT-D COSMO calculations have predicted much larger (ca. 2.5 times) reaction enthalpies - ΔH_r values from c-a. -22 kcal/mol to -31 kcal/mol, the computed ΔH_r values are mutually in accordance (regarding their structural and electronic characteristics). Such overestimation might be a consequence of not taking into account the explicit interactions of chlorobenzene with the reactants, especially with the complex. The computed Gibbs free energies (ΔG_r values from ca. -8 kcal/mol to -17 kcal/mol) suggest the possibility of quite spontaneous interactions.

III. Amination of Fischer carbenes

Fischer type carbenes can be drawn by a general structural formula of $(CO)_5M=C(X)R$ wherein carbene carbon atom is connected to a low-valent transition metal from VI-VIII group of PTE. The nature of the metal-carbene carbon atom bond could be described as σ-donating/π-back-donating, while nature of binding within M-C-X as (weak) three-centered four-electron bonding interaction. The group *X* is usually an electron donating group having a stabilizing effect to electron deficient carbene carbon atom while *R* group could be either a saturated or unsaturated organic group. To stabilize a low valent metal center many π accepting ligands could be employed. In the typical Fischer carbene complex these π accepting ligands are carbonyls. Due to such constitution of the carbene, its general chemical characteristic could be described as electrophilic, containing few potential reactive sites. As a consequence of possessing such versatile chemical properties, accompanied by adjustable electronic characteristics of the substituents (*X*, *R*) on the carbene carbon atom, the Fischer carbenes have been found as very important precursors in both organic and inorganic synthesis as well as in the synthesis of biological active substrates. The aminolysis reaction of the Fischer carbenes, the mechanism of which as well as kinetics is well established, could be considered similar to the amination of esters. Intriguingly, although a lot was done both experimentally and theoretically regarding the mechanisms of action as well as structure features and structure-reactivity relationship of the Fisher carbenes, a little has been published about actual thermochemistry of any transformation including Fischer carbenes.

The aminolysis reaction, in general, (auto) catalyzed addition-substitution reaction sequence, has been studied on a series of Fischer's carbenes (Scheme A 1) by the experimental and theoretical tools.

The results suggest an equilibrium nature of the amination process as well as no side reaction products. The thermodynamic ITC results (ΔH_r values larger than -15 kcal/mol) suggested energetically favorable transformations within the amination process in the systems **3.2a-c**/**3.3a** and **3.2a-c**/**3.3b**, while the systems **3.2a-c**/**3.3b** were found to be non-exploitable. Clear dependence of the type of a metal atom on the reaction enthalpy could not be drawn. The kinetic ITC results rather confirmed partial second reaction order with respect to the amine.

The calculated reaction enthalpies (ranged from ca. -5.5 kcal/mol up to -20 kcal/mol), are in excellent accordance with the experimental values, while the calculated Gibbs free energies

have suggested a spontaneous process within all the systems. In addition, the calculation revealed that the amination of the herein investigated Fischer carbenes by phenylamine (**3.3b**) is not thermodynamically possible in normal conditions, confirming the ITC observations.

IV. Insertion of alkynes into palladacycles

Metallacycles contain a direct metal-carbon bond, wherein the carbon atom is part of one of metal ligands. As the activation of C-H bond is one of the most important subjects within organometallic chemistry, resulting metallacycles found to be of great importance in many domains: from synthesis and catalysis to medicine and materials. In general, the cyclo-metalation reaction in case of palladium follows a base-assisted electrophilic pathway. Among transition metals, palladium has been one of most used metals within metallacycle chemistry so far. An insertion of various kinds of alkynes into Pd-C bond has been observed by Pfeffer and co-workers. That finding has found to be a quite useful preparative method for the range of palladacycles containing various functionalities. The mechanism of the insertion of the alkynes into the palladacycles suggests step-wise process beginning with a coordination of the alkyne to the palladium and subsequent migratory insertion of the alkyne into Pd-C bond. While kinetics of the insertion reactions of the alkynes into the palladacycles are described, no information of actual thermochemistry has been provided yet.

Within this study, a round of isothermal calorimetric measurements supplemented with theoretical estimations, was engaged. Two highly active substrates (**4.4a-b**) were used to study kinetics and thermodynamics of the step-wise insertion reaction into the charged cyclopalladated complexes (Scheme A1). The latter one is even more active and presents a double insertion capability.

Kinetic ITC study showed partial first reaction order with respect to **4.4b**, that is in accordance with published data.

The obtained ITC ΔH_r value of a double insertion (ca. -38 kcal/mol) is reasonably larger than ITC ΔH_r value of a single insertion (ca. -24 - -28 kcal/mol). DFT-D predicted ΔH_r and ΔG_r values are around 10-15 kcal/mol larger than the experimental ITC data, suggesting that chlorobenzene might have a significant competitive influence, interacting non-covalently, within the insertion sequence. Considering the complexity of nature of the reactants and the chemical transformations within the insertion reaction, it could be concluded that there is good accordance between experimental and theoretical results.

V. Affinity of Lewis donors to hexafluoroisopropanol

Recently, 1,1,1,3,3,3-hexafluoropropan-2-ol (HFIP) was found to be an exceptional medium, either as solvent or co-solvent, that allows many reactions to occur. It is known that HFIP possesses an acidic and polar feature and hydrogen bonding abilities, but still, an exact role of HFIP in various chemical transformations is not fully and reasonably explained.

To figure out the possible role of HFIP, a formation of a potential donor-acceptor complex between HFIP and a series of different substrates (Scheme A1) was examined by ITC experiments and DFT-D calculations. The scope of the calculations was extended even to some other substrates (amines, ketone, aldehyde, chlorobenzene and HFIP)

The ITC results have suggested on quite strong to strong non-covalent interactions (range of ITC ΔH_a -5 – -13 kcal/mol) within the examined systems. In addition, concluded on ΔG_a (ranged -1.4 – -3.2 kcal/mol), all considered Lewis donors might interact spontaneously with HFIP. Altogether, that might have a huge influence on an additional polarization of bonds within the Lewis donor molecule that could be of crucial importance in key steps of various chemical transformations, suggesting that HFIP might have a catalytic role.

Although the results of the calculations ΔH_a in a gas phase are consistent with the experimental ΔH_a ITC results within the error bar, it was shown that even better accordance of the results could be achieved applying continuum model solvation treatment (COSMO) within the computations. Additionally, it was shown that chlorobenzene could considerably interact with HFIP as well as that quite strong interactions between HFIP molecules are possible. The calculations showed that nitrogen is stronger H bonding acceptor than oxygen, while the later one is stronger than sulfur. In addition, HFIP would rather prefer to interact with aliphatic than aromatic hydrogen atoms.

Regarding the achieved results, it can be concluded that the Thesis' goals are accomplished.

The ITC experiments, extended to organic and organometallic chemistry, proved to be a powerful technique for obtaining reliable kinetic as well as thermodynamic reaction data.

The DFT-D calculations showed up capabilities in the accurate modelling of the reaction systems as well as in good to excellent prediction the thermochemical parameters of reactions.

Subsequently, a huge experimental database of thermochemistry of a number of reactions is produced, which can be used as the reference in further improvements of DFT and quantum chemical calculations.

The research sheds some light on existing FLPs and HFIP chemistry by introducing molecular clusters and by proving a formation of relatively strong donor-acceptor complexes, respectively. These findings can be the potentially important base of their chemical reactivity.

It is shown that various chemical transformations within organometallic complexes, (such as migration-insertion, many step-wise insertions, auto catalyzed addition-elimination reaction sequences), can be properly investigated and described experimentally – by kinetic and thermodynamic ITC experiments and theoretically – by static DFT-D calculations.

The covalent interactions play very important or crucial role within the examined systems.

Абстракт

Израда ове докторске дисертације била је вођена следећим циљевима: а) формирање обимне термохемијске базе података формирања ахиралних органских или органометалних адуката органских фрустрираних Lewis-ових парова помоћу изотермалне титрационе калориметрије (енг. isothermal titration calorimetry (ITC)); б) теоријско моделовање молекулских система и њихових термохемијских параметара DFT-D методом; ц) допринос референтној бази (benchmark) рачунских метода формирањем раније поменуте експерименталне термохемијске базе.

До сада су у литератури добро описани многи аспекти различитих типова хемијске везе, али неке од њих, попут нековалентних интеракција, и даље остају изазов за научни свет. Поновно интересовање за разумевање неких непознатих аспеката хемијске везе подстакнуто је развојем нових теоријских метода, посебно дисперзионо-коригованих метода теорије функционала густине (DFT-D), које омогућују да се на физички релевантан начин опишу ефекти дисперзије на средњим и дугим растојањима.

London-ова сила (названа по физичару Fritz London-у) или дисперзија, је свеприсутна у природи. Она представља важан допринос енергији стабилизације терцијарне структуре протеина, других природних полимера, као и спонтане агрегације атомских кластера или неполарних молекула. Специфичност London-ове силе је у томе што је везана за дуга растојања и увек је привлачна, те је такође ефикасна унутар молекула. У многим ситуацијама одређује конформационо понашање органских и органометалних молекула. У комбинацији са електростатичким и орбиталним интеракцијама помаже у дефинисању стереохемијског тока многих реакција; она игра кључну улогу у процесима препознавања и хиралне дискриминације.

Топлота је једна од ретких физичких величина која прати сваку (унутрашњу) промену материје и може се пренети са система на околину или обрнуто (апсорбовати из околине од стране система). Стога је мерење промене топлоте проучаваног система једна од веома моћних експерименталних техника за праћење промена у датом систему. Једна од најпопуларнијих експерименталних техника која омогућава мерење протока топлоте унутар одређеног система је калориметрија. Према термодинамичким законима (Gibbs-ове једначине), на основу познавања промене топлоте током одређеног процеса који се

одвија у испитиваном систему (енталпија, Δ*H*), могуће је одредити и друге термохемијске параметре (Δ*G*, Δ*S*) датог система.

Формирање базе експерименталних термохемијских података великог броја различитих хемијских реакција биће употребљено за тестирање и корекцију постојећих рачунарских метода.

Познавање експериментално одређених термохемијских параметара система који су у складу са рачунарски предвиђеним параметрима, може помоћи у расветљавању улоге нековалентних интеракција у посматраном систему.

Основну експерименталну технику у овој тези представљали су експерименти изотермалне титрационе калориметрије (ITC). За потребе ITC експеримената коришћен је Nano ITC (*TA Instrument* ®) уређај. Од теоријских метода коришћени су статички DFT-D прорачуни. Поред ових метода, урађена је и претрага Кембричке базе структурних података (енг. Cambridge Structural Database (CSD)), као комплементарна и помоћна метода рачунарским методама.

Током рада на овој тези истраживање је било фокусирано на хемијске реакције приказане схемом А1. Реакциони системи били су изабрани уколико: а) представљају важну тему у области хемије или је у току хемијске трансформације у систему претпостављен/доказан вишестепени реакциони механизам (што може представљати изазов и за експерименталне и за теоријске хемичаре); б) утицај нековалентних интеракција у систему је значајан.

Поред ITC и теоријских студија, већина реакција (реактанти и реакциони производи) у потпуности су окарактерисане стандардним експерименталним методама (НМР спектроскопија, масена спектроскопија, елементална анализа, дифракција рендгенских зрака, ИЦ спектроскопија). Реакције (F)LP-а праћене су и 2D NMR - DOSY експериментима.

ITC истраживање обухватило је кинетичке (одређивање парцијалног реда реакције реактаната, почетне константе брзине реакција, у реакционим системима где је то било могуће) и термодинамичке студије (Δ*H*, Δ*G*, Δ*S*) реакционих система. Помоћу DFT-D прорачуна израчунати су термохемијски параметри (Δ*H*, Δ*G*, Δ*S*) реакционих система како

у гасној фази тако и у раствору хлорбензена. Претраживање CSD-а извршено је само у случају (F)LP-а.

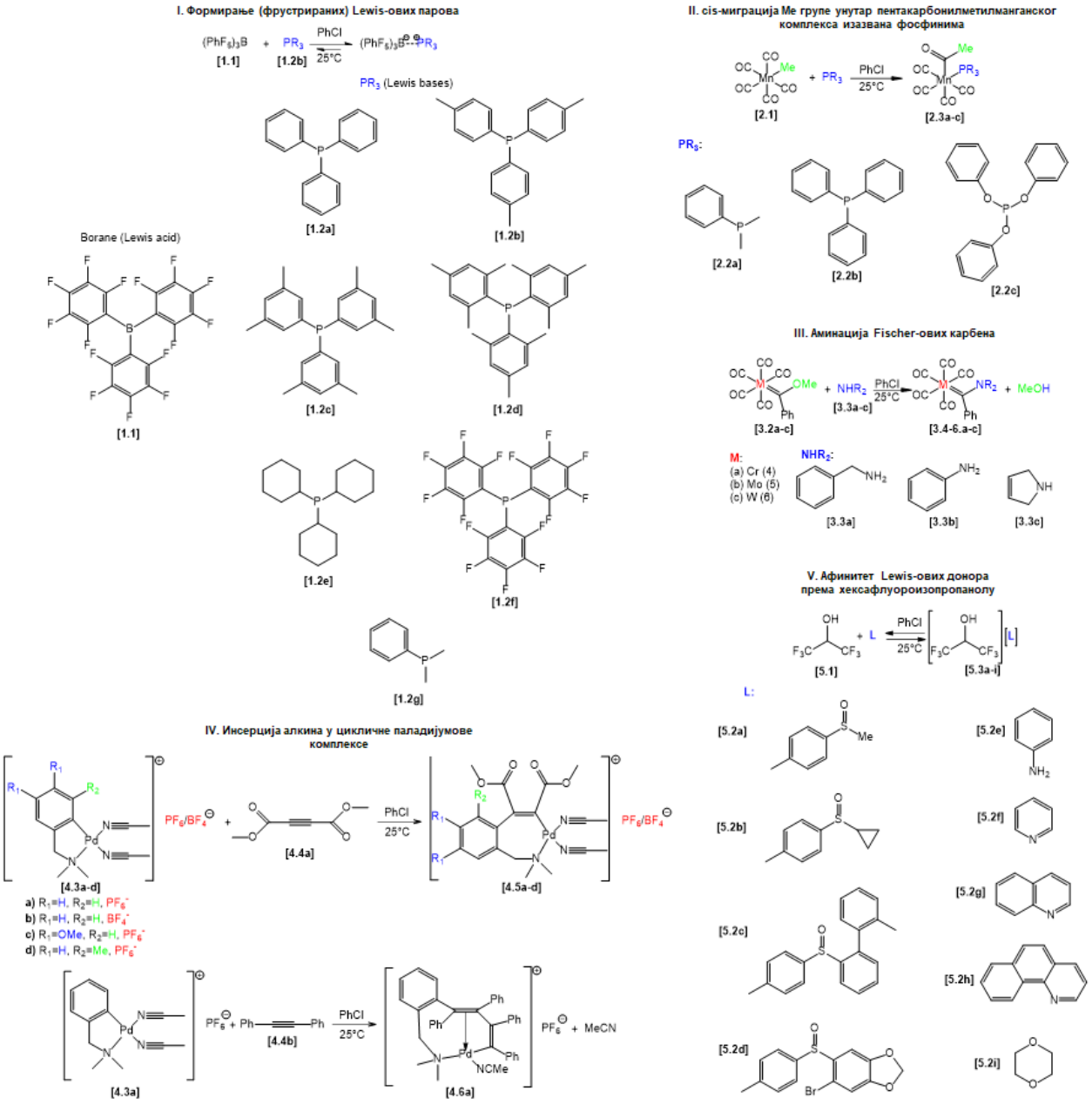

Схема А1. Схематски приказ реакционих система проучаваних током израде тезе.

I. Формирање (фрустрираних) Lewis-ових парова

Откриће „фрустрираних“ Lewis-ових киселинско-базних парова (енг. frustrated Lewis pair - FLP), међу којима су најпознатији трис(пентафлуорофенил)боран са различитим фосфинама, указало је на велики утицај нековалентних интеракција у овим системима и

отворило ново поље истраживања у хемији. Концепт FLP-а, који је установио Stephan, изазвао је велико интересовање током последње деценије. Концепт је заснован на открићу да системи који садрже Lewis-ове киселине и базе, код којих су класичне донорско-акцепторске интеракције спречене стерним (и електронским) факторима, задржавају своја кисело-базна својства, те стога могу интераговати са трећим молекулом. Фосфин-борански парови, посебно "фрустрирани", пронашли су широку примену у различитим доменима: од синтезе и катализе до складиштења водоника и материјала. Многи научни радови бавили су се прорачунима у системима фосфин-боран, а посебно: енергијама њихових интеракција и растојањима између киселинских и базних центара; утицајем супституената на атомима бора и фосфора на њихову реактивност; реакционим каталитичким механизмом, као и улогом нековалентних интеракција. Упркос великом броју научних радова који су се бавили FLP-ма, неки аспекти хемијског понашања FLP-а још увек нису у потпуности схваћени, а посебно термохемија интеракција међумолекулских парова у раствору и начин агрегације таквих „лабавих“ парова (FLP) у растворима.

Као што је већ поменуто, у току израде ове дисертације углавном су коришћена истраживања заснована на изотермалној титрационој калориметрији. Из ових истраживања проистекли су прилично интересантани и, на неки начин, изненађујући резултати. Наиме, системи **1.1**/**1.2a-c** формирају кохерентне парове, систем **1.1**/**1.2d** постоји у равнотежној фази, систем **1.1**/**1.2f** не показује било какву тенденцију за стварањем стабилног пара, док систем **1.1**/**1.2e** формира један реакциони производ када је употребљено мање од 0,2 еквивалента фосфина. Претпоставка о формирању кластера (највероватније састављеног од једног молекула фосфина и најмање два молекула борана) произашла је из ITC термограма, а потврђена је и 2D DOSY NMR експериментима и DFT-D прорачунима. Резултати ITC Δ*H* су показали да је међу свим формираним адукатима, највећа топлота произведена при формирању $mes_3PB(PhF_5)_3$ (**1.1/1.2d**, веома познати FLP адукт), што указује на огроман утицај нековалентних интеракција унутар ових система. Теоријске вредности Δ*H* израчунате DFT-D методом, које укључују и утицај хлоробензена, у доброј су сагласности са експерименталним ITC подацима. На основу анализе структура пронађених претрагом CSD-а, добијени су корисни геометријски параметри за класичне и фрустриране фосфин-боран парове. На основу анализе ових параметара, а разматрајући међусобну оријентацију и растојање у фосфин-боран паровима, било је могуће објаснити разлике између њих.

II. Cis-миграција метил групе унутар комплекса метил-манган-пентакарбонила изазвана фосфинима

Комплекс метил-манган-пентакарбонил представља први синтетисан комплекс који садржи карбонилне лиганде. Након открића комплекс је интензивно проучаван различитим експерименталним техникама које су биле доступне. У реакцији са нуклеофилима долази до миграције метил групе на суседни карбонилни лиганд, а потом до инсерције нуклеофила у комплекс. Касније је утврђено да миграционо-инсерциона секвенца представља важну секвенцу у катализи. Како би се објаснио механизам ове реакције, као и кинетика инсерционог корака многих нуклеофилних лиганада, урађена су различита експериментална и теоријска истраживања. Утврђено је да је комплекс значајан за синтезу и као прекурсор и као катализатор. Упркос томе, публиковано је мало резултата о термохемији миграцино-инсерционе вишестепене реакције метил-манган-пентакарбонила са Lewis-овим базама.

Миграцино-инерциона реакциона секвенца унутар метил-манган-пентакарбонила **2.1**, изазвана низом фосфина (**2.2a-c**, схема A1) испитивана је помоћу експерименталних кинетичких и термодинамичких ITC метода и теоријских DFT-D метода.

Реакциони тестови указали су да се нежељене реакције (тј. изомеризација и декарбонилација *cis* производа) могу избећи при нижим реакционим температурама и краћим временским периодима реакције.

ITC термодинамички резултати (ITC сирове (raw) ΔH_r вредости у распону од -9 до -12,5 kcal/mol) указали су да би се разумно јаче интеракције могле успоставити посредством испитиване *cis* миграционо-инсерционе реакционе секвенце, али такође и на разлике међу изабраним фосфинима, тј. на њихове различите способности успостављања нековалентних интеракција и на њихове различите нуклеофилне афинитете. ITC кинетички резултати потврдили су да се ради о реакцији првог реда у односу на комплекс **2.1**.

Иако су на основу резултата статичких DFT-D COSMO прорачуна предвиђене много веће (око 2,5 пута) реакционе енталпије, ΔH_r вредности од око -22 kcal/mol до -31 kcal/mol, израчунате ΔH_r вредности међусобно су усклађене (с обзиром на структурне и електронске карактеристике испитиваних система). Оваква прецењивања могу бити последица чињенице да нису експлицитно узете у обзир интеракције хлоробензена са

реактантима, а посебно са комплексом (**2.1**). Израчунате вредности Gibbs-ове слободне енергије (ΔG_r вредности од око -8 kcal/mol до -17 kcal/mol) указују на могућност прилично спонтаних интеракција.

III. Аминовање Fischer-ових карбена

Карбени Fischer-овог типа могу се представити општом структурном формулом $(CO)_5M=C(X)R$ где је карбенски угљеников атом повезан са нисковалентним прелазним металом VI-VIII групе ПСЕ. Веза метал-карбенски угљеник може се описати као σ-донорска/π-повратно-донорска (енг. σ-donating/π-back-donating), а природа везивања унутар M-C-X као (слаба) трицентрична-четвороелектронска везивна интеракција. Група *X* је обично електрон-донорска група која има стабилишући ефекат на електрон-дефицитарни карбенски угљеников атом, док *R* група може бити или засићена или незасићена органска група. За стабилизацију нисковалентног метала могу се користити многи π-акцепторски лиганди. У типичном Fischer-овом карбенском комплексу као π-акцепторски лиганди служе карбонили (CO). Због такве структуре Fischer-ог карбена, његове опште хемијске карактеристике могу се описати као електрофилне са неколико потенцијалних реактивних места. Као последица таквих хемијских особина, а у комбинацији са подесивим електронским карактеристикама супституената (*X*, *R*) на карбенском угљениковом атому, Fischer-ови карбени се користе као врло важни прекурсори у органској и неорганској синтези, као и у синтези биолошки активних супстрата. Реакција аминолизе Fischer-ових карбена, чији су механизам и кинетика добро познати, може се сматрати сличном аминовању естара. Без обзира на велики број експерименталних и теоријских истраживања реакционог механизма, структурних карактеристика, као и односа између структуре и реактивности Fischer-ових карбена, изненађујуће је да је веома мало резулатата публиковано о термохемији било које трансформације која укључује Fischer-ове карбене.

Реакција аминолизе, уопштено (ауто) катализоване адиционо-елиминационе реакционе секвенце, проучавана је на серијама Fischer-ових карбена (схема A1) помоћу експерименталних и теоријских метода. Резултати указују на равнотежну природу процеса аминације, као и на непостојање споредних реакционих производа. ITC термодинамички резултати (ΔH_r вредности веће од -15 kcal/mol) указују на енергетски повољне трансформације у процесу аминације у системима **3.2a-c**/**3.3a** и **3.2a-c**/**3.3c**, док су системи **3.2a-c**/**3.3b** окарактерисани као неупотребљиви. Јасна зависност ентлапије

реакције од типа метала није опажена. ITC кинетички резултати потврдили су да се ради о реакцији другог реда у односу на амине.

Израчунате реакционе енталпије (у распону од око -5,5 kcal/mol до -20 kcal/mol) су у одличној сагласности са експерименталним вредностима, док израчунате вредности Gibbs-ове слободне енергије указују да се ради о спонтаним процесима у свим системима. Поред тога, на основу квантнохемијских прорачуна је закључено да аминовање испитиваних Fischer-ових карбена помоћу фениламина (**3.3b**) није термодинамички могуће на 25ºC, што је потврдило исправност резултата добијених ITC методом.

IV. Инсерција алкина у цикличне комплексе паладијума

Циклични комплекси метала садрже директну везу између метала и угљеника, при чему је атом угљеника део једног од лиганада на металу. Како је активација C-H везе једна од најважнијих тема у органометалној хемији, циклични комплекси метала имају велики значај у многим доменима: од синтезе и катализе до медицине и материјала. Генерално, реакција циклометалације у случају паладијума се одвија према базно-потпомогнутим електрофилном рекционом путу/механизаму. Међу прелазним металима, паладијум је до сада био један од најчешће коришћених у хемији цикличних комплекса метала. Pfeffer и сарадници су уочили инсерцију различитих врста алкина у везу Pd-C. Тај проналазак се показао као прилично корисна препаративна метода за палету паладијумових цикличних комплекса који садрже различите функционалне групе. Механизам инсертовања алкина у паладијумове цикличне комплексе представља вишестепени процес који почиње координацијом алкина за паладијум, док касније долази до инсертовања алкина у везу Pd-C. Иако је кинетика реакција инсертовања алкина у паладијумове цикличне комплексе описана, још увек нису познате информације о њиховој термохемији.

За проучавање ове проблематике, у оквиру ове дисертације употребљена су изотермална калориметријска мерења и квантнохемијски прорачуни. Два врло активна супстрата (**4.4a-b**) коришћена су за проучавање кинетике и термодинамике вишестепене инсерционе реакције у наелектрисаним паладијумовим цикличним комплексима (схема A1). Други супстрат (**4.4b**) је активнији и има могућност двоструке инсерције.

Кинетичка ITC студија показала је да се ради о реакцији првог реда у односу на реактант **4.4b**, што је у складу са објављеним резултатима.

Добијена ITC ΔH_r вредност за двоструку инсерцију (око -38 kcal/mol) је разумно већа од ITC ΔH_r вредности једноструке инсерције (од -24 до -28 kcal/mol). Вредности ΔH_r и ΔG_r предвиђене DFT-D методом су око 10-15 kcal/mol веће од експерименталних ITC вредности, што указује на то да хлоробензен интерагујући нековалентно, може имати значајан компетитивни утицај унутар инсерционе секвенце. С обзиром на сложену природу реактаната и хемијске трансформације у инсерционој реакцији, може се закључити да постоји добра сагласност између експерименталних и теоријских резултата.

V. Афинитет Lewis-ових донора према хексафлуороизопропанолу

Недавно је утврђено да 1,1,1,3,3,3-хексафлуоропропан-2-ол (HFIP) представља изузетну средину, било као растварач или кораствараč, која омогућава одвијање многих реакција. Познато је да HFIP поседује киселе и поларне особине и могућност водоничног везивања, али тачна улога HFIP-а у различитим хемијским процесима још увек није у потпуности објашњена.

Да би се открила могућа улога HFIP, формирање потенцијалног донорско-акцепторског комплекса између HFIP-а и серије различитих супстрата (схема A1) испитивано је ITC експериментима и DFT-D прорачунима. Прорачуни су урађени чак и за неке друге супстрате (амине, кетон, алдехид, хлоробензен и HFIP).

Резултати ITC експеримената указали су на постојање прилично јаких до јаких нековалентних интеракција (опсег ITC ΔH_a вредности је између -5 и -13 kcal/mol) у испитиваним системима. Осим тога, на основу ΔG_a вредности (у опсегу између -1,4 и -3,2 kcal/mol), закључено је да сви разматрани Lewis-ови донори могу спонтано да интерагују са HFIP. Све то може имати велики утицај на додатну поларизацију веза унутар Lewis-овог донорског молекула што би могло бити од пресудне важности у кључним корацима различитих хемијских трансформација, а истовремено указује да HFIP може имати и каталитичку улогу.

Иако су резултати прорачуна ΔH_a вредности у гасној фази у складу са експерименталним резултатима ITC ΔH_a унутар границе грешке, показано је се да се може постићи још боља сагласност резултата применом COSMO (continuum model solvation treatment) континуалног солватационог модела. Поред тога, показано је да хлоробензен може значајно да интерагује са HFIP-ом, као и да су могуће снажне интеракције између самих молекула HFIP. Прорачуни су показали да при формирању водоничне везе атом азота

има израженије акцепторске способности у односу на атом кисеоника, док је атом кисеоника бољи акцептор од атома сумпора. Такође је показано да HFIP радије гради интеракције са алифатичним него са ароматичним атомима водоника.

У складу са добијеним резултатима, може се закључити да су циљеви докторске тезе испуњени.

ITC експерименти, проширени на органску и органометалну хемију, показали су се као моћна техника за добијање поузданих кинетичких и термодинамичких реакционих података.

DFT-D прорачуни показали су се као веома добри за прецизно моделовање реакционих система, као и за добро до одлично предвиђање термохемијских реакционих параметара.

Осим тога, формирана је огромна база експерименталних термохемијских података бројних реакција, која се може користити за даље побољшање квантнохемијских прорачуна.

Истраживање је донекле „расветлило“ постојећу FLP и HFIP хемију увођењем молекуларних кластера односно доказивањем формирања релативно јаких донорско-акцепторских комплекса. Добијени резултати могу представљати потенцијално важну базу за проучавање њихове хемијске реактивности.

Показано је да различите хемијске трансформације у органометалним комплексима (као што су миграционо-инсерционе, једноструке и двоструке инсерционе и аутокатализоване адиционо-елиминационе реакционе секвенце) могу бити правилно истражене и описане експериментално - кинетичким и термодинамичним ITC експериментима, и теоријски - статичким DFT-D прорачунима.

Улога нековалентних интеракција у испитиваним системима може се описати као веома значајна до кључна.

Résumé

Cette thèse a été guidée par les objectifs suivants: a) l'acquisition d'une vaste bibliothèque de données thermochimiques pour la formation d'adduits organiques ou organométalliques achiraux avec une extension aux paires de Lewis frustrées organiques au moyen de la calorimétrie de titration isotherme (ITC); b) modélisation théorique des systèmes moléculaires et de leurs paramètres thermochimiques par les méthodes DFT-D; c) contribution à l'évaluation ou "benchmark" des méthodes de calcul par la constitution d'une base thermochimique expérimentale, mentionnée précédemment.

Jusqu'à présent, de nombreux aspects de divers types de liaisons chimiques ont été bien décrits dans la littérature, mais certains d'entre eux, en particulier les interactions non-covalentes faibles, restent encore un défi pour le monde scientifique. La réémergence de ce sujet fondamental dans la compréhension de certains aspects inconnus de la liaison chimique est rendue possible par de nouveaux outils théoriques, notamment les méthodes dites DFT-D, c'est-à-dire DFT corrigées pour la dispersion; ces méthodes permettent de rendre compte de manière physiquement pertinente des effets de la dispersion à moyenne et longue distance.

La force de London (nommée d'après le physicien Fritz London) ou dispersion, est omniprésente dans la nature. Elle constitue une partie importante de la contribution énergétique à la stabilisation de la structure tertiaire des peptides, d'autres polymères naturels ainsi que la coalescence spontanée des amas atomiques ou des molécules apolaires. La spécificité de la force de London est qu'elle est liée à de longues distances et qu'elle est toujours attractive, elle est donc également efficace au niveau intramoléculaire et détermine dans de nombreuses situations le comportement conformationnel des molécules organiques et des organométalliques.

Combinée aux interactions électrostatiques et orbitales, elle contribue à définir l'évolution stéréochimique de nombreuses réactions, jouant un rôle essentiel dans les processus de reconnaissance et de discrimination chirale.

La chaleur est l'une des rares observables qui accompagne tout changement (intrinsèque) de la matière et qui peut être libérée de la matière vers son environnement ou inversement. Par conséquent, mesurer la variation de chaleur d'un système d'intérêt est l'une des techniques expérimentales les plus puissantes pour suivre les changements dans le système étudié.

D'autre part, parmi les techniques les plus effectives pour l'enregistrement des flux de chaleur dans un certain système la calorimétrie est particulièrement recommandée. Selon les lois thermodynamiques (équations de Gibbs), connaissant les changements de chaleur au cours d'un processus particulier qui se déroule dans un système étudié (enthalpie, Δ*H*), il est possible de connaître d'autres paramètres thermochimiques (Δ*G*, Δ*S*) du système.

L'acquisition d'une base de données thermochimiques expérimentales pour une vaste gamme de réactions chimiques est la clé pour le développement ultérieur de méthodes de calcul précises et ayant une valeur prédictive fiable.

Dans le meilleur des cas l'acquisition des paramètres thermochimiques expérimentaux du système permettrait la validation des méthodes de calcul et assurerait une meilleure prise en compte des interactions non-covalentes.

Dans la présente thèse, les expériences de calorimétrie par titration isotherme (ITC) ont été utilisées comme principal outil expérimental. Pour les expériences ITC, un dispositif Nano ITC (TA Instrument ®) a été utilisé. En tant qu'outil théorique, les calculs statiques DFT-D ont été effectués. Outre ces techniques, une recherche de Cambridge Structural Database (CSD) a été effectuée comme une méthode complémentaire et d'aide aux calculs.

Tout au long de la thèse, la recherche s'est concentrée sur les réactions chimiques suivantes décrites dans le Schéma A1. Les systèmes réactionnels ont été sélectionnés si: a) ils présentent un sujet important dans le monde chimique, ou dans leur transformation chimique un mécanisme de réaction par étapes est supposé/documenté; b) l'influence des interactions non-covalentes dans le système est significative.

Outre les études ITC et théoriques, la plupart des réactions (réactifs et produits de réaction) ont été entièrement caractérisées par des méthodes analytiques standard (spectroscopie RMN, spectroscopie de masse, analyze élémentaire, diffraction des rayons X, spectroscopie IR). De plus, les réactions des (F)LP ont été suivies par des expériences 2D RMN-DOSY.

Les études par ITC ont couvert à la fois l'aspect cinétique (ordre relatifs, constantes de vitesse initiale la réaction, si possible, selon les conditions réactionnelles utilisées) et l'étude thermodynamique (Δ*H*, Δ*G*, Δ*S*) des systèmes réactionnels, tandis que par les calculs DFT-D seuls les paramètres thermochimiques (Δ*H*, Δ*G*, Δ*S*) des systèmes réactionnels en phase

gazeuse et/ou chlorobenzène ont été obtenus. La recherche CSD a été effectuée uniquement dans le cas des LP(F).

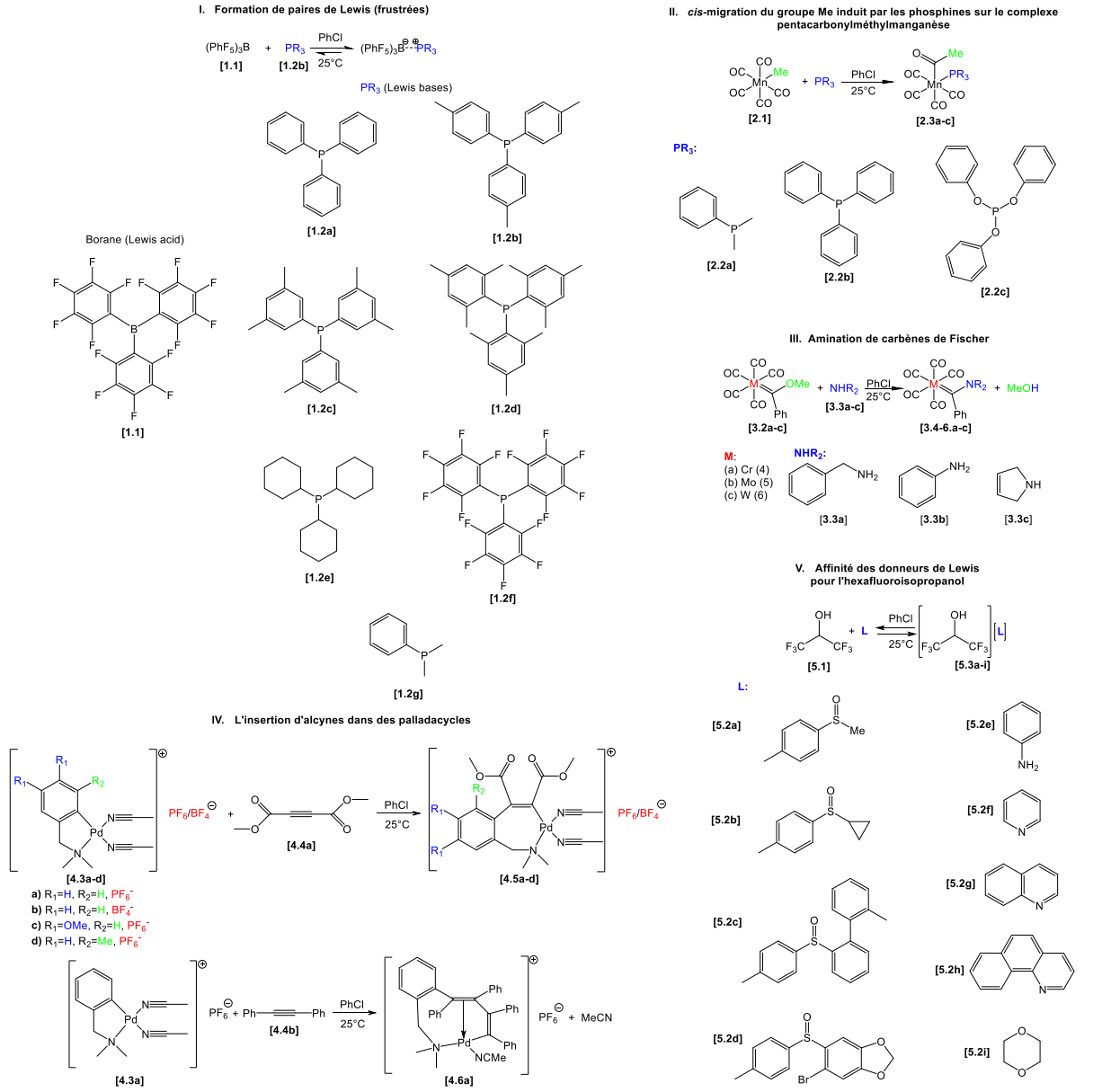

Schéma A1. Représentation schématique des systèmes réactionnels étudiés au cours de la thèse.

I. Formation de paires de Lewis (frustrées)

La découverte de paires acide-base de Lewis (FLP) "frustrées", parmi lesquelles le tris (pentafluorophényl) borane avec une variété de phosphines sont les plus étudiées, a montré une grande influence des interactions non-covalentes dans ces systèmes et a ouvert un

nouveau domaine de recherche en chimie. Le concept FLP, établi par Stephan, a suscité un grand intérêt au cours de la dernière décennie. Le concept est basé sur la constatation que les systèmes contenant des acides et des bases de Lewis, qui sont empêchés par des facteurs stériques (et électroniques) d'interactions donneur-récepteur classiques, conservent leur acidité et leur basicité de Lewis et sont donc disponibles pour interagir avec une troisième molécule. Les paires phosphine-borane, en particulier celles "frustrées", ont trouvé une grande utilité dans les domaines de la synthèse et de la catalyse jusqu'au stockage de l'hydrogène et aux matériaux. De nombreux rapports ont traité des calculs sur les systèmes phosphine-borane, en particulier leurs énergies d'interaction et les distances connexes entre les centers acide et base; les influences des substituants sur les atomes de bore et de phosphore sur leur réactivité; les mécanismes de réaction catalytique, ainsi que l'importance des interactions non covalentes. En dépit d'un grand nombre d'articles qui ont abordé les FLP, certains aspects du comportement chimique des FLP ne sont pas encore entièrement compris, en particulier la thermochimie réelle des interactions en solution de paires intermoléculaires et le mode d'agrégation réel pour ces paires (FLPs) en solutions.

Comme mentionné précédemment, l'approche utilisée ici est principalement basée sur l'investigation ITC. La recherche a révélé des résultats assez intéressants et, dans certains cas, surprenants. A savoir, les systèmes **1.1/1.2a-c** forment des paires cohérentes, le système **1.1/1.2d** existe dans un équilibre, alors que le système **1.1/1.2f** ne montre aucune tendance à former une paire stable. Une hypothèse de formation de clusters (très probablement composée d'une molécule de phosphine et d'aux moins deux molécules de borane), relevée à partir des thermogrammes ITC, est confirmée à la fois par des expériences RMN DOSY 2D et des calculs DFT-D.

Les valeurs d'enthalpies Δ*H* résultats déduites des mesures par ITC ont montré que, parmi toutes les formations d'adduit étudiées ici, la plus forte enthalpie libérée l'est pendant la formation de $mes_3PB(PhF_5)_3$ (**1.1/1.2d**, produit d'addition FLP bien connu), suggérant que les interactions non-covalentes ont une énorme influence au sein de ces systèmes. Les valeurs Δ*H* prédites par DFT-D qui expliquent l'influence du chlorobenzène sont en bon accord avec les données expérimentales ITC. De nombreux paramètres géométriques utiles de paires phosphine-borane classiques et frustrées ont été obtenus par la recherche CSD. Ces paramètres ont permis de rationaliser les différences entre eux, compte tenu de leur orientation mutuelle et des distances.

II. Cis-migration du groupe Me induit par les phosphines sur le complexe pentacarbonylméthylmanganèse.

Le complexe pentacarbonylméthylmanganèse a été parmi l'un des premiers complexes contenant des ligands carbonyle jamais synthétisés. Depuis cette découverte, ce complexe a été étudié intensivement en utilisant diverses techniques expérimentales disponibles à ce moment-là. Il a été trouvé qu'en réaction avec des nucléophiles, une migration du groupe méthyle vers le ligand carbonyle adjacent est induite et suivie par l'insertion des nucléophiles dans le complexe. Plus tard, la séquence d'insertion migratoire s'est avérée être une séquence importante en catalyse. Par conséquent, de nombreuses recherches expérimentales et théoriques ont été réalisées afin de trouver son mécanisme ainsi qu'une cinétique de l'étape d'insertion de nombreux ligands nucléophiles. Le complexe s'est avéré être important en synthèse en tant que précurseur et catalyseur. Néanmoins, peu a été publié sur la thermochimie actuelle de la réaction d'insertion-migration impliquant le complexe pentacarbonylméthylmanganèse avec des bases de Lewis.

La séquence de réaction d'insertion-migration dans le pentacarbonylméthylmanganèse, induite par la série de phosphines (**2.2a-c**, Schéma A1), a été étudiée dans le sens des recherches expérimentales cinétiques et thermodynamiques et des recherches théoriques DFT-D.

Les essais de réaction ont suggéré que les réactions secondaires (c'est-à-dire l'isomérisation et la décarbonylation du produit cis) pouvaient être évitées à des températures de réaction plus basses dans des périodes de temps de réaction plus courtes.

Les résultats thermodynamiques ITC (gamme de ITC raw ΔH_r -9 - -12,5 kcal/mol) suggèrent que des interactions raisonnablement plus fortes pourraient être établies grâce à la séquence de migration cis-insertion étudiée, indiquant une différence entre les phosphines choisies: leur capacité à établir interactions non-covalentes et l'affinité nucléophile. Les résultats cinétiques ITC ont confirmé un premier ordre partiel dans le complexe **2.1**.

Bien que les calculs de COSMO DFT-D statiques aient prédit des enthalpies de réaction beaucoup plus grandes (environ 2,5 fois) - les valeurs de ΔH_r d'environ de -22 kcal/mol à -31 kcal/mol et les valeurs ΔH_r calculées sont conformes (en ce qui concerne leurs caractéristiques structurelles et électroniques). Une telle surestimation découle probablement de la non prise en compte des interactions explicites du chlorobenzène avec les réactifs, en particulier avec le

complexe. Les énergies libres de Gibbs calculées (valeurs de ΔG_r environ de -8 kcal/mol à -17 kcal/mol) suggèrent la possibilité d'interactions tout à fait spontanées.

III. Amination de carbènes de Fischer

Les carbènes de type Fischer peuvent être décrit par une formule structurale générale de $(CO)_5M=C(X)R$, dans laquelle l'atome de carbone carbènique est lié à un métal de transition faiblement valent provenant du groupe VI-VIII de PTE. La nature de la liaison C-M peut être décrite comme σ-donneur/π-accepteur (σ-donating/π-back-donating), tandis que la nature de la liaison dans M-C-X comme (faible) interaction trois-centré de quatre électrons. Le groupe X est habituellement un groupe donneur d'électrons ayant un effet stabilisant sur un atome de carbone de carbène déficient en électrons tandis que le groupe R peut être un groupe organique saturé ou insaturé. Pour stabiliser un center métallique à faible valence, de nombreux ligands accepteurs de π pourraient être utilisés. Dans le complexe de carbène de Fischer typique, ces ligands accepteurs de type π sont des carbonyles. En raison de cette constitution du carbène, sa caractéristique chimique générale pourrait être décrite comme électrophile, contenant peu de sites réactifs potentiels. En conséquence de telles propriétés chimiques polyvalentes, associées à des caractéristiques électroniques accordables au niveau des substituants (X, R), les carbènes de Fischer sont des précurseurs très importants en synthèse organique et inorganique aussi bien que dans la synthèse de substrats biologiques actifs. L'accent sera exclusivement mis sur une réaction typique. La réaction d'aminolyse des carbènes de Fischer, dont le mécanisme et la cinétique sont bien établis. Elle peut être considérée comme analogue à l'amination d'esters. Curieusement, bien que beaucoup ait été fait expérimentalement et théoriquement concernant les mécanismes d'action ainsi que les caractéristiques de structure et la relation structure-réactivité des carbènes de Fischer, peu a été publié sur la thermochimie réelle de toute transformation incluant les carbènes de Fischer.

La réaction d'aminolyse, en général, la séquence de réaction d'addition-substitution (auto-) catalysée, a été étudiée sur des séries de carbènes de Fischer (Schéma A1) par des outils expérimentaux et théoriques.

Les résultats suggèrent une nature d'équilibre du processus d'amination ainsi que des produits de réaction secondaire. Les résultats des investigation la thermodynamique de cette réaction par l'ITC (valeurs de ΔH_r supérieures à -15 kcal / mol) suggèrent des transformations favorables dans le processus d'amination dans les systèmes **3.2a-c/3.3a** et **3.2a-c/3.3b**, tandis que les

systèmes **3.2ac / 3.3b** ont été trouvés non-exploitables. La dépendance claire du type de métal sur l'enthalpie de la réaction n'a pas pu être clairement établie. Les résultats des mesures cinétique par ITC ont plutôt confirmé un deuxième ordre partiel en amine.

Les enthalpies de réaction calculées (allant de -5,5 kcal/mol jusqu'à -20 kcal/mol) sont en excellent accord avec les valeurs expérimentales, tandis que les énergies libres de Gibbs calculées ont suggéré un processus spontané dans tous les systèmes. De plus, le calcul a révélé que l'amination des carbènes de Fischer étudiés ici par le phénylamine (**3.3b**) n'est pas thermodynamiquement possible dans des conditions normales, ce qui confirme les observations ITC.

IV. L'insertion d'alcynes dans des palladacycles.

Les métallocycles contiennent une liaison métal-carbone directe, dans laquelle l'atome de carbone fait partie de l'un des ligands métalliques. Comme l'activation des liaisons C-H est l'un des sujets les plus importants de la chimie organométallique, les métallacycles qui en résultent ont une grande importance dans de nombreux domaines: de la synthèse et la catalyse à la médecine et aux matériaux. En général, la réaction de cyclo-métallation dans le cas du palladium suit une voie électrophile assistée par une base. Parmi les métaux de transition, le palladium a été jusqu'à présent l'un des métaux les plus utilisés dans la chimie des métallacycles. Une insertion de divers types d'alcynes dans la liaison Pd-C a été observée par Pfeffer et ses collègues. Cette découverte s'est révélée comme une méthode préparatoire très utile pour la gamme de palladacycles contenant diverses fonctionnalités. Le mécanisme de l'insertion des alcynes dans les palladacycles suggère un processus par étapes commençant par une coordination de l'alcyne au palladium et une insertion migratoire subséquente de l'alcyne dans la liaison Pd-C. Bien que la cinétique des réactions d'insertion des alcynes dans les palladacycles soit décrite, aucune information de thermochimie réelle n'a encore été fournie.

Dans le cadre de cette étude, une série de mesures calorimétriques isothermes complétées par des estimations théoriques a été engagée. Deux substrats hautement actifs (**4.4a-b**) ont été utilisés pour étudier la cinétique et la thermodynamique de la réaction d'insertion par étapes dans les complexes cyclopalladiés chargés (Schéma A1). Ce dernier est encore plus actif et présente une double capacité d'insertion.

L'étude CTI cinétique a montré que la réaction était un pseudo premier ordre dans le cas de **4.4b**, ce qui est conforme aux données publiées.

La valeur de ΔH_r ITC obtenue d'une double insertion (environ -38 kcal/mol) est raisonnablement plus grande à la valeur ITC ΔH_r d'une seule insertion (d'environ -24 - -28 kcal/mol). Les valeurs de ΔH_r et ΔG_r prédites par DFT-D sont d'environ -10 - -15 kcal/mol plus grandes que les données ITC expérimentales, suggérant que le chlorobenzène pourrait avoir une influence compétitive significative, interagissant de manière non covalente, dans la séquence d'insertion par la solvatation de certains centers réactifs. Compte tenu de la complexité de la nature des réactifs et des transformations chimiques dans la réaction d'insertion, on peut conclure qu'il existe une bonne concordance entre les résultats expérimentaux et théoriques.

V. Affinité des donneurs de Lewis pour l'hexafluoroisopropanol.

Récemment, le 1,1,1,3,3,3-hexafluoropropan-2-ol (HFIP) s'est révélé comme un milieu exceptionnel, soit comme solvant, soit comme co-solvant, qui rend possible de nombreuses réactions. Il est connu que le HFIP possède une caractéristique acide et polaire et des capacités de liaison hydrogène, mais encore, son rôle exact de HFIP dans diverses transformations chimiques n'est pas entièrement et raisonnablement expliqué.

Pour déterminer le rôle possible du HFIP, la formation d'un complexe donneur-accepteur potentiel entre HFIP et une série de substrats différents (schéma A1) a été examinée par des expériences ITC et des calculs DFT-D. La portée des calculs a été étendue même à d'autres substrats (amines, cétones, aldéhydes, chlorobenzènes et HFIP).

Les résultats des analyzes ITC ont suggéré des interactions non-covalentes assez fortes à fortes (gamme de ITC ΔH_a -5 - -13 kcal/mol) dans les systèmes examinés. De plus, il a été conclu sur la base des valeurs de ΔG_a (compris entre -1,4 et -3,2 kcal/mol) déterminées que tous les donneurs de Lewis considérés pourraient interagir spontanément avec le HFIP. Au total, cela pourrait avoir une influence énorme sur la polarisation des liaisons au sein de la molécule donneuse de Lewis, qui pourrait être d'une importance cruciale dans les étapes clés de diverses transformations chimiques, suggérant que HFIP pourrait avoir un rôle non innocent dans les processus catalytiques.

Bien que les résultats des calculs de ΔH_a dans une phase gazeuse soient cohérents avec les résultats expérimentaux (ITC ΔH_a) dans la barre l d’erreur, il a été démontré que le traitement par le modèle de solvatation COSMO pouvait être le mieux adapté. De plus, il a été démontré que le chlorobenzène interagissait considérablement avec le HFIP et que le HFIP pouvait interagir assez fortement avec lui-même. Les calculs ont montré que l'azote est un accepteur de

liaison H plus fort que l'oxygène, tandis que le dernier est plus fort que le soufre et que HFIP préférerait plutôt interagir avec les atomes d'hydrogène aliphatiques que les atomes d'hydrogène aromatiques.

En ce qui concerne les résultats obtenus, on peut conclure que les objectifs de la thèse sont atteints.

Les expériences ITC, étendues à la chimie organique et organométallique, constituent une technique puissante pour obtenir des données de réaction cinétiques et thermodynamiques fiables.

Les calculs DFT-D ont montré des capacités dans la modélisation précise des systèmes de réaction ainsi que dans la bonne à l'excellente prédiction des paramètres thermochimiques des réactions.

Par la suite, une énorme base de données expérimentale de thermochimie d'un certain nombre de réactions est produite, et peut être utilisée comme référence dans d'autres améliorations des calculs de DFT et de chimie quantique.

La recherche apporte un éclairage sur les FLP existantes et la chimie du HFIP en révélant la possible existence d’agrégats moléculaires dans un cas et prouvant une formation de complexes donneur-accepteur relativement forts dans l’autre.

Il est montré que diverses transformations chimiques dans des complexes organométalliques (comme la migration-insertion, de nombreuses insertions par étapes, des séquences de réaction d'addition-élimination auto-catalysées) peuvent être étudiées et décrites expérimentalement - par des expériences ITC cinétiques et thermodynamiques et théoriquement - par des calculs statiques DFT-D.

Le rôle des interactions non-covalentes dans les systèmes examinés est important à crucial.

Table of Contents

List of Abbreviations

ADF – Amsterdam density functional
BJ – Becke-Johnson
BSSE – basis set superposition error
CC – coupled-cluster
CCSD – CC, single, double (excitations)
CCSD(T) – CC, single, double (triple) (excitations)
CI – configuration interaction
CISD – CI, single, double (excitations)
COSMO – conductor like screening model
COSMO-RS – COSMO for real solvents
CPCM – conductor-like PCM
CSD – Cambridge structural database
DFT – density functional theory
DFT-D – DFT corrected for dispersion
DMAD – dimethyl acetylenedicarboxylate
DOSY – diffusion-ordered spectroscopy
DPCM – dielectric PCM
EC – electron correlation
ESI – electron-spray ionization
FCI – full configuration interaction
FCISD(T) – FCI, single, double (triple) (excitations)
FLP – frustrated Lewis pair
GGA – generalized-gradient approximation
GM – generalized Born
H-bond – hydrogen bond
HF – Hartree-Fock
IEF – integral equation formalism
IEFPCM – integral equation formalism PCM
IR – infrared
ITC – isothermal titration xalorimetry
KS – Kohn-Sham
LC – long-range correction
LDA – local density approximation
LP – Lewis pair
MC – Monte Carlo
MD – molecular dynamics
Me – methyl
MM – molecular mechanics

MO – molecular orbital
MP2 – Møller-Plesset second order
MP4 – Møller-Plesset forth order
MP4SDQ – MP4, single, double, quadruple (excitations)
MP4SDSTQ – MP4, single, double, triple, quadruple (excitations)
MPE – multipole expansion
MW – micro wave
NCIs – non-covalent interactions
NMR – nuclear magnetic resonance
PBE – Perdew-Burke-Erzenhof
PCM – polarizable continuum model
ppm – part per milion
QCI – quadratic configuration interaction
QCISD – QCI, single, double (excitations)
QCISD(T) – QCI, single, double (triple) (excitations)
QMC – quantum Monte Carlo
REMPI – resonance-enhanced multiphoton ionization
SAPT – symmetry-adapted perturbation theory
SCF – self-consistent field
SCRF – self-consistent reaction filed
SVPE – surface and volume polarization for electrostatics
SS(V)PE – surface and simulation of volume polarization for electrostatics
TPSS – Tap-Perdew-Staroverov-Scuseria
TS – Tkatchenko-Scheffer
TS-SCS – TS self-consisted screening
UV – ultra violet
vdW – van der Waals
VRT – vibration-rotation-tunnelling
WFT – wave function theory
XDM – exchange-hole dipole moment
ZEKE – zero electron kinetic energy
ZORA – zeroth order regular approximation

Chapter 1

General Introduction

1.1. The problematics, the aims and the tools of the Thesis.

Question: *What is the problematics of the Thesis' research*?

Answer: It can be said that the chemical bond, in its the broadest sense, is one of the crucial points of research in chemistry. Up to date, many aspects of various kinds of chemical bond have well been described, but some of them, especially weak non-covalent interactions, still remain a challenge for the scientific world. Although, the re-emergence of this fundamental subject of the understanding of some unknown aspects of the chemical bond is made possible by the availability of powerful computers, even though their power is not sufficient for calculations based on the CCSD(T) or FCISD(T) method (golden standard in theoretical chemistry)[1] within a reasonable time, especially for the calculations of larger molecular systems. Therefore, new theoretical tools have been developed, in particular, the methods known as DFT-D, i.e. DFT corrected for dispersion; allow to account for in a physically relevant way the effects of dispersion at medium to long distances[2] However, to have reliable theoretical data, they must be supported by experimental ones. In other words, caused by a lack of experimental data, especially the data on reactions in solution involving metals, there is a need to benchmark newly developed methods. On the other hand, although there are several approaches of modelling the solvation[3] still there is a need for their improvement. Namely, the approaches are mainly based on implicit (continuum) modelling of the solvent effects: in cases wherein a coordination of a solvent molecule to a metal center is possible or when a solvent molecule can concurrently and significantly interact with a reactant, the risk of improper modelling of the solvent effects is high. Thus, in some cases additional calculations including explicit solvent molecule might refine the theoretical estimations.

Question: *What is the importance of the Thesis' research?*

Answer: London force (named after the physicist Fritz London) or dispersion[4] is ubiquitous in nature. It constitutes an important part of the energy contribution to the stabilization of the tertiary structure of peptides, other natural polymers as well as the spontaneous coalescence of atomic clusters or apolar molecules. The specificity of the London force is that it is related to

[1] [N^0 1] P. Hobza, *Acc. Chem. Res*. **2012**, *45*, 663.
[2] [N^0 2] R. Huenerbein, B. Schirmer, J. Moellmann, S. Grimme, *Phys. Chem. Chem. Phys.* **2010**, *12*, 6940.
[3] [N^0 3] see section *1.4.2.1.3. Solvation treatment* for the details.
[4] [N^0 4] F. London, *Z. Physik* **1930**, *63*, 245.

long distances and is always attractive, thus, it is also effective intra-molecularly and determines in many situations the conformational behavior of organic molecules and organometallics. Combined with electrostatic and orbital interactions, it helps to define the stereochemical course of many reactions; it plays an essential role in the processes of recognition and chiral discrimination.[5] Consequently, a proper accounting for the dispersion and the other non-covalent interactions is found to be of crucial importance. In addition, since almost all chemical and biochemical processes take place in solution, it was found to be important to experimentally/theoretically study the processes in solution.

By gathering the need for experimental data to benchmark the theoretical methods with the needs for the proper accounting the non-covalent interactions for studying chemical reaction in solution, it seems that if the research would provide, first of all, a base of the experimental data of huge scope of chemical reactions (in solution), it can be extremely useful for validation of the existing theoretical methods as well as for a further develop of the better ones.

Additionally, by having the experimental data of the system which are in accordance with computationally predicted ones (because of right reasons), the role of non-covalent interactions in the considered system could be rationally elucidated.

Question: *What kind of experimental data can be used to benchmark the theoretical methods?*

Answer: There are several experimental methods, mainly spectroscopy based, which can provide information about vibration frequencies, rotational constants, energies of excitation states, and stabilization energies of various kinds of systems.[6]

Since all these quantities can be computed to some accuracy by conventional theoretical methods, they have been used for actual benchmarking the quantum chemical methods (besides theory benchmarking theory). However, none the method provides an easy access to the structure and stabilization energy of (especially on non-covalently bonded) system, except Zero Electron Kinetic Energy (ZEKE) spectroscopy which accurately determines the stabilization energy. In addition, all the techniques available do not deal with chemical reactions.[7]

---

[5] [N^0 5] A. J. Stone, *The Theory of Intermolecular Forces*; Oxford University Press. Oxford, **2002**. P.
[N^0 6] Hobza, K. Müller-Dethlefs, In *Non-Covalent Interactions: Theory and Experiment*; The Royal Society of Chemistry, **2009**
[6] [N^0 7] see section *1.4.1. Experimental tools* for the details.
[7] [N^0 8] see section *1.4.2. Theoretical tools* for the details.

On the other hand, heat is one of the rare observables that accompanies every (intrinsic) change of the matter and it could be liberated from the matter to its surroundings or reverse (absorbed from the surroundings by the matter). Hence, measuring the heat change of the system of interest is one of the very powerful experimental techniques for monitoring the changes in the researched system. One of the most popular experimental techniques which allows recording of heat flow produced by a reaction is calorimetry.[8]

According to the well-known thermodynamic laws (Gibbs equations), by knowing the heat changes during a particular process which takes place within a researched system (i.e. enthalpy, Δ*H*) it is possible to know other thermodynamic parameters (i.e. Gibbs free energy, Δ*G*, and entropy, Δ*S*) of the system.[9] Since the theoretical calculations can also provide the thermodynamic parameters of the system (in both gas and solution phase), it seems that the thermodynamic parameters can be the good meeting point of the theory and experiments.

Therefore, acquiring a large base of the thermodynamic parameters of reactions/interactions in solution can be the solution for the benchmarking of the theoretical methods.

This methodology has proven rather useful by Dr. Petrović, a former PhD student in the group of Dr. Djukic, within his PhD thesis, which was based on experimental and theoretical investigation of the intermetallic interactions of transition metal coordination and organometallic complexes.

Question: *What are the suitable reaction systems?*

Answer: The reaction systems were selected if:

a) either they represent an important topic in the chemical world or in their course of chemical transformation a step-wise reaction mechanism is assumed/documented (which can be challenging for both experimental and theoretical chemists), and

b) an influence of non-covalent interactions in the system is significant.

Question: *What are the main aims of the Thesis' research?*

Answer: The thesis' research work was guided by the following goals:

[8] [N^0 9] see section *1.3. Thermochemistry and Thermodynamics*. for the details.
[9] [N^0 10] I. Müller, *A History of Thermodynamics – the Doctrine of Energy and Entropy*; Springer. **2007**.

a) acquiring an extensive thermochemical data library for the achiral organic or organometallic adduct formation with an extension to the organic frustrated Lewis pairs by means of the isothermal titration calorimetry (ITC);

b) theoretical modelling of the molecular systems and their thermochemical parameters by the DFT-D methods;

c) contribution to the benchmark of the computational methods by the constitution of experimental thermochemical base, mentioned earlier.

Question: *What are the tools used in the Thesis' research?*

Answer: Isothermal titration calorimetry (ITC) experiments were used as the main experimental tool. As a theoretical tool, static DFT-D calculations were performed. Besides those techniques, a search of Cambridge Structural Database (CSD) was performed as a complementary and helping method to the calculations, but only in the case of (frustrated) Lewis pairs ((F)LPs). Additionally, most of the reactions (reactants and reaction products) were fully characterized by standard experimental characterization methods (NMR spectroscopy, Mass spectroscopy, Elemental analysis, X-Ray diffraction, IR spectroscopy). Moreover, the reactions of interest were monitored by 2D NMR - DOSY (diffusion ordered spectroscopy) experiments. The ITC technique covered both kinetic (partial reaction orders, initial rate constants of the reactions, where possible, according to the used reaction conditions) and thermodynamic studies (ΔH, ΔG, ΔS) of the reaction systems, while DFT-D calculations aimed exclusively at the thermochemical parameters (ΔH, ΔG, ΔS) of the reaction systems in gas or/and chlorobenzene phase.

The herein mentioned topics will be discussed in more details in the following subchapters.

1.2. Chemical bonds.

1.2.1. Generalities.

It can be said that a chemical bond is an attraction between atoms leading to formation of chemical compounds. Regarding the nature of chemical bonds, they could be divided in few main types of bonding: ionic bonds (which are purely electrostatic in nature, attracting the oppositely charged ions); covalent bonds (which are characterized by sharing valence electrons between atoms); metallic bonds (are those in which there is a large delocalization of bonding

electrons over a lattice of metal atoms); coordinate covalent bonds (are basically covalent bonds in which the shared valence electrons come from only one atom); non-covalent interactions (which, according to one of most accurate formulations[10] include all other intra- and, especially, intermolecular interactions). However, herein, a (brief) discussion will only be given on covalent and non-covalent interactions (NCIs).

It can be said that covalent[11] and non-covalent interactions differ, even significantly, due to their origins. Namely, covalent interaction is a result of distribution and delocalization of electrons over whole regarded molecule as well as of sharing valence electrons (popularly valence pair(s)) of electrons between two atoms that constitute the molecule. Form theoretical point of view, a covalent bond is formed if two subsystems (atoms) carrying unfiled orbitals start to overlap, increasing electron density in a bonding region, and consequently, increasing a bond strength. Accordingly, an increasing of electron density in anti-bonding region leads to weakening of a bond. It was found that the orbital overlapping is the most efficient when interatomic distance is less then 2 Å, while over 4 Å the orbital overlapping becomes negligible.[12]

The formation and breaking chemical bonds, especially covalent ones, can be described at different level of theory (e.g. *ab initio* and Density Functional Theory (DFT) calculations) as well as experimentally using various spectroscopic experimental techniques that provide (mostly indirect) a look at a molecule (e.g. supersonic expansion jet technique coupled with high-resolution spectroscopic methods).

1.2.2. Non-covalent Interactions (NCIs)

1.2.2.1. Generalities.

Historically speaking, the story about non-covalent interactions has been started in mid of 19th century (1857) when Johannes Diderik van der Waals[13] has, for the first time, realized the main reasons that caused different behavior of real gases in comparison to behavior of ideal ones (that can be described by Boyle's law). Namely, he concluded that the reasons are the attraction

[10] [N^0 11] K. Müller-Dethlefs, P. Hobza, *Chem. Rev*. **2000**, *100*, 143.
[11] [N^0 12] G. N. Lewis, *J. Am. Chem. Soc*. **1916**, *38*, 762.
[12] [N^0 6] P. Hobza, K. Müller-Dethlefs, In *Non-Covalent Interactions: Theory and Experiment*; The Royal Society of Chemistry, **2009**.
[13] [N^0 13] L. M. Brown, A. Pais, B. Pippard, *Twentieth Century Physics*; Institute of Physics Pub.; American Institute of Physics Press, Bristol; Philadelphia; New York, **1995**.

between moving particles, and their proper volume.[14] He compiled this in the following state function for real gases equation:

$$p = \frac{RT}{V - b} - \frac{a}{V^2}$$

where *p* is the pressure, *R* is the universal gas constant, *T* is the temperature, *V* is the molar volume, while *a* and *b* are empirical parameters related to particular gas. Although, this equation is not the most precise equation describing state function for real gases, it contributed considerably in understanding of new type of bonding. Another important moment was in 1908 when Kamerlingh-Omnes managed to do liquefaction of helium,[15] which decisively supported the existence of attractive interactions even between molecules barring no charge or permanent dipole moments. Further, two decades after Fritz London,[16] and soon after Hans Hellman,[17] gave important contributions in understanding and describing these interactions. London rationalized that these interactions have quantum origin. Basic principles of hydrogen bonding (one kind of NCIs) was described for the first time by Linus Pauling.[18] Beside these above-mentioned pioneers, there were other scientists during last century who contributed as well.[19]

Although it is possible to relate stability of, for instance, non-covalent complexes to the stabilizing role of NCI, it is not such easy to localize these interactions in space. Moreover, the understanding of the nature of NCIs is still not clear, as theoretical and experimental results are frequently in contradiction. Although many efforts have been made during last decades in both theoretical and experimental description of NCIs, improving theoretical methods and

---

[14] [N^0 14] J. D. van der Waals, In *Nobel Lecture: The Equation of State for Gases and Liquids*; NobelPrize.org. Nobel Media AB 2018. Wed. 22 Aug 2018. https://www.nobelprize.org/prizes/physics/1910/waals/lecture/
[15] [N^0 15] H. Kamerlingh Onnes, *Proc. R. Netherlands Acad. Arts Sci. (KNAW) 11* **1909**, 168.
[16] [N^0 16] F. London, *Trans. Faraday Soc*. **1937**, *33*, 8.
[N^0 4] F. London, *Z. Physik* **1930**, *63*, 245.
[N^0 17] R. Eisenschitz, F. London, *Z. Physik* **1930**, *60*, 491.
[17] [N^0 18] H. Hellmann, *Acta Physicochim*. **1935**, 273.
[18] [N^0 19] L. Pauling, *J. Am. Chem. Soc*. **1931**, *53*, 1367.
[19] [N^0 20] P. Hobza, R. Zahradnik, K. Müller-Dethlefs, *Collect Czech Chem. C* **2006**, *71*, 443.
[N^0 21] I. G. Kaplan, *Intermolecular Interactions; Physical Picture, Computational Methods and Model Potentials*; Wiley, Chichester, **2006**.
[N^0 5] A. J. Stone, *The Theory of Intermolecular Forces*; Oxford University Press, Oxford, **2002**.
[N^0 11] K. Müller-Dethlefs, P. Hobza, *Chem. Rev*. **2000**, *100*, 143.
[N^0 22] J. O. Hirschfelder, C. F. Curtiss, R. B. Bird, *Molecular Theory of Gases and Liquids*; Wiley, New York, **1954**.
[N^0 23] P. Debye, *Phys. Z*. **1921**, *22*, 302.
[N^0 24] I. E. Dzyaloshinskii, E. M. Lifshitz, P. P. Lev, *Sov. Phys. Usp*. **1961**, *4*, 153.
[N^0 25] D. Lanfbein, *Phys. Rev. B* **1970**, *2*, 3371.
[N^0 26] H. C. Hamaker, *Physica* **1937**, *4*, 1058.
[N^0 16] F. London, *Trans. Faraday Soc*. **1937**, *33*, 8.

experimental techniques, science is still quite far away from fully description and understanding of NCIs without any ambiguity. However, it is well established that NCIs can act, in comparison to the covalent interactions, at much larger distances, even at more than 10 Å (in biomacromolecules even at more than 100 Å). Therefore, NCIs do not, in general, require orbital overlapping, even overlapping of filled orbitals would lead to repulsive interactions. Accordingly, the origin of NCIs, i.e. the attraction between interacting "subsystems", should lie in purely electrical, and to some extent, magnetic properties of the "subsystems", meaning that the attraction originates from interactions between: permanent multipoles, permanent multipole and induced multipole, induced multipole and instantaneous multipole or, finally, instantaneous multipoles. All these types of NCIs will be briefly described in the following sections.

In addition, a nice overview about NCIs as well as a significant contribution to understanding of NCIs within some heterodox and atypical situations in transition metal chemistry has been given by C. Werlé, a former PhD student in Djukic's group. P. Petrović, also a former PhD student in Djukic's group, has gave important impact to the field of NCIs. His PhD thesis was based on experimental and theoretical investigation of the intermetallic interactions of transition metal coordination and organometallic complexes.

1.2.2.2. NCIs: basic interactions.

1.2.2.2.1. Permanent multipole/permanent multipole interactions.

This type of interactions is also known as *electrostatic interactions*, in which the electrostatic term predominates over other energy terms. All energy consideration within this type of interactions can be derived form so called Coulomb's law[20] and Coulombic potential energy which, for two point changes, can be expressed as:

$$V = \frac{q_1 q_2}{4\pi\varepsilon r}$$

where q_1 and q_2 represent these two charges, r distance between the charges and ε dielectric permittivity of the medium. Based on this equation the expression of (electrostatic) potential

[N^0 27] Y. Zheng, A. Narayanaswamy, *Phys. Rev. A* **2011**, *83*, 042504.

[20] [N^0 28] C. A. Coulomb, *Premier mémoire sur l'électicité et le magnétisme*; Histoire de l'Académie Royale des Sciences, Imprimerie Royale, **1785**, 569-577.

[N^0 29] C. A. Coulomb, *Second mémoire sur l'électicité et le magnétisme*; Histoire de l'Académie Royale des Sciences, Imprimerie Royale, **1785**, 578-611.

energy of other cases (permanent dipole/point charge; permanent dipole/permanent dipole, or interactions of higher order of multipoles) can readily be adapted.[21] Although such extension will not be given, it is important to note that by increasing the number of poles (*n*) the potential energy falls off by $1/r^n$. It is worth mentioning that there is no zero average interaction energy (which theoretically can happen due to rotation of systems) as lower energy orientations are always favoured, which can be expressed by so called Keesom interaction equation:

$$\langle V \rangle = -\frac{C}{r^6}$$

where C is expressed as:

$$C = \frac{2\mu_1^2\mu_1^2}{3(4\pi\varepsilon)^2 kT}$$

In fact, herein mentioned case of interaction between two point (permanent) charges corresponds to more familiar term – *ion-ion* interactions, while the terms permanent dipole/point charge interactions to *ion-dipole* interactions and permanent dipole/permanent dipole interactions to *dipole-dipole* interactions.

Ion-ion interactions are established when two ions with opposite and fully permanent charge interact. Typical examples of such interactions (bonds) is table salt NaCl. Although these interactions are among the strongest interactions (ranged 100-1000 kcal/mol), they can readily be split through interacting with polar solvent molecules. Namely, during solvation process many ion-dipole interactions do compensate such strong ion-ion bonds. Energy of these interactions falls off slowly as the energy is proportional to $1/r$.

Ion-dipole interactions occur when an ion interacts with a polar molecule (i.e. molecule having an electric dipole or multipole moment). Example of this type of interactions is the interaction of ions such as Na^+ with water molecule. Energy of these interactions is in range from 10 to 250 kcal/mol and depends of the ion charge, the molecule dipole moment and their mutual distance. The energy falls off by $1/r^2$. Normally, the dipole moment within a molecule is caused by the difference in electronegativity of atoms in the molecule. Atom having larger electronegativity attracts the electrons becoming more negative, while the other becomes more positive. During

[N^0 30] J. D. Jackson, *Classical Electrodynamics*; John Wiley & Sons Ltd, **1962**.

the interactions the negative end of the dipole is attracted by cations while the positive end is attracted by anions.

Dipole-dipole interactions are interactions between two polar molecules, i.e. two permanent dipoles. Example of such interactions can be any polar molecule interacting with itself (e.g. liquid water). The energy of this type of interactions is usually ranged 1-5 kcal/mol. Existence of these interactions force molecules to align with reverse direction of the dipoles in order to minimize the potential energy of the system. Caused by these interactions highly polar molecules (if liquids) have higher boiling points than molecules of the same molar weight. These interactions are quite short ranged, as their interaction energy falls off by $1/r^3$.

1.2.2.2.2. Permanent multipole/induced multipole interactions.

This type of interaction is known as *induction (polarization) interaction*, as well. In principle, these interactions are electrostatic in nature. These interactions occur due to fact that molecule with permanent dipole moment approaching to neighbouring polarizable atom/molecule without dipole moment (e.g. non-polar, neutral or spherically symmetric atom/molecule) can induce polarization (i.e. temporal dipole/multipole moment) in that atom/molecule. Consequently, the strength of these interactions depends on dipole moment of first molecule and polarizability of second one as well as on their mutual distance and orientation, but, by contrast to permanent multipole/permanent multipole interactions, these interactions do not depend on temperature (see the following equation of Debye force (parameter *C*).

$$C = \frac{\mu_1^2 \alpha'_2}{4\pi\varepsilon}$$

μ_1 is permanent dipole moment of first molecule and α'_2 is polarizability volume of second one. Energy of these interaction is rather relatively small (up to ca. 0.5 kcal/mol) and proportional to $1/r^4$.

1.2.2.2.3. Instantaneous multipole/induced multipole interactions.

This type of interactions, also called London dispersion interactions (named by Fritz London),[22] are consequence of oscillations/fluctuations of electron “clouds” and nuclei. Namely, as

[21] [N^0 31] P. Atkins, J. de Paula, *Physical Chemistry for the Life Science*; Oxford University Press, Oxford. **2006**.
[22] [N^0 16] F. London, *Trans. Faraday Soc*. **1937**, *33*, 8.

suggested by London,[23] the motion of electrons within (non-polar) systems (atoms/molecules) can result in formation of instantaneous dipole moment (μ_1^*), which, subsequently, can induce polarization in neighbouring atom/molecule, i.e. similar instantaneous dipole moment (μ_2^*). Consequently, these two dipoles show mutual attraction, and moreover, they are mutually direction correlated. The strength of these interactions is highly dependent on polarizability of both subsystems. These dispersive interactions occur between any molecules (even non-polar) and they are always attractive by nature (similar to the two previously described types of interactions). That was exactly the case in very surprising, in that time, condensation of dihydrogen,[24] liquefication of noble gases,[25] liquid state of benzene at room temperature.[26] Energy of these interactions (which can be approximated by London formula, see below) are usually very small (0.1-1 kcal/mol), but the net effect (in energy contribution) can be rather significant due to the possibility for a large number of these interactions (e.g. in proteins). Dispersion interaction energy is proportional to $1/r^6$.

$$C = \frac{3}{2}\alpha_1'\alpha_2'\frac{I_1 I_2}{I_1 + I_2}$$

α'_1 and α'_2 are polarizability volumes of the subsystems, while I_1 and I_2 are their ionization energies. As above-mentioned, it was shown that dispersion energy has important contribution to interaction energy of (aromatic) systems with delocalized π electrons, which significantly influenced further considerations on the stabilization of biomacromolecules. Discussion on theoretical modelling of these very important interactions will be given in next sections (see section Theoretical tools.)

1.2.2.2.4. Repulsive interactions.

Repulsion (electrostatic) interactions, as a balance to so far mentioned attractive interactions, are a result of overlapping of (occupied) orbitals of two non-bonded systems (atoms/molecules) when two systems (and their electron "clouds") approach each other. Basically, the origin of

---

[N^0 4] F. London, *Z. Physik*, **1930**, *63*, 245.
[23] [N^0 32] F. London, *Z. Physik Chem*. **1930**, *11*, 222.
[N^0 16] F. London, *Trans. Faraday Soc*. **1937**, *33*, 8.
[N^0 4] F. London, *Z. Physik* **1930**, *63*, 245.
[24] [N^0 33] J. W. Leachman, R. T. Jacobsen, S. G. Penoncello, E. W. Lemmon, *J. Phys. Chem. Ref. Data* **2009**, 38, 721.
[25] [N^0 34] H. Kamerlingh Onnes, In *Nobel Lecture: Investigation into the Properties of Substances at Low Temperatures, which Have Led, amongst Other Things, to the Preparation of Liquid Helium*; NobelPrize.org. Nobel Media AB 2018. Wed. 22 Aug 2018. https://www.nobelprize.org/prizes/physics/1913/onnes/lecture/

these interactions can be explained by Pauli exclusion principle and Heisenberg uncertainty principle.[27] Beside electron repulsions, there is a possibility for repulsion of incomplete shielded nuclei. Energy of the repulsion interaction is extremely dependent on mutual distance of the systems and it is approximately proportional to $1/r^{12}$. Consequently, it seems that the smallest distance between two non-bonded atoms cannot be less than the sum of their vdW radii. Although it is hard task to find exact formula describing the repulsion energy, especially for more complex systems, it is possible to do that employing some approximations that include few adjustable parameters (such as hard-sphere potential approximation).

1.2.2.3. NCIs: systemic interactions.

Intuitively, it could be concluded that systemic NCIs are results of simultaneous effect of several simple NCIs that take place in simple or more complex molecular systems. Herein, a couple of such systemic interactions will be briefly discussed.

1.2.2.3.1. Hydrogen bonds.

Generally, hydrogen bonds[28] (H-bonds) are a kind of electrostatic interactions, which can occur when there is a possibility to establish a link *D-H ·A* (where *D* represents an atom that is formally a donor of hydrogen atom, while *A* represents an atom that is formally an acceptor of hydrogen atom).

Although both *D* and *A* atoms are usually highly electronegative atoms (such as N, O, F etc,) while *D* also possesses a lone pair of electrons, there is no strict limitation in that regard. Thus, other atoms and ions can participate in H-bonding as well. In general, hydrogen bond formation can be considered in two ways: a) as an array of point charges (partial positive on H atom and partial negative on *D* and *A* atoms); b) as formation of three new delocalized orbitales (as each atom participate with one orbital).[29] Whatever approach is, it is noticeable that a strength of H-bonds is highly dependent on the nature of donor (*D*) and acceptor (*A*) atoms as well as on mutual position of all the three constituents (i.e. bond angle and distance). Certain structural

[26] [N^0 35] C. J. Benmore, B. Tomberli, P. A. Egelstaff, J. Neuefeind, *Mol. Phys*. **2001**, *99*, 787.
[27] [N^0 36] E. Pavarini, E. Koch, F, Anders, In *Correlated electrons: From Models to Materials* 2012.
[N^0 37] V. F. Weisskopf, *Science* **1975**, *187*, 605.
[N^0 38] H. C. Andersen, D. Chandler, J. D. Weeks, *J. Chem. Phys*. **1972**, *56*, 3812.
[N^0 39] P. A. M. Dirac, *Proc. Royal. Soc. Lond. S. A* **1926**, *112*, 661.
[28] [N^0 40] In IUPAC. Compendium of Chemical Terminology, Version 2.3.3. – 2014-02-24 – the "Gold Book" ed. XML version: Web.
[29] [N^0 31] P. Atkins, J. de Paula, *Physical Chemistry for the Life Science*; Oxford University Press, Oxford. **2006**.

evidence of hydrogen bonding can be found if the interatomic distance is less than sum of their vdW contacts.

Typical example of H-bonds is condensed water, where a hydrogen atom from one water molecule is shared with an adjacent water molecule. Energy of H-bond can vary form relatively very weak (0.25-0.5 kcal/mol, for example in proteins) to relatively quite strong (ca. 40 kcal/mol, for example in HF_2^-).

1.2.2.3.2. Hydrophobic interactions.

So-called hydrophobic effect, related to hydrophobic interactions,[30] represent special relation between polar water molecules and non-polar molecules (so-called hydrophobes) occurring when non-polar molecules are present in polar water medium. Namely, it is *well-known* that non-polar molecules are almost insoluble in polar solvents as a consequence of no possibility for strong interactions between polar and non-polar molecules. This results in a formation of some kind of solvent cages (so-called clathrates) around individual solute molecule, i.e. interface regions with low entropy (high order) of the solvent, as the solvent is translationally and rotationally constrained. However, according to the equation of Gibbs free energy this is not thermodynamically favorable situation ($\Delta G > 0$), as the change in entropy ($\Delta S < 0$) is large and cannot be compensated with the change in enthalpy (that is usually even positive, $\Delta H > 0$). However, by interaction between non-polar molecules through so-called hydrophobic interactions, this situation changes. Indeed, when two hydrophobes interact firstly the solvent cage should be deformed which leads to increasing of enthalpy ($\Delta H > 0$) but also to increasing in entropy ($\Delta S > 0$).

Once again, the enthalpy change is not so large (as the enthalpy also decreases due to attractive hydrophobic interactions) but the entropy change is. Therefore, resulting change in Gibbs free energy is negative, meaning that the aggregation of non-polar molecules in polar medium (water) is spontaneous process. In brief, the hydrophobic effect (hydrophobicity) leads to minimum exposed surface area of non-polar molecules (by aggregation) to polar (water) molecules[31] where the driving force of aggregation of hydrophobic molecules is an increase of entropy of aqueous phase and not (intrinsic) attraction of hydrophobic solutes. Good example of

[30] [N^0 41] D. Chandler, *Nature* **2005**, *437*, 640.
[N^0 42] C. Tanford *Prot. Sci*. **1997**, *6*, 1358.
[31] [N^0 40] In IUPAC. Compendium of Chemical Terminology, Version 2.3.3. – 2014-02-24 – the “Gold Book” ed. XML version: Web.

this kind of interactions is mixing of oil and water. Hydrophobic interactions are important in biology,[32] especially in the processes of protein folding.

1.2.2.3.3. Aromatic interactions.

Purely aromatic interactions are those attractive non-covalent forces between aromatic rings. Prototypical example of such interactions is benzene dimer.[33] These interactions are, in general, relatively weak (up to few kcal/mol) and acts outside the sum of relevant vdW radii. Although first attempts in description of these so-called π-π stacking interactions suggested that electrostatics forces are reasonable,[34] later studies showed important role of London dispersion forces.[35] In addition, it was noticed that substituents on benzene ring have considerable influence[36] which can be interpreted by Hunter-Senders model[37] or by model proposed by Wheeler and Huok.[38]

Experimentally, aromatic interactions in solution were observed by NMR[39] as well as by Double Mutant experiment.[40] Besides studies dealing with aromatics mostly organized in sandwich, T-shaped or displaced arrangements, it was found that interactions of aromatic molecules at large horizontal displacement are significantly strong.[41]

Another kind of aromatic interactions are cation-π interactions that represents interactions between ion and aromatic ring.[42] In some cases, the strength of cation-π interactions are even larger than the strength of salt bridges (which are, in principle, formed by H-bonds).[43] Most

---

[32] [N^0 43] H. J. Dyson, P. E. Wright, H. A. Scheraga, *Proc. Natl. Acad. Sci. USA* **2006**, *103*, 13057.
[33] [N^0 44] M. Rapacioli, F. Calvo, F. Spiegelman, C. Joblin, D. J. Wales, *J. Phys. Chem. A* 2005, *109*, 2487.
[N^0 45] J. Grant hill, J. A. Platts, H.-J. Werner, *Phys. Chem. Chem. Phys*. **2006**, *8*, 4072.
[N^0 46] R. Podeszwa, R. Bukowski, K. Szalewicz, *J. Phys. Chem. A* **2006**, *110*, 10345.
[34] [N^0 47] F. Cozzi, M. Cinquini, R. Annunziata, T. Dwyer, J. S. Siegel, *J. Am. Chem. Soc*. **1992**, *114*, 5729.
[N^0 48] C. A. Hunter, J. K. M. Snaders, *J. Am. Chem. Soc*. **1990**, *112*, 5525.
[35] [N^0 49] E.-I. Kim. S. Paliwal, C. S. Wilcox, *J. Am. Chem. Soc*. **1998**, *120*, 11192.
[N^0 50] S. Grimme, *Angew. Chem. Int. Ed.* **2008**, *47*, 3430.
[36] [N^0 51] M. O. Sinnokrot, C. D. Sherrill, *J. Phys. Chem. A* **2003**, *107*, 8377.
[N^0 52] M. O. Sinnokrot, C. D. Sherrill, *J. Am. Chem. Soc.* **2004**, *12*, 7690.
[37] [N^0 48] C. A. Hunter, J. K. M. Snaders, *J. Am. Chem. Soc*. **1990**, *112*, 5525.
[38] [N^0 51] M. O. Sinnokrot, C. D. Sherrill, *J. Phys. Chem. A* **2003**, *107*, 8377.
[N^0 52] M. O. Sinnokrot, C. D. Sherrill, *J. Am. Chem. Soc.* **2004**, *12*, 7690.
[N^0 53] S. E. Wheeler. K. N. Houk, *J. Am. Chem. Soc*. **2008**, *130*, 10854.
[39] [N^0 47] F. Cozzi, M. Cinquini, R. Annunziata, T. Dwyer, J. S. Siegel, *J. Am. Chem. Soc*. **1992**, *114*, 5729.
[N^0 54] F. Cozzi, R. Annunziata, M. Banaglia, K. K. Baldridge, G. Aguirre, J. Estrada, Y. Sritana-Anant, J. S. Siegel, *Phys. Chem. Chem. Phys.* **2008**, *10*, 2686.
[40] [N^0 55] S. L. Cockroft, C. A. Hunter, *Chem. Soc. Rev*. **2007**, *36*, 172.
[41] [N^0 56] D. B. Ninković, J. M. Andrić, S. D. Zarić, *ChemPhysChem* **2013**, *14*, 237.
[N^0 57] D. B. Ninković, G. V. Janjić, D. Ž. Veljković, D. N. Sredojević, S. D. Zarić, *ChemPhysChem* **2011**, *12*, 3511.
[42] [N^0 55] S. L. Cockroft, C. A. Hunter, *Chem. Soc. Rev*. **2007**, *36*, 172.
[43] [N^0 58] J. P. Gallivan, D. A. Dougherty, *J. Am. Chem. Soc*. **2000**, *122*, 870.

probably, these interactions are dispersive but also, to some extent, induced electrostatic in the nature[44] as well as dependent on mutual orientation of the interacting units.[45]

Similar to the pure aromatic interactions (π-π stacking), the cation-π interactions are influenced by the presence of substituents.[46] In addition, the associative interactions of metal cations and aromatics are well documented.[47]

Additional kind of the interactions are aromatic/chelate interactions. The chelate ring contains (transition) metal atom and can be planar having π delocalized system. It was found that the chelates can interact through π-π stacking[48] or to form XH-π interactions.[49] In addition, many significant information about chelates and their interactions have been provided by Zarić *et al.*[50] Recently, interactions of aromatic/H-bridged rings have been found as well.[51] In addition, it has been shown that stacking interactions of H-bridged rings are stronger than corresponding

[44] [N^0 59] S. Tsuzuki, M. Yoshida, T. Uchimaru, M. Mikami, *J. Phys. Chem. A* **2001**, *105*, 769.
[45] [N^0 60] C. D. Sherrill, T. Takatani, E. G. Hohestein, *J. Phys. Chem. A* **2009**, *113*, 10146.
[46] [N^0 61] S. Mecozzi, A. P. West. Jr., D. A. Dougherty, *Proc. Nat. Acad. Sci. USA*, **1996**, *93*, 10566.
[N^0 62] S. Mecozzi, A. P. West. Jr., D. A. Dougherty, *J. Am. Chem. Soc*. **1996**, *118*, 2307.
[N^0 63] S. E. Wheeler. K. N. Houk, *J. Am. Chem. Soc*. **2009**, *131*, 3126.
[47] [N^0 64] S. D. Zarić, *Eur. J. Inorg. Chem.* **2003**, 2197.
[N^0 65] C. Rapp, E. Goldberger, N. Tishbi, R. Kirshenbaum, *Proteins: Struct., Funct., Bioinf*. **2014**, *82*, 1494.
[N^0 66] K. K. Bania, A. K. Guha, P. K. Bhattacharyya, S. Sinha, *Dalton Trans*. **2014**, *43*, 1769.
[N^0 67] D. A. Dougherty, *Science*, **1996**, 271, 163.
[N^0 68] D. A. Dougherty, *J. Nutr*. **2007**, *137*, 1504.
[N^0 69] S. A. Pless, A. P. Hanek, K. L. Price, J. W. Lynch, H. A. Lester, D. A. Dougherty, S. C. Lummis, *Mol. Pharmaco*l. **2011**, *79*, 742.
[48] [N^0 70] T. J. Anderson, G. D. Jones, D. A. Vicic, *J. Am. Chem. Soc*. **2004**, *126*, 8100.
[N^0 71] B. C. De Petar, H.-W. Fruehauf, K. Vrieze, R. De Gelder, E. J. Baerends, D. McCormack, M. Lutz, [N^0 70] L. Spek, F. Hartl, *Eur. J. Inorg, Chem*. **2004**, 1675.
[N^0 72] G. V. Janjić, J. M. Andrić, A. Kapor, Z. D. Bugarčić, S. D. Zarić, *CrystEngComm* **2010**, *12*, 3773.
[N^0 73] G. V. Janjić, P. V. Petrović, D. B. Ninković, S. D. Zarić, *J. Mol. Mod*. **2011**, *17*, 2083.
[N^0 74] D. N. Sredojević, Z. D. Tomić, S. D. Zarić, *Ctyst. Growth Des*. **2010**, *10*, 3901.
[N^0 75] D. N. Sredojević, D. Z. Vojislavljević, Z. D. Tomić, S. D. Zarić, *Acta Crystallogr.* **2012**, *B68*, 261.
[49] [N^0 76] G. A. Bogdanović, A. Spasojević-de Biré, S. D. Zarić, *Eur. J. Inorg. Chem*. **2002**, 1599.
[N^0 77] G. A. Bogdanović V. B. Medaković, M. K. Milčić, S. D. Zarić, *Int. J. Mol. Sci*. **2004**, *5*, 174.
[N^0 78] V. B. Medaković, M. K. Milčić, G. A. Bogdanović, S. D. Zarić, *J. Inorg. Biochem*. **2004**, *98*, 1867.
[N^0 79] M. K. Milčić, V. B. Medaković, D. N. Sredojević, N. O. Juranić, S. D. Zarić, *Inorg. Chem*. **2006**, *45*, 4755.
[N^0 80] S. Đ. Stojanović, V. B. Medaković, G. Predović, M. Beljanski, S. D. Zarić, J. Biol. *Inorg. Chem*. **2007**, *12*, 1063.
[N^0 81] M. K. Milčić, V. B. Medaković, S. D. Zarić, *Inorg. Chim. Acta* **2006**, *359*, 4427.
[50] [N^0 72] G. V. Janjić, J. M. Andrić, A. Kapor, Z. D. Bugarčić, S. D. Zarić, *CrystEngComm* **2010**, *12*, 3773.
[N^0 73] G. V. Janjić, P. V. Petrović, D. B. Ninković, S. D. Zarić, *J. Mol. Mod*. **2011**, *17*, 2083.
[N^0 82] D. P. Malenov, D. B. Ninković, D. N. Sredojević, S. D. Zarić, *ChemPhysChem* **2014**, *15*, 2458.
[N^0 83] D. P. Malenov, D. B. Ninković, S. D. Zarić, *ChemPhysChem* **2015**, *16*, 761.
[N^0 84] D. N. Sredojević, D. B. Ninković, G. V. Janjić, J. Zhou, M. B. Hall, S. D. Zarić, *ChemPhysChem* **2013**, *14*, 1797.
[N^0 85] Z. D. Tomić, S. B. Novaković, S. D. Zarić, *Eur. J. Inorg. Chem*. **2004**, 2215.
[N^0 86] Z. D. Tomić, D. N. Sredojević, S. D. Zarić, *Cryst. Growth Des*. **2006**, *6*, 29.
[N^0 87] D. P. Malenov, S. D. Zarić, *Phys. Chem. Chem. Phys.* **2018**, *20*, 14053.
[N^0 88] D. P. Malenov, M. B. Hall, S. D. Zarić, *Int. J. Quantum Chem*. **2018**; e25629.
[N^0 89] D. P. Malenov, G. V. Janjić, V. B. Medaković, M. B. Hall, S. D. Zarić, *Coord. Chem. Rev*. **2017**, *345*, 318.

interactions of benzene molecules.[52] There are increasing number of theoretical studies dealing the substitution effects, the effect of heteroatoms introduced in aromatic ring, and the effects of transition metal coordination.[53]

1.2.2.4. Importance of NCIs.

Everywhere where molecules are presented - non-covalent interactions are presented as well. Although weaker than covalent interactions, NCIs are omnipresent. If NCIs would not exist, condensed phase of matter would not exist neither. NCIs are responsible for wide range of properties of molecules and processes as well. Solvation process is undoubtedly attributed to NCIs. Highly dynamic behavior of systems is caused by presence of a large number of NCIs. Perhaps one of the most important examples of the significance of NCIs is liquid water, which survives in liquid state at wide range of temperatures due to the presence of hydrogen bonds. Another amazing example of crucial importance of NCIs in nature is an animal called gecko,[54] which can climb everywhere regardless of the surface.[55] It has been shown that (several thousand) of keratinous setae incorporated on its feet, form NCIs (i.e. dispersion interactions) with the surface and consequently strong adhesive force.[56]

The structure and (re)activity of biomacromolecules, such as DNA, RNA, proteins etc., are significantly determined by NCIs (i.e. hydrophobic effect, aromatic interactions, hydrogen bonding etc.). Processes of molecular recognition, which are highly important in many fundamental life processes, show very important role on NCIs. In particular, aromatic interactions play significant role in many chemical and biological process such as molecular recognition, molecular transport, and catalysis.[57] In addition, interactions of heteroaromatics

---

[51] [N^0 90] J. P. Blagojević, D. Ž. Veljković, S. D. Zarić, *CrystEngComm* **2017**, *19*, 40.
[52] [N^0 91] J. P. Blagojević, S. D. Zarić, *Chem. Commun.* **2015**, *51*, 12989.
[53] [N^0 51] M. O. Sinnokrot, C. D. Sherrill, *J. Phys. Chem. A* **2003**, *107*, 8377.
[N^0 53] S. E. Wheeler. K. N. Houk, J. *Am. Chem. Soc*. **2008**, *130*, 10854.
[N^0 63] S. E. Wheeler. K. N. Houk, J. Am. Chem. Soc. **2009**, *131*, 3126.
[N^0 92] S. A. Arnstein, C. D. Sherrill, *Phys. Chem. Chem. Phys*. **2008**, *10*, 2646.
[N^0 93] S. T. Mutter, J. A: Platts, *Chemistry*, **2010**, *16*, 5391.
[54] [N^0 94] P. Forbes, *The gecko's foot: How scientists are taking a leaf form nature's book*; Harper Perennial. **2006**.
[55] [N^0 95] A. P. Russell, *J. Zool*. **1975**, *176*, 437.
[N^0 96] P. F. A. Maderson, *Nature* **1964**, *203*, 780.
[56] [N^0 97] S. Hu, S. Lopez, P. H. Niewiarowski, Z. Xia, *J. Royal Soc. Inter*. **2012**.
[N^0 98] B. N. J. Persson, *MRS Bulletin* **2007**, *32*, 486.
[N^0 99] K. Autumn, A. M. Peattie, *Intergr. Comp. Biol*. **2002**, *42*, 1081.
[N^0 100] K. Autumn, Y. A. Liang, S. T. Hsieh, W. Zesch, W. P. Chan, T. W. Kenny, R. Fearilng, R. J. Full, *Nature* **2000**, *405*, 681.
[N^0 101] E. E. Williams, J. A. Peterson, *Science*, **1982**, *215*, 1509.
[57] [N^0 102] C. Bissantz, B. Kuhn, M. Stahl*, J. Med. Chem*. **2010**, *53*, 5061.

have important role in protein structure and protein-ligand recognition[58] as well as DNA structure.[59]

It has been shown that NCIs, have great contribution to stereospecificity of chemical processes,[60] drug design,[61] design of supramolecular assemblies,[62] design of coordination polymers and materials,[63] synthesis of organic molecules.[64] In addition, it was shown that properties of nitrogen heterocycles (e.g. pyridine, bipyridine, phenanthroline, etc.) as well as pyridine- and pyrazine- derivate chelate complexes can be: a) changed by coordination to metal ions and, b) controlled by changing a coordination mode of chelating ligands in coordination sphere of metal ions.[65] Although great efforts have been put to better understand and describe NCIs, it still remains hard task for both experimentalists and theoreticians.

1.3. Thermochemistry and Thermodynamics.

Thermochemistry, heat, calorimetry and thermodynamics are intimately connected. Semantically speaking, *thermo* in Greek represent a heat that makes more than obvious connection between

---

[N^0 103] M. Ma, Y. Kuang, Y. Gao, Y. Zhang, P. Gao, B. Xu, *J. Am. Chem. Soc*. **2010**, *132*, 2719.
[N^0 104] L. M. Salonen, M. Ellermann, F. Diederich, *Angew. Chem. Int. Ed*. **2011**, *50*, 4808.
[N^0 105] H.-J. Schneider, *Angew. Chem. Int. Ed*. **2009**, 48, 3924.
[N^0 106] M. O. Sinnokrot, E. F. Valeev, C. D. Sherrill, *J. Am. Chem. Soc*. **2002**, *124*, 10887.
[58] [N^0 107] R. Chelli, F. L. Gervasio, P. Procacci, V. Schettino, *J. Am. Chem. Soc*. **2002**, *124*, 6133.
[N^0 108] U. Samanta, P. Chakrabarti, *Protein Eng*. **2001**, *14*, 7.
[N^0 109] S. K. Burley, G. A. Petsko, *Science* **1985**, *229*, 23.
[59] [N^0 48] C. A. Hunter, J. K. M. Snaders, *J. Am. Chem. Soc*. **1990**, *112*, 5525.
[N^0 109] S. K. Burley, G. A. Petsko, *Science* **1985**, 229, 23.
[N^0 110] V. L. Malinovskii, F. Samain, R. Haner*, Angew. Chem. Int. Ed*. **2007**, *46*, 4464.
[60] [N^0 111] C. A. Eckert, D. L. Bergmann, D. L. Tomasko, M. P. Ekart, *Acc. Chem. Res*. **1993**, *26*, 621.
[N^0 112] O. Schuster, U. Monkowius, H. Schmidbaur, R. S. Ray, S. Krueger, N. Roesch, *Organometallics* **2006**, *25*, 1004.
[N^0 113] T. R. Ward, J. Collot, J. Gradinaru, A. Loosli, M. Skander, C. Letondor, E. Joseph, G. Klein, *Chimia* **2003**, *57*, 586.
[61] [N^0 114] S. Li, Y. Xu, Q. Shen, X. Liu, J. Lu, Y. Chen, T. Lu, C. Luo, X. Luo, M. Zheng, H. Jiang, *Curr. Pharm. Des*. **2013**, *19*, 6522.
[N^0 115] A. K. Patri, J. F. Kukowska-Latallo, J. R. Baker Jr., *Adv. Drug Delivery Rev*. **2005**, *57*, 2203.
[N^0 116] P. Zhou, J. Huang, F. Tian. *Curr. Med. Chem*. **2012**, *19*, 226.
[62] [N^0 117] D. B. Amabilino, J. Veciana, *Top. Curr. Chem*. **2006**, *265*, 253.
[N^0 118] C. G. Claessens, J. F. Stoddart, *J. Phys. Org. Chem*. **1997**, *10*, 254.
[N^0 119] J. A. A. W. Elemans, A. E. Rowan, R. J. M. Nolte, *J. Mater. Chem*. **2003**, *13*, 2661.
[63] [N^0 120] A. S. Borovik, *Comments Inorg. Chem.* **2002**, *23*, 45.
[N^0 121] L. H. Doerrer, *Comments Inorg. Chem.* **2008***, 29, 93.*
[N^0 122] C. A. Hunter, *Chem. Soc. Rev*. **1994**, *23*, 101.
[N^0 123] J. K. Klosterman, Y. Yamauchi, M. Fujita, *Chem Soc. Rev*. **2009**, *38*, 1714.
[N^0 124] J. M. Pollino, M. Weck, *Chem. Soc. Rev*. **2005**, *34*, 193.
[N^0 125] S. Zhang, D. M. Marini, W. Hwang, S. Santoso, *Curr. Opin. Chem. Biol*. **2002**, *6*, 865.
[64] [N^0 126] T. L. Brown, *Chemistry: the central science*; Prentice Hall, Boston, **2012**.
[N^0 127] D. H. Guston, *Encyclopedia of nanoscience and society*; Sage, Thousand Oaks, Calif, **2010**.
[65] [N^0 128] A. Rajput, R. Mukherjee, *Coord. Chem. Rev*. **2013**, *257*, 350.
[N^0 129] C. Janiak, *Dalton Trans*. **2000**, 3885.

the first two. On the other hand, calorimetry – the oldest experimental technique, founded by Black, Lavoisier and Laplace in 18th century, for studying the thermodynamics of chemical reactions, inseparably dealing with a measuring of heat (changes).[66]

It can be said that the thermochemistry is ground base for a proper understanding of chemical structures, dynamics and synthesis. If one would like to deal with molecular stability, the thermodynamics must be employed, as it provides a necessary framework to discuss such issue. However, theory without reliable data is useless. Therefore, it seems that a major concern are the reliable data as well as methods that can provide such data.

It has also been suggested to use a term *energetics* instead *thermochemistry* in order, from one hand, to emphasize that not all experimental methods involve determination of heat (such as equilibrium and kinetic experiments), and from another hand, to avoid traditional link between thermochemistry and calorimetry. Anyway, the laws of thermodynamics provide required theoretical background to deal with nearly all concepts relevant for discussion of either energetics or thermochemistry.[67]

Basically, two main outcomes from the laws of thermodynamics for chemistry can perhaps be represented in two equations:

$$\Delta_r G = -RT\ln K \quad \text{(equation 1)}$$

$$\Delta_r G = \Delta_r H - T\Delta_r S \quad \text{(equation 2)}$$

The first equation relates the reaction Gibbs free energy ($\Delta_r G$) with the equilibrium constant (K), while the second one relates the reaction Gibbs free energy ($\Delta_r G$) with the reaction enthalpy ($\Delta_r H$) and reaction entropy ($\Delta_r S$). These equations can be used to calculate the yields of chemical reactions, the equilibrium constants, the thermodynamic reaction parameters, etc. It should be noted that the quality of $\Delta_r G$ values are highly dependent on the quality of K values as well as that activity coefficients of solutes (γ) should be used in order to get more reliable results. In addition, kinetic characteristics of reaction (e.g. reaction rate constant (k)) can readily

[66] [N^0 130] J. A. Martinho Simoes, M. E. Minas da Piedade, *Molecular Energetics: condensed phase thermochemical techniques*; Oxford University Press, Inc, New York, **2008**. and related references therein.
[67] [N^0 130] J. A. Martinho Simoes, M. E. Minas da Piedade, *Molecular Energetics: condensed phase thermochemical techniques*; Oxford University Press, Inc, New York, **2008**. and related references therein.

be connected to thermodynamic ones.[68] However, due to the consistency such excursion will be avoided. More about experimental tools and methods which can be used to obtain thermochemical data as well as on an assessment of reliability of the data will be given in the following sections.

1.4. The tools.

1.4.1. Experimental tools.

1.4.1.1. Generalities.

Like mentioned in the early introduction to the thesis, experimental methods/techniques suitable for achieving the aims of this thesis would be those which can provide some (new) inside of the molecular structures, emphasizing a possible role of non-covalent interactions, especially for reactions in solution, and, in turn, generating such quantities that can accurately be estimated by quantum chemical (in particular by DFT) calculations.

In present state of science, there is no experimental technique providing direct measurement of strength of non-covalent interactions. Widely used experimental methods for studying non-covalent interactions of molecular clusters (which are said to be ideal systems for experimentally studying non-covalent interactions[69] are supersonic jet expansion[70] combined with additional, mainly spectroscopy-based techniques, such as vibrational – rotational (and its extensions – VRT, ER, MW), UV, IR, Raman and ZEKE spectroscopies, Resonance-Enhanced Multiphoton Ionization (REMPI), mass spectroscopy. Consequently, information about vibration frequencies,[71] rotational constants,[72] energies of excitation states,[73] stabilization energies,[74] mass signature[75] of various kinds of systems can be obtained.

---

[68] [N^0 130] J. A. Martinho Simoes, M. E. Minas da Piedade, *Molecular Energetics: condensed phase thermochemical techniques*; Oxford University Press, Inc, New York, **2008**. and related references therein.
[69] [N^0 11] K. Müller-Dethlefs, P. Hobza, *Chem. Rev*. **2000**, *100*, 143.
[70] [N^0 131] P. Hobza, H. L. Selzle, E. W. Schlag, *Chem. Rev.* **1994**, 94, 1767.
[N^0 132] P. Hobza, R. Zahradnik, *Chem. Rev*. **1988**, *88*, 871.
[71] [N^0 133] B. C. Garrett, D. A. Dixon, D. M. Camaioni, D. M. Chipman, M. A. Johnson, C. D. Jonah, G. A. Kimmel, J. H. Miller, T. N. Rescigno, P.J. Rossky, S. S. Xantheas, S. D. Colson, A. H. Laufer, D. Ray, P. F. Barbara, D. M. Bartels, K. H. Becker, K. H. Bowen, Jr., S. E. Bradforth, I. Carmichael, J. V. Coe, L. R. Corrales, J. P. Cowin, M. Dupuis, K. B. Eisenthal, J. A. Franz, M. S. Gutowski, K. D. Jordan, B. D. Kay, J. A. LaVerne, S. V. Lymar, T. E. Madey, C. W. McCurdy, D. Meisel, S. Mukamel, A. R. Nilsson, T. M. Orlando, N. G. Petrik, S. M. Pimblott, J. R. Rustad, G. K. Schenter, S. J. Singer, A. Tokmakoff, L.-S. Wang, C. Wittig, T. S. Zwier, *Chem. Rev*. **2005**, *105*, 355.
[N^0 134] A. B. E. H. Abou El-Nasr, A. Fujii, T. Ebata, N. Mikami, *Mol. Phys*. **2005**, *103*, 1561.
[N^0 135] P. Imhof, D. Krugler, R. Brause, K. Kleinermanns, *J. Chem. Phys.* **2004**, *121*, 2598.
[N^0 136] R. H. Wu, B. Brutschy, *J. Phys. Chem. A* **2004**, *108*, 9715.

Even though quite sophisticated, no technique provides an easy access to the structure and stabilization energy of (especially on non-covalently bonded) system giving unambiguous answers, except ZEKE spectroscopy which accurately determines the stabilization energy. Although vibrational frequencies are direct observables, often straightforwardly determined, providing information about the structure and strength of non-covalent systems,[76] sometimes not all the frequencies may be seen due to symmetry selection rules or Franck-Condon factors.[77] In addition, these experimental techniques do not, in principle, handle chemical reactions (in solution). Besides these, there are well-known NMR spectroscopy and X-Ray diffraction analysis, which are able to provide a lot of information regarding molecular structures.

[N^0 137] E. A. El-Hakam, A. El-Nasr, A. Fujii, T. Yahagi, T. Ebata, N. Mikami, *J. Phys. Chem. A* **2005**, *109*, 2498.
[72] [N^0 138] B. M. Giuliano, P. Ottaviani, W. Caminati, M. Schnell, D. Banser, J. U. Grabow, *Chem. Phys*. **2005**, *312*, 111.
[N^0 139] R. Sanchez, S. Blanco, A. Lesarri, J. C. Lopez, J. L. Alonso, *Chem. Phys. Lett*. **2005**, *401*, 259.
[N^0 140] S. Blanco, J. C. Lopez, A. Lesarri, W. Caminati, J. L. Alonso, *Mol. Phys.* **2005**, *103*, 1473.
[N^0 141] B. M. Giuliano, W. Caminati, *Angew. Chem. Int. Ed. Engl*. **2005**, *44*, 603.
[N^0 142] W. Caminati, J. C. Lopez, J. L. Alonso, J. U. Grabow, Angew. *Chem. Int. Ed. Engl*. **2005**, *44*, 3840.
[N^0 143] A. Lesarri, E. J. Cocinero, J. C. Lopez, J. L. Alonso, Angew. *Chem. Int. Ed. Engl*. **2004**, *43*, 605.
[N^0 144] J. L. Alonso, S. Antolinez, S. Blanco, A. Lesarri, J. C. Lopez, *J. Am. Chem. Soc*. **2004**, *126*, 3244.
[N^0 145] G. C. Cole, A. C. Legon, *J. Chem. Phys*. **2004**, *121*, 10467.
[N^0 146] P. W. Fowler, A. C. Legon, J. M. A. Thumwood, E. R. Waclawik, *Coord. Chem. Rev*. **2000**, *197*, 231.
[N^0 147] N. Goldman, C. Leforestier, R. J. Saykally, *Philos. Trans. Roy. Soc. A* **2005**, *363*, 493.
[N^0 148] F. N. Keutsch, J. D. Cruzan. R. J. Saykally, *Chem. Rev*. **2003**, *103*, 2533.
[N^0 149] J. D. Cruzan. L. B. Braly, K. Liu, M. G. Brown, J. G. Loeser, R. J. Saykally, *Science*, **1996**, *271*, 59.
[N^0 150] S. Chervenkov, P. Q. Wang, J. E. Braun, S. Georgiev, H. J. Neusser, C. K. Nandi, T. Chakraborty, *J. Chem. Phys*. **2005**, 122.
[N^0 151] T. V. Nguyen, T. M. Korter, D. W. Pratt, *Mol. Phys.* **2005**, *103*, 2453.
[N^0 151] S. Georgiev, H. J. Neusser, *J. Electron Spect*. **2005**, *142*, 207.
[N^0 153] C. Kang, D. W. Pratt, *Int. Rev. Phys. Chem*. **2005**, *24*, 1.
[N^0 154] D. W. Pratt, *Science* **2002**, *296*, 2347.
[N^0 155] M. S. Ford, K. Müler-Dethlefs, *Phys. Chem. Chem. Phys*. **2004**, *6*, 23.
[N^0 156] Y. H. Lee, J. W. Jung, B. Kim, P. Butz, L. C. Snoek, R. T. Kroemer, J. P. Simons, *J. Phys. Chem. A* **2004**, *108*, 69.
[N^0 157] X. Tong, M. S. Ford, C. E. H. Dessent, K. Müler-Dethlefs, *J. Chem. Phys*. **2003**, *119*, 12908.
[N^0 158] M. S. Ford, X. Tong, C. E. H. Dessent, K. Müler-Dethlefs, *J. Chem. Phys*. **2003**, *119*, 12914.
[73] [N^0 159] D. A. Beattie, R. J. Donovan, *Prog. React. Kinet. Mec*. **1998**, *23*, 281.
[N^0 160] S. Leutwyler, J. Bosiger, *Chem. Rev*. **1990**, *90*, 489.
[N^0 161] R. B. Bernstein, *J. Phys. Chem*. **1982**, *86*, 1178.
[74] [N^0 162] C. E. H. Dessent, K. Müler-Dethlefs, *Chem. Rev*. **2000**, *100*, 3999.
[N^0 163] K. Müler-Dethlefs, *J. Chem. Phys*, **1991**, *95*, 4821.
[N^0 164] K. Müler-Dethlefs, M. Sadner, E. W. Z. Schlag, *Z. Naturforsch. A* **1984**, *39*, 1089.
[N^0 165] K. Müler-Dethlefs, M. Sadner, E. W. Z. Schlag, *Chem. Phys. Lett*. **1984**, *112*, 291.
[N^0 166] W. Hebanicht, G. Reiser, K. Müler-Dethlefs, *J. Chem. Phys*. **1991**, *95*, 4809.
[75] [N^0 167] H. Krause, H. J. Neusser, *J. Chem. Phys*. **1993**, *99*, 6278.
[N^0 168] L. Zhu, P. Johnson, *J. Chem. Phys*. **1991**, *94*, 5769.
[N^0 169] D. M. Chapman, K. Müler-Dethlefs, J. B. Peel, *J. Chem. Phys*. **1999**, *111*, 1955.
[76] [N^0 170] M. Schmitt, C. Ratzer, W. L. Meerts, *J. Chem. Phys*. **2004**, *120*, 2752.
[N^0 171] A. Westphal, C. Jacoby, C. Ratzer, A. Reichelt, M. Schmitt, *Phys. Chem. Chem. Phys.* **2003**, *5*, 4114.
[N^0 172] M. Schmitt, C. Jacoby, M. Gerhards, C. Unterberg, W. Roth, K. Kleinermanns, *J. Chem. Phys*. **2000**, *113*, 2995.
[N^0 173] C. Jacoby, W. Roth, M. Schmitt, C. Janzen, D. Spangenberg, K. Kleinermanns, *J. Phys. Chem. A* **1998**, *102*, 4471.
[N^0 174] W. Roth, C. Jacoby, M. Schmitt, D. Spangenberg, C. Janzen, K. Kleinermanns, *Chem. Phys*. **1998**, *239*, 1.

In addition, dynamic NMR experiments can provide information related to reaction thermochemistry (based on determination of equilibrium constant). However, due to issues related with their use, they are not so practical for large series of experiments.

Since another approach, i.e. isothermal titration calorimetry (ITC), is used as a main experimental technique in this thesis' research, more details about calorimetry will be given in the following sections.

1.4.1.2. Calorimetry.

1.4.1.2.1. Generalities.

All chemical reactions are followed, at least on some parts on their course, by absorption or release of heat, from and into surrounding, respectively. Consequently, is seems that calorimeters, instruments which can precisely measure such heat changes taking please in reaction vessel, are ideal instruments for thermochemical studies. Therefore, it is not so surprising that most published enthalpies of formation and reaction in the condensed phase were determined by calorimetry.[78]

Although the term of heat dates back from ancient times, its first scientific description has been given by Lavoisier in 18th century.[79] The first calorimeter has been constructed by Lavoisier and Laplace, after the discovery of latent heat by Black. Generally, the main part of calorimeters is the reaction vessel, which is normally surrounded by a temperature-controlled jacket. Other usual parts are thermometers, stirring device, cooling, heating and ignition devices

In spite of the number of differently designed calorimeters, intended for various needs (in respect to the type and reaction conditions, to the sort of information pursued), all these can be put in few categories.[78] If they are based on heat exchange, three classes of calorimeters can be distinguished: adiabatic, heat conduction and isoperibol.[78]

Three different types of calorimeters based on different techniques of measuring the heat change (flow) will be briefly described in the following:

---

[77] [N^0 175] E. Condon, *Phys. Rev*. **1926**, *28*, 1182.
[78] [N^0 130] J. A. Martinho Simoes, M. E. Minas da Piedade, *Molecular Energetics: condensed phase thermochemical techniques*; Oxford University Press, Inc, New York, **2008**.
[79] [N^0 176] M. Kleibeer, in *The fire of life: an introduction to animal energetics*; ed. E. R. Krieger, Pub. Co, Huntington, New York, **1987**.
[N^0 177] A. C. Buchholz, D. A. Schoeller, *Am. J. Clin. Nutr*. **2004**, *79*, 899.

a) Temperature change instrument. This type of instruments measures the change of temperature of the calorimeter's (reaction) cell as reaction takes place in the latter. The resulting raw signal represents the temperature change of the reaction cell as a function of time. In order to obtain heat change of reaction, the measured temperature change (ΔT) should be multiplied by the energy equivalent of the calorimeter (ε_c), which can be determined by chemical and/or electrical calibration of the calorimeter.

b) *Heat conduction instrument*. This type of instruments is constructed in such a way that the reaction cell (in which a reaction takes place) is maintained at constant temperature by coupling it with a heat sink (which is actively controlled at constant temperature) through heat flow sensors. The raw data corresponds to a voltage developed within the heat flow sensors as the result of absorbed/released heat of the chemical reaction of interest. That voltage is subsequently converted into the heat change of reaction.

c) *Power compensation instrument*. The working principle of this class of instruments is based on whole time active maintenance the sample (reaction) cell at constant temperature by constant cooling/heating the sample cell. Once temperature change within the sample cell is detected (by sensor) the power is applied (by thermo-controller) to the (reaction) heater (which subsequently heat/cool the sample cell) so that the temperature of the sample cell is always the same. Therefore, the heat input of the reaction is efficiently compensated by the power required to maintain the sample cell at constant temperature. The resulting raw data represent exactly that power as a function of time. To obtain the heat change, the area of the measured signals should be integrated.

More details about this type of instrument as well as about related experimental details will be reported in the Methodology chapter.

Calorimetry was found to be very useful in various fields, from biology and biochemistry to chemistry and supramolecular chemistry. The first reports dealing with simultaneous determination of equilibrium constant (K_{eq}) and reaction enthalpy (ΔH) using titration calorimetry has been given by Christensen and Izatt.[80] However, due to the design of calorimeters (which were not too much sensitive) at that time, a determination of K_{eq} values was limited to values less than ca. 10^5. Use of calorimetry in binding studies on biological systems has been reported

[80] [N^0 178] J. J. Christensen, R. M. Izatt, L. D. Hansen, J. A. Partridge, *J. Phys. Chem*. **1966**, *70*, 2003.
[N^0 179] L. D. Hansen, J. J. Christensen, R. M. Izatt, *Chem. Commun*. **1965**, 36.

for first time by Langerman and Beaudette.[81] The first commercially available (isothermal) titration calorimeter specially designed for biological studies was released by MicroCal.[82]

In the last years, many improvements have been introduced in modern microcalorimeters, so that they became much more sensitive with faster responses making possible to measure very small heat effects (0.1 μcal) and, in the same time, very large binding constants (up to 10^{12}). Thank to these improvements, ITC is now routinely used for: thermodynamic characterization of biopolymer binding interaction;[83] estimating kinetic parameters in enzymatic studies;[84] investigation of interaction between DNA and cationic ligands[85] etc. In addition, there are many reports in literature dealing with benefits, drawbacks and progress (almost annually) of ITC[86] as well as with ITC experimental design and analysis of the data.[87] However, little has been published on the use of ITC in organic and organometallic chemistry.[88]

---

[81] [N^0 180] N. V. Beaudette, N. Langerman, *Anal. Biochem*. **1978**, *90*, 693.
[82] [N^0 181] T. Wiseman, S. Williston, J. F. Brandts, L. N. Lin, *Anal. Biochem*. **1989**, *179*, 131.
[83] [N^0 182] E. Freire, O. L. Mayorga, M. Straume, *Anal. Chem*. **1990**, *62*, 950A.
[N^0 183] M. W. Freyer, E. A. Lewis, in *Methods in Cell Biology*; eds. J. C. John, H. William Detrich, III, Academic Press, **2008**, vol. 87, 79-113.
[84] [N^0 184] C. Spink, I. Wadso, *Methods Biochem. Anal*. **1976**, *23*, 1.
[N^0 185] M. J. Todd, J. Gomez, *Anal. Biochem*. **2001**, *296*, 179.
[N^0 186] B. A. Williams, E. J. Toone, *J. Org. Chem*. **1993**, *58*, 3507.
[N^0 187] N. A. Demarse, M. C. Killian, L. D. Hansen, C. F. Quinn, *Methods Mol. Biol*. **2013**, *978*, 21.
[85] [N^0 188] T. Ehtezazi, U. Rungsardthong, S. Stolnik, *Langmuir* **2003**, *19*, 9387.
[N^0 189] M. Keller, M. R. Jorgensen, E. Perouzel, A. D. Miller, *Biochemistry* **2003**, *42*, 6067.
[N^0 190] D. Matulis, I. Rouzina, V. A. Bloomfield, *J. Am. Chem. Soc*. **2002**, *124*, 7331.
[N^0 191] C. K. Nisha, S. V. Manorama, M. Ganguli, S Maiti, J. N. Kizahakkedathu, *Langmuir* **2004**, *20*, 2386.
[N^0 192] E. Pozharski, R. C. MacDonald, *Biophys. J*. **2002**, *83*, 556.
[N^0 193] U. Rungsardthong, T. Ehtezazi, L. Bailey, S. P. Armes, M. C. Garnett, S. Stolnik, *Biomacromolecules* **2003**, *4*, 683.
[N^0 194] M. Keller, T. Tagawa, M. Preuss, A. D. Miller, *Biochemistry* **2002**, *41*, 652.
[86] [N^0 195] A. Velazquez Campoy, E. Freire, *Biophys. Chem*. **2005**, *115*, 115.
[N^0 196] G. A. Holdgate, *BioTechniques* **2001**, *31*, 164.
[N^0 197] I. Jelesarov, H. R. Bosshard, *J Mol. Recognit*. **1999**, *12*, 3.
[N^0 198] J. E. Ladbury, *Thermochim. Acta*. **2001**, *380*, 209.
[N^0 199] E. A. Lewis, K. P. Murphy, *Methods Mol. Biol*. **2005**, *305*, 1.
[N^0 200] F. P. Schmidtchen, in *Macrocyclic Chemistry*; ed. K. Gloe, Springer Netherlands, **2005**, ch. 19, pp. 291-302.
[N^0 201] P. C. Weber, F. R. Salemme, *Curr. Opin. Chem. Biol*. **2003**, *13*, 115.
[N^0 202] A. Ababou, J. E. Ladbury, *J. Mol. Recognit*. **2007**, *20*, 4.
[N^0 203] M. J. Cliff, A. Gutierrez, J. E. Ladbury, *J. Mol. Recognit*. **2004**, *17*, 513.
[N^0 204] J. E. Ladbury, *Biochem. Soc. Trans*. **2010**, *38*, 888.
[87] [N^0 205] E. A. Lewis, K. P. Murphy, *Methods Mol. Biol*. **2005**, *305*, 1.
[N^0 206] D. R. Bundle, B. W. Sigurskjold, *Methods Enzymol*. **1994**, *247*, 288.
[N^0 207] P. Puja, K. S. Gopinatha, *Photochem. Photobiol. Sci*. **2014**, *13*, 1192.
[N^0 208] E. Freire, *Drug Discovery Today: Technol*. **2014**, *1*, 295.
[N^0 209] L. Indyk, H. F. Fisher, *Methods Enzymol*. **1998**, *295*, 350.
[88] [N^0 210] M. Hamdaoui, M. Ney, V. Sarda, L. Karmazin, C. Bailly, N. Sieffert, S. Dohm, A. Hansen, S. Grimme, and J.-P. Djukic, *Organometallics* **2016**, *35*, 2207.
[N^0 211] A. Hansen, C. Bannwarth, S. Grimme, P. Petrović, C. Werlé, J.-P. Djukic, *ChemistryOpen* **2014**, *3*, 177.
[N^0 212] P. V. Petrović, S. Grimme, S. D. Zarić, M. Pfeffer, J.-P. Djukic, *Phys. Chem. Chem. Phys*. **2014**, *16*, 14688.
[N^0 213] H. Fischer, P. Hofmann, *Organometallics* **1999**, *18,* 2590.

The main features of the ITC, the technique of choice of the thesis' experimental research, will be given in the following section.

1.4.1.2.2. Isothermal titration calorimetry (ITC).

One of the main advantages of calorimetry-based techniques, especially modern ITC, against other experimental techniques is their ability for a direct and highly precise measure of heat of the process that takes place in the measuring cell. ITC measurements can be done: over a range of experimental conditions (for instance, at various temperatures, pH values etc.); with spectroscopically non-active reactants (there is no need for a chromophore or a fluorophore); in heterogeneous solution. Multiple (and very precise in modern ITC) addition of one of the reactants is one more benefit. All relevant thermodynamic parameters of reaction/interaction are obtainable in a single ITC experiment. Indeed, in simple binding process, obtained reaction/interaction enthalpy $\Delta_r H_{obs}$ corresponds to number of molecules involved in the reaction/interaction. From this, it can be concluded on the extent of the reaction/interaction as well as the binding/association constant ($K_{b/a}$) can be determined. Subsequently, form the $K_{b/a}$ value obtained and according to well-known Gibbs equations, other thermodynamic parameters (i.e. $\Delta_r G_{obs}$, $\Delta_r S_{obs}$) can be easily calculated. In addition, stoichiometry of reaction/interaction n (i.e. molar ration of reactants) is directly measurable, as well. It should be noted that all these thermodynamic parameters do not represent quantities related just for one single event (e.g. formation of complex), as heat of all potentional events (e.g. conformational changes, protonation/deprotonation, solvent rearrangement, etc.) is included in the measured total heat. Accordingly, to emphasize this a subscript *obs* is used. On the other hand, due to the fact that the ITC signal (heat rate), after multiplying with a particular calorimeter constant, is a direct measure of reaction rate, ITC experiments are also suitable for estimation of kinetic parameters (i.e. initial rate, initial rate constant, partial order with respect to reactants) of reaction. One of the potentially main weak points of ITC experiment is the duration of experiments (may practically take more than 24 hours), since it is very dependent on a nature of the studied system.

However, in spite of all above-mentioned benefits, ITC is a "black box". Therefore, one must know what (chemical/physical) processes take place. In addition, an experimentalist should perform an optimal design of the experiment and proper analyzing of the data obtained as well as reasonably estimate data uncertainties.

More practical details related to the design of ITC experiment and data analysis will be provided in the Methodology chapter.

1.4.2. Theoretical tools.

1.4.2.1. Generalities.

The core of most approaches in quantum chemistry is based on solving the well-known non-relativistic, time independent Schrödinger equation:[89]

$$\hat{\mathrm{H}}\Psi(r_1, \ldots, r_N) = \mathrm{E}\Psi(r_1, \ldots, r_N)$$

where $\Psi(r_1,\ldots,r_N)$, many electron wave function, is function of 3N variables (N is number of electrons). If this equation can be solved exactly, all the information of any electronic system can be obtained. Unfortunately, the exact solution is only accessible for the simplest systems, i.e. dihydrogen molecule, while for any larger system it is impossible due to existence of too many degrees of freedom. Consequently, in order to solve the equation, some approximation had to be introduced. Regarding to the employed approximation(s), the quantum chemical methods differ in the accuracy and computational time cost.

Earlier methods, exclusively based on the Hartree-Fock (HF) scheme,[90] rose up the fact that one of the main problems within the calculations is an estimation of contribution of interactions between electrons (termed the electron correlation). During the years, a large variety of computational schemes dealing with the electron correlation problem has been developed.[91] One of popular methods which account for the electron correlation most economically is given by Møller and Plesset through their second order perturbation theory (abbreviated as MP2).[92] Often used MP4 method (forth order Møller-Plesset perturbation theory) is more accurate but significantly more computational time costly than MP2. Other frequently used methods, which are based on configuration interaction (CI), quadratic CI (QCI), full CI (FCI) and coupled cluster (CC) approaches in principle can provide exact wave functions and related energies. Their extensions that account for single and double excitations (abbreviated as CISD, QCISD and CCSD, respectively) as well as even more sophisticated triple excitations (QCISD(T) and

[89] [N^0 214] E. Schrödinger, *Annalen der Physik* **1926**, *79*, 361.
[90] [N^0 215] C. Froese Fischer, *Comp. Phis. Comm*. **1987**, *43*, 355.
[91] [N^0 216] W. Koch, M. C. Holthausen, *A Chemist's Guide to Density Functional Theory*; Wiley-VCH, Weinheim, **2001**, and related references therein.

CCSD(T)) are used as well.[93] The latter two, known as golden standards in quantum chemistry, are the most accurate but also the most time demanding computational wave function based methods generally available. There are also related higher levels of MP perturbation theory, i.e. MP4SDQ and MP4SDSTQ, which are generally highly time demanding.[94]

In principle, energies of non-covalent interactions (NCIs) can be estimated in quite similar ways as energies of covalent interactions by means of standard quantum chemical methods, which are generally based on two approaches: perturbation or variational theory. The main difference between these two approaches is the way the calculation of the stabilization energy of the system is done.

The methods based on the perturbation theory give the stabilization energy separated into a few physically meaningful contribution parts (i.e. electrostatic, induction, exchange-repulsion and dispersion energy) considering a studied system in whole, while the variational method determines the stabilization energy as a difference between the energy of whole system (cluster) and the energies of the isolated subsystems. The main disadvantage of the perturbation method based calculations lies in the fact that they are more time demanding than variational calculations. Consequently, this has implications of the size of the system that can be studied in reasonable time by the perturbation method. Therefore, the perturbation method, especially those methods based on symmetry-adapted perturbation theory (SAPT),[95] is more suitable for more rigid systems, while the evaluation of the stabilization energy of larger systems is almost exclusively done by variational method, in which the stabilization energy is represented as a sum of HF and electron correlation (EC) energies. The detailed explanation of the herein mentioned approaches and methods is omitted and can be found elsewhere.[96]

---

[92] [N^0 217] C. Møller, M. S. Plesset *Phys. Rev*. **1934**, *46*, 618.
[93] [N^0 218] J. Čižek, *J. Chem. Phys*. **1966**, *45*, 4256.
[N^0 219] J. Čižek, J. Paldus, *Int. J. Quantum Chem*. **1971**, *5*, 359.
[N^0 220] J. Paldus, J. Čižek, I. Shavitt, *Phys. Rev. A*, **1972**, *5*, 50.
[N^0 221] R. J. Bartlett, M. Musial, *Rev. Mod. Pys*, **2007**, 79, 291.
[N^0 222] K. Raghavachari, G. W. Trucks, J. A. Pople, M. Head-Gordon, *Chem. Phys. Lett*. **1989**, *157*, 479.
[94] [N^0 223] R. J. Bartlett, *An. Rev. Phys. Chem*. **1981**, *32*, 359.
[95] [N^0 224] B. Jeziorski, R, Moszinsky, K. Szalewicz, *Chem. Rev.* **1994**, *94*, 1887.
[96] for example see: [N^0 225] R, J. Barllet, J. F. Stanton, *Rev. Comput. Chem*. **1995**, *5*, 65.
[N^0 226] A. Szabo, N. S. Ostlund, *Modern Quantum Chemistry: Introduction to Advanced Electronic Structure Theory*; MacMillan Publishing Co., New York, **1982**.
[N^0 227] R. Mc Wenny, *Methods of Molecular Quantum Mechanics*; 2nd Edition, Academic Press, London, **1992**.
[N^0 228] P. W. Atkins, R. S. Friedman, *Molecular Quantum Mechanics*; 3rd Edition, Oxford University Press, Oxford, **1997**.
[N^0 229] F. Jansen, *Introduction to Computational Chemistry*; Wiley, Chichester, **1999**.

In contrast to all the wave function-based approaches and methods mentioned-above, there is the famous so-called density functional theory (DFT) that was introduced by Hohenberg, Kohn and Sham in the mid-sixties.[97] Besides the wave function theory (WFT) and DFT schemes, there is one more procedure dealing with the electronic structure determination, i.e. Quantum Monte Carlo (QMC) method.[98] This method is based on multielectron wave function explicitly including the correlation energy. The QMC method is variational, size consistent and guessed as cubic scaling. Generally, it can only give the total energy of the system,[99] while there is no easy way, for example, for geometry optimization. Fortunately, within QMC calculations NCIs are usually cancelled out.

As the DFT is the theoretical method of choice of this Thesis, the DFT will be discussed in more details in the following section.

1.4.2.1. Density functional theory (DFT).

1.4.2.1.1. Generalities.

The electron density plays a key role within the DFT. Unlike in the wave function theory, the electron density is an observable which can be measured experimentally, by X-Ray diffraction.

Although there were attempts to use the electron density instead the wave function much earlier, in 1927 (works of Thomas and Fermi as well as of Slater),[100] the electron (pair) density (more correctly the probability of the density of electrons) has found its usefulness for obtaining information of atomic and molecular systems after two publications of Kohn: one with Hohenberg and another with Sham, in 1964 and 1965, respectively.[101] Through those two major publications two theorems and set of equations derived from these theorems, representing the basis of the DFT, have been introduced. In general, the first theorem states that all the ground-state properties of the system are determined by the electron density of the system (in form of a

---

[97] [N^0 230] P. Hohenberg, W. Kohn, *Phys. Rev.* **1964**, *136*, B864.
[N^0 231] W. Kohn, L. J. Sham, *Phys. Rev.* **1965**, *140,* A1133.
[98] [N^0 232] V. G. Rousseau, *Phys. Rev. E* **2008**, *77,* 056705.
[N^0 233] M. Mella, J. B. Anderson, *J. Chem. Phys*. **2003**, *119*, 8225.
[N^0 234] W. M. C. Foulkes, L. Mitas, R. J. Needs, G. Rajagopal, *Rev. Mod. Phys*. **2001**, *73*, 33.
[99] [N^0 235] C. Diedrich, A. Luchow, S. Grimme, *J. Chem. Phys. Chem*. **2005**, *123*, 184106.
[100] [N^0 236] E. Fermi*, Rend. Accad. Lincei* **1927**, *6*, 602.
[N^0 237] L. H. Tomas, *Proc. Camb. Phil. Soc*. **1927**, *23*, 542.
[N^0 238] J. C. Slater, *Phys. Rev.* **1951**, *81*, 385.
[101] [N^0 230] P. Hohenberg, W. Kohn, *Phys. Rev.* **1964**, *136*, B864.
[N^0 231] W. Kohn, L. J. Sham, *Phys. Rev.* **1965**, *140,* A1133.

functional), without giving an explanation about the nature of the functional. The second theorem introduces a general way on how the right electron density can be found by minimization of energy of the functional. Finally, it has been shown that the problem of obtaining the right election density can be solved by using (and solving using iterative technique by self-consistent field method) the set of Kohn-Sham (KS) equations.

Since that time (when the DFT was introduced) and especially over the past years, the DFT has been developed largely. Nowadays DFT is established as one of most successful approaches for calculating electronic structure of matter due to its much less computational time demands, less basis set dependence and reasonably high accuracy.[102]

Basically, in its original formulation, DFT is able to provide the ground-state properties of the system as a function of the electron (pair) density, while the results are significantly dependent on the employed approximate exchange-correlation functional (i.e. functional derivative of exchange-correlation energy (E_{xc}) with respect to the electron density). Worthy to note, unlike the HF model, where the approximation is introduced right from the start, the KS approach is in principle exact and the approximation enters only when the exact form of unknown (non-classical) exchange-correlation functional (and related exchange-correlation potential (V_{xc})) has to be found. The exchange-correlation functional should account for everything unknown, i.e. non-classical effects of self-interaction, exchange and correlation of electrons (which contribute to the potential energy) as well as a portion that belong to the kinetic energy (which is not accounted for through the non-interacting kinetic energy). However, building such a functional is rather quite challenging task. Therefore, it seems that the central goal of the modern DFT is to improve the approximation for that quantity. So far, several approaches giving the approximate functionals have been developed, such as Local Density Approximation (LDA), Generalized Gradient Approximation (GGA), meta-GGA, or Hybrid Functionals.

The LDA method is based on an assumption that the system's behavior is local. Surprisingly, in some cases it gives reasonably good results for such a method, but usually it highly overestimates the bond energies and provides poor thermochemistry. Therefore, its use is rather limited. In the GGA approach the exchange-correlation functional depends on both the

---

[102] [N^0 239] S. Sirois, E. I. Proynov, D. T. Nguyen, D.R. Salahub, *J. Chem. Phys*. **1997**, *107*, 6770.
[N^0 240] F. Sim, A. St. Amant, I. Papai, D. R. Salahub, *J. Am. Chem. Soc*. **1992**, *114*, 4391.
[N^0 241] M. S. Liao, Y. Lu, V. D. Parker, S. Scheiner, *J. Chem. Phys*. **2003**, *107*, 8939.
[N^0 242] C. Desplanches, E. Ruiz, A. Rodríguez-Fortea, S. Alvarez, *J. Am. Chem. Soc*, **2002**, *124*, 5197.
[N^0 64] S. D. Zarić, *Eur. J. Inorg. Chem.* **2003**, 2197.

value and the gradient of the electron density. Due to the fact that GGA approach does not give a unique expression of the E_{xc}, there are a number of the GGA functionals which differ in the number of adjustable parameters, the amount of the used empiricism and constrains within they are constructed. Generally, in comparison to LDA method, they give more accurate results of various properties, while the reaction energies they provide are not sufficiently good. More flexibility within the GGA frame of calculations of E_{xc}, introduced by adding local KS kinetic energy density, usually leads to an improvement of the accuracy of the calculations. These class of functionals are known as meta-GGA functionals. It has been shown by Becke[103] that a great improvement of computed molecular thermochemistry can be obtained if the functionals based on GGA approach use fraction of exact exchange (calculated as HF exchange energy but using KS orbitals). In opposite to so far mentioned local and semi-local functionals, these so-called hybrid functionals are no longer local.

Hence the calculation of the exact exchange involves double integration over real space, the hybrid functionals are much more computational time demanding. That has limited their wide spread use. In addition, there is one class of functionals, so-called long-range correction (LC) functionals,[104] that was developed to deal with the self-interaction of electrons, a possible problem of the hybrid functionals. Similar to the hybrid functionals, the LC functionals combine the semi local functionals with the exact exchange while separate the electron-correlation term in two: as short and long range. Consequently, the LC functionals made improvements in a modeling of non-dispersive electron-electron interactions.

Generally, DFT produces good results in molecular structure geometries, vibrational frequencies, electric and magnetic properties, ionization energies etc. However, the local DFT based investigation of the systems where the NCI have significant influence was precluded for a long time since DFT failed to properly describe non-local dispersion interaction energy, although that has not been recognized for a long time. The first papers suggesting this drawback have appeared in 1990s.[105] For a long period of time the community of DFT users denied the failure of DFT to provide correct agreement between DFT computed and reference energies for H-bonded systems. However, it appears that error cancelation, where attractive dispersion interaction is partially compensated by an attractive overestimation in some exchange

[103] [N^0 243] A. D. Becke, *J. Chem. Phys*, **1993**, *98*, 1372.
[104] [N^0 244] P. M. W. Gill, R. D. Adamson, J. A. Pople, *Mol. Phys.* **1996**, *88*, 1005.
[105] [N^0 245] P. Hobza, J. Sponer, T. Reschel, *J. Comput. Chem*. **1995**, *16*, 1315.
[N^0 246] S. Kristyan, P. Pulay, *Chem. Phys. Lett*. **1994**, *229*, 175.

functionals[106] or by the basis set superposition error (BSSE)[107] was unphysically producing the right results. On the other hand, when a dispersion-bound complex is the system of interest, the results are rather meaningless. This is supported by a recent review of DiLabio *et al.*[108] in which an extensive comparison of the performance of different functionals dealing with NCI has been reported. Consequently, determining the way to include (correctly) dispersion into DFT was found to be of primary importance.

Besides the aforementioned problem of dealing with dispersion, there is one more issue that is related to solvation. Namely, nearly all chemical and biochemical processes take place in the condensed phase, especially in fluids. However, during the last couple of years the calculations have greatly been improved for prediction of a range of molecular properties in gas phase, while not to such extent for the treatment of the molecules in solution. Therefore, the proper treatment of solute-solvent behavior is one of actual challenges and tasks in modern computational chemistry.[109]

Like mentioned above, DFT calculations provide rather good results in molecular structure geometries as well as in harmonic vibrational frequencies, which are of great importance for the context of the thesis' research. Namely, the optimization of structure geometries and calculating of the harmonic vibrational frequencies were the core of all the theoretical studies of the thesis. It should be mentioned that calculating the harmonic vibrational frequencies is essential for obtaining thermodynamic reaction/interaction parameters (ΔH, ΔG, ΔS)[110] which were of particular interest for fulfilling the thesis' aims.

1.4.2.1.2. Dispersion treatment.

Like pointed out above, finding a way to correctly account for the dispersion within DFT calculations was one of major task in modern DFT. Generally, the attempts made to find the solution followed three main directions: a) non-empirical (theoretically, by avoiding the empiricism); b) reparameterization of the existing functionals; c) empirical (by applying of

[106] [N^0 247] Y. K. Zhang. W. Pan, W. T. Yang, *J. Chem. Phys*, **1997**, *107*, 7921.
[107] [N^0 6] P. Hobza, K. Müller-Dethlefs, In *Non-Covalent Interactions: Theory and Experiment*; The Royal Society of Chemistry, **2009.**
[N^0 248] R. M. Balabin, *J. Chem. Phys*. **2008**, *129*, 164101.
[N^0 249] B. Paizs, S. Suhai, *J. Comput. Chem.* **1998**, *19*, 575.
[N^0 131] P. Hobza, H. L. Selzle, E. W. Schlag, *Chem. Rev.* **1994**, 94, 1767.
[108] [N^0 250] G. A. DiLabio, A. Otero-de-la-Roza, *arXiv:1405.1771 [physics.chem-ph]* **2014**.
[109] [N^0 251] J. Tomasi, B. Mennucci, R. Cammi, *Chem. Rev*. **2005**, *150*, 2999.

empirical expression for dispersion in the existing functionals). In the last fifteen years a number of approximations have been proposed. Some of the efficiently implemented ones are: DFT-D, i.e. family of the empirical dispersion corrections developed by Grimme *et al.*;[111] the empirical dispersion corrections developed by Hobza *et al.*;[112] the method by Tao, Perdew and Ruzsinszky;[113] Tkatchenko-Scheffer (TS)[114] and Tkatchenko-Scheffer-self-consisted screening (TS-SCS) methods,[115] exchange-hole dipole moment (XDM) model of dispersion.[116]

In addition, there is a number of papers aiming to extend benchmarking of the dispersion corrections in DFT.[117] Essentially, the aim of all the approaches is to find the dispersion coefficient C_6^{AB} (or even the coefficients of higher order) which depends on the polarizabilities of the particular atoms, while the polarizabilities are proportional to the number of valence electrons and the size of atom.[118] In principle, the dispersion coefficients can be calculated theoretically using MP2 theoretical methods[118] or Casimir-Polder formula,[119] while an estimation of the dispersion coefficients by London's formula has little practical value. It should be noted that the dispersion coefficients used in classical force fields are not adequate.[120] In the expression of the dispersion energy term generalized to intermolecular or intramolecular interactions, where all the atoms interact with one another in a pairwise fashion, there is a so-called dumping function, i.e. factor f_6. Its role is triple: a) to correct the error introduced by the

---

[110] [N^0 252] W. J. Hehre, L. Radom, P. v. R. Schleyer, J. A. Pople, *Ab Initio Molecular Orbital Theory*, Wiley, New York, **1986**.
[111] [N^0 253] S. Grimme, *J. Comput. Chem*. **2004**, *25*, 1463.
[N^0 254] S. Grimme, *J. Comput. Chem*. **2006**, *27*, 1787.
[N^0 255] S. Grimme, J. Antony, S. Ehrlich, H. Krieg, *J. Chem. Phys*. **2010**, *132*, 154104.
[N^0 256] E. Caldeweyher, C. Bannwarth, S. Grimme, *J. Chem. Phys*. **2017**, *147*, 034112.
[112] [N^0 257] P. Jurecka, J. Cerny, P. Hobza, D. R. Salahub, *J. Comput. Chem*. **2007**, *28*, 555.
[113] [N^0 258] J. Tao, J. P. Perdew, A. Ruzsinszky, *Proc. Nat. Acad. Sc*i. **2012**, *109*, 18.
[114] [N^0 259] A. Tkatchenko, M. Scheffer, *Phys. Rev. Lett*. **2009**, *102*, 073005.
[115] [N^0 260] A. Tkatchenko, A. Ambrosetti, R. A. DiStasio, *J. Chem. Phys.* **2013***, 138,* 074106*.*
[116] [N^0 261] A. Otero-de-la-Roza, R. R. Johnson, *J. Chem. Phys*. **2013**, *138*, 054103.
[117] [N^0 262] J. Luder, B. Sanyal, O. Eriksson, C. Puglia, B. Brena, *Phys. Rev. B* **2014**, *89*, 045416.
[N^0 263] G. A. DiLabio, E. R. Johnson, A. Otero-de-la-Roza, *Phys. Chem. Chem. Phys*. **2013**, *15*, 12821.
[N^0 264] N. Marom, A. Tkatchenko, M. Rossi, V. V. Gobre, O. Hod, M. Scheffer, L. Kronik, *J. Chem. Theory Comput.* **2011**, *7*, 3944.
[N^0 265] G. DiLibio, M. Koleini, E. Torres, *Theor. Chem. Acc*. **2013**, *132*,1.
[N^0 266] S. Grimme, *WIREs: Comput. Mol. Sci*. **2011**, *1*, 211.
[N^0 267] W. Hujo, S. Grimme, *Phys. Chem. Chem. Phys.* **2011**, *13*, 13942.
[N^0 268] S. Grimme, S. Ehrlich, L. Goerigk, *J. Comput. Chem*. **2011**, *32*, 1456.
[N^0 269] S. Grimme, M. Steinmetz, *Phys. Chem. Chem. Phys.* **2013**, *15*, 16031.
[N^0 270] S. Grimme, R. Huenerbein, S. Ehrlich, *ChemPhysChem* **2011**, *12*, 1258
[118] [N^0 228] P. W. Atkins, R. S. Friedman, *Molecular Quantum Mechanics*; 3rd Edition, Oxford University Press, Oxford, **1997**.
[119] [N^0 271] H. B. G. Casimir, D. Polder, *Phys. Rev*. **1948**, *73*, 360.
[120] [N^0 272] Q. Wu, W. Yang, *J. Chem. Phys*. **2002**, *116*, 515.
[N^0 273] T. A. Halgren, *J. Am. Chem. Soc*. **1992**, *114*, 7827.

approximation; b) to deactivate the dispersion contribution at very short range; c) to fix problems in reproducing other terms in intermolecular energy.

Hobza *et al.*[121] have greatly reported the experienced issues related to the dispersion correction. In brief: a) even a simple empirical dispersion correction improves considerably the description of the intermolecular interactions; b) a critical point – the dumping function, related to double counting of the correlation energy; c) an increasing of the basis set quality leads to more obvious impact of the empirical dispersion correction; d) the BSSE of the sets of DZ quality indirectly reveal the precise role of the dispersion in hydrogen-bonded systems; e) it is recommended to add the empirical dispersion correction only if larger basis set (at least TZV(P) quality) is used; f) when combined with the empirical dispersion correction, more advanced functionals give better results than simple ones; g) the results are highly dependent on the exchange-correlation functional used; the best results seem to be produced by the TPSS functional (especially meta-GGA).

Although D4 Grimme's dispersion correction has been developed recently, due to the fact that the work of this thesis has started in 2014, all the theoretical studies within the thesis used D3 Grimme's dispersion correction.

1.4.2.1.3. Solvation treatment.

Proper modelling of solvation is a rather hard task due to the fact that a solute molecule typically interacts with several solvent molecules, while these interact with others and so on. This means that for proper description of solute solvent system several thousands of atoms should be considered. Additionally, a few limiting factors make the modelling even harder: a) the surface effects have a huge influence; b) calculations of the ground state of the system are, actually, determined by the thermodynamic average of conformationally excited states; c) computational time cost of such calculations, since the molecular orbital (MO) calculations are scaled to third power regard to number of atoms. Therefore, as usually, some approximations had to be developed.

So far, the treatment of solvation is based on two main approaches, namely explicit and implicit (continuum) approaches.

[121] [N^0 257] P. Jurecka, J. Cerny, P. Hobza, D. R. Salahub, *J. Comput. Chem*. **2007**, *28*, 555.

Explicit approach

Intuitively, the explicit approach is based on the use of explicit solvent molecules, employing molecular mechanics (MM) and molecular dynamics (MD). Inter- and intra-molecular interactions are approximated by force fields while thermodynamic averring by MD and random Monte Carlo (MC) sampling of relevant states. Accordingly, the solvent effects are parametrized. The potential energy is considered as a sum of bonding and non-bonding interactions, arising from all atoms of the solute and all the molecules of solvent that are loaded in the simulation box. While intramolecular and dispersion interactions seem to be well parametrized, the fact that the electrostatic interactions are usually calculated by using dielectric constant of vacuum limits considerably the application of MD and MC methods for description of the solvation. Generally, the explicit model of the solvation can give reasonably accurate and physically meaningful information for the system consisting of nonpolarizable solute and solvent molecules, while it is usually quite computational time demanding (requiring orders of magnitude more computational time than corresponding gas phase calculations).

The implicit (continuum) approach

The implicit (continuum) approach, based on early works of Born, Krikwood and Onsager,[122] accounts for only the solute molecule (or small cluster of the solute) and few solvent molecules, while the influence of the rest of solvent is approximated by an effective continuum surrounding. Dispersion interactions can be accounted for accurately by a term that is proportional to exposed surface area (of the solute), while a (proper) description of electrostatic interactions/electrostatic screening (the main task of the approach) is based on dielectric theory for macroscopic systems. Within this approach, solvent is considered as a uniform polarizable medium with particular dielectric constant (ε) containing a solute molecule placed in a suitably shaped cavity (which is a basic concept of all continuum models). Models developed within the frame of this dielectric continuum solvation approach are usually called self-consistent reaction filed (SCRF) models. The implicit approach is mostly used for an estimation of Gibbs free energy of solute-solvent interactions in various chemical and biochemical processes.

[122] [N^0 274] M. Born, *Z. Phys*. **1920**, *1*, 45.
[N^0 275] J. G. Krikwood, *J. Chem. Phys*. **1934**, *2* 351.
[N^0 276] L. Onsager, *J. Am. Chem. Soc*. **1936**, *58*, 1486.

The Gibbs free energy of solute-solvent interactions is defined as a sum of bonding interactions, non-bonding interactions and solvation contributions. The solvation contribution is constituted of electric (representing electrostatic interactions caused by polarization between solute and solvent), dispersion (representing dispersion interactions between solute and solvent) and cavity (representing creation of the cavity in the medium) Gibbs free energies.

The computational cost of the calculations based on the implicit approach is highly dependent on how the cavity is modeled. The cavity should not only be a mathematical creation, but also should have a physical meaning, containing (within its boundaries) as much as possible of the solute charge distribution and none of solvent. Thus, there are several models defining the shape of the cavity.[123] The above-mentioned electrostatic problem, a challenging task for the proper solvation treatment, can be described by Poisson or Poison-Boltzmann equations. For their solving several approaches were employed, such as Finite Difference method or so-called Generalized Born (GM) model.

In the last decades, several implicit (continuum) approach models have been developed, such as: Polarizable Continuum Model (PCM) family of codes, sharing the same basis and many features, developed for general use or some specific purpose (there are Dielectric PCM (DPCM), Conductor-like PCM (CPCM), Integral Equation Formalism PCM (IEFPCM); Conductor like Screening Model (COSMO),[124] which uses scaled conductor boundary condition inserted much more complicated dielectric boundary condition; Conductor like Screening Model for Real Solvents (COSMO-RS),[125] an extension to the COSMO. Besides these models, there are others that are based on different approaches, such as: MultiPole Expansion (MPE);[126] Integral Equation Formalism (IEF),[127] Surface and Volume Polarization for Electrostatic (SVPE and SS(V)PE);[128] Generalized Born (GB).[129]

---

[123] [N^0 251] J. Tomasi, B. Mennucci, R. Cammi, *Chem. Rev*. **2005**, *150*, 2999.
[N^0 275] J. G. Krikwood, *J. Chem. Phys*. **1934**, *2*, 351.
[N^0 276] L. Onsager, *J. Am. Chem. Soc*. **1936**, *58*, 1486.
[124] [N^0 277] A. Klamt, G. Schueuermann, *J. Chem. Soc. Perkin Trans. 2* **1993**, 799.
[125] [N^0 278] A. Klamt, *Phys. Chem*. **1955**, *99*, 2224.
[126] [N^0 276] L. Onsager, *J. Am. Chem. Soc*. **1936**, *58*, 1486.
[N^0 279] J. G. Krikwood, *J. Chem. Phys*. **1939**, *7*, 911.
[N^0 280] K. V. Mikkelsen, H. Aagren, H. J. A. Jensen, T. Helgaker, *J. Chem. Phys*. **1988**, *89*, 3086.
[N^0 281] J. L. Rivail. D. Rinaldi, *Chem. Phys*. 1976, *18*, 233.
[N^0 282] M. W. Wong, M. J. Frisch, K. B. Wiberg, *J. Am. Chem. Soc*. **1991**, *113*, 4776.
[N^0 283] M. W. Wong, K. B. Wiberg, M. J. Frisch, *J. Am. Chem. Soc*. **1992**, *114*, 523.
[127] [N^0 284] B. Mennucci, E. Cances, J. Tomasi, *J. Phys. Chem. B* **1997**, *101*, 10506.
[N^0 285] E. Cances, B. Mennucci, J. Tomasi, *J. Chem. Phys*. **1997**, *107*, 3032.
[128] [N^0 286] D. M. Chipman, *J. Chem. Phys*. **1999**, *110*, 8012.
[N^0 287] D. M. Chipman, *J. Chem. Phys.* **2000**, *112*, 5558.

In general, the SCRF continuum models differs in several aspects: the size and shape of the cavity, the way of calculation the dispersion and the cavity contribution (within the solvation contribution to total Gibbs free energy), the representation of the solute charge distribution, the description of the dielectric medium.

DPCM and COSMO-RS are probably among the best models for the solvation treatment available. DPCM is said to be able to describe an unlimited number of solutes, permitting an extension to association-dissociation phenomena.[130]. COSMO-RS, method which does not depend on too much of experimental data, provides good predictions of thermodynamic properties of pure and mixed liquids.[131]

However, during the work on this thesis, due to available computational resources, COSMO procedure was exclusively used.

[N^0 288] D. M. Chipman, *J. Chem. Phys*. **2002**, *116*, 10129.
[129] [N^0 289] D. Bashford, D. A. Case, *Annu. Rev. Phys. Chem*. **2000**, *51*, 129.
[N^0 290] A. Onufriev, D. Bashford, D. A. Case, *J. Phys. Chem. B*, **2000**, *104*, 3712.
[130] [N^0 251] J. Tomasi, B. Mennucci, R. Cammi, *Chem. Rev*. **2005**, *150*, 2999.
[131] [N^0 291] A. Klamt, V. Jonas, T. Burger, J. C. W. Lohrenz, *J. Phys. Chem. A*, **1998**, *102*, 5074.
[N^0 292] R. Putnam, R. Taylor, A. Klamt, F. Eckert, M. Schiller, *Ind. Eng. Chem. Res*. **2003**, *42*, 3635.

Chapter 2

Methodology

2.1. Generalities.

In order to achieve the aims of the thesis, i.e. to make the base for the improvement of the theoretical calculations, for better understanding of non-covalent interactions, used methodology was the following:

- at the beginning all the studied reactions were tested by standard Schlenk line technique.
- after proving suitability of particular reaction system, the system was investigated using Isothermal Titration Calorimetry (ITC), the main employed experimental technique during the work of the thesis.
- in parallel to the ITC measurements, the static DFT-D calculations, method of choice of this thesis, were performed on all the investigated systems.
- in addition, the search and analysis of Cambridge Structural Database were used where appropriate.

Within this section the principles of the ITC measurements, instrumentation and data treatment as well as employed procedures within the calculations, the CSD search and data analysis will be explained.

2.2. Isothermal titration calorimetry (ITC).

2.2.1. Principles and instrumentation.

Calorimetric titration (a.k.a ITC)[132] has been proven as a very accurate and sensitive technique capable of achieving in some cases a $\pm$ 0.1 kcal/mol precision for the determination of reaction enthalpies.

ITC measurements were carried out on a Waters-SAS nano-ITC device[133] (TA Instruments ®) (see Figure M1). The Nano ITC machine consists of the measuring unit (containing calorimeter block and two nonremovable reaction vessels - two stainless steel Hastelloy cells (reference and sample call) of 1 mL volume each) and the buret assembly including the stirring system (see Figure M2). The measuring unit is placed in an air/thermal-tight canister previously purged

[132] [N^0 181] T. Wiseman, S. Williston, J. F. Brandts, L. N. Lin, *Anal. Biochem.* **1989**, *179*, 131.
[N^0 182] E. Freire, O. L. Mayorga, M. Straume, *Anal. Chem.* **1990**, *62*, 950A.
[133] [N^0 293] www.tainstruments.com

and filed with dry nitrogen, ensuring no evaporation and condensation of moisture, and leading proper base line response. A Cleaning/degassing system is provided as an accessory to the ITC instrument. All functions of the Nano ITC are controlled remotely by the computer through the USB connection, except the power on/off switch that is located on the back of the calorimeter unit. Additional part of the instrument is a calibration heater that is located outside of the sample cell. It is used for precise electric calibration of the instruments and for testing its performance.

Figure M1 Picture of the TA Instruments ® nano-ITC device

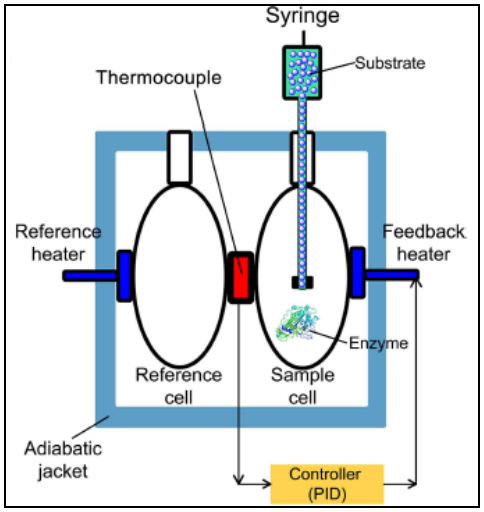

Figure M2 Schematic representation of the ITC measuring unit.[134]

[134] [N^0 294] K. H. Ebrahimi, P.-L. Hagedoorn, D. Jacobs, W. R. Hagen, *Scientific Reports*, 5:16380.

The principle on which the use of the nano-ITC instrument is based is differential power compensation. In that way maximum sensitivity and responsiveness can be achieved. To provide right differential power compensation few additional parts are included within the instrument. Firstly, a semiconducting thermoelectric device (TED) is employed to detect difference in temperature between sample and reference cell as well as for temperature control. Once the temperature difference is observed, a proportional/integral/derivative (PID) control loop employs a heater located on the sample cell to maintain the reference and sample cell on the same temperature. The power required for the maintaining the zero-temperature difference between the cells is a calorimetric signal that is monitored as a function of time. The calorimetric signal is directly proportional to the heat released/absorbed of the reaction that occurs in the sample cell.

The reference cell is constructed to match the sample cell as much as possible. Accordingly, it has the same volume as the reference cell as well as the reference needle that is placed into the reference cell during the measurements to correspond to the titrant syringe needle. The cells are connected via the thermal controller. In addition, the reference cell requires the same solvent as used in sample and titrant syringe solutions.

The buret assembly holding the titrant syringe has two main functions: a) delivery of very precise aliquots (syringe of 100 μL - min. delivery volume is 0.11 μL) of “titrant” solution at specified time into the sample cell containing the “titrand” solution; b) appropriate stirring of the sample cell solution through titrant syringe needle.

An access to the cells is provided by platinum tubes that connect the cells with the buret cavity. The access tubes enable the delivery of titrant, manipulations with the filing syringe, displacing the reference needle. They also serve as a thermal barrier to the outside of calorimeter.

2.2.2. Measurements.

The main prerequisites for getting reasonable results are ITC measurements

- well-defined reaction product;
- no side reaction products;
- no production of gases/solids;
- homogeneousness of all reactants and reaction product(s) in chlorobenzene (solvent of choice);

- fast enough reaction.

Consequently, if one of these prerequisites is not fulfilled, the conditions of the reaction of interest should be reconsidered.

In general, ITC measurements can be run in two modes: a) sequential injection; b) continuous. However, regardless of the chosen mode, every ITC experiment involves the following: a) preparing the titrant syringe and sample cell solutions of well-defined concentrations; b) appropriate preparing the sample cell, reference cell and the titrant syringe; c) mounting the buret; d) pre-equilibration of the solutions; e) running the stirring and equilibration of the solutions to a stable base line; f) running the experiment; g) data collection; h) cleaning the calorimeter; i) performing data analysis.

The first step for fruitful ITC experiment is defining reaction conditions, i.e. concentration of the solutions, number of injections, volume of injection, time between two consecutive injections, temperature and stirring rate. The properly chosen parameters should allow obtaining of ITC thermogram containing well-defined heat responses as well as the base line (see an example depicted in Figure M3 – left side). Otherwise, the parameters should be refined. The base line is the heat flow before and after the injection, it shows the power required to maintain zero-temperature difference between the cells. Consequently, the base line is used to calculate the area of heat released/absorbed after the injection. Resulting from successfully performed ITC measurement, a heat change plot as function of time is obtained. In order to get reliable data, the heat effects caused by dilution of the titrant and any temperature differences between titrant and sample cell solution must be accounted for, as well. This can be achieved most easily by preforming blank ITC experiments and by subtracting the blank heat data from the experimental one. By integrating newly heat peak areas, the heat data as a function of molar ratio of the reactants rises up, which can be subsequently analyzed (see an example depicted in Figure M3 – right side).

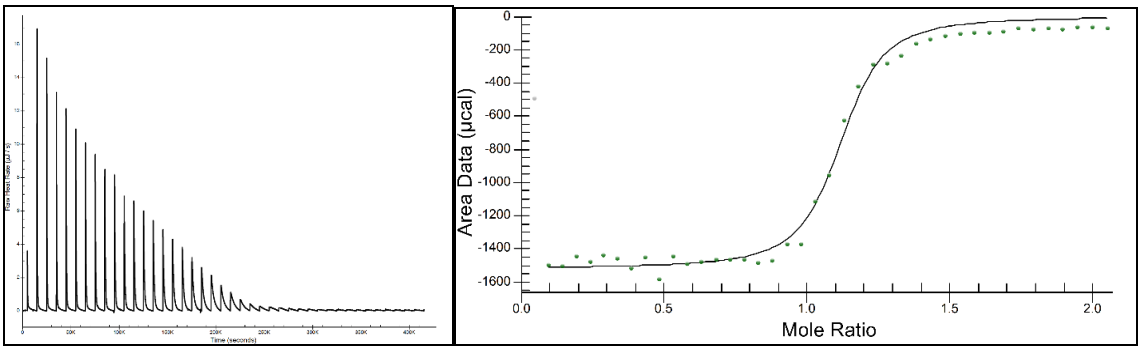

Figure M3. *left side* – ITC thermogram representing well-defined heat responses and base line. *right side* – ITC integrated and fitted heat peaks of the thermogram shown on the left side.

2.2.3. Data analysis.

2.2.3.1. Generalities.

Like mentioned above, the heat change/rate data as a function of time is early result of ITC experiment. In general, this ITC data could be analyzed in two ways:

a) thermodynamic;
b) kinetic.

Herein, both methodologies will be briefly discussed.

2.2.3.2. Thermodynamic study.

By integrating heat change areas, the heat data as a function of molar ratio of reactants is obtainable. In order to analyze this data and get all the thermodynamic parameters of interaction/reaction of interest, first of all, one should know what kind of process takes place in calorimeter (competitive replacement, one or multiple site bonding, dimmer dissociation, etc.), because only proper understanding of chemical process will lead to reliable thermodynamic parameters. Extraction of all the thermodynamic parameters is only possible by employing appropriate models. The models, implemented in Nano-analyzes software, are mathematical representations of possible chemical, physical or biological processes that take place in calorimeters and in which a heat/heat rate, a dependent variable, is defined as a function of some independent variable (for instance molar ratio of reactants) and one or more model parameters. Fitting the ITC data to the model and determining the best model parameters (e.g. n, K, ΔH) can be done using a nonlinear regression procedure along with equations

implemented in a particular model. From these parameters (K and Δ*H*) the other thermodynamic parameters (i.e. Δ*G* and Δ*S*) are easily obtainable.

The nonlinear regression is an iterative process, which begins by guessing model parameters and generating a theoretical curve. Subsequently the theoretical curve is compared to the actual heat data by calculating an error as a sum of squared deviations between the model curve and the data. The process is repeated until the error is changed insignificantly. That final error (as standard deviation) is used to calculate the errors of the obtained model parameters, as well.

It is worthy to note that the quality of the model parameters is largely dependent of starting assumptions, first of all, of starting concentrations of the used solutions. Therefore, preparation of solutions of well-defined concentrations of reactants is rather quite important.

If no model fits the integrated heat data, only one choice remains to obtain the thermodynamic parameters. Namely, the heat data can be analyzed manually. Unfortunately, this method can provide only raw values of the reaction/interaction enthalpy (raw Δ*H*). To obtain reliable raw Δ*H* values, one should follow a rather simple procedure: summing up all the integrated areas (peaks) of the released/absorbed heat against a molar content introduced by injection(s) before the athermicity point is reached.

In addition, regardless of the used method for analyzing ITC heat data, the molar ratio (*n*, also known as stoichiometric coefficient) of the reactants can be precisely monitored during the whole course of the reaction/interaction process.

2.2.3.3. Estimation of an error of the ITC measurements.

Herein, the used procedure of estimation of the error of the ITC measurements will be briefly discussed. The base of the used procedure are well-known mathematical formulas and facts:

Firstly, the used mathematical formulas are:

- The variance σ of x is the square of the standard deviation, $\sigma = sd(x)^2$,

followed by:

Rule 1: Variances add on addition or subtraction:

$$sd\,(z)^2 = sd\,(x)^2 + sd\,(y)^2$$

Rule 2: Relative variances add on multiplication or division:

$$sd\ (z)^2/\ z^2 = sd\ (x)^2/x^2 + sd\ (y)^2/\ y^2$$

Second, the used standard uncertainties (deviations - sd) of the instruments:

Vol. flask [mL]	± [mL]	**Balance**	± [g]
2	0.015	analytical	0.0001
5	0.02	**Injection syringe [µL]**	± [µL]
10	0.02	100	0.1
20	0.03	**Cell syringe [mL]**	± [mL]
25	0.03	2.5	0.025
50	0.05	**ITC machine**	± [µJ]
100	0.08	nano	0.1

while for **Molar mass** it was ± 0.01 [g/mol].

Later, the used chemical formulas:

- number of mol - $n = m/M$ [mol]
- concentration - $c = n/V$ [mol/L]
- number of injected mol per injection - $n_{injected} = c_{syringe} * V_{of\ injection}$ [mol]
- enthalpy - $\Delta H = Q_{produced}/n_{injected}$

where :

m – weighted mass of a compound on the analytical balance
M – molar mass of a compound
V – volume of used volumetric flask
$n_{injected}$ – number of mol injected into sample cell by titration syringe during ITC experiment
$c_{syringe}$ – concentration of a solution it the titration syringe
$V_{of\ injection}$ – volume of a solution in the titration syringe injected per single titration
$Q_{produced}$ – heat produced during ITC experiment – average value

In order to get the error of obtained ΔH by ITC measurements standard deviations (*sd*) and relative variance of every single factor in the above listed chemical-mathematical formulas, should be figured out. For achieving that goal, above listed rules (rule 1 and rule 2) should be followed.

Accordingly, firstly it was found: *sd* of **n**:

$$sd(\mathrm{n}) = \sqrt{\frac{sd\,(\mathrm{m})^2}{\mathrm{m}^2} + \frac{sd\,(\mathrm{M})^2}{\mathrm{M}^2}}\,\mathrm{n}$$

secondly, *sd* of ***c***:

$$sd(\mathrm{c}) = \sqrt{\frac{sd\,(\mathrm{n})^2}{\mathrm{n}^2} + \frac{sd\,(\mathrm{V})^2}{\mathrm{V}^2}}\,\mathrm{c}$$

then *sd* of $\boldsymbol{n_{injected}}$:

$$sd(\mathrm{n_{injected}}) = \sqrt{\frac{sd\,(\mathrm{c})^2}{\mathrm{c}^2} + \frac{sd\left(\mathrm{V_{of\,injection}}\right)^2}{\mathrm{V_{of\,injection}}^2}}\,\mathrm{n_{injected}}$$

and finally *sd* of **Δ*H***:

$$sd(\Delta\mathrm{H}) = \sqrt{\frac{sd\left(\mathrm{Q_{produced}}\right)^2}{\mathrm{Q_{produced}}^2} + \frac{sd\left(\mathrm{n_{injected}}\right)^2}{\mathrm{n_{injected}}^2}}\,\Delta\mathrm{H}$$

Used values of:

- *sd*(m) = 0.0001 g
- *sd*(M) = 0.01 g/mol
- *sd*(V_{5ml}) = 0.02 ml
- *sd*($V_{of\ injection}$) = 0.1 µL
- *sd*($Q_{produced}$) = 0.1 µJ

In order to find *sd* of the mean value of Δ*H*, following formula was used:

$$sd(\Delta\mathrm{H_{mean}}) = \sqrt{\frac{sd\,(\Delta\mathrm{H_1})^2}{\Delta\mathrm{H_1}^2} + \frac{sd\,(\Delta\mathrm{H_2})^2}{\Delta\mathrm{H_2}^2} + \frac{sd\,(\Delta\mathrm{H_3})^2}{\Delta\mathrm{H_3}^2} + \frac{sd\,(\Delta\mathrm{H_4})^2}{\Delta\mathrm{H_4}^2}}\,\Delta\mathrm{H_{mean}}$$

with consideration that a relative variance of natural numbers could be excluded.

In addition, it was assumed that the fluctuations in detected heat arise from the diffusion of titration solution from the titration syringe during the stirring process and from an uncertainty on the injected volume by the titration syringe. Thus, it was considered that the minimum of

detectable heat by ITC should be chosen for the error on detected heat (*Q*), while for the error of $V_{of\ injecton}$ it should be the minimum of injectable volume by ITC injection mechanism.

During the thesis' work, these calculations were done for all related ITC experimental data, producing a large set of **Δ*H* ± sd** values.

2.2.3.4. Kinetic study.

Besides fruitful use in thermodynamic studies, ITC measurements found to be useful in kinetic studies, as well. Namely, the use of the ITC on the kinetic studies is based on the capability of the calorimeter to record a heat change every single second during the experiment. Consequently, a rich base of the heat experimental data arises, carrying information about a rate of transformation of reactants into reaction products. Although it has been reported that the obtained rate of the transformation is not the exact rate, but directly proportional to the exact rate with the constant of proportionality inherent to the ITC device and type of the experiment, the heat change data during a time found to be exploitable in terms of initial rate and initial rate constant.[135]

The method of kinetic study adapted in this thesis provides information about initial rate constants and partial reaction orders. The method is based on well-known facts about flooding method of simplifying reaction kinetics. Basically, the flooding method – carrying out reactions in presence of one of reactants in a large excess with respect to other one (limiting reactant) – makes the reaction kinetics directly dependent only in the change of concentration of the limiting reactant. This situation can be described in the following[136]:

Imagining a fictitious reaction:

$$aA + bB \xrightarrow{k} cC$$ (equation 3.1),

its reaction rate in stoichiometric condition of the reactants can be expressed as:

$$\frac{d[A]}{dt} = k[A]^a[B]^b$$ (equation 3.2),

[135] [N^0 294] K. H. Ebrahimi, P.-L. Hagedoorn, D. Jacobs, W. R. Hagen, *Scientific Reports*, 5:16380.
[136] [N^0 295] J. H. Espenson, *Chemical Kinetics and Reaction Mechanisms*; McGraw-Hill series in advanced chemistry, eds. J. Ricci, J.W. Bradley, McGraw-Hill, Inc, **1981**.

while if the reaction is carried out in a large excess of reactant *B*, the rate becomes simplified:

$$-\frac{d[A]}{dt} = k'[A]^a$$ (equation 3.3),

where

$$k' = k[B]^b$$ (equation 3.4).

Therefore, all the ITC experiments dealing with the kinetics were carried out in a large excess in reactant placed in the sample cell.

In general, to figure out the initial rate constants and partial reaction order with respect to reactant in excess the following procedure[137] was employed. By integrating the equation 3.3 the integrated rate expression is obtained:

$$\ln\frac{[A]}{[A_0]} = -ak't.$$

By plotting ln[A_t] against time and its linear fitting, the initial rate constant ***k'*** is obtained. Consequently, pseudo-first-order kinetics are reachable as well as the partial first reaction order with respect to the limiting reactant. According to equation 3.4, by plotting ln[*B*] against the obtained ***k'*** values of various starting concentrations of reactant *B* and its linear fitting, partial reaction order with respect to reactant *B*, i.e. the reactant in excess, is obtained. The same method can be used for the reaction product *C* as it was for the limiting reactant *A*.

Within the kinetic studies of this thesis, the initial rate constant derived from the limiting reactant is denoted by k_{obs} while the initial rate constant derived from the reaction product by ***k***. The difference between their values is due to the fact that ***k*** includes concentration contributions of both reactants.

Like mentioned at the beginning of this section, ITC experiment provides the heat change per second, which can be easily transformed to rate of transformation of the reactants to the product by employing a direct relation between the change of enthalpy (Δ*H*) [µcal/mol] and the rate v_{ITC} [µM/s] through the change of applied compensate power (Δ*p*) [µcal/s] and volume of sample cell (*V*) [L], see equation 3.5. The exact concentrations of the reactants are assumed as known.[138]

---

[137] [N^0 295] J. H. Espenson, *Chemical Kinetics and Reaction Mechanisms*; McGraw-Hill series in advanced chemistry, eds. J. Ricci, J.W. Bradley, McGraw-Hill, Inc, **1981**.

[138] [N^0 181] T. Wiseman, S. Williston, J. F. Brandts, L. N. Lin, *Anal. Biochem.* **1989**, *179*, 131.

The only prerequisite for the ITC kinetic study is well defined first, or eventually second, titration heat released/absorbed peak.

$$v_{ITC} = \frac{\Delta p}{\Delta H\, V} \quad \text{(equation 3.5)}$$

Then, by plotting the early first changes of concentrations of the limiting reactant (A_t) or the product (C_t) after lag time (response time that is a characteristic of the ITC device) against time (***t***), the initial rate constants $\boldsymbol{k_{obs}}$ and ***k***, respectively, can be observed. Subsequently, by plotting the obtained rate constants ($\boldsymbol{k_{obs}}$ and ***k***) against the starting concentration of the reactant in excess (B_0) the partial reaction order with respect to reactant *B* can be obtained.

2.3 Static DFT-D calculations

Like mentioned in the Introductory chapter, to achieve the Thesis' aims, the work during the thesis has been conceived to be collaborative – between the groups of Prof. Dr. Grimme, Dr. Djukic and Prof. Dr. Zarić. The latter two were supposed to be represented by myself, while the Grimme's group by PhD candidate Mr. Hansen. According to non-written collaborative agreement, the produced data by each group might be only published in scientific journals. Therefore, the theoretical part of this thesis is significantly shorter than the overall produced theoretical data.

As discussed in the Introductory chapter, although several methods being developed to treat dispersion correction, only most widely-used Grimme's dispersion corrections were used within this thesis. In particular, Grimme's third development (D3)[139] was employed. Due to the fact explained above, a number of tested methods were limited.

The calculations were performed either using the Amsterdam Density Functional package (ADF2013 version)[140] or Gaussian 09 program package.[141], due to the joint nature of the thesis

---

[N^0 182] E. Freire, O. L. Mayorga, M. Straume, *Anal. Chem.* **1990**, *62*, 950A.
[139] [N^0 255] S. Grimme, J. Antony, S. Ehrlich, H. Krieg, *J. Chem. Phys*. **2010**, *132*, 154104.
[140] [N^0 296] G. te Velde, F.M. Bickelhaupt, S. J. A. van Gisbergen, C. Fonseca Guerra, E. J. Baerends, J. G. Snijders, T. Ziegler, *J. Comput. Chem.* **2001**, *22*, 931.
[N^0 297] C. Fonseca Guerra, J. G. Snijders, G. te Velde, E. J. Baerends, *Theor. Chem. Acc.* **1998**, *99*, 391.
[N^0 298] ADF2013, SCM, Theorical Chemistry, Vrije Universiteit, Amsterdam, The Netherlands, http://www.scm.com The following list of authors and contributors:
E.J. Baerends, T. Ziegler, J. Autschbach, D. Bashford, A. Bérces, F. M. Bickelhaupt, C. Bo, P. M. Boerrigter, L. Cavallo, D. P. Chong, L. Deng, R. M. Dickson, D. E. Ellis, M. van Faassen, L. Fan, T. H. Fischer, C. Fonseca Guerra, M. Franchini, A. Ghysels, A. Giammona, S. J. A. van Gisbergen, A. W. Götz, J.A. Groeneveld, O. V. Gritsenko, M. Grüning, S. Gusarov, F. E. Harris, P. van den Hoek, C. R. Jacob, H. Jacobsen, L. Jensen, J. W. Kaminski, G. van

work and an accessibility to supercomputer resources in particular country. All the calculations were performed employing rather known DFT-D methods in both gas and solution phase. The main purpose of such calculations was to estimate the thermodynamic parameters of all the systems that were previously experimentally studied. The interaction energies were calculated for some systems, as well. By comparison to the experimentally obtained values of the thermodynamic parameters, the extent of mutual accordance of the theoretical and experimental values was estimated and lately critically discussed.

The general calculation procedure involved the following:

a) constructing starting geometries of the investigated reactants;
b) constructing starting geometries of the assumed pairs/reaction products;
c) performing geometry optimization calculations on the starting geometries employing chosen static DFT-D method;
d) performing vibrational frequency calculations at the same level of theory;
e) calculating the thermodynamic parameters from statistical data (internal energy and entropy) generated by vibrational frequency calculations.
f) estimating interaction/reaction enthalpies (ΔH), Gibbs free energies (ΔG) and entropies (ΔS) from a difference between corresponding values of the pair/product and free reactants.

All further details of the performed calculations are given in Chapter 3, while the calculation results are given within the Chapters 4-8.

Kessel, F. Kootstra, A. Kovalenko, M. V. Krykunov, E. van Lenthe, D. A. McCormack, A. Michalak, M. Mitoraj, S.M. Morton, J. Neugebauer, V. P. Nicu, L. Noodleman, V. P. Osinga, S. Patchkovskii, M. Pavanello, P. H. T. Philipsen, D. Post, C.C. Pye, W. Ravenek, J. I. Rodríguez, P. Ros, P. R. T. Schipper, G. Schreckenbach, J. S. Seldenthuis, M. Seth, J. G. Snijders, M. Solà, M. Swart, D. Swerhone, G. te Velde, P. Vernooijs, L. Versluis, L. Visscher, O. Visser, F. Wang, T. A. Wesolowski, E. M. van Wezenbeek, G. Wiesenekker, S. K. Wolff, T. K. Woo, A. L. Yakovlev

[141] [N^0 299] M. J. Frisch, G. W. Trucks, H. B. Schlegel, G. E. Scuseria, M. A. Robb, J. R. Cheeseman, G. Scalmani, V. Barone, B. Mennucci, G. A. Petersson, H. Nakatsuji, M. Caricato, X. Li, H. P. Hratchian, A. F. Izmaylov, J. Bloino, G. Zheng, J. L. Sonnenberg, M. Hada, M. Ehara, K. Toyota, R. Fukuda, J. Hasegawa, M. Ishida, T. Nakajima, Y. Honda, O. Kitao, H. Nakai, T. Vreven, J. A. Montgomery, Jr., J. E. Peralta, F. Ogliaro, M. Bearpark, J. J. Heyd, E. Brothers, K. N. Kudin, V. N. Staroverov, R. Kobayashi, J. Normand, K. Raghavachari, A. Rendell, J. C. Burant, S. S. Iyengar, J. Tomasi, M. Cossi, N. Rega, J. M. Millam, M. Klene, J. E. Knox, J. B. Cross, V. Bakken, C. Adamo, J. Jaramillo, R. Gomperts, R. E. Stratmann, O. Yazyev, A. J. Austin, R. Cammi, C. Pomelli, J. W. Ochterski, R. L.

2.4. Cambridge Structural Database (CSD)

The Cambridge Structural Database (CSD),[142] established in 1965, represents a large base of crystal structures of small organic and organometallic molecules. The CSD contains over 650000 structures derived as results of both X-Ray and neutron diffraction analysis. The precisely determined 3D structures are accompanied with all relevant crystallographic data of the structures, enabling the interpretation of structures in chemically meaningful way. Analysis of crystal structures from the CSD has found to be a useful method in investigating geometrical characteristic of various systems. In this way, some non-covalent interactions were recognized and described, such as cation-π interactions of transition metal complexes,[143] interactions of chelate[144] and hydrogen-bridged rings,[145] as well as interactions of aromatic rings at large horizontal displacements[146] Based on CSD study the importance of several other types of non-covalent interaction was recognized as well as their influence on crystal packing.[147] The CSD data analysis has also been used in a systematic study of various types of chemical bonds,[148] and specifically, a metal-ligand bond.[149] A knowledge gained by analysis data from CSD

Martin, K. Morokuma, V. G. Zakrzewski, G. A. Voth, P. Salvador, J. J. Dannenberg, S. Dapprich, A. D. Daniels, Ö. Farkas, J. B. Foresman, J. V. Ortiz, J. Cioslowski, and D. J. Fox, *Gaussian 09* (Gaussian, Inc., Wallingford CT, **2009**).

[142] [N^0 300] C. R. Groom, I. J. Bruno, M. P. Lightfoot, S. C. Ward, *Acta Cryst*. **2016**, *B72*, 171.

[143] [N^0 301] S. D. Zarić, *Chem. Phys. Lett.* **1999**, *311*, 77.
[N^0 302] S. D. Zarić, *Chem. Phys*. **2000**, *256*, 213.
[N^0 303] S. D. Zarić, D. Popović, E. W. Knapp, *Chem. Eur. J.* **2000**, *6*, 3935.
[N^0 64] S. D. Zarić, *Eur. J. Inorg. Chem.* **2003**, 2197.

[144] [N^0 76] G. A. Bogdanović, A. Spasojević-de Biré, S. D. Zarić, *Eur. J. Inorg. Chem*. **2002**, 1599.
[N^0 78] V. B. Medaković, M. K. Milčić, G. A. Bogdanović, S. D. Zarić, *J. Inorg. Biochem.* **2004**, *98*, 1867.
[N^0 85] Z. D. Tomić, S. B. Novaković, S. D. Zarić, *Eur. J. Inorg. Chem.* **2004**, 2215.
[N^0 86] Z. D. Tomić, D. N. Sredojević, S. D. Zarić, *Cryst. Growth Des.* **2006**, *6*, 29.

[145] [N^0 91] J. P. Blagojević, S. D. Zarić, *Chem. Commun.* **2015**, *51*, 12989.
[N^0 90] J. P. Blagojević, D. Ž. Veljković, S. D. Zarić, *CrystEngComm* **2017**, *19*, 40.
[N^0 304] C. I. Yeo, S. N. A. Halim, S. W. Ng, S. L. Tan, J. Zukerman-Schpector, M. A. B. Ferreira, E. R. T. Tiekink, *Chem. Commun.* **2014**, *50*, 5984.

[146] [N^0 57] D. B. Ninković, G. V. Janjić, D. Ž. Veljković, D. N. Sredojević, S. D. Zarić, *ChemPhysChem* **2011**, *12*, 3511.
[N^0 305] D. P. Malenov, J. Lj. Dragelj, G. V. Janjić, S. D. Zarić, *Cryst. Growth Des.* **2016**, *16*, 4169.

[147] [N^0 306] T. Steiner, G. R. Desiraju, *Chem. Commun.* **1998**, *8*, 891.
[N^0 307] A. Nangia, *Cryst. Eng.* **2001**, *4*, 49.
[N^0 308] T. Steiner, *Chem. Commun.* **1997**, *8*, 727.
[N^0 309] T. Steiner, *Angew. Chem. Int. Ed.* **2002**, *41*, 48.
[N^0 310] A. Bauzá, R. Ramis, A. Frontera, *J. Phys. Chem. A* **2014**, *118*, 2827.
[N^0 311] J. Huang, S. Kingsbury, M. Kertesz, *Phys. Chem. Chem. Phys.* **2008**, *10*, 2625.
[N^0 312] T. J. Mooibroek, P. Gamez, J. Reedijk, *CrystEngComm* **2008**, *10*, 1500.
[N^0 313] E. R. T. Tiekink, *Coord. Chem. Rev.* **2017**, 345, 209.
[N^0 314] A. Bauzá, T. J. Mooibroek, A. Frontera, *ChemPhysChem* **2015**, *16*, 2496.
[N^0 315] R. Taylor, *CrystEngComm* **2014**, 16, 6852.

[148] [N^0 316] Santiago Alvarez, *Dalton Trans.* **2013**, 42, 8617.

[149] [N^0 317] G. Kuppuraj, M. Dudev, C. Lim, *J. Phys. Chem. B* **2009**, *113*, 2952.
[N^0 318] A. Nimmermark, L. Öhrström, J. Reedijk, *Z. Kristallogr.* **2013**, *228*, 3113.
[N^0 319] R. K. Hocking, T. W. Hambley, *Inorg. Chem.* **2003**, *42*, 2833.

underpins huge areas of fundamental and applied science. Similar to CSD, the Protein Data Base[150] (PDB) is found to be important for studying non-covalent interactions within proteins.[151]

In this Thesis, CSD analysis was used only in case of study of the interactions within phosphine-borane Lewis pairs.

The CSD (November 2015 released, version 5.37)[152] search was performed on the crystal structures involving phosphine and borane molecules screening for their intermolecular or intramolecular contacts. The CSD search program ConQuest 1.18[153] was used to retrieve structures satisfying the following criteria: (a) the crystallographic R factor < 10%, (b) the error-free coordinates according to the criteria used in the CSD, (c) no polymer and ionic structures, (d) structures with the disorder and (e) structure solved from powder were not included.

The phosphine-borane interactions were analyzed by using the geometrical parameters defined in Figure M4. The structures where the distance between phosphorus and boron atoms ($\mathbf{d_{B\text{-}P}}$) was less than 2.5 Å were extracted from the CSD. The additional geometrical parameters were: the dihedral angle – an angle between the planes formed by atoms directly bound to phosphorus and boron atoms (**φ**), the normal distance between phosphorus atom and the plane formed by atoms directly bound to boron atom (**R**) and the offset distance between the projection of phosphorus atom on the plane formed by atoms directly bound to boron atom and the centroid of atoms directly bound to boron atom (**r**).

The results and analysis of the results of the performed search are given in Chapter 4, Subchapter 2.

---

[150] [N^0 320] www.rcsb.org; H. M. Berman, J. Westbrook, Z. Feng, G. Gilliland, T. N. Bhat, H. Weissig, I. N. Shindyalov, P. E. Bourne, The Protein Data Bank *Nucleic Acids Research* **2000**, *28*, 235.

[151] see some examples: [N^0 321] I. M. Stanković, D. M. Božinovski, E. N. Brothers, M. R. Belić, M. B. Hall, S. D. Zarić, *Cryst. Growth Des*. **2017**, *17*, 6353.
[N^0 322] J. Lj. Dragelj, I. M. Stanković, D. M. Božinovski, T. Meyer, D. Ž. Veljković, V. B. Medaković, E.-W. Knapp, S. D. Zarić, *Cryst. Growth Des*. **2016**, *16*, 1948.
[N^0 323] D. B. Ninković, D. P. Malenov, P. V. Petrović, E. N. Brothers, S. Niu, M. B. Hall, M. R. Belić, S. D. Zarić, *Chem. Eur. J*. **2017**, *23*, 11046 – 11053.

[152] [N^0 300] C. R. Groom, I. J. Bruno, M. P. Lightfoot, S. C. Ward, *Acta Cryst*. **2016**, *B72*, 171.

[153] [N^0 324] I. J. Bruno, J. C. Cole, P. R. Edgington, M. Kessler, C. F. Macrae, P. McCabe, J. Pearson, R. Taylor, *Acta Cryst*. **2002**, *B58*, 389.

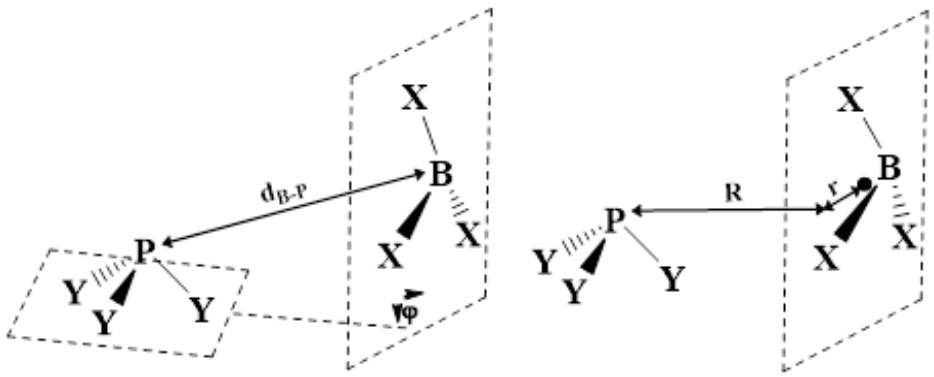

Figure M4 The geometrical parameters describing phosphine-borane interactions: a) $d_{B\text{-}P}$ distance and angle φ, b) normal distance R and offset distance r. The X and Y are substituents on boron and phosphorus atoms, respectively. The dihedral angle **φ** is an angle between the planes formed by atoms directly bound to phosphorus and boron atoms.

Chapter 3

Experimental section

3.1. NMR details.

All 1D NMR measurements (^{1}H (300, 400, 500, and 600 MHz), ^{11}B (128 MHz), ^{13}C (75 and 126 MHz), ^{19}F (282 MHz), ^{31}P (121 and 162 MHz), were performed on Bruker DPX 300 and 400, Avance I 500, and Avance III 600 spectrometers. Used deuterated solvents were chloroform-d_1 dichloromethane-d_2 or toluene-d_8. NMR spectra were recorded at 25°C and referenced to the residual proton and carbon signals of the deuterated solvent (^{1}H, ^{13}C) or to phosphorus, boron and fluorine signal of the external reference standards (^{31}P, ^{11}B, ^{19}F), i.e. to $CF_3C_6H_5$ in chloroform-*d*for ^{19}F, and to $NaBH_4$ in D_2O for ^{11}B. ^{1}H and ^{13}C signals are reported relative to $SiMe_4$ (TMS). Chemical shifts δ and coupling constants are expressed in parts per million (ppm) and hertz (Hz), respectively. Multiplicity: s = singlet, d = doublet, t = triplet, q = quadruplet, sept = septuplet, dt = triplet of doublets, td = doublet of triplets, m = multiplet. Relevant NMR spectra are given throughout the Chapters 4-8 or in Supplementary Information.

3.2. X-Ray diffraction analysis details.

Structural X-Ray diffraction analysis was performed on the Bruker APEX II DUO Kappa-CCD diffractometer equipped with an Oxford Cryosystem liquid N_2 device, using Mo Kα radiation (λ = 0.71073 Å). The crystal−detector distance was 38 mm. The cell parameters were determined (APEX2 software)1 from reflections taken from 3 sets of 12 frames, each at 10 s exposure. The structures were solved by direct methods using the program SHELXS-2013.2. The refinement and all further calculations were carried out using SHELXL-2013. Recording and resolving of the crystal structures were done by X-Ray service at Unistra.

3.3. ESI-MS details.

ESI-MS analysis of the samples was performed on a Bruker Daltonik GmgH (Bremen, Germany) microTOF spectrometer equipped with an orthogonal electrospray (ESI) interface. Relevant MS spectra are given throughout the Chapters 4-8 or in Supplementary Information.

3.4. IR details.

The infra-red spectra of powder amorphous samples were recorded on an ATR spectrometer provided by Bruker optics and analyzed with OPUS software. Relevant IR spectra are given throughout the Chapters 4-8 or in Supplementary Information.

3.5. ITC experimental details.

Isothermal titration calorimetry (ITC) experiments were carried out on a Waters-SAS nano-ITC device[154] (TA Instruments ®) equipped with two stainless steel Hastelloy cells of 1 mL volume each). Auto equilibration of the ITC was performed before every experiment to reach an acceptable baseline.

3.6. Static DFT-D calculations.

All computations were performed by the methods of the density functional theory (DFT) using Amsterdam Density Functional package (ADF2013 version)[155] or Gaussian 09 program package.[156]

All the geometry optimizations and computing of interaction energies were employed Perdew-Burke-Ernzerhof (PBE)[157] GGA functional augmented with Grimme's D3[158] inclusion of mid-to-long range dispersion force with a Becke-Johnson (BJ),[159] unless stated otherwise.

---

[154] [N^0 293] www.tainstruments.com

[155] [N^0 296] G. te Velde, F.M. Bickelhaupt, S. J. A. van Gisbergen, C. Fonseca Guerra, E. J. Baerends, J. G. Snijders, T. Ziegler, *J. Comput. Chem.* **2001**, *22*, 931.
[N^0 297] C. Fonseca Guerra, J. G. Snijders, G. te Velde, E. J. Baerends, *Theor. Chem. Acc.* **1998**, *99*, 391.
[N^0 298] ADF2013, SCM, Theorical Chemistry, Vrije Universiteit, Amsterdam, The Netherlands, http://www.scm.com
The following list of authors and contributors:
E.J. Baerends, T. Ziegler, J. Autschbach, D. Bashford, A. Bérces, F. M. Bickelhaupt, C. Bo, P. M. Boerrigter, L. Cavallo, D. P. Chong, L. Deng, R. M. Dickson, D. E. Ellis, M. van Faassen, L. Fan, T. H. Fischer, C. Fonseca Guerra, M. Franchini, A. Ghysels, A. Giammona, S. J. A. van Gisbergen, A. W. Götz, J.A. Groeneveld, O. V. Gritsenko, M. Grüning, S. Gusarov, F. E. Harris, P. van den Hoek, C. R. Jacob, H. Jacobsen, L. Jensen, J. W. Kaminski, G. van Kessel, F. Kootstra, A. Kovalenko, M. V. Krykunov, E. van Lenthe, D. A. McCormack, A. Michalak, M. Mitoraj, S.M. Morton, J. Neugebauer, V. P. Nicu, L. Noodleman, V. P. Osinga, S. Patchkovskii, M. Pavanello, P. H. T. Philipsen, D. Post, C.C. Pye, W. Ravenek, J. I. Rodríguez, P. Ros, P. R. T. Schipper, G. Schreckenbach, J. S. Seldenthuis, M. Seth, J. G. Snijders, M. Solà, M. Swart, D. Swerhone, G. te Velde, P. Vernooijs, L. Versluis, L. Visscher, O. Visser, F. Wang, T. A. Wesolowski, E. M. van Wezenbeek, G. Wiesenekker, S. K. Wolff, T. K. Woo, A. L. Yakovlev

[156] [N^0 299] M. J. Frisch, G. W. Trucks, H. B. Schlegel, G. E. Scuseria, M. A. Robb, J. R. Cheeseman, G. Scalmani, V. Barone, B. Mennucci, G. A. Petersson, H. Nakatsuji, M. Caricato, X. Li, H. P. Hratchian, A. F. Izmaylov, J. Bloino, G. Zheng, J. L. Sonnenberg, M. Hada, M. Ehara, K. Toyota, R. Fukuda, J. Hasegawa, M. Ishida, T. Nakajima, Y. Honda, O. Kitao, H. Nakai, T. Vreven, J. A. Montgomery, Jr., J. E. Peralta, F. Ogliaro, M. Bearpark, J. J. Heyd, E. Brothers, K. N. Kudin, V. N. Staroverov, R. Kobayashi, J. Normand, K. Raghavachari, A. Rendell, J. C. Burant, S. S. Iyengar, J. Tomasi, M. Cossi, N. Rega, J. M. Millam, M. Klene, J. E. Knox, J. B. Cross, V. Bakken, C. Adamo, J. Jaramillo, R. Gomperts, R. E. Stratmann, O. Yazyev, A. J. Austin, R. Cammi, C. Pomelli, J. W. Ochterski, R. L. Martin, K. Morokuma, V. G. Zakrzewski, G. A. Voth, P. Salvador, J. J. Dannenberg, S. Dapprich, A. D. Daniels, Ö. Farkas, J. B. Foresman, J. V. Ortiz, J. Cioslowski, and D. J. Fox, *Gaussian 09* (Gaussian, Inc., Wallingford CT, **2009**).

[157] [N^0 325] J. P. Perdew, K. Burke, M. Ernzerhof, *Phys. Rev. Lett.* **1996**, *77*, 3865.
[N^0 326] J. P. Perdew, K. Burke, M. Ernzerhof, *Phys. Rev. Lett.* **1997**,*78*, 1396.

[158] [N^0 255] S. Grimme, J. Antony, S. Ehrlich, H. Krieg, *J. Chem. Phys.* **2010**, *132*, 154104.
[N^0 268] S. Grimme, S. Ehrlich, L. Goerigk, *J. Comput. Chem.* **2011**, *32*, 1456.

[159] [N^0 268] S. Grimme, S. Ehrlich, L. Goerigk, *J. Comput. Chem.* **2011**, *32*, 1456.

All computations performed in ADF used the scalar relativistic Zeroth Order Regular Approximation (ZORA)[160] and were carried out with single polarized triple-ζ (TZP)[161] basis set while in Gaussian 09 were carried out with Karlsruhe's valence polarized triple-ζ (def2-TZVP)[162] unless stated otherwise.

Geometry optimizations by energy gradient minimization were carried out in all cases with an integration grid accuracy spanned 4 - 6.5 (ultra-fine in Gaussian09), an energy gradient convergence criterion of 1e-3 au and tight SCF convergence criterion ($1e^{-7}$ au), unless stated otherwise.

Solvation by chlorobenzene in ADF was accounted for using the COSMO procedure with Klamt's values of van der Waals radii for atoms,[163] i.e. epsilon - 5.62, radius - 3.48 Å, while in Gaussian by employing standard solvation method - Polarizable Continuum Model (PCM)[164] with default solvent parameters.

All the geometry optimizations were confirmed as true energy minima by calculating vibrational modes.

Calculations of vibrational modes (analytical second derivative of vibrational frequencies)[165] were performed at 298.15 K at the same level of theory as the geometry optimizations calculations (i.e. ZORA-GGAPBE-D3(BJ)/TZP level in ADF, PBE-D3(BJ)/def2-TZVP level in Gaussian), unless stated otherwise.

The vibrational modes were also used for obtaining thermodynamic parameters of the systems, namely internal energy and entropy, by statistical thermal analysis. Enthalpies and Gibbs free energies of the systems are deduced from the internal energies and entropies. Reaction enthalpies (Δ*H*), Gibbs free energies (Δ*G*) and entropies (Δ*S*) of the pair formation are

---

[160] [N^0 327] E. van Lenthe, E. J. Baerends, J. G. Snijders, *J. Chem. Phys.* **1993**, *99*, 4597.
[N^0 328] E. van Lenthe, E. J. Baerends, J. G. Snijders, *J. Chem. Phys.* **1994**,*101*, 9783.
[N^0 329] E. van Lenthe, A. E. Ehlers, E. J. Baerends, *J. Chem. Phys.* **1999**,*110*, 8943.
[161] [N^0 330] E. van Lenthe and E. J. Baerends, *J. Comput. Chem.* **2003**, *24*, 1142.
[162] [N^0 331] F. Weigend, R. Ahlrichs, *Phys. Chem. Chem. Phys.* **2005**, *7*, 3297.
[N^0 332] F. Weigend, *Phys. Chem. Chem. Phys.* **2006**, *8*, 1057.
[163] [N^0 333] C. C. Pye, T. Ziegler, *Theor. Chem. Acc.* **1999**, *101*, 396-408.
[164] [N^0 334] S. Miertuš, E. Scrocco, J. Tomasi, *Chem. Phys.* **1981**, *55*, 117-129.
[165] [N^0 335] A. Bérces, R. M. Dickson, L. Fan, H. Jacobsen, D. Swerhone, T. Ziegler, *Comput. Phys. Commun.* **1997**, *100*, 247.
[N^0 336] H. Jacobsen, A. Bérces, D. Swerhone, T. Ziegler, *Comput. Phys. Commun.* **1997**, *100*, 263.
[N^0 337] S. K. Wolff, *Int. J. Quantum Chem.* **2005**, *104*, 645.

estimated as a difference between corresponding values of the pair and free reactants. In the same manner E_{int} was obtained.

The basis set superposition error (BSSE) was not calculated and accounted for unless stated otherwise.

Graphical representations of molecular structures were drawn using ADFview v13 implemented in ADF 13 package[153] or Mercury v3.9.[166]

[166] [N^0 338] C. F. Macrae, P. R. Edgington, P. McCabe, E. Pidcock, G. P. Shields, R. Taylor, M. Towler, J. van de Streek, *J. Appl. Cryst.* **2006**, *39*, 453.

Chapter 4

Formation of (Frustrated) Lewis pairs ((F)LPs)

4.1. Subchapter 1. - Experimental and theoretical approach.

4.1.1. Introduction.

It has been known that most of the phosphine-borane (Lewis acid-base) pairs among themselves make a classical covalent bond.[167] However, the discovery of “frustrated” Lewis acid - base pairs (FLPs), among which tris(pentafluorophenyl)borane with a variety of phosphines are the most studied ones, showed a great influence of the non-covalent interactions in these systems, and opened a new field of research in chemistry.[168]

FLP concept, established by Stephan, has found great interest over past decade.[169]The concept is based on the finding that systems containing Lewis acids and bases that are prevented from classical donor-acceptor interactions by steric (and electronic) factors keep their Lewis acidity and basicity and, consequently, are available for interaction with another molecule. In that way

[167] [N^0 339] E. Gamble, P. Gilmont, *J. Am. Chem. Soc.* **1940**, *62*, 717.
[N^0 340] A. Cowley, M. Damasco, *J. Am. Chem. Soc.* **1971**, *93*, 6815.
[N^0 341] R. Foester, K. Cohn, *Inorg. Chem.* **1972**, 11, 2590.
[168] [N^0 342] G. C. Welch, L. Cabrera, P. A. Chase, E. Hollink, J. D. Masuda, P. Wei, D. W. Stephan, *Dalton Trans.* **2007**, 3407.
[N^0 343] P. Spies, R. Fröhlich, G. Kehr, G. Erker, S. Grimme, *Chem. Eur. J.* **2008**, *14*, 333.
[N^0 344] D. W. Stephan, *Dalton Trans*. **2009**, 3129.
[N^0 345] G. Erker, *Dalton Trans*. **2011**, *40*, 7475.
[N^0 346] D. W. Stephan, *Dalton Trans*. **2012**, *41*, 9015.
[N^0 347] T. H. Warren, G. Erker, *Top. Curr. Chem*. **2013**, *334*, 219.
[N^0 348] D. W. Stephan, G. Erker, *Chem. Sci*. **2014**, *5*, 2625.
[169] [N^0 349] J. S. J. McCahill, G. C. Welch, D. W. Stephan, *Angew. Chem. Int. Ed*. **2007**, *46*, 4968.
[N^0 342] G. C. Welch, L. Cabrera, P. A. Chase, E. Hollink, J. D. Masuda, P. Wei, D. W. Stephan, *Dalton Trans.* **2007**, 3407.
[N^0 350] M. A. Dureen, A. Lough, T. M. Gilbert, D. W. Stephan, *Chem. Commun.* **2008**, 4303.
[N^0 351] D. W. Stephan, *Org. Biomol. Chem*. **2008**, *6*, 1535.
[N^0 352] M. A. Dureen, D. W. Stephan, *J. Am. Chem. Soc*. **2009**, 131, 8396.
[N^0 353] M. A. Dureen, G. C. Welch, T. M. Gilbert, D. W. Stephan, *Inorg. Chem*. **2009**, 9910.
[N^0 354] J. S. J. McCahill, G. C. Welch, D. W. Stephan, *Dalton Trans*. **2009**, 8555
[N^0 355] C. M. Momming, E. Otten, G. Kehr, R. Frohlich, S. Grimme, D. W. Stephan, G. Erker, *Angew. Chem. Int. Ed. Engl*. **2009**, *48*, 6643.
[N^0 356] E. Otten, R. C. Neu, D. W. Stephan, *J. Am. Chem. Soc.* **2009**, *131*, 9918.
[N^0 357] M. Ullrich, K. S. H. Seto, A. J. Lough, D. W. Stephan, *Chem. Commun*. **2009**, 2335.
[N^0 358] B. Birkmann, T. Voss, S. J. Geier, M. Ullrich, G. Kehr, G. Erker, D. W. Stephan, *Organometallics* **2010**, *29*, 5310.
[N^0 359] C. Chen, R. Froehlich, G. Kehr, G. Erker, *Chem. Commun.* **2010**, *46*, 3580.
[N^0 360] T. Voss, C. Chen, G. Kehr, E. Nauha, G. Erker, D. W. Stephan, *Chem. - Eur. J*. **2010**, *16*, 3005.
[N^0 361] T. Holtrichter-Roessmann, C. Roesener, J. Hellmann, W. Uhl, E.-U. Wuerthwein, R. Froehlich, B. Wibbeling, *Organometallics* **2012**, *31*, 3272.
[N^0 362] E. Y. X. Chen, *Top. Curr. Chem.* **2013**, *334*, 239.
[N^0 363] M. Sajid, A. Klose, B. Birkmann, L. Liang, B. Schirmer, T. Wiegand, H. Eckert, A. J. Lough, R. Froehlich, C. G. Daniliuc, S. Grimme, D. W. Stephan, G. Kehr, G. Erker, *Chem. Sci*. **2013**, *4*, 213.
[N^0 364] A. L. Travis, S. C. Binding, H. Zaher, T. A. Q. Arnold, J.-C. Buffet, D. O'Hare, *Dalton Trans*. **2013**, *42*, 2431.
[N^0 365] T. H. Warren, A. J. P. Cardenas, *American Chemical Society*, **2013**, pp. CATL.

FLPs can activate H_2 or other small molecules.[170] Access to free electron donor and acceptor centers is provided either by introducing steric demanding groups or by dissociative equilibrium. An overall electron content of both donor and acceptor is found to be important for FLP behavior, as well.[171] The correlation between the loose character of the bimolecular pair and the related catalytic reactivity led to propose the possible existence of van der Waals complexes[172] wherein optimal covalent connection between the donor and the acceptor would be basically prevented –or frustrated- by steric cluttering, leading to a dynamic assembly in which a highly polarized interspace would ease the concerted cleavage[173] of weakly polarized bonds.[174]

The phosphine-borane pairs, especially "frustrated" ones, have found great use in different domains: from the synthesis and catalysis to the hydrogen storage and materials.[175] Further

[170] [N^0 366] D. P. Huber, G. Kehr, K. Bergander, R. Froehlich, G. Erker, S. Tanino, Y. Ohki, K. Tatsumi, *Organometallics* **2008**, *27*, 5279.
[N^0 367] T. A. Rokob, A. Hamza, A. Stirling, T. Soos, I. Papai, *Angew. Chem. Int. Ed*. **2008**, *47*, 2435.
[N^0 368] V. Sumerin, F. Schulz, M. Nieger, M. Leskela, T. Repo, B. Rieger, *Angew. Chem. Int. Ed*. **2008**, *47*, 6001.
[N^0 369] C. Jiang, O. Blacque, H. Berke, *Organometallics* **2009**, *28*, 5233.
[N^0 370] A. Ramos, A. J. Lough, D. W. Stephan, *Chem. Commun*. **2009**, 1118.
[N^0 371] M. Ullrich, A. J. Lough, D. W. Stephan, *Organometallics* **2010**, *29*, 3647.
[N^0 372] S. Kronig, E. Theuergarten, D. Holschumacher, T. Bannenberg, C. G. Daniliuc, P. G. Jones, M. Tamm, *Inorg. Chem*. **2011**, *50*, 7344.
[N^0 373] A. Schaefer, M. Reissmann, A. Schaefer, W. Saak, D. Haase, T. Mueller, *Angew. Chem. Int. Ed*. **2011**, *50*, 12636.
[N^0 374] T. J. Herrington, A. J. W. Thom, A. J. P. White, A. E. Ashley, *Dalton Trans.* **2012**, *41*, 9019.
[N^0 375] G. Menard, D. W. Stephan, *Angew. Chem. Int. Ed*. **2012**, *51*, 8272.
[N^0 376] S. Schwendemann, S. Oishi, S. Saito, R. Froehlich, G. Kehr, G. Erker, *Chem. - Asian J*. **2013**, *8*, 212.
[N^0 377] D. J. Scott, M. J. Fuchter, A. E. Ashley, *Chem. Soc. Rev*. 2017, *46*, 5689.
[N^0 378] C. Jiang, O. Blacque, T. Fox, H. Berke, *Organometallics* **2011**, *30*, 2117.
[N^0 379] B. Schirmer, S. Grimme, *Chem. Commun*. **2010**, *46*, 7942.
[N^0 380] Z. Lu, Z. Cheng, Z. Chen, L. Weng, Z. H. Li, H. Wang, *Angew. Chem. Int. Ed.* **2011**, *50*, 12227.
[N^0 381] D. W. Stephan, S. Greenberg, T. W. Graham, P. Chase, J. J. Hastie, S. J. Geier, J. M. Farrell, C. C. Brown, Z. M. Heiden, G. C. Welch, M. Ullrich, *Inorg. Chem.* **2011**, *50*, 12338.
[171] [N^0 382] D. W. Stephan, G. Erker, *Angew. Chem. Int. Ed.* **2015**, *54*, 6400.
[N^0 383] D. W. Stephan, *Science* **2016**, *354*, aaf7229.
[172] [N^0 384] B. Schirmer, S. Grimme, *Top. Curr. Chem*. **2013**, *332*, 213.
[173] [N^0 385] T. A. Rokob, I. Bako, A. Stirling, A. Hamza, I. Papai, *J. Am. Chem. Soc*. **2013**, *135*, 4425.
[N^0 386] T. A. Rokob, I. Papai, *Top. Curr. Chem*. **2013**, *332*, 157.
[174] [N^0 379] B. Schirmer, S. Grimme, *Chem. Commun.* **2010**, *46*, 7942.
[N^0 387] R. Ponec, P. Beran, *J. Phys. Chem. A* **2013**, *117*, 2656.
[N^0 388] M. Pu, T. Privalov, *J. Chem. Phys*. **2013**, *138*, 154305/1.
[175] [N^0 389] T. Imamoto, *Pure Appl. Chem.* **1993**, *65*, 655.
[N^0 390] T. Imamoto, T. Oshiki, T. Onozawa, M. Matsuo, T. Hikosaka, M. Yanagawa, *Heteroat. Chem.* **1992**, *3*, 563.
[N^0 391] D. Mimeau, O. Delacroix, B. Join, A.-C. Gaumont, *C. R. Chimie*, **2004**, *7*, 845.
[N^0 392] J.-M. Denis, H. Forintos, H. Szelke, L. Toupet, T.-N. Pham, P.-J. Madec, A.-C. Gaumont, *Chem. Commun.* **2003**, 54.
[N^0 393] Z. M. Heiden, M. Schedler, D. W. Stephan, *Inorg. Chem.* **2011**, *50*, 1470.
[N^0 394] K. Izod, C. M. Dixon, E. McMeekin, L. Rodgers, R. W. Harrington, U. Baisch, *Organometallics* **2014**, *33*, 378.
[N^0 395] T. Özgön, G.-Q. Chen, C. G. Daniliuc, A. C. McQuilken, T. H. Warren, R. Knitsch, H. Eckert, G. Kehr, G. Erker, *Organometallics* **2016**, *35*, 3667.
[N^0 396] C.-H. Lim, A. M. Holder, J. T. Hynes, C. B. Musgrave, *Inorg. Chem.* **2013**, *52*, 10062.
[N^0 397] C. M. Thomas, J. C. Peters, *Inorg. Chem.* **2004**, *43*, 80.

cases including frustrated azaheterocycles/borane[176] pairs were also reported and further supplemented with a large variety of alternative pairs.[177] The syntheses of molecules containing intramolecular frustrated Lewis partners have paved the way to a rich organocatalysis bringing organoboron chemistry into a new era.[178]

Many reports have dealt with calculations on phosphine-borane systems, particularly their interaction energies and related distances between acid and base centers; the influences of the substituents on the boron and phosphorus atoms on their reactivity; the catalytic reaction mechanisms, as well as the importance of non-covalent interactions.[179] Also, some advances

---

[N^0 342] G. C. Welch, L. Cabrera, P. A. Chase, E. Hollink, J. D. Masuda, P. Wei, D. W. Stephan, *Dalton Trans.* **2007**, 3407.
[N^0 398] S. J. Geier, M. A. Dureen, E. Y. Ouyang, D. W. Stephan, *Chem. Eur. J.* **2010**, *16*, 988.
[N^0 399] T. Agou, J. Kobayashi, T. Kawashima, *Inorg. Chem.* **2006**, *45*, 9137.
[N^0 400] A. J. Lough, D. W. Stephan, *J. Am. Chem. Soc.* **2009**, *131*, 523.
[N^0 401] D. Chen, Y. Wang, J. Klankermayer, *Angew. Chem. Int. Ed*. **2010**, *49*, 9475;
[N^0 402] S. Schwendemann, T. A. Tumay, K. V. Axenov, I. Peuser, G. Kehr, R. Frohlich, G. Erker, *Organometallics* **2010**, *29*, 1067.
[N^0 403] D. W. Stephan, G. Erker, *Angew. Chem. Int. Ed*. **2010**, *49*, 46.
[N^0 404] G. Erker, *C. R. Chim*. **2011**, 14, 831.
[N^0 405] T. Mahdi, D. W. Stephan, *J. Am. Chem. Soc*. **2014**, *136*, 15809.
[N^0 406] J. Paradies, *Angew. Chem. Int. Ed*. **2014**, *53*, 3552.
[176] [N^0 407] A. E. Ashley, A. L. Thompson, D. O'Hare, *Angew. Chem. Int. Ed*. **2009**, *48*, 9839.
[177] [N^0 408] K. V. Axenov, G. Kehr, R. Frohlich, G. Erker, *Organometallics* **2009**, *28*, 5148.
[N^0 409] P. A. Chase, A. L. Gille, T. M. Gilbert, D. W. Stephan, *Dalton Trans*. **2009**, 7179.
[N^0 410] S. J. Geier, A. L. Gille, T. M. Gilbert, D. W. Stephan, *Inorg. Chem*. **2009**, *48*, 10466.
[N^0 411] S. J. Geier, D. W. Stephan, *J. Am. Chem. Soc*. **2009**, *131*, 3476.
[N^0 412] M. Alcarazo, C. Gomez, S. Holle, R. Goddard, *Angew. Chem. Int. Ed*. **2010**, *49*, 5788.
[N^0 413] R. S. Chellappa, T. Autrey, M. Somayazulu, V. V. Struzhkin, R. J. Hemley, *ChemPhysChem* **2010**, *11*, 93.
[N^0 414] F. Schulz, V. Sumerin, M. Leskelae, T. Repo, B. Rieger, *Dalton Trans*. **2010**, *39*, 1920.
[N^0 415] D. P. Curran, A. Solovyev, M. M. Brahmi, L. Fensterbank, M. Malacria, E. Lacote*, Angew. Chem. Int. Ed.* **2011**, *50*, 10294.
[N^0 378] C. Jiang, O. Blacque, T. Fox, H. Berke, *Organometallics* **2011**, *30*, 2117.
[N^0 416] F. Schulz, V. Sumerin, S. Heikkinen, B. Pedersen, C. Wang, M. Atsumi, M. Leskelae, T. Repo, P. Pyykkoe, W. Petry, B. Rieger, *J. Am. Chem. Soc*. **2011**, *133*, 20245.
[N^0 417] J. Iglesias-Siguenza, M. Alcarazo, *Angew. Chem. Int. Ed*. **2012**, *51*, 1523.
[N^0 418] S. Khan, M. Alcarazo, *Top. Curr. Chem.* **2013**, *334*, 157.
[N^0 419] E. L. Kolychev, E. Theuergarten, M. Tamm, *Top. Curr. Chem.* **2013**, *334*, 121.
[N^0 420] Z. Lu, H. Ye, H. Wang, *Top. Curr. Chem*. **2013**, *334*, 59.
[178] [N^0 421] S. Froemel, R. Froehlich, C. G. Daniliuc, G. Kehr, G. Erker, *Eur. J. Inorg. Chem*. **2012**, 3774;
[N^0 422] M. Sajid, G. Kehr, T. Wiegand, H. Eckert, C. Schwickert, R. Poettgen, A. J. P. Cardenas, T. H. Warren, R. Froehlich, C. G. Daniliuc, G. Erker, *J. Am. Chem. Soc*. **2013**, *135*, 8882.
[179] [N^0 423] T. Özgön, K.-Y. Ye, C. G. Daniliuc, B. Wibbeling, L. Liu, S. Grimme, G. Kehr, G. Erker, *Chem. Eur. J*. **2016**, *22*, 5988.
[N^0 424] A. Skancke, P. N. Skancke, *J. Phys. Chem.* **1996**, *100*, 15079.
[N^0 425] C. Bannwarth, A. Hansen, S. Grimme, *Isr. J. Chem.* **2015**, *55*, 235.
[N^0 426] V. Horváth, A. Kovács, I. Hargittai, *J. Phys. Chem. A* **2003**, *107*, 1197.
[N^0 427] T. A. Rokob, A. Hamza, I. Pápai, *J. Am. Chem. Soc*. **2009**, *131*, 10701.
[N^0 428] Z. X. Lu, G. Wang, H. X. Li, L. L. Zhao, *Chinese Sci. Bull.* **2010**, *55*, 239.
[N^0 429] S. Gao, W. Wu, Y. Mo, *Int. J. Quantum Chem.* **2011**, *111*, 3761.
[N^0 430] D. Wu, D. Jia, A. Liu, L. Liu, J. Guo, *Chem. Phys. Lett.* **2012**, *541*, 1.
[N^0 378] C. Jiang, O. Blacque, T. Fox, H. Berke, *Organometallics* **2011**, *30*, 2117.
[N^0 379] B. Schirmer, S. Grimme, *Chem. Commun*. **2010**, *46*, 7942.
[N^0 380] Z. Lu, Z. Cheng, Z. Chen, L. Weng, Z. H. Li, H. Wang, *Angew. Chem. Int. Ed.* **2011**, *50*, 12227.

were made in the synthesis of various kinds of phosphine-borane pairs and in their use, especially the use as the metal-free catalysts of a bond cleavage in small molecules (H_2, CO_2, etc.).[180] Review given by Stephan in 2016 outlines the major advances over the past decade in FLP chemistry as well as its application areas.[181] Recently, it has been found that a mode of action of FLPs could proceed through radical mechanism, as well, that would lead to homolytic cleavage of concreted bond.[182]

Although annual reports on the boron chemistry[183] gives a great overview on arising boron chemistry and huge contribution in chemistry overall, a systematic structural description of the phosphine-borane systems has not been given yet.

Manners and co-workers gave in 2010 a detailed overview on (amine-) and phosphine-borane adducts.[184] They described phosphine-borane adducts: in general; their history; reactivity and functionalization; coordination chemistry with transition metals as well as their polymeric chemistry.

The nature of boron-donor (so-called triel) bonds is explained by π-hole concept (as π-hole bonds). Depending on the nature of the donor, boron-donor bonds may vary from strong and (partially) covalent bond to weak interactions.[185]

Quite intriguing, whilst a great number of articles have dealt with the possible modes of action of FLPs over small molecule activation[186] or structure-activity relationships[187] in FLP's for hydrogen

---

[N^0 381] D. W. Stephan, S. Greenberg, T. W. Graham, P. Chase, J. J. Hastie, S. J. Geier, J. M. Farrell, C. C. Brown, Z. M. Heiden, G. C. Welch, M. Ullrich, *Inorg. Chem*. **2011**, *50*, 12338.
[180] [N^0 431] S. Tamke, Z.-W. Qu, N. A. Sitte, U. Flörke, S. Grimme, J. Paradies, *Angew. Chem. Int. Ed.* **2016**, *55*, 4336.
[N^0 432] G. E. Arnott, P. Moquist, C. G. Daniliuc, G. Kehr, G. Erker, *Eur. J. Inorg. Chem.* **2014**, 1394.
[N^0 433] G.-Q. Chen, G. Kehr, C. Mück-Lichtenfeld, C. G. Daniliuc, G. Erker, *J. Am. Chem. Soc.* **2016**, *138*, 8554.
[N^0 434] M. Sajid, L.-M. Elmer, C. Rosorius, C. G. Daniliuc, S. Grimme, G. Kehr, G. Erker, *Angew. Chem. Int. Ed.* **2013**, *52*, 2243.
[N^0 435] A. Tlili, A. Voituriez, A. Marinetti, P. Thuérya, T. Cantat, *Chem. Commun.* **2016**, 52, 7553.
[181] [N^0 383] D. W. Stephan, *Science* **2016**, *354*, aaf7229.
[182] [N^0 436] L. Liu, L. L. Cao, Y. Shao, G. Ménard, D. W. Stephan, *Chem.* **2017**, *3*, 259.
[183] [N^0 437] R. T. Paine, H. Nöth, *Chem. Rev.* **1995**, *95*, 343.
[N^0 438] B. Carboni, L. Monnier, *Tetrahedron* **1999**, *95*, 1197.
[N^0 439] J. M. Brune, B. Faure, M. Maffei, *Coord. Chem. Rev.* **1998**, *178-180*, 665.
[N^0 440] Y. Zhu, N. S. Hosmane, *Coord. Chem. Rev.* **2015**, *293–294*, 357.
[N^0 441] G. Duret, R. Quinlan, P. Bisseret, N. Blanchard, *Chem. Sci.* **2015**, *6*, 5366.
[N^0 442] H. DeFrancesco, J. Dudley, A. Coca, *Boron Chemistry: An Overview*; ACS Symposium Series, American Chemical Society, Washington, DC, **2016**, vol. 1236, ch. 1, pp 1–25.
[184] [N^0 443] A. Staubitz, A. P. M. Robertson, M. E. Sloan, I. Manners, *Chem. Rev.* **2010**, *110*, 4023.
[185] [N^0 444] S. J. Grabowski, *ChemPhysChem* **2014**. *15*, 2985.
[N^0 445] S. J. Grabowski, *J. Comp. Chem.* **2018**, *39*, 472.

activation catalysis and its thermochemistry[188] little has been published on the actual thermochemistry of the interactions in solution of intermolecular pairs and particularly on the actual aggregation mode for such loose "pairs" (FLPs) in solution. An article by Macchioni *et al.* in 2014 presented one rare attempt at determining the enthalpy of interaction of intermolecular FLPs by means of ^{1}H and ^{19}F NMR techniques.[189]

The research within the study of the formation of the Lewis pairs from the borane **1.1** (acting as Lewis acid) and various phosphines **1.2a-g** (acting as Lewis base) was done by experimental (mainly using ITC measurements and DOSY NMR experiments) and theoretical tools (using static DFT-D calculations). Among used phosphines there are those which, interacting with the borane **1.1**, should give classical Lewis pair (notorious example is the phosphine **2.2a**) as well as those which form notorious frustrated Lewis pairs (example is the phosphine **2.2d**). Regarding the others, in the literature[190] the only known pair is **2.1**/**2.2e**, which instead of forming classical Lewis pair rather form a frustrated one derived from nucleophilic substitution of fluorine atom in *para* position by phosphorous (see Scheme 1.1.2). This fact might be an issue within the investigation. All other systems should not, in principle, exhibit any unusual behavior. Therefore, in order to settle right conditions for ITC experiments, a round of the reaction tests was carried out on all considered reaction systems **1.1**/**1.2a-g**.

---

[186] [N^0 372] S. Kronig, E. Theuergarten, D. Holschumacher, T. Bannenberg, C. G. Daniliuc, P. G. Jones, M. Tamm, *Inorg. Chem.* **2011**, *50*, 7344.
[N^0 378] C. Jiang, O. Blacque, T. Fox, H. Berke, *Organometallics* **2011**, *30*, 2117.
[N^0 379] B. Schirmer, S. Grimme, *Chem. Commun.* **2010**, *46*, 7942.
[N^0 380] Z. Lu, Z. Cheng, Z. Chen, L. Weng, Z. H. Li, H. Wang, *Angew. Chem. Int. Ed*. **2011**, *50*, 12227.
[N^0 381] D. W. Stephan, S. Greenberg, T. W. Graham, P. Chase, J. J. Hastie, S. J. Geier, J. M. Farrell, C. C. Brown, Z. M. Heiden, G. C. Welch, M. Ullrich, *Inorg. Chem*. **2011**, *50*, 12338.
[187] [N^0 446] F. Bertini, V. Lyaskovskyy, B. J. J. Timmer, F. J. J. de Kanter, M. Lutz, A. W. Ehlers, J. C. Slootweg, K. Lammertsma, *J. Am. Chem. Soc.* **2012**, *134*, 201;
[N^0 447] R. C. Neu, E. Y. Ouyang, S. J. Geier, X. Zhao, A. Ramos, D. W. Stephan, *Dalton Trans.* **2010**, 39, 4285.
[188] [N^0 448] S. Kronig, E. Theuergarten, D. Holschumacher, T. Bannenberg, C. G. Daniliuc, P. G. Jones, M. Tamm, *Inorg. Chem.* **2011**, *50*, 7344;
[N^0 449] A. Hamza, A. Stirling, T. A. Rokob, I. Papai*, Int. J. Quantum Chem.* **2009**, *109*, 2416;
[N^0 427] T. A. Rokob, A. Hamza, I. Pápai, *J. Am. Chem. Soc.* **2009**, *131*, 10701.
[N^0 450] S. M. Kathmann, H. Cho, T.-M. Chang, G. K. Schenter, K. Parab, T. Autrey, *J. Phys. Chem. B* **2014**, *118*, 4883.
[N^0 451] S. M. Whittemore, G. Edvenson, D. M. Camaioni, A. Karkamkar, D. Neiner, K. Parab, T. Autrey, *Catal. Today* **2015**, 251, 28;
[N^0 452] A. Y. Houghton, T. Autrey, *J. Phys. Chem. A* **2017**, *121*, 8785.
[189] [N^0 453] L. Rocchigiani, G. Ciancaleoni, C. Zuccaccia, A. Macchioni, *J. Am. Chem. Soc*. **2014**, *136*, 112.
[190] [N^0 454] G. C. Welch, R. Prieto, M. A. Dureen, A. J. Lough, O. A. Labeodan, T. Holtrichter-Rössmann, D. W. Stephan, *Dalton Trans*. **2009**, 1559.

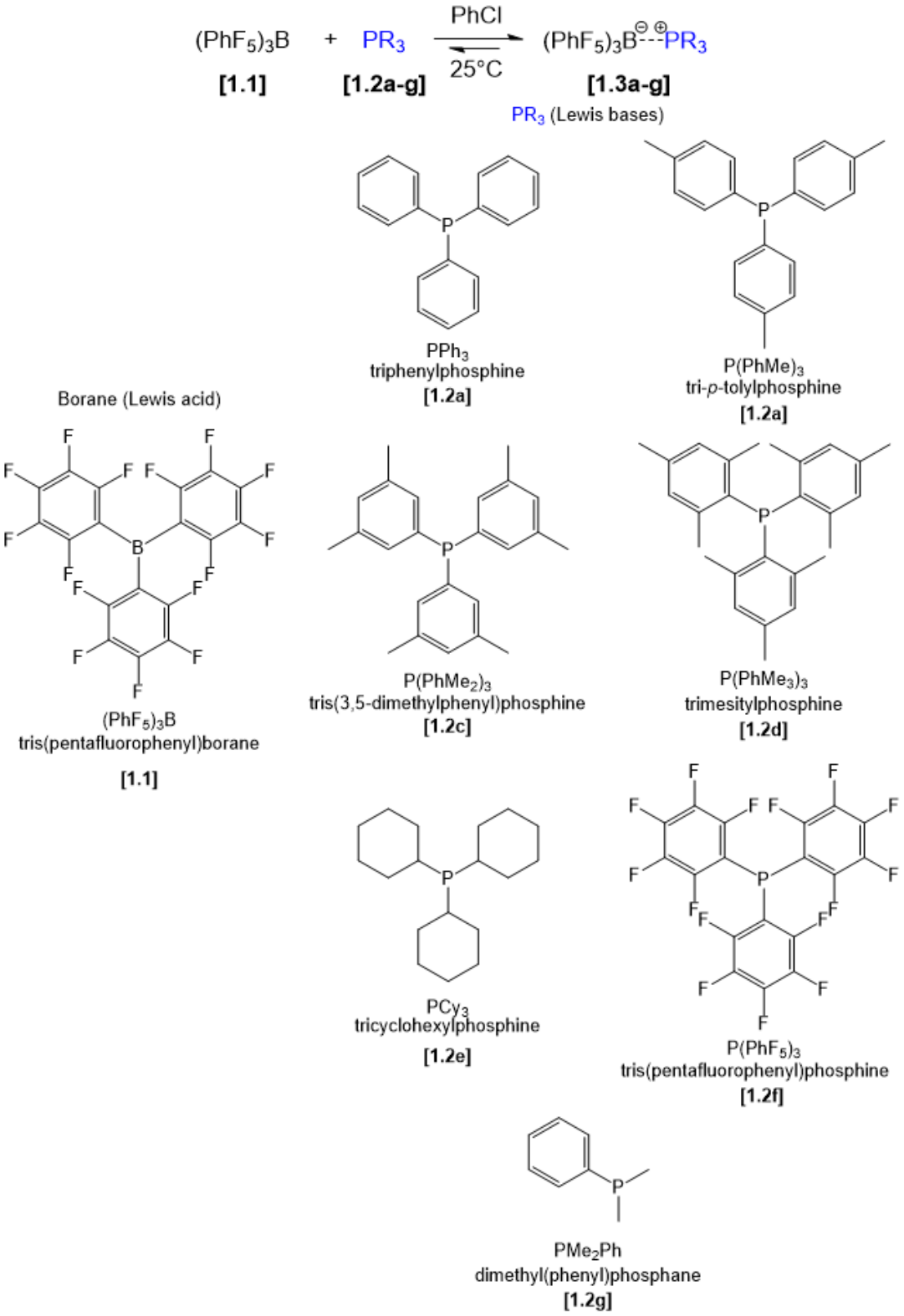

Scheme 1.1.1 Schematic representation of the investigated reactions within the study of formation of the (frustrated) Lewis pairs from the borane **1.1** and various phosphines **1.2a-g**.

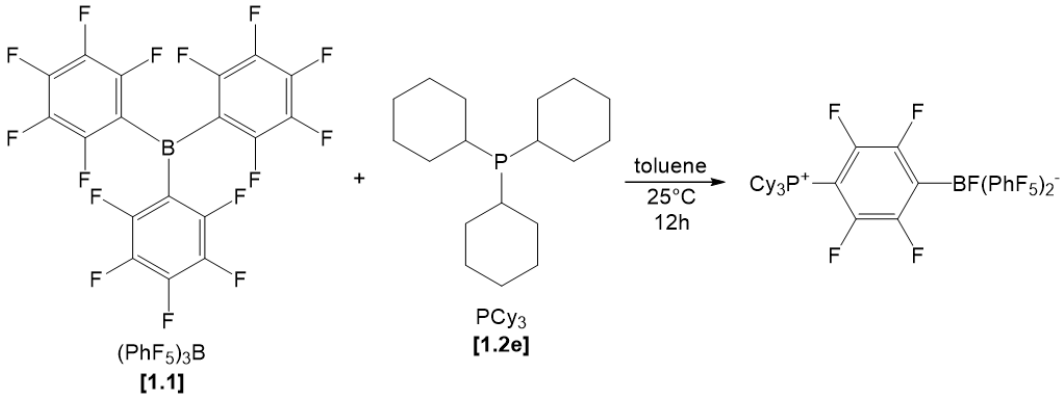

Scheme 1.1.2 Simplified schematic representation of the possible side reaction – nucleophilic aromatic substitution of fluorine atom in *para* position within tris(pentafluorophenyl)borane (**1.1**) induced by tricyclohexylphosphine (**1.2e**) and long reaction times.

4.1.2. Experimental section.

4.1.2.1. Generalities.

The experiments considered an (equilibrium) reaction between the tris(perfluorophenyl)-borane (**1.1**, Scheme 1.1) and particular phosphine (**1.2a-g**, Scheme 1.1).

4.1.2.2. Techniques.

The interaction of interests was examined experimentally and theoretically. The main employed experimental technique was ITC. Before doing ITC experiments every studied reaction system was examined into the conventional Schlenk line using standard experimental techniques. The reactions and the reaction products were monitored and characterized by standard experimental techniques: NMR (^{1}H, ^{13}C, ^{31}P, ^{19}F, ^{11}B) spectroscopy, X-Ray crystallography (where possible), mass spectrometry (where possible) and elemental analysis (where possible). Additionally, all studied reactions except a reaction between tris(perfluorophenyl)borane and tris (perfluorophenyl) phosphine were monitored by Diffusion-Ordered Spectroscopy (DOSY) NMR experiment. As theoretical tools the static DFT-D calculations were employed. The calculations were performed for each considered system.

4.1.2.3. Materials.

All used compounds were stored into a dry, argon filled glove box or under argon. Chlorobenzene was purchased from Sigma Aldrich and distillated over calcium hydride and

degassed prior to use. Tris(perfluorophenyl)borane (**1.1**) was ordered from TCI and used as received. All used phosphines (**1.2a-g**) were ordered from Sigma Aldrich and used as received. All solvents used in the synthesis and reaction tests (dichloromethane, pentane, hexene, heptane) were ordered from Sigma Aldrich and distillated over an appropriate drying agent prior to use. All deuterated solvents were ordered from Sigma Aldrich and dried through neutral alumina prior to use.

4.1.2.4. Reaction tests

The reaction tests were performed in two approaches – synthetic and monitoring.

Since the reaction examinations within all the herein considered systems were conducted in the same manner, only a general procedure is given.

Synthesis: The reactions were carried out under argon using standard Schlenk line technique at ambient temperature. Tris (perfluorophenyl) borane (**1.1**) (0.0300 g, 0.057 mol) (or 30 mg, 57 mmol) was dissolved in 2 mL of dichloromethane and one equivalent (0.057 mol) of the phosphine was added. After stirring for one hour, the solvent was removed under reduced pressure to yield white residue. The residue was washed with 3 x 5 mL of pentane or hexane and dried under reduced pressure for several hours giving white powder in almost quantitative yield.

Monitoring: The same reactions (1:1 equivalent) were also carried out in deuterated solvent (chloroform-d_1), but without any further treatment and NMR spectra were subsequently (after one hour) recorded at 25ºC.

Crystals suitable for X-Ray diffraction analysis were obtained only in cases of tris (4-methylphenyl) phosphine (**1.2b**), tris (3,5-dimethylphenyl)phosphine (**1.2c**) and tricyclohexylphosphine (**1.2e**) (see Figure SI 1.39-41). However, in the cases of resolved X-Ray structures of tris (4-methylphenyl) phosphine (**1.2b**) and tricyclohexylphosphine (**1.2e**) it is obtained that the structures do not correspond to the expected reaction products - Lewis pairs **1.3b** and **1.3e**, respectively. These structures show an activation of EtOH promoted by the Lewis pair and the unexplainable case of phosphane-borane adduct. Correct structure of the phosphine-borane Lewis pair is obtained only in case of tris (3,5-dimethylphenyl)phosphine **1.2c** (Figure SI 1.41).

4.1.2.5. DOSY 2D NMR details.

All DOSY NMR experiments were performed on a Bruker Avance III 600 MHz spectrometer, equipped with a PABBI *z* diff probe, developing a pulse field gradient of 29 G A^{-1} cm^{-1}. All samples are prepared in a glove box at ambient temperature, charged in a micro (2.5 mm) NMR tube and tightly closed. The sample contained 1:1 equivalent of both reactants, borane (**1.1**) and phosphine (**1.2a-e**), in final concentration around 20 mmol/L in chloroform-d_1. The ^{1}H, ^{31}P, ^{19}F NMR spectra were acquired at 25 °C. Exclusively, the system **1.1**/**1.2a** was probed in molar ratio 10:1 (in final concentrations around 100 mmol/L: 10 mmol/L). Diffusion coefficients were extracted in both a) manually by a visual peaking the peaks generated by module implemented in the software MNova12[191] and applying well-known Stoke-Einstein equation and b) analytically by plotting the curves of the changing in NMR signal ($\ln(I/I_0)$ versus G^2) and its integral fitting. DOSY spectra were generated by DOSY module of the software MNova12.[189] Related DOSY NMR spectra are given throughout the chapter or in Supporting Information.

4.1.2.6. X-Ray diffraction analysis details.

Crystals for the X-Ray diffraction analysis were grown using diffusion crystal growing technique from pentane, hexane or heptane at -25 ºC. The crystallographic data of the obtained and resolved structures are given in Supplementary Information (see Figure SI 1.1.39-41)

4.1.2.7. ESI-MS details.

The details were the following:

Negative mode
Acquisition parameters:
Source Type - ESI Capillary 4500 V Nebulizer 0.4 Bar Corona 195 nA
Ion Polarity - Negative Set Capillary Exit -160.0 V Dry Gas 4.0 l/min Set Hexapole RF 60.0 V
Scan Range - n/a Set Skimmer - 1 -50.0 V Dry Heater 180 °C APCI Heater 514 °C
Positive mode
Acquisition parameters:
Source Type - ESI Capillary 4500 V Nebulizer 0.4 Bar Corona 195 nA

[191] [N^0 455] Mestrelab Reasearch S.L. www.mestrelab.caom

Ion Polarity - Positive Set Capillary Exit 80.0 (or 150) V Dry Gas 4.0 l/min Set Hexapole RF 60.0 (or 220) V

Scan Range - n/a - Set Skimmer 1 50.0 V Dry Heater 180 (or 200) °C APCI Heater 514 °C

Mass Spectrum Molecular Formula Report

Acquisition parameters:

Set Corrector Fill 65 V

Source Type ESI Ion Polarity Positive Set Pulsar Pull 817 V

Scan Range n/a Capillary Exit 80.0 V Set Pulsar Push 817 V

Scan Begin 50 m/z Hexapole RF 60.0 V Set Reflector 1700 V

Scan End 3000 m/z Skimmer 1 50.0 V Set Flight Tube 8600 V

Hexapole 1 24.3 V Set Detector TOF 2275 V

Sum Formula Sigma m/z Err [ppm] Mean Err [ppm] rdb N Rule e"

4.1.2.8. ITC experimental details.

The solutions of reactants (borane and phosphines) were prepared by dissolving a mass of substrate in pure, freshly distilled and degassed chlorobenzene. The ITC experiments were performed in sequential injection manner at 25ºC with a moderate stirring rate (150-200 rpm). The concentrations of the borane solutions were around 3.5 mmol/L, while the concentrations of the phosphine's solutions were between i.e. 20-80 mmol/L. The solution of tris (perfluorophenyl) borane (**1.1**) was introduced in the sample cell (1.0 mL) while the servo-controlled ITC syringe (100 µL) was filled with the solution of the phosphine (**1.2a-g**). The reference cell (1.0 mL) was entirely filled with pure chlorobenzene. The auto equilibrating mode was allowed before the experiment. The content of the syringe was injected into the sample cell through 45-90 equivalent injections (1.03 µL or 2.06 µL per injection) while a time delay between two consecutive injections was 600-3000s (mostly 2000s), depending on the nature of a certain system. After successfully finished ITC experiment a ratio between borane and phosphine in the sample cell was up to 1:2 equivalents. For each studied system, at least three experiments under the same conditions were done. Besides these, the blank (i.e. dilution) experiments of each phosphine were performed, as well. Enthalpy of reaction (ΔH_r) (as result of experiment) was obtained by calculating the ratio of the heat released (obtained by integration of the heat response - peak surfaces employing NanoAnalyze software[192]) and number of mols of the phosphine injected until reaching a stationary response point (i.e. a point after which there is no

heat changes during time). The heat of dilution of the particular phosphine is encountered in each corresponding enthalpy calculation. Enthalpy of reaction (ΔH_r) obtained in such way is so-called raw enthalpy of reaction (raw ΔH_r). Resulting ΔH_r value represents an average value of three corresponding experiments. Where possible, the fitting of the ITC thermograms by the Independent model (implemented in NanoAnalyze software[190]) was employed rising up all the thermodynamic parameters of the reaction (ΔH_r, ΔG_r, ΔS_r). Additionally, from the stationary response point molar (stoichiometric) ratio of the reactants is estimated.

Experiments with reverse order of the reactants were checked out, as well. However, satisfactory results were not obtained. Namely, in most of the cases it was not possible to reach proper stationary point under the employed experimental conditions. Additionally, in case of Cy_3P (**1.2e**) the employed experimental conditions readily allowed a secondary reaction (a substitution of the fluorine in para position) to happen.

4.1.2.9. Static DFT-D calculation details.

The computations were performed by the DFT methods using Amsterdam Density Functional package (ADF2013 version) and Gaussian 09 program package.

Starting geometries of the monomers (phosphines and borane) were taken from the CSD and optimized as singlet ground states in the gas phase (in Gaussian 09) and chlorobenzene solution phase (in ADF 13 and Gaussian 09). Geometries of the pairs (dimers) were constructed from the previously optimized monomers in proposed orientations (a - face to face and b - face to back) by Grimme[193] and optimized as singlet ground states in the gas phase (in Gaussian 09) and chlorobenzene solution phase (in ADF 13). Trimer geometry of the **2-1a-2** was optimized in both, the gas phase and chlorobenzene solution phase in Gaussian 09.

The interaction energies (E_{int}) were computed only in Gaussian09 at PBE-D3(BJ)/def2-TZVP level of theory.

[192] [N^0 293] www.tainstruments.com
[193] [N^0 425] C. Bannwarth, A. Hansen, S. Grimme, *Isr. J. Chem.* **2015**, *55*, 235.

4.1.3. Results and discussion.

4.1.3.1. Reaction tests.

As mentioned, the reaction tests were carried out to give preliminary inside view of the investigated systems (**1.1**/**1.2a-f**). The additional investigated system **1.1**/**1.2g** was not probed. Herein, as results of the tests, ^{1}H, ^{19}F, ^{31}P, ^{11}B NMR spectra of notorious classical **1.1**/**1.2a** and frustrated **1.1**/**1.2d** Lewis pairs as well as the spectra of the starting materials will be reported and comparatively commented in detail, while for the other investigated systems only major drawbacks will be given. The representations of all the spectra will be given in Supplementary Information.

*System **1.1**/**1.2a** - (1:1).*

The ^{1}H NMR spectrum shows an upfield shifting of the signals compared to the free Ph_3P (**1.2a**). Namely, there are two main broad signals at 7.58 ppm and 7.45, while in the free Ph_3P there is a multiplet of signals from 7.34-7.29 ppm. Additionally, at around 7.37 ppm a broad and overlapped signal can be observed (see Figure SI 1.1.1)

From the ^{19}F NMR spectrum a downfield shifting (compared to the free borane) of all the signals and multiplying some of them are noticeable. Most probably the signal at -130.4 (*ortho* fluorenes) is moved to -136.8 ppm while the signal at -146.0 ppm (*-p* fluorine) is moved to -159.8. The third signal (-161.2 ppm *meta*-fluorenes) is probably divided into four signals: two singlets (-160.2, -165.3) or one doublet -162.9 (J = 30 Hz) and two triplets (-159.8 (J = 20 Hz) and -165.8 (t, J = 37 Hz) or, eventually, one triplet of doublets. (see Figure SI 1.1.2)

The ^{31}P NMR spectrum shows a shifting the signal from -5.2 ppm (free phosphine) to 1.1 ppm (pair), while ^{11}B NMR spectrum shows a change in the signal position - from 57.3 ppm (free borane) to -3.4 ppm (pair). (see Figure SI 1.1.3-4)

From these observations it could be concluded that the ITC measurements might be performed in stoichiometric conditions reliably expecting the formation of cohesive pair.

*System **1.1**/**1.2d** - (1:1)*

The ^{1}H NMR spectrum shows existence of two species (the free phosphine and a pair). Their signals appear at very similar chemical shifts and are partially overlapped: three singlets (6.76

(s, Ar-H), 2.25 (s, -*p*-Me), 2.02 (s, -*o*-Me) ppm) belong to the free phosphine while the singlets at 6.77, 2.28 and 2.04 ppm correspond to the pair. However, one can notice some extra signals: two doublets (one at 8.23 ppm (J = 48 Hz) and one at 7.11 (d, J = 54 Hz) larger in abundance) and two singlets (6.63 and 2.38 ppm), which might correspond to activated impurities by the pair. (see Figure SI 1.1.13)

The ^{19}F NMR spectrum suggests on at least two kinds of binding modes of the borane to the phosphine. Namely, there are two sets of signals – an upfielded and a downfielded compared to the free borane (-130.4, -145.9, -161.2 ppm). The upfielded set consists of three relatively sharp singlets (at -128.7, -143.4, -160.8 ppm) while the downfielded one contains one relatively broad singlet (at -133.9 ppm) and two triplets (the well-defined at -160.1 ppm (J = 20 Hz) and the fused at -166.0 ppm (J = 21 Hz)). (see Figure SI 1.1.14)

The ^{31}P NMR spectrum shows, as well, an existence of two species: a pair with upfield shifted signal - from -36.2 ppm (free phosphine) to -27.3 ppm (the pair) and free phosphine. (see Figure SI 1.1.15)

From these observations one could conclude on rational possibilities of performing the ITC measurements within stoichiometric conditions expecting rather the equilibrium mixture.

*System **1.1/1.2b** - (1:1)* and *system **1.1/1.2c** - (1:1)*

Similar to the system **1.1**/**1.2a** the NMR spectra of the systems **1.1**/**1.2b-c** (see Figure SI 1.1.5-12) revealed the slight shifting and broadening of the signals in the proton spectra and a clear shift of the signal in the related phosphorous and boron spectra indicating the existence of the pair without the presence of the free reactants. The ^{19}F NMR spectra showed a multiplying of the signals what might suggest the coupling with protons or/and the existence of molecular clusters. Nonetheless, the spectra allowed the conclusion that these systems might be exploited within ITC measurements in stoichiometric conditions expecting the formation of the cohesive pairs.

*System **1.1/1.2e** - (1:0.2-1.3 equivalents; 0.5h-46.5h)*

To figure out when and within what molar ratio the side reaction of nucleophilic aromatic substitution occurs, a series of the tests were carried out within various molar ratios of the reactants and reaction times at ambient temperature. The reaction mixtures were mainly

monitored by ^{31}P NMR. The results (see Figure SI 1.1.16-17) suggested that within a molar ratio of around 1:0.2 equivalents in favor of the borane, the mixture is rather clean giving only one reaction product, probably a cohesive pair, regardless the employed reaction times. However, in molar ratio close to stoichiometry (1:0.7) after longer reaction times (for instance 10h) the mixture starting to be contaminated by other reaction products. Therefore, the results suggest that within ITC experiments stoichiometric ratio of the reactants as well as long reaction times should be avoided in order to raise chances to get reliable data.

*System **1.1/1.2f** - (1:1-2)*

According to the results of ^{19}F and ^{31}P NMR spectra (see Figure SI 1.1.18-19) it could be concluded that no formation of the pair is likely to happen within up to two equivalents of the phosphine and 48h of the reaction time. Therefore, it is not likely to expect some other behavior of the system neither within ITC stoichiometric measurements.

4.1.3.2. ITC experiments.

Following the main conclusion of the reaction tests (that shows that the reactions could be satisfactory performed in stoichiometric conditions), all the ITC measurements within this study were carried out in stoichiometric condition, with the final molar ratio of the reactants 1:2. The main issue was the order of the reactants. As any choice, basically, had no significant favor, both possible orders of the reactants were probed. However, lately it was found that more appropriate order is titration of the borane (**1.1**) by the phosphine (**1.2a-g**). Therefore, the ITC results (raw ΔH_r values as well as Model ITC values of all thermodynamic parameters of the reaction, where possible) of these experiments are reported in the main text (Table 1.1.1, Figure 1.1.1 and Figure SI 1.1.36) while the results of the reverse ITC experiments are given in Supplementary Information (see Table SI 1.1.1, Figure SI 1.1.37). In addition, the stoichiometric coefficients, i.e. molar ratio of the reactants at a stationary point (n) of all the examined systems are reported, as well.

Table 1.1.1 ITC results – reaction enthalpy values (raw ΔH_r) and stoichiometric coefficient (n) – obtained from the sequential addition of the phosphine **1.2a-g** into the cell contained the solution of the borane **1.1**.

System	***n*** and ITC **raw ΔH_r** ± error	
	"substoichiometric" stage	stationary point
1.1/1.2a	0.13-0.14 -19.2 ± 2.1	1 -12.4 ± 1.3
1.1/1.2b$_3$	0.11-0.13 -16.9 ± 1.8	1 -12.9 ± 1.4
1.1/1.2c	0.14-0.16 -21.4 ± 2.3	1 -13.3 ± 1.4
1.1/1.2d	0.11-0.13 -29.3 ± 4.7	0.18-0.20 -22.8 ± 3.7
1.1/1.2e	0.17-0.19 -24.1 ± 2.6	1 -34.4 ± 3.7
1.1/1.2f	/	no stationary state (-0.3 ± 0.1)
1.1/1.2g	/	1 -14.0 ± 2.1

The ITC results revealed few quite interesting things. Firstly, the obtained raw ΔH_r values of (supposedly) classical Lewis pairs (**1.1**/**1.2a-c,g**) do not show such a high exothermicity as it has been published in the literature[192] – the values are valued around -13 - -14 kcal/mol. Secondly, the supposed classical Lewis pairs (**1.1**/**1.2a-c**) showed an upsurge of heat release in early (substoichiometric) stages of the reaction. The estimated raw ΔH_r values of these substoichiometric stages (up to 6:1 of molar ratio of the reactants - **1.1**:**1.2a-c**) are ranged from around -17 kcal/mol to -21.5 kcal/mol. Rather expectedly, all these systems (**1.1**/**1.2a-c,g**) reached the stationary point (athermicity) within the ITC measurements at stoichiometry around 1:1.

Further, in opposite to the classical Lewis pairs, the frustrated pair **1.1**/**1.2d** showed higher exothermicity than predicted by the theory[194] and even much higher than the obtained reaction

[194] [N^0 456] G. Skara, B. Pinter, J. Top, P. Geerlings, F. De Proft, F. De Vleeschouwer, *Chem. Eur. J.* **2015**, *21*, 5510.

enthalpy of the classical Lewis pairs – the raw ΔH_r value of the system **1.1**/**1.2d** is ca. -23 kcal/mol. Even more interestingly, the athermicity is reached within $n \approx 0.2$ ruling out the existence of 1:1 pair as the dominant type of association and rather suggesting the formation of aggregates containing over two (even up to five) molecules of the borane (**1.1**) per one molecule of the phosphine (**1.2d**).

The results of the reverse ordered ITC experiments (see Figure SI 1.1.1 and Table SI 1.1.37) roughly confirmed herein explained results (as Model ITC ΔH_r values are ranged from ca. -13 to -15 kcal/mol), suggesting that reliable data could be obtained for the **1.1**/**1.2a-c** system whatever the order of the reactants is. On the opposite side, the **1.1**/**1.2d** system is not exploitable in the reverse order of the reactants within employed ITC conditions, as it shows a releasing of heat after stoichiometry, while that fact is in accordance with the observation that suggests the occurrence of large molecular assemblies within the system **1.1**/**1.2d**.

The results of the system **1.1**/**1.2e** (see the shape of the related thermogram - Figure 1.1.1e) readily suggest on the occurrence of two different processes – probably a formation of the truly frustrated pair (or mixture of the classical and truly frustrated pair) as well as of the frustrated one derived from the aromatic nucleophilic substitution. Therefore, although it is not totally certainly, the heat released in early stages could correspond to the heat of the formation of the classical/truly frustrated pair, while the rest of heat release might correspond to formation of the frustrated pair as a product of an aromatic nucleophilic substitution.

Last but not least, the results of the system **1.1**/**1.2f** clearly tell that the system does not reach any athermicity neither before, at nor after stoichiometry. Thus, it suggests that the medium permanently adjusts its composition through new intermolecular interactions as the phosphine is added. Therefore, it is not possible to state that a “pair”, even frustrated, that is stabilized predominantly by non-covalent attractive interactions, is the dominating molecular assembly.

[N^0 429] S. Gao, W. Wu, Y. Mo, *Int. J. Quantum Chem.* **2011**, *111*, 3761.
[N^0 425] C. Bannwarth, A. Hansen, S. Grimme, *Isr. J. Chem.* **2015**, *55*, 235.

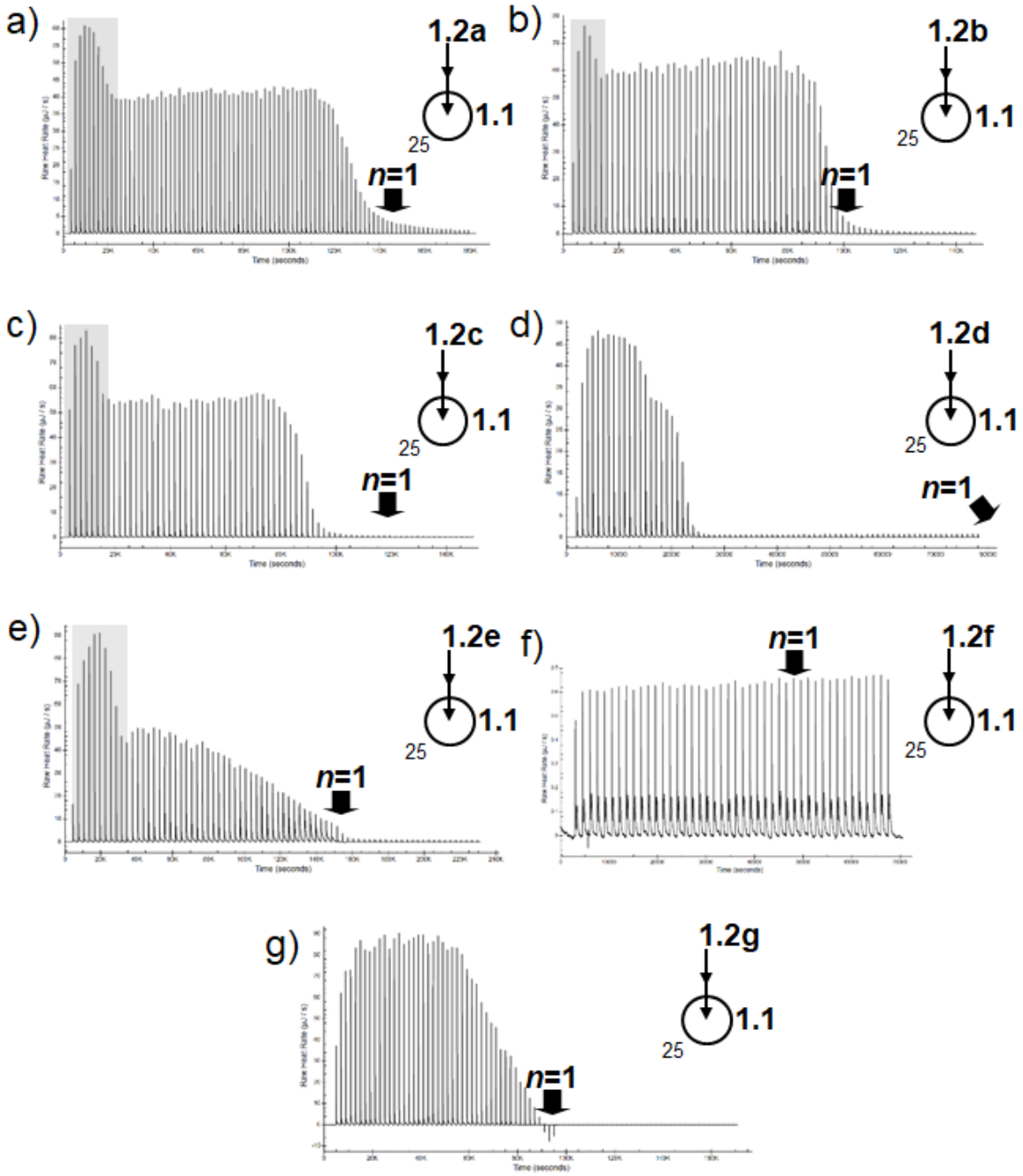

Figure 1.1.1 ITC thermograms in chlorobenzene at 25ºC a) reaction between **1.1** (sample cell, *c*= 3.82 mM) and **1.2a** (syringe, *c*= 47.43 mM) through 90 sequential additions (of 1.03 µL each), with a time delay of 2000 s; b) reaction between **1.1** (sample call, *c*= 3.63 mM) and **1.2b** (syringe, *c*= 6.63 mM) through 90 sequential additions (of 1.03 µL each) with a time delay of 2000 s; c) reaction between **1.1** (sample cell, *c*= 3.13 mM) and **1.2c** (syringe, *c*= 57.20 mM) through 90 sequential additions (of 1.03 µL each) with a time delay of 2000 s; d) reaction between **1.1** (sample cell, *c*= 3.01 mM) and **1.2d** (syringe, *c*= 21.11 mM) through 90 sequential additions (of 1.03 µL each) with a time delay of 1000 s; e) reaction between **1.1** (sample call, *c*= 3.10 mM) and **1.2e** (syringe, *c*= 55.25 mM) through 90 sequential additions (of 1.03 µL each) with a time delay of 3000 s; f) reaction between **1.1** (sample call, *c*= 3.04 mM) and **1.2f**

(syringe, *c*= 55.36 mM) through 45 sequential additions (of 2.06 µL each) with a time delay of 1500 s; g) reaction between **1.1** (sample call, *c*= 3.76 mM) and **1.2g** (syringe, *c*= 80.20 mM) through 90 sequential additions (of 2.06 µL each) with a time delay of 2000s. Heat flow is expressed in µJ/s *vs* time in s and *n* represents the molar ratio between reactants, i.e. $n = n_{injected}/n_{cell}$. The greyed part of thermograms a), b), c) and e) outlines unusual exothermicity i.e. the upsurge of heat release in the early "substoichiometric" stages of the reaction, a characteristic feature of most stable pair formation.

4.1.3.3. DOSY NMR experiments.

The 2D DOSY NMR experiments were carried out as complement to the ITC measurements in order to try to confirm the observations noticed from the ITC experiments, i.e. to confirm the assumed existence of larger molecular assemblies, especially within the supposed frustrated Lewis pair systems. The DOSY experiments considered the systems **1.1**/**1.2a-d**. The case of **1.1**/**1.2e** was not included within the investigation due to issue of possible contamination of the main, herein desired, reaction of the pair formation by side aromatic substitution reaction, while the system **1.1**/**1.2f** was not included because of no pair formation observed by ITC.

As mentioned in the introductory chapter, there is one rare example[195] that considered 2D DOSY NMR study of the FPLs. One case investigated therein - the $(mes)_3P/B(C_6F_5)_3$ (herein **1.1**/**1.2d**) pair, considering a large excess of one of the reactants, revealed clear dynamic behavior that was treated assuming the exclusive population of the system by equilibrium depicted in Scheme 1.1.1. One of the major drawbacks in this chemical system is that the putative formation of the FLP does not result in major chemical shift changes. The authors concluded that the pair formation was most probably not a selective process favoring special orientations of the Lewis base and acid and that the energy of association was only slightly endergonic with a Gibbs free energy of ca. +0.4 kcal/mol.

Herein, the considered molar ratio of the reactants was 1:1. Exclusively, the system **1.1**/**1.2a** was examined within the molar ratio of 1:0.1, as well. The results of the DOSY experiments are summarized in Table 1.1.2, while all the corresponding DOSY spectra are given in Supplementary Information (see Figure SI 1.1.20-35).

Table 1.1.2 DOSY NMR results – final spherical volumes of noticed particles - of the reactions of **1.1** with various phosphines **1.2a-d** carried out within either molar ratio of the reactants of 1:1 or 2:0.1 in deuterated chloroform at 25°C.

[195] [N^0 453] L. Rocchigiani, G. Ciancaleoni, C. Zuccaccia, A. Macchioni, *J. Am. Chem. Soc*. **2014**, *136*, 112.

System	Spectra	*V* molecule (angstrom^3)
1.1/1.2a [1:1eqv]	Ph_3P - ^1H	214
	$B(PhF_5)_3$ - ^{19}F	214
	$B(PhF_5)_3/Ph_3P$ - ^1H	628
		371
	$B(PhF_5)_3/Ph_3P$ - ^{19}F	1866
		1085
1.1/1.2a [0.1:1eqv]	Ph_3P - ^1H	214
	$B(PhF_5)_3$ - ^{19}F	365
	$B(PhF_5)_3/Ph_3P$ - ^1H	1866
		1090
	$B(PhF_5)_3/Ph_3P$ - ^{19}F	No information
1.1/1.2b [1:1eqv]	(*p*-MePh)$_3$P - ^1H	365
	$B(PhF_5)_3$ - ^{19}F	214
	$B(PhF_5)_3$/(*p*-MePh)$_3$P - ^1H	628
		1866
	$B(PhF_5)_3$/(*p*-MePh)$_3$P - ^{19}F	628
		1866
1.1/1.2c [1:1eqv]	(*m,m*-Me_2Ph)$_3$P - ^1H	365
	$B(PhF_5)_3$ - ^{19}F	214
	$B(PhF_5)_3$/(*m,m*-Me_2Ph)$_3$P - ^1H	628
		1866
		633-683
	$B(PhF_5)_3$/(*m,m*-Me_2Ph)$_3$P - ^{19}F	1866
		635-697
1.1/1.2d [1:1eqv]	(*o,p,o*-Me_3Ph)$_3$P - ^1H	628
	$B(PhF_5)_3$ - ^{19}F	214
	$B(PhF_5)_3$/(*o,p,o*-Me_3Ph)$_3$P - ^1H	1866
		365
	$B(PhF_5)_3$/(*o,p,o*-Me_3Ph)$_3$P - ^{19}F	1866
		365

The results derived from both ^1H and ^{19}F spectral domains revealed that in the cases of strong cohesive pairs (**1.1**/**1.2a-c**), within stoichiometric conditions, there are species which are roughly

equivalent in spherical volume to a sum of volumes of the free reactants, as well as much larger ones which are roughly 2-4 times bigger than the simple pair, suggesting that, apart forming and existing of the cohesive pairs, formation of the larger molecular aggregates (clusters) is rather possible. Quite interestingly, by mixing **1.1** and **1.2a** in molar ratio of around 10:1, that is about the ratio for which a typical upsurge of heat is released in the early stages of the ITC experiment (see Figure 1.1.1), DOSY ^{1}H domain reveals the raise of a large molecular aggregate about up to 5 times larger than a sum of the volumes of the free reactants, telling that even the pairs known as strongly cohesive could form rather quite large molecular assemblies. The results of the known frustrated Lewis pair (**1.1**/**1.2d**) suggest on the existing of a dynamic equilibrium between larger assemblies (roughly up to 2.5 times larger in size of spherical volume) and free reactants. Although the DOSY results did not find such large assemblies (5 times larger than the free reactants) as roughly observed within the ITC experiments in case of **1.1**/**1.2d**, they showed dynamic behavior of the system that does not strictly exclude the existence of even larger species. In addition, the DOSY results showed, in comparison to the results of Macchioni *et al*.[196] that 1:1 mixture of the reactants could allow the observation of larger assemblies than the simple pairs.

4.1.3.4. Static DFT-D calculations.

Within the theoretical study of the formation of the (frustrated) Lewis pairs from the borane (**1.1**, see Scheme 1.1.1) and various phosphines (**1.2a-g**, see Scheme 1.1.1) computations were performed at ZORA-GGAPBE-D3(BJ)/TZP level of theory in chlorobenzene solution (COSMO) phase as well as at GGAPBE-D3/Def2TZVP level of theory in gas phase and, in some cases, in chlorobenzene solution (PCM) phase. The geometry optimizations were done on both the reactants and, according to Grimme[197], two possible corresponding reaction products (Figure 1.1.2) and conformed as true minima by performing calculations of vibrational modes. Exclusively, the “sandwich” trimer (see Figure SI 1.1.38) constituted of the molecules of the borane **1.1** and one molecule of the phosphine **1.2a** was computed. In addition, the interactions of the pair formed of one/two molecule(s) of chlorobenzene and the borane **1.1** were theoretically estimated. The resulting thermodynamic parameters of the studied reaction of the pair formation (ΔH_r, ΔG_r, ΔS_r) are reported in Table 1.1.3. The related Cartesian coordinates of the optimized structure geometries are given in Supplementary Information (see section

[196] [N^0 453] L. Rocchigiani, G. Ciancaleoni, C. Zuccaccia, A. Macchioni, *J. Am. Chem. Soc*. **2014**, *136*, 112.
[197] [N^0 425] C. Bannwarth, A. Hansen, S. Grimme, *Isr. J. Chem.* **2015**, *55*, 235.

A.1.1.7.), while the optimized structure geometries of the pairs in orientation “a” as well as of the computed pairs **1.1**/**PhCl** are displayed in Figure 1.1.3 and Figure 1.1.4, respectively.

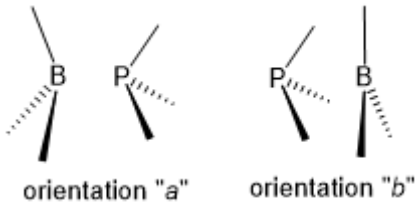

Figure 1.1.2 Schematic representation of the face-to-face orientations of Lewis partners in (F)LPs according to Grimme *et al.* [196]

Noticeably, regardless of the constitution of the system, all the computed ΔH_r values are negative (ranged from ca. -3.5 kcal/mol to -24 kcal/mol) suggesting that the formation of both classical and frustrated pairs is rather energetically favorable in both gas and chlorobenzene solution phase. A quite interesting fact is that both considered orientations (orientation “a” and orientation “b”, see Scheme 1.1.X) showed aggregatory potentials. Namely, by comparison of the ΔH_r values of the two orientations, it seems that within the supposed classical Lewis pairs (**1.1**/**1.2a-c,g**) the orientation “a” could be 2.5 times more stable than the opposite orientation (the orientation “b”). However, within known and suspected frustrated Lewis pairs (**1.1**/**1.2d-f**) both the orientations are energetically almost equal. According to these facts, it could be concluded that it would not be surprising to have larger molecular aggregates than simple stoichiometry pair. This assumption is confirmed by the calculation of the thermodynamic parameters of the theoretical trimer **1.1**/**1.2a**/**1.1**. Namely, even the theoretical trimer of known classical Lewis pair (**1.1**/**1.2a**) showed quite large ΔH_r value (ca. -35 kcal/mol) accompanied with favorable Gibbs free energy (ΔG_r value of ca. -3.5 kcal/mol).

Although all the systems showed significant formation enthalpies, calculated Gibbs free energies tell that only formation of the classical Lewis pairs (**1.1**/**1.2a-c,g**) might be spontaneous process (ΔG_r values ranged from ca. -0.3 kcal/mol to -15.5 kcal/mol). Nonetheless, within certain experimental conditions (for instance in presence of a large excess of the borane) the possibility of formation of those frustrated pairs or even larger molecular aggregates should not be excluded. Worthy to note, the calculation predicted formation of (covalent) bond between phosphorus and boron centers within the supposed classical Lewis pairs **1.1**/**1.2a-c,g** while within the others (supposedly frustrated) the predicted B-P distances are significantly longer (see Figure 1.1.3).

Table 1.1.3 Results of static DFT-D calculations. The calculations were performed at ZORA-GGAPBE-D3-BJ/TZP level of theory in chlorobenzene solution (COSMO) phase and at GGAPBE-D3/Def2TZVP level of theory in gas phase and chlorobenzene solution (PCM) phase.

System	Level of theory	ΔH_r [kcal/mol]	ΔG_r [kcal/mol]	ΔS_r [cal/Kmol]	ΔE_r [kcal/mol]
1.1/1.2a $a_{orientation}$	GGAPBE-D3/Def2TZVP -gas	-23.0	-5.0	-60.3	-24.7
	ZORA-GGAPBE-D3(BJ)/TZP - PhCl	-23.8	-8.8	-50.1	
1.1/1.2a $b_{orientation}$	GGAPBE-D3/Def2TZVP -gas	-12.4	0.8	-44.3	-14.0
	ZORA-GGAPBE-D3(BJ)/TZP - PhCl	-9.5	6.1	-52.4	
1.1/1.2a/1.1	GGAPBE-D3/Def2TZVP -gas	-35.9	-5.0	-103.6	-39.2
	GGAPBE-D3/Def2TZVP -PhCl	-35.3	-3.4	-107.1	-38.7
1.1/1.2b $a_{orientation}$	GGAPBE-D3/Def2TZVP -gas	-17.6	0.4	-60.3	-19.3
	ZORA-GGAPBE-D3(BJ)/TZP - PhCl	-17.7	-0.3	-58.5	
1.1/1.2b $b_{orientation}$	GGAPBE-D3/Def2TZVP -gas	-12.1	2.1	-47.5	-13.7
	ZORA-GGAPBE-D3(BJ)/TZP - PhCl	-6.2	11.2	-58.6	
1.1/1.2c $a_{orientation}$	GGAPBE-D3/Def2TZVP -gas	-20.2	-0.4	-66.4	-22.0
	ZORA-GGAPBE-D3(BJ)/TZP - PhCl	-18.2	-3.7	-48.7	
1.1/1.2c $b_{orientation}$	GGAPBE-D3/Def2TZVP -gas	-11.6	4.0	-52.4	-13.1
	ZORA-GGAPBE-D3(BJ)/TZP - PhCl	-3.4	4.2	-25.7	
1.1/1.2d $a_{orientation}$	GGAPBE-D3/Def2TZVP -gas	-10.0	2.3	-41.1	-11.4
	ZORA-GGAPBE-D3(BJ)/TZP - PhCl	-7.3	11.5	-63.1	
1.1/1.2d $b_{orientation}$	GGAPBE-D3/Def2TZVP -gas	-10.1	2.3	-41.5	-11.6
	ZORA-GGAPBE-D3(BJ)/TZP - PhCl	-7.7	13.9	-72.4	
1.1/1.2e $a_{orientation}$	GGAPBE-D3/Def2TZVP -gas	-13.7	-0.2	-45.0	-15.3
	ZORA-GGAPBE-D3(BJ)/TZP - PhCl	-11.3	6.0	-53.4	
1.1/1.2e $b_{orientation}$	GGAPBE-D3/Def2TZVP -gas	-12.2	0.5	-42.6	-13.7
	ZORA-GGAPBE-D3(BJ)/TZP - PhCl	-10.4	7.4	-59.7	
1.1/1.2f $a_{orientation}$	GGAPBE-D3/Def2TZVP -gas	-9.9	2.0	-40.0	-11.2
	ZORA-GGAPBE-D3(BJ)/TZP - PhCl	-8.8	8.1	-56.6	
1.1/1.2f $b_{orientation}$	GGAPBE-D3/Def2TZVP -gas	-10.9	1.3	-40.8	-12.2
	ZORA-GGAPBE-D3(BJ)/TZP - PhCl	-8.2	7.0	-50.9	
1.1/1.2g $a_{orientation}$	GGAPBE-D3/Def2TZVP -gas				
	ZORA-GGAPBE-D3(BJ)/TZP - PhCl	-28.1	-15.5		
1.1/1.2g $b_{orientation}$	GGAPBE-D3/Def2TZVP -gas				
	ZORA-GGAPBE-D3(BJ)/TZP - PhCl				

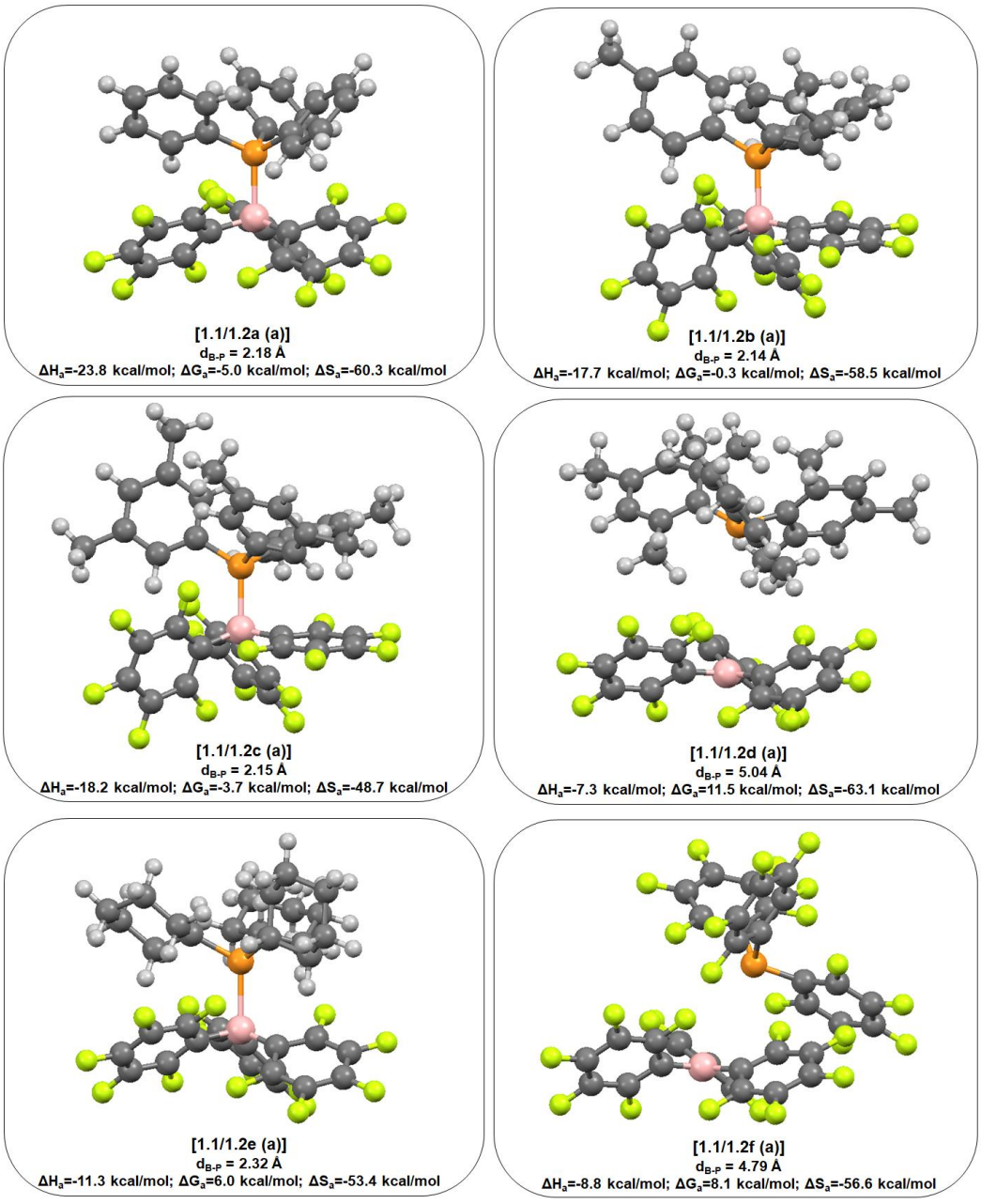

Figure 1.1.3 Graphic representations of optimized geometries of the investigated systems in orientation “a” at ZORA-GGAPBE-D3-BJ/TZP level of theory in chlorobenzene solution (COSMO) phase. P: orange; B: pink; F: yellowish; C: grey; H: white.

By comparison of the experimentally obtained and theoretically computed reaction enthalpies, significant differences in the corresponding ΔH_r values of all the systems could be noticed. To figure out a possible reason for such discrepancy between experimental and theoretical ΔH_r values, a round of the calculations of possible non-covalent pair(s) constituted of molecule(s) of

the solvent[198] (chlorobenzene that could be considered as weak Lewis base) and molecule of the borane was performed. The computed results are summarized in Figure 1.1.4. The results revealed that moderate enthalpy of interaction (Δ*H* value is ca. 6 kcal/mol) might be reached within the system **1.1**/**PhCl** (**1.4**) as well as that even two molecules of chlorobenzene (**1.5**) might be appropriately adapted for interaction with boron atom through chlorine (Δ*H* value is ca. 12 kcal/mol). Although it is reasonable to assume that more than two molecules of chlorobenzene could surround molecule of the borane, herein the calculated attractive interactions (see Figure 1.1.4.) might help in a final estimation of thermodynamic parameters of the reaction/interaction within the investigated systems (**1.1**/**1.2a-g**). Therefore, such estimation assumed "decoordination" of one or both chlorobenzene molecules from the borane before subsequent borane-phosphine reaction/interaction giving new values of the thermodynamic parameters herein labeled Δ*H**/Δ*G** and Δ*H***/Δ*G***, respectively. The newly estimated values of the thermodynamic parameters accompanied with corresponding experimental values are reported in Table 1.1.4.

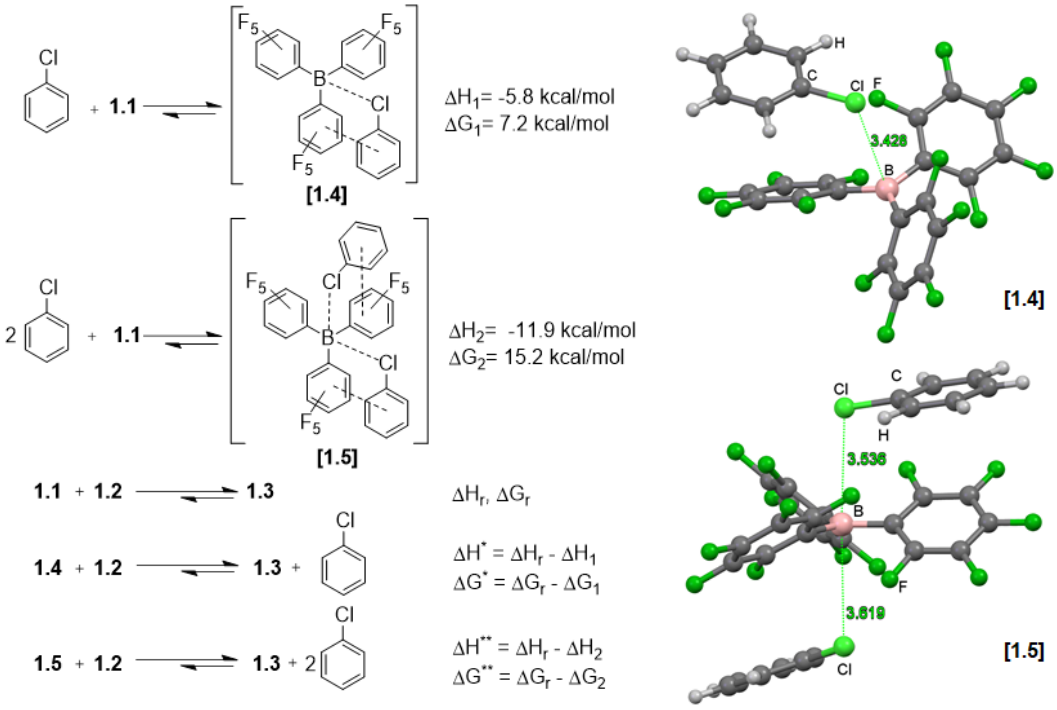

Figure 1.1.4 *left side* – Schematic representation of the computed theoretical pair(s) **1.1**/(**2**)**PhCl** (**1.4-5**) accompanied with the obtained results (Δ*H* and Δ*G*). *right side* – Graphic representations of optimized geometries of the investigated systems (**1.4-5**) at ZORA-GGAPBE-D3-BJ/TZP level of theory in chlorobenzene solution (COSMO) phase. Cl: greenish; B: pink; F: green; C: grey; H: white.

[198] [N^0 457] H. J. Kwon, H. W. Kim, Y. M. Rhee, *Chem. Eur. J.* **2011**, *17*, 6501.

Table 1.1.4 Results of static DFT-D calculations of the orientation “a” corrected by the estimated values for the decoordination of chlorobenzene (Figure 1.1.4). The calculations were performed at ZORA-GGAPBE-D3-BJ/TZP level of theory in chlorobenzene solution (COSMO) phase.

System	ΔH_r [kcal/mol]	ΔG_r [kcal/mol]	ΔH_r* [kcal/mol]	ΔG_r* [kcal/mol]	ΔH_r** [kcal/mol]	ΔG_r** [kcal/mol]	raw ITC ΔH_r [kcal/mol]
1.1/1.2a (a)	-23.8	-8.8	-18.0	-16.0	-11.9	-24.0	-12.4 ± 1.3
1.1/1.2b (a)	-17.7	-0.3	-11.9	-7.3	-5.8	-15.5	-12.9 ± 1.4
1.1/1.2c (a)	-18.2	-3.7	-12.4	-10.9	-6.3	-19.2	-13.3 ± 1.4
1.1/1.2d (a)	-7.3	11.5	-1.4	4.3	4.6	-3.7	-22.8 ± 3.7
1.1/1.2e (a)	-11.3	6.0	-5.5	-1.2	0.6	-9.2	-24.1 ± 2.6
1.1/1.2f (a)	-8.8	8.1	-2.0	0.9	3.1	-7.1	-0.3 ± 0.1
1.1/1.2g (a)	-28.1	-15.5	-22.3	-22.7	-16.2	-30.7	-14.0 ± 2.1

According to the roughly estimated values ($\Delta H^*/\Delta G^*$ and $\Delta H^{**}/\Delta G^{**}$) and the experimental ITC enthalpy values of the supposed classical Lewis pairs (**1.1**/**1.2a-c**,**g**) it seems that within the bulkier pairs (**1.1**/**1.2b-c**) the decoordination of one molecule of chlorobenzene is more likely to happen while within the pairs **1.1**/**1.2a,g** the decoordination of two molecules of chlorobenzene is more appropriate. Regarding the corresponding values of the system **1.1/1.2f,** by decoordination of one molecule of chlorobenzene the experimental and theoretical values are found to be quite close to each other. Noticeably, the related values of the two other systems (**1.1/1.2d-e**) are not directly comparable due to the fact that the calculation did not take into consideration: a) the observation derived from the ITC experiments which revealed probable molecular clustering (case **1.1/1.2d**); b) the probable nucleophilic aromatic substitution reaction that might bias the obtained ITC results. Nevertheless, the corrected results of the **1.1/1.2d-e** might suggest dynamic rearrangement of the solvent molecules in such a way that one solvent molecule is being shared between two molecules of the borane what would lead to decreasing of the loss of enthalpy caused by full decoordination of the solvent molecule.

In addition, these investigations showed that the interaction abilities of the solvent (interacting competitively with the substrate of interest), could significantly bias the theoretically predicted thermodynamic parameters of the reaction/interactions. This suggests that, in some cases, the solvent interactions should be accounted for within theoretical calculations explicitly.

4.1.4. Subchapter conclusion.

Within this study, the formation and behavior of the Lewis phosphine-borane pairs (**1.1**/**1.2a-g**, Scheme 1.1.1) in chlorobenzene and deuterated chloroform solution were investigated by experimental means using isothermal titration calorimetry (ITC) and 1D/2D NMR spectroscopy as well as theoretically using static DFT-D calculations in both gas and chlorobenzene solution phase. In addition, the thermochemical characteristics of theoretical trimer "sandwich" complex **1.1**/**1.2a**/**1.1** were calculated.

The reaction tests, i.e. monitoring the reaction systems by 1D NMR spectroscopy, revealed that the systems **1.1**/**1.2a-c** form cohesive pairs, the system **1.1**/**1.2d** exist within an equilibrium, the system **1.1**/**1.2f** do not show any tendency to form any stable pair, while the system **1.1**/**1.2e** only with less than 0.2 equivalents of the phosphine form single reaction product. In addition, the results of the reaction tests suggested that all the investigated pairs might be exploitable in stoichiometric conditions within ITC measurements.

Due to the shape of the obtained ITC thermograms, in most of the investigated cases only reaction enthalpies could be extracted. The resulting raw ΔH_r, ranged from ca. -0.3 kcal/mol – -24 kcal/mol, suggested that a variety of chemical features is incorporated within the studied systems. Worthy to note, the well-known FLP **1.1**/**1.2d** and supposed one **1.1**/**1.2e** showed much higher reaction enthalpies in comparison to known and supposed classical LPs (**1.1**/**1.2a-c**), which suggests that non-covalent interactions have a huge influence within these systems. The ITC experiments of the **1.1**/**1.2d** shed some light on actual situation into the solution ruling out the 1:1 stoichiometry and suggesting a 5:1 molar ratio in favor to the borane as more likely scenario. In addition, the system **1.1**/**1.2f** showed no tendency to forming any stable pair.

The DOSY experiments have discovered the existence of molecular assemblies/clusters larger than simple pair within the solution of the pairs. This observation is in accordance with an assumption derived from ITC thermograms (and liberated heat) that, at least at the beginning of the reaction between borane and phosphine (when there is an excess of borane), the formation of clusters occurs. Additionally, in the case of mes_3P (**1.2d**) an addition of ca. 0.2 equivalent of the phosphine leads to chemical equilibrium. Moreover, DFT-D calculations suggest on cluster formation by significantly higher ΔH_r value for trimer than for dimer.

The performed calculations, in comparison to the experimental results, predicted higher reaction enthalpy values for assumed classical LPs **1.1**/**1.2a-c,g** (ΔH_r values ranged from ca. -18 kcal/mol to -28 kcal/mol), while lower enthalpies are obtained for assumed FLPs **1.1**/**1.2d-e** (ΔH_r values ranged from ca. -7.5 kcal/mol to -11.5 kcal/mol). Discordance was obtained for the system **1.1**/**1.2f**, as its predicted ΔH_r value is significantly higher. By the predicted Gibbs free energy values only the systems **1.1**/**1.2a-c,g** might interact spontaneously. The estimation of the thermodynamic parameters of interaction of chlorobenzene (weak Lewis base and solvent of choice) with the borane (**1.1**) revealed significant interaction enthalpy (ca. -6 kcal/mol per molecule of chlorobenzene) that brings the theoretical values much closer to the experimental ones, suggesting the importance of accounting for explicit interactions of the solvent with substrate within the calculations.

In addition, new Lewis pair **1.3c** was synthesized and fully characterized (by ^{1}H and ^{13}C NMR, elemental analysis, MS and X-Ray).

Outlook. Performing the DOSY experiments within deuterated chlorobenzene solution is highly desirable. The estimation of the thermodynamic parameters of all possible interactions of chlorobenzenes with the borane would be important. Calculating the electrostatic potential of chlorobenzene and all the reactants would be quite useful. Isolation and characterization of the reaction products **1.3b** are desirable.

4.1.5. Закључак потпоглавља.

У оквиру ове студије, формирање и понашање Lewis-ових парова (енг. Lewsi pair - LP) фосфин-боран (**1.1**/**1.2a-g**, схема 1.1.1) у хлоробензенском и деутерирсном хлороформском раствору истраживано је експериментално, коришћењем изотермалне титрационе калориметрије, (ITC) и 1D/2D NMR спектроскопије, и теоријски, коришћењем статичких DFT-D прорачуна у гасној фази и у раствору хлоробензена. Поред тога, израчунате су термохемијске карактеристике теоријског тримера - "сендвич" комплекса **1.1**/**1.2a**/**1.1.**

Реакциони тестови, односно праћење реакционих система помоћу 1D NMR спектроскопије, открили су да системи **1.1**/**1.2a-c** формирају кохерентне парове, систем **1.1**/**1.2d** постоји у равнотежи, систем **1.1**/**1.2f** не показује било какву тенденцију ка формирању икаквог стабилног пара док систем **1.1**/**1.2e** формира један реакциони производ када је употребљено мање од 0,2 еквивалента фосфина. Поред тога, резултати реакционих тестова указују на то да се сви системи могу испитивати у стехиометријским условима у оквиру ITC мерења.

Због облика добијених ITC термограма, у већини испитаних случајева могу се добити само вредности за реакционе енталпије. Добијене сирове (raw) ΔH_r вредности, које су у опсегу од око -0.3 kcal/mol до -24 kcal/mol, указују на различита хемијска својства проучаваних система. Треба напоменути да су познати FLP **1.1**/**1.2d** и претпостављени FLP **1.1**/**1.2e** показали много веће реакционе енталпије у односу на познате и претпостављене класичне LP-ове (**1.1**/**1.2a-c**), што указује да нековалентне интеракције имају огроман утицај у овим системима. ITC експерименти за систем **1.1**/**1.2d** унеколико су расветлили стање у раствору овог FLP-а искључујући 1:1 стехиометрију и указујући на моларни однос 5:1 у корист борана, као више вероватан. Поред тога, систем **1**/**1.2f** није показао тенденцију ка формирању било каквог стабилног пара.

На основу DOSY експеримената показано је да у растворима испитиваних парова постоје молекулски агрегати/кластери који су већи од простих парова. Ово опажање је у складу са претпоставком изведеном на основу ITC термограма (и ослобођене топлоте) да бар на почетку реакције између борана и фосфина (када постоји вишак борана) долази до формирања кластера. Поред тога, у случају mes_3P (**1.2d**) додатак од око 0,2 еквивалента фосфина доводи до успостављања хемијске равнотеже. Штавише, DFT-D прорачуни

указују на формирање кластера, на основу значајно веће ΔH_r вредности за тример него за димер.

Резултати прорачуна су, у поређењу са резултатима експеримента, предвидели веће вредности реакционих енталпија за претпостављене класичне LP-ове **1.1**/**1.2a-c,g** (ΔH_r вредности кретале су се од око -18 kcal/mol to -28 kcal/mol), а мање реакционе енталпије за претпостављене FLP-ове **1.1**/**1.2d-e** (ΔH_r вредности кретале су се од око -7,5 kcal/mol до -11,5 kcal/mol). Добијени резултати за систем **1.1**/**1.2f** такође нису у сагласности, јер је теоријски предвиђена ΔH_r вредност значајно већа од експериментално одређене ΔH_r вредности. На основу предвиђених вредности Gibbs-ових слободних енергија само би системи **1.1**/**1.2a-c,g** могли да интерагују спонтано. Проценом термодинамичких параметара интеракције хлоробензена (који је слаба база Lewis-ова и растварач избора) са бораном (**1.1**) добијена је значајна енталпија интеракције (око -6 kcal/mol по молекулу хлоробензена) која теоријске вредности значајно приближава експерименталним, што указује на значај урачунавања експлицитних интеракција растварача са супстратом у оквиру прорачуна.

Поред тога, нови Lewis-ов пар **1.3c** је синтетисан и потпуно окарактерисан (^{1}H и ^{13}C NMR спектроскопијом, елементалном анализом, масеном спектроскопијом и рендгенском структурном анализом).

Перспектива. Извођење DOSY експеримената у деутерисаном хлоробензенском раствору је веома пожељно. Процена термодинамичких параметара свих могућих интеракција хлоробензена са бораном би била од значаја. Израчунавање електростатичког потенцијала хлоробензена и свих реактаната било би корисно. Пожељна је изолација и карактеризација реакционог производа **1.3b**.

4.1.6. Conclusion du sous-chapitre

Dans cette étude, la formation et le comportement des paires Lewis phosphine-borane (**1.1/1.2a-g**, schéma 1.1.1) dans le chlorobenzène et la solution chloroforme deutérée ont été étudiés par des méthodes expérimentales utilisant la calorimétrie isotherme par titration (ITC) et la spectroscopie RMN 1D/2D, ainsi que théoriquement utilisant des calculs statiques DFT-D à la fois dans la phase de solution de gaz et de chlorobenzène. De plus, les caractéristiques thermochimiques du complexe "sandwich" trimère **1.1/1.2a/1.1** ont été calculées.

Les tests de réaction, i.e. la suite des systèmes réactionnels par spectroscopie RMN 1D, ont révélé que les systèmes **1.1/1.2ac** forment des couples cohésifs, le système **1.1/1.2d** existe dans un équilibre, le système **1.1/1.2f** ne montre aucune tendance à former toute paire stable, tandis que le système **1.1/1.2e** au-delà de 0.2 équivalents de la phosphine forme un seul produit de réaction. En outre, les résultats des essais de réaction ont suggéré que tous les essais pourraient être exploitables dans des conditions stoechiométriques dans les mesures de l'ITC.

En raison de la forme des thermogrammes ITC obtenus, dans la plupart des cas étudiés, seules les enthalpies réactionnelles ont pu être extraites. Le ΔH_r brut résultant, va d'environ de -0,3 kcal/mol à -24 kcal/mol suggérant que diverses caractéristiques chimiques sont incorporées dans les systèmes étudiés. Il est intéressant de noter que les célèbres FLP **1.1/1.2d** et **1.1/1.2e** supposés ont montré des enthalpies de réaction beaucoup plus élevées que les LP classiques connues et supposées (**1.1**/**1.2a-c**), ce qui suggère que les interactions non-covalentes ont une influence au sein de ces systèmes. Les expériences ITC du **1.1** / **1.2d** ont révélé la situation réelle dans la solution excluant la stoechiométrie 1:1 et suggérant un rapport molaire de 5:1 en faveur du borane comme scénario plus probable. De plus, le système **1.1**/**1.2f** n'a montré aucune tendance à former une paire stable.

Les expériences DOSY ont découvert l'existence d'assemblages / clusters moléculaires plus gros que la simple paire dans la solution des paires. Cette observation est en accord avec une hypothèse dérivée des thermogrammes ITC (et de la chaleur libérée) qui se produit, au moins, au début de la réaction entre le borane et la phosphine (quand il y a un excès de borane). De plus, dans le cas de l'addition de mes_3P (**1.2d**) de ca. 0,2 équivalent de la phosphine conduit à l'équilibre chimique. De plus, les calculs DFT-D suggèrent la formation de grappes par une valeur de ΔH_r significativement plus élevée pour le trimère que pour le dimère.

Les calculs effectués, comparés aux résultats expérimentaux, prédisaient des valeurs d'enthalpie de réaction plus élevées pour les LP classiques supposées **1.1**/**1.2a-c**,**g** (les valeurs de ΔH_r allaient de -18 kcal/mol à -28 kcal/mol), tandis que les enthalpies inférieures pour les FLP supposées **1.1**/**1.2d,e** (les valeurs de ΔH_r allaient de -7,5 kcal/mol à -11,5 kcal/mol). La discordance a été obtenue pour le système **1.1**/**1.2f**, car sa valeur prédite de ΔH_r est significativement plus élevée. D'après les valeurs d'énergie libre de Gibbs prédites, seuls les systèmes **1.1/1.2a-c**,**g** pourraient interagir spontanément. L'estimation des paramètres thermodynamiques de l'interaction du chlorobenzène (base de Lewis faible et solvant de choix) avec le borane (1.1) révèle une enthalpie d'interaction significative (environ -6 kcal/mol par molécule de chlorobenzène) qui rapproche beaucoup plus les valeurs théoriques expérimentaux, suggérant l'importance de tenir compte des interactions explicites du solvant avec le substrat dans les calculs.

De plus, la nouvelle paire de Lewis **1.3c** a été synthétisée et entièrement caractérisée (par RMN ^{1}H et ^{13}C, analyze élémentaire, MS et rayons X).

Perspective. L'exécution des expériences DOSY dans une solution de chlorobenzène deutéré est hautement souhaitable. L'estimation des paramètres thermodynamiques de toutes les interactions possibles des chlorobenzènes avec le borane serait importante. Le calcul du potentiel électrostatique du chlorobenzène et de tous les réactifs serait très utile. L'isolement et la caractérisation des produits de réaction **1.3b** sont souhaitables.

4.2. Subchapter 2. – Analysis of the Cambridge Structural Database.

4.2.1. Introduction.

As an addition to the ITC and static DFT-D investigations, CSD analysis was used to study the interactions within phosphine-borane Lewis pairs. Within this subchapter the CSD analysis' results that have been recently published[199] are reported.

Like mentioned in the Methodology chapter, the CSD (November 2015 released, version 5.37)[200] search was performed. The crystal structures involving phosphine and borane molecules were screened for intermolecular or intramolecular contacts. The CSD search program ConQuest 1.18[201] was used to retrieve structures satisfying the following criteria: (a) the crystallographic R factor < 10%, (b) the error-free coordinates according to the criteria used in the CSD, (c) no polymer and ionic structures, (d) structures with the disorder and (e) structure solved from powder were not included.

The phosphine-borane interactions were analyzed by using the geometrical parameters defined in Figure 1.2.1. The structures where the distance between phosphorus and boron atoms ($\mathbf{d_{B\text{-}P}}$) was less than 2.5 Å were extracted from the CSD. The additional geometrical parameters were: the dihedral angle – an angle between the planes formed by atoms directly bound to phosphorus and boron atoms (**φ**), the normal distance between phosphorus atom and the plane formed by atoms directly bound to boron atom (**R**) and the offset distance between the projection of phosphorus atom on the plane formed by atoms directly bound to boron atom and the centroid of atoms directly bound to boron atom (**r**).

[199] [N^0 458] M. R. Milovanović, J. M. Andrić, V. B. Medaković, J.-P. Djukic, S. D. Zarić, *Acta Cryst.* **2018**, *B74*, 255.
[200] [N^0 300] C. R. Groom, I. J. Bruno, M. P. Lightfoot, S. C. Ward, *Acta Cryst*. **2016**, *B72*, 171.
[201] [N^0 324] I. J. Bruno, J. C. Cole, P. R. Edgington, M. Kessler, C. F. Macrae, P. McCabe, J. Pearson, R. Taylor, *Acta Cryst*. **2002**, *B58*, 389.

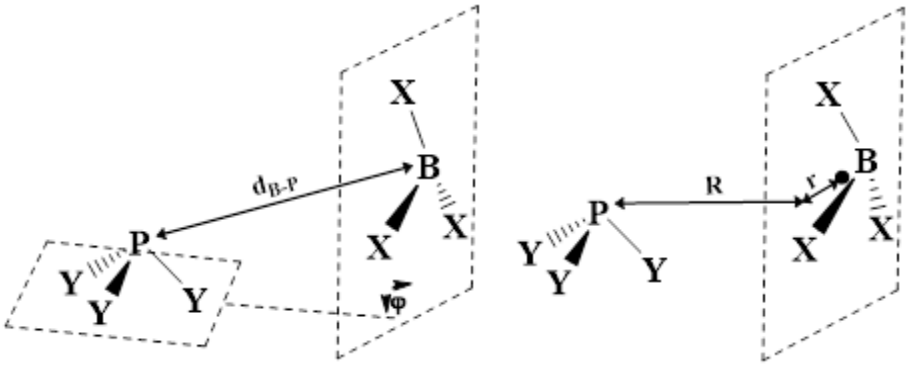

Figure 1.2.1 The geometrical parameters describing phosphine-borane interactions: a) d_{B-P} distance and angle φ, b) normal distance R and offset distance r. The X and Y are substituents on boron and phosphorus atoms, respectively. The dihedral angle **φ** is an angle between the planes formed by atoms directly bound to phosphorus and boron atoms.

4.2.2. Results and discussion.

By searching the CSD, using the criteria described in the Methodology section, 571 contacts between phosphine and borane molecules were found. The initial set of the contacts was divided into three sets; two sets were made depending on substituents on boron atom, while in the third set were frustrated Lewis pairs (FLPs). By analyzing the obtained data, it was noticed that most of the structures contain BH_3 as borane molecule, hence it was the first set, while the second set contained other found structures (except FLPs ones). The data on frustrated phosphine-borane Lewis pairs show that they depend more on substituents on the boron atom than on the phosphorus' substituents.[202] For the first set, BH_3 - $P(Y_1Y_2Y_3)$, we obtained 447 contacts from the CSD, for the second set, $B(X_1X_2X_3)$ - $P(Y_1Y_2Y_3)$, 99 contacts, while for the third set, FLPs, 25 contacts.

4.2.2.1. The BH_3 - $P(Y_1Y_2Y_3)$ set.

The distribution of the dihedral angle φ (Figure 1.2.1) values of the analyzed contacts in the BH_3 - $P(Y_1Y_2Y_3)$ set is shown in Figure 1.2.2. The results of the statistical analysis show that the majority of contacts have the dihedral angle from 0˚ to 10˚ what indicates the preference for parallel orientation of the planes defined in Figure 1.2.1.

[202] [N^0 382] D. W. Stephan, G. Erker, *Angew. Chem. Int. Ed.* **2015**, *54*, 6400.

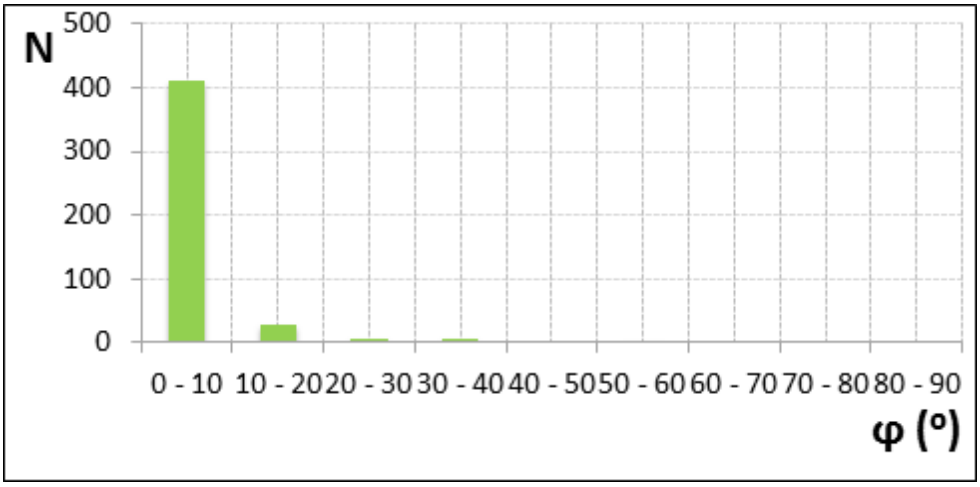

Figure 1.2.2 The distribution of the dihedral angle ***φ*** (Figure 1.2.1) of the interacting molecules in the BH_3 - $P(Y_1Y_2Y_3)$ set.

The distribution of the distance between boron and phosphorus atoms $\mathbf{d_{B\text{-}P}}$ (Figure 1.2.1) values of the contacts in the BH_3 - $P(Y_1Y_2Y_3)$ set is shown in Figure 1.2.3. The $\mathbf{d_{B\text{-}P}}$ peaks are in the range of 1.8–2.0 Å, which corresponds to the length of strong classical covalent bond.[203] More precisely, in most of the structures, the $\mathbf{d_{B\text{-}P}}$ value is around 1.9 Å.

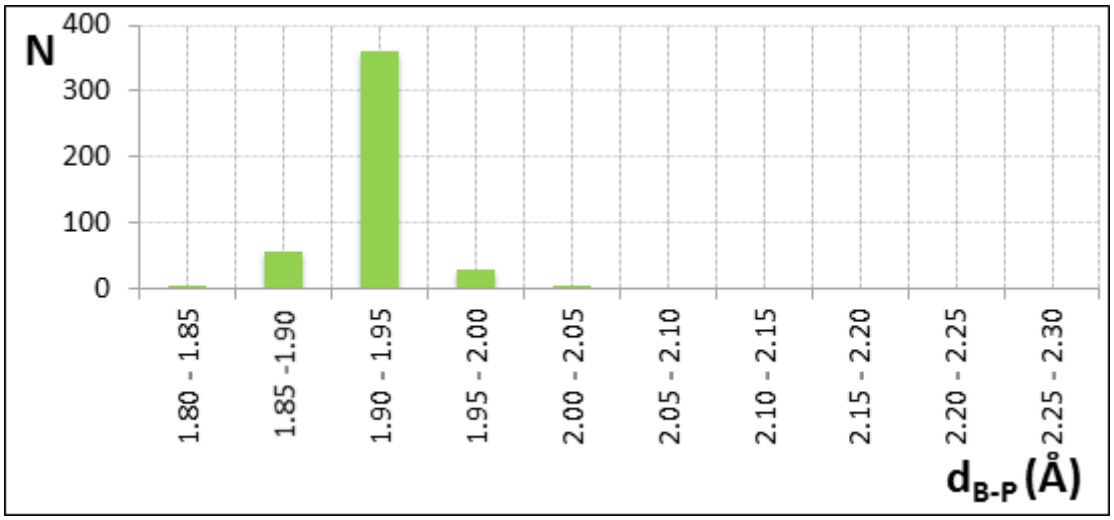

[203] [N⁰ 459] H. Jacobsen, H. S. Berke, Döring, G. Kehr, G. Erker, R. Fröhlich, O. Meyer, *Organometallics* **1999**, *18*, 1724.
[N⁰ 460] A. G. Massey, A. J. Park, *J. Organomet. Chem.* **1964**, *.2*, 245.
[N⁰ 461] A. G. Massey, A. J. Park, F. G. A. Stone, *Proc. Chem. Soc*. **1963**, 212.
[N⁰ 462] W. Van Doorne, A. W. Cordes, G. W. Hunt, *Inorg. Chem.* **1973**, *12*, 1686.
[N⁰ 463] J. C. Huffman, W. A. Skupinski, K. G. Caulton, *Cryst. Struct. Commun.* **1982**, *11*, 1435.
[N⁰ 464] M. Lutz, A. L. Spek, A. Azghay, J. C. Slootweg, *CSD Commun*. **2009**.
[N⁰ 371] M. Ullrich, A. J. Lough, D. W. Stephan, *Organometallics* **2010**, *29*, 3647.
[N⁰ 465] S. R. Ghanta, M. H. Raoa, K. Muralidharan. *Dalton Trans.* **2013**, *42*, 8420.

Figure 1.2.3 The distribution of the distance between boron and phosphorus atoms $\mathbf{d_{B\text{-}P}}$ (Figure 1.2.1) of the interacting molecules in the BH_3 - $P(Y_1Y_2Y_3)$ set.

The distribution of the offset distance **r** (Figure 1.2.1) values of the contacts in the BH_3 - $P(Y_1Y_2Y_3)$ set is shown in Figure 1.2.4. The results show that most of the contacts have **r** values in the range of 0.0-0.2 Å, which means that phosphorus atom is placed right above the boron atom.

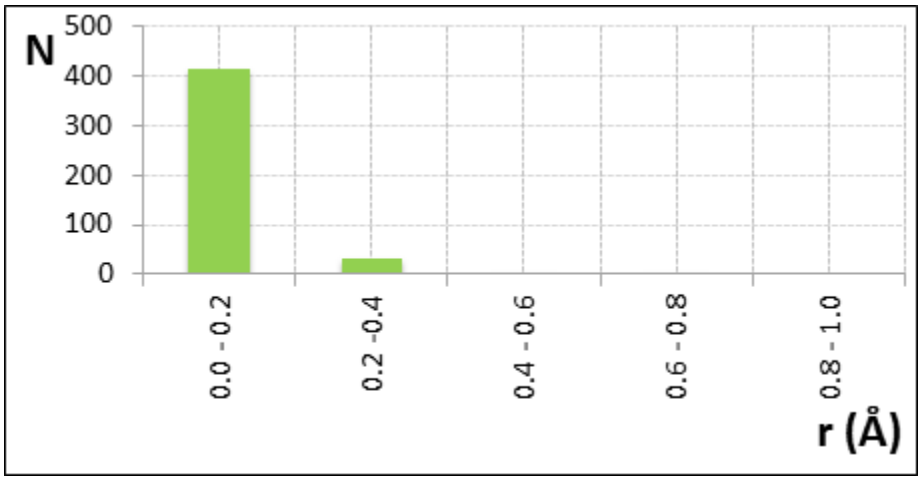

Figure 1.2.4 The distribution of the offset distance **r** (Figure 1.2.1) of the interacting molecules in the BH_3 - $P(Y_1Y_2Y_3)$ set.

The distribution of the normal distance **R** (Figure 1.2.1) values of the contacts in the BH_3 - $P(Y_1Y_2Y_3)$ set is shown in Figure 1.2.5. The results show that in most of the contacts normal distances are in the range of 2.20-2.30 Å (with the peak in the range 2.20-2.25 Å). Since r value is close to 0.0 Å, the comparison of the distributions of the $\mathbf{d_{B\text{-}P}}$ (Figure 1.2.3) and **R** (Figure 1.2.5) values shows that in the borane molecules boron atom is not in the plane with the substituents; the geometry around boron atoms is pyramidal.

Considering known problems in applying neutron diffraction with boron containing compounds, it can be expected that positions of hydrogen atoms were not determined with high accuracy. Hence, the parameter that depend on positions of hydrogen atoms, dihedral angle **φ** (Figure 1.2.1), is not very reliable in this first set, BH_3 - $P(Y_1Y_2Y_3)$.

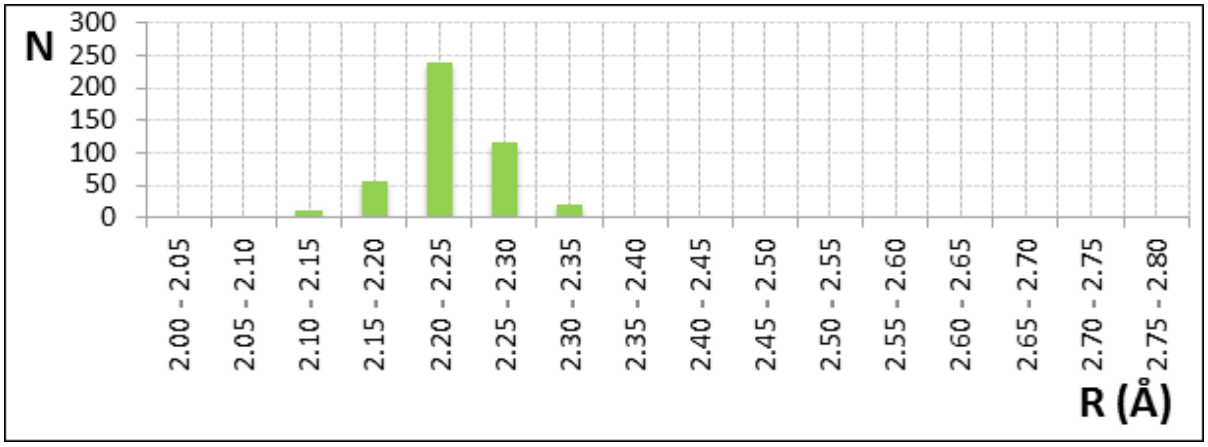

Figure 1.2.5 The distribution of the normal distances **R** (Figure 1.2.1) of the interacting molecules in the BH_3 - $P(Y_1Y_2Y_3)$ set.

4.2.2.2. The $B(X_1X_2X_3)$ - $P(Y_1Y_2Y_3)$ set.

Analyzing data in the $B(X_1X_2X_3)$ - $P(Y_1Y_2Y_3)$ set two factors that can have significant influence on geometric parameters in this set were noticed. The first one is the presence of aromatic rings on boron atom, while the second one is a bridge between phosphorus and boron atoms. (The **bridge** represents an atomic chain between phosphorus and boron centers that connect these two centers besides their direct covalent bond connection.) Hence, within this set the results are presented in two different ways: **aromatic** (the structures which *contain* aromatic substituent(s) on the boron atom vs. **other** (the structures which *do not contain* any aromatic substituent on the boron atom) (Figures 1.2.6-9) and **bridged** (the structures for which *there is* an atomic chain between phosphorus and boron centers besides their direct covalent bond connection) vs. **non-bridged** (the structures for which *there is no* such atomic chain between phosphorus and boron centers) (Figures 1.2.10-13).

Data in the Figures 1.6-9 indicate small differences in the systems with and without aromatic rings. The dihedral angle **φ** is quite similar it the two systems, in most of the structures the angle is close to zero, however, in significant number of structures the angle can have values up to 40˚ (Figure 1.2.6). The distribution of the distance $\mathbf{d_{B\text{-}P}}$ (Figure 1.2.7) shows again very similar behavior of the two systems with tendency for slightly lower values for non-aromatic systems with maximum of the distribution at 1.95-2.00 Å, while systems with aromatic rings have maximum at 2.00-2.05 Å. Values of the offset **r** (Figure 1.2.8) are similar with small tendency for aromatic systems for somewhat larger **r** values. The largest difference was observed for the

normal distance **R** (Figure 1.2.9), with values significantly lower for aromatic system, indicating compactness of these structures.

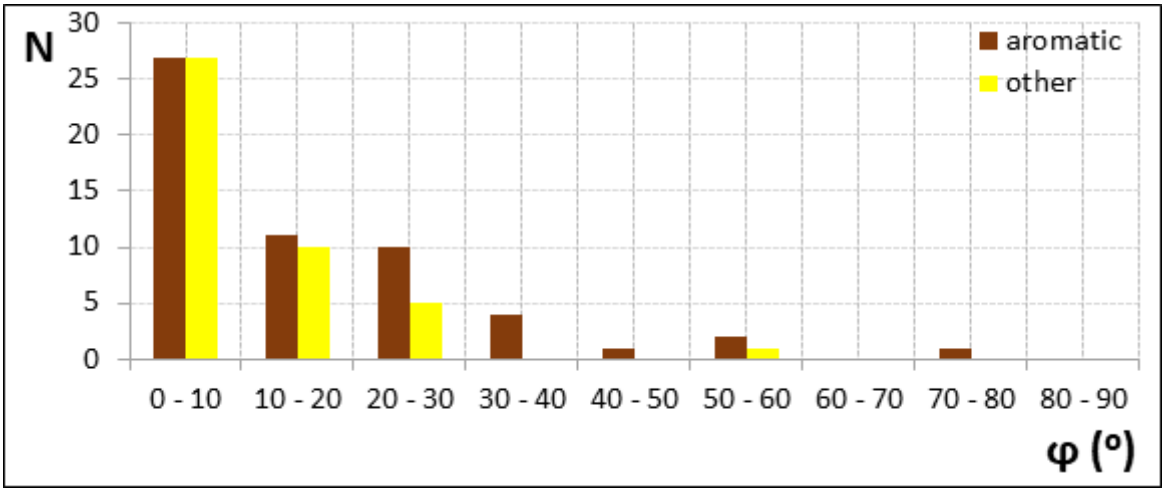

Figure 1.2.6 The distribution of the dihedral angle **φ** (Figure 1.2.1) of the interacting molecules in the $B(X_1X_2X_3)$ - $P(Y_1Y_2Y_3)$ set.

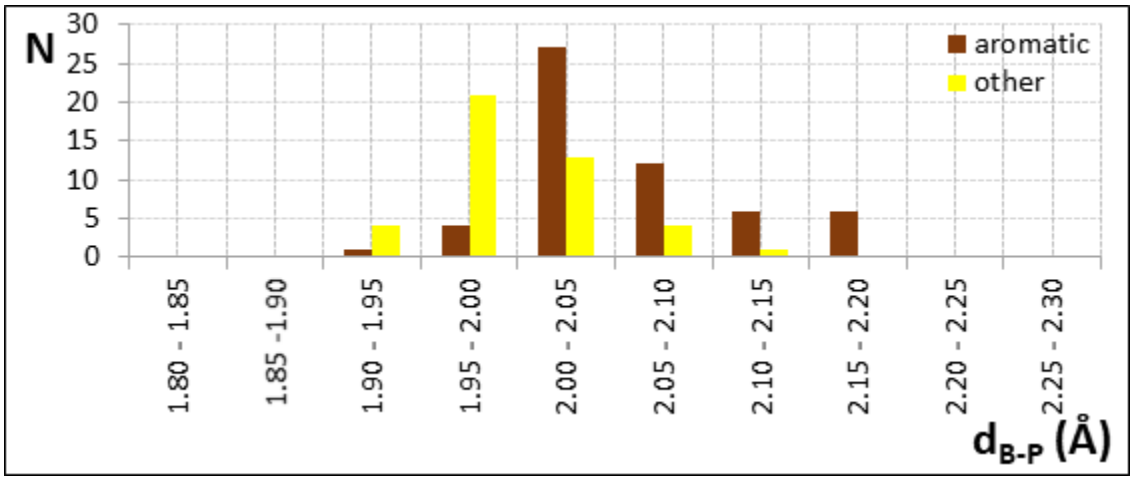

Figure 1.2.7 The distribution of the distance between phosphorus and boron atoms $\mathbf{d_{B\text{-}P}}$ (Figure 1.2.1) of the interacting molecules in the $B(X_1X_2X_3)$ - $P(Y_1Y_2Y_3)$ set.

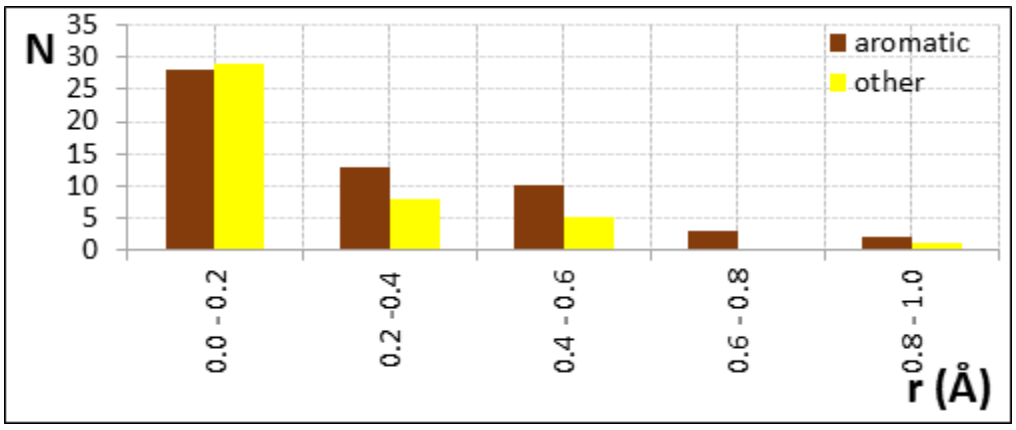

Figure 1.2.8 The distribution of the offset distance **r** (Figure 1.2.1) of the interacting molecules in the $B(X_1X_2X_3)$ - $P(Y_1Y_2Y_3)$ set.

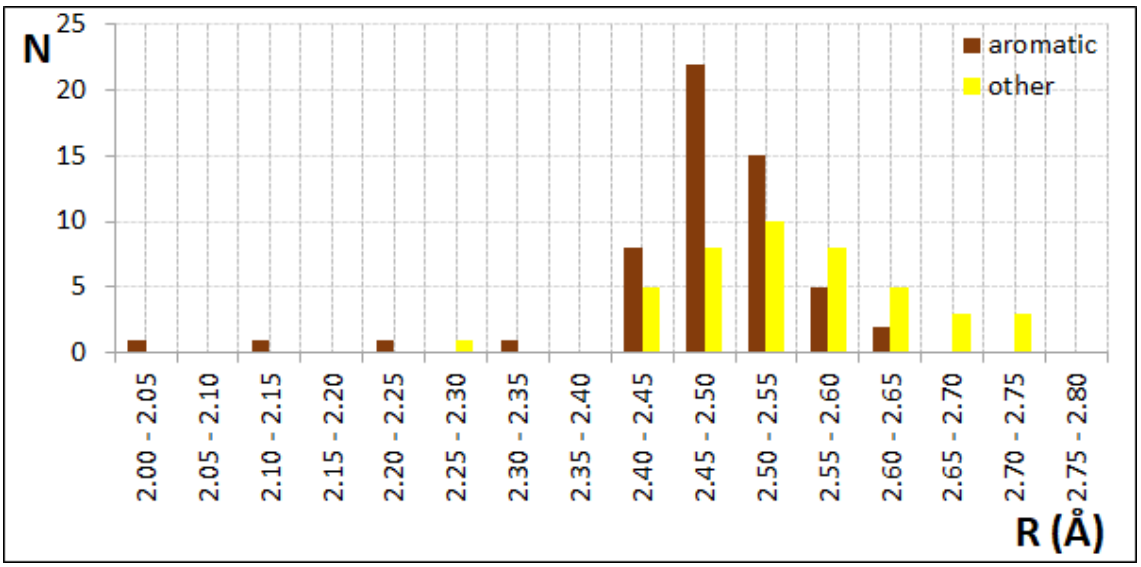

Figure 1.2.9 The distribution of the normal distance **R** (Figure 1.2.1) of the interacting molecules in the $B(X_1X_2X_3)$ - $P(Y_1Y_2Y_3)$ set.

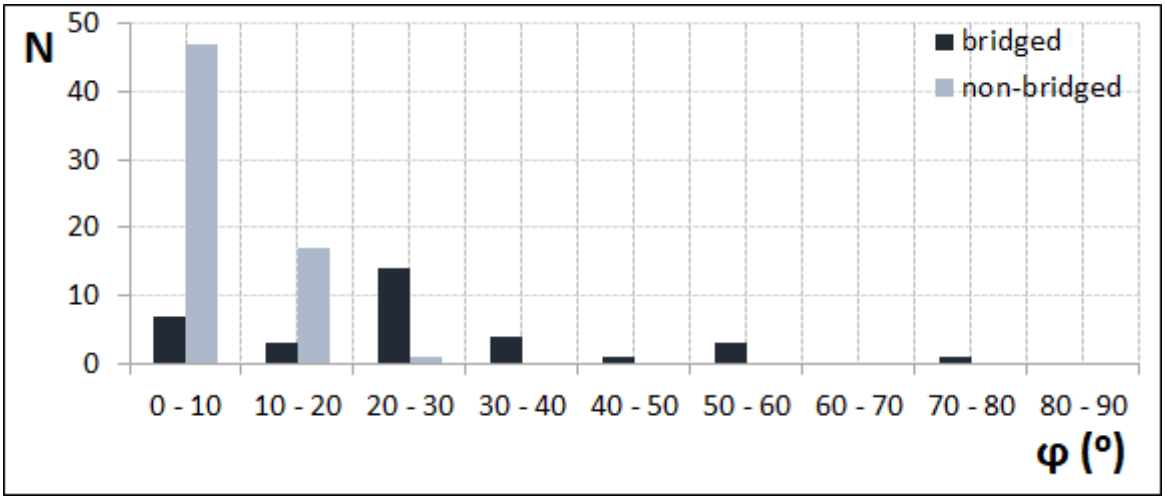

Figure 1.2.10 The distribution of the dihedral angle ***φ*** (Figure 1.2.1) of the interacting molecules in the $B(X_1X_2X_3)$ - $P(Y_1Y_2Y_3)$ set.

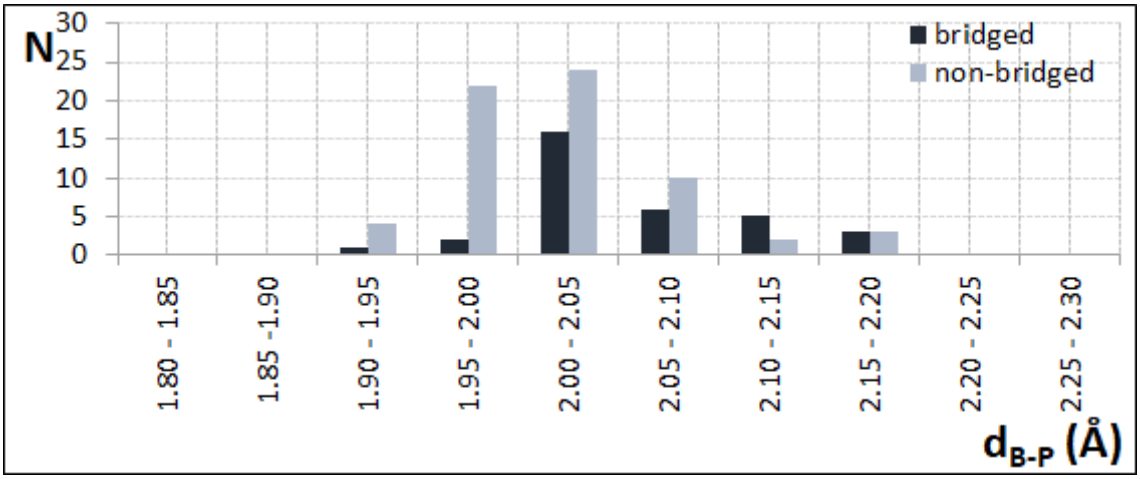

Figure 1.2.11 The distribution of the distance between phosphorus and boron atoms $\mathbf{d_{B\text{-}P}}$ (Figure 1.2.1) of the interacting molecules in the $B(X_1X_2X_3)$ - $P(Y_1Y_2Y_3)$ set.

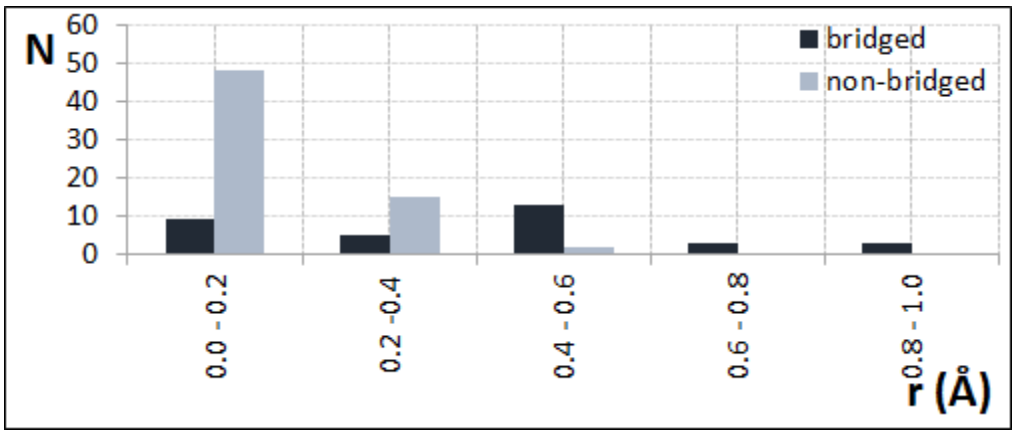

Figure 1.2.12 The distribution of the offset distance **r** (Figure 1.2.1) of the interacting molecules in the $B(X_1X_2X_3)$ - $P(Y_1Y_2Y_3)$ set.

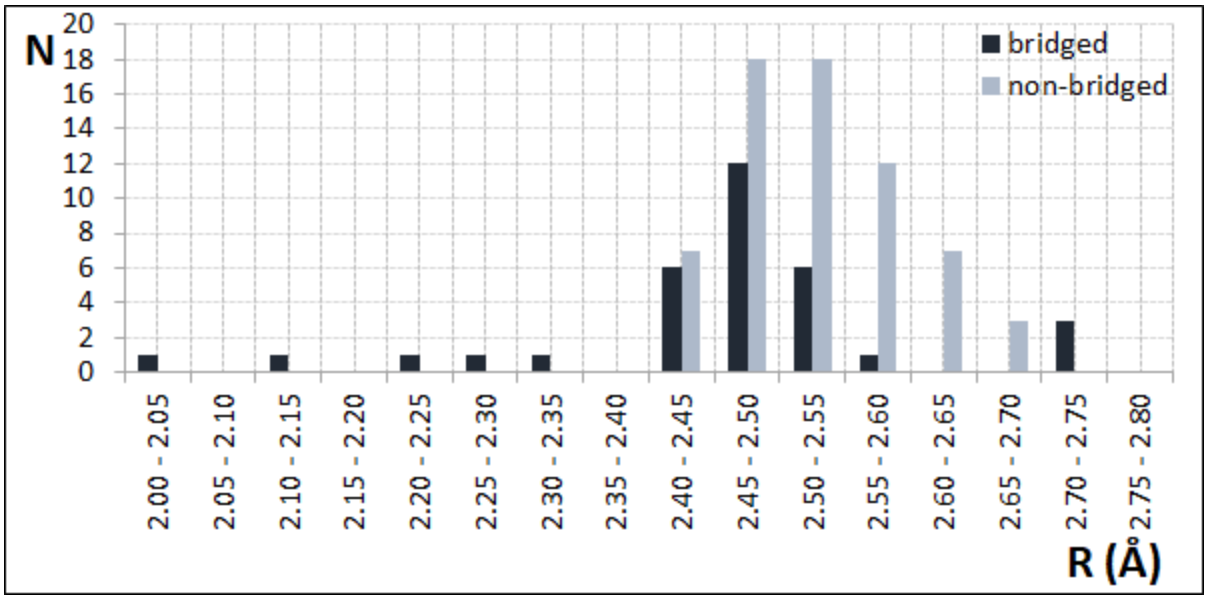

Figure 1.2.13 The distribution of the normal distance **R** (Figure 1.2.1) of the interacting molecules in the $B(X_1X_2X_3)$ - $P(Y_1Y_2Y_3)$ set.

Comparison of data in the $B(X_1X_2X_3)$ - $P(Y_1Y_2Y_3)$ set considering presence of the bridge between phosphorus and boron atoms indicate some significant differences in studied geometrical parameters (Figure 1.2.10-13). The non-bridged structures have tendency for values of the dihedral angle **φ** close to zero, while bridged structures have large **φ** values (Figure 1.2.10). The bridged and non-bridged structures have the maxima of the distribution of the distance $\mathbf{d_{B\text{-}P}}$ in the same range (2.00 - 2.05 Å), however, the non-bridged ones show tendency for somewhat shorter distances, while the bridged ones have significant number of structures with larger distances (Figure 1.2.11). Non-bridges structures also have tendency for shorter offsets **r** (Figure 1.2.12). The bridged structures have shorter normal distances **R** (Figure 1.2.13), the maximum in the distribution of the bridged structures is in the range 2.45-2.55 Å, while for non-bridged ones it is 2.45-2.55. In addition, significant number of the non-bridged structures has distances above 2.55 Å.

One can notice that both, the presence of the aromatic rings and the presence of the bridge in the structure influence on shortening the normal distance **R**.

4.2.2.3. The frustrated Lewis pairs (FLPs) set.

In order to study crystal structures of frustrated Lewis pairs (FLPs), the related literature has been comprehensively screened. The presence of, at least, two pentafluorophenyl (-PhF_5) or, eventually, tetrafluorophenyl (-p-PhF_4H) substituents on the boron atom, is found to be one of

the most important criteria for the existence of frustrated phosphine-borane pairs.[204] Based on the literature, the FLPs structures with experiment evidence, such as the ability to activate (small) molecules by heterolytic cleavage of the chemical bond, were found. In addition, to find structures of the FLPs, although experiments were not performed to confirm it, visual analysis of the set of structures with three cyclic substituents on the boron atom was done. The pair was marked as "frustrated" if a particular structure was similar to a structure for which there is experimental evidence for FLPs. The description of the considered FLPs structures is shown in Table 1.2.1, while the structures are shown in Supplementary Information (Figure SI 1.2.1–20).

In this study 25 contacts of FLPs structures in total were considered; 15 contacts of the structures with experimental evidence in the literature that they belong to the class of frustrated Lewis pairs (termed **experimental FLPs**) and 10 contacts of the structures without experimental evidence in the literature that they belong to the class of frustrated Lewis pairs, but they are structurally very similar to the documented ones (termed **evaluated FLPs**). The large fraction (13 of 20 structures) of considered FLPs structures are the bridged phosphine-boranes pairs. In five structures with pairs that are not bridged, heteroatoms (O, N, Si for instance)) are bound to the phosphorus atom, that support the formation of the pairs in the crystal structure by electronic effect. In addition, there are just two FLPs structures (probably more suitable "Confused" Lewis Pairs-CLPs,[205] as a boundary cases between classical and frustrated Lewis pair) without any other heteroatom, which exist in equilibrium as non-bridged ones (and could be isolated).

On another hand, according to the criteria of the CSD search (Methodology Section) it might be that some of FLPs structures were excluded, especially the structures with the "disorder" in the crystal structure, which could be found in the literature.

[204] [N^0 382] D. W. Stephan, G. Erker, *Angew. Chem. Int. Ed.* **2015**, *54*, 6400.
[205] [N^0 466] A. C. McQuilken, Q. M. Dao, A. J. P. Cardenas, J. A. Bertke, S. Grimme, T.H. Warren, *Angew. Chem. Int. Ed.* **2016**, *55*, 14335.

Table 1.2.1 Summary description of structures found in the Cambridge Structural Database of phosphine-borane FLPs. In some of the structures FLPs, were confirmed based on experimental evidence, while some of the structures were chosen based on structural similarity (evaluated FLPs).

Entry	REFCODE	Experimental evidence of FLP activity	Bridged or not	State of existing	Reference
1	SEZKAL	Yes – Coordination of alkyl isocyanides	Yes	Covalently bound FLP	Ekkert *et al.*, 2013[204]
2	FUWKUF	Yes – Coordination of NO	Yes	Covalently bound FLP	Liedtke *et al.*, 2014[204]
3	SEZJUE	Yes – Coordination of alkyl isocyanides	Yes	Covalently bound FLP	Ekkert *et al.*, 2013[204]
4	ODUJUU	Yes – Activating of ketones	No	Post reaction product in stoichiometric reaction or an intermediate in catalytic reaction	Takeuchi *et al.*, 2013[204]
5	FAPGIO	Yes – Addition to alkynes	No	In equilibria	Caputo *et al.*, 2012[204]
6	FAPGEK	Yes – Addition to PhCCH	No	In small equilibria	Caputo *et al.*, 2012[204]
7	OSUZEI	Yes – Activation of H_2 at elevated temperatures	Yes	Covalently bound FLP	Heiden *et al.*, 2011[204]
8	OLAJOB	Yes – Activation of H_2	No	In equilibria	Ullrich *et al.*, 2010[204]
9	OLAJUH	Yes – Activation of H_2	No	In equilibria	Ullrich *et al.*, 2010[204]
10	MIKDER	Yes – FLP activity (CO_2 capturing) thanks to isomerization on another PN	No	Air stable acyclic FLP	Barry *et al.*, 2013[204]

11	FUWLEQ	No – Probably lower FLP activity	Yes	Covalently bound FLP	Liedtke *et al.*, 2014[204]
12	BIRXAD	No	Yes	Covalently bound FLP Post reaction product of FLP activity (H_2) at higher temperatures	Yu *et al.*, 2013[204]
13	XUPZAK	No	No	Post reaction product of FLP activity (reduction of phosphines and activation of silanes (and H_2))	Geier & Stephan, 2010[204]
14	EWETAC	No	Yes	Covalently bound FLP	Ekkert *et al.*, 2011[204]
15	MIKCUG	No	Yes	Cyclic B-PNP	Barry *et al.*, 2013[204]
16	ROVLAR	No	Yes	Covalently bound FLP	Moquist *et al.*, 2015[204]
17	YORPAX	No (but negative for H_2 activation)	Yes	Covalently bound FLP	Spies *et al.*, 2009[204]
18	EWESUV	No	Yes	Covalently bound FLP	Ekkert *et al.*, 2011[204]
19	TACHAI	No (but negative for H_2 activation)	Yes	Covalently bound FLP	Chapman *et al.*, 2010[204]
20	SIGVUB01	No	Yes	Covalently bound FLP	Beckmann *et al.*, 2013[206]

[206] [N^0 467] O. Ekkert, G. G. Miera, T. Wiegand, H. Eckert, B. Schirmer, J. L. Petersen, C. G. Daniliuc, R. Fröhlich, S. Grimme, G. Kehra, G. Erker, *Chem. Sci*. **2013**, *4*, 2657.
[N^0 468] R. Liedtke, F. Scheidt, J. Ren, B. Schirmer, A. J. P. Cardenas, C. G. Daniliuc, H. Eckert, T. H. Warren, S. Grimme, G. Kehr, G. Erker, *J. Am. Chem. Soc.* **2014**, *136*, 9014.
[N^0 469] K. Takeuchi, L. J. Hounjet, D. W. Stephan, *Organometallics* **2013**, *32*, 4469.
[N^0 470] C. B. Caputo, S. J. Geier, E. Y. Ouyang, C. Kreitner, D. W. Stephan, *Dalton Trans.* **2012**, *41*, 237.
[N^0 471] Z. M. Heiden, M. Schedler, D. W. Stephan, *Inorg. Chem.* **2011**, *50*, 1470.
[N^0 371] M. Ullrich, A. J. Lough, D. W. Stephan, *Organometallics* **2010**, *29*, 3647.
[N^0 472] B. M. Barry, D. A. Dickie, L. J. Murphy, J. A. C. Clyburne, R. A. Kemp, *Inorg. Chem*. **2013**, *52*, 8312.
[N^0 473] J. Yu, G. Kehr, C. G. Daniliuc, G. Erker, *Inorg. Chem.* **2013**, *52*, 11661.
[N^0 474] S. J. Geier, D. W. Stephan, *Chem. Commun.* **2010**, *46*, 1026.
[N^0 475] O. Ekkert, G. Kehr, R. Fröhlich, G. Erker, *J. Am. Chem. Soc*. **2011**, *133*, 4610.
[N^0 476] P. Moquist, G.-Q. Chen, C. Mück-Lichtenfeld, K. Bussmann, C. G. Daniliuc, G. Kehr, G. Erker, *Chem. Sci.* **2015**, *6*, 816.
[N^0 477] P. Spies, G. Kehr, K. Bergander, B. Wibbeling, R. Fröhlich, G. Erker, *Dalton Trans.* **2009**, *9*, 1534.
[N^0 478] A. M. Chapman, M. F. Orton, J. P. H. Haddow, D. F. Wass, *Dalton Trans.* **2010**, *39*, 6184.
[N^0 479] J. Beckmann, E. Hupf, E. Lork, S. Mebs, *Inorg. Chem.* **2013**, *52*, 11881.

Separated distributions of the analyzed geometrical parameters of both, **experimental** and **evaluated FPLs** are given in Figure 1.2.14–17). It could be noticed that both, **experimental** and **evaluated FLPs** have a very similar distribution of the studied geometrical parameters.

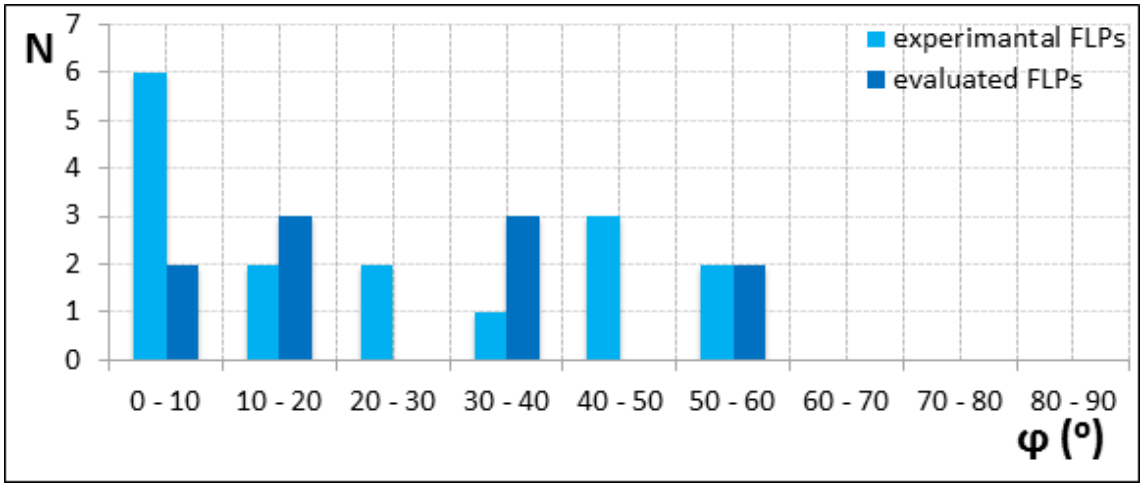

Figure 1.2.14. The distribution of the dihedral angle ***φ*** (Figure 1.2.1) of the interacting molecules in the contacts in the FLPs set.

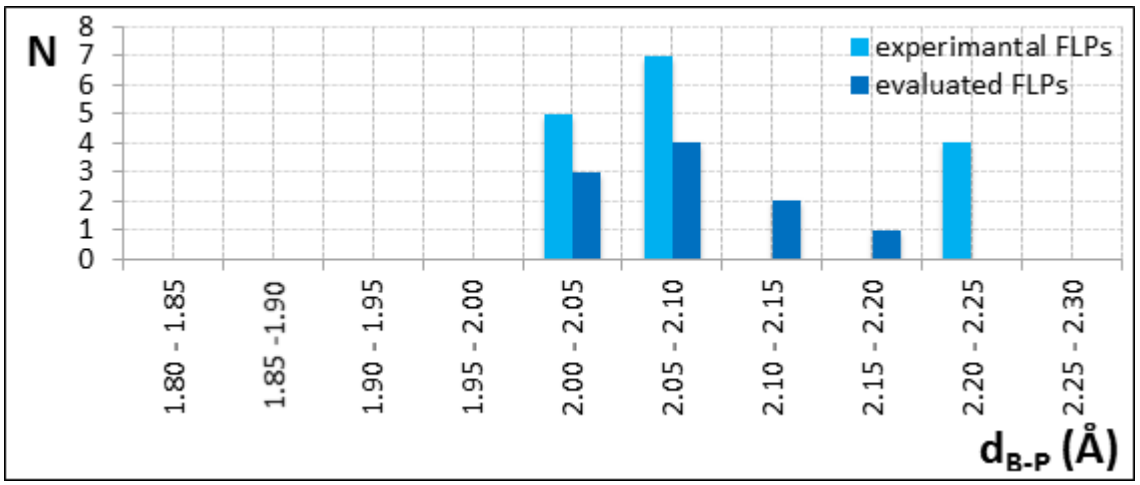

Figure 1.2.15. The distribution of the *distance between phosphorus and boron atoms* $\mathbf{d_{B\text{-}P}}$ (Figure 1.2.1) of the interacting molecules in the FLPs set.

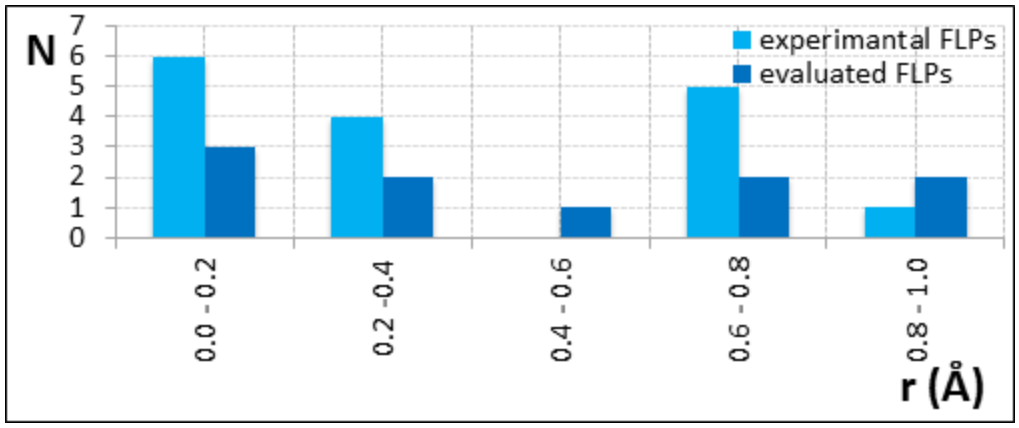

Figure 1.2.16. The distribution of the *offset distance* ***r*** (Figure 1.2.1) of the interacting molecules in the FLPs set.

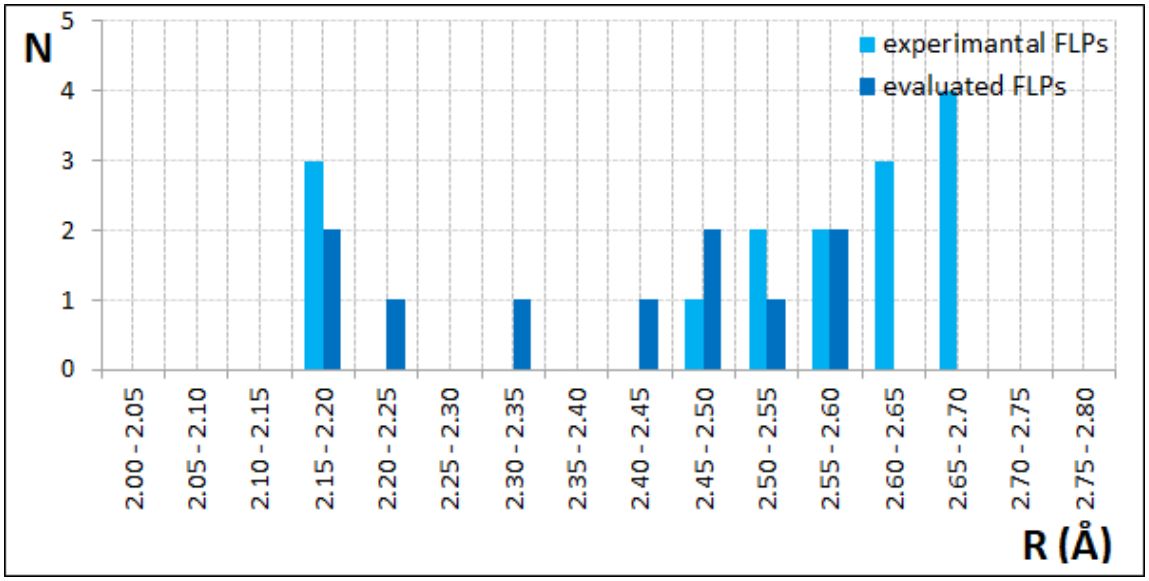

Figure 1.2.17. The distribution of the *normal distance* ***R*** (Figure 1.2.1) of the interacting molecules in the FLPs set.

To show possible influence on geometrical arrangement of the interacting phosphine and borane units in **bridged** (the structures for which *there is* an atomic chain between phosphorus and boron centers besides their direct covalent bond connection) and **non-bridged** (structures for which *there is no* an atomic chain between phosphorus and boron centers besides their direct covalent bond connection) FLPs, separated distributions of the analyzed geometrical parameters (Figure 1.2.1) for both (**bridged** and **non-bridged** FLPs) are shown in Figures 1.2.18 – 21. The influence of the bridge in FLPs structures is quite similar to the influence in the $B(X_1X_2X_3)$ - $P(Y_1Y_2Y_3)$ set (Figures 1.2.10 – 13). The results indicate that the **bridged** FPLs show larger discrepancy in the dihedral angle ***φ*** (up to 60º, mainly between 30º-60º) while the

non-bridged FLPs prefer ***φ*** values up to 20º (Figure 1.2.18). The **bridged** FLPs have slightly lower the $\mathbf{d_{B\text{-}P}}$ distance values (maximum of the distribution is around 2.0 Å) in comparison to the **non-bridged** FLPs which have tendency for $\mathbf{d_{B\text{-}P}}$ values around 2.05 Å and 2.10 Å. (Figure 1.2.19). The offset **r** values are higher for the **bridged** FLPs (mainly between 0.6 Å and 1.0 Å) than for the **non-bridged** FLPs (between 0.0 Å and 0.4 Å) (Figure 1.2.20). The normal distance **R** values in case of the **bridged** FLPs have the maximum around 2.2 Å, while for the **non-bridged** FLPs the maximum is around 2.7 Å (Figure 1.2.21). Overall, in can be concluded that the presence of the bridge has a huge influence on the geometric parameters in FLPs structures.

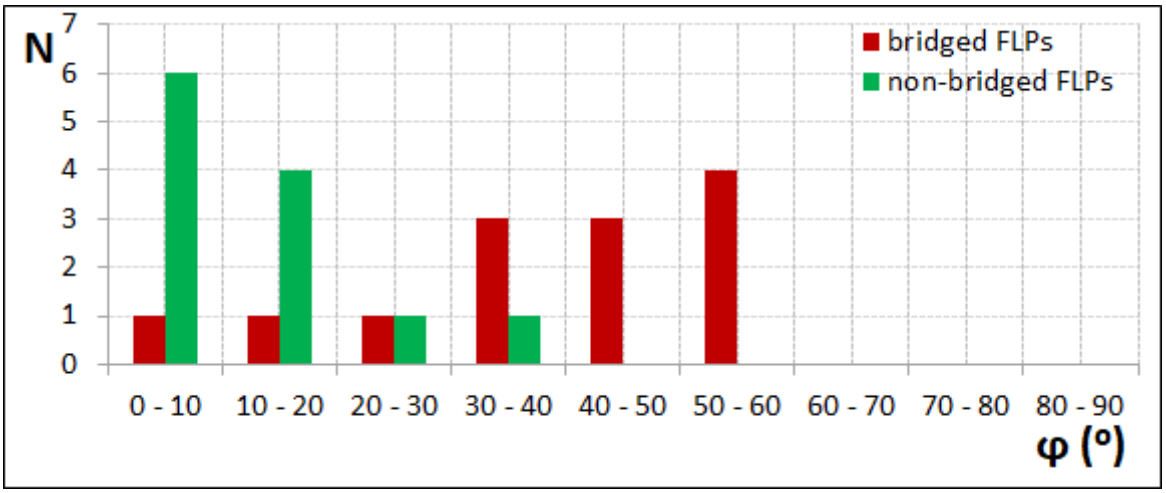

Figure 1.2.18 The distribution of the dihedral angle ***φ*** (Figure 1.2.1) of the interacting molecules in the FLPs set.

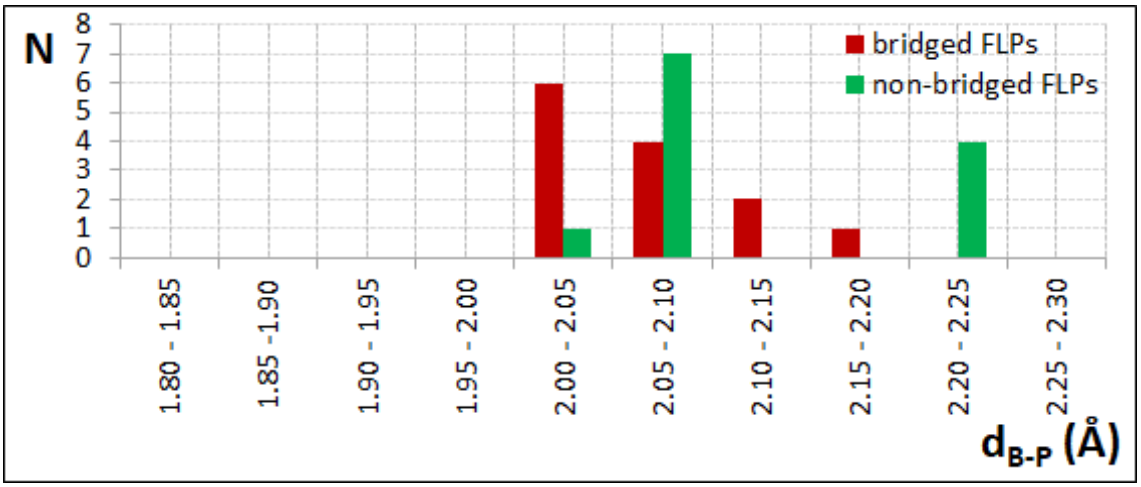

Figure 1.2.19 The distribution of the distance between phosphorus and boron atoms $\mathbf{d_{B\text{-}P}}$ (Figure 1.2.1) of the interacting molecules in the FLPs set.

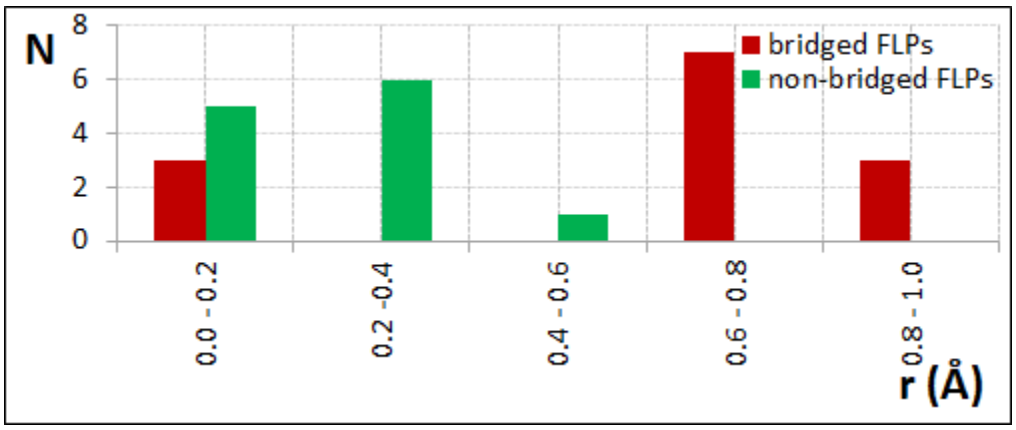

Figure 1.2.20 The distribution of the offset distance **r** (Figure 1.2.1) of the interacting molecules in the FLPs set.

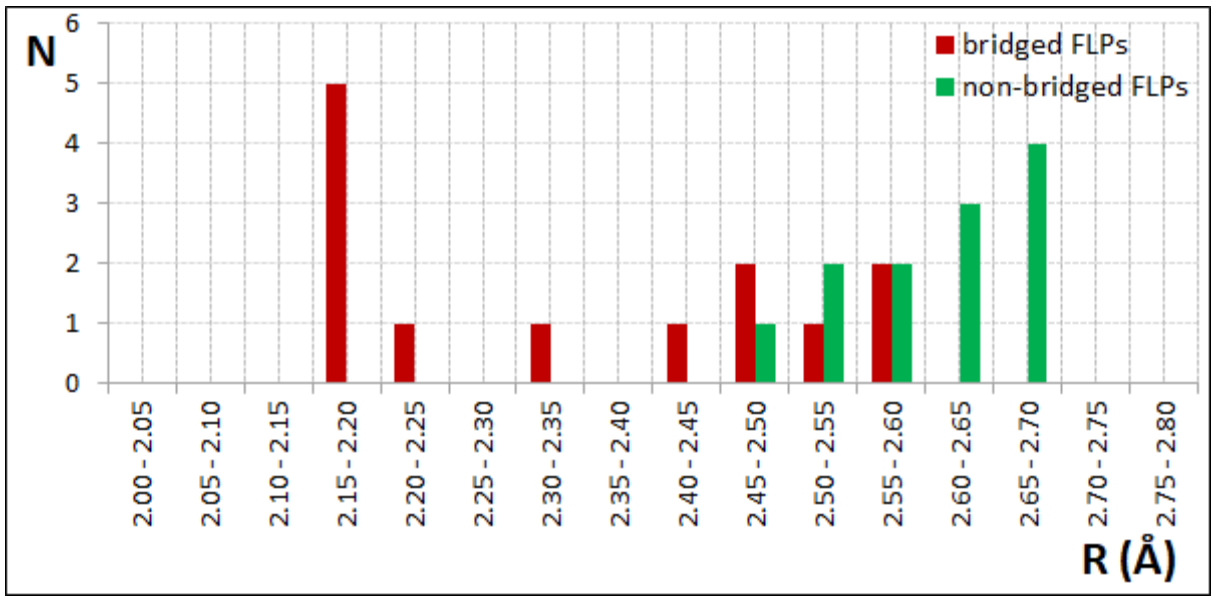

Figure 1.2.21 The distribution of the normal distance **R** (Figure 1.2.1) of the interacting molecules in the FLPs set.

4.2.2.4. Comparison of the sets.

In general, the contacts in the $B(X_1X_2X_3)$ - $P(Y_1Y_2Y_3)$ set have greater tendency for the larger **φ** values (especially in the range from 10˚ to 30˚ (Figure 1.2.6 or Figure 1.2.10) than the contacts in the BH_3 - $P(Y_1Y_2Y_3)$ set (almost all contacts have ***φ*** below 10˚ (Figure 1.2.2)). In comparison to the BH_3 - $P(Y_1Y_2Y_3)$ set (preferred $\mathbf{d_{B\text{-}P}}$ values around 1.9 Å (Figure 1.2.3)) preferred $\mathbf{d_{B\text{-}P}}$ of the $B(X_1X_2X_3)$ - $P(Y_1Y_2Y_3)$ set (Figure 1.2.7 or Figure 11) are longer. The BH_3 - $P(Y_1Y_2Y_3)$ set has a strong preference for **r** values ranged from 0.0 Å to 0.2 Å (Figure 1.2.4)), while the $B(X_1X_2X_3)$ - $P(Y_1Y_2Y_3)$ set has a wider distribution of **r** values (Figure 1.2.8 or Figure 1.2.12).

The normal distances are longer for the contacts in the $B(X_1X_2X_3)$ - $P(Y_1Y_2Y_3)$ set (Figure 1.2.9 or Figure 1.2.13) than for the contacts in the BH_3 - $P(Y_1Y_2Y_3)$ set (2.20-2.30 Å (Figure 1.2.5)). As in the BH_3 - $P(Y_1Y_2Y_3)$ set, the longer **R** (Figure 1.2.9 or Figure 13) in comparison to the $\mathbf{d_{B\text{-}P}}$ (Figure 1.2.7 or Figure 1.2.11) indicate a pyramidal geometry around the boron atom.

Comparison of the data of the FLPs set with the other two sets show that FLPs have slight preference for parallel orientation of the planes (Figure 1.2.18) that differs from both, the structures in the $B(X_1X_2X_3)$ - $P(Y_1Y_2Y_3)$ set (that have the contacts with **φ** values up to 30˚ (Figure 1.2.6)) and the structures in the BH_3 - $P(Y_1Y_2Y_3)$ set (that prefers only the lowest ***φ*** values: 0˚-10˚ (Figure 12)).

It is interesting to note that only in FLPs set there are $\mathbf{d_{B\text{-}P}}$ values slightly above 2.2 Å (Figure 1.2.19). Overall, among all the sets of the structures the FLPs have, in average, the longest B-P bond.

In comparison to the BH_3 - $P(Y_1Y_2Y_3)$ set (Figure 1.2.4) and the $B(X_1X_2X_3)$ - $P(Y_1Y_2Y_3)$ set (Figure 1.2.8), the FLPs set has a wider range of the **r** values (Figure 1.2.20).

The distribution of the normal distance **R** (Figure 1.2.1) values of the contacts in the FLPs set is shown in Figure 1.2.21. The results show that most of the contacts have tendency for two different regions of the **R** values. First region is around 2.20 Å (2.15-2.20 Å), that differs slightly from the BH_3 - $P(Y_1Y_2Y_3)$ set (Figure 1.2.5) and differs strongly from the $B(X_1X_2X_3)$ - $P(Y_1Y_2Y_3)$ set (that has no preference for such low **R** values, (Figure 1.2.9)). Second region is in the range of 2.50-2.70 Å, that is similar to the preferred **R** values of the $B(X_1X_2X_3)$ - $P(Y_1Y_2Y_3)$ set (Figure 1.2.9) and different from the BH_3 - $P(Y_1Y_2Y_3)$ set (Figure 1.2.5). In the first preferred region of **R** values (around 2.20 Å) of FLPs set there are a C_2-bridged type of FLPs structures (one example of such structure is given in Figure 1.2.22).

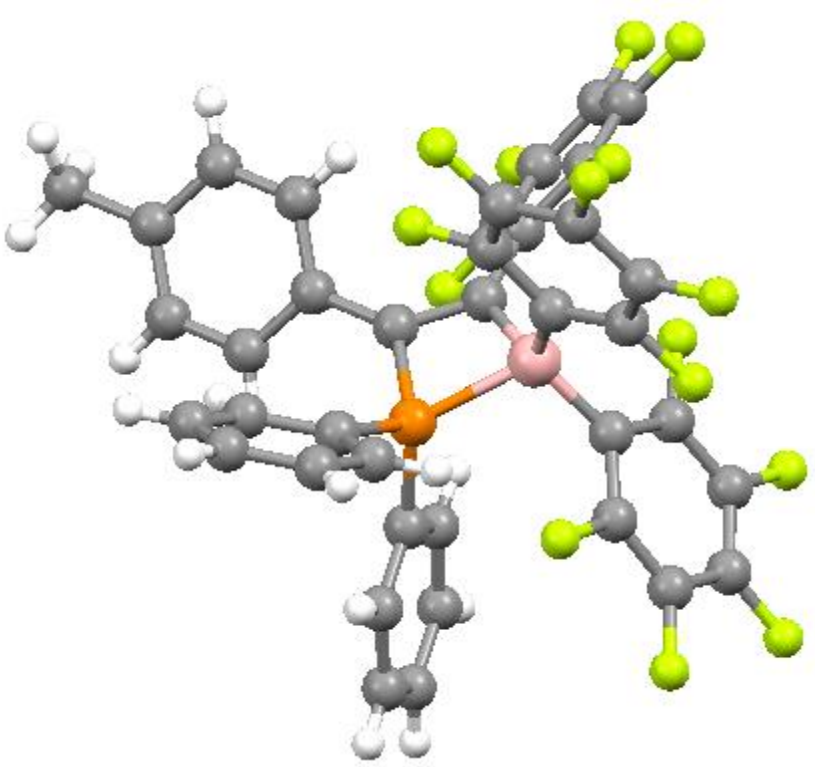

Figure 1.2.22 Crystal structure **SEZKAL**[207] with C_2-bridge as an example of FLP structure with short (2.17(4) Å) normal distance **R** (Figure 1.2.1). P: orange; B: pink; F: yellow; C: grey; H: white.

4.2.3. Subchapter conclusion.

Study of the interactions between phosphine and borane based on the analysis of the structures archived in Cambridge Structural Database (CSD) was performed. Three sets of the structures were considered: the BH_3 - $P(Y_1Y_2Y_3)$ set containing BH_3 as borane molecule; the $B(X_1X_2X_3)$ - $P(Y_1Y_2Y_3)$ set with all other borane molecules, and the frustrated Lewis (phosphine-borane) pairs set. The obtained data enabled the comparison of the geometrical parameters of the classical and frustrated Lewis pairs. The results show that presence of aromatic substituents on boron atom has small influence, while presence of the bridge (an atomic chain between phosphorus and boron centers) has more significant influence on the geometries of phosphine-borane interactions in crystals.

The results show that most of the found structures (78.1 %) contain BH_3 as borane. In the BH_3 - $P(Y_1Y_2Y_3)$ set preferred mutual phosphorus – boron distances ($\mathbf{d_{B\text{-}P}}$, values) are around 1.9 Å,

[207] [N^0 480] R. Fröhlich, S. Grimme, G. Kehra, G. Erker, *Chem. Sci*. **2013**, *4*, 2657.

preferred angles between the planes formed by the atoms directly bound to phosphorus and boron atoms (***φ)*** are in the range from 0˚ to 10˚.

FLPs structures prefer a bit higher $\mathbf{d_{B\text{-}P}}$ values (the peak is at 2.05-2.10 Å) and among all here studied sets only FLPs have some structures with $\mathbf{d_{B\text{-}P}}$ slightly above 2.2 Å. FLPs structures have angle **φ** values in the larger region, up to 60˚. It should be noted that majority of the phosphine-borane FLPs found in the crystal structures from the CSD are "bridged" structures. The only exceptions in crystal structures are the non-bridged frustrated phosphine-borane adducts containing other heteroatoms (oxygen, nitrogen, silicon) bound to the phosphorus atom.

It is worth to note that all the considered FLPs, as matter of fact, do not show the "frustration" as it is defined in the literature.[208] Despite the experimental and theoretical finding that "frustration" in FLP chemistry does not mean the complete suppression of covalent interactions between the Lewis acid and base centers,[209] it could be concluded that the capabilities of the pairs caused by "frustration" cannot be recognized from the pairs' crystal structures. Hence, it seems to be more suitable to term these pairs as Loose Lewis Pairs (LLPs) rather than the Frustrated Lewis Pairs (FLPs).

[208] [N^0 342] G. C. Welch, L. Cabrera, P. A. Chase, E. Hollink, J. D. Masuda, P. Wei, D. W. Stephan, *Dalton Trans.* **2007**, 3407.
[N^0 343] P. Spies, R. Fröhlich, G. Kehr, G. Erker, S. Grimme, *Chem. Eur. J.* **2008**, *14*, 333.
[N^0 382] D. W. Stephan, G. Erker, *Angew. Chem. Int. Ed.* **2015**, *54*, 6400.
[209] [N^0 481] T. Wiegand, H. Eckert, O. Ekkert, R. Fröhlich, G. Kehr, G. Erker, S. Grimme, *J. Am. Chem. Soc.* **2012**, *134*, 4236.

4.2.4. Закључак потпоглавља.

У циљу проучавања интеракција између фосфина и борана извршена је анализа структура архивираних у Кембричкој бази структурних података (енг. Cambridge Structural Database (CSD)). Разматране су три групе структура: BH_3 - $P(Y_1Y_2Y_3)$ сет који садржи BH_3 као молекул борана; $B(X_1X_2X_3)$ - $P(Y_1Y_2Y_3)$ сет који садржи све остале молекуле борана, и сет фрустрираних Lewis-ових (фосфин-боран) парова. Добијени подаци омогућили су упоређивање геометријских параметара класичних и фрустрираних Lewis-их парова. Резултати показују да присуство ароматичних супституената на атому бора има мали утицај, док присуство моста (атомски ланац између фосфора и бора) има значајан утицај на геометрију интеракција фосфин-борана у кристалима.

Резултати показују да већина пронађених структура (78,1%) садржи BH_3 као молекул борана. У BH_3 - $P(Y_1Y_2Y_3)$ сету преферентна међусобна растојања између фосфора и бора ($\mathbf{d_{B\text{-}P}}$ вредности) су око 1,9 Å, а преферентни углови између равни формираних од атома директно везаних за атоме фосфора и бора ($\boldsymbol{\varphi}$) су у опсегу од 0˚ до 10˚.

Структуре FLP-а преферирају нешто веће $\mathbf{d_{B\text{-}P}}$ вредности (пик је на 2,05-2,10 Å), а међу свим овде описаним сетовима само у FLP сету постоје структуре са $\mathbf{d_{B\text{-}P}}$ мало већим од 2,2 A. Структуре FLP-а имају вредности угла $\boldsymbol{\varphi}$ у већем распону, до 60˚. Треба напоменути да су већина фосфин-боран FLP-ова пронађених у кристалним структурама у CSD, „премошћене“ структуре. Изузеци у кристалним структурама, који су непремошћени фрустрирани фосфин-борански адукти, садрже хетероатоме (кисеоник, азот, силицијум) везане за атом фосфора.

Важно је напоменути да сви разматрани FLP-и, у ствари, не показују „фрустрацију“ како је то дефинисано у литератури.[208] Упркос резултатима експерименталних и теоријских истраживања, који указују на то да „фрустрација“ у хемији FLP не значи потпуно непостојање ковалентних интеракција између Lewis-их киселинско-базних центара,[209] може се закључити да се карактеристике парова узроковане "фрустрацијом" не могу препознати из кристалних структура тих парова. Стога, изгледа да је погодније да се ови парови називају „лабави“ Lewis-ови парови (енг. Loose Lewis Pairs (LLPs)), а не „фрустрирани“ Lewis-ови парови (енг. Frustrated Lewis Pairs (FLPs)).

4.2.5. Conclusion du sous-chapitre

Pour étudier les interactions entre la phosphine et le borane sur la base de l'analyze des structures archivées dans la base de données Cambridge Structural Database (CSD) a été réalisée. Trois ensembles de structures ont été considérés: l'ensemble BH_3-P($Y_1Y_2Y_3$) contenant BH_3 comme molécule de borane; l'ensemble B($X_1X_2X_3$)-P($Y_1Y_2Y_3$) avec toutes les autres molécules de borane et les paires frustrées de Lewis (phosphine-borane). Les données obtenues ont permis de comparer les paramètres géométriques des paires de Lewis classiques et frustrées. Les résultats montrent que la présence de substituants aromatiques sur l'atome de bore a peu d'influence, alors que la présence du pont (une chaîne atomique entre les centers de phosphore et de bore) a une influence plus significative sur les géométries des interactions phosphine-borane dans les cristaux.

Les résultats montrent que la plupart des structures trouvées (78,1%) contiennent du BH_3 sous forme de borane. Dans l'ensemble BH_3-P($Y_1Y_2Y_3$), les distances préférées phosphore-bore ($\mathbf{d_{B\text{-}P}}$ valeurs) sont d'environ 1,9 Å, les angles préférés entre les plans formés par les atomes directement liés aux atomes de phosphore et de bore ($\boldsymbol{\varphi}$) sont compris de 0˚ à 10˚.

Les structures FLP préfèrent des valeurs $\mathbf{d_{B\text{-}P}}$ un peu plus élevées (le pic est à 2.05-2.10 Å) et parmi tous les ensembles étudiés ici, seules les FLP ont des structures avec un $\mathbf{d_{B\text{-}P}}$ légèrement supérieur à 2,2 Å. Les structures FLP ont des valeurs d'angle $\boldsymbol{\varphi}$ dans la plus grande région, jusqu'à 60˚. Il convient de noter que la majorité des FLP phosphine-borane trouvées dans les structures cristallines de la CSD sont des structures «pontées». Les seules exceptions dans les structures cristallines sont les adduits phosphine-borane frustrés non pontés contenant d'autres hétéroatomes (oxygène, azote, silicium) liés à l'atome de phosphore.

Il vaut la peine de noter que tous les FLP considérés, en fait, ne montrent pas la "frustration" telle qu'elle est définie dans la littérature.[208] Malgré la découverte expérimentale et théorique que la "frustration" dans la chimie FLP ne signifie pas la suppression complète des interactions covalentes entre l'acide de Lewis et les centers de base,[209] on pourrait conclure que les capacités des paires provoquées par la "frustration" ne peuvent pas être reconnues à partir des structures cristallines des paires. Par conséquent, il semble plus approprié de qualifier ces paires comme paires de Lewis lâches (LLP) plutôt que de paires de Lewis frustrées (FLPs).

Chapter 5

Cis-migration of Me group within pentacarbonylmethylmanganese complex induced by phosphines

5.1. Introduction.

The first evidence of the pentacarbonylmethylmanganese complex has been given in mid-fifties (1957) by Coffield *et al.*[210] The pentacarbonylmethylmanganese complex has been the first mononuclear complex containing carbonyl ligands ever synthetized. Since that discovery, the complex has been intensively investigated using various experimental techniques available at that time.[211] It was found that in reaction with nucleophiles a migration of the methyl group to adjacent carbonyl ligand is induced and followed by insertion of the nucleophiles into the complex.[212] Later, the migratory insertion sequence was found to be an important sequence in organometallic synthesis and catalysis.[213] Therefore, many experimental and theoretical

[210] [N^0 482] R. D. Closson, J. Kozikowski, T. H. Coffield, J. *Org. Chem.* **1957**, *22*, 598.
[211] see selected examples: [N^0 483] P. M. Treichel, F. G. A. Stone, *Advan. Ovganometal. Chem.* **1964**, *1*, 143.
[N^0 484] F. A. Cotton, R. M. Wing, *J. Ovganometal. Chem.* **1967**, *9*, 511.
[N^0 485] M. B. Hall, M. F. Guset, I. H. Hillier, *Chem. Phys. Lett*. **1972**, *15*, 592.
[N^0 486] S. Evans, J. C. Green, M. L. H. Green, A. F. Orchard, D. W. Turner, *Discuss. Faraday Soc*. **1969**, *41,* 112.
[N^0 487] D. L. Lichtenberger, R. F. Fenske *Inorg. Chem.* **1974**, *13*, 486.
[N^0 488] Z. Mahmood, M. Azam, A. Mushtaq, R. Kausar, S. Kausar, S. R. Gilani, *Spectrochim. Acta A* **2006**, *65*, 445.
[N^0 489] L. González, C. Daniel, *J Comput Chem*. **2006**, *27*, 1781.
[N^0 490] T. Leyssens, D. Peeters, A. Guy Orpen, J. N. Harvey, *Organometallics* **2007**, *26,* 2637.
[N^0 491] K. W. Feindel, K. J. Ooms, R. E. Wasylishen, *Phys. Chem. Chem. Phys*. **2007**, *9*, 1226.
[N^0 492] A.G. Algarra, V. V. Grushin, S. A. Macgregor, *Organometallics* **2012**, *31*, 1467.
[212] see selected examples: [N^0 482] T. H. Coffield, J. Kozikowski, R. D. Closson, *J. Org. Chem*. **1957**, *22*, 598.
[N^0 493] F. Calderazzo, F. A. Cotton, *Inorg. Chem*. **1962**, *1*, 30.
[N^0 494] K. A. Keblys, A. H. Filbey, *J. Am. Chem. Soc.* **1960**, *82*, 4202.
[N^0 495] R. J. Mawby, F. Basolo, R. G. Pearson, *J. Am. Chem. Soc.* **1964**, *86*, 3994.
[N^0 496] F. Calderazzo, F. A. Cotton, *Chim. Ind. (Milano)* **1964**, *46*, 1165.
[N^0 497] F. Calderazzo, K. Noack, *Coordin. Chem. Rev.* **1966**, *1*, 118.
[213] see selected examples: [N^0 498] L.S. Reich, A. Schindler, *Polymerization by Organometallic Compounds*; Wiley–Interscience, New York, **1966**.
[N^0 499] C. Masters, *Adv. Organomet. Chem*. **1969**, *17*, 61.
[N^0 500] R. C. Brady, R. Pettit, *J. Am. Chem. Soc*. **1980**, *102*, 6181.
[N^0 501] J. R. Blackborow, R. J. Daroda, G. Wilkinson, *Coord. Chem. Rev.* **1982**, *43*, 17.
[N^0 502] E. J. Kuhlmann, J. J. Alexander, *Coord. Chem. Rev.* **1980**, *33*, 195.
[N^0 503] A. Wojciki, *Adv. Organomet. Chem*. **1973**, *11*, 87.
[N^0 504] F. Calderazzo, *Angew. Chem. Int. Ed. Engl*. **1977**, *16*, 299.
[N^0 495] R. J. Mawby, F. Basolo, R. G. Pearson, *J. Am. Chem. Soc.* **1964**, *86*, 3994.
[N^0 505] J. J. Wax, R. G. Bergman, *J. Am. Chem. Soc.* **1981**, *103*, 7028.
[N^0 493] F. Calderazzo, F. A. Cotton, *Inorg. Chem.* **1962**, *1*, 30.
[N^0 506] K. Noack, F. Calderazzo, *J. Organomet. Chem.* **1967**, *10*, 101.
[N^0 507] T. C. Flood, J. E. Jensen, J. A. Statler, *J. Am. Chem. Soc.* **1981**, *103*, 4410.
[N^0 508] T. H. Cotfield, J. Kozikowske, R. N. Closson, *J. Org. Chem.* **1957**, *22*, 598.
[N^0 509] T. H. Cotfield, J. Kozikowske, R. N. Closson, *Spec. Publ. Chem. Soc*. **1959**, *13*, 126.
[N^0 510] T. M. McHugh, A. J. Rest, *J. Chem. Soc., Dalton Trans.* **1980**, 2323.
[N^0 511] K. Nickolas, S. Raghu, M. Rosenblum, *J. Organomet. Chem.* **1974**, *78*, 133.
[N^0 512] K. Mashima. A. Nakamura, *J. Organomet. Chem.* **1992**, *428*, 49.
[N^0 513] M. Brookhart, M. L. H. Green, L. L. Wong, *Prog. Inorg. Chem.* **1988**, *36*, 1.
[N^0 514] H. Berke, R. Hoffmann, *J. Am. Chem. Soc.* **1978**, *100*, 7224.
[N^0 515] T. Ziegler, L. Versluis, V. Tschinke, *J. Am. Chem. Soc.* **1986**, *108*, 612.
[N^0 516] D. Saddei, H. J. Freund, G. G. Holnecher, *J. Organomet. Chem.***1980**, *186*, 63.
[N^0 517] M. E. Ruiz, A. Flores-Riveros, O. Novaro, *J. Catal. **1980***, *64*, 1.
[N^0 518] F. U. Axe, D. S. Marynick, *Organometallics* **1987**, *6*, 572.

researches have been done in order to find its mechanism as well as kinetics of the insertion step of many nucleophilic ligands.[214] The complex has been found to be important in synthesis as a precursor as well as a catalyst.[215]

Nevertheless, little has been published[216] on the actual thermochemistry of the insertion-migration step-wise reaction of the pentacarbonylmethylmanganese complex with Lewis bases.

[N^0 519] F. U. Axe, D. S. Marynick, *J. Am. Chem. Soc.* **1988**, *110*, 3728.
[214] see selected examples: [N^0 520] R. J. Ruszczyk, B.-L. Huang, J. D. Atwood, *J. Organomet.Chem*. **1986**, *299*, 205.
[N^0 521]. M. Andersen, J. R. Moss, *Organometallics* **1994**, *13*, 5013.
[N^0 514] H. Berke, R. Hoffmann*, J. Am. Chem. Soc*. **1978**, *100*, 7224.
[N^0 518] F. U. Axe, D. S. Marynick, *Organometallics* **1987**, *6*, 572.
[N^0 515] T. Ziegler, L. Versluis, V. Tschinke, *J. Am. Chem. Soc.* **1986**, *108*, 612.
[N^0 522] A. Derecskei-Kovacs, D. S. Marynick, J*. Am. Chem. Soc*. **2000**, *122*, 2078.
[N^0 523] X. H. Wang, E. Weitz, *J. Phys. Chem. A*. **2002**, *106*, 11782.
[N^0 524] X. Wang, E. Weitz, *J. Organomet. Chem*. **2004**, *689*, 2354.
[N^0 525] S. L. Webb, C. M. Giandomenico, J. Halpern, *J. Am. Chem. Soc.* **1986**, *108*, 34.
[N^0 526] W. T. Boese, B. Lee, D. W. Ryba, S. T. Belt, P. C. Ford, *Organometallics* **1993***, 12*, 4739.
[N^0 527] W. T. Boese, P. C. Ford, *J. Am. Chem. Soc.* **1995**, *117*, 8381.
[N^0 528] T. L Bent, J. D. Cotton, *Organometallics* **1991**, *10*, 3156.
[N^0 529] J. N. Cawse, R. A. Fiato, R. L. Pruett, *J. Organomet. Chem*. **1979**, *172*, 405. and related references therein.
[N^0 530] T. G. Richmond, F. Basolo, D. F. Shriver, *Inorg. Chem.* **1982**, *21*, 1272.
[215] see selected examples: [N^0 531] R. L. Pruett, *Adv. Organomet. Chem*. **1979**, *17*, 1.
[N^0 532] D. Forster, *Adv. Organomet. Chem*. **1979**, *17*, 255.
[N^0 533] G. W. Parshall, *Homogeneous Catalysis*; John Wiley, New York, **1980**.
[N^0 534] C. Masters, *Homogeneous Transition-Metal Catalysis*; Chapman and Hall, **1981**.
[N^0 535] T. G. Richmond, F. Basolo, D.F. Shriver, *Inorg. Chem*. **1982**, *21*, 1272.
[N^0 536] J. P. Collman, R. G. Finke, J. N. Cawse, J. I. Brauman, *J. Am. Chem. Soc*. **1978**, *100*, 4766.
[N^0 520] R. J. Ruszczyk, B.-L. Huang, J. D. Atwood, *J. Organomet.Chem*. **1986**, *299*, 205.
[N^0 537] J. R. Moss, *J. Molecular Catal. A: Chemical* **1996**, *107*, 169.
[N^0 538] P. L. Motz, D. J. Sheeran, M. Orchin, *J. Organomet. Chem.* **1990**, *383*, 201.
[N^0 539] M. A. Gonzalez, S. J. Carrington, N. L. Fry, J. L. Martinez, P. K. Mascharak, *Inorg. Chem.* **2012**, *51*, 11930.
[N^0 540] H. J. Haupt, G. Lohmann, U. Floerke, *Z. Anorg. Allg. Chem.* **1985**, *526*, 103.
[N^0 541] W. Ping, J. D. Atwood, *Organometallics* **1993**, *12*, 4247.
[N^0 542] I. J. Hart, J. C. Jeffery, R. M. Lowry, F. G. A. Stone, *Angew. Chem. Int. Ed. Engl.* **1988**, *27*, 1703.
[N^0 543] K. E. Warner, J. R. Norton, *Organometallics* **1985**, *4*, 2150.
[N^0 544] R. M. Bullock, B. J. Rappoli, *J. Am. Chem. Soc.* **1991**, *113*, 1659.
[N^0 545] G. D. Vaughn, K. A. Krein, J. A. Gladysz, *Organometallics* **1986**, *5*, 936.
[N^0 546] F. Carré, G. Cerveau, E. Colomer, R. J. P. Corriu, *J. Organomet. Chem.* **1982**, *229*, 257.
[N^0 547] P. DeShong, G. A. Slough, A. Rheingold, *Tetrahedron Lett.* **1987**, *28*, 2229.
[N^0 548] P. DeShong, D. R. Sidler, *J. Org. Chem.* **1988**, *53*, 4892.
[N^0 549] R. M. Ceder, J. Sales, X. Solans, M. Font-Altaba, *J. Chem. Soc., Dalton Trans.* **1986**, 1351.
[N^0 550] M. E. Dowler, T. X. Le, P. DeShong, W. von Philipsborn, M. Vöhler, D. Rentsch, *Tetrahedron* **1993**, *49*, 5673.
[N^0 551] B. Zhou, Y. Hu, C. Wang, *Angew. Chem. Int. Ed.* **2015**, 54, 13659.
[N^0 552] S. A. Llewellyn, M. L. H. Green, A. R. Cowley, *Dalton Trans.* **2006**, 1776.
[N^0 553] A. Fernández 1, J. M. Vila, *J. Organomet. Chem.* **2005**, *690*, 3638.
[N^0 554] J. Albert, J. Cadena, J. Granell, X. Solans, M. Font-Bardia, *J. Organomet. Chem.* **2004**, 689, 4889.
[216] [N^0 514] H. Berke, R. Hoffmann, *J. Am. Chem. Soc.* **1978**, *100*, 7224.
[N^0 555] E. Folga, T. Ziegler, *J. Am. Chem. Soc.* **1993**, *115*, 5169.
[N^0 518] F. U. Axe, D. S. Marynick, *Organometallics* **1987**, *6*, 572.
[N^0 519] F. U. Axe, D. S. Marynick, *J. Am. Chem. Soc.* **1988**, *110*, 3728.
[N^0 515] T. Ziegler, L. Versluis, V. Tschinke, *J. Am. Chem. Soc.* **1986**, *108*, 612.
[N^0 556] R. S. Drago, N. M. Wong, D. C. Ferris, *J. Am. Chem. Soc.* **1992**, *114*, 91.
[N^0 557] J. A. Connor, M. T. Zefarani-Moattar, J. Bickerton, N. I. El Saied, S. Suradi, R. Carson, G. Al Takhin, H. A. Skinner, *Organometallics* **1982**, *1*, 1166.

Thus, in this study the reactions of the manganese complex with various organo-phosphorous Lewis bases were investigated experimentally and theoretically.

The migration-insertion reaction sequence into the pentacarbonylmethylmanganese complex (**2.1**) induced by a series of organo-phosphorous Lewis bases (Scheme 2.1), has been studied in the sense of experimental kinetic and thermodynamic ITC and theoretical static DFT-D studies. The reaction supposedly goes through the *cis-migration* of the methyl group to carbon-monoxide ligand and subsequent insertion of the Lewis base into the manganese complex (see Scheme 2.2). It has been reported that concurrent *trans* migration of the methyl group is possible as well as decarbonylation of the resulting product of the migration-insertion step-wise reaction.[217] It has been shown that *trans* migration of methyl group occurs in reaction of **2.1** with variety of nucleophilic substrates[218] (see Scheme 2.3), while with many other Lewis bases exclusively the *cis-migration* takes place.[219] The reaction conditions that allow the *trans* migration and/or the decarbonylation are longer reaction time periods (more than three hours) as well as higher reaction temperatures[220] (these side reactions, i.e. *trans* migration/decarbonylation, are schematically shown in Scheme 2.3). Importantly, it has been documented therein that the Lewis bases of interest in this study (**2.2a,c**) exclusively, whatever the condition, gave *cis-migration* product, while **2.2b** often gave a mixture of *cis*/*trans* products. Therefore, is seems that the chosen Lewis bases **2.2a,c** are rather good candidates for the ITC research, while **2.2.b** might be tricky one (see Scheme 2.1.3)

In order to verify whether the chosen Lewis bases (**2.2a-c**) are suitable candidates to **2.1**, so that their interaction leads to only one reaction product (preferably the product of the *cis-migration*) which would be, therefore, desirable for further ITC investigations, preliminary reaction tests were done.

[N^0 558] G. P. Smith, *Polyhedron* **1988**, *7*, 1605.
[217] [N^0 559] C. S. Krainhanzel, P. K. Maples, *J. Chem. Soc.* **1965**, *87*, 5267.
[N^0 560] R. N. Haszeldine, *J. Chem. Soc.* (*A*), **1969**, 698.
[218] [N^0 495] R. J. Mawby, F. Basolo, R. G. Pearson, *J. Am. Chem. Soc*. **1964**, *86*, 3994.
[N^0 561] C. S. Krainhanzel, P. K. Maples, K. Peter, *Inorg. Chem.,* **1968**, *7*, 1806.
[219] [N^0 495] R. J. Mawby, F. Basolo, R. G. Pearson, *J. Am. Chem. Soc*. **1964**, *86*, 3994.
[N^0 561] C. S. Krainhanzel, P. K. Maples, K. Peter, *Inorg. Chem.,* **1968**, *7*, 1806.
[220] [N^0 559] C. S. Krainhanzel, P. K. Maples, *J. Chem. Soc.* **1965**, *87*, 5267.
[N^0 560] R. N. Haszeldine, *J. Chem. Soc.* (*A*), **1969**, 698.

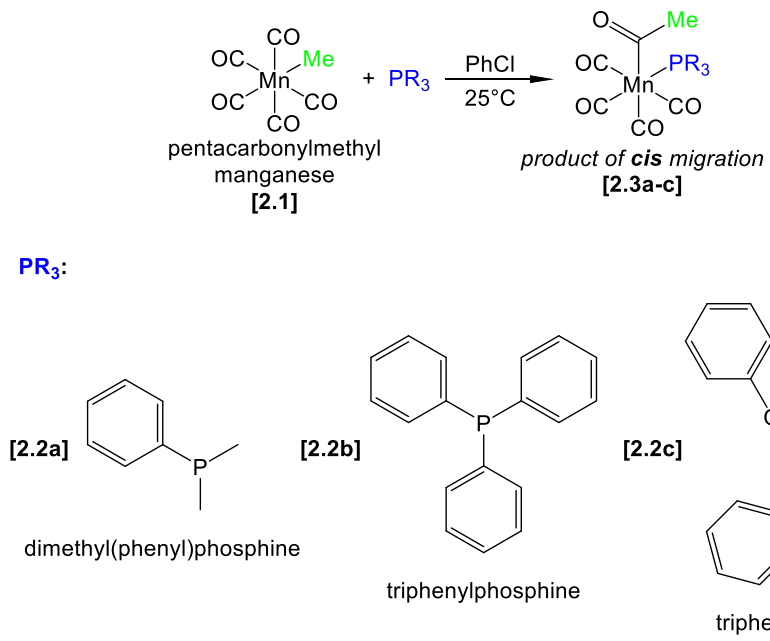

Scheme 2.1 Schematic representation of the investigated reactions within the study of cis-migration of the methyl group within **2.1** complex induced by organophosphorous Lewis bases (**2.2a-c**) and 2D representations of used Lewis bases throughout ITC experiments and static DFT-D calculations.

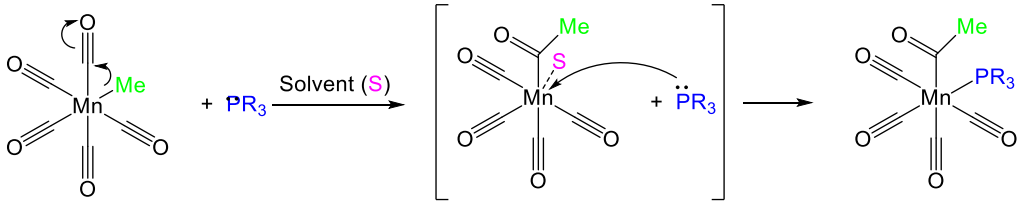

Scheme 2.2 Simplified schematic representation of the mechanism of the investigated reactions within the study of cis-migration of the methyl group within **2.1** complex induced by organo-phosphorous Lewis bases (**2.2a-c**).

5.2. Experimental section.

5.2.1. Generalities.

As mentioned in the introductory chapter, the experiments considered a reaction of the pentacarbonylmethylmanganese complex (**2.1**) with various Lewis bases - organophosphorous compounds (**2.2a-c**) (see Scheme 2.1). The reaction supposedly involves the *cis-migration* of the methyl group to carbon-monoxide ligand and subsequent insertion of the Lewis base into the manganese complex.

5.2.2. Techniques.

The investigations within the study of the reaction of the pentacarbonylmethylmanganese complex (**2.1**) with various of Lewis bases (**2.2a-c**) were preformed using ITC measurements and static DFT-D calculations, while the synthesis and the reaction tests were carried out using standard Schlenk line experimental technique.

The chemical characterizations were done employing Nuclear Magnetic Resonance (NMR) and Infrared (IR) spectroscopy.

5.2.3. Materials.

All used compounds were stored and used into a dry and argon filled glove box or under argon. Chlorobenzene was purchased from Sigma Aldrich and distillated over calcium hydride and degassed prior to use. The pentacarbonylmethylmanganese complex (**2.1**) was prepared by modified literature procedure.[221] Decacarbonyl-dimanganese was purchased from Sigma Aldrich and used as received. Methyl-iodide was purchased from Sigma Aldrich and used as received. The phosphines (**2.2a-b**) and the phosphite (**2.2c**) were purchased from Sigma Aldrich and used as received after checking their purity by NMR. All used solvents in the synthesis and reaction tests (CH_2Cl_2, THF) were purchased from Sigma Aldrich and distillated over an appropriate drying agent prior to use. Deuterated chloroform was purchased from Sigma Aldrich and dried through neutral alumina prior to use

5.2.4. Reaction tests.

The reaction tests were carried out using standard Schlenk line experimental technique. Hence the tests of all the investigated systems (**2.1**/**2.2a-c**) were performed in the same manner, only the general procedure is given.

The tests considered few different experiments:

-*Tests in chlorobenzene as the solvent*:

The Schlenk tube was charged with 0.08 mmol of **2.1** (16.8 mg) and ca. 0.07-0.075 mmol of **2.2a-c**. To the reactants 20 mL of chlorobenzene was added and the mixture was allowed to stir for 4.5-30 hours at 25-35ºC. Then, the solvent and the slight excess of **2.1** was evaporated under reduced pressure. The residue was washed with pentane (3x5 mL) and dried for several

[221] [N^0 482] R. D. Closson, J. Kozikowski, T. H. Coffield, *J. Org. Chem.* **1957**, *22*, 598.

hours under reduced pressure. The resulting product was checked by NMR (as solution in deuterated chloroform) and IR (as powder) spectroscopy.

-*Tests in deureated* chloroform *as the solvent*:

The Schlenk tube was charged with 0.08 mmol of **2.1** (16.8 mg) and ca. 0.07-0.075 mmol of **2.2a-c**. To the reactants 3-5 mL of deuterated chloroform was added and the mixture was allowed to stir for 4.5h-30 hours at 2-35ºC. The reaction mixture was subsequent, without any further treatment, checked by NMR spectroscopy.

In addition, the same type of the experiments in deuterated chloroform was carried out with different starting molar ratio of the reactants (**2.1**:**2.2a-c** – 2:1 and 1:2).

The relevant NMR and IR spectra are reported either throughout the main text or in Supplementary Information.

5.2.5. ITC experimental details.

The solutions of the reactants (**2.1** and **2.2a-c**, see Scheme 5.1) were prepared by dissolving a mass of substrate in pure, freshly distilled and degassed chlorobenzene. The ITC experiments were performed using sequential injection at 25°C with a moderate stirring rate (150-200 rpm). In a typical ITC experiment, the solution of the complex **2.1** was introduced in the ITC sample cell while the servo-controlled ITC syringe (100 µL) contained the solution of Lewis base (**2.2a-c**). The reference (1.0 mL) was entirely filled with pure PhCl. As the experiments considered a large excess of the complex **2.1**, the concentration of its solution in pure PhCl spanned from around 20 mmol/L to 100 mmol/L, while the concentration of **2.2a-c** solutions were comprised between 10-20 mmol/L. The content of the syringe was injected into the sample cell through 7-10 equivalent injections (either 5.03 µL or 6.97 per injection, accordingly to the concentration of the Lewis base solution) with time delay between two consecutive injections of 2000-3000s, depending on the nature of the system. For each studied system at least three experiments under the same condition were done (with an exception in the concentration of the solutions of **2.1**, accordingly to the kinetic (in parallel to the thermodynamic) purpose of the performed experiments). A heat dilution of each investigated Lewis base (**2.2a-c**) in neat PhCl was estimated from the blank experiments (basically, the titration of the Lewis base in pure PhCl) performed under the same condition as the main experiments. Afterwards, the obtained heat of blank experiments was subtracted from all the corresponding titration curves. Enthalpy of reaction (ΔH_r) was obtained as a result of the experiment by summing up the heat released upon first three injections against molar content introduced during those three injections.

Resulting ΔH_r values represent an average value of three corresponding experiments. Unfortunately, this methodology of performing ITC experiment does not allow extracting reaction free energies (ΔG_r) and entropies (ΔS_r), while kinetics parameters of reaction, i.e. the initial rates and constants of reaction (v_{init} and k_{init}, respectively) as well as partial reaction order with respect to reactant in excess, might be obtained.

5.2.6. Static DFT-D calculation details.

All computations were performed by the DFT methods using Amsterdam Density Functional package (ADF2013 version).

Starting geometries of the reactants (**2.1** and **2.2a-c**, see Scheme 2.1) were taken from the CSD and optimized as singlet ground states in the chlorobenzene solution phase. Geometries of the reaction products (**2.3a-c**) were built up from the previously optimized reactants by changing the methyl group within the complex **2.1** with particular Lewis base (**2.2a-c**) and making acetyl group from the CO ligand in *cis* position regarding to the position of introduced Lewis base. All those manipulations were done using the software provided within the ADF package. The geometries of the reaction products constructed in such way were optimized as singlet ground states in the chlorobenzene solution phase.

5.2.7. Synthesis.

5.2.7.1. Synthesis of **2.1**

Synthesis of the pentacarbonylmethylmanganese complex was done following a modified literature procedure[222] Reaction scheme of the synthesis is depicted in Scheme ES 2.1.

$$Mn_2(CO)_{10} \xrightarrow[\text{THF, 0°C, 4h}]{\text{Hg/Na amalgam}} Na^+[Mn(CO)_5]^- \xrightarrow[\text{THF, 0°C, 2h}]{\text{MeI}} \underset{[\mathbf{2.1}]}{MeMn(CO)_5} + NaI$$

Scheme ES 2.1 Simplified schematic representation of the synthesis of the pentacarbonylmethylmanganese complex (**2.1**)

The modified procedure was the following: about 10 mL of liquid mercury (≈150 g, ≈0.67 mol) was put in a laboratory glass of 100 ml and washed with previously prepared ca. 18% HCl

solution (3x20 mL), then with distilled water (3x20 mL) and with acetone (3x20 mL). Washed mercury was transferred into a Schlenk tube and dried under reduced pressure over a night. Tiny pieces of sodium (2.22g, 0.097mol), washed with pentane (3x10 mL) and dried with a tissue paper, were carefully introduced into the Schlenk tube contained the mercury. After every portion, the Schlenk tube was immediately evacuated under reduced pressure. Then, the tube was allowed to cool down while the amalgam was displaced on the walls. Subsequently, 40 mL of freshly distilled THF was added. After adding decacarbonyldimanganese (4.00 g, 0.010 mol) a resulting mixture was allowed to stir for 4 hours at 0ºC. Resulting mixture is transferred via canula into another Schlenk tube that was charged with 2ml of methyl-iodide (4.56 g, 0.032 mol) and allowed to stir next 2 hours at 0ºC. To ensure the reaction completeness, the mixture was subsequently heated for 10 minutes. Then, the content is reduced to a half by evaporation under reduced pressure. After adding silica (ca. four spatulas), the evaporation was continued until dryness. The crude product was purified by chromatography (through silica) with pentane as an eluent. The solvent was removed under reduced pressure causing a crystallization of the product. After recrystallization from pentane, **2.1** was dried under reduced pressure for several hours at -20ºC.

Yield: 1.68g (39%).

^{1}H NMR (500 MHz, chloroform-*d*, δ, ppm) -0.11 (s, 3H). ^{13}C NMR (126 MHz, chloroform-*d,* δ, ppm) 251.6, 213.3. IR (solid phase – powder, ν, cm^{-1}) 2915, 2109, 1949, 1175.

5.3. Results and discussion.

5.3.1. Reaction tests.

Before performing the ITC experiments all the reaction systems (**2.1**/**2.2a-c**, Scheme 2.1) were investigated by standard Schlenk line technique in order to check whether the chosen reaction systems are suitable for further ITC investigations. Namely, to check whether as the reaction product only product of cis-migration-insertion sequence raises up as well as whether the acquiring of the product is enough swift.

[222] [N^{0} 482] R. D. Closson, J. Kozikowski, T. H. Coffield, *J. Org. Chem.* **1957**, *22*, 598.

According to the literature,[223] the system **2.1/2.2b** could be problematic, as it frequently gives a mixture of the cis/trans migration-insertion products. The other two systems **2.1/2.2a** and **2.1/2.2c** supposedly give only the *cis* product. If longer reaction time periods are applied, the product of the decarbonylation could be noticed, as well. Such possible reactions are schematically displayed in Scheme 2.3

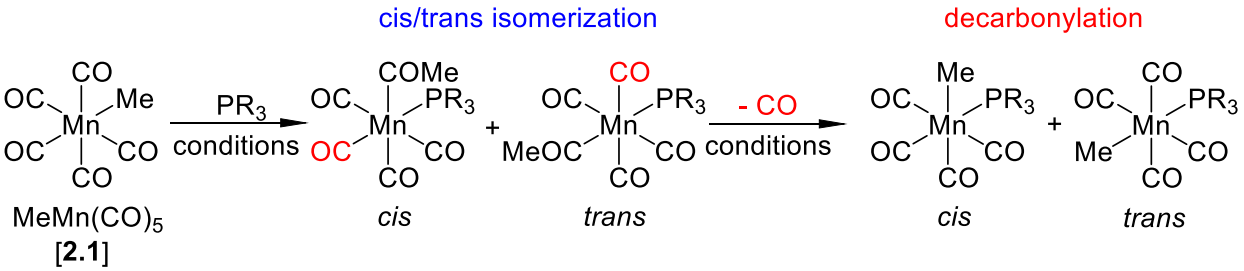

Scheme 2.3 Schematic representation of the possible side reactions (cis/trans isomerization and decarbonylation) within the study of cis-migration of the methyl group within **2.1** complex induced by organo-phosphorous Lewis bases (**2.2a-c**).

This investigation was based on the carrying out of the reaction of **2.1** with the chosen organo-phosphorous Lewis bases (**2.2a-c**) under various experimental conditions, i.e. reaction temperatures, reaction times and molar ratios between the reactants. After reactions, the reaction products were isolated and characterized by NMR and IR spectroscopy.

[223] [N^0 559] C. S. Krainhanzel, P. K. Maples, *J. Chem. Soc.* **1965**, *87*, 5267.
[N^0 560] R. N. Haszeldine, *J. Chem. Soc.* (*A*), **1969**, 698.

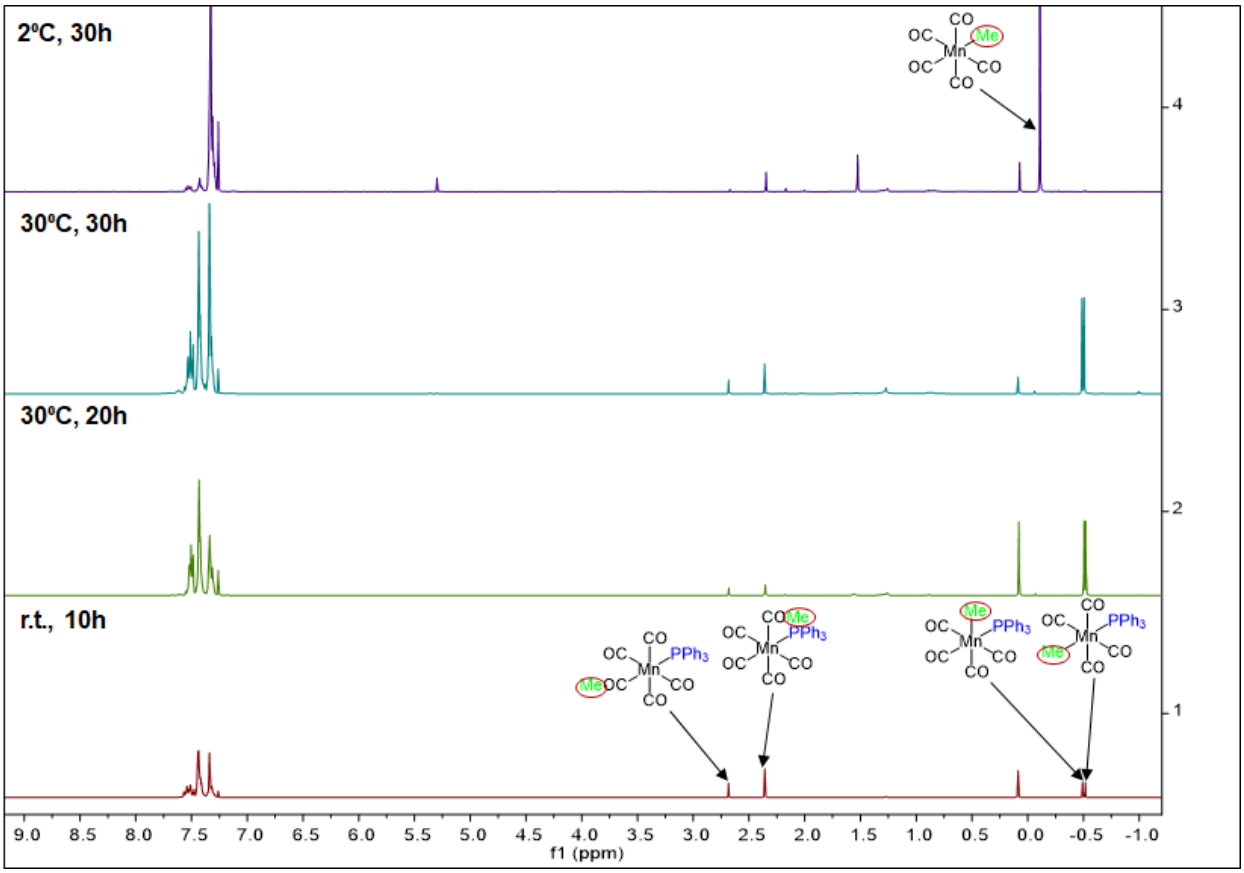

Figure 2.1 Superimposed ^{1}H NMR spectra of the reaction of **2.1** with **2.2b** carried out at various reaction temperatures (2ºC, ambient temperature and 30ºC) within various reaction times (10h, 20h and 30h). The spectra are recorded in deuterated chloroform at 400 MHz.

Figure 2.1 displays the ^{1}H NMR spectra of the obtained reaction products of the system **2.1**/**2.2b** by carrying out the reaction at the various reaction temperatures (at room temperature, 30ºC and 2ºC, respectively) within 10h, 20h and 30h, respectively. Noticeably, in the cases when the reaction was carried out at the room temperature or at the higher one within 10h or more, the reaction product was constituted of the mixture of the cis/trans products as well as of the products of the decarbonylation. Otherwise, the reaction preformed at 2ºC even within 30h gave almost only the *cis* reaction product without the product of the decarbonylation process. In all the cases a certain amount of the starting materials is always noticeable, which means that an equilibrium takes place (as an addition, see ^{31}P NMR spectra of the same reactions that are shown in Figure 2.2). The reaction of **2.1** with **2.2b** was carried out with different starting molar ratios of the reactants, as well. The corresponding NMR spectra are given in Supplementary Information (see Figures SI 2.1-7). Nonetheless, the same conclusions could be drawn (occurrence of the cis/trans products and reaction equilibrium). Altogether, the results of the

reaction tests of the system **2.1**/**2.2b** suggest the existence of an equilibrium between the reactants and reaction products as well as the possibility to avoid the cis/trans isomerization and decarbonylation of the (cis) reaction product by performing the reaction at lower temperature or within shorter reaction time periods. Therefore, the ITC measurements of the system **2.1**/**2.2b** should be constrained to relatively short reaction time (at most to one hour) and, in order to reach the reaction completion, to the presence of one of the reactants in excess.

The results of the reaction tests of the systems **2.1**/**2.2a** and **2.1**/**2.2c** confirmed the results from the literature. There is no formation of the trans isomer, only cis-migration-insertion product is noticed, as it can be seen from the ^{1}H NMR spectrum of **2.1**/**2.2a** shown in Figure 2.3. The ^{31}P NMR spectrum of **2.1**/**2.2a** is displayed in Figure 2.4. As the NMR spectra of **2.1**/**2.2a** and **2.1**/**2.2c** are similar, the spectra of the latter one are provided in Supplementary Information (see Figure SI 2.8-9). Expectedly, the equilibrium between the reactants and the product is observed. Due to a higher reaction temperature (up to 35ºC) and longer reaction time periods (especially in the case of **2.1**/**2.2c**) a small amount of the decarbonylated product is noticed. Regarding to the NMR spectra, the more pronounced equilibrium in **2.1**/**2.2c**. is the only difference between these two systems (**2.1**/**2.2a** and **2.1**/**2.2c**).

Supplementary to the NMR characterization, solid state (powder) IR experiments of all the systems are done. The IR results are in accordance with the observations (discussed above) provided by NMR spectroscopy. The IR spectra of all the investigated system are given in Supplementary Information (see Figures SI 2.12-15)

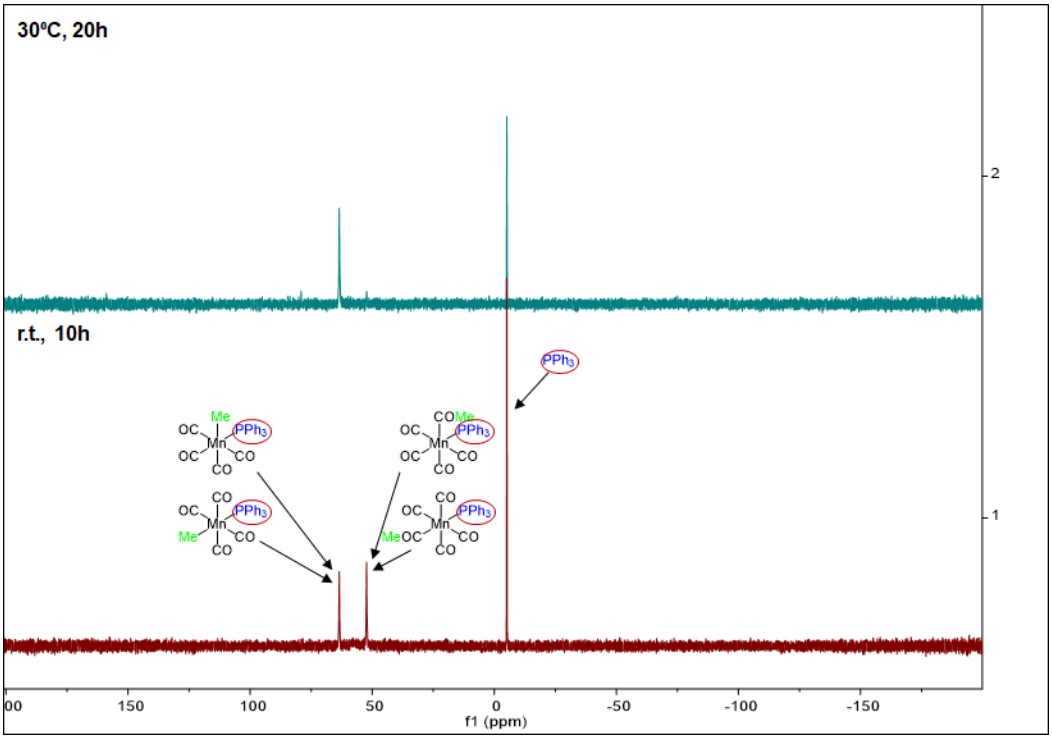

Figure 2.2 Superimposed ^{31}P NMR spectra of the reaction of **2.1** with **2.2b** carried out at various reaction temperatures (ambient temperature and 30ºC) within various reaction times (10h and 20h). The spectra are recorded in deuterated chloroform at 121 MHz.

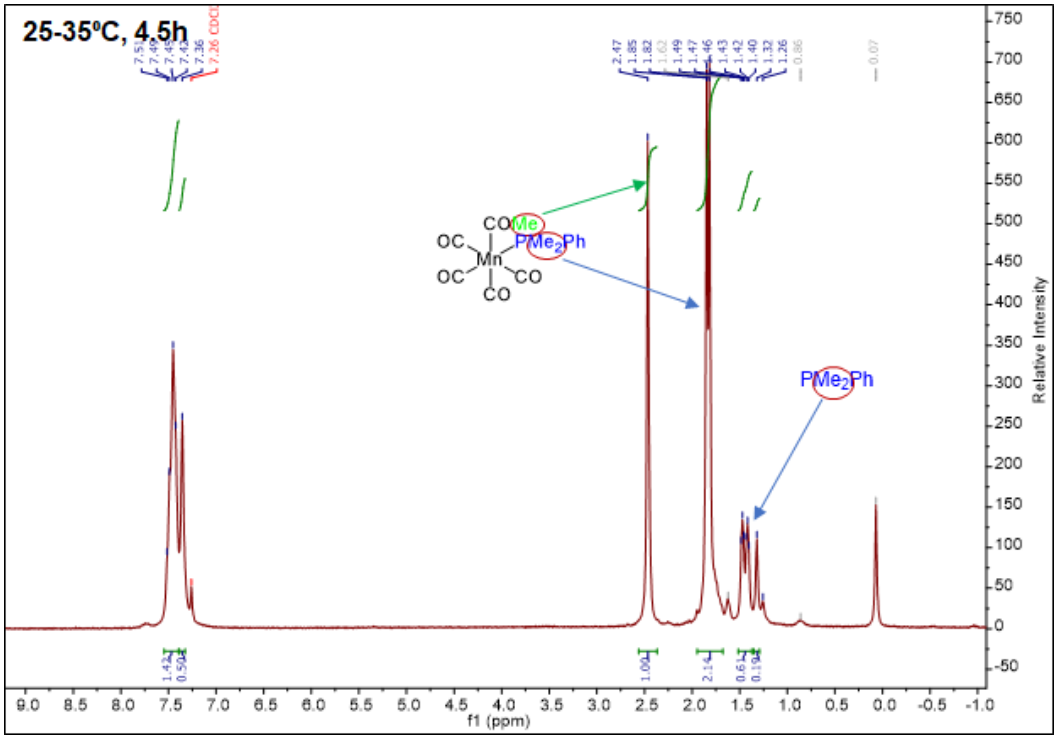

Figure 2.3 ^{1}H NMR spectra of the reaction of **2.1** with **2.2a** carried out in the temperature span from 25ºC to 35ºC within 4.5h. The spectrum is recorded in deuterated chloroform at 400 MHz.

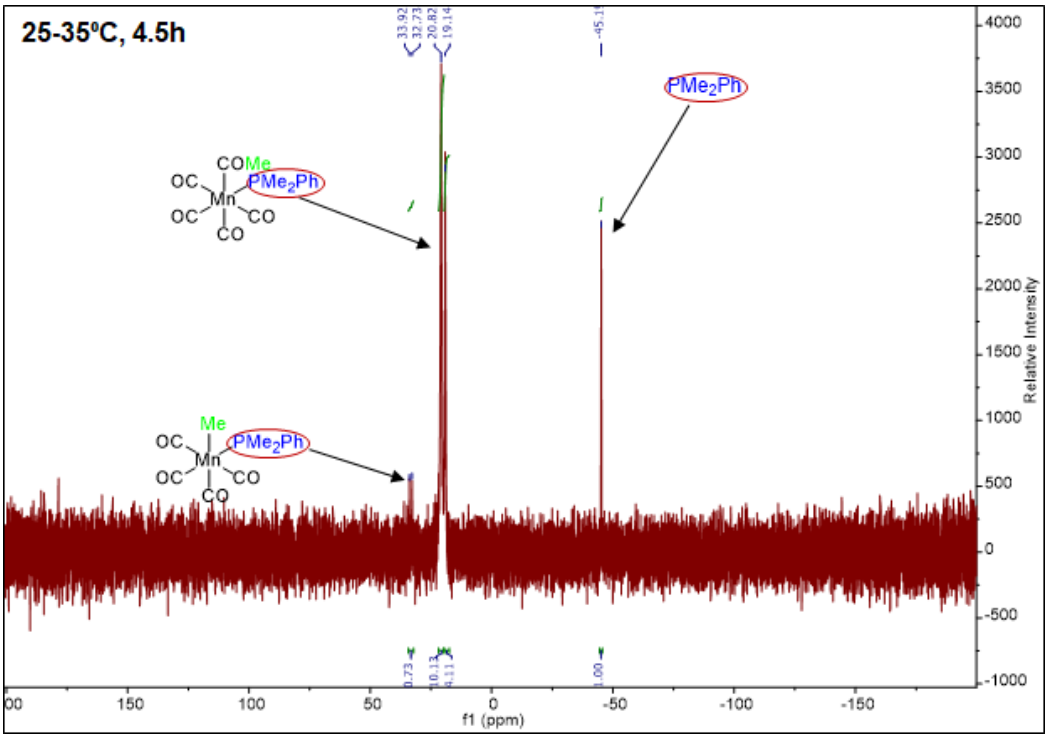

Figure 2.4 ^{31}P NMR spectra of the reaction of **2.1** with **2.2a** carried out in the temperature span from 25ºC to 35ºC within 4.5h. The spectrum is recorded in deuterated chloroform at 121 MHz.

5.3.2. ITC experiments.

5.3.2.1. Generalities.

The first challenge which has been met in the optimization of ITC experimental conditions was the reaction rate as well as the temperature at which the reactions should be performed. Namely, the reaction rate appeared to be quite low in rather standard ITC conditions (concentration of the sample cell's solution 1-5 mmol/L; concentration of the syringe's solution around 25 times higher). The changing of the order of reactants, i.e. what kind of solution (either the solution of **2.1** or Lewis base (**2.2a-c**)) contained the sample cell and the syringe, respectively, did not give a satisfying heat response (see the examples shown in Figure SI 2.16-17). The increase of the reaction temperature did not produce enough swift heat release, as well. As neither the change of order of the reactants nor the change of temperature made these reaction systems exploitable under ITC investigation, only one possibility was left. Namely, to increase the rate of an equilibrium reaction and to hurry the reaction to completion, the increase of the concentration of the sample cell's solution to a level of an excess regarding the conditions of the sequential injection mode of ITC experiment, might be helpful. In accordance to that fact

and to the prominent equilibrium features of the reactions (observed from the performed independent reaction tests), all ITC investigations within the study of the *cis-migration* – insertion reaction sequence were performed with large, but precisely defined, an excess of **2.1** (that was placed in the sample cell). In order to get kinetic characteristics of the particular reactions, in parallel to thermodynamic ones, the value of a large excess of **2.1** was varied. Accordingly, it was found that to reach the aim of ITC experiment, in other words, to get readable and reliable ITC thermograms, the concentration of the **2.1** solution, relative to the concentration of the **2.2a-c** solutions, should be at least three times larger (see Figure SI 2.19).

5.3.2.2. Thermodynamic study.

According to the employed conditions of the ITC experiments (mainly, the large excess of **2.1** in sample cell) reaction enthalpies (ΔH_r) only could be obtained. Namely, the reason why the other thermodynamic parameters (ΔG_r, ΔS_r, k_r) could not be obtained lies in the fact that it was not possible to fit the ITC thermograms (what would result in all the thermodynamic parameters) with any available *ad-hoc* logarithm. Thus, as the results of ITC thermodynamic study of the *cis-migration* – insertion reaction sequence only raw ΔH_r values are given (Table 2.1). In fact, to make a difference between the ΔH_r values resulted from a fitting of released and integrated ITC heat by an appropriate *ad-hoc* algorithm form these ΔH_r values, it should be more properly to call these ΔH_r values raw reaction enthalpy values (raw ΔH_r), as they are derived from a "raw" ITC data, that are, subsequently, manually transformed into ΔH_r (for more details of herein mentioned transformation, see ITC introductory chapter). As the ITC thermograms of all herein studied systems (**2.1**/**2.2a-c**) are quite similar, only the thermogram of **2.1**/**2.2a** is shown (Figure 2.5) in main text, while the others are given in Supplementary Information (Figure SI 2.18-19). It is important to notice that, according to the shape of the ITC thermogram of the system **2.1**/**2.2b** (Figure SI 2.18), the possible isomerization of the product **2.3b** (Scheme 2.1) is rather unlikely to happen.

Table 2.1 ITC results obtained as raw values from the sequential addition ITC experiments that considered an excess of **2.1** interacting with organo-phosphorous Lewis base (**2.2a-c**).

System	raw ΔH_r ± error [kcal/mol]
2.3a	-12.4 ± 0.3
2.3b	-10.6 ± 0.2
2.3c	-9.1 ± 0.2

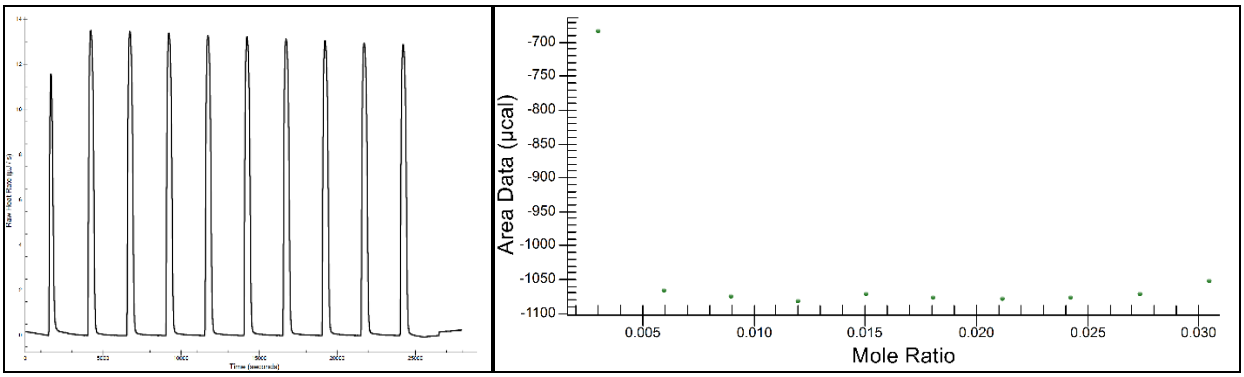

Figure 2.5. *left side* – ITC thermogram of the reaction between **2.1** (sample call, c=20.91 mM) and **2.2a** (syringe, c=12.31 mM) in chlorobenzene. The titration was performed at 25ºC through 10 sequential additions (of 5.03 µL each). Time between two consecutive injections was 2800 s. Heat released is expressed in µJ/s versus time in s. *right side* – ITC integrated heat peaks of the thermogram shown on the left side. Integrated heats are expressed in µcal versus molar ratio of the reactants.

Although the obtained ITC results (raw ΔH_r) are similar, ranged from ca. -9 kcal/mol to -12.5 kcal/mol, they are rather consistent. Namely, the relatively small difference (of ca. 3.5 kcal/mol) between their raw ΔH_r values, might be directly related to their structural characteristics. In comparison to the others, **2.2c** possesses most flexible, but, in the same time, the biggest substituents (-*OPh*). It seems that its bulkiness could not be compromised by its flexibility, as the system **2.1**/**2.2c** showed the lowest raw ΔH_r values (-9.1 kcal/mol). Therefore, by decreasing the steric cluttering around the phosphorous atom (from **2.2c** to **2.2a**) the availability of the phosphorous atom (as most reactive part within the molecule) for reaction with **2.1** increases, what apparently leads to larger raw ΔH_r values alongside the series (from **2.2c** to **2.2a**).

A possible interference of chlorobenzene (which could be considered as a weak Lewis base, as well) on the investigated reaction sequence was not estimated. One more issue that might be addressed is a capability of chlorobenzene to promote the *cis-migration* of the methyl group within **2.1**. complex.

5.3.2.3. Kinetic study.

As mentioned in the ITC introductory chapter, one of the prerequisites of the ITC kinetic study is a gradually changing of concentration in one reactant retaining a concentration of second one as constant. As well, a heat response of the first or, furthest, the second injection, should be properly established, in order to avoid the complications related to the accuracy of concentration of solutions that are present in the calorimeter. Herein the imposed conditions (a large excess of

2.1) of ITC experiments allowed such kinetic study, as each ITC experiment within each studied system (**2.1**/**2.2a-c**) were carried out with different concentration in **2.1** complex. As the experiments were performed in the presence of a large excess of **2.1**, further manipulations of the ITC data and the obtaining kinetic parameters were simplified, according to the well-known fact of kinetics with one reactant in excess. Consequently, only initial rate constants and partial reaction order with respect to reactant in excess could be derived.

Caused by not well established first two heat peaks in the systems **2.1**/**2.2a** and **2.1**/**2.2c** as well as by lack of starting materials to redo the ITC experiments, only the data of **2.1**/**2.2b** were managed.

The results of the kinetic ITC study of the system **2.1**/**2.2b** are summarized in Table 2.2 including the used concentration of each reactant solution. It can be noticed that the concentration of **2.1** was ca. 3-6 times larger from the concentration of **2.2b**, but under the used ITC experimental conditions that ratio is multiplied representing the molar ration ca. 1:500-1000 in favor to **2.1** (see right side of Figure SI 2.18 or Figure 2.5, as the illustrative example). By plotting the initial ITC rates of reaction (ITC Rate) of the very first few seconds after the ITC lag time against time (t) and subsequent linear fitting the data, the value of *k* could be obtained from the slope. Similarly, by plotting the logarithmic values of exact concentration of **2.2b** in given time ($\ln(c_t(\mathbf{2.2b}))$ against time (t) the value k_{obs} could be obtained. The plots *ITC Rate* against *t* and $ln(c_t(\mathbf{2.2b}))$ against *t* are displayed in Figure 2.6 and in Figures SI 2.20-21. To gain the partial reaction order with respect to **2.1**, *k* or k_{obs} values of at least three independent ITC experiments should be linearly correlated with logarithmic values of the used concentrations of **2.1** within these ITC experiments ($ln(c_0(\mathbf{2.2b}))$). Thus, Figure 2.7 shows a dependence between *k* (and k_{obs}) values and $ln(c_0(\mathbf{2.2b}))$. For more details what *k* and k_{obs} exactly represent as well as how their values could be obtained see Methodology chapter (page 87).

Table 2.2 Results of the ITC kinetic study obtained from the sequential addition ITC experiments that considered an excess of **2.1** interacting with organo-phosphorous Lewis base **2.2a**.

Nº exp	[**2.2b**] mmol/L	[**2.1**] mmol/L	Molar ratio under ITC conditions	**k**	**order** with respect to **2.1**	$\mathbf{k_{obs}}$	**order** with respect to **2.1**
1	16.93	101.43	1:855	$3.3*10^{-3} \pm 3*10^{-4}$		$2.8*10^{-5} \pm 2*10^{-6}$	
2	18.61	74.57	1:572	$2.5*10^{-3} \pm 2*10^{-4}$	**0.94 ± 0.03**	$1.9*10^{-5} \pm 2*10^{-6}$	**0.93 ± 0.16**
3	17.46	54.57	1:446	$1.8*10^{-3} \pm 2*10^{-4}$		$1.6*10^{-5} \pm 1*10^{-6}$	

For more details what do *k* and k_{obs} exactly represent as well as how their values could be obtained see ITC methodology chapter.

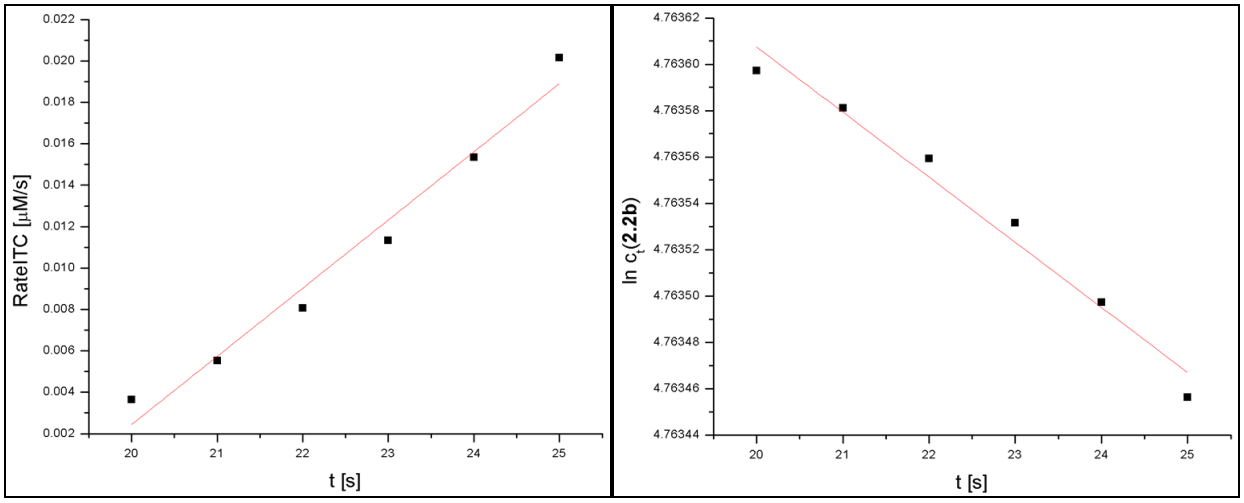

Figure 2.6 *left side* - Linear fit of the plot of the ITC Rate as a function of time for the reaction of **2.1** (sample call, c=101.43 mM) with **2.2b** (syringe, c=16.93 mM) carried out in ITC calorimeter. ITC Rate is expressed in µM/s and time in s. Obtained $\boldsymbol{k = 3.3*10^{-3} \pm 3*10^{-4}}$, as the result of the fitting. *right side* - Linear fit of the plot of logarithm of **2.2b** concentration as a function of time for the same reaction. Obtained $\boldsymbol{k_{obs} = 2.8*10^{-5} \pm 2*10^{-6}}$ as the result of the fitting.

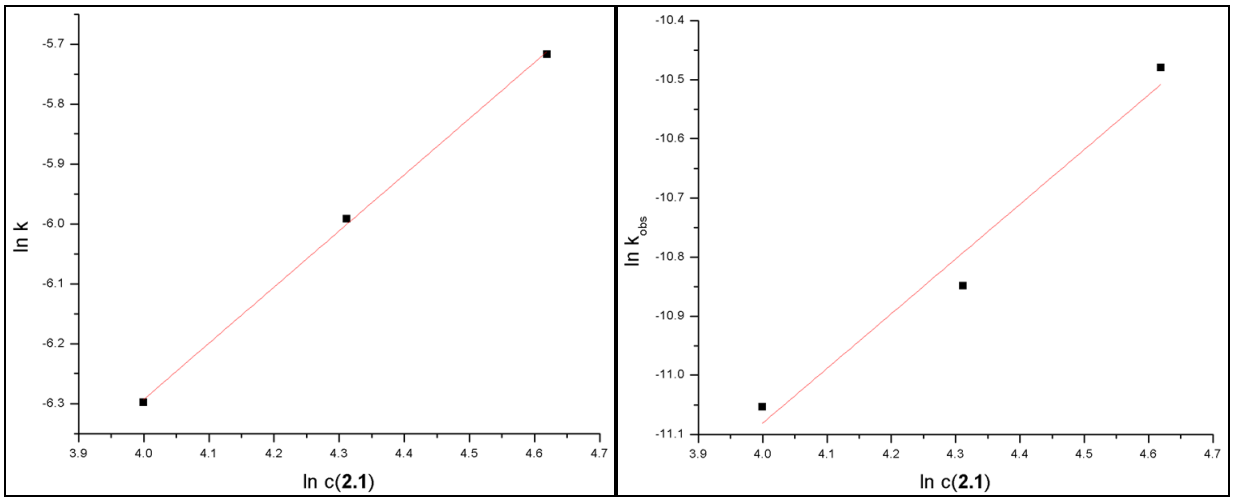

Figure 2.7 *left side* - Linear fit of the plot of logarithm of obtained *k* values as a function of the logarithm of **2.1** starting concentrations for the reaction of **2.1** with **2.2b** carried out in ITC calorimeter. Obtained partial reaction order with respect to **2.1** is **0.94 ± 0.03**, as the result of the fitting. *right side* - Linear fit of the plot of logarithm of obtained k_{obs} values as a function of the logarithm of **2.1** starting concentrations for the reaction of **2.1** with **2.2b** carried out in ITC calorimeter. Obtained partial reaction order with respect to **2.1** is **0.93 ± 0.16**, as the result of the fitting.

Based on the obtained *k* or k_{obs} values, that are rather small (ranged from $1.8*10^{-3}$ to $3.3*10^{-3}$ and from $1.6*10^{-5}$ to $2.8*10^{-5}$, respectively), one could conclude that the cis-migration of the methyl group induced by **2.2b** and following insertion of **2.2b** into **2.1** is a rather slow process. The obtained order value of ca. 0.94, as the final result of the kinetic ITC investigation, suggests partial first reaction order with respect to **2.1**. According to the similar structures of the Lewis base along herein studied series (**2.2a-c**), it could be concluded that partial first reaction order with respect to **2.1** takes place in the reaction of **2.1** with the two other Lewis bases (**2.2a** and **2.2c**). Although such result has been already proven by other experimental techniques,[224] this investigation showed again ITC's powerful abilities in accurate measurement of released heat and, in turn, in precise determination of initial rates/rate constants of reaction as well as of partial reaction orders.

5.3.3. Static DFT-D calculations.

All computations within the study of cis-migration of the methyl group (to CO ligand) followed by insertion of the organo-phosphorous compound (**2.2a-c**) to the pentacarbonylmethylmanganese complex (**2.1**) were performed at ZORA-GGAPBE-D3(BJ)/TZP level of theory in chlorobenzene solution (COSMO) phase. The geometry optimizations were done for all the reactants (**2.1**, **2.2a-c**) and corresponding products (**2.3a-c**, Scheme 2.1) and conformed as true minima by performing calculations of vibrational modes. The resulting optimized geometries of the products are shown in Figure 2.8 while Cartesian's coordinates of all the optimized geometries within this study are given in Supplementary Information (see SI, section A.2.4.). Thermodynamic parameters (ΔH_r, ΔG_r, ΔS_r), derived as results of the performed static DFT-D calculations, are reported in Table 2.3.

Table 2.3 Results of static DFT-D calculations. The calculations were performed at ZORA-GGAPBE-D3-BJ/TZP level of theory in chlorobenzene solution (COSMO) phase.

System	Level of theory	ΔH_r [kcal/mol]	ΔG_r [kcal/mol]	ΔS_r [cal/Kmol]
2.3a	ZORA-GGAPBE-D3(BJ)/TZP - PhCl	-31.3	-17.0	-48.1
2.3b	ZORA-GGAPBE-D3(BJ)/TZP - PhCl	-25.4	-9.5	-53.5
2.3c	ZORA-GGAPBE-D3(BJ)/TZP - PhCl	-21.6	-7.9	-46.1

[224] [N^0 495] R. J. Mawby, F. Basolo, R. G. Pearson, *J. Am. Chem. Soc*. **1964**, *86*, 3994.

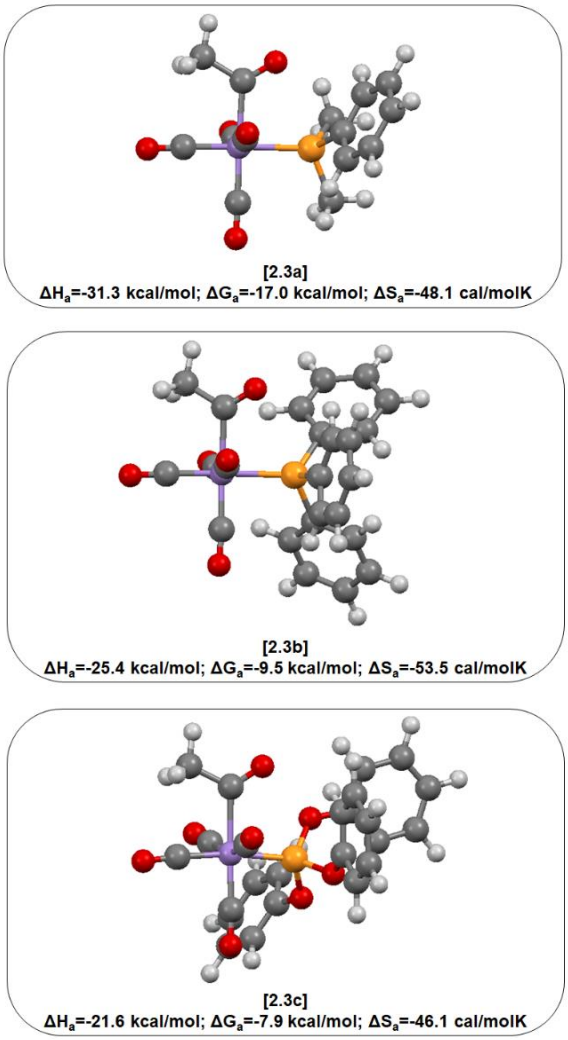

Figure 2.8 Graphic representations of optimized geometries of the investigated systems at ZORA-GGAPBE-D3-BJ/TZP level of theory in chlorobenzene solution (COSMO) phase. P: orange; O: red; Mn: violet; C: grey; H: white.

The results of the ΔH_r, ranged from ca. -22 kcal/mol to -31 kcal/mol, suggest that strong to very strong chemical attraction takes place in the chemical transformation of **2.1** with the Lewis bases **2.2a-c** to the corresponding products **2.3a-c**. The particular values of the reaction entropy are rather consistent. Namely, similarly to the results of ITC experiments, the largest ΔH_r belongs to the system **2.1**/**2.2a**, that possesses the smallest substituents (one phenyl and two methyl) compared to the other systems (Scheme 2.1). Most probably that fact allows the phosphorus atom to establish more efficient connection to the manganese as well as more appropriate interactions between the substituents of the reactants. Regarding the other two studied Lewis bases (**2.2b-c**), that possess larger substituents (three -Ph and three -OPh groups, respectively), it could be concluded that repulsive interactions within the systems

2.1/**2.2b-c** are more expressed. In addition, the presence of three electronegative oxygen atoms directly connected to the phosphorous atom (**2.2c**) might decrease the availability of the phosphorous' free electron pair that would be reflected on the strength of P-Mn bond. The computed Gibbs free enthalpies (ca. -8 kcal/mol - -17 kcal/mol) confirmed rather spontaneous process of the studied chemical transformation. The obtained negative values of ΔS_r (ca. -50 cal/Kmol) are in accordance with the fact of the reducing of entropy during the regarded chemical transformation.

By comparing the ΔH_r values obtained by static DFT-D calculations and ITC measurements, it could be noticed that the calculations do overestimate the ΔH_r values of all the systems for ca. 2.5 times (see Table 2.4). One of possible reasons for such difference between the experimental and theoretical ΔH_r values might be poor solvation treatment within the calculations. Namely, chlorobenzene as a weak nucleophile could, in principle, interact with the **2.1** after the cis-migration step as well as with Lewis bases (**2.2a-c**) by its aromatic ring, but rather differently according to the structures of the **2.2a-c**. Therefore, an estimation of the interactions of the reactants (**2.1**, **2.2a-c**) with chlorobenzene is necessary.

Table 2.4 Ratio of ΔH_r values of the systems **2.1/2a-c** obtained as the results of static DFT-D calculations (ZORA-GGAPBE-D3-BJ/TZP (COSMO)) and sequential injection ITC measurements.

System	Static DFT-D ΔH_r/ITC raw ΔH_r
2.3a	2.5
2.3b	2.4
2.3c	2.4

5.4. Chapter conclusion.

The supposed *cis-migration* of the methyl group within the pentacarbonylmethylmanganese complex (**2.1**, Scheme 2.1) induced by various organo-phosphorous Lewis bases (**2.2a-c**, Scheme 2.1) and subsequent insertion of the Lewis bases into the complex **2.1** were examined experimentally (by the reaction tests using standard Schlenk line technique, Nuclear Magnetic Resonance (NMR) spectroscopy, Infrared (IR) spectroscopy and Isothermal Titration Calorimetry (ITC)), and theoretically (by static Density Functional Theory (DFT) with Grimme's dispersion correction – D3).

The reaction tests were done in order to verify whether the chosen reaction systems are suitable for the ITC investigations. The tests were carried out in chlorobenzene (with

subsequent isolation of the products) and deuterated chloroform (without the isolation of the product) as the solvent in the temperature span 2-35 ºC within 4.5-30h. The ITC experiments considered sequential addition of **2a-c** into a large excess (ca. 450-850 times) of **2.1**. The static DFT-D calculations were performed at ZORA-GGAPBE-D3(BJ)/TZP level of theory in chlorobenzene solution (COSMO) phase. As ITC results partial reaction order with respect to **2.1** and raw ΔH_r values are obtained while the calculations gave the values of all thermodynamic parameters of the reaction (ΔH_r, ΔG_r, ΔS_r).

The reaction tests suggested that the side reactions (i.e. the isomerization and decarbonylation of the *cis* product) could be avoided at lower reaction temperatures within shorter reaction times.

The ITC thermodynamic results (range of ITC raw ΔH_r -9 – -12.5 kcal/mol) suggested that reasonably stronger interactions could be established through the examined *cis-migration*-insertion reaction sequence. The particular raw ΔH_r values are rather consistent in terms of the structural differences among the used Lewis bases (**2.2a-c**), representing the influence of steric hindrance on achieving of more appropriate interactions. The ITC kinetic results have confirmed partial first reaction order with respect to the complex **2.1**.

Although, the static DFT-D COSMO calculations predicted much larger reaction enthalpies - ΔH_r values from ca. -22 kcal/mol to -31 kcal/mol, the computed ΔH_r values are mutually in accordance (regarding their structural and electronic (manly phosphorous' free electron pair availability) characteristics) and ca. 2.5 times larger than ITC raw ΔH_r values. Such overestimation might be the consequence of improper treatment of the solvation through the computations. Regarding to the computed Gibbs free energies (ΔG_r values from ca. -8 kcal/mol to -17 kcal/mol), all the examined systems (**2.1/2.2a-c**) might give the reaction products (**2.3a-c**) quite spontaneously.

Outlook. The research should be supplemented with reaction tests carried out in ITC conditions, i.e. when **2.1** is present in (large) excess. A possible interference of chlorobenzene on the investigated reaction sequence to be estimated, especially by the calculations. It would be interesting to address the ability of chlorobenzene to promote the *cis-migration* of the methyl group within **2.1**. complex itself. An estimation of BSSE as well as a calculation of interaction energies of all herein studied systems would be appreciable.

5.5. Закључак поглавља.

Претпостављена *cis* миграција метил групе унутар комплекса метил-манган-пентакарбонила (**2.1**, схема 2.1) узрокована различитим органофосфорним базама (**2.2a-c**, схема 2.1) и накнадна инсерција Lewis-ових база у комплекс **2.1** испитана је експериментално (реакционим тестовима применом стандардне Schlenk line технике, нуклеарном магнетном резонанционом (енг. NMR) спектроскопијом, инфрацрвеном (енг. IR) спектроскопијом и изотермалном титрационом калориметријом (енг. ITC)), и теоријски (помоћу статичке теорије функционала густине (енг. DFT) са Grimme-овом корекцијом за дисперзију - D3).

Реакциони тестови су извршени како би се проверило да ли су изабрани реакциони системи погодни за испитивање помоћу ITC-а. Тестови су изведени у хлоробензену (уз накнадно изоловање производа) и деутерисаном хлороформу (без изоловања производа) као растварачу у распону температуре од 2-35 ºC у периоду од 4,5-30h. ITC експерименти подразумевали су постерено додавање **2a-c** у велики вишак (око 450-850 пута) комплекса **2.1**. Статички DFT-D прорачуни урађени су на ZORA-GGAPBE-D3(BJ)/TZP теоријском нивоу у раствору хлоробензена (COSMO). Као ITC резултати добијени су парцијални ред реакције у односу на **2.1** и сирове (raw) ΔH_r вредности, док су прорачунима добијене вредности свих термодинамичких реакционих параметара (ΔH_r, ΔG_r, ΔS_r).

Реакциони тестови указују на то да се нежељене реакције (тј. изомеризовање и декарбониловање *cis* производа) могу избећи при нижој реакционој температури и краћем трајању реакције.

ITC термодинамички резултати (ITC сирове (raw) ΔH_r вредости у распону од -9 до -12,5 kcal/mol) указали су да би се разумно јаче интеракције могле успоставити посредством испитиване *cis* миграционе-инсерционе реакционе секвенце. Појединачне сирове (raw) ΔH_r вредности прилично су конзистентне у погледу структурних разлика међу коришћеним Lewis-овим базама (**2.2a-c**), што одражава утицај стерних сметњи на формирање јачих интеракција. ITC кинетички резултати потврдили су први ред реакције у односу на комплекс **2.1**.

Иако су статички DFT-D COSMO прорачуни предвидели много веће (око 2,5 пута) реакционе енталпије - ΔH_r вредности од око -22 kcal/mol до -31 kcal/mol, израчунате ΔH_r

вредности међусобно су усклађене (с обзиром на структурне и електронске (углавном доступност слободног електронског пара на фосфору) карактеристике испитиваних система) и око 2,5 пута веће од ITC сирове (raw) ΔH_r вредности. Таква прецењивања могу бити последица неправилног третмана растварача у оквиру теоријских прорачуна. Израчунате вредности Gibbs-ове слободне енергије (ΔG_r вредности од око -8 kcal/mol до -17 kcal/mol), указују на то да би сви испитивани системи (**2.1/2.2a-c**) могли дати реакционе производе (**2.3a-c**) прилично спонтано.

Перспектива. Истраживање би требало допунити реакционим тестовима изведеним у ITC условима, тј. у присуству **2.1** у (великом) вишку. Требало би проценити могући утицај хлоробензена на испитивану реакциону смешу, нарочито прорачунима. Било би интересантно испитати способност хлоробензена да самостално промовише *cis* миграцију метил групе унутар комплекса **2.1**. Такође би била пожељна процена BSSE-а, као и израчунавање енергије интеракције свих проучаваних система у овој студији.

5.6. Conclusion du chapitre

La migration *cis* supposée du groupe méthyle dans le complexe pentacarbonylméthylmanganèse (**2.1**, schéma 2.1) induite par diverses bases de Lewis organophosphorées (**2.2a-c**, schéma 2.1) et l'insertion ultérieure des bases de Lewis dans le complexe **2.1** ont été examinées expérimentalement (par des tests de réaction utilisant la technique de la ligne de Schlenk standard, la spectroscopie par résonance magnétique nucléaire (RMN), la spectroscopie infrarouge (IR) et la calorimétrie par titrage isotherme (ITC)) et théoriquement (DFT) avec la correction de la dispersion de Grimme – D3.

Les tests de réaction ont été effectués afin de vérifier si les systèmes réactionnels choisis sont appropriés pour les investigations ITC. Les tests ont été effectués dans du chlorobenzène (avec isolation subséquente des produits) et du chloroforme deutérié (sans isolement du produit) en tant que solvant dans l'intervalle de température de 2 à 35 ° C dans un espace de 4,5 à 30 heures. Les expériences ITC ont considéré l'addition séquentielle de **2a-c** en large excès (environ 450-850 fois) de **2.1.** Les calculs DFT-D statiques ont été effectués au niveau de théorie ZORA-GGAPBE-D3 (BJ) / TZP dans la phase solution de chlorobenzène (COSMO). En tant que résultats ITC, l'ordre partiel en **2.1** et les valeurs brutes ΔH_r sont obtenus tandis que les calculs donnent les valeurs de tous les paramètres thermodynamiques de la réaction (ΔH_r, ΔG_r, ΔS_r).

Les essais de réaction ont suggéré que les réactions secondaires (c'est-à-dire l'isomérisation et la décarbonylation du produit cis) pourraient être évitées à des températures de réaction plus basses dans des temps de réaction plus courts.

Les résultats thermodynamiques de l'ITC (fourchette de ΔH_r -9 - -12,5 kcal/mol de l'ITC raw) suggèrent que des interactions raisonnablement plus fortes pourraient être établies grâce à la séquence de réaction de l'insertion et de la migration *cis* examinée. Les valeurs brutes de ΔH_r sont plutôt cohérentes en termes de différences structurelles parmi les bases de Lewis utilisées (**2.2a-c**), représentant l'influence de l'empêchement stérique sur l'obtention d'interactions plus appropriées. Les résultats cinétiques de l'ITC sont confirmés au premier ordre dans le complexe **2.1**.

Bien que, les calculs statiques DFT-D COSMO prédisent des enthalpies de réaction beaucoup plus grandes - les valeurs de ΔH_r d'environ de -22 kcal/mol à -31 kcal/mol, les valeurs calculées

de ΔH_r sont mutuellement conformes (en ce qui concerne leurs caractéristiques structurelles et électroniques (disponibilité des paires d'électeurs libres de phosphore)) et environ 2,5 fois plus grand que les valeurs ΔH_r brutes ITC. Une telle surestimation pourrait être la conséquence d'un mauvais traitement de la solvatation à travers les calculs. En ce qui concerne les énergies libres de Gibbs calculées (valeurs de ΔG_r comprises entre environ -8 kcal/mol et -17 kcal/mol), tous les systèmes examinés (**2.1**/**2.2a-c**) pourraient donner les produits de réaction (**2.3a-c**) de manière très spontanée.

Perspective. La recherche devrait être complétée par des tests de réaction effectués dans des conditions ITC, c'est-à-dire lorsque **2.1** est présent en excès (important). Une éventuelle interférence du chlorobenzène sur la séquence de réaction étudiée doit être estimée, notamment par les calculs. Il serait intéressant d'aborder la capacité du chlorobenzène de favoriser la migration *cis* du groupe méthyle au sein de **2.1** complexe lui-même. Une estimation de la BSSE ainsi qu'un calcul des énergies d'interaction de tous les systèmes étudiés ici seraient appréciables.

Chapter 6

Amination of Fischer carbenes

6.1. Introduction.

Fischer type carbenes, discovered by Fischer and Maasböl in 1964,[225] could be expressed by general structural formula of $(CO)_5M=C(X)R$ wherein carbene carbon atom is connected to a low-valent transition metal from VI-VIII group of PTE. The nature of the metal-carbene bond could be described as σ-donating/π-back-donating, while nature of binding within M-C-X as (weak) three-centered four-electron bonding interaction.[226] The group *X* is usually electron donating group having a stabilizing effect to electron deficient carbene carbon atom while *R* group could be either a saturated or unsaturated organic group. To stabilize low valent metal center many π accepting ligands could be employed. In the typical Fischer carbene complex these π accepting ligands are carbonyls.[227] Due to such constitution of the carbene, its general chemical characteristic could be described as electrophilic, opposite to Schrock type carbenes[228] that are nucleophilic. In particular, within the Fischer carbenes there are few potential reactive sites.[229] It has been found that a reacting mode of the Fischer carbenes could be an abstraction of methyl group from the methoxy substituent,[230] as well. As a consequence of possessing such versatile chemical properties, accompanied with adjustable electronic characteristics of the substituents (*X*, *R*) on the carbene carbon atom, Fischer carbenes have been found as very important precursors in both organic and inorganic synthesis[231] as well as in the synthesis of biological active substrates.[232]

---

[225] [N^0 562] E. O. Fischer, A. Maasböl, *Angew*. *Chem. Int. Ed. Engl*. **1964**, *3*, 580.
[226] [N^0 563] K. H. Dötz, H. Fischer, P. Hofmann, F.R. Kreissl, U. Schubert, K. Weiss, *Transition Metal Carbene Complexes*; VCH, Weinheim, **1983**.
[N^0 564] C.-C. Wang, Y. Wang, H.-J. Liu, K.-J. Lin, L.-K. Chou, K.-S. Chan, *J. Phys. Chem*. *A* **1997**, *101*, 8887.
[N^0 565] T. F. Block, R. F. Fenske, *J. Am. Chem. Soc*. **1977**, *99*, 4321.
[N^0 566] J. Poater, M. Cases, X. Fradera, M. Duran, M. Solà, *Chem. Phys*. **2003**, *294*, 129.
[227] [N^0 562] E. O. Fischer, A. Maasböl, *Angew*. *Chem. Int. Ed. Engl*. **1964**, *3*, 580.
[228] [N^0 567] R. R. Schrock, *Chem. Rev.* ***2002***, *102*, 145.
[N^0 568] C. P. Casey, *J. Chem. Educ*. **2006**, *83*, 192.
[N^0 569] C. D. Montgomery, *J. Chem. Educ*. **2015**, *92*, 1653.
[229] [N^0 570] U. Klabunde, *Thesis,* Northwestern University **1967**.
[N^0 571] H. Werner, H. Rascher, *Helv. Chim. Acta,* **1968**, *51*, 1765.
[N^0 572] E. Lindner, H. Behrens, *Spectrochim. Acta* **1967**, *23*, 3025.
[N^0 573] U. Klabunde, E. O. Fischer. *J. Am. Chem. Soc.* **1967**, *89*, 7141.
[N^0 574] B. Heckl, H. Werner, E. O. Fischer, *Angew. Chem. Int. Ed.* **1968**, *7,* 817.
[N^0 575] E. O. Fischer, V. Kiener, *Angew. Chem. Int. Ed.* **1967**, *6*, 961.
[N^0 576] C. G. Kreiter, *Angew. Chem. Int. Ed.* **1968**, *7,* 390.
[230] [N^0 577] L. M. Toomey, J. D. Atwood, *Organometallics* **1997**, *16,* 490.
[231] [N^0 578] K. H. Dötz, *Angew. Chem. Int. Ed. Engl*. **1984**, *23*, 587.
[N^0 579] W. D. Wulff, in *Comprehensive Organic Synthesis*, Pergamon Press, Oxford, **1991**. vol. 5.
[N^0 580] W. D. Wulff, *Comprehensive Organometallic Chemistry II*; Pergamon Press, Oxford, **1995**.
[N^0 581] A. de Meijere, *Pure Appl. Chem.* **1996**, *68*, 61.
[N^0 582] J. Barluenga, *J. Pure Appl. Chem*. **1996**, *68*, 543.
[N^0 583] D. F. Harvey, D.M. Sigano, *Chem. Rev*. **1996**, *96*, 271.

For the sake of consistency, a detailed referring to all chemical transformations (such as cycloaddition, metathesis, cross-coupling etc.), wherein the Fischer carbenes are involved, will be avoided. The focus will be only given to the chosen aminolysis reaction[233] of the Fischer carbenes, which mechanism[234] as well as kinetics[235] is well established. From the point of view of the mechanism, in general, the amination of the Fischer carbenes could be considered similar to the amination of esters.[236] Intriguingly, although it has been done a lot both experimentally and theoretically regarding the mechanisms of action,[237] structural features and structure-reactivity relationship[238] of Fischer carbenes, little has been published[239] about the actual thermochemistry of any transformation including Fischer carbenes.

[N^0 584] R. Aumann, *Eur. J. Org. Chem.* **2000**, 17.
[N^0 585] M. A. Sierra, *Chem. Rev.* **2000**, *100*, 3591.
[N^0 586] A.de Meijere, H. Schirmer, M. Duetsch, *Angew. Chem. Int. Ed*. **2000**, 39, 3964.
[N^0 587] M. W. Davies, C. N. Johnson, J. P. A. Harrity, *J. Org. Chem.* **2001**, *66*, 3525.
[N^0 588] J. Barluenga, J. Santamaría, M. Tomás, *Chem. Rev*. **2004**, *104*, 2259.
[N^0 589] Y.-T. Wu, T. Kurahashi, A. de Meijere, *J. Organomet. Chem.* **2005**, *690*, 5900.
[N^0 590] H. K. Dötz, *Stendel. Chem. Rev.* **2009**, *109*, 3227.
[N^0 591] S. Lafollée-Bezzenine, A. Parlier, H. Rudler, J. Vaissermann, J.-C. Daran, *J. Organomet. Chem.* **1998**, 567, 83.
[232] [N^0 592] K. H. Dötz, I. Pruskil, J. Mühlemeier*, Chem. Ber.* **1982**, *115*, 1278.
[N^0 593] M. P. López-Alberca, Israel Fernández, M. J. Mancheño, M. Gómez-Gallego, L. Casarrubios, M. A. Sierra, *Eur. J. Org. Chem.* **2011**, 3293.
[N^0 594] G. M. Chu, A. Guerrero-Martínez, I. Fernández, M. A. Sierra, *Chem. Eur. J.* **2014**, *20*, 1367.
[N^0 595] P. Dutta, S. Sawoo, N. Ray, O. Bouloussa, A. Sarkar, *Bioconjugate Chem.* **2011**, *22*, 1202.
[N^0 596] K. H. Dötz, C. Jäkel, W.-C. Haase, *J. Organomet. Chem.* **2001**, *617–618*, 119.
[233] [N^0 597] E. O. Fischer, B. Heckl, H. Werner, *J. Organomet. Chem.* **1971**, *28*, 359.
[N^0 598] J. A. Connor, P. D. Rose, *J. Organomet. Chem*. **1972**,*46*, 329.
[234] [N^0 599] H. Werner, E. O. Fischer, B. Heckl, C. G. Kreiter, *J. Orgonomet. Chem.* **1971**, *28,* 367.
[N^0 600] D. M. Andrada, J. O. C. Jimenez-Halla, M. Solà, *J. Org. Chem*. **2010**, *75*, 5821.
[N^0 601] D. M. Andrada, M. E. Zoloff Michoff, R. H. de Rossib, A. M. Granados, *Dalton Trans*., **2015**, *44*, 5520.
[N^0 602] C. F. Bernasconi, M. W. Stronach, *J. Am. Chem. Soc*. **1993**, *115*, 1341.
[235] [N^0 599] H. Werner, E. O. Fischer, B. Heckl, C. G. Kreiter, *J. Orgonomet. Chem.* **1971**, *28,* 367.
[N^0 603] D. M. Andrada, M. E. Zoloff Michoff, R. H. de Rossi, A. M. Granados, *Phys. Chem. Chem. Phys*. **2010**, *12*, 6616.
[N^0 574] B. Heckl, H. Werner, E. O. Fischer, *Angew. Chem. Int. Ed.* **1968**, *7*, 817.
[N^0 604] C. F. Bernasconi, S. Bhattacharya, *Organometallics* **2003**, *22,* 1310.
[N^0 605] C. F. Bernasconi, C. Whitesell, R. A. Johnson, *Tetrahedron* **2000**, *56*, 4917.
[236] [N^0 602] C. F. Bernasconi, M. W. Stronach, *J. Am. Chem. Soc*. **1993**, *115*, 1341.
[237] [N^0 606] K. Gu, G. Yang, W. Zhang, X. Liu, Z. Yu, X. Han, X. Bao, *J. Organomet. Chem.* **2006**, *691*, 1984.
[N^0 607] G. M. Chu, I. Fernández, M. A. Sierra, *J. Org. Chem.* **2013**, *78*, 865.
[N^0 608] M. A. Sierra, J. C. del Amo, M. J. Mancheño, M. Gómez-Gallego, *Tetrahedron Lett.* **2001**, *42*, 5435.
[N^0 591] S. Lafollée-Bezzenine, A. Parlier, H. Rudler, J. Vaissermann, J.-C. Daran, *J. Organomet. Chem.* **1998**, 567, 83.
[N^0 213] H. Fischer, P. Hofmann, *Organometallics* **1999**, *18,* 2590.
[238] [N^0 609] W. W. Schoeller, D. Eisner, S. Grigoleit, A. B. Rozhenko, A. Alijah, *J. Am. Chem. Soc.* **2000**, *122,* 10115.
[N^0 610] B. Karatas, I. Hyla-Kryspin, R. Aumann, *Organometallics* **2007**, *26,* 4983.
[N^0 611] M. L. Lage, I. Fernández, M. J. Mancheño, M. A. Sierra, *Inorg. Chem*. **2008**, *47*, 5253.
[N^0 612] N. Fey, M. F. Haddow, J. N. Harvey, C. L. McMullin, A. G. Orpen, *Dalton Trans.* **2009**, 8183.
[N^0 613] J. O. C. Jimenez-Halla, M. Solà, *Chem. Eur. J.* **2009**, *15*, 12503.
[N^0 614] I. Hoskovcová, J. Roháčová, D. Dvořák, T. Tobrman, S. Záliš, R. Zvěřinová, J. Ludvík, *Electrochimica Acta* **2010**, *55*, 8341.
[N^0 615] M. Landman, R. Pretorius, B. E. Buitendach, P. H. van Rooyen, J. Conradie, *Organometallics* **2013**, *32*, 5491.

Thus, within the study of the amination of the Fischer carbenes (**3.2a-c**, see Scheme 3.1) by various amines (**3.3a-c**, see Scheme 3.1) the experimental and theoretical estimations of thermodynamic parameters of the aminolysis reaction are provided.

The aminolysis reaction[240] of Fischer carbene complexes[241] (**3.2a-c**, Scheme 3.1) induced by the series of the amines (**3.3a-c**, Scheme 3.1) was investigated by experimental means (the reaction tests and ITC measurements) as well as by theoretical means (static DFT-D calculations). The well established mechanism of the aminolysis reaction,[242] which is, in general, quite similar to the mechanism of the reaction of carboxylic esters with amines, implies the nucleophilic attack of the amine to carbene carbon atom, subsequent transfer of proton from the amine to the methoxy group by an external molecule (for instance amine, solvent or cosolvent) followed by the departure of the methanol giving the final product of the amination. Supposedly, the rate of this equilibrium step-wise reaction is determined by the nucleophilicity (or pK_a values) of the amine in question. According to the literature,[243] no side reaction occurs.

Therefore, it seems that, in terms of ITC measurements, the only issue might be the rate of the amination. Thus, before performing the ITC experiments, reaction tests were carried out to estimate whether the reaction of interest could be satisfactorily used with the ITC as well as to confirm that there is no side reaction product.

[N^0 616] H. Kvapilová, I. Hoskovcová, M. Kayanuma, C. Daniel, S. Záliš, *J. Phys. Chem. A* **2013**, *117*, 11456.
[N^0 617] K. Yamamoto, C. P. Gordon, W.-C. Liao, C. Copéret, C. Raynaud, O. Eisenstein, *Angew. Chem. Int. Ed.* **2017**, *56*, 10127.
[N^0 618] D. Munz, *Organometallics* **2018**, *37*, 275.
[N^0 619] D. B. Grotjahn, F. E. K. Kroll, T. Schäfer, K. Harms, K. H. Dötz, *Organometallics* **1992**, *11*, 298.
239 [N^0 213] H. Fischer, P. Hofmann, *Organometallics* **1999**, *18,* 2590.
240 [N^0 597] E. O. Fischer, B. Heckl, H. Werner, *J. Organomet. Chem.* **1971**, *28*, 359.
[N^0 598] J. A. Connor, P. D. Rose, *J. Organomet. Chem*. **1972**,*46*, 329.
241 [N^0 573] U. Klabunde, E. O. Fischer. *J. Am. Chem. Soc.* **1967**, *89*, 7141.
242 [N^0 599] H. Werner, E. O. Fischer, B. Heckl, C. G. Kreiter, *J. Orgonomet. Chem.* **1971**, *28,* 367.
[N^0 600] D. M. Andrada, J. O. C. Jimenez-Halla, M. Solà, *J. Org. Chem*. **2010**, *75*, 5821.
[N^0 601] D. M. Andrada, M. E. Zoloff Michoff, R. H. de Rossib, A. M. Granados, *Dalton Trans*., **2015**, *44*, 5520.
[N^0 602] C. F. Bernasconi, M. W. Stronach, *J. Am. Chem. Soc*. **1993**, *115*, 1341.
243 [N^0 597] E. O. Fischer, B. Heckl, H. Werner, *J. Organomet. Chem.* **1971**, *28*, 359.
[N^0 598] J. A. Connor, P. D. Rose, *J. Organomet. Chem*. **1972**,*46*, 329.

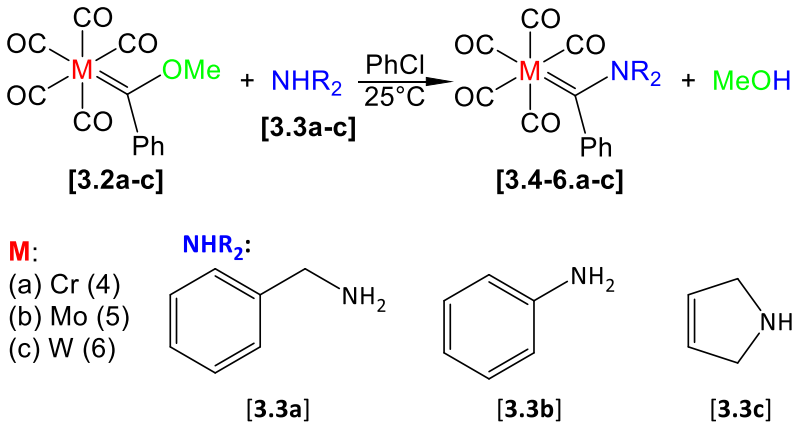

Scheme 3.1 Schematic representation of the investigated reactions within the study of amination of the Fischer carbenes **3.2a-c** by amines **3.3a-c**.

6.2. Experimental section.

6.2.1. Generalities.

Generally, the experiments within this study considered nucleophilic substitution reaction of the methoxy group (leaving as methanol) within Fischer's carbene complexes (**3.2a-c**) are induced by various amines (**3.3a-c**) (see Scheme 3.1).

6.2.2. Techniques.

The investigations within the study of amination of the Fischer carbenes (**3.2a-c**) by various amines (**3.3a-c**) were performed experimentally (using ITC measurements) and theoretically (using static DFT-D calculations) while the reaction tests were carried out using standard Schlenk line experimental technique. Analytical characterizations of the known products were done employing NMR and IR spectroscopies.

6.2.3. Materials.

All used compounds were stored and used into a dry and argon filled glove box or under argon. Chlorobenzene was purchased from Sigma Aldrich and distillated over calcium hydride and degassed prior to use. Fischer's carbene complexes (**3.2a-c**) were prepared using modified literature procedure.[244] Starting carbonyl complexes (**3.1a-c**) were purchased from Sigma Aldrich, stored into a fridge and used as received. Phenyl-lithium (PhLi) and trimethyloxonium

tetrafluoroborate ($(MeO)_3BF_4$) were purchased from Sigma Aldrich, stored into a fridge and used as received. Amines (**3.3a-c**) were purchased from Sigma Aldrich and used as received after checking their purity by NMR. All used solvents in the synthesis and reaction tests (CH_2Cl_2, Et_2O, pentane, hexane) were purchased from Sigma Aldrich and distillated over an appropriate drying agent prior to use. Deuterated chloroform was purchased from Sigma Aldrich and dried through neutral alumina prior to use.

6.2.4. Reaction tests.

Due to the aim of the research (estimating thermodynamic and kinetic parameters of the reaction) and the fact that the studied aminolysis reaction is rather very well-known, the reactions were only monitored. Namely, all the reaction tests were carried out in $CDCl_3$ without isolating the reaction product while the reaction was monitored by ^{1}H NMR spectroscopy. The tests considered various reaction times (1 hour – 5 days) as well as molar ratios of the reactants (up to four equivalents in favor of the amine).

As all the reaction tests were carried out in the same manner, only a general procedure is given herein. Into the solution of the Fischer carbene complex (**3.2a**; **3.2c**) (0.15 mmol) in 1 mL of the deuterated chloroform solution of the amine (**3.3a-c**) containing 0.15 mmol of the amine was added by syringe. The mixture was allowed to stir at ambient temperature. After one hour, a second equivalent of the amine was added in the same manner. The reaction mixture was monitored by ^{1}H NMR spectra after one hour as well as after two hours of the beginning of the reaction. Exclusively, the system **3.2a**/**3.3b** was monitored by ^{1}H NMR spectra in presence of the excess of the amine **3.3b** (5 equivalents) after 1 day, 2 days and 5 days of the reaction.

6.2.5. ITC experimental details.

The solutions of the reactants (**3.2a-c** and **3.3a-c**, see Scheme 3.1) were prepared by dissolving a mass of substrate in pure, freshly distilled and degassed chlorobenzene. The ITC experiments were performed using sequential injection at 25ºC with a moderate stirring rate (150-200 rpm).

The ITC measurements were done in the presence of an excess of the amine. Therefore, the solution of the amine (**3.3a-c**) was introduced in the ITC sample cell while the servo-controlled ITC syringe (100 µL) contained the solution of the Fischer carbene complex (**3.2a-c**). The

[244] [N^0 562] E. O. Fischer, A. Maasböl, Angew. *Chem. Int. Ed. Engl*. **1964**, *3*, 580.

reference (1.0 mL) was entirely filled with pure PhCl. The concentration of the Fischer carbene complex (**3.2a-c**) in pure PhCl was 16-19 mmol/L, while the concentrations of the amine (**3.3a-c**) solutions were from around 30 mmol/L to 130 mmol/L. The content of the syringe was injected into the sample cell through 10 equivalent injections (6.97 µL per injection) while time delay between two consecutive injections was in the range of 1500-3000s, depending on the nature of the amine.

For each studied system at least three experiments were done under identical condition, with an exception in the concentrations of the amine solutions that were varied according to the kinetic purpose of the performed experiments. A heat dilution of the Fischer carbene complexes in neat PhCl was estimated from blank experiments (basically, the titration of the complex in pure PhCl) performed under the same condition as the main experiments. Afterwards, the obtained heat of blank experiments was subtracted from all the corresponding titration curves. The enthalpy of reaction (ΔH_r) of the considering systems **3.2a-c**/**3.3a-c** was obtained by summing up the heat released upon first three injections against a molar content introduced during those three injections. Resulting ΔH_r values represent an average value of three corresponding experiments. As mentioned throughout the manuscript, this methodology of ITC measurements (presence of one of reactants in excess) and subsequent treatment of the ITC data does not allow extraction of reaction free energies (ΔG_r) and entropies (ΔS_r), whereas kinetics parameters of reaction might be obtained.

6.2.6. Static DFT-D calculation details.

All computations were performed by the DFT methods using Amsterdam Density Functional package (ADF2013 version).

Starting geometries of the reactants (**3.2a-c** and **3.3a-c**, see Scheme 3.1) and the reaction products (**3.4-6a-c**, see Scheme 3.1) were taken from the CSD or built up from the similar structures and optimized as singlet ground states in the chlorobenzene solution (COSMO) phase. In addition, within the study of the mechanism of the aminolysis reaction, the supposed reaction intermediates (see Figure 3.11) were built up from the previously optimized geometries of the reactants and subsequently optimized as singlet ground states in the chlorobenzene solution (COSMO) phase. All the starting geometries were built using the software provided within the ADF package.

6.2.7. Synthesis.

6.2.7.1. Synthesis of the Fischer carbenes **3.2a-c**.

Since all the used Fischer carbenes were synthesized in the same way, using modified literature procedure[245] only the general procedure is given. Synthetic scheme is depicted in Scheme ES 3.1.

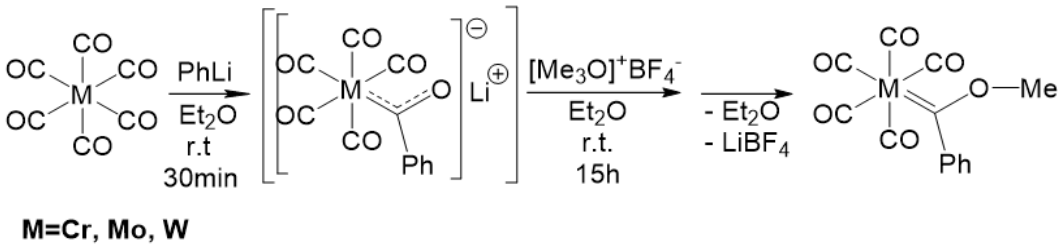

Scheme ES 3.1 Simplified schematic representation of the synthesis of the Fischer carbenes **3.2a-c**.

Into the solution of previously dried metal carbonyl complex (**$M(CO)_6$**, M=Cr, Mo, W) (4.5 mmol) in 20 mL freshly distilled diethyl-ether, 3 ml of 1.8M solution of phenyl-lithium in diethyl-ether (0.45g, 5.4 mmol) were slowly added by syringe. After 30 minutes of stirring at ambient temperature into the dark-colored reaction mixture trimethyloxonium tetrafluoroborate ($(MeO)_3BF_4$) (0.86 g, 4.5 mmol) was added. The resulting mixture was allowed to stir over the night and the solvent was evaporated under reduced pressure. The crude product was subsequently chromatographically purified through neutral silica with 300 mL of pentane and mixture of 250 mL pentane/100 mL of dichloromethane as the eluents. The product was characterized by ^{1}H and ^{13}C NMR spectra as well as IR spectroscopy (related spectra are given is Supplementary Information, Figures SI 13-17; 20-22).

Yield: **3.2a** = 0.53g (38%); **3.2b** = 0.59g (37%); **3.2c** = 0.7g (35%).

NMR: **3.2a** ^{1}H NMR (300 MHz, chloroform-*d*, δ, ppm) 7.48 – 7.34 (m, 3H), 7.34 – 7.20 (m, 2H), 4.70 (s, 3H).^{13}C NMR (126 MHz, chloroform-*d*, δ, ppm) 351.0, 224.1, 216.2, 153.7, 130.4, 128.2, 123.1, 67.2. **3.2b** ^{1}H NMR (400 MHz, chloroform-*d*, δ, ppm) 7.61 – 7.51 (m, 2H), 7.50 – 7.38 (m, 3H), 4.87 (s, 3H). **3.2c** ^{1}H NMR (500 MHz, chloroform-*d*, δ, ppm) 7.59 – 7.51 (m, 2H),

[245] [N^0 562] E. O. Fischer, A. Maasböl, Angew. *Chem. Int. Ed. Engl*. **1964**, *3*, 580.

7.50 – 7.39 (m, 3H), 4.77 (s, 3H). ^{13}C NMR (126 MHz, chloroform-*d*, δ, ppm) 203.6, 197.3, 155.2, 131.8, 128.1, 126.4, 70.2.

IR (solid phase – powder, ν, cm^{-1}): **3.2a** 2061, 1985, 1959, 1888, 1438, 1428, 1247, 1209, 1140, 1126. **3.2b** 2068, 1988, 1962, 1887, 1438, 1428, 1250, 1222, 1141, 1129. **3.2c** 2068, 1982, 1956, 1881, 1437, 1426, 1246, 1221, 1139, 1127.

6.3. Results and discussion.

6.3.1. Reaction tests.

Due to the similarities of the series of the investigated Fischer carbene complexes (**3.2a-c**, Scheme 3.1) the reactions of chromium complex (**3.2a**) with all the amines (**3.3a-c**, Scheme 3.1) were fully studied, while the tungstene complex (**3.2c**) was monitored only for its reaction with the amine **3.3b**. The molybdenum complex (**3.2b**) was only synthetized.

The reaction tests considered various molar ratios of the reactants and reaction time periods. In the following figures (Figure 3.1-3) the monitored reactions of the systems **3.2a**/**3.3a-c** are shown.

Noteworthy, all the systems within stoichiometric conditions exist in an equilibrium consisting of the amination reaction product (**3.4a-c**, see Scheme 3.1) and the free reactants. Expectedly, if two equivalents of the amine are used, the equilibrium of the systems **3.2a**/**3.3a** and **3.2a**/**3.3c** is displaced, in some higher extent, towards the reaction product, while the system **3.2a**/**3.3b**, even in larger excess of the amine, does not show any reaction product. By comparison of systems **3.2a**/**3.3a** and **3.2a**/**3.3c**, it seems that the system **3.2a**/**3.3a** is more likely to give the expected amination reaction product. To estimate the influence of the reaction time for the system **3.2a**/**3.3b**, reaction tests were carried out in a large excess of amine **3.3b** (more than 5 equivalents) within the reaction time of up to 5 days. Related 1H NMR spectra are given in Supplementary Information (see Figure SI 3.18-19). However, no amination reaction products are obtained. Thus, it seems that this reaction, carried out at ambient temperature, rather could not give the expected product. It is worth mentioning, within all the investigated systems there is no occurrence of any side reaction products. In addition, system **3.2c**/**3.3b** was probed as well. However, the same conclusion as for the system **3.2a**/**3.3b** could be drawn – no reaction product is obtainable within the used conditions.

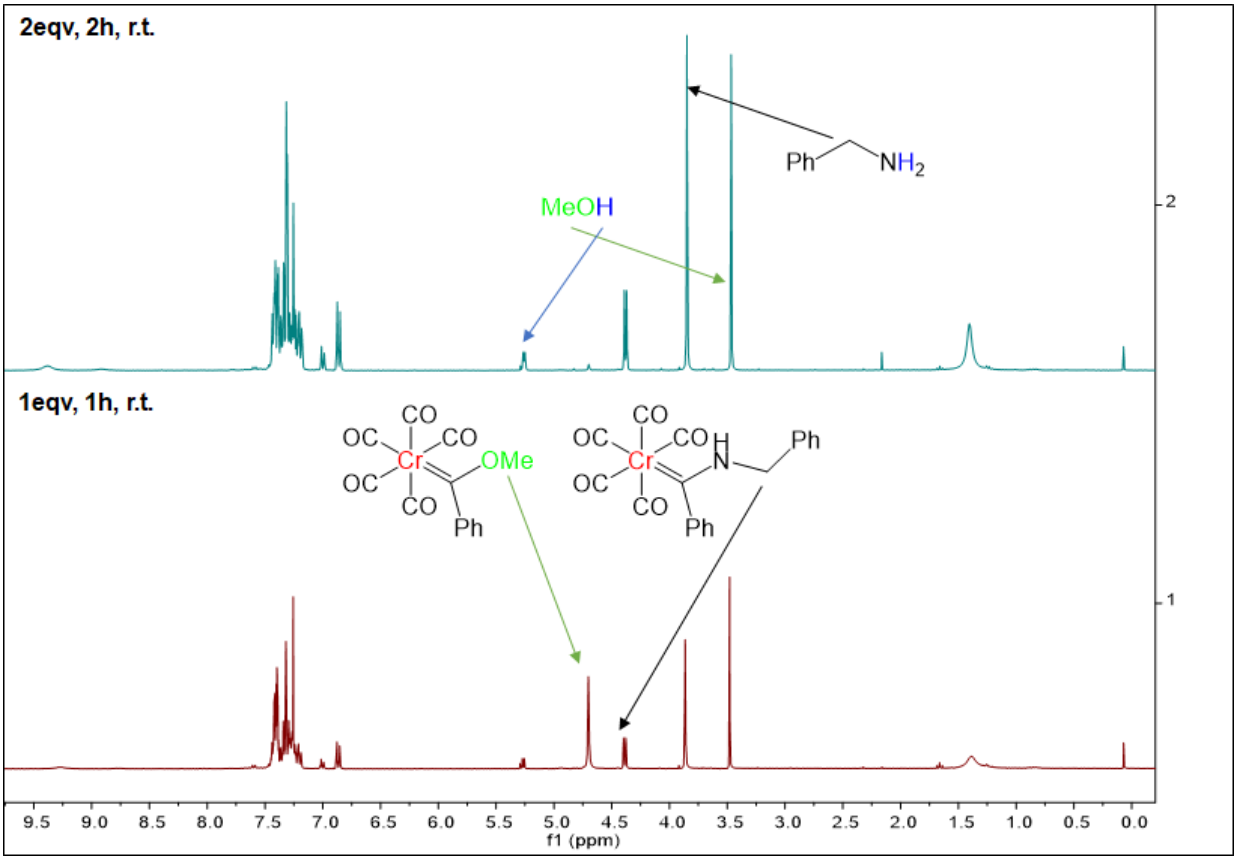

Figure 3.1 Superimposed ^{1}H NMR spectra of the reaction of **3.2a** with **3.3a** carried out in various molar ratios of the reactants (1:1 and 1:2) within various reaction times (1h and 2h). The spectra are recorded in deuterated chloroform at 300 MHz.

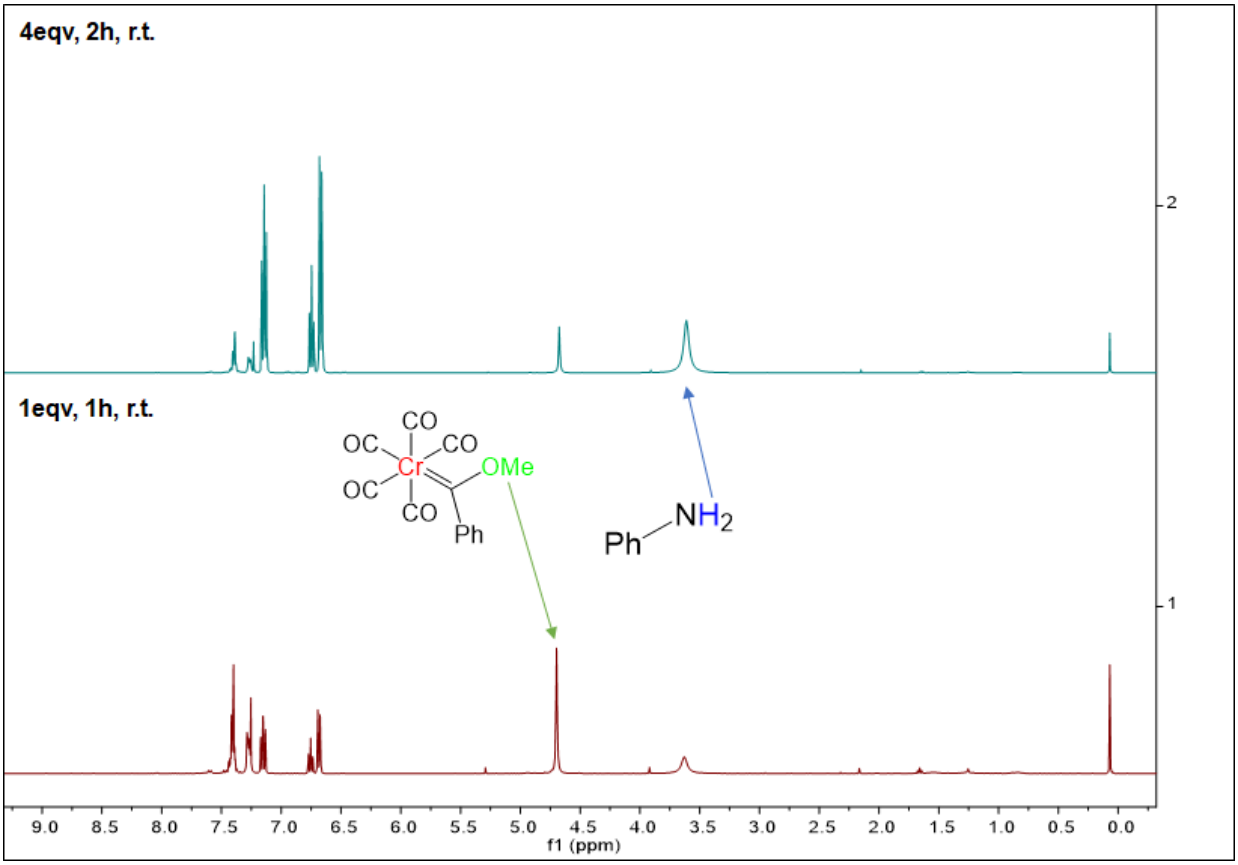

Figure 3.2 Superimposed ^{1}H NMR spectra of the reaction of **3.2a** with **3.3b** carried out in various molar ratios of the reactants (1:1 and 1:4) within various reaction times (1h and 2h). The spectra are recorded in deuterated chloroform at 400 MHz.

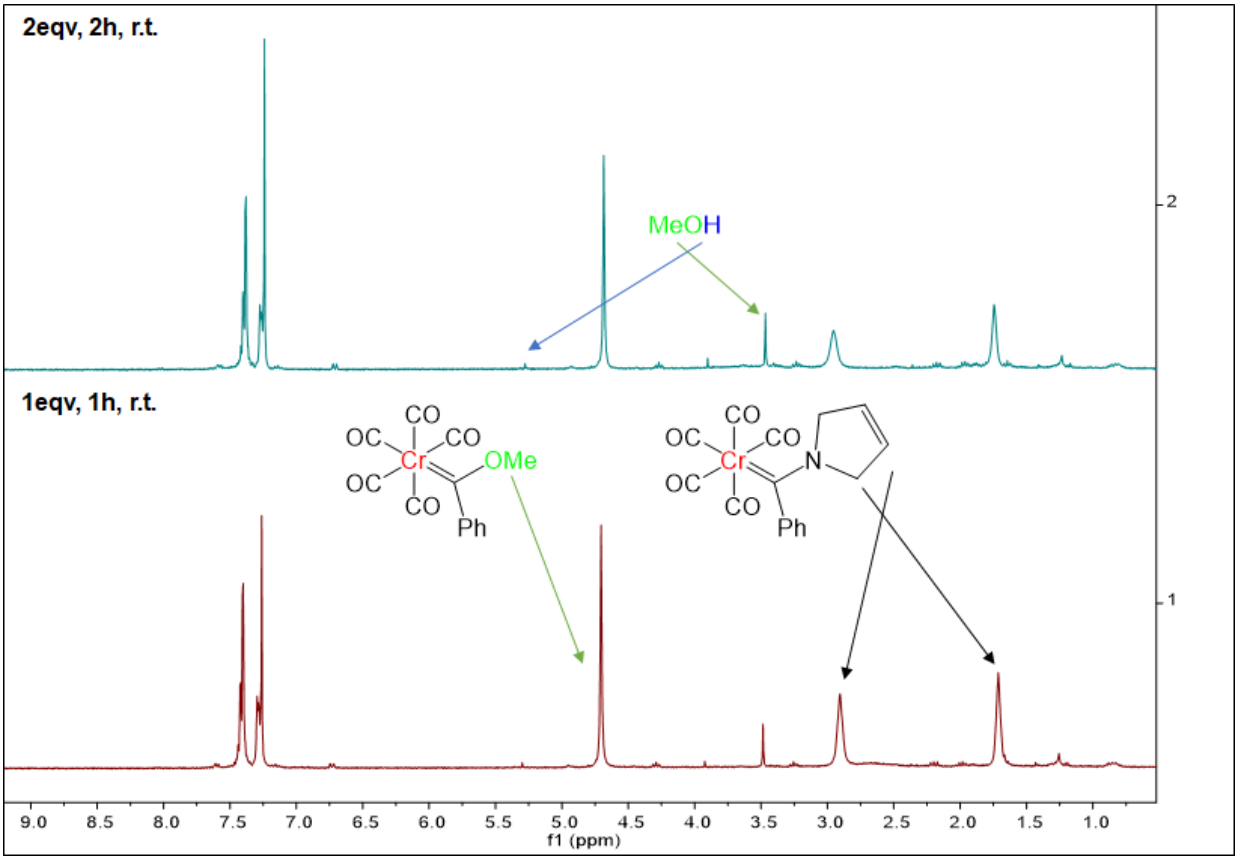

Figure 3.3 Superimposed ^{1}H NMR spectra of the reaction of **3.2a** with **3.3c** carried out in various molar ratios of the reactants (1:1 and 1:2) within various reaction times (1h and 2h). The spectra are recorded in deuterated chloroform at 300 MHz.

6.3.2. ITC experiments.

6.3.2.1. Generalities.

Governed by the suggestion of the reaction tests on the investigated systems, ITC measurements were performed with an excess of amine (**3.3a-c**) with respect to the Fischer carbene complex (**3.2a-c**). In that way, the equilibrium nature of the reaction should be minimized as well as the issues caused by quite low reaction rate could be overcome. To ensure proper base line before subsequent injection takes place, relatively long time-delay (1500s-3000s) between two consecutive injections was employed. To confirm the chosen condition as optimal, ITC measurements in stoichiometric conditions were done as well. From the preformed ITC experiments, only the raw ΔH_r values are derived as thermodynamic parameters of the reaction, while the initial rate constant and the partial reaction order with respect to the amine in excess are obtained as kinetic parameters of the reaction.

6.3.2.2. Thermodynamic study.

Although the studied reaction was clean in terms of the expected reaction products, its equilibrium nature was the major issue for ITC measurements. Considering the mechanism of the reaction, the only way to overcome the issue and obtain a satisfactory fast heat response was employing an excess of the amine accompanied with relatively long time-delay between consecutive injections. Consequently, only raw ΔH_r values are obtained. For illustration purpose, in Figure SI 3.1 the ITC thermogram of the reaction of **3.2a** with **3.3a** in stoichiometric condition is given. It can be noticed that the rate of the amination (nucleophilic substitution reaction) is too low that does not allow extracting thermodynamic parameters of the reaction. The ITC results (raw ΔH_r values) of herein studied systems (**3.2a-c**/**3.3a-c**, see Scheme 3.1) are summarized in Table 3.1. Noticeably, in all the systems when the amine is **3.3b**, no enthalpy values are obtained. It suggests that, even though the ITC experiments performed in large excess of **3.3b**, the energetic barrier of the transition/intermediary state in the course of the reaction could not be overcame (see ITC thermogram depicted in Figure 3.5 that show mainly just heat of dilution of the amine). To confirm that assumption, static DFT-D calculations were employed (see detailed explanation in the following chapter that deals with the theoretical calculations). Considering the obtained ΔH_r values (that are in range from around -15 kcal/mol to -20 kcal/mol) in general, it could be concluded that the amination of the Fischer carbenes is energetically quite favorable. Comparison of the raw ΔH_r values of the reaction of the amine **3.3a** with the series of the Fischer carbenes **3.2a-c** (ranged around 16 kcal/mol) one could conclude that metal atom has no large influence on the enthalpy of the reaction. Regarding the raw ΔH_r values of the reaction of the amine **3.3c** with the same carbenes (ranged around 18 kcal/mol to 20.5 kcal/mol) the influence of the metal is more pronounced but not consistent with their size (as intermediary large metal – molybdenum has the raw ΔH_r value – 18 kcal/mol). However, comparing the obtained trends, it seems that the molybdenum carbene complex exhibits lowest enthalpy values, while tungstene one tends to highest ΔH_r values. The examples of the ITC thermograms of the investigated systems are shown in Figure 3.4-6, while, due to their similarities, the ITC thermograms of other systems are given in Supplementary Information (see Figure SI 3.2-5).

Table 3.1 ITC results obtained from the sequential addition ITC experiments that considered an excess of the amine **3.3a-c** interacting with the Fischer carbene complex **3.2a-c**.

System	raw ΔH_r ± error [kcal/mol]
3.2a/3.3a	-15.5 ± 0.5
3.2a/3.3b	/
3.2a/3.3c	-19.1 ± 0.6
3.2b/3.3a	-15.3 ± 0.6
3.2b/3.3b	/
3.2b/3.3c	-18.1 ± 0.5
3.2c/3.3a	-16.3 ± 0.3
3.2c/3.3b	/
3.2c/3.3c	-20.5 ± 0.8

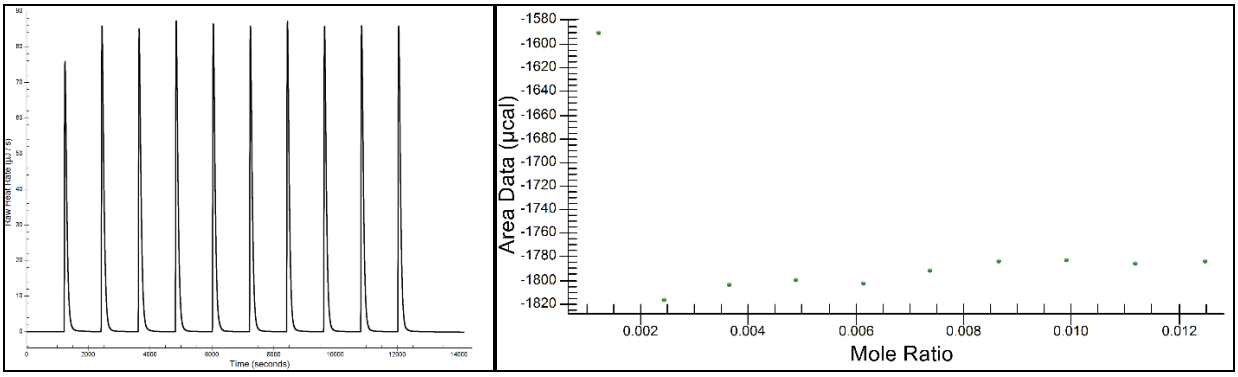

Figure 3.4. *left side* – ITC thermogram of the reaction between **3.3a** (sample call, c=94.48 mM) and **3.2a** (syringe, c=16.27 mM) in chlorobenzene. The titration was performed at 25ºC through 10 sequential additions (of 6.97 µL each). Time between two consecutive injections was 1000 s. Heat released is expressed in µJ/s versus time in s. *right side* – ITC integrated heat peaks of the thermogram shown on the left side. Integrated heats are expressed in µcal versus molar ratio of the reactants.

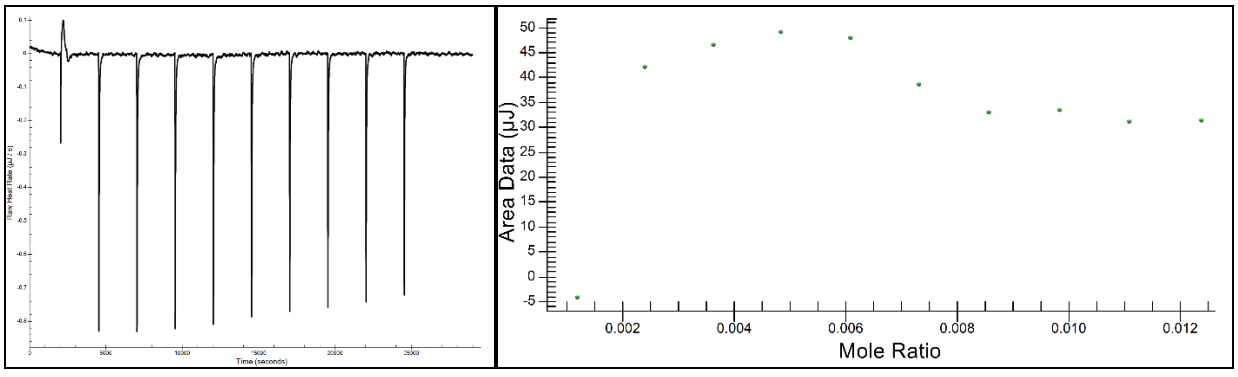

Figure 3.5. *left side* – ITC thermogram of the reaction between **3.3b** (sample call, c=570.92 mM) and **3.2c** (syringe, c=16.04 mM) in chlorobenzene. The titration was performed at 25ºC through 10 sequential additions (of 6.97 µL each). Time between two consecutive injections was 3000 s. Heat released is expressed in µJ/s versus time in s. *right side* – ITC integrated heat peaks of the

thermogram shown on the left side. Integrated heats are expressed in µcal versus molar ratio of the reactants.

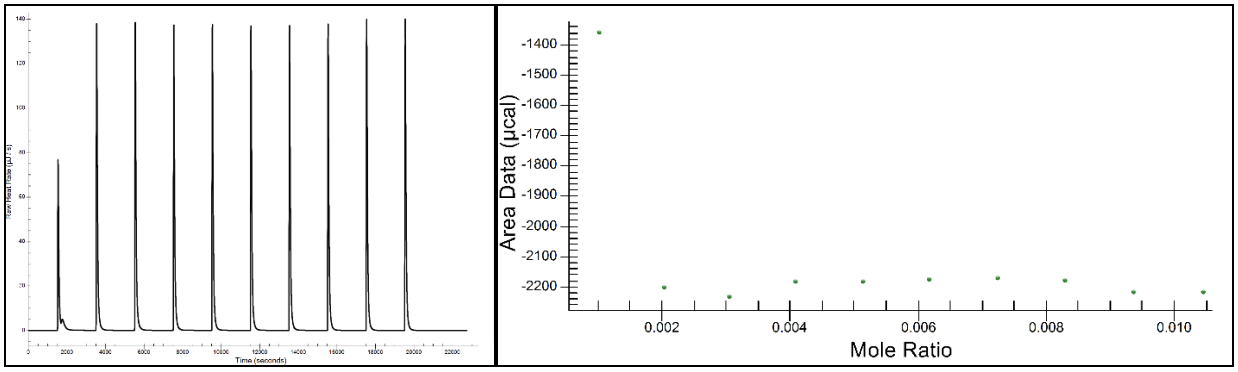

Figure 3.6. *left side* – ITC thermogram of the reaction between **3.3c** (sample call, c=109.12 mM) and **3.2c** (syringe, c=15.73 mM) in chlorobenzene. The titration was performed at 25ºC through 10 sequential additions (of 6.97 µL each). Time between two consecutive injections was 2000 s. Heat released is expressed in µJ/s versus time in s. *right side* – ITC integrated heat peaks of the thermogram shown on the left side. Integrated heats are expressed in µcal versus molar ratio of the reactants.

6.3.2.3. Kinetic study.

The employed ITC conditions (the excess of the amine) allowed determining the reaction kinetic parameters (the initial rate constant and the partial reaction order with respect to amine), as well. As mentioned in the introductory chapter, to obtain reliable kinetic parameters, the first or eventually the second titration within ITC measurement must be proper. Due to that fact, only exploitable thermograms within this study were those of the following systems: **3.2a-c**/**3.3a** and **3.2c**/**3.3c**. Expectedly, as it was the case within the thermodynamic analyzes, the systems that included the amine **3.3b** could neither be analyzed in sense of the kinetics. The results of the kinetic analysis are reported in Table 3.2 while the corresponding plots are displayed in Figures 3.7-8 as well as in Figure SI 3. 6-11.

The obtained initial rate constant (*k*) values of the systems **3.2a-c**/**3.3a** (spanned from $6.6*10^{-4}$ to $6.8*10^{-2}$) suggest on moderately swift transformation within the amination reaction process. It seems that the transformation is roughly ten times slower with the tungstene carbene complex (**3.2c**) than with the other ones. The transformation of system **3.2c**/**3.3c** is approximately ten times faster than the transformation of the system **3.2c**/**3.3a**. This observation might be caused by the difference of the pKa values of the used amines (pKa(**3.3a**) = 9.34; pKa(**3.3c**) ≈ 11). Considering the obtained partial orders in the amine, that are within the error bar, valued around 2, it could be concluded partial second reaction order with respect to amine, which is in perfect

accordance with the literature.[246] Therefore, once again, the established method of estimating kinetic parameters of reaction is found to be satisfactorily accurate.

Table 3.2 Results of the ITC kinetic study obtained from the sequential addition ITC experiments that considered an excess of **4.4b** interacting with the palladacycle **4.3a**.

System	[**Fischer carbene**] mmol/L	[**amine**] mmol/L	Molar ratio under ITC conditions	**k**	**order** with respect to **amine**	k_{obs}	**order** with respect to **amine**
3.2a/3.3a	16.27	94.48	1:833	$4.5*10^{-2} \pm 3*10^{-3}$	**2.13 ± 0.24**	$2.7*10^{-4} \pm 2*10^{-5}$	**1.58 ± 0.22**
	16.21	28.23	1:250	$4.1*10^{-3} \pm 2*10^{-4}$		$3.6*10^{-5} \pm 2*10^{-6}$	
	35.23	93.46	1:381	$4.5*10^{-2} \pm 2*10^{-3}$		$1.9*10^{-4} \pm 1*10^{-5}$	
	35.49	93.46	1:378	$6.8*10^{-2} \pm 3*10^{-3}$		$2.8*10^{-4} \pm 1*10^{-5}$	
3.2b/3.3a	17.02	50.67	1:427	$1.5*10^{-2} \pm 1*10^{-3}$	**2.18 ± 0.14**	$1.2*10^{-4} \pm 9*10^{-6}$	**2.24 ± 0.12**
	17.24	29.16	1:243	$3.8*10^{-3} \pm 3*10^{-4}$		$3.2*10^{-5} \pm 2*10^{-6}$	
	18.03	64.02	1:509	$1.9*10^{-2} \pm 2*10^{-3}$		$1.5*10^{-4} \pm 1*10^{-5}$	
	18.42	105.82	1:824	$7.7*10^{-2} \pm 3*10^{-3}$		$6.1*10^{-4} \pm 3*10^{-5}$	
3.2c/3.3a	16.09	95.32	1:850	$7.8*10^{-3} \pm 8*10^{-4}$	**2.02 ± 0.42**	$7.0*10^{-5} \pm 7*10^{-6}$	**2.02 ± 0.42**
	16.09	47.59	1:424	$2.9*10^{-3} \pm 3*10^{-4}$		$2.6*10^{-5} \pm 3*10^{-6}$	
	16.09	28.79	1:257	$6.6*10^{-4} \pm 7*10^{-5}$		$5.9*10^{-6} \pm 6*10^{-7}$	
3.2c/3.3c	15.84	134.59	1:1219	$7.0*10^{-2} \pm 2*10^{-3}$	**1.72 ± 0.31**	$6.4*10^{-4} \pm 2*10^{-5}$	**1.70 ± 0.32**
	15.73	109.12	1:995	$6.2*10^{-2} \pm 2*10^{-3}$		$5.7*10^{-4} \pm 2*10^{-5}$	
	15.62	60.78	1:558	$1.9*10^{-2} \pm 2*10^{-3}$		$1.8*10^{-4} \pm 1*10^{-5}$	

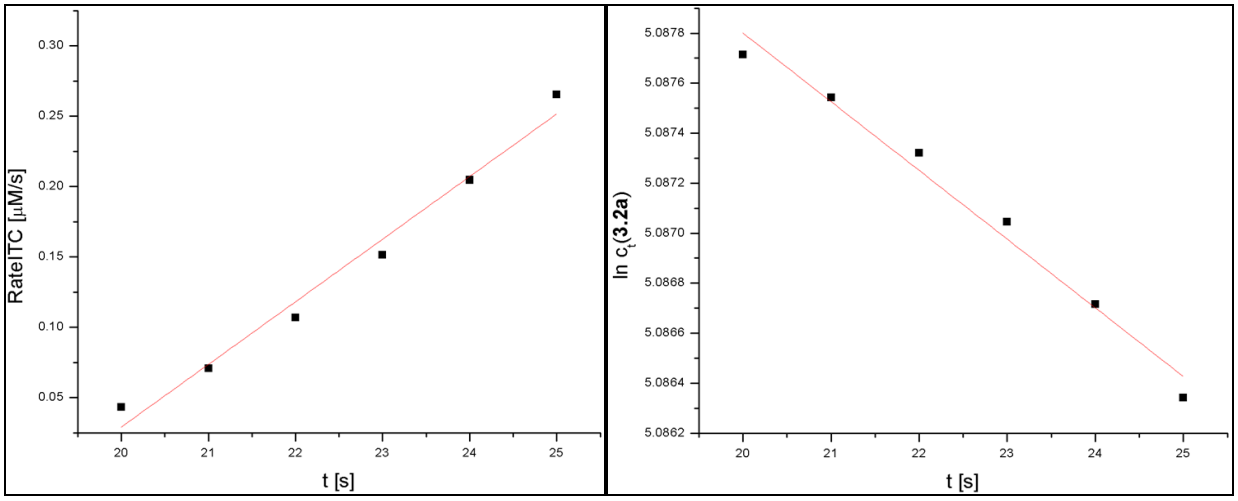

Figure 3.7 *left side* - Linear fit of the plot of the ITC Rate as a function of time for the reaction of **3.3a** (sample call, c=94.48 mM) with **3.2a** (syringe, c=16.27 mM) carried out in ITC calorimeter. ITC Rate is expressed in µM/s and time in s. Obtained $\boldsymbol{k = 4.5*10^{-2} \pm 3*10^{-3}}$, as the result of the fitting. *right side* - Linear fit of the plot of logarithm of **3.2a** concentration as a function of time for the same reaction. Obtained $\boldsymbol{k_{obs} = -2.7*10^{-4} \pm 2*10^{-5}}$, as the result of the fitting.

[246] [N^0 599] H. Werner, E. O. Fischer, B. Heckl, C. G. Kreiter, *J. Orgonomet. Chem.* **1971**, *28,* 367.
[N^0 603] D. M. Andrada, M. E. Zoloff Michoff, R. H. de Rossi, A. M. Granados, *Phys. Chem. Chem. Phys*. **2010**, *12*, 6616.
[N^0 574] B. Heckl, H. Werner, E. O. Fischer, *Angew. Chem. Int. Ed.* **1968**, *7*, 817.
[N^0 604] C. F. Bernasconi, S. Bhattacharya, *Organometallics* **2003**, *22,* 1310.
[N^0 605] C. F. Bernasconi, C. Whitesell, R. A. Johnson, *Tetrahedron* **2000**, *56*, 4917.

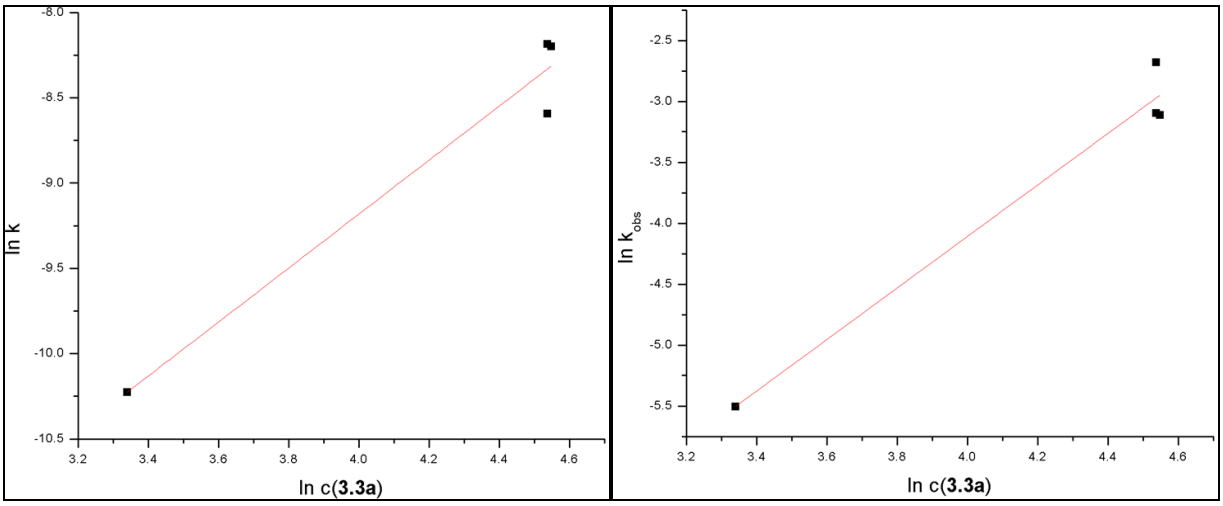

Figure 3.8 *left side* - Linear fit of the plot of logarithm of obtained *k* values as a function of the logarithm of **3.3a** starting concentrations for the reaction of **3.2a** with **3.3a** carried out in ITC calorimeter. Obtained partial reaction order with respect to **3.3a** – **2.13 ± 0.24**, as the result of the fitting. *right side* - Linear fit of the plot of logarithm of obtained k_{obs} values as a function of the logarithm of **3.3a** starting concentrations for the reaction of **3.2a** with **3.3a** carried out in ITC calorimeter. Obtained partial reaction order with respect to **3.3a** – **1.58 ± 0.22**, as the result of the fitting.

6.3.3. Static DFT-D calculations.

The theoretical investigations of the amination of the Fischer carbenes were done on the series of the Fischer carbenes (**3.2a-c**, see Scheme 3.1) and various amines (**3.3a-c**, see Scheme 3.1). All the computations were performed at ZORA-GGAPBE-D3(BJ)/TZP level of theory in chlorobenzene solution (COSMO) phase. The geometry optimizations were done on both reactants (**3.2a-c** and **3.3a-c**) and corresponding products (**3.4-6.a-c**, see Scheme 3.1) and confirmed as true minima by performing calculations of vibrational modes. In addition, the calculation of the intermediary states within the course of the aminolysis reaction on the systems **3.2a-c**/**3.3b** were performed (at the same level of theory). The derived thermodynamic parameters (ΔH_r, ΔG_r, ΔS_r) of the aminolysis reaction are shown in Table 3.3. The corresponding optimized structure geometries are displayed in Figure 3.9 while the Cartesian coordinates of all related optimized geometries are given in Supplementary Information (see SI, section A.3.5.).

Table 3.3 Results of static DFT-D calculations. The calculations were performed at ZORA-GGAPBE-D3-BJ/TZP level of theory in chlorobenzene solution (COSMO) phase.

System	Level of theory	ΔH_r [kcal/mol]	ΔG_r [kcal/mol]	ΔS_r [cal/Kmol]
3.4.a	ZORA-GGAPBE-D3(BJ)/TZP - PhCl	-16.2	-16.8	2.0
3.4.b	ZORA-GGAPBE-D3(BJ)/TZP - PhCl	-6.7	-7.0	1.1
3.4.c	ZORA-GGAPBE-D3(BJ)/TZP - PhCl	-19.8	-19.7	-0.3
3.5.a	ZORA-GGAPBE-D3(BJ)/TZP - PhCl	-17.0	-15.5	-4.8
3.5.b	ZORA-GGAPBE-D3(BJ)/TZP - PhCl	-6.1	-4.4	-5.8
3.5.c	ZORA-GGAPBE-D3(BJ)/TZP - PhCl	-20.6	-18.6	-6.7
3.6.a	ZORA-GGAPBE-D3(BJ)/TZP - PhCl	-16.1	-16.6	1.6
3.6.b	ZORA-GGAPBE-D3(BJ)/TZP - PhCl	-5.5	-5.7	0.9
3.6.c	ZORA-GGAPBE-D3(BJ)/TZP - PhCl	-20.1	-20.1	-0.2

Noticeably, all the calculated reaction enthalpies (ΔH_r,) are negative (ranged from -5.5 kcal/mol to -20.5 kcal/mol) meaning that all herein investigated aminolysis reactions might be energetically favorable in comparison to the reverse reaction. Regarding calculated Gibbs free energies of reaction (ΔG_r values ranged ca. 4 kcal/mol - 20 kcal/mol) it could be concluded that all considered transformations are spontaneous in chlorobenzene solution. By comparison within the related systems (i.e. the systems **3.2a-c**/**3.3a**, **3.2a-c**/**3.3b** and **3.2a-c**/**3.3c**) quite similar reaction enthalpies are noticeable. As opposed to the obtained ITC trends (ΔH_r values of the **3.2b**/**3.3a,c3.2a-c**/**3.3** are lowest among all related systems), predicted theoretical ΔH_r values suggest highest exothermicity in case of the Fischer carbene **3.2b**. Interestingly, the systems, for which experimental ITC values were not obtained (i.e. system that include the amine **3.3b**), theoretically have lowest reaction enthalpies (in range 5.5-6.7 kcal/mol) as well Gibbs free energies (in range 4.4-7.0 kcal/mol) with decreasing values from chromium (**3.2a**) to tungstene (**3.2c**) carbene complex. Worthy to note that, although the ITC experimental values (raw ITC ΔH_r) suggested different trends from the calculated ones, it could be concluded that the experimental (see Table 3.1) and calculated (see Table 3.3) reaction enthalpy values are in very good accordance.

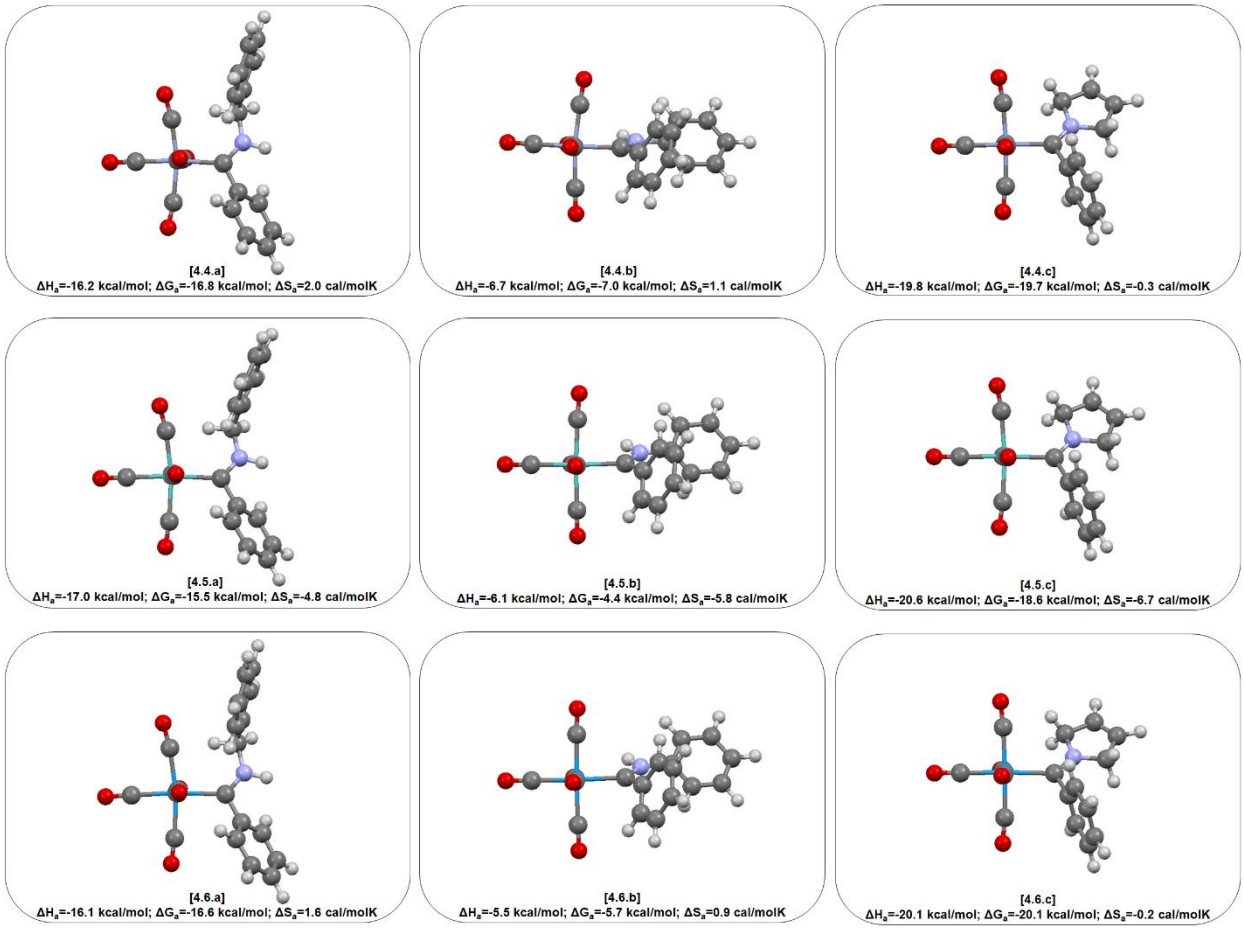

Figure 3.9 Graphic representations of optimized geometries of the investigated systems at ZORA-GGAPBE-D3-BJ/TZP level of theory in chlorobenzene solution (COSMO) phase. N: bluish; O: red; Cr: violet; Mo: greenish; W: blue; C: grey; H: white.

In order to explain experimental observations related to the systems **3.2a-c**/**3.3b** (no experimental values were obtained), a round of calculations was performed on the supposed intermediary states appearing within the course of the amination process. The calculation included the systems **3.2a**/**3.3a-c** as well as the systems **3.2b-c**/**3.3b**. The resulted values of the thermodynamic parameters (Δ*H* and Δ*G*) of the intermediary states relative to the reactants are shown graphically in Figure 3.10 and Figure SI 3.12, while the graphic representations of the considered intermediary states are depicted in Figure 3.11. The results clearly show the differences between used amines. Namely, the nucleophilic attack of the amines **3.3a** and **3.3c** (establishing intermediary state T1) is energetically negligible (Δ*H* values are 0.2 kcal/mol and -1.5 kcal/mol, respectively) while the attack of the amine **3.3b** is energetically quite unfavorable (Δ*H* values are 9.4 kcal/mol). The calculated Gibbs free energy values of the first step (intermediary state T1) of all the studied cases suggest the thermodynamically unfavorable

process. However, the calculated Δ*H* and Δ*G* values (roughly higher than -10 kcal/mol) of the second step show that the proton transfer and potential departure of methanol from the complex (intermediary state T2 (products)) are thermodynamically favorable. Again, the exception is the system involving the amine **3.3b** that shows positive Δ*G* value (2.5 kcal/mol). The same conclusion can be drawn for the systems **3.2b-c**/**3.3b**, as it can be seen in the Figure SI 3.12.

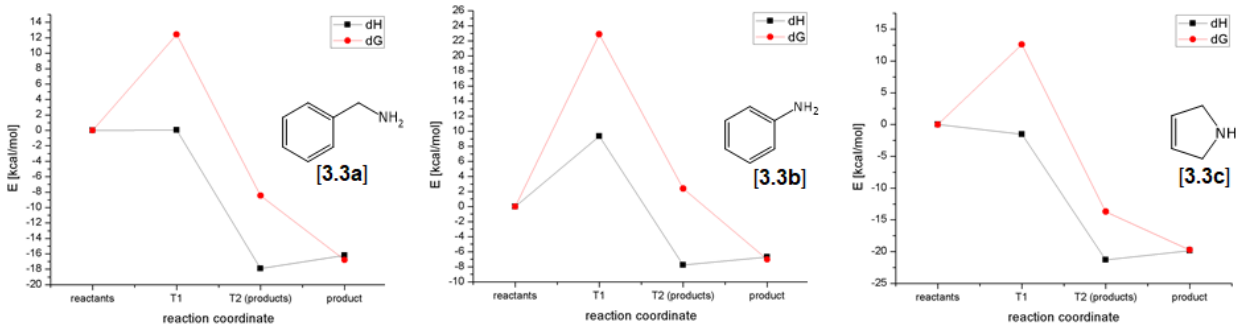

Figure 3.10 Graphic representation of the Δ*H* and Δ*G* values (given as energy expressed in kcal/mol) for particular states (given through reaction coordinate, see also Figure 3.11) within the course of the amination process of the Fischer carbene complex **3.2a** induced by various amines **3.3a-c**. The calculations were performed at ZORA-GGAPBE-D3-BJ/TZP level of theory in chlorobenzene solution (COSMO) phase at 298.15K.

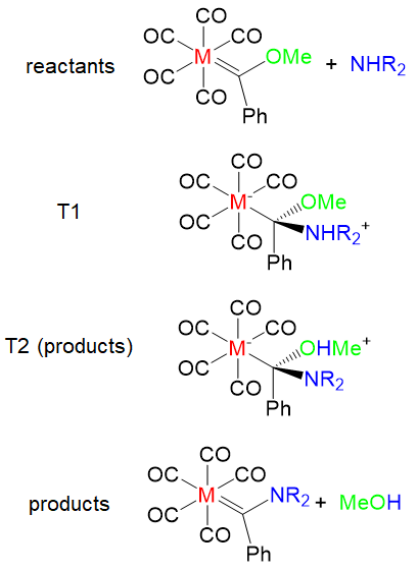

Figure 3.11 Schematic representation of the considered particular states within the theoretical study of the course of amination process of the Fischer carbenes **3.2a-c** induced by various amines **3.3a-c** (see also Figure 3.10).

These two facts related to the system **3.2a-c**/**3.3b**, i.e. relatively high energy barrier of the first reaction step (herein T1) accompanied with an unfavorable second step (herein T2 (products))

can rationally explain lack of possibility of obtaining experimental thermodynamic reaction parameters (by ITC measurements). In addition, the results of the first step of the systems **3.2a**/**3.3a** (ΔH = 0.2 kcal/mol) and **3.2a**/**3.3c** (ΔH = -1.5 kcal/mol) might explain, in general, the difference in the reaction rate (obtained by kinetic analysis of the ITC results) of the amines **3.3a** and **3.3c** with the herein investigated Fischer carbenes (see subchapter ITC experiments – kinetic study).

6.4. Chapter conclusion.

The amination of the Fischer carbenes **3.2a-c** (Scheme 3.1) induced by the series of amine **3.3a-c** (Scheme 3.1) was investigated experimentally using the reaction tests and Isothermal Titration Calorimetry (ITC) as well as theoretically employing static Density Functional Theory with Grimme's dispersion correction (DFT-D3) calculations.

The reaction tests, carried out in deuterated chloroform within various molar ratios of the reactants and reaction times without the isolation of the reaction products, confirmed the equilibrium nature of the amination process and no existence of side reaction products. They suggested that a large excess of one of the reactants should be employed in ITC measurements in order to overcome the existing equilibrium.

The ITC measurements, performed in large excess of the amine, allowed estimation of the reaction enthalpies as well as the initial rate constants and the partial reaction order with respect to used amine. The thermodynamic parameters of the reaction (ΔH_r, ΔG_r, ΔS_r) as well as the thermodynamic parameters (ΔH, ΔG) of the particular intermediary states (see Figure 3.11) on the course of the amination process are obtained as results of the performed calculations.

The thermodynamic ITC results (ΔH_r values larger than -15 kcal/mol, Table 3.1) suggested on energetically favorable transformations within the amination process in the systems **3.2a-c**/**3.3a** and **3.2a-c**/**3.3b**, while the systems **3.2a-c**/**3.3b** were found to be non-exploitable even in tremendously large excess of the amine **3.3b**. In addition, regarding the results, clear dependence of the type of metal atom on the reaction enthalpy could not be drawn. The kinetic ITC results rather confirmed partial second reaction order with respect to the amine as well as a moderate swift of the transformations in the early stages of the reaction.

The calculated reaction enthalpies (ranged from around -5.5 kcal/mol up to -20 kcal/mol), similarly to the experimental ones, show that in all the investigated systems the overall energetics might be favorable, while the calculated Gibbs free energies (ranged from around -4.5 kcal/mol up to -20 kcal/mol) suggested on spontaneous process within all the systems. Although the calculations predicted different influence of the type of metal atom on the reaction enthalpies than the ITC experiments did, within the error bar the experimental and the theoretical reaction enthalpy values are rather in excellent accordance. In addition, the calculation revealed that the amination of the herein investigated Fischer carbenes by phenylamine (**3.3b**) is not thermodynamically possible at 25ºC, as both the enthalpy and the Gibbs free energy of the first reaction step (nucleophilic attack of the amine) are largely positive (ΔH value larger than 2.5 kcal/mol; ΔG value larger than 20 kcal/mol) as well as the Gibbs free energy of the second step (transfer of proton and potential leaving of methanol) (ΔG valued around 8 kcal/mol).

6.5. Закључак поглавља.

Анминовање Fischer-ових карбена **3.2a-c** (схема 3.1) узрокована серијом амина **3.3a-c** (схема 3.1) испитивана је експериментално - коришћењем реакционих тестова и изотермалне титрационе калориметрије (ITC), и теоријски - коришћењем прорачуна заснованих на теорији функционала густине са Grimme-овом корекцијом за дисперзију (енг. DFT-D3).

Реакциони тестови, изведени у деутерисаном хлороформу при различитим моларним односима реактаната и реакционим временима, без изоловања реакционих производа, потврдили су равнотежну природу процеса аминовања и непостојање споредних реакционих производа. Резултати реакционих тестова указали су на то да би требало у ITC мерењима да се користи велики вишак једног од реактаната како би се превазишла постојећа равнотежа.

ITC мерења изведена у великом вишку амина омогућила су процену реакционих енталпија, као и иницијалних константи брзина и парцијалног реда реакције у односу на коришћени амин. Као резултат теоријских прорачуна добијени су термодинамички реакциони параметри (ΔH_r, ΔG_r, ΔS_r), као и термодинамички параметри (ΔH, ΔG) појединачних интермедијера (види слику 3.11) у току процеса аминовања.

Термодинамички ITC резултати (ΔH_r вредности веће од -15 kcal/mol, табела 3.1) указали су на енергетски повољне промене унутар процеса аминовања у системима **3.2a-c**/**3.3a** и **3.2a-c**/**3.3c**, док су системи **3.2a-c**/**3.3b** окарактерисани као неупотребљиви чак и уз коришћење изузетно великог вишка амина **3.3b**. На основу добијених резултата, није било могуће извести јасне закључке о утицају типа метала на реакциону ентлапију. ITC кинетички резултати су потврдили други ред реакције у односу на амине, као и умерено брзе хемијске промене у раним фазама реакције.

Израчунате реакционе енталпије (у распону од око -5,5 kcal/mol до -20 kcal/mol), слично експерименталним вредностима, указују на то да у свим испитиваним системима укупна енергетика процеса трансформације може бити повољна, док су израчунате Gibbs-ове слободне енергије (у распону од око -4,5 kcal/mol до -20 kcal/mol) указале на спонтане реакционе процесе у свим системима. Иако су прорачуни предвидели различит утицај типа атома метала на реакционе енталпије у поређењу са ITC експериментима, може се

закључити да су, у оквиру експерименталне грешке, експерименталне и теоријске вредности реакционих енталпија у одличној сагласности. Поред тога, резултати прорачуна су показали да аминовање испитиваних Fischer-ових карбена фениламином (**3.3b**) није термодинамички могуће на 25 ºC, јер и енталпија и Gibbs-ова слободна енергија првог реакционог корака (нуклеофилни напад амина) имају позитивне вредности (Δ*H* вредност већа од 2,5 kcal/mol, Δ*G* вредност већа од 20 kcal/mol), као и Gibbs-ова слободна енергија другог корака који укључује пренос протона и потенцијално отпуштање метанола (Δ*G* вредност око 8 kcal/mol).

6.6. Conclusion du chapitre

L'amination des Fischer carbènes **3.2c** (Schéma 3.1) induite par la série d'amine **3.3a-c** (Schéma 3.1) a été étudiée expérimentalement utilisant les tests de réaction et la Calorimétrie par Titration Isotherme (ITC) et théoriquement par la Théorie Fonctionnelle de Densité Statique avec les calculs de correction de la dispersion de Grimme (DFT-D3).

Les essais de réaction, effectués dans du chloroforme deutéré dans différents rapports molaires des réactifs et les temps de réaction sans isolement des produits de réaction, ont confirmé la nature d'équilibre du procédé d'amination et l'absence de produits de réaction secondaire. Ils ont suggéré qu'un grand excès de l'un des réactifs devrait être utilisé dans les mesures de l'ITC afin de surmonter l'équilibre existant.

Les mesures d'ITC, réalisées dans un large excès d'amine, ont permis d'estimer les enthalpies de réaction ainsi que les constantes de vitesse initiales et l'ordre partiel dans l'aminé utilisée. Les paramètres thermodynamiques de la réaction (ΔH_r, ΔG_r, ΔS_r) ainsi que les paramètres thermodynamiques (ΔH, ΔG) des états intermédiaires particuliers (voir Figure 3.11) sur le déroulement du processus d'amination sont obtenus comme résultats des calculs effectués.

Les résultats de l'ITC thermodynamique (valeurs de ΔH_r supérieures à -15 kcal / mol, tableau 3.1) suggèrent des transformations favorables à l'énergie dans le processus d'amination dans les systèmes **3.2a-c/3.3a** et **3.2a-c/3.3c,** tandis que les systèmes **3.2a-c/3.3b** ont été trouvés non exploitables même dans un excès extrêmement important de l'amine **3.3b**. De plus, en ce qui concerne les résultats, une dépendance claire du type d'atome de métal sur l'enthalpie de réaction n'a pas pu être établie. Les résultats de l'ITC cinétique ont plutôt confirmé le second ordre partiel dans l'amine ainsi qu'un mouvement modéré des transformations dans les premiers stades de la réaction.

Les enthalpies de réaction calculées (allant d'environ 5,5 kcal/mol jusqu'à 20 kcal/mol), de même que les entonnages expérimentaux, indiquent que dans tous les systèmes étudiés, l'énergie globale peut être favorable, tandis que les énergies libres de Gibbs calculées (entre 4,5 kcal / mol et 20 kcal / mol) suggèrent un processus spontané dans tous les systèmes. Bien que les calculs prédisaient une influence différente du type d'atome de métal sur les enthalpies de réaction que les expériences ITC, dans la barre d'erreur, les valeurs d'enthalpie de réaction expérimentale et théorique sont plutôt en accord excellent. De plus, le calcul a révélé que

l'amination des carbènes Fischer étudiés ici par le phénylamine (**3.3b**) n'est pas thermodynamiquement possible à 25°C, car l'énergie libre de l'enthalpie et de la première étape de réaction (attaque nucléophile de l'amine) largement positive (valeur Δ*H* supérieure à 2,5 kcal/mol, valeur Δ*G* supérieure à 20 kcal/mol) ainsi que l'énergie libre de la seconde étape de Gibbs (transfert du proton et départ potentiel du méthanol) (Δ*G* évalué à environ 8 kcal/mol).

Chapter 7

Insertion of alkynes into palladacycles

7.1. Introduction.

First metallacycles were synthetized in 1965 by Cope and Siekman[247] by activating aromatic C-H bond, through so-called cyclo-metalation reaction. Consequently, metallacycles contain a direct metal-carbon bond, wherein the carbon atom is part of one of metal ligands. As the activation of C-H bond is one of the most important subjects within organometallic chemistry, resulting metallacycles found to be of great importance in many domains: from synthesis[248] and catalysis[249] to medicine[250] and materials.[251] Among transition metals, palladium has been one of most used metal within metallacycle chemistry so far. In general, the cyclo-metalation reaction in case of palladium follows a base-assisted electrophilic pathway.[252] An insertion of various kinds of alkynes into Pd-C bond has been observed by Pfeffer and co-workers.[253]

That finding has found to be quite useful preparative method for range of palladacycles containing various functionalities.[254] The mechanism of the insertion of the alkynes into the

[247] [N^0 620] A. C. Cope, R. W. J. Siekman, *Am. Chem. Soc.* 1965, *87*, 3272.
[248] [N^0 621] J. Spencer, M. Pfeffer, *Adv. Met-Org. Chem.* **1998**, *6*, 103.
[N^0 622] M. Pfeffer, *Recl. Trav. Chim. Pays-Bas* **1990**, *109*, 567.
[N^0 623] *Palladacycles: Synthesis, Characterization and Applications*; Eds. J. Dupont, M. Pfeffer, Wiley-VCH: Weinheim, Germany, **2008**.
[N^0 624] W. A. Herrmann, V. P. W. Bohm, C. P. J. Reisinger, *J. Organomet. Chem.* **1999**, 576, 23.
[N^0 625] J.-P. Djukic, A. Hijazi, H. D. Flack, G. Bernardinelli, *Chem. Soc. Rev.* **2008**, *37*, 406.
[N^0 626] R. F. Heck, *Palladium Reagents in Organic Syntheses*; Academic Press: New York, **1985**.
[N^0 627] *Comprehensive Organometallic Chemistry II*; Eds. G. Wilkinson, F. G. Stone, E. W. Abel, Pergamon Press: New York, **1995**; vol. 12.
[249] [N^0 628] M. Ohff, A. Ohff, D. Milstein, *Chem. Commun.* **1999**, 357.
[N^0 629] Y. J. Wu, J. J. Hou, H. Y. Yun, X. L. Cui, R. J. Yuan, *J. Organomet. Chem.* **2001**, *637*, 793.
[N^0 630] J. Dupont, M. Pfeffer, J. Spencer, *Eur. J. Inorg. Chem.* **2001**, 1917.
[N^0 631] R. B. Bedford, *Chem. Commun.* **2003**, 1787.
[N^0 632] W. A. Herrmann, C. Brossmer, K. K. Öfele. C.-P. Reisinger, T. Priermeier. M. Beller, H. Fischer, *Angew. Chem. Int. Ed.* **1995**, *34*, 1844.
[N^0 633] T. Rosner, J. Le Bars, A. Pfaltz, D. G. Blackmond, *J. Am. Chem. Soc.* **2001**, *123,* 1848.
[N^0 634] A. V. Cheprakov, I. P. Beletskaya, *J. Organomet. Chem.* **2004**, *689*, 4055.
[N^0 635] J. Dupont, C. S. Consorti, Spencer, *J. Chem. Rev.* **2005**, 105,2527.
[250] [N^0 636] D. M. Fan, C. T. Yang, J. D. Ranford, J. J. Vittal, P. F. Lee, *Dalton Trans.* **2003**, 3376.
[N^0 637] A. Gómez Quiroga, C. Navarro Ranninger, *Coord. Chem. Rev.* **2004**, *248*, 119.
[251] [N^0 638] M. Albrecht, M. Lutz, A. L. Spek, G. van Koten, *Nature* **2000**, *406*, 970.
[N^0 639] M. Ghedini, D. Pucci, G. Barberio, *Liq. Cryst.* **2000**, *27*, 1277.
[N^0 640] L. Diez, P. Espinet, J. A. Miguel, M. B. Ros, *J. Mater. Chem.* **2002**, *12*, 3694.
[252] [N^0 641] A. D. Ryabov, *Chem. Rev.* **1990**, *90*, 403.
[N^0 642] D. L. Davies, S. M. A. Donald, S. A. Macgregor, *J. Am. Chem. Soc*. **2005**, 127, 13754.
[N^0 643] Y. Boutadla, D. L. Davies, S. A. Macgregor, A. I. Poblador-Bahamonde*, Dalton Trans.* **2009**, 5820.
[253] [N^0 644] A. Bahsoun, J. Dehand, M. Pfeffer, M. Zinsius, *J. Chem. Soc*. *Dalton Trans*. **1979**, 547.
[N^0 645] A. D. Ryabov, *Synthesis* **1985**, 233.
[N^0 622] M. Pfeffer, *Recl. Trav. Chim*. *Pays-Bas* **1990**, *109*, 567.
[254] [N^0 646] M.-J. Oliva-Madrid, J.-A. García-López, I. Saura-Llamas, D. Bautista, José Vicente, *Organometallics* **2014**, *33*, 33.
[N^0 647] R. B. Bedford, Chem. Commun. **2003**, 1787.
[N^0 648] R. Ratti, *Can. Chem. Trans.* **2014**, *2*, 467.

palladacycles has been intensively studied.[255] In general, the insertion of the alkynes is a step-wise process beginning with a coordination of the alkyne to the palladium and subsequent migratory insertion of the alkyne into Pd-C bond. Usually, the first insertion is rate determining step within multiple insertions. It was found that electron deficient alkynes (for instance dimethyl acetylenedicarboxylate (DMAD) (**4.4a**, see Scheme 4.1)) do single insertion while the electron rich alkynes (for instance diphenyl-ethyne (**4.4b**, see Scheme 4.1)) give double inserted reaction product.[256]

[N^0 649] C. López, R. Bosque, X. Solans, M. Font-Bardía, J. Silver, G. Fern, *J. Chem. Soc.*, *Dalton Trans*. **1995**, 1835.
[N^0 650] R. C. Larock, E. K. Yum, M. J. Doty, K. K. C. J. Sham, *Org. Chem.* **1995**, *60*, 3270.
[N^0 651] A.-E. Gies, M. Pfeffer, C. Sirlin, J. Spencer, *Eur. J. Org. Chem*. **1999**, 1957.
[N^0 652] J. Vicente, J. A. Abad, R. Fernández-de-Bobadilla, P. G. M. Jones, C. Ramírez de Arellano, *Organometallics* **1996**, *15*, 24.
[N^0 653] J. Vicente, J. A. Abad, R. Bergs, P. G. Jones, M. C. Ramírez de Arellano*, Organometallics* **1996**, *15*, 1422.
[N^0 654] J. Vicente, J. A. Abad, J. Gil-Rubio, *Organometallics* **1996**, *15*, 3509.
[N^0 655] J. A. Abad, *Gazz. Chim. Ital.* **1997**, *127*, 119.
[N^0 656] R. C. Larock, E. K. Yum, M. D. Refvik, *J. Org. Chem.* **1998**, *63*, 7652.
[N^0 657] S. Cacchi, *J. Organomet. Chem.* **1999**, *576*, 42.
[N^0 658] J. Vicente, J. A. Abad, R. Bergs, M. C. Ramírez de Arellano, E. Martínez-Viviente, P. G. Jones*, Organometallics* **2000**, *19*, 5597.
[N^0 659] J. Vicente, J. A. Abad, B. López-Peláez, E. Martínez-Viviente, *Organometallics* **2002**, *21*, 58.
[N^0 660] J. Vicente, J. A. Abad, W. Förtsch, M.-J. López-Sáez, P. G. Jones, *Organometallics* **2004**, *23*, 4414.
[N^0 661] J. Vicente, J. A. Abad, J. López-Serrano, P. G. Jones, C. Nájera, L. Botella-Segura, *Organometallics* **2005**, *24*, 5044.
[N^0 662] J. Albert, J. Granell, A. Luque, M. Font-Bardia, X. Solans, *Polyhedron* **2006**, *25*, 793.
[N^0 663] G. Z. Wu, S. J. Geib, A. L. Rheingold, R. F. Heck, *J. Org. Chem*. **1988**, *53*, 3238.
[N^0 664] Y. Zhang, E. Negishi, *J. Am. Chem. Soc*. **1989**, *111*, 3454.
[N^0 665] L. S. Liebeskind, J. R. Gasdaska, J. S. McCallum, S. J. Tremont, *J. Org. Chem.* **1989**, *53*, 669.
[N^0 666] R. C. Larock, E. K. Yum, *J. Am. Chem. Soc.* **1991**, *113*, 6689.
[N^0 667] J. Vicente, J. A. Abad, J. Gil-Rubio, *J. Organomet. Chem*. **1992**, *436*, C9.
[N^0 668] J. Vicente, J. A. Abad, J. Gil-Rubio, P. G. Jones, *Organometallics* **1995**, *14*, 2677.
[N^0 669] J. Vicente, J. A. Abad, K. F. Shaw, J. Gil-Rubio, M. C. Ramírez de Arellano, P. G. Jones, *Organometallics* **1997**, *16*, 4557.
[N^0 670] K. R. Roesch, R. C. Larock, *J. Org. Chem*. **1998**, *63*, 5306.
[N^0 671] R. C. Larock, *J. Organomet. Chem*. **1999**, *576*, 111.
[N^0 672] J. Vicente, J. A. Abad, E. Martínez-Viviente, M. C. Ramírez de Arellano, P. G. Jones, *Organometallics* **2000**, *19*, 752.
[255] [N^0 673] C. Arlen, M. Pfeffer, O. Bars, D. Grandjean, *J. Chem. Soc., Dalton Trans*. **1983**,1535.
[N^0 674] G. Z. Wu, A. L. Rheingold, S. J. Geib, R. F. Heck, *Organometallics* **1987**, *6*, 1941.
[N^0 675] F. Maassarani, M. Pfeffer, G. Le Borgne, *Organometallics* **1987**, *6*, 2029.
[N^0 676] W. Tao, L. J. Silverberg, A. L. Rheingold, R. F. Heck, *Organometallics* **1989**, *8*, 2550.
[N^0 622] M. Pfeffer, *Recl. Trav. Chim. Pays-Bas* **1990**, *109*, 567.
[N^0 677] M. Pfeffer, *Pure Appl. Chem.* **1992**, *64*, 335.
[N^0 678] J. Spencer, M. Pfeffer, *Tetrahedron*: *Asymmetry* **1995**, *6*, 419.
[N^0 679] E. G. Samsel, J. R. Norton, *J. Am. Chem. Soc*. **1984**, *106*, 5505.
[N^0 680] P. de Vaal, A. Dedieu, *J. Organomet. Chem*. **1994**, *478*, 121.
[N^0 681] F. Maassarani, M. Pfeffer, G. J. Le Borgne, *Chem. Soc. Chem. Commun*. **1986**, 488.
[N^0 682] G. Z. Wu, A. L. Rheingold, R. F Heck, *Organometallics* **1986**, *5*, 1922.
[N^0 683] A. D. Ryabov, R. van Eldik, G. Le Borgne, M. Pfeffer, *Organometallics* **1993**, *12*, 1386.
[256] [N^0 683] A. D. Ryabov, R. van Eldik, G. Le Borgne, M. Pfeffer, *Organometallics* **1993**, *12*, 1386.

While kinetics of the insertion reactions of the alkynes into the palladacycles are described[257] no information of actual thermochemistry has been provided yet. Thus, within this study a round of isothermal calorimetric measurements on the various insertion reactions (see Scheme 4.1), supplemented with theoretical estimations, was engaged.

The insertion reactions of the alkynes (**4.4a-b**, Scheme 4.1) into the palladacyclic complexes (**4.3a-d** Scheme 4.1)) were studied experimentally (by carrying out the reaction tests and ITC measurements) and theoretically by performing static DFT-D calculations. The mechanism of the investigated insertion reactions, which is rather quite known[258] implies a perpendicular approach of the alkyne to the palladium followed by labile coordination of the alkyne by means of triple carbon – carbon bond and a decoordination of an adjacent MeCN ligand. From that point the system might either go back or to a further step that starts with a nucleophilic attack of the carbon, directly connected to the palladium, on the alkyne's triple bonded carbon establishing new carbon-carbon bond, while another triple bonded carbon connects to the palladium. If the alkyne is **4.4a**, this stair-case sequence finishes by coordination of the MeCN resulting in single inserted product (**4.5a**-**d**). However, if the used alkyne is **4.4b**, the sequence cannot be stopped here due to the extreme reactivity of the formed single inserted product which would rather react with another molecule of alkyne forming a new carbon-carbon bond leading to the insertion of second alkyne into the palladacycle by "kicking out" one of the coordinated MeCN molecules. According to the literature[259] the insertion of the alkyne **4.4b** should lead exclusively to the double inserted product (**4.6a**) whatever the molar ratio of the reactants (**4.3a** and **4.4b**) is, while the insertion of the alkyne **4.4a** is dependent of the molar ratio, as additional (side) reactions (i.e. ligand exchange and double/triple insertion of the alkyne, see Scheme 4.2-3) are, in presence of an excess of the alkyne, possible to happen.

Therefore, within this study the reaction tests were carried out to figure out whether the chosen reaction system could be used in the ITC measurements as well as to check the literature statements in the ITC conditions.

[257] [N^0 683] A. D. Ryabov, R. van Eldik, G. Le Borgne, M. Pfeffer, *Organometallics* **1993**, *12*, 1386.
[258] [N^0 678] J. Spencer, M. Pfeffer, *Tetrahedron*: *Asymmetry* **1995**, *6*, 419.
[N^0 683] A. D. Ryabov, R. van Eldik, G. Le Borgne, M. Pfeffer, *Organometallics* **1993**, *12*, 1386.
[259] [N^0 683] A. D. Ryabov, R. van Eldik, G. Le Borgne, M. Pfeffer, *Organometallics* **1993**, *12*, 1386.

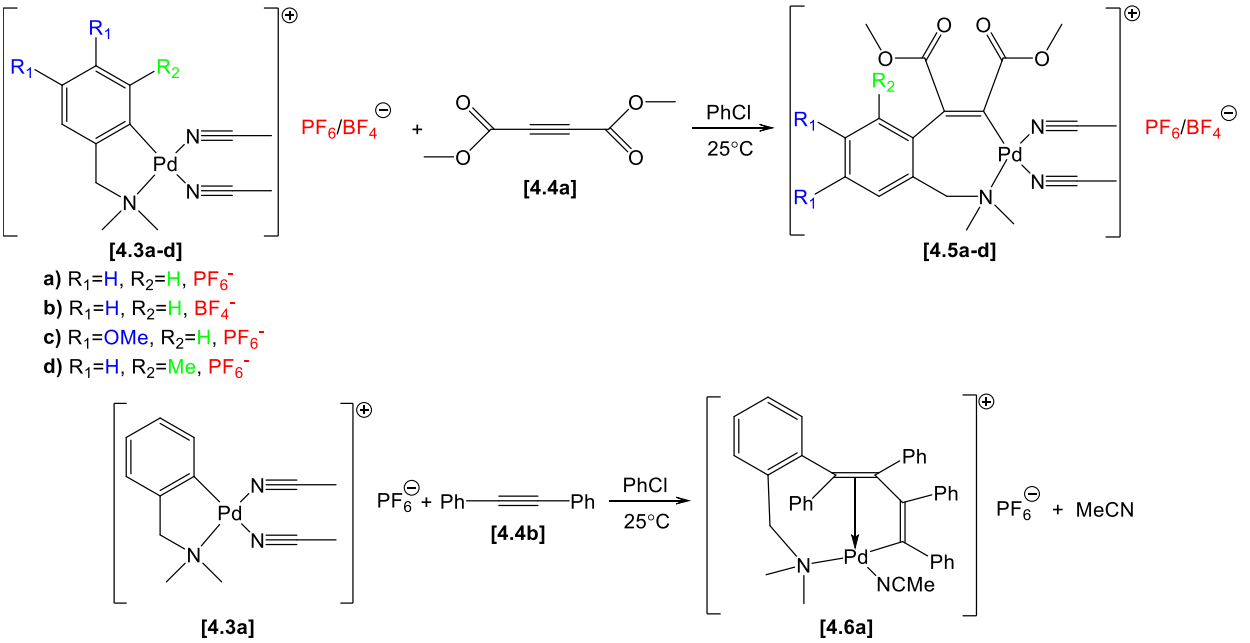

Scheme 4.1 Schematic representation of the investigated reactions within the study of the single/double insertion of the alkyne **4.4a-b** into the palladacycle **4.3a-d**.

7.2. Experimental section.

7.2.1. Generalities.

As mentioned in the introductory chapter, the experiments considered single insertion reaction of dimethyl acetylenedicarboxylate (**4.4a**) into the palladacyclic complexes (**4.3a-d**) as well as double insertion reaction of diphenylethyne (**4.4b**) into the palladacyclic complex (**4.3a**) (see Scheme 4.1).

7.2.2. Techniques.

The investigations within the study of the insertion reactions of the alkynes (**4.4a-b**) into the palladacycles (**4.3a-d**) were performed using ITC measurements and static DFT-D calculations, while the synthesis and the reaction tests were carried out using standard Schlenk line experimental technique. The chemical characterizations of the products were done employing Nuclear Magnetic Resonance (NMR) spectroscopy, Elemental Analysis (EA), Mass Spectrometry (MS) and X-Ray diffractometry (X-Ray).

7.2.3. Materials.

All used compounds were stored and used into a dry and argon filled glove box or under argon. Chlorobenzene was purchased from Sigma Aldrich and distillated over calcium hydride and degassed prior to use. Alkynes (**4.4a-b**) were purchased from Sigma Aldrich and used as received after checking their purity by NMR. If needed a purification of the alkynes was done through silica with pentane as an eluent. Palladacyclic complexes (**4.3a-d**) were prepared by modified literature procedure.[260] Starting amino ligand 1-(3,4-dimethoxyphenyl)-N,N-dimethylmethanamine (**4.1c**) were prepared by modified literature procedure.[261] Palladium-chloride was purchased from Sigma Aldrich and used as received. Lithium-chloride was purchased from Sigma Aldrich and used as received. (3,4-dimethoxyphenyl)methanamine was purchased from Sigma Aldrich and used as received. N,N-dimethyl-1-phenylmethanamine (**4.1a**) was purchased from Sigma Aldrich and used as received. m-tolylmethanamine (**4.1d**) was purchased from Sigma Aldrich and used as received. Formic acid (88%) and formaldehyde (37%) were purchased from Sigma Aldrich and used as received. Triethylamine was purchased from Sigma Aldrich and used as received. All used solvents in the synthesis and reaction tests (CH_2Cl_2, MeOH, MeCN, pentane, hexane) were purchased from Sigma Aldrich and distillated over an appropriate drying agent prior to use. Deuterated chloroform was purchased from Sigma Aldrich and dried through neutral alumina prior to use.

7.2.4. Reaction tests.

The reaction tests were carried out in two methodologies: a) in CH_2Cl_2 followed by the isolation of the reaction product and its subsequent characterization (mainly by ^{1}H NMR spectroscopy) and b) in $CDCl_3$ without the isolation of the reaction product while the reaction was monitored by ^{1}H NMR spectroscopy.

[260] [N^0 684] Pfeffer, M, Goel, A. B. *Cyclopalladated Compounds in Inorganic Syntheses*; ed H. D. Kaesz, John Wiley & Sons, Inc., Hoboken, New York, **1989**, vol. 26, ch. 38, and related references therein.
[261] [N^0 685] E. L. Eliel, T. N. Ferdinand, M. C. Herrmann, *J. Org. Chem.* 1954,*19*, 1693.

7.2.4.1. *Synthetic approach.*

7.2.4.1.1. Synthesis of **4.1c.**

The synthesis of the precursor – tertiary amine **4.1c** was done following modified literature procedure.[262] Reaction scheme of the synthesis is depicted in Scheme ES 4.1.

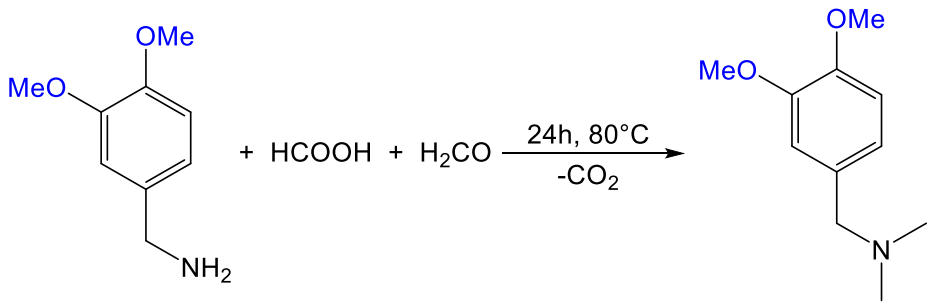

Scheme ES 4.1 Simplified schematic representation of the synthesis of the amine **4.1c**.

Schlenk tube was put in a cold ice bath and loaded with starting materials: amine (1.50 g, 0.009 mol), formic acid 88% (1.44 g, 0.025 mol) and formaldehyde 37% (2.04 g, 0.025 mol). The reaction mixture was refluxed (at 80°C) for 24 hours. To the reaction mixture 3 mL of HCl 6M was added. The crude product was extracted with 3 x 5 mL of Et_2O. Subsequently, to the water layer a solution of sodium-hydroxide (ca. 2g in 3 mL of water) was added and a remained product was extracted with 3 x 5 mL of Et_2O. The resulting ether fraction was mixed, dried on anh. magnesium-sulphate and filtrated. Hence, the solvent was evaporated resulting in colorless oily product that was further dried under reduced pressure for several hours.

Yield: 0.97g (56%).

^{1}H NMR (400 MHz, chloroform-*d*, δ, ppm) 6.87 (t, *J* = 1 Hz, 1H), 6.80 (d, *J* = 1 Hz, 2H), 3.95 (d, *J* = 8.8 Hz, 1H), 3.87 (d, *J* = 8 Hz, 6H), 3.35 (s, 2H), 2.22 (s, 6H).

7.2.4.1.2. Synthesis of **4.2a-d.**

As all these compounds were synthetized in the same manner, only a general procedure is explained. The used procedure followed the literature procedure.[263] Reaction scheme of the synthesis is depicted in Scheme ES 4.2.

[262] [N^0 685] E. L. Eliel, T. N. Ferdinand, M. C. Herrmann, *J. Org. Chem.* 1954,*19*, 1693.

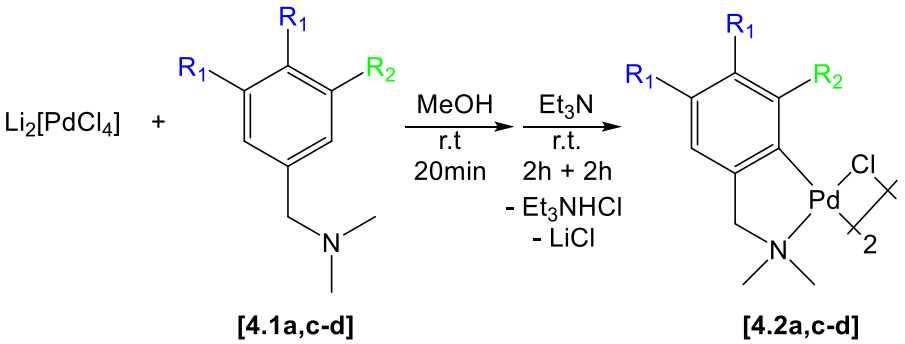

[4.1a,c-d] **[4.2a,c-d]**

a) R_1=H, R_2=H
c) R_1=OMe, R_2=H
d) R_1=H, R_2=Me

Scheme ES 4.2 Simplified schematic representation of the synthesis of the palladacycles **4.2a, 4.2c** and **4.2d**.

The flask was loaded with 37.5 mL of previously prepared solution of $PdCl_2$ (1.88 g, 0.011 mol) and LiCl (2.5 g, 0.059 mol) in MeOH. The amine (**4.1a**,**c**,**d**) (0.011 mol) was added into the solution of the palladium salt. After few minutes of stirring a cream-colored precipitate appeared. Then, the solution of Et_3N was added into the mixture drop-wisely within 80 minutes. The resulting mixture was allowed to stir for 6 hours. Resulting yellow precipitate was filtrated through *Celite*, washed with 3 x 10 mL of MeOH and with 2 x 10 mL of Et_2O and dried under reduced pressure for several hours. The product was obtained as pale-yellow powder.

Yield: 83-85%.

NMR

4.2a ^{1}H NMR (500 MHz, chloroform-*d*, δ, ppm) 7.22 – 6.81 (m, 8H), 3.93 (s, 4H), 2.85 (d, *J* = 13 Hz, 12H).^{13}C NMR (126 MHz, chloroform-*d*, δ, ppm) 146.9 (d, *J* = 16 Hz), 143.0 (d, *J* = 15 Hz), 133.5, 132.9, 125.2 (d, *J* = 6 Hz), 124.7, 121.5 (d, *J* = 4 Hz), 73.25 (d, *J* = 20 Hz), 52.76 (d, *J* = 36.3 Hz).

4.2c ^{1}H NMR (300 MHz, chloroform-*d*, δ, ppm) 6.70 (d, *J* = 11 Hz, 2H), 6.48 (d, *J* = 2 Hz, 2H), 3.89 (d, *J* = 3 Hz, 4H), 3.81 (d, 12H), 2.85 (d, *J* = 9 Hz, 12H).

4.2d ^{1}H NMR (400 MHz, chloroform-*d*, δ, ppm) 6.99 (d, *J* = 24 Hz, 2H), 6.76 (q, *J* = 8 Hz, 4H), 3.89 (s, 4H), 2.84 (d, *J* = 15 Hz, 12H), 2.26 (d, *J* = 10 Hz, 6H).

[263] [N^0 684] Pfeffer, M, Goel, A. B. *Cyclopalladated Compounds in Inorganic Syntheses*; ed H. D. Kaesz, John Wiley & Sons, Inc., Hoboken, New York, **1989**, vol. 26, ch. 38, and related references therein.

Corresponding NMR spectra are given in Supplementary Information (see Figure SI 4.10-14).

7.2.4.1.3. Synthesis of **4.3a-d.**

As all these compounds were synthesized in the same manner, only a general procedure is described in detail. The used procedure followed the literature procedure.[264] Reaction scheme of the synthesis is depicted in Scheme ES 4.3.

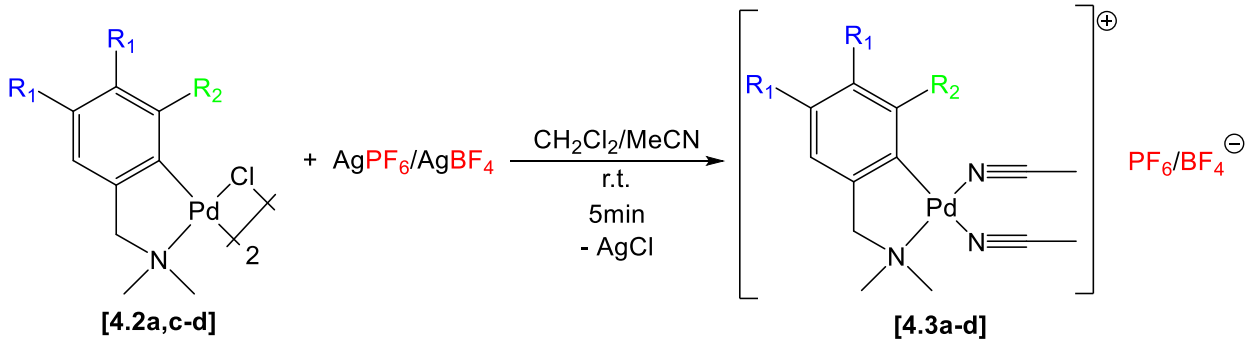

a) R_1=H, R_2=H, PF_6^-
b) R_1=H, R_2=H, BF_4^-
c) R_1=OMe, R_2=H, PF_6^-
d) R_1=H, R_2=Me, PF_6^-

Scheme ES 4.3 Simplified schematic representation of the synthesis of the palladacycles **4.3a-d**.

Into the solution containing the compound **2a-d** (0.5 mmol) and 2 mL of MeCN in 20 mL of CH_2Cl_2, the solution that contained PF_6 or BF_4 (1.0 mmol) and 1 mL of MeCN in 5 mL of CH_2Cl_2 was added. These solutions were prepared in separate Schlenk tubes. The resulting mixture was allowed to stir for few minutes, i.e. until a precipitate (AgCl) was observed. Then the mixture was filtrated through *Celite*. The solvents of the resulting solution were evaporated under reduced pressure. The crude product was then dissolved in minimal amount of CH_2Cl_2 and around 2 mL of pentane was added in order to induce precipitation of the product. After adding the additional 5 mL of pentane the solvent was decanted and the product was dried under reduced pressure for two hours. The product was obtained as a pale-brown powder.

Yield: 91-94%.

[264] [N^0 684] Pfeffer, M, Goel, A. B. *Cyclopalladated Compounds in Inorganic Syntheses*; ed H. D. Kaesz, John Wiley & Sons, Inc., Hoboken, New York, **1989**, vol. 26, ch. 38, and related references therein.

NMR

4.3a ^{1}H NMR (300 MHz, chloroform-*d*, δ, ppm) 7.09 – 6.84 (m, 4H), 3.91 (s, 2H), 2.80 (s, 6H), 2.44 (s, 3H), 2.34 (s, 3H). ^{13}C NMR (126 MHz, chloroform-*d*, δ, ppm) 145.1, 130.8, 123.7, 123.5, 120.1, 118.5, 70.8, 50.3, 20.0, 11.7.

4.3b ^{1}H NMR (400 MHz, chloroform-*d*, δ, ppm) 7.06 (ddd, *J* = 8, 7, 2 Hz, 1H), 6.96 – 6.86 (m, 3H), 3.94 (s, 2H), 2.84 (s, 6H), 2.50 (s, 3H), 2.34 (s, 3H).

4.3c ^{1}H NMR (300 MHz, chloroform-*d*, δ, ppm) 6.52 (s, 1H), 6.38 (s, 1H), 3.91 (s, 2H), 3.82 (d, *J* = 9 Hz, 6H), 2.82 (s, 6H), 2.48 (s, 3H), 2.19 (s, 3H).

4.3d ^{1}H NMR (400 MHz, chloroform-*d*, δ, ppm) 6.90 – 6.65 (m, 3H), 3.91 (s, 2H), 2.81 (s, 6H), 2.48 (s, 3H), 2.27 (s, 3H), 2.14 (s, 3H).

Corresponding NMR spectra are given in Supplementary Information (see Figure SI 4.15-19).

7.2.4.1.4. Synthesis of **4.5a-c.**

As all these compounds were synthesized in the same manner, only a general procedure is explained. The used procedure followed the literature procedure.[265] Reaction scheme of the synthesis is depicted in Scheme ES 4.4.

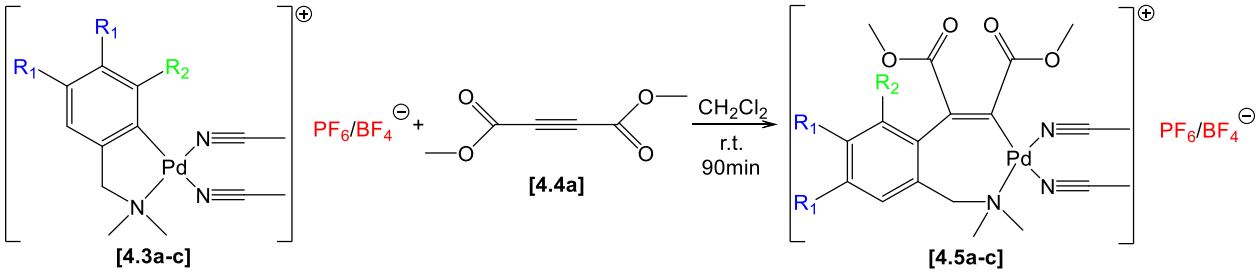

Scheme ES 4.4 Simplified schematic representation of the synthesis of the palladacycles **4.5a-c**.

The palladacycle (**4.3a-c**) (0.1 mmol) was dissolved in 10 mL of CH_2Cl_2 and subsequently the solution that contained (14.2 mg, 0.1 mmol) of the alkyne **4.4a** in 1 mL of CH_2Cl_2 was added. After stirring the reaction mixture for 90 minutes, the solvent evaporated under reduced

pressure. The resulting yellow residue was washed with 3 x 5 mL of hexane. After evaporation of hexane under reduced pressure, a yellow-orange product appeared and was consecutively dried under reduced pressure for several hours.

Yield: 62-64%.

NMR

4.5a ^{1}H NMR (400 MHz, chloroform-*d*, δ, ppm) 7.68 (d, *J* = 8 Hz, 1H), 7.55 (t, *J* = 7 Hz, 1H), 7.48 – 7.36 (m, 1H), 7.32 (d, *J* = 7 Hz, 1H), 3.83 (d, *J* = 12 Hz, 1H), 3.83 (d, 6H), 2.99 (d, *J* = 12 Hz, 1H), 2.96 (s, 3H), 2.90 (d, *J* = 5 Hz, 1H), 2.56 (s, 3H), 2.26 (d, *J* = 15 Hz, 6H).

4.5b ^{1}H NMR (300 MHz, chloroform-*d*, δ, ppm) 7.68 (dd, *J* = 8, 1 Hz, 1H), 7.56 (td, *J* = 8, 1 Hz, 1H), 7.44 (td, *J* = 8, 2 Hz, 1H), 7.32 (dd, *J* = 8, 1 Hz, 1H), 3.91 (s, 3H), 3.69 (s, 3H), 2.99 (s, 3H), 2.99 (d, *J* = 12 Hz, 1H), 2.63 (s, 3H), 2.34 (s, 3H), 2.28 (s, 3H).

4.5c ^{1}H NMR (300 MHz, chloroform-*d*, δ, ppm) 7.21 (s, 1H), 6.78 (s, 1H), 3.96 (d, *J* = 8 Hz, 6H), 3.89 (s, 3H), 3.69 (s, 3H), 2.96 (s, 3H), 2.92 (d, *J* = 12 Hz, 1H), 2.63 (s, 3H), 2.32 (s, 3H), 2.24 (s, 3H).

Corresponding NMR spectra are given in Supplementary Information (see Figure SI 4.20-21).

3.5.4.1.5. Synthesis of **4.6a.**

The synthesis of palladacycle **4.6a** was done following a modified literature procedure.[266] Reaction scheme of the synthesis is depicted in Scheme ES 4.5.

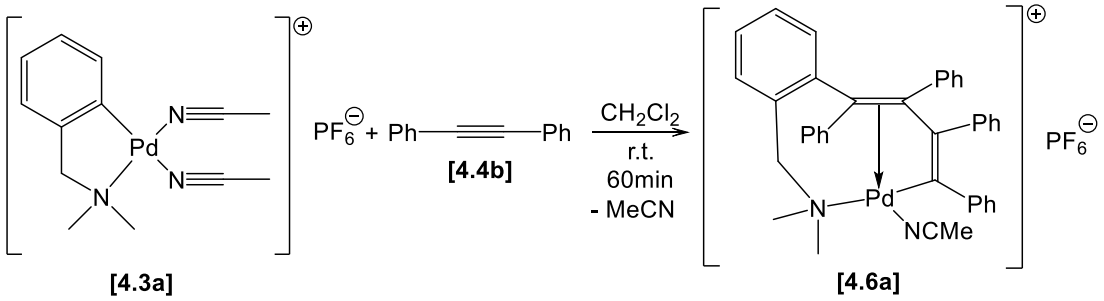

[4.3a] **[4.6a]**

Scheme ES 4.5 Simplified schematic representation of the synthesis of the palladacycles **4.6a**.

[265] [N^0 684] Pfeffer, M, Goel, A. B. *Cyclopalladated Compounds in Inorganic Syntheses*; ed H. D. Kaesz, John Wiley & Sons, Inc., Hoboken, New York, **1989**, vol. 26, ch. 38, and related references therein.
[266] [N^0 684] Pfeffer, M, Goel, A. B. *Cyclopalladated Compounds in Inorganic Syntheses*; ed H. D. Kaesz, John Wiley & Sons, Inc., Hoboken, New York, **1989**, vol. 26, ch. 38, and related references therein.

The palladacycle (**4.3a**) (0.1000 g, 0.2 mmol) was dissolved in 10 mL of CH_2Cl_2 and subsequently the solution that contained (0.0930 g, 0.4 mmol) of the alkyne **4.4b** in 1 mL of CH_2Cl_2 was added. After stirring of the reaction mixture for 60 minutes, the solvent was evaporated under reduced pressure. The resulting yellow residue was washed with 3 x 5 mL of hexane. After evaporation of hexane under reduced pressure, a yellow-orange product appeared. Consecutively, the product was dried under reduced pressure for several hours.

Yield: 0.13g (80%).

NMR

4.6a ^{1}H NMR (500 MHz, chloroform-*d*, δ, ppm) 7.45 – 7.13 (m, 24H), 7.07 – 6.89 (m, 3H), 6.62 (d, *J* = 9 Hz, 1H), 2.78 (s, 2H), 2.53 (d, *J* = 139 Hz, 6H), 1.96 (s, 6H). ^{13}C NMR (126 MHz, chloroform-*d*, δ, ppm) 145.7, 144.0, 137.0, 134.9, 134.6, 134.5, 132.5, 131.8, 131.0, 130.9, 129.6, 129.1, 128.4, 127.4, 127.3, 127.1, 126.7, 126.3, 126.0, 125.4, 125.1, 124.9, 124.3, 124.2, 124.17, 123.7, 123.5, 122.8, 120.0, 74.9, 74.7, 74.4, 70.9, 64.6, 49.8, 44.1, 29.3, 20.3, 11.8, 0.7, -0.0, -1.3.

Corresponding NMR spectra are given in Supplementary Information (see Figure SI 4.22-23).

7.2.4.2. *Monitoring approach.*

7.2.4.2.1. Synthesis of **4.5a-c.**

The reactants - the palladacycle (**4.3a-c**) (0.1 mmol) and alkyne **4.4a** (0.2 mmol) were separately dissolved into 2.5 mL and 1.0 mL of deuterated chloroform, respectively. The solution of the alkyne was sequentially injected into the stirred solution of the palladacycle. ^{1}H NMR spectra was recorded immediately after injection of 1 eqv of alkyne as well as after 3.5 hours. Additionally, the reaction was monitored by ^{1}H NMR upon adding of 2 eqv of alkyne within 1h and 15h of the reaction time. Related ^{1}H NMR spectra are given either in the main text of the manuscript (see Chapter 7) or in Supplementary Information (see Figure SI 4.20-21). Reaction scheme of the monitored synthesis is depicted in Scheme ES 4.6.

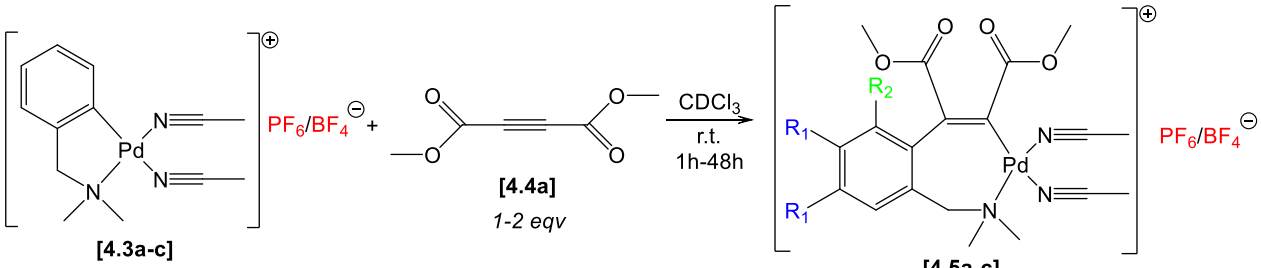

a) R_1=H, R_2=H, PF_6^-
b) R_1=H, R_2=H, BF_4^-
c) R_1=OMe, R_2=H, PF_6^-

Scheme ES 4.6 Simplified schematic representation of the monitoring approach of the synthesis of the palladacycles **4.5a-c** in deuterated chloroform.

3.5.4.2.2. Synthesis of **4.6a.**

The reactants - the palladacycle (**4.3a**) (46.8 mg, 0.1 mmol) and alkyne **4.4b** (178.2 mg, 1.0 mmol) were separately dissolved into 2.5 mL and 3.0 mL of deuterated chloroform, respectively. The solution of the alkyne was sequentially injected into the stirred solution of the palladacycle. The reaction was monitored by ^{1}H NMR upon adding of 1-10 eqv of alkyne within 0.7h to 24h of the reaction time. Related ^{1}H NMR spectra are given either in the main text of the manuscript (see Chapter 7) or in the Supplementary Information (see Figure SI 4.22-23).

Reaction scheme of the monitored synthesis is depicted in Scheme ES 4.7.

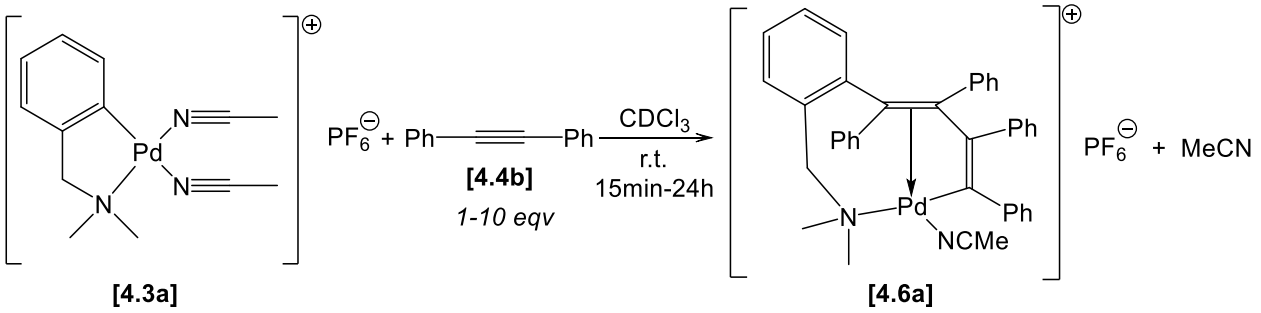

Scheme ES 4.7 Simplified schematic representation of the monitoring approach of the synthesis of the palladacycles **4.6a** in deuterated chloroform.

7.2.5. ESI-MS details.

The details were the following:

Positive mode
Acquisition parameters:
Method - Standard m/Mid m
Operator - BDAL@DE
Source Type - ESI Capillary 4500 V Nebulizer 0.3 Bar Set Hexapole RF 55.0 Vpp / 330.0 Vpp

Ion Polarity - Positive Dry Heater 200 °C Dry Gas 3.0 l/min Set Capillary Exit 100.0 V / 150.0 V

7.2.6. X-Ray diffraction analysis details.

For the crystal structures see Figure SI 4.6-7

7.2.7. ITC experimental details.

The solutions of the reactants (**4.3a-b** and **4.4a-b**, see Scheme 4.1) were prepared by dissolving a mass of substrate in pure, freshly distilled and degassed chlorobenzene. The ITC experiments were performed using sequential injection at 25ºC with a moderate stirring rate (150-200 rpm).

Due to the nature of the investigated reactions, two kinds of ITC experiments were performed. In a first one, that considered reaction of the palladacycle complex (**4.3a-b**) with the alkyne **4.4a**, the solution of the complex was introduced in the ITC sample cell while the servo-controlled ITC syringe (100 µL) contained the solution of the alkyne **4.4a**. The reference cell (1.0 mL) was entirely filled with pure PhCl. The concentration of the palladacycle complex (**4.3a-b**) in pure PhCl was around 1.1 mmol/L, while the concentration of **4.4a** solution were around 25.3 mmol/L. The content of the syringe was injected into the sample cell through 45 equivalent injections (2.06 µL per injection) with time delay between two consecutive injections of either 3000s or 10000s.

In a second one, that considered reaction of the palladacycle complex **4.3a** with the alkyne **4.4b**, the solution of the complex **4.3a** in pure PhCl was placed in the servo-controlled ITC syringe (100 µL) while the ITC sample was charged with the solution of the alkyne **4.4b**. The reference (1.0 mL) was entirely filled with pure PhCl. As the experiments considered a large excess of the alkyne **4.4b**, the concentration of the alkyne solution in pure PhCl spanned from around 3.3 mmol/L to 16.9 mmol/L, while the concentration of the solution of the complex were around 2.3 mmol/L. The content of the syringe was injected into the sample cell through 10 equivalent injections (first nine of 10.06 µL per injection while tenth of 5.03 µL) with time delay between two consecutive injections of 3000s.

For each studied system at least three experiments under the same condition were done (with an exception in the concentration of the solutions of **4.4b**, accordingly to the kinetic (in parallel to the thermodynamic) purpose of the performed experiments). A heat dilution of **4.3a** and **4.4a**

in neat PhCl was estimated from the blank experiments (basically, the titration of the **4.3a**/**4.4a** in pure PhCl) preformed under the same condition as the main experiments. Afterwards, the obtained heat of blank experiments was subtracted from all the corresponding titration curves. Enthalpy of reaction (ΔH_r) of the system **4.3a**/**4.4b** was obtained as a result of the experiment by summing up the heat released until the stoichiometry point against molar content introduced theretofore, while ΔH_r of the system **4.3a**/**4.4b** was obtained by summing up the heat released upon first three injections against molar content introduced during those three injections. Resulting ΔH_r values represent an average value of three corresponding experiments. As mentioned in the chapter two, this manner of treating ITC experiment data does not allow extracting reaction free energies (ΔG_r) and entropies (ΔS_r), while the kinetics parameters of reaction might be obtained. Although the use of the fitting models on an irreversible reaction is not reliable, the ITC data of the **4.3a**/**4.4b** were fitted using the independent *ad-hoc* logarithm (implemented within NanoITC software), that provided all the thermodynamic parameters.

7.2.8. Static DFT-D calculation details.

All computations were performed by the DFT methods using Amsterdam Density Functional package (ADF2013 version).

Starting geometries of the reactants (**4.3a** and **4.4a-b**, see Scheme 4.1) and the reaction products (**4.5a** and **4.6a**, see Scheme 4.1) were taken from the CSD or built up from the similar structures and optimized as singlet ground states in the chlorobenzene solution (COSMO) phase. All constructions of the starting geometries were done using the software provided within the ADF package. The geometries of the reaction products constructed in such a way were optimized as singlet ground states in the chlorobenzene solution phase.

7.3. Results and discussion.

7.3.1. Reaction tests.

The reaction tests were done in order to find most optimal conditions for the ITC measurements. They included two kinds of the experiments: a) experiments carried out into dichloromethane having the isolation (of the reaction products, supposedly **4.5a-c** and **4.6a**, see Scheme SI 4.4-5) purpose; b) the experiments carried out into deuterated chloroform with different molar ratios of the reactants (the palladacycles **4.3a-c** and the alkynes **4.4a-b**, see Scheme SI 4.6-7) within

various reaction times having monitoring purpose. In addition, **4.2a** was probed as the palladacycle by both approaches (the isolation and monitoring).

According to the literature[267] within these systems two kinds of additional reactions (ligand exchange and double/triple insertions) might happen if the alkyne is in an excess. Schematic representations of these side reactions are given in Scheme 4.2-3. Therefore, the aim of the tests was broadened to examination of possibility for such reactions within ITC conditions.

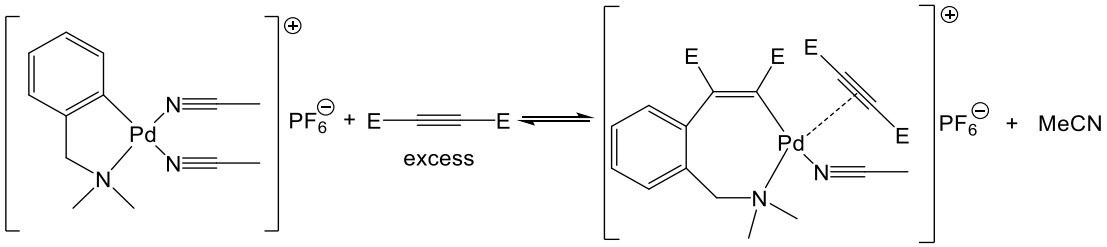

Scheme 4.2 Simplified schematic representation of the possible (side) reaction – exchanging of the ligands within the palladacycles in presence of an excess of the alkyne.

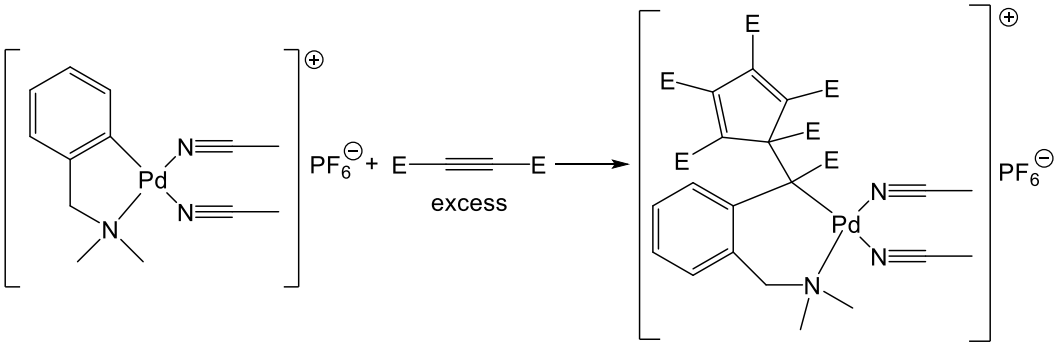

Scheme 4.3 Simplified schematic representation of the possible (side) reaction – double/triple insertion of the alkyne into the palladacycles in presence of an excess of the alkyne.

[267] [N^0 684] Pfeffer, M, Goel, A. B. *Cyclopalladated Compounds in Inorganic Syntheses*; ed H. D. Kaesz, John Wiley & Sons, Inc., Hoboken, New York, **1989**, vol. 26, ch. 38, and related references therein.

7.3.1.1. Approach one – the isolation.

In the Figure 4.1 ^{1}H NMR spectrum of the product (**4.5a**) of the stoichiometric reaction of **4.3a** with **4.4a**.

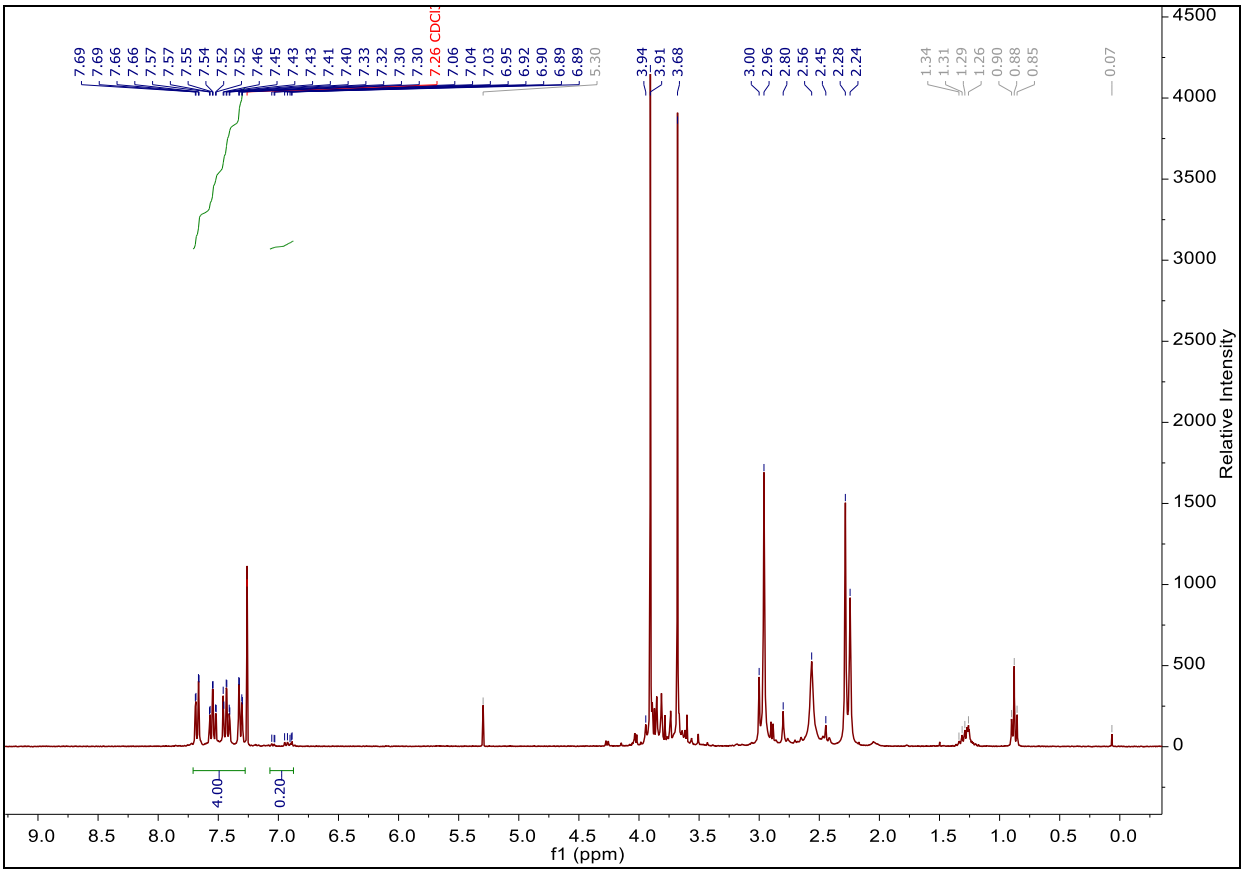

Figure 4.1 ^{1}H NMR spectrum of the reaction of **4.3a** with **4.4a** carried out at 25ºC within 90 minutes. The spectrum is recorded in deuterated chloroform at 300 MHz. ^{1}H NMR (300 MHz, chloroform-*d*, δ, ppm) 7.68 (dd, *J* = 8, 2 Hz, 1H), 7.55 (td, *J* = 8, 2 Hz, 1H), 7.43 (td, *J* = 8, 2 Hz, 1H), 7.31 (dd, *J* = 8, 2 Hz, 1H), 3.79 (d, *J* = 68 Hz, 6H), 2.99 (d, *J* = 12 Hz, 1H), 2.90 (d, *J* = 5 Hz, 1H)., 2.96 (s, 3H), 2.56 (s, 3H), 2.26 (d, *J* = 12 Hz, 6H).

Although a little excess of **4.3a** could be noticed on the shown spectrum, the spectrum suggests that the adduct **4.5a** could be obtained without interference of the side products (products of multiple insertions, see Scheme 4.3), as the aromatic region seems to be rather clear. The same conclusion could be drawn for the system **4.3b**/**4.4a** reacting stoichiometrically, by looking at ^{1}H NMR spectra of the reaction product **4.5b**, depicted in Figure 4.2. Therefore, it seems that both systems (**4.3a-b**/**4.4a**) could be used within ITC measurements in stoichiometric condition.

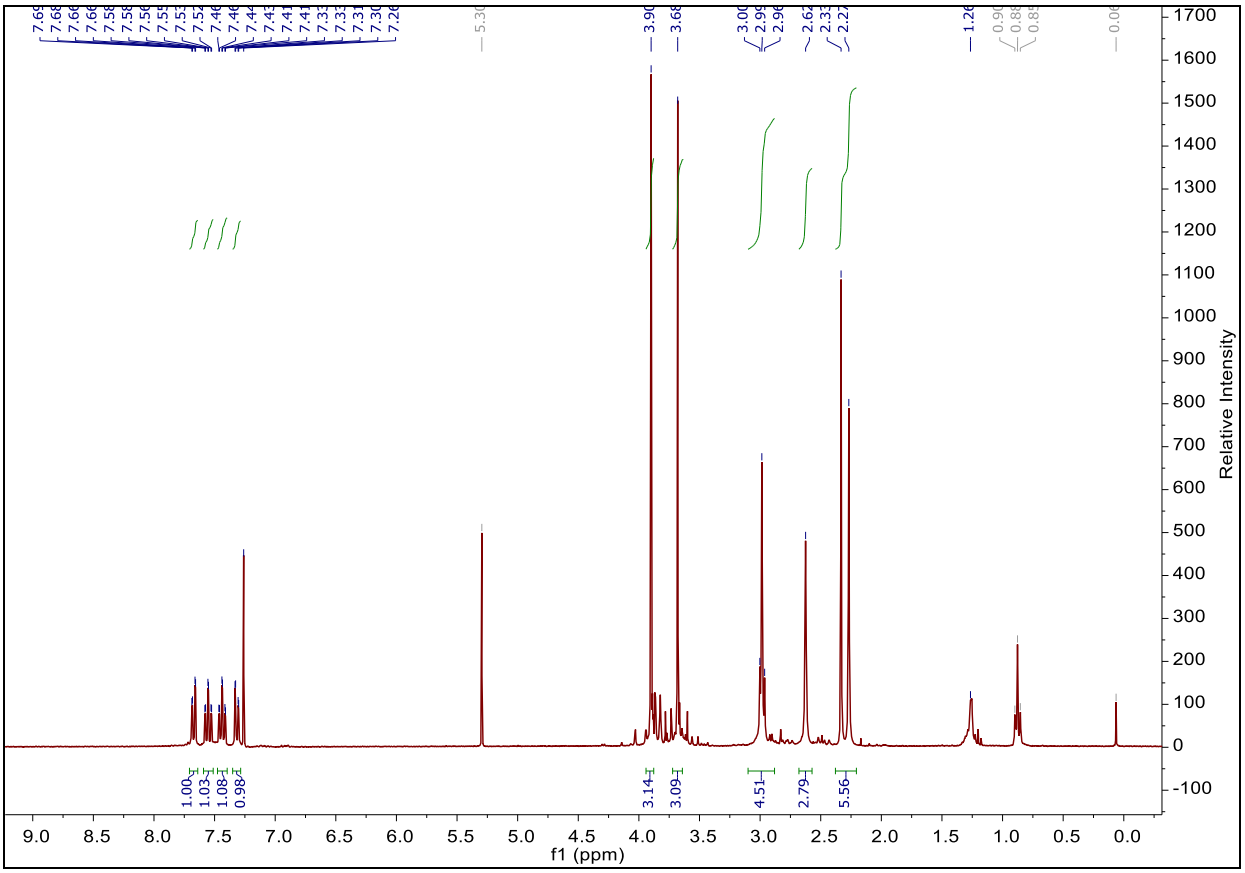

Figure 4.2 ^{1}H NMR spectrum of the reaction of **4.3b** with **4.4a** carried out at 25ºC within 45 minutes. The spectrum is recorded in deuterated chloroform at 300 MHz. ^{1}H NMR (300 MHz, chloroform-*d*, δ, ppm) δ 7.67 (dd, *J* = 8, 1 Hz, 1H), 7.55 (td, *J* = 8, 1 Hz, 1H), 7.44 (td, *J* = 8, 1 Hz, 1H), 7.32 (dd, *J* = 8, 1 Hz, 1H), 3.90 (s, 3H), 3.68 (s, 3H), 2.99 (s, 3H), 2.98 (d, *J* = 12 Hz, 2H), 2.62 (s, 3H), 2.30 (d, *J* = 19 Hz, 6H).

Unfortunately, the isolation of the reaction product **4.5c** has failed.

The ^{1}H NMR spectrum of the reaction product the reaction of **4.3a** with **4.4b** with the ratio of the reactant ca. 1:1.9 is reported in Figure 4.3, while its ^{13}C NMR spectrum is given in Supplementary Information (Figure SI 4.23). Markedly, the single inserted product is not observed. Exclusively the product of double insertion and some amount of the started palladacycle remained. This observation confirmed already found features of the alkyne **4.4b**[268] that has been pointed out as quite reactive alkyne giving only the double inserted product. This also suggests that this system might be examined within ITC experiments considering 1:2 molar ratio in favor to the alkyne.

[268] [N^{0} 683] A. D. Ryabov, R. van Eldik, G. Le Borgne, M. Pfeffer, *Organometallics* **1993**, *12*, 1386.

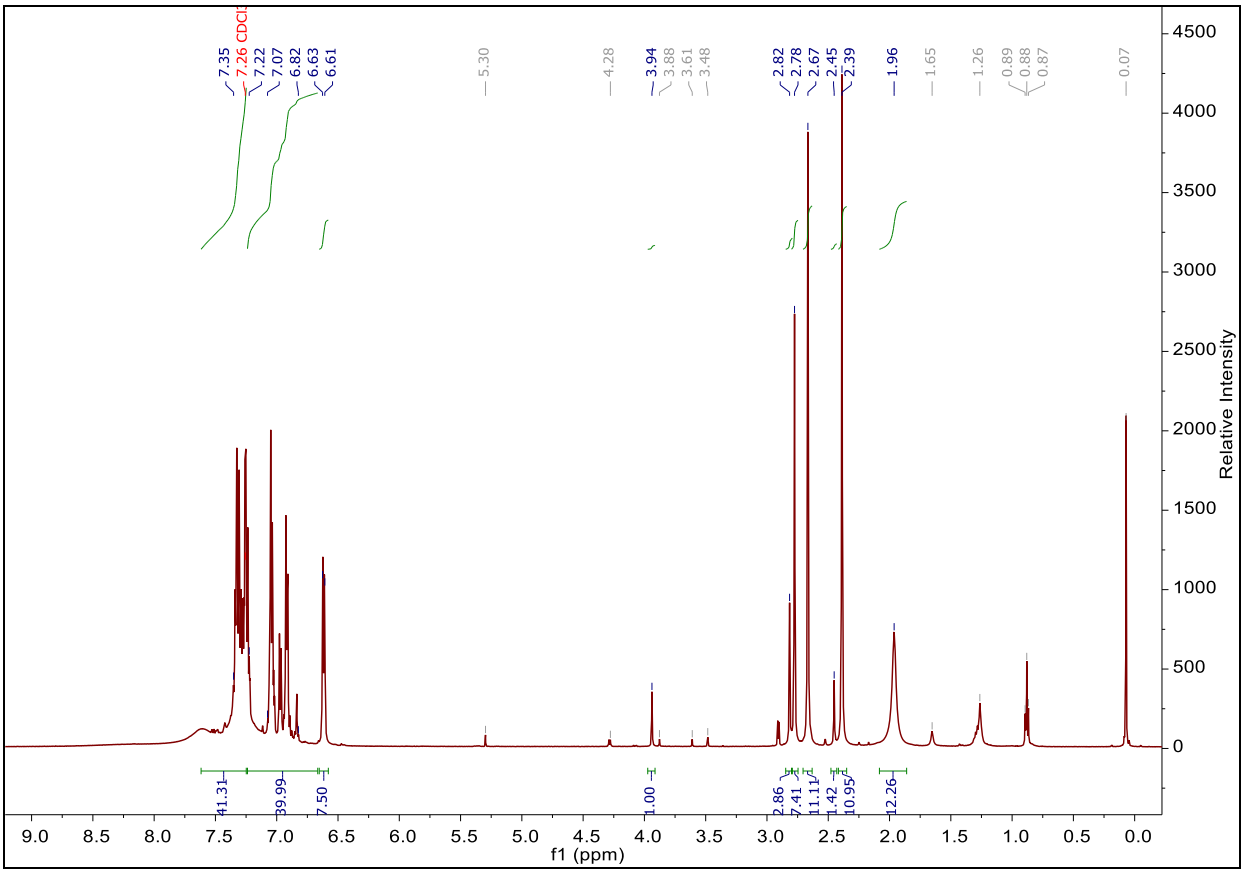

Figure 4.3 ^{1}H NMR spectrum of the reaction of **4.3a** with **4.4b** carried out at 25ºC within 60 minutes. The spectrum is recorded in deuterated chloroform at 500 MHz. ^{1}H NMR (500 MHz, chloroform-*d*, δ, ppm) 7.45 – 7.13 (m, 24H), 7.07 – 6.89 (m, 3H), 6.62 (d, *J* = 9.2 Hz, 1H), 2.78 (s, 2H), 2.53 (d, *J* = 139 Hz, 6H), 1.96 (s, 6H).

7.3.1.2. Approach two – the monitoring.

Like mentioned at the beginning, the monitoring approach was used to test the studied systems within various reaction time periods and ratios of the reactants without the isolation of the products.

Accordingly, the system **4.3a**/**4.4a** was examined within the following conditions:

a) 1:1 equivalent of the reactants while the ^{1}H NMR spectra were recorded immediately after mixing the reactants and after reaction time of 3.5h. Related spectra are shown in Figure 4.4. and Figure SI 4.27-28). It could be noticed that the supposed reaction product **4.5a** is obtainable even after few minutes and that the product is stable within the considered-reaction time.

[N^{0} 684] Pfeffer, M, Goel, A. B. *Cyclopalladated Compounds in Inorganic Syntheses*; ed H. D. Kaesz, John Wiley & Sons, Inc., Hoboken, New York, **1989**, vol. 26, ch. 38, and related references therein.

b) 1:2 equivalents in favor of the alkyne while the ^{1}H NMR spectra were recorded after reaction time of 1h and 15h. In the Figure 4.5 that displays the corresponding spectra it is noticeable that double/triple insertion of **4.4a** (see Scheme 4.3) occurs after fifteen hours (see spectral region 3.5-4 ppm). The separated spectra accompanied with chemical shifts are given in Supplementary Information (Figure SI 4.29-30). Although considered reaction time was 15h, the double/triple insertion might probably occur earlier. Therefore, considering ITC measurements this system (**4.3a**/**4.4a**) should not be allowed to interact within such long reaction times as well as within an excess of the alkyne. In accordance with both manners of the reaction tests, it could be concluded that the system **4.3a**/**4.4a** might be usable within ITC measurements carried out in stoichiometric condition within shorter reaction times.

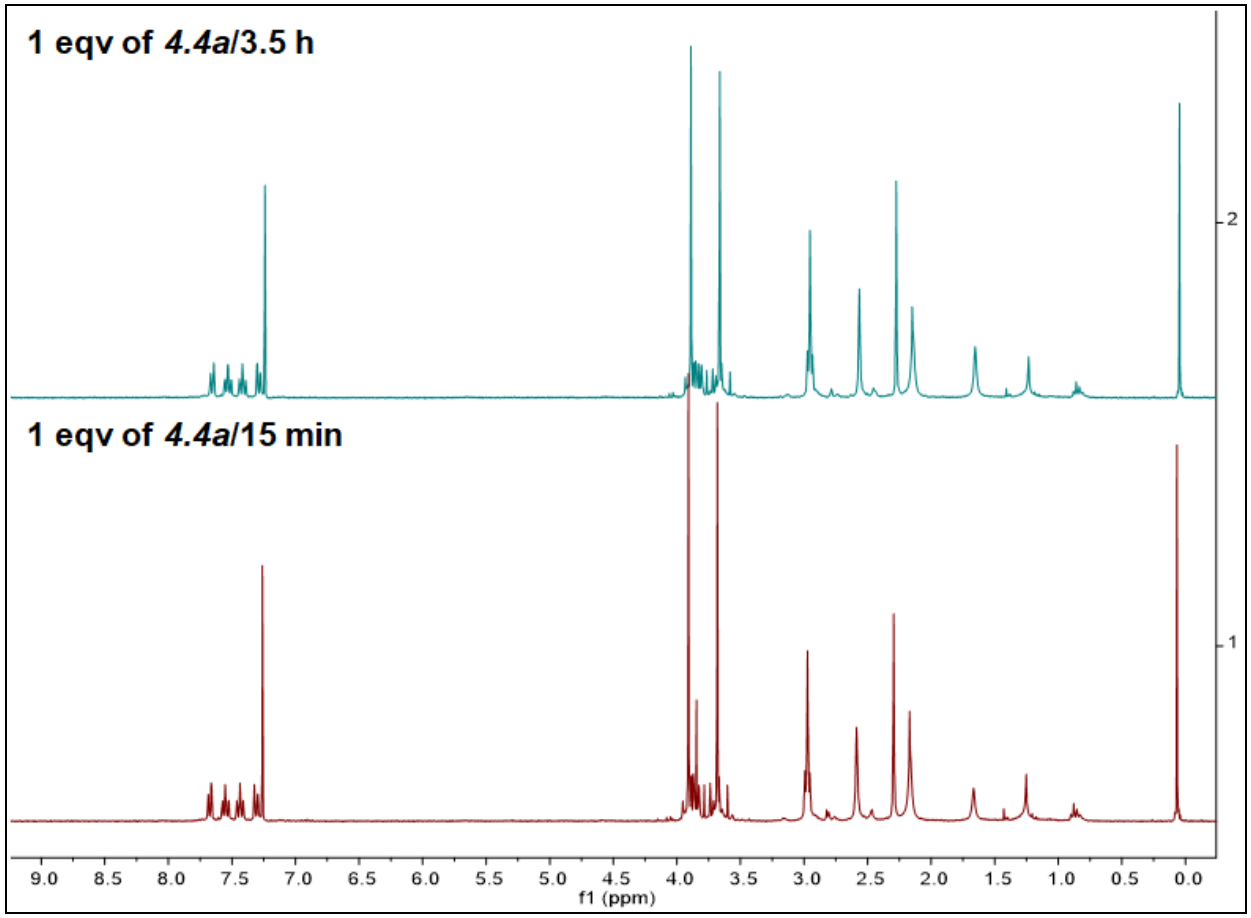

Figure 4.4 Superimposed ^{1}H NMR spectra of the reaction of **4.3a** with **4.4a** carried out in molar ratio of the reactants 1:1, recorded at various reaction times (15 min, 3.5 h). The spectra are recorded in deuterated chloroform at 300 MHz.

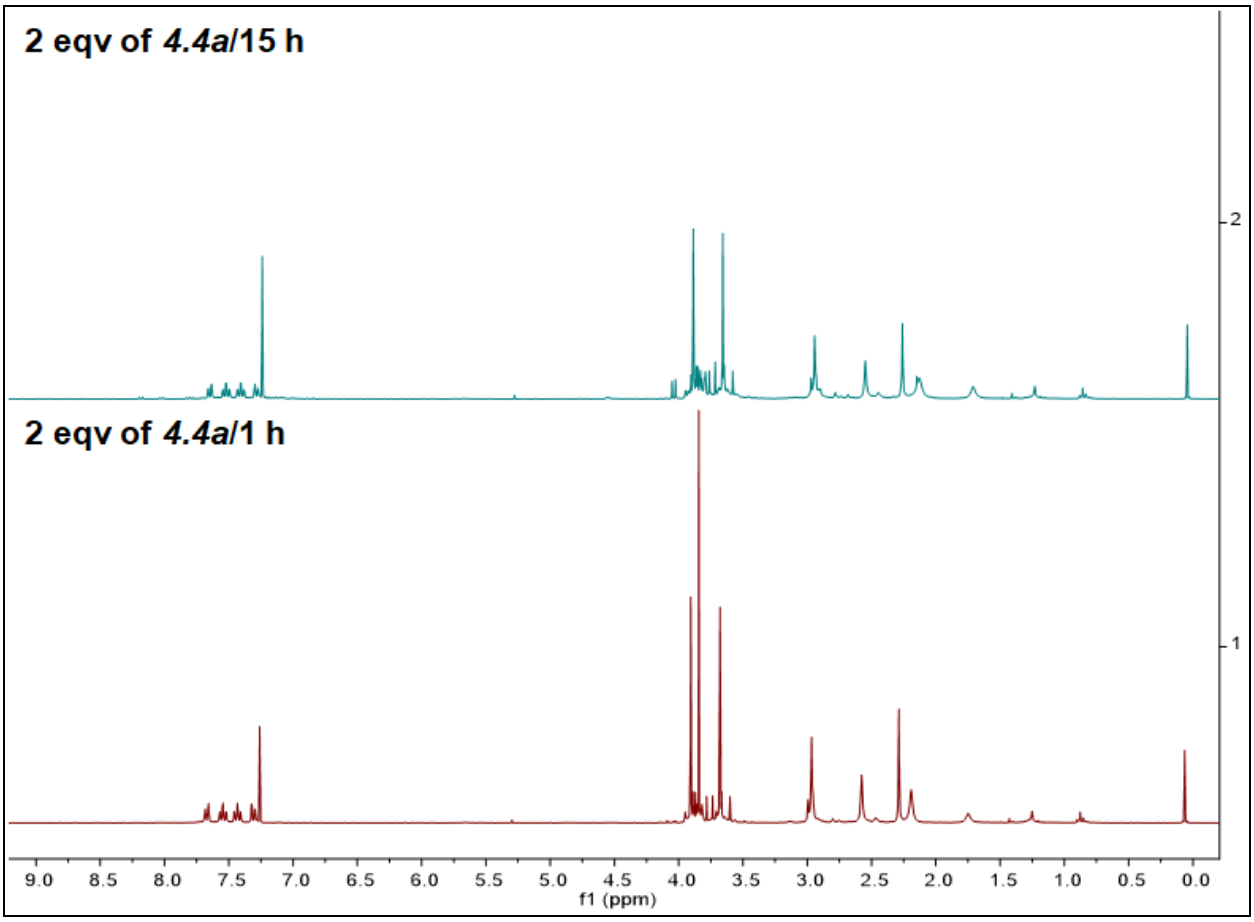

Figure 4.5 Superimposed ^{1}H NMR spectra of the reaction of **4.3a** with **4.4a** carried out in molar ratio of the reactants 1:2, recorded at various reaction times (1 h and 15 h). The spectra are recorded in deuterated chloroform at 300 MHz.

Considering the system **4.3b**/**4.4a** the same conclusions could be drawn as for the system **4.3a**/**4.4a** due to almost the same ^{1}H NMR of the two systems. For the illustrative purpose, its ^{1}H NMR spectra are given in Supplementary Information (Figure SI 4.31-32).

The system **4.3c**/**4.4a** was examined within two molar ratios of the reactants (1:1 and 1:2) and various reaction times (immediately upon injection of the alkyne, 1h, 3.5h and 15h). The stacked ^{1}H NMR spectra of the system **4.3c**/**4.4a** is shown in Figure 4.6, while the separated spectra are shown in Figure SI 4.33. Regarding the spectra, it seems that first insertion of the alkyne **4.4a** exclusively occur in stoichiometric condition within reasonable reaction times, while in the presence of the excess of the alkyne multiple insertions (noticeable in the region 2-4 ppm of the spectra) are likely to happen. Therefore, similarly to the previous systems (**4.3a-b**/**4.4a**), this system might be examined by ITC within stoichiometric condition and reasonably long reaction time periods.

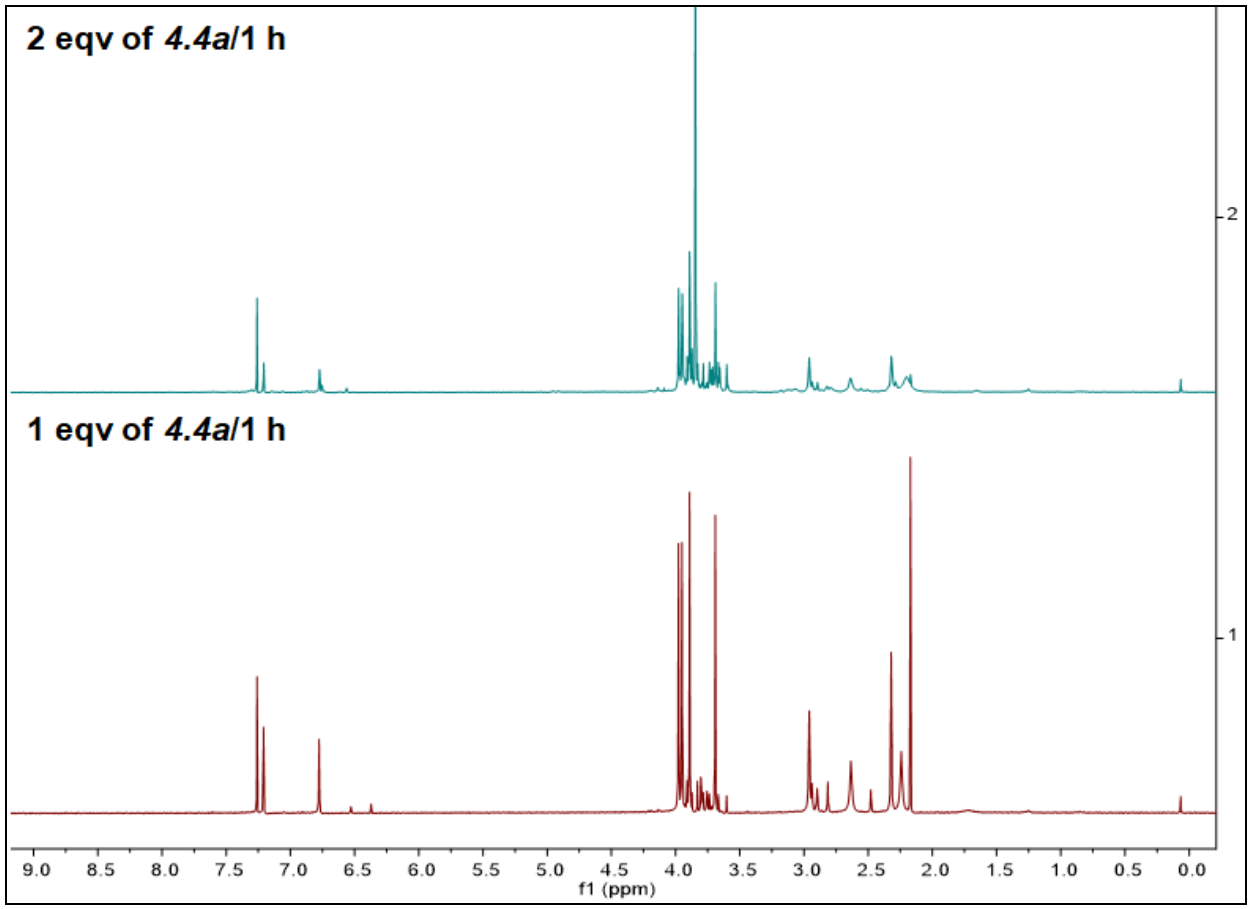

Figure 4.6 Superimposed ^{1}H NMR spectra of the reaction of **4.3c** with **4.4a** carried out in molar ratio of the reactants 1:1 as well as 1:2, recorded at reaction times of 1 h. The spectra are recorded in deuterated chloroform at 400 MHz.

The supposed double insertion of the alkyne **4.4b** into the palladacycle **4.3a** was examined within the reaction times of 1.8h, 3h and 24h as well as in molar ratios of the reactants of 1:1, 1:2 and 1:4 (in favor to the alkyne). From the relevant ^{1}H NMR spectra, displayed in Figure 4.7 and Figure SI 4.34-36, it could be concluded that the double insertion of the alkyne exclusively occurs, as no single inserted product is observed (proved by presence of the palladacycle when the stoichiometric conditions employed). These observations just confirmed long time known features of the alkyne **4.4b** that govern it to double insertion into similar palladacycles.

Additionally, the tests considered a large excess (up to 10 equivalents) of the alkyne and time span from 0.7h to 20.5h. The corresponding ^{1}H NMR spectra are shown in Figure 4.8. According to the spectra, it could be concluded that the reaction gives solely double inserted product **4.6a** regardless the excess of the alkyne and quite long reaction times. Altogether, the

system **4.3a**/**4.4b** might be investigated within the ITC in both stoichiometric conditions (in respect with the exclusive double inserted product) and a large excess of the alkyne.

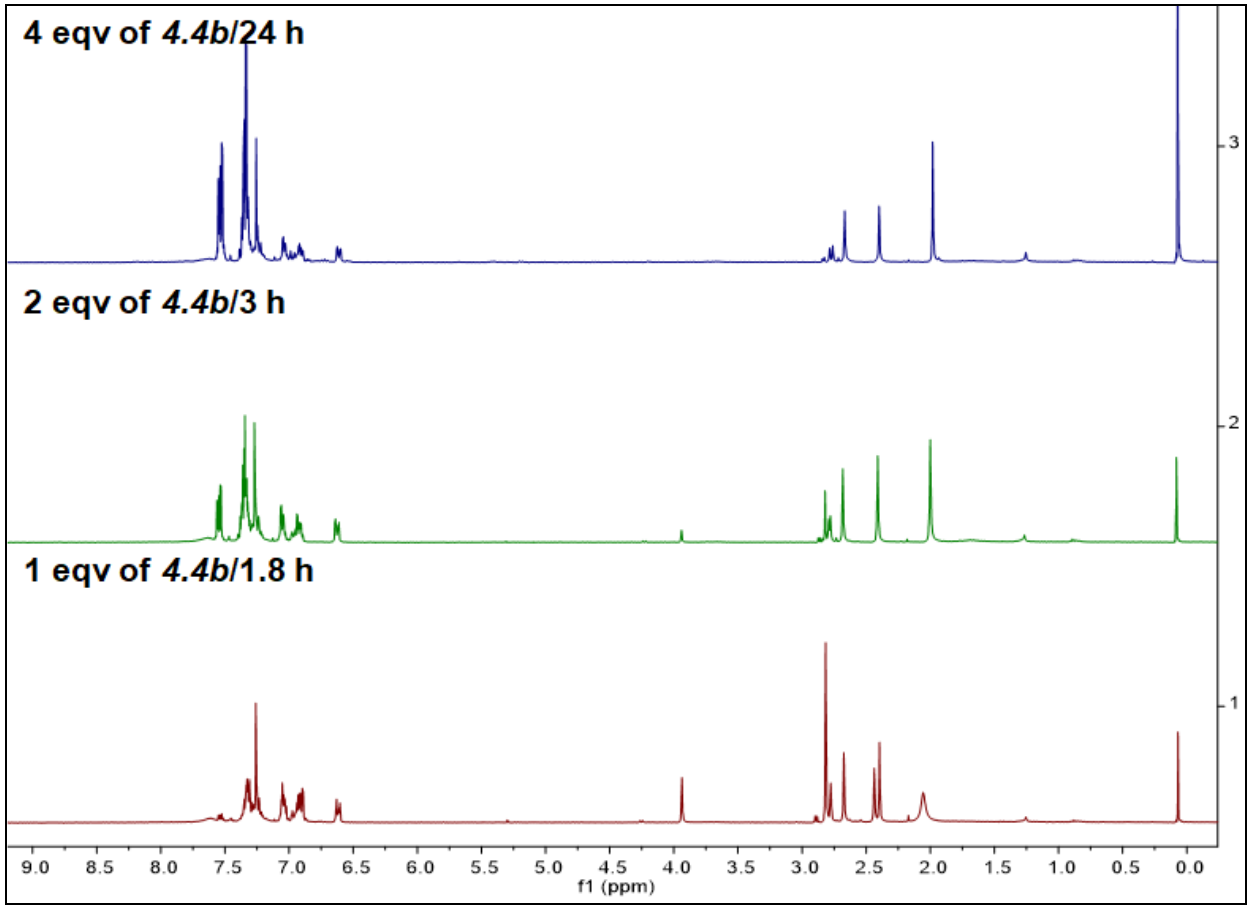

Figure 4.7 Superimposed ^{1}H NMR spectra of the reaction of **4.3a** with **4.4b** carried out in molar ratio of the reactants 1:1, 1:2 and 1:4, recorded at various reaction times (1,8 h, 3 h and 24 h). The spectra are recorded in deuterated chloroform at 400 MHz.

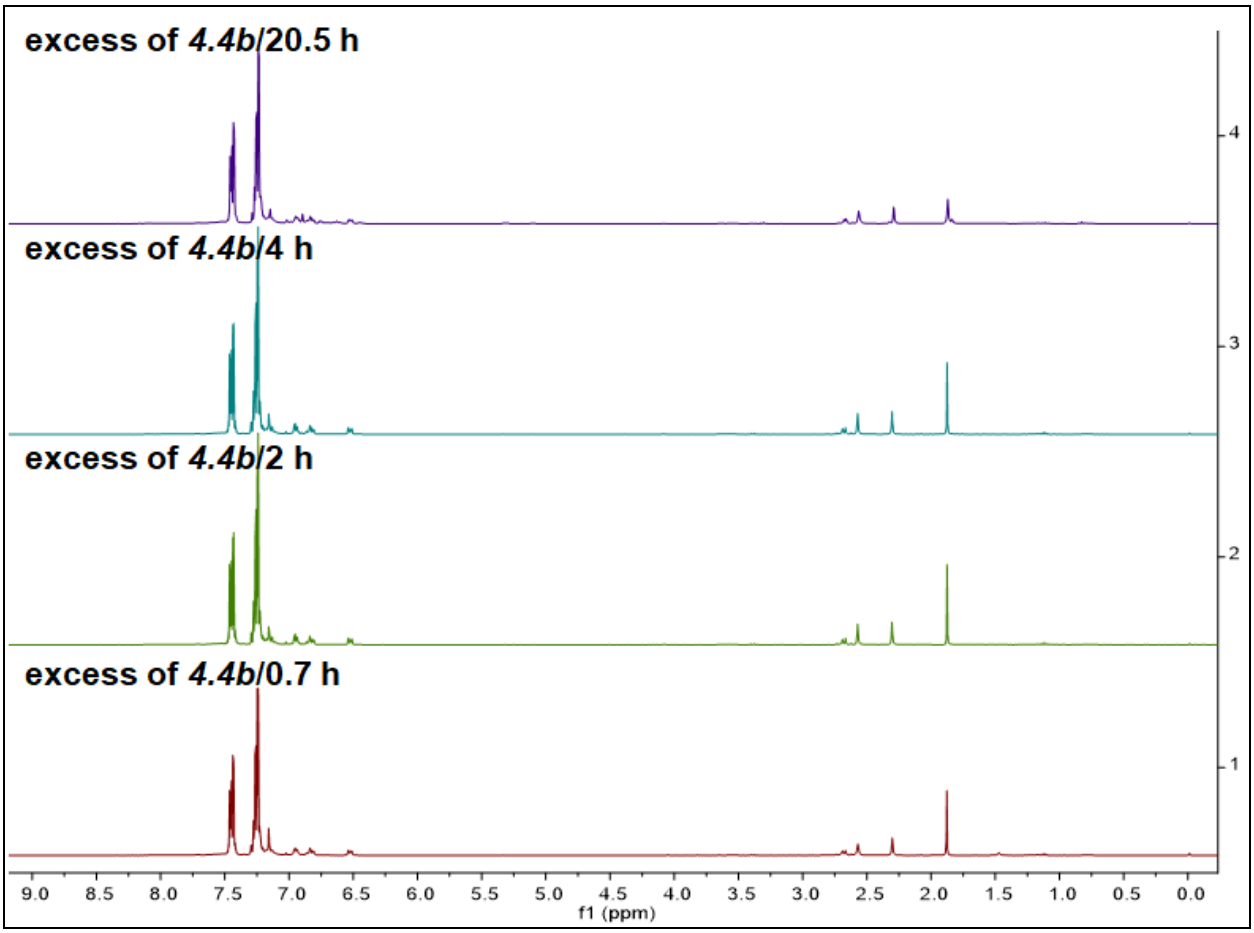

Figure 4.8 Superimposed ^{1}H NMR spectra of the reaction of **4.3a** with **4.4b** carried out in the excess of the alkyne **4.4b** (10 eqv), recorded at various reaction times (0.7 h, 2 h, 4 h and 20.5 h). The spectra are recorded in deuterated chloroform at 400 MHz.

As mentioned previously, the palladacycle **4.2a** was probed in the reaction with **4.4a**, as well. The ^{1}H NMR spectrum of the reaction product of the system **4.2a**/**4.4a** obtained from stoichiometric condition is given in Supplementary Information (Figure SI 4.24). It could be noticed that aromatic region is rather not clear, indicating slower transformation and/or incomplete insertion of the **4.4a** into the **4.2a**. To reduce complexity of the spectra, the chloro-bridge of the **4.2a** was cleaved by pyridine. Related ^{1}H NMR spectrum is shown in Figure SI 4.25. Expectedly, the spectrum is clearer and shows the possibility of obtaining the product **4.7a** (see Figure SI 4.24-5). The previously obtained palladacycle **4.7a** was also verified with $AgPF_6$, which basically could be an alternative way to access palladacycle **4.5a**. The corresponding spectrum is displayed in Figure SI 4.26. As previously, the spectrum showed that it is possible to synthesize the compound **4.7a** from **4.2a** and **4.4a** as well as the inserted palladacycle **4.5a** in the reverse way (through **4.7a**), but with the presence of some small amount of the starting

palladacycle. Although it is shown that there is some possibility of using the palladacycle **4.2a** within ITC measurements, the palladacycle **4.2a** is not used because of slow transformation of interest within ITC conditions and difficulties to proof the purity of the obtained product by ^{1}H NMR (see Figure SI 4.24.).

7.3.2. ITC experiments.

7.3.2.1. Generalities.

As the preformed reaction tests on the investigated systems have suggested, only exploitable reactions within ITC measurements were the reactions of the complexes **4.3a-b** with the alkyne **4.4a** within stochiometric conditions as well as the reaction of **4.3a** with the alkyne **4.4b** either within stochiometric conditions or in the conditions that implied a large excess of the alkyne. Therefore, to optimize the ITC experiments of the system **4.3a**/**4.4a**, first challenge was an overcoming of relatively slow chemical transformation taking place within the system. Another constraint was the quite low solubility of the palladacycles in chlorobenzene. It was found that only longer time delays between two subsequent injections are helpful. Thus, quite long relaxation times (3000-10000s) were employed. Due to the similarities between the palladacycles **4.3a** and **4.3b**, the same condition was also used for the system **4.3b**/**4.4a**. The investigation of system **4.3a/4.4b** possessed similar challenges. However, as this system allows a large excess of the alkyne, that was the choice for ITC conditions. To ensure a proper base line before subsequent injection, 3000s of time delay was employed. As the large excess in one reactant simplifies achieving of the reaction kinetics, the concentration of the **4.4b** was varied. Therefore, for the system **4.3a/4.4b** besides the reaction enthalpy (ΔH_r) the reaction kinetic parameters (k_{int} and partial reaction order with respect to reactant in an excess) are obtained. As the results of the preformed ITC measurements of the systems **4.3a-b/4.4a** raw ΔH_r as well as model ITC ΔH_r, ΔG_r and ΔS_r were obtained.

7.3.2.2. Thermodynamic study.

As mentioned above, according to the employed ITC conditions, raw ΔH_r values of all herein examined systems (**4.3a-b**/**4.4a** and **4.3a**/**4.4b**) are obtained as the results of the preformed ITC measurements within the thermodynamic study, while for the systems **4.3a-b**/**4.4a** additional model ITC values are achieved as well. The ITC thermodynamic results are depicted in Table

4.1. Examples of the corresponding ITC thermograms are shown in Figure 4.9–10 as well as in Figure SI 1-3.

Table 4.1 ITC results obtained from the sequential addition ITC experiments that considered either stoichiometric condition for the systems **4.3a-b**/**4.4a** or an excess of **4.4b** interacting with the palladacycle **4.3a**. The model values are obtained by employing independent model on integrated heat peaks.

System	raw ΔH_r ± error [kcal/mol]	Model ITC ΔH_r ± error [kcal/mol]	Model ITC ΔG_r ± error [kcal/mol]	Model ITC ΔS_r ± error [cal/molK]
4.3a/**4.4a**	-28.1 ± 2.6	-31.1 ± 1.1	-7.0 ± 3.5	-81.5 ± 41.1
4.3b/**4.4a***	-24.2 ± 1.3	-24.7 ± 0.3	-7.4 ± 1.4	-60.0 ± 13.2
4.3a/**4.4b**	-38.1 ± 0.8	/	/	/

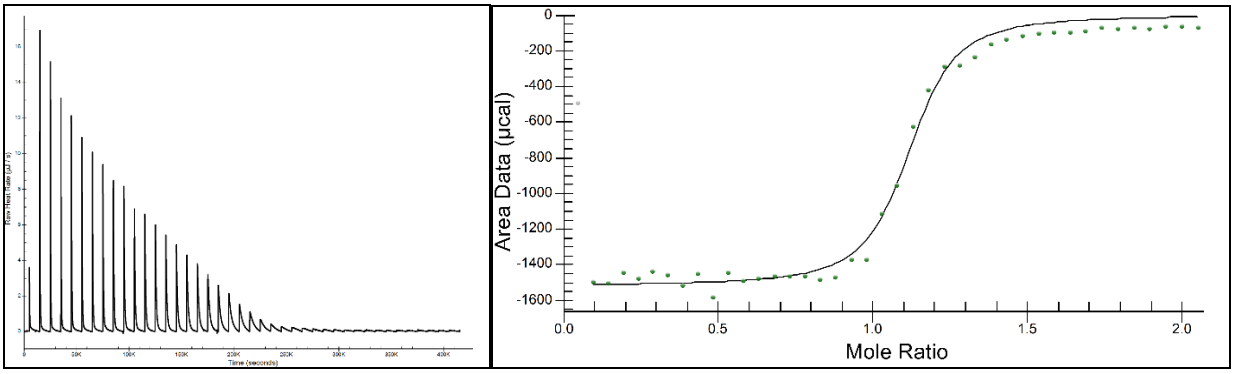

Figure 4.9. *left side* – ITC thermogram of the reaction between **4.3a** (sample cell, c=1.09 mM) and **4.4a** (syringe, c=25.37 mM) in chlorobenzene. The titration was performed at 25ºC through 45 sequential additions (of 2.06 µL each). Time between two consecutive injections was 10000 s. Heat released is expressed in µJ/s versus time in s. *right side* – ITC integrated and fitted, by independent model; heat peaks of the thermogram shown on the left side. Integrated heats are expressed in µcal versus molar ratio of the reactants.

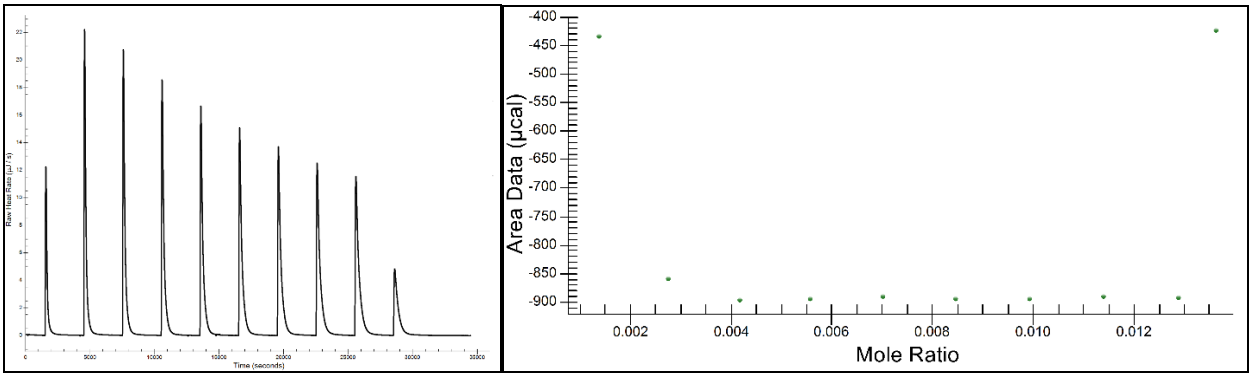

Figure 4.10. *left side* – ITC thermogram of the reaction between **4.4b** (sample cell, c=16.91 mM) and **4.3a** (syringe, c=2.29 mM) in chlorobenzene. The titration was performed at 25ºC through 10 sequential additions (of 10.06 µL first nine titrations and of 5.03 µL the last one). Time between two consecutive injections was 3000 s. Heat released is expressed in µJ/s versus time in s. *right side* – ITC integrated heat peaks of the thermogram shown on the left side. Integrated heats are expressed in µcal versus molar ratio of the reactants.

The raw ΔH_r values of the systems **4.3a-b/4.4a** (ca. -28 kcal/mol and -24 kcal/mol, respectively) suggest on quite strong exothermic chemical transformation taking place within the insertion reaction sequence. In other words, it seems that the formation of aromatic carbon – aliphatic carbon bond and aliphatic carbon – palladium bond is energetically favorable in comparison to the cleavage of aromatic carbon – palladium bond and aliphatic carbon – aliphatic carbon bond (within the alkyne). Non-covalent interactions of the esters group have probably positive influence on the overall enthalpy of the transformation. Although only one ITC measurement of the system **4.3b/4.4a** was found to be acceptable, the comparison of the systems **4.3a/4.4a** (ΔH_r is around -28 kcal/mol) and **4.3b/4.4a** (ΔH_r is around -24 kcal/mol) might lead to a conclusion that the nature of the anion could have significant influence on the reaction enthalpy. Considering the system **4.3a-b/4.4a**, its obtained raw ΔH_r value (ca. -38 kcal/mol) might be reasonable regarding to the chemical formation/cleavage of the bonds as well as to the establishing of non-covalent interactions within the transformation. In comparison to the previous systems **4.3a-b/4.4a**, within this system **4.3a/4.4b** there is the formation of an additional aliphatic carbon - aliphatic carbon bond (between the alkynes) as well as an additional cleavage of the aliphatic carbon - aliphatic carbon bond (within second alkyne). This transformation is accompanied with the decoordination of MeCN ligand and subsequent coordination of first alkyne to palladium through its double carbon-carbon bond. An influence of the phenyl rings, interacting in π-π stacking manner, probably is cohesive. In addition, it is worth to note that, according to the literature,[269] chlorobenzene, herein the solvent of the ITC experiments, might be the competitive ligand to palladium. Therefore, its interaction enthalpy with the palladacycle should not be put aside.

7.3.2.3. Kinetic study.

According to the used conditions within the ITC experiments (i.e. a large excess of the alkyne **4.4b**), the ITC of the system **4.3a/4.4b** could be analyzed in sense of the kinetics. As mentioned throughout the manuscript, the kinetic analysis rises up the initial rate constant as well as the partial reaction order with respect to reactant in an excess. The results of such analysis of the double insertion of the alkyne **4.4b** into the palladacycle **4.3a** are shown in Table 4.2. Related plots from which the results were derived are displayed in Figures 4.11-12 and in Figure SI 4-5.

[269] [N^0 84] D. N. Sredojević, D. B. Ninković, G. V. Janjić, J. Zhou, M. B. Hall, S. D. Zarić, *ChemPhysChem* **2013**, *14*, 1797.

Table 4.2 Results of the ITC kinetic study obtained from the sequential addition ITC experiments that considered an excess of **4.4b** interacting with the palladacycle **4.3a**.

Nº exp	[**4.3a**] mmol/L	[**4.4b**] mmol/L	Molar ratio under ITC conditions	***k***	**order** with respect to **2.1**	k_{obs}	**order** with respect to **2.1**
1	2.29	16.91	1:734	$9.6*10^{-4} \pm 9*10^{-5}$		$3.0*10^{-5} \pm 3*10^{-6}$	
2	2.35	8.45	1:357	$7.1*10^{-4} \pm 7*10^{-5}$	**0.97 ± 0.25**	$4.2*10^{-5} \pm 4*10^{-6}$	**0.98 ± 0.24**
3	2.33	3.37	1:144	$2.1*10^{-4} \pm 2*10^{-5}$		$9.0*10^{-5} \pm 7*10^{-7}$	

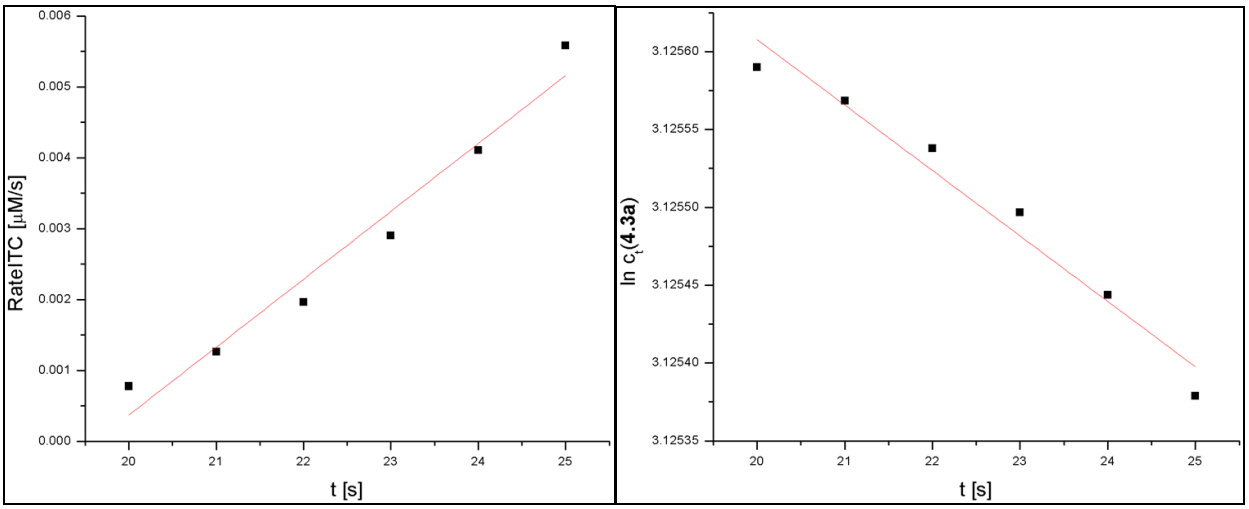

Figure 4.11 *left side* - Linear fit of the plot of the ITC Rate as a function of time for the reaction of **4.4b** (sample call, c=16.91 mM) with **4.3a** (syringe, c=2.29 mM) carried out in ITC calorimeter. ITC Rate is expressed in µM/s and time in s. Obtained $\boldsymbol{k = 9.6*10^{-4} \pm 9*10^{-5}}$, as the result of the fitting. *right side* - Linear fit of the plot of logarithm of **2.2b** concentration as a function of time for the same reaction. Obtained $\boldsymbol{k_{obs} = -3.0*10^{-5} \pm 3*10^{-6}}$ as the result of the fitting.

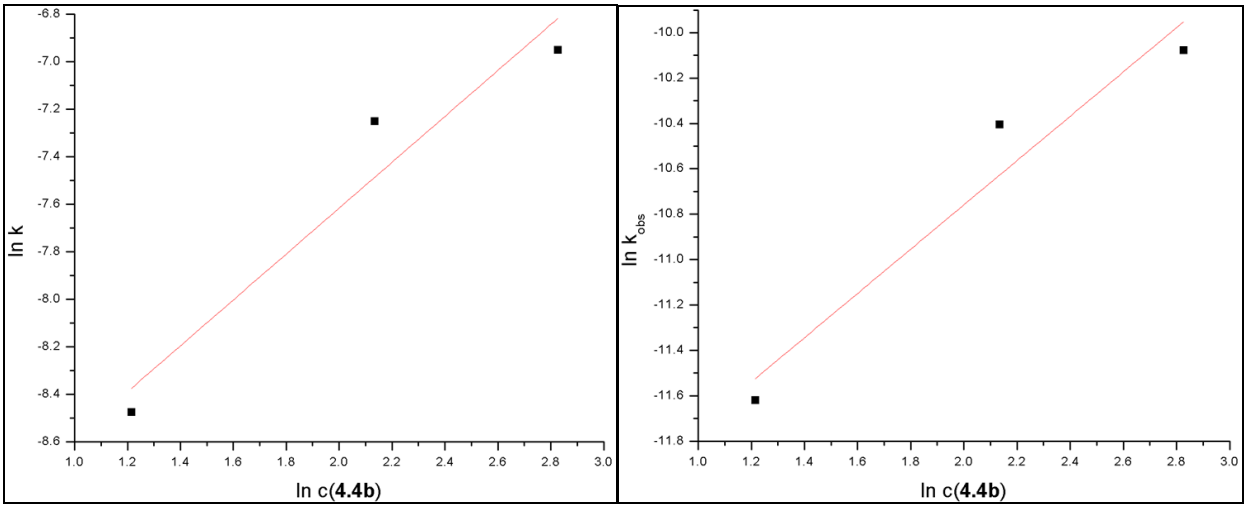

Figure 4.12 *left side* - Linear fit of the plot of logarithm of obtained *k* values as a function of the logarithm of **4.4b** starting concentrations for the reaction of **4.3a** with **4.4b** carried out in ITC calorimeter. Obtained partial reaction order with respect to **4.4b** - **0.97 ± 0.25**, as the result of the fitting. *right side* - Linear fit of the plot of logarithm of obtained k_{obs} values as a function of the logarithm of **4.4b** starting concentrations for the reaction of **4.3a** with **4.4b** carried out in ITC

calorimeter. Obtained partial reaction order with respect to **4.4b** - **0.98 ± 0.24**, as the result of the fitting.

The values of either *k* (ranged from $2.1*10^{-4}$ to $9.6*10^{-4}$) or k_{obs} (ranged from $9.0*10^{-6}$ to $3.0*10^{-5}$) suggest that the rate of the double insertion of the alkyne **4.4b** into the palladacycle **4.3a** is reasonably low. The results of the partial reaction order with respect to **4.4b** that are very close to one (0.98) tell that the examined step-wise double insertion of the alkyne is rate dependent only in insertion of the first molecule of the alkyne while the second insertion goes instantaneously. These observations are in perfect accordance with the literature. Once again, the established method of the ITC kinetic study is proved as useful.

7.3.3. Static DFT-D calculations.

Within the study of the single/double insertion of the alkynes (**4.4a**/**b**) into the palladacycles only the insertion into **4.3a** was investigated. All the computations were performed at ZORA-GGAPBE-D3(BJ)/TZP level of theory in chlorobenzene solution (COSMO) phase. The geometry optimizations were done for all the reactants (**4.3a**, **4.4a-b**) and corresponding products (**4.5a** **4.6a**, Scheme 4.1) and confirmed as true minima by performing calculations of vibrational modes. The results, i.e. thermodynamic parameters of the studied single/double insertion reaction sequences (ΔH_r, ΔG_r, ΔS_r) obtained by the performed calculations, are shown in Table 4.3. The related optimized structure geometries are displayed in Figure 4.13 while their Cartesian coordinates are given in Supplementary Information (see SI, section A.4.6.).

Table 4.3 Results of static DFT-D calculations. The calculations were performed at ZORA-GGAPBE-D3-BJ/TZP level of theory in chlorobenzene solution (COSMO) phase.

System	Level of theory	ΔH_r [kcal/mol]	ΔG_r [kcal/mol]	ΔS_r [cal/Kmol]
4.5a	ZORA-GGAPBE-D3(BJ)/TZP - PhCl	-37.1	-18.9	-61.2
4.6a	ZORA-GGAPBE-D3(BJ)/TZP - PhCl	-51.5	-26.3	-84.3

The resulting values of the reaction enthalpies ΔH_r of both the systems **4.3a**/**4.4a** and **4.3a**/**4.4a-b** (-37.1 kcal/mol and -51.5 kcal/mol, respectively) suggest on quite energetically favorable chemical transformation within the insertion sequence of alkynes into the palladacycle. The difference of ca. 14 kcal/mol between the single and double insertion reaction might be reasonable regarding the nature of the transformations (for more details of the considered transformations see the explanation given it the ITC thermodynamic study part of this chapter or in the introductory chapter). Regarding to the computed Gibbs ΔG_r energies (-18.9 kcal/mol and -26.3 kcal/mol), it could be concluded that the investigated reactions in solution should be, in

principle, rather spontaneous, what is in accordance to the observations derived from both the reactions tests and ITC measurements. Negative ΔS_r values are expected.

In comparison to the obtained ITC raw ΔH_r values (ca. -24 kcal/mol and -28 kcal/mol, see Table 4.1) the computed ΔH_r values seem to be overestimated. Possible reason for such overestimation might lie in the fact that chlorobenzene could generally interact with palladacycle through coordination to palladium[270]. Consequently, its decoordination, that must take place before subsequent interaction of the palladacycle with the alkyne, would lead to decreasing in overall enthalpy of the insertion reaction. Therefore, an accounting of the explicit interaction of the solvent with the reactants within the calculations might, even significantly, bring the experimental and theoretical values closer to each other. Unfortunately, such research within this study was not carried out.

[270] [N^0 84] D. N. Sredojević, D. B. Ninković, G. V. Janjić, J. Zhou, M. B. Hall, S. D. Zarić, *ChemPhysChem* **2013**, *14*, 1797.

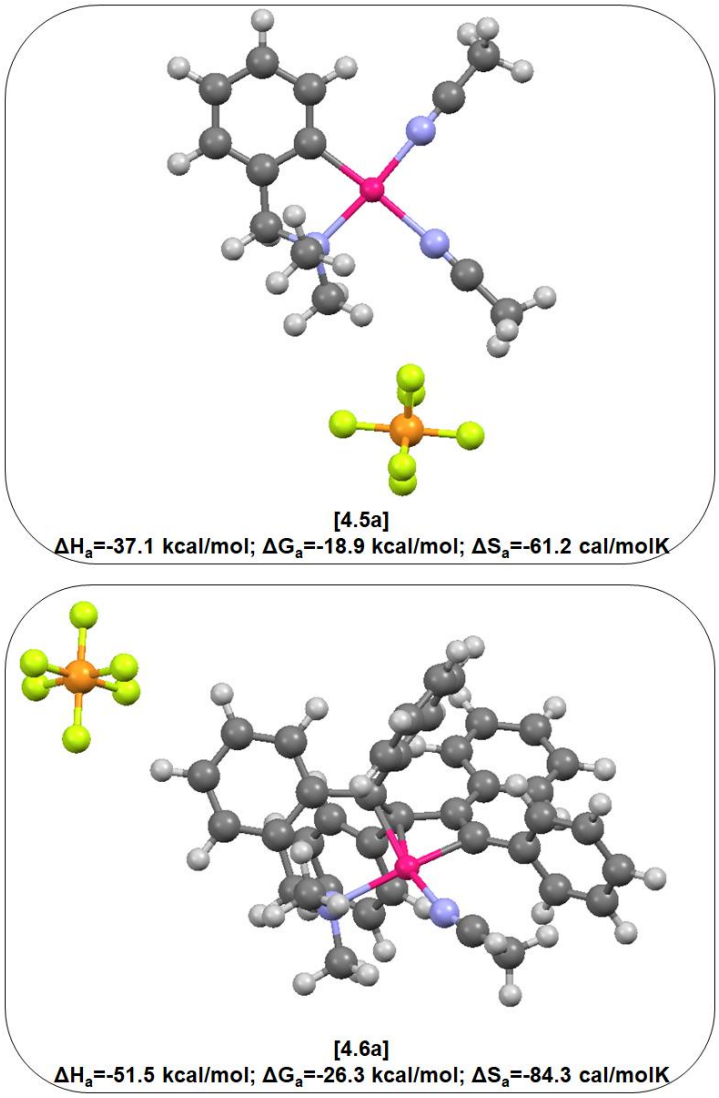

Figure 4.13 Graphic representations of optimized geometries of the investigated systems at ZORA-GGAPBE-D3-BJ/TZP level of theory in chlorobenzene solution (COSMO) phase. P: orange; F: yellowish; N: violet; Pd: pink, C: grey; H: white.

7.4. Chapter conclusion.

The single/double insertion of the alkynes **4.4a-b** (Scheme 4.1) into the palladacycles **4.3a-b** (Scheme 4.1) were investigated by experimental tools i.e. by the reaction tests using standard Schlenk line technique, Nuclear Magnetic Resonance (NMR) spectroscopy and Isothermal Titration Calorimetry (ITC) and by theoretical tools i.e. by static Density Functional Theory (DFT) with Grimme's dispersion correction – D3. In addition, new complexes (**4.3a** and **4.6a**, Scheme 4.1) were synthesized and fully characterized.

The reaction tests were done in order to establish suitable reaction conditions that will be used within ITC measurements as well as to verify the extent of possible side reactions. The tests were carried out at room temperature in two methodologies: a) in chlorobenzene and dichloromethane with the isolation of the reaction products, and b) in deuterated chloroform without the isolation of the reaction products considering various molar ratios of the reactants and reaction times.

The ITC measurements considered two kinds of experimental conditions: a) the experiments performed in stoichiometric conditions (systems **4.3a-b**/**4.4a**) and b) the experiments performed in a large excess of one reactant (system **4.3a**/**4.4b**), while all the experiments are carried out in a sequential addition manner. All the computations were performed at ZORA-GGAPBE-D3(BJ)/TZP level of theory in chlorobenzene solution (COSMO) phase. The obtained ITC results of the systems **4.3a-b**/**4.4a** were raw ΔH_r values as well as Model ITC values of ΔH_r, ΔG_r, ΔS_r, while for the system **4.3a**/**4.4b** the ITC measurements allowed obtaining raw ΔH_r values as well as estimating of the partial reaction order with respect to the alkyne **4.4b**. The static DFT-D calculations of both single (systems **4.3a-b**/**4.4a**) and double insertion sequence (system **4.3a**/**4.4b**) computed the values of all thermodynamic parameters of the reactions (ΔH_r, ΔG_r, ΔS_r).

The reaction tests showed that the single insertion of the alkynes (**4.4a-b**) regardless of kind of the palladacycle (**4.3a-c**) is dependent on the concentration of the alkyne. Namely, with nearly stoichiometric ratio of the reactants the side reactions (the isomerization and second insertion) might happen. On another hand, the double insertion of the **4.4b** into the **4.3a** is independent of the concentration of the alkyne giving only the double inserted product. These observations helped in designing of the ITC experiment suggesting that the single insertion should be carried out in stoichiometric condition as well as that the double insertion could be carried out even in an excess of the alkyne.

The obtained raw ΔH_r of both studied reactions of single (ΔH_r values of the systems **4.3a-b**/**4.4a** are ca. -28 kcal/mol and -24 kcal/mol, respectively) and double (ΔH_r value of the system **4.3a**/**4.4b** is -38 kcal/mol) insertion of the alkynes into the palladacycles suggest energetically quite favorable transformations within the insertion sequence. These enthalpy values might be rather reasonable regarding the nature of the transformations accounting cleavage of carbon-carbon bond and formation of carbon-palladium bond as well as attractive non-covalent interactions. The Model ITC ΔH_r values of the systems **4.3a-b**/**4.4a** (ca. -31 kcal/mol and -25

kcal/mol, respectively) are in accordance with the raw ΔH_r values, confirming significance of the raw ones. The Model ITC ΔG_r values of the systems **4.3a-b**/**4.4a** (ca. -7 kcal/mol for both systems) show that the insertion reactions are favorable from a thermodynamic point of view, as well. Kinetic study showed the partial first reaction order with respect to the alkyne **4.4b** within the double insertion sequence. Consequently, it was shown that the second insertion is much faster than the first one. These findings are in excellent accordance with already published data.[271]

The computed values of the thermodynamic parameters ΔH_r and ΔG_r of both examined systems (**4.3a**/**4.4a-b**; with the ΔH_r values of ca. -37 kcal/mol and -51 kcal/mol, respectively; and with the ΔG_r values of ca. -19 kcal/mol and -26 kcal/mol, respectively) are, in comparison to the obtained ITC ones, overestimated. The reason of such overestimation (over 10 kcal/mol in both ΔH_r and ΔG_r values) might lie in no consideration of the explicit interaction of the chlorobenzene with the palladacycle, that has been shown (on similar models)[272] as not negligible (as its values of interaction energies are up to few kcal/mol).

In addition, new complexes **4.3a** and **4.6a** were synthesized and fully characterized (by 1H NMR, elemental analysis, MS and X-Ray).

Outlook. The estimation of the thermodynamic parameters of the interactions of chlorobenzenes with the palladacycles is necessary. X-ray diffraction analysis of the product **4.5a** is desirable.

[271] [N^0 683] A. D. Ryabov, R. van Eldik, G. Le Borgne, M. Pfeffer, *Organometallics* **1993**, *12*, 1386.
[272] [N^0 84] D. N. Sredojević, D. B. Ninković, G. V. Janjić, J. Zhou, M. B. Hall, S. D. Zarić, *ChemPhysChem* **2013**, *14*, 1797.

7.5. Закључак поглавља.

Једнострука/двострука инсерција алкина **4.4a-b** (схема 4.1) у цикличним паладијумовим комплексима **4.3a-b** (схема 4.1) испитана је помоћу експерименталних метода тј. реакционим тестовима коришћењем стандардне Schlenk line технике, нуклеарне магнетне резонанционе (NMR) спектроскопије и изотермалне титрационе калориметрије (ITC) и теоријским методама, тј. прорачунима заснованим на теорији функционала густине са Grimme-овом корекцијом за дисперзију (енг. DFT-D3). Поред тога, нови комплекси (**4.3a** и **4.6a**, схема 4.1) су синтетисани и потпуно окарактерисани.

Реакциони тестови урађени су како би се пронашли погодни реакциони услови који ће се користити у оквиру ITC мерења, као и да би се утврдио степен могућих споредних реакција. Тестови су изведени на собној температури применом две методологије: а) у хлоробензену и дихлорометану са изоловањем реакционих производа, и б) у деутерисаном хлороформу без изоловања реакционих производа узимајући у обзир различите моларне односе реактаната и различита реакциона времена.

У оквиру ITC мерења разматране су две врсте експерименталних услова: а) експерименти изведени у стехиометријским условима (системи **4.3a-b**/**4.4a**) и б) експерименти изведени у великом вишку једног реактанта (систем **4.3a-b**/**4.4a**), при чему су сви експерименти изведени секвенцијалним начином додавања (титранта). Сви прорачуни изведени су на ZORA-GGAPBE-D3(BJ)/TZP теоријском нивоу у хлоробензену (COSMO). ITC мерењима за систем **4.3a-b**/**4.4a** добијене су сирове (raw) ΔH_r вредности као и модел ITC ΔH_r, ΔG_r, ΔS_r вредности, док су ITC мерења за систем **4.3a**/**4.4b** омогућила добијање сирових (raw) ΔH_r вредности као и процену парцијалног реда реакције у односу на алкин **4.4b**. Статичким DFT-D прорачунима израчунате су вредности свих термодинамичких реакционих параметара (ΔH_r, ΔG_r, ΔS_r) једноструке (системи **4.3a-b**/**4.4a**) и двоструке инсерционе секвенце (систем **4.3a**/**4.4b**).

Реакциони тестови показали су да једнострука инсерција алкина (**4.4a-b**) без обзира на врсту цикличног паладијумовог комплекса (**4.3a-c**) зависи од концентрације алкина. Наиме, при скоро стехиометријском односу реактаната може доћи до споредне реакције (изомеризовање и инсертовање другог молекула алкина). С друге стране, двострука инсерција **4.4b** у **4.4b** независна је од концентрације алкина, и даје једино двоструко инсертовани реакциони производ. Ова запажања су помогла планирање ITC

експеримента и указала на то да би једностурку инсерцију требало изводити у стехиометријским реакционим условима, а да се двострука инсерција може изводити чак и у вишку алкина.

Добијене сирове (raw) ΔH_r вредности проучаваних реакција једноструке (ΔH_r вредности система **4.3a-b**/**4.4a** су око -28 kcal/mol односно -24 kcal/mol) и двоструке (ΔH_r вредности система **4.3a**/**4.4b** је -38 kcal/mol) инсерције алкина у цикличне паладијумове комплексе сугеришу енергетски прилично повољне промене унутар инсерционе секвенце. Ове вредности енталпије могу бити прилично рационалне и у вези са природом трансформације узимајући у обзир раскидање везе угљеник-угљеник и формирање угљеник-паладијум везе, као и привлачних нековалентних интеракција. Модел ITC ΔH_r вредности система **4.3a-b**/**4.4a** (око -31 kcal/mol односно -25 kcal/mol) у складу су са сировим (raw) ΔH_r вредностима, потврђујући значај истих. Модел ITC ΔG_r вредности система **4.3a-b**/**4.4a** (око -7 kcal/mol за оба система) указују да су реакције инсерције повољне и са термодинамичке тачке гледишта. Процењено је да је парцијални ред реакције алкина **4.4b** једнак један у оквиру двоструке инсерционе секвенце, као и да је друга инсерција много бржа. Ови налази су у одличној сагласности са већ објављеним експерименталним подацима.[271]

Теоријски израчунате вредности термодинамичких параметара ΔH_r и ΔG_r за оба испитана система (**4.3a**/**4.4a-b**, са вредностима ΔH_r од око -37 kcal/mol односно -51 kcal/mol, и са вредностима ΔG_r од око -19 kcal/mol односно -26 kcal/mol) су, у поређењу са добијеним ITC вредностима, прецењене. Разлог томе (преко 10 kcal/mol и у ΔH_r и у ΔG_r вредностима) може бити неукључивање експлицитне интеракције хлоробензена са цикличним паладијумовим комплексом, за коју је показано (на сличним моделима)[272] да није занемарљива (јер су вредности енергије интеракције до неколико kcal/mol).

Поред тога, синтетисани су нови комплекси **4.3a** и **4.6a** и потпуно окарактерисани (^{1}H NMR-ом, елементалном анализом, масеном спектроскопијом и дифракцијом рендгенских зрака).

Перспектива. Потребна је процена термодинамичких параметара интеракције хлоробензена са цикличним паладијумовим комплексима. Пожељна је анализа реакционог производа **4.5a** дифракцијом рендгенских зрака.

7.6. Conclusion du chapitre

L'insertion simple /double des alcynes **4.4ab** (schéma 4.1) dans les palladacycles **4.3a-b** (schéma 4.1) a été étudiée par des outils expérimentaux, à savoir par des tests de réaction utilisant les techniques sur ligne de Schlenk, la spectroscopie de résonance magnétique nucléaire et la calorimétrie par titrage isotherme (ITC) et par des outils théoriques, c.-à-d. la DFT (Density Functional Theory) avec la correction de la dispersion de Grimme - D3. En outre, de nouveaux complexes (**4.3a** et **4.6a**, schéma 4.1) ont été synthétisés et entièrement caractérisés.

Les tests de réaction ont été effectués afin de déterminer les conditions de réaction appropriées qui seront utilisées dans les mesures de l'ITC et de vérifier l'étendue des réactions secondaires possibles. Les essais ont été réalisés à température ambiante dans deux méthodes: a) dans du chlorobenzène et du dichlorométhane avec isolement des produits de réaction et b) dans du chloroforme deutérié sans isolement des produits de réaction en considérant divers rapports molaires des réactifs et divers temps de réaction.

Les mesures ITC ont pris en compte deux types de conditions expérimentales: a) les expériences réalisées dans des conditions stoechiométriques (systèmes **4.3ab/4.4a**) et b) les expériences réalisées avec un large excès d'un réactif (système **4.3a/4.4b**), tandis que les expériences sont réalisées de manière séquentielle. Tous les calculs ont été effectués au niveau de théorie ZORA-GGAPBE-D3(BJ)/TZP en considérant une solvation modèle dans le chlorobenzène (COSMO). Les résultats ITC obtenus pour les systèmes **4.3a-b/4.4a** étaient des valeurs brutes de ΔH_r ainsi que des valeurs issues d'un modèle thermochimique de ΔH_r, ΔG_r, ΔS_r, tandis que pour le système **4.3a/4.4b**, les mesures ITC ont permis d'obtenir des valeurs brutes ΔH_r ainsi que l'ordre partiel en alcyne **4.4b.** Les calculs de DFT-D des séquences de réaction simples (systèmes **4.3a-b/4.4a**) et de celles impliquant une double insertion (système **4.3a/4.4b**) ont donné accès aux valeurs de tous les paramètres thermodynamiques des réactions (ΔH_r, ΔG_r, ΔS_r).

Les tests de réaction ont montré que l'insertion d'un alcyne (**4.4a-b**), quel que soit le type de palladacycle (**4.3a-c**), dépend de la concentration de l'alcyne. A savoir, avec un rapport presque stoechiométrique des réactifs, les réactions secondaires (l'isomérisation et la seconde insertion) peuvent se produire. D'autre part, la double insertion de **4.4b** dans **4.3a** est indépendante de la concentration de l'alcyne etne donne que le produit doublement inséré. Ces observations ont

aidé à la conception de l'expérience ITC suggérant que l'insertion unique pourrait être favorisé si des conditions stoechiométriques étaient respectées alors que la double insertion quant à elle ne nécessiterait qu'un excès d'alcyne.

L'enthalpie (raw ΔH_r) obtenu pour les deux réactions étudiées impliquant une insertion simple (valeurs ΔH_r des systèmes **4.3a-b/4.4a** sont environ -28 kcal/mol et -24 kcal/mol, respectivement) et double (valeur ΔH_r du système **4.3a/4.4b** est de -38 kcal/mol) d'alcynes dans le palladacycle suggère des transformations énergétiquement très favorables. Ces valeurs d'enthalpie sot plutôt raisonnables, tenant compte du clivage de la liaison carbone-carbone et de la formation de la liaison carbone-palladium, ainsi que des interactions attractives non-covalentes. Les valeurs ΔH_r du modèle ITC des systèmes **4.3a-b/4.4a** (environ -31 kcal/mol et -25 kcal/mol, respectivement) sont en accord avec les valeurs de raw ΔH_r. Les valeurs de ΔG_r du modèle ITC des systèmes **4.3a-b/4.4a** (environ -7 kcal/mol pour les deux systèmes) indiquent que les réactions d'insertion sont également favorables du point de vue thermodynamique. L'ordre estimé de l'alcyne **4.4b** (la valeur est un) dans la séquence d'insertion double, ainsi que le second est beaucoup plus rapide. Ces résultats correspondent parfaitement aux données déjà publiées.[271]

Les valeurs calculées des paramètres thermodynamiques ΔH_r et ΔG_r des deux systèmes examinés (**4.3a/4.4a-b**, avec les valeurs de ΔH_r environ -37 kcal/mol et -51 kcal/mol, respectivement, et avec les valeurs de ΔG_r environ -19 kcal/mol et -26 kcal/mol, respectivement) sont surestimés par rapport aux ITC obtenus. La raison d'une telle surévaluation (plus de 10 kcal/mol dans les deux les valeurs ΔH_r et les valeurs ΔG_r) pourrait se trouver dans l'absence de considération de l'interaction explicite du chlorobenzène avec le palladacycle, pour laquelle il est montré (sur des modèles similaires),[272] qu'elle n'est pas négligeable (puisque les valeurs de l'énergie de l'interaction peuvent atteindre plusieurs kcal/mol).

De plus, de nouveaux complexes **4.3a** et **4.6a** ont été synthétisés et entièrement caractérisés (par RMN ^{1}H, analyze élémentaire, MS et rayons X).

Perspective. L'estimation des paramètres thermodynamiques des interactions du chlorobenzène avec les palladacycles est nécessaire. Une analyze par diffraction des rayons X du produit **4.5a** est souhaitable.

Chapter 8

Affinity of Lewis donors to hexafluoroisopropanol

8.1. Introduction.

Recently, due to its features:[273] acidic and polar character, strong hydrogen bonding capabilities, high ionizing and stabilizing ability as well as low boiling point, low viscosity, and recyclability, 1,1,1,3,3,3-hexafluoropropan-2-ol (HFIP) was found to be an exceptional medium, either as solvent or co-solvent, that allows many reactions to occur.[274] However, the exact role and mode of action of HFIP in various chemical transformations is not still fully and reasonably explained. It is shown that aqueous alcohol mixture, especially aqueous mixture of HFIP, has a stabilizing effect on α-helical structure of proteins and peptides[275] as well as on their separation.[276]

---

[273] [N^0 686] I. Colomer, A. E. R. Chamberlain, M. B. Haughey, T. J. Donohoe, *Nat. Rev. Chem.* **2017**, *1*, 0088.
[N^0 687] H. Li, H. Yin, X. Liu, Y. Shi, M. Jin, D. Ding *Spectrochim. Acta* A: Molecular and Biomolecular Spectroscopy **2017**, *184*, 270.
[N^0 688] P. G. Seybold W. C. Kreye *Int. J. Quantum Chem.* **2012**, *112*, 3769.
[N^0 689] A. Berkessel, J. A. Adrio, D. Hüttenhain, J. M. Neudörfl, *J. Am. Chem. Soc.* **2006**, *128*, 8421.
[N^0 690] K. S. Ravikumar, F. Barbier, J.-P. Bégué, D. Bonnet-Delpon, *J. Fluorine Chem*. **1999**, *95*, 123.
[N^0 691] D. Vuluga, J. Legros, B. Crousse, A. M. Z. Slawin, C. Laurence, P. Nicolet, D. Bonnet-Delpon, *J. Org. Chem.* **2011**, *76*, 1126.
[N^0 692] R. Cabot, C. A. Hunter, L. M. Varley, *Org. Biomol. Chem.* **2010**, *8*, 1455.
[N^0 693] J. Graton, F. Besseau, A.-M. Brossard, E. Charpentier, A. Deroche, J.-Y. Le Questel, *J. Phys. Chem. A* **2013**, *117*, 13184.
[274] For selected examples, see: [N^0 694] C. Zhang, Y. Rao, *Org. Lett.* **2015**, *17*, 4456.
[N^0 695] D. Leow, G. Li, T.-S. Mei, J.-Q. Yu, *Nature* **2012**, *486*, 518.
[N^0 696] G. Li, D. Leow, L. Wan, J.-Q. Yu, *Angew. Chem. Int. Ed*. **2013**, *52*, 1245.
[N^0 697] L. Wan, N. Dastbaravardeh, G. Li, J.-Q. Yu, *J. Am. Chem. Soc.* **2013**, *135*, 18056.
[N^0 698] W. Gong, G. Zhang, T. Liu, R. Giri, J.-Q. Yu, J*. Am. Chem. Soc.* **2014**, *136*, 16940.
[N^0 699] G. Chen, T. Shigenari, P. Jain, Z. Zhang, Z. Jin, J. He, S. Li, C. Mapelli, M. M. Miller, M. A. Poss, P. M. Scola, K.-S. Yeung, J.-Q. Yu, *J. Am. Chem. Soc.* **2015**, *137*, 3338.
[N^0 700] Q. Dherbassy, G. Schwertz, M. Chessé, C. K. Hazra, J. Wencel-Delord, F. Colobert, *Chem. Eur.J.* **2016**, 22, 1735.
[N^0 701] L. Eberson, M. P. Hartshorn, O. Persson, F. Radner, *Chem. Commun*. **1996**, 2105.
[N^0 702] A. Berkessel, J. A. Adrio, *J. Am. Chem. Soc*. **2006**, *128*, 13412.
[N^0 703] B. Elsler, A. Wiebe, D. Schollmeyer, K. M. Dyballa, R. Franke, S. R. Waldvogel, *Chem. - Eur. J.* **2015**, *21*, 12321.
[N^0 704] H. F. Motiwala, R. H. Vekariya, J. Aubé, *Org. Lett.* **2015**, *17*, 5484.
[N^0 705] S. J. Khaksar, *Fluorine Chem*. **2015**, *172*, 51.
[N^0 706] H. F. Motiwala, M. Charaschanya, V. W. Day, J. Aubé, *J. Org. Chem*. **2016**, *81*, 1593.
[N^0 707] R. H. Vekariya, J. Aubé, *J. Org. Lett*. **2016**, *18*, 3534.
[N^0 708] K. Kushwaha, B. Pinter, S. A. Shehzadi, C. C. Malakar, C. M. L. Vande Velde, F. de Proft, K. A. Tehrani, *Adv.Synth. Catal*. **2016**, *358*, 41.
[N^0 709] S. Možina, S. Stavber, J. Iskra, *Eur. J. Org*. *Chem*. 2017, **2017**, 448.
[N^0 710] V. D. Vuković, E. Richmond, E. Wolf, J. Moran, *Angew. Chem., Int. Ed*. **2017**, *56*, 3085.
[N^0 711] M. Ochiai, K. Miyamoto, T. Kaneaki, S. Hayashi, W. Nakanishi, *Science* **2011**, *332*, 448.
[N^0 712] L. Lu, H. Liu, R. Hua, *Org. Lett.* **2018**, *20*, 3197.
[N^0 689] A. Berkessel, J. A. Adrio, D. Hüttenhain, J. M. Neudörfl, *J. Am. Chem. Soc.* **2006**, *128*, 8421.
[275] [N^0 713] D. Hong, M. Hoshino, R. Kuboi, Y. Goto, *J. Am. Chem. Soc*. **1999**, *121*, 8427.
[N^0 714] T. Fujinaga, S. Nakamura, S. Krishtal, K. Yoshida, S. Lee, K. Kanazawa, T. Nemoto, T. Yamaguchi, *Fukuoka Univ. Sci. Rep*. **2007**, *37*, 23.
[N^0 715] K. Yoshida, J. Kawaguchi, S. Lee, T. Yamaguchi, *Pure Appl. Chem*. **2008**, *80*, 1337.
[N^0 716] M. Buck, H. Schwalbe, C. M. Dobson, *Biochem.* **1995**, *34*, 13219.
[N^0 717] J. W. Nelson, N.R. Kallenbach, *Biochem.* **1989**, 28, 5256.

It has been found that HFIP is useful in the generation of intermediate conformation of proteins[277] within investigations of Alzheimer and prion diseases[278] as well as in other applications within biochemical researches.[279] Even though there have been many attempts to reveal molecular structure and properties of water-HFP mixture[280] mainly suggesting micellar aggregates with fluoroalkyl group located in micelle, detailed structure has remained unexplored. It has been reported that the water-HFP mixture existing within microheterogeneities of HFIP and water clusters are dependent on mole fraction of the HFIP.[281]

Despite many papers dealing with water/HFIP complexes, little has been published on other complexes as well as on thermochemistry of the formation of the complexes.[282] In a rare example given by Maiti at al., among other characteristics, the enthalpies of H-bond formation within complexes of HFIP and tertiary amines have been reported. Thus, within this study the affinity of various Lewis donors to HFIP (see Scheme 5.1-2), are investigated experimentally by means of ITC as well as theoretically using static DFT-D calculations.

[N^0 718] T. Banerjee, N. Kishore, *J. Phys. Chem*. *B* **2005**, *109*, 22655.
[N^0 719] S. M. M. Reddy, G. Shanmugam, A. B. Mandal, *Org. Biomol. Chem*., **2014**, *12*, 6181.
[276] [N^0 720] Y. Mengerink, S. van der Wal, H. A. Claessens, C. A. Cramers, *J. Chromatogr*. *A* **2000**, *871*, 259.
[N^0 721] J. Aussenac, D. Chassagne, C. Claparols, M. Charpentier, B. Duteurtre, M. Feuillat and C. Charpentier, *J. Chromatogr*. *A*, **2001**, *907*, 155.
[N^0 722] M. R. Nilsson, L. L. Nguyen, D. P. Raleigh, *Anal. Biochem*. **2001**, *288*, 76.
[N^0 723] A. Abedini, G. Singh, D. P. Raleigh, *Anal. Biochem*. **2006**, *351*, 181.
[277] [N^0 724] A. Kundu, N. Kishore, *Biopolymers* **2004**, *73*, 405.
[278] [N^0 725] S. W. Snyder, U. S. Ladror, W. S. Wade, G. T. Wang, L. W. Barrett, E. D. Matayoshi, H. J. Huffaker, G. Krafft, T. F. Holzman, *Biophys. J.* **1994**, *67*, 1216.
[N^0 726] H. Zhang, K. Kaneko, J. T. Nguyen, T. L. Livshits, M. A. Baldwin, F. E. Cohen, T. L. James, S. B. Prusiner*, J. Mol. Biol*. **1995**, *250*, 514.
[279] [N^0 727] J. R. Cort, N. H. Andersen, *Biochem. Biophys. Res. Commun*. **1997**, *233*, 687.
[N^0 728] H. S. Mchaourab, J. S. Hyde, J. B. Feix, *Biochem.* **1993**, *32*, 11895.
[N^0 729] A. Galat, J. P. Degelaen, C. C. Yang, E. R. Blout, *Biochem.* **1981**, *20*, 7415.
[N^0 730] I. Sirangelo, F. D. Piaz, C. Malmo, M. Cassilo, L. Birolo, P. Pucci, G. Marino, G. Irace, *Biochem*. **2003**, *42*, 312.
[N^0 731] N. Hirota, K. Mizuno, Y. Goto, *Protein Sci.* **1997**, *6*, 416.
[280] [N^0 732] M. Fioroni, K. Burger, A. E. Mark, D. Roccatano, *J. Phys. Chem*. *B* **2001**,*105*, 10967.
[N^0 733] K. Yoshida, T. Yamaguchi, T. Adachi, T. Otomo, D. Matsuo, T. Takamuku, N. Nishi, *J. Chem. Phys*. **2003**, *119*, 6132.
[N^0 734] K. Kinugawa, K. Nakanishi, *J. Chem. Phys*. **1988**, 89, 5834.
[N^0 735] Y. Mizutani, K. Kamogawa, T. Kitagawa, A. Shimizu, Y. Taniguchi, K. Nakanishi, *J. Phys. Chem*. **1991**, *95*, 1790.
[N^0 736] T. Takamuku, H. Wada, C. Kawatoko, T. Shimomura, R. Kanzakib, M. Takeuchic, *Phys. Chem. Chem. Phys.* **2012**, *14*, 8335.
[N^0 737] T. Takamuku, M. Tobiishi, H. Saito, *J. Solution Chem*. **2011**, *40*, 2046.
[N^0 738] A. Shahi, E. Arunan, *Phys. Chem. Chem. Phys.* **2015**, *17*, 24774.
[281] [N^0 739] T. Yamaguchi, S. Imura, T. Kai, K. Yoshida, *Z. Naturforsch*. **2013**, *68a*, 145.
[N^0 733] K. Yoshida, T. Yamaguchi, T. Adachi, T. Otomo, D. Matsuo, T. Takamuku, N. Nishi*, J. Chem. Phys*. **2003**, *119*, 6132.
[282] [N^0 740] N. C. Maiti, R. Carey, V. E. Anderson, *J. Phys. Chem. A* **2003**, *107,* 9910.

To figure out the possible role of HFIP, a formation of a potential donor-acceptor complex between HFIP and a series of ligands[283] (Scheme 5.1-2) was investigated by ITC experiments and static DFT-D calculations in gas phase.

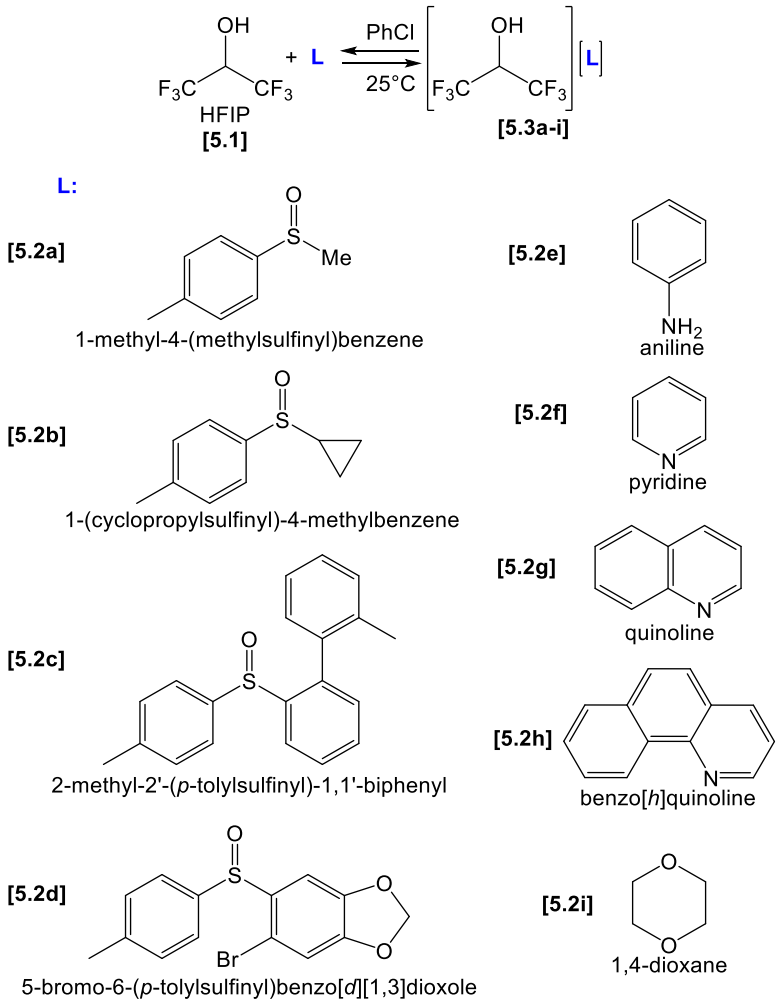

Scheme 5.1. Schematic representation of the investigated reactions within the study of the affinity of various Lewis donors (**5.2a-j**) to HFIP (**5.1**) and 2D representations of used Lewis donors throughout ITC experiments and static DFT-D calculations.

[283] [N^0 700] Q. Dherbassy, G. Schwertz, M. Chessé, C. K. Hazra, J. Wencel-Delord, F. Colobert, *Chem. Eur.J.* **2016**, 22, 1735.

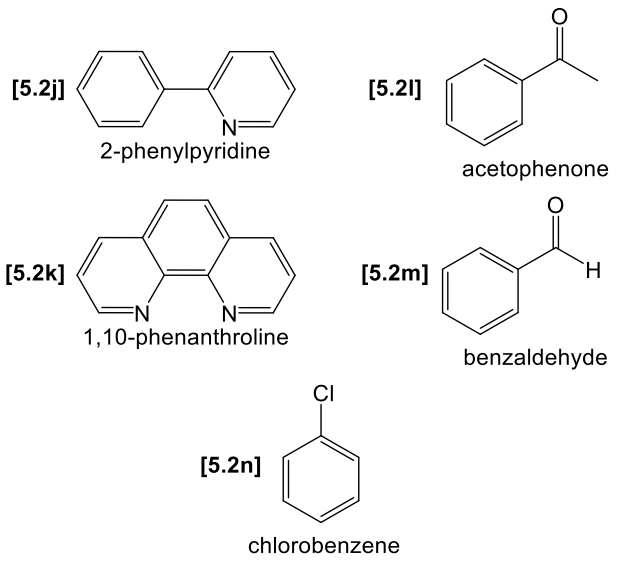

Scheme 5.2. 2D representations of additional Lewis donors used throughout static DFT-D calculations.

8.2. Experimental section.

8.2.1. Generalities.

The experiments considered an equilibrium dissociation reaction of complex formed between 1:1 equivalents of 1,1,1,3,3,3-hexafluoropropan-2-ol (HFIP) with different substrates (ligands) (Scheme 5.1).

8.2.2. Techniques.

All the investigations on the affinity of various Lewis donors to HFIP were done using ITC measurements and static DFT-D calculations.

8.2.3. Materials.

All used compounds were stored and used into a dry and argon filled glove box. Chlorobenzene was purchased from Sigma Aldrich and distilled over calcium hydride and degassed prior to use. HFIP (**5.1**) was purchased from Sigma Aldrich and used as received. The sulfoxides (**5.2a-d**) were prepared by the group of Françoise Colobert (ECPM-Strasbourg) and used as received under argon after checking their purity by NMR. Amines: aniline (**5.2e**) and pyridine (**5.2f**) were purchased from Sigma Aldrich, purified over silica and degassed prior to use. Quinoline (**5.2g**) and Benzo[h]quinoline (**5.2h**) were purchased from Sigma Aldrich and purified over silica and

recrystallized from pentane under argon and used checking its purity by NMR. Dioxane (**5.2i**) was purchased from Sigma Aldrich, distillated over calcium hydride and degassed prior to use.

8.2.4. ITC experimental details.

The solutions of the adducts (**5.3a-i**) were prepared by dissolving a mass of substrates in pure, freshly distilled and degassed chlorobenzene in the same volumetric flask and contained the same number of mol of each substrate. The concentrations of the solutions in pure PhCl were around 130 mmol/L. The ITC experiments were performed using sequential injection at 25ºC with a moderate stirring rate (150-200 rpm). Auto equilibration of the ITC was performed before every experiment to reach an acceptable baseline. In the typical ITC experiment, the solution of the adduct was introduced in the servo-controlled ITC syringe (100 µL) while the reference and sample cell were entirely filled with pure PhCl (1.0 mL each cell). The content of the syringe was injected into the sample cell through 45 equivalent injections (2.06 µL per injection) with time delay between two consecutive injections of 1500-3000s, depending on a nature of the particular system. For each studied system at least three experiments under the same condition were done. A heat of dilution of each substrate in neat PhCl was estimated from the blank experiments of HFIP in neat PhCl (preformed under the same condition as the main experiments), which, supposedly, has the major contribution to the heat of dilution. That was confirmed by comparison to the heats of dilution of other substrates (ligands) that were significantly lower. Therefore, a heat of 100 µJ was subtracted from all the corresponding titration curves. Enthalpy of dissociation (ΔH_d) was obtained as result of an experiment using an *ad-hoc* logarithm – dimer dissociation model - implemented in NanoITC Analyze software. Resulting ΔH_d values represents an average value of three corresponding experiments.

8.2.5. Static DFT-D calculation details.

All computations were performed by the methods DFT using Amsterdam Density Functional package (ADF2013 version).

Starting geometries of the monomers (**5.1** and **5.2a-i**, see Scheme 5.1) were taken from the CSD or built up from similar ones and optimized as singlet ground states in the gas phase. Geometries of the complexes (dimers) were constructed from the previously optimized monomers following two main possible orientations: - in case of the sulfoxides (**5.2a-d**) a) when the OH group of HFIP is close to the sulfur atom or b) when the OH of HFIP group is close to

the oxygen atom; - in case of amines/dioxane (**5.2e-i**) a) when the OH group of HFIP is close to the nitrogen/oxygen atom while the rest of the HFIP molecule is above the aromatic/aliphatic ring of the amine/dioxane or b) when the OH group of HFIP is close to the nitrogen/oxygen atom while the rest of the HFIP molecule is outside of the aromatic/aliphatic ring of the amine/dioxane, and optimized as singlet ground states in the gas phase.

The calculations were performed on larger scope of the ligands compared to the ITC investigation. Accordingly, the calculations took into consideration the ligands showed in the Scheme 5.2. Similar to the studied system by ITC, new ligands (**5.2.j-n**) were optimized as monomers and as dimers with HFIP with respect to the previously explained choices of the starting dimer geometries and at the same level of theory. When reasonable, theoretical trimers were also considered. Namely, if the ligand possesses two potential proton acceptors, like the sulfoxides (**5.2a-d**) and phenanthroline (**5.2k**) do possess, two molecules of the HFIP are included into the structure optimization. The theoretical trimers (**5.3a-d** and **5.3j-n**) were also optimized in the gas phase at the same level of theory. Special case was HFIP itself, where up to four molecules of HFIP were simultaneously optimized as one system (**5.3.1**)

8.3. Results and discussion.

8.3.1. ITC experiments.

To find optimal conditions for ITC measurements two approaches were employed. Like previously, the first choice considered a separation of the substrates. Namely, first tests used either HFIP as reagent in the sample cell, while the ligands (**5.1a-i**) were injecting through the ITC syringe, or the reverse. However, it is shown that whatever the order and concentrations of the substrates were, no exploitable ITC heat response was obtained (i.e. no possibility to fit the curve). Some examples of these results are summarized in Figure SI 5.1 (see Supplementary Information).

Thus, the second approach, for first time used in this PhD study, had to be utilized. That approach considered a making previously (outside of the ITC instrument) quite concentrated mixture solutions of HIFP (**5.1**) and the ligand (**5.2a-i**) in pure chlorobenzene, supposedly resulting in some kind of relatively labile non-covalent complex with respect of 1:1 equivalent in each substrate. Such solutions were afterwards put in the servo-controlled ITC syringe and sequentially injected into the ITC sample cell fulfilled with pure chlorobenzene. Basically, in this

approach a dilution of the concentrated solution takes place in the ITC instrument. That dilution leads to dissociation of that labile bonded complex and certainly to a forming of new complexes of the substrates with chlorobenzene. The concentrations of these solutions that generated reasonable ITC thermograms are found to be 80-130 mM. The heat of dilution, i.e. heat of dissociation of the investigated complex upon dilution, was subsequently threated by an *ad-hoc* algorithm (dimer dissociation model) implemented in NanoITC Analyze software. One should be aware that the obtained heat was resulted from, among others, two main processes: a) the dissociation of the complex (**5.3a-i**) which, if such complex exists within its concentrated solution, must be an endothermic process; b) the solvation of the substrates by infinitely concentrated chlorobenzene, which is most probably an exothermic process. As it was shown separately, by doing the blank experiments (dilution of each substrate separately under the same condition), the heat of solvation is mostly negligible (around 100 μJ) compared to the heat of dissociation (a couple of mJ). For sake of consistency, that solvation heat is roughly subtracted from the obtained ITC heat during its treatment by NanoITC Analyze software.

Results of the dissociation of the investigated complexes using dimer dissociation model are depicted in Table 5.1. As it was mentioned above, these heats, and therefore, dissociation enthalpies (ΔH_d) have to be with endothermic (i.e. positive by convention) sign. Hence, in Table SI. 5.1 (see Supplementary Information) one can find dissociation enthalpies (ΔH_d), dissociation entropies (ΔS_d) and dissociation Gibbs energies (ΔG_d) while the corresponding association (reaction) thermochemical parameters, which are basically the opposite to the dissociation ones, are reported in Table 5.1. Figure 5.1 displays ITC thermogram of dissociation of the **5.1/5.2a** complex in chlorobenzene and its integrated heat peaks fitted by dimer dissociation model, as an example of the shape of ITC thermogram, considering very similar shape within of all herein the investigated Lewis donors (**5.2.a-i**). The ITC thermograms of other herein studied systems are given in Supplementary Information (see Figures SI 5.2 – 9).

Table 5.1 Results of ITC experiments obtained by employing dimer dissociation model on integrated heat peaks and transformed to association thermodynamic parameters.

System	ΔH_a ± error		ΔG_a ± error		ΔS_a ± error		K_a ± error	
	kcal/mol	kcal/mol	kcal/mol	kcal/mol	cal/molK	cal/molK	M	M
5.3a	-12.9	0.8	-3.2	0.6	-32.4	5.9	$2.3*10^2$	4*10
5.3b	-10.1	0.6	-2.9	0.5	-24.3	4.5	$1.3*10^2$	2*10
5.3c	-10.1	0.4	-2.7	0.4	-24.8	4.2	8.9*10	1*10
5.3d	-4.6	0.5	-2.2	1.3	-8.3	5.1	3.8*10	2*10
5.3e	-9.9	0.0						
5.3f	-14.3	1.2	-3.2	0.8	-37.1	8.7	$2.2*10^2$	5*10
5.3g	-11.8	0.3	-1.9	0.4	-33.0	6.4	2.7*10	5
5.3h	-12.3	0.8	-1.4	0.3	-36.5	8.1	1.1*10	2
5.3i	-9.3	0.3	-1.4	0.2	-26.6	3.4	1.0*10	1

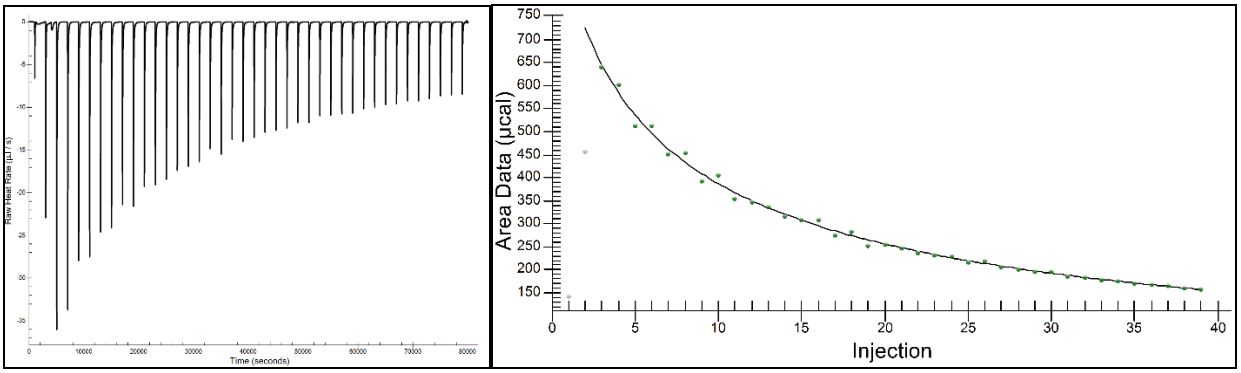

Figure 5.1. *left side* – ITC thermogram of the dissociation of the complex **5.1/5.2a** (syringe, c=82.44 mM) in chlorobenzene. The titration was performed at 25ºC through 39 sequential additions (of 2.06 µL each). Time between two consecutive injections was 2000 s. Heat released is expressed in µJ/s versus time in s. *right side* – ITC integrated heat peaks of the thermogram shown on the left side. Integrated heats are expressed in µcal versus number of injections and fitted by dimer dissociation model implemented in NanoAnalyze software.

As a dissociation process is an equilibrium process it could be, in general, expressed with an equilibrium constant K_d or K_a:

$$[AB] \underset{K_a}{\overset{K_d}{\rightleftharpoons}} A + B \qquad K_d = [A]*[B]/[[AB]] \qquad K_a = [[AB]]/[A]*[B]$$

Therefore, the shape of ITC thermogram of the dissociation of the complex **5.1/5.2a** shown in Figure 5.1, is reasonable. Namely, at the beginning of the sequential titrations (by the introducing of the solution of the complex through the ITC syringe into the sample cell fulfilled with pure chlorobenzene), the heat response (endothermic) due to the dissociation of the complex is the highest. As long as new portions of the complex are being injected, the equilibrium mixture simultaneously adapts itself accordingly to the equilibrium constant (either K_d or K_a), what leads to a decreasing of the relative heat change per injection.

By integration the heat peaks of the recorded ITC thermograms and by applying the dimer dissociation model, implemented in NanoAnalyze software, on these integrated heats, the thermochemical parameters of the dissociation process of the complex (ΔH_d, ΔG_d, ΔS_d) were obtained (as results of the fitting).

Intuitively, one can expect that HFIP interacting with the sulfoxides (**5.2a-d**) would be challenged by at least two possible proton acceptors (sulfur and oxygen atom). The rest of the HFIP molecule, i.e. fluorine atoms might interact with hydrogen atoms either from aromatic or aliphatic residue of the sulfoxide molecule. On the other hand, an increasing of steric cluttering around the sulfur atom would force HFIP molecule to move towards the oxygen atom adapting its fluorine atoms accordingly.

The amines (**5.2e-h**) should, in principle, be simpler in terms of their possible interactions with HFIP. Basically, basicity of the nitrogen atom accompanied with a possibility of delocalization of its electron pair through aromatic ring would govern its capability to hydrogen bonding. On the other hand, the aromatic (condensed) ring size might have an influence on the polarizability of an aromatic ring and corresponding hydrogen atoms, and therefore on the strength of subsequent interactions with the third party, i.e. fluorine atoms of HFIP molecule.

In the case of dioxane (**5.2i**) the interacting picture is even more predictable. Most probably, the OH group of HFIP is oriented toward an oxygen atom, while the fluorine atoms interact with the hydrogen atom of dioxane.

Moreover, the solvation interactions of chlorobenzene with the reactants should not be excluded and treated as negligible. Thus, it must be assumed that a competition between these sources of attractive (non-covalent) interactions always takes place.

The ITC results of the interactions of sulfoxides (**5.2a-d**) with HFIP in chlorobenzene as a reaction medium suggest on a discriminatory influence of second substituent on sulfur atom. Namely, it can be seen that if methyl group is the substituent, the association enthalpy (ΔH_a) is the highest, around -13 kcal/mol. That might be accompanied with small bulkiness of the methyl group giving a possibility for relatively strong F-H interactions and a chance to the OH group to properly interact with the oxygen or sulfur atom. As the bulkiness of the substituent increases, the association enthalpy decreases. The same ΔH_a value (around -10 kcal/mol) for **5.2b** and **5.2c** is probably caused by two opposite effects: the substituent bulkiness and the strength of aliphatic hydrogen atom against aromatic hydrogen atom with a fluorine atom. The lowest ΔH_a

value of **5.2d** (around -5 kcal/mol) is most probably due to the bromine substituent in *ortho* position of aromatic ring directly connected to the sulfur. Namely, this bromine, to some extent, can prevent most proper interaction of the sulfoxide with HFIP.

Expectedly, the ΔH_a value of an association of aniline (**5.2e**) with HFIP is the lowest (around -10 kcal/mol), most probably due to its the lowest basicity among the series of investigated amines (**5.2e-h**) and possible interference of nitrogen's hydrogen atoms on achieving optimal orientation of HFIP. Structural differences between the three other aromatic amines could rationally explain the differences in their ΔH_a values. Namely, in case of pyridine (**5.2f**), which exhibits the highest association tendency to HFIP (with ΔH_a around -14 kcal/mol and ΔG_a around -1.3 kcal/mol), its moderately high basicity and molecular simplicity might allow preferable orientation of HFIP achieving, relatively strong non-covalent interactions, i.e. OH-N hydrogen bond and a couple of F-H interactions. Although quinoline (**5.2g**), compared to benzo[h]quinoline (**5.2h**) possesses an aromatic ring less, it seems that the number of the condensed aromatic rings has no significant influence on the ΔH_a value, as their ΔH_a values are very similar, -11.8 kcal/mol and -12.3 kcal/mol, respectively. Quite interestingly, in comparison to ΔH_a values of **5.2f** (ca. -14 kcal/mol) is seems that larger electron delocalization (through condensed aromatic rings) leads to decreasing ΔH_a values for ca. 2 kcal/mol.

Considering the dioxane (**5.2i**) case and its ΔH_a around -9 kcal/mol one could conclude that relative flexibility of heteroaliphatic ring might have a disrupting influence on herein considered interactions with HFIP.

From the obtained ITC Gibbs enthalpies of association (ΔG_a), that are negative (ranged from around -1.4 kcal/mol to -3.2 kcal/mol) in all the studied systems (**5.3a-i**), it can be concluded that all Lewis donors (**5.2a-i**) would spontaneously interact with HFIP (**5.1**). This information, accompanied with relatively large association enthalpies (ranged from around -5 kcal/mol to -13 kcal/mol), might have a huge influence on an additional polarization of bonds within sulfoxide (or other) molecule, what would ease its further transformations with third party.

So, to treat the ITC data properly, one must be aware of the complexity of interactions/reaction in solution.

8.3.2. Static DFT-D calculations.

All computations within the study of the affinity of Lewis donors (**5.2a-i**) to HFIP were performed at ZORA-GGAPBE-D3(BJ)/TZP level of theory in gas phase, while some calculations were performed in chlorobenzene solution (COSMO) phase as well. As explained in detail in the experimental section of the manuscript, the geometry optimization was done for all the monomers (**5.1**, **5.2a-i**), corresponding complexes (**5.1/5.2a-i**) and, in the cases where there are two possible proton acceptors (**5.2a-d**), even trimers (**2x5.1/5.2a-d**) were considered. The geometry optimizations were confirmed as true minima by performing calculations of vibrational modes. In accordance to the fact that a starting geometry has huge directing course to geometry optimization (as frequently it stops into some of local energetic minimum), to find most optimal orientation, a couple of starting positions of HFIP (regarding the second substrate) were probed. The scope of the calculations was extended to few Lewis donors (**5.2j-n**) which have not been tackled by ITC investigations. The thermodynamic parameters (ΔH_a, ΔG_a, ΔS_a), as results of the performed calculations, for all the systems were obtained. It is worthy to note that this study is rather made for qualitatively-comparative purpose.

Graphic representations of the selected optimized geometries are shown in Figure 5.2 and Figure 5.3 while their Cartesian coordinates are given in Supplementary Information.

The computational results of the studied systems by ITC (**5.1/5.2a-i**) are compiled in Table 5.2. The data of the sulfoxides include results for various orientations of HFIP (primarily the orientation of the OH group) regarding the molecule of sulfoxide. Otherwise, the data of (potentially) most stable geometries are only given. Table 5.3 displays the results of the additional systems (**5.1/5.2j-n**).

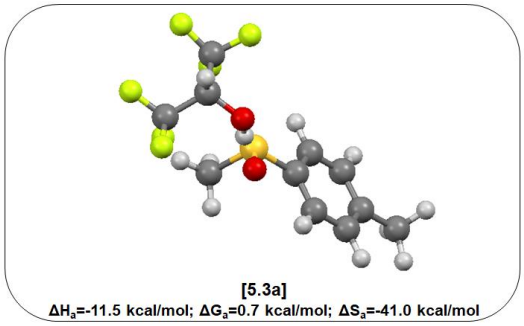

[5.3a]
ΔH_a=-11.5 kcal/mol; ΔG_a=0.7 kcal/mol; ΔS_a=-41.0 kcal/mol

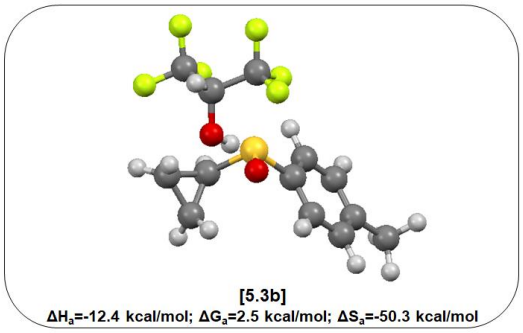

[5.3b]
ΔH_a=-12.4 kcal/mol; ΔG_a=2.5 kcal/mol; ΔS_a=-50.3 kcal/mol

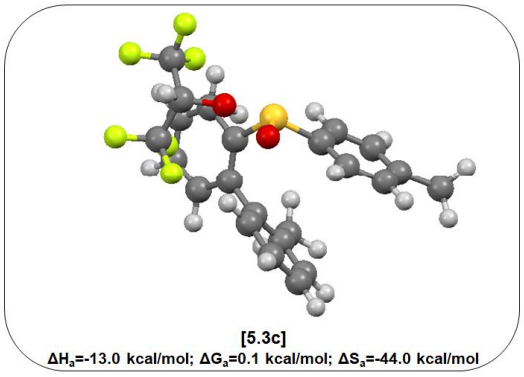

[5.3c]
ΔH_a=-13.0 kcal/mol; ΔG_a=0.1 kcal/mol; ΔS_a=-44.0 kcal/mol

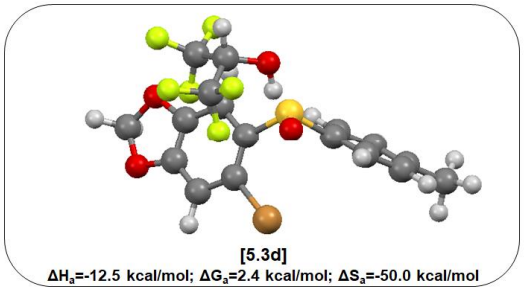

[5.3d]
ΔH_a=-12.5 kcal/mol; ΔG_a=2.4 kcal/mol; ΔS_a=-50.0 kcal/mol

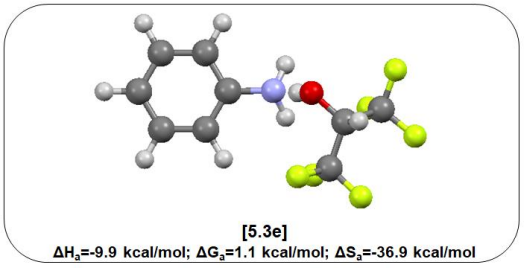

[5.3e]
ΔH_a=-9.9 kcal/mol; ΔG_a=1.1 kcal/mol; ΔS_a=-36.9 kcal/mol

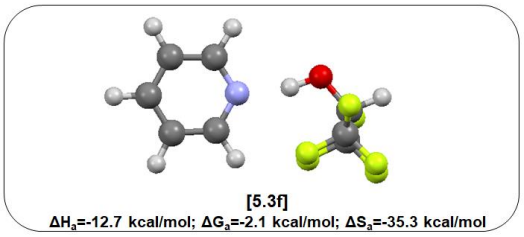

[5.3f]
ΔH_a=-12.7 kcal/mol; ΔG_a=-2.1 kcal/mol; ΔS_a=-35.3 kcal/mol

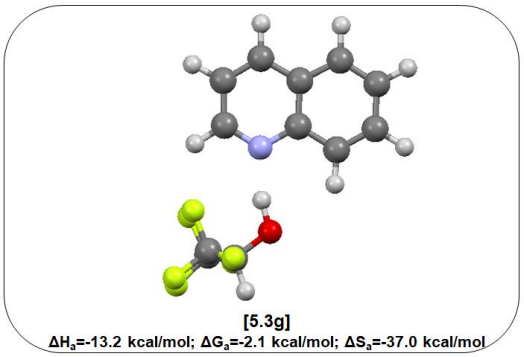

[5.3g]
ΔH_a=-13.2 kcal/mol; ΔG_a=-2.1 kcal/mol; ΔS_a=-37.0 kcal/mol

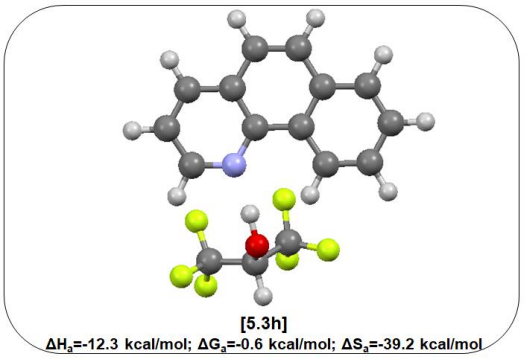

[5.3h]
ΔH_a=-12.3 kcal/mol; ΔG_a=-0.6 kcal/mol; ΔS_a=-39.2 kcal/mol

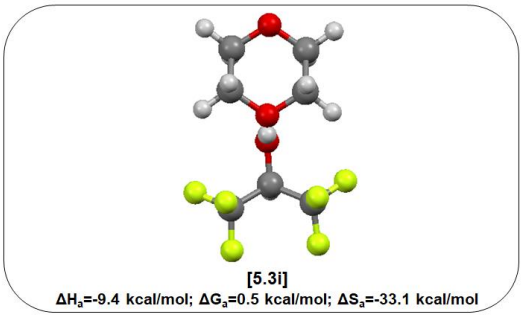

[5.3i]
ΔH_a=-9.4 kcal/mol; ΔG_a=0.5 kcal/mol; ΔS_a=-33.1 kcal/mol

Figure 5.2 Graphic representations of selected optimized geometries of the investigated systems at ZORA-GGAPBE-D3-BJ/TZP level of theory in gas and chlorobenzene solution (COSMO) phase. S: orange; O: red; N: violet; F: yellowish; Br: brown; C: grey; H: white.

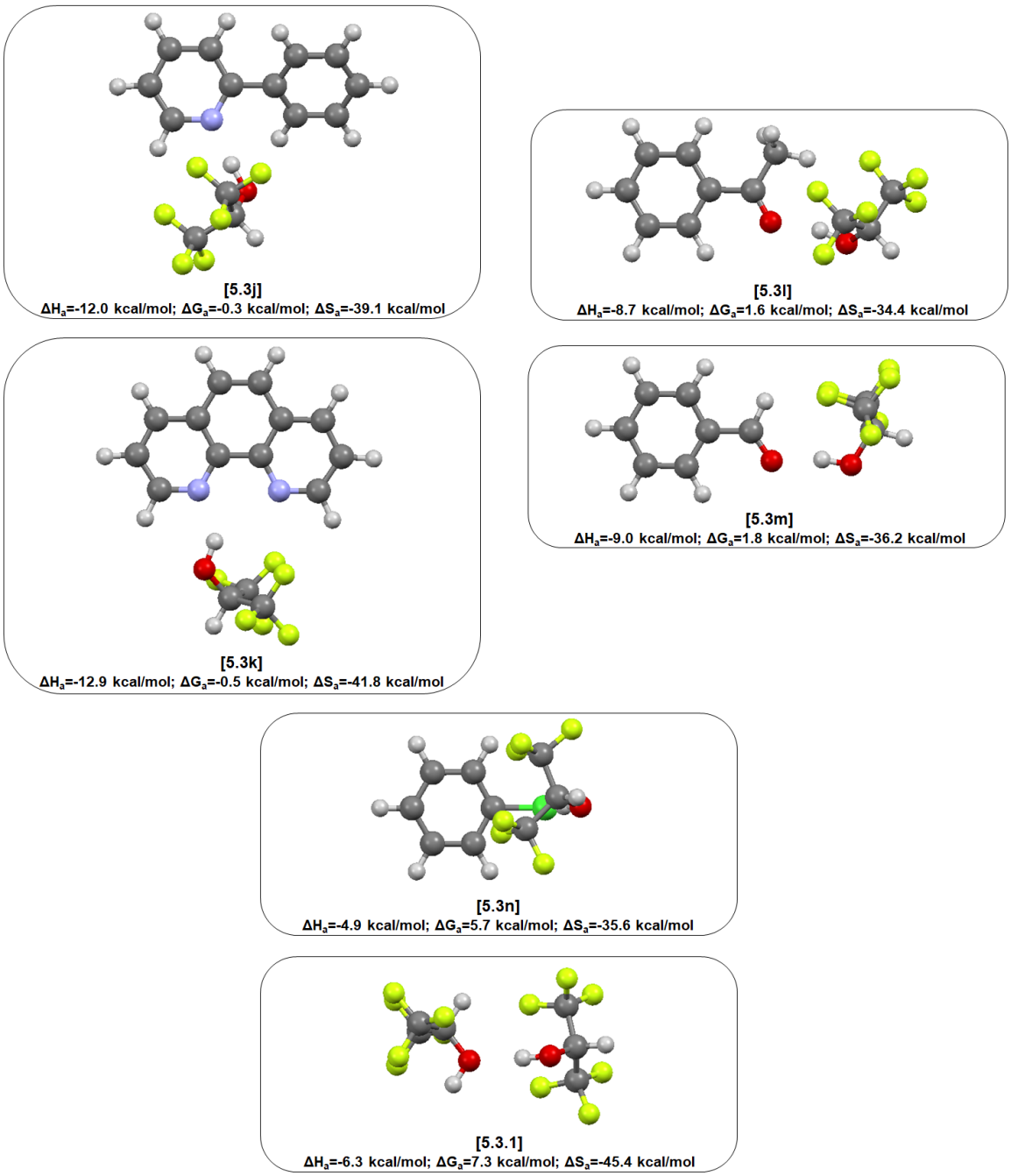

Figure 5.3 Graphic representations of selected optimized geometries of the investigated system at ZORA-GGAPBE-D3-BJ/TZP level of theory in gas phase. O: red; N: violet; F: yellowish; Cl: green; C: grey; H: white.

Noticeably, in all the sulfoxides (**5.2a-d**) stronger (even twofold) association enthalpies ΔH_a are obtained when HFIP is positioned toward oxygen atom than toward sulfur atom (see Figure SI 5.10 as an example). In addition, in the case of **5.2d** a difference in ΔH_a among differently substituted oxygen atoms could be seen; if HFIP is oriented to the heterocyclic ring a resulting ΔH_a is significantly lower than ΔH_a of the case in which HFIP is pointed to the oxygen doubly bonded to the sulfur (see Figure SI 5.11 as an example). If two molecules of HFIP (positioned towards oxygen and sulfur, respectively) were optimized together with the molecule of sulfoxide (**5.2a-c**), ΔH_a value is roughly a sum of the separated association enthalpies, what means that two HFIP molecules are able to accommodate themselves in such a way to not bother each other's optimal interactions with the sulfoxide. The results (of **5.1/5.2a-d**) showed that the ΔH_a values of most optimal orientation within the complexes are similar and ranged from -11.5 kcal/mol to -13.0 kcal/mol. It seems that, theoretically in a gas phase, in terms of ΔH_a and ΔG_a, most probably the complex **5.1/5.2c** (ΔH_a = -13 kcal/mol and ΔG_a = 0.1 kcal/mol) would exist within an equilibrium, while the complexes **5.1/5.2a** (ΔH_a = -11.5 kcal/mol and ΔG_a = 0.7 kcal/mol), **5.1/5.2b** (ΔH_a = -12.4 kcal/mol and ΔG_a = 2.5 kcal/mol) and **5.1/5.2d** (ΔH_a = -12.5 kcal/mol and ΔG_a = 2.4 kcal/mol) would unlikely be in a single form. For the complex **5.1/5.2c** the thermochemical parameters were calculated for chlorobenzene solution state as well. The results revealed that in solution ΔG_a value got increased while ΔH_a value got decreased for, almost the same value (ca. 3.5 kcal/mol) compared to the gas phase values.

Calculated ΔH_a values of the amines (**5.2e-h**) interactions with HFIP are span from -9.9 kcal/mol to -13.2 kcal/mol. Again, the lowest value (-9.9 kcal/mol) belongs to aniline (**5.2e**). An influence of a size of delocalized π system (number of condensed aromatic rings) on the association enthalpies cannot be clearly stated since an inconsistency in the ΔH_a values is noticeable. As the calculated ΔH_a values of quinoline (**5.2g**) and benzo[h]quinoline are -13.2 kcal/mol and -12.3 kcal/mol, respectively, it seems that largely delocalized systems (containing more than two condensed rings) have no significant stabilizing influence on the interactions amine-HFIP. Considering the ΔG_a values, that are slightly negative (-0.6 - -2.1 kcal/mol), it could be concluded that these pairs (**5.1/5.2f-g**) would rather exist in gas phase, what is not the case for the **5.1/5.2e** (ΔG_a = 1.1 kcal/mol).

Results of **5.1/5.2i** (ΔH_a = -9.4 kcal/mol; ΔG_a = 0.5 kcal/mol) suggest a moderately association enthalpy value and not spontaneous formation of the pair. Regarding the discussed results

above, one could conclude that oxygen is weaker proton acceptor than nitrogen while stronger than sulfur.

Table 5.2 Results of static DFT-D calculations supplemented with ITC results. The calculations were performed at ZORA-GGAPBE-D3-BJ/TZP level of theory in gas and chlorobenzene solution (COSMO) phase.

System	Type of main interaction	ITC		Level of theory	DFT		
		ΔH_a kcal/mol	ΔG_a kcal/mol		ΔH_a kcal/mol	ΔG_a kcal/mol	ΔS_a cal/molK
5.3a	OH-S	-12.9 ± 0.8	-3.2 ± 0.6	GGAPBE-D3-BJ/TZP-gas	-6.0	5.5	-38.8
	OH-O				-11.5	0.7	-41.0
	OH-O + OH-S				-17.8	8.6	-88.7
5.3b	OH-S	-10.1 ± 0.6	-2.9 ± 0.5		-6.8	6.0	-42.9
	OH-O				-12.4	2.5	-50.3
	OH-O + OH-S				-17.5	6.1	-79.2
5.3c	OH-S	-10.1 ± 0.4	-2.7 ± 0.4	GGAPBE-D3-BJ/TZP-PhCl	-5.9	6.5	-41.6
	OH-O				-13.0	0.1	-44.0
	OH-O + OH-S				-18.0	7.6	-85.7
5.3d	OH-S	-4.6 ± 0.5	-2.2 ± 1.3		-3.5	10.7	-47.8
	OH-O				-9.7	3.7	-44.9
	OH-S				-6.6	8.0	-48.8
	OH-O				-12.5	2.4	-50.0
	OH-*m*O				-7.3	8.9	-54.2
	OH-*p*O				-6.1	8.2	-48.2
5.3e	OH-N	-9.9 ±		GGAPBE-D3-BJ/TZP-gas	-9.9	1.1	-36.9
5.3f	OH-N	-14.3 ± 1.2	-3.2 ± 0.8		-12.7	-2.1	-35.3
5.3g	OH-N	-11.8 ± 0.3	-1.9 ± 0.4		-13.2	-2.1	-37.0
5.3h	OH-N	-12.3 ± 0.8	-1.4 ± 0.3		-12.3	-0.6	-39.2
5.3i	OH-O	-9.3 ± 0.3	-1.4 ± 0.2		-9.4	0.5	-33.1

Table 5.3 Results of static DFT-D calculations. The calculations were performed at ZORA-GGAPBE-D3-BJ/TZP level of theory in gas phase.

System	Type of main interaction	Level of theory	ΔH_a kcal/mol	ΔG_a kcal/mol	ΔS_a cal/molK
5.3j	OH-N	GGAPBE-D3-BJ/TZP-gas	-12.0	-0.3	-39.1
5.3k	OH-N		-12.9	-0.5	-41.8
	2 x OH-N		-20.2	5.1	-85.0
5.3l	OH-O		-8.7	1.6	-34.4
5.3m	OH-O		-9.0	1.8	-36.2
5.3n	out of ring_*p*-H		-3.9	4.8	-29.2
	out of ring_Cl		-3.8	5.0	-29.3
	in ring_*p*-H		-5.3	7.1	-41.5
	in ring_Cl		-4.9	5.7	-35.6
5.3.1	2 x HFIP		-6.3	7.3	-45.4
	3 x HFIP		-13.5	12.7	-87.8
	4 x HFIP		-21.7	15.3	-124.0

Comparing the results of the additionally studied amines (**5.2j** and **5.3k**) a slight difference in their ΔH_a (-12 kcal/mol and -12.9 kcal/mol, respectively) might be caused by a presence of

another nitrogen atom in the latter amine. If two HFIP molecules interact with **5.2k** ((2x**5.1**)/**5.2k**), the resulting Δ*H*a value is not a simple sum of the two dimer (**5.1/5.2k**) ΔH_a values (see Table 5.3. and ΔH_a related values: -20.2 kcal/mol against 2*(-12.9 kcal/mol)) suggesting that in the dimer case (**5.1/5.2k**) both nitrogen atoms are involved in the interactions with the HFIP molecule.

Supplemented theoretical calculations included: two molecules that contain carbonyl group (i.e. acetophenone (**5.2l**) and benzaldehyde (**5.3m**)), chlorobenzene (**5.2n**) and HFIP (**5.1**), each interacting with HFIP.

As HFIP molecule rather prefers to interact with aliphatic than aromatic hydrogen atom (confirmed on these cases by additional calculations, see Figure SI 5.12), a tiny difference between the ΔH_a values of **5.2l** (ΔH_a = -8.7 kcal/mol) and **5.2m** (ΔH_a = -9.0 kcal/mol) is rather expected scenario.

Within a theoretical study of interactions between chlorobenzene and HFIP, a few orientations of HFIP to PhCl were considered. The results, reported in Table 5.3, reveal that in the all taken orientations no negligible association enthalpies (ΔH_a is up to -5.3 kcal/mol) are obtained. Interestingly, in most stable orientations, OH group (from HFIP) is oriented, either to carbon atom in *para* position or to chlorine atom (**Figure 5.3**), while a rest of the HFIP molecule lies above the aromatic ring.

The special case of theoretical part are interactions of HFIP itself. The results exhibited a relatively large ΔH_a values (-6.3 kcal/mol) for HFIP's dimer and up 21.7 kcal/mol for the quatromer, suggesting on a cooperative effect and a probability of large molecular clusters of HFIPs. However, according to quite positive ΔG_a values (from 7.3 kcal/mol), the clustering (in diluted solutions) is unlikely to happen.

In accordance to the decrease of the number of molecules during an association process, the obtained ΔS_a values, negative in all the systems, are rather expected. They are ranged ca. -40 - -50 cal/molK.

8.4. Subchapter conclusion.

The affinity of various Lewis donors to 1,1,1,3,3,3-hexafluoropropan-2-ol (HFIP) were estimated experimentally (by Isothermal Titration Calorimetry – ITC) and theoretically (by static Density Functional Theory – DFT, with Grimme's dispersion correction – D3).

ITC experiments considered a dissociation of the pair formed between HFIP and Lewis donor and were carried out in sequential addition manner. Static DFT-D calculations were performed at ZORA-GGAPBE-D3(BJ)/TZP level of theory (in principle, relatively fast and acceptably accurate for organic components) mostly in gas phase. As results of both, experimental and theoretical approach, thermodynamic parameters of the association (ΔH_a, ΔG_a, ΔS_a) are obtained.

In ITC study a couple of sulfoxides (**5.2a-d**, Scheme 5.1), amines (**5.2e-g**, Scheme 5.1) and dioxane (**5.2i**, Scheme 5.1) were studied, while the scope of static DFT-D calculations were extended to some other amines (**5.2j-k**, Scheme 5.2), ketone (**5.2l**, Scheme 5.2) aldehyde (**5.2m**, Scheme 5.2) as well as to chlorobenzene and HFIP (**5.2n**, Scheme 5.2 and **5.1**, Scheme 5.1, respectively).

The ITC results suggested on quite strong to strong non-covalent interactions (range of ITC ΔH_a -5 – -13 kcal/mol) within the studied systems. In addition, concluded on ΔG_a (ranged -1.4 – -3.2 kcal/mol) all considered Lewis donors might interact spontaneously with HFIP. Altogether, that might have a huge influence on an additional polarization of bonds within the Lewis donor molecule, what could be of a crucial importance in key steps of various chemical transformations. Therefore, HFIP might have a catalytic role.

Although, the results of the calculations ΔH_a in gas phase are consistent with the experimental ΔH_a ITC results within the error bar, it is shown that even better accordance of the results could be achieved applying continuum model solvation treatment (COSMO) within the computations. Compared to the ITC results, static DFT-D calculations at used level of theory do overestimate ΔS_a value.

It is shown that chlorobenzene, solvent of choice for ITC experiments, could considerably interacts with HFIP as well as that quite strong interactions between HFIP molecules are possible, what one should be aware of. Additionally, the calculations showed that nitrogen is

stronger H bonding acceptor than oxygen, while the later one is stronger than sulfur. HFIP rather prefer to interact with aliphatic than aromatic hydrogen atoms.

Outlook. The investigation should be supplemented with solution (COSMO, or better) thermodynamic parameters for non-treated systems. An estimation of BSSE as well as a calculation of interaction energies of all herein studied systems would be appreciable. 2D NMR – Diffusion ordered spectroscopy (DOSY) investigation is highly desirable.

8.5. Закључак поглавља.

Афинитет различитих Lewis-ових донора према 1,1,1,3,3,3-хексафлуоропропан-2-олу (HFIP) процењен је експериментално (помоћу изотермалне титрационе калориметрије (енг. ITC) и теоријски (прорачунима заснованим на теорији функционала густине са Grimme-овом корекцијом за дисперзију (енг. DFT-D3)).

ITC експериментима проучавана је дисоцијација пара формираног између HFIP Lewis-ових донора, а изведени су секвенцијалним начином додавања. Статички DFT-D прорачуни изведени су на ZORA-GGAPBE-D3(BJ)/TZP теоријском нивоу (у принципу, релативно брзом и прихватљиво тачном за органске компоненте) углавном у гасној фази. Као резултат експерименталног и теоријског приступа добијени су термодинамички параметри асоцијације (ΔH_a, ΔG_a, ΔS_a).

У ITC студији проучавано је неколико сулфоксида (**5.2a-d**, схема 5.1), амина (**5.2e-g**, схема 5.1) и диоксан (**5.2i**, схема 5.1), док је обим статичких DFT-D прорачуна проширен на неке друге амине (**5.2j-k**, схема 5.2), кетон (**5.2l**, схема 5.2) алдехид (**5.2m**, схема 5.2), као и хлоробензен и HFIP (**5.2n**, схема 5.2, односно **5.1**, схема 5.1).

ITC резултати указали су на постојање прилично јаких до јаких нековалентних интеракција (опсег ΔH_a вредности од -5 до -13 kcal/mol) у проучаваним системима. Поред тога, на основу ΔG_a вредности (у опсегу од -1,4 до -3,2 kcal/mo), закључено је да сви разматрани Lewis-ови донори могу да интерагују спонтано са HFIP-ом. Све то може имати велики утицај на додатну поларизацију веза унутар молекула Lewis-ових донора, што би могло бити од пресудног значаја у кључним корацима различитих хемијских промена. Стога, HFIP може имати каталитичку улогу.

*И*ако су резултати прорачуна ΔH_a у гасној фази у складу са експерименталним ΔH_a ITC резултатима унутар границе грешке, показано је да би се могла постићи још боља усклађеност између резултата применом континуалног солватационог модела (енг. continuum model solvation treatment (COSMO)). У поређењу са ITC резултатима, статички DFT-D прорачуни на коришћеном теоријском нивоу прецењују ΔS_a вредности.

Показано је да би и хлоробензен, изабрани растварач за ITC експерименте, могао значајно интераговати са HFIP-ом, као и да су могуће снажне интеракције између самих

молекула HFIP, што треба узети у обзир. Поред тога, прорачуни су показали да је при грађењу водоничних веза атом азота јачи акцептор него атом кисеоника, док је атом кисеоника јачи акцептор од атома сумпора, као и да HFIP радије гради интеракције са алифатичним него са ароматичним атомима водоника.

Перспектива. Истраживање треба допунити термодинамичким параметрима интеракција испитиваних система у раствору (COSMO, или боља метода). Процена BSSE-а, као и израчунавање енергије интеракције проучаваних система, било би значајно. 2D NMR DOSY испитивање проучаваних система је веома пожељно.

8.6. Conclusion du chapitre.

L'affinité de divers donneurs de Lewis pour le 1,1,1,3,3,3-hexafluoropropane-2-ol (HFIP) a été estimée expérimentalement (par calorimétrie de titrage isotherme - ITC) et théoriquement (par la théorie de la densité statique fonctionnelle - DFT, avec Correction de la dispersion de Grimme – D3).

Les expériences ITC ont considéré une dissociation du couple formé entre le HFIP et le donneur de Lewis et ont été réalisées de manière séquentielle. Les calculs de DFT-D statiques ont été réalisés au niveau de théorie ZORA-GGAPBE-D3(BJ)/TZP (en principe, relativement rapide et acceptable pour les composants organiques), principalement en phase gazeuse. Comme résultats de l'approche expérimentale et théorique, les paramètres thermodynamiques de l'association (ΔH_a, ΔG_a, ΔS_a) sont obtenus.

Dans l'étude ITC, quelques sulfoxydes (**5.2a-d**, schéma 5.1), des amines (**5.2e-g**, schéma 5.1) et du dioxane (**5.2i,** schéma 5.1) ont été étudiés, tandis que la portée des calculs de DFT-D statique a été étendue à d'autres amines (**5.2j-k**, schéma 5.2), une cétone (**5.2l**, schéma 5.2), un aldéhyde (**5.2m**, schéma 5.2) ainsi que le chlorobenzène et le HFIP (**5.2n**, schémas 5.2 et 5.1, schéma 5.1, respectivement).

Les résultats de l'ITC suggèrent des interactions non-covalentes assez fortes à fortes (fourchette de ITC ΔH_a -5 - -13 kcal/mol) dans les systèmes étudiés. En outre, sur la base des valeurs de ΔG_a (compris entre -1,4 et -3,2 kcal/mol), tous les donneurs de Lewis considérés pourraient bien interagir spontanément avec HFIP. Au total, cela pourrait avoir une influence sur une polarisation supplémentaire des liaisons au sein de la molécule donneuse de Lewis, ce qui pourrait être d'une importance cruciale dans les étapes clés de diverses transformations chimiques. Par conséquent, l'HFIP pourrait avoir un rôle de catalyseur.

Bien que les résultats des calculs de ΔH_a en phase gazeuse soient cohérents avec les résultats expérimentaux (ITC ΔH_a) dans la barre d'erreur, il est démontré que les résultats peuvent être encore meilleurs en appliquant le modèle de solvatation COSMO dans les calculs. Comparés aux résultats de l'ITC, les calculs statiques de DFT-D au niveau de la théorie utilisé surestiment la valeur de ΔS_a.

Il est montré que le chlorobenzène, solvant de choix pour les expériences ITC, pourrait interagir considérablement avec HFIP ainsi que HFIP est capable d'interagir assez fortement avec lui-même, ce que l'on devrait être au courant. De plus, les calculs ont montré que l'azote est un accepteur de liaison H plus fort que l'oxygène, alors que le plus tardif est plus fort que le soufre, alors que le HFIP préfèrerait plutôt interagir avec des atomes d'hydrogène aliphatiques que aromatiques.

Perspective. L'étude devrait être complétée par des paramètres thermodynamiques en solution (COSMO, ou mieux) pour les systèmes non traités. Une estimation de la BSSE ainsi qu'un calcul des énergies d'interaction de tous les systèmes étudiés ici seraient appréciables. RMN 2D - L'étude de la spectroscopie par diffusion (DOSY) est hautement souhaitable.

Chapter 9

Conclusion

Version in English.

To address the main questions posed as the aims of the Thesis – how the theory could be rationally improved, and consequently, how the theory and experiments could meet each other as well as how to rationalize a role and importance of non-covalent interactions – heat and related thermodynamics were chosen as a central part. Therefore, the core of the Thesis's research was the acquiring a huge thermochemical data base of various reaction systems which could be, in the broadest sense, considered as Lewis donor-acceptor pairs.

The reaction systems were selected in a way that: a) either they represent an important topic in the chemical world or in their course of chemical transformation a step-wise reaction mechanism is assumed/documented (which can be challenging for both experimental and theoretical chemists); b) an influence of non-covalent interactions within the system might be significant.

In the present Thesis, the isothermal titration calorimetry (ITC) experiments were employed, as the main experimental tool. For the purpose of ITC experiments a Nano ITC (*TA Instrument* ®), device was used. As a theoretical tool, the static DFT-D calculations were performed. As a complementary and helping method, a search of Cambridge Structural Database (CSD) was performed. Besides the ITC and theoretical studies, most of the reactions (reactants and reaction products) were fully characterized by standard experimental characterization methods (NMR spectroscopy, Mass spectroscopy, Elemental analysis, X-Ray diffraction, IR spectroscopy). Moreover, the reactions of (F)LPs were monitored by 2D NMR - DOSY experiments.

The ITC journey covered both, kinetic (partial order, initial rate constants of reaction, where possible, according to the used reaction conditions) and thermodynamic study (ΔH, ΔG, ΔS) of the reaction systems, while by the DFT-D calculations only the thermochemical parameters (ΔH, ΔG, ΔS) of the reaction systems in gas or/and chlorobenzene phase were obtained. The CSD search was performed only in case of the (F)LPs.

The research of the **(F)LPs** revealed the following: **1.1**/**1.2a-c** form cohesive pairs, the system **1.1**/**1.2d** exist within an equilibrium, the system **1.1**/**1.2f** does not show any tendency to forming any stable pair, while the system **1.1**/**1.2e** only with less than 0.2 equivalents of the phosphine form single reaction product. An assumption of forming clusters (most probably consisted of one

molecule of the phosphine and, at least, two molecules of the borane), rose up from the ITC thermograms, is confirmed by both 2D DOSY NMR experiments and DFT-D calculations. The ITC Δ*H* results showed that, among all herein studied adduct formations, the highest heat release (ca. -22 kcal/mol) is obtained during the formation of $mes_3PB(PhF_5)_3$ (**1.1/1.2d**, well-known FLP adduct), suggesting that non-covalent interactions have a huge influence within these systems. The theoretically estimated interaction/reaction Δ*H* values (that account for the influence of chlorobenzene explicitly) are in good agreement with the experimental ITC data. Many useful geometrical parameters of classical and frustrated phosphine-borane pairs were obtained by the CSD search. These parameters helped in rationalizing the differences between them considering their mutual orientation and distances.

The ITC thermodynamic results (range of ITC raw ΔH_r -9 – -12.5 kcal/mol) have suggested that reasonably stronger interactions could be established through the investigated ***cis-migration*-insertion reaction sequence**, indicating a difference between chosen phosphines: their ability to establish non-covalent interactions and nucleophilic affinity. The ITC kinetic results have confirmed partial first reaction order with respect to the complex **2.1**. Although the static DFT-D COSMO calculations have predicted much larger (ca. 2.5 times) reaction enthalpies (computed ΔH_r values are ranged from ca. -22 kcal/mol to -31 kcal/mol), the computed ΔH_r values are mutually in accordance (regarding their structural and electronic characteristics). Such overestimation might be a consequence of not taking into account explicit interactions of chlorobenzene with the reactants, especially with the complex. The computed Gibbs free energies (ΔG_r values from ca. -8 kcal/mol to -17 kcal/mol) suggest the possibility of quite spontaneous interactions.

The results suggest on an equilibrium nature of the **amination process** as well as no side reaction products. The thermodynamic ITC results (ΔH_r values larger than -15 kcal/mol) suggested energetically favorable transformations within the amination process in the systems **3.2a-c/3.3a** and **3.2a-c/3.3b**, while the systems **3.2a-c/3.3b** were found to be non-exploitable. Clear dependence between the type of metal atom and the reaction enthalpy could not be drawn. The kinetic ITC results rather confirmed partial second reaction order with respect to the amine. The calculated reaction enthalpies (ranged from ca. -5.5 kcal/mol up to -20 kcal/mol), are in excellent accordance with the experimental ones, while the calculated Gibbs free energies have suggested on spontaneous process within all the systems. In addition, the calculation revealed that the amination of the herein investigated Fischer carbenes by aniline (**3.3b**) is not thermodynamically possible in normal conditions, confirming the ITC observations.

Obtained ITC Δ*H* value of the double insertion (ca. -38 kcal/mol) is reasonably larger than ITC Δ*H* value of the single insertion (ca. -24 – -28 kcal/mol) of the alkynes within the **palladacycle complexes**. Kinetic ITC study confirmed the pseudo first order of reaction in case of **4.4b**. The DFT-D predicted Δ*H* and Δ*G* values are around 10-15 kcal/mol larger than the experimental ITC data, suggesting that chlorobenzene has a significant competitive influence, interacting non-covalently, within the insertion sequence. Considering the complexity of nature of the reactants and the chemical transformations within the insertion reaction, it could be concluded that there is a good accordance between experimental and theoretical results.

The ITC results of the affinity of various Lewis bases to **HFIP** suggested quite strong to strong non-covalent interactions (range of ITC ΔH_a -5 – -13 kcal/mol) within the studied systems. In addition, concluded on ΔG_a (ranged -1.4 – -3.2 kcal/mol), all considered Lewis donors might interact spontaneously with HFIP. Altogether, that might have a huge influence on an additional polarization of bonds within the Lewis donor molecule that could be of crucial importance in key steps of various chemical transformations, suggesting that HFIP might have a catalytic role. Although the calculated ΔH_a values in gas phase are consistent with the experimental ΔH_a ITC results within the error bar, it was shown that even better accordance of the results could be achieved applying continuum model solvation treatment (COSMO) within the computations. Additionally, it was shown that chlorobenzene could considerably interacts with HFIP as well as that quite strong interactions between HFIP molecules are possible. The calculations showed that nitrogen is stronger H bonding acceptor than oxygen, while the latter one is stronger than sulfur. In addition, HFIP would rather prefer to interact with aliphatic than aromatic hydrogen atoms.

Although nor the interaction energies have been calculated neither the energy decomposition analysis has been performed on any investigated system, it could be concluded from the obtained interaction enthalpies, especially of the systems including formation of Lewis pairs of $(PhF_5)_3B$ and HFIP with various Lewis donors/acceptors (where, in general, there is no possibility for covalent bonding), that the importance of non-covalent interactions is great to crucial.

Overall, it could be concluded that:

- The ITC experiments, extended to organic and organometallic chemistry, were proved as a powerful technique for obtaining reliable thermodynamic as well as kinetic reaction data.

- The DFT-D calculations showed up capabilities in an accurate modelling of the reaction systems as well as in good to excellent prediction of the thermochemical parameters of reactions.

- Subsequently, a huge experimental database of thermochemistry of a number of reactions is produced, which can be used as the reference in further improvements of DFT calculations.

- The research shed some light on existing FLPs and HFIP chemistry by introducing molecular clusters and by proving a formation of relatively strong donor-acceptor complexes, respectively. These findings can be the potentially important base of their chemical reactivity.

- It is shown that various chemical transformation within organometallic complexes, (such as migration-insertion, many step-wise insertions, auto catalyzed addition-elimination reaction sequences), can be properly studied and described experimentally – by kinetic and thermodynamic ITC experiments and theoretically – by static DFT-D calculations.

- Additionally, it was shown that the influence of the solvent, interacting non-covalently with solutes, is not negligible in many cases, suggesting that accounting for the explicit solvent interactions leads to better accordance between the theoretically and experimentally obtained results.

- Non-covalent interactions play important or even crucial role within the investigated systems.

- For the sake of authority on produced data of our collaborators – colleagues from prof. Grimme group, the additional calculated data of all herein studied systems are not reported. Due to that fact, a comprehensive estimation of the role and importance of non-covalent interactions, especially of London's dispersion forces, was not possible.

General outlook.

Calculating the energy of interactions of all the studied systems as well as performing the energy decomposition analysis is highly desirable. The analysis of the interactions by the Ziegler-Rauch decomposition technique in repulsive and attractive energy terms would make it possible to enter further into the nature of the interactions and the point that represents for example the dispersion Calculating electrostatic potentials of all the reactants/products would be rather important, because it can help significantly in rationalizing the potential reactive sites by visualizing the distribution of the electron density.

Version in Serbian.

Да би се одговорило на главна питања која су постављена као циљеви тезе – како би се теорија могла унапредити, како се теорија и експеримент могу међусобно допуњавати, као и како рационализовати улогу и значај нековалентних интеракција – проучавање топлоте реакција и одговарајућих термодинамичких реакционих параметара изабрано је за експерименталну и теоријску основу истраживања. Стога је језгро истраживања у оквиру ове докторске дисертације било формирање огромне термохемијске базе података различитих реакционих система, који би се у најширем смислу могли сматрати Lewis-овим донорско-акцепторским паровима.

Реакциони системи су избарани уколико испуњавају следеће услове: а) представљају важну тему у области хемије или ако је у току хемијске промене у систему претпостављен/доказан вишестепени реакциони механизам (што може представљати изазов и за експерименталне и за теоријске хемичаре); б) у систему је значајан утицај нековалентних интеракција.

У овој докторској дисертацији као главна експериментална техника коришћена је изотермална титрациона калориметрија. За потребе ITC експеримената коришћен је Nano ITC (*TA Instrument* ®) уређај. Теоријска проучавања заснована су углавном на статичким DFT-D прорачунима. Као комплементарни и помоћни метод извршена је и претрага Кембричке базе структурних података. Поред ITC и теоријских студија, већина реакција (реактанти и реакциони производи) у потпуности су окарактерисане стандардним методама експерименталне карактеризације (НМР спектроскопија, масена спектроскопија, елементална анализа, дифракција рендгенских зрака, ИЦ спектроскопија). Реакције (F)LP-а праћене су и 2D NMR - DOSY експериментима.

ITC истраживање обухватило је кинетичке (одређивање парцијалног реда реакције у односу на одговарјуће реактанте, константе почетне брзине реакције, где је то било могуће зависно од реакционих услова) и термодинамичке студије (одређивање Δ*H*, Δ*G*, Δ*S*) реакционих система, док су помоћу DFT-D прорачуна добијени само термохемијски параметри (Δ*H*, Δ*G*, Δ*S*) реакционих система у гасној и/или хлоробензенској фази. Претраживање CSD-а извршено је само у случају (F)LP-а.

Проучавање **(F)LPs** показало је следеће: **1.1**/**1.2a-c** формирају кохерентне парове, систем **1.1**/**1.2d** постоји у равнотежи, систем **1.1**/**1.2f** не показује тенденцију ка формирању стабилног пара, док систем **1.1**/**1.2e** у присуству до 0,2 еквивалента фосфина формира један реакциони производ. Претпоставка о формирању кластера (највероватније састављених од једног молекула фосфина и, барем, два молекула борана), која је произашла из ITC термограма, потврђена је и 2D DOSY NMR експериментима и DFT-D прорачунима. ITC Δ*H* резултати показали су да је, при формирању адуката, највећа количина топлоте (око -22 kcal/mol) ослобођена током формирања $mes_3PB(PhF_5)_3$ (**1.1/1.2d**, добро познатог FLP адукта), указујући на чињеницу да нековалентне интеракције имају огроман утицај у овим системима. Предвиђене DFT-D Δ*H* вредности, које узимају у обзир и утицај хлоробензена, у доброј су сагласности са експерименталним ITC вредностима. Много корисних геометријских параметара за класичне и фрустриране парове фосфина и борана добијено је претрагом CSD-а. Имајући у виду њихову међусобну оријентацију и растојање, ови параметри су помогли у дефинисању разлика између њих.

ITC термодинамички резултати (опсег ITC сирових (raw) ΔH_r вредсности од -9 до -12,5 kcal/mol) показали су да би се разумно јаче интеракције могле успоставити преко испитиване *cis* **миграционе-инсерционе реакционе секвенце**, истовремено указујући и на разлику између изабраних фосфина: на њихову различиту способност успостављања нековалентних интеракција и њихов различити нуклеофилни афинитет. ITC кинетички резултати потврдили су да се ради о реакцији првог реда у односу на комплекс **2.1**. Иако су статички DFT-D COSMO прорачуни предвидели много веће (око 2,5 пута) реакционе енталпије - ΔH_r вредности од око -22 kcal/mol до -31 kcal/mol, израчунате ΔH_r вредности међусобно су усклађене (с обзиром на структурне и електронске карактеристике испитиваних система). Оваква прецењивања могу бити последица неузимања у обзир експлицитних интеракција хлоробензена са реактантима, а посебно са комплексом (**2.1**). Израчунате вредности Gibbs-ове слободне енергије (ΔG_r од око -8 kcal/mol до -17 kcal/mol) указују на могућност прилично спонтаних интеракција.

Резултати указују на равнотежну природу **процеса аминивања**, као и на непостојање споредних реакционих производа. ITC термодинамички резултати (ΔH_r вредности веће од -15 kcal/mol) указали су на енергетски повољне промене у процесу аминовања у системима **3.2a-c**/**3.3a** и **3.2a-c**/**3.3c**, док су системи **3.2a-c**/**3.3b** окарактерисани као

неупотребљиви. Јасна зависност реакционе ентлапије од типа метала није опажена. ITC кинетички резултати су потврдили да се ради о реакцији другог реда у односу на амине.

Израчунате реакционе енталпије (у распону од око -5,5 kcal/mol до -20 kcal/mol) су у одличној сагласности са експерименталним вредностима, док израчунате Gibbs-ове слободне енергије указују на спонтане процесе у свим системима. Поред тога, на основу прорачуна је закључено да аминовање испитиваних Fischer-ових карбена помоћу фениламина (**3.3b**) није термодинамички могућа на 25 ºC, што је потврдило резултате добијене ITC методом.

Добијена ITC ΔH_r вредност двоструке инсерције (око -38 kcal/mol) је разумно већа од ITC ΔH_r вредности једноструке инсерције (око -24 до -28 kcal/mol) алкина унутар **цикличних паладијумових комплекса**. Кинетичка ITC студија потврдила је да се ради о реакцији првог реда у односу на **4.4b**. Вредности ΔH_r и ΔG_r предвиђене DFT-D методом су за око 10-15 kcal/mol веће од експерименталних ITC вредности, што указује на то да хлоробензен, интерагујући нековалентно, може имати значајан компетитивни утицај унутар инсерционе секвенце. С обзиром на сложену природу реактаната и хемијске трансформације у инсерционој реакцији, може се закључити да постоји добра сагласност између експерименталних и теоријских резултата.

ITC резултати афинитета различитих Lewis-ових база према **HFIP** указали су на прилично јаке до јаке нековалентне интеракције (опсег ITC ΔH_a вредности од -5 до -13 kcal/mol) у испитиваним системима. Осим тога, на основу ΔG_a вредности (у опсегу од -1,4 до -3,2 kcal/mol), закључено је да сви разматрани Lewis-ови донори могу спонтано интераговати са HFIP. Све то може имати велики утицај на додатну поларизацију веза унутар Lewis-овог донорског молекула што би могло бити од пресудне важности у кључним корацима различитих хемијских промена, а истовремено указује да HFIP може имати каталитичку улогу. Иако су резултати прорачуна ΔH_a вредности у гасној фази у складу са експерименталним резултатима ITC ΔH_a унутар границе грешке, показано је се да се може постићи још боља сагласност резултата применом континуалног модела третмана растварача (continuum model solvation treatment (COSMO)). Поред тога, показано је да хлоробензен може да интерагује у значајној мери са HFIP-ом, као и да су могуће снажне интеракције између самих молекула HFIP. Прорачуни су показали да при формирању водоничне везе атом азота има израженије акцепторске способности у односу на атом

кисеоника, док је атом кисеоника бољи акцептор од атома сумпора. Такође је показано да HFIP радије гради интеракције са алифатичним него са ароматичним атомима водоника.

Иако енергије интеракција нису израчунате нити је урађена декомпозиција енергије на било ком испитиваном систему, на основу измерених/израчунатих енталпија интеракција, нарочито у системима који укључују формирање Lewis-ових парова $(PhF_5)_3B$ и HFIP са различитим Lewis-овим донорима/акцепторима (где у принципу, нема могућности за ковалентно везивање), може се закључити да је важност нековалентних интеракција веома велика до круцијална.

На основу свега изнетог, може се закључити да:

- ITC експерименти, проширени на органску и органометалну хемију, су се показали као моћна техника за добијање поузданих кинетичких и термодинамичких реакционих података.

- DFT-D прорачунима је могуће прецизно моделовање реакционих система, као и добро до одлично предвиђање термохемијских реакционих параметара.

- Формирана је огромна експериментална база термохемијских података бројних реакција, која се може користити за даље побољшање DFT прорачуна.

- Истраживање је донекле „расветлило“ постојећу хемију FLP и HFIP увођењем молекулских кластера односно доказивањем формирања релативно јаких донорско-акцепторских комплекса. Ови резултати могу бити потенцијално важна основа за проучавање њихове хемијске реактивности.

- Показано је да различите хемијске промене у органометалним комплексима (као што су миграционо-инсерционе, једноструке и двоструке вишестепене инсерционе, аутокатализоване адициono-елиминационе реакционе секвенце) могу бити правилно истражене и описане експериментално - кинетичким и термодинамичним ITC експериментима и теоријски - статичким DFT-D прорачунима.

- Поред тога, показано је да утицај растварача, који интерагују нековалентно са раствореним супстанцама, у многим случајевима није занемарљив, као и да урачунавање експлицитних интеракција између растварача и растворених супстанци (реактаната)

доводи до боље усаглашености између теоријски и експериментално добијених резултата.

- Улога нековалентних интеракција у испитиваним системима може се описати као важна или чак кључна.

- Због ауторских права о подацима наших сарадника - колега из групе проф. Grimme-a, додатни резултати теоријских прорачуна овде проучаваних система нису приказани. Због те чињенице, свеобухватна процена улоге и важности нековалентних интеракција, посебно London-ових дисперзионих сила, није била могућа.

Општа перспектива.

Требало би израчунати енергије интеракција свих проучаваних система, као и урадити декомпозицију енергије интеракција. Анализа интеракција помоћу Ziegler-Rauch-ове декомпозиционе технике, која омогућава разлагање укупне енргије интеракције на одбојене и привлачне енергетске доприносе, омогућила би боље разумевање природе интеракција, као и, на пример, дисперзије. Такође би било веома важно израчунати електростатичке потенцијале свих реактаната и производа, јер би визуализација расподеле електронске густине могла знатно да помогне у рационализацији потенцијално реактивних места.

Version in French.

Pour aborder les questions principales posées comme objectifs de la thèse – comment la théorie pourrait être améliorée rationnellement et, par conséquent, comment la théorie et les expériences pourraient se rencontrer et comment rationaliser le rôle et l'importance des interactions non-covalentes – la chaleur et la thermodynamique connexe ont été choisies comme partie centrale. Par conséquent, le cœur de la recherche réalisée dans le cadre de cette thèse consistait à accumuler une base de données thermochimiques de divers systèmes réactionnels qui pourraient être, au sens le plus large, considérés comme des paires donneur-accepteur de Lewis.

Dans la présente thèse, la calorimétrie par titration isotherme (ITC) a été utilisée en tant qu'outil expérimental principal. Aux fins des expériences ITC, un appareil Nano ITC (TA Instrument ®) a été utilisé. Comme outil théorique des calculs DFT-D statiques ont été effectués. Comme méthode complémentaire et d'aide, une recherche de Cambridge Structural Database (CSD) a été effectuée. Outre les études ITC et théoriques, la plupart des réactions (réactifs et produits de réaction) ont été entièrement caractérisées par des méthodes de caractérisation expérimentales standard (spectroscopie RMN, spectroscopie de masse, analyze élémentaire, diffraction des rayons X, spectroscopie IR). De plus, les réactions de (F)LP ont été suivies par des expériences 2D RMN-DOSY.

Le parcours ITC a couvert à la fois l'étude cinétique (ordre partiel, constantes de vitesse initiales de la réaction, si possible selon les conditions de réaction utilisées) et l'étude thermodynamique (ΔH, ΔG, ΔS) des systèmes réactionnels, tandis que par les calculs DFT-D seulement les paramètres thermochimiques (ΔH, ΔG, ΔS) des systèmes réactionnels en phase gazeuse et / ou chlorobenzène ont été obtenus. La recherche CSD a été effectuée uniquement dans le cas des (F)LP.

La recherche des LP(F) a révélé ce qui suit: **1.1/1.2a-c** forment des paires cohésives, le système **1.1/1.2d** existe dans un équilibre, le système **1.1/1.2f** ne montre aucune tendance à former une paire stable, alors que le système **1.1/1.2e** au-delà de 0.2 équivalent de la phosphine forme un produit réactionnel unique. Une hypothèse de formation de grappes (probablement constituée par une molécule de phosphine et au moins deux molécules de borane) supramoléculaire, suggérée par les thermogrammes ITC, est confirmée par des expériences de RMN 2D DOSY et des calculs DFT-D. Les valeurs d'enthalpie obtenues par les

expériences d'ITC Δ*H* ont montré que, parmi toutes les formations d'adduits étudiées ici, l'enthalpie libérée la plus élevée (environ 22 kcal/mol) est obtenue lors de la formation de $mes_3PB(PhF_5)_3$ (adduit FLP bien connu **1.1**/**1.2d**), suggérant que les interactions non-covalentes ont une influence énorme dans ces systèmes. Les valeurs Δ*H* prédites par DFT-D qui tiennent compte de l'influence du chlorobenzène sont en bon accord avec les données expérimentales de l'ITC. De nombreux paramètres géométriques utiles de paires phosphine-borane classiques et frustrées ont été obtenus par la recherche CSD. Ces paramètres ont permis de rationaliser les différences entre eux, compte tenu de leur orientation mutuelle et des distances.

Les résultats thermodynamiques ITC (gamme de ITC raw ΔH_r -9 à -12,5 kcal/mol) ont suggéré que les interactions raisonnablement solides pourraient être établies par la **séquence réactionnelle de cis-migration-insertion** étudiée, ce qui indique une différence entre les phosphines choisies: leur aptitude à établir les interactions non-covalentes et l'affinité nucléophile. Les résultats des études cinétiques menées par ITC ont confirmé un premier ordre partiel pour les réactions impliquant le complexe **2.1**. Bien que les calculs statiques DFT-D COSMO aient prévu des enthalpies de réaction beaucoup plus grandes (environ 2,5 fois - les ΔH_r valeurs d'environ -22 kcal/mol à -31 kcal/mol), les valeurs calculées de ΔH_r sont conformes (en ce qui concerne leurs caractéristiques structurelles et électroniques). Une telle surestimation pourrait être une conséquence de la non prise en compte les interactions explicites du chlorobenzène avec les réactifs, en particulier avec le complexe. Les énergies libres de Gibbs calculées (valeurs de ΔG_r d'environ de -8 kcal/mol à -17 kcal/mol) suggèrent la possibilité d'interactions assez spontanées.

Les résultats suggèrent que **processus d'amination** est un équilibre. Les résultats (valeurs thermodynamiques ITC ΔH_r supérieure à -15 kcal/mol) des études thermochimiques suggèrentdes transformations énergétiquement favorables dans les systèmes **3.2a-c**/**3.3a** et **3.2a-c**/**3.3b**, tandis que les systèmes **3.2a-c**/**3.3b** se sont avérés non exploitables. Une dépendance claire du métal sur l'enthalpie de réaction n'a pas pu être établie. Les résultats cinétiques de l'ITC ont plutôt confirmé un deuxième ordre partiel en amine. Les enthalpies de réaction calculées à distance (à partir d'environ de -5,5 kcal/mol jusqu'à -20 kcal/mol), sont en excellent accord avec ceux expérimentaux, tandis que les énergies libres de Gibbs calculées ont suggéré un processus spontané à l'intérieur de tous les systèmes. De plus, le calcul a

révélé que l'amination des carbènes de Fischer par le phénylamine (**3.3b**) est thermodynamiquement impossible dans des conditions normales, confirmant les ITC.

La valeur d'enthalpie obtenues par ITC pour la double insertion (environ -38 kcal/mol) est relativement plus grande que la valeur pour une insertion unique ITC Δ*H* (environ -24 à -28 kcal/mol) d'alcynes dans les **complexes palladacycliques**. L'étude cinétique ITC a confirmé le pseudo-premier ordre de réaction dans le cas de **4.4b**. Les valeurs de Δ*H* et Δ*G* prédites par DFT-D sont supérieures d'environ 10 à 15 kcal/mol aux données expérimentales de l'ITC, ce qui suggère que le chlorobenzène a une influence concurrentielle significative, interagissant de manière non covalente dans la séquence d'insertion. Compte tenu de la complexité de la nature des réactifs et des transformations chimiques au cours de la réaction d'insertion, on peut conclure qu'il existe un bon accord entre les résultats expérimentaux et les résultats théoriques.

Les résultats ITC de l'affinité de diverses bases de Lewis pour **HFIP** ont suggéré des interactions non-covalentes assez fortes à fortes (fourchette de ITC ΔH_a -5 - -13 kcal/mol) dans les systèmes étudiés. En outre, sur la base de la valeur de ΔG_a (allant de -1,4 à -3,2 kcal/mol), tous les donneurs de Lewis considérés pourraient interagir spontanément avec le HFIP. Bien que les valeurs de ΔH_a calculées en phase gazeuse soient cohérentes avec les résultats expérimentaux de ΔH_a ITC dans la barre d'erreur, il a été montré qu'une meilleure concordance des résultats pouvait être obtenue en appliquant un traitement de solvatation continu (COSMO). En outre, il a été montré que le chlorobenzène pouvait interagir considérablement avec HFIP et que le HFIP pouvait interagir assez fortement avec lui-même. Les calculs ont montré que l'azote est un accepteur de liaison H plus fort que l'oxygène, tandis que le dernier est plus fort que le soufre et que le HFIP préférerait interagir avec les atomes d'hydrogène aliphatiques qu'avec les atomes d'hydrogène.

Dans l'ensemble, on pourrait conclure que:

- Les expériences ITC, étendues à la chimie organique et organométallique, se sont révélées comme une technique puissante pour obtenir des données de réaction thermodynamiques et cinétiques fiables.

- Les calculs DFT-D ont mis en évidence des capacités dans une modélisation précise des systèmes de réaction ainsi qu'une prédiction excellente des paramètres thermochimiques des réactions

Par la suite, une énorme base de données expérimentale sur la thermochimie d'un certain nombre de réactions est produite, qui peut être utilisée comme référence pour d'autres améliorations des calculs DFT.

- La recherche a permis de mieux comprendre la chimie existante des FLP et des HFIP en introduisant des agrégats moléculaires et en démontrant la formation de complexes donneurs-accepteurs relativement forts, respectivement. Ces résultats peuvent constituer la base potentiellement importante de leur réactivité chimique.

- Il est démontré que diverses transformations chimiques au sein de complexes organométalliques (comme la migration-insertion, de nombreuses insertions par étapes, des séquences de réaction d'addition-élimination auto-catalysées) peuvent être correctement étudiées et décrites expérimentalement - par des expériences ITC cinétiques et thermodynamiques – et par des calculs DFT-D statiques.

- En outre, il a été montré que l'influence du solvant, interagissant de manière non covalente avec les solutés, n'est pas négligeable dans de nombreux cas, ce qui suggère que la prise en compte des interactions explicites conduit à une meilleure concordance entre les résultats théoriquement et expérimentalement obtenus.

- Le rôle des interactions non-covalentes dans les systèmes étudiés est important crucial.

- Par souci d'autorité sur les données produites par nos collaborateurs - collègues du groupe de prof. Grimme, les données calculées supplémentaires de tous les systèmes étudiés ici ne sont pas rapportées. De ce fait, une estimation complète du rôle et de l'importance des interactions non covalentes, en particulier des forces de dispersion de Londres, n'était pas possible.

Perspectives générales.

Le calcul des énergie d'interactions pour tous les systèmes étudiés ainsi que l'analyze de ces mêmes interactions par la technique de Ziegler–Rauch de décomposition en termes énergétiques répulsifs et attractifs permettrait d'entrer plus en avant dans la nature des interactions et dans le point que représente par exemple la dispersion. Le calcul des potentiels électrostatiques de tous les réactifs/produits serait plutôt important car cela peut aider significativement à rationaliser les sites réactifs potentiels en visualisant la distribution de la densité électronique.

Chapter 10

Appendix

A.1. Supplementary information to Chapter 4.

A.1.1. Supplementary information to Subchapter 1.

A.1.1.1. 1D NMR spectra.

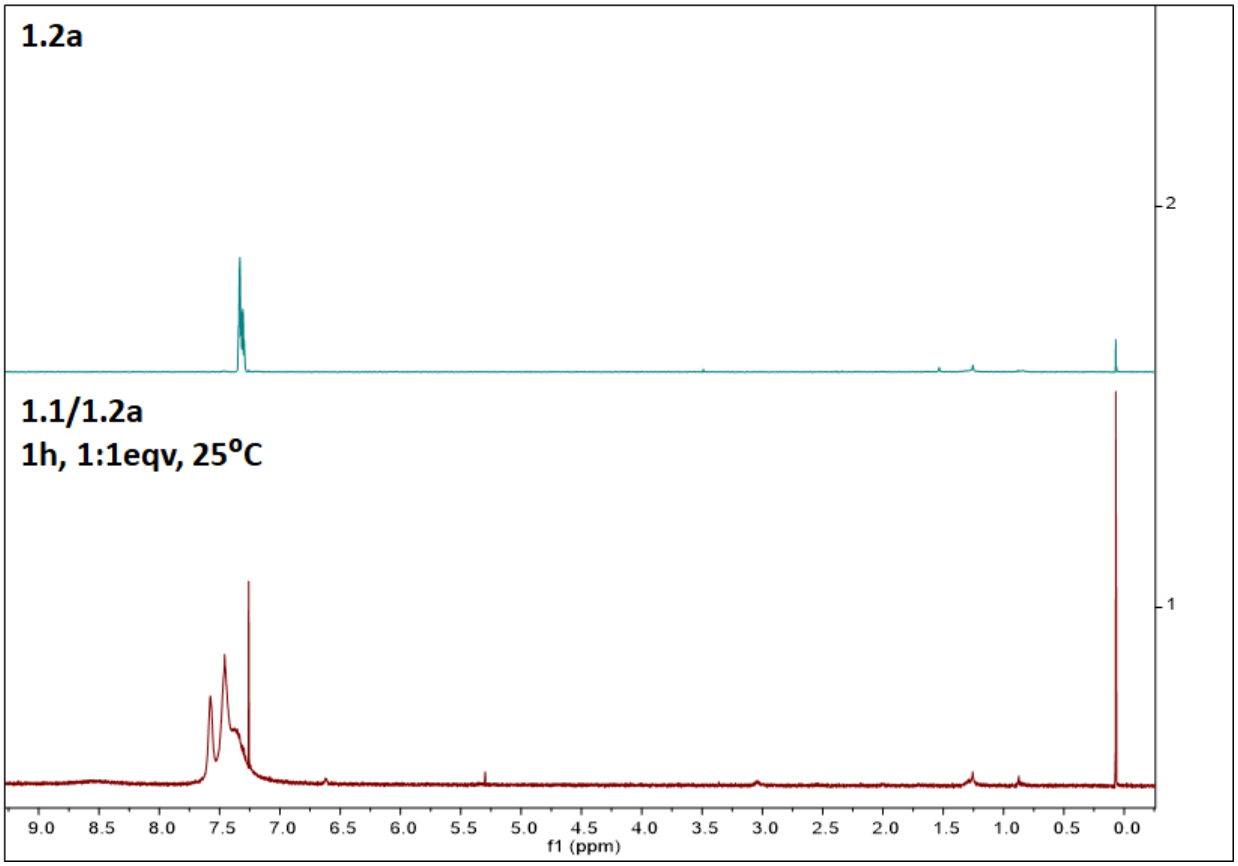

Figure SI 1.1.1 *down* – ^{1}H NMR spectrum of the reaction of **1.1a** with **1.2a** carried out in molar ratio of the reactants 1:1, recorded after 1h of reaction time at 25ºC. ^{1}H NMR (600 MHz, chloroform-*d*, δ, ppm) 7.58, - 7.28 (m, 15H). *up* – ^{1}H NMR spectrum of free **1.2a**. ^{1}H NMR (600 MHz, chloroform-*d*, δ, ppm) 7.34 – 7.29 (m, 15H).

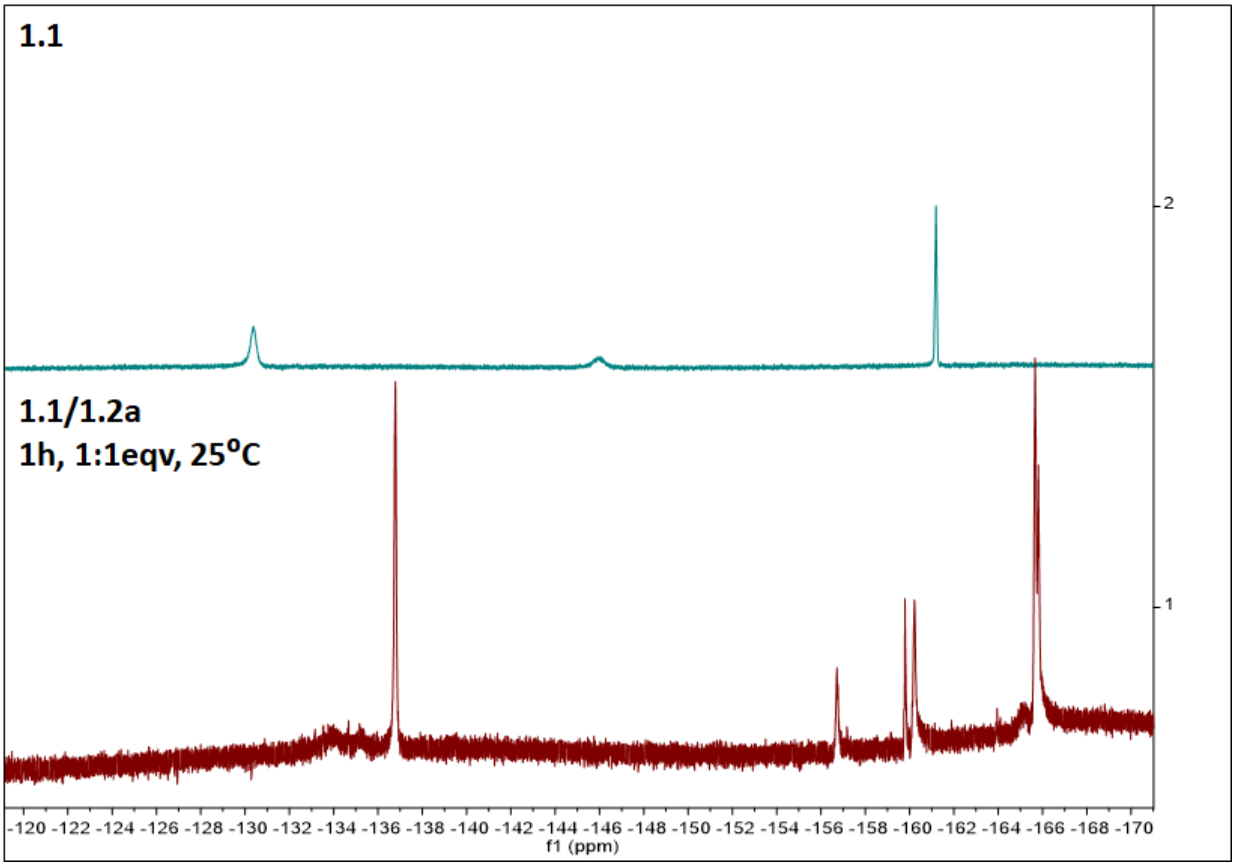

Figure SI 1.1.2 *down* – ^{19}F NMR spectrum of the reaction of **1.1a** with **1.2a** carried out in molar ratio of the reactants 1:1, recorded after 1h of reaction time at 25ºC. ^{19}F NMR (565 MHz, chloroform-*d*, δ, ppm) -136.8, -156.7, -159.8 (t, *J* = 20 Hz), -160.2, -165.7, -165.1 (t, *J* = 37 Hz). *up* – ^{19}F NMR spectrum of free **1.1**. ^{19}F NMR (565 MHz, chloroform-*d*, δ, ppm) -130.4, -146.0, -161.2.

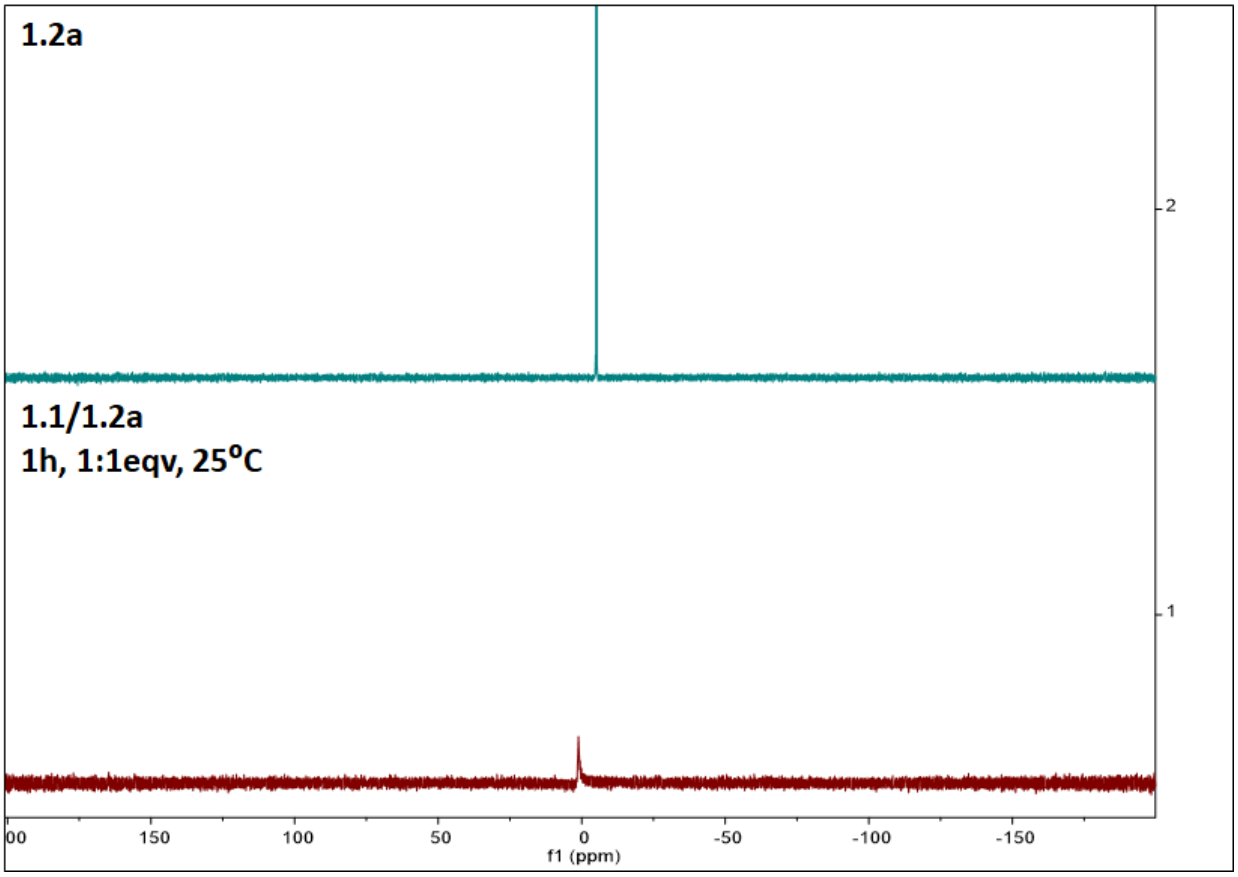

Figure SI 1.1.3 *down* – ^{31}P NMR spectrum of the reaction of **1.1a** with **1.2a** carried out in molar ratio of the reactants 1:1, recorded after 1h of reaction time at 25ºC. ^{31}P NMR (121 MHz, chloroform-*d*, δ, ppm) 1.1. *up* – ^{31}P NMR spectrum of free **1.2a**. ^{31}P NMR (121 MHz, chloroform-*d*, δ, ppm) -5.2.

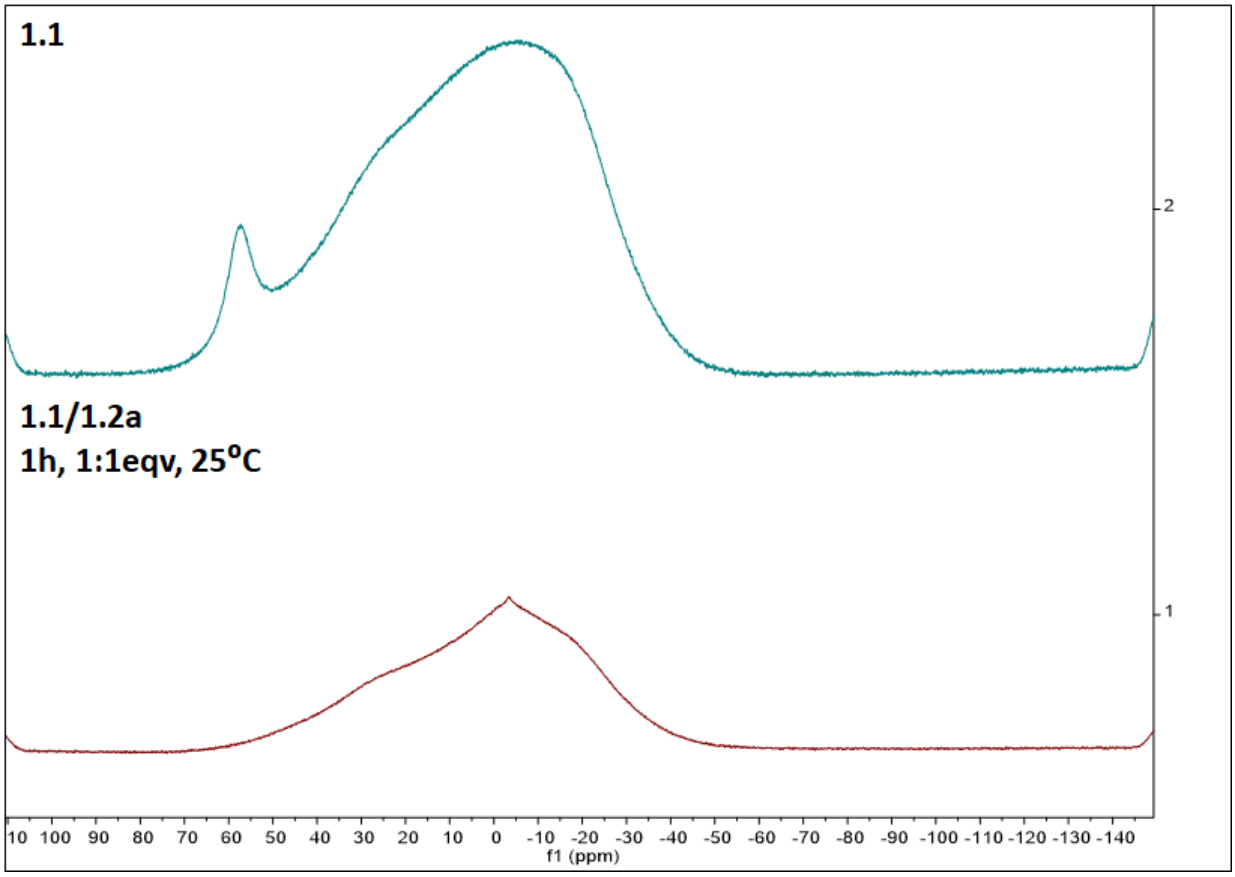

Figure SI 1.1.4 *down* – ^{11}B NMR spectrum of the reaction of **1.1a** with **1.2a** carried out in molar ratio of the reactants 1:1, recorded after 1h of reaction time at 25ºC. ^{11}B NMR (128 MHz, chloroform-*d*, δ, ppm) -3.4. *up* – ^{11}B NMR spectrum of free **1.1**. ^{11}B NMR (128 MHz, chloroform-*d*, δ, ppm) 57.3.

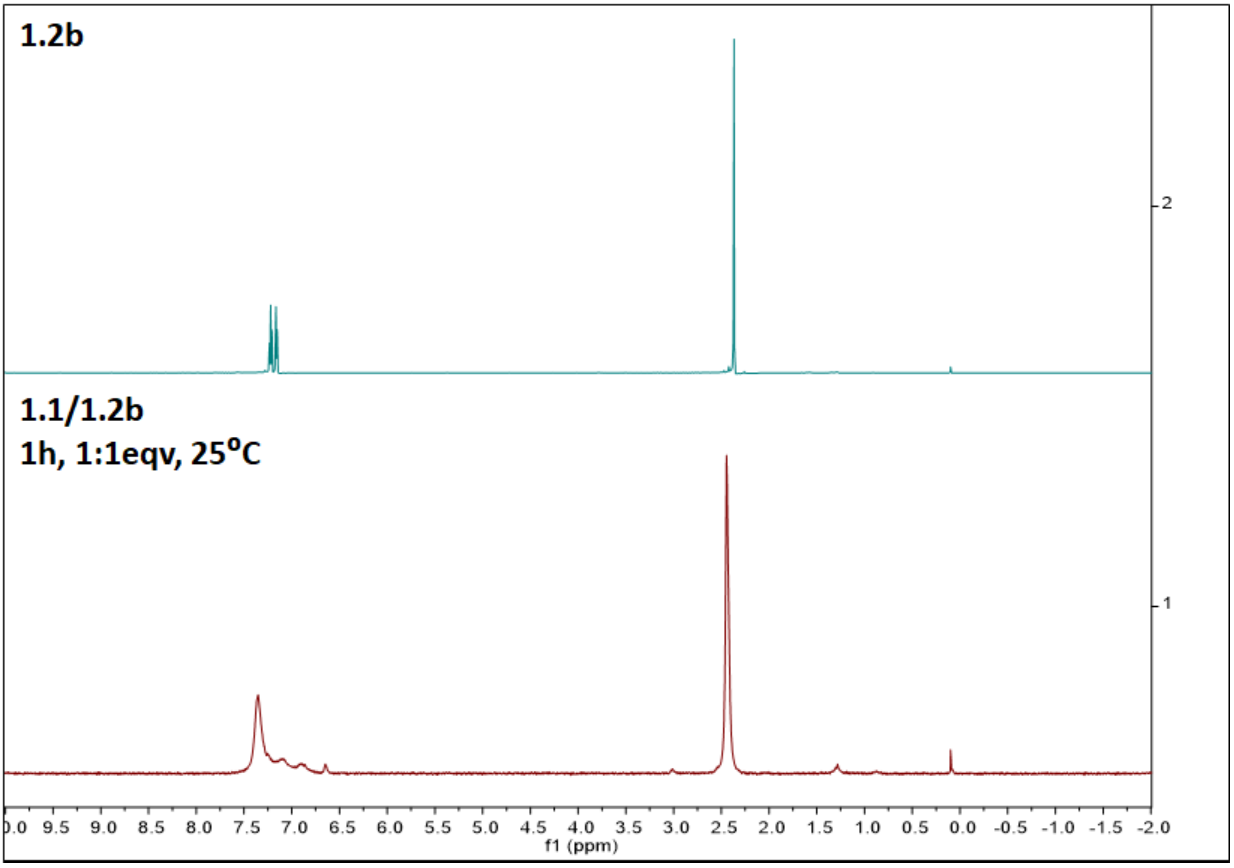

Figure SI 1.1.5 *down* – ^{1}H NMR spectrum of the reaction of **1.1a** with **1.2b** carried out in molar ratio of the reactants 1:1, recorded after 1h of reaction time at 25ºC. ^{1}H NMR (600 MHz, chloroform-*d*, δ, ppm) 7.26 – 6.55 (m, 12H), 2.35 (s, 9H). *up* – ^{1}H NMR spectrum of free **1.2b**. ^{1}H NMR (600 MHz, chloroform-*d*, δ, ppm) 7.20 (t, *J* = 8 Hz, 6H), 7.14 (d, *J* = 8 Hz, 6H), 2.34 (s, 9H).

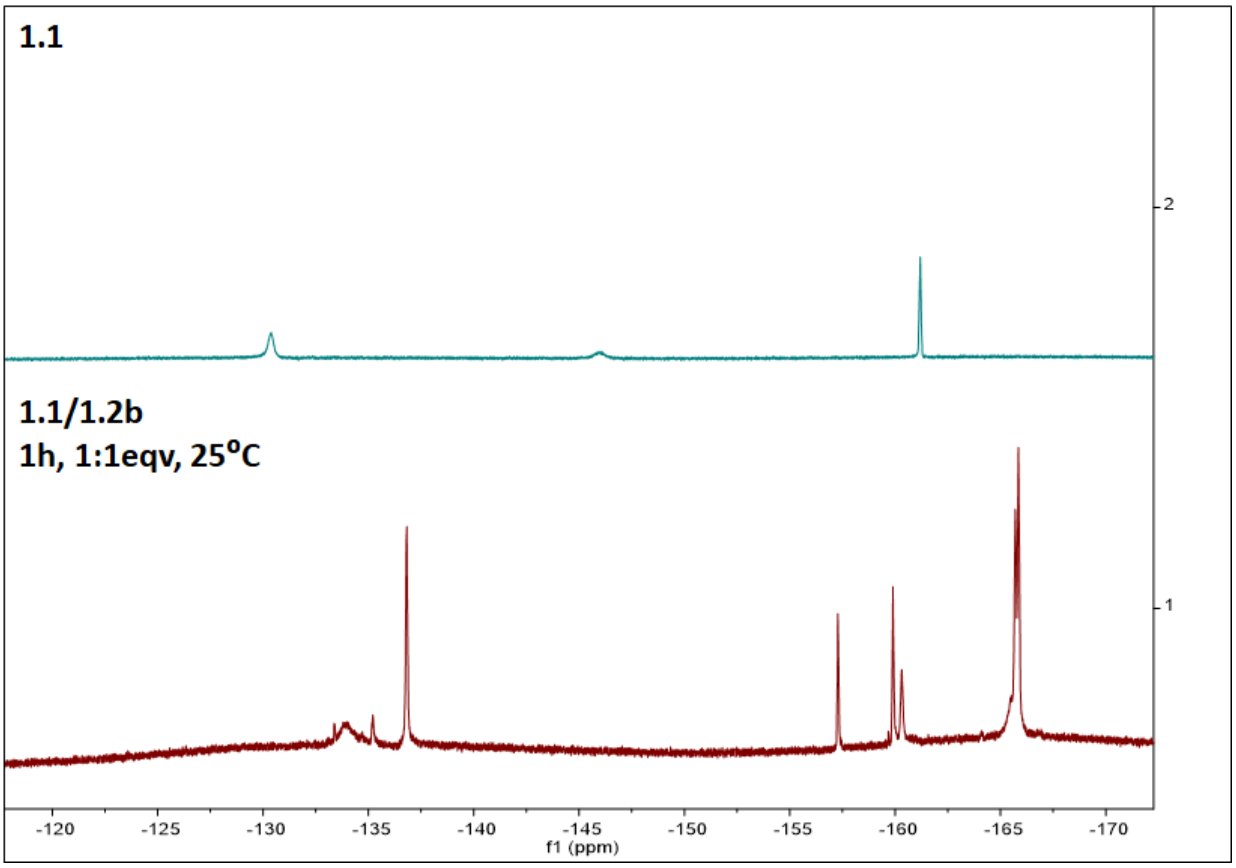

Figure SI 1.1.6 *down* – ^{19}F NMR spectrum of the reaction of **1.1a** with **1.2b** carried out in molar ratio of the reactants 1:1, recorded after 1h of reaction time at 25ºC. ^{19}F NMR (565 MHz, chloroform-*d*, δ, ppm) 133.3, -133.9, -135.2, -136.8, -157.2, -157.3, 159.9, -160.3, -165.7, -165.9. *up* – ^{19}F NMR spectrum of free **1.1**. ^{19}F NMR (565 MHz, chloroform-*d*, δ, ppm) -130.4, -146.0, -161.2.

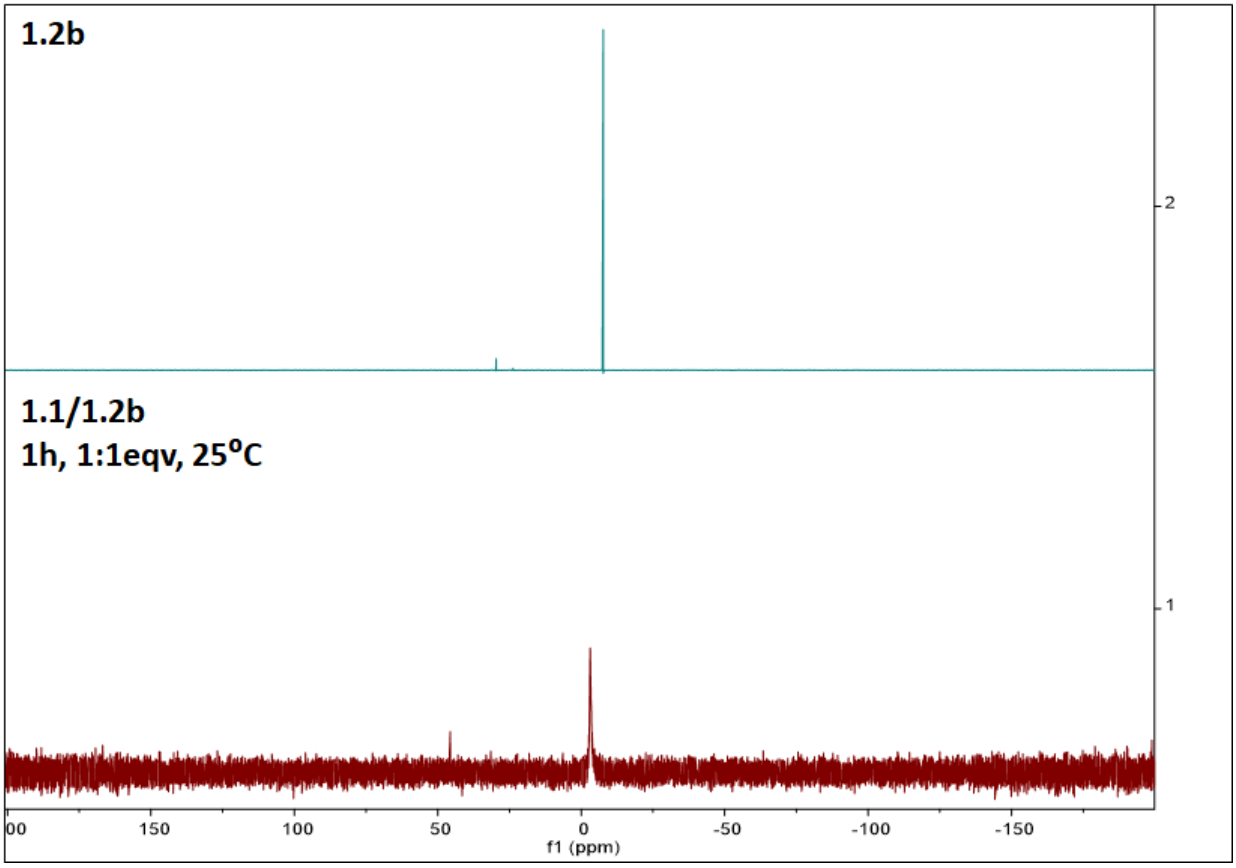

Figure SI 1.1.7 *down* – ^{31}P NMR spectrum of the reaction of **1.1a** with **1.2b** carried out in molar ratio of the reactants 1:1, recorded after 1h of reaction time at 25ºC. ^{31}P NMR (121 MHz, chloroform-*d*, δ, ppm) -3.2. *up* – ^{31}P NMR spectrum of free **1.2b**. ^{31}P NMR (121 MHz chloroform-*d*, δ, ppm) -7.7.

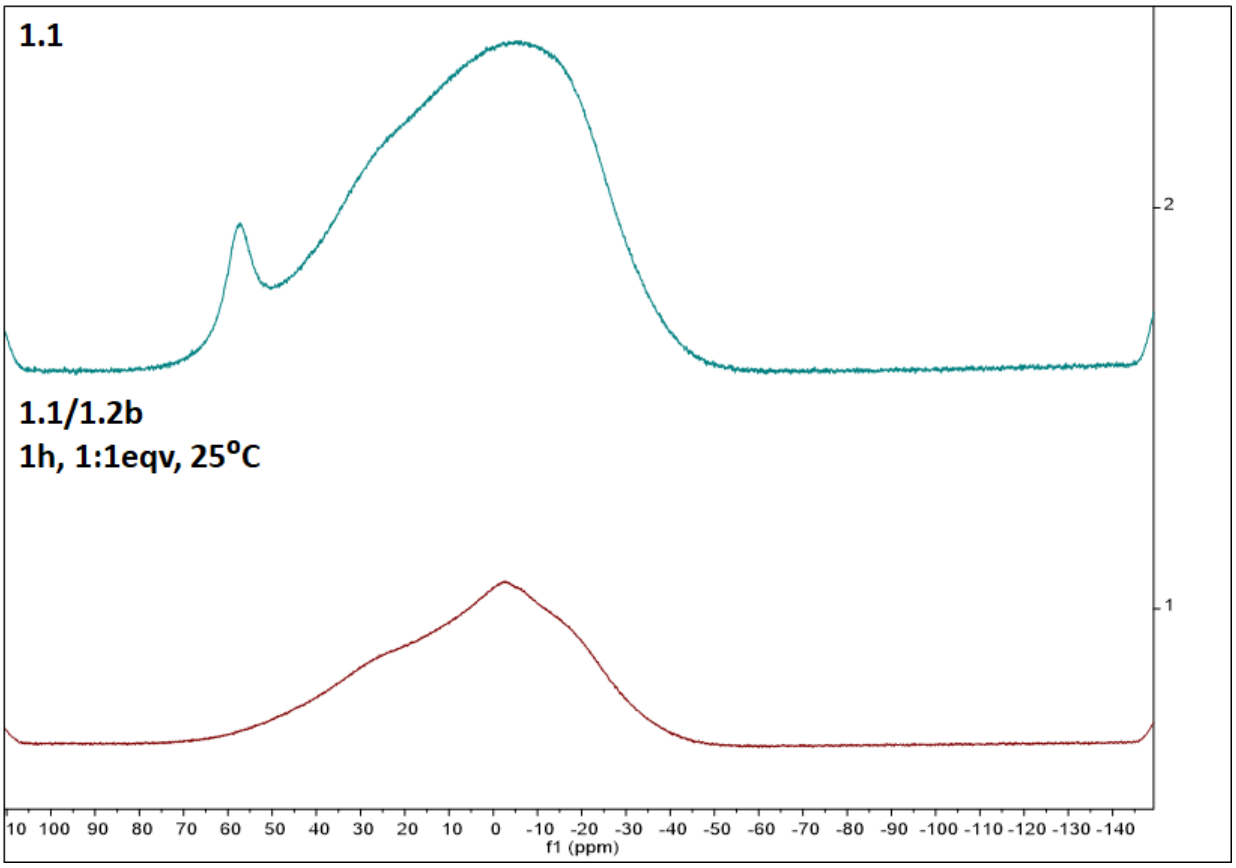

Figure SI 1.1.8 *down* – ^{11}B NMR spectrum of the reaction of **1.1a** with **1.2b** carried out in molar ratio of the reactants 1:1, recorded after 1h of reaction time at 25ºC. ^{11}B NMR (128 MHz, chloroform-*d*, δ, ppm) -3.7. *up* – ^{11}B NMR spectrum of free **1.1**. ^{11}B NMR (128 MHz, chloroform-*d*, δ, ppm) 57.3.

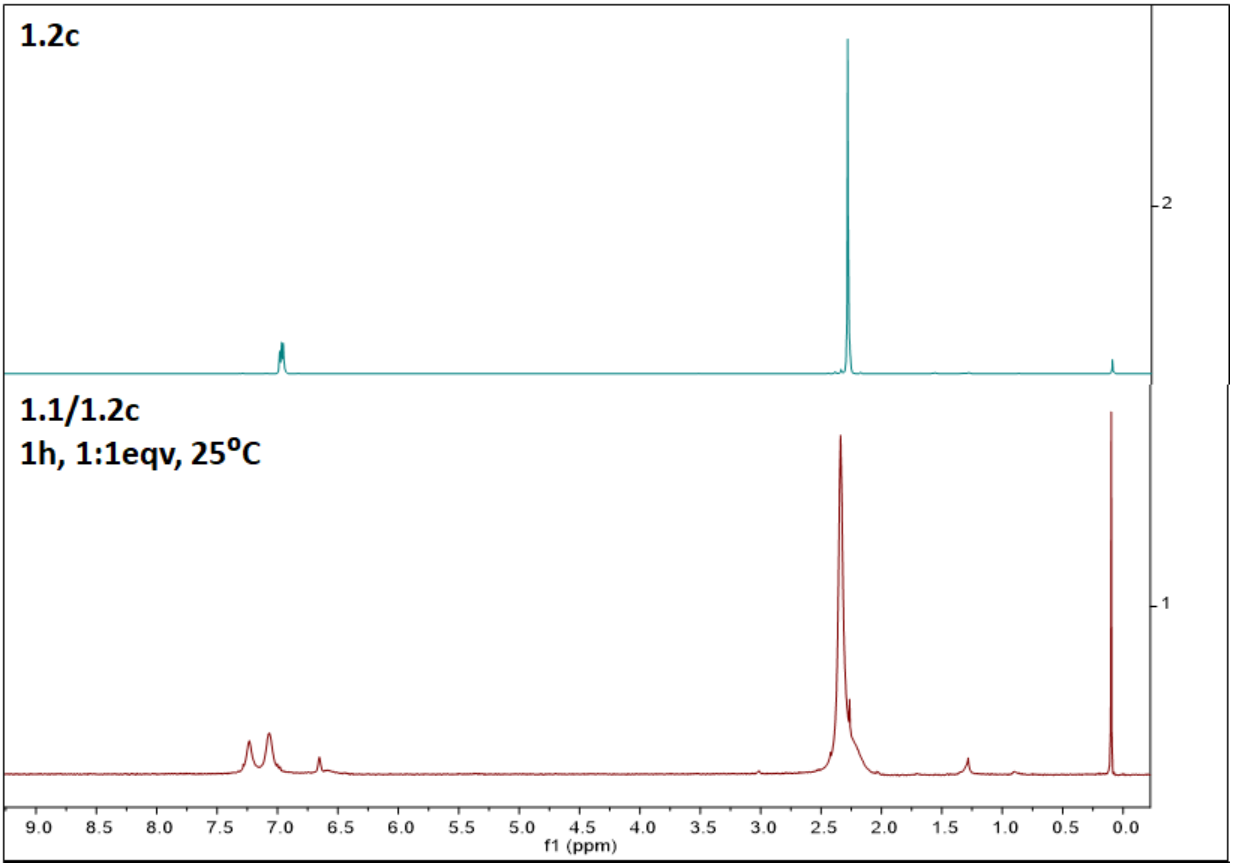

Figure SI 1.1.9 *down* – ^{1}H NMR spectrum of the reaction of **1.1a** with **1.2c** carried out in molar ratio of the reactants 1:1, recorded after 1h of reaction time at 25ºC. ^{1}H NMR (600 MHz, chloroform-*d*, δ, ppm) 7.21 (s, 3H), 7.04 (s, 6H), 2.31 (s, 18H). *up* – ^{1}H NMR spectrum of free **1.2c**. ^{1}H NMR (600 MHz, chloroform-*d*, δ, ppm) 6.95 – 6.93 (m, 9H), 2.26 (s, 18H).

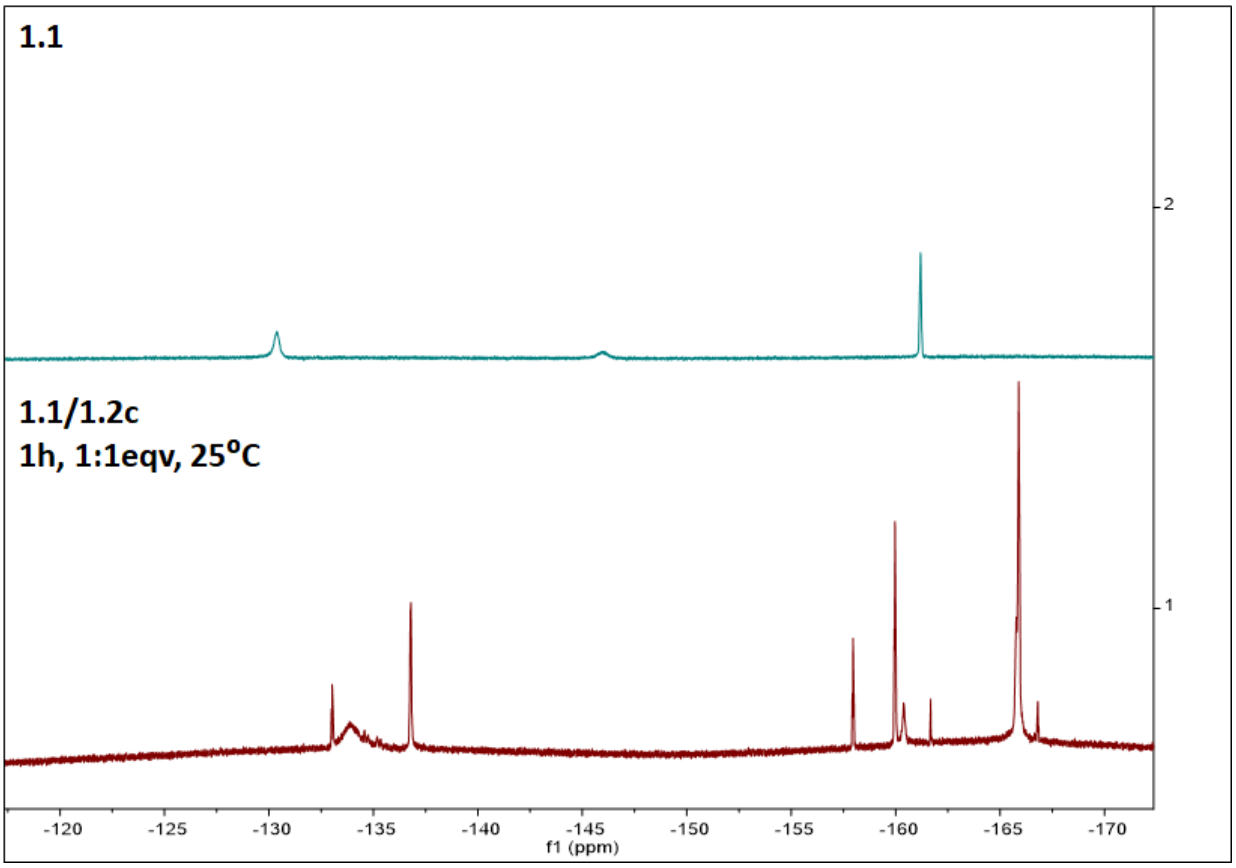

Figure SI 1.1.10 *down* – ^{19}F NMR spectrum of the reaction of **1.1a** with **1.2c** carried out in molar ratio of the reactants 1:1, recorded after 1h of reaction time at 25ºC. ^{19}F NMR (565 MHz, chloroform-*d*, δ, ppm) -132.3 – -133.5 (m), -133.9, -136.8 (d, *J* = 23 Hz), -157.96 (t, *J* = 20 Hz), -156.0 (t, *J* = 21 Hz), -160.4, -161.7 (t, *J* = 20.4 Hz), -165.9 (t, *J* = 22 Hz), -166.47 – -167.04 (m). *up* – ^{19}F NMR spectrum of free **1.1**. ^{19}F NMR (565 MHz, chloroform-*d*, δ, ppm) -130.4, -146.0, -161.2.

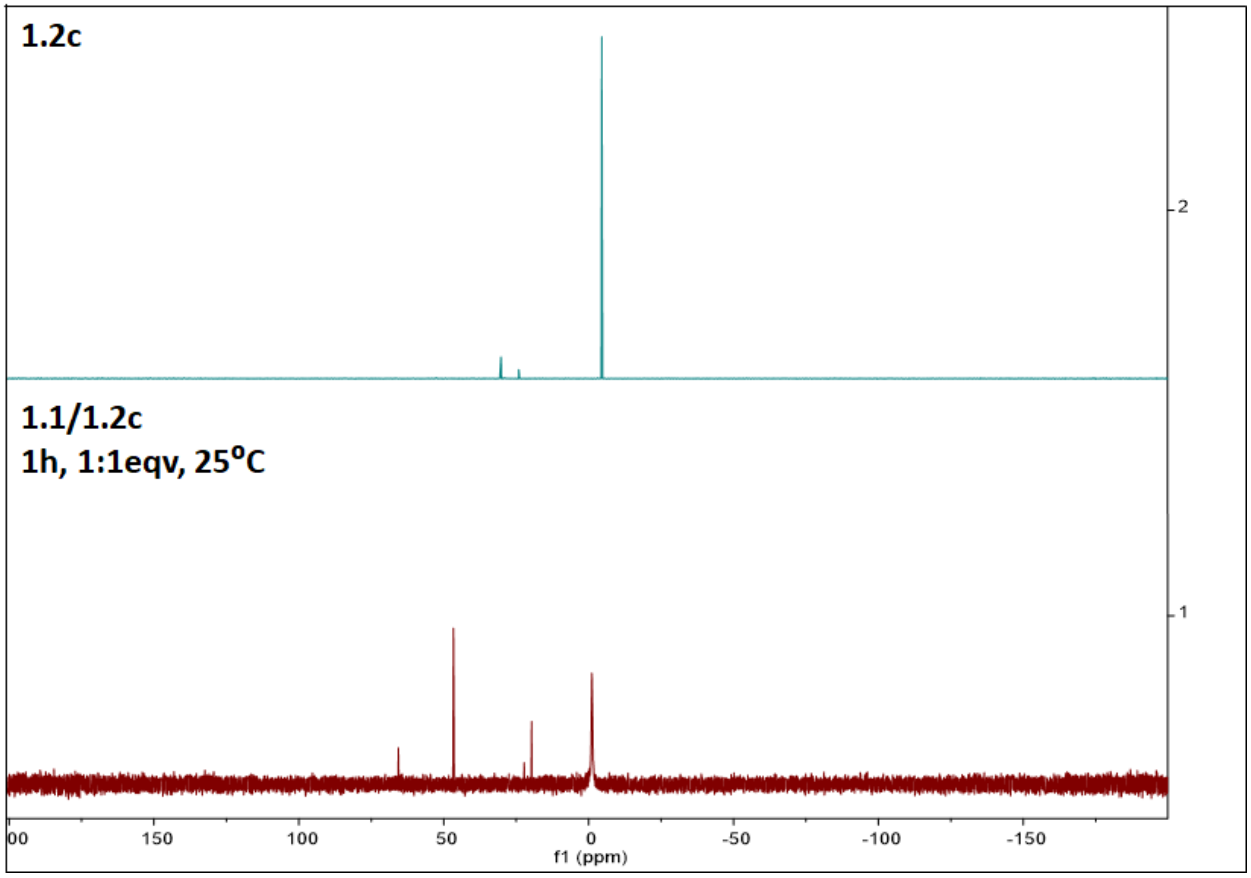

Figure SI 1.1.11 *down* – ^{31}P NMR spectrum of the reaction of **1.1a** with **1.2c** carried out in molar ratio of the reactants 1:1, recorded after 1h of reaction time at 25ºC. ^{31}P NMR (121 MHz, chloroform-*d*, δ, ppm) -1.1. *up* – ^{31}P NMR spectrum of free **1.2c**. ^{31}P NMR (121 MHz chloroform-*d*, δ, ppm) -4.8.

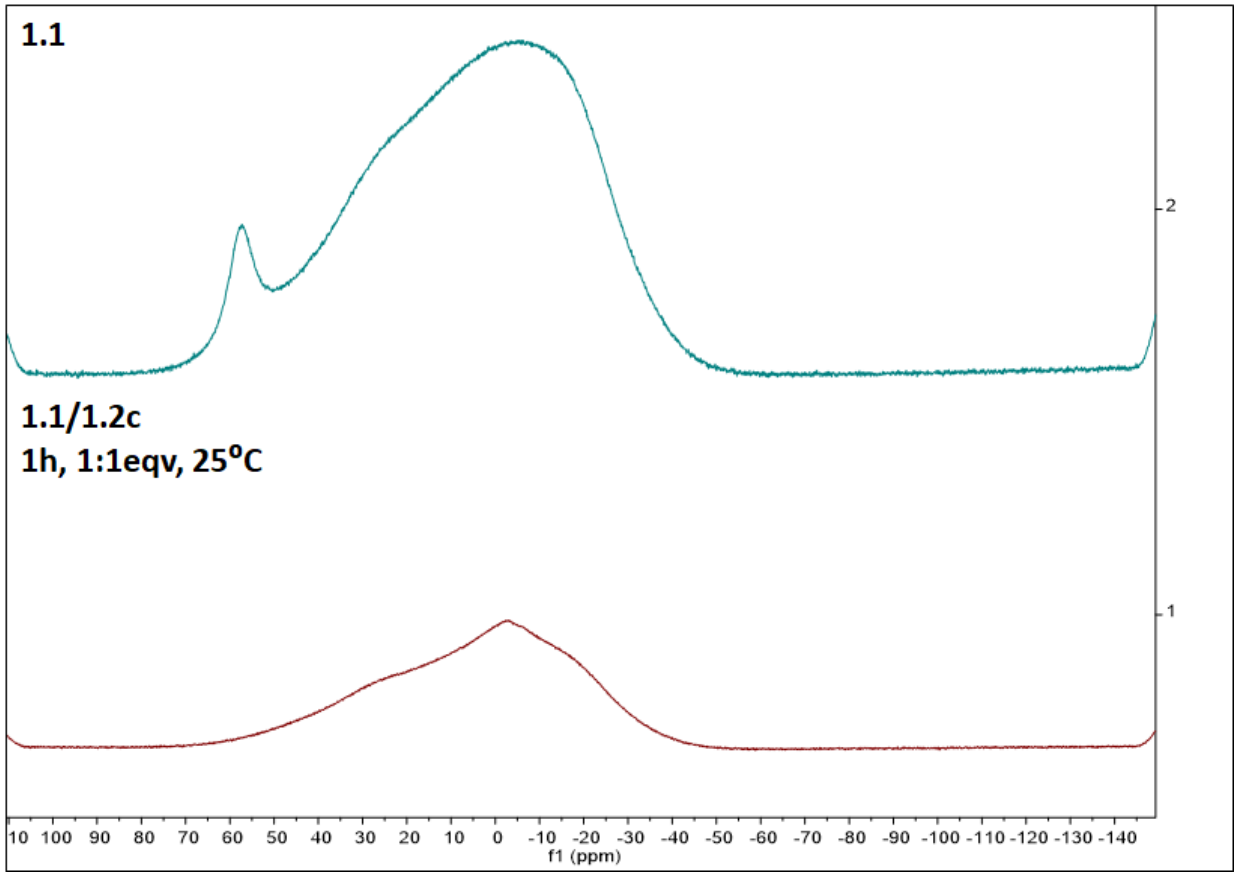

Figure SI 1.1.12 *down* – ^{11}B NMR spectrum of the reaction of **1.1a** with **1.2c** carried out in molar ratio of the reactants 1:1, recorded after 1h of reaction time at 25ºC. ^{11}B NMR (128 MHz, chloroform-*d*, δ, ppm) -2.9. *up* – ^{11}B NMR spectrum of free **1.1**. ^{11}B NMR (128 MHz, chloroform-*d*, δ, ppm) 57.3.

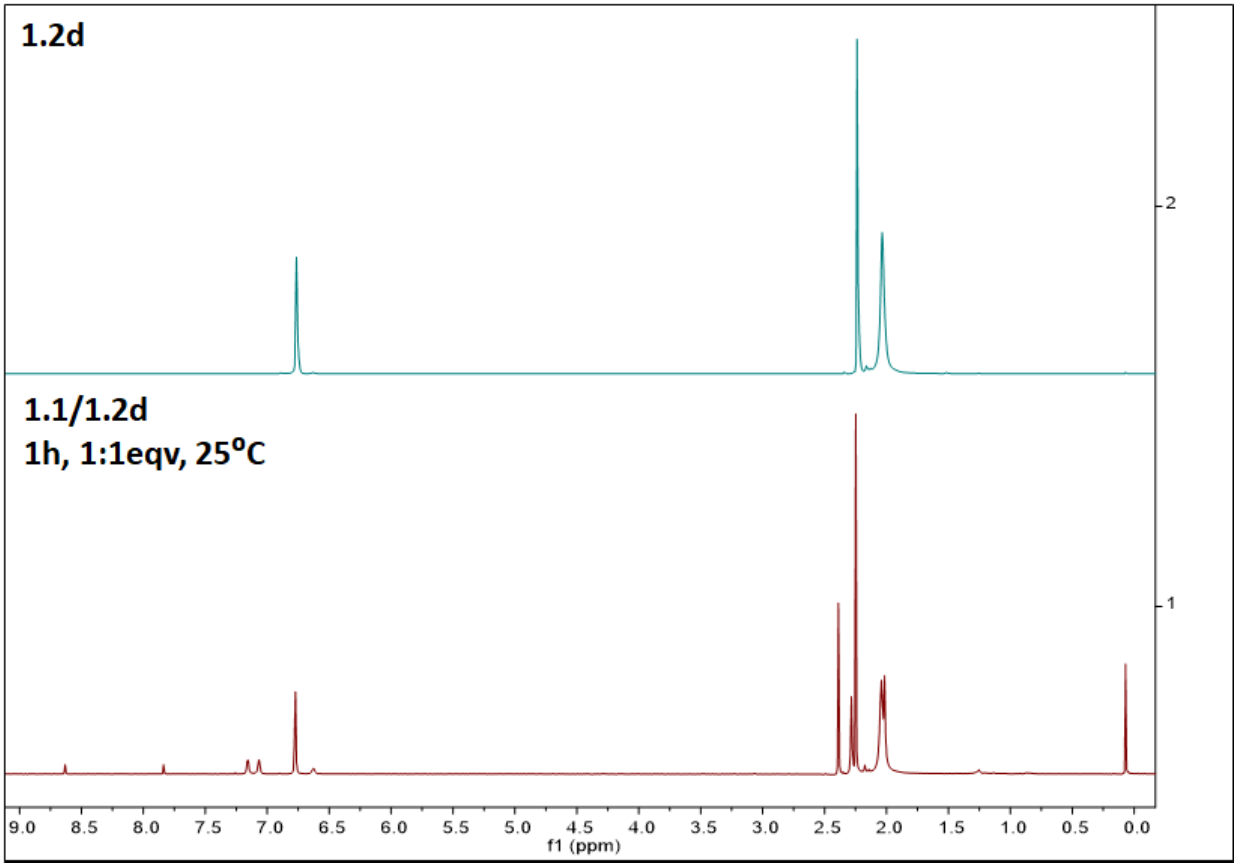

Figure SI 1.1.13 *down* – ^{1}H NMR spectrum of the reaction of **1.1a** with **1.2d** carried out in molar ratio of the reactants 1:1, recorded after 1h of reaction time at 25ºC. ^{1}H NMR (600 MHz, chloroform-*d*, δ, ppm) 8.23 (d, *J* = 477 Hz), 7.11 (d, *J* = 53 Hz), 6.77 (d, *J* = 3 Hz), 6.63 (s), 2.39 (s), 2.28 (s), 2.25 (s), 2.03 (d, *J* = 16 Hz).*up* – ^{1}H NMR spectrum of free **1.2d**. ^{1}H NMR (600 MHz, chloroform-*d*, δ, ppm) 6.76 (s, 6H), 2.24 (s, 9H), 2.03 (s, 18H).

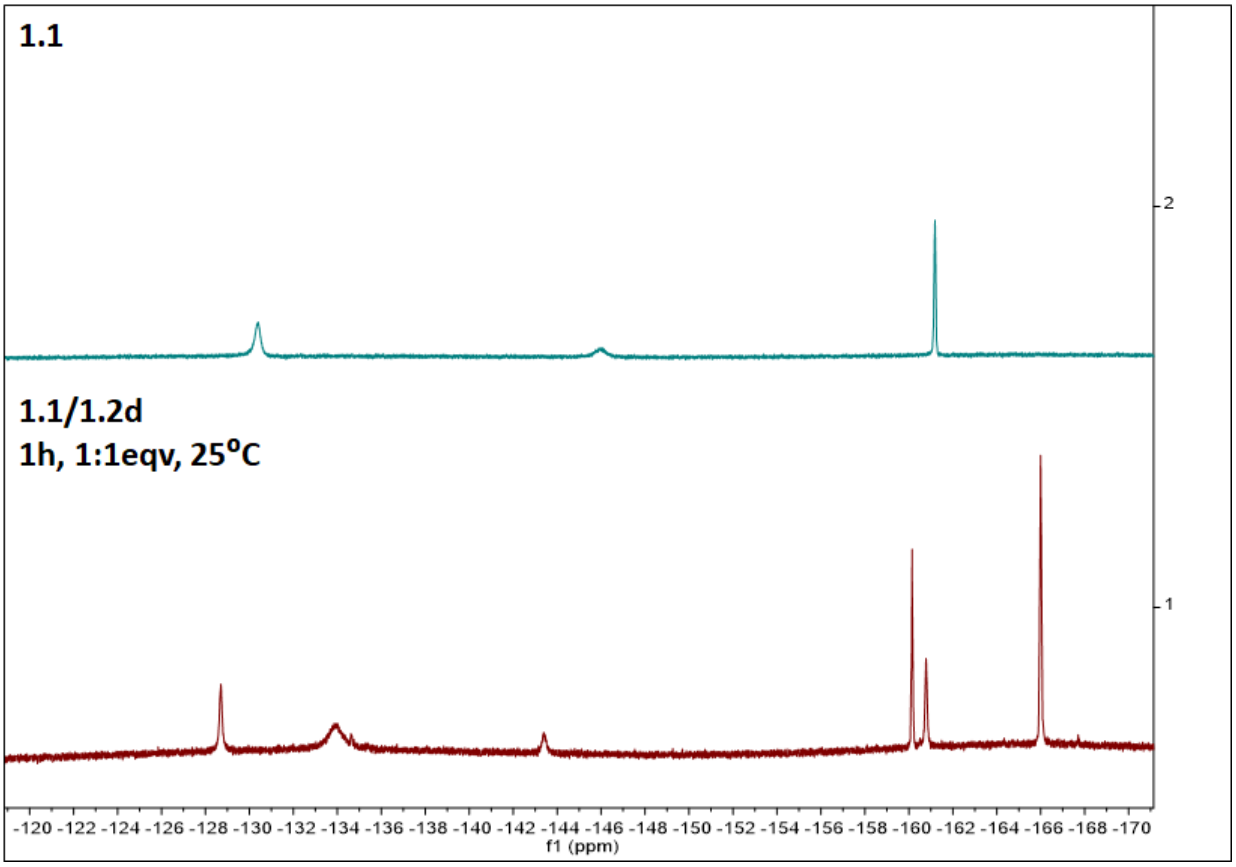

Figure SI 1.1.14 *down* – ^{19}F NMR spectrum of the reaction of **1.1a** with **1.2d** carried out in molar ratio of the reactants 1:1, recorded after 1h of reaction time at 25ºC. ^{19}F NMR (565 MHz, chloroform-*d*, δ, ppm) -128.7, -133.9, -143.4, -160.1 (t, *J* = 20 Hz), -160.8, -166.0 (t, *J* = 2 H2z). *up* – ^{19}F NMR spectrum of free **1.1**. ^{19}F NMR (565 MHz, chloroform-*d*, δ, ppm) -130.4, -146.0, -161.2.

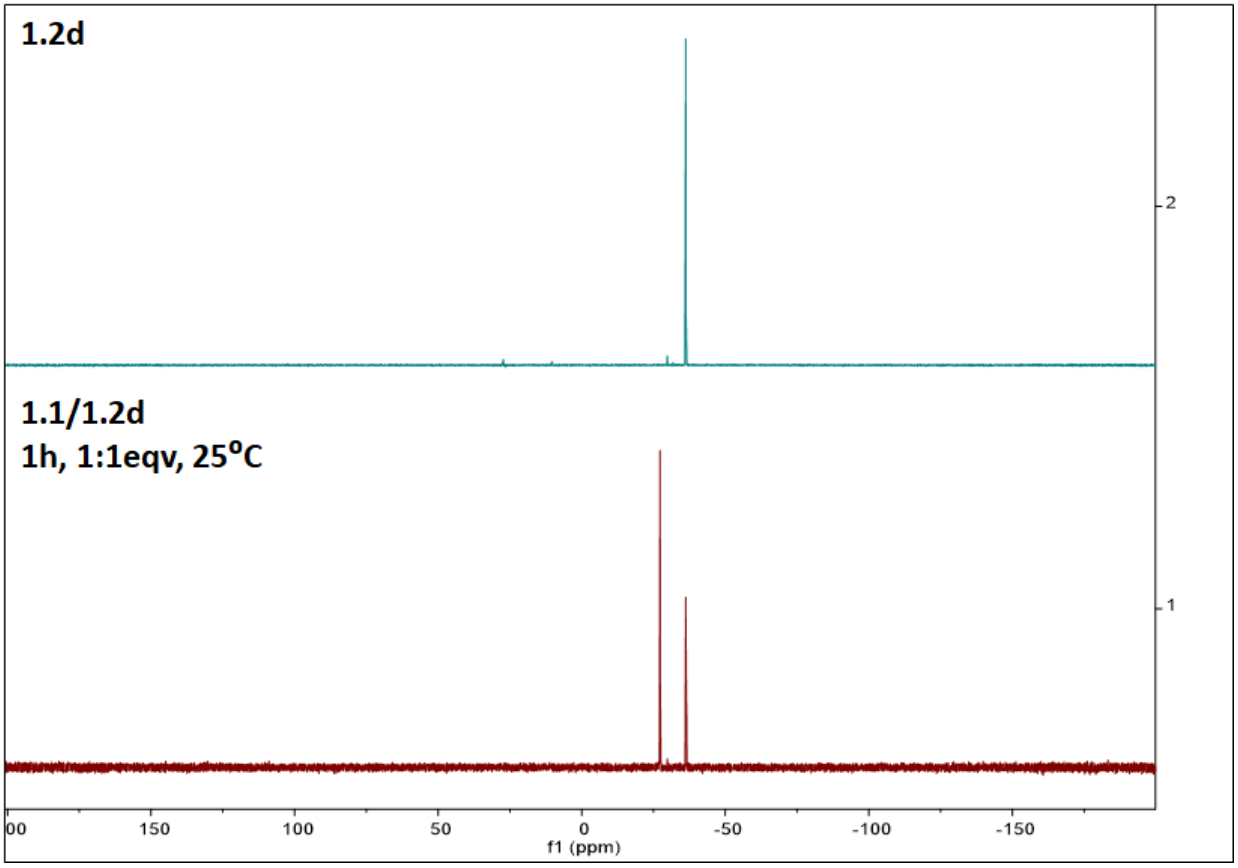

Figure SI 1.1.15 *down* – ^{31}P NMR spectrum of the reaction of **1.1a** with **1.2d** carried out in molar ratio of the reactants 1:1, recorded after 1h of reaction time at 25ºC. ^{31}P NMR (121 MHz, chloroform-*d*, δ, ppm) -27.3, -36.3. *up* – ^{31}P NMR spectrum of free **1.2d**. ^{31}P NMR (121 MHz chloroform-*d*, δ, ppm) -36.2.

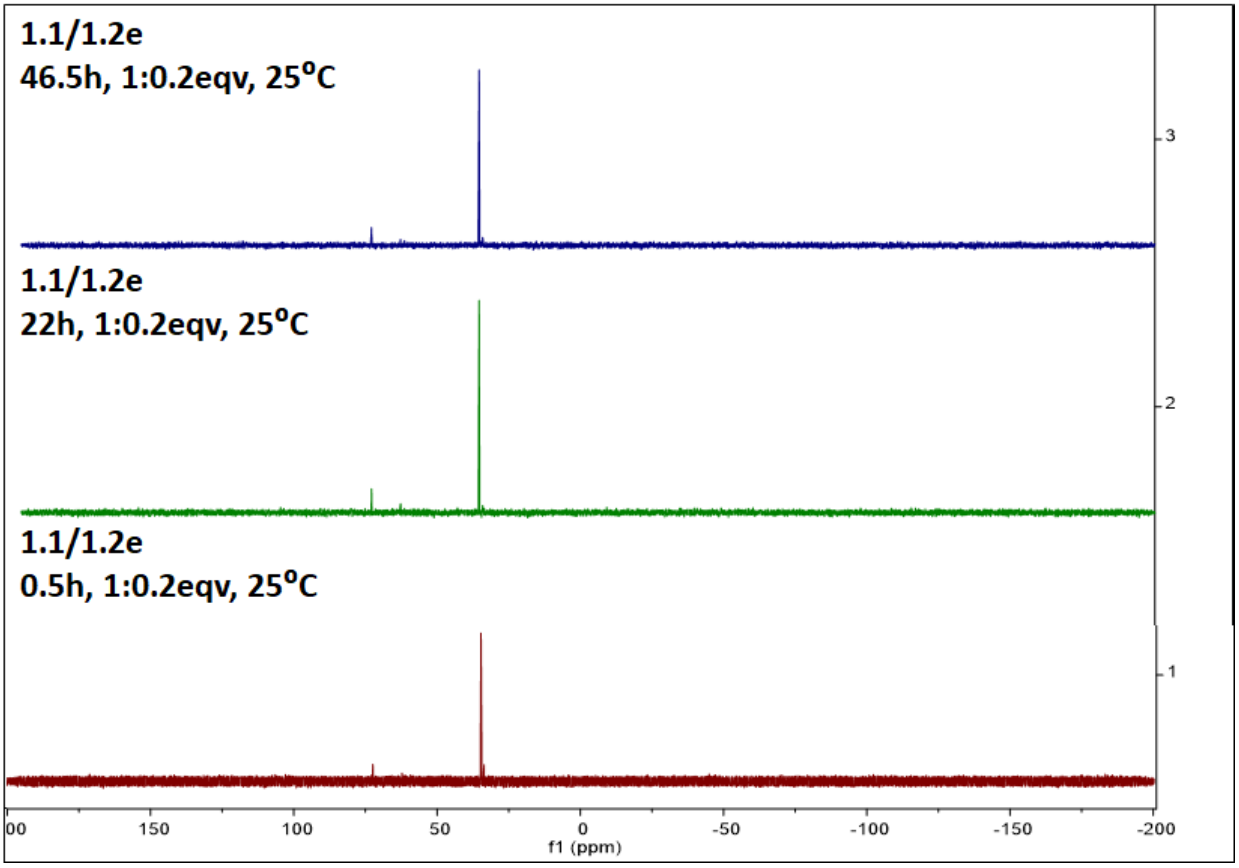

Figure 1.16 Superimposed ^{31}P NMR spectra of the reaction of **1.1** with **1.2e** carried out within molar ratio of the reactants 1:0.2, recorded at various reaction times (0.5 h, 22 h and 46.5 h). The spectra are recorded in deuterated chloroform at 121 MHz at 25ºC. ^{31}P NMR (122 MHz, chloroform-*d*, δ, ppm) 72.4, 34.7; ^{31}P NMR (122 MHz, chloroform-*d*, δ, ppm) 72.4, 62.2, 34.7; ^{31}P NMR (162 MHz, chloroform-*d*, δ, ppm) 72.4, 62.2, 34.8; Free **1.1e** ^{31}P NMR (121 MHz, chloroform-*d*, δ, ppm) 11.2.

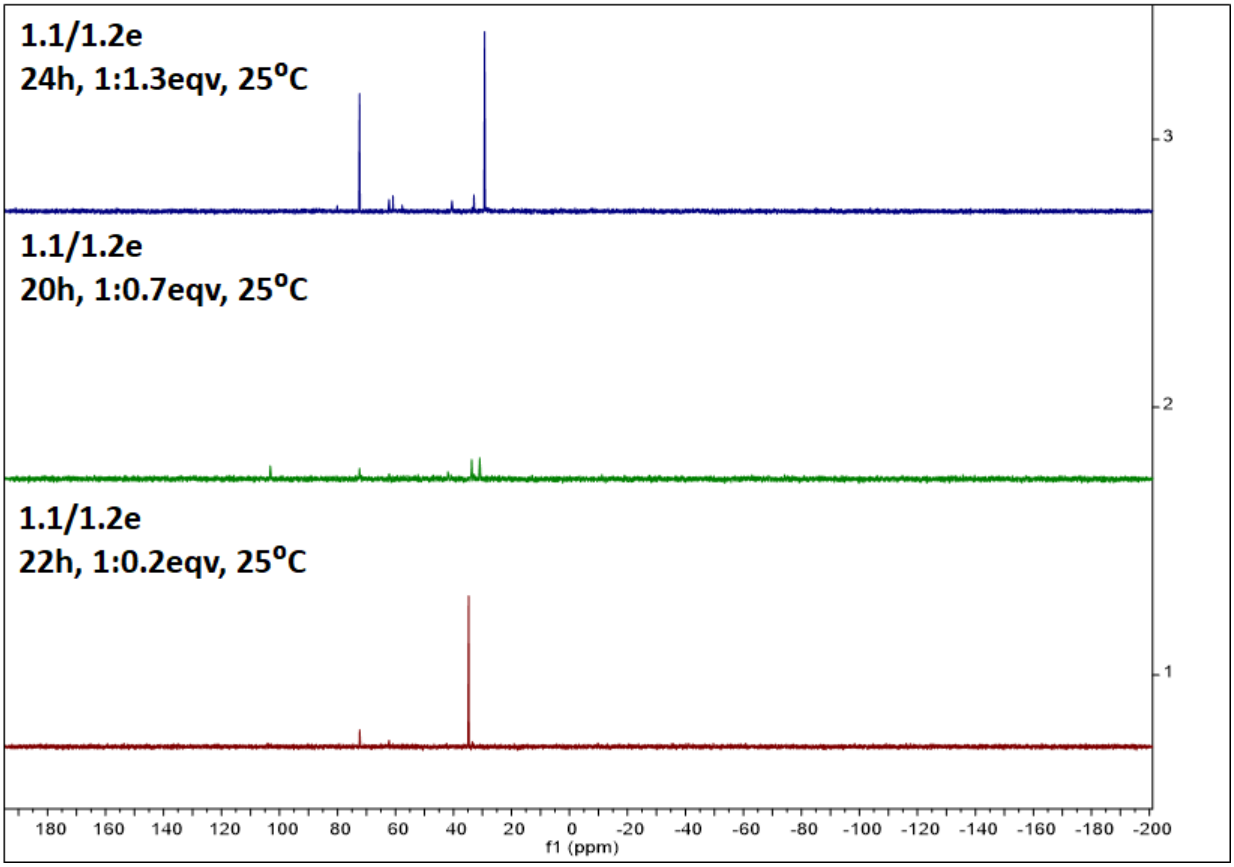

Figure 1.17 Superimposed ^{31}P NMR spectra of the reaction of **1.1** with **1.2e** carried out within various molar ratios of the reactants (1:0.2, 1:0.7 and 1:1.3). The spectra are recorded in deuterated chloroform at 121 MHz at 25ºC. Signals: ^{31}P NMR (122 MHz, chloroform-*d*, δ, ppm) 72.38, 62.20, 34.66; ^{31}P NMR (162 MHz, chloroform-*d*, δ, ppm) 103.1, 72.4, 41.9, 33.7, 31.0; ^{31}P NMR (162 MHz, chloroform-*d*, δ, ppm) 80.1, 72.4, 62.2, 60.9, 57.7, 40.5, 33.1, 33.0, 29.3; Free **1.1e** ^{31}P NMR (121 MHz, chloroform-*d*) 11.2.

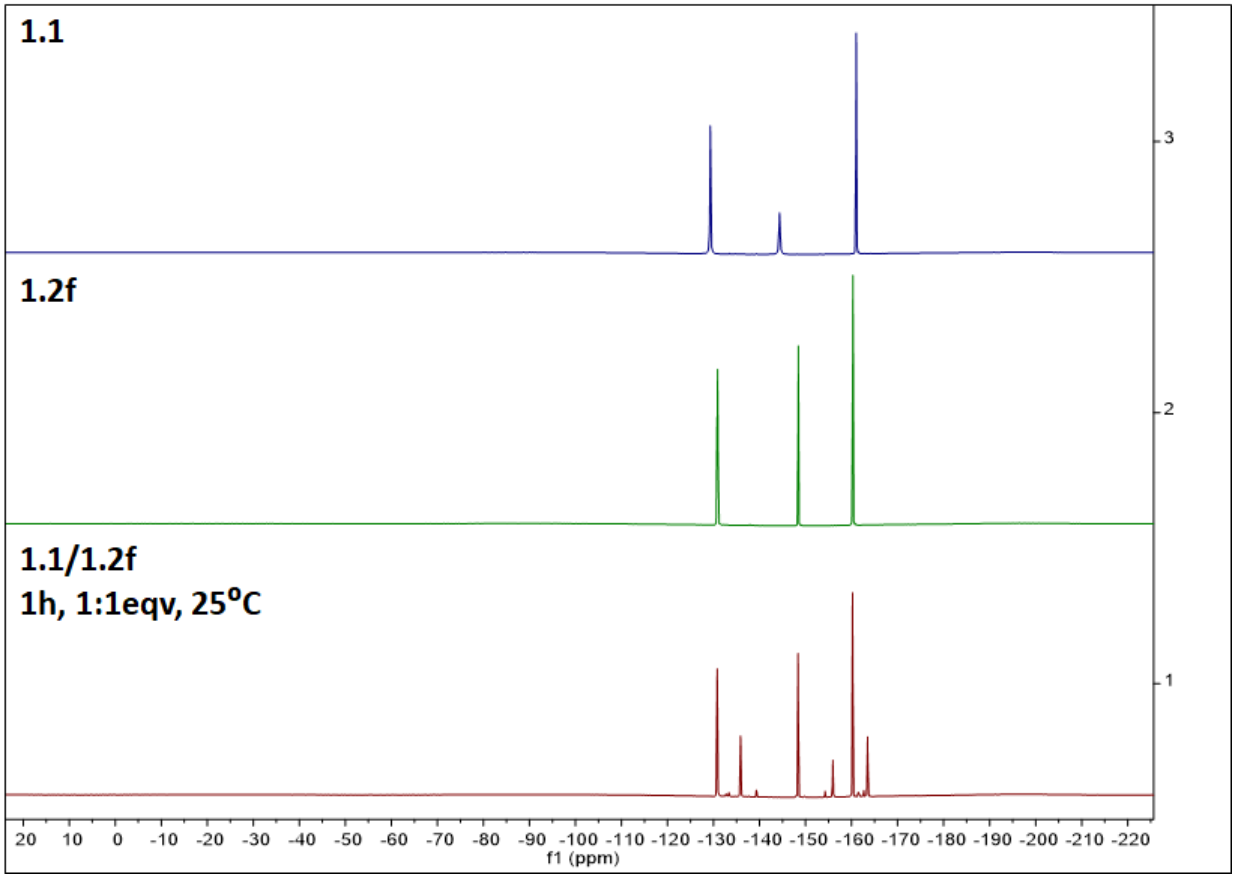

Figure SI 1.1.18 *down* – ^{19}F NMR spectrum of the reaction of **1.1a** with **1.2f** carried out in molar ratio of the reactants 1:1, recorded after 1h of reaction time at 25ºC. ^{19}F NMR (565 MHz, chloroform-*d*, δ, ppm) -130.5 – -131.3 (m), -134.8, -148.4 (t, *J* = 20 Hz), -153.5, -160.3 (t, *J* = 21 Hz), -162.2 – -163.0 (m). Middle – ^{19}F NMR spectrum of free **1.2f**. ^{19}F NMR (565 MHz, chloroform-*d*, δ, ppm) -130.9 (t, *J* = 29 Hz), -148.4 (t, *J* = 21 Hz), -160.3 (t, *J* = 20 Hz). *up* – ^{19}F NMR spectrum of free **1.1**. ^{19}F NMR (565 MHz, chloroform-*d*, δ, ppm) -130.4, -146.0, -161.2.

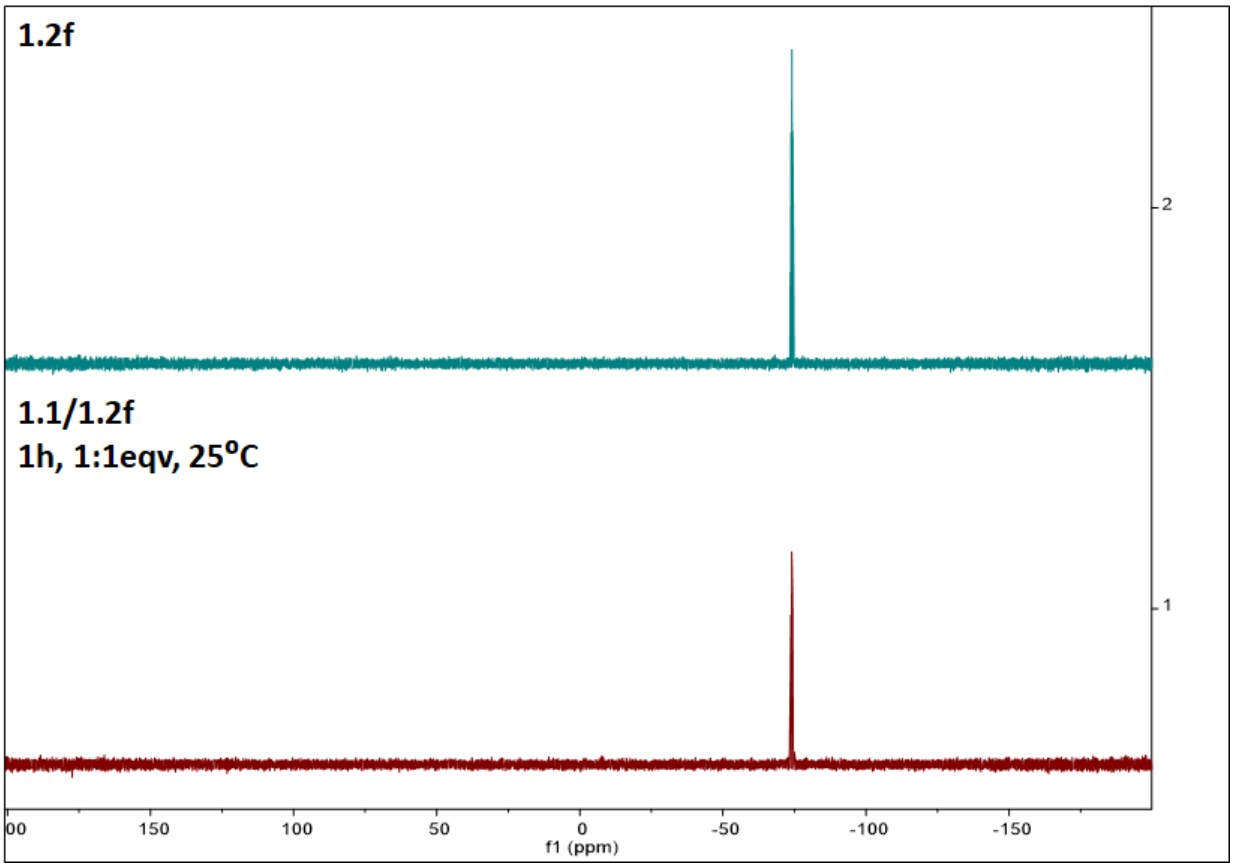

Figure SI 1.1.19 *down* – ^{31}P NMR spectrum of the reaction of **1.1a** with **1.2f** carried out in molar ratio of the reactants 1:1, recorded after 1h of reaction time at 25ºC. ^{31}P NMR (121 MHz, chloroform-*d*, δ, ppm) -73.6, -73.9, -74.1, -74.4, -74.7. *up* – ^{31}P NMR spectrum of free **1.2f**. ^{31}P NMR (121 MHz, chloroform-*d*, δ, ppm) -73.5, -73.8, -74.1, -74.4, -74.7, -75.00.

A.1.1.2. 2D NMR spectra.

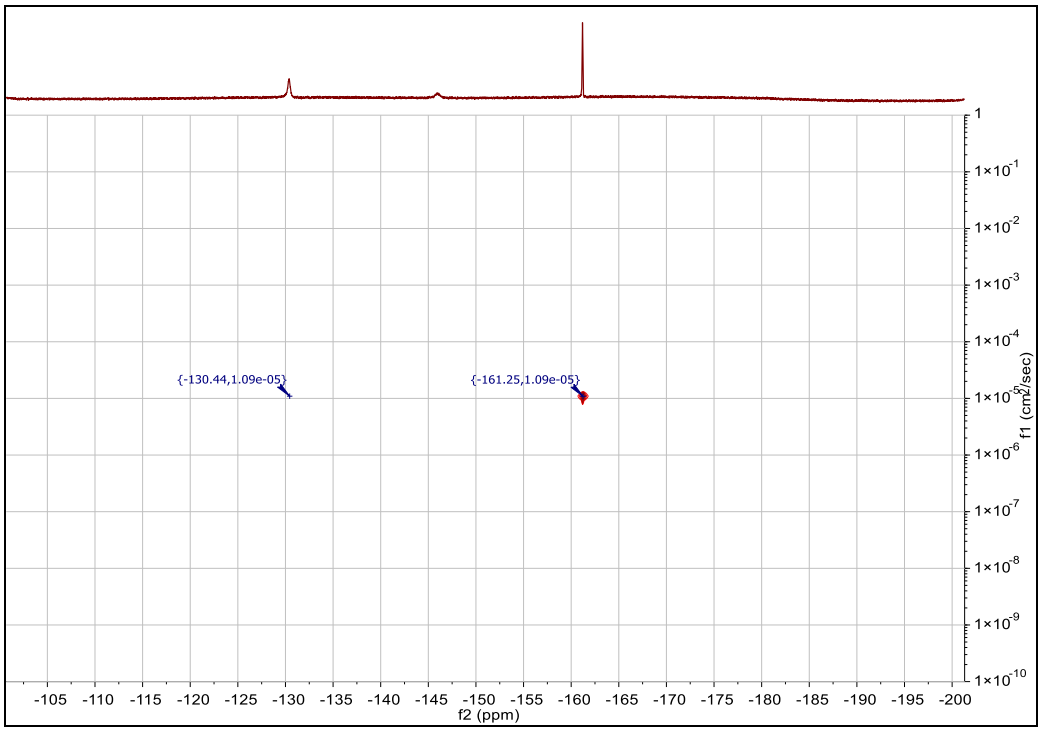

Figure SI 1.1.20 ^{19}F DOSY NMR spectrum of **1.1** (c≈20 mM). The spectrum is recorded in deuterated chloroform at 565 MHz at 25ºC. Obtained signals: D=1.09 e^{-9} m^2/s, V=214 $Å^3$.

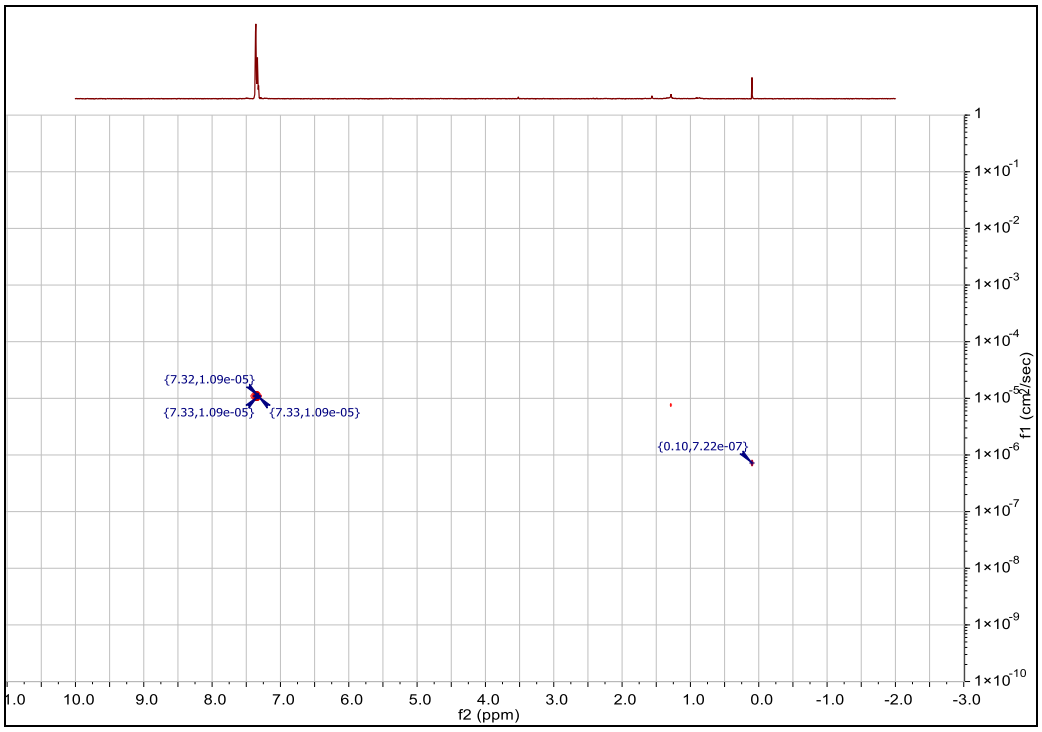

Figure SI 1.1.21 ^{1}H DOSY NMR spectrum of **1.2a** (c≈20 mM). The spectrum is recorded in deuterated chloroform at 600 MHz at 25ºC. Obtained signals: D=1.09 e^{-9} m^2/s, V=214 Å^3.

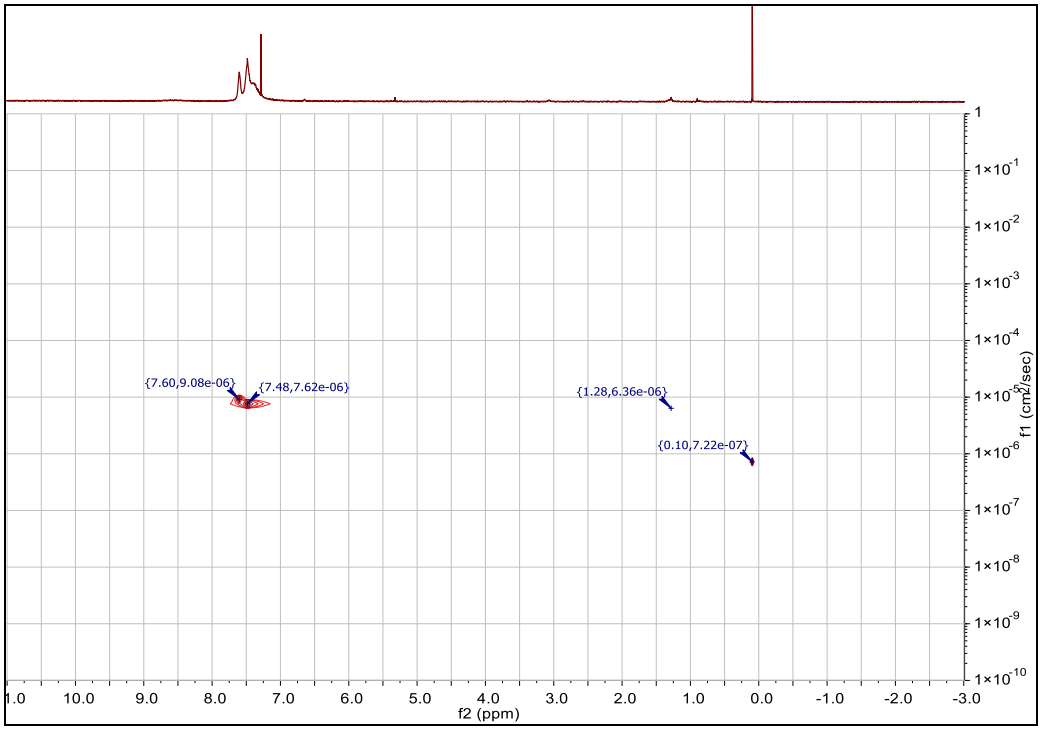

Figure SI 1.1.22 ^{1}H DOSY NMR spectrum of the reaction of **1.1** (c≈20 mM) with **1.2a** (c≈20 mM). The spectrum is recorded in deuterated chloroform at 600 MHz at 25ºC. Obtained signals: D=7.62 e^{-10} m^2/s, V=628 Å^3; D=9.08 e^{-10} m^2/s, V=371 Å^3.

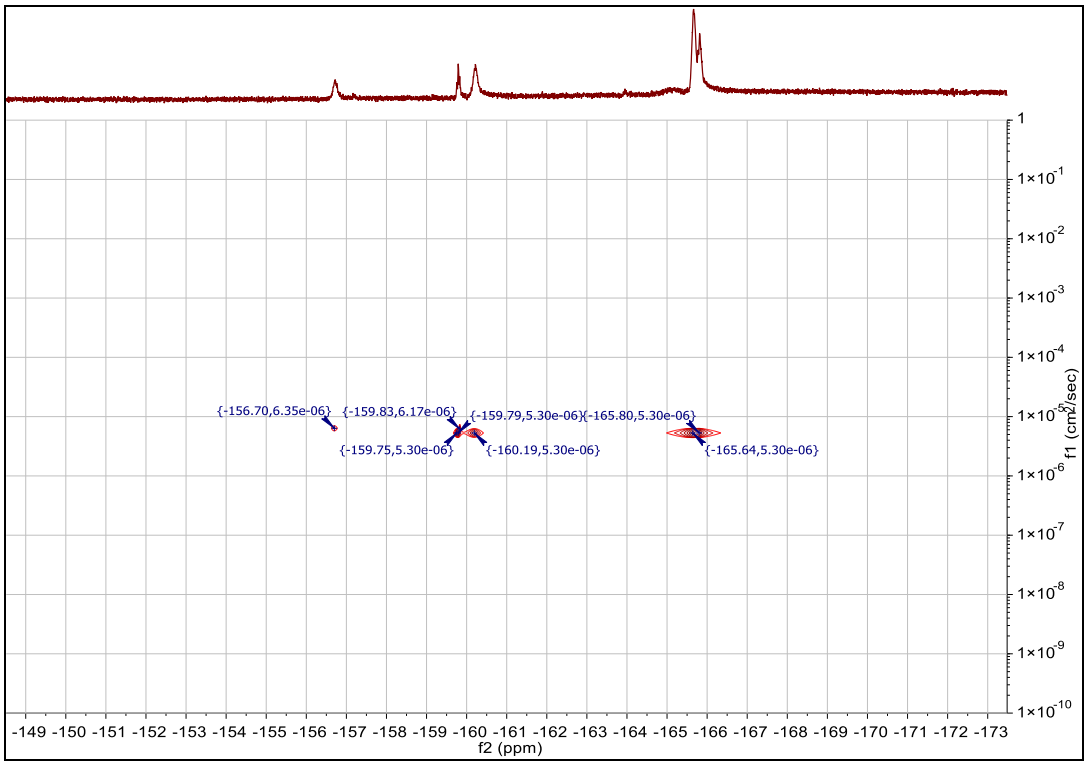

Figure SI 1.1.23 ^{19}F DOSY NMR spectrum of the reaction of **1.1** (c≈20 mM) with **1.2a** (c≈20 mM). The spectrum is recorded in deuterated chloroform at 565 MHz at 25ºC. Obtained signals: D=5.30 e^{-10} m^2/s, V=1866 $Å^3$; D=6.35 e^{-10} m^2/s, V=1085 $Å^3$.

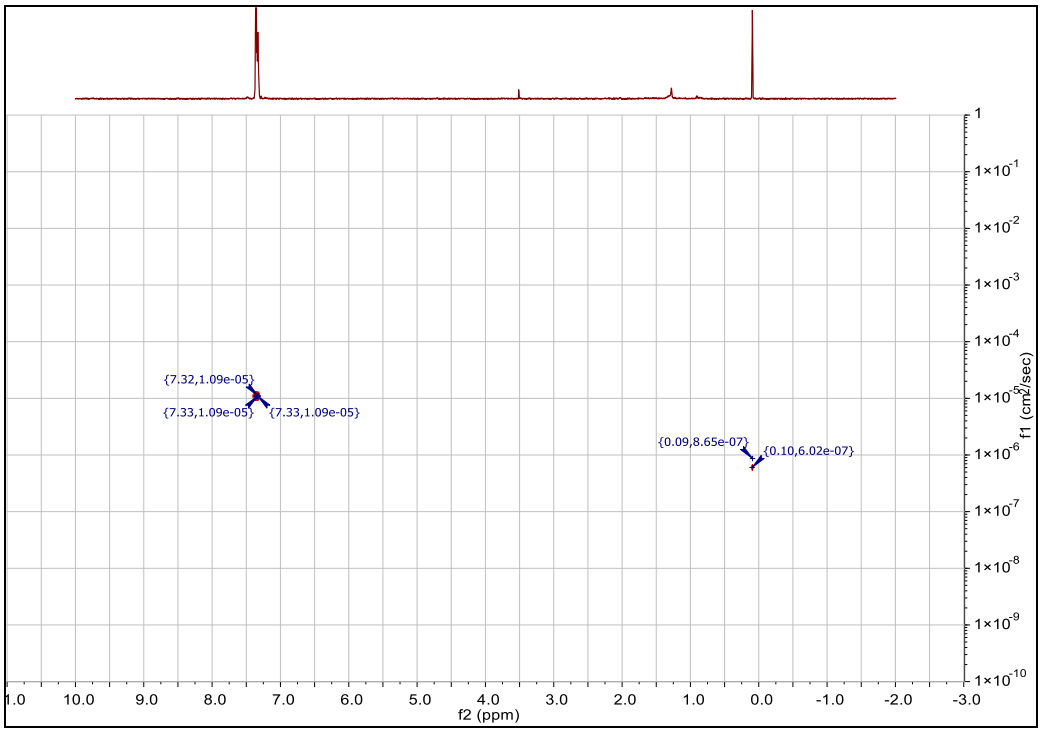

Figure SI 1.1.24 ^{1}H DOSY NMR spectrum of **1.2a** (c≈10 mM). The spectrum is recorded in deuterated chloroform at 600 MHz at 25ºC. Obtained signals: D=1.09 e^{-9} m^2/s, V=214 $Å^3$.

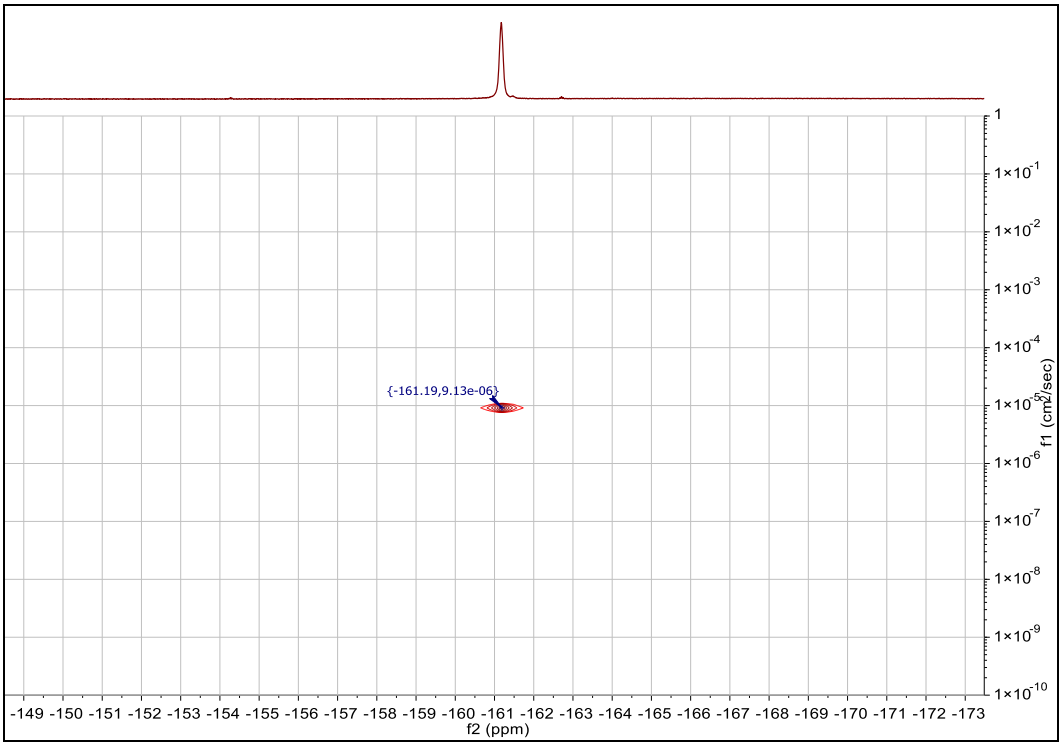

Figure SI 1.1.25 ^{19}F DOSY NMR spectrum of **1.1** (c≈100 mM). The spectrum is recorded in deuterated chloroform at 565 MHz at 25ºC. Obtained signals: D=9.13 e^{-10} m^2/s, V=365 $Å^3$.

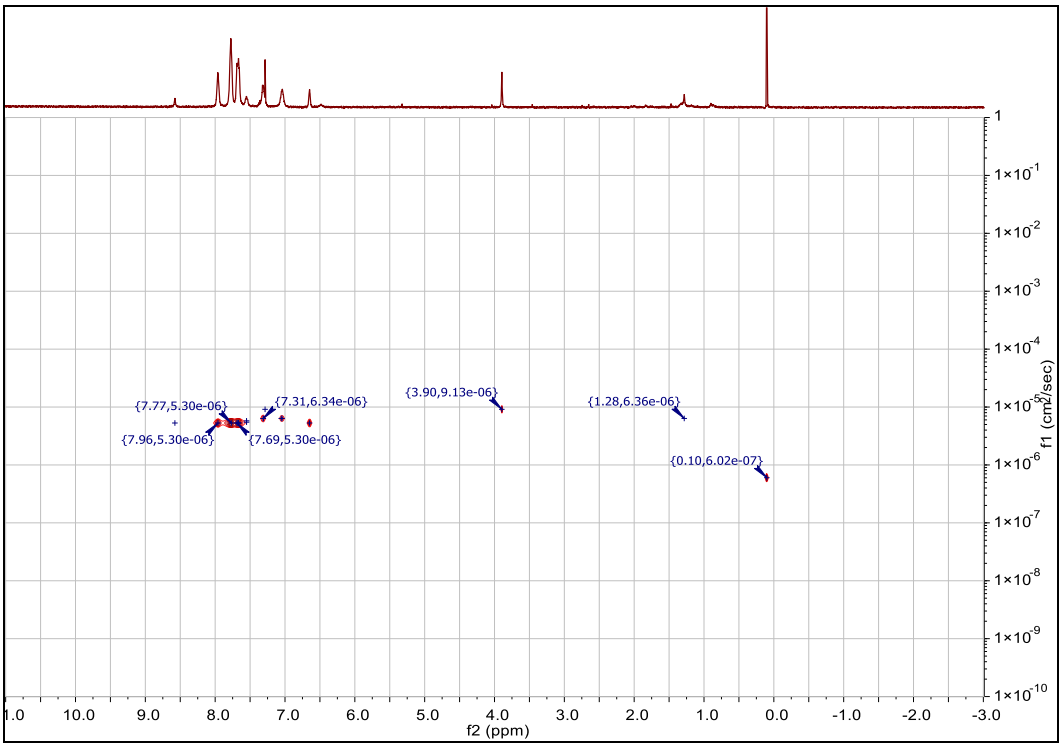

Figure SI 1.1.26 ^{1}H DOSY NMR spectrum of the reaction of **1.1** (c≈100 mM) with **1.2a** (c≈10 mM). The spectrum is recorded in deuterated chloroform at 600 MHz at 25ºC. Obtained signals: D=5.30 e^{-10} m^2/s, V=1866 $Å^3$; D=6.34 e^{-10} m^2/s, V=1090 $Å^3$.

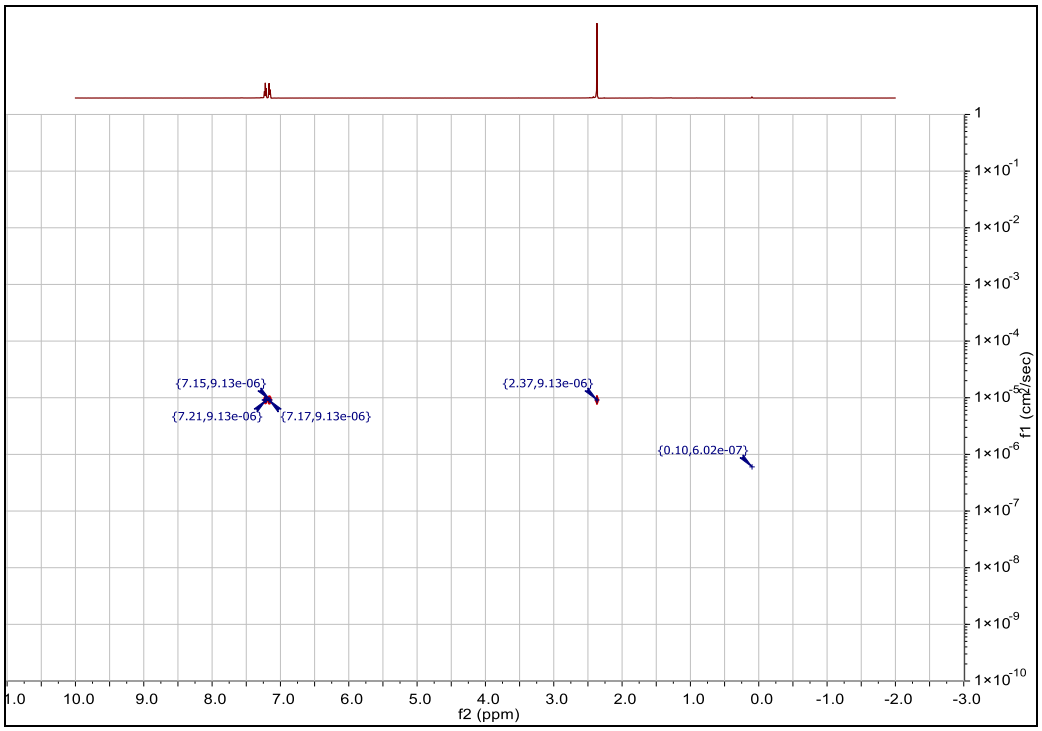

Figure SI 1.1.27 ^{1}H DOSY NMR spectrum of **1.2b** (c≈20 mM). The spectrum is recorded in deuterated chloroform at 600 MHz at 25ºC. Obtained signals: D=9.13 e^{-10} m^2/s, V=365 $Å^3$.

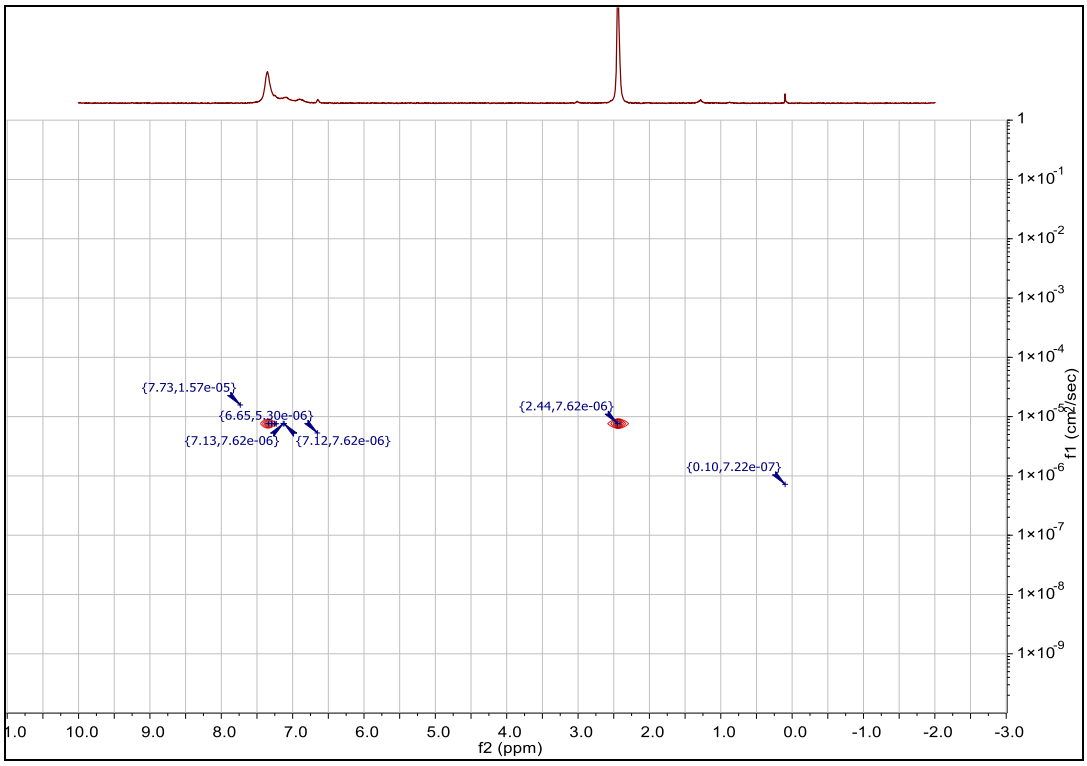

Figure SI 1.1.28 ^{1}H DOSY NMR spectrum of the reaction of **1.1** (c≈20 mM) with **1.2b** (c≈20 mM). The spectrum is recorded in deuterated chloroform at 600 MHz at 25ºC. Obtained signals: D=7.62 e^{-10} m^2/s, V=628 Å^3; D=5.30 e^{-10} m^2/s, V=1866 Å^3.

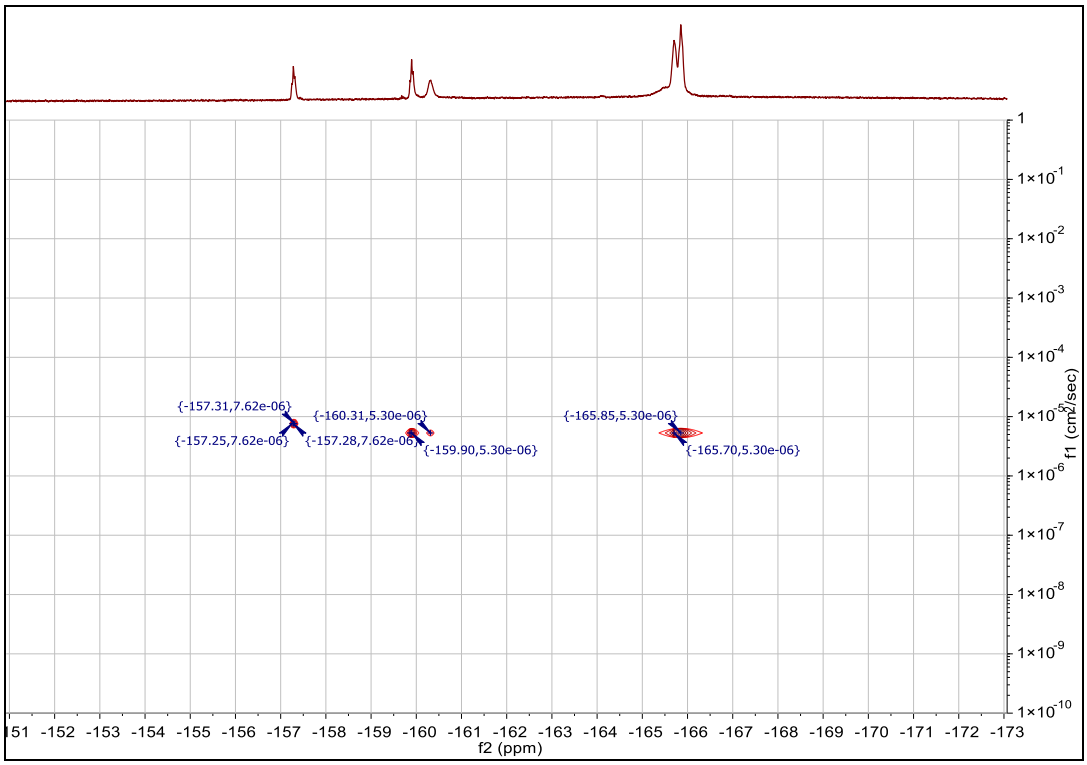

Figure SI 1.1.29 ^{19}F DOSY NMR spectrum of the reaction of **1.1** (c≈20 mM) with **1.2b** (c≈20 mM). The spectrum is recorded in deuterated chloroform at 565 MHz at 25ºC. Obtained signals: D=7.62 e^{-10} m^2/s, V=628 $Å^3$; D=5.30 e^{-10} m^2/s, V=1866 $Å^3$.

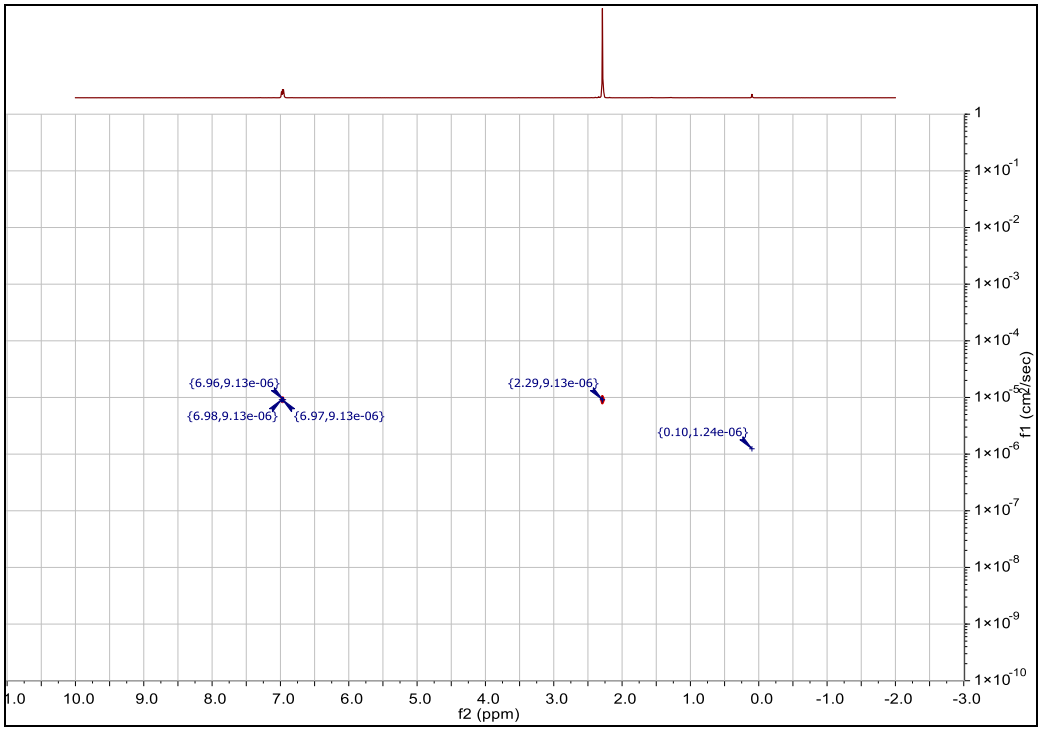

Figure SI 1.1.30 ^{1}H DOSY NMR spectrum of **1.2c** (c≈20 mM). The spectrum is recorded in deuterated chloroform at 600 MHz at 25ºC. Obtained signals: D=9.13 e^{-10} m^2/s, V=365 $Å^3$.

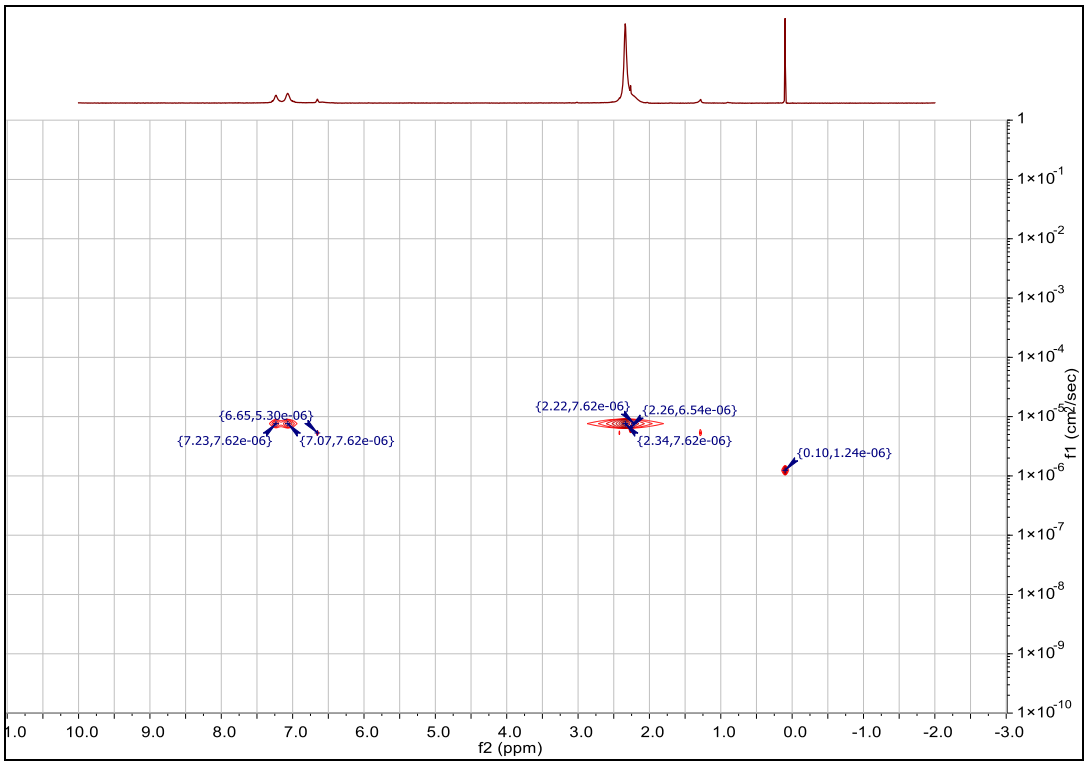

Figure SI 1.1.31 ^{1}H DOSY NMR spectrum of the reaction of **1.1** (c≈20 mM) with **1.2c** (c≈20 mM). The spectrum is recorded in deuterated chloroform at 600 MHz at 25ºC. Obtained signals: D=7.62 e^{-10} m^2/s, V=628 Å^3; D=5.30 e^{-10} m^2/s, V=1866 Å^3.

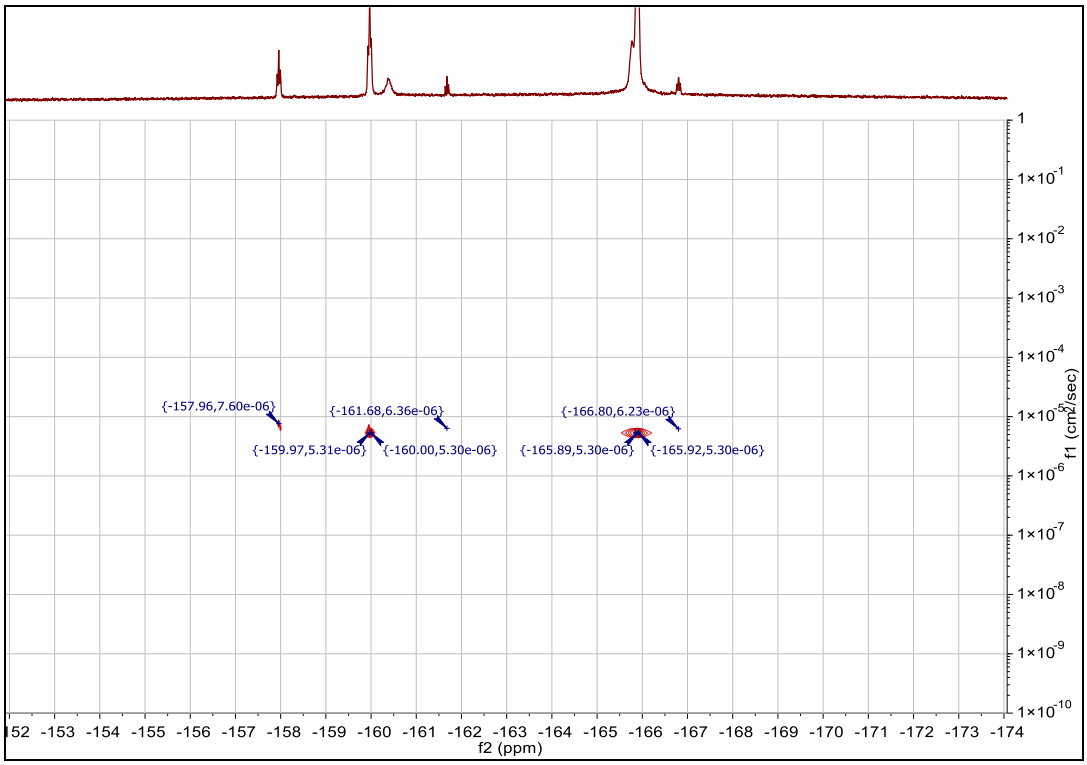

Figure SI 1.1.32 ^{19}F DOSY NMR spectrum of the reaction of **1.1** (c≈20 mM) with **1.2c** (c≈20 mM). The spectrum is recorded in deuterated chloroform at 565 MHz at 25ºC. Obtained signals: D=7.62-7.41 e^{-10} m^2/s, V=633-683 $Å^3$; D=5.30 e^{-10} m^2/s, V=1866 $Å^3$; D=7.36-7.23 e^{-10} m^2/s, V=697-635 $Å^3$.

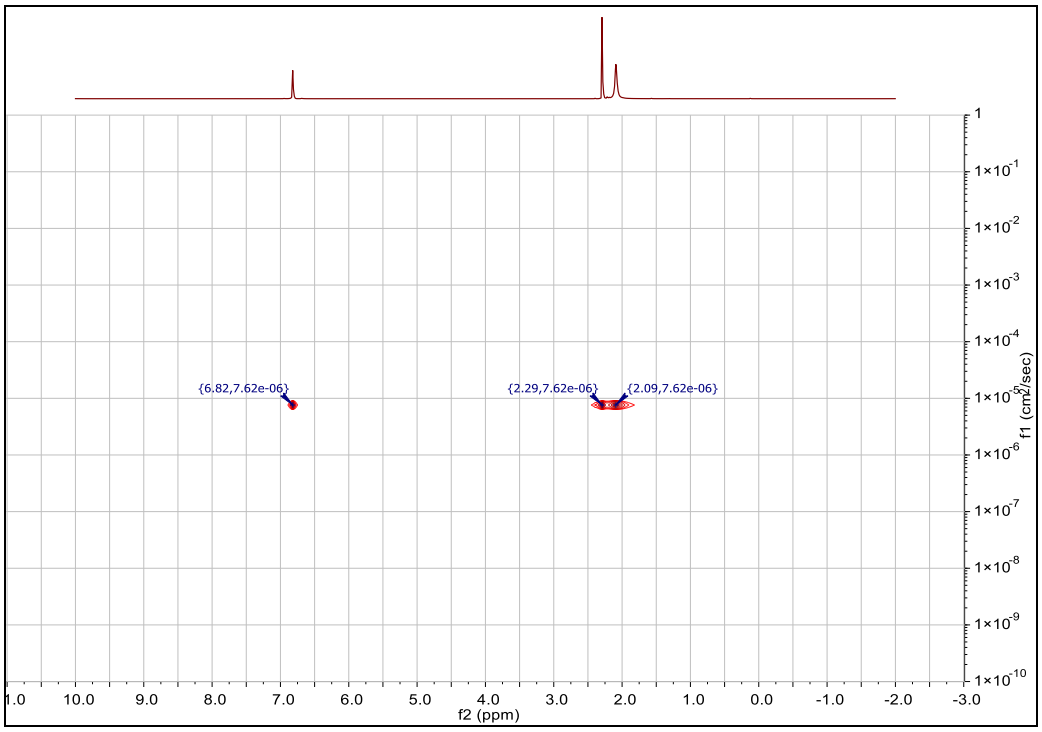

Figure SI 1.1.33 ^{1}H DOSY NMR spectrum of **1.2d** (c≈20 mM). The spectrum is recorded in deuterated chloroform at 600 MHz at 25ºC. Obtained signals: D=7.62 e^{-10} m^2/s, V=628 $Å^3$.

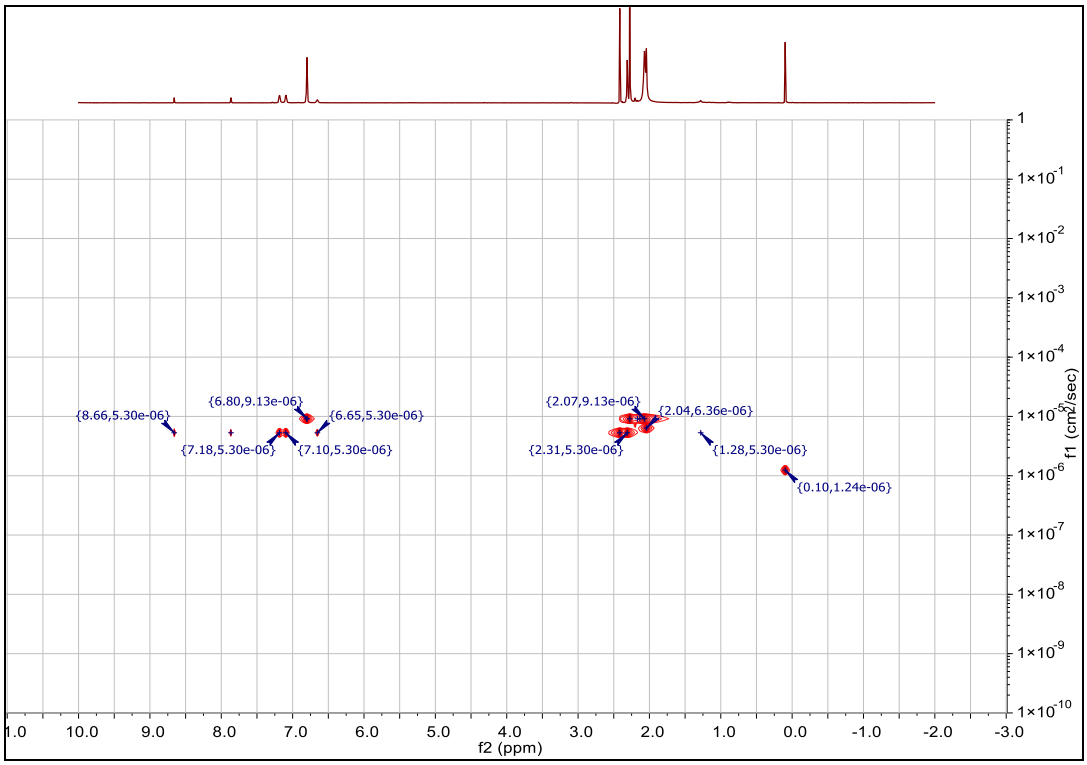

Figure SI 1.1.34 ^{1}H DOSY NMR spectrum of the reaction of **1.1** (c≈20 mM) with **1.2d** (c≈20 mM). The spectrum is recorded in deuterated chloroform at 600 MHz at 25ºC. Obtained signals: D=5.30 e^{-10} m^2/s, V=1866 Å^3; D=9.13 e^{-10} m^2/s, V=365 Å^3; D=6.36 e^{-10} m^2/s, V=1080 Å^3.

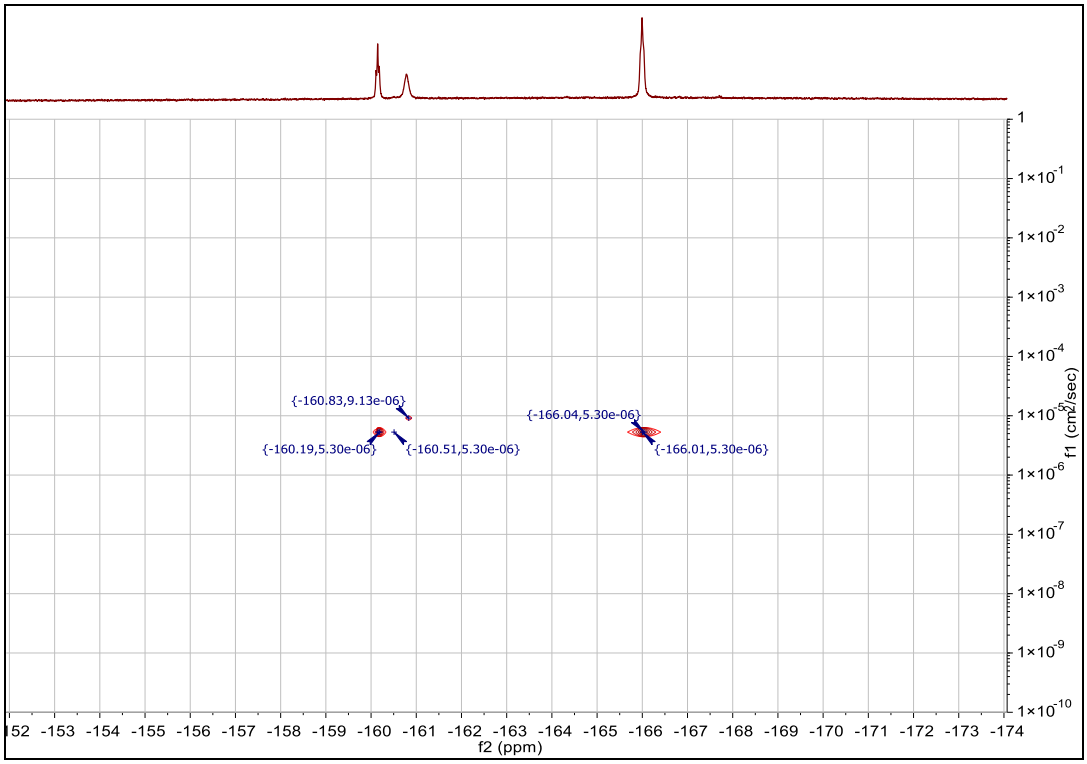

Figure SI 1.1.35 ^{19}F DOSY NMR spectrum of the reaction of **1.1** (c≈20 mM) with **1.2d** (c≈20 mM). The spectrum is recorded in deuterated chloroform at 565 MHz at 25ºC. Obtained signals: D=5.30 e^{-10} m^2/s, V=1866 Å^3; D=9.13 e^{-10} m^2/s, V=365 Å^3.

A.1.1.3. ITC thermodynamic data.

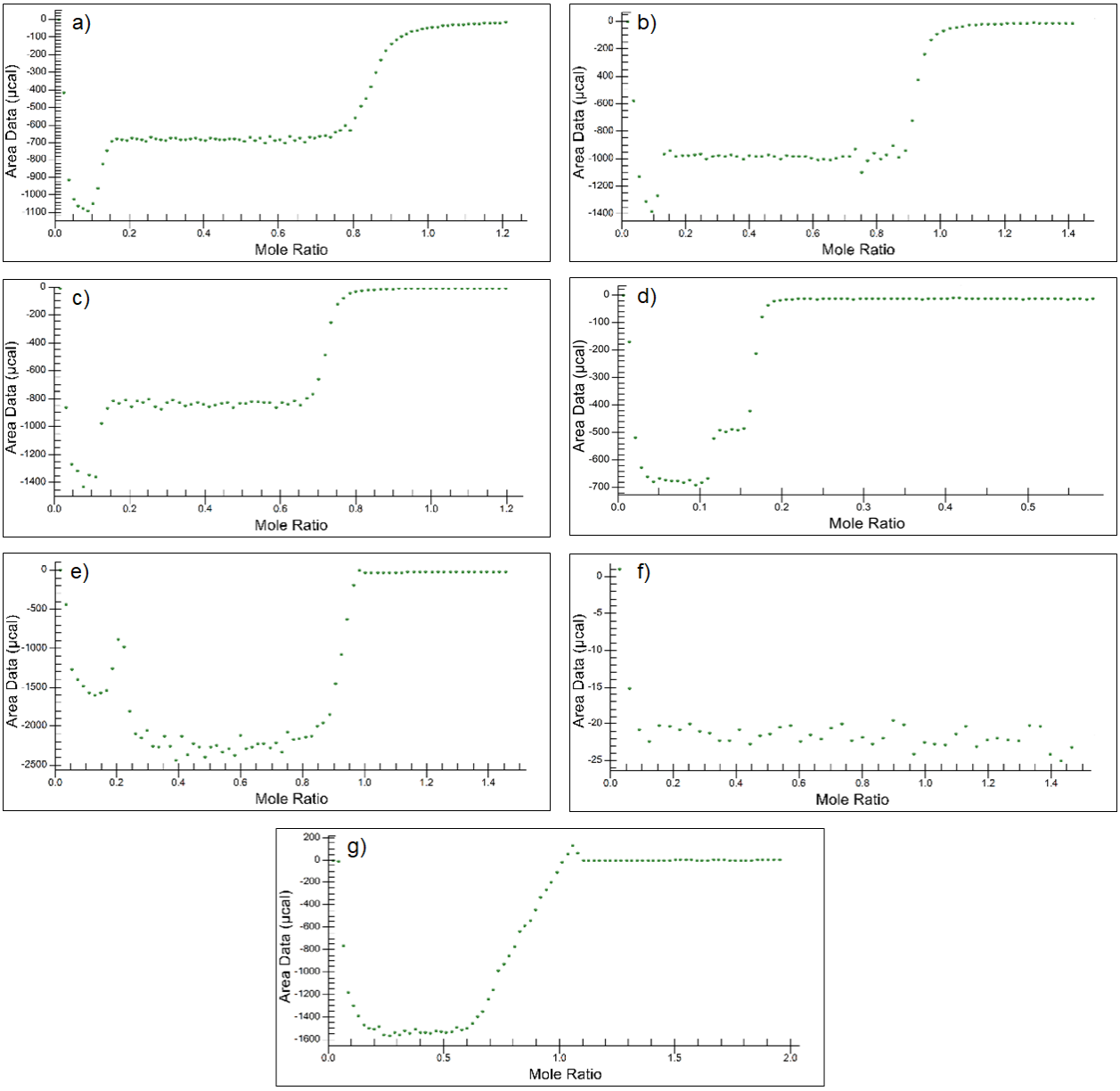

Figure SI 1.1.36 ITC integrated heat peaks of the thermograms shown in Figure 1.X. Integrated heats are expressed in µcal versus molar ratio of the reactants. a) reaction between **1.1** (sample cell, *c*= 3.82 mM) and **1.2a** (syringe, *c*= 47.43 mM) through 90 sequential additions (of 1.03 µL each), with a time delay of 2000 s; b) reaction between **1.1** (sample call, *c*= 3.63 mM) and **1.2b** (syringe, *c*= 6.63 mM) through 90 sequential additions (of 1.03 µL each) with a time delay of 2000 s; c) reaction between **1.1** (sample cell, *c*= 3.13 mM) and **1.2c** (syringe, *c*= 57.20 mM) through 90 sequential additions (of 1.03 µL each) with a time delay of 2000 s; d) reaction between **1.1** (sample cell, *c*= 3.01 mM) and **1.2d** (syringe, *c*= 21.11 mM) through 90 sequential additions (of 1.03 µL each) with a time delay of 1000 s; e) reaction between **1.1** (sample call, *c*= 3.10 mM) and **1.2e** (syringe, *c*= 55.25 mM) through 90 sequential additions (of 1.03 µL each) with a time delay of 3000 s; f) reaction between **1.1** (sample call, *c*= 3.04 mM) and **1.2f**

(syringe, *c*= 55.36 mM) through 45 sequential additions (of 2.06 µL each) with a time delay of 1500 s; g) reaction between **1.1** (sample call, *c*= 3.76 mM) and **1.2g** (syringe, *c*= 80.20 mM) through 90 sequential additions (of 2.06 µL each) with a time delay of 2000s.

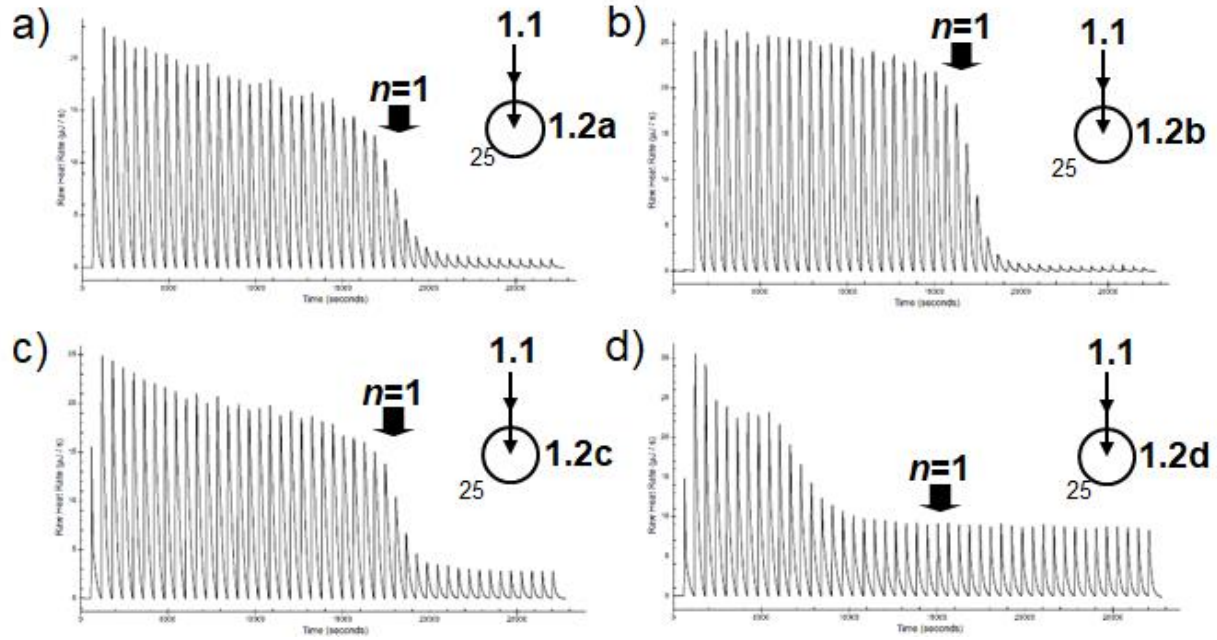

Figure SI 1.1.37. ITC thermograms in chlorobenzene at 25ºC a) reaction between **1.2a** (sample cell, c=2.00 mM) and **1.1** (syringe, c=40.00 mM) through 45 sequential additions (of 2.06 µL each) with a time delay between two consecutive injections of 600 s; b) thermogram of the reaction between **1.2b** (sample call, c= 2.00 mM) and **1.1** (syringe, *c*= 40.00 mM) through 45 sequential additions (of 2.06 µL each) with a 600 s time delay; c) thermogram of the reaction of **1.2c** (sample call, *c*= 2 mM) and **1.1** (syringe, *c*= 40 mM) through 45 sequential additions (of 2.06 µL each) with a 600 s time delay; d) ITC thermogram of the reaction between **1.2d** (sample cell, *c*=2.00 mM) and **1.1** (syringe, *c*= 40.00 mM) through 45 sequential additions (of 2.06 µL each) with a time delay of 600 s; Heat flow is expressed in µJ/s *vs* time in s and *n* represents the molar ratio between reactants, i.e. $n = n_{injected}/n_{cell}$.

Table SI 1.1.1 ITC results –model thermodynamic parameters - obtained from the sequential addition of the borane **1.1** into the cell contained the solution of the phosphine **1.2a-c** as well as from the sequential addition of the phosphine **1.2g** into the cell contained the solution of the borane **1.1**. The model values are obtained by employing independent model on integrated heat peaks.

System	ITC Model Δ*H* ± error		ITC Model Δ*G* ± error		ITC Model Δ*S* ± error		ITC Model n ± error		ITC Model K_a ± error		ITC Model K_d ± error	
	kcal/mol	kcal/mol	kcal/mol	kcal/mol	cal/molK	cal/molK			M^{-1}	M^{-1}	M	M
1.2a/1.1	-12.9	0.2	-7.0	-1.8	-19.7	-5.0	1.230	0.010	1.5E+05	3.7E+04	6.9E-06	1.7E-06
1.2b/1.1	-15.1	0.1	-7.6	-1.2	-25.2	-3.9	1.183	0.004	3.5E+05	5.3E+04	2.9E-06	4.4E-07
1.2c/1.1	-13.3	0.3	-7.0	-2.9	-21.2	-8.8	1.257	0.015	1.4E+05	5.7E+04	7.3E-06	3.0E-06
1.1/1.2g	-19.0	0.5	-6.4	-1.7	-42.4	-11.6	0.795	0.011	4.8E+04	1.3E+04	2.1E-05	5.7E-06

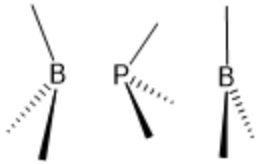

Figure SI 1.1.38 Schematic representation of the theoretical trimer considered within the calculation of the thermodynamic parameters of the system **1.1**/**1.2a**/**1.1**.

A.1.1.4. X-Ray data.

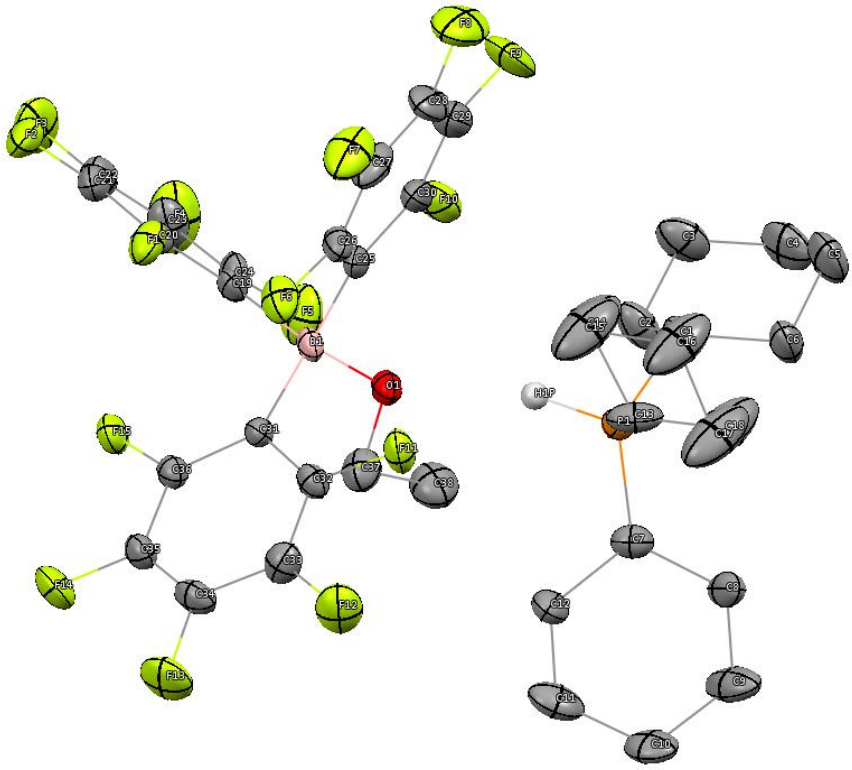

Figure SI 1.1.39 Ellipsoid type plot of the structure of **$(PhF_5)_3B$-OEt H-PCy_3** drawn at 30% of possibility level. Fully atom labelling is included. Atoms of hydrogen of the cyclohexyl groups are omitted for the sake of clarity.

Selected angles

Nº	Angle	Value [º]
1	P_1-H_1P-O_1	150.5
2	B_1-O_1-H_1P	111.5
3	P_1-H_1P -B_1	173.1

Selected distances

Nº	Distance	Value [Å]
1	B_1-P_1	4.585
2	H_1P- P_1	1.259
3	O_1-B_1	1.462
4	O_1-H_1P	2.506

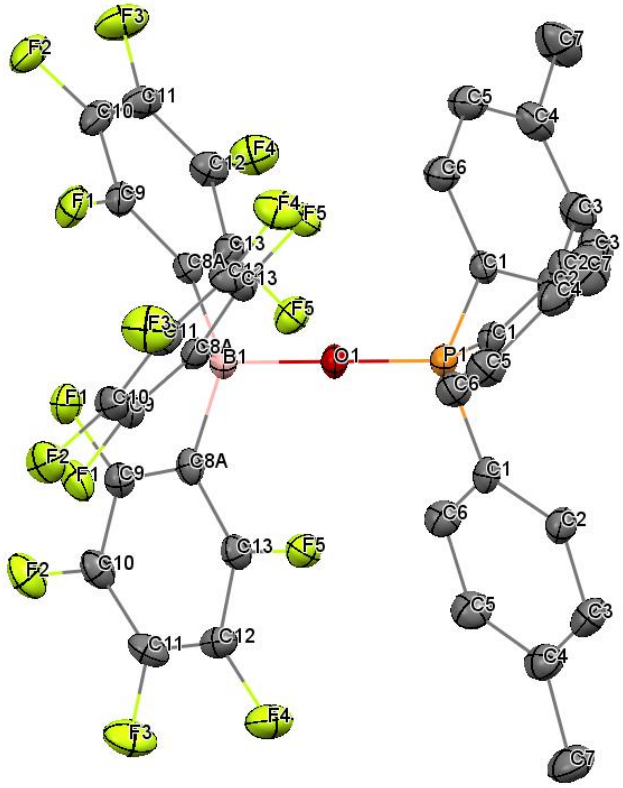

Figure SI 1.1.40 Ellipsoid type plot of the structure of (**$PhF_5)_3B$-O-P(*p*-MePh)$_3$** drawn at 30% of possibility level. Fully atom labelling is included. Atoms of hydrogen of the methyl-phenyl groups are omitted for the sake of clarity.

Selected distances

Nº	Distance	Value [Å]
1	B_1-O_1	1.526
2	P_1-O_1	1.502
3	B_1-P_1	3.028

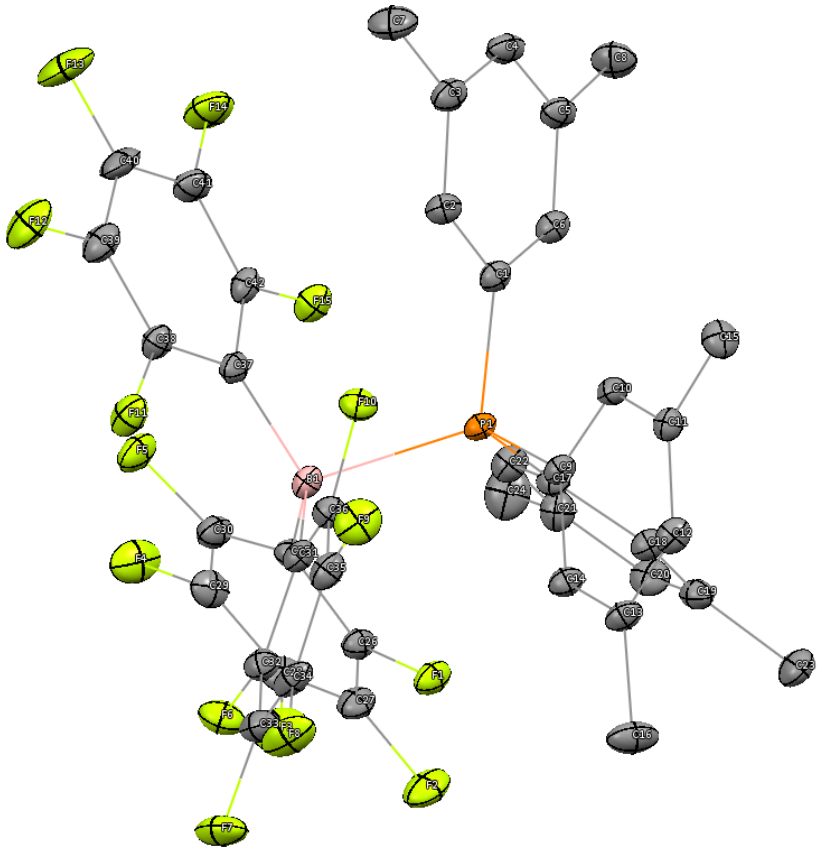

Figure SI 1.1.41 Ellipsoid type plot of the structure of **1.3c** ($(PhF_5)_3B$-P(*m*,*m*-$Me_2Ph)_3$) drawn at 30% of possibility level. Fully atom labelling is included. Atoms of hydrogen of the dimethyl-phenyl groups are omitted for the sake of clarity.

Selected distances

Nº	Distance	Value [Å]
1	B_1-P_1	2.199(4)

A.1.1.5. Mass spectra.

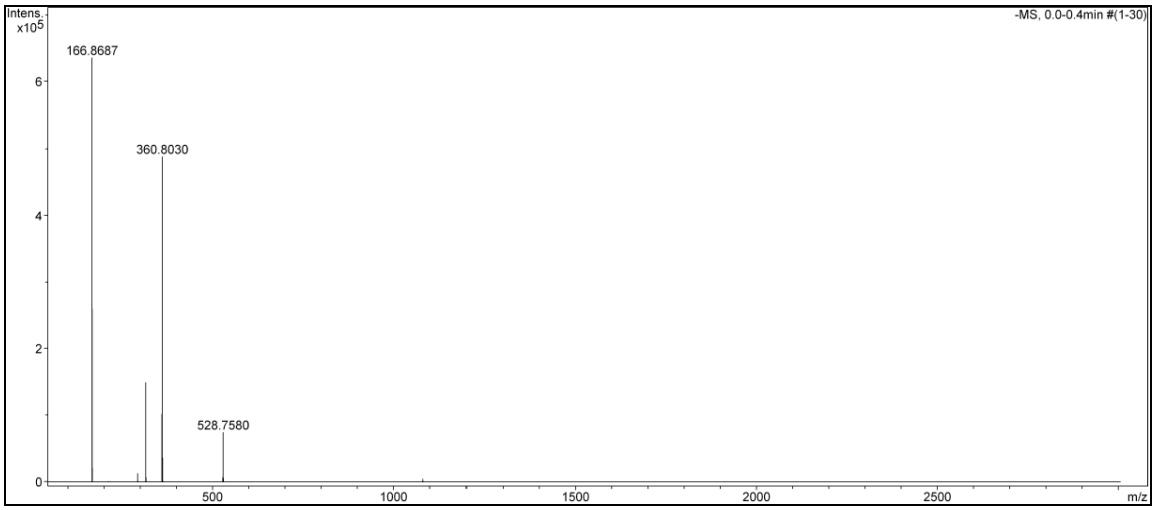

Figure SI 1.1.42a. Mass spectra of the Lewis pair **1.3a** ($(PhF_5)_3B$-PPh_3) recorded in negative charge mode. Molecular masses: **1.1** ($(PhF_5)_3B$) = 511.99; **1.2a** (PPh_3) = 262.09.

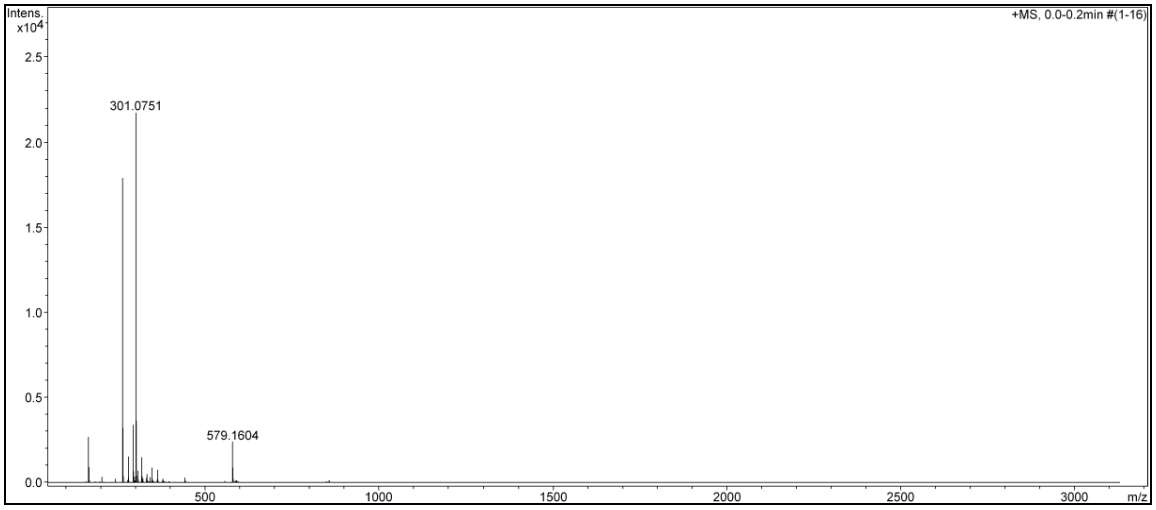

Figure SI 1.1.42b. Mass spectra of the Lewis pair **1.3a** ($(PhF_5)_3B$-PPh_3) recorded in positive charge mode. Molecular masses: **1.1** ($(PhF_5)_3B$) = 511.99; **1.2a** (PPh_3) = 262.09.

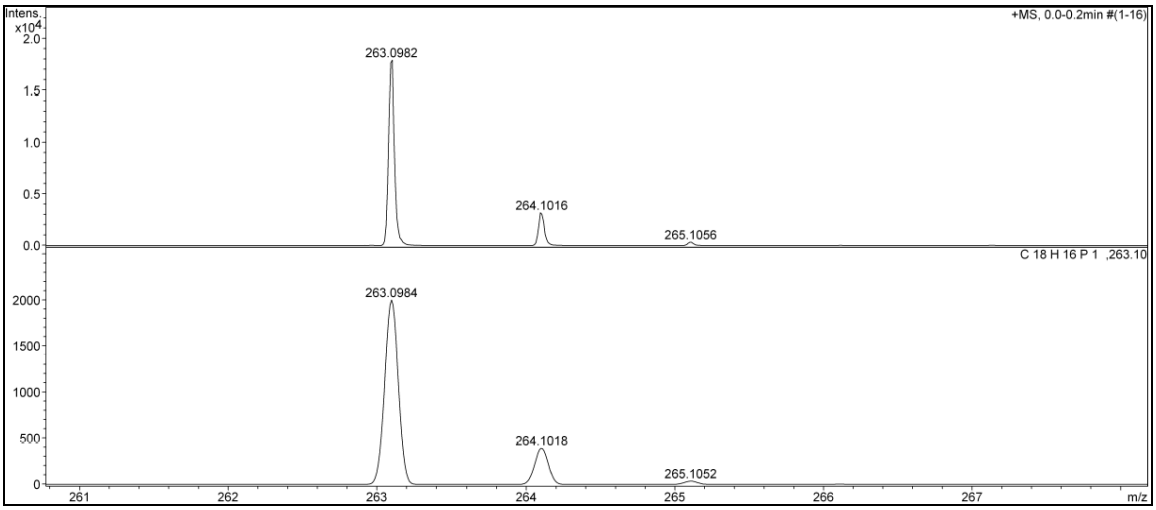

Figure SI 1.1.42c. Mass spectra of the Lewis pair **1.3a** ($(PhF_5)_3B$-PPh_3) – simulated; positive charge mode. Molecular masses: **1.1** ($(PhF_5)_3B$) = 511.99; **1.2a** (PPh_3) = 262.09.

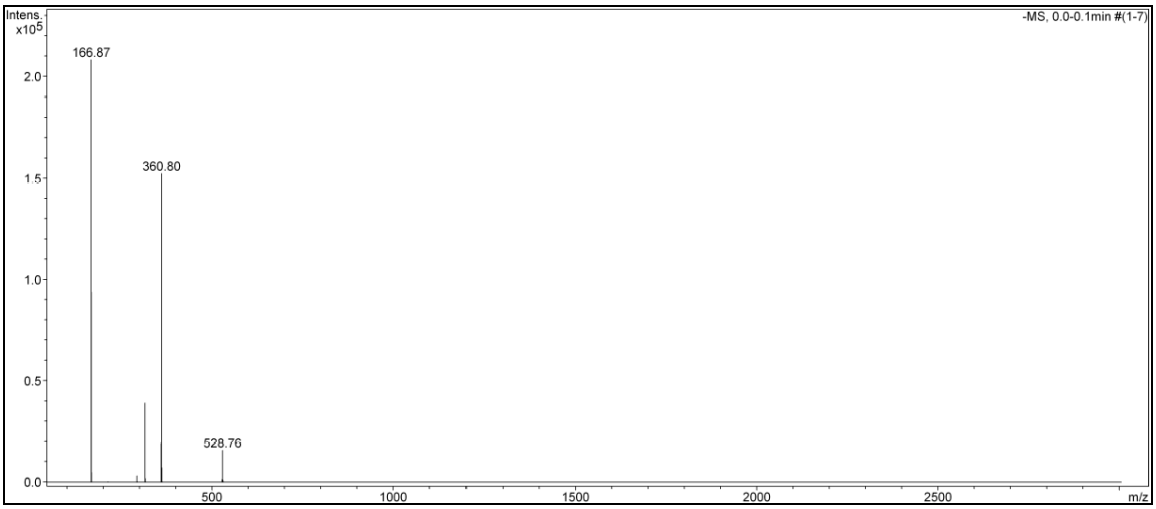

Figure SI 1.1.43a. Mass spectra of the Lewis pair **1.3b** ($(PhF_5)_3B$-P(*p*-MePh)$_3$) recorded in negative charge mode. Molecular masses: **1.1** ($(PhF_5)_3B$) = 511.99; **1.2b** (P(*p*-MePh)$_3$) = 304.14.

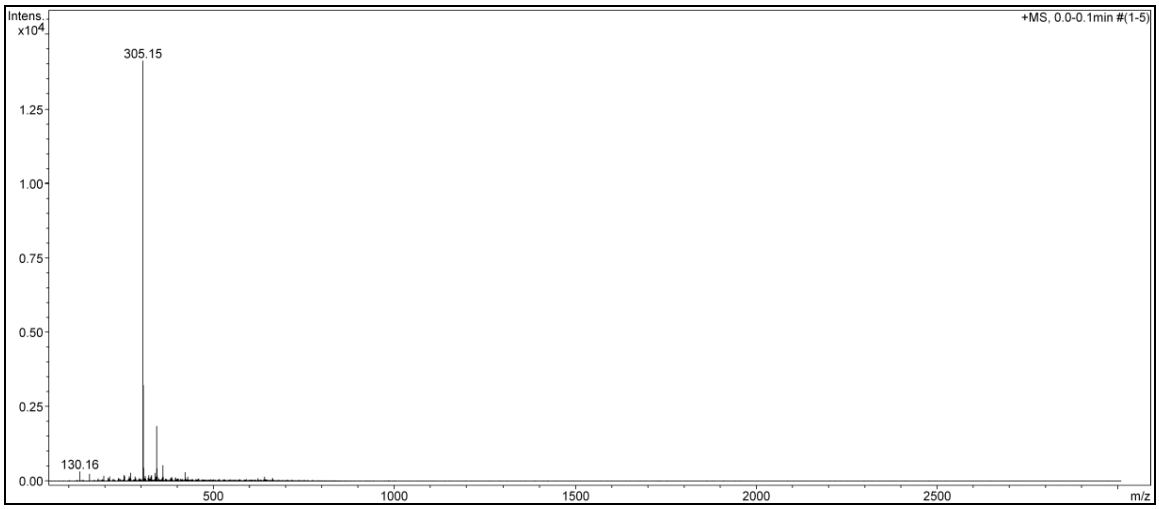

Figure SI 1.1.43b. Mass spectra of the Lewis pair **1.3b** ($(PhF_5)_3B$-P(*p*-MePh)$_3$) recorded in positive charge mode. Molecular masses: **1.1** ($(PhF_5)_3B$) = 511.99; **1.2b** (P(*p*-MePh)$_3$) = 304.14.

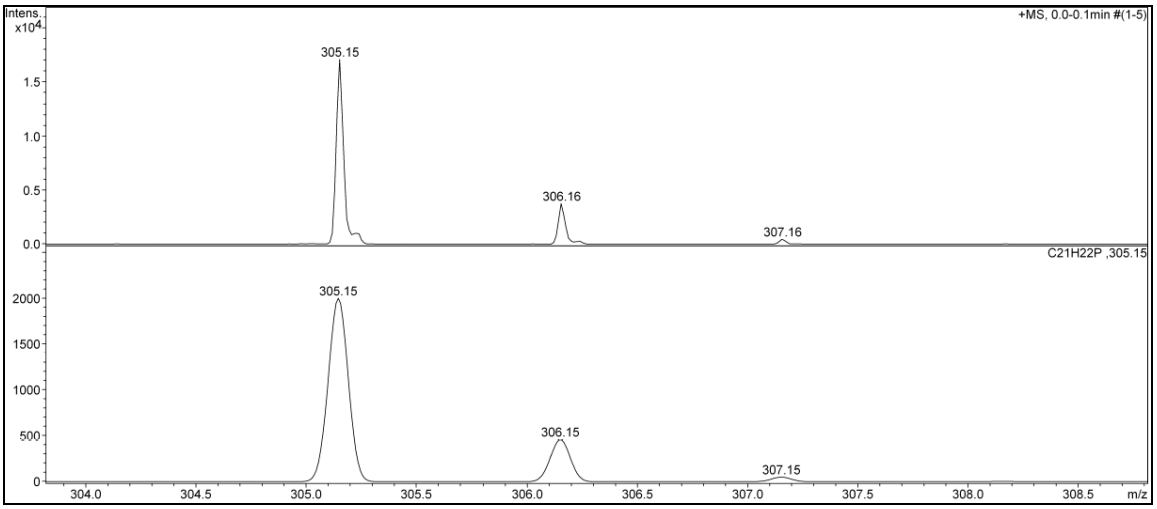

Figure SI 1.1.43c. Mass spectra of the Lewis pair **1.3b** ($(PhF_5)_3B$-P(*p*-MePh)$_3$) – simulated; positive charge mode. Molecular masses: **1.1** ($(PhF_5)_3B$) = 511.99; **1.2b** (P(*p*-MePh)$_3$) = 304.14.

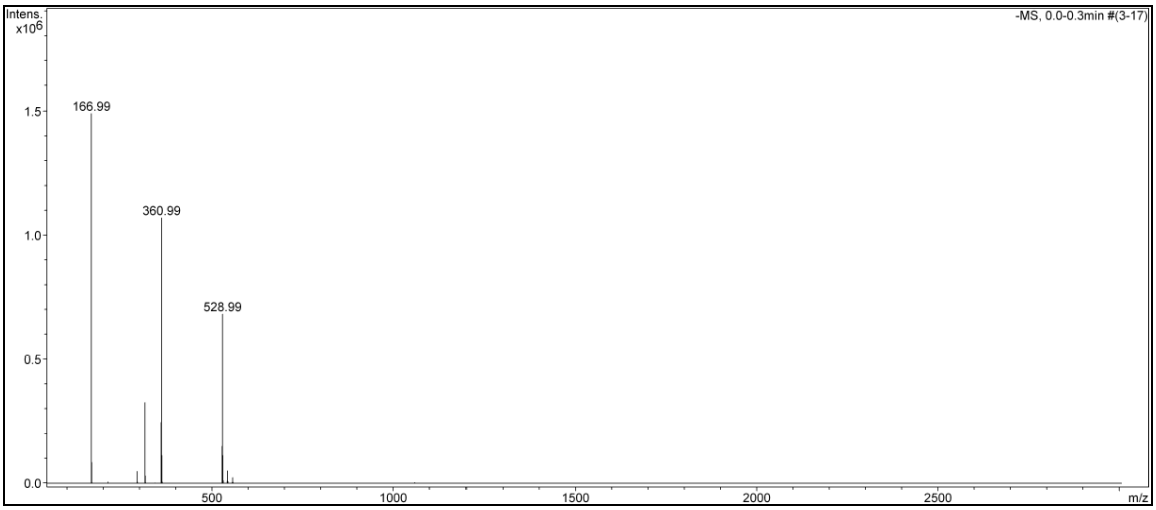

Figure SI 1.1.44a. Mass spectra of the Lewis pair **1.3c** ($(PhF_5)_3B$-P(*m*,*m*-$Me_2Ph)_3$) recorded in negative charge mode. Molecular masses: **1.1** ($(PhF_5)_3B$) = 511.99; **1.2c** (P(*m*,*m*-$Me_2Ph)_3$) = 346.19.

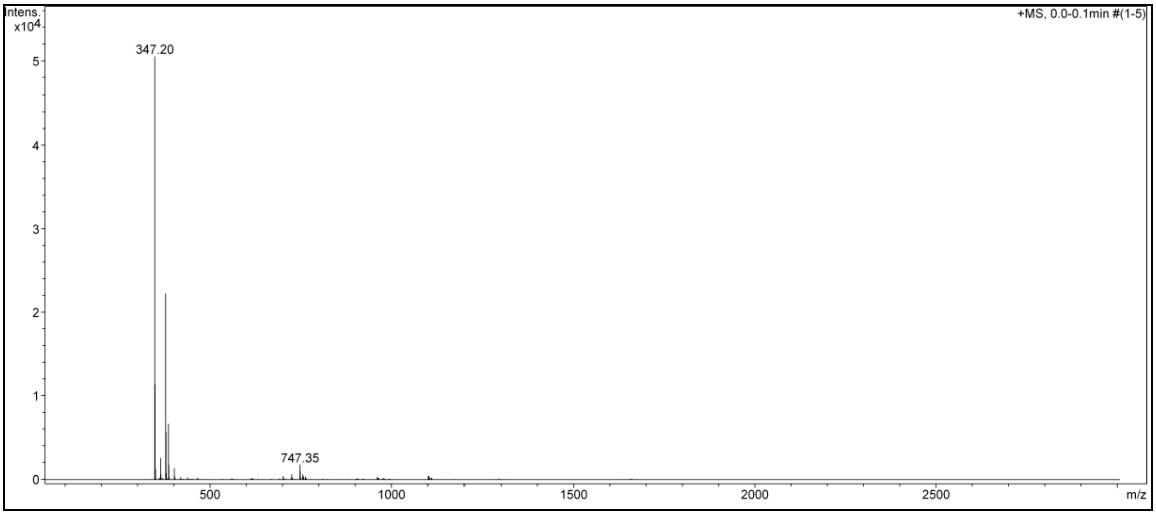

Figure SI 1.1.44b. Mass spectra of the Lewis pair **1.3c** ($(PhF_5)_3B$-P(*m*,*m*-$Me_2Ph)_3$) recorded in positive charge mode. Molecular masses: **1.1** ($(PhF_5)_3B$) = 511.99; **1.2c** (P(*m*,*m*-$Me_2Ph)_3$) = 346.19.

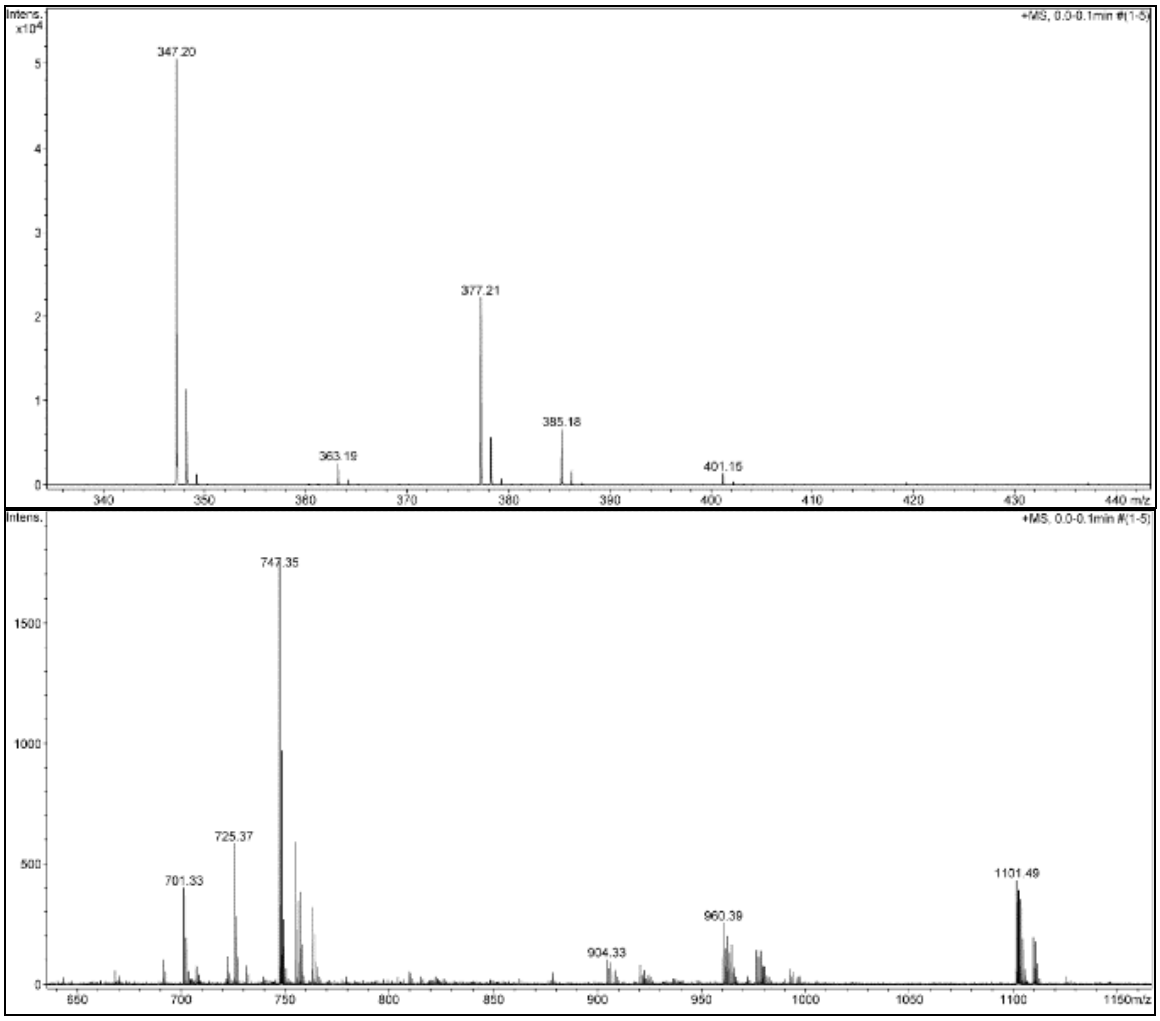

Figure SI 1.1.44c. Mass spectra of the Lewis pair **1.3c** ($(PhF_5)_3B$-P(*m*,*m*-$Me_2Ph)_3$) recorded in positive charge mode – zoomed. Molecular masses: **1.1** ($(PhF_5)_3B$) = 511.99; **1.2c** (P(*m*,*m*-$Me_2Ph)_3$) = 346.19.

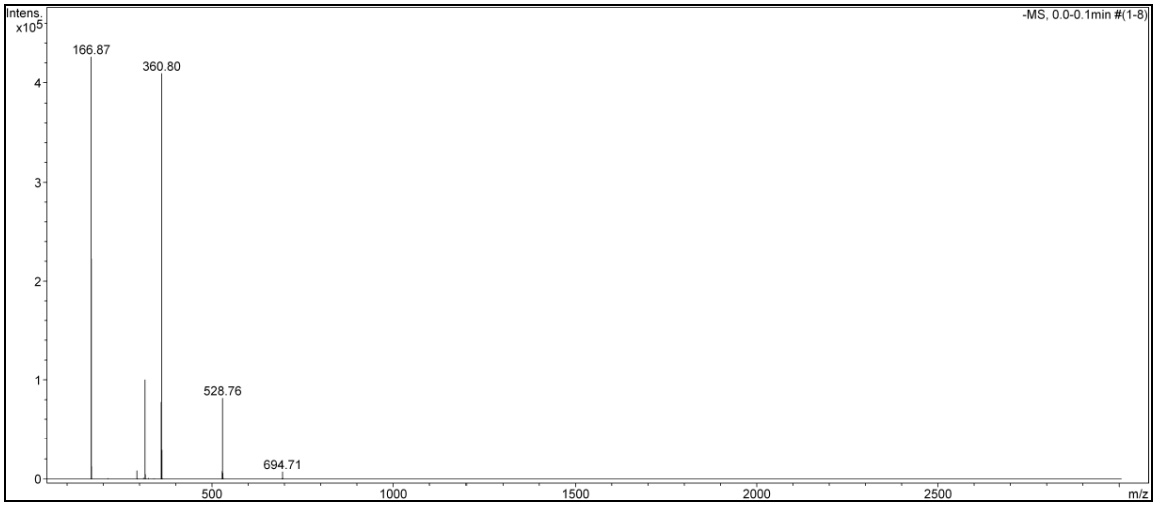

Figure SI 1.1.45a. Mass spectra of the Lewis pair **1.3d** ($(PhF_5)_3B$-P(*o*,*p*,*o*-$Me_3Ph)_3$) recorded in negative charge mode. Molecular masses: **1.1** ($(PhF_5)_3B$) = 511.99; **1.2d** (P(*o*,*p*,*o*-$Me_3Ph)_3$) = 388.23.

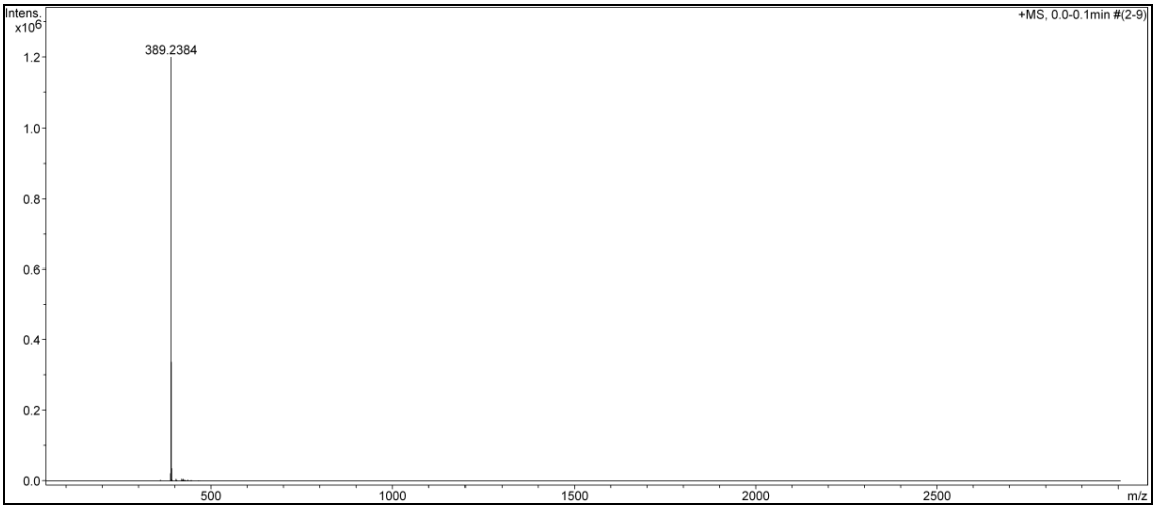

Figure SI 1.1.45b. Mass spectra of the Lewis pair **1.3d** ($(PhF_5)_3B$-P(*o*,*p*,*o*-$Me_3Ph)_3$) recorded in positive charge mode. Molecular masses: **1.1** ($(PhF_5)_3B$) = 511.99; **1.2d** (P(*o*,*p*,*o*-$Me_3Ph)_3$) = 388.23.

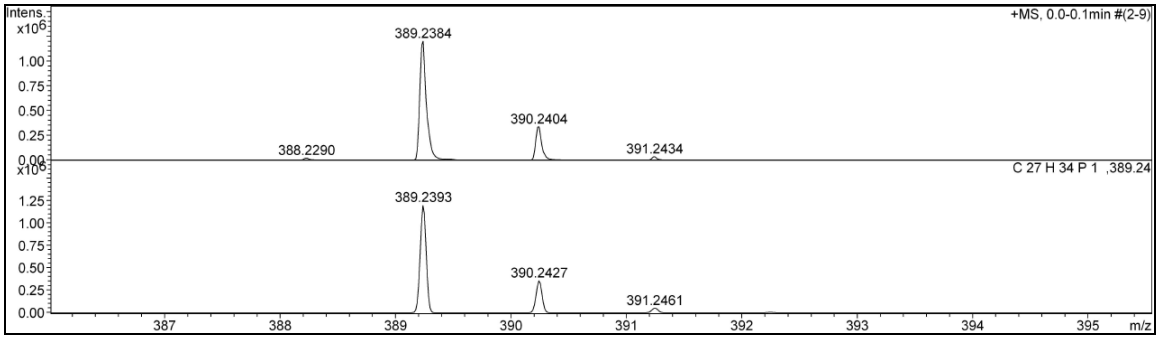

Figure SI 1.1.45c. Mass spectra of the Lewis pair **1.3d** ($(PhF_5)_3B$-P(*o*,*p*,*o*-$Me_3Ph)_3$) – Mass Spectrum Molecular Formula Report. Molecular masses: **1.1** ($(PhF_5)_3B$) = 511.99; **1.2d** (P(*o*,*p*,*o*-$Me_3Ph)_3$) = 388.23.

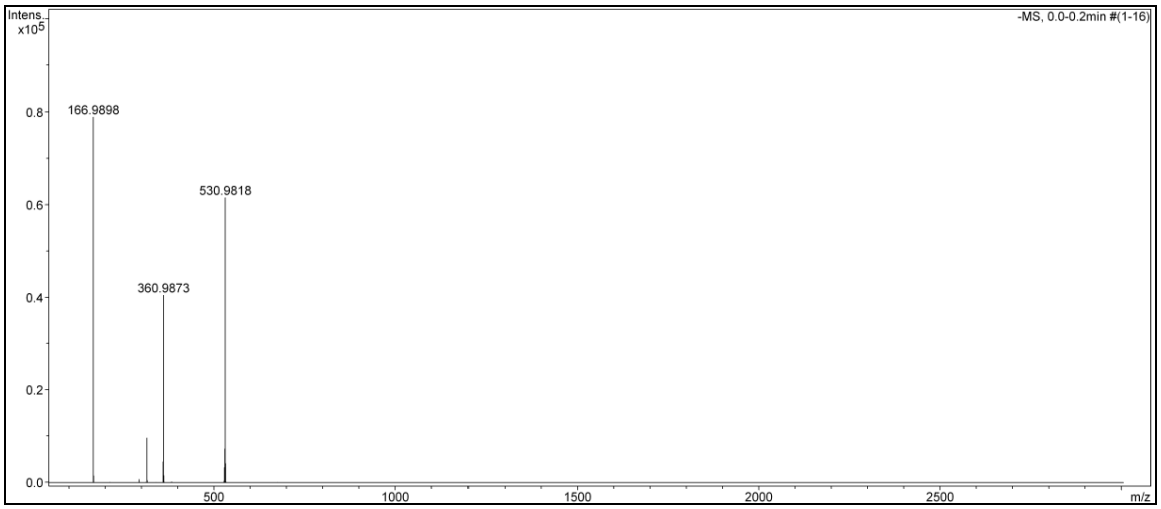

Figure SI 1.1.46a. Mass spectra of the Lewis pair **1.3e** ($(PhF_5)_3B$-PCy_3) recorded in negative charge mode. Molecular masses: **1.1** ($(PhF_5)_3B$) = 511.99; **1.2e** (PCy_3) = 280.23.

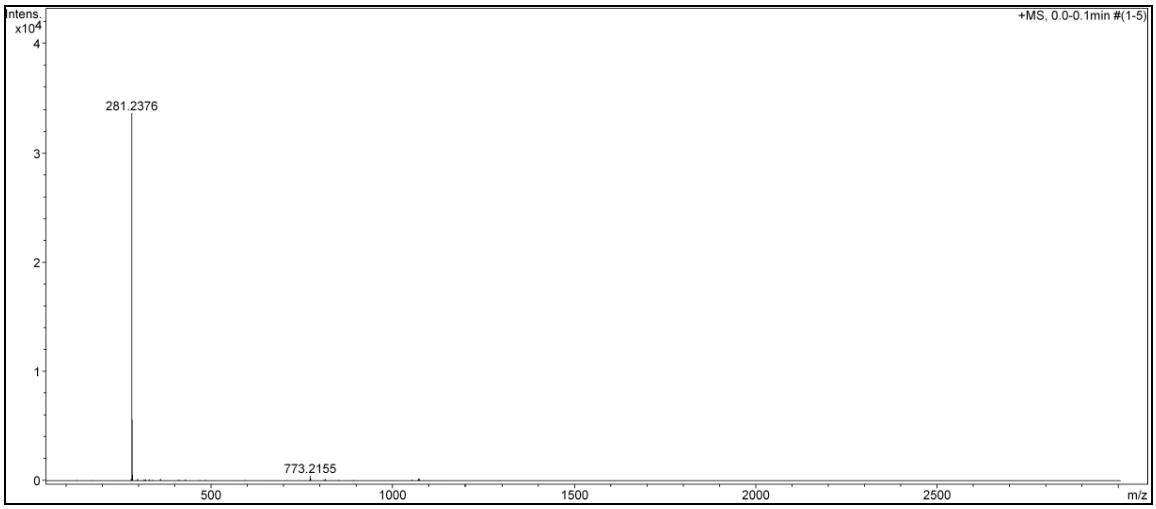

Figure SI 1.1.46b. Mass spectra of the Lewis pair **1.3e** ($(PhF_5)_3B$-PCy_3) recorded in positive charge mode. Molecular masses: **1.1** ($(PhF_5)_3B$) = 511.99; **1.2e** (PCy_3) = 280.23.

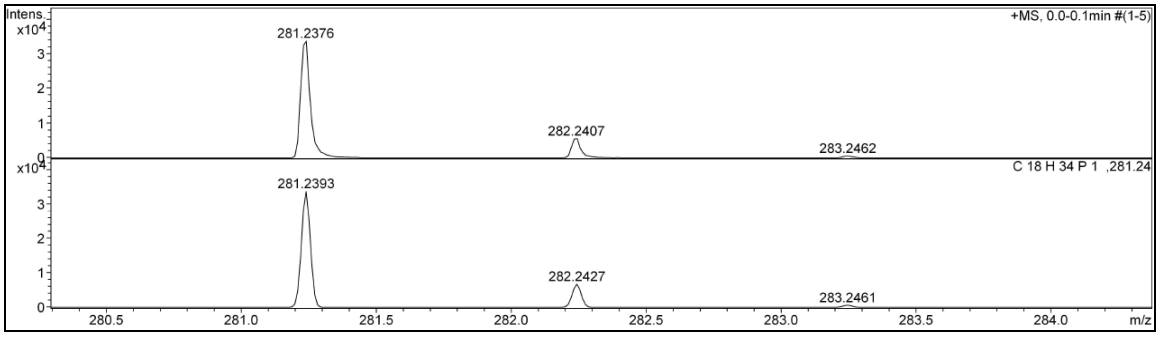

Figure SI 1.1.46b. Mass spectra of the Lewis pair **1.3e** ($(PhF_5)_3B$-PCy_3) – Mass Spectrum Molecular Formula Report. Molecular masses: **1.1** ($(PhF_5)_3B$) = 511.99; **1.2e** (PCy_3) = 280.23.

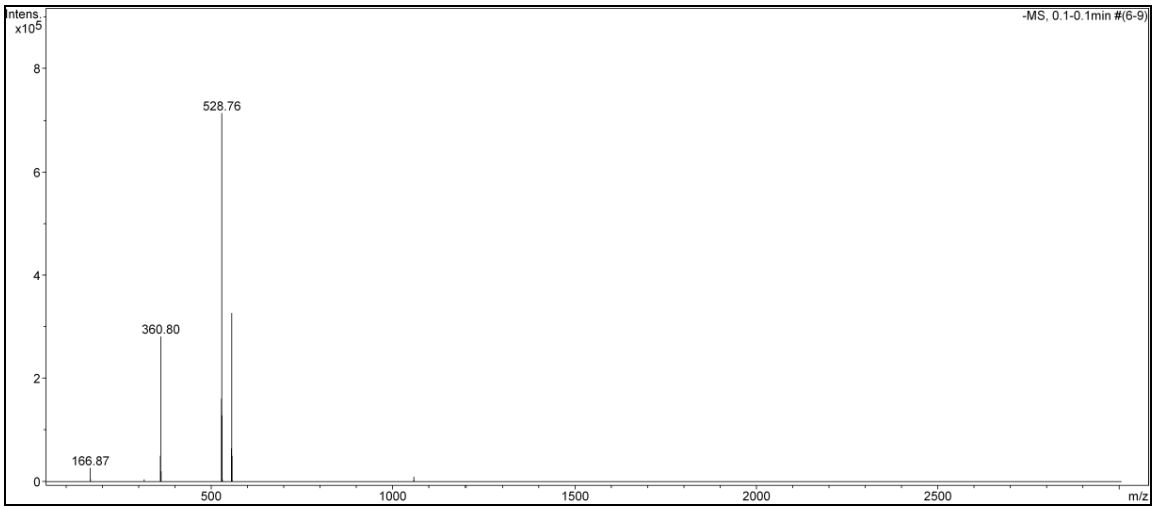

Figure SI 1.1.47a. Mass spectra of the Lewis pair **1.3f** ($(PhF_5)_3B$-$P(PhF_5)_3$) recorded in negative charge mode. Molecular masses: **1.1** ($(PhF_5)_3B$) = 511.99; **1.2f** ($P(PhF_5)_3$) = 531.95.

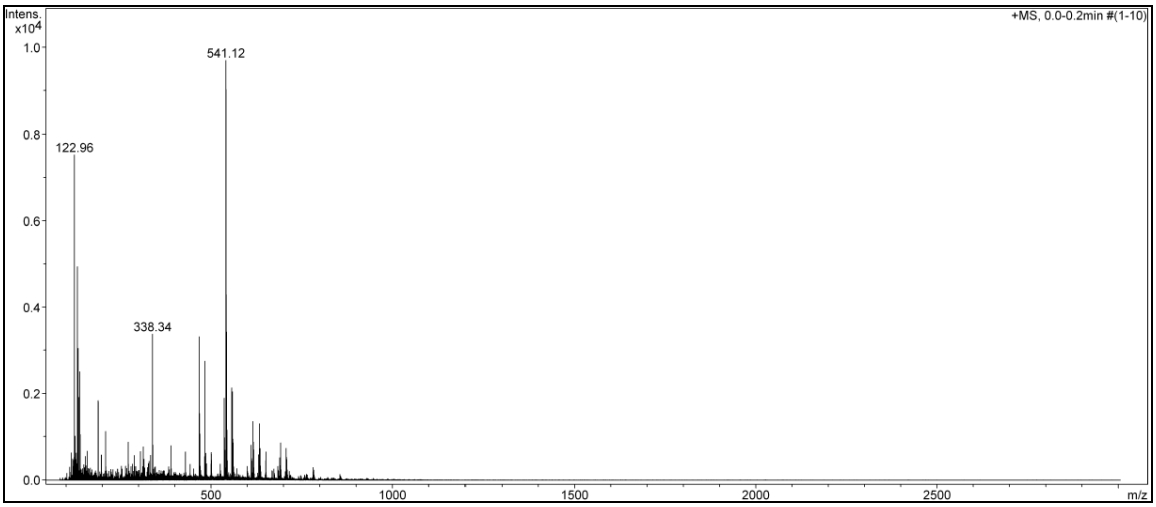

Figure SI 1.1.47b. Mass spectra of the Lewis pair **1.3f** ($(PhF_5)_3B$-$P(PhF_5)_3$) recorded in positive charge mode. Molecular masses: **1.1** ($(PhF_5)_3B$) = 511.99; **1.2f** ($P(PhF_5)_3$) = 531.95.

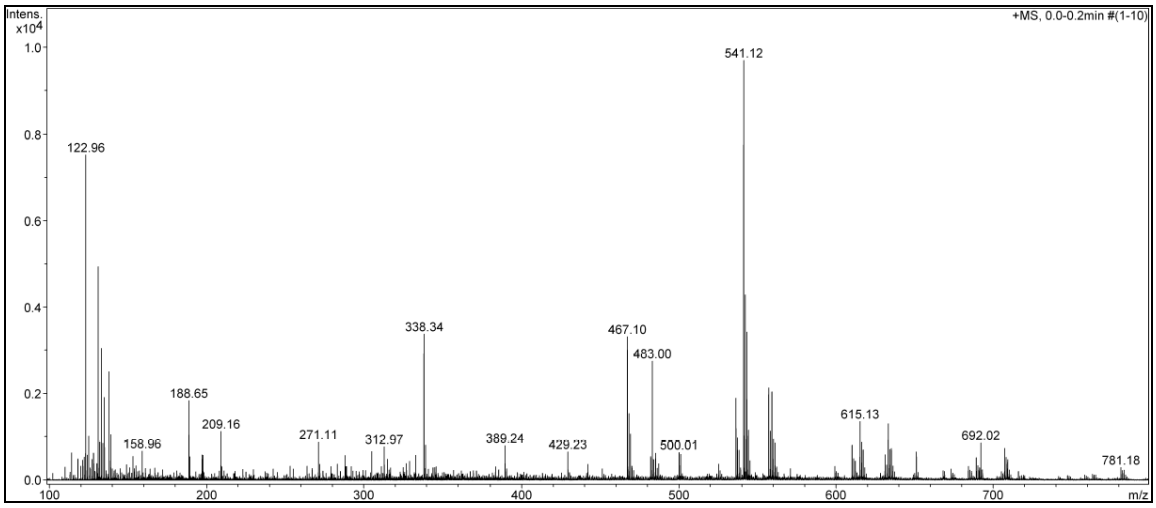

Figure SI 1.1.47b. Mass spectra of the Lewis pair **1.3f** ($(PhF_5)_3B$-$P(PhF_5)_3$) recorded in positive charge mode - zoomed. Molecular masses: **1.1** ($(PhF_5)_3B$) = 511.99; **1.2f** ($P(PhF_5)_3$) = 531.95.

A.1.1.6. Elemental analysis data.

Compound		%N	%C	%H
1.3b	Valeur Théorique		57.1	2.94
			56.76	2.86
	Attendue		**57.38**	**2.59**
1.3c	Valeur Théorique		59.71	3.31
			59.62	3.27
	Attendue		**58.77**	**3.17**
1.3f	Valeur Théorique		42.87	1.03
			42.6	1.19
	Attendue		**41.41**	**0**
1.3e	Valeur Théorique		54.2	3.88
			54.36	3.93
	Attendue		**54.57**	**4.2**

A.1.1.7. Cartesian's coordinates of the optimized geometries of the investigated systems within the study of the formation the (frustrated) Lewis pairs form the borane (1.1) and various phosphines (1.2a-g).

[**1.1**] - tris(pentafluorophenyl)borane ($B(PhF_5)_3$) - GGAPBE-D3/def2TZVP_gas phase

F	5.104167	1.191482	-0.426605
F	2.564948	0.301779	-0.427615
F	0.666124	1.568279	-1.926361
F	1.327445	3.751908	-3.426449
F	3.853925	4.676867	-3.430155
C	4.596831	2.976472	-1.928330
C	4.206589	1.846839	-1.188106
C	2.898222	1.369387	-1.165100
C	1.922519	2.018393	-1.926979
C	2.263463	3.139056	-2.689545
C	3.577409	3.601015	-2.667900
B	6.070462	3.504739	-1.928418
F	4.552121	5.497782	-0.424425
F	8.555686	3.823675	-0.424307
F	5.051236	8.141776	-0.425524
F	10.596077	2.069830	-0.425165
F	7.095605	9.153194	-1.926669
F	10.450007	-0.206809	-1.925642
F	8.654212	7.488936	-3.428924
F	8.229371	-0.725207	-3.427581
F	8.192061	4.838248	-3.432330
F	6.164645	1.000076	-3.431328
C	6.349866	5.045089	-1.928331
C	7.264856	2.492752	-1.928000
C	5.567561	5.947664	-1.187019
C	8.437678	2.719268	-1.186798
C	5.808273	7.319467	-1.164073
C	9.505465	1.825057	-1.163671
C	6.857229	7.840056	-1.927183
C	9.431909	0.656112	-1.926425

C	7.656373	6.984596	-2.690880
C	8.291462	0.391402	-2.689965
C	7.399546	5.615688	-2.669085
C	7.234265	1.298145	-2.668382

[**1.1**] - tris(pentafluorophenyl)borane ($B(PhF_5)_3$) - GGAPBE-D3/def2TZVP_PhCl (PCM) phase

F	5.099721	1.189965	-0.426018
F	2.560443	0.303039	-0.429289
F	0.663643	1.570781	-1.930576
F	1.328610	3.754474	-3.430056
F	3.854666	4.677546	-3.431021
C	4.596251	2.976178	-1.928501
C	4.203738	1.847304	-1.188902
C	2.895386	1.371447	-1.167555
C	1.921136	2.020279	-1.929812
C	2.264147	3.139981	-2.691230
C	3.577802	3.601017	-2.668652
B	6.070330	3.503442	-1.927261
F	4.561013	5.496121	-0.412260
F	8.555155	3.822367	-0.420283
F	5.059445	8.139836	-0.415135
F	10.596256	2.071000	-0.421264
F	7.094270	9.153010	-1.929213
F	10.454107	-0.204718	-1.924564
F	8.644444	7.489131	-3.441573
F	8.233901	-0.724407	-3.427920
F	8.184244	4.838674	-3.441976
F	6.167806	0.997673	-3.431163
C	6.350105	5.043982	-1.927228
C	7.265118	2.491698	-1.926053
C	5.572542	5.946154	-1.181296
C	8.437265	2.718135	-1.184277
C	5.813086	7.317439	-1.159727
C	9.505419	1.825217	-1.161795
C	6.856308	7.838901	-1.928475

C	9.434329	0.657510	-1.925015
C	7.650380	6.983948	-2.696313
C	8.294889	0.392819	-2.688445
C	7.394820	5.615385	-2.673507
C	7.236834	1.297684	-2.666916

[**1.2a**] - triphenylphosphine (Ph_3P) - GGAPBE-D3/def2TZVP_gas phase

P	3.324746	0.711719	0.052217
C	4.188183	1.449715	1.504693
C	3.745002	2.713137	1.932964
C	5.234419	0.828719	2.203598
C	4.347908	3.350061	3.017828
H	2.919391	3.199625	1.407030
C	5.827178	1.460585	3.299859
H	5.588220	-0.154442	1.888279
C	5.390234	2.723067	3.706824
H	3.995742	4.334084	3.333496
H	6.638874	0.963764	3.835322
H	5.855641	3.215238	4.562791
C	3.977661	-1.012674	0.059797
C	3.316019	-1.938783	0.884817
C	5.068522	-1.450158	-0.706618
C	3.748253	-3.262996	0.959681
H	2.454457	-1.613962	1.473982
C	5.490836	-2.780599	-0.642969
H	5.591441	-0.746129	-1.356333
C	4.836686	-3.688572	0.192521
H	3.227091	-3.967874	1.610455
H	6.339947	-3.106826	-1.247117
H	5.169279	-4.727076	0.241559
C	4.248088	1.460019	-1.357456
C	3.701703	1.282786	-2.640478
C	5.436051	2.194881	-1.225264
C	4.338947	1.806875	-3.765324
H	2.767692	0.726441	-2.754548

C	6.065134	2.732980	-2.350940
H	5.872249	2.346514	-0.236349
C	5.522573	2.536972	-3.622781
H	3.904535	1.654536	-4.755297
H	6.987856	3.304680	-2.231978
H	6.016538	2.957210	-4.500799

[**1.2a**] - triphenylphosphine (Ph_3P) - GGAPBE-D3/def2TZVP_PhCl (PCM) phase

P	3.331527	0.711760	0.051823
C	4.189573	1.452036	1.505930
C	3.738353	2.711383	1.939001
C	5.241693	0.835437	2.200520
C	4.338866	3.348420	3.025978
H	2.909534	3.196386	1.416686
C	5.832616	1.467269	3.298385
H	5.603076	-0.143698	1.881223
C	5.387042	2.725629	3.711081
H	3.980727	4.328927	3.345561
H	6.649033	0.974384	3.830119
H	5.850668	3.217925	4.567858
C	3.978756	-1.014433	0.060715
C	3.313872	-1.939796	0.884645
C	5.070550	-1.453030	-0.704262
C	3.743727	-3.265483	0.958880
H	2.452482	-1.615599	1.474473
C	5.490942	-2.784615	-0.641105
H	5.597115	-0.750052	-1.352174
C	4.833134	-3.692454	0.192730
H	3.220526	-3.969752	1.608543
H	6.340825	-3.111622	-1.243593
H	5.163945	-4.731458	0.241682
C	4.250463	1.460251	-1.360142
C	3.699834	1.286773	-2.642285
C	5.441508	2.190900	-1.229189
C	4.336131	1.811740	-3.768061

H	2.764534	0.732732	-2.757361
C	6.070172	2.729372	-2.355514
H	5.882093	2.338803	-0.241636
C	5.523099	2.537819	-3.626832
H	3.898908	1.662553	-4.757188
H	6.995364	3.297159	-2.237790
H	6.016405	2.957851	-4.505238

[**1.2b**] - tri-p-tolylphosphine $((PhMe)_3P)$ - GGAPBE-D3/def2TZVP_gas phase

P	0.447958	0.133167	0.022747
C	1.284017	0.876507	1.486685
C	0.844640	2.144612	1.903727
C	2.316207	0.262282	2.210018
C	1.433230	2.783146	2.993222
H	0.033735	2.637964	1.361297
C	2.891433	0.900986	3.310490
H	2.677277	-0.722811	1.908643
H	1.080154	3.773908	3.291503
H	3.695978	0.403169	3.858568
C	1.086299	-1.594720	0.060609
C	0.405276	-2.514477	0.876393
C	2.192162	-2.050571	-0.670948
C	0.830590	-3.837718	0.972266
H	-0.466309	-2.184120	1.447719
C	2.603766	-3.382005	-0.582518
H	2.740198	-1.358383	-1.312939
C	1.935251	-4.299022	0.239394
H	0.289919	-4.531055	1.622039
H	3.469790	-3.714395	-1.161330
C	1.409110	0.860935	-1.370401
C	0.888940	0.698452	-2.665714
C	2.612564	1.565450	-1.223471
C	1.561698	1.205220	-3.775702
H	-0.053608	0.161918	-2.803221
C	3.273925	2.084044	-2.338458

H	3.039697	1.707062	-0.228907
C	2.764895	1.913572	-3.632912
H	1.141299	1.056738	-4.773920
H	4.211746	2.628782	-2.199610
C	2.464632	2.170629	3.722004
C	3.067766	2.844881	4.925751
H	4.072096	2.456081	5.143696
H	3.142861	3.932423	4.782547
H	2.448929	2.677924	5.822487
C	3.466115	2.498297	-4.830315
C	2.364880	-5.740418	0.311562
H	4.535862	2.654448	-4.633628
H	3.369028	1.847677	-5.711245
H	3.035712	3.476472	-5.100370
H	3.417465	-5.861609	0.020456
H	2.238512	-6.147961	1.324890
H	1.762139	-6.365937	-0.366968

[**1.2c**] - tris(3,5-dimethylphenyl)phosphine ($(PhMe_2)_3P$) - GGAPBE-D3/def2TZVP_gas phase

P	-1.254646	-0.164244	-0.118391
C	-0.343364	0.603647	-1.525451
C	-0.960899	1.693615	-2.161011
C	0.903060	0.164852	-1.986071
C	-0.341669	2.359216	-3.223132
H	-1.942133	2.031463	-1.814603
C	1.537878	0.798479	-3.064959
H	1.392372	-0.681795	-1.499063
C	0.906717	1.893873	-3.663899
H	1.396927	2.398012	-4.502636
C	-0.258919	-1.685513	0.188064
C	0.756763	-1.779624	1.146198
C	-0.560268	-2.808859	-0.599678
C	1.472599	-2.973040	1.324374
H	0.999492	-0.912381	1.764548
C	0.152063	-4.003829	-0.460844

H	-1.363454	-2.745558	-1.339865
C	1.162937	-4.067825	0.510332
H	1.719925	-5.001261	0.638356
C	-0.744015	0.909552	1.290758
C	-1.425882	0.727882	2.505467
C	0.262739	1.878565	1.214596
C	-1.098473	1.476895	3.639625
H	-2.223982	-0.017945	2.566699
C	0.596982	2.661492	2.329878
H	0.799552	2.028642	0.275086
C	-0.086116	2.442634	3.530862
H	0.171752	3.044744	4.407731
C	2.861193	0.290197	-3.576911
C	-0.989371	3.552840	-3.876536
C	-0.146796	-5.193440	-1.336421
C	2.535920	-3.073426	2.387800
C	1.655245	3.729294	2.222625
C	-1.804832	1.251015	4.951560
H	-0.956664	3.477341	-4.973604
H	-2.039599	3.655833	-3.571972
H	-0.469860	4.484671	-3.601174
H	2.714154	-0.526344	-4.302448
H	3.429441	1.082196	-4.084474
H	3.479451	-0.109757	-2.760728
H	2.453055	3.433925	1.526474
H	1.226006	4.670883	1.843245
H	2.111297	3.945989	3.198764
H	-2.106722	2.202337	5.414318
H	-2.703683	0.633290	4.821819
H	-1.147836	0.736011	5.670711
H	0.642541	-5.336275	-2.091847
H	-0.202493	-6.121473	-0.748342
H	-1.098407	-5.069094	-1.870623
H	3.056276	-2.115019	2.525603
H	2.094254	-3.345572	3.360245
H	3.283604	-3.840088	2.140747

[**1.2d**] - trimesitylphosphine ($(PhMe_3)_3P$) - GGAPBE-D3/def2TZVP_gas phase

P	0.227048	-0.340256	0.466590
C	-0.334766	-2.086559	0.452253
C	0.156629	-2.862093	1.540673
C	-1.076821	-2.732937	-0.570568
C	-0.087096	-4.238115	1.576043
C	-1.273804	-4.118295	-0.493490
C	-0.787691	-4.894728	0.560764
H	0.289137	-4.814288	2.426483
H	-1.852797	-4.603964	-1.284726
C	0.065460	0.404832	-1.202323
C	-0.875734	1.387108	-1.607186
C	1.090735	0.018312	-2.111575
C	-0.745621	1.969325	-2.875252
C	1.160660	0.618450	-3.372162
C	0.262128	1.610729	-3.773250
H	-1.481002	2.720731	-3.178186
H	1.948986	0.299537	-4.060361
C	-0.720978	0.632145	1.700272
C	-1.921429	0.242796	2.349758
C	-0.078607	1.836515	2.105590
C	-2.417675	1.037957	3.391541
C	-0.629659	2.601498	3.137719
C	-1.792301	2.214809	3.809593
H	-3.347185	0.730593	3.880130
H	-0.127241	3.529253	3.426865
C	-0.996036	-6.385267	0.594210
C	0.909987	-2.236524	2.685739
C	-1.719978	-2.009369	-1.725546
C	-2.737801	-0.959986	1.952229
C	-2.340903	3.027639	4.951765
C	1.171027	2.337134	1.428876
C	2.093480	-1.052723	-1.768995
C	0.385929	2.279212	-5.116391
C	-2.054237	1.814821	-0.770938

H	2.885084	-1.103436	-2.528517
H	2.551301	-0.867172	-0.784107
H	1.621699	-2.046497	-1.703592
H	-1.764447	2.471252	0.062870
H	-2.777611	2.360258	-1.392029
H	-2.569451	0.955970	-0.319820
H	0.784138	1.589849	-5.874497
H	-0.584237	2.656670	-5.469039
H	1.073023	3.139848	-5.066088
H	-0.990057	-1.696722	-2.486880
H	-2.456362	-2.661528	-2.214382
H	-2.234679	-1.094898	-1.401036
H	-1.090802	-6.755910	1.624831
H	-1.897664	-6.678214	0.038075
H	-0.143269	-6.912531	0.135837
H	1.333204	-3.008513	3.342251
H	1.723753	-1.590250	2.319413
H	0.259302	-1.590565	3.297109
H	1.594140	3.191482	1.973986
H	1.930814	1.542080	1.360529
H	0.972882	2.659344	0.393813
H	-2.282318	-1.906499	2.278957
H	-3.739883	-0.898108	2.397810
H	-2.852036	-1.035457	0.862307
H	-2.136469	4.099497	4.818339
H	-3.426904	2.893945	5.055759
H	-1.881270	2.724931	5.906980

[**1.2e**] - tricyclohexylphosphine (Cy_3P) - GGAPBE-D3/def2TZVP_gas phase

P	0.827271	-0.192202	-0.087749
C	1.768208	0.486304	1.415543
C	1.068277	1.780073	1.882314
C	1.889844	-0.478630	2.606322
H	2.793269	0.739554	1.083240
C	1.800613	2.443135	3.054212

H	0.038624	1.522877	2.188643
H	0.962818	2.490040	1.048661
C	2.615315	0.173361	3.792676
H	0.879837	-0.794480	2.926811
H	2.428986	-1.392965	2.318085
C	1.944461	1.477141	4.233334
H	1.265472	3.354707	3.365427
H	2.803701	2.766458	2.721367
H	2.665982	-0.537290	4.633524
H	3.659248	0.384661	3.498385
H	2.514886	1.944648	5.051736
H	0.941668	1.250480	4.638091
C	1.225934	-2.034773	-0.033143
C	0.227487	-2.862458	-0.865526
C	2.671459	-2.462437	-0.326203
H	1.011731	-2.284939	1.022481
C	0.426815	-4.365709	-0.631921
H	0.356841	-2.647089	-1.939596
H	-0.802251	-2.563590	-0.614542
C	2.867213	-3.967273	-0.093870
H	2.918534	-2.230848	-1.376712
H	3.380162	-1.887256	0.291536
C	1.871240	-4.792968	-0.915254
H	-0.273768	-4.942125	-1.257321
H	0.178343	-4.603183	0.418430
H	3.901859	-4.257378	-0.338959
H	2.724794	-4.188509	0.979481
H	2.002039	-5.867265	-0.709176
H	2.085834	-4.651685	-1.990195
C	1.936325	0.441237	-1.477472
C	1.448254	-0.078274	-2.841191
C	2.000798	1.979022	-1.490580
H	2.960396	0.062279	-1.300856
C	2.293025	0.457547	-4.004300
H	0.394512	0.223317	-2.980951
H	1.459413	-1.177832	-2.859564
C	2.845124	2.511156	-2.656380

H	0.974914	2.383534	-1.566288
H	2.417757	2.353945	-0.544006
C	2.344425	1.987131	-4.004446
H	1.891855	0.083509	-4.960023
H	3.320547	0.059937	-3.918545
H	2.842747	3.613054	-2.644422
H	3.895251	2.198324	-2.513619
H	2.985064	2.352585	-4.822789
H	1.331330	2.384570	-4.195547

[**1.2f**] - tris(pentafluorophenyl)phosphine ($(PhF_5)_3P$) - GGAPBE-D3/def2TZVP_gas phase

F	3.796383	2.013918	0.641974
F	1.353558	1.426497	-0.346403
F	0.790257	1.895689	-2.978044
F	2.693542	2.948493	-4.626664
F	5.152441	3.525179	-3.662269
C	4.557246	2.812533	-1.470959
C	3.558293	2.262937	-0.655873
C	2.289267	1.950289	-1.148463
C	1.998921	2.189875	-2.492674
C	2.974602	2.734263	-3.334403
C	4.231913	3.033638	-2.815872
P	6.146464	3.287593	-0.665801
F	4.839952	5.600328	0.453730
F	9.012674	3.770422	-0.486818
F	4.989268	8.234425	-0.144792
F	11.123703	2.361448	-1.428567
F	6.543263	9.075909	-2.236563
F	10.704936	0.139880	-2.978373
F	7.922308	7.253332	-3.731556
F	8.153046	-0.640588	-3.573424
F	7.766974	4.639126	-3.183508
F	6.051584	0.735998	-2.661239
C	6.313691	5.013967	-1.317370
C	7.452508	2.335489	-1.554053

C	5.617384	5.983500	-0.578858
C	8.777633	2.684618	-1.253456
C	5.677392	7.344306	-0.871859
C	9.876673	1.974028	-1.726107
C	6.468441	7.775292	-1.939508
C	9.665155	0.842467	-2.518295
C	7.174246	6.840770	-2.699213
C	8.361410	0.448038	-2.820165
C	7.083860	5.481519	-2.390492
C	7.278624	1.187833	-2.337334

[**1.1**/1**.2a**] (orientation a) - $B(PhF_5)_3/Ph_3P$_a - GGAPBE-D3/def2TZVP_gas phase

6	4.756529	2.661351	4.377319
6	4.541178	1.363788	4.860332
6	3.414122	0.592363	4.596152
6	2.419137	1.111539	3.769135
6	2.595140	2.379360	3.218636
6	3.746017	3.116286	3.516778
5	6.092977	3.508634	4.784366
6	6.030138	5.088869	4.374030
6	7.494830	2.772657	4.380442
6	5.015271	5.926978	4.854245
6	8.726587	3.234100	4.863130
6	4.913506	7.288420	4.587240
6	9.957507	2.641141	4.601342
6	5.862453	7.887002	3.759780
6	10.004398	1.517783	3.777189
6	6.871476	7.097622	3.211846
6	8.818127	1.037065	3.226678
6	6.931436	5.733002	3.512940
6	7.605312	1.668081	3.522184
9	11.088479	3.134078	5.133092
9	11.172941	0.919898	3.506974
9	8.850537	-0.023796	2.402887
9	6.527938	1.150155	2.892550

9	8.765100	4.346020	5.641485
9	5.483872	0.776896	5.642087
9	3.275823	-0.633328	5.128471
9	1.318895	0.396622	3.496469
9	1.661301	2.879873	2.392461
9	3.835683	4.308495	2.887543
9	7.918531	5.056011	2.886244
9	7.773695	7.652701	2.385410
9	5.796101	9.196839	3.484260
9	3.921889	8.023883	5.116985
9	4.034120	5.407157	5.635892
15	6.087887	3.512221	6.994613
6	5.998089	5.181411	7.749629
6	6.873456	6.195410	7.323189
6	5.070053	5.462301	8.764201
6	6.812895	7.464425	7.899702
1	7.602397	5.999590	6.540116
6	5.012825	6.735052	9.333790
1	4.384519	4.688532	9.108993
6	5.879952	7.739907	8.901330
1	7.495526	8.242461	7.554101
1	4.282179	6.939479	10.118106
1	5.828578	8.736336	9.343326
6	4.685644	2.602672	7.750335
6	3.370374	2.849422	7.319476
6	4.905429	1.664230	8.770436
6	2.301384	2.164234	7.897581
1	3.175910	3.573308	6.531400
6	3.831524	0.980048	9.341595
1	5.917886	1.460612	9.118305
6	2.528355	1.224525	8.905040
1	1.286753	2.362968	7.548581
1	4.019106	0.249585	10.130277
1	1.690845	0.683213	9.348248
6	7.574938	2.756346	7.757041
6	8.021567	1.493761	7.329717
6	8.272700	3.417843	8.779311

6	9.147559	0.912243	7.913147
1	7.494666	0.962471	6.540476
6	9.400186	2.831525	9.356014
1	7.940215	4.396478	9.124590
6	9.842963	1.580541	8.922786
1	9.485048	-0.065993	7.566852
1	9.935103	3.360488	10.146487
1	10.728947	1.127166	9.370404

[**1.1**/**1.2a**] (orientation b) - $B(PhF_5)_3/Ph_3P$_b - GGAPBE-D3/def2TZVP_gas phase

6	4.771164	2.659089	4.472940
6	4.663852	1.450065	5.183122
6	3.493431	0.698449	5.240147
6	2.365306	1.142257	4.547625
6	2.423790	2.326459	3.807715
6	3.608874	3.057910	3.787947
5	6.082622	3.518905	4.464931
6	5.994592	5.084632	4.472868
6	7.482848	2.812782	4.468059
6	5.005480	5.782731	5.188276
6	8.584806	3.322311	5.177788
6	4.942372	7.172182	5.247787
6	9.820570	2.683583	5.232168
6	5.888697	7.926727	4.551914
6	9.998551	1.485789	4.537334
6	6.880349	7.283370	3.806247
6	8.942616	0.946630	3.797399
6	6.918975	5.891331	3.784452
6	7.717161	1.608220	3.780097
9	10.831436	3.196429	5.944609
9	11.174681	0.854764	4.582954
9	9.121188	-0.194682	3.117733
9	6.742875	1.050323	3.035457
9	8.473289	4.464668	5.881964
9	5.710658	0.976436	5.885298

9	3.434173	-0.432914	5.953539
9	1.231379	0.438390	4.595780
9	1.344280	2.741700	3.130480
9	3.610325	4.180951	3.043811
9	7.886560	5.328048	3.035111
9	7.777623	8.010102	3.125685
9	5.848385	9.260674	4.601939
9	3.996318	7.789597	5.966293
9	4.073678	5.113659	5.893472
15	6.098577	3.501155	10.444437
6	7.483410	2.601634	9.623021
6	8.784792	2.848005	10.096148
6	7.309536	1.678460	8.582088
6	9.884042	2.208558	9.522943
1	8.935773	3.553434	10.917397
6	8.409214	1.021901	8.023200
1	6.309626	1.468526	8.203642
6	9.699222	1.288155	8.486447
1	10.888537	2.420301	9.894047
1	8.250962	0.302547	7.216558
1	10.559068	0.780550	8.044972
6	4.622254	2.752936	9.630213
6	4.177538	1.509868	10.114928
6	3.913196	3.359822	8.583828
6	3.069481	0.879551	9.548416
1	4.710469	1.030802	10.940360
6	2.789570	2.738588	8.032413
1	4.237887	4.324640	8.195642
6	2.367510	1.495250	8.507451
1	2.744616	-0.090722	9.928677
1	2.247327	3.232018	7.222662
1	1.493942	1.006456	8.071742
6	6.183472	5.154444	9.630935
6	5.319025	6.154978	10.110295
6	7.068330	5.471843	8.590569
6	5.321380	7.429742	9.543959
1	4.633681	5.927917	10.931037

6	7.085500	6.755569	8.038737
1	7.750267	4.713634	8.206903
6	6.209450	7.736261	8.508087
1	4.635417	8.191119	9.919887
1	7.786627	6.983232	7.232649
1	6.217670	8.737034	8.071887

[**1.1**/**1.2b**] (orientation a) - $B(PhF_5)_3$/$(PhMe)_3P$_a - GGAPBE-D3/def2TZVP_gas phase

6	4.801619	2.612404	-1.197642
6	4.113192	1.555335	-0.591658
6	3.116758	0.796721	-1.203350
6	2.775978	1.061098	-2.528475
6	3.457195	2.070489	-3.203829
6	4.445517	2.806985	-2.543026
5	5.959365	3.537263	-0.477220
6	5.848524	5.070299	-1.067995
6	7.473744	2.910265	-0.551759
6	4.766376	5.906587	-0.782390
6	8.618025	3.671198	-0.249452
6	4.592965	7.192931	-1.293923
6	9.917864	3.166514	-0.251782
6	5.531795	7.699550	-2.188067
6	10.132756	1.825075	-0.569444
6	6.604357	6.890544	-2.560036
6	9.037642	1.025070	-0.884145
6	6.730181	5.609781	-2.019937
6	7.750315	1.571075	-0.867608
9	10.962000	3.957199	0.048483
9	11.372255	1.315413	-0.567811
9	9.224458	-0.272076	-1.179203
9	6.764089	0.697586	-1.160285
9	8.510765	4.979137	0.071171
9	4.420173	1.190143	0.677455
9	2.495934	-0.189752	-0.532602
9	1.823902	0.346961	-3.144438

9	3.167942	2.322178	-4.491250
9	5.080542	3.716274	-3.314080
9	7.740832	4.875766	-2.532396
9	7.493300	7.340779	-3.461474
9	5.396505	8.932401	-2.696753
9	3.535659	7.940487	-0.926854
9	3.789894	5.482398	0.061544
15	5.728447	3.593358	1.668737
6	6.710055	4.981808	2.352240
6	6.263032	6.295271	2.127033
6	7.884401	4.795635	3.092770
6	6.995570	7.382119	2.593048
1	5.321935	6.475698	1.610508
6	8.611808	5.892602	3.554912
1	8.237820	3.792193	3.325307
6	8.193877	7.204465	3.301558
6	6.355260	2.085068	2.515546
6	5.495472	1.337152	3.336283
6	7.676331	1.630046	2.360909
6	5.940783	0.178983	3.969316
1	4.461654	1.650530	3.475460
6	8.111667	0.470003	2.998889
1	8.385762	2.180617	1.747577
6	7.253777	-0.283640	3.810198
6	4.085752	3.860176	2.443559
6	2.879550	3.523746	1.815002
6	4.042480	4.359500	3.755967
6	1.667144	3.681591	2.483007
1	2.873590	3.160340	0.789765
6	2.825202	4.511640	4.415846
1	4.967095	4.627941	4.269147
6	1.613972	4.177220	3.793136
1	0.739913	3.415477	1.970159
1	2.816835	4.898588	5.437660
1	6.625391	8.392747	2.404674
1	9.525809	5.720450	4.128186
1	5.245251	-0.381373	4.598651

1	9.145558	0.145890	2.856981
6	9.005086	8.385353	3.758783
6	0.298351	4.375852	4.494662
6	7.716849	-1.558111	4.460579
1	9.647350	8.752323	2.941925
1	8.361733	9.221944	4.065832
1	9.660714	8.123782	4.600332
1	0.410142	4.317024	5.585992
1	-0.120366	5.368075	4.260619
1	-0.442543	3.627983	4.179941
1	8.787426	-1.520504	4.705068
1	7.156531	-1.767368	5.382093
1	7.566768	-2.414589	3.783482

[**1.1**/**1.2b**] (orientation b) - $B(PhF_5)_3$/$(PhMe)_3P$_b - GGAPBE-D3/def2TZVP_gas phase

6	4.009659	2.468870	-1.311233
6	3.791763	1.568311	-0.253947
6	2.847391	0.546078	-0.307197
6	2.092217	0.374858	-1.470472
6	2.282409	1.233603	-2.556302
6	3.218267	2.261124	-2.455262
5	5.036549	3.650243	-1.220053
6	4.646598	5.027413	-1.868275
6	6.419763	3.487196	-0.511512
6	3.373828	5.592945	-1.699995
6	7.078349	4.568827	0.108259
6	3.016582	6.831509	-2.228247
6	8.320712	4.452058	0.724961
6	3.945778	7.537926	-2.995748
6	8.963928	3.212757	0.741468
6	5.219522	7.003777	-3.212076
6	8.357711	2.110276	0.134609
6	5.547485	5.776637	-2.640533
6	7.111993	2.260967	-0.467546
9	8.906808	5.516196	1.292228

9	10.153759	3.081328	1.328813
9	8.982671	0.923518	0.139808
9	6.597148	1.163732	-1.053356
9	6.513804	5.787569	0.144509
9	4.489976	1.687069	0.887257
9	2.657197	-0.275167	0.735623
9	1.192671	-0.608570	-1.545023
9	1.566255	1.059631	-3.675376
9	3.367541	3.047755	-3.538956
9	6.786871	5.302962	-2.879256
9	6.105353	7.677629	-3.958293
9	3.618560	8.721225	-3.521374
9	1.801446	7.351436	-2.005189
9	2.440381	4.958155	-0.959016
15	6.063500	3.287164	5.372866
6	7.868695	3.650414	5.347432
6	8.652152	3.040500	6.341195
6	8.514292	4.458063	4.400420
6	10.035007	3.213388	6.368387
1	8.170279	2.414166	7.096538
6	9.897502	4.638329	4.439961
1	7.931016	4.953173	3.623140
6	10.684403	4.018209	5.420210
6	5.383504	4.511644	4.173160
6	4.640367	4.136373	3.044732
6	5.508885	5.885125	4.449398
6	4.059619	5.097284	2.216391
1	4.510276	3.081558	2.807164
6	4.948641	6.840182	3.601963
1	6.060884	6.213837	5.333644
6	4.214747	6.466776	2.465749
6	5.993857	1.730535	4.385538
6	4.827344	0.953235	4.472743
6	7.022969	1.286785	3.541800
6	4.679898	-0.205288	3.709836
1	4.019214	1.269863	5.137373
6	6.878024	0.116355	2.797067

1	7.947840	1.862346	3.467096
6	5.701379	-0.643989	2.855837
1	3.751538	-0.778352	3.774965
1	7.692188	-0.208751	2.144031
1	10.623488	2.718444	7.145383
1	10.375584	5.265116	3.682920
1	3.472677	4.772324	1.353015
1	5.076653	7.901043	3.832661
6	12.173395	4.234316	5.472730
6	5.549704	-1.899857	2.039924
6	3.643733	7.496844	1.528179
1	12.424330	5.093920	6.115489
1	12.693435	3.357742	5.884055
1	12.584036	4.442594	4.474834
1	5.905380	-2.781121	2.598156
1	4.498631	-2.080961	1.775673
1	6.134769	-1.844389	1.110869
1	4.344327	7.699536	0.700672
1	2.698821	7.156531	1.080914
1	3.457400	8.451391	2.039404

[**1.1**/**1.2c**] (orientation a) - $B(PhF_5)_3$/$(PhMe_2)_3P$_a - GGAPBE-D3/def2TZVP_gas phase

15	0.084946	-0.483393	-8.355901
6	1.018263	0.948032	-9.020104
6	2.411534	0.965001	-8.841891
6	0.395325	2.028559	-9.650015
6	3.173898	2.063260	-9.243701
1	2.919231	0.103511	-8.410795
6	1.136744	3.148071	-10.055571
1	-0.679269	2.016970	-9.830810
6	2.516767	3.151608	-9.837640
1	3.101620	4.024026	-10.143916
6	-1.561608	-0.439468	-9.182093
6	-1.938176	-1.495474	-10.025762
6	-2.463988	0.614620	-8.976331

6	-3.187829	-1.509062	-10.653896
1	-1.259120	-2.331277	-10.192333
6	-3.723361	0.623497	-9.589671
1	-2.198870	1.454547	-8.338543
6	-4.066448	-0.442312	-10.427133
1	-5.045074	-0.443149	-10.916246
6	0.915647	-1.912821	-9.156077
6	1.015298	-3.159575	-8.535782
6	1.382870	-1.755032	-10.471905
6	1.567303	-4.256999	-9.211101
1	0.686249	-3.291002	-7.506705
6	1.939633	-2.831719	-11.167041
1	1.306549	-0.783930	-10.964556
6	2.017109	-4.075757	-10.521989
1	2.445340	-4.927300	-11.059270
6	0.437028	4.331540	-10.670291
6	4.667286	2.074150	-9.048118
6	-4.688868	1.746546	-9.314238
6	-3.588676	-2.668382	-11.528255
6	2.456214	-2.660814	-12.571777
6	1.679689	-5.587601	-8.514540
1	4.999254	3.013912	-8.582773
1	4.994499	1.243343	-8.408558
1	5.194714	1.985512	-10.011018
1	-0.052845	4.937274	-9.890846
1	1.139553	4.983971	-11.205945
1	-0.345469	4.014206	-11.374586
1	2.150578	-1.695789	-12.997288
1	3.556638	-2.702820	-12.594028
1	2.089255	-3.459454	-13.233246
1	2.471784	-5.562782	-7.749598
1	0.742566	-5.847910	-8.000739
1	1.920881	-6.393748	-9.220080
1	-5.405235	1.874550	-10.137082
1	-5.269586	1.544753	-8.399489
1	-4.165417	2.700726	-9.159373
1	-2.709937	-3.194361	-11.925484

1	-4.180558	-3.401080	-10.956518
1	-4.207152	-2.338727	-12.375051
6	-0.431623	-1.750378	-5.494662
6	-0.052718	-2.062071	-4.177806
6	-0.340930	-3.277884	-3.549033
6	-1.060430	-4.257237	-4.228731
6	-1.499012	-3.985156	-5.523149
6	-1.195547	-2.754278	-6.101832
6	-1.147201	0.861881	-6.081863
6	1.465971	0.135571	-5.634697
6	-2.492146	0.625490	-5.757897
6	1.661607	1.139631	-4.671492
6	-3.474184	1.620789	-5.736160
6	2.912792	1.514698	-4.180470
6	-3.137123	2.933728	-6.052264
6	4.057999	0.850954	-4.618315
6	-1.811598	3.229925	-6.368779
6	3.915738	-0.198398	-5.521232
6	-0.861722	2.208983	-6.372608
6	2.641391	-0.536333	-5.977495
9	3.022067	2.494798	-3.267622
9	5.269157	1.203440	-4.163968
9	4.999891	-0.869553	-5.955312
9	2.591778	-1.594213	-6.828171
9	0.614272	1.776904	-4.105355
9	0.601130	-1.169438	-3.403324
9	0.064012	-3.504450	-2.288321
9	-1.339583	-5.431105	-3.645425
9	-2.212103	-4.904202	-6.199503
9	-1.707557	-2.555921	-7.340452
9	0.392574	2.596565	-6.689090
9	-1.464122	4.491921	-6.677091
9	-4.072580	3.893619	-6.067367
9	-4.750923	1.313749	-5.448133
9	-2.939222	-0.613468	-5.465615
5	-0.013438	-0.319016	-6.194416

[**1.1**/**1.2c**] (orientation b) - $B(PhF_5)_3/(PhMe_2)_3P$_b - GGAPBE-D3/def2TZVP_gas phase

15	0.301985	0.211178	-5.328658
6	1.270492	1.580188	-4.560051
6	1.139270	2.852779	-5.145248
6	2.154117	1.417775	-3.490164
6	1.850673	3.951366	-4.658726
1	0.461421	2.989709	-5.992988
6	2.889059	2.501875	-2.985731
1	2.266696	0.437830	-3.022901
6	2.726007	3.756540	-3.577810
1	3.295767	4.607593	-3.192254
6	0.552019	-1.188317	-4.153938
6	-0.446508	-1.657331	-3.289794
6	1.782367	-1.863903	-4.196999
6	-0.239278	-2.787247	-2.488076
1	-1.410403	-1.146395	-3.247223
6	2.035230	-2.966811	-3.372373
1	2.560496	-1.524253	-4.887432
6	1.008621	-3.422467	-2.532891
1	1.183043	-4.303257	-1.908331
6	-1.429241	0.711491	-4.936852
6	-2.448061	0.171947	-5.735844
6	-1.770643	1.551903	-3.870017
6	-3.795856	0.446709	-5.474144
1	-2.183092	-0.475963	-6.576403
6	-3.110694	1.845413	-3.583587
1	-0.980623	1.982893	-3.252902
6	-4.106065	1.283271	-4.392813
1	-5.155437	1.508323	-4.178656
6	3.796992	2.312693	-1.798452
6	1.688520	5.317544	-5.273833
6	3.382802	-3.642223	-3.390254
6	-1.358581	-3.324027	-1.632697
6	-3.468053	2.718264	-2.407047
6	-4.884813	-0.111048	-6.353798

1	2.658535	5.732514	-5.587610
1	1.031972	5.286014	-6.153645
1	1.252198	6.027462	-4.553585
1	4.540206	3.118261	-1.723403
1	3.221092	2.307728	-0.858755
1	4.335043	1.355260	-1.851097
1	-3.413000	2.148563	-1.464400
1	-2.778289	3.569389	-2.315169
1	-4.490142	3.111886	-2.491680
1	-5.179754	0.618128	-7.125771
1	-4.555002	-1.021951	-6.871939
1	-5.786887	-0.352334	-5.773453
1	4.125610	-3.063944	-2.816288
1	3.337397	-4.646197	-2.947686
1	3.771657	-3.732415	-4.414750
1	-2.007336	-2.515019	-1.268275
1	-1.995328	-4.011258	-2.213095
1	-0.977149	-3.882355	-0.767498
6	-0.851203	-1.826161	2.243057
6	-0.430757	-2.688221	3.268342
6	-1.283143	-3.593674	3.895392
6	-2.615297	-3.675182	3.479111
6	-3.078773	-2.843621	2.456020
6	-2.201945	-1.931154	1.873510
6	-0.396620	0.635625	1.236705
6	1.574176	-1.241220	1.159725
6	-1.225764	1.337156	2.129248
6	2.650052	-0.333020	1.117704
6	-1.674254	2.634639	1.888818
6	3.933283	-0.686900	0.710660
6	-1.299704	3.276042	0.705713
6	4.184071	-2.002263	0.310079
6	-0.479862	2.618703	-0.215653
6	3.158177	-2.947745	0.352675
6	-0.054002	1.321564	0.058501
6	1.891876	-2.560474	0.783721
9	4.927343	0.211465	0.698490

9	5.403517	-2.355104	-0.101996
9	3.402169	-4.212177	-0.017771
9	0.953236	-3.524360	0.800931
9	2.478562	0.945167	1.506456
9	0.842629	-2.643418	3.706997
9	-0.845434	-4.385552	4.883668
9	-3.444208	-4.546226	4.059444
9	-4.353577	-2.930723	2.052540
9	-2.699088	-1.156765	0.887483
9	0.702764	0.718112	-0.873147
9	-0.118592	3.244933	-1.343350
9	-1.725187	4.516068	0.452757
9	-2.451871	3.271945	2.774889
9	-1.594838	0.778705	3.298954
5	0.119799	-0.811160	1.547771

[**1.1**/**1.2d**] (orientation a) - $B(PhF_5)_3/(PhMe_3)_3P$_a - GGAPBE-D3/def2TZVP_gas phase

6	4.465899	3.065069	2.801257
6	4.055870	1.931290	3.526217
6	2.725178	1.533086	3.629545
6	1.740534	2.264714	2.961945
6	2.098406	3.385041	2.206830
6	3.436642	3.765807	2.147334
5	5.958731	3.541649	2.756926
6	6.292502	5.073566	2.764412
6	7.118915	2.488140	2.715841
6	5.558474	6.002367	3.524083
6	8.331755	2.673772	3.404128
6	5.881357	7.355539	3.592252
6	9.346598	1.720160	3.430440
6	6.963871	7.836408	2.852325
6	9.182091	0.529480	2.719310
6	7.710700	6.958764	2.061456
6	8.005659	0.306637	1.998324
6	7.371637	5.608222	2.038394

6	7.003852	1.273828	2.015824
9	10.467174	1.925998	4.135373
9	10.146419	-0.394280	2.727259
9	7.856786	-0.830302	1.303735
9	5.897787	1.008464	1.293519
9	8.543288	3.790310	4.123605
9	4.953293	1.195479	4.205937
9	2.379986	0.468868	4.366607
9	0.460011	1.894722	3.043555
9	1.153436	4.076213	1.553731
9	3.722159	4.846606	1.395084
9	8.120352	4.812383	1.249829
9	8.739603	7.425580	1.339870
9	7.284778	9.131876	2.899224
9	5.176005	8.194095	4.363195
9	4.516538	5.598557	4.272936
15	6.103873	3.466724	7.522327
6	5.625674	1.786950	8.080939
6	4.663985	1.475054	9.077511
6	6.188596	0.727983	7.314269
6	4.255190	0.143313	9.230289
6	5.754717	-0.584050	7.519466
6	4.769872	-0.900998	8.458651
1	3.514366	-0.085312	10.002283
1	6.200950	-1.382455	6.919412
6	7.819638	3.861600	8.035040
6	8.425707	4.920243	7.301430
6	8.608398	3.130878	8.961661
6	9.786498	5.189155	7.467764
6	9.971829	3.433866	9.077028
6	10.589162	4.443468	8.335141
1	10.231952	6.007263	6.894234
1	10.569688	2.864699	9.795135
6	4.930189	4.724707	8.156244
6	3.684614	4.769395	7.468795
6	5.207527	5.712721	9.136945
6	2.782839	5.803084	7.733556

6	4.272890	6.734743	9.351317
6	3.063580	6.813651	8.656923
1	1.831155	5.818098	7.194388
1	4.496654	7.490083	10.110559
6	4.274214	-2.312515	8.623319
6	4.085090	2.486442	10.033566
6	7.277507	0.976945	6.306520
6	3.289000	3.702915	6.483965
6	2.103845	7.950363	8.884991
6	6.432972	5.705172	10.014407
6	8.057811	2.072998	9.883384
6	12.065318	4.711065	8.455762
6	7.627477	5.793026	6.371641
1	8.761834	1.890555	10.706567
1	7.093079	2.369154	10.316567
1	7.884029	1.113851	9.373173
1	6.985693	6.497830	6.924941
1	8.288290	6.375048	5.715122
1	6.952791	5.183431	5.752203
1	12.453180	4.396625	9.434818
1	12.628035	4.156847	7.686752
1	12.294266	5.777644	8.319782
1	8.244664	1.181470	6.793937
1	7.404971	0.110400	5.643716
1	7.046140	1.863356	5.697299
1	3.880376	-2.485925	9.634604
1	3.459052	-2.526839	7.912852
1	5.071674	-3.044805	8.432851
1	3.622519	1.972351	10.886954
1	4.852362	3.170242	10.420931
1	3.315745	3.119731	9.567390
1	6.274348	6.356786	10.884339
1	6.668840	4.696773	10.379948
1	7.332513	6.060135	9.489805
1	3.022919	2.760232	6.989356
1	2.427595	4.023465	5.882541
1	4.127129	3.466081	5.811815

1	2.221128	8.381478	9.889089
1	2.276588	8.760765	8.157950
1	1.059882	7.626430	8.767859

[**1.1**/**1.2d**] (orientation b) - $B(PhF_5)_3/(PhMe_3)_3P$_b - GGAPBE-D3/def2TZVP_gas phase

6	5.348077	4.042614	10.989038
6	4.711742	2.985179	11.665162
6	3.348242	2.975055	11.948551
6	2.557167	4.048962	11.533828
6	3.137347	5.114429	10.840933
6	4.506709	5.095406	10.588129
5	6.893485	4.061454	10.730829
6	7.694191	5.404999	10.811869
6	7.642846	2.717890	10.420318
6	7.384637	6.414594	11.742946
6	8.907493	2.418689	10.955495
6	8.125873	7.587856	11.864160
6	9.541852	1.192685	10.770706
6	9.208285	7.804356	11.007515
6	8.927449	0.218460	9.980339
6	9.542048	6.842533	10.049971
6	7.685299	0.480452	9.395452
6	8.794579	5.669730	9.976580
6	7.067398	1.706009	9.632417
9	10.729208	0.938695	11.340095
9	9.527334	-0.956763	9.779799
9	7.104398	-0.448320	8.624342
9	5.871557	1.904108	9.044528
9	9.553578	3.317406	11.726338
9	5.424661	1.933416	12.111303
9	2.789418	1.961048	12.622345
9	1.250600	4.060032	11.805073
9	2.374146	6.139024	10.436144
9	5.007623	6.142105	9.904140
9	9.156383	4.782964	9.029171

9	10.572330	7.058688	9.220936
9	9.919445	8.929993	11.100108
9	7.809670	8.511893	12.781947
9	6.354174	6.267386	12.592883
15	5.649269	3.418356	17.330875
6	4.032336	2.553545	17.250064
6	3.702665	1.439589	16.434413
6	3.079466	3.017598	18.200323
6	2.459623	0.816682	16.607905
6	1.847410	2.367525	18.318833
6	1.517619	1.253859	17.541893
1	2.212650	-0.033590	15.965255
1	1.123542	2.746763	19.046103
6	5.531650	5.061019	16.516519
6	6.564180	5.967111	16.885507
6	4.486355	5.521803	15.671255
6	6.535119	7.282991	16.409572
6	4.496860	6.854039	15.242813
6	5.506322	7.755080	15.592980
1	7.347822	7.959043	16.690533
1	3.693933	7.191279	14.580078
6	6.953459	2.400259	16.534442
6	7.391349	1.293905	17.317139
6	7.620295	2.678739	15.314003
6	8.459090	0.509030	16.871423
6	8.700185	1.873644	14.927243
6	9.140150	0.785071	15.682205
1	8.768698	-0.345498	17.480383
1	9.207726	2.103218	13.986439
6	0.202758	0.541978	17.716160
6	4.593337	0.905314	15.343381
6	3.341194	4.223423	19.065346
6	6.710130	0.915392	18.606339
6	10.313331	-0.047942	15.239098
6	7.207762	3.772427	14.366013
6	3.378426	4.642706	15.151311
6	5.477981	9.177609	15.102873

6	7.724224	5.542614	17.748291
1	2.852391	5.150023	14.330808
1	3.759604	3.682752	14.777988
1	2.634639	4.394972	15.922478
1	8.392887	4.844193	17.219079
1	8.320144	6.412361	18.055692
1	7.376169	5.008961	18.647094
1	5.233043	9.224110	14.031553
1	4.714954	9.766334	15.637092
1	6.446957	9.672946	15.251177
1	3.361693	5.152760	18.473225
1	2.562403	4.329295	19.832402
1	4.324066	4.153664	19.558033
1	-0.114031	0.049133	16.786194
1	0.277484	-0.238801	18.490817
1	-0.592111	1.234274	18.027977
1	4.014397	0.269343	14.660898
1	5.048870	1.709413	14.752153
1	5.427669	0.306410	15.738506
1	7.680975	3.611272	13.388736
1	6.120465	3.808367	14.223658
1	7.502530	4.772798	14.714660
1	5.699121	0.513848	18.430203
1	7.288391	0.152056	19.143840
1	6.580468	1.793708	19.258978
1	10.490630	0.049409	14.158664
1	11.236778	0.266469	15.752342
1	10.161710	-1.112318	15.469974

[**1.1**/**1.2e**] (orientation a) - $B(PhF_5)_3/Cy_3P$_a - GGAPBE-D3/def2TZVP_gas phase

6	4.782557	2.908997	-1.669581
6	4.457840	1.735124	-0.967833
6	3.167937	1.215081	-0.907917
6	2.135357	1.860635	-1.591826
6	2.411805	3.011758	-2.331560

6	3.714518	3.508184	-2.357725
5	6.236815	3.508200	-1.680631
6	6.471027	5.062283	-1.755971
6	7.472008	2.536030	-1.768770
6	5.638310	5.986049	-1.099834
6	8.699001	2.809918	-1.141061
6	5.890855	7.355239	-1.063267
6	9.787414	1.942465	-1.176135
6	6.997013	7.866361	-1.744349
6	9.687897	0.748608	-1.893287
6	7.827156	6.999269	-2.457674
6	8.501149	0.442659	-2.562715
6	7.553947	5.632637	-2.450939
6	7.426848	1.327662	-2.486020
9	10.918335	2.230474	-0.514018
9	10.723025	-0.095118	-1.939984
9	8.409282	-0.693270	-3.269500
9	6.318802	0.979740	-3.170581
9	8.857907	3.935405	-0.419410
9	5.399719	1.071742	-0.269008
9	2.901007	0.112471	-0.189183
9	0.890990	1.375397	-1.539844
9	1.427472	3.622097	-3.007341
9	3.919410	4.609453	-3.107329
9	8.385536	4.860791	-3.177926
9	8.872862	7.489343	-3.138898
9	7.249732	9.178035	-1.726363
9	5.084006	8.186696	-0.384802
9	4.547740	5.568057	-0.433666
15	5.903086	3.508579	2.003839
6	4.184932	3.280664	2.777855
6	3.133347	3.956088	1.873360
6	3.794071	1.812859	3.025818
1	4.193121	3.797837	3.756395
6	1.710321	3.824340	2.425629
1	3.180595	3.487299	0.875898
1	3.378004	5.014463	1.715987

6	2.362682	1.680185	3.565364
1	3.879699	1.240713	2.085167
1	4.484739	1.342737	3.741083
6	1.337232	2.358601	2.654914
1	0.999006	4.302952	1.733596
1	1.635729	4.374099	3.381397
1	2.118457	0.613976	3.696775
1	2.313940	2.139461	4.569222
1	0.326974	2.276682	3.085885
1	1.306804	1.832386	1.683708
6	6.894385	2.123228	2.812926
6	8.172745	1.775683	2.033332
6	7.184680	2.259340	4.314484
1	6.222408	1.257373	2.675999
6	8.848074	0.518724	2.596268
1	8.886769	2.615323	2.067369
1	7.917085	1.620620	0.976172
6	7.853001	0.993314	4.869765
1	7.860682	3.115974	4.481412
1	6.259867	2.477821	4.873129
6	9.130637	0.652611	4.095698
1	9.779971	0.315977	2.043916
1	8.186735	-0.350312	2.427678
1	8.074606	1.124016	5.941201
1	7.145287	0.147995	4.795801
1	9.580635	-0.273481	4.486789
1	9.874194	1.454421	4.254688
6	6.521075	5.061709	2.878567
6	7.888127	5.470761	2.300407
6	5.535442	6.240800	2.804612
1	6.650038	4.809197	3.946760
6	8.446471	6.735474	2.963067
1	7.776645	5.644589	1.216191
1	8.611364	4.648131	2.401547
6	6.103129	7.502042	3.469152
1	5.301469	6.466781	1.751855
1	4.582653	5.976427	3.286862

6	7.455163	7.897823	2.871029
1	9.406927	7.005723	2.495940
1	8.662441	6.525755	4.026221
1	5.379886	8.327007	3.369582
1	6.225451	7.319053	4.551928
1	7.855453	8.789799	3.378138
1	7.315513	8.176342	1.810448

[**1.1**/**1.2e**] (orientation b) - $B(PhF_5)_3/Cy_3P$_b - GGAPBE-D3/def2TZVP_gas phase

6	5.531283	1.996874	-0.413444
6	6.095668	1.044189	0.453798
6	5.574604	-0.234202	0.628995
6	4.429207	-0.607354	-0.078219
6	3.831110	0.299038	-0.957766
6	4.383210	1.569752	-1.106458
5	6.140170	3.429138	-0.603141
6	5.197106	4.656047	-0.847438
6	7.692665	3.636649	-0.525744
6	3.960354	4.796634	-0.194329
6	8.271765	4.776244	0.062092
6	3.135413	5.906321	-0.355682
6	9.646843	4.941149	0.212245
6	3.524249	6.923127	-1.231178
6	10.509856	3.949944	-0.260175
6	4.734294	6.820411	-1.923553
6	9.986794	2.812322	-0.881469
6	5.544810	5.707218	-1.714163
6	8.605955	2.676248	-0.998568
9	10.147972	6.034413	0.803180
9	11.829228	4.090731	-0.122929
9	10.815644	1.871310	-1.352018
9	8.162098	1.566582	-1.619824
9	7.497669	5.764886	0.547338
9	7.181468	1.350973	1.189199
9	6.153636	-1.103811	1.468273

9	3.908676	-1.824298	0.086104
9	2.741138	-0.063700	-1.646259
9	3.777430	2.386741	-1.988526
9	6.695162	5.656400	-2.413147
9	5.098716	7.790085	-2.772969
9	2.743214	7.990928	-1.405071
9	1.985202	6.014164	0.322622
9	3.536986	3.854637	0.671356
15	6.002486	3.373101	5.156472
6	4.948573	2.125207	4.185978
6	4.873564	0.819347	5.004241
6	3.525394	2.587602	3.836891
1	5.474280	1.917668	3.235135
6	4.091464	-0.282119	4.279188
1	4.384213	1.047096	5.967905
1	5.883031	0.461955	5.258524
6	2.747999	1.494940	3.089762
1	2.984248	2.846080	4.765714
1	3.545476	3.495560	3.218759
6	2.688455	0.188482	3.885512
1	4.030875	-1.179259	4.916050
1	4.644972	-0.584958	3.374101
1	1.732378	1.852914	2.856298
1	3.242429	1.311165	2.118430
1	2.168006	-0.591551	3.306726
1	2.090981	0.351639	4.800274
6	5.329560	5.033561	4.566711
6	5.669614	6.175310	5.543408
6	5.641504	5.443401	3.121998
1	4.237089	4.886079	4.647552
6	4.936920	7.466317	5.154579
1	6.756427	6.364992	5.543462
1	5.409805	5.875817	6.570668
6	4.914528	6.736430	2.730324
1	6.726102	5.604517	3.011657
1	5.378470	4.631467	2.425130
6	5.237260	7.872191	3.707324

1	5.211060	8.280140	5.844885
1	3.848776	7.310820	5.268766
1	5.191702	7.026924	1.703542
1	3.824236	6.554818	2.726817
1	4.675202	8.780532	3.437975
1	6.308565	8.127971	3.617814
6	7.631187	3.225358	4.214343
6	8.657916	4.242923	4.741639
6	8.214234	1.803665	4.294894
1	7.431960	3.443651	3.148332
6	10.005059	4.135293	4.016359
1	8.805337	4.071457	5.823010
1	8.272704	5.268258	4.641865
6	9.556187	1.698775	3.557026
1	8.356050	1.529605	5.356085
1	7.511575	1.071915	3.870522
6	10.573138	2.715765	4.080993
1	10.718867	4.858906	4.441359
1	9.866644	4.422547	2.959036
1	9.951923	0.674374	3.645914
1	9.387926	1.875834	2.479475
1	11.513392	2.650905	3.510033
1	10.823977	2.472439	5.128964

[**1.1**/**1.2f**] (orientation a) - $B(PhF_5)_3$/$(PhF_5)_3P$_a - GGAPBE-D3/def2TZVP_gas phase

6	4.106817	4.039427	13.302858
6	3.521863	3.500833	14.458371
6	2.147530	3.446371	14.670041
6	1.288779	3.926725	13.677357
6	1.819386	4.460459	12.499820
6	3.203119	4.517176	12.338649
5	5.662392	4.136223	13.107421
6	6.250397	5.436976	12.461020
6	6.605850	2.972987	13.555999
6	5.768501	6.714328	12.793625

6	7.920002	3.201457	14.011101
6	6.290727	7.886039	12.249559
6	8.760989	2.182851	14.452002
6	7.316970	7.800575	11.305041
6	8.303259	0.864137	14.441873
6	7.816200	6.550442	10.927690
6	7.009064	0.581822	13.996559
6	7.287327	5.403696	11.514507
6	6.194025	1.625831	13.568247
9	9.991050	2.453570	14.908539
9	9.093870	-0.121209	14.867574
9	6.567641	-0.684025	13.993950
9	4.968108	1.283336	13.127261
9	8.412565	4.449711	14.084442
9	4.302742	3.022223	15.450072
9	1.643719	2.934506	15.802427
9	-0.033188	3.872872	13.852237
9	0.995494	4.910498	11.544354
9	3.655950	5.030916	11.178726
9	7.796753	4.222480	11.112698
9	8.792826	6.472380	10.013591
9	7.819684	8.911886	10.761986
9	5.819465	9.086254	12.613921
9	4.781695	6.855085	13.700243
6	6.079854	4.439444	18.181893
6	5.939365	5.493802	17.269844
6	5.743792	4.704435	19.515978
6	5.479219	6.754294	17.654378
6	5.286199	5.952734	19.931540
6	5.153024	6.981598	18.992910
6	8.103874	2.558920	18.814570
6	8.080149	1.701376	19.922071
6	9.315503	3.219245	18.556763
6	9.207838	1.495756	20.720135
6	10.452326	3.043335	19.342286
6	10.396449	2.168908	20.430795
6	5.515726	1.565440	17.885786

6	4.158447	1.759331	18.170168
6	5.902580	0.251908	17.581783
6	3.240912	0.705830	18.155532
6	5.016056	-0.819785	17.566385
6	3.668251	-0.587950	17.855018
15	6.784988	2.858052	17.555904
9	4.713739	8.181577	19.378766
9	5.356372	7.741128	16.758204
9	6.252594	5.323614	15.972605
9	5.831039	3.733559	20.439523
9	4.962027	6.175685	21.211658
9	3.665382	2.979018	18.451722
9	6.963639	1.041388	20.271561
9	9.153179	0.667470	21.771722
9	11.475254	1.983267	21.196665
9	11.586869	3.698890	19.066301
9	9.397419	4.072698	17.516272
9	1.949466	0.932951	18.427920
9	2.795191	-1.599598	17.842808
9	5.439594	-2.056755	17.279125
9	7.198527	0.000575	17.289097

[**1.1**/**1.2f**] (orientation b) - $B(PhF_5)_3$/$(PhF_5)_3P$_b - GGAPBE-D3/def2TZVP_gas phase

6	5.460598	2.867524	3.092740
6	5.545547	1.634443	3.765447
6	4.456504	1.037958	4.394274
6	3.209075	1.662422	4.339917
6	3.063830	2.874067	3.659417
6	4.182768	3.457882	3.070023
5	6.706510	3.547466	2.438329
6	6.852638	5.111070	2.447537
6	7.826783	2.686519	1.765552
6	6.580421	5.889080	3.582370
6	9.188721	3.019890	1.872179
6	6.737531	7.272091	3.613142

6	10.202912	2.259307	1.294227
6	7.158918	7.936453	2.458220
6	9.865195	1.126639	0.548659
6	7.430611	7.206699	1.297693
6	8.523564	0.763051	0.400059
6	7.287439	5.820275	1.316398
6	7.539477	1.533997	1.013661
9	11.490348	2.599498	1.441059
9	10.822727	0.393127	-0.022516
9	8.203750	-0.316904	-0.325255
9	6.262800	1.146192	0.829466
9	9.572830	4.095618	2.585895
9	6.724385	0.995299	3.874237
9	4.594752	-0.113753	5.067680
9	2.159196	1.108530	4.951926
9	1.863437	3.461915	3.599061
9	3.987137	4.627791	2.432262
9	7.555257	5.165233	0.169659
9	7.826242	7.844689	0.188452
9	7.303489	9.263243	2.464538
9	6.492768	7.970416	4.732915
9	6.180393	5.298025	4.728617
6	6.994971	3.392411	8.525056
6	8.134980	3.543805	9.323927
6	7.200166	3.184433	7.156219
6	9.424206	3.501089	8.785349
6	8.469624	3.145261	6.589320
6	9.589180	3.305637	7.412717
6	4.740392	4.983402	8.163531
6	3.859523	4.903162	7.078708
6	5.236064	6.261577	8.466029
6	3.483023	6.027654	6.342339
6	4.887210	7.400461	7.743485
6	3.997053	7.281066	6.674097
6	4.350230	2.158984	8.831191
6	4.842479	0.907657	8.439399
6	2.968988	2.235160	9.063093

6	4.003236	-0.191995	8.242454
6	2.105282	1.162873	8.862205
6	2.628861	-0.063632	8.444668
15	5.339144	3.643661	9.302802
9	10.814709	3.266401	6.884598
9	10.498057	3.650807	9.570759
9	8.021574	3.743358	10.645993
9	6.145354	2.996259	6.345367
9	8.632876	2.949001	5.272020
9	6.158428	0.702449	8.235725
9	3.348139	3.725566	6.673639
9	2.655751	5.904295	5.294636
9	3.654300	8.356988	5.960968
9	5.400649	8.596287	8.057798
9	6.108886	6.409692	9.483665
9	4.512516	-1.369577	7.859827
9	1.819556	-1.108722	8.250820
9	0.788559	1.296108	9.066057
9	2.435751	3.405811	9.471976

[**1.1**/**1.2a**/**1.1**] - $B(PhF_5)_3/Ph_3P/B(PhF_5)_3$ - GGAPBE-D3/def2TZVP_gas phase

6	4.526279	2.682387	4.822829
6	4.393422	1.376880	5.313757
6	3.259573	0.583703	5.171196
6	2.167565	1.087495	4.466038
6	2.255072	2.362348	3.910393
6	3.416856	3.121473	4.084458
5	5.879890	3.556726	5.089681
6	5.738177	5.139674	4.711910
6	7.247543	2.857112	4.534525
6	4.756487	5.944962	5.304383
6	8.512206	3.345768	4.888057
6	4.598040	7.307682	5.074330
6	9.722110	2.782571	4.495608
6	5.446832	7.942630	4.168884

6	9.707926	1.663638	3.664190
6	6.413698	7.186801	3.508967
6	8.481759	1.157395	3.237768
6	6.534079	5.819334	3.777274
6	7.292474	1.758517	3.662762
9	10.890927	3.299821	4.909387
9	10.854980	1.094203	3.269635
9	8.451962	0.100643	2.408778
9	6.166823	1.218016	3.147102
9	8.606465	4.456419	5.663951
9	5.431074	0.803926	5.976833
9	3.207248	-0.648377	5.704250
9	1.058343	0.351510	4.312240
9	1.224535	2.848479	3.198699
9	3.412017	4.319351	3.459797
9	7.468043	5.176555	3.042758
9	7.216376	7.776816	2.607613
9	5.324286	9.254751	3.926045
9	3.647581	8.009941	5.713321
9	3.868362	5.388695	6.168157
15	6.113096	3.540410	7.288288
6	6.053977	5.202284	8.063851
6	6.865855	6.241331	7.575138
6	5.203076	5.454923	9.149589
6	6.819849	7.504917	8.164585
1	7.533818	6.068607	6.734226
6	5.156542	6.723367	9.729850
1	4.566772	4.664964	9.543725
6	5.960131	7.752688	9.236957
1	7.454817	8.301574	7.774038
1	4.483659	6.901062	10.570726
1	5.921149	8.745634	9.688579
6	4.827122	2.580132	8.177878
6	3.464349	2.814817	7.922197
6	5.185968	1.604788	9.119574
6	2.486942	2.083281	8.597368
1	3.162012	3.566824	7.196841

6	4.203203	0.871483	9.786100
1	6.234572	1.407004	9.333101
6	2.852157	1.104400	9.524125
1	1.433645	2.275963	8.388051
1	4.503364	0.113389	10.511811
1	2.083657	0.528372	10.042835
6	7.698518	2.825290	7.873237
6	8.119987	1.564282	7.414954
6	8.506752	3.526422	8.779848
6	9.327601	1.023921	7.857761
1	7.509748	1.001848	6.711736
6	9.717078	2.983258	9.213074
1	8.199403	4.503631	9.147008
6	10.133554	1.733972	8.750369
1	9.642148	0.045004	7.492865
1	10.334198	3.547104	9.915012
1	11.082003	1.310820	9.086327
6	8.073759	2.706828	12.942455
6	9.283993	3.154170	13.503815
6	10.492251	2.478476	13.348166
6	10.524339	1.303541	12.591864
6	9.349011	0.813135	12.018923
6	8.159537	1.510056	12.209287
5	6.732320	3.502009	13.103746
6	6.745865	5.069896	13.111227
6	5.373755	2.730649	13.236351
6	7.616625	5.822632	12.303922
6	4.181841	3.194310	12.652346
6	7.613561	7.213875	12.266395
6	2.976612	2.501763	12.721299
6	6.718652	7.914673	13.077808
6	2.925657	1.291984	13.417019
6	5.844308	7.215933	13.914991
6	4.076876	0.795446	14.034913
6	5.868624	5.823084	13.912778
6	5.267225	1.511464	13.930335
9	1.875302	2.972776	12.122663

9	1.780870	0.609118	13.486393
9	4.022243	-0.357415	14.714537
9	6.338991	0.992674	14.559280
9	4.169385	4.344386	11.949404
9	9.311727	4.270087	14.256913
9	11.617780	2.938852	13.909588
9	11.676494	0.654080	12.412116
9	9.381805	-0.308270	11.287922
9	7.065671	0.995699	11.613059
9	5.015341	5.204712	14.751272
9	4.997308	7.890258	14.703541
9	6.695324	9.248952	13.049095
9	8.445074	7.884107	11.458615
9	8.488846	5.205352	11.482260

[**1.1**/**1.2a**/**1.1**] - $B(PhF_5)_3/Ph_3P/B(PhF_5)_3$ - GGAPBE-D3/def2TZVP_PhCl (PCM) phase

6	4.528288	2.685620	4.807699
6	4.387620	1.380015	5.296659
6	3.252115	0.591184	5.144747
6	2.166663	1.097201	4.432874
6	2.263023	2.370841	3.878744
6	3.425508	3.125700	4.061145
5	5.882491	3.558416	5.090932
6	5.741424	5.140557	4.699848
6	7.250483	2.858117	4.530791
6	4.758720	5.949690	5.285711
6	8.515330	3.347779	4.882988
6	4.602421	7.311091	5.047419
6	9.724693	2.783239	4.491462
6	5.452726	7.941707	4.141717
6	9.712147	1.662598	3.663807
6	6.419494	7.181821	3.488717
6	8.486722	1.156192	3.239115
6	6.537831	5.816229	3.763797
6	7.297878	1.758309	3.661770

9	10.894888	3.303517	4.902907
9	10.860496	1.092267	3.269824
9	8.456610	0.095889	2.410913
9	6.172558	1.214257	3.143646
9	8.610795	4.462268	5.651657
9	5.418642	0.800620	5.962508
9	3.192721	-0.643116	5.676019
9	1.055554	0.363643	4.269930
9	1.238156	2.861285	3.157535
9	3.426537	4.324163	3.433030
9	7.473696	5.170364	3.030531
9	7.225653	7.766948	2.583880
9	5.330774	9.253727	3.890955
9	3.648581	8.017753	5.679907
9	3.865167	5.399215	6.146188
15	6.108909	3.543640	7.279204
6	6.047276	5.205686	8.051536
6	6.852141	6.249486	7.561405
6	5.206213	5.448548	9.147846
6	6.806102	7.510463	8.156805
1	7.516268	6.084678	6.715946
6	5.161608	6.713610	9.735890
1	4.578938	4.653432	9.546311
6	5.955989	7.748846	9.239359
1	7.435168	8.311068	7.764986
1	4.500956	6.884320	10.587628
1	5.918761	8.738318	9.698217
6	4.819602	2.584762	8.162492
6	3.457366	2.812387	7.897876
6	5.178288	1.627701	9.123335
6	2.479102	2.088981	8.580804
1	3.153637	3.553082	7.161637
6	4.194702	0.904847	9.800292
1	6.226559	1.438956	9.346861
6	2.843857	1.128820	9.527595
1	1.426179	2.275462	8.364463
1	4.492332	0.165060	10.545372

1	2.075451	0.561941	10.056004
6	7.694064	2.827782	7.860592
6	8.113124	1.563796	7.408264
6	8.500498	3.530178	8.768493
6	9.318324	1.021866	7.855993
1	7.504161	0.997911	6.706877
6	9.707183	2.984264	9.208970
1	8.193302	4.508157	9.133953
6	10.122179	1.732506	8.750596
1	9.630966	0.040673	7.495799
1	10.321552	3.544696	9.915712
1	11.066827	1.307266	9.093948
6	8.079029	2.707450	12.943038
6	9.287894	3.155333	13.505812
6	10.494798	2.476812	13.357537
6	10.528875	1.299517	12.606656
6	9.355637	0.810826	12.029440
6	8.166393	1.509396	12.212662
5	6.734352	3.496700	13.107197
6	6.739744	5.064492	13.113484
6	5.381545	2.717233	13.251707
6	7.607047	5.820855	12.306070
6	4.183123	3.169968	12.673157
6	7.605918	7.211975	12.277685
6	2.980669	2.475791	12.764942
6	6.717413	7.909669	13.097707
6	2.938600	1.276273	13.477730
6	5.844875	7.206952	13.931859
6	4.097509	0.790234	14.087432
6	5.865918	5.814676	13.921033
6	5.285145	1.505930	13.959998
9	1.870593	2.938048	12.172283
9	1.794615	0.594085	13.572244
9	4.052940	-0.354653	14.784069
9	6.364878	0.995480	14.583956
9	4.160754	4.311128	11.955807
9	9.315797	4.274676	14.255258

9	11.619697	2.937703	13.923442
9	11.680603	0.645662	12.436837
9	9.389247	-0.314305	11.301457
9	7.073723	0.994528	11.614038
9	5.013463	5.193949	14.759831
9	5.001319	7.878182	14.729274
9	6.698728	9.244695	13.080240
9	8.436775	7.886104	11.470047
9	8.475100	5.207246	11.477140

[**1.1**] - tris(pentafluorophenyl)borane ($B(PhF_5)_3$) - ZORA-GGAPBE-D3(BJ)/TZP_PhCl (COSMO) phase

C	4.13870491	4.20517719	13.37944176
C	3.59040676	3.66397890	14.55610837
C	2.22402186	3.64454051	14.81877214
C	1.33906137	4.16065894	13.87000302
C	1.83232703	4.69813056	12.67929830
C	3.20652561	4.72247203	12.46201697
B	5.67741006	4.23055247	13.10898582
C	6.32527150	5.45969215	12.39436212
C	6.56802970	3.02734462	13.55744285
C	5.89377484	6.77796015	12.62808210
C	7.86672999	3.20160475	14.06872519
C	6.46726655	7.88602311	12.01203513
C	8.66758946	2.14310354	14.48624619
C	7.50556107	7.69736876	11.09756229
C	8.18434612	0.83757795	14.37741435
C	7.96294020	6.40717143	10.82166181
C	6.90590771	0.60988731	13.86434485
C	7.38076091	5.32495352	11.47439326
C	6.12425281	1.69483786	13.47958919
F	4.89552163	7.02469401	13.50961961
F	8.94746740	-0.19668824	14.76536543
F	6.44564300	-0.65280646	13.75209024
F	4.89644764	1.41070866	12.98359455
F	8.38695565	4.44470429	14.20569172

F	4.39884217	3.15560229	15.51661266
F	1.74559102	3.13424486	15.97179662
F	0.01692643	4.14016249	14.10220933
F	0.97488831	5.18842552	11.76094943
F	3.62472838	5.24993827	11.28673286
F	7.86174365	4.09859236	11.15980768
F	8.96026396	6.22717133	9.93172506
F	8.06320878	8.75393482	10.48527390
F	6.03386541	9.13397944	12.28380793
F	9.89958339	2.36049758	14.99014899

[**1.2a**] - triphenylphosphine (Ph_3P) - ZORA-GGAPBE-D3(BJ)/TZP_PhCl (COSMO) phase

P	0.69118574	2.23174602	-2.33564951
H	-0.03311515	2.71702511	0.56499795
H	2.16986673	0.64270882	-0.22527697
H	2.69562716	3.78774613	-0.67874795
C	2.52860938	2.26857376	-2.21010677
C	3.24456786	1.41796164	-3.07276556
C	4.64142626	1.40947104	-3.06354915
C	5.34256900	2.26727487	-2.20559692
C	4.63783677	3.12191816	-1.35061262
C	3.23856711	3.12040215	-1.35028992
H	2.70281257	0.76366193	-3.75970198
H	5.18421094	0.74434310	-3.73726518
H	6.43411048	2.27333109	-2.20922883
H	5.17648464	3.79423161	-0.68054566
C	0.25483480	0.83963470	-1.21177241
C	-1.04999720	0.32280473	-1.30989095
C	-1.45131039	-0.74897998	-0.50854865
C	-0.54724245	-1.32917111	0.39074296
C	0.75507619	-0.82594079	0.48835488
C	1.15303532	0.25457436	-0.30599725
H	-1.75255004	0.75967823	-2.02330323
H	-2.46637949	-1.14028138	-0.59443973
H	-0.85501408	-2.17578561	1.00721702
H	1.46602496	-1.27547306	1.18379323

C	0.19876044	3.70486348	-1.34602196
C	0.09262586	4.92900365	-2.03126867
C	-0.29801153	6.08887038	-1.35700082
C	-0.60376937	6.03618489	0.00916707
C	-0.50788844	4.82053189	0.69621794
C	-0.10574955	3.66177320	0.02325792
H	0.31137481	4.97081014	-3.10077190
H	-0.37548403	7.03204748	-1.90035674
H	-0.92204011	6.93862406	0.53433075
H	-0.74704420	4.77143866	1.75996023

[**1.2b**] - tri-p-tolylphosphine ($(PhMe)_3P$) - ZORA-GGAPBE-D3(BJ)/TZP_PhCl (COSMO) phase

C	5.44976578	4.54678020	4.21517598
C	5.17921871	4.30008026	2.85994994
C	5.12461657	5.80750387	4.74390316
C	4.59449483	5.28402461	2.06032093
H	5.41720060	3.32608202	2.42927429
C	4.55205354	6.79351325	3.93670533
H	5.31015390	6.01670927	5.79974930
C	4.26814778	6.54764240	2.58274784
C	5.97158581	1.74117736	4.38576045
C	4.74361146	1.05847395	4.45046572
C	7.00152933	1.19270507	3.60813093
C	4.55175690	-0.13163495	3.74769141
H	3.93032005	1.46361802	5.05674817
C	6.80949404	-0.00712868	2.91728313
H	7.96219972	1.70600794	3.54147657
C	5.58529128	-0.69276447	2.97589758
H	3.58719826	-0.64177969	3.80722376
H	7.62721711	-0.41715493	2.31928826
H	10.73698746	2.76862423	7.07474089
H	10.38210330	5.32527156	3.62156158
H	4.38087700	5.06323285	1.01133792
H	4.30170355	7.76484817	4.36990012
C	12.22024245	4.37519259	5.41811063

C	5.39695707	-2.00872185	2.26485157
C	3.63276308	7.60161756	1.71145936
H	12.41555170	5.24927881	6.05933100
H	12.77802364	3.52960313	5.84116816
H	12.62446119	4.60403632	4.42347193
H	5.64022134	-2.84858625	2.93477839
H	4.35726104	-2.14336929	1.93896816
H	6.05527624	-2.08757115	1.39003815
H	4.35876115	8.00109600	0.98690649
H	2.79749603	7.18455503	1.13153642
H	3.25675869	8.44121875	2.30925165
P	6.13434996	3.28745611	5.36871975
C	7.94279161	3.61366014	5.29204998
C	8.75080132	3.01996838	6.27822209
C	8.55186500	4.44215877	4.33836340
C	10.12818642	3.24359852	6.30151395
H	8.29593307	2.37758442	7.03548595
C	9.92969795	4.67380081	4.37345948
H	7.94516206	4.91217487	3.56252751
C	10.74219759	4.08429316	5.35596343

[**1.2c**] - tris(3,5-dimethylphenyl)phosphine ($(PhMe_2)_3P$) - ZORA-GGAPBE-D3(BJ)/TZP_PhCl (COSMO) phase

P	-0.00134068	-0.11345957	-5.09435149
C	1.15590937	1.08484346	-4.31104993
C	1.28270187	2.34521534	-4.92332355
C	1.91130177	0.79692995	-3.17025014
C	2.13866132	3.31851558	-4.39741672
H	0.70168120	2.57065040	-5.82165033
C	2.79233939	1.74928526	-2.62938261
H	1.81613106	-0.18085671	-2.69245403
C	2.88857795	3.00077236	-3.25002863
H	3.56978081	3.74985712	-2.83421488
C	0.44937652	-1.69130418	-4.26035586
C	-0.14236761	-2.13465172	-3.07349838

C	1.43166566	-2.48431476	-4.88112311
C	0.23140412	-3.36025869	-2.49573929
H	-0.90828928	-1.52236371	-2.59157940
C	1.83400614	-3.70174270	-4.32156138
H	1.88655439	-2.14615667	-5.81598146
C	1.21840406	-4.12547137	-3.12945006
H	1.51353465	-5.08275961	-2.68840736
C	-1.59928411	0.31139855	-4.28317182
C	-2.76162678	-0.28426009	-4.80633757
C	-1.71104686	1.21979534	-3.22583789
C	-4.02238076	0.00791464	-4.27569753
H	-2.68159798	-0.98059938	-5.64551406
C	-2.96607173	1.54417205	-2.68248276
H	-0.81237607	1.69133797	-2.82176222
C	-4.10610670	0.93142194	-3.21715400
H	-5.08907642	1.18681280	-2.80893615
C	3.62293858	1.41312800	-1.41547207
C	2.27488999	4.67188023	-5.04928983
C	2.88994974	-4.55284636	-4.98171152
C	-0.43291172	-3.83773355	-1.22799105
C	-3.06948206	2.52071722	-1.53676247
C	-5.26879412	-0.63806878	-4.82753939
H	3.30208542	4.83401455	-5.40856854
H	1.59441564	4.77327010	-5.90390326
H	2.05431431	5.47834583	-4.33500790
H	4.10214328	2.30756729	-0.99807231
H	3.01020731	0.94758367	-0.63073180
H	4.41617873	0.69419385	-1.67195158
H	-2.76055660	2.04892641	-0.59110934
H	-2.41222864	3.38739687	-1.69269643
H	-4.09820993	2.88089388	-1.40968794
H	-6.02900174	0.11588947	-5.07726643
H	-5.04944950	-1.22132574	-5.73061826
H	-5.71992330	-1.31580718	-4.08717617
H	3.75963355	-4.68408856	-4.32107329
H	2.50360755	-5.55768583	-5.20690766
H	3.23790245	-4.10064984	-5.91877700

H	-1.49247329	-4.07566724	-1.40675134
H	0.05459000	-4.73900409	-0.83581151
H	-0.40636495	-3.06200418	-0.44940087

[**1.2d**] - trimesitylphosphine ($(PhMe_3)_3P$) - ZORA-GGAPBE-D3(BJ)/TZP_PhCl (COSMO) phase

C	3.32710740	4.27030994	19.03303326
C	6.72125034	0.96491973	18.67574773
C	10.37775963	-0.02213751	15.37141726
C	7.07699828	3.58683746	14.27562986
C	3.39143337	4.59321488	15.07238865
C	5.37317899	9.19220617	15.21603869
C	7.69603098	5.50132120	17.71906518
H	2.86730683	5.09888452	14.25156133
H	3.80153876	3.64751301	14.69384015
H	2.64909341	4.32247073	15.83741583
H	8.35002771	4.79556487	17.18434367
H	8.30002078	6.36484064	18.02293118
H	7.34329235	4.97056830	18.61667980
H	4.96557392	9.30271192	14.20199264
H	4.71188863	9.75569684	15.89332546
H	6.36192218	9.66775583	15.25149998
H	3.35745993	5.17139778	18.40166656
H	2.55644464	4.41486395	19.79991848
H	4.31347993	4.20346761	19.51722879
H	-0.08077933	-0.14073081	17.08406946
H	0.27674396	-0.14888447	18.82057780
H	-0.63146405	1.20021717	18.12457417
H	3.92157217	0.13800587	14.78081948
H	4.87682117	1.64132574	14.73479500
H	5.38109078	0.32180042	15.78118414
H	7.55534963	3.40433108	13.30509231
H	5.98812909	3.54475335	14.14071315
H	7.30982069	4.61668808	14.58361834
H	5.70279386	0.57608003	18.52423733
H	7.29737006	0.21132169	19.22630111

H	6.61428209	1.86647888	19.29835746
H	10.60509810	0.08903882	14.30343647
H	11.26078454	0.31560161	15.93649359
H	10.24493494	-1.09029048	15.59236173
P	5.60989449	3.38793984	17.30295722
C	3.97610745	2.54587619	17.25640241
C	3.63287514	1.40274800	16.49073952
C	3.04549684	3.03603048	18.21677446
C	2.40427980	0.76751176	16.72797810
C	1.82458534	2.37888396	18.40005982
C	1.48757736	1.22654727	17.67903766
H	2.15143320	-0.11138966	16.12793906
H	1.12059645	2.77841340	19.13583618
C	5.51567383	5.02341901	16.46772591
C	6.53612354	5.93404276	16.86100399
C	4.47352169	5.48453536	15.62200872
C	6.48671121	7.26390484	16.42677222
C	4.45932231	6.83068694	15.23043797
C	5.44466270	7.74295098	15.62502783
H	7.28613866	7.94491931	16.73267245
H	3.65212946	7.17057411	14.57500349
C	6.90507654	2.33992733	16.52486105
C	7.38546178	1.29419305	17.36449704
C	7.54891869	2.57220518	15.28334681
C	8.48697086	0.53174912	16.96385291
C	8.66355802	1.79265226	14.93722296
C	9.15839248	0.77549444	15.75877338
H	8.83337564	-0.27227998	17.61976064
H	9.14899463	1.98152317	13.97546803
C	0.19206137	0.49871991	17.93351299
C	4.49703548	0.84627241	15.39008587

[**1.2e**] - tricyclohexylphosphine (Cy_3P) - ZORA-GGAPBE-D3(BJ)/TZP_PhCl (COSMO) phase

H	1.77964507	2.29092809	1.76988685
C	7.38634810	2.62068305	2.79245580

C	8.67436954	2.33310244	1.99516843
C	7.67614543	2.72989495	4.29622200
H	6.73271904	1.74330387	2.63734148
C	9.38502519	1.08006654	2.52562950
H	9.36197866	3.19161623	2.06589180
H	8.43135106	2.21471498	0.92764561
C	8.38819940	1.47418499	4.82090658
H	8.32056678	3.60639424	4.48141151
H	6.74351295	2.90260652	4.85659631
C	9.67106324	1.18858795	4.02929071
H	10.32032320	0.91291031	1.96751272
H	8.74337336	0.19901983	2.34205810
H	8.61524243	1.58987802	5.89293807
H	7.70615315	0.60916183	4.73158444
H	10.15040672	0.26671042	4.39562031
H	10.39030525	2.01021765	4.20115982
C	6.97196980	5.55022455	2.94226174
C	8.42335129	5.88937050	2.55680607
C	6.04695183	6.74928181	2.66303509
H	6.93133271	5.33229937	4.02486534
C	8.91852713	7.18030673	3.22247635
H	8.48419536	5.99761013	1.45889560
H	9.09216593	5.06010652	2.82619876
C	6.55061917	8.03723943	3.32941581
H	5.97918948	6.90699757	1.57126790
H	5.02876887	6.53431823	3.01711797
C	7.99100240	8.36163445	2.91924356
H	9.94585830	7.39834210	2.88919560
H	8.96544172	7.02742265	4.31581732
H	5.87778041	8.87211390	3.07547216
H	6.50544322	7.91589937	4.42679270
H	8.34267312	9.27078851	3.43257395
P	6.38469329	4.01492610	2.01710788
C	4.66696120	3.79112371	2.78706843
C	3.62283938	4.40723549	1.83162185
C	4.28560359	2.33203197	3.08682373
H	4.65317445	4.35150084	3.74041684

C	2.19949207	4.31724431	2.39473608
H	8.01983201	8.57595332	1.83527688
H	3.87509868	5.45158434	1.59994352
C	2.85801790	2.22267825	3.64424013
H	4.36029825	1.73819158	2.15771481
H	4.98677208	1.88628089	3.80651740
C	1.82377566	2.86544854	2.71295284
H	1.48502937	4.75233470	1.67758425
H	2.13399648	4.92381668	3.31615717
H	2.61017463	1.16386980	3.82254888
H	2.82208482	2.72606895	4.62728242
H	0.81938041	2.81461176	3.16292871
H	3.67021204	3.85929794	0.87377930

[**1.2f**] - tris(pentafluorophenyl)phosphine ($(PhF_5)_3P$) - ZORA-GGAPBE-D3(BJ)/TZP_PhCl (COSMO) phase

C	5.92634302	4.38636228	18.19256868
C	5.67297068	5.40135743	17.25772403
C	5.61254353	4.66473628	19.53076539
C	5.13772530	6.63593689	17.62608410
C	5.08066950	5.88838727	19.92665321
C	4.84348385	6.87734260	18.96791823
C	8.07475528	2.62857030	18.84719814
C	8.07525455	1.76674453	19.95329922
C	9.27602627	3.30908894	18.58811660
C	9.21100658	1.57746495	20.74196197
C	10.41829046	3.15324948	19.36824931
C	10.38492144	2.27260075	20.45075430
C	5.58441426	1.48413469	17.89036086
C	4.22667221	1.56563029	18.22647389
C	6.06029360	0.20821492	17.54872879
C	3.39856313	0.44090282	18.23881516
C	5.26336082	-0.93039627	17.56293374
C	3.91596607	-0.81116897	17.91043901
P	6.75830798	2.86772085	17.57025845

F	4.32467248	8.05832710	19.34362033
F	4.90537106	7.59082408	16.70298026
F	5.94322672	5.20790025	15.94610682
F	5.78925232	3.72128813	20.48118205
F	4.77469915	6.12963052	21.21770125
F	3.64548408	2.74321039	18.55290125
F	6.96891872	1.07735048	20.30958764
F	9.18087293	0.73388191	21.79469505
F	11.47818938	2.09692954	21.21388389
F	11.54839268	3.83288763	19.08511874
F	9.34602303	4.16071897	17.53466879
F	2.09617050	0.55986558	18.57127625
F	3.12248901	-1.89760127	17.92388083
F	5.77393994	-2.13646321	17.24062515
F	7.36328392	0.06622503	17.19420710

[**1.2g**] - dimethyl(phenyl)phosphane ($PhMe_2P$) - ZORA-GGAPBE-D3(BJ)/TZP_PhCl (COSMO) phase

P	0.80352751	2.28245828	-2.38864513
H	0.74584465	2.94430414	0.56816081
H	0.16190133	0.90413239	-0.41296141
C	-0.70299066	5.98574852	-1.37639148
H	3.15977178	2.87405119	-2.06128199
C	-0.27117395	4.85115881	-2.07468110
C	-0.61386145	6.02288632	0.01906050
C	-0.09142218	4.92270913	0.71317965
C	0.33903580	3.79262407	0.01264425
H	-0.34199369	4.82231592	-3.16469250
C	0.25411890	3.74258806	-1.38984711
H	-1.10883908	6.83888895	-1.92279885
H	-0.95007603	6.90531303	0.56639440
H	-0.01948647	4.94711121	1.80209133
C	-0.05002765	0.89816762	-1.49221413
H	-1.13443555	0.97665272	-1.65100621
H	0.29480913	-0.05482683	-1.91963597
C	2.52565421	2.03806788	-1.73573174

H	2.54909959	1.96689147	-0.63836709
H	2.92855177	1.10891612	-2.16487836

[**1.1**/**1.2a**] (orientation a) - $B(PhF_5)_3/Ph_3P$_a - ZORA-GGAPBE-D3(BJ)/TZP_PhCl (COSMO) phase

C	4.75457343	2.67178742	4.41140462
C	4.54277129	1.36711901	4.87785789
C	3.43210420	0.58481033	4.58327238
C	2.44087575	1.10452005	3.75330966
C	2.60767243	2.38243831	3.22821994
C	3.74677554	3.12678587	3.54902637
B	6.09288966	3.50680905	4.83498231
C	6.04103815	5.08295705	4.40881855
C	7.48422843	2.76293606	4.41160612
C	5.01460823	5.91970061	4.86830847
C	8.72169557	3.23148546	4.87375665
C	4.89599814	7.27308337	4.57395487
C	9.95325754	2.65905249	4.57719007
C	5.84804996	7.87117730	3.75099918
C	9.99571653	1.53898595	3.74948891
C	6.87361832	7.08681129	3.23194316
C	8.80377612	1.04414412	3.22894357
C	6.94504113	5.72788917	3.55238729
C	7.59102445	1.66022282	3.55174638
F	11.10141752	3.18158530	5.06540451
F	11.17424318	0.95900299	3.43980851
F	8.83026180	-0.02270391	2.39552990
F	6.50340023	1.12163617	2.93797311
F	8.76414436	4.35717092	5.64246851
F	5.49614695	0.77147242	5.65033050
F	3.31091373	-0.66908523	5.07613389
F	1.34967885	0.37228702	3.44612275
F	1.67037461	2.88926213	2.39270210
F	3.82379419	4.33612831	2.93166912
F	7.95698635	5.05616279	2.94045407
F	7.78726375	7.64450354	2.40263754

F	5.76342162	9.18271497	3.44450088
F	3.86839782	8.00586857	5.06072643
F	4.01638222	5.39285162	5.63391010
P	6.08953546	3.51192829	7.01386589
C	6.01710636	5.18433762	7.75707006
C	6.92546298	6.18093199	7.35720839
C	5.07142764	5.47589060	8.75263489
C	6.88099969	7.44798299	7.94197229
H	7.67282977	5.97293794	6.59647386
C	5.02787620	6.74698968	9.33102862
H	4.36605577	4.71266911	9.07897641
C	5.92875566	7.73679457	8.92547299
H	7.59267924	8.21059460	7.62323333
H	4.28605414	6.95924877	10.10210162
H	5.89129798	8.72992535	9.37626779
C	4.67815831	2.61865593	7.76526174
C	3.36053480	2.89610952	7.35909032
C	4.90044182	1.67185270	8.77756636
C	2.28705910	2.23049500	7.95411480
H	3.16500932	3.63381971	6.58571801
C	3.82289350	1.00574384	9.36686260
H	5.91457344	1.45075301	9.10792378
C	2.51484869	1.27975332	8.95489870
H	1.27037762	2.45604350	7.62990222
H	4.01152551	0.27102517	10.15080170
H	1.67466824	0.75575783	9.41364152
C	7.56882857	2.74025246	7.76897751
C	7.98667797	1.45860582	7.36791195
C	8.27692103	3.40947235	8.77947908
C	9.09850757	0.86299435	7.96652112
H	7.44551379	0.91798430	6.59624314
C	9.39118873	2.81044993	9.37244975
H	7.96110195	4.39932796	9.10648464
C	9.80729667	1.53882209	8.96561611
H	9.41066410	-0.13210584	7.64700663
H	9.93214666	3.34301996	10.15582146
H	10.68013600	1.07397098	9.42713034

[**1.1**/**1.2a**] (orientation b) - $B(PhF_5)_3/Ph_3P$_b - ZORA-GGAPBE-D3(BJ)/TZP_PhCl (COSMO) phase

C	4.74515524	2.70682587	4.52735282
C	4.60369057	1.47694035	5.19796098
C	3.41773780	0.74922805	5.21985938
C	2.30101398	1.24585255	4.54714885
C	2.38933782	2.45430993	3.85415321
C	3.59156501	3.15427145	3.85644109
B	6.08400145	3.51921287	4.52590730
C	6.05289033	5.08471537	4.52842901
C	7.45451660	2.76204819	4.51387947
C	5.06008160	5.82503028	5.19877026
C	8.59506443	3.24098304	5.18557057
C	5.02524297	7.21597462	5.21851357
C	9.81467750	2.57089197	5.19563517
C	6.01512815	7.93247417	4.54539110
C	9.93446763	1.36205374	4.50980005
C	7.01695990	7.24913687	3.85432157
C	8.83820664	0.84743838	3.81568223
C	7.01946891	5.85799466	3.85776975
C	7.63471137	1.54515586	3.82938151
F	10.87927362	3.07429835	5.85070269
F	11.10249952	0.69774464	4.51321708
F	8.95993259	-0.31241457	3.13606371
F	6.62129984	1.00257371	3.11249067
F	8.54598438	4.40072700	5.88025047
F	5.64349241	0.94421297	5.87991478
F	3.33466223	-0.42638031	5.87335467
F	1.14481764	0.56127919	4.56336666
F	1.31365216	2.92495797	3.18827487
F	3.61472858	4.30456066	3.14102527
F	8.00316580	5.26139204	3.14274519
F	7.96303321	7.94282284	3.18685719
F	6.00167373	9.27598266	4.55890829
F	4.04976601	7.87852983	5.87101633

F	4.07803810	5.19245163	5.88071225
P	6.09197287	3.50790207	10.31601741
C	7.56357093	2.73207024	9.53078813
C	8.83188959	3.13173237	9.99424200
C	7.48109800	1.71188650	8.57237114
C	9.99085715	2.53473736	9.49404322
H	8.91001662	3.91485273	10.75167559
C	8.64165408	1.09550986	8.09231611
H	6.50665961	1.39184686	8.20402119
C	9.89896424	1.50544537	8.54772529
H	10.96739525	2.86129114	9.85496375
H	8.55780905	0.28980512	7.35971936
H	10.80415885	1.02446109	8.17251826
C	4.68254933	2.62410602	9.53056408
C	4.39475544	1.32382311	9.98871524
C	3.83629830	3.21091806	8.57876023
C	3.29444796	0.62284347	9.49062234
H	5.03661333	0.85990528	10.74099355
C	2.71749285	2.51940571	8.10238324
H	4.04687305	4.21603247	8.21386077
C	2.44421321	1.22373418	8.55273073
H	3.08939580	-0.38758232	9.84766158
H	2.05821167	2.99985367	7.37621544
H	1.57105724	0.68410125	8.18123831
C	6.03109549	5.17201938	9.53432000
C	5.05396048	6.07272514	10.00005165
C	6.95559422	5.60927640	8.57512219
C	4.99454469	7.37557538	9.50126604
H	4.33629212	5.74982574	10.75740294
C	6.91339858	6.92360640	8.09761924
H	7.71711498	4.92319838	8.20490939
C	5.93241770	7.80944507	8.55491897
H	4.22537040	8.05945522	9.86355846
H	7.65357017	7.25245301	7.36486385
H	5.89888095	8.83455085	8.18126147

[**1.1**/**1.2b**] (orientation a) - $B(PhF_5)_3$/$(PhMe)_3P$_a - ZZORA-GGAPBE-D3(BJ)/TZP_PhCl (COSMO) phase

C	4.79567829	2.63166480	-1.19242560
C	4.06368132	1.60358001	-0.58838539
C	3.02183649	0.90493146	-1.19359525
C	2.67488972	1.20278686	-2.50916765
C	3.40200390	2.17707120	-3.18555284
C	4.43867106	2.85035759	-2.53378300
B	5.97528539	3.51626564	-0.46144260
C	5.91071144	5.04694867	-1.06304232
C	7.46585324	2.84487879	-0.54390336
C	4.85404818	5.91297736	-0.77287558
C	8.63804622	3.57630708	-0.28615294
C	4.71592309	7.20632752	-1.27487329
C	9.92223319	3.03811443	-0.33011496
C	5.66533207	7.69215980	-2.16727256
C	10.09153345	1.68717289	-0.62737054
C	6.71012991	6.85332857	-2.54789958
C	8.96612069	0.91079582	-0.88174884
C	6.80125386	5.56774473	-2.01556283
C	7.69639471	1.49209872	-0.83497817
F	11.00603578	3.81254303	-0.09112647
F	11.32511064	1.14378994	-0.66772351
F	9.11035036	-0.40363137	-1.16588419
F	6.67343002	0.63698023	-1.08727787
F	8.57329682	4.89408022	0.02636702
F	4.37054809	1.21029348	0.67801338
F	2.35515497	-0.06209576	-0.52067253
F	1.66776127	0.54708314	-3.12142840
F	3.10535871	2.45688169	-4.47572029
F	5.12238751	3.72728216	-3.31518494
F	7.79356445	4.80485149	-2.54593632
F	7.61407940	7.28494047	-3.45964038
F	5.56326115	8.93923750	-2.67346861
F	3.67247371	7.98512523	-0.90122008
F	3.85463309	5.50398290	0.06154082
P	5.73447221	3.58858969	1.66316731

C	6.64860554	5.02701746	2.33477958
C	6.07556998	6.30453563	2.19007243
C	7.88209884	4.91721997	2.98854265
C	6.74150512	7.43599972	2.65166318
H	5.08548446	6.41526763	1.75327495
C	8.54380430	6.05809472	3.44919680
H	8.33529282	3.94414486	3.16103766
C	7.99728256	7.33752517	3.27739524
C	6.41173424	2.11119532	2.51907511
C	5.55821269	1.31762399	3.30532373
C	7.76527433	1.73825326	2.43310966
C	6.04411885	0.20037239	3.98359142
H	4.50198846	1.56731109	3.39014408
C	8.24499744	0.62330509	3.12009691
H	8.46764039	2.31888809	1.84082114
C	7.39589036	-0.17117868	3.90584881
C	4.08182184	3.79455688	2.42752008
C	2.87224371	3.54100428	1.77123441
C	4.05048151	4.17488607	3.78204836
C	1.65930654	3.66355136	2.45244124
H	2.85656435	3.27079257	0.71840532
C	2.83839675	4.28985428	4.45612181
H	4.98068408	4.37688995	4.31352230
C	1.61717394	4.03663280	3.80390835
H	0.72725358	3.46967920	1.91744788
H	2.84081719	4.58272288	5.50836905
H	6.27239640	8.41526745	2.53171374
H	9.50451056	5.94490708	3.95593897
H	5.35416694	-0.39285643	4.58795621
H	9.30499288	0.37101384	3.04442307
C	8.72040995	8.57115193	3.74933364
C	0.30979710	4.17439893	4.53804875
C	7.91115155	-1.39382536	4.61741174
H	9.01457584	9.19817308	2.89422590
H	8.07362209	9.18785074	4.38933795
H	9.62645735	8.31446706	4.31129525
H	0.28600565	3.52148794	5.42256342

H	0.17210437	5.20449707	4.89830138
H	-0.53982156	3.91809210	3.89398024
H	8.96960942	-1.28413169	4.88579961
H	7.33205930	-1.60085012	5.52631224
H	7.82785123	-2.27853886	3.96688955

[**1.1**/**1.2b**] (orientation b) - $B(PhF_5)_3$/$(PhMe)_3P$_b - ZORA-GGAPBE-D3(BJ)/TZP_PhCl (COSMO) phase

C	4.18572314	2.42652697	-1.11246528
C	3.32455550	2.00360794	-0.10109887
C	2.54119926	0.85492243	-0.21408716
C	2.63352429	0.07674691	-1.36880420
C	3.48560474	0.46635693	-2.40389689
C	4.23041536	1.63461222	-2.26067616
B	5.09369334	3.72120523	-1.02497604
C	4.56835171	5.01904266	-1.72627523
C	6.48073128	3.66845209	-0.34234630
C	3.23873141	5.45520994	-1.60318239
C	7.14563446	4.82693429	0.12453385
C	2.74440404	6.58302848	-2.25359336
C	8.40742317	4.79986341	0.70349484
C	3.58804302	7.30487444	-3.10008877
C	9.08207499	3.58059887	0.81967698
C	4.91335397	6.89837161	-3.27266492
C	8.46262628	2.40223487	0.39949726
C	5.37907089	5.78328012	-2.58330120
C	7.18997395	2.45828204	-0.15914306
F	8.99714226	5.93619224	1.12619869
F	10.32640775	3.54450367	1.30696717
F	9.11404819	1.22743825	0.51938683
F	6.68155344	1.28591764	-0.58847502
F	6.56327314	6.04003575	0.02667330
F	3.20377287	2.74423654	1.02915331
F	1.68825339	0.49418156	0.76882247
F	1.89531125	-1.04540241	-1.48790517
F	3.57863362	-0.28745750	-3.52142947

F	5.06694029	1.98859146	-3.27538779
F	6.66948800	5.43077600	-2.79355157
F	5.72219640	7.59142839	-4.09925115
F	3.12834524	8.38801324	-3.74724870
F	1.46969186	6.98444534	-2.07327017
F	2.38632678	4.80767818	-0.77236012
P	6.09140206	3.16258393	5.18716456
C	7.90997102	3.27399018	4.94195869
C	8.71097725	2.25397830	5.48852111
C	8.54465378	4.35478308	4.31393526
C	10.10027530	2.30537003	5.38304543
H	8.24129175	1.40659605	5.99267136
C	9.93934064	4.41363589	4.23491828
H	7.94598682	5.15985855	3.88510638
C	10.74262264	3.39110528	4.75990383
C	5.48067301	4.65121601	4.29943740
C	4.92655822	4.60127959	3.01272696
C	5.51417330	5.88758122	4.96760052
C	4.41987811	5.75431221	2.41298320
H	4.88009946	3.64909326	2.48576708
C	5.03213719	7.04416806	4.34918845
H	5.92159237	5.94822313	5.97906834
C	4.47247013	6.99897033	3.06061351
C	5.61641671	1.79106894	4.05502729
C	4.29547629	1.31616721	4.12456044
C	6.50627349	1.15705887	3.17388638
C	3.87789584	0.24784793	3.32837019
H	3.58416912	1.78816004	4.80581411
C	6.08939623	0.07649737	2.39412204
H	7.53880269	1.50365459	3.11031344
C	4.76927866	-0.40054936	2.45726648
H	2.84326742	-0.09615478	3.39199210
H	6.80225477	-0.40645616	1.72132196
H	10.69948961	1.49109010	5.79820895
H	10.41017650	5.26539403	3.73816520
H	3.97266087	5.68864851	1.41767953
H	5.07601062	7.99674949	4.88254801

C	12.24616735	3.46101864	4.67870393
C	4.34200709	-1.59307279	1.63948479
C	3.95571399	8.24202141	2.38180593
H	12.67392880	3.81015774	5.63157126
H	12.68071245	2.47339290	4.47274116
H	12.57069110	4.15761190	3.89512860
H	4.74628434	-2.52389507	2.06601600
H	3.24960746	-1.68916160	1.60852180
H	4.72096635	-1.52449647	0.60969020
H	4.65026126	8.57013295	1.59263990
H	2.98428572	8.05906195	1.90122076
H	3.84147831	9.07038712	3.09197849

[**1.1**/**1.2c**] (orientation a) - $B(PhF_5)_3$/$(PhMe_2)_3P$_a - ZORA-GGAPBE-D3(BJ)/TZP_PhCl (COSMO) phase

P	0.08089812	-0.48844689	-8.34825994
C	1.05366548	0.91280591	-9.02104102
C	2.45271124	0.84136460	-8.92721071
C	0.45866773	2.03973971	-9.59898786
C	3.25667809	1.89897681	-9.36693575
H	2.93001087	-0.06188751	-8.55013871
C	1.24091733	3.11419689	-10.04504122
H	-0.62106899	2.09134259	-9.72504680
C	2.63373799	3.03048063	-9.91628389
H	3.25268063	3.86105741	-10.26860462
C	-1.56775603	-0.40687153	-9.16330377
C	-1.98704900	-1.48049449	-9.96592850
C	-2.41701738	0.70090708	-9.01626320
C	-3.22454762	-1.45403059	-10.62012100
H	-1.34692920	-2.35351880	-10.08866503
C	-3.66045659	0.75403294	-9.66161401
H	-2.12106365	1.55191150	-8.40713559
C	-4.04668405	-0.32776915	-10.46283223
H	-5.01029558	-0.29206476	-10.98003105
C	0.87212320	-1.93905249	-9.14369119
C	1.07582277	-3.15542933	-8.49019859

C	1.20559106	-1.81446822	-10.50384843
C	1.60294071	-4.26026454	-9.17721861
H	0.85205084	-3.25894149	-7.43033569
C	1.73026611	-2.89808570	-11.21228592
H	1.04722984	-0.86504460	-11.01728637
C	1.91840641	-4.11519282	-10.53265032
H	2.32788246	-4.97125967	-11.07740534
C	0.58264550	4.34182873	-10.62221355
C	4.75583751	1.82377076	-9.22699839
C	-4.56417350	1.94573947	-9.46736103
C	-3.67077883	-2.62619721	-11.45737183
C	2.09767411	-2.76430703	-12.66806385
C	1.81256109	-5.56707203	-8.45423612
H	5.06739238	2.17982650	-8.23235008
H	5.11635904	0.79177055	-9.33098520
H	5.26068081	2.45028942	-9.97307520
H	0.26529289	5.02268886	-9.81667993
H	1.27064148	4.89743055	-11.27168711
H	-0.31389530	4.08142961	-11.20062848
H	1.66601619	-3.58300307	-13.26045648
H	1.74639544	-1.81151028	-13.08306738
H	3.18895219	-2.81219243	-12.80078618
H	2.42727305	-5.42576864	-7.55362312
H	0.85245244	-5.99301871	-8.12592778
H	2.30810971	-6.30387031	-9.09783936
H	-5.26557188	2.05597550	-10.30365536
H	-5.16228661	1.83358551	-8.54907403
H	-3.98866588	2.87642340	-9.37028873
H	-2.81618732	-3.22949956	-11.78915561
H	-4.33670757	-3.28451477	-10.87828740
H	-4.23056539	-2.29350723	-12.34144705
C	-0.40315221	-1.74315984	-5.49243301
C	-0.04046497	-2.02268476	-4.16406552
C	-0.28162614	-3.24401537	-3.52854284
C	-0.94110774	-4.26225571	-4.21000866
C	-1.37048198	-4.02250375	-5.51313345
C	-1.11111917	-2.78639147	-6.10054347

C	-1.16695342	0.84173883	-6.09371633
C	1.45206192	0.17122290	-5.64164039
C	-2.51170756	0.57017694	-5.80031787
C	1.62650283	1.16910962	-4.66910413
C	-3.51139764	1.54514304	-5.75292655
C	2.86717382	1.56875196	-4.17402441
C	-3.19371110	2.87391612	-6.01280154
C	4.02835509	0.94065642	-4.61892262
C	-1.87227508	3.20288003	-6.30840037
C	3.91126066	-0.10060952	-5.53317981
C	-0.90503851	2.20036241	-6.34482445
C	2.64547628	-0.46463257	-5.99199127
F	2.95254001	2.54647043	-3.24031166
F	5.23785565	1.31746086	-4.15238489
F	5.01732215	-0.75122554	-5.96843950
F	2.62192022	-1.52804856	-6.84549032
F	0.55988618	1.78018932	-4.08821344
F	0.55164129	-1.08444264	-3.37938639
F	0.11127651	-3.44116272	-2.24853430
F	-1.17831299	-5.44917752	-3.61416530
F	-2.04019499	-4.98377656	-6.19188973
F	-1.61602950	-2.61982336	-7.35227735
F	0.34837644	2.62019396	-6.64748970
F	-1.54255754	4.49155419	-6.55866362
F	-4.14801788	3.82647769	-5.98528801
F	-4.79076597	1.20594022	-5.47326072
F	-2.94085946	-0.69290459	-5.55264008
B	-0.01346583	-0.31456484	-6.21167031

[**1.1**/**1.2c**] (orientation b) - $B(PhF_5)_3$/$(PhMe_2)_3P$_b - ZORA-GGAPBE-D3(BJ)/TZP_PhCl (COSMO) phase

P	0.047093	-0.464298	-4.864115
C	1.273132	0.831221	-4.419723
C	1.374646	1.905436	-5.322727
C	2.097548	0.804531	-3.290333
C	2.272561	2.955116	-5.101502

H	0.741908	1.918556	-6.214388
C	3.033144	1.828017	-3.061009
H	2.024818	-0.030947	-2.590566
C	3.102705	2.891806	-3.969170
H	3.831456	3.689686	-3.796114
C	0.539599	-1.949576	-3.892618
C	-0.396302	-2.729168	-3.196598
C	1.851515	-2.432966	-4.039475
C	-0.045721	-3.978394	-2.667251
H	-1.419210	-2.369555	-3.074332
C	2.238419	-3.659373	-3.483070
H	2.586166	-1.850342	-4.600671
C	1.275742	-4.425074	-2.809189
H	1.561253	-5.396289	-2.392953
C	-1.491148	0.131443	-4.051376
C	-2.682611	-0.567635	-4.314624
C	-1.545133	1.319391	-3.308748
C	-3.911314	-0.114522	-3.816674
H	-2.657890	-1.468373	-4.933035
C	-2.768782	1.819553	-2.840984
H	-0.626631	1.877305	-3.113193
C	-3.937509	1.088865	-3.095502
H	-4.896189	1.471695	-2.731943
C	3.948899	1.781410	-1.863816
C	2.353815	4.125359	-6.049355
C	3.662421	-4.142843	-3.598077
C	-1.070202	-4.840696	-1.972083
C	-2.825834	3.107421	-2.058982
C	-5.176999	-0.900207	-4.049505
H	3.397019	4.416673	-6.233589
H	1.879483	3.894805	-7.011716
H	1.842770	5.004275	-5.626567
H	4.647349	2.627239	-1.862818
H	3.371848	1.816838	-0.927940
H	4.538194	0.851978	-1.852453
H	-2.888510	2.901012	-0.978588
H	-1.931993	3.721054	-2.233012

H	-3.711522	3.699547	-2.325366
H	-6.038213	-0.235176	-4.198652
H	-5.085618	-1.558551	-4.923056
H	-5.403091	-1.534365	-3.177706
H	4.241798	-3.854738	-2.707338
H	3.707268	-5.237278	-3.676090
H	4.164170	-3.707386	-4.472010
H	-2.048595	-4.344462	-1.933212
H	-1.201059	-5.798005	-2.497701
H	-0.758869	-5.083284	-0.945306
C	-1.104126	-1.054822	0.984691
C	-0.804416	-2.353079	1.444419
C	-1.672043	-3.430549	1.305029
C	-2.900607	-3.241425	0.668174
C	-3.251500	-1.975790	0.197461
C	-2.369114	-0.913096	0.375984
C	-0.643797	1.604517	1.239115
C	1.444608	-0.089282	1.073207
C	-1.705509	1.938316	2.094821
C	2.325318	0.688271	1.848713
C	-2.170139	3.240730	2.257229
C	3.706468	0.508928	1.843316
C	-1.579931	4.271942	1.522996
C	4.263876	-0.470451	1.019981
C	-0.531539	3.987554	0.646238
C	3.434817	-1.262237	0.223752
C	-0.078317	2.676599	0.529583
C	2.056620	-1.070267	0.269862
F	4.509208	1.268309	2.618218
F	5.595406	-0.647833	0.989464
F	3.981484	-2.201101	-0.575711
F	1.307851	-1.866694	-0.517472
F	1.847571	1.644598	2.681490
F	0.361759	-2.603960	2.083988
F	-1.340017	-4.655121	1.766237
F	-3.742142	-4.276010	0.509317
F	-4.443719	-1.797287	-0.407951

F	-2.779117	0.284238	-0.086397
F	0.934264	2.458358	-0.341764
F	0.023631	4.980672	-0.079646
F	-2.024529	5.533501	1.655389
F	-3.179203	3.517924	3.109477
F	-2.311330	0.977743	2.834768
B	-0.105583	0.138077	1.098978

[**1.1**/**1.2d**] (orientation a) - $B(PhF_5)_3$/$(PhMe_3)_3P$_a - ZORA-GGAPBE-D3(BJ)/TZP_PhCl (COSMO) phase

C	4.38799219	3.16627463	2.66413625
C	3.88640251	2.04516880	3.34978795
C	2.53174535	1.73078807	3.40356452
C	1.61555825	2.53812259	2.72726694
C	2.06495551	3.65180450	2.01481099
C	3.42426666	3.94862332	2.00351411
B	5.91000125	3.52577073	2.65047368
C	6.35820008	5.02087051	2.72162969
C	6.97428387	2.38342514	2.57265440
C	5.66137819	5.98135852	3.47966157
C	8.19947941	2.44171735	3.26232794
C	6.06567918	7.30922740	3.58092209
C	9.13526526	1.41196004	3.23941187
C	7.19818553	7.73394174	2.88443904
C	8.87751369	0.27059724	2.47839098
C	7.91415063	6.82515188	2.10266144
C	7.68542277	0.17171244	1.75806904
C	7.49311179	5.50063323	2.04205074
C	6.76268508	1.21098855	1.82377949
F	10.28189649	1.50075410	3.94356898
F	9.77412850	-0.72851224	2.43665806
F	7.44449834	-0.92495909	1.01002826
F	5.63144571	1.05828773	1.09490881
F	8.50507099	3.51479633	4.02545038
F	4.72244619	1.23129829	4.03356663
F	2.09411510	0.66239595	4.10054416

F	0.30538769	2.24375412	2.75952910
F	1.17966984	4.42228949	1.34915316
F	3.79917068	5.03621654	1.28818950
F	8.22203580	4.67263847	1.25656879
F	8.99919050	7.24166613	1.41735227
F	7.59780031	9.01360954	2.96366282
F	5.38271320	8.18670613	4.34326047
F	4.56510015	5.63174246	4.18728438
P	6.20161576	3.47549857	7.68139081
C	5.85106702	1.77033261	8.26995117
C	4.92445193	1.39843099	9.27653837
C	6.47986223	0.74981446	7.50268006
C	4.62466949	0.03968914	9.45684614
C	6.16079806	-0.59117119	7.73350560
C	5.21706622	-0.97210809	8.69442139
H	3.91012730	-0.23381421	10.23866104
H	6.65947523	-1.35886393	7.13474602
C	7.86335221	4.03018013	8.23754352
C	8.40685719	5.09825931	7.47012023
C	8.67799319	3.40846041	9.21828368
C	9.73114112	5.49803642	7.67184060
C	10.00560833	3.83539320	9.37030745
C	10.56074354	4.86621923	8.60477383
H	10.12576595	6.32385452	7.07278582
H	10.62130254	3.34943642	10.13279537
C	4.89976020	4.64116063	8.24901864
C	3.68750922	4.56590638	7.50660754
C	5.05392851	5.67789433	9.20449406
C	2.69212914	5.52798977	7.69871394
C	4.03128287	6.62783173	9.34863620
C	2.85023754	6.58651612	8.60055358
H	1.76963640	5.45043174	7.11591362
H	4.16299286	7.42178107	10.08955893
C	4.83921388	-2.41908640	8.88342066
C	4.26601036	2.38252423	10.20689864
C	7.50063735	1.07645371	6.44711438
C	3.43580732	3.45503177	6.52537850

C	1.79329085	7.65155174	8.74405667
C	6.24345480	5.79815345	10.12032805
C	8.18505425	2.33625197	10.15381771
C	12.00482492	5.26868143	8.76250035
C	7.58156742	5.83304410	6.45028306
H	8.89785231	2.19774796	10.97654531
H	7.20625098	2.59333956	10.58043997
H	8.05567752	1.36925107	9.64613294
H	6.78299859	6.42575860	6.92235173
H	8.21006377	6.50959000	5.85747690
H	7.07927126	5.11942959	5.78026540
H	12.38057227	5.03036951	9.76622917
H	12.63891694	4.73157443	8.03910190
H	12.14436514	6.34265077	8.57982406
H	8.41378591	1.51149998	6.88075443
H	7.77987485	0.17611950	5.88549434
H	7.10154063	1.83176599	5.75407812
H	4.42527494	-2.59830359	9.88427489
H	4.07237905	-2.71889943	8.15141701
H	5.70258526	-3.08186843	8.73558479
H	3.82331892	1.85523732	11.06141477
H	4.98352332	3.12204505	10.58639776
H	3.46950819	2.95418387	9.70793209
H	6.01364188	6.48226298	10.94704061
H	6.52846162	4.82489427	10.54152254
H	7.13311173	6.18021142	9.59813624
H	3.29640267	2.48818698	7.03258948
H	2.54147856	3.66246725	5.92456417
H	4.30294387	3.32781250	5.86036782
H	1.86753037	8.16285982	9.71266448
H	1.90361267	8.41589751	7.95835981
H	0.78342152	7.23084679	8.64470458

[**1.1**/**1.2d**] (orientation b) - $B(PhF_5)_3$/$(PhMe_3)_3P$_b - ZORA-GGAPBE-D3(BJ)/TZP_PhCl (COSMO) phase

C	5.176129	3.615034	10.873513

C	4.841155	2.337058	11.362887
C	3.532129	1.932847	11.609894
C	2.482279	2.808062	11.329613
C	2.756216	4.072189	10.803147
C	4.078082	4.449574	10.590990
B	6.659527	4.087327	10.707874
C	7.055658	5.576317	10.976857
C	7.758505	3.052722	10.282615
C	6.408944	6.380561	11.936825
C	9.054588	3.054832	10.829551
C	6.751552	7.708014	12.175286
C	10.020072	2.107358	10.502860
C	7.789017	8.289524	11.445275
C	9.718436	1.120415	9.562419
C	8.461688	7.539537	10.479500
C	8.454115	1.089595	8.971017
C	8.089758	6.215884	10.264982
C	7.505926	2.038042	9.343166
F	11.241427	2.136340	11.073646
F	10.643238	0.207822	9.224040
F	8.167743	0.144366	8.053036
F	6.299657	1.957096	8.733673
F	9.411329	3.984767	11.745295
F	5.804368	1.432663	11.646890
F	3.266402	0.707957	12.104730
F	1.213229	2.431269	11.553619
F	1.740051	4.908923	10.509192
F	4.272139	5.682321	10.066127
F	8.765748	5.557869	9.293861
F	9.452517	8.107023	9.761745
F	8.129180	9.569751	11.663801
F	6.081379	8.450107	13.080078
F	5.403400	5.879805	12.688035
P	6.095414	3.146809	17.312969
C	4.270836	3.331224	17.452572
C	3.292221	2.767394	16.595480
C	3.846700	4.006554	18.631826

C	1.938576	2.861960	16.952092
C	2.483260	4.091962	18.931882
C	1.506851	3.509675	18.113902
H	1.193606	2.427456	16.279217
H	2.178362	4.627402	19.835646
C	6.857665	4.707183	16.703016
C	8.260708	4.795121	16.930231
C	6.177333	5.835966	16.176341
C	8.945081	5.974302	16.614583
C	6.905226	7.003681	15.909077
C	8.286333	7.098378	16.104529
H	10.025480	6.012895	16.781019
H	6.366347	7.865961	15.509909
C	6.508595	1.759589	16.178734
C	6.366920	0.466806	16.756174
C	7.081920	1.873317	14.886782
C	6.800055	-0.661494	16.049488
C	7.524420	0.715367	14.233493
C	7.400104	-0.561306	14.788940
H	6.666739	-1.647497	16.503872
H	7.956802	0.818149	13.234049
C	0.046012	3.566703	18.481674
C	3.613955	2.114904	15.277240
C	4.830762	4.672038	19.558211
C	5.729107	0.271003	18.106360
C	7.902264	-1.779305	14.056055
C	7.197460	3.174606	14.141629
C	4.711472	5.850158	15.830810
C	9.039019	8.351606	15.736054
C	9.050701	3.632394	17.471241
H	4.475214	6.740573	15.235696
H	4.427112	4.962577	15.250573
H	4.070443	5.852899	16.723796
H	9.112826	2.814137	16.737241
H	10.071935	3.940296	17.726595
H	8.565300	3.206675	18.362767
H	8.411063	9.245226	15.849483

H	9.940670	8.475533	16.350274
H	9.365752	8.313263	14.684013
H	5.331482	5.521568	19.068838
H	4.328147	5.044002	20.459241
H	5.630053	3.974008	19.849896
H	-0.593777	3.409032	17.603689
H	-0.202369	2.784096	19.215983
H	-0.214793	4.531365	18.937799
H	2.693717	1.975938	14.695211
H	4.313536	2.724409	14.688607
H	4.091251	1.131980	15.398460
H	7.366043	2.966693	13.078434
H	6.291555	3.785157	14.241867
H	8.032243	3.796195	14.495990
H	4.657450	0.521376	18.083623
H	5.831188	-0.768872	18.439768
H	6.183060	0.938575	18.854908
H	7.711068	-1.701829	12.976620
H	8.990226	-1.894407	14.183940
H	7.427160	-2.695981	14.428598

[**1.1**/**1.2e**] (orientation a) - $B(PhF_5)_3/Cy_3P$_a - ZORA-GGAPBE-D3(BJ)/TZP_PhCl (COSMO) phase

C	4.773256	2.878305	-1.199229
C	4.394163	1.623172	-0.707677
C	3.186291	0.993245	-0.981453
C	2.269947	1.623860	-1.822294
C	2.608900	2.851833	-2.381601
C	3.840160	3.441716	-2.078921
B	6.218315	3.507553	-0.782750
C	6.456821	5.054391	-1.277592
C	7.466146	2.539707	-1.221519
C	5.562410	6.071421	-0.920663
C	8.783484	2.841260	-0.849848
C	5.678524	7.413128	-1.268241
C	9.908376	2.111508	-1.213824

C	6.745203	7.815813	-2.067910
C	9.755136	0.984073	-2.017390
C	7.638665	6.847652	-2.512143
C	8.478374	0.646738	-2.451356
C	7.474882	5.510284	-2.134422
C	7.379616	1.425056	-2.071130
F	11.140772	2.475928	-0.786224
F	10.823547	0.244139	-2.378785
F	8.310043	-0.427051	-3.258766
F	6.204047	1.025573	-2.625672
F	9.020025	3.929007	-0.071657
F	5.273086	0.922529	0.067889
F	2.898799	-0.223146	-0.459735
F	1.087497	1.039794	-2.107720
F	1.747051	3.459997	-3.230080
F	4.086393	4.608085	-2.732229
F	8.375775	4.669547	-2.709427
F	8.657571	7.204582	-3.329458
F	6.888703	9.107725	-2.428703
F	4.756965	8.317558	-0.858823
F	4.447015	5.747158	-0.216840
P	6.048966	3.525633	1.527141
C	4.306010	3.334293	2.329174
C	3.147078	4.120662	1.688727
C	3.839390	1.894257	2.630640
H	4.511800	3.811837	3.305227
C	1.898288	4.104033	2.583259
H	2.902361	3.683411	0.707911
H	3.428655	5.159929	1.512949
C	2.600436	1.895379	3.539060
H	3.583786	1.378331	1.695369
H	4.621523	1.302375	3.118316
C	1.445814	2.682575	2.917466
H	1.093767	4.663426	2.080778
H	2.121978	4.645027	3.520950
H	2.304152	0.853487	3.736818
H	2.867647	2.341414	4.514135

H	0.578662	2.700094	3.595904
H	1.117952	2.176046	1.991694
C	6.922660	2.097700	2.430229
C	8.318025	1.647052	1.974647
C	6.917049	2.290273	3.961037
H	6.250951	1.259852	2.191706
C	8.736300	0.359259	2.703419
H	9.063196	2.436463	2.161954
H	8.311340	1.440376	0.901361
C	7.306102	0.988871	4.676550
H	7.652373	3.066493	4.228664
H	5.940287	2.633396	4.327897
C	8.687513	0.505304	4.225863
H	9.746192	0.070860	2.372050
H	8.057898	-0.456114	2.394135
H	7.284921	1.153026	5.764949
H	6.551472	0.212776	4.455746
H	8.939805	-0.449726	4.712345
H	9.448411	1.239023	4.547166
C	6.661536	5.047329	2.473779
C	8.125070	5.418124	2.192791
C	5.774700	6.304486	2.458829
H	6.611544	4.657216	3.504922
C	8.633064	6.460680	3.198775
H	8.203290	5.826440	1.173174
H	8.765985	4.528697	2.232851
C	6.285040	7.328933	3.483823
H	5.794701	6.770203	1.464334
H	4.730380	6.056382	2.684943
C	7.745093	7.708291	3.219214
H	9.672550	6.726418	2.951325
H	8.651908	6.009563	4.207281
H	5.639718	8.220699	3.454059
H	6.194159	6.902435	4.498947
H	8.101491	8.422730	3.977413
H	7.814627	8.219353	2.242071

[**1.1**/**1.2e**] (orientation b) - $B(PhF_5)_3/Cy_3P$_b - ZORA-GGAPBE-D3(BJ)/TZP_PhCl (COSMO) phase

C	5.075346	2.322111	-0.466126
C	5.753078	1.190325	0.026511
C	5.181830	-0.075213	0.094741
C	3.867971	-0.256794	-0.340639
C	3.150038	0.829863	-0.843576
C	3.754875	2.082723	-0.895059
B	5.739940	3.735605	-0.549024
C	4.873673	5.022255	-0.346209
C	7.277043	3.868082	-0.816034
C	3.826771	5.090695	0.590360
C	8.062073	4.868194	-0.211301
C	3.077585	6.240737	0.814502
C	9.439463	4.967431	-0.385437
C	3.340958	7.384967	0.059200
C	10.091389	4.054541	-1.215434
C	4.355433	7.364409	-0.900133
C	9.355514	3.060291	-1.863163
C	5.101515	6.202855	-1.076712
C	7.982345	2.983209	-1.653084
F	10.147556	5.935067	0.231935
F	11.418218	4.137650	-1.397794
F	9.982381	2.191273	-2.681377
F	7.326772	2.005443	-2.321596
F	7.497504	5.783071	0.609268
F	7.022563	1.294120	0.484098
F	5.883189	-1.125686	0.567339
F	3.300413	-1.470701	-0.280810
F	1.886604	0.652416	-1.278697
F	3.009998	3.083897	-1.417870
F	6.065734	6.242945	-2.026329
F	4.598728	8.465081	-1.640048
F	2.618639	8.499809	0.251535
F	2.103287	6.262312	1.746619
F	3.520580	4.015710	1.355398

P	6.922448	2.684511	4.941172
C	5.571711	1.684481	4.062471
C	5.632055	0.232192	4.581823
C	4.147676	2.234995	4.242122
H	5.805329	1.688280	2.981751
C	4.593914	-0.674593	3.910090
H	5.446526	0.252050	5.670494
H	6.640948	-0.185061	4.451307
C	3.103782	1.337098	3.562455
H	3.918507	2.306060	5.320870
H	4.068273	3.250613	3.831451
C	3.176869	-0.110168	4.061069
H	4.653269	-1.688931	4.336085
H	4.837585	-0.772861	2.838391
H	2.095832	1.751615	3.723816
H	3.279412	1.355912	2.471019
H	2.451330	-0.739269	3.520619
H	2.890135	-0.139005	5.127978
C	6.258726	4.446952	4.876242
C	6.936687	5.355262	5.920912
C	6.238879	5.115855	3.496287
H	5.213511	4.325011	5.211876
C	6.265140	6.735264	5.969434
H	8.003434	5.483663	5.674428
H	6.899698	4.874594	6.910862
C	5.568515	6.495383	3.545933
H	7.272818	5.241310	3.136882
H	5.730332	4.466925	2.765530
C	6.239118	7.400551	4.587004
H	6.783008	7.381273	6.696408
H	5.227952	6.615851	6.332247
H	5.606728	6.966965	2.550010
H	4.500228	6.372505	3.802747
H	5.723512	8.372784	4.638099
H	7.276330	7.607550	4.265579
C	8.269237	2.675903	3.620595
C	9.461650	3.543831	4.061598

C	8.737596	1.242628	3.310407
H	7.841501	3.100920	2.694216
C	10.611884	3.514537	3.046833
H	9.826148	3.177027	5.037881
H	9.140810	4.583064	4.218957
C	9.884545	1.221748	2.290184
H	9.073655	0.761851	4.246824
H	7.901266	0.642098	2.926855
C	11.066909	2.083015	2.746322
H	11.453069	4.120532	3.419383
H	10.273951	3.990923	2.109553
H	10.205980	0.182807	2.114242
H	9.511017	1.604850	1.323345
H	11.860292	2.083838	1.981572
H	11.505822	1.643237	3.660345

[**1.1**/**1.2f**] (orientation a) - $B(PhF_5)_3$/$(PhF_5)_3P$_a - ZORA-GGAPBE-D3(BJ)/TZP_PhCl (COSMO) phase

C	4.10526228	4.20500912	13.36750006
C	3.52188314	3.63373253	14.51199835
C	2.15678044	3.65833206	14.77460675
C	1.29837457	4.25989433	13.85093398
C	1.82164085	4.83145815	12.68925021
C	3.19735968	4.80452809	12.47322283
B	5.64780467	4.19425309	13.11258350
C	6.31263506	5.42105817	12.40383095
C	6.53405547	2.98589630	13.55646873
C	5.95073081	6.74637260	12.70019119
C	7.85663572	3.15507616	14.00946948
C	6.53405761	7.84844700	12.08202474
C	8.66120480	2.09850706	14.42463702
C	7.50733986	7.64536302	11.10139169
C	8.15818103	0.79787244	14.38101820
C	7.89331620	6.34666515	10.76384576
C	6.85318284	0.57377307	13.93684637
C	7.30641064	5.27002691	11.42224041

C	6.07334994	1.65576090	13.54042729
F	9.91103809	2.31662240	14.88125348
F	8.92306741	-0.23381582	14.76894501
F	6.36967260	-0.68480829	13.89389372
F	4.82645562	1.36903203	13.09898506
F	8.39831035	4.39081579	14.10331170
F	4.30127314	3.03426873	15.44582277
F	1.65592953	3.10583053	15.89854542
F	-0.02373290	4.28598754	14.07731896
F	0.99080084	5.40254710	11.79436499
F	3.63577192	5.36603475	11.32266992
F	7.71644142	4.03253740	11.05214596
F	8.82744292	6.15319235	9.81020866
F	8.07161583	8.69631232	10.48432715
F	6.16992447	9.10419383	12.41417995
F	5.01588713	7.00428221	13.64650161
C	5.94667654	4.36647698	18.21217703
C	5.81355695	5.44578802	17.32643186
C	5.51977094	4.57315079	19.53136355
C	5.26664469	6.66818468	17.71835798
C	4.96953555	5.78077813	19.95147672
C	4.84282139	6.83196164	19.03805816
C	8.10646330	2.64055572	18.82295313
C	8.14908458	1.81091858	19.95138006
C	9.28214330	3.34919412	18.52310327
C	9.30076717	1.68345999	20.73017691
C	10.44049959	3.25030879	19.28784585
C	10.44816367	2.40549028	20.39987951
C	5.59275022	1.46194194	17.92377260
C	4.21377631	1.55647727	18.15766917
C	6.08290114	0.17377333	17.65517647
C	3.37971423	0.43619196	18.14061157
C	5.27992023	-0.96105750	17.64078672
C	3.91096630	-0.82746396	17.88547614
P	6.76014232	2.84496676	17.57469247
F	4.31289005	8.00115375	19.43425690
F	5.15298952	7.68672779	16.84291424

F	6.23236345	5.33784587	16.04259535
F	5.60614396	3.57246975	20.43446387
F	4.54851190	5.94748279	21.22154825
F	3.61455695	2.74591473	18.39393552
F	7.07211365	1.09093277	20.33599318
F	9.30988588	0.87216079	21.80822572
F	11.55709252	2.29223391	21.15216759
F	11.54531280	3.95381108	18.96663365
F	9.30558447	4.17461441	17.44554722
F	2.05744464	0.57196559	18.37075235
F	3.11255328	-1.90976404	17.87308487
F	5.80679319	-2.17665443	17.38974427
F	7.40667603	0.01277696	17.39359415

[**1.1**/**1.2f**] (orientation b) - $B(PhF_5)_3/(PhF_5)_3P$_b - ZORA-GGAPBE-D3(BJ)/TZP_PhCl (COSMO) phase

C	5.497193	2.875775	3.124287
C	5.620981	1.639079	3.786341
C	4.547855	0.980552	4.376174
C	3.273514	1.545751	4.299461
C	3.095137	2.771958	3.656855
C	4.196156	3.414605	3.098683
B	6.707549	3.574422	2.429471
C	6.810386	5.133675	2.365169
C	7.830233	2.716797	1.758958
C	6.460093	5.957609	3.448200
C	9.187335	3.078531	1.825003
C	6.567798	7.344197	3.418109
C	10.198780	2.347213	1.209463
C	7.018287	7.967178	2.251732
C	9.865692	1.212543	0.466739
C	7.366026	7.194559	1.141730
C	8.531310	0.813553	0.368510
C	7.270819	5.807365	1.219840
C	7.549690	1.555576	1.018462
F	11.490231	2.722233	1.316008

F	10.826283	0.506414	-0.151384
F	8.211196	-0.280375	-0.352737
F	6.272423	1.126185	0.878266
F	9.571096	4.166937	2.534668
F	6.830601	1.045289	3.908487
F	4.722227	-0.193594	5.017324
F	2.223115	0.914072	4.845119
F	1.864680	3.317512	3.589482
F	3.953470	4.593859	2.481043
F	7.612756	5.113242	0.108095
F	7.789519	7.798396	0.012566
F	7.115346	9.305226	2.198477
F	6.241835	8.093252	4.492732
F	6.020350	5.403379	4.602722
C	7.029704	3.356044	8.585740
C	8.123449	3.382078	9.462549
C	7.315242	3.235566	7.219404
C	9.440326	3.293424	9.006813
C	8.616553	3.155009	6.734452
C	9.684753	3.182541	7.637100
C	4.780035	4.998408	8.161197
C	3.896717	4.932856	7.075960
C	5.237861	6.279779	8.511321
C	3.486826	6.073024	6.383628
C	4.858425	7.432669	7.829375
C	3.968868	7.326548	6.758349
C	4.347251	2.181763	8.788904
C	4.809150	0.935156	8.344734
C	2.981712	2.255566	9.106485
C	3.956763	-0.162863	8.202401
C	2.106459	1.186153	8.958824
C	2.601235	-0.037822	8.502507
P	5.353832	3.643994	9.288555
F	10.946756	3.099317	7.183567
F	10.473336	3.318511	9.873144
F	7.930552	3.502914	10.795833
F	6.304176	3.168331	6.326770

F	8.860367	3.038778	5.412017
F	6.110870	0.727346	8.039458
F	3.404120	3.752074	6.636925
F	2.647749	5.967052	5.331697
F	3.586239	8.426321	6.085779
F	5.334661	8.640782	8.193211
F	6.094172	6.417090	9.555164
F	4.439772	-1.348454	7.778613
F	1.775685	-1.090172	8.359900
F	0.798016	1.316790	9.257537
F	2.477998	3.428645	9.567774

A.1.2. Supplementary information to Subcapter 2.

A.1.2.1. The crystal structures of experimental and evaluated FLPs.

The representation of crystal structures of both, experimental (Figures SI 1.2.1 – SI 1.2.10) and evaluated FLPs (Figures SI 1.2.11 – SI 1.2.20) are given to illustrate the considered structures (see related references at the end of this section).

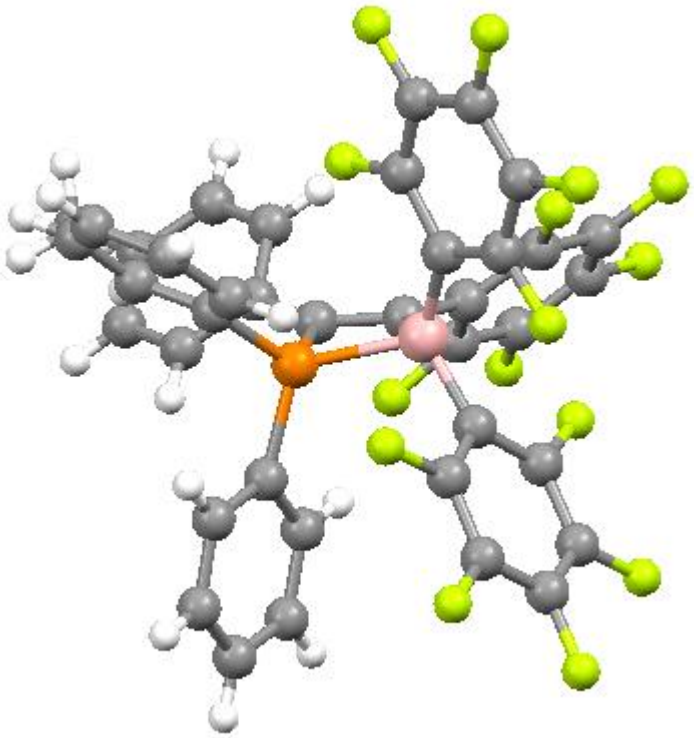

Figure SI 1.2.1. Crystal structure SEZKAL (Ekkert *et al.*, 2013).[284] P: orange; B: pink; F: yellow; C: grey; H: white. This structure corresponds to the **experimental** FLP.

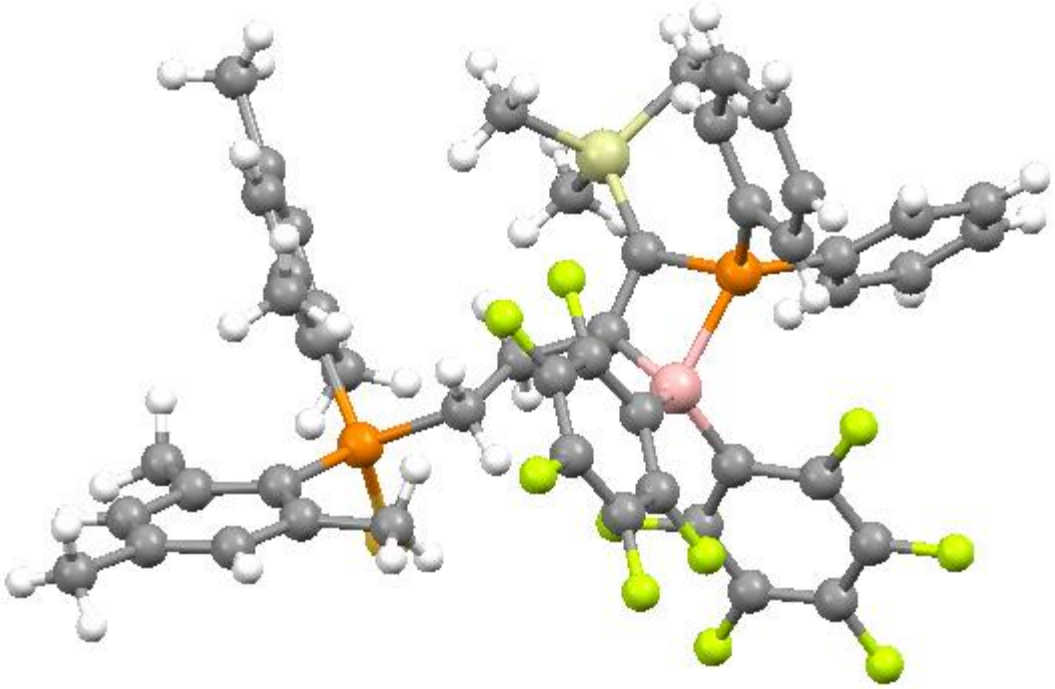

Figure SI 1.2.2. Crystal structure FUWKUF (Liedtke *et al.*, 2014).[284] P: orange; B: pink; F: yellow; Si: light green; Cl: green; C: grey; H: white. This structure corresponds to the **experimental** FLP.

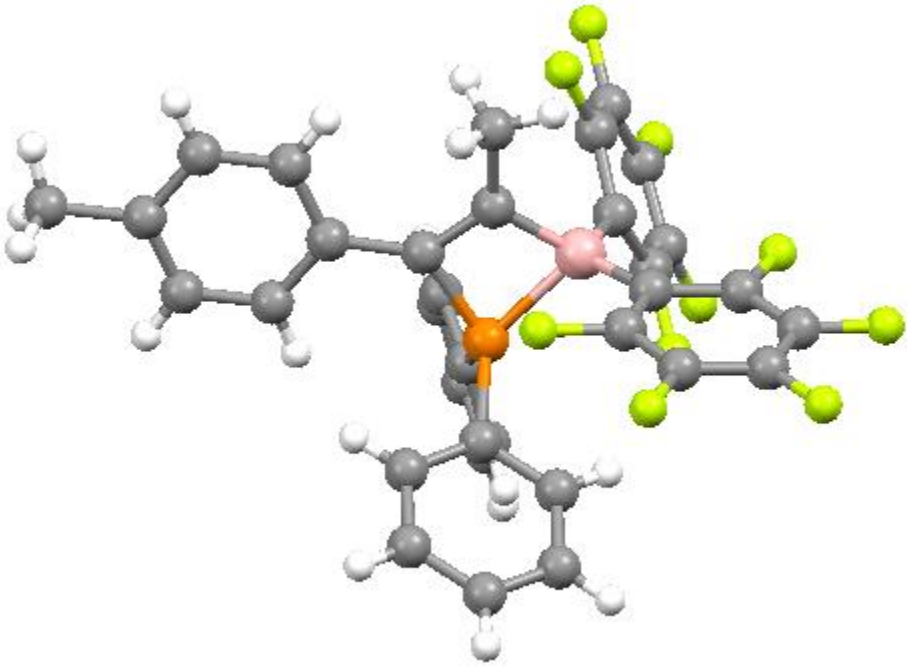

Figure SI 1.2.3. Crystal structure SEZJUE (Ekkert *et al.*, 2013).[284] P: orange; B: pink; F: yellow; C: grey; H: white. This structure corresponds to the **experimental** FLP.

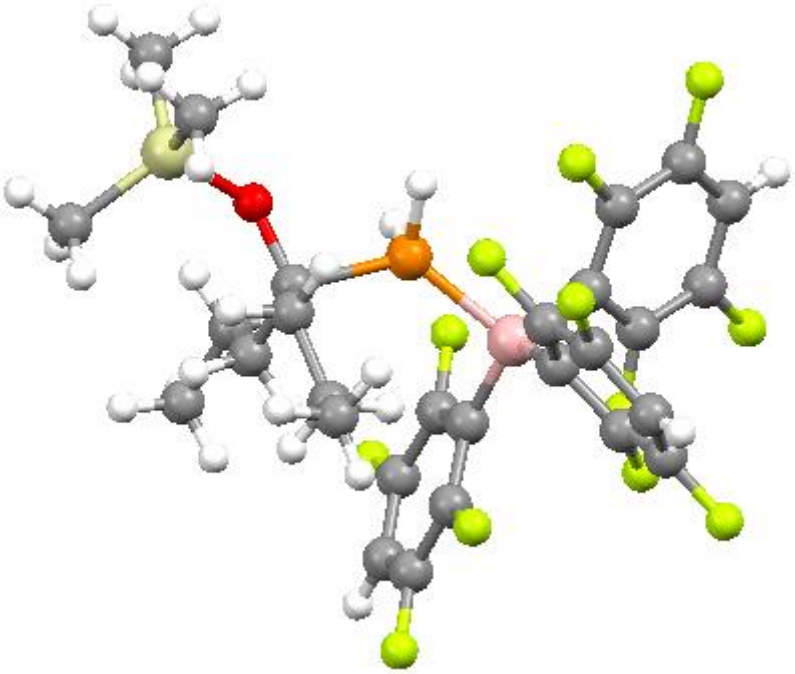

Figure SI 1.2.4. Crystal structure ODUJUU (Takeuchi *et al.*, 2013).[284] P: orange; B: pink; F: yellow; Si: light green; O: red; C: grey; H: white. This structure corresponds to the **experimental** FLP.

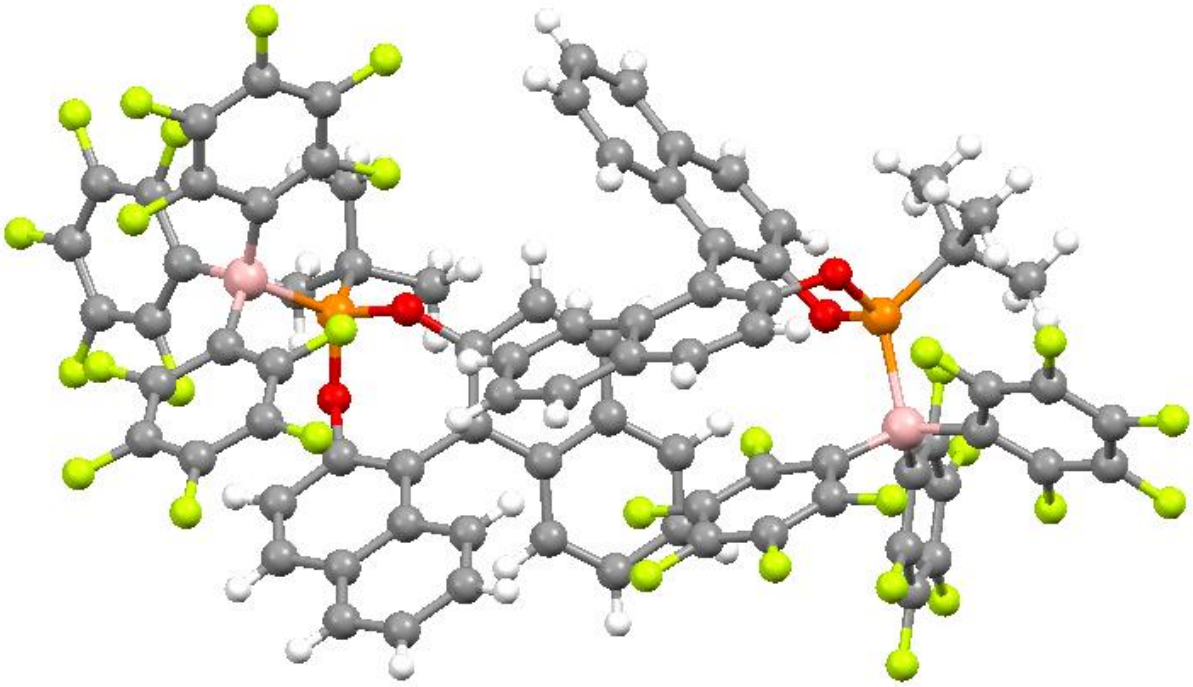

Figure SI 1.2.5. Crystal structure FAPGIO (Caputo *et al.*, 2013).[284] P: orange; B: pink; F: yellow; O: red; C: grey; H: white. This structure corresponds to the **experimental** FLP.

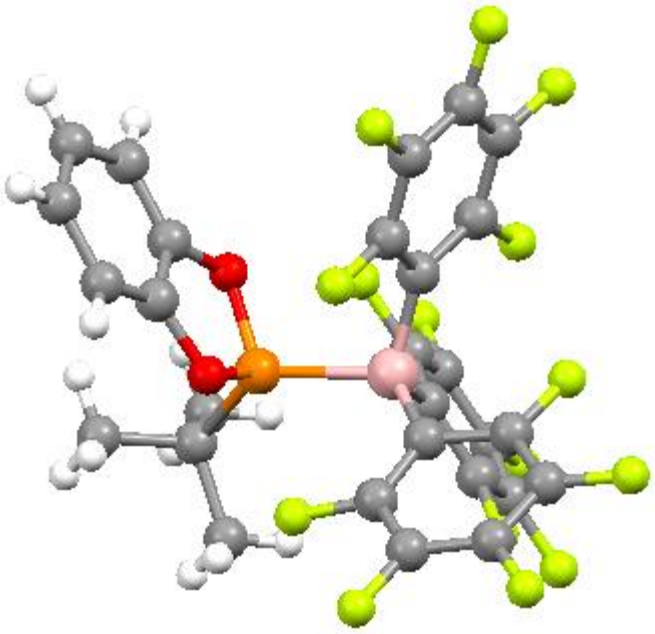

Figure SI 1.2.6. Crystal structure FAPGEK (Caputo *et al.*, 2013).[284] P: orange; B: pink; F: yellow; O: red; C: grey; H: white. This structure corresponds to the **experimental** FLP.

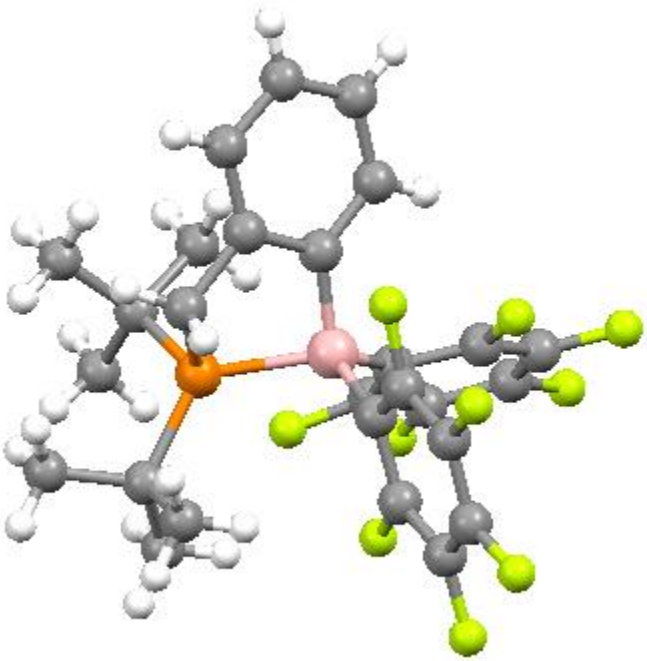

Figure SI 1.2.7. Crystal structure OSUZEI (Heiden *et al.*, 2011).[284] P: orange; B: pink; F: yellow; C: grey; H: white. This structure corresponds to the **experimental** FLP.

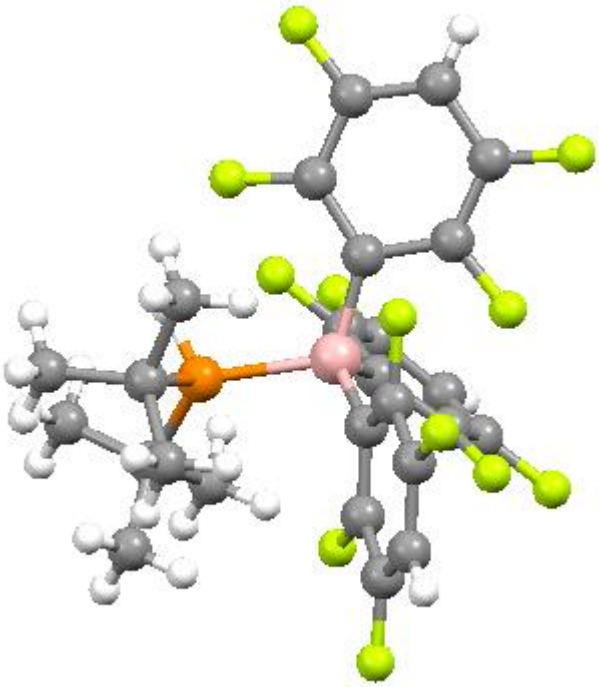

Figure SI 1.2.8. Crystal structure OLAJOB (Ullrich *et al.*, 2010).[284] P: orange; B: pink; F: yellow; C: grey; H: white. This structure corresponds to the **experimental** FLP.

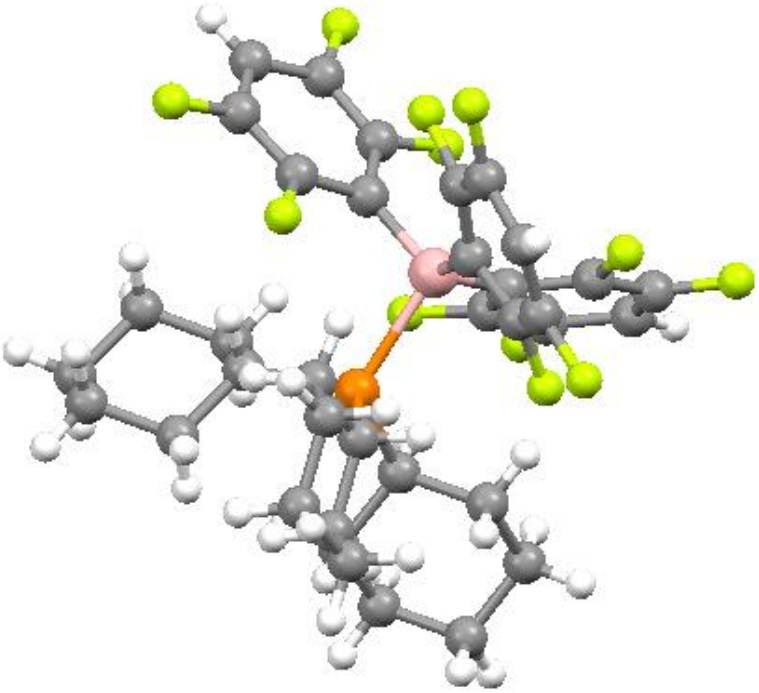

Figure SI 1.2.9. Crystal structure OLAJUH (Ullrich *et al.*, 2010).[284] P: orange; B: pink; F: yellow; C: grey; H: white. This structure corresponds to the **experimental** FLP.

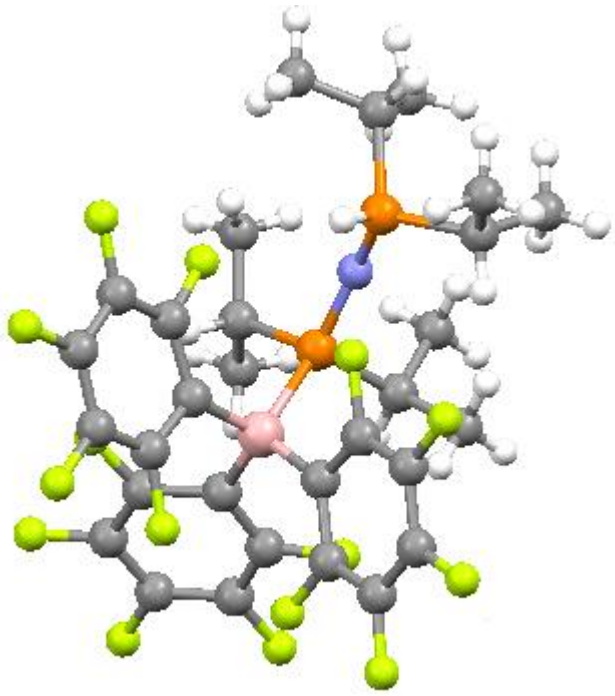

Figure SI 1.2.10. Crystal structure MIKDER (Barry *et al.*, 2013).[284] P: orange; B: pink; F: yellow; the nitrogen atoms - blue, C: grey; H: white. This structure corresponds to the **experimental** FLP.

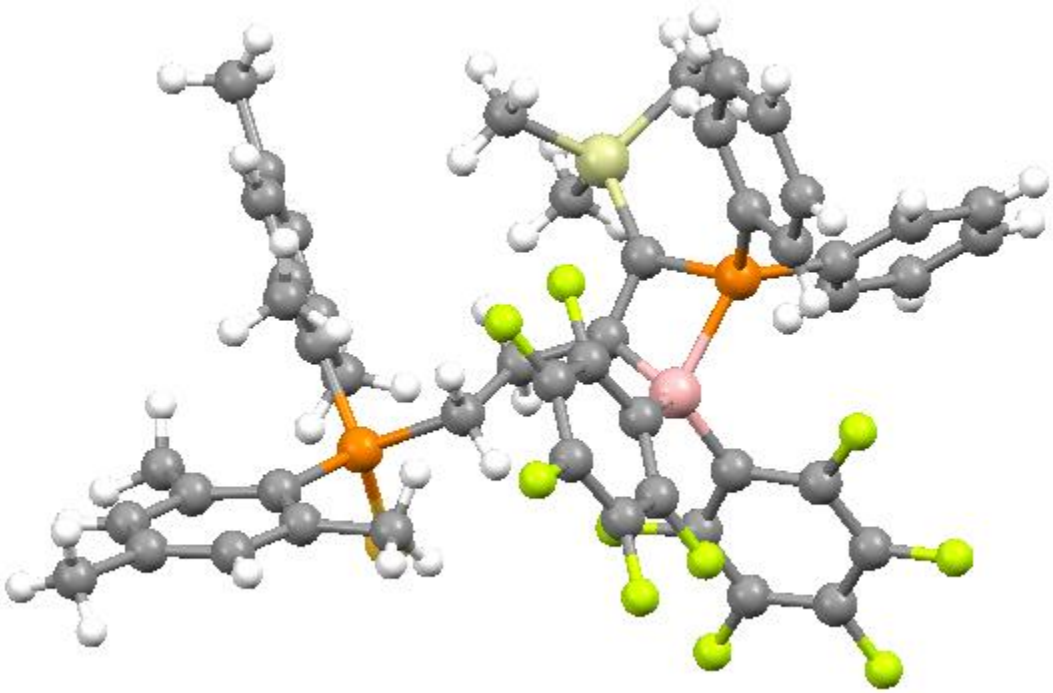

Figure SI 1.2.11. Crystal structure FUWLEQ (Liedtke *et al.*, 2014).[284] P: orange; B: pink; F: yellow; Si: light green; the sulfur brown, C: grey; H: white. This structure corresponds to the **evaluated** FLP.

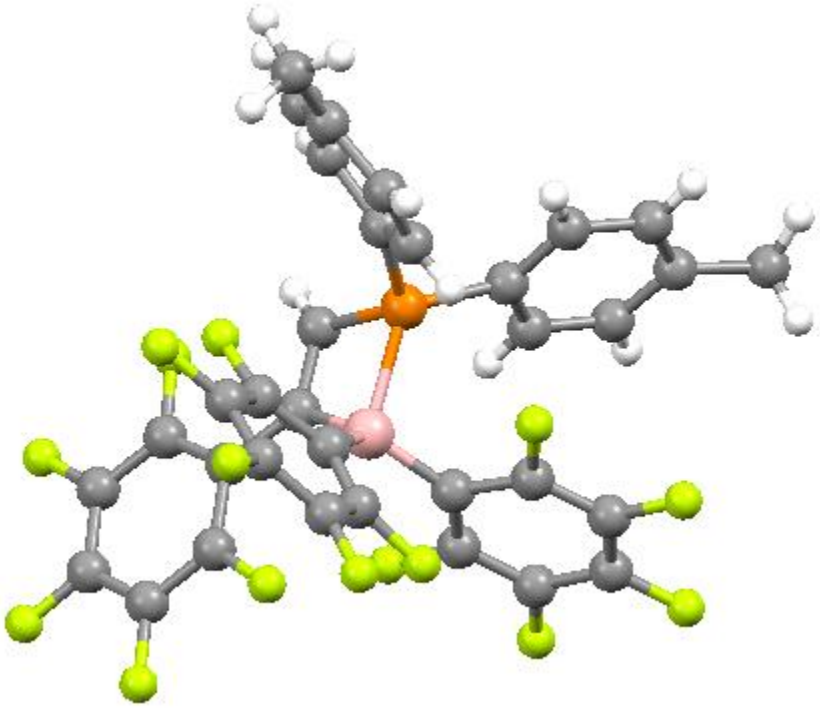

Figure SI 1.2.12. Crystal structure BIRXAD (Yu *et al.*, 2013).[284] P: orange; B: pink; F: yellow; C: grey; H: white. This structure corresponds to the **evaluated** FLP.

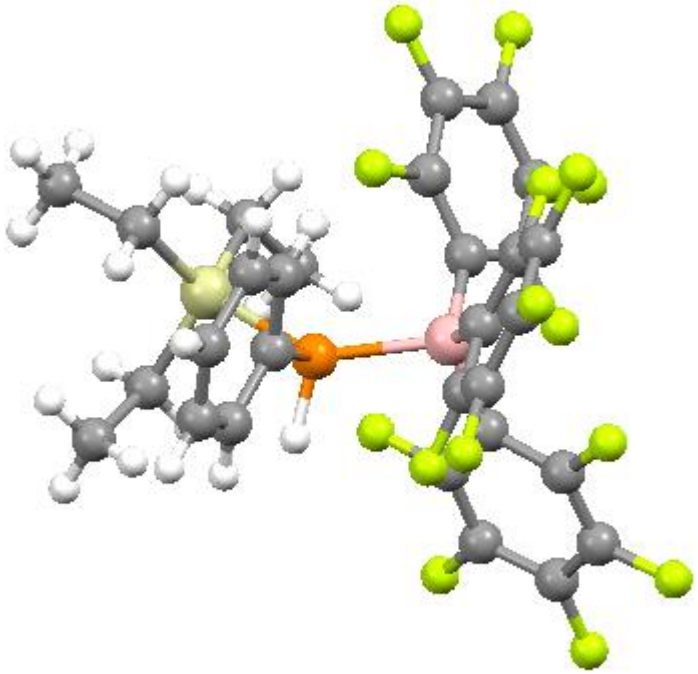

Figure SI 1.2.13. Crystal structure XUPZAK (Geier & Stephan, 2010).[284] P: orange; B: pink; F: yellow; Si: light green; C: grey; H: white. This structure corresponds to the **evaluated** FLP.

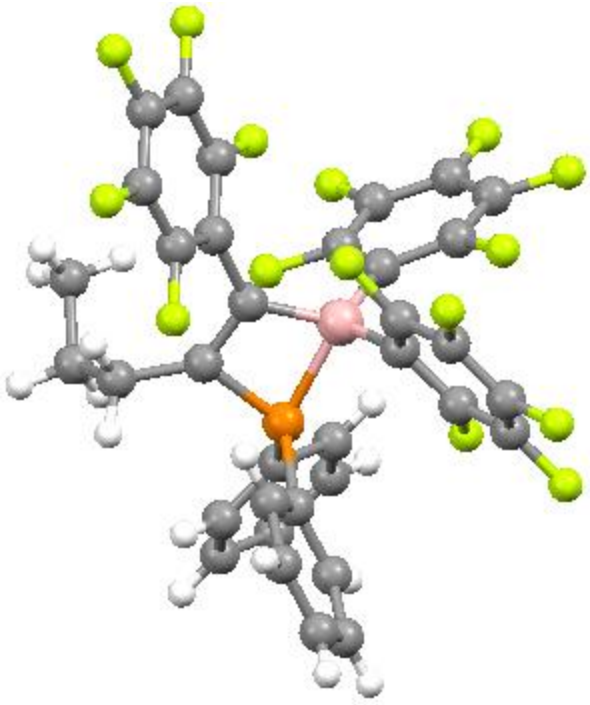

Figure SI 1.2.14. Crystal structure EWETAC (Ekkert *et al.*, 2011).[284] P: orange; B: pink; F: yellow; C: grey; H: white. This structure corresponds to the **evaluated** FLP.

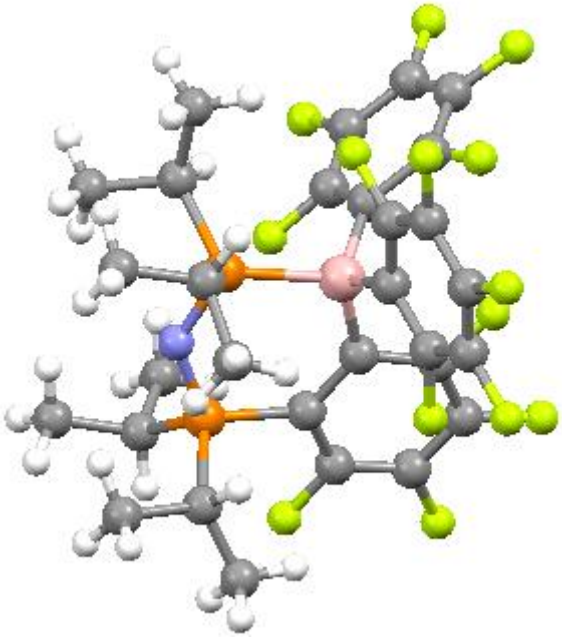

Figure SI 1.2.15. Crystal structure MIKCUG (Barry *et al.*, 2013).[284] P: orange; B: pink; F: yellow; N: blue; C: grey; H: white. This structure corresponds to the **evaluated** FLP.

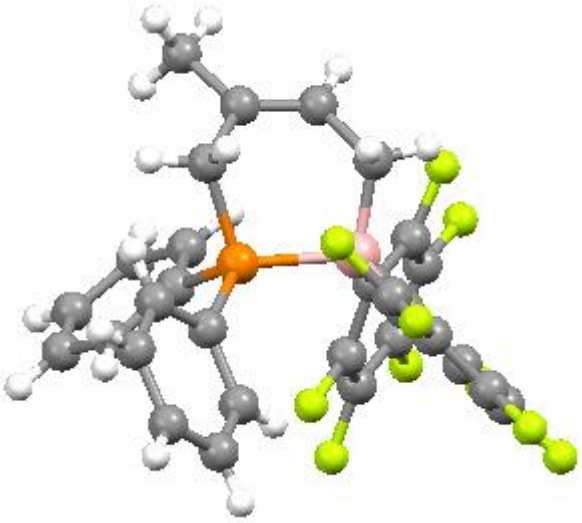

Figure SI 1.2.16. Crystal structure ROVLAR (Moquist *et al.*, 2015).[284] P: orange; B: pink; F: yellow; C: grey; H: white. This structure corresponds to the **evaluated** FLP.

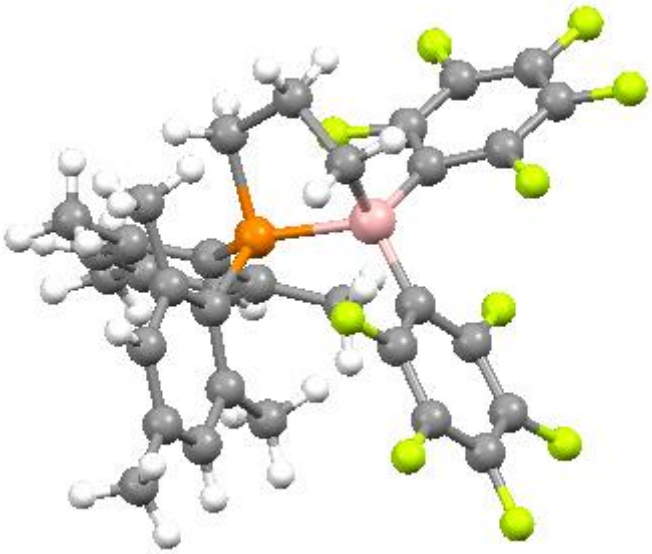

Figure SI 1.2.17. Crystal structure YORPAX (Spies *et al.*, 2009).[284] P: orange; B: pink; F: yellow; C: grey; H: white. This structure corresponds to the **evaluated** FLP

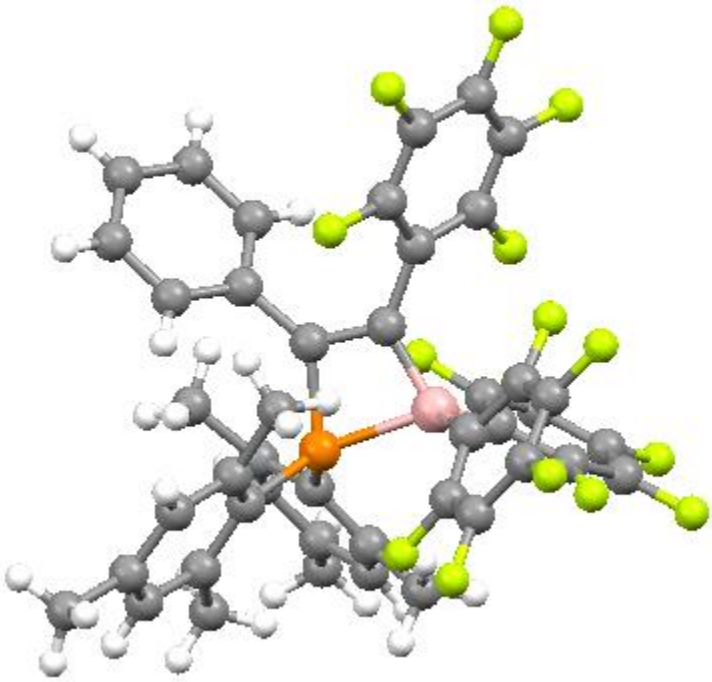

Figure SI 1.2.18. Crystal structure EWESUV (Ekkert *et al.*, 2011).[284] P: orange; B: pink; F: yellow; C: grey; H: white. This structure corresponds to the **evaluated** FLP.

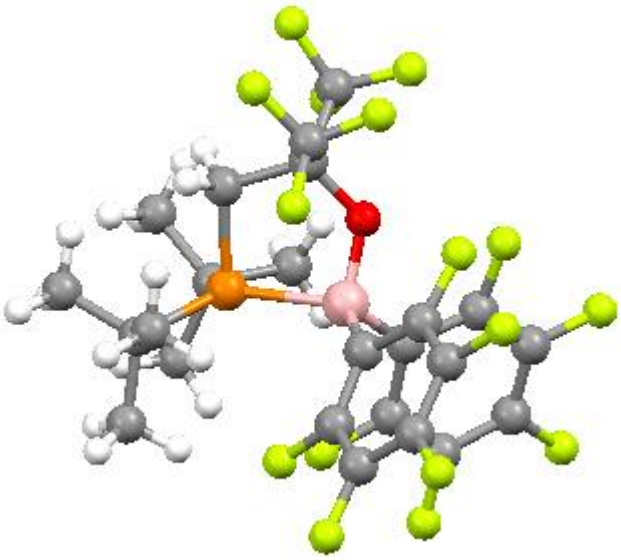

Figure SI 1.2.19. Crystal structure TACHAI (Chapman *et al.*, 2010).[284] P: orange; B: pink; F: yellow; O: red; C: grey; H: white. This structure corresponds to the **evaluated** FLP.

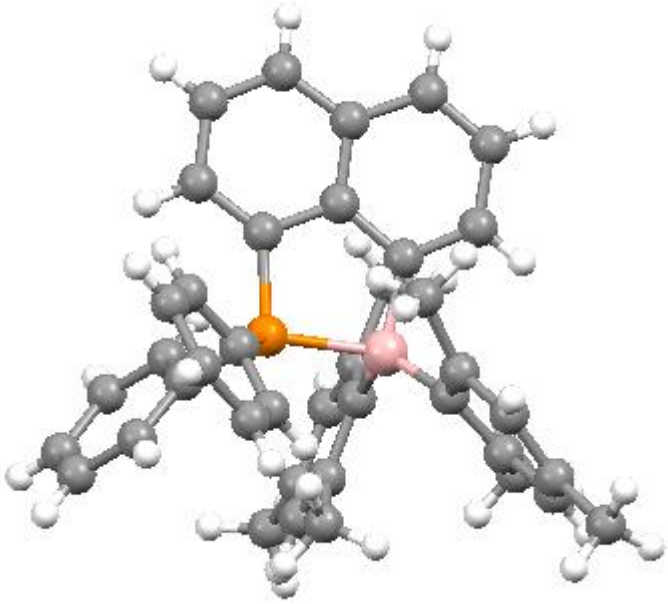

Figure SI 1.2.20. Crystal structure SIGVUB01 (Beckmann *et al.*, 2013).[284] P: orange; B: pink; C: grey; H: white. This structure corresponds to the **evaluated** FLP.

[284] [N^0 467] O. Ekkert, G. G. Miera, T. Wiegand, H. Eckert, B. Schirmer, J. L. Petersen, C. G. Daniliuc, R. Fröhlich, S. Grimme, G. Kehra, G. Erker, *Chem. Sci*. **2013**, *4*, 2657.
[N^0 468] R. Liedtke, F. Scheidt, J. Ren, B. Schirmer, A. J. P. Cardenas, C. G. Daniliuc, H. Eckert, T. H. Warren, S. Grimme, G. Kehr, G. Erker, *J. Am. Chem. Soc.* **2014**, *136*, 9014.
[N^0 469] K. Takeuchi, L. J. Hounjet, D. W. Stephan, *Organometallics* **2013**, *32*, 4469.
[N^0 470] C. B. Caputo, S. J. Geier, E. Y. Ouyang, C. Kreitner, D. W. Stephan, *Dalton Trans.* **2012**, *41*, 237.
[N^0 471] Z. M. Heiden, M. Schedler, D. W. Stephan, *Inorg. Chem.* **2011**, *50*, 1470.
[N^0 371] M. Ullrich, A. J. Lough, D. W. Stephan, *Organometallics* **2010**, *29*, 3647.
[N^0 472] B. M. Barry, D. A. Dickie, L. J. Murphy, J. A. C. Clyburne, R. A. Kemp, *Inorg. Chem*. **2013**, *52*, 8312.
[N^0 473] J. Yu, G. Kehr, C. G. Daniliuc, G. Erker, *Inorg. Chem.* **2013**, *52*, 11661.
[N^0 474] S. J. Geier, D. W. Stephan, *Chem. Commun.* **2010**, *46*, 1026.
[N^0 475] O. Ekkert, G. Kehr, R. Fröhlich, G. Erker, *J. Am. Chem. Soc*. **2011**, *133*, 4610.
[N^0 476] P. Moquist, G.-Q. Chen, C. Mück-Lichtenfeld, K. Bussmann, C. G. Daniliuc, G. Kehr, G. Erker, *Chem. Sci.* **2015**, *6*, 816.
[N^0 477] P. Spies, G. Kehr, K. Bergander, B. Wibbeling, R. Fröhlich, G. Erker, *Dalton Trans.* **2009**, *9*, 1534.
[N^0 478] A. M. Chapman, M. F. Orton, J. P. H. Haddow, D. F. Wass, *Dalton Trans.* **2010**, *39*, 6184.
[N^0 479] J. Beckmann, E. Hupf, E. Lork, S. Mebs, *Inorg. Chem.* **2013**, *52*, 11881.

A.2. Supplementary information to Chapter 5.

A.2.1. NMR spectra.

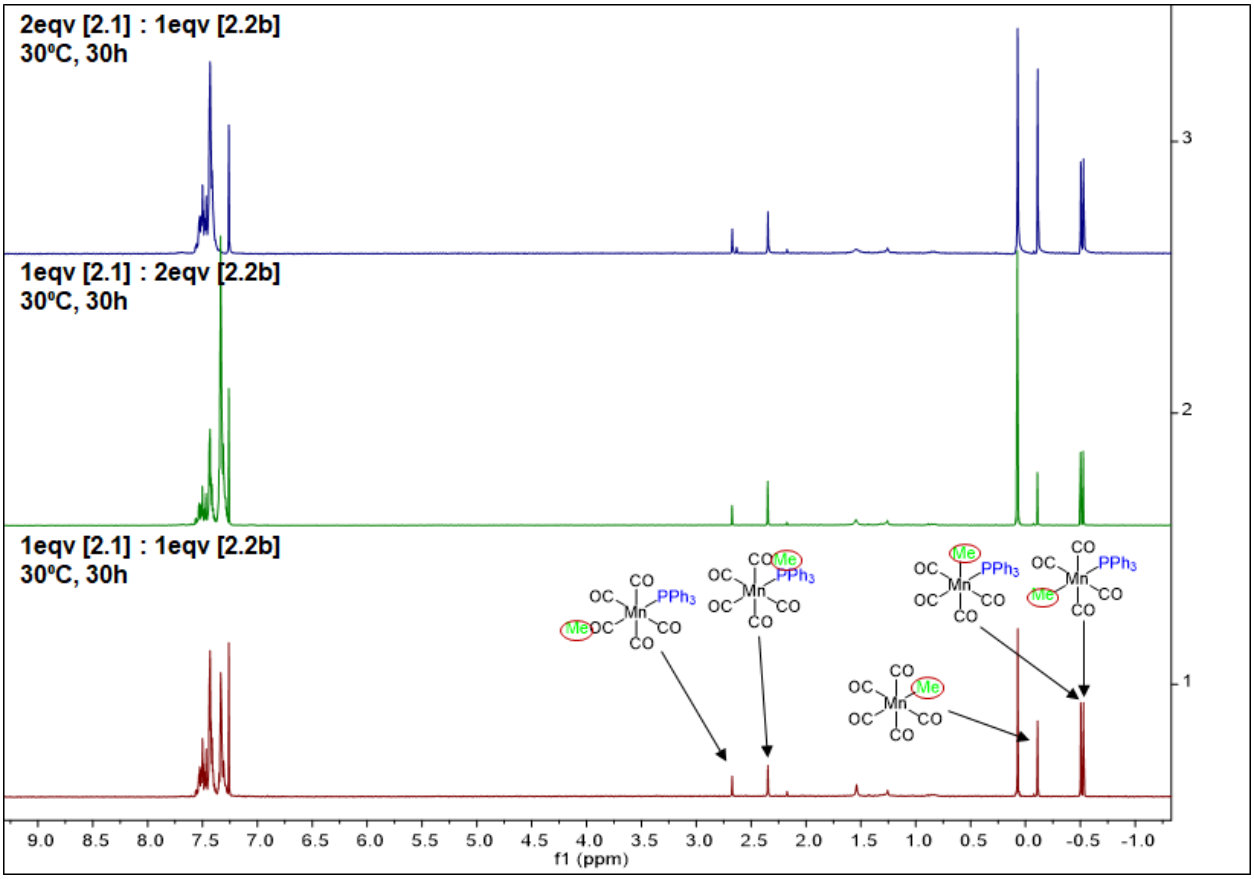

Figure SI 2.1 Superimposed ^{1}H NMR spectra of the reaction of **2.1** with **2.2b** carried out with various starting molar ratios of the reactants (1:1; 1:2 and 2:1) at 30ºC within 30h. The spectra are recorded in deuterated chloroform at 400 MHz.

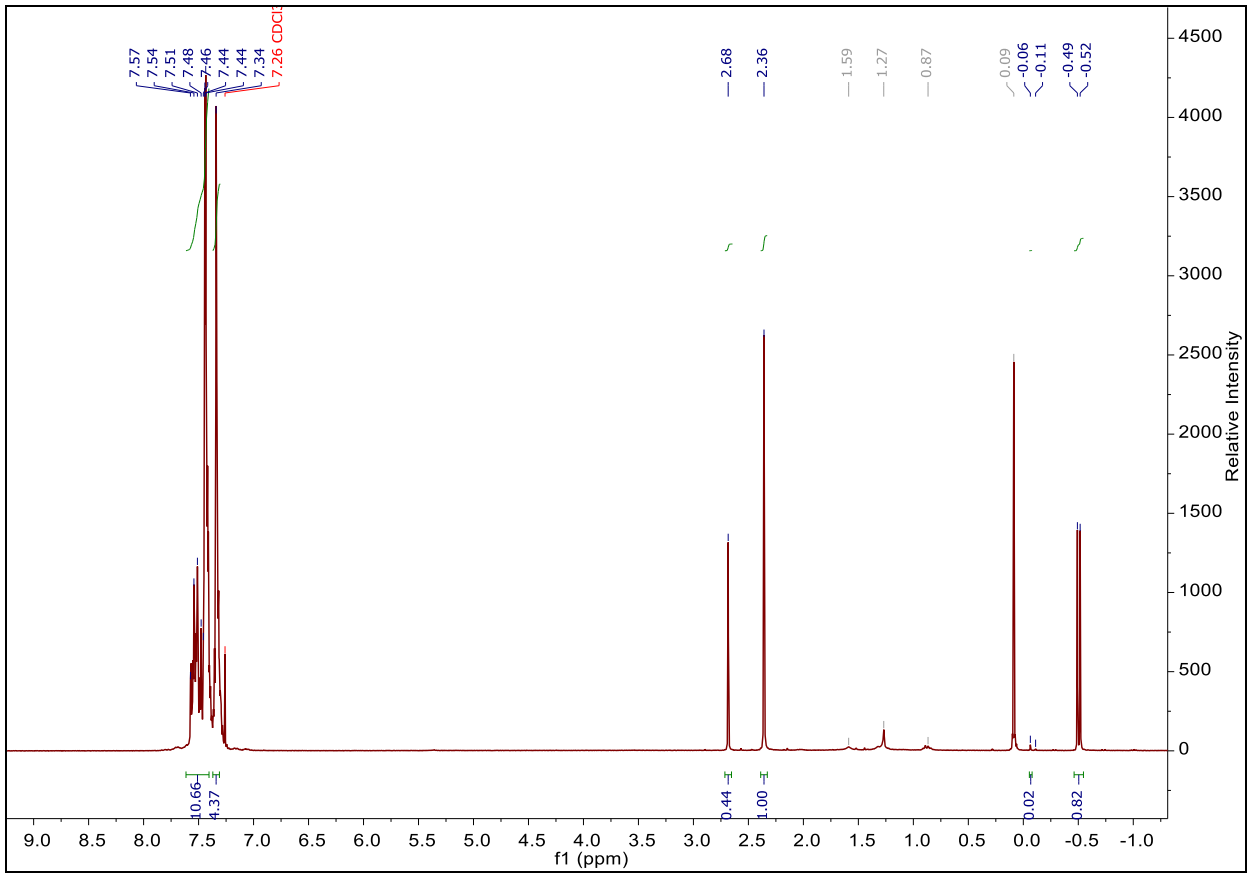

Figure SI 2.2 ^{1}H NMR spectrum of the reaction of **2.1** with **2.2b** carried out at ambient temperature within 10h. The spectrum is recorded in deuterated chloroform at 400 MHz.

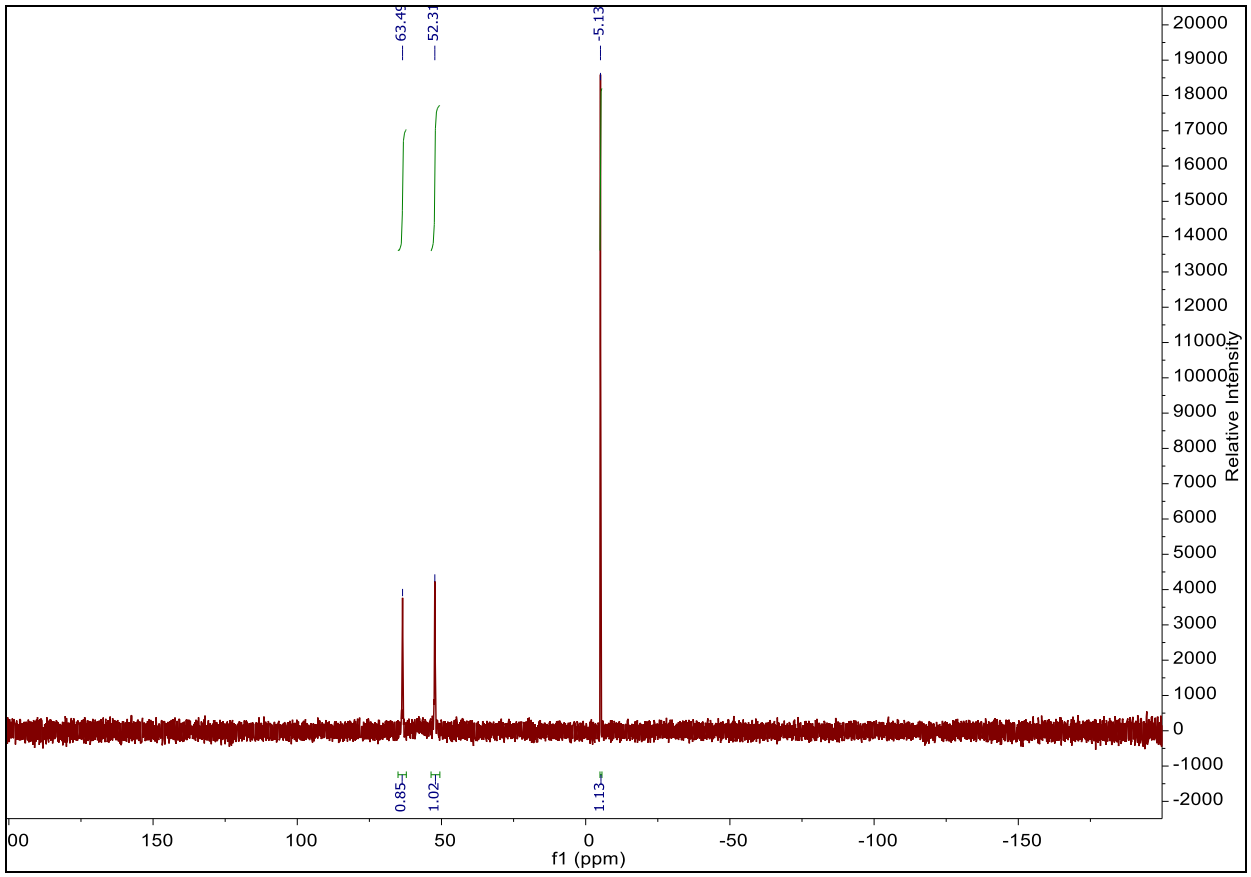

Figure SI 2.3 ^{31}P NMR spectrum of the reaction of **2.1** with **2.2b** carried out at ambient temperature within 10h. The spectrum is recorded in deuterated chloroform at 121 MHz.

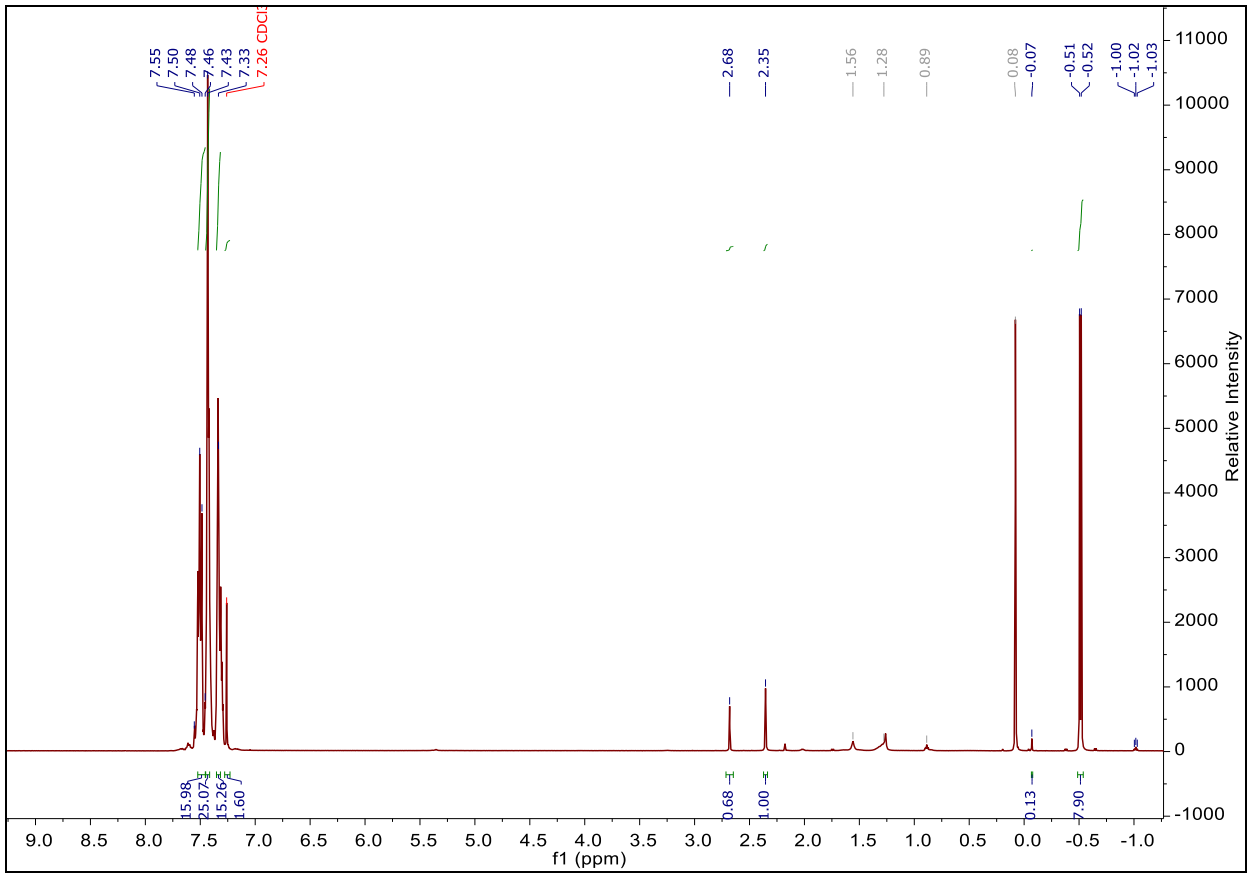

Figure SI 2.4 ^{1}H NMR spectrum of the reaction of **2.1** with **2.2b** carried out at 30ºC within 20h. The spectrum is recorded in deuterated chloroform at 400 MHz.

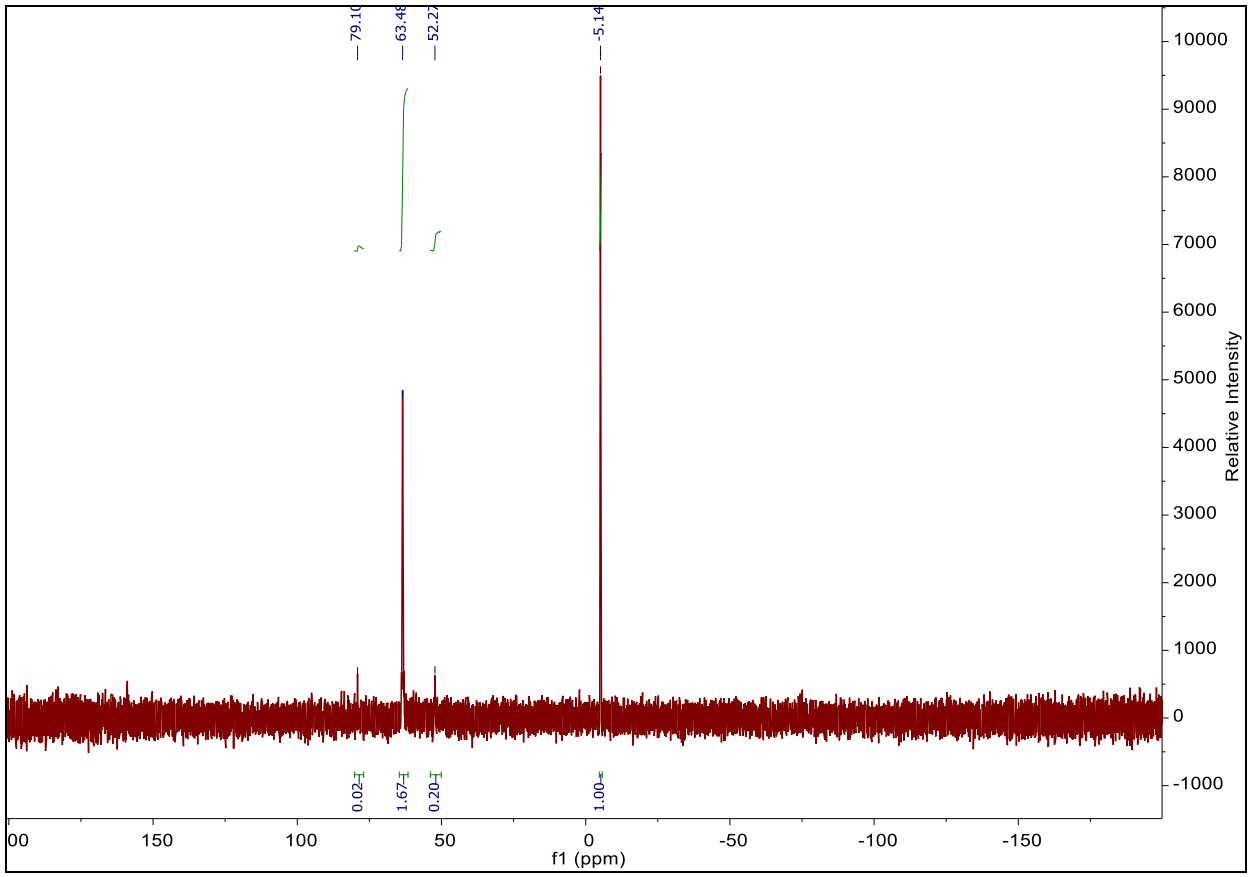

Figure SI 2.5 ^{31}P NMR spectrum of the reaction of **2.1** with **2.2b** carried out at 30ºC within 20h. The spectrum is recorded in deuterated chloroform at 121 MHz.

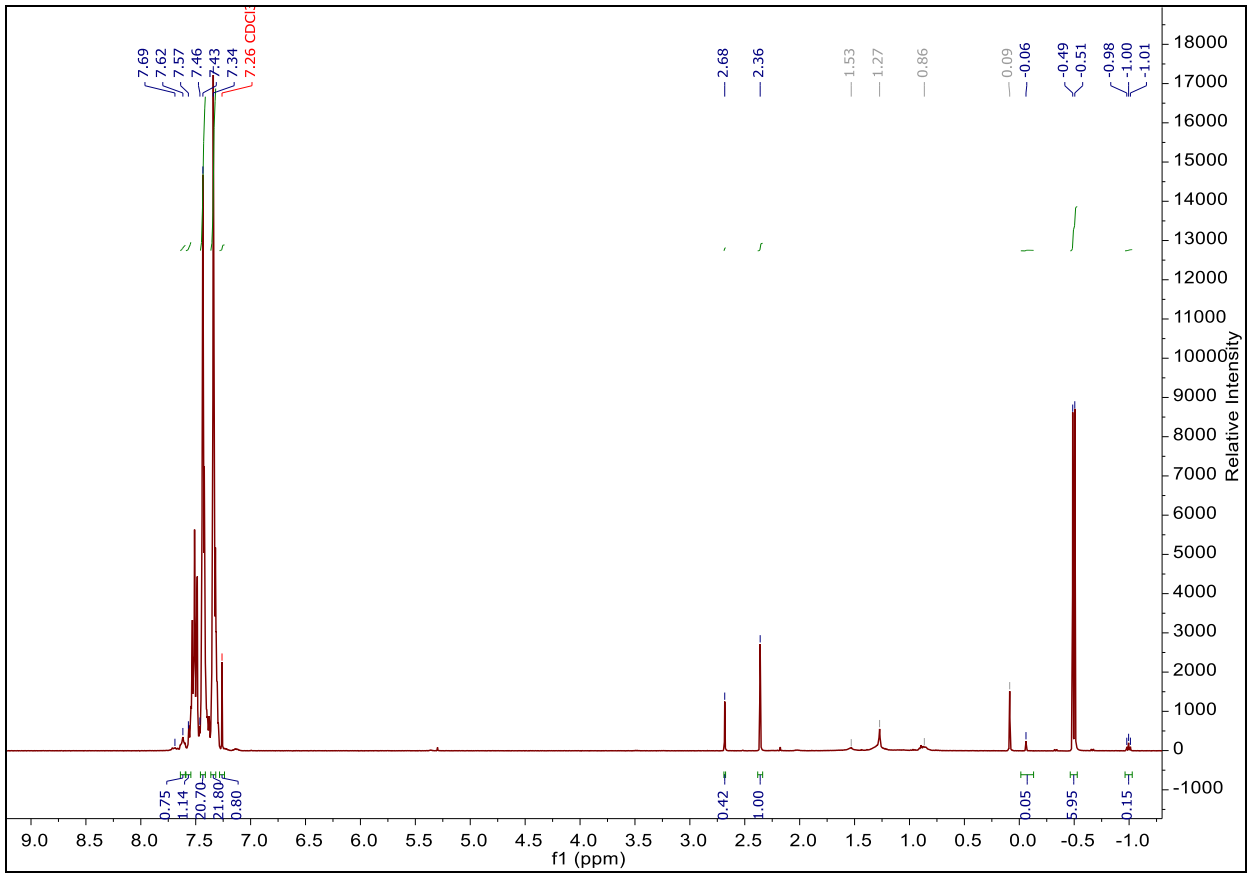

Figure SI 2.6 ^{1}H NMR spectrum of the reaction of **2.1** with **2.2b** carried out at 30ºC within 30h. The spectrum is recorded in deuterated chloroform at 400 MHz.

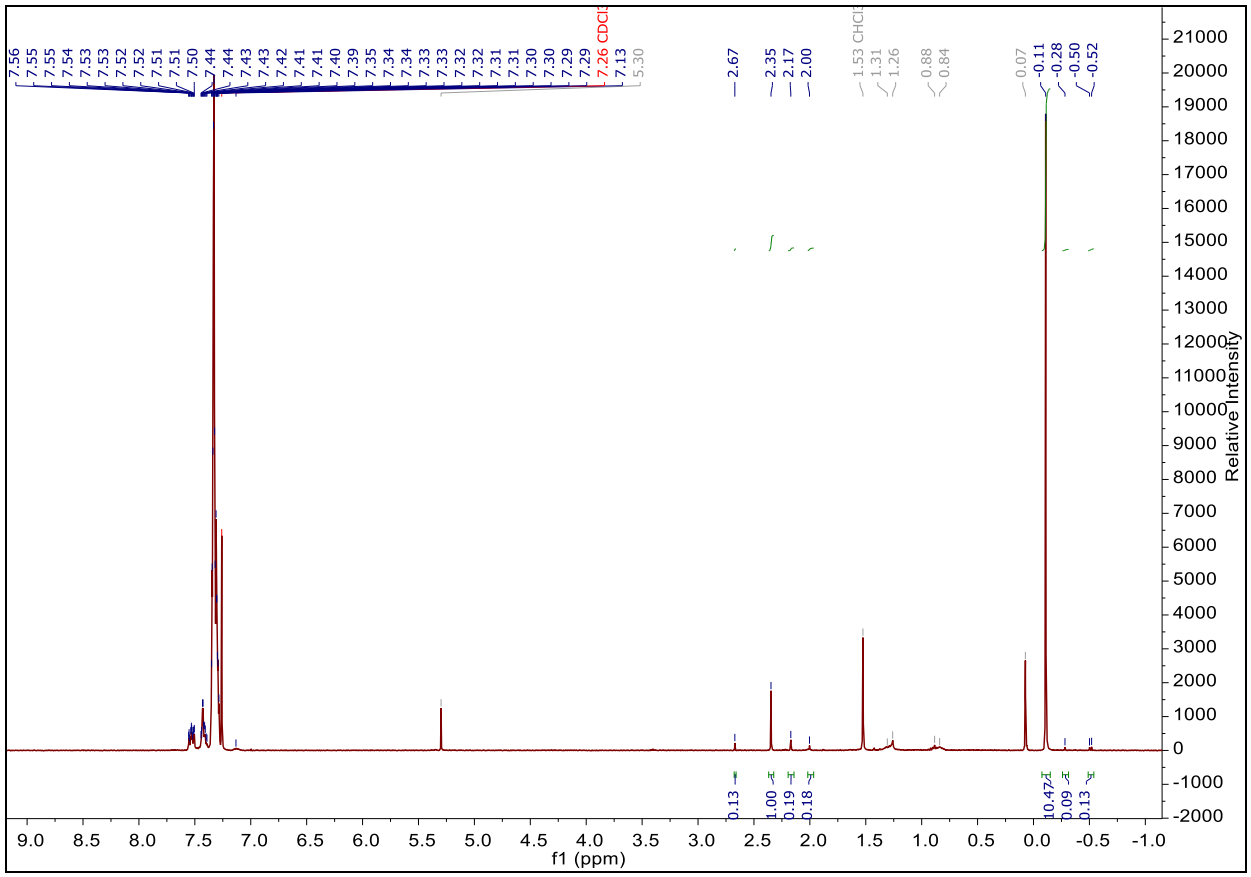

Figure SI 2.7 ^{1}H NMR spectrum of the reaction of **2.1** with **2.2b** carried out at 2ºC within 30h. The spectrum is recorded in deuterated chloroform at 400 MHz.

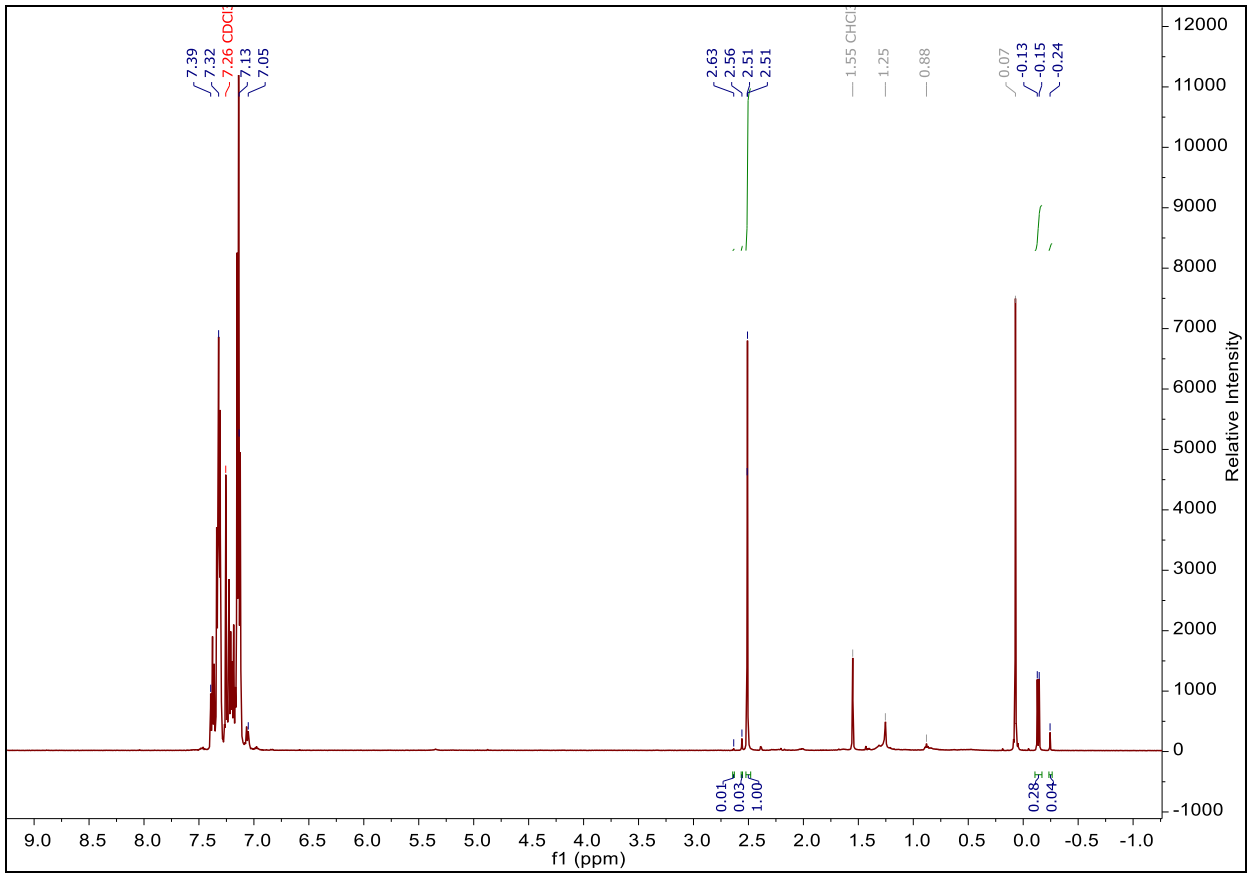

Figure SI 2.8 ^{1}H NMR spectrum of the reaction of **2.1** with **2.2c** carried out at 30-35ºC within 14.5h. The spectrum is recorded in deuterated chloroform at 400 MHz.

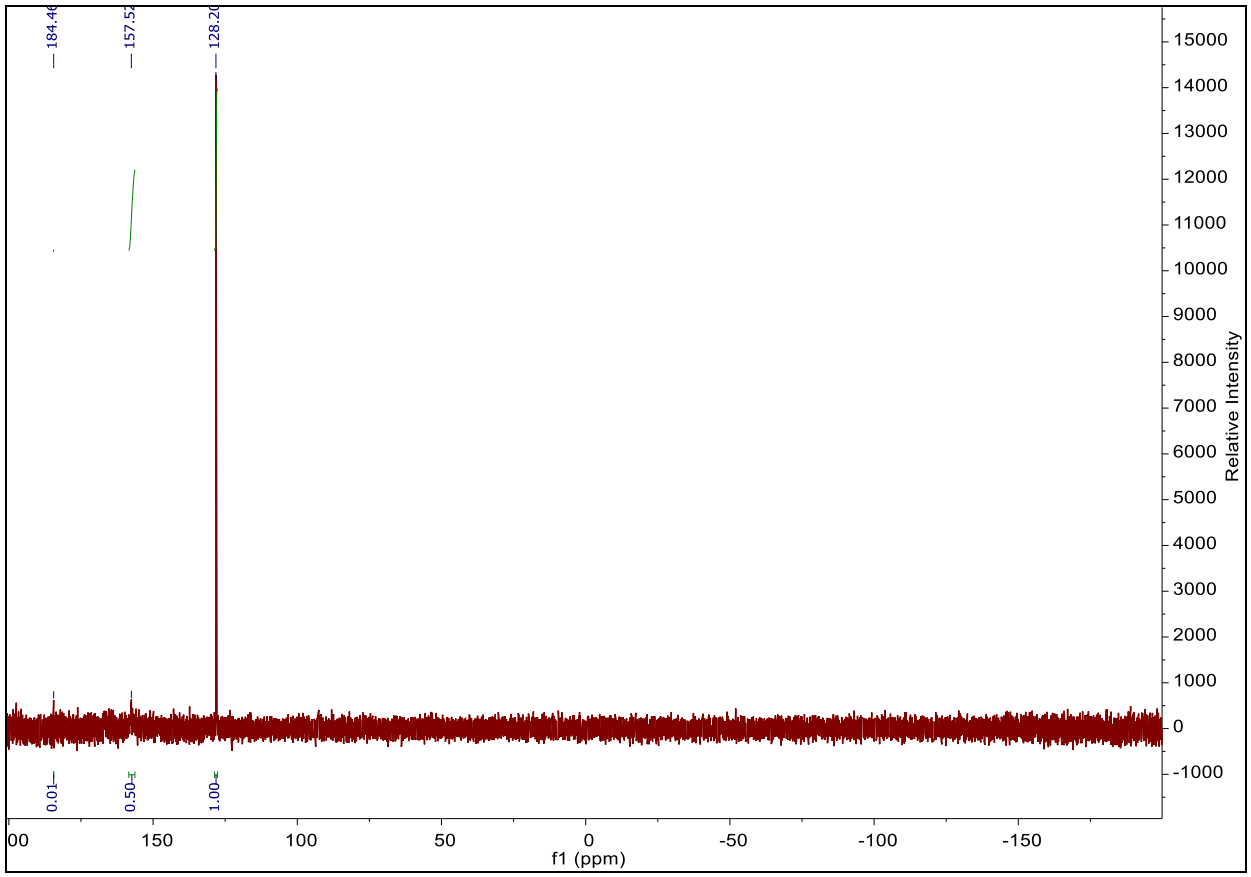

Figure SI 2.9 ^{31}P NMR spectrum of the reaction of **2.1** with **2.2c** carried out at 30-35ºC within 14.5h. The spectrum is recorded in deuterated chloroform at 121 MHz.

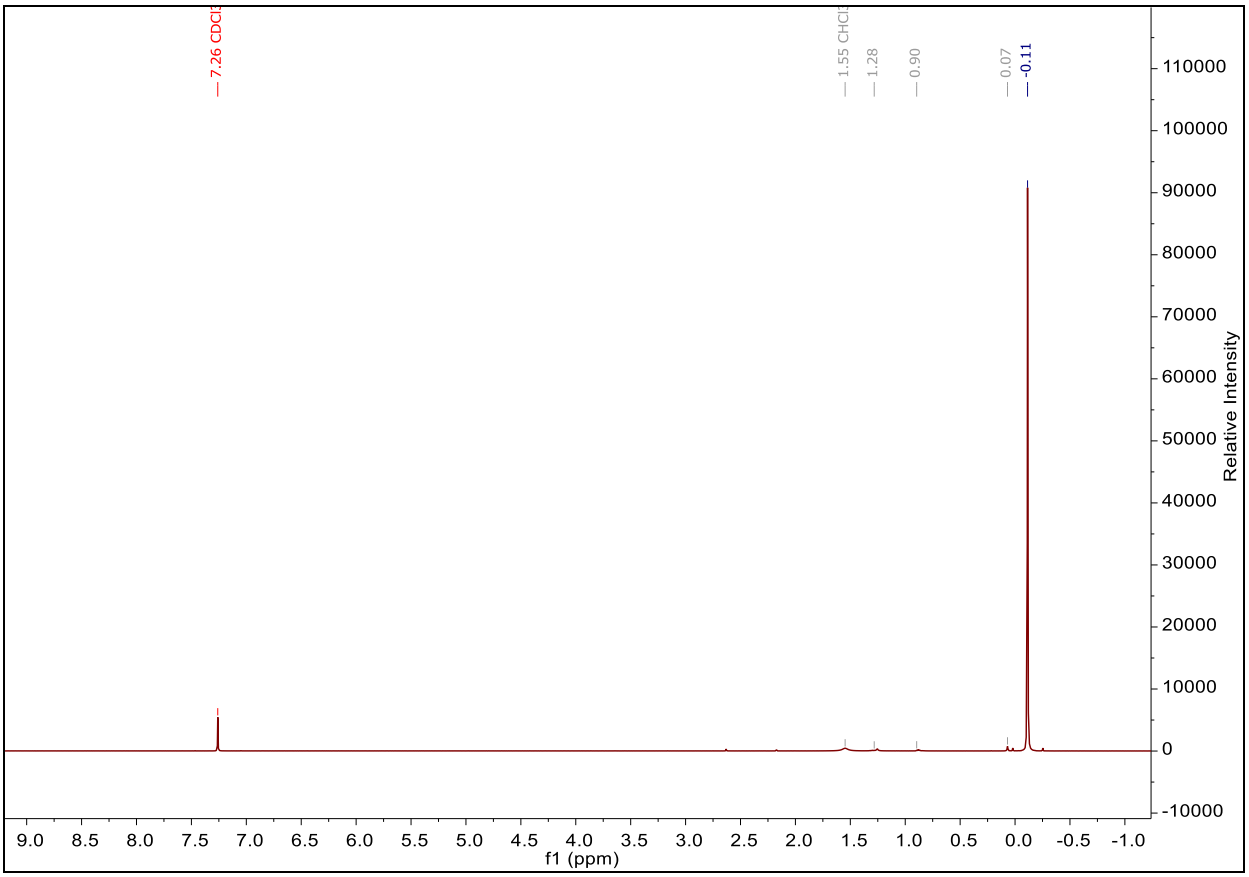

Figure SI 2.10 ^{1}H NMR spectrum of the synthesized complex **2.1** by modified literature procedure[285] (for the details of the synthesis, see Experimental section, page 163). The spectrum is recorded in deuterated chloroform at 400 MHz.

[285] [N^{0} 482] R. D. Closson, J. Kozikowski, T. H. Coffield, *J. Org. Chem.* **1957**, *22*, 598.

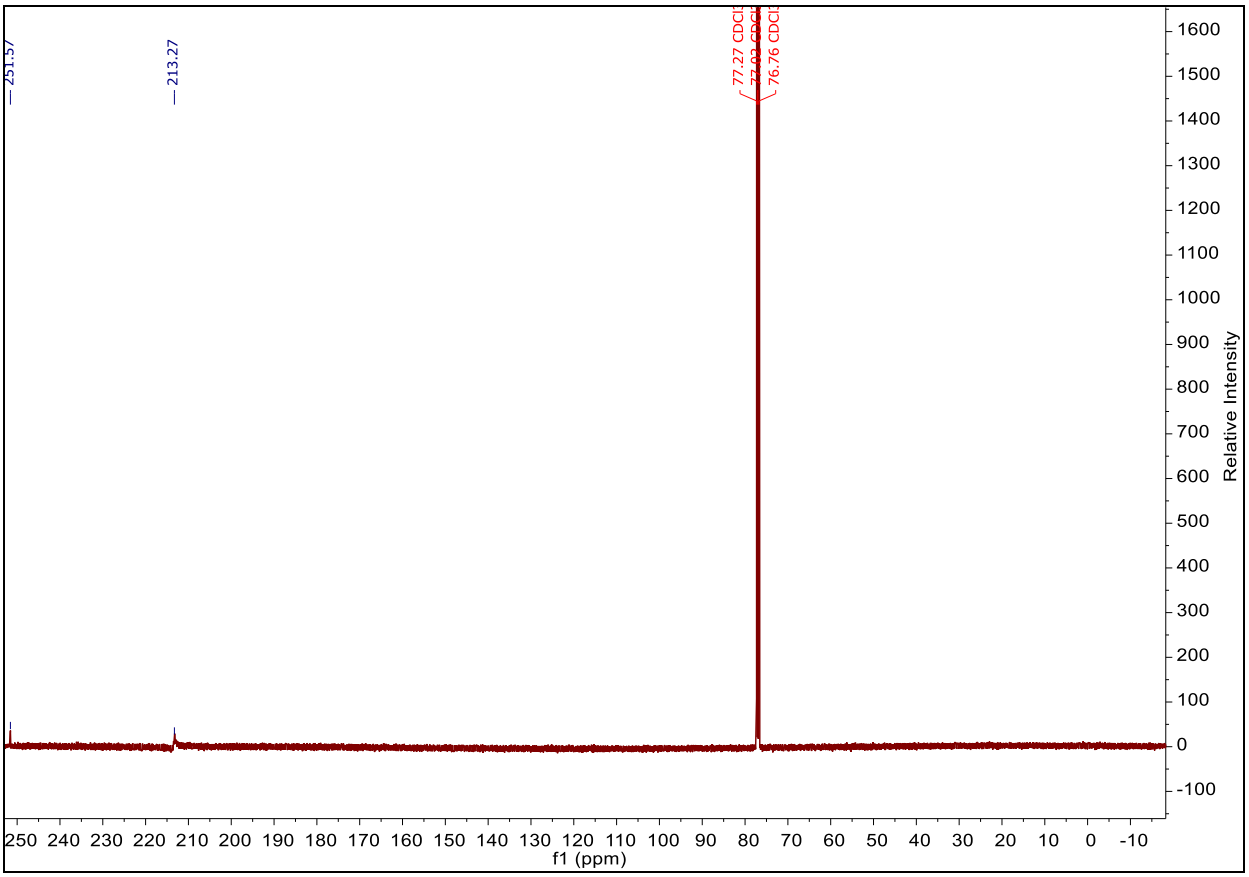

Figure SI 2.11 ^{13}C NMR spectrum of the synthesized complex **2.1** by modified literature procedure[285] (for the details of the synthesis, see Experimental section, page 163). The spectrum is recorded in deuterated chloroform at 500 MHz.

A.2.2. IR spectra.

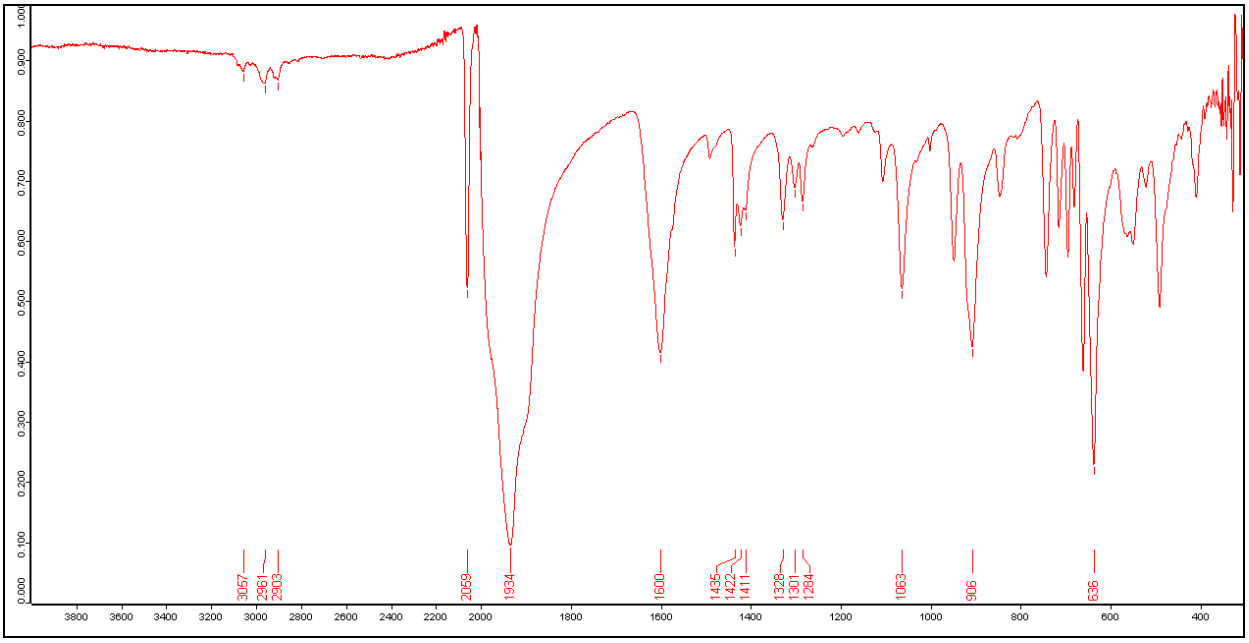

Figure SI 2.12 IR solid state (powder) spectrum of the reaction product of the reaction of **2.1** with **2.2a** carried out at 30-35ºC within 14.5h.

IR (solid phase – powder, ν, cm^{-1}) 3055, 2961, 2903, 2059, 1934, 1600.

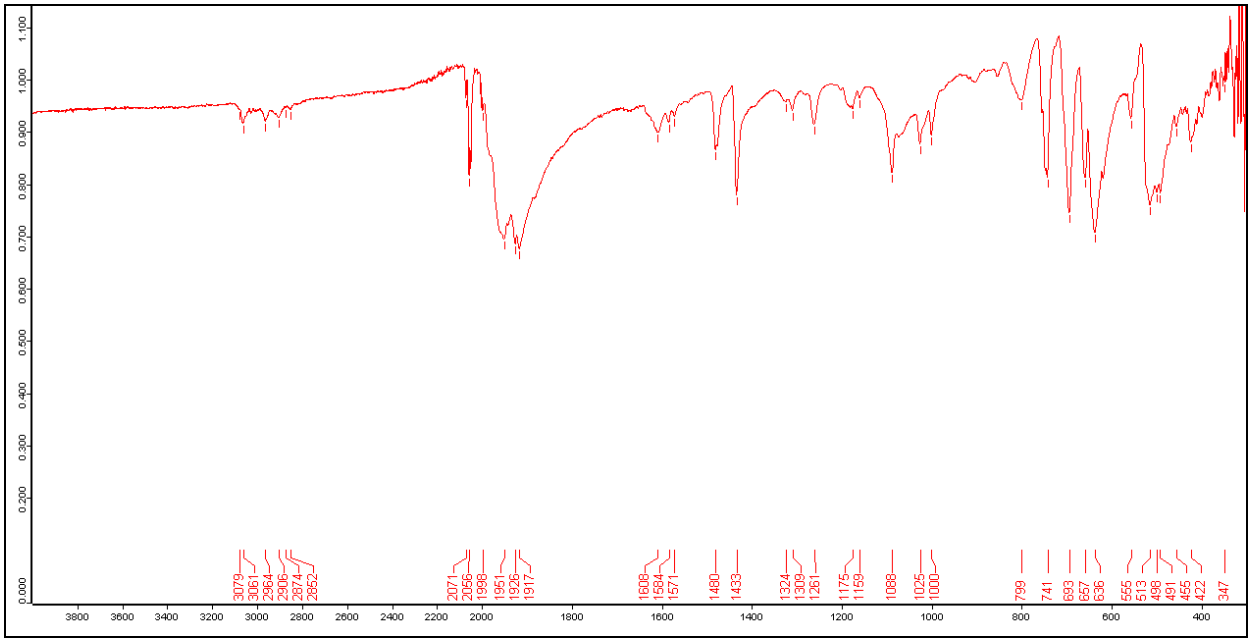

Figure SI 2.13 IR solid state (powder) spectrum of the reaction product of the reaction of **2.1** with **2.2b** carried out at 30-35ºC within 14.5h.

IR (solid phase – powder, ν, cm^{-1}) 3079, 2964, 2906, 2056, 1998, 1951, 1917, 1608, 1480, 1433.

Figure SI 2.14 IR solid state (powder) spectrum of the reaction product of the reaction of **2.1** with **2.2c** carried out at 30-35ºC within 14.5h.

IR (solid phase – powder, ν, cm^{-1}) 3067, 3041, 2079, 2004, 1964, 1635, 1622, 1588, 1486, 1455,1215, 1184, 1161.

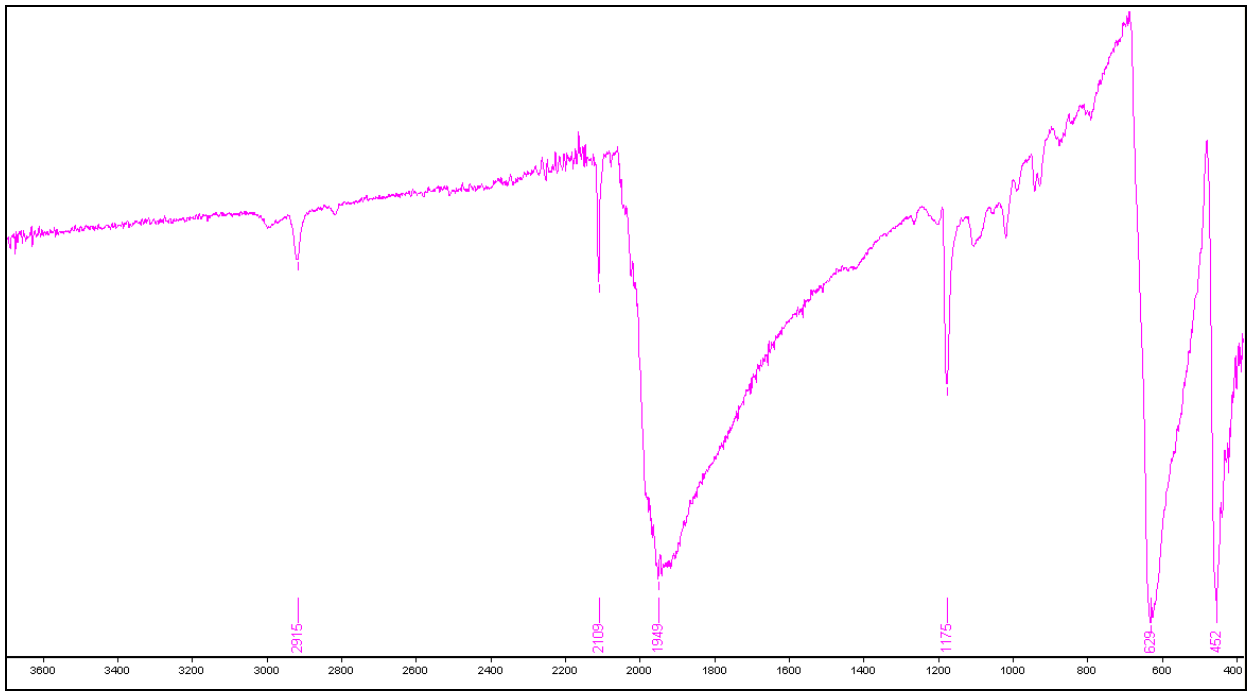

Figure SI 2.15 IR solid state (powder) spectrum of the synthesized complex **2.1** by modified literature procedure[285] (for the details of the synthesis, see Experimental section, page 163).

IR (solid phase – powder, ν, cm^{-1}) 2915, 2109, 1949, 1175.

A.2.3. ITC data.

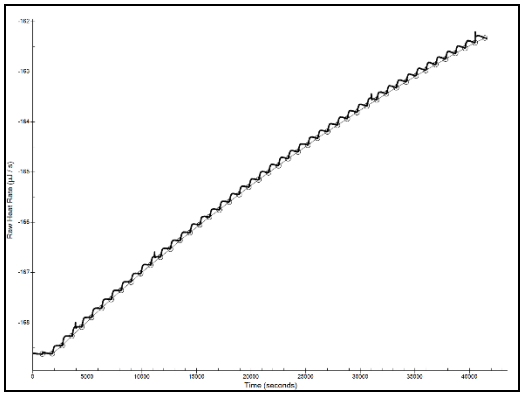

Figure SI 2.16 ITC thermogram of the reaction between **2.2a** (sample call, c=4.00 mM) and **2.1** (syringe, c=100.00 mM) in chlorobenzene. The titration was performed at 30ºC through 45 sequential additions (of 2.06 µL each). Time between two consecutive injections was 600 s. Heat released is expressed in µJ/s versus time in s.

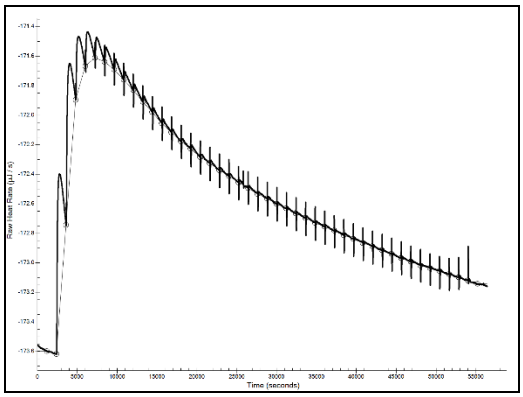

Figure SI 2.17 ITC thermogram of the reaction between **2.1** (sample call, c=4.00 mM) and **2.2b** (syringe, c=100.00 mM) in chlorobenzene. The titration was performed at 30ºC through 45 sequential additions (of 2.06 µL each). Time between two consecutive injections was 1200 s. Heat released is expressed in µJ/s versus time in s.

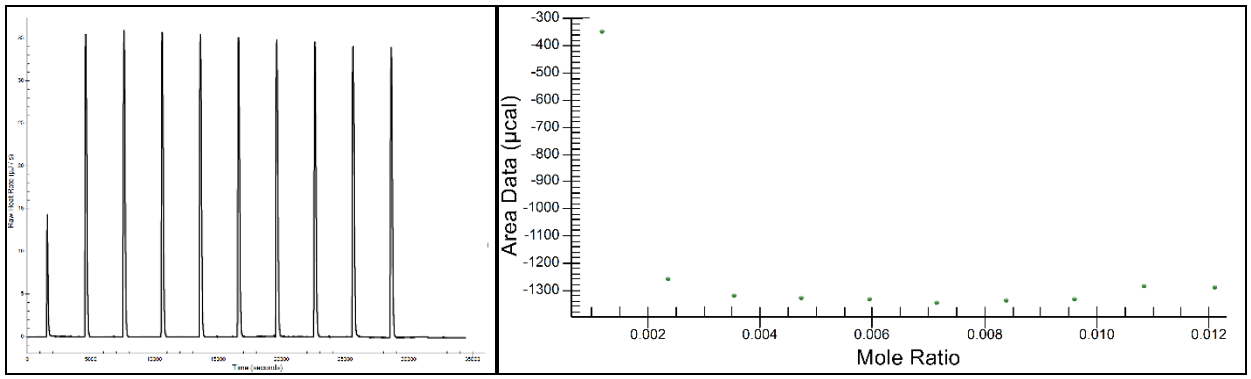

Figure SI 2.18 *left side* – ITC thermogram of the reaction between **2.1** (sample call, c=101.43 mM) and **2.2b** (syringe, c=16.93 mM) in chlorobenzene. The titration was performed at 25ºC through 10 sequential additions (of 6.97 µL each). Time between two consecutive injections was 3000 s. Heat released is expressed in µJ/s versus time in s. *right side* – ITC integrated heat peaks of the thermogram shown on the left side. Integrated heats are expressed in µcal versus molar ratio of the reactants.

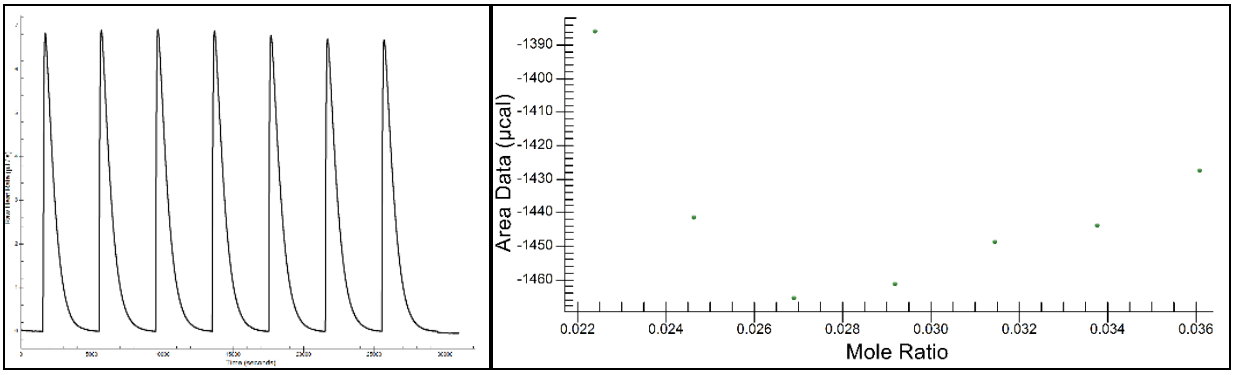

Figure SI 2.19 *left side* – ITC thermogram of the reaction between **2.1** (sample call, c=52.28 mM) and **2.2c** (syringe, c=22.11 mM) in chlorobenzene. The titration was performed at 25ºC through 7 sequential additions (of 5.03 µL each). Time between two consecutive injections was 2000 s. Heat released is expressed in µJ/s versus time in s. *right side* – ITC integrated heat peaks of the thermogram shown on the left side. Integrated heats are expressed in µcal versus molar ratio of the reactant

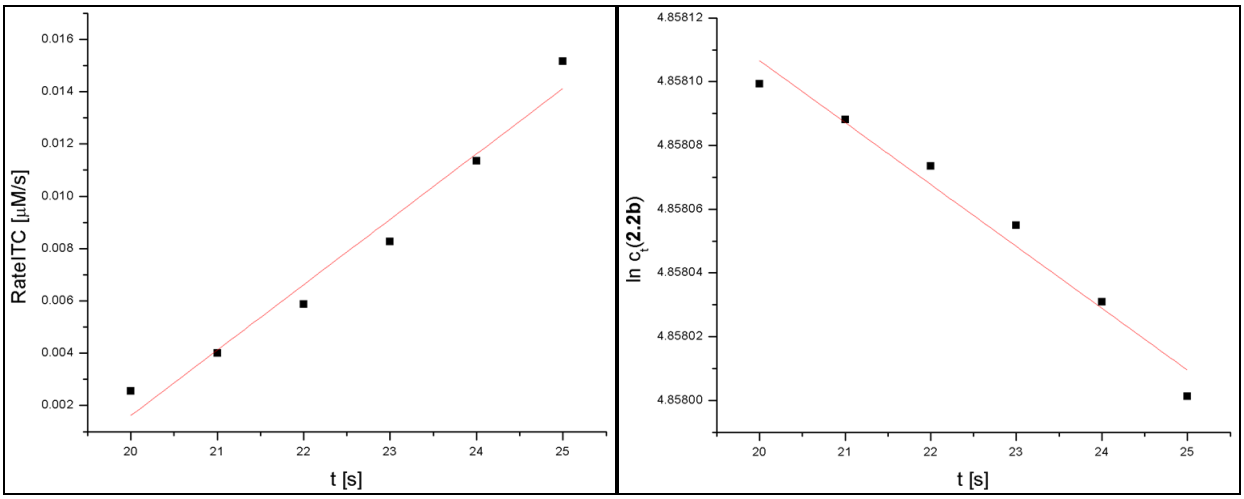

Figure SI 2.20 *left side* - Linear fit of the plot of the ITC Rate as a function of time for the reaction of **2.1** (sample call, c=74.57 mM) with **2.2b** (syringe, c=18.61 mM) carried out in ITC calorimeter. ITC Rate is expressed in µM/s and time in s. Obtained $\boldsymbol{k = 2.5*10^{-3} \pm 2*10^{-4}}$, as the result of the fitting. *right side* - Linear fit of the plot of logarithm of **2.2b** concentration as a function of time for the same reaction. Obtained $\boldsymbol{k_{obs} = -1.9*10^{-5} \pm 2*10^{-6}}$, as the result of the fitting.

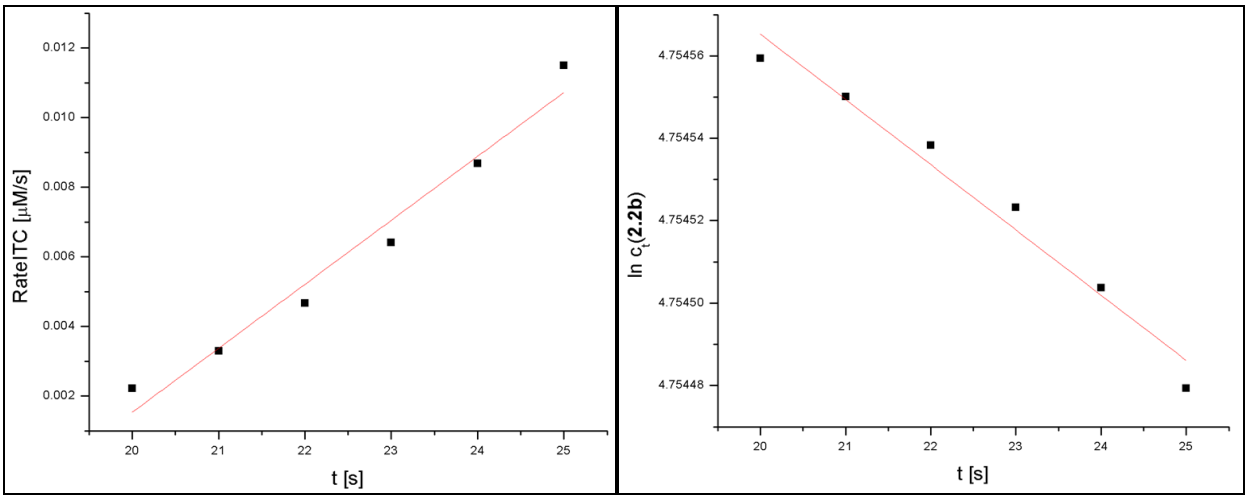

Figure SI 2.21 *left side* - Linear fit of the plot of the ITC Rate as a function of time for the reaction of **2.1** (sample call, c=54.57 mM) with **2.2b** (syringe, c=16.78 mM) carried out in ITC calorimeter. ITC Rate is expressed in µM/s and time in s. Obtained $\boldsymbol{k = 1.8*10^{-3} \pm 2*10^{-4}}$, as the result of the fitting. *right side* - Linear fit of the plot of logarithm of **2.2b** concentration as a function of time for the same reaction. Obtained $\boldsymbol{k_{obs} = -1.6E*10^{-5} \pm 1*10^{-6}}$, as the result of the fitting.

A.2.4. Cartesian's coordinates of the optimized geometries of the investigated systems within the study of cis-migration-insertion reaction sequence within the pentacarbonylmethylmanganese complex.

[**2.1**] - pentacarbonylmethylmanganese - ZORA-GGAPBE-D3(BJ)/TZP_PhCl (COSMO) phase

Mn	-0.39673228	3.19548324	-1.02391999
O	2.56950799	3.51785816	-0.78666942
O	-0.67228856	6.17489667	-0.99462863
O	-3.34036358	2.97360979	-0.53633414
H	0.63260227	2.97363970	1.63026052
O	-0.10860862	0.30146336	-0.31743846
O	-0.48490679	2.85493943	-3.97377863
C	-0.45054825	2.99018540	-2.82055963
C	-0.21921842	1.41237964	-0.61754941
C	-2.20736275	3.05663312	-0.75109062
C	-0.56598071	5.02421094	-1.03066247
C	1.42636976	3.39007027	-0.90254265
C	-0.31425557	3.40912712	1.30093207
H	-0.37056221	4.47630195	1.52786338
H	-1.17019483	2.86246444	1.70489464

[**2.2a**] - dimethyl(phenyl)phosphine - ZORA-GGAPBE-D3(BJ)/TZP_PhCl (COSMO) phase

P	0.80352751	2.28245828	-2.38864513
H	0.74584465	2.94430414	0.56816081
H	0.16190133	0.90413239	-0.41296141
C	-0.70299066	5.98574852	-1.37639148
H	3.15977178	2.87405119	-2.06128199
C	-0.27117395	4.85115881	-2.07468110
C	-0.61386145	6.02288632	0.01906050
C	-0.09142218	4.92270913	0.71317965
C	0.33903580	3.79262407	0.01264425
H	-0.34199369	4.82231592	-3.16469250
C	0.25411890	3.74258806	-1.38984711
H	-1.10883908	6.83888895	-1.92279885
H	-0.95007603	6.90531303	0.56639440
H	-0.01948647	4.94711121	1.80209133
C	-0.05002765	0.89816762	-1.49221413
H	-1.13443555	0.97665272	-1.65100621
H	0.29480913	-0.05482683	-1.91963597
C	2.52565421	2.03806788	-1.73573174
H	2.54909959	1.96689147	-0.63836709
H	2.92855177	1.10891612	-2.16487836

[**2.2b**] - triphenylphosphine - ZORA-GGAPBE-D3(BJ)/TZP_PhCl (COSMO) phase

P	0.69118574	2.23174602	-2.33564951
H	-0.03311515	2.71702511	0.56499795
H	2.16986673	0.64270882	-0.22527697

H	2.69562716	3.78774613	-0.67874795
C	2.52860938	2.26857376	-2.21010677
C	3.24456786	1.41796164	-3.07276556
C	4.64142626	1.40947104	-3.06354915
C	5.34256900	2.26727487	-2.20559692
C	4.63783677	3.12191816	-1.35061262
C	3.23856711	3.12040215	-1.35028992
H	2.70281257	0.76366193	-3.75970198
H	5.18421094	0.74434310	-3.73726518
H	6.43411048	2.27333109	-2.20922883
H	5.17648464	3.79423161	-0.68054566
C	0.25483480	0.83963470	-1.21177241
C	-1.04999720	0.32280473	-1.30989095
C	-1.45131039	-0.74897998	-0.50854865
C	-0.54724245	-1.32917111	0.39074296
C	0.75507619	-0.82594079	0.48835488
C	1.15303532	0.25457436	-0.30599725
H	-1.75255004	0.75967823	-2.02330323
H	-2.46637949	-1.14028138	-0.59443973
H	-0.85501408	-2.17578561	1.00721702
H	1.46602496	-1.27547306	1.18379323
C	0.19876044	3.70486348	-1.34602196
C	0.09262586	4.92900365	-2.03126867
C	-0.29801153	6.08887038	-1.35700082
C	-0.60376937	6.03618489	0.00916707
C	-0.50788844	4.82053189	0.69621794
C	-0.10574955	3.66177320	0.02325792
H	0.31137481	4.97081014	-3.10077190
H	-0.37548403	7.03204748	-1.90035674
H	-0.92204011	6.93862406	0.53433075
H	-0.74704420	4.77143866	1.75996023

[**2.2c**] - triphenylphosphite - ZORA-GGAPBE-D3(BJ)/TZP_PhCl (COSMO) phase

H	2.20849666	4.97200563	-0.23252152
P	-0.42197149	2.68091785	0.76659601
H	0.46340553	5.67047472	3.61721320
H	1.51705850	-0.59786734	1.98396319
O	-0.02219229	1.48571123	1.87093988
O	-0.00026397	3.84910495	1.88848179
O	0.87635192	2.70234156	-0.27188179
C	-0.45087535	0.18067895	1.58463949
C	-1.78094583	-0.10115054	1.25508754
C	-2.15683236	-1.42786764	1.01758764
C	-1.21944215	-2.46130841	1.12013036
C	0.10300407	-2.16511720	1.46896961
C	0.49344517	-0.84278873	1.69990141
H	-2.51526673	0.70327649	1.20005335
H	-3.19316573	-1.65039880	0.76028013
H	-1.51932780	-3.49341362	0.93506178
H	0.83946345	-2.96465621	1.56011204
C	-0.14972826	5.20526964	1.60647861
C	-0.55073396	5.69847496	0.35911314
C	-0.67651623	7.08167163	0.17893419

C	-0.39025383	7.96594482	1.22283275
C	0.02486486	7.45813572	2.46059227
C	0.14299090	6.08113898	2.65863388
H	-0.76613473	5.02217968	-0.46925463
H	-0.99825372	7.46249427	-0.79139458
H	-0.48641431	9.04232029	1.07356303
H	0.25821607	8.13740828	3.28191635
C	2.21954828	2.84794351	0.13421202
C	2.95414131	1.72351757	0.51228540
C	4.30384485	1.87485634	0.84867832
C	4.90806074	3.13636334	0.79733036
C	4.15777124	4.25157510	0.40726832
C	2.80629333	4.11313258	0.07544107
H	2.47343975	0.74633920	0.52542508
H	4.88398535	1.00019955	1.14641535
H	5.96191099	3.24930516	1.05545192
H	4.62363685	5.23675507	0.35596357

[**2.3a**] - pentacarbonylmethylmanganese/dimethyl(phenyl)phosphine - ZORA-GGAPBE-D3(BJ)/TZP_PhCl (COSMO) phase

Mn	-0.64327750	2.97445288	-0.98273939
O	1.36150602	5.09912731	-0.41728123
O	-2.38364463	5.36299801	-1.40212902
O	-2.79947012	0.99715987	-0.44799170
H	0.90869071	5.89432370	2.24184094
O	1.73117167	1.18809204	-0.73621358
O	-0.94319433	2.26326626	-3.84333311
C	-0.80177470	2.56926553	-2.72747187
C	0.79505897	1.87630039	-0.81571534
C	-1.94880779	1.77425838	-0.62806396
C	-1.71404617	4.43536448	-1.19819988
H	0.43625666	4.98950244	-3.35132372
H	-4.00935112	6.65013032	2.45645504
H	-2.43313644	8.44884671	3.17662911
H	0.02867166	8.05634578	3.06016042
P	-0.44647152	3.40479760	1.32212567
H	-3.13971447	4.48851610	1.64137888
C	-0.16830327	6.04897971	2.29631143
C	-0.66676920	7.27334138	2.75356880
H	1.93114283	3.88747587	1.50597869
C	0.86166591	4.44455497	-1.32087510
C	-1.05127084	5.03111154	1.90554436
C	1.30260678	4.67834669	-2.74914689
C	-2.04704186	7.49315664	2.81765534
C	-2.93177373	6.48496836	2.41522569
H	-1.05296163	1.21300461	2.16036116
H	2.08684589	5.44635870	-2.79389648
H	1.66772184	3.73653800	-3.18322305
C	-2.43700913	5.26157455	1.95829198
C	-1.40083330	2.23484858	2.36626084
H	-1.24078460	2.47630926	3.42558568
H	-2.47113755	2.29337436	2.13479439
C	1.22925579	3.24004811	2.04094947

H	1.19787501	3.50452385	3.10643040
H	1.54516195	2.19349557	1.93582021

[**2.3b**] - pentacarbonylmethylmanganese/triphenylphosphine - ZORA-GGAPBE-D3(BJ)/TZP_PhCl (COSMO) phase

Mn	-0.59044686	3.04058648	-0.91670033
O	1.42857648	5.19644390	-0.60261152
O	-1.94951668	5.68186414	-1.25397422
O	-3.10834751	1.57108601	-0.32237878
H	0.60605790	6.19815912	1.78106417
O	1.34881323	0.78152559	-0.98067632
O	-1.15145553	2.48338103	-3.77017380
C	-0.91003558	2.72437280	-2.65678819
C	0.59373497	1.66642027	-0.91029352
C	-2.10241249	2.12741756	-0.50468792
C	-1.43085136	4.66151898	-1.07528922
H	1.02495759	4.46714050	-3.49668719
H	-4.28486516	5.92674600	2.67574502
H	-3.11281513	8.12904011	2.80183894
H	-0.66078275	8.25281337	2.34896949
P	-0.22463210	3.40085147	1.38099799
H	-3.01946815	3.87517498	2.12295159
H	-1.35198521	3.36729646	4.13376759
H	0.80042567	4.50434636	3.90145941
C	1.47969164	3.60056376	2.04779071
C	2.59652910	3.12926059	1.34554699
C	3.87194106	3.19600757	1.91382954
C	4.04315009	3.73821913	3.19183611
C	2.93090320	4.20839752	3.90090600
C	1.65606563	4.13586722	3.33538734
H	2.48371161	2.71621062	0.34561463
H	4.73169109	2.82774807	1.35212856
H	5.03920600	3.79402038	3.63452476
H	3.05252594	4.63205812	4.89888790
C	-0.87076463	2.06135747	2.46955422
C	-0.83631037	0.72782365	2.03210452
C	-1.25050651	-0.30787382	2.87423273
C	-1.70880548	-0.02116239	4.16435169
C	-1.74099947	1.30564936	4.61005962
C	-1.31892626	2.33993980	3.77168538
H	-0.49338564	0.48599374	1.02692911
H	-1.22040832	-1.33793966	2.51619339
H	-2.04130642	-0.82788560	4.81992838
H	-2.09642367	1.53972044	5.61457325
C	-1.11269548	4.89596920	1.94647620
C	-0.45971109	6.13619991	1.99677783
C	-1.17900397	7.29357097	2.30754505
C	-2.55370913	7.22379163	2.55820341
C	-3.21182926	5.98965623	2.48908209
C	-2.49693417	4.83125426	2.17870665
C	1.05746523	4.31910438	-1.36624423
C	1.73198923	4.15804935	-2.71153897
H	2.63364538	4.78301127	-2.76750529

H	1.97748710	3.10428192	-2.90099940

[**2.3c**] - pentacarbonylmethylmanganese/triphenylphosphite - ZORA-GGAPBE-D3(BJ)/TZP_PhCl (COSMO) phase

Mn	-0.38980791	3.01284453	-0.92302598
O	1.32915281	5.47897922	-1.02331712
O	-2.34522902	5.25607512	-1.17633389
O	-2.30918144	0.99757553	0.12739202
H	1.78148228	5.38404714	-3.49887537
O	2.10321374	1.49185030	-1.53178091
O	-1.35911367	2.12612489	-3.58379070
C	-0.96213177	2.51119296	-2.56250279
C	1.13497742	2.05138237	-1.22080600
C	-1.53025132	1.77457253	-0.25098035
C	-1.57950647	4.40565838	-0.98914776
H	0.11291484	4.75168102	-3.71195142
C	0.85491792	4.59920301	-1.71436638
C	1.07884052	4.59132436	-3.20974156
H	1.45058778	3.61065409	-3.53679524
H	1.48594823	3.02445866	3.93054321
P	0.26167849	3.31899598	1.20757133
H	-3.15825075	4.58116848	2.93861399
H	3.01665373	1.88858225	1.97833853
O	0.33633201	1.95616782	2.12821550
O	-0.73008497	4.03734705	2.28818730
O	1.71370706	4.02397414	1.39382469
C	1.13171500	0.85129376	1.75791438
C	0.47971307	-0.35388648	1.49054741
C	1.24329763	-1.48621998	1.19005427
C	2.64025322	-1.40796487	1.16021465
C	3.27549299	-0.19453754	1.44271042
C	2.52483558	0.94411761	1.74976679
H	-0.60821303	-0.39870876	1.52691282
H	0.73994434	-2.43105024	0.98147438
H	3.23225070	-2.29320146	0.92445088
H	4.36384450	-0.12768106	1.43034606
C	-1.32469839	5.29092718	2.05860120
C	-0.62317635	6.34983384	1.48202554
C	-1.27189787	7.57944802	1.32972851
C	-2.59122367	7.74603629	1.76097119
C	-3.27438991	6.67090465	2.34267675
C	-2.64461507	5.43296959	2.49110899
H	0.39954067	6.21460453	1.13287147
H	-0.73457142	8.41054668	0.87174573
H	-3.08725066	8.71032295	1.64436137
H	-4.30405750	6.79173175	2.68126837
C	2.27890459	4.52376636	2.58452389
C	3.07625675	5.66016888	2.43189707
C	3.72644377	6.18852668	3.55006498
C	3.57309556	5.58683121	4.80494835
C	2.76457017	4.45379946	4.93682436
C	2.11015272	3.90914417	3.82619526
H	3.18182185	6.10898879	1.44353341

H	4.35409475	7.07317369	3.43645228
H	4.08263573	5.99969820	5.67643010
H	2.63950955	3.97802156	5.91021722

A.3. Supplementary information to Chapter 6.

A.3.1. ITC data.

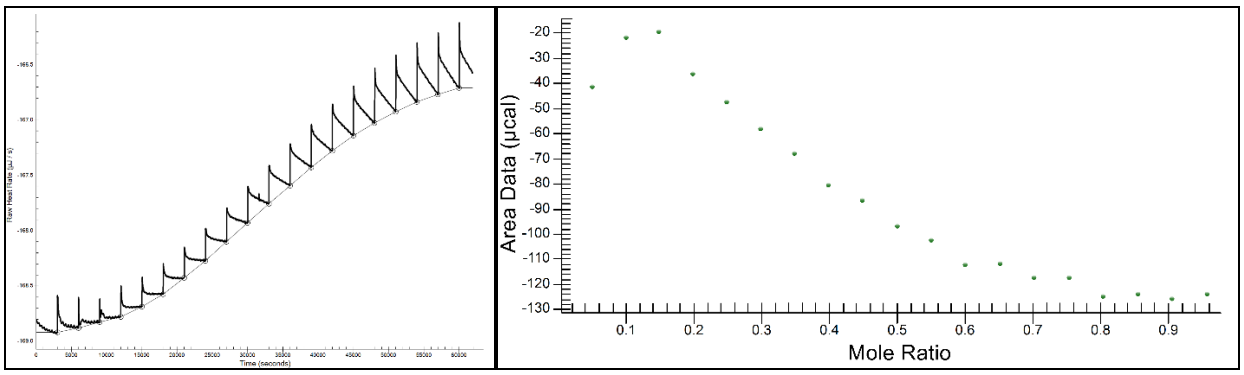

Figure SI 3.1 *left side* – ITC thermogram of the reaction between **3.2a** (sample call, c=4.00 mM) and **3.3a** (syringe, c=95.93 mM) in chlorobenzene. The titration was performed at 25ºC through 19 sequential additions (of 2.06 µL each). Time between two consecutive injections was 3000 s. Heat released is expressed in µJ/s versus time in s. *right side* – ITC integrated heat peaks of the thermogram shown on the left side. Integrated heats are expressed in µcal versus molar ratio of the reactants.

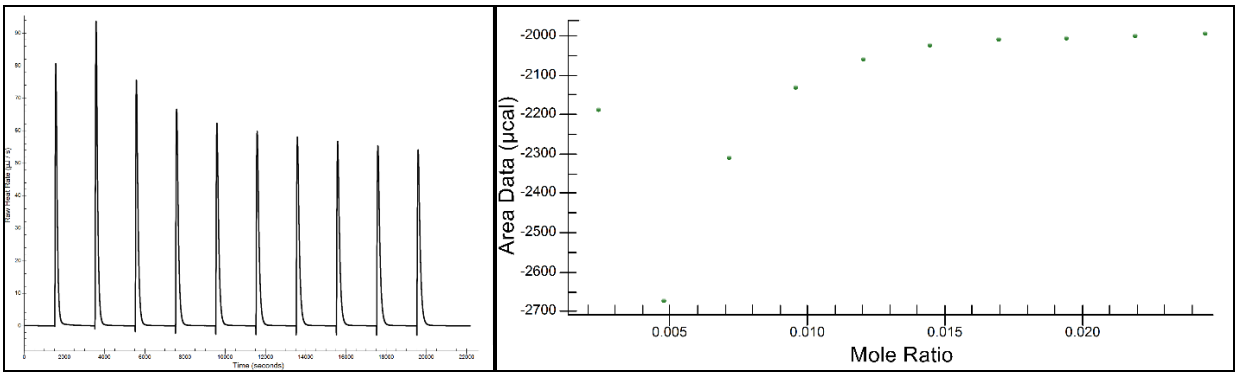

Figure SI 3.2. *left side* – ITC thermogram of the reaction between **3.3c** (sample call, c=47.83 mM) and **3.2a** (syringe, c=16.14 mM) in chlorobenzene. The titration was performed at 25ºC through 10 sequential additions (of 6.97 µL each). Time between two consecutive injections was 2000 s. Heat released is expressed in µJ/s versus time in s. *right side* – ITC integrated heat peaks of the thermogram shown on the left side. Integrated heats are expressed in µcal versus molar ratio of the reactants.

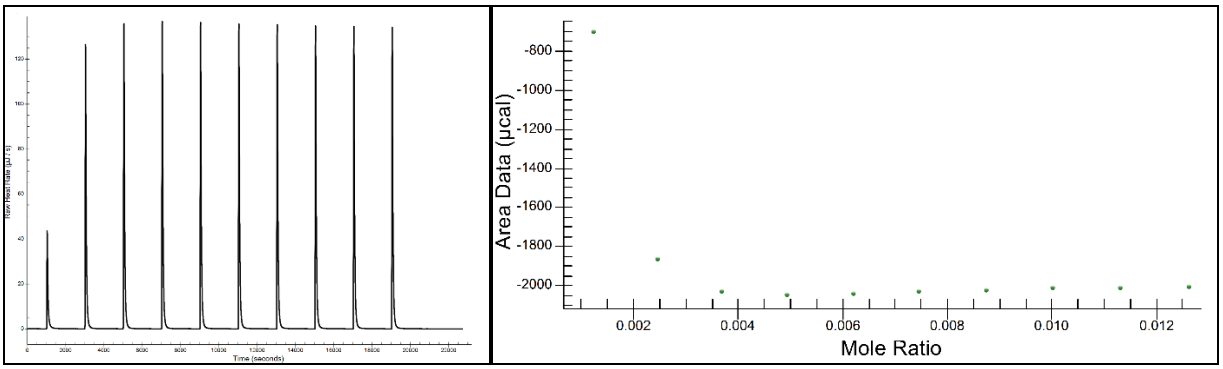

Figure SI 3.3. *left side* – ITC thermogram of the reaction between **3.3a** (sample call, c=105.82 mM) and **3.2b** (syringe, c=18.42 mM) in chlorobenzene. The titration was performed at 25ºC through 10 sequential additions (of 6.97 µL each). Time between two consecutive injections was 2000 s. Heat released is expressed in µJ/s versus time in s. *right side* – ITC integrated heat peaks of the thermogram shown on the left side. Integrated heats are expressed in µcal versus molar ratio of the reactants.

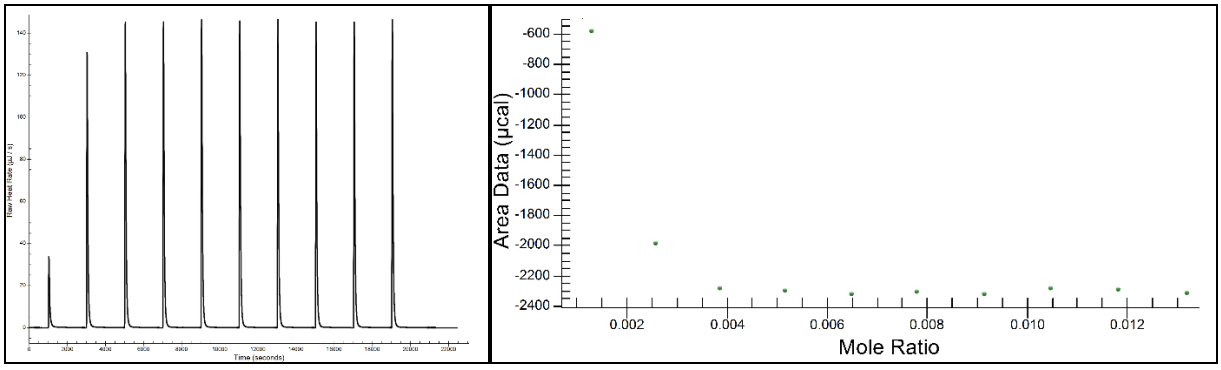

Figure SI 3.4. *left side* – ITC thermogram of the reaction between **3.3c** (sample call, c=99.12 mM) and **3.2b** (syringe, c=18.03 mM) in chlorobenzene. The titration was performed at 25ºC through 10 sequential additions (of 6.97 µL each). Time between two consecutive injections was 2000 s. Heat released is expressed in µJ/s versus time in s. *right side* – ITC integrated heat peaks of the thermogram shown on the left side. Integrated heats are expressed in µcal versus molar ratio of the reactants.

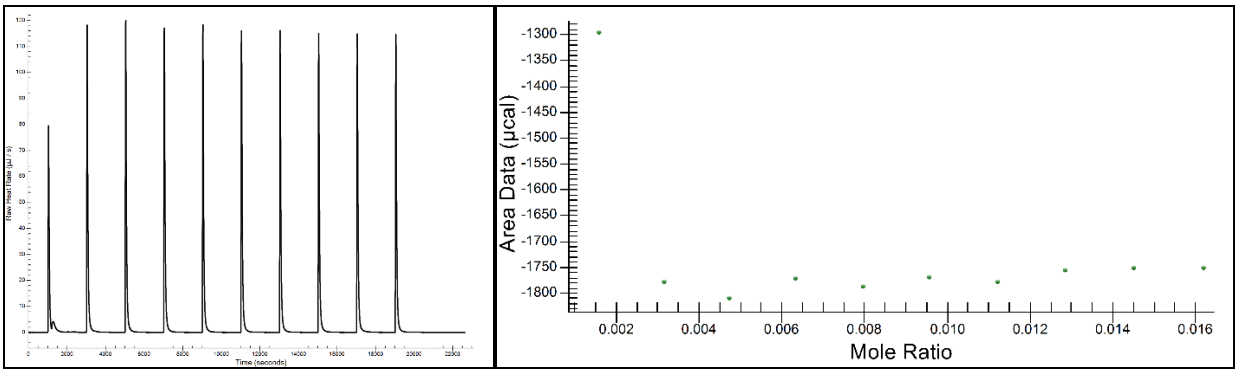

Figure SI 3.5. *left side* – ITC thermogram of the reaction between **3.3a** (sample call, c=72.04 mM) and **3.2c** (syringe, c=16.09 mM) in chlorobenzene. The titration was performed at 25ºC through 10 sequential additions (of 6.97 µL each). Time between two consecutive injections was 2000 s. Heat released is expressed in µJ/s versus time in s. *right side* – ITC integrated heat peaks of the thermogram shown on the left side. Integrated heats are expressed in µcal versus molar ratio of the reactants.

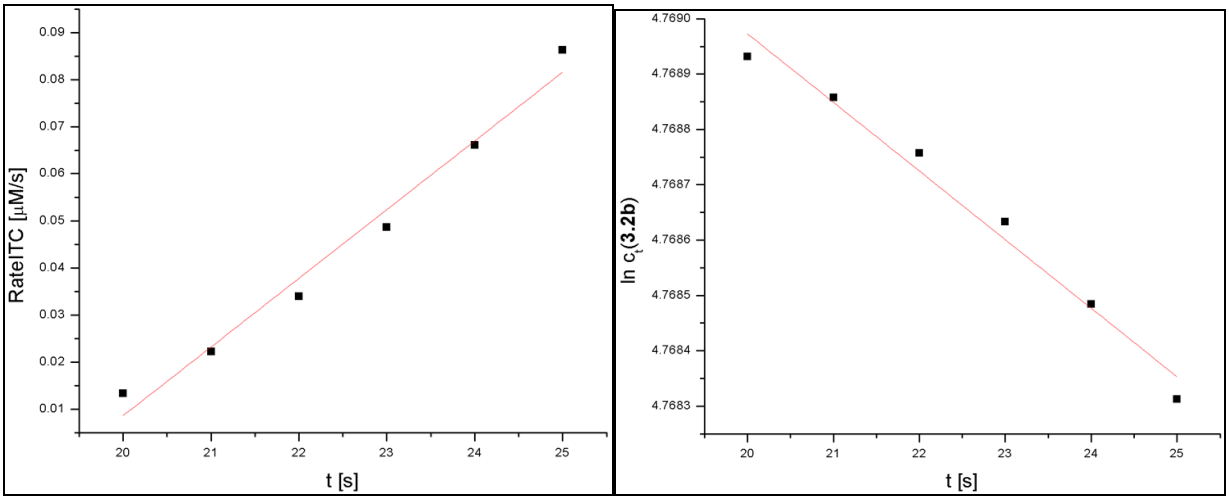

Figure SI 3.6 *left side* - Linear fit of the plot of the ITC Rate as a function of time for the reaction of **3.3a** (sample call, c=50.67 mM) with **3.2b** (syringe, c=17.02 mM) carried out in ITC calorimeter. ITC Rate is expressed in µM/s and time in s. Obtained ***k* = 1.5E-02 ± 1E-03**, as the result of the fitting. *right side* - Linear fit of the plot of logarithm of **3.2b** concentration as a function of time for the same reaction. Obtained $\boldsymbol{k_{obs}}$ **= -1.2E-04 ± 9E-06**, as the result of the fitting.

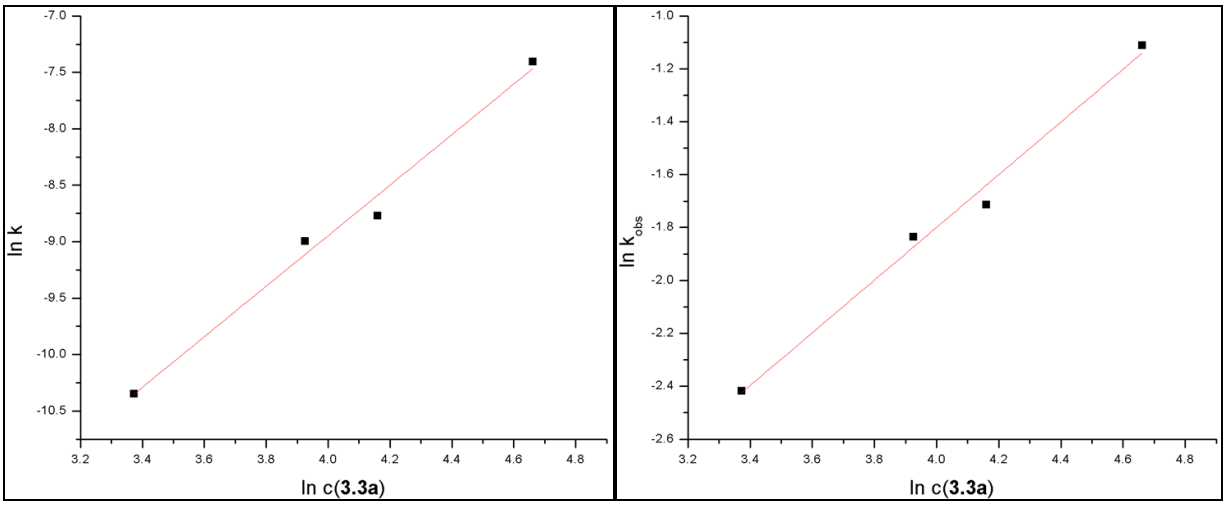

Figure SI 3.7 *left side* - Linear fit of the plot of logarithm of obtained *k* values as a function of the logarithm of **3.3a** starting concentrations for the reaction of **3.2b** with **3.3a** carried out in ITC calorimeter. Obtained partial reaction order with respect to **3.3a** – **2.18 ± 0.14**, as the result of the fitting. *right side* - - Linear fit of the plot of logarithm of obtained k_{obs} values as a function of the logarithm of **3.3a** starting concentrations for the reaction of **3.2a** with **3.3b** carried out in ITC calorimeter. Obtained partial reaction order with respect to **3.3a** – **2.24 ± 0.12**, as the result of the fitting.

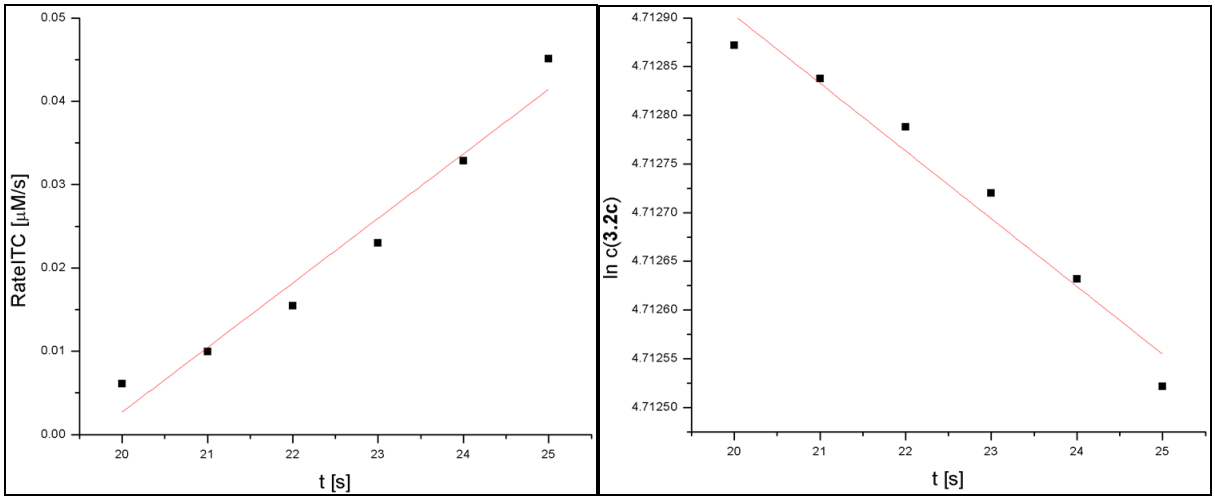

Figure SI 3.8 *left side* - Linear fit of the plot of the ITC Rate as a function of time for the reaction of **3.3a** (sample call, c=95.32 mM) with **3.2c** (syringe, c=16.09 mM) carried out in ITC calorimeter. ITC Rate is expressed in µM/s and time in s. Obtained ***k* = 7.8E-03 ± 8E-04**, as the result of the fitting. *right side* - Linear fit of the plot of logarithm of **3.2c** concentration as a function of time for the same reaction. Obtained ***k*$_{obs}$ = -7.0E-05 ± 7E-06**, as the result of the fitting.

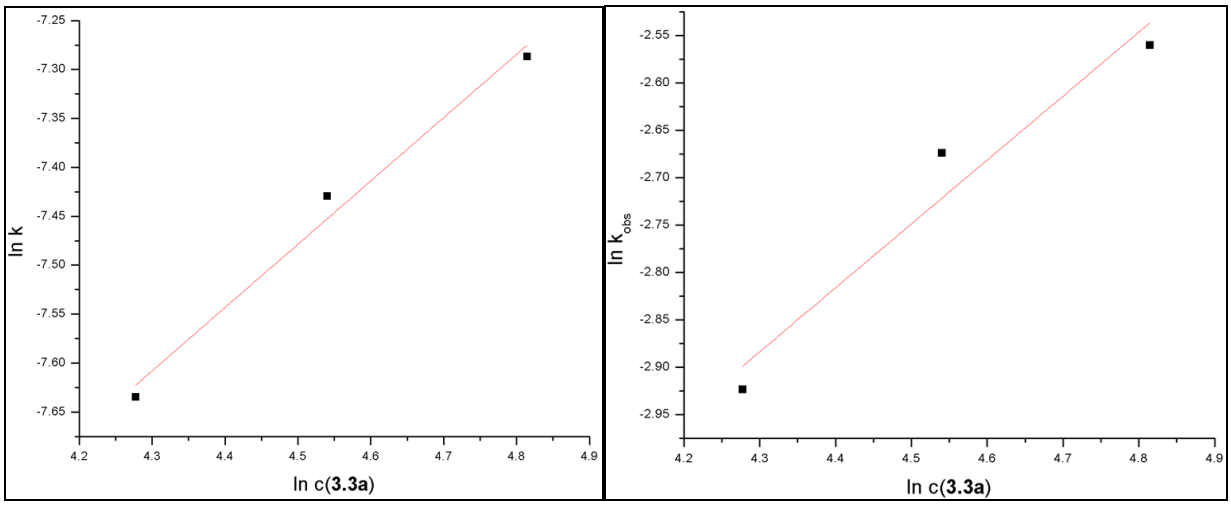

Figure SI 3.9 *left side* - Linear fit of the plot of logarithm of obtained *k* values as a function of the logarithm of **3.3a** starting concentrations for the reaction of **3.2c** with **3.3a** carried out in ITC calorimeter. Obtained partial reaction order with respect to **3.3a** – **2.02 ± 0.42**, as the result of the fitting. *right side* - - Linear fit of the plot of logarithm of obtained k_{obs} values as a function of the logarithm of **3.3a** starting concentrations for the reaction of **3.2c** with **3.3a** carried out in ITC calorimeter. Obtained partial reaction order with respect to **3.3a** – **2.02 ± 0.42**, as the result of the fitting.

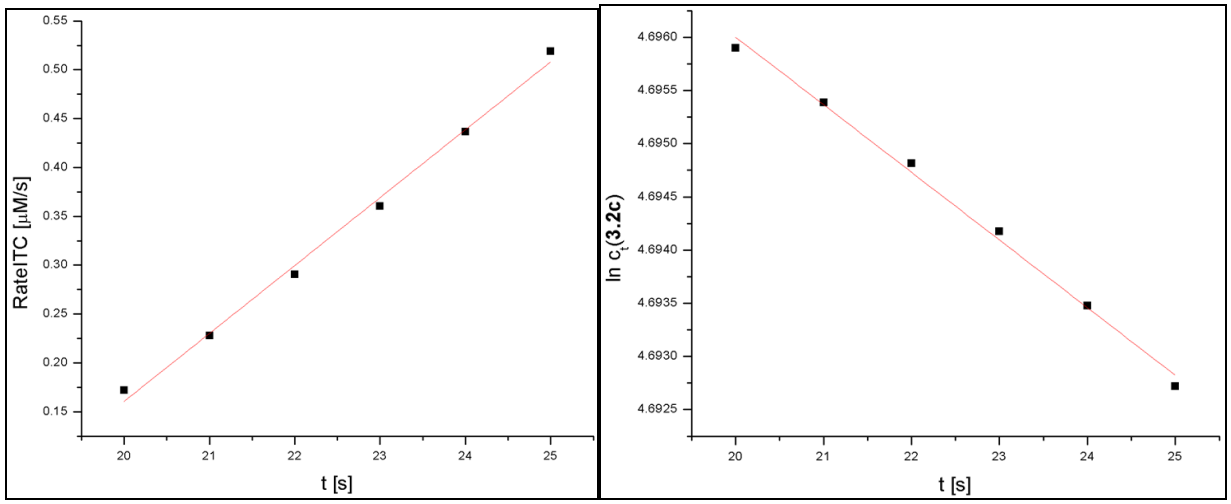

Figure SI 3.10 *left side* - Linear fit of the plot of the ITC Rate as a function of time for the reaction of **3.3c** (sample call, c=134.59 mM) with **3.2c** (syringe, c=15.84 mM) carried out in ITC calorimeter. ITC Rate is expressed in µM/s and time in s. Obtained ***k* = 7.0E-02 ± 2E-03**, as the result of the fitting. *right side* - Linear fit of the plot of logarithm of **3.2c** concentration as a function of time for the same reaction. Obtained $\boldsymbol{k_{obs}}$ **= -6.4E-04 ± 2E-05**, as the result of the fitting.

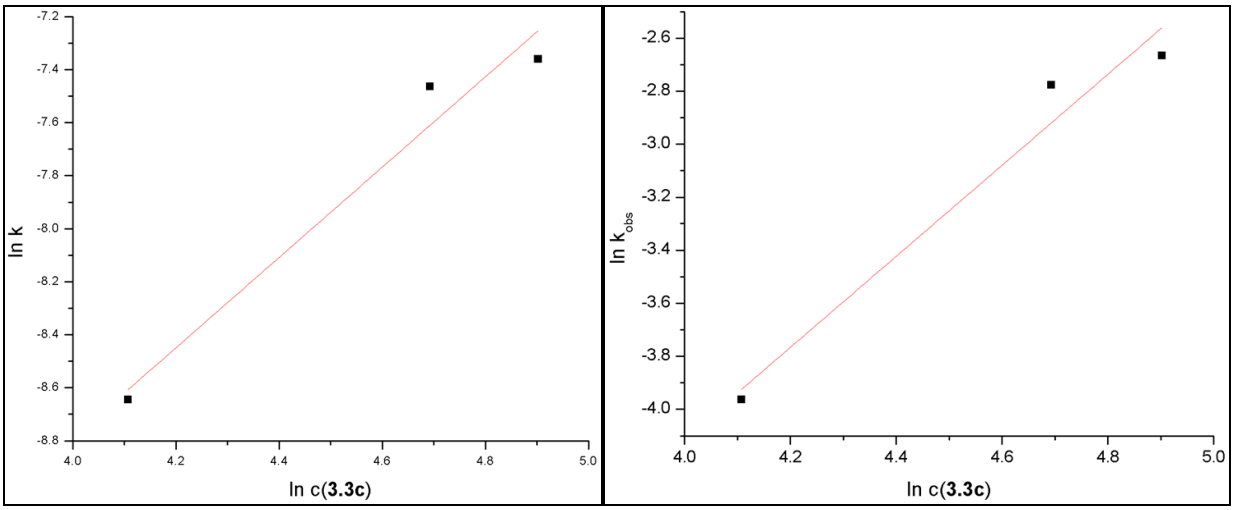

Figure SI 3.11 *left side* - Linear fit of the plot of logarithm of obtained *k* values as a function of the logarithm of **3.3c** starting concentrations for the reaction of **3.2c** with **3.3c** carried out in ITC calorimeter. Obtained partial reaction order with respect to **3.3c** – **1.72 ± 0.31**, as the result of the fitting. *right side* - - Linear fit of the plot of logarithm of obtained k_{obs} values as a function of the logarithm of **3.3c** starting concentrations for the reaction of **3.2c** with **3.3c** carried out in ITC calorimeter. Obtained partial reaction order with respect to **3.3c** – **1.70 ± 0.32**, as the result of the fitting.

A.3.2. Calcualtion data.

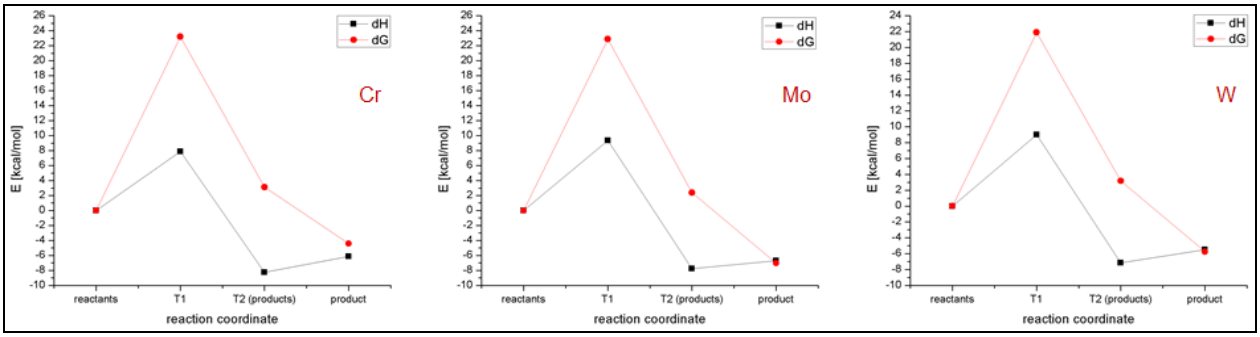

Figure SI 3.12 Graphic representation of the Δ*H* and Δ*G* values (given as energy expressed in kcal/mol) for particular states (given through reaction coordinate, see also Figure 3.10) within the course of the amination process of the Fischer carbene complex **3.2a-c** induced by the amines **3.3b**. The calculated were performed at ZORA-GGAPBE-D3-BJ/TZP level of theory in chlorobenzene solution (COSMO) phase at 298.15K.

A.3.3. NMR spectra.

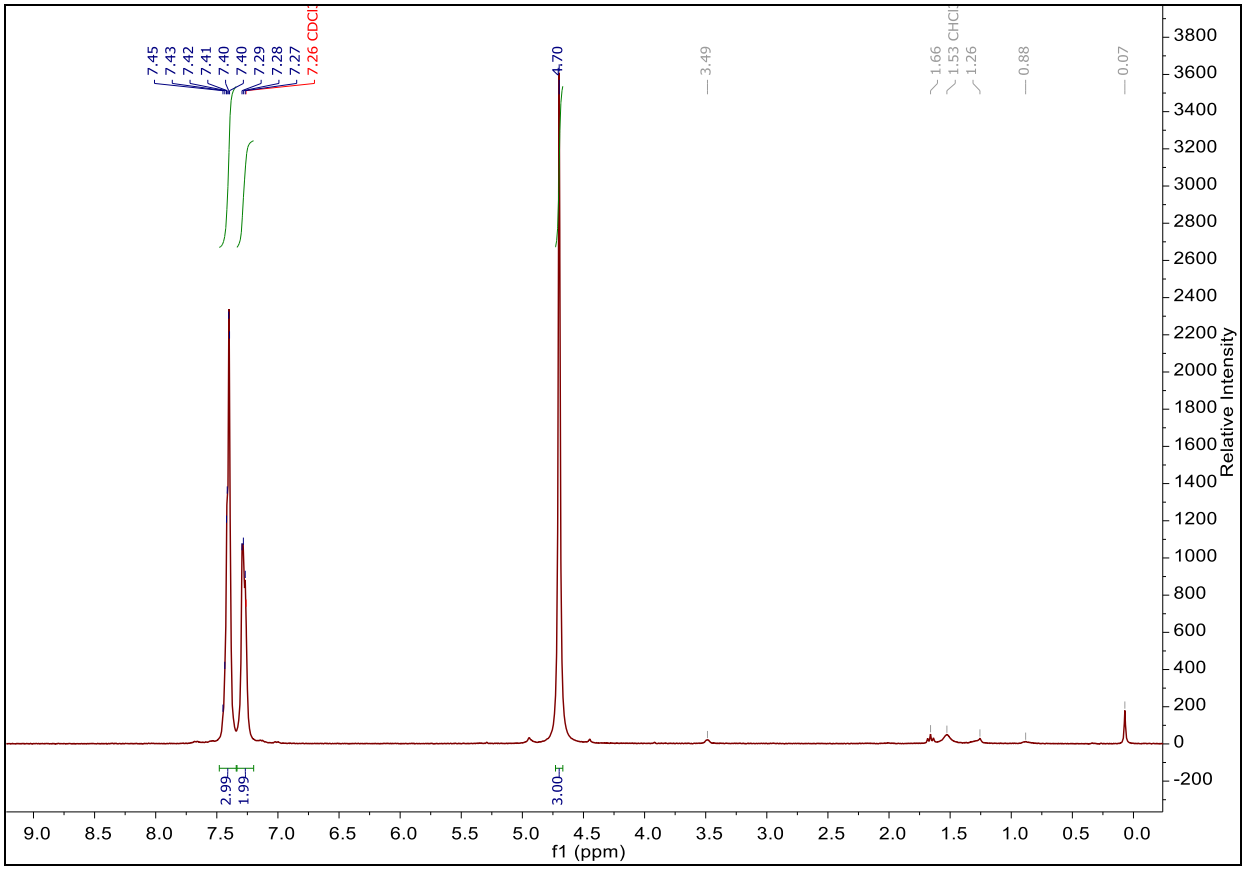

Figure SI 3.13 ^{1}H NMR spectrum of the synthesized Fischer carbene complex **3.2a** by modified literature procedure[286] (for the details of the synthesis, see Experimental section, page 191). The spectrum is recorded in deuterated chloroform at 300 MHz.

[286] [N^{0} 562] E. O. Fischer, A. Maasböl, Angew. *Chem. Int. Ed. Engl*. **1964**, *3*, 580.

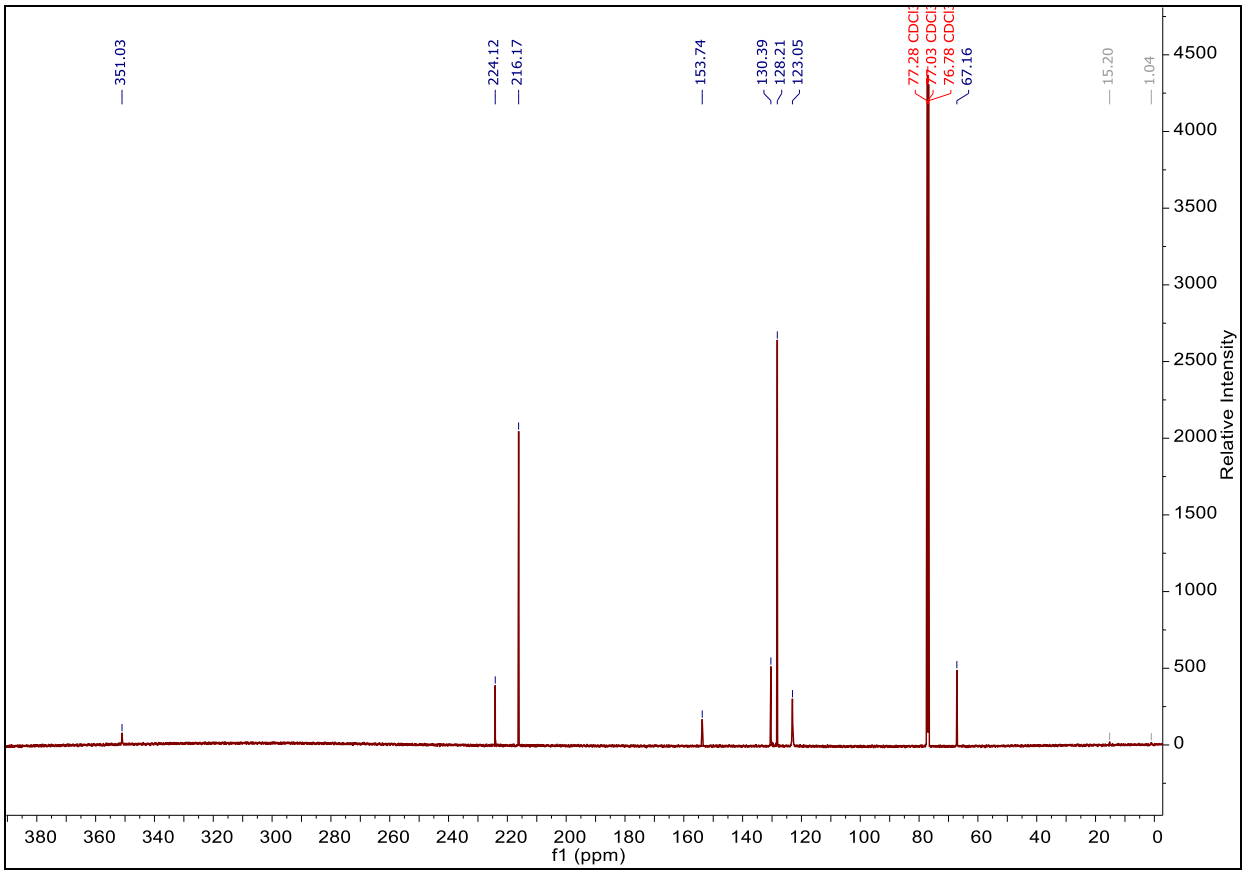

Figure SI 3.14 ^{13}C NMR spectrum of the synthesized Fischer carbene complex **3.2a** by modified literature procedure[286] (for the details of the synthesis, see Experimental section, page 191). The spectrum is recorded in deuterated chloroform at 126 MHz.

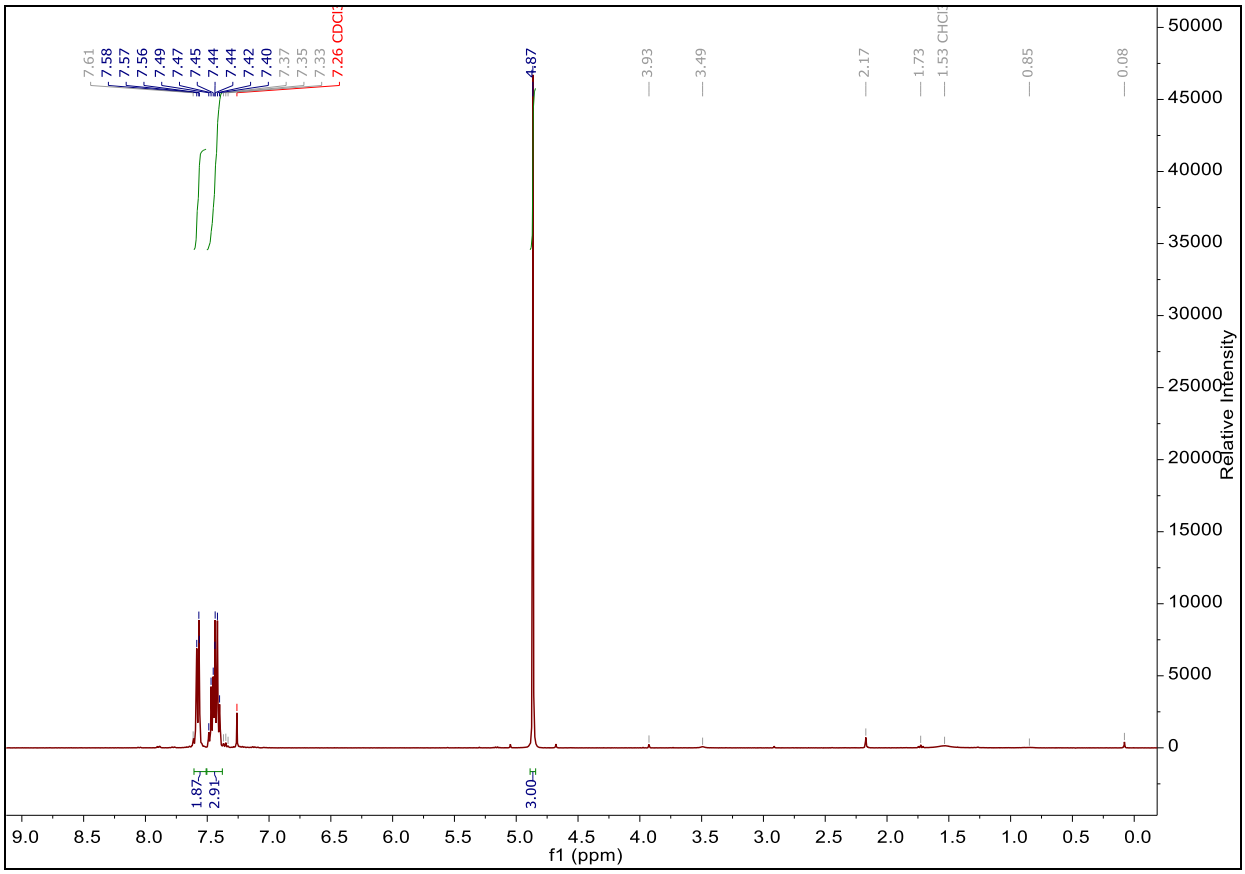

Figure SI 3.15 ^{1}H NMR spectrum of the synthesized Fischer carbene complex **3.2b** by modified literature procedure[286] (for the details of the synthesis, see Experimental section, page 191). The spectrum is recorded in deuterated chloroform at 400 MHz.

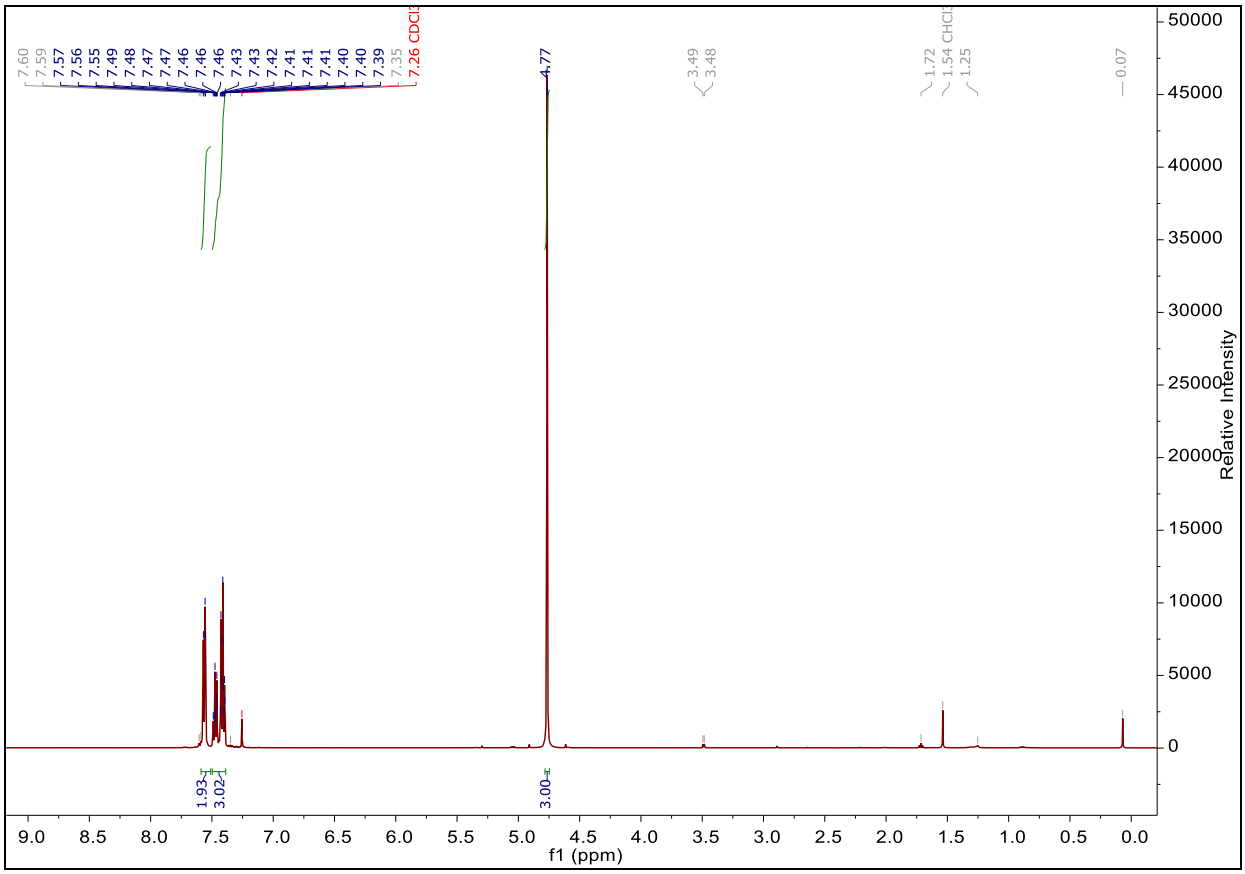

Figure SI 3.16 ^{1}H NMR spectrum of the synthesized Fischer carbene complex **3.2c** by modified literature procedure[286] (for the details of the synthesis, see Experimental section, page 191). The spectrum is recorded in deuterated chloroform at 500 MHz.

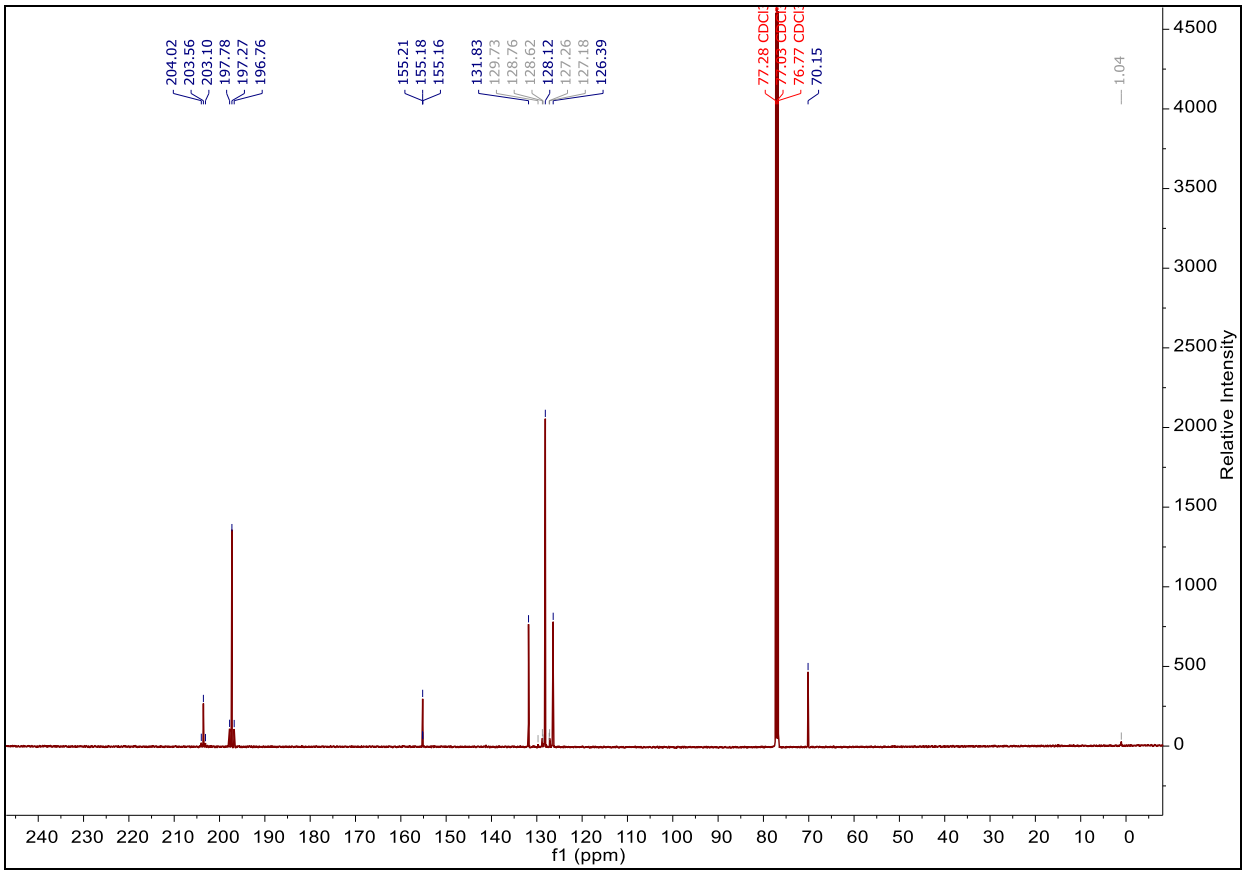

Figure SI 3.17 ^{13}C NMR spectrum of the synthesized Fischer carbene complex **3.2c** by modified literature procedure[286] (for the details of the synthesis, see Experimental section, page 191). The spectrum is recorded in deuterated chloroform at 126 MHz.

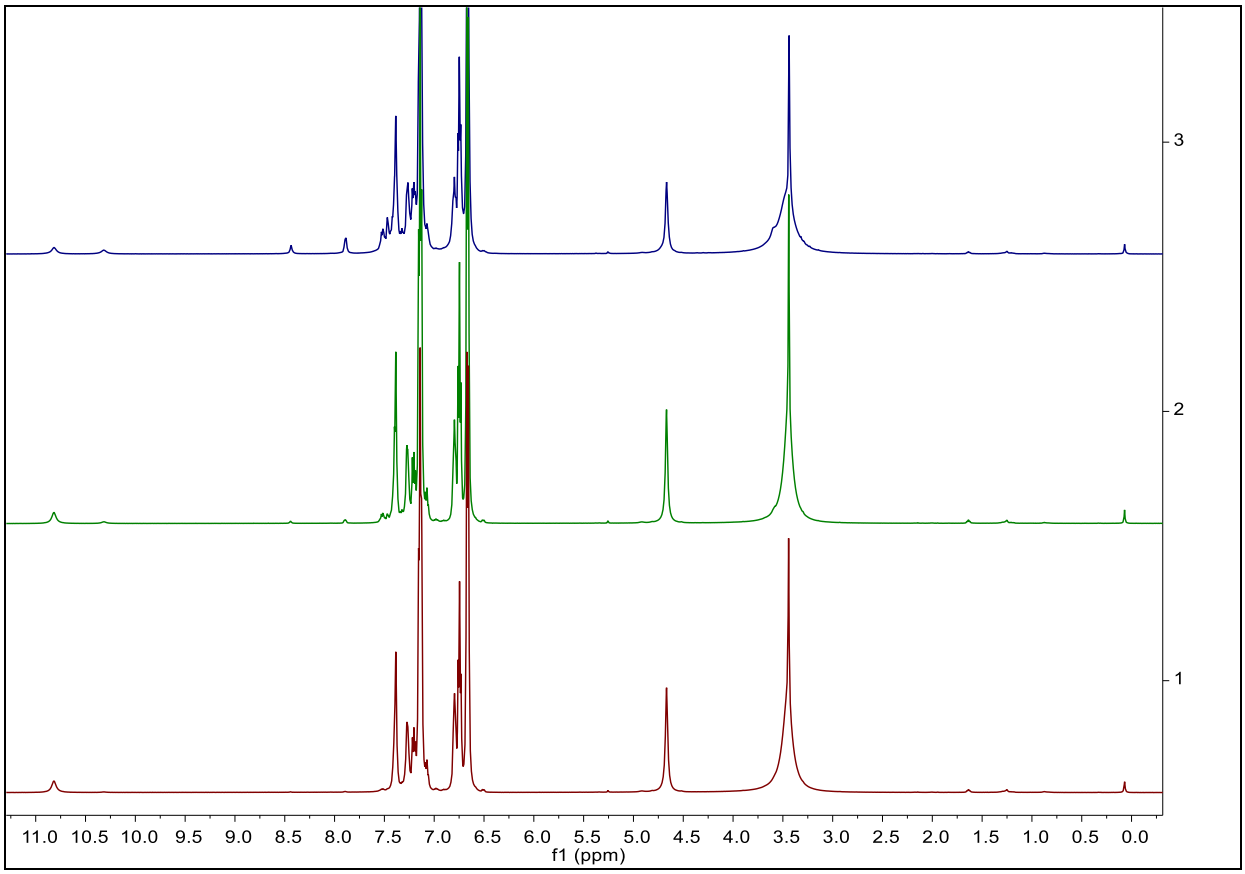

Figure SI 3.18 Superimposed ^{1}H NMR spectra of the reaction of **3.2a** with **3.3b** carried out in molar ratios of the reactants 1:5 within various reaction times (1 day, 2 days and 5 days). The spectra are recorded in deuterated chloroform at 400 MHz.

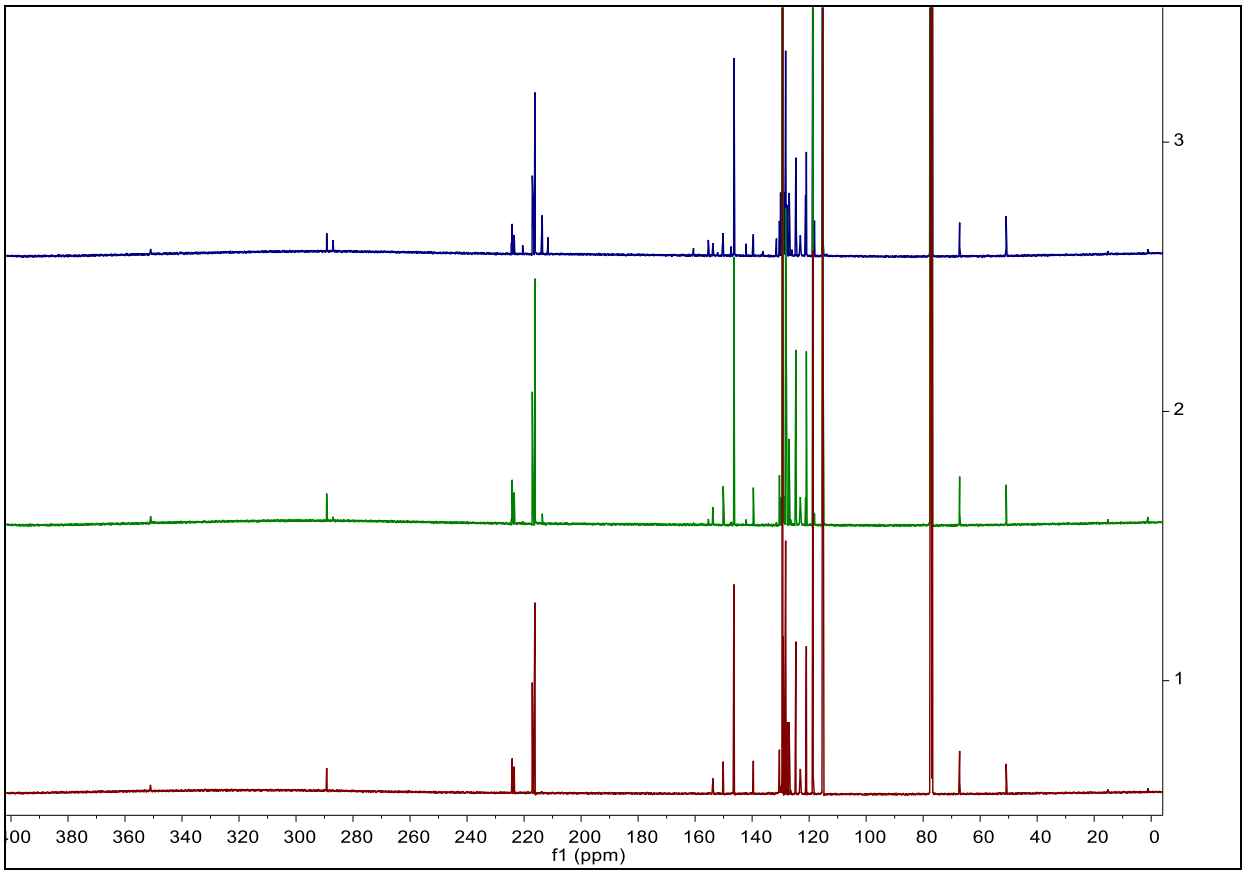

Figure SI 3.19 Superimposed ^{1}H NMR spectra of the reaction of **3.2a** with **3.3b** carried out in molar ratios of the reactants 1:5 within various reaction times (1 day, 2 days and 5 days). The spectra are recorded in deuterated chloroform at 126 MHz.

A.3.4. IC spectra.

Figure SI 3.20 IR solid state (powder) spectrum of the Fischer carbene **3.2a**.

IR (solid phase – powder, ν, cm^{-1}) 2061, 1985, 1959, 1888, 1438, 1428, 1247, 1209, 1140, 1126.

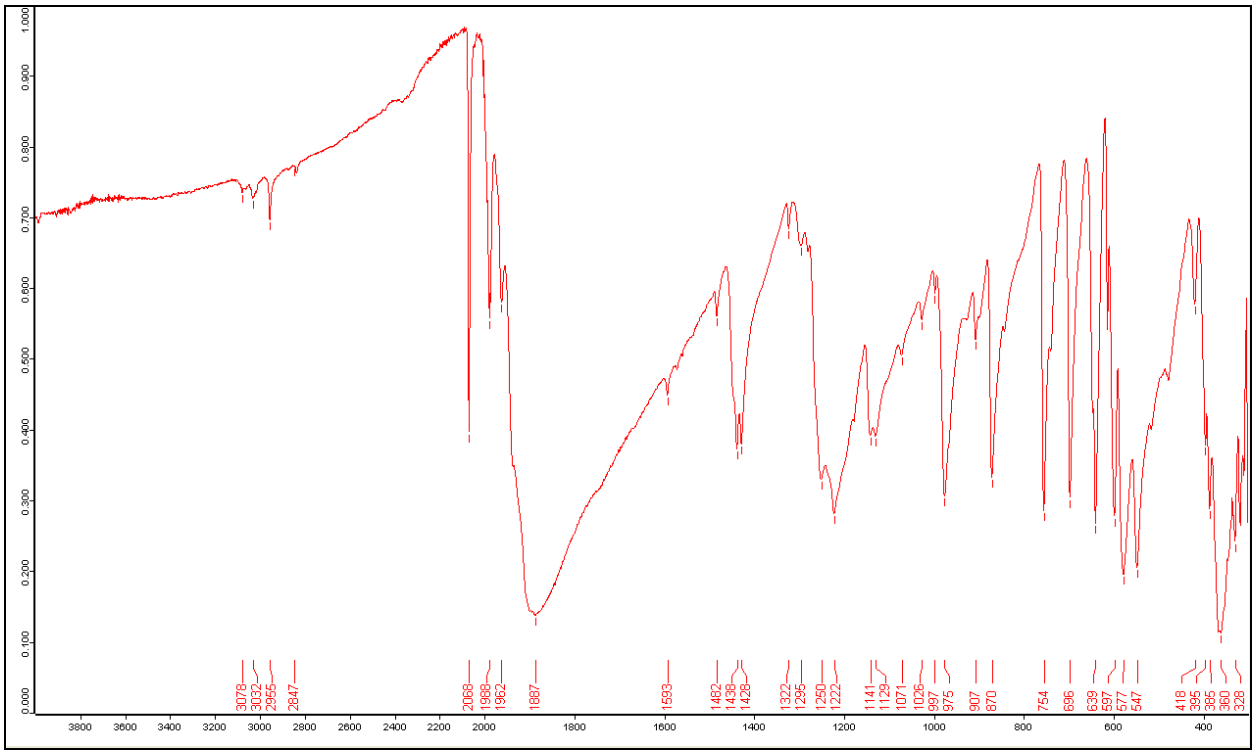

Figure SI 3.21 IR solid state (powder) spectrum of the Fischer carbene **3.2b**.

IR (solid phase – powder, ν, cm^{-1}) 2068, 1988, 1962, 1887, 1438, 1428, 1250, 1222, 1141, 1129.

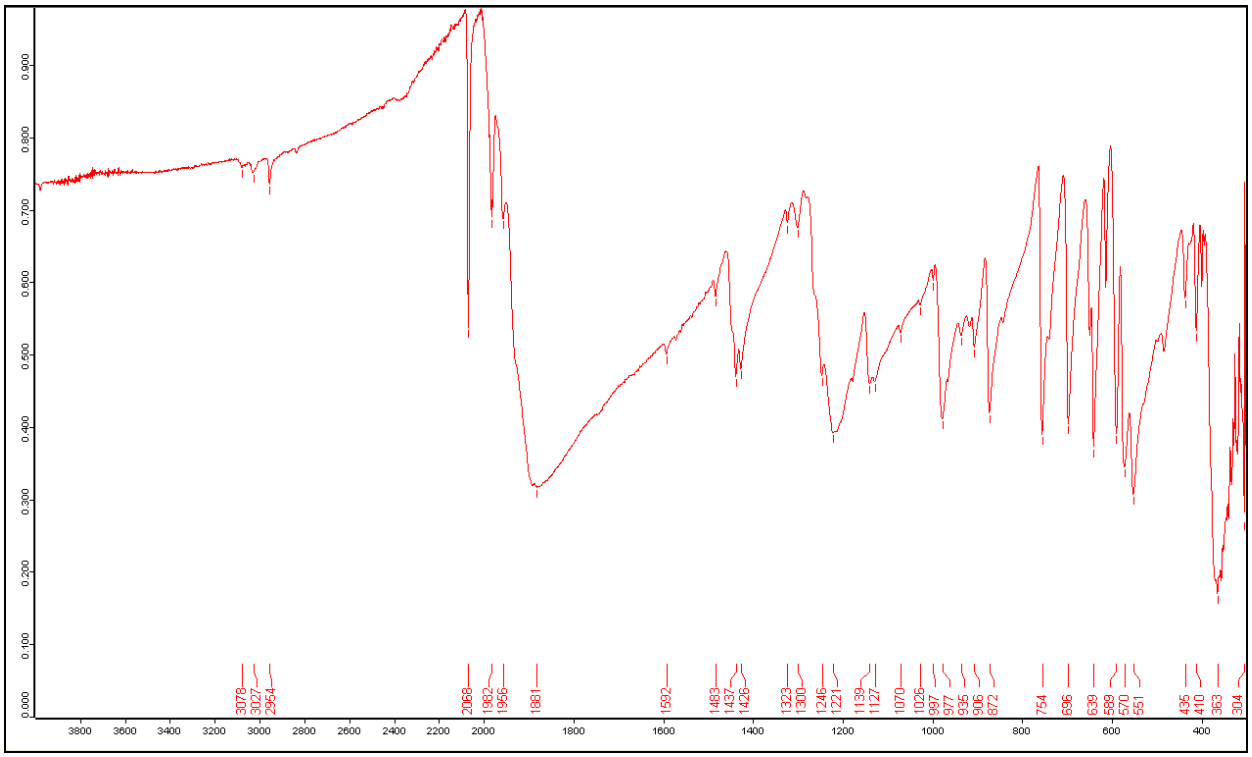

Figure SI 3.22 IR solid state (powder) spectrum of the Fischer carbene **3.2c**.

IR (solid phase – powder, ν, cm^{-1}) 2068, 1982, 1956, 1881, 1437, 1426, 1246, 1221, 1139, 1127.

A.3.5. Cartesian's coordinates of the optimized geometries of the investigated systems within the study of the amination of the Fischer carbenes by various amines.

[**3.2a**] - $(CO)_5Cr=C(OMe)Ph$ - ZORA-GGAPBE-D3(BJ)/TZP_PhCl (COSMO) phase

Cr	3.60834799	-1.30391777	-0.30324097
C	1.87541040	-0.59492924	-0.08027373
O	0.81865178	-0.18928098	0.18966858
C	5.32900626	-2.08029274	-0.28953566
O	6.36526813	-2.59568364	-0.19487318
C	3.90239340	-0.66315762	-2.24294243
O	2.99555836	-0.52152064	-3.19941139
C	3.43773103	-1.95531467	1.44069054
O	3.33272921	-2.36737466	2.52505369
C	4.26599556	0.33581494	0.35437857
O	4.63813348	1.34424851	0.79563910
C	2.90126897	-2.91681935	-0.97931862
O	2.47035534	-3.92334907	-1.36891713
C	1.58386000	-0.77592683	-3.01871746
H	1.17974288	-0.84606391	-4.03262469
H	1.41660178	-1.70843673	-2.47429733
H	1.13276555	0.07131128	-2.49214068
C	5.21866912	-0.36057826	-2.86660672
C	6.30155319	0.13775327	-2.11648018
C	7.51913592	0.43632495	-2.72584032
C	7.69364260	0.21390550	-4.09557559
C	6.63553617	-0.30013824	-4.85495997
C	5.40939550	-0.57227546	-4.25305974
H	6.18993796	0.32015325	-1.05094068
H	8.33541406	0.84101292	-2.12690117
H	8.65121498	0.43584129	-4.56907120
H	6.76730743	-0.48822253	-5.92139538
H	4.59188014	-0.97412984	-4.85049219

[**3.2a** O**H**$^+$] - $(CO)_5Cr=C(^+$**H**$OMe)Ph$ - ZORA-GGAPBE-D3(BJ)/TZP_PhCl (COSMO) phase

Cr	3.62113073	-1.29266930	-0.31267001
C	1.87594308	-0.57123115	-0.11609946
O	0.81948556	-0.15686629	0.11362867
C	5.36318845	-2.05184910	-0.29137442
O	6.41442772	-2.52673604	-0.23586064
C	4.00627859	-0.66941528	-2.11004568
O	2.96720939	-0.59439906	-3.20939428
C	3.42726846	-2.01970657	1.45151865
O	3.31712233	-2.46359763	2.51025653
C	4.29235753	0.31595455	0.45591447
O	4.67423036	1.29703359	0.93021943
C	2.86800121	-2.90036186	-0.99806924
O	2.40346702	-3.87333369	-1.41396237
C	1.49310491	-0.68572906	-3.06955958
H	1.12814978	-0.71611739	-4.09918276
H	1.28008578	-1.62049802	-2.55361240
H	1.13501060	0.19445163	-2.53258411
C	5.23854319	-0.36509767	-2.81854671
C	6.28897837	0.30598920	-2.14618581
C	7.47332616	0.60318544	-2.80833550

C	7.65512691	0.21208015	-4.14104397
C	6.64054727	-0.47837561	-4.81421504
C	5.43920939	-0.75699682	-4.17198815
H	6.15803841	0.62764859	-1.11600301
H	8.26000639	1.14518040	-2.28410318
H	8.59148165	0.43815518	-4.65224711
H	6.79027621	-0.81181045	-5.84098427
H	4.68111746	-1.33829817	-4.69784691
H	3.22499317	0.09557068	-3.86847914

[**3.2a**/**3.3a**] - $(CO)_5CrC(NHCH_2Ph)Ph$ - ZORA-GGAPBE-D3(BJ)/TZP_PhCl (COSMO) phase

Cr	3.74857485	-1.55346134	-0.20723131
C	1.98689806	-1.13281276	0.29985954
O	0.92735434	-0.96055966	0.75311272
C	5.52860785	-2.17188341	-0.36252547
O	6.60007708	-2.62182150	-0.33962686
C	3.88237284	-0.54096354	-2.03404469
H	1.37063449	3.80053366	-0.17467301
C	3.77020062	-2.52750879	1.37770392
O	3.78820504	-3.14163367	2.37001105
C	4.28548876	0.05276673	0.60659079
O	4.58054553	1.06570405	1.09888869
C	3.11857960	-2.98343903	-1.25805642
O	2.71409364	-3.83263392	-1.94205561
C	1.46362708	-0.21888871	-2.61460271
H	1.02724492	-0.52396012	-3.57434955
H	1.28458309	-1.03062532	-1.90251614
H	2.51454686	1.76329971	-1.00017215
C	5.20304812	-0.33509293	-2.68572110
C	6.27189236	0.30057123	-2.03001465
C	7.49429776	0.47652214	-2.67740899
C	7.68513325	-0.01183819	-3.97565604
C	6.63540380	-0.66096703	-4.63199452
C	5.39801888	-0.80715572	-3.99981118
H	6.14446852	0.67361066	-1.01520077
H	8.30626195	0.98968826	-2.16092215
H	8.65018370	0.10833773	-4.47015194
H	6.77678510	-1.05701349	-5.63845959
H	4.58711612	-1.32815178	-4.51304276
N	2.90409990	-0.10866213	-2.80920079
H	3.16838416	0.39056276	-3.66570002
C	0.81474455	1.06643931	-2.14296687
C	-0.50738606	1.34072997	-2.52170679
C	-1.15527091	2.48717274	-2.05285708
C	-0.48367944	3.37553962	-1.20497582
C	0.83823002	3.11092078	-0.83137351
C	1.48343762	1.96154356	-1.29739427
H	-1.03228402	0.65162386	-3.18733503
H	-2.18364711	2.68990138	-2.35581114
H	-0.98649948	4.27342690	-0.84215999

[**3.2a**/**3.3b**] - $(CO)_5CrC(NHPh)Ph$ - ZORA-GGAPBE-D3(BJ)/TZP_PhCl (COSMO) phase

Cr	3.63967290	-1.34716166	-0.15433312
C	2.42241669	0.08426000	-0.30372134
O	1.67165348	0.96081416	-0.44145449
C	4.87049780	-2.76780596	-0.25915574

O	5.62811248	-3.64658039	-0.33995209
C	3.82380667	-1.15956683	-2.20883758
H	2.06424547	-2.01473132	-2.58015600
C	3.46977118	-1.46814165	1.70185862
O	3.35644879	-1.54411110	2.86022163
C	5.04461514	-0.12363005	0.17988325
O	5.88496562	0.61645090	0.48650664
C	2.23052999	-2.57763907	-0.26987082
O	1.35072498	-3.34371338	-0.27846681
H	0.67375695	-1.22309229	-4.38783889
H	2.35280294	-1.85330616	-8.31435344
H	0.38692391	-1.35930869	-6.85557855
H	4.59220733	-2.23609644	-7.28470974
C	4.93580326	-0.40519087	-2.82386519
C	6.27333688	-0.80034598	-2.65787483
C	7.30560505	-0.03746127	-3.20431605
C	7.02043430	1.15212944	-3.88417025
C	5.69168069	1.56585213	-4.02908172
C	4.65349197	0.78560764	-3.51923474
H	6.50651625	-1.71491548	-2.11290569
H	8.33859605	-0.36604960	-3.08392206
H	7.83069950	1.75877398	-4.29134536
H	5.45934233	2.49777915	-4.54635325
H	3.61818982	1.11024392	-3.63895486
N	2.88128113	-1.60418538	-3.03204589
C	2.79533191	-1.63488962	-4.46583507
C	3.90058901	-1.93046550	-5.27185388
C	3.73293059	-2.00155108	-6.65581046
C	2.47492806	-1.79094910	-7.23241587
C	1.37280954	-1.51455206	-6.41671344
C	1.52965697	-1.43897866	-5.03124768
H	4.87641768	-2.11493525	-4.82351216

[**3.2a/3.3c**] - $(CO)_5CrC$(3-en-pirolidone)Ph - ZORA-GGAPBE-D3(BJ)/TZP_PhCl (COSMO) phase

Cr	3.56919059	-1.25075517	-0.23640974
C	1.90001181	-0.40153274	-0.05630420
O	0.88616451	0.13050997	0.16021371
C	5.26077405	-2.09014969	-0.23090786
O	6.28762643	-2.62590034	-0.13314627
C	3.70484726	-0.90399431	-2.30171802
H	6.81463986	2.32960869	-3.57364697
C	3.50739370	-1.55370844	1.59610256
O	3.46090791	-1.74653502	2.74737565
C	4.40665325	0.41349923	0.06867278
O	4.91163991	1.43124490	0.31251027
C	2.77680140	-2.93038502	-0.53539889
O	2.31531228	-3.99134198	-0.66990333
H	7.94720984	-1.81063230	-4.02116888
H	4.60504755	1.62991343	-2.69304028
H	8.50303156	0.61349391	-4.23836041
H	-0.29182981	-1.70949736	-4.48714454
C	5.02570732	-0.48723773	-2.85202623
C	5.97459530	-1.44895986	-3.23296757
C	7.21759582	-1.05258598	-3.73243413
C	7.52841703	0.30606229	-3.85629597
C	6.58293641	1.26736632	-3.48230323
C	5.33694620	0.87528588	-2.98624308
H	5.74055447	-2.51005775	-3.13141830

N	2.76620930	-0.99910533	-3.21618014
C	1.35517147	-1.38385680	-2.96188889
C	2.96635354	-0.75403221	-4.68335179
C	1.63107857	-1.08271854	-5.27108941
C	0.74866582	-1.42901194	-4.32973310
H	0.87666651	-0.63589598	-2.31519701
H	1.31653316	-2.34912526	-2.44155048
H	1.44600877	-1.02808746	-6.34304948
H	3.78008248	-1.39247262	-5.05781278
H	3.26496082	0.29246117	-4.84855237

[**3.2a/3.3b** N**H**$^{+}$] - $(CO)_5CrC(+N\mathbf{H}_2Ph)Ph(OMe)$ - ZORA-GGAPBE-D3(BJ)/TZP_PhCl (COSMO) phase

Cr	3.62246088	-1.30509516	-0.29087807
C	1.87694699	-0.66992003	-0.54411705
O	0.78718276	-0.28586439	-0.70927264
C	5.36136343	-2.01882467	-0.14398571
O	6.40195900	-2.51215107	0.01985743
C	4.00684089	-0.37750989	-2.34555688
O	3.04279886	-0.57409980	-3.36479624
C	3.17877457	-1.93259843	1.38184415
O	2.88342381	-2.31893559	2.44778399
C	4.23022087	0.24174429	0.56240481
O	4.63432422	1.16468183	1.15880099
C	3.16642799	-3.02092941	-0.92847361
O	2.92408986	-4.13362977	-1.17718440
C	2.51408052	-1.88091437	-3.56920343
H	2.00573456	-1.84101218	-4.54027968
H	3.29911189	-2.64877894	-3.60766274
H	1.78215393	-2.14214812	-2.79109679
C	5.41516479	-0.53382699	-2.88617088
C	6.52874750	-0.09301022	-2.14789624
C	7.82259357	-0.21081556	-2.65153441
C	8.03800690	-0.80056762	-3.90385455
C	6.94206475	-1.24642090	-4.64602561
C	5.64198093	-1.09978961	-4.14938473
H	6.39426377	0.33741214	-1.15226318
H	8.66610029	0.14511790	-2.05868606
H	9.05117513	-0.91136342	-4.29344340
H	7.09336764	-1.70097713	-5.62666122
H	4.79533358	-1.41228958	-4.75803021
H	5.70697353	3.82071352	-5.45708640
H	3.47089317	4.39864566	-6.39777550
H	1.40295723	3.47308340	-5.35215519
H	2.96175236	1.30276877	-1.58801688
N	3.81748467	1.19466820	-2.14370117
H	4.59008026	1.50295460	-1.54444203
H	1.57659623	1.96369090	-3.37542030
C	3.73475087	2.06427688	-3.33072413
C	4.90394256	2.57176206	-3.89674600
C	4.80068031	3.41310610	-5.00844357
C	3.54505618	3.73590263	-5.53460665
C	2.38354857	3.21824399	-4.94944169
C	2.47460589	2.37360881	-3.84051298
H	5.87906783	2.32070784	-3.47611872

[**3.2a/3.3b** O**H**$^{+}$] - $(CO)_5CrC(NHPh)Ph(^{+}\mathbf{H}OMe)$ - ZORA-GGAPBE-D3(BJ)/TZP_PhCl (COSMO) phase

Cr	3.70465112	-1.17793533	-0.14645903
C	1.90980134	-0.64964279	-0.30556305
O	0.78836914	-0.34096602	-0.38145980
C	5.48188327	-1.79878252	0.05912415
O	6.54900361	-2.21799840	0.24593147
C	4.23112536	-0.07776292	-1.82560937
O	2.24425803	-1.44077064	-4.09838107
C	3.25670073	-2.11705113	1.40440854
O	2.97087144	-2.69412373	2.37842414
C	4.11941342	0.37766513	0.83175868
O	4.37447898	1.35684131	1.40647134
C	3.31823755	-2.68055768	-1.22366385
O	3.07685067	-3.63253857	-1.84569053
C	2.71929786	-2.27544071	-5.16587861
H	1.98687066	-2.35507305	-5.98472553
H	3.67838067	-1.91408932	-5.57429692
H	2.87924636	-3.27305813	-4.73887047
C	5.46779205	-0.35410849	-2.58716920
C	6.50678809	0.59560113	-2.57063015
C	7.71582425	0.32910949	-3.21433892
C	7.89386079	-0.87126942	-3.91066965
C	6.86185129	-1.81615915	-3.93469350
C	5.66663155	-1.57062330	-3.25859272
H	6.37082862	1.53716057	-2.03518423
H	8.51852543	1.06699192	-3.17736728
H	8.83487943	-1.07304382	-4.42463757
H	6.99206284	-2.75593074	-4.47311006
H	4.87048584	-2.31170021	-3.27212590
H	4.38060814	2.05276486	-6.61657754
H	3.77044552	4.44087065	-6.23489690
H	3.07073750	5.18966824	-3.95711814
H	2.78113318	1.26170139	-1.56126558
N	3.55296323	1.00995447	-2.17876362
H	4.31878143	0.42768213	-4.74140343
H	3.00375373	3.56171535	-2.07929260
C	3.67050688	1.90286442	-3.29546109
C	4.05073608	1.47022011	-4.57264523
C	4.08603616	2.39023817	-5.62247291
C	3.74039878	3.72949537	-5.40880857
C	3.34814218	4.15010616	-4.13378902
C	3.30859531	3.23845445	-3.07718370
H	2.09537149	-0.55201081	-4.47149654

[**3.2a/3.3b** + **MeOH**] - $(CO)_5CrC(NHPh)Ph$ + **HOMe** - ZORA-GGAPBE-D3(BJ)/TZP_PhCl (COSMO) phase

Cr	3.70598326	-1.18083560	-0.14881975
C	1.90697731	-0.68103297	-0.35154980
O	0.78432200	-0.38782454	-0.46014266
C	5.49233578	-1.76563165	0.08154398
O	6.56683469	-2.16026728	0.27889594
C	4.24009534	-0.07824868	-1.82452493
O	2.23059740	-1.42524355	-4.06818973
C	3.24772076	-2.12062085	1.39867304
O	2.95606284	-2.69794719	2.37080365
C	4.07488972	0.38269908	0.83499175
O	4.30042473	1.36647623	1.41424542
C	3.35919237	-2.69673746	-1.22022585
O	3.13764782	-3.65625099	-1.83843464

C	2.68441951	-2.28049033	-5.12861476
H	1.94050555	-2.36633225	-5.93638726
H	3.64100721	-1.93392655	-5.55507635
H	2.84109377	-3.27267535	-4.68787164
C	5.47098727	-0.36041754	-2.59341846
C	6.51763488	0.58083932	-2.57677948
C	7.71994540	0.31004764	-3.23111036
C	7.88386831	-0.88626446	-3.93792263
C	6.84458599	-1.82312278	-3.96127829
C	5.65613994	-1.57337576	-3.27495843
H	6.39268973	1.51924056	-2.03321066
H	8.52844584	1.04157418	-3.19451255
H	8.81954617	-1.09104776	-4.46035171
H	6.96348274	-2.75945269	-4.50821457
H	4.85356470	-2.30714010	-3.28997102
H	4.38216447	2.07297534	-6.60779990
H	3.77852012	4.46066367	-6.21486037
H	3.08831293	5.20232571	-3.93162412
H	2.80268577	1.27223350	-1.54749188
N	3.56903724	1.01642463	-2.17013806
H	4.32491924	0.44078083	-4.73937945
H	3.02416642	3.56694176	-2.06018999
C	3.68461171	1.91165256	-3.28478034
C	4.05911251	1.48298924	-4.56506341
C	4.09195297	2.40711993	-5.61133102
C	3.74995692	3.74629508	-5.39130439
C	3.36306590	4.16292173	-4.11329196
C	3.32561030	3.24715658	-3.06031151
H	2.09065513	-0.53976262	-4.45238847

[**3.2b**] - $(CO)_5Mo=C(OMe)Ph$ - ZORA-GGAPBE-D3(BJ)/TZP_PhCl (COSMO) phase

Mo	3.59483210	-1.30741683	-0.27575727
C	1.70646632	-0.54298759	-0.05082443
O	0.64081825	-0.14556955	0.19256353
C	5.47026972	-2.14446849	-0.29580159
O	6.51337703	-2.64913087	-0.23397634
C	3.91994951	-0.62238182	-2.36139458
O	3.01714728	-0.49728411	-3.32680112
C	3.40960356	-2.01834587	1.62234470
O	3.31148685	-2.42983521	2.70679672
C	4.31956270	0.46349923	0.46598031
O	4.70378353	1.46435751	0.91142839
C	2.81486813	-3.06874039	-0.98898872
O	2.37225213	-4.07437112	-1.36478673
C	1.61068474	-0.74436597	-3.10250753
H	1.16022777	-0.75237563	-4.09885989
H	1.46342659	-1.70556874	-2.60294395
H	1.19304323	0.07199867	-2.50480014
C	5.24213829	-0.33186537	-2.97182179
C	6.30392221	0.17876714	-2.20125225
C	7.53531327	0.47283586	-2.78378630
C	7.74231372	0.23258249	-4.14646435
C	6.70409334	-0.29348326	-4.92554611
C	5.46381724	-0.56044028	-4.35034867
H	6.15638741	0.36905378	-1.14109343
H	8.33647788	0.88780400	-2.17157735
H	8.71019063	0.45163906	-4.59997204
H	6.86247870	-0.49301161	-5.98630572

H	4.65987070	-0.97042999	-4.96111431

[**3.2b**/**3.3a**] - $(CO)_5MoC(NHCH_2Ph)Ph$ - ZORA-GGAPBE-D3(BJ)/TZP_PhCl (COSMO) phase

Mo	3.77046126	-1.60322280	-0.13719909
C	1.91523350	-1.01258317	0.48767815
O	0.88702350	-0.75626896	0.96947944
C	5.65617923	-2.35324930	-0.47128775
O	6.70856096	-2.83631141	-0.55781413
C	3.88496497	-0.47964497	-2.08416364
H	1.16585069	3.84546133	-0.30219479
C	3.80089895	-2.70903605	1.55606991
O	3.82211051	-3.35459671	2.52788744
C	4.51522831	0.03736981	0.83290679
O	4.90000856	0.98537263	1.38582879
C	2.93446302	-3.12866403	-1.22412492
O	2.44236826	-3.96255351	-1.86601182
C	1.45428184	-0.23177442	-2.61113647
H	1.00673192	-0.65257544	-3.52070438
H	1.33948883	-0.96906881	-1.80999120
H	2.34544435	1.75635049	-0.93788813
C	5.19553074	-0.22454100	-2.73771961
C	6.26561953	0.36401795	-2.04129187
C	7.48246635	0.60298790	-2.67867274
C	7.66853610	0.22197813	-4.01308908
C	6.62086970	-0.38590361	-4.71159342
C	5.38973196	-0.59441552	-4.08516927
H	6.13683985	0.65273021	-0.99985275
H	8.29367218	1.08061559	-2.12793481
H	8.62877430	0.39124086	-4.50259253
H	6.76078353	-0.70216091	-5.74610270
H	4.58347002	-1.08675940	-4.63316143
N	2.88474695	-0.07637488	-2.84738630
H	3.11045163	0.43539765	-3.70827764
C	0.77075574	1.07041961	-2.25337606
C	-0.49119772	1.36283765	-2.78908765
C	-1.15985064	2.53680586	-2.42705251
C	-0.56666788	3.43340460	-1.53166983
C	0.69662044	3.14962617	-0.99921252
C	1.36086797	1.97375261	-1.35731933
H	-0.95263953	0.66671920	-3.49329811
H	-2.14171867	2.75337513	-2.85054607
H	-1.08438849	4.35254004	-1.25265760

[**3.2b**/**3.3b**] - $(CO)_5MoC(NHPh)Ph$ - ZORA-GGAPBE-D3(BJ)/TZP_PhCl (COSMO) phase

Mo	3.63372806	-1.35021538	-0.10650897
C	2.18210676	0.09538997	-0.22719877
O	1.35746395	0.90675534	-0.33081793
C	5.08690801	-2.79668532	-0.09881028
O	5.90901620	-3.61796552	-0.09256013
C	3.81987970	-1.15858494	-2.31161456
H	2.00465591	-1.89253090	-2.67396453
C	3.44264051	-1.46656883	1.91435703
O	3.32104781	-1.53334769	3.07217824
C	5.07094763	0.09842219	0.17588309
O	5.86947958	0.90937021	0.40043039
C	2.21460183	-2.80389669	-0.28450695

O	1.40345840	-3.63820538	-0.34545347
H	0.65692197	-0.98114399	-4.47405367
H	2.27138534	-1.69655357	-8.41373632
H	0.35149410	-1.07554929	-6.94216803
H	4.48219253	-2.24539421	-7.39734073
C	4.97533498	-0.46860081	-2.92433527
C	6.28559246	-0.94524721	-2.75322363
C	7.36763731	-0.23988393	-3.28014395
C	7.16197341	0.97498087	-3.94417559
C	5.86200458	1.47043711	-4.09365566
C	4.77340357	0.74737651	-3.60456566
H	6.45510426	-1.88016174	-2.21990376
H	8.37765804	-0.63297433	-3.15699980
H	8.01138905	1.53714631	-4.33523852
H	5.69136764	2.42208846	-4.59911211
H	3.76130108	1.13771639	-3.72632783
N	2.84184857	-1.53142230	-3.13131039
C	2.74318762	-1.54187329	-4.56486888
C	3.82167782	-1.90761208	-5.37878029
C	3.64424150	-1.95536719	-6.76261045
C	2.40199321	-1.65143116	-7.33189490
C	1.32549188	-1.30446651	-6.50879307
C	1.49267087	-1.25177103	-5.12322788
H	4.78346077	-2.16382527	-4.93534966

[**3.2b**/**3.3c**] - $(CO)_5$MoC(3-en-pirolidone)Ph - ZORA-GGAPBE-D3(BJ)/TZP_PhCl (COSMO) phase

Mo	3.56365286	-1.25187909	-0.19805374
C	1.70286373	-0.43144044	0.02297812
O	0.65773369	0.02332925	0.26323284
C	5.43522875	-2.10029155	-0.18374338
O	6.47832667	-2.60029560	-0.07807419
C	3.71346165	-0.87558854	-2.40469026
H	6.94026483	2.24629417	-3.65849105
C	3.51175198	-1.58095367	1.79739928
O	3.47253064	-1.77212103	2.94867391
C	4.39600001	0.60194050	0.10486173
O	4.85905870	1.64956793	0.29612622
C	2.75643289	-3.10039414	-0.54644335
O	2.31499505	-4.16182189	-0.72633429
H	7.94552906	-1.93146447	-4.06081024
H	4.69676833	1.62324690	-2.80272350
H	8.58046713	0.47235528	-4.29068384
H	-0.32390464	-1.58510500	-4.53001895
C	5.04989747	-0.50705891	-2.94813785
C	5.97428214	-1.50132530	-3.30467861
C	7.23609928	-1.14829625	-3.78944733
C	7.59158582	0.19891447	-3.91975520
C	6.67258171	1.19272259	-3.56470331
C	5.40773984	0.84408814	-3.08433058
H	5.70552103	-2.55329699	-3.19274875
N	2.76525386	-0.92524558	-3.31176308
C	1.35003784	-1.26912297	-3.03009940
C	2.94591807	-0.68015383	-4.77978055
C	1.59701131	-0.99513914	-5.34588701
C	0.72282815	-1.31994015	-4.38847289
H	0.90404475	-0.49712106	-2.38729856
H	1.30014053	-2.22203418	-2.48690454
H	1.39580620	-0.94679318	-6.41532092

H	3.74870457	-1.32488305	-5.16695556
H	3.25046334	0.36433411	-4.94883764

[**3.2b**/**3.3b** N**H**$^{+}$] - (CO)$_5$MoC($^{+}$N**H**$_2$Ph)Ph(OMe) - ZORA-GGAPBE-D3(BJ)/TZP_PhCl (COSMO) phase

Mo	3.60715318	-1.33296462	-0.26667948
C	1.71438625	-0.60857938	-0.48659445
O	0.63110916	-0.20389215	-0.64045266
C	5.49397960	-2.13701327	-0.14373817
O	6.53550504	-2.63585327	-0.02011035
C	4.01271034	-0.35010438	-2.43155742
O	3.07653599	-0.56568437	-3.47900351
C	3.18206383	-2.01403530	1.56653210
O	2.92073668	-2.39109511	2.64362447
C	4.29698581	0.34799624	0.64514147
O	4.72195631	1.26051543	1.23967480
C	3.04071352	-3.18955700	-0.93924108
O	2.75822203	-4.28941066	-1.19272717
C	2.50238546	-1.86162667	-3.61060824
H	1.97091039	-1.85181284	-4.57014796
H	3.26498557	-2.65394774	-3.63183387
H	1.78561350	-2.06661666	-2.80165321
C	5.43359533	-0.48312241	-2.94348240
C	6.52641344	-0.02811074	-2.18201880
C	7.83370053	-0.15028311	-2.64793581
C	8.08474481	-0.76171638	-3.88359827
C	7.01055916	-1.22557017	-4.64664592
C	5.69673178	-1.07396924	-4.18847122
H	6.36162063	0.41160738	-1.19486380
H	8.66050640	0.21632334	-2.03804988
H	9.10858821	-0.87660147	-4.24311262
H	7.19081105	-1.69985889	-5.61311703
H	4.86517157	-1.40762447	-4.80753665
H	5.73531256	3.91752931	-5.43965308
H	3.52187277	4.45362330	-6.45671690
H	1.43877626	3.47613699	-5.49119582
H	2.92008783	1.30518752	-1.68365133
N	3.79065827	1.21894055	-2.21875717
H	4.53942874	1.53213327	-1.59253252
H	1.57419549	1.95668094	-3.51977680
C	3.72698708	2.10222523	-3.39657448
C	4.90376569	2.63988434	-3.91779776
C	4.82235722	3.48739031	-5.02662906
C	3.57959764	3.78700903	-5.59522157
C	2.40964253	3.23998144	-5.05495776
C	2.47928948	2.38944239	-3.94874889
H	5.86853982	2.40567266	-3.46485739

[**3.2b**/**3.3b** O**H**$^{+}$] - (CO)$_5$MoC(NHPh)Ph($^{+}$**H**OMe) - ZORA-GGAPBE-D3(BJ)/TZP_PhCl (COSMO) phase

Mo	3.67461667	-1.20651067	-0.18752017
C	1.72396803	-0.99095084	-0.77002712
O	0.61797362	-0.84436655	-1.09813068
C	5.66105347	-1.35752592	0.33289482
O	6.77798413	-1.43972769	0.63776182
C	4.28446104	0.04834551	-1.92161022
O	2.12793741	-1.84259935	-4.41946130
C	3.11895130	-2.32552095	1.41614237

O	2.78630223	-2.95825125	2.33903818
C	3.51601420	0.48996341	0.94355342
O	3.42542570	1.45735736	1.58508948
C	3.85985771	-2.95055635	-1.26269597
O	3.96213830	-3.97321588	-1.80410582
C	1.41007476	-3.00944259	-3.97820514
H	0.43708340	-3.10574845	-4.48508353
H	1.99479957	-3.93014159	-4.13461584
H	1.23389129	-2.88745999	-2.90389637
C	5.43062709	-0.32453968	-2.78446376
C	6.63819552	0.38597336	-2.65644373
C	7.76283173	-0.00083141	-3.38837878
C	7.68997869	-1.08034161	-4.27515799
C	6.48509873	-1.77964901	-4.41412002
C	5.36655410	-1.41808313	-3.66179424
H	6.70036829	1.22932364	-1.96579397
H	8.69726249	0.54939529	-3.26815215
H	8.56730712	-1.37674188	-4.85231686
H	6.41728161	-2.61836301	-5.10903447
H	4.42114424	-1.94872286	-3.78041540
H	4.24885748	2.43266730	-6.59392905
H	4.44160970	4.84471861	-5.99438347
H	4.29699641	5.54428479	-3.60233742
H	3.01926023	1.53478544	-1.49767089
N	3.73332822	1.23139977	-2.15976419
H	3.91912248	0.72249567	-4.81123395
H	3.98840059	3.82994889	-1.82177055
C	3.96509126	2.17927405	-3.21716184
C	4.02616573	1.77664462	-4.55551925
C	4.20370948	2.74183571	-5.54913669
C	4.30736560	4.09651595	-5.21219848
C	4.22532267	4.49022608	-3.87213206
C	4.05051982	3.53235481	-2.87064950
H	2.25004512	-1.93683143	-5.38158851

[**3.2b**/**3.3b** + **MeOH**] - $(CO)_5MoC(NHPh)Ph$ + **HOMe** - ZORA-GGAPBE-D3(BJ)/TZP_PhCl (COSMO) phase

Mo	3.69539682	-1.19823161	-0.09220462
C	1.75263235	-0.59665242	-0.28195167
O	0.63777640	-0.27250769	-0.37540766
C	5.63373064	-1.86597852	0.11076104
O	6.71155009	-2.26976080	0.26294794
C	4.26764592	-0.01475929	-1.88639127
O	2.25156839	-1.44639629	-4.16942837
C	3.18972340	-2.24173895	1.57796478
O	2.88961688	-2.82831093	2.54139232
C	4.13190415	0.47244163	1.01569397
O	4.37673611	1.43740444	1.61663257
C	3.26549804	-2.83211640	-1.26408584
O	3.02025147	-3.77301016	-1.89971155
C	2.78476993	-2.25177777	-5.23120814
H	2.10154966	-2.30322324	-6.09382340
H	3.76791439	-1.88509654	-5.57189381
H	2.91579720	-3.26219656	-4.82470695
C	5.49266180	-0.30913398	-2.65911422
C	6.53123412	0.64135286	-2.70048863
C	7.73016428	0.34889700	-3.35135263
C	7.89906952	-0.88007448	-3.99903501

C	6.86875173	-1.82680341	-3.96514719
C	5.68520630	-1.55398256	-3.27948105
H	6.40351417	1.60405133	-2.20203849
H	8.53282097	1.08771990	-3.35754015
H	8.83240790	-1.10272835	-4.51837411
H	6.99267869	-2.78945852	-4.46310608
H	4.89067494	-2.29619452	-3.24260689
H	4.35070972	2.07136799	-6.69176948
H	3.75601558	4.46674966	-6.32897839
H	3.09568222	5.24506244	-4.04945924
H	2.83235452	1.33361029	-1.60296981
N	3.59412210	1.08030351	-2.23129857
H	4.31702494	0.47062650	-4.79592651
H	3.05316948	3.64046529	-2.15105121
C	3.69562348	1.96444347	-3.35690410
C	4.05325074	1.51572495	-4.63530844
C	4.07416938	2.42216956	-5.69706495
C	3.73664702	3.76533741	-5.49407308
C	3.36653884	4.20236911	-4.21790525
C	3.34073200	3.30359021	-3.14962372
H	2.14087868	-0.54244531	-4.51854598

[**3.2c**] - $(CO)_5W=C(OMe)Ph$ - ZORA-GGAPBE-D3(BJ)/TZP_PhCl (COSMO) phase

W	3.59560107	-1.29686240	-0.28473738
C	1.71224287	-0.54295597	-0.05457998
O	0.64119203	-0.15254882	0.18168429
C	5.46691122	-2.12381346	-0.31646984
O	6.51497386	-2.62100129	-0.26339777
C	3.91794472	-0.60737990	-2.35686134
O	3.01822467	-0.47565592	-3.32543215
C	3.42418756	-2.02312632	1.60098264
O	3.33503289	-2.44723551	2.68269548
C	4.32353473	0.45670259	0.47353117
O	4.71922220	1.44864788	0.93122233
C	2.80730877	-3.04777046	-0.99280879
O	2.35301462	-4.05061167	-1.36443596
C	1.60984616	-0.71945920	-3.10966826
H	1.16160372	-0.69321029	-4.10666370
H	1.45413377	-1.69632071	-2.64258958
H	1.19544773	0.08046422	-2.48787683
C	5.24245733	-0.32401774	-2.96338420
C	6.29737406	0.21496082	-2.20216400
C	7.53109958	0.49478908	-2.78636456
C	7.74730294	0.21353968	-4.13968949
C	6.71527679	-0.33859359	-4.90843986
C	5.47230494	-0.59222320	-4.33281170
H	6.14406577	0.44105863	-1.14942864
H	8.32698895	0.93145415	-2.18239120
H	8.71778653	0.42031813	-4.59323703
H	6.88069044	-0.57058026	-5.96138146
H	4.67312937	-1.02333584	-4.93505545

[**3.2c**/**3.3a**] - $(CO)_5WC(NHCH_2Ph)Ph$ - ZORA-GGAPBE-D3(BJ)/TZP_PhCl (COSMO) phase

W	3.73987493	-1.56206143	-0.18864712
C	1.83748535	-1.04727017	0.33318998
O	0.76877459	-0.84014464	0.74842085

C	5.65380283	-2.25193677	-0.41608584
O	6.72531281	-2.70229093	-0.44191825
C	3.89615956	-0.48434126	-2.13938866
H	1.37174496	3.78323192	-0.21253749
C	3.74726048	-2.61153623	1.53404468
O	3.75747576	-3.22450745	2.52855211
C	4.38589600	0.12868311	0.75070836
O	4.72809017	1.10871841	1.27729776
C	3.00826122	-3.14746289	-1.25164182
O	2.57292517	-4.02514199	-1.87777813
C	1.48316359	-0.19596695	-2.71604628
H	1.03487611	-0.49858490	-3.67087671
H	1.33038308	-1.01696169	-2.00658524
H	2.53481290	1.78057877	-1.09692941
C	5.22394656	-0.26478354	-2.77125447
C	6.28330009	0.34595065	-2.07746717
C	7.52008763	0.53126848	-2.69371671
C	7.73383041	0.07762872	-4.00100046
C	6.69329041	-0.54488167	-4.69686332
C	5.44266582	-0.70142531	-4.09383911
H	6.13272232	0.69106851	-1.05546443
H	8.32535400	1.02324358	-2.14701984
H	8.71013181	0.20320013	-4.47136077
H	6.85366509	-0.91475329	-5.71034134
H	4.64072598	-1.20703982	-4.63562238
N	2.91888007	-0.06730834	-2.92613049
H	3.17625986	0.43149082	-3.78445512
C	0.82394808	1.07309770	-2.21568566
C	-0.51161231	1.32740230	-2.55952799
C	-1.17044409	2.45300768	-2.05666120
C	-0.49655865	3.34038114	-1.20949974
C	0.83839228	3.09550903	-0.87040687
C	1.49480704	1.96701183	-1.37062537
H	-1.03862834	0.63832660	-3.22351268
H	-2.20963028	2.63982212	-2.33154962
H	-1.00860669	4.22121615	-0.81891455

[**3.2c**/**3.3b**] - $(CO)_5WC(NHPh)Ph$ - ZORA-GGAPBE-D3(BJ)/TZP_PhCl (COSMO) phase

W	3.63591892	-1.34907391	-0.12272842
C	2.20320621	0.10784484	-0.20964643
O	1.38464355	0.92991702	-0.28116553
C	5.06775148	-2.80627947	-0.11517662
O	5.88434691	-3.63437279	-0.10452322
C	3.82328705	-1.14852142	-2.31633092
H	2.00926790	-1.88392942	-2.67679872
C	3.44767779	-1.47646775	1.89015307
O	3.32776307	-1.54979019	3.04912569
C	5.08136029	0.07515265	0.17126938
O	5.88766929	0.87701694	0.40582760
C	2.19839061	-2.77494577	-0.30449325
O	1.36957744	-3.59325552	-0.36742457
H	0.65516563	-1.01206262	-4.48145728
H	2.27506163	-1.75077369	-8.41418935
H	0.34894917	-1.13726101	-6.94755804
H	4.49320087	-2.26138368	-7.39398453
C	4.97651096	-0.45436452	-2.92920109
C	6.29067837	-0.91125072	-2.73716955
C	7.36938668	-0.19769771	-3.25953247

C	7.15488452	1.00430157	-3.94347417
C	5.85002054	1.47838056	-4.11805973
C	4.76606581	0.74760146	-3.63086228
H	6.46643744	-1.83785118	-2.19117512
H	8.38311950	-0.57424410	-3.11775235
H	8.00117786	1.57326533	-4.33124548
H	5.67261150	2.41972872	-4.63987587
H	3.75038167	1.12172117	-3.77132258
N	2.84532526	-1.52406173	-3.13661529
C	2.74819341	-1.54858060	-4.56795704
C	3.83030360	-1.91044066	-5.37892128
C	3.65233960	-1.97468752	-6.76176364
C	2.40597626	-1.69223643	-7.33310613
C	1.32597113	-1.34960405	-6.51289854
C	1.49355984	-1.27974148	-5.12838178
H	4.79552907	-2.15116392	-4.93419702

[**3.2c/3.3c**] - $(CO)_5$WC(3-en-pirolidone)Ph - ZORA-GGAPBE-D3(BJ)/TZP_PhCl (COSMO) phase

W	3.56465135	-1.26062918	-0.21483994
C	1.78914710	-0.26893593	-0.05549781
O	0.78514405	0.29969858	0.10778401
C	5.35322531	-2.25550332	-0.26658086
O	6.35979781	-2.83557643	-0.23360233
C	3.72148640	-0.90241061	-2.40725084
H	6.77227320	2.45213925	-3.50517279
C	3.51221431	-1.55818564	1.78023471
O	3.47613598	-1.73216944	2.93565754
C	4.55527192	0.49582779	0.13494099
O	5.11200856	1.48169984	0.39820019
C	2.59276181	-3.04135191	-0.43284907
O	2.05081487	-4.07207388	-0.47769230
H	7.98794149	-1.64003272	-4.14108366
H	4.57230867	1.66796338	-2.66874685
H	8.49688240	0.80274820	-4.24043501
H	-0.25211087	-1.80864299	-4.58420602
C	5.03254165	-0.42900585	-2.93608028
C	6.00150957	-1.35369164	-3.35630321
C	7.24093912	-0.91050762	-3.82481252
C	7.52584765	0.45840149	-3.88146690
C	6.55974940	1.38268559	-3.46844399
C	5.31930377	0.94359251	-2.99874659
H	5.78710226	-2.42287975	-3.30526034
N	2.80090601	-1.05432257	-3.33300041
C	1.41547524	-1.51474265	-3.07446198
C	2.98636489	-0.78931815	-4.79535187
C	1.64569972	-1.11611135	-5.37367540
C	0.78488738	-1.51342742	-4.43194977
H	0.92214120	-0.83033430	-2.37041797
H	1.43602030	-2.51058221	-2.61057437
H	1.44200602	-1.02707245	-6.43985328
H	3.79656150	-1.42164049	-5.18889454
H	3.28291359	0.25966541	-4.94783614

[**3.2c/3.3b** + N**H**$^+$] - $(CO)_5$WC($^+$N**H**$_2$Ph)Ph(OMe) - ZORA-GGAPBE-D3(BJ)/TZP_PhCl (COSMO) phase

W	3.61526630	-1.32572508	-0.29266883
C	1.74266753	-0.55768898	-0.45293683

O	0.66196486	-0.12552452	-0.55786042
C	5.48052460	-2.17115959	-0.21569298
O	6.51526383	-2.69162846	-0.12133502
C	4.03701308	-0.34281278	-2.43426919
O	3.15635919	-0.56331306	-3.52376996
C	3.21215816	-2.01239935	1.53776232
O	2.96375185	-2.39541445	2.61722284
C	4.34791462	0.32866871	0.62062742
O	4.78928202	1.23757329	1.21099792
C	2.97698905	-3.15022707	-0.96325624
O	2.63672388	-4.23147804	-1.23120167
C	2.45267652	-1.79819525	-3.61621915
H	1.92672763	-1.76014932	-4.57795229
H	3.13375660	-2.66171639	-3.61514070
H	1.71693561	-1.90943811	-2.80630255
C	5.47616008	-0.46844645	-2.89577875
C	6.54208300	0.06255248	-2.14537754
C	7.86378354	-0.08651026	-2.56133564
C	8.15634766	-0.79628246	-3.73310728
C	7.10861765	-1.33500614	-4.48393517
C	5.78102609	-1.16123155	-4.07654957
H	6.35304247	0.58187167	-1.20201718
H	8.66856384	0.33917595	-1.96058705
H	9.19106202	-0.92919139	-4.05279280
H	7.32105146	-1.88830194	-5.40046803
H	4.97087756	-1.56164971	-4.68412480
H	5.61934617	3.94069384	-5.50562463
H	3.37407593	4.42331799	-6.47834602
H	1.33249278	3.41193282	-5.46043912
H	2.93282173	1.30773149	-1.67367383
N	3.79585397	1.23474458	-2.22283855
H	4.54938649	1.56740300	-1.61194424
H	1.54174917	1.91473405	-3.47857940
C	3.69334346	2.10477053	-3.40368819
C	4.84777664	2.66006578	-3.95519462
C	4.72472918	3.49568470	-5.06936687
C	3.46398610	3.76518092	-5.61324381
C	2.31716926	3.19974519	-5.04330239
C	2.42851069	2.36069530	-3.93209197
H	5.82674755	2.45036014	-3.52089938

[**3.2c**/**3.3b** O**H**$^{+}$] - $(CO)_5$WC(NHPh)Ph(**$^{+}$H**OMe) - ZORA-GGAPBE-D3(BJ)/TZP_PhCl (COSMO) phase

W	3.59300463	-1.06704283	-0.27954033
C	1.92457874	-1.63236831	-1.32207337
O	0.95912160	-1.96065479	-1.88109691
C	5.23432755	-0.46232706	0.77930627
O	6.16203093	-0.09766946	1.37832806
C	4.27113010	0.24441611	-1.92831444
O	2.80841818	-4.38334670	-3.97518577
C	3.05064193	-2.29870050	1.23687025
O	2.74432459	-3.00455607	2.11511635
C	2.52214441	0.45464151	0.55207240
O	1.91336168	1.31849543	1.04259406
C	4.68441495	-2.59493557	-1.10017568
O	5.30815727	-3.47361221	-1.53606363
C	2.71760563	-5.20188400	-2.79617372
H	3.68462441	-5.66455673	-2.54348229
H	2.35622738	-4.62829581	-1.92683824

H	1.99334996	-5.99495219	-3.01592719
C	4.68412573	-0.33287204	-3.22758632
C	6.04291213	-0.31021852	-3.58988793
C	6.47353432	-0.95270404	-4.75160830
C	5.55300633	-1.59572561	-5.58527380
C	4.19638352	-1.60521609	-5.23982549
C	3.76634584	-0.99727240	-4.05838093
H	6.76711999	0.18981154	-2.94427025
H	7.53388970	-0.94495193	-5.00744555
H	5.88958527	-2.08996973	-6.49751731
H	3.46855993	-2.09360639	-5.88925610
H	2.70913386	-1.01329440	-3.79429238
H	4.62166969	3.71927520	-5.84360219
H	6.07561723	5.51653255	-4.90913040
H	6.75585381	5.43576154	-2.50705666
H	4.29572349	1.89605047	-0.81717602
N	4.47437949	1.54726764	-1.75888821
H	3.85825753	1.84935829	-4.40437601
H	6.00428993	3.55240283	-1.06591308
C	4.91148861	2.57749732	-2.65746627
C	4.50860577	2.62272863	-3.99726632
C	4.93670538	3.68139351	-4.80044560
C	5.74958727	4.69197957	-4.27415418
C	6.13090019	4.64837289	-2.92904886
C	5.70983431	3.59359454	-2.11697427
H	3.45888068	-3.67564887	-3.80155322

[**3.2c**/**3.3b** + **MeOH**] - $(CO)_5WC(NHPh)Ph$ + **HOMe** - ZORA-GGAPBE-D3(BJ)/TZP_PhCl (COSMO) phase

W	3.69404136	-1.18962243	-0.11050966
C	1.75570051	-0.58705384	-0.26125260
O	0.63832738	-0.25742981	-0.31615610
C	5.62526142	-1.85183153	0.08333693
O	6.70464934	-2.25431391	0.23587259
C	4.25523911	-0.00942062	-1.89603781
O	2.27374308	-1.46695921	-4.16756765
C	3.20372335	-2.24118914	1.54993917
O	2.91240413	-2.83706098	2.51200631
C	4.12760192	0.45893781	1.01769680
O	4.36950584	1.40828373	1.64554395
C	3.26752004	-2.81790561	-1.27661398
O	3.02979647	-3.76301267	-1.91043179
C	2.78686810	-2.31527428	-5.20670696
H	2.07726504	-2.41882665	-6.04281024
H	3.75212020	-1.95007277	-5.59623414
H	2.94706737	-3.30292834	-4.75719602
C	5.48459546	-0.30065635	-2.66446404
C	6.52415295	0.64809432	-2.69293472
C	7.72588000	0.35767512	-3.33958508
C	7.89559535	-0.86702943	-3.99492617
C	6.86265846	-1.81113338	-3.97529303
C	5.67577737	-1.54007621	-3.29490886
H	6.39498584	1.60790054	-2.18937700
H	8.52985194	1.09495758	-3.33674377
H	8.83122641	-1.08804656	-4.51069804
H	6.98618187	-2.76926306	-4.48187268
H	4.87683852	-2.27815741	-3.27255452
H	4.37452890	2.07176761	-6.70139756

H	3.80226621	4.47199245	-6.33818898
H	3.13069654	5.25293763	-4.06324806
H	2.81682941	1.33881573	-1.62299748
N	3.58096966	1.08353517	-2.24791813
H	4.30688486	0.46679592	-4.80890600
H	3.05865979	3.64573913	-2.16773489
C	3.69353774	1.96572120	-3.37219314
C	4.05537389	1.51492908	-4.64856290
C	4.09435058	2.42326637	-5.70795240
C	3.76913111	3.76943980	-5.50473562
C	3.39240584	4.20788730	-4.23114862
C	3.34993416	3.30774130	-3.16481643
H	2.12848543	-0.58567468	-4.55897089

MeOH - ZORA-GGAPBE-D3(BJ)/TZP_PhCl (COSMO) phase

O	0.17046538	-1.15784252	0.00773108
H	1.14310993	-1.09632705	0.00773108
C	-0.16344508	-2.55830173	0.00773108
H	0.22096816	-3.06845379	0.90557114
H	0.22096816	-3.06845379	-0.89010899
H	-1.25816939	-2.62355669	0.00773108

MeO^- - ZORA-GGAPBE-D3(BJ)/TZP_PhCl (COSMO) phase

O	0.16873568	-1.18276374	0.00773108
H	-1.27124745	-2.72757083	0.00773108
C	-0.16034692	-2.51134645	0.00773108
H	0.22278833	-3.09823202	0.89643378
H	0.22278833	-3.09823202	-0.88097163

NH_2CH_2Ph - ZORA-GGAPBE-D3(BJ)/TZP_PhCl (COSMO) phase

N	-0.00606477	2.48572298	1.00865731
H	-0.58824099	2.49277116	1.85140104
H	-0.64322093	2.27054504	0.23676682
H	1.59062069	1.42705320	0.19099203
C	1.00222596	1.42862736	1.12162577
H	1.70792765	1.71455076	1.91642077
H	2.53800572	-0.75646719	1.59213072
C	0.52341022	0.00601061	1.39199646
C	-0.83538072	-0.33384350	1.42629051
C	-1.23889198	-1.65353010	1.67289034
C	-0.28564345	-2.65259105	1.88760755
C	1.07632470	-2.32289043	1.85609199
C	1.47356679	-1.00698332	1.61007637
H	-1.59307743	0.43618185	1.26389074
H	-2.30236395	-1.89749942	1.69565517
H	-0.59843497	-3.67963545	2.08247110
H	1.82954231	-3.09361288	2.02919068

NH_2Ph - ZORA-GGAPBE-D3(BJ)/TZP_PhCl (COSMO) phase

H	-2.29518553	-1.74895263	1.80492431
H	-0.65733766	-3.63418339	1.94401402
H	1.78991981	-3.13677765	1.78687663
H	1.98195432	1.54072420	1.58706824

N	1.03755512	1.36048273	1.25290444
H	0.39581826	2.07829903	1.58279942
H	2.58141317	-0.80783768	1.49090617
C	0.59291707	0.05108260	1.48076982
C	-0.78404222	-0.23601154	1.57014527
C	-1.22416833	-1.55124545	1.73379002
C	-0.30929189	-2.60909845	1.81187194
C	1.06014678	-2.32765203	1.72332622
C	1.51064231	-1.01603461	1.55945162
H	-1.50725653	0.58116116	1.50988537

NH_2^+Ph - ZORA-GGAPBE-D3(BJ)/TZP_PhCl (COSMO) phase

H	-2.29532251	-1.74925778	1.80535313
H	-0.65636821	-3.63427730	1.94677669
H	1.79030277	-3.13625124	1.78752034
H	2.00412707	1.52226580	1.51836423
N	1.03399528	1.36189454	1.25528851
H	0.42918239	2.08003602	1.64827970
H	2.58152301	-0.80612311	1.49825004
C	0.59266860	0.05113405	1.47917790
C	-0.78478540	-0.23694389	1.56555545
C	-1.22424802	-1.55148463	1.73423596
C	-0.30883472	-2.60926898	1.81296477
C	1.06024256	-2.32739601	1.72348088
C	1.51057690	-1.01530565	1.56131862
H	-1.50770588	0.58006352	1.50001645

NH_3^+Ph - ZORA-GGAPBE-D3(BJ)/TZP_PhCl (COSMO) phase

H	-2.29761435	-1.74801171	1.79931284
H	-0.64953596	-3.61280401	1.94395843
H	1.79298564	-3.13674182	1.79143857
H	1.99898753	1.52617863	1.64550555
N	1.04736521	1.39462323	1.27958557
H	0.44104470	2.07216452	1.75987807
H	2.58929080	-0.79144146	1.49049128
C	0.57727085	0.00466811	1.47869720
C	-0.79188565	-0.22744498	1.55969907
C	-1.22938819	-1.54425964	1.72907466
C	-0.30176332	-2.58824580	1.80999629
C	1.06909365	-2.32495316	1.72383970
C	1.52236989	-1.01275621	1.55664246
H	-1.50426397	0.59713608	1.49768769
H	1.06508204	1.64887469	0.28113306

NH^-Ph - ZORA-GGAPBE-D3(BJ)/TZP_PhCl (COSMO) phase

H	-2.30246813	-1.76358232	1.81639221
H	-0.65493075	-3.65997445	1.96664334
H	1.79517350	-3.12880274	1.77994005
H	-1.53835400	0.55692429	1.50347255
N	1.07558386	1.36212999	1.29727647
H	0.26416828	1.99659620	1.26578730
H	2.57527659	-0.81385361	1.46722520
C	0.60033057	0.10780612	1.45891096
C	-0.79946196	-0.25000938	1.56445629

C	-1.22907766	-1.56371316	1.74125166
C	-0.31491592	-2.63271537	1.82651291
C	1.05649392	-2.32347982	1.72035767
C	1.50261021	-1.01664249	1.54295740

3-en-pirolidone - ZORA-GGAPBE-D3(BJ)/TZP_PhCl (COSMO) phase

N	0.41803382	-1.99864229	0.00000000
C	-0.13272552	-1.29503879	1.19209365
C	-0.13272552	-1.29503879	-1.19209365
C	-0.63735797	0.03097193	-0.66957335
C	-0.63735797	0.03097193	0.66957335
H	0.63600396	-1.19926389	1.97275920
H	-0.96638953	-1.87231087	1.63411336
H	1.42460963	-1.82147088	0.00000000
H	-0.96638953	-1.87231087	-1.63411336
H	0.63600396	-1.19926389	-1.97275920
H	-1.00077614	0.83349652	-1.31368860
H	-1.00077614	0.83349652	1.31368860

A.4. Supplementary information to Chapter 7.

A.4.1. ITC data.

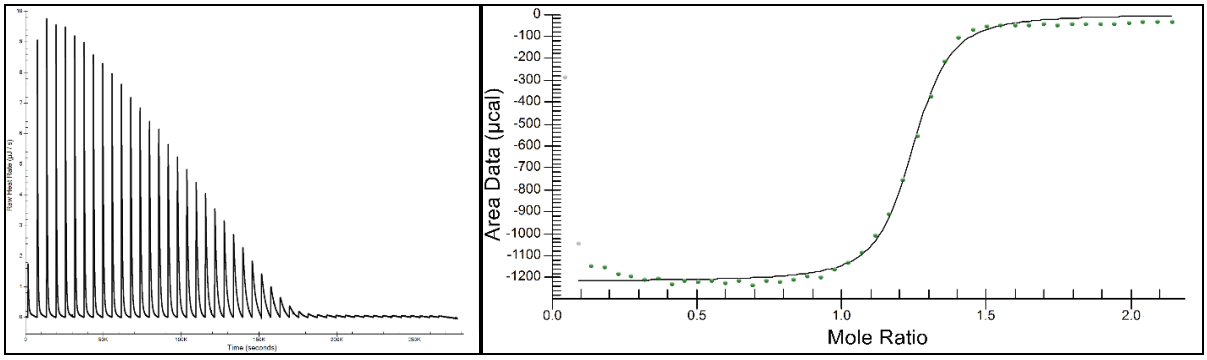

Figure SI 4.1. ITC thermogram of the reaction between **4.3b** (sample call, c=1.09 mM) and **4.4a** (syringe, c=23.93 mM) in chlorobenzene. The titration was performed at 25ºC through 45 sequential additions (of 2.06 µL each). Time between two consecutive injections was 10000 s. Heat released is expressed in µJ/s versus time in s. *right side* – ITC integrated and fitted, by independent model, heat peaks of the thermogram shown on the left side. Integrated heats are expressed in µcal versus molar ratio of the reactants.

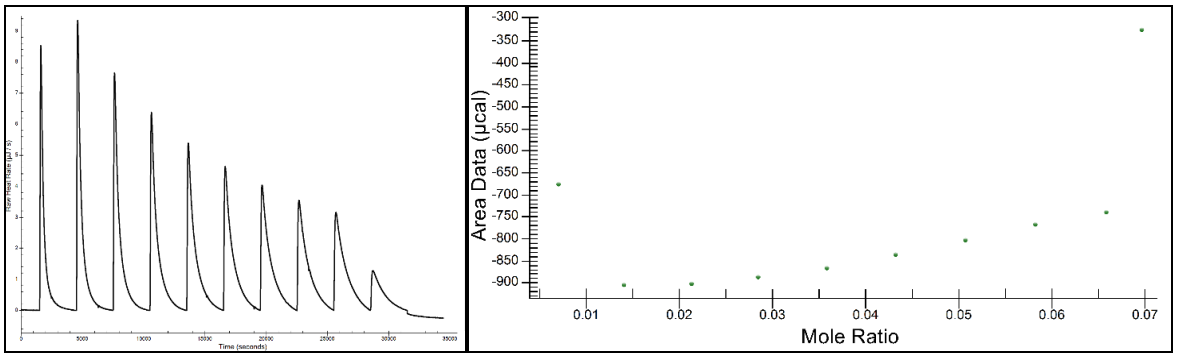

Figure 4.2. *left side* – ITC thermogram of the reaction between **4.4b** (sample call, c=3.37 mM) and **4.3a** (syringe, c=2.33 mM) in chlorobenzene. The titration was performed at 25ºC through 10 sequential additions (of 10.06 µL first nine titrations and of 5.03 µL the last one). Time between two consecutive injections was 3000 s. Heat released is expressed in µJ/s versus time in s. *right side* – ITC integrated heat peaks of the thermogram shown on the left side. Integrated heats are expressed in µcal versus molar ratio of the reactants.

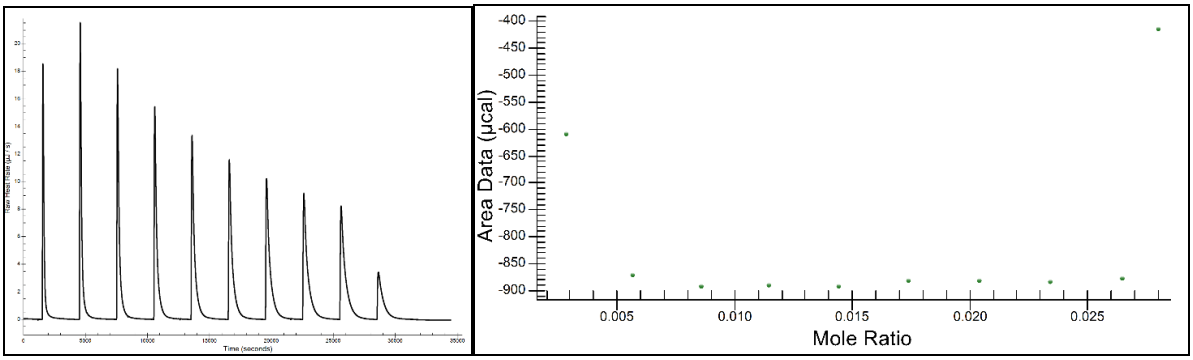

Figure 4.3. *left side* – ITC thermogram of the reaction between **4.4b** (sample call, c=8.45 mM) and **4.3a** (syringe, c=2.35 mM) in chlorobenzene. The titration was performed at 25ºC through 10 sequential additions (of 10.06 µL first nine titrations and of 5.03 µL the last one). Time between two consecutive injections was 3000 s. Heat released is expressed in µJ/s versus time in s. *right side* – ITC integrated heat peaks of the thermogram shown on the left side. Integrated heats are expressed in µcal versus molar ratio of the reactants.

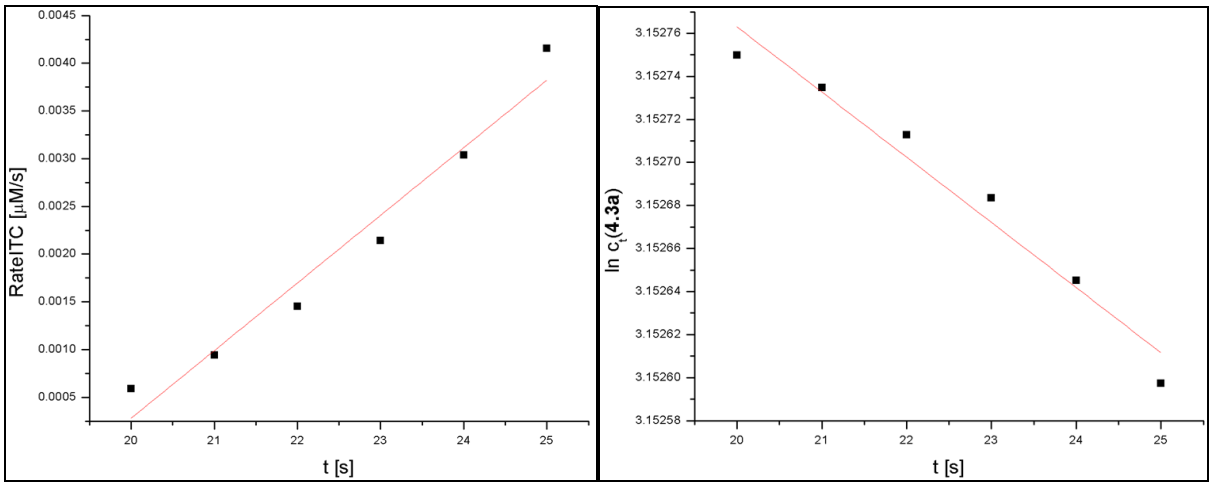

Figure SI 4.4 *left side* - Linear fit of the plot of the ITC Rate as a function of time for the reaction of **4.4b** (sample call, c=8.45 mM) with **4.3a** (syringe, c=2.35 mM) carried out in ITC calorimeter. ITC Rate is expressed in µM/s and time in s. Obtained $\boldsymbol{k = 7.1*10^{-4} \pm 7*10^{-5}}$, as the result of the fitting. *right side* - Linear fit of the plot of logarithm of **2.2b** concentration as a function of time for the same reaction. Obtained $\boldsymbol{k_{obs} = -4.2*10^{-5} \pm 4*10^{-6}}$, as the result of the fitting.

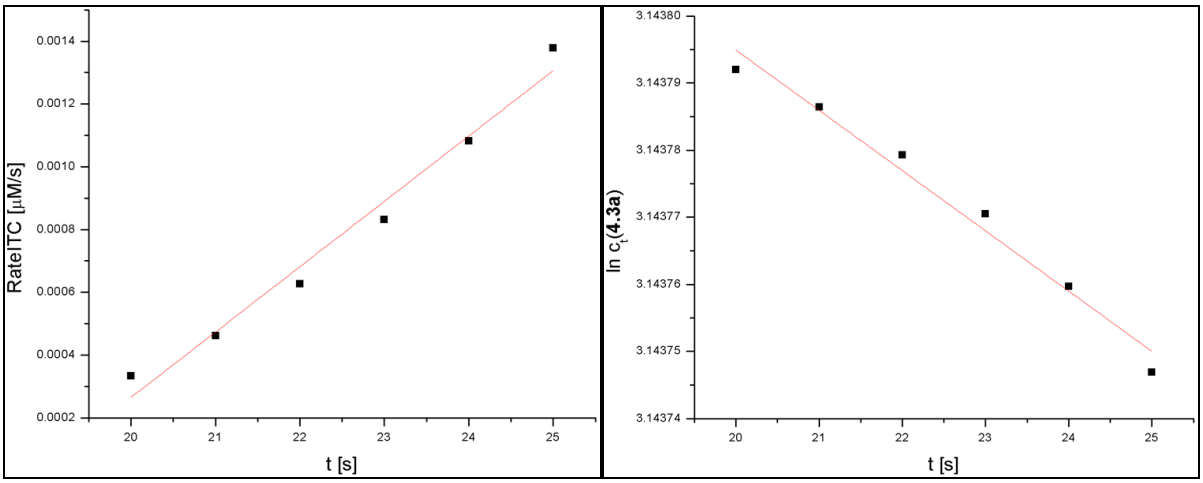

Figure SI 4.5 *left side* - Linear fit of the plot of the ITC Rate as a function of time for the reaction of **4.4b** (sample call, c=2.33 mM) with **4.3a** (syringe, c=3.37 mM) carried out in ITC calorimeter. ITC Rate is expressed in µM/s and time in s. Obtained $\boldsymbol{k = 2.1*10^{-4} \pm 2*10^{-5}}$, as the result of the fitting. *right side* - Linear fit of the plot of logarithm of **2.2b** concentration as a function of time for the same reaction. Obtained $\boldsymbol{k_{obs} = -9.0*10^{-6} \pm 7*10^{-7}}$, as the result of the fitting.

A.4.2. X-Ray structures.

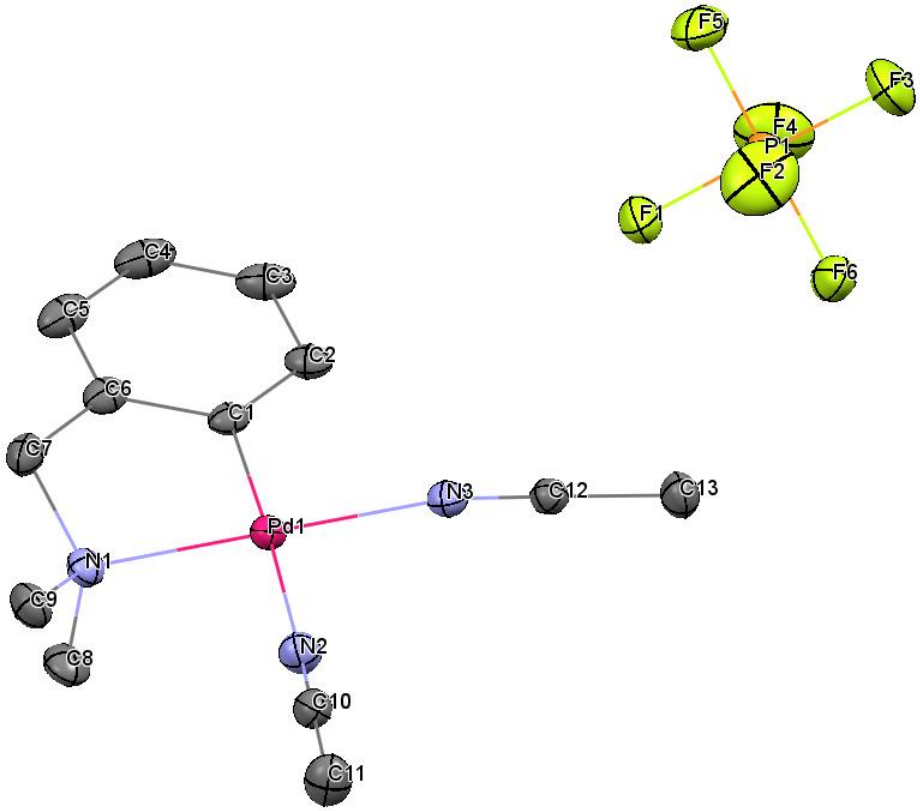

Figure SI 4.6. Ellipsoid type plot of the structure of **4.3a** drawn at 30% of possibility level. Fully atom labelling is included. Atoms of hydrogen of the cyclohexyl groups are omitted for the sake of clarity.

Selected angles

Nº	Angle	Value [º]
1	N_1-Pd_1-N_2	94.73(9)
2	N_2-Pd_1-N_3	88.16(9)
3	N_3-Pd_1-C_1	94.75(9)
4	C_1-Pd_1-N_1	82.45(9)

Selected distances

Nº	Distance	Value [Å]
1	Pd_1-N_1	2.070(3)
2	Pd_1-N_2	2.127(2)
3	Pd_1-N_3	2.025(3)
4	Pd_1-C_1	1.970(2)

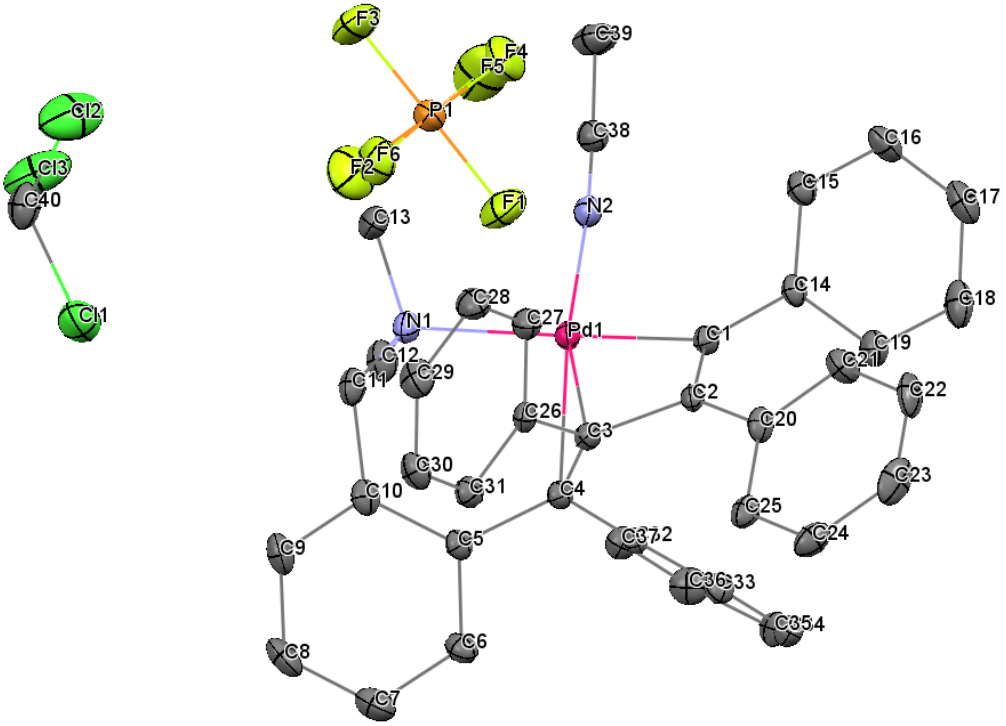

Figure SI 4.7. Ellipsoid type plot of the structure of **4.6a** drawn at 30% of possibility level. Fully atom labelling is included. Atoms of hydrogen of the cyclohexyl groups are omitted for the sake of clarity.

Selected angles

Nº	Angle	Value [º]
1	N_1-Pd_1-N_2	88.5(3)
2	N_2-Pd_1-C_1	95.7(3)
3	C_1-Pd_1-C_3	65.8(3)
4	C_1-Pd_1-C_4	85.1(3)
5	N_1-Pd_1-C_3	108.0(3)
6	N_1-Pd_1-C_4	93.6(2)
7	C_3-Pd_1-C_4	36.6(2)
8	Pd_1-C_3-C_4	72.5(4)
9	Pd_1-C_4-C_3	70.9(4)

Selected distances

Nº	Distance	Value [Å]
1	Pd_1-N_1	2.214(7)
2	Pd_1-N_2	2.043(7)
3	Pd_1-C_1	2.001(7)
4	Pd_1-C_2	2.588(7)
5	Pd_1-C_3	2.215(7)
6	Pd_1-C_4	2.236(7)

A.4.3. Mass spectra.

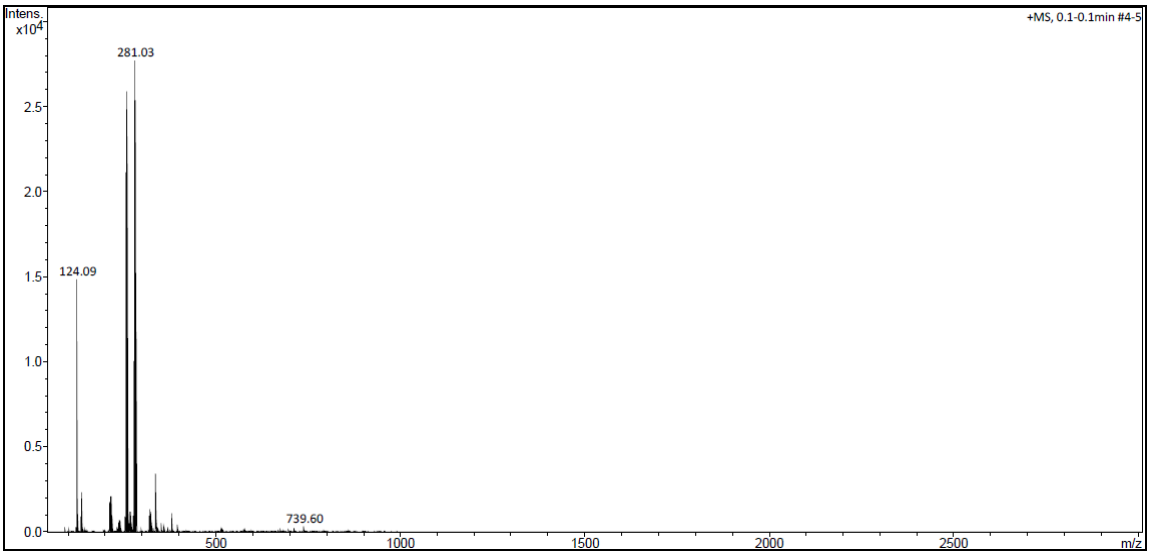

Figure SI 4.8a. Mass spectra of the palladacycle **4.3a** recorded in positive charge mode.

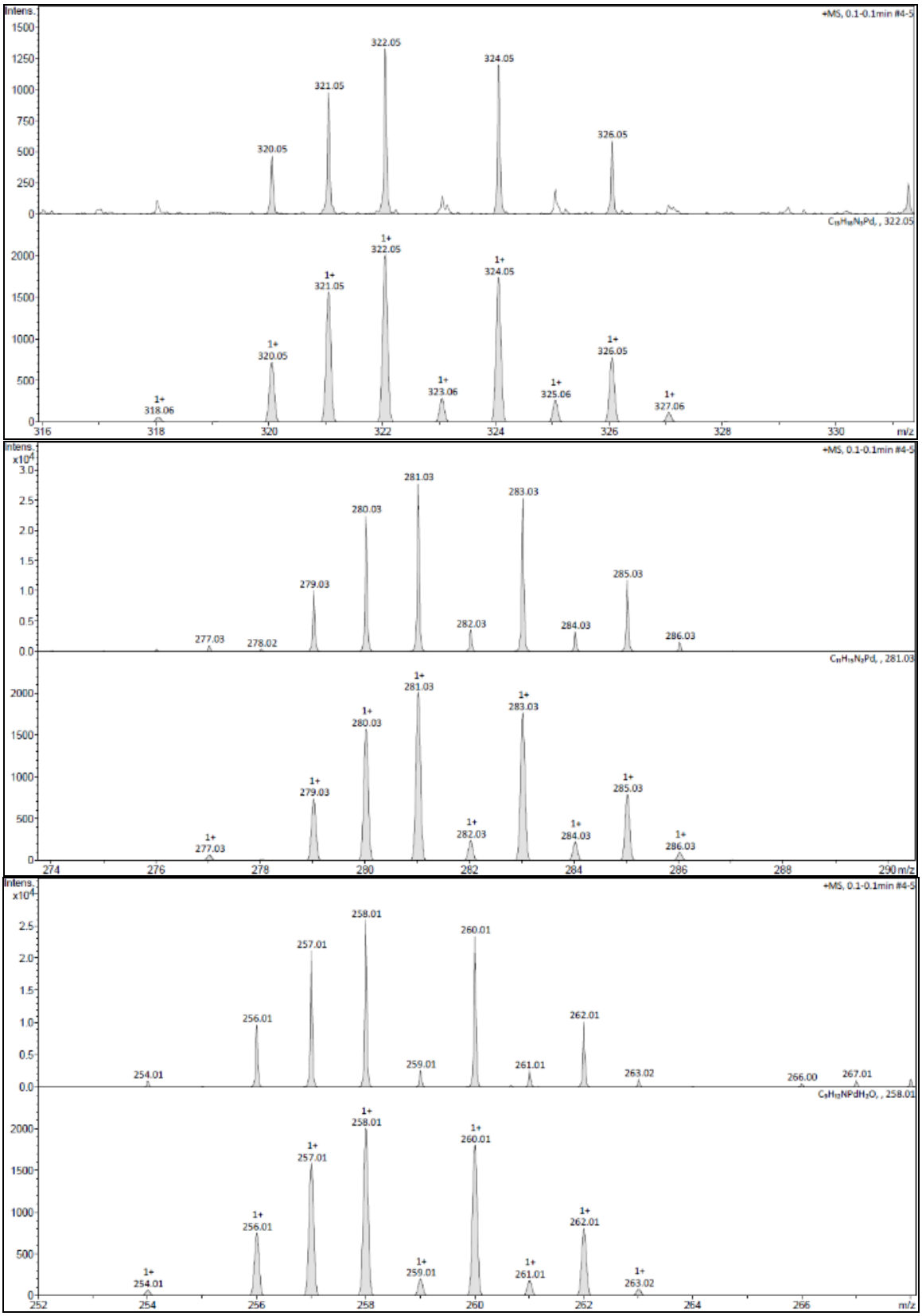

Figure SI 4.8b. Mass spectra of the palladacycle **4.3a** recorded in positive charge mode – zoomed.

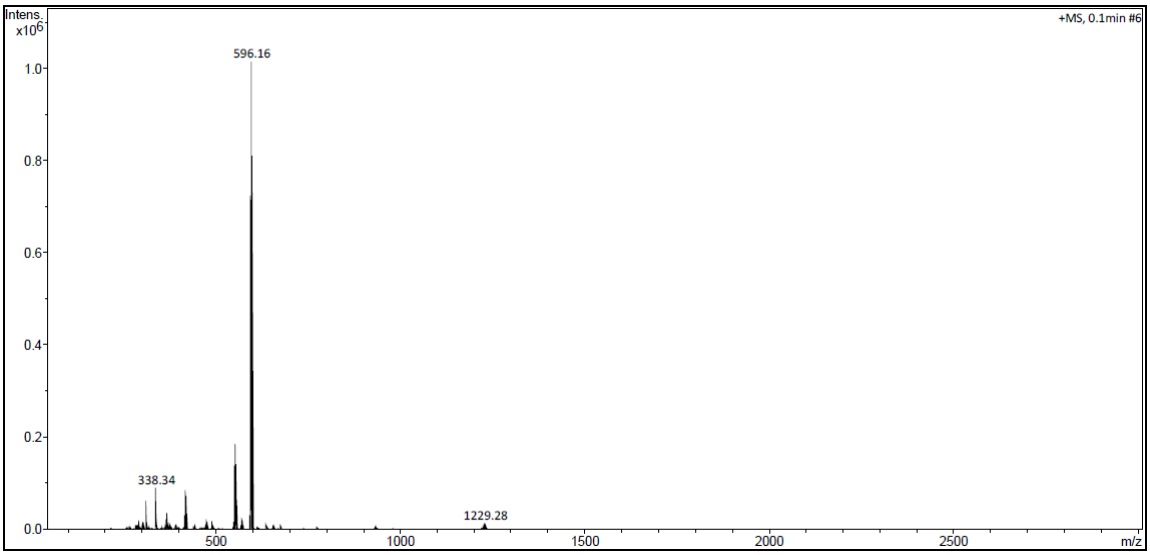

Figure SI 4.9a. Mass spectra of the palladacycle **4.6a** recorded in positive charge mode.

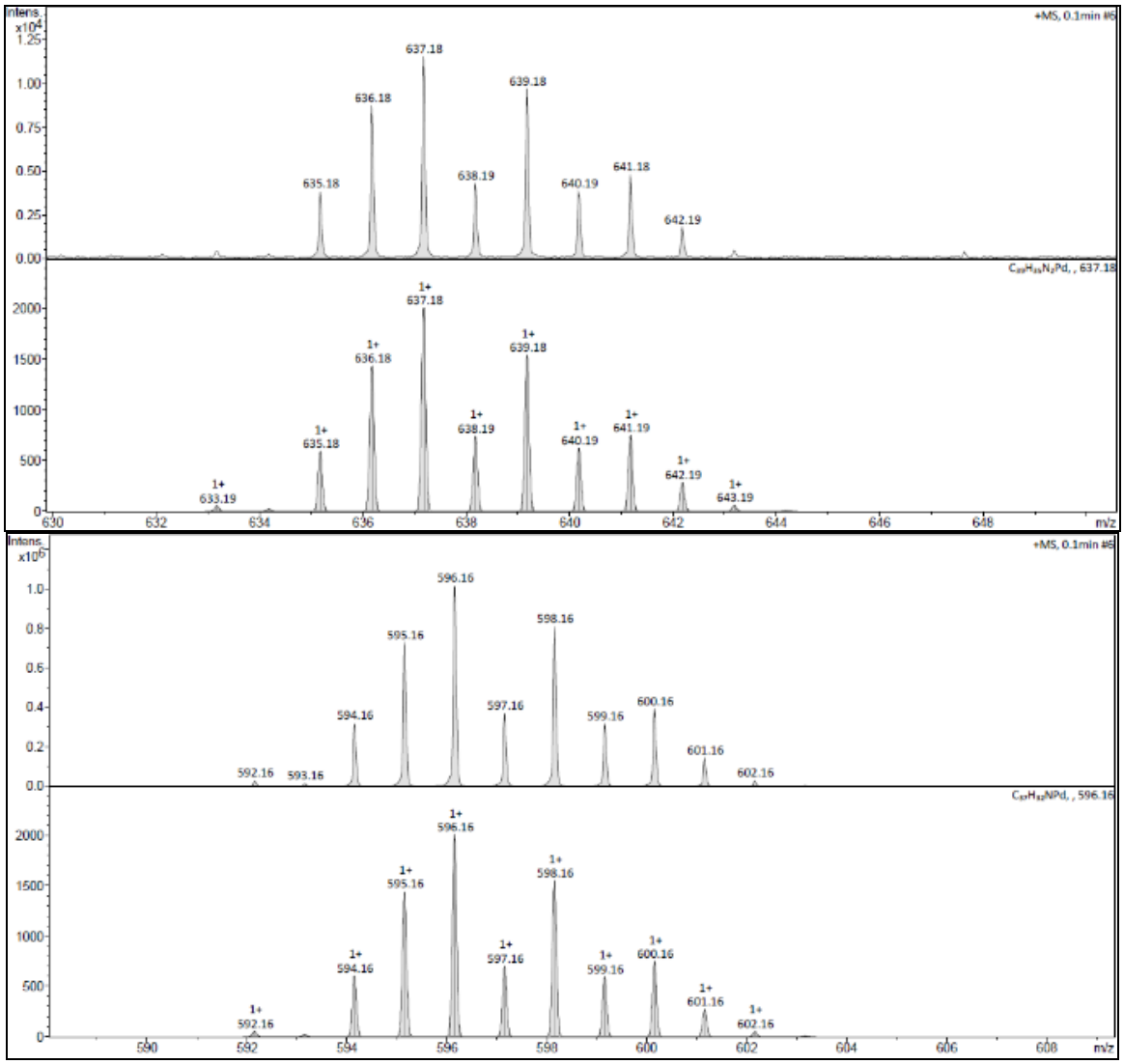

Figure SI 4.9b. Mass spectra of the palladacycle **4.6a** recorded in positive charge mode – zoomed.

A.4.4. Elemental analysis.

Compound		%N	%C	%H
		8.56	33.55	4.04
4.3a		8.52	33.5	4.02
	Valeur Théorique Attendue	**8.98**	**33.39**	**3.88**
		5.54	36.75	4.11
4.5a		5.53	36.85	4.14
	Valeur Théorique Attendue	**6.89**	**37.42**	**3.97**
		4.11	56.48	4.56
4.6a		4.13	56.44	4.57
	Valeur Théorique Attendue	**3.58**	**59.82**	**4.51**

A.4.5. NMR spectra.

A.4.5.1. *Synthesis.*

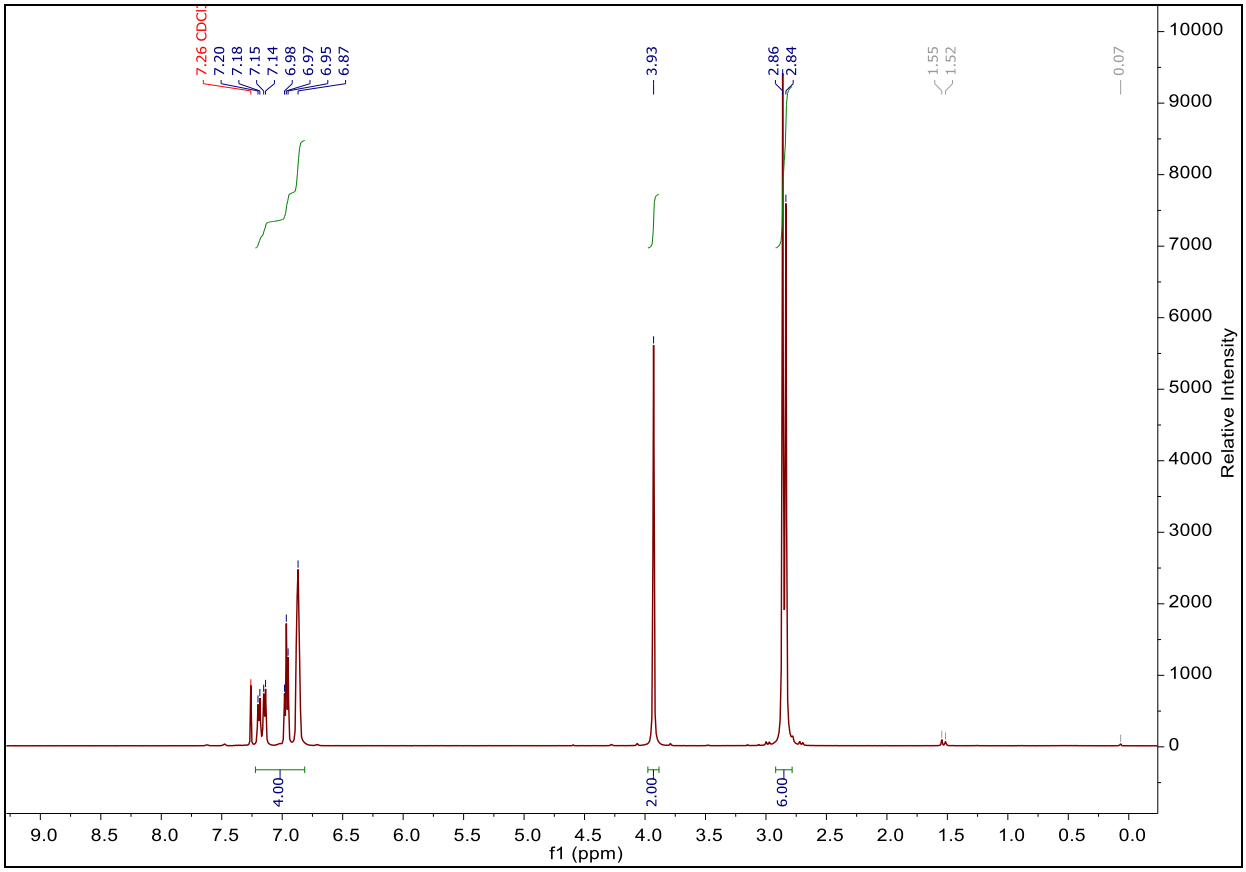

Figure SI 4.10 ^{1}H NMR spectrum of the palladacycle **4.2a**. The spectrum is recorded in deuterated chloroform at 500 MHz. ^{1}H NMR (500 MHz, chloroform-*d*, δ, ppm) 7.22 – 6.81 (m, 8H), 3.93 (s, 4H), 2.85 (d, *J* = 13.2 Hz, 12H).

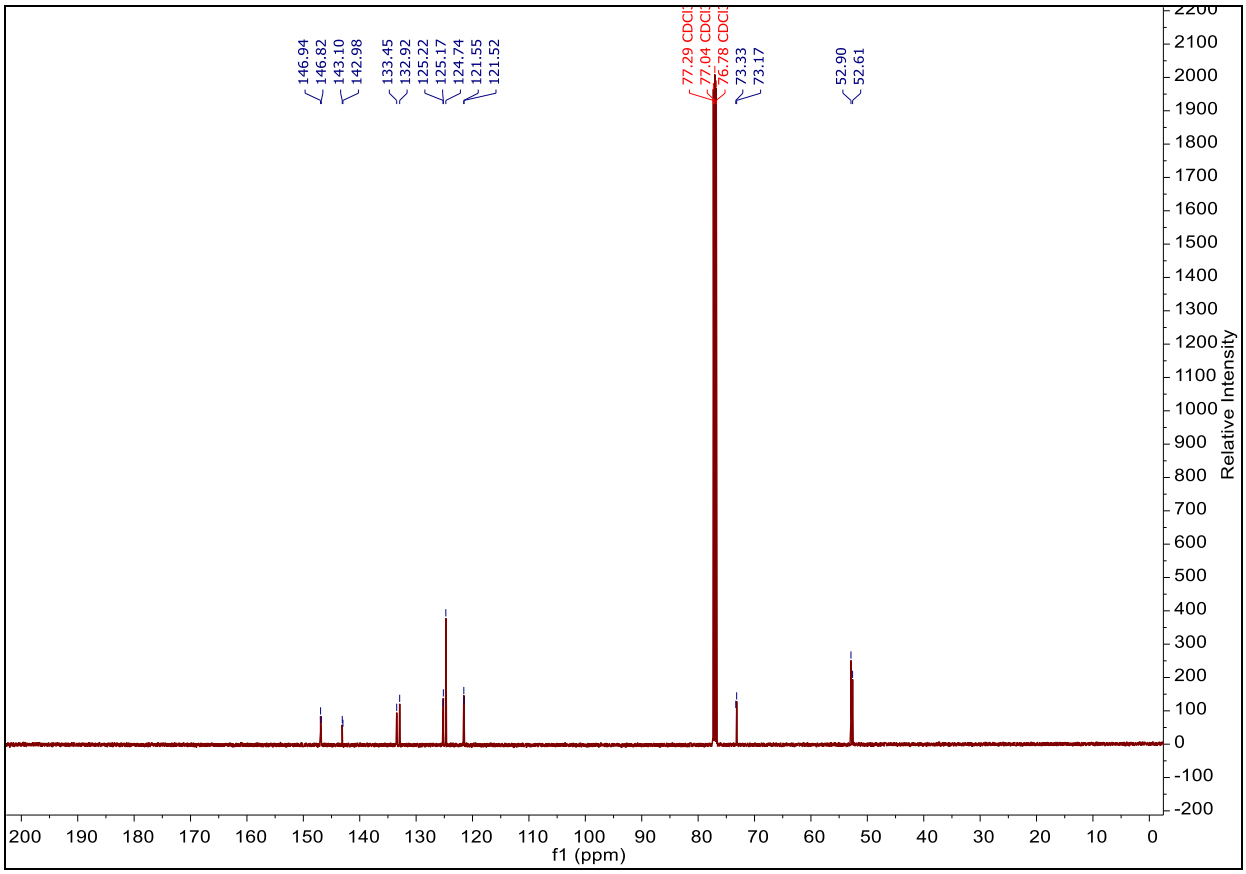

Figure SI 4.11 ^{13}C NMR spectrum of the palladacycle **4.2a**. The spectrum is recorded in deuterated chloroform at 500 MHz. ^{13}C NMR (126 MHz, chloroform-*d*, δ, ppm) 146.88 (d, *J* = 16 Hz), 143.04 (d, *J* = 16 Hz), 133.45, 132.92, 125.20 (d, *J* = 6 Hz), 124.74, 121.53 (d, *J* = 4 Hz), 73.25 (d, *J* = 20 Hz), 52.76 (d, *J* = 36 Hz).

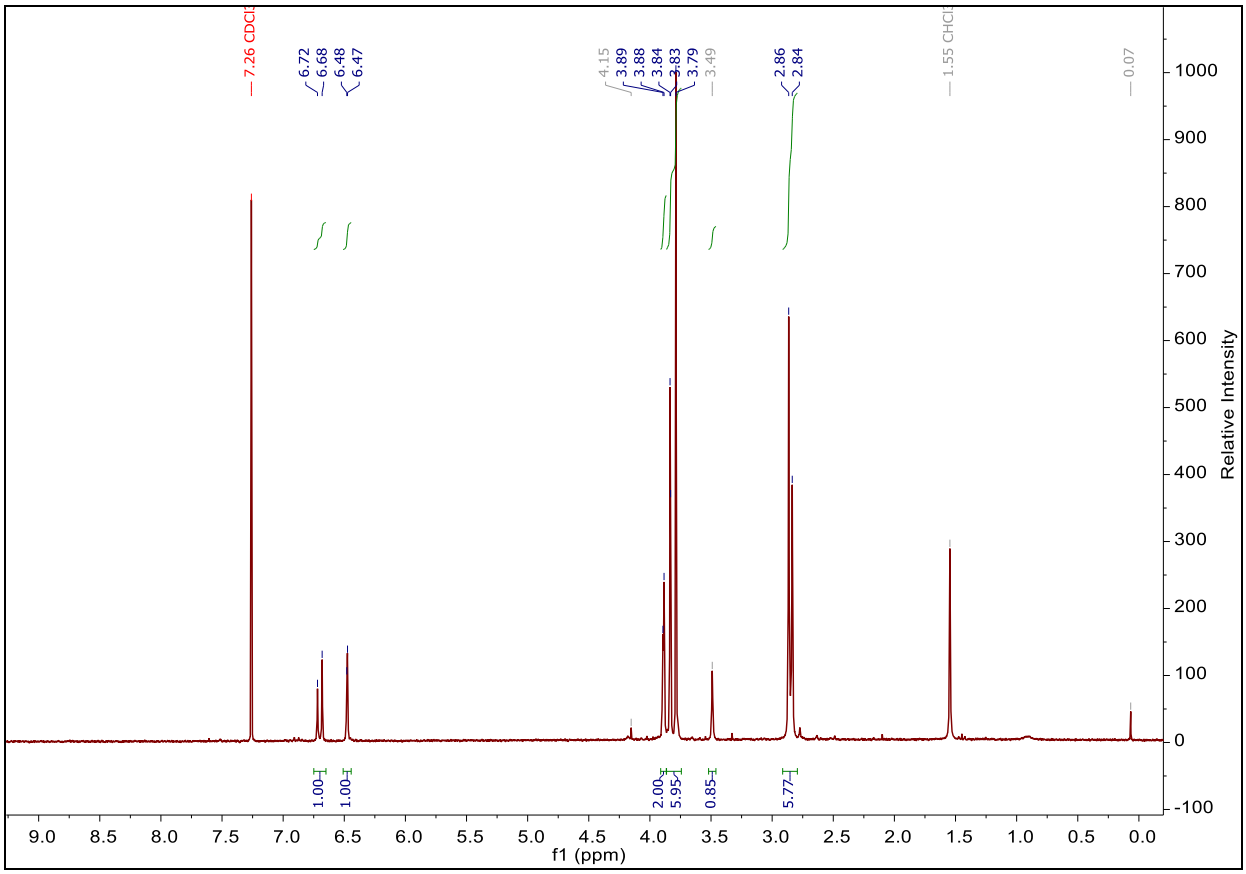

Figure SI 4.12 ^{1}H NMR spectrum of the palladacycle **4.2c**. The spectrum is recorded in deuterated chloroform at 300 MHz. ^{1}H NMR (300 MHz, chloroform-*d*, δ, ppm) 6.70 (d, *J* = 11.4 Hz, 2H), 6.48 (d, *J* = 2 Hz, 2H), 3.89 (d, *J* = 3 Hz, 4H), 3.81 (d, 12H), 2.85 (d, *J* = 9 Hz, 12H).

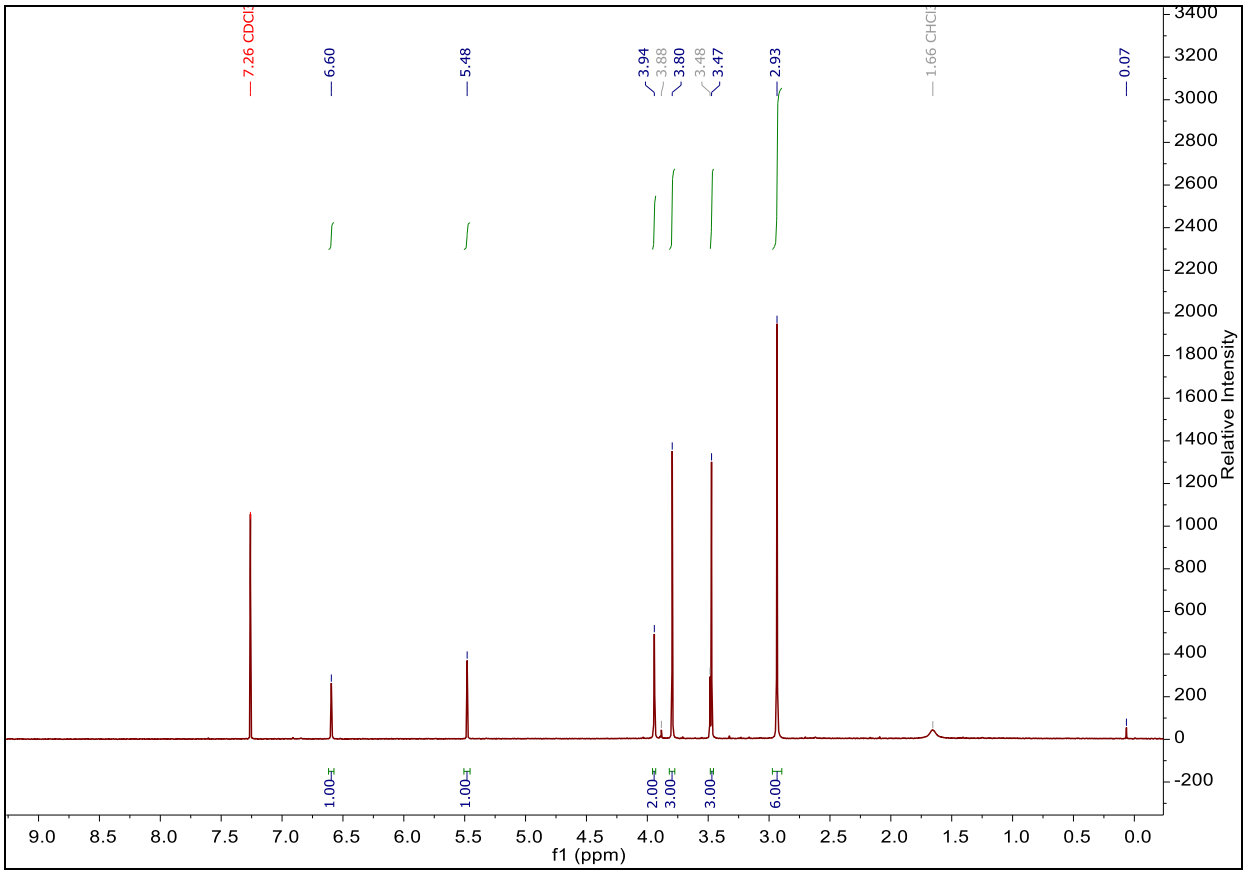

Figure SI 4.13 ^{1}H NMR spectrum of the palladacycle **4.2c.1**. The spectrum is recorded in deuterated chloroform at 300 MHz. ^{1}H NMR (300 MHz, chloroform-*d*, δ, ppm) 6.60 (s, 1H), 5.48 (s, 1H), 3.94 (s, 2H), 3.80 (s, 3H), 3.47 (s, 3H), 2.93 (s, 6H).

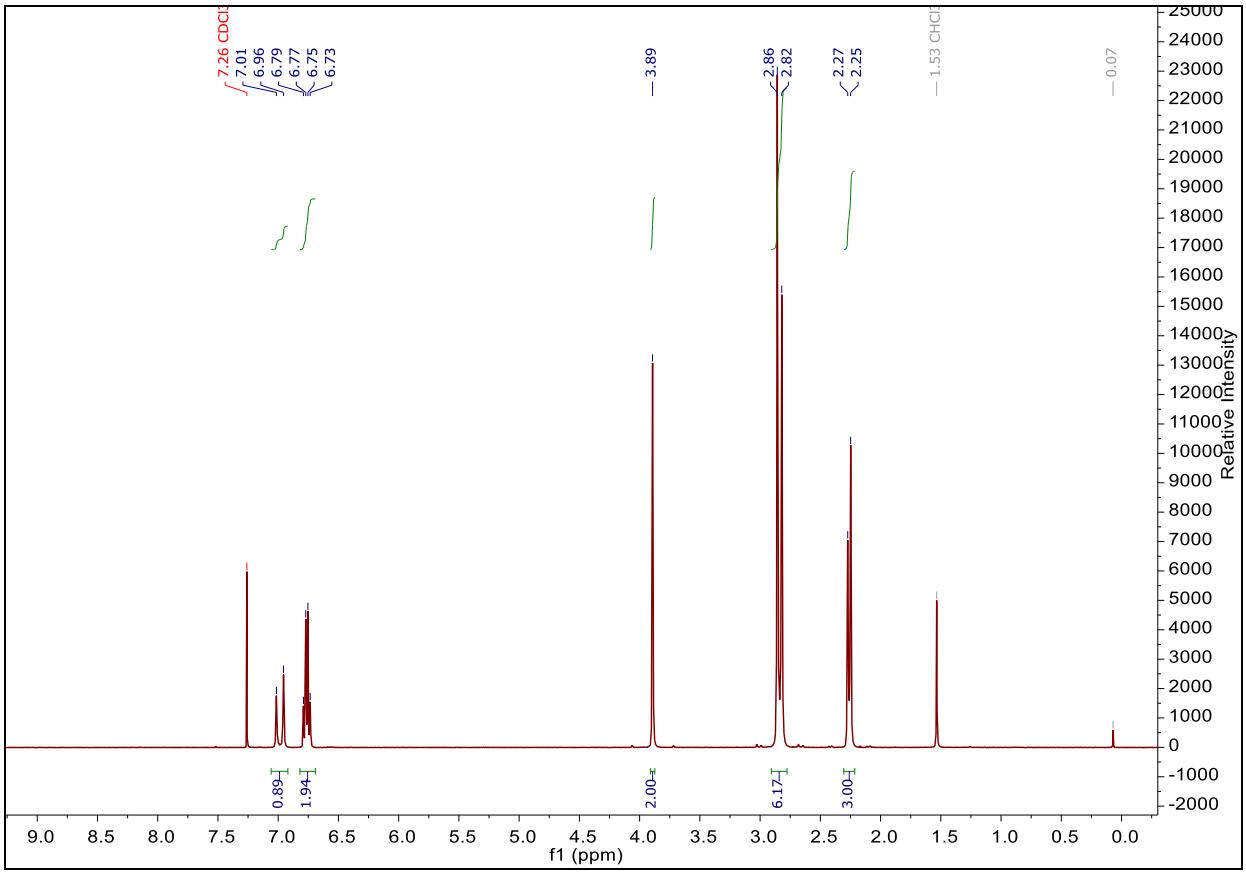

Figure SI 4.14 ^{1}H NMR spectrum of the palladacycle **4.2d**. The spectrum is recorded in deuterated chloroform at 400 MHz. ^{1}H NMR (400 MHz, chloroform-*d*, δ, ppm) 6.99 (d, *J* = 24 Hz, 2H), 6.76 (q, *J* = 8 Hz, 4H), 3.89 (s, 4H), 2.84 (d, *J* = 15 Hz, 12H), 2.26 (d, *J* = 10 Hz, 6H).

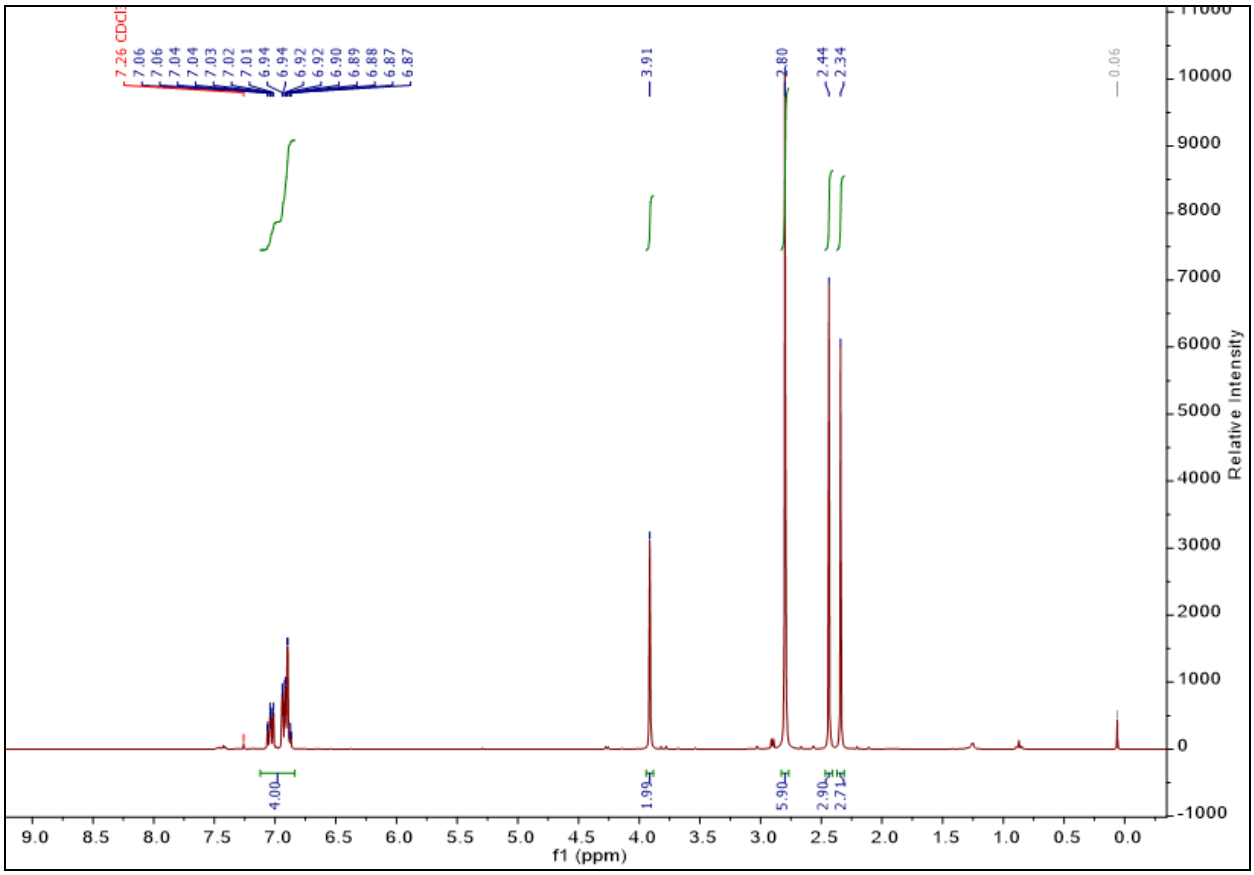

Figure SI 4.15 ^{1}H NMR spectrum of the palladacycle **4.3a**. The spectrum is recorded in deuterated chloroform at 300 MHz. ^{1}H NMR (300 MHz, chloroform-*d*, δ, ppm) 7.09 – 6.84 (m, 4H), 3.91 (s, 2H), 2.80 (s, 6H), 2.44 (s, 3H), 2.34 (s, 3H).

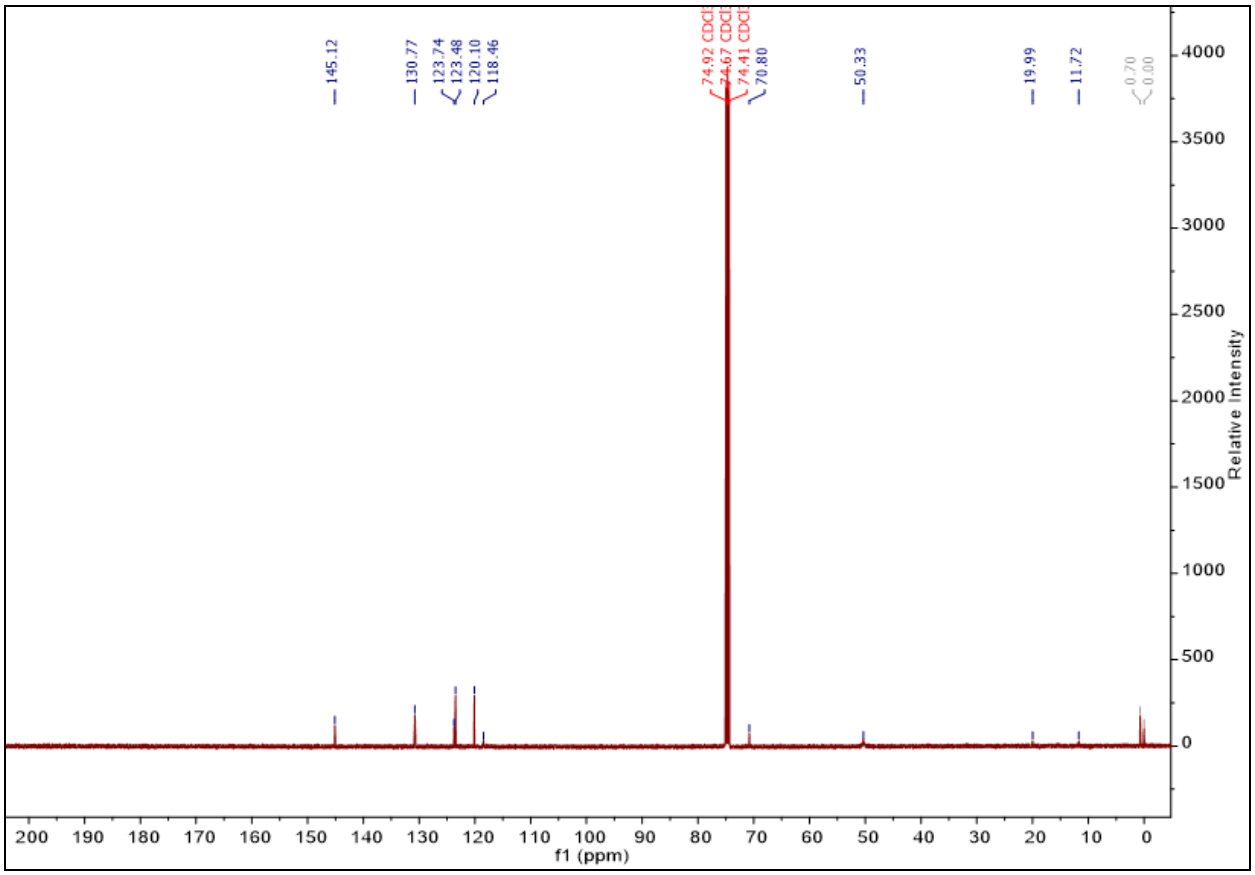

Figure SI 4.16 ^{13}C NMR spectrum of the palladacycle **4.3a**. The spectrum is recorded in deuterated chloroform at 126 MHz. ^{13}C NMR (126 MHz, chloroform-*d*, δ, ppm) 145.12, 130.77, 123.74, 123.48, 120.10, 118.46, 70.80, 50.33, 19.99, 11.72.

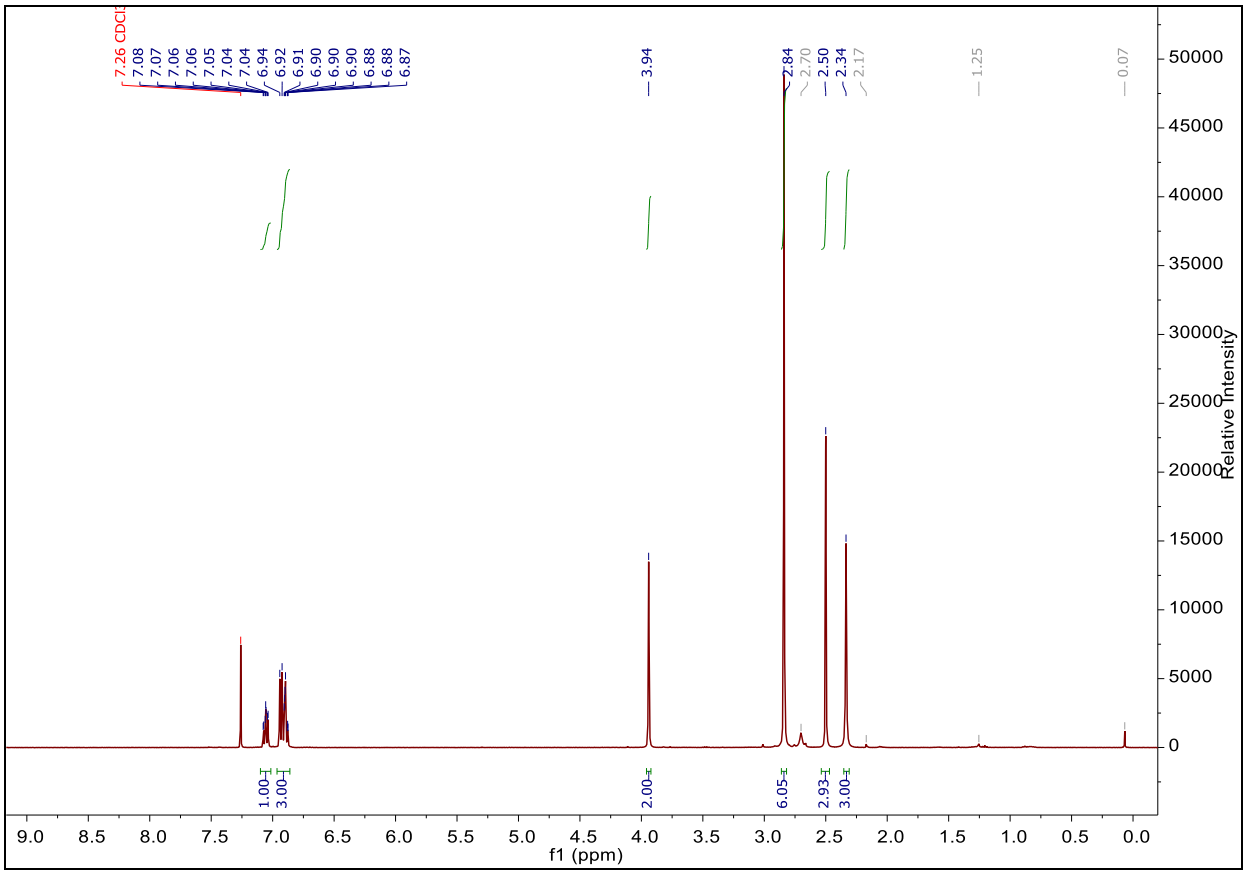

Figure SI 4.17 ^{1}H NMR spectrum of the palladacycle **4.3b**. The spectrum is recorded in deuterated chloroform at 400 MHz. ^{1}H NMR (400 MHz, chloroform-*d*, δ, ppm) 7.06 (ddd, *J* = 8, 7, 2 Hz, 1H), 6.96 – 6.86 (m, 3H), 3.94 (s, 2H), 2.84 (s, 6H), 2.50 (s, 3H), 2.34 (s, 3H).

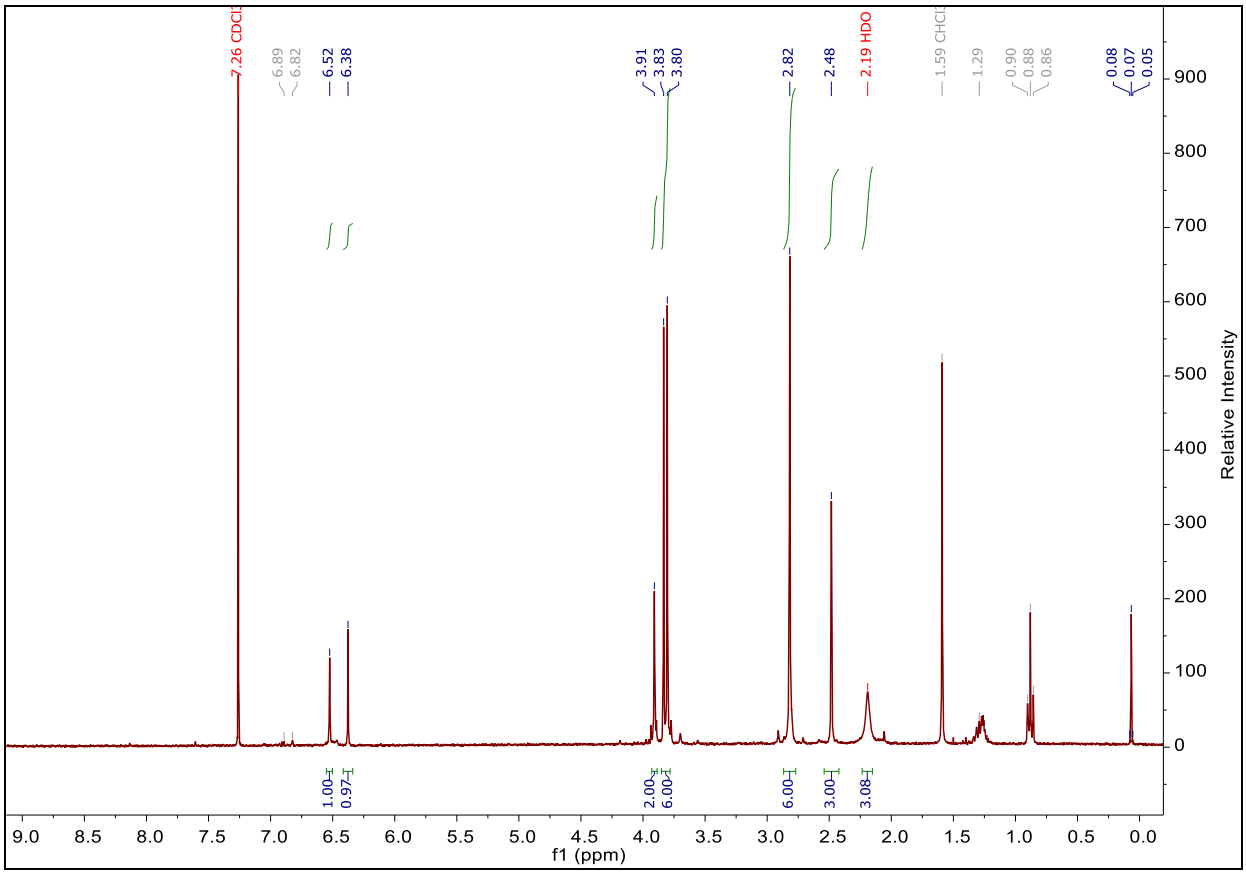

Figure SI 4.18 ^{1}H NMR spectrum of the palladacycle **4.3c**. The spectrum is recorded in deuterated chloroform at 400 MHz.^{1}H NMR (300 MHz, chloroform-*d*, δ, ppm) 6.52 (s, 1H), 6.38 (s, 1H), 3.91 (s, 2H), 3.82 (d, *J* = 9 Hz, 6H), 2.82 (s, 6H), 2.48 (s, 3H), 2.19 (s, 3H).

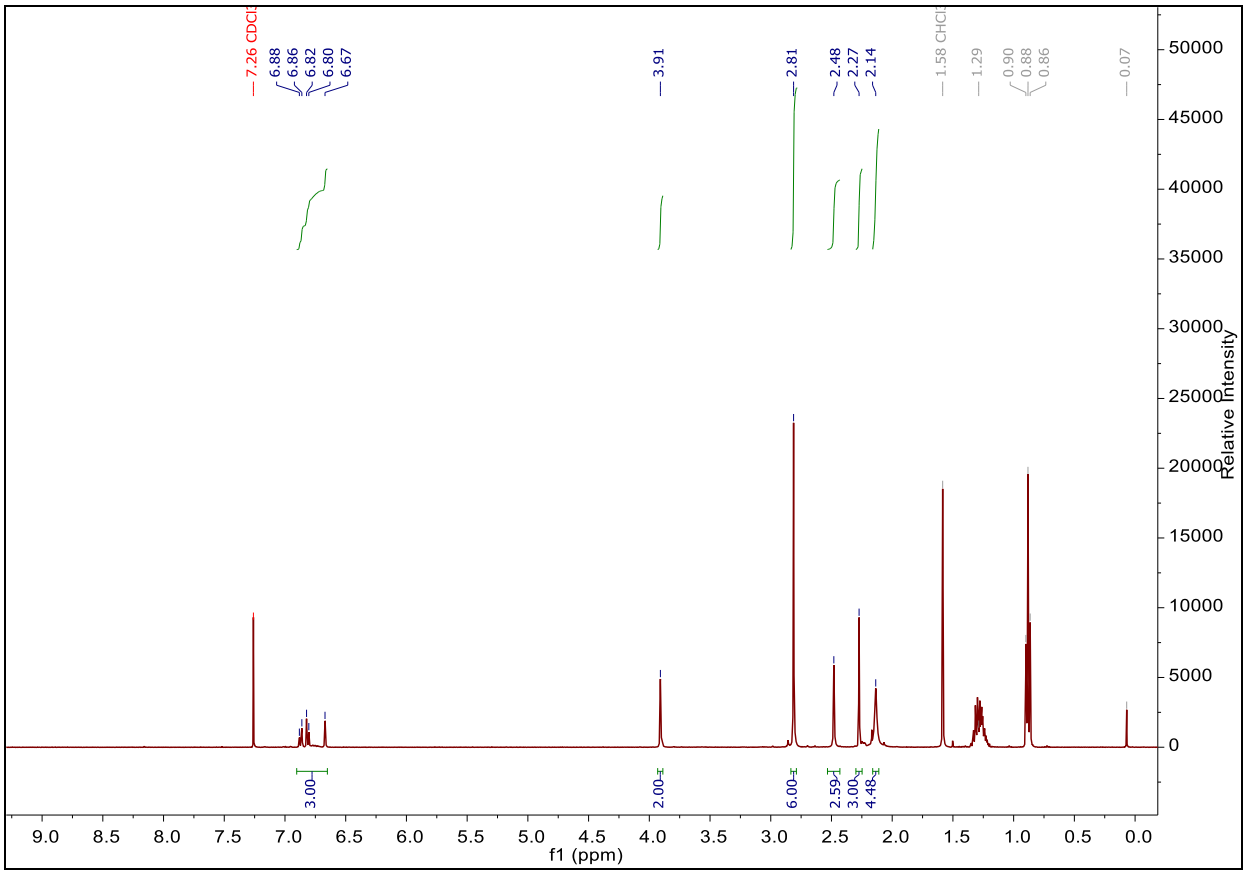

Figure SI 4.19 ^{1}H NMR spectrum of the palladacycle **4.3d**. The spectrum is recorded in deuterated chloroform at 400 MHz. ^{1}H NMR (400 MHz, chloroform-*d*, δ, ppm) 6.90 – 6.65 (m, 3H), 3.91 (s, 2H), 2.81 (s, 6H), 2.48 (s, 3H), 2.27 (s, 3H), 2.14 (s, 3H).

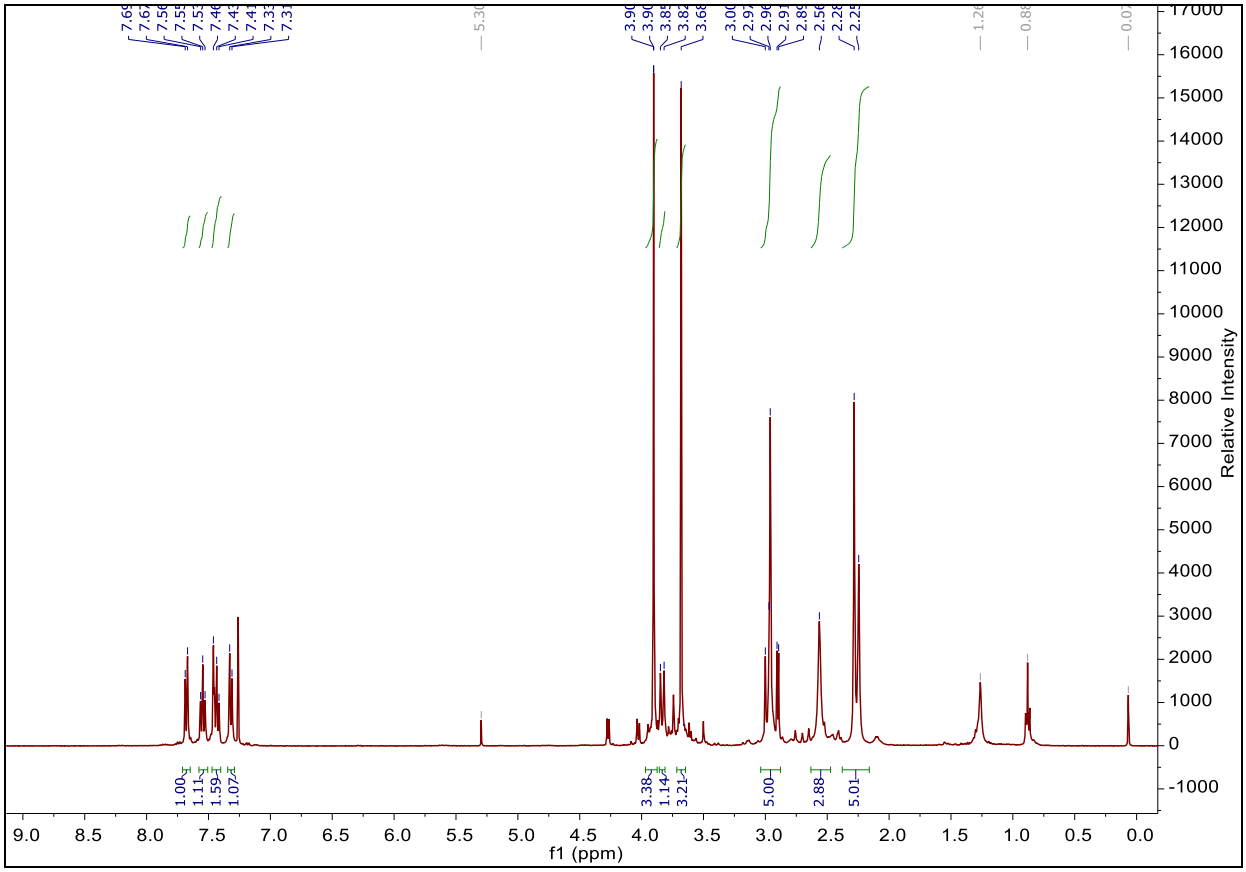

Figure SI 4.20 ^{1}H NMR spectrum of the palladacycle **4.5a**. The spectrum is recorded in deuterated chloroform at 400 MHz.^{1}H NMR (400 MHz, chloroform-*d*, δ, ppm) 7.68 (d, *J* = 8 Hz, 1H), 7.55 (t, *J* = 7 Hz, 1H), 7.48 – 7.36 (m, 1H), 7.32 (d, *J* = 7 Hz, 1H), 3.83 (d, *J* = 12 Hz, 1H), 3.83 (d, 6H), 2.99 (d, *J* = 12 Hz, 1H), 2.96 (s, 3H), 2.90 (d, *J* = 5 Hz, 1H), 2.56 (s, 3H), 2.26 (d, *J* = 15 Hz, 6H).

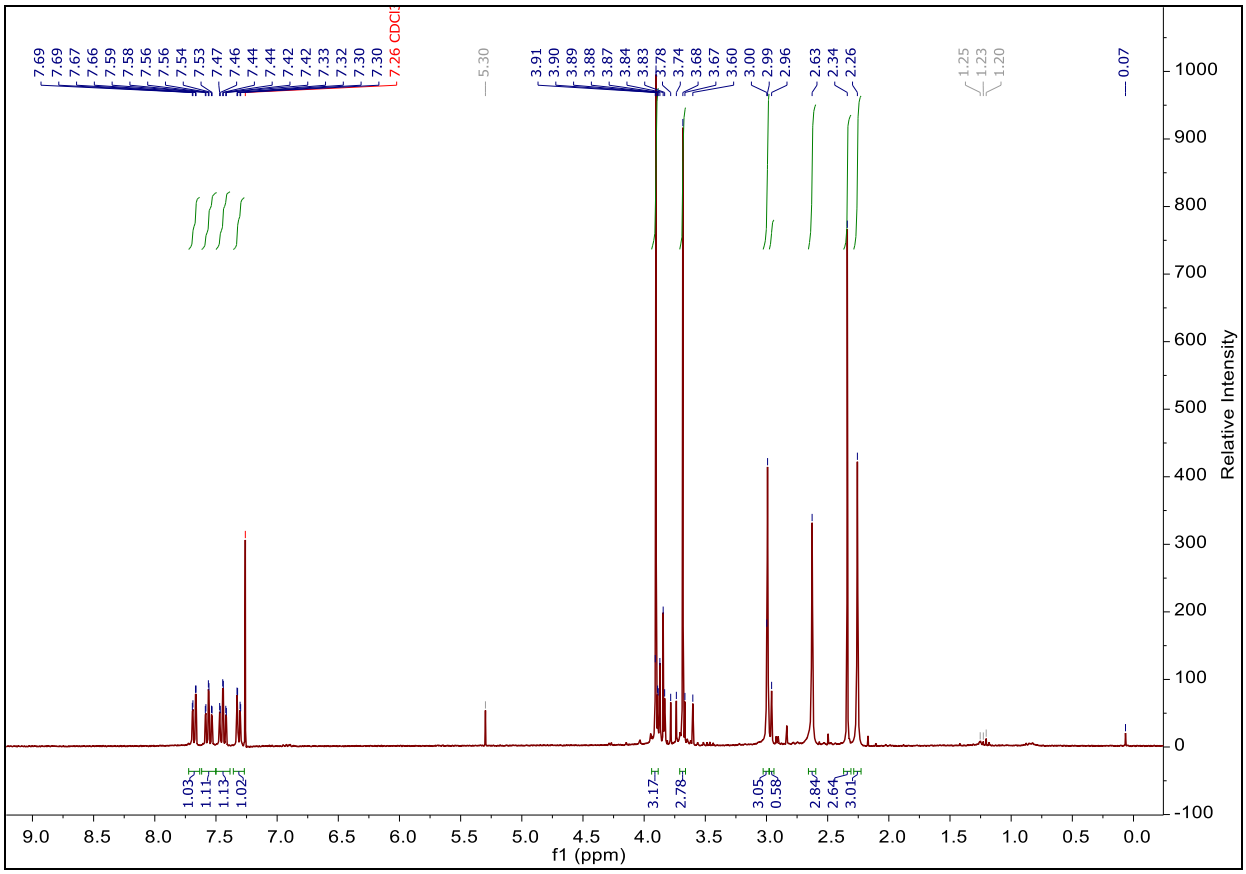

Figure SI 4.21 ^{1}H NMR spectrum of the palladacycle **4.5b**. The spectrum is recorded in deuterated chloroform at 300 MHz. ^{1}H NMR (300 MHz, chloroform-*d*, δ, ppm) 7.68 (dd, *J* = 8, 1 Hz, 1H), 7.56 (td, *J* = 7.6, 1.4 Hz, 1H), 7.44 (td, *J* = 7.5, 1.5 Hz, 1H), 7.32 (dd, *J* = 8, 1 Hz, 1H), 3.91 (s, 3H), 3.69 (s, 3H), 2.99 (s, 3H), 2.99 (d, *J* = 12 Hz, 1H), 2.63 (s, 3H), 2.34 (s, 3H), 2.28 (s, 3H).

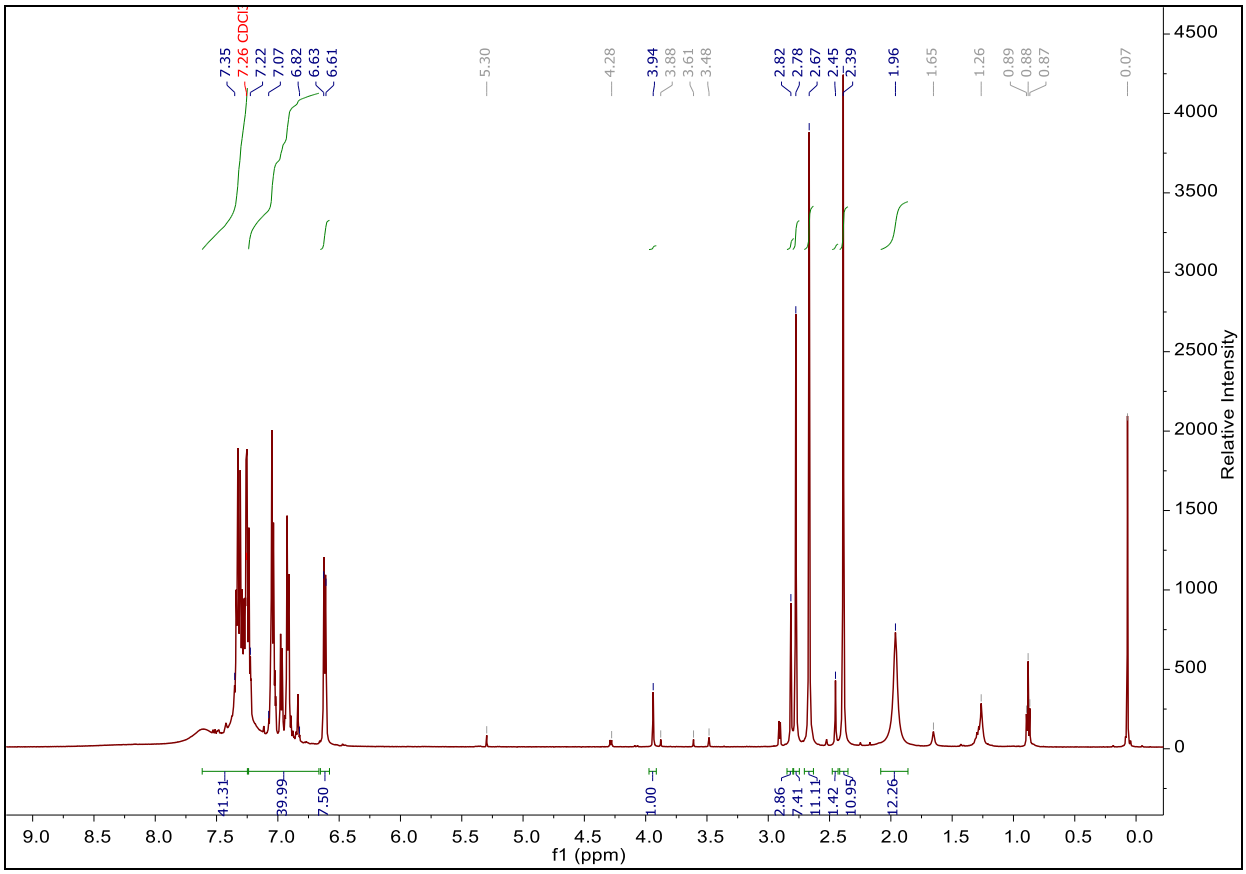

Figure 4.22 ^{1}H NMR spectrum of the palladacycle **4.6a**. The spectrum is recorded in deuterated chloroform at 500 MHz. ^{1}H NMR (500 MHz, chloroform-*d*, δ, ppm) 7.45 – 7.13 (m, 24H), 7.07 – 6.89 (m, 3H), 6.62 (d, *J* = 9 Hz, 1H), 2.78 (s, 2H), 2.53 (d, *J* = 139 Hz, 6H), 1.96 (s, 6H).

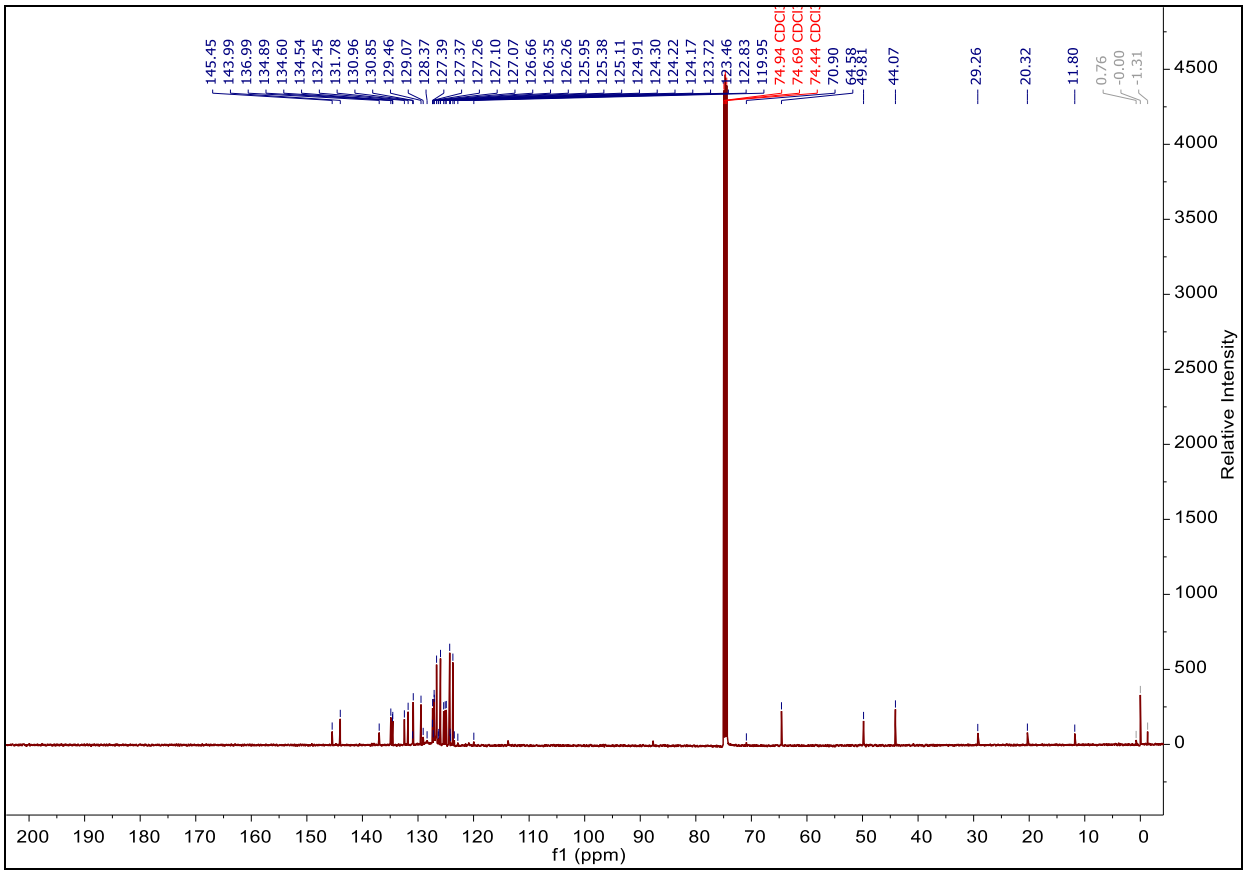

Figure SI 4.23 ^{13}C NMR spectrum of the palladacycle **4.6a**. The spectrum is recorded in deuterated chloroform at 126 MHz. ^{13}C NMR (126 MHz, chloroform-*d*, δ, ppm) 145.45, 143.99, 136.99, 134.89, 134.60, 134.54, 132.45, 131.78, 130.96, 130.85, 129.46, 129.07, 128.37, 127.39, 127.37, 127.26, 127.10, 127.07, 126.66, 126.35, 126.26, 125.95, 125.38, 125.11, 124.91, 124.30, 124.22, 124.17, 123.72, 123.46, 122.83, 119.95, 74.94, 74.69, 74.44, 70.90, 64.58, 49.81, 44.07, 29.26, 20.32, 11.80, 0.76, -0.00, -1.31.

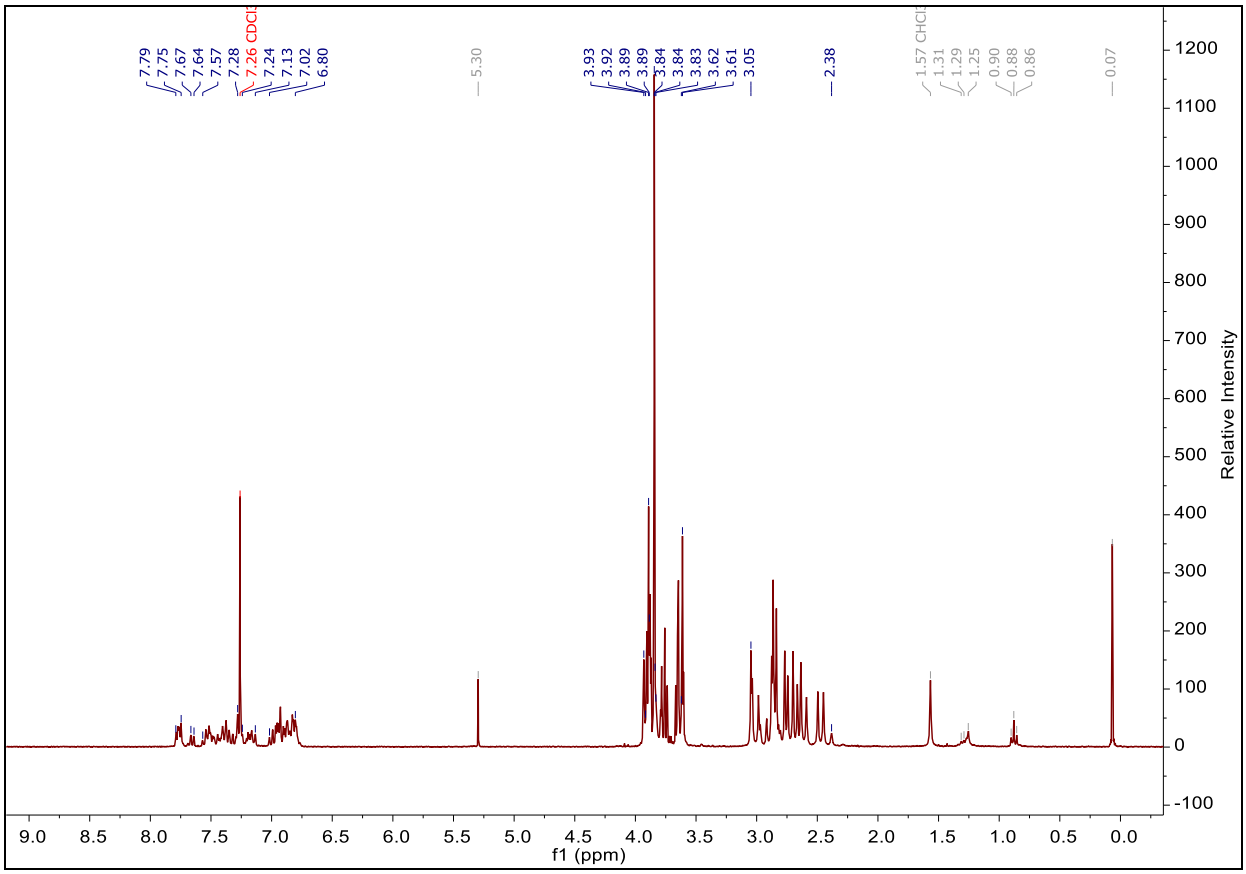

Figure 4.24 ^{1}H NMR spectrum of the palladacycle **4.7a**. The spectrum is recorded in deuterated chloroform at 300 MHz.

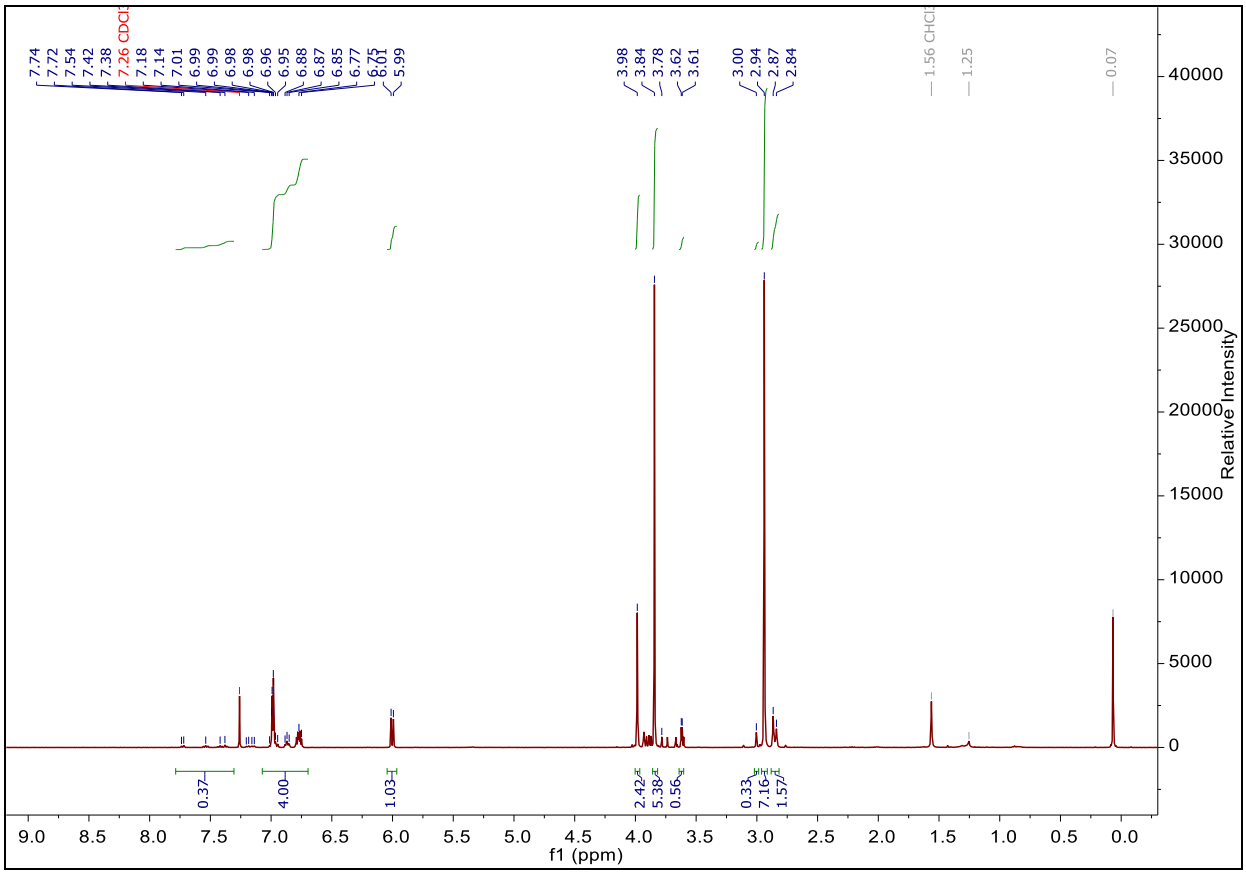

Figure 4.25 ^{1}H NMR spectrum of the palladacycle **4.7a.1**. The spectrum is recorded in deuterated chloroform at 300 MHz.

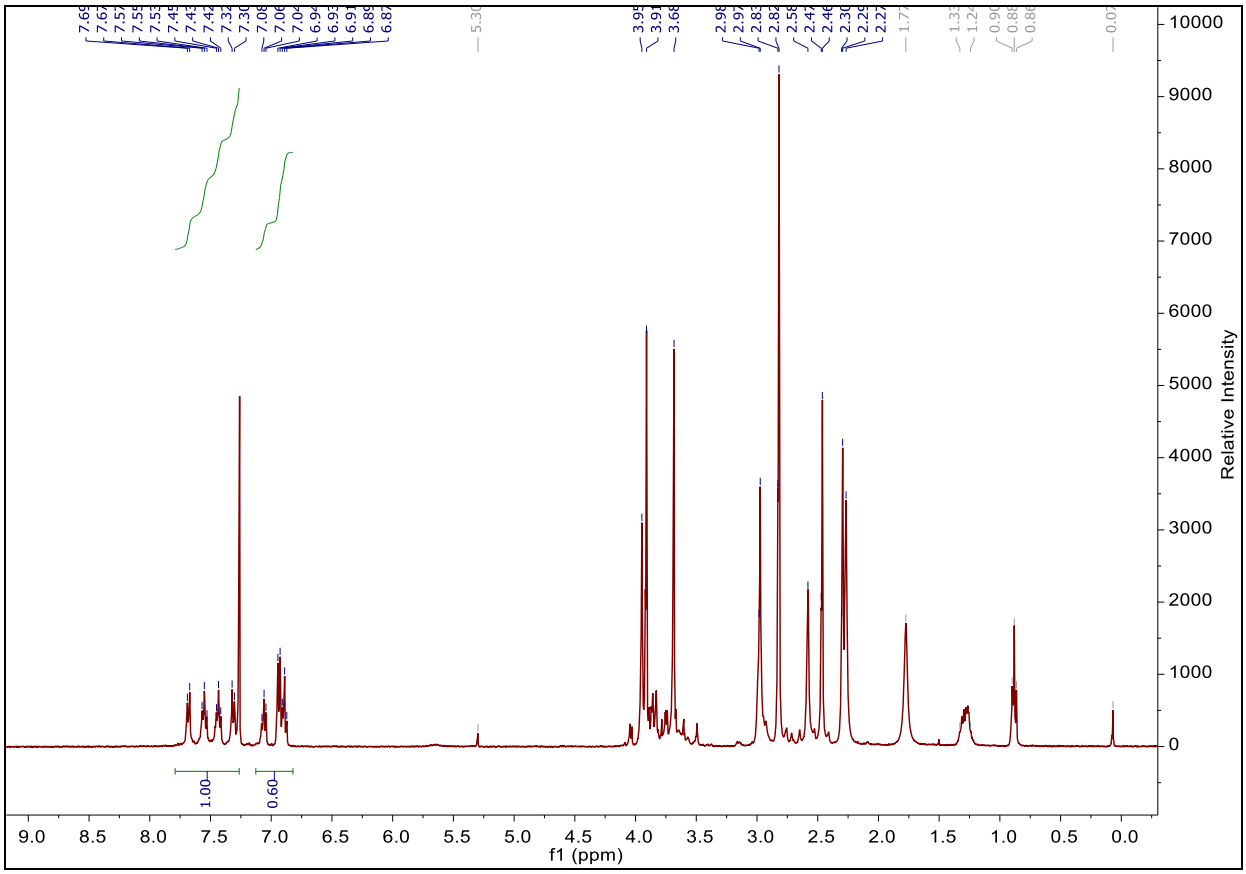

Figure 4.26 ^{1}H NMR spectrum of the palladacycle **4.5a**, obtained in the reverse way – from **4.2a** through **4.7a**. The spectrum is recorded in deuterated chloroform at 400 MHz.

A.4.5.2. *Monitoring.*

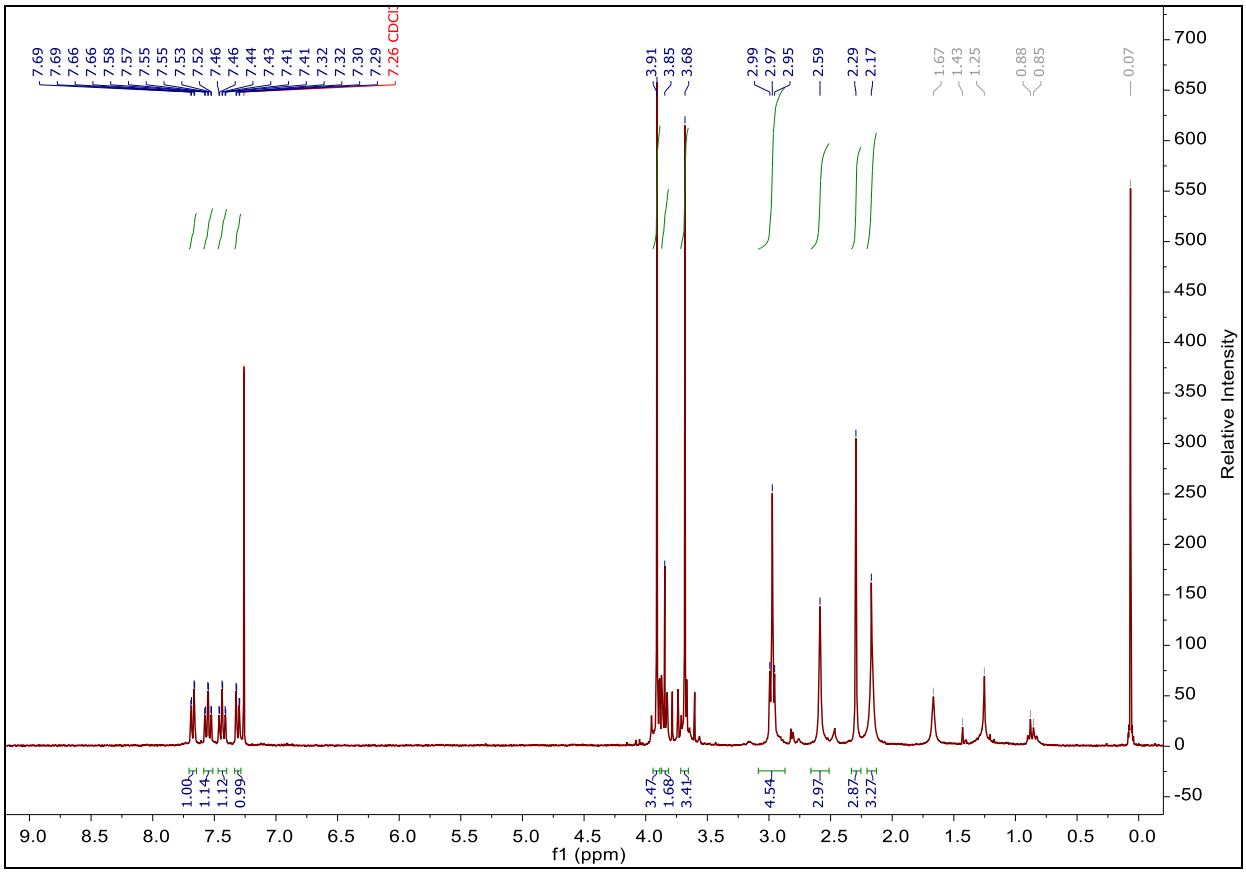

Figure SI 4.27 ^{1}H NMR spectra of the reaction of **4.3a** with **4.4a** carried out at 25ºC in molar ratio of the reactants 1:1. The spectra are recorded in deuterated chloroform at 300 MHz after 15 minutes of reaction.

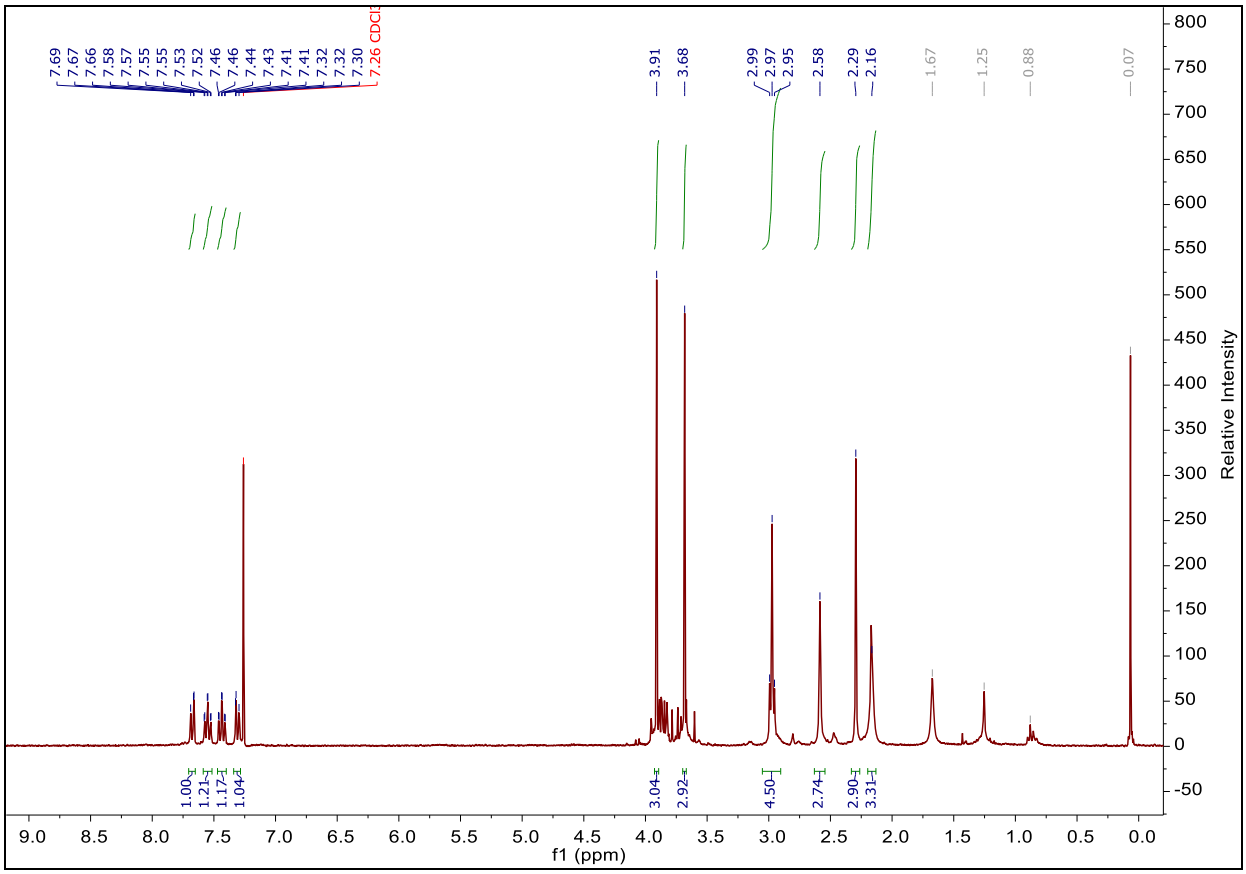

Figure SI 4.28 ^{1}H NMR spectra of the reaction of **4.3a** with **4.4a** carried out at 25ºC in molar ratio of the reactants 1:1. The spectra are recorded in deuterated chloroform at 300 MHz after 3.5 hours of reaction.

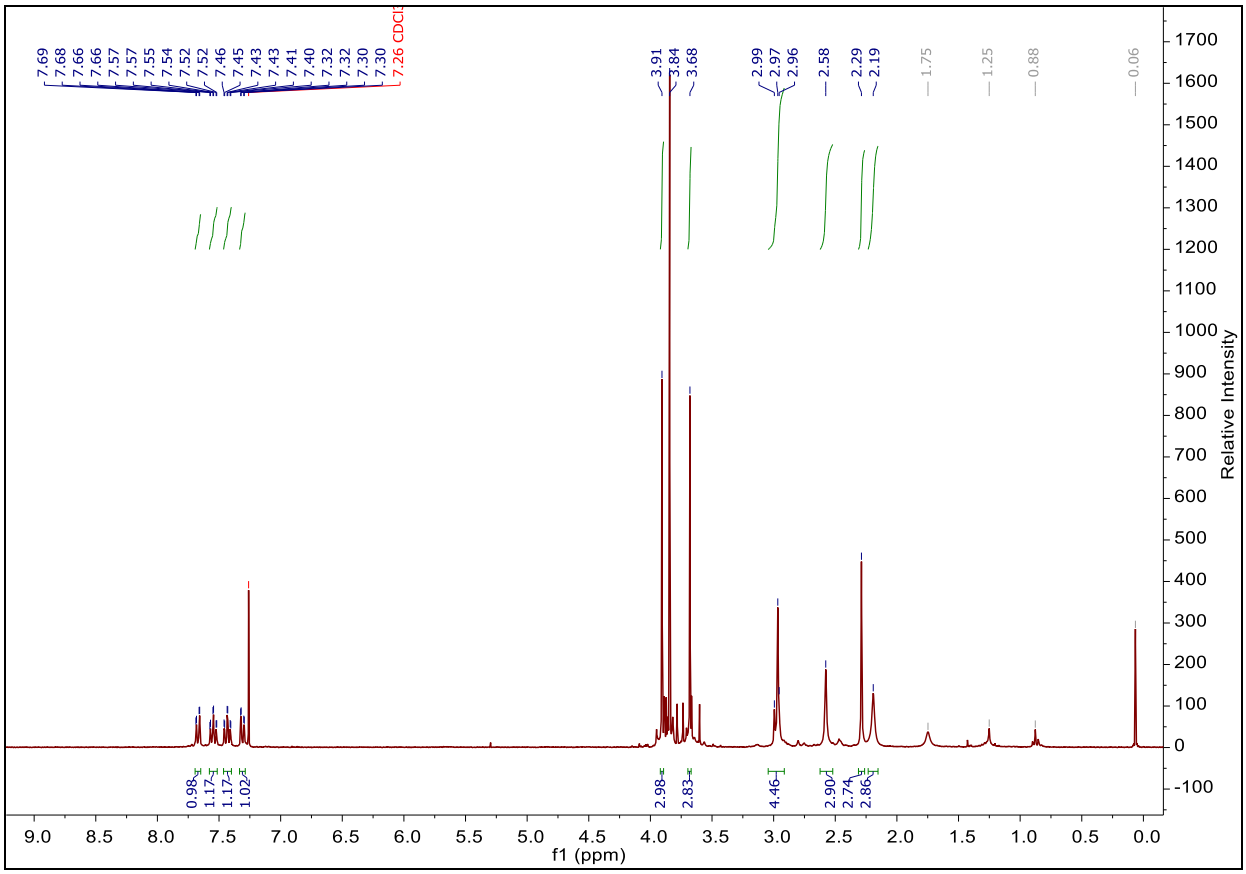

Figure SI 4.29 ^{1}H NMR spectra of the reaction of **4.3a** with **4.4a** carried out at 25ºC in molar ratio of the reactants 1:2. The spectra are recorded in deuterated chloroform at 300 MHz after one hour of reaction.

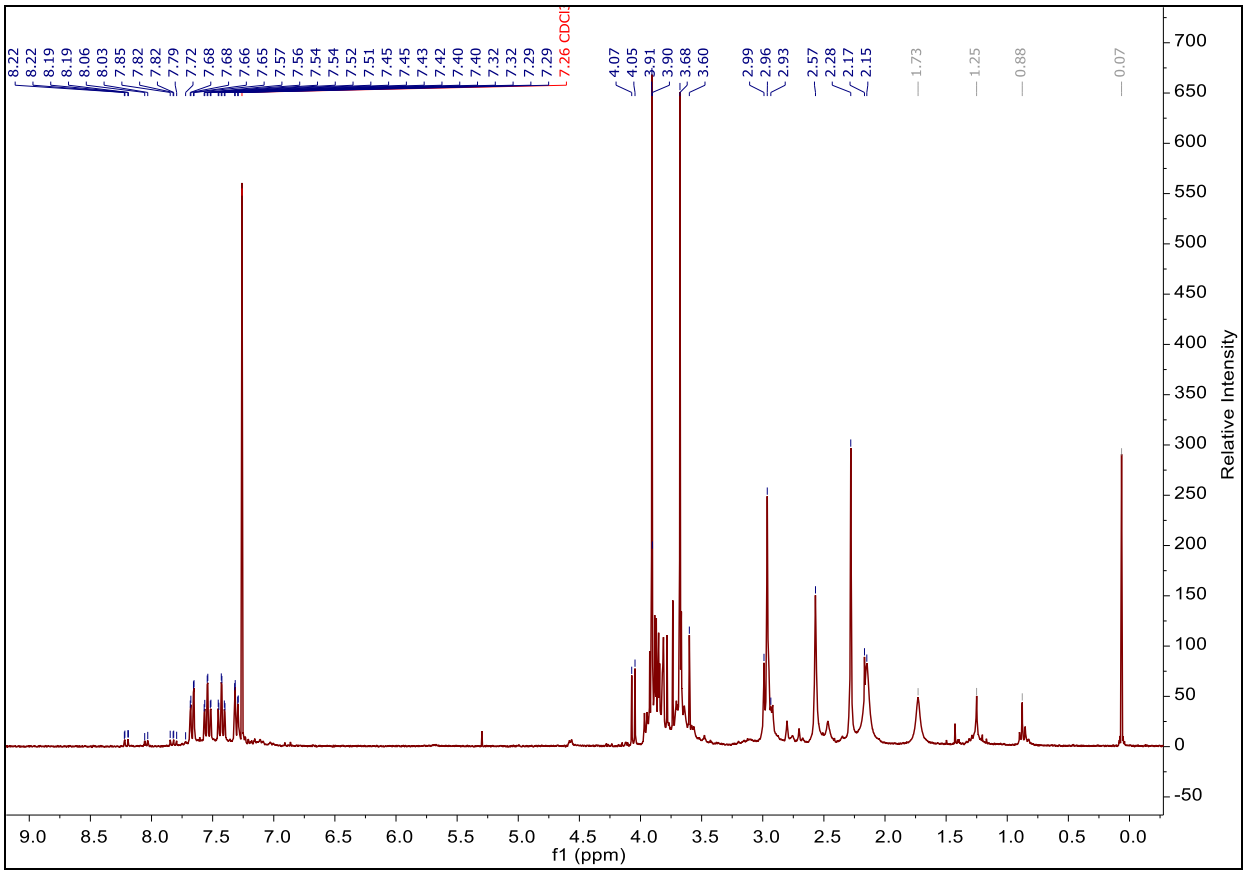

Figure SI 4.30 ^{1}H NMR spectra of the reaction of **4.3a** with **4.4a** carried out at 25°C in molar ratio of the reactants 1:2. The spectra are recorded in deuterated chloroform at 300 MHz after 15 hours of reaction.

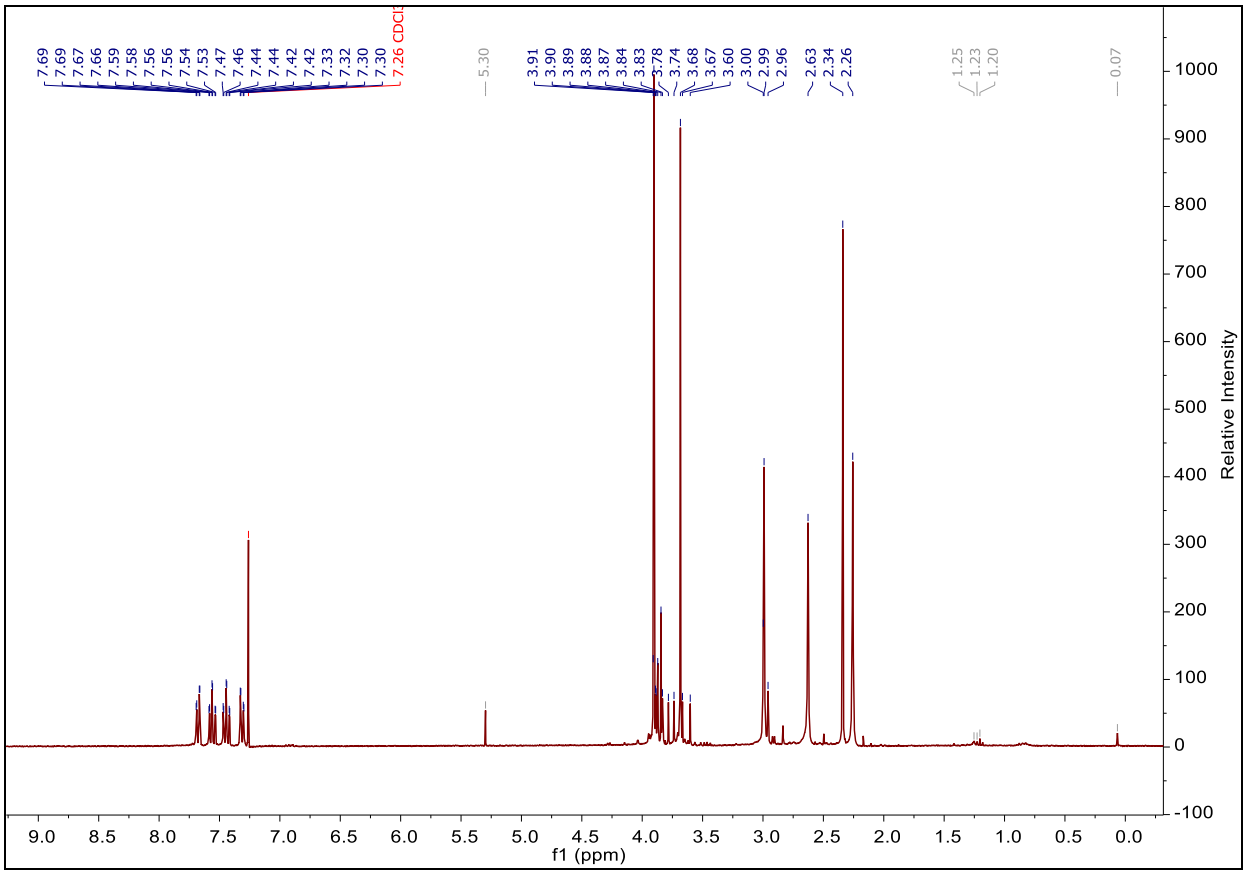

Figure SI 4.31 ^{1}H NMR spectra of the reaction of **4.3b** with **4.4a** carried out at 25ºC in molar ratio of the reactants 1:1. The spectra are recorded in deuterated chloroform at 300 MHz after 0.5 hours of reaction.

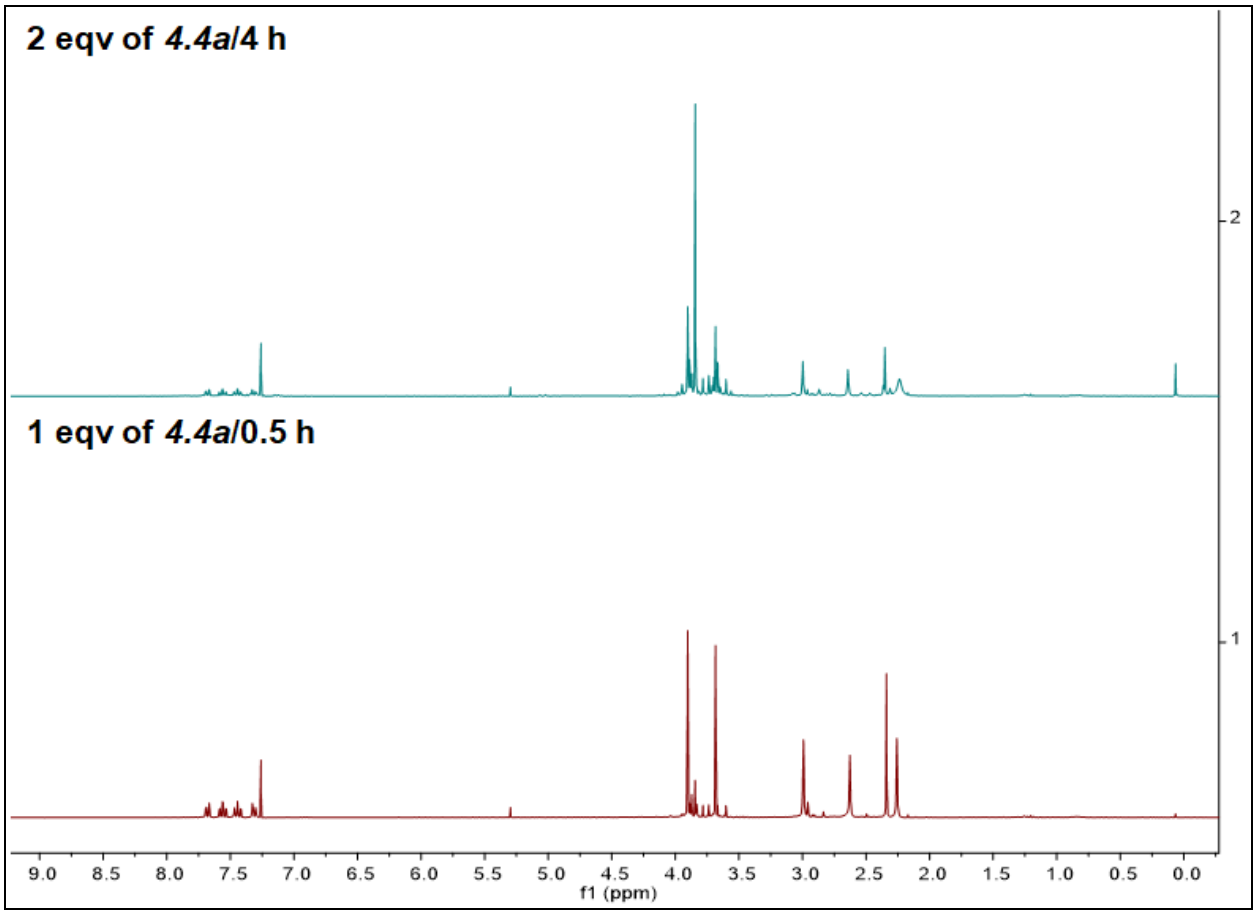

Figure 4.SI 32 Superimposed ^{1}H NMR spectra of the reaction of **4.3b** with **4.4a** carried out in molar ratio of the reactants 1:1 and 1:2, recorded at various reaction times (0.5 h and 4 h). The spectra are recorded in deuterated chloroform at 400 MHz.

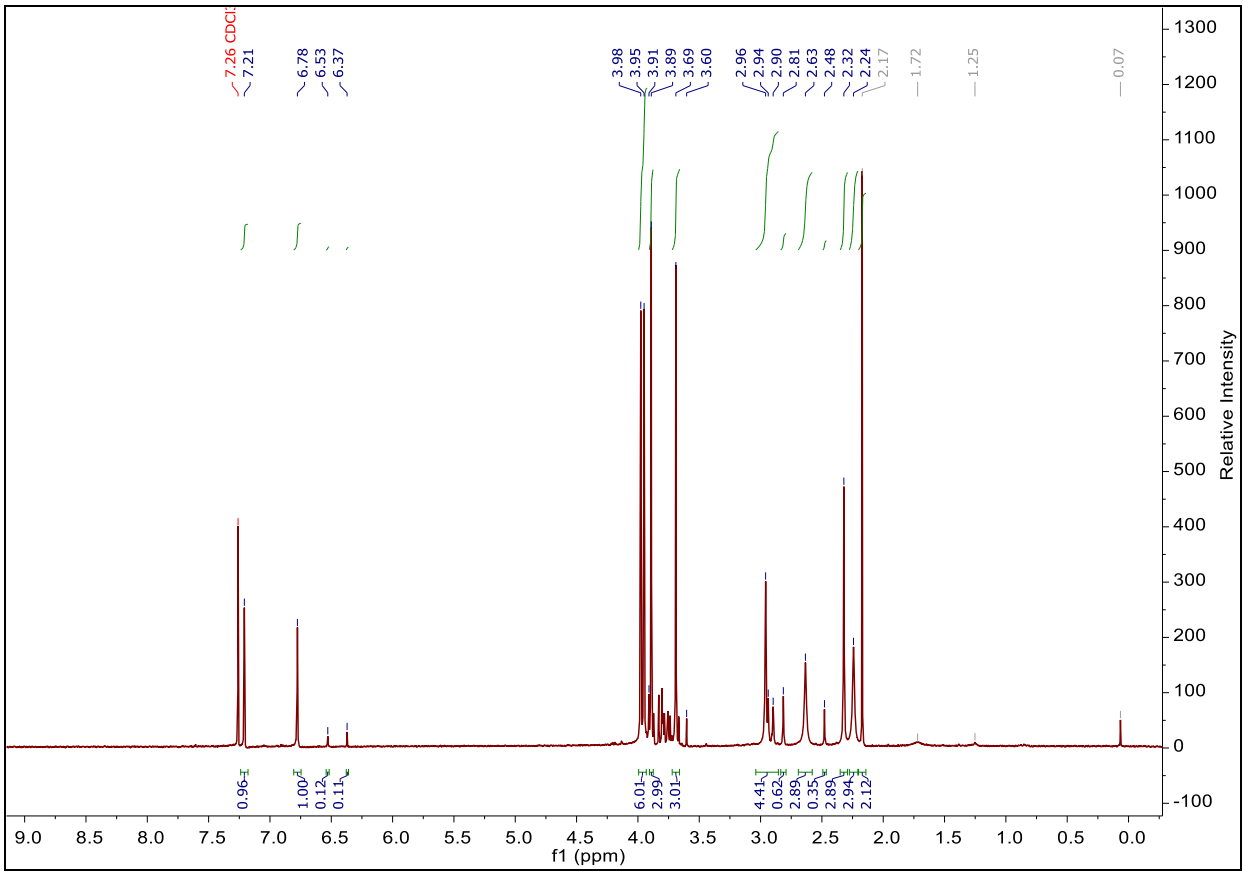

Figure SI 4.33 ^{1}H NMR spectra of the reaction of **4.3c** with **4.4a** carried out at 25ºC in molar ratio of the reactants 1:1. The spectra are recorded in deuterated chloroform at 300 MHz after 0.5 hours of reaction.

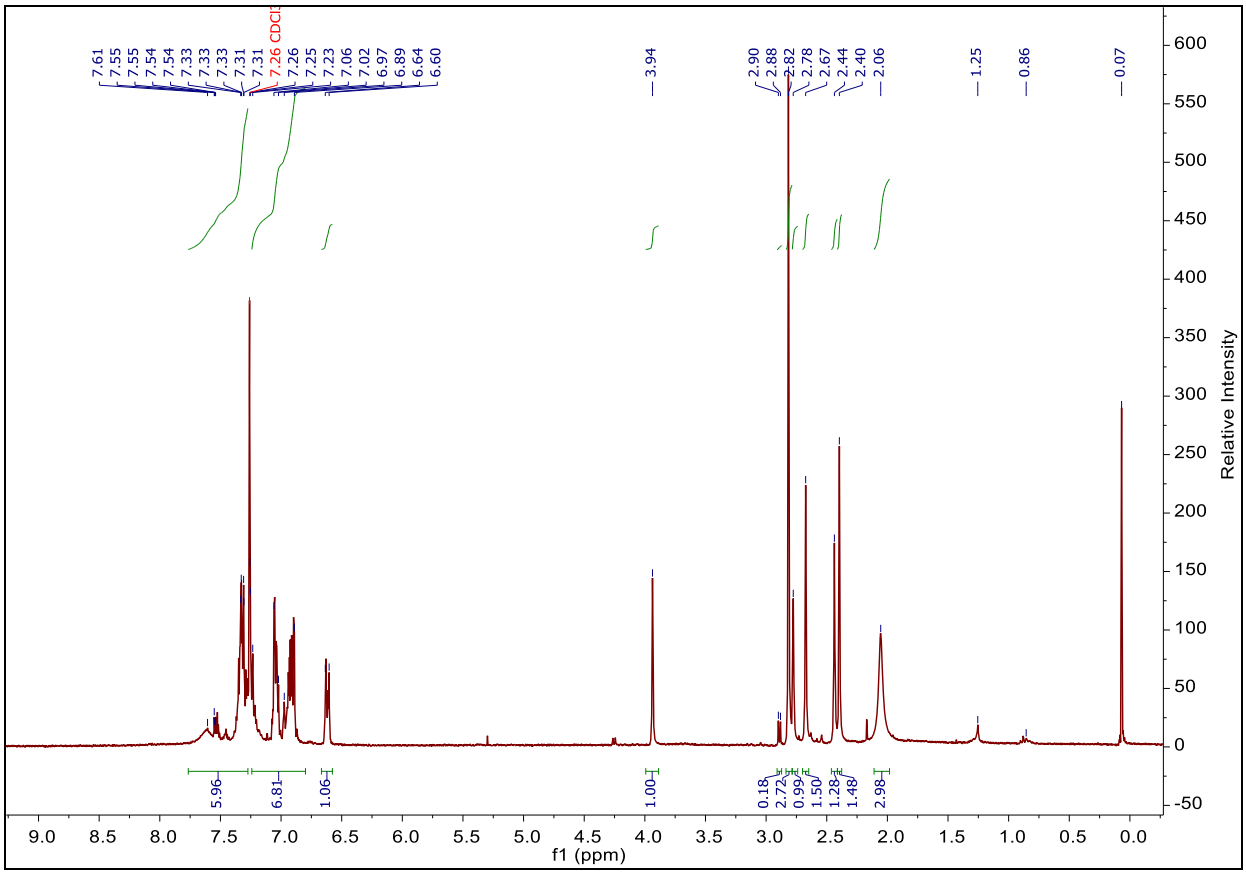

Figure SI 4.34 ^{1}H NMR spectra of the reaction of **4.3a** with **4.4b** carried out at 25ºC in molar ratio of the reactants 1:1. The spectra are recorded in deuterated chloroform at 300 MHz after 1.8 hours of reaction.

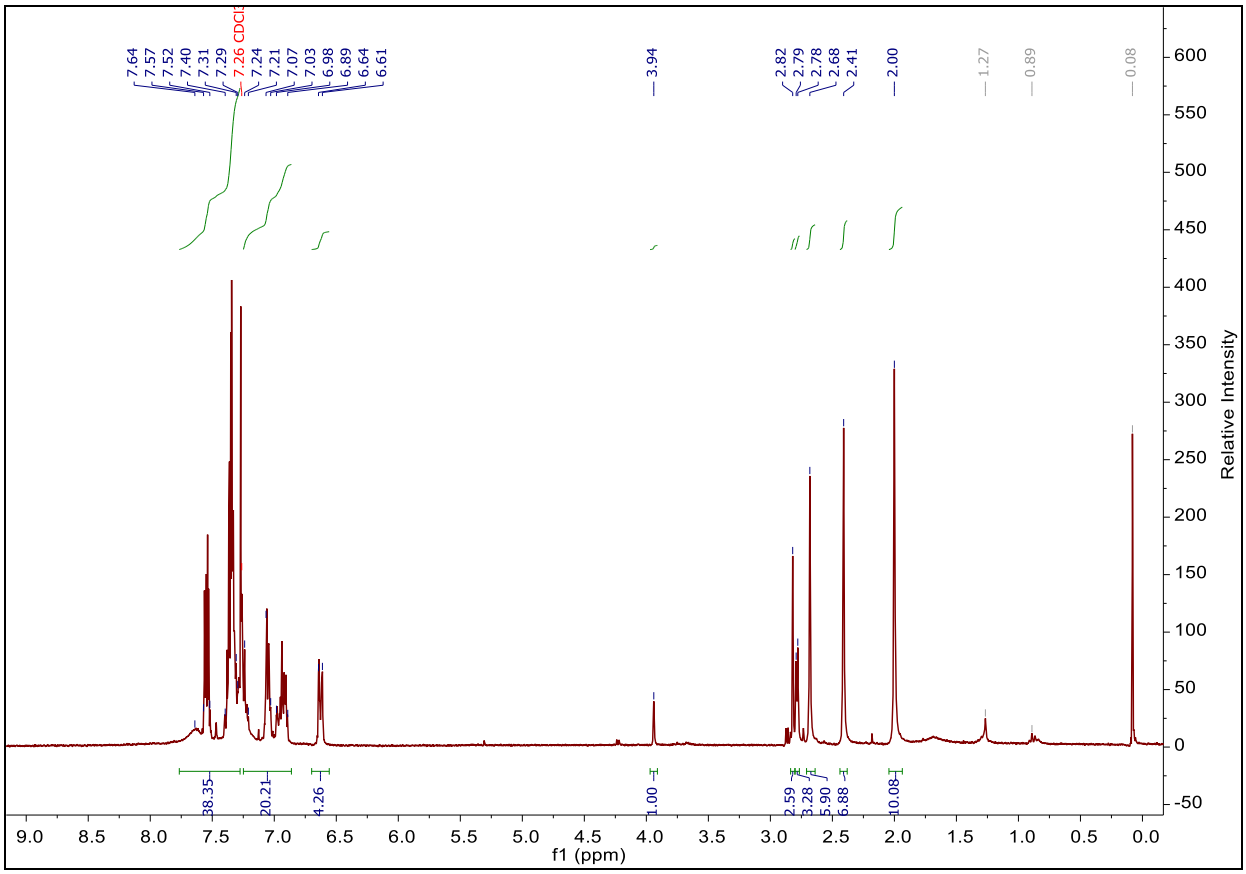

Figure SI 4.35 ^{1}H NMR spectra of the reaction of **4.3a** with **4.4b** carried out at 25°C in molar ratio of the reactants 1:2. The spectra are recorded in deuterated chloroform at 300 MHz after 3 hours of reaction.

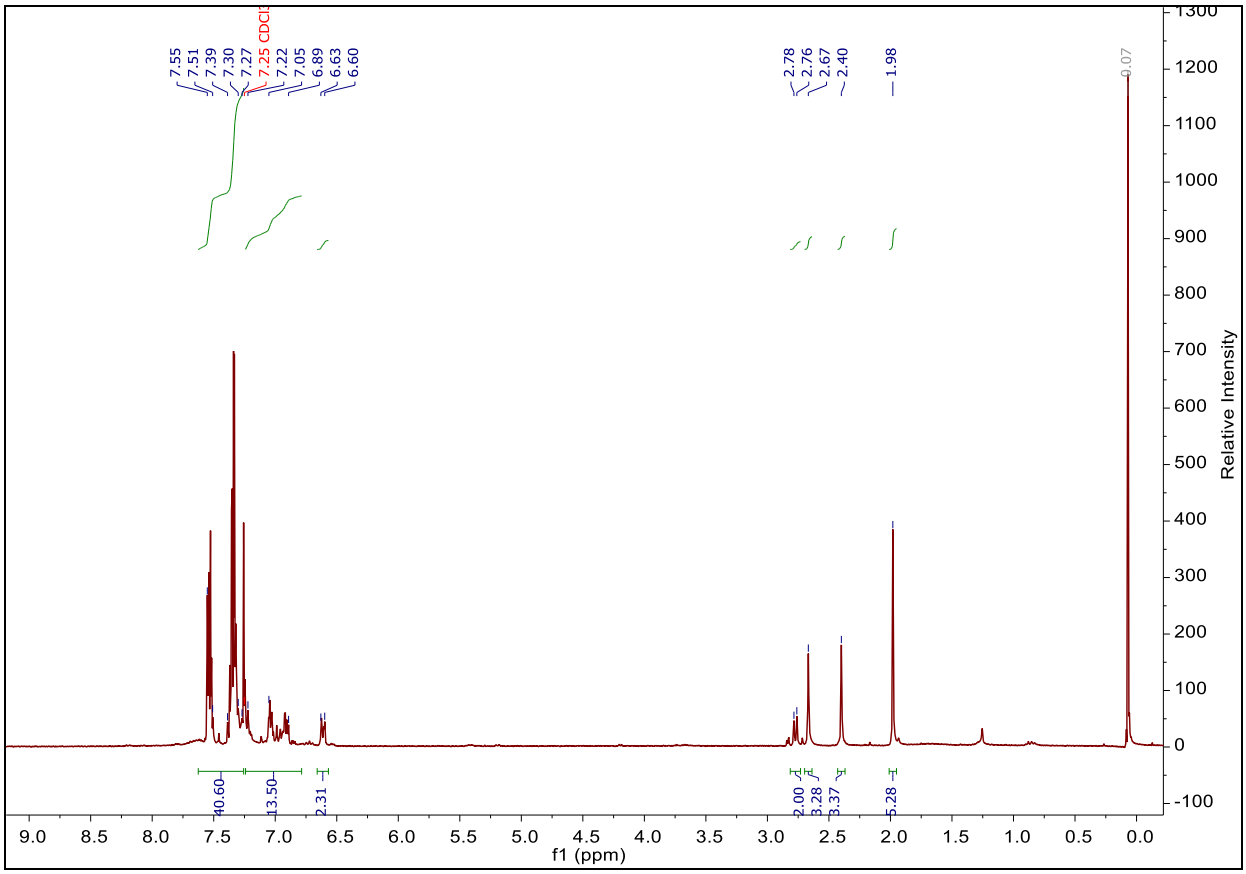

Figure SI 4.36 ^{1}H NMR spectra of the reaction of **4.3a** with **4.4b** carried out at 25ºC in molar ratio of the reactants 1:4. The spectra are recorded in deuterated chloroform at 300 MHz after 1.8 hours of reaction.

A.4.6. Cartesian's coordinates of the optimized geometries of the investigated systems within the study the insertion of the alkyne into the palladacycle.

[4.3a] - [Pd($C_6H_4CH_2NMe_2$-kC,N)$(NCMe)_2$]PF_6 -GGAPBE-D3(BJ)/TZP_PhCl (COSMO) phase

C	-2.60553680	-2.49343869	-1.17467435
C	-3.75434451	-2.59488672	-1.96757862
C	-3.63673801	-2.86924201	-3.33510849
C	-2.36995501	-3.02942753	-3.90727285
C	-1.21384406	-2.91920719	-3.11929059
C	-1.32459670	-2.65580129	-1.74639403
H	-4.74033591	-2.45908109	-1.51708188
H	-4.53225107	-2.94982627	-3.95290771
H	-2.27563132	-3.23631605	-4.97508095
H	-0.23681670	-3.03740671	-3.58725454
P	0.17054748	-2.37610037	-0.44809598
C	-2.63796935	-2.24497649	0.29836499
H	-3.50784845	-1.65663287	0.62849725
H	-2.64779058	-3.19820014	0.84405318
N	-1.37491082	-1.53594104	0.69952478
H	-0.32115303	-1.09006458	2.49036770
H	-0.53675423	0.41256593	0.59901371
C	-1.18211543	-1.67835584	2.16892801
H	-2.07866559	-1.30733297	2.68891515
H	-1.02409190	-2.73361036	2.41556651

C	-1.48419257	-0.08523776	0.36418070
H	-1.70586988	0.02580165	-0.70270143
H	-2.29249357	0.36578369	0.96319064
N	1.67714511	-1.95331556	0.99524030
C	3.40225479	-1.27511942	2.82938631
H	3.06546095	-1.66469696	3.79871157
H	3.45279189	-0.18070308	2.89720997
H	4.39233451	-1.67932921	2.58339218
C	2.44946251	-1.64904848	1.80880579
N	1.50507655	-3.27637145	-1.64597171
C	3.21548027	-4.57165357	-3.12881327
H	3.42671325	-3.99582430	-4.03974444
H	2.79767784	-5.54919863	-3.40498029
H	4.14925149	-4.72136445	-2.57069694
C	2.26717597	-3.85321938	-2.30548582
F	0.91200708	0.64077963	3.71844988
F	2.25949927	0.16757682	5.55975296
F	0.36525626	-0.31169196	6.82669755
F	-0.98381661	0.16138041	4.98740186
F	0.55293809	1.74258037	5.74029771
F	0.72398266	-1.41226237	4.80325077
P	0.63501205	0.16767691	5.27789705

[4.4a] - DMAD - ZORA-GGAPBE-D3(BJ)/TZP_PhCl (COSMO) phase

C	-1.31646443	-0.17010700	-0.08978176
C	-0.11452111	-0.01793755	0.00481133
H	-4.75989328	-2.55996640	-1.20994575
H	3.56195758	1.47902802	0.07710386
C	-2.75910538	-0.23420634	-0.17740688
O	-3.48779696	0.70075696	0.12703978
O	-3.16535655	-1.43180698	-0.63939902
C	-4.61196697	-1.57178290	-0.76864524
H	-5.07928928	-1.50789905	0.22061774
H	-5.00404806	-0.78434874	-1.42179882
O	2.04810741	-0.49140010	-0.78107898
H	3.34333675	1.86757519	1.82592083
C	1.32725528	0.10113607	0.01088724
O	1.74230961	0.94070465	0.97828765
C	3.18876227	1.12154767	1.04320826
H	3.66821261	0.17121193	1.30386541

[4.4b] - 1,2-diphenylethyne - ZORA-GGAPBE-D3(BJ)/TZP_PhCl (COSMO) phase

C	-1.32320405	-0.12633979	-0.10780139
C	-0.11160198	0.00637707	-0.02585600
H	-2.63686706	-2.44901145	-0.34594925
H	1.24814333	2.31858643	-0.07887003
C	-2.73152776	-0.28963961	-0.20788789
C	-3.58959858	0.83237177	-0.18763278
C	-4.97041649	0.66310228	-0.28122359
C	-5.51954562	-0.61962409	-0.40147817
C	-4.67650117	-1.73751542	-0.42534557
C	-3.29481598	-1.57957996	-0.32912271
H	-3.16060084	1.83032156	-0.09389201
H	-5.62232265	1.53743959	-0.26277630
H	-6.60060041	-0.74765955	-0.47047641
H	-5.09810611	-2.73943450	-0.51681845

C	1.29867376	0.15794526	0.06438715
C	2.13365479	-0.97406727	0.19486784
C	3.51660907	-0.82147374	0.28343005
C	4.09186181	0.45457800	0.23727054
C	3.27225144	1.58249253	0.10624415
C	1.88784354	1.44121273	0.02182123
H	1.68414499	-1.96684196	0.22672579
H	4.14970717	-1.70370289	0.38693133
H	5.17433661	0.56966817	0.30862777
H	3.71387646	2.57938283	0.07234248

[4.5a] - [Pd{C(CO_2Me)=C(CO_2Me)$C_6H_4CH_2NMe_2$-kC,N}$(NCMe)_2$]PF_6 - ZORA-GGAPBE-D3(BJ)/TZP_PhCl (COSMO) phase

C	0.01690497	-2.99997972	1.20810180
C	-0.25733569	-3.75942688	2.36477128
C	-0.23265241	-5.14976836	2.37075756
C	0.07382369	-5.83293206	1.18966345
C	0.35447441	-5.10222453	0.04195167
C	0.34667008	-3.68916936	0.01801375
H	-0.49738240	-3.22499997	3.28615076
H	-0.44709183	-5.69472284	3.29071730
H	0.10307717	-6.92260637	1.16465487
H	0.61099089	-5.63419191	-0.87595220
Pd	2.37874811	-1.10841994	0.12816666
C	-0.18482328	-1.51246302	1.46841103
H	-1.26997552	-1.31237054	1.53127356
H	0.22935026	-1.30913376	2.46178127
N	0.39358410	-0.48425269	0.55293258
H	0.88528498	1.57769511	0.64817081
H	-0.04009405	0.41123910	-1.32851031
C	0.44139591	0.81423274	1.29542252
H	-0.58328703	1.11076958	1.56381137
H	1.03008284	0.70180992	2.20515076
C	-0.51993399	-0.25969194	-0.60960436
H	-0.75725137	-1.20226611	-1.10220257
H	-1.44659824	0.19689141	-0.23126847
N	4.20209288	-1.78727818	-0.38012675
C	6.46257431	-2.62852684	-1.36456699
H	6.35124080	-3.66489902	-1.71000023
H	7.25145478	-2.58229022	-0.60249279
H	6.74051672	-1.99116957	-2.21483426
C	5.21051323	-2.16537377	-0.80919945
F	0.76826086	-1.65073408	6.58014132
F	-0.73580528	0.12162833	6.69858917
F	-0.14378200	0.76210387	4.54092961
F	1.50108914	0.52296089	6.17135875
F	-0.8759629	-1.41157641	4.94517244
P	0.30667680	-0.44623984	5.56601752
F	1.35865183	-1.01052503	4.42264539
C	0.75010324	-3.09022038	-1.28578667
C	1.62168216	-2.06849583	-1.43814870
H	1.13647830	-4.30852401	-5.50209587
H	1.71505323	-1.06473410	-5.35260334
C	0.08597308	-3.68661335	-2.49377236
O	-1.10402334	-3.97381296	-2.54451041
O	0.94227421	-3.84582822	-3.53131101
C	0.32010114	-4.25659698	-4.77692230
H	-0.15639844	-5.23665783	-4.65852908

H	-0.42918713	-3.51755250	-5.08557397
O	3.19601196	-1.58144334	-3.20068421
H	0.48236431	0.20578515	-5.01549766
C	2.05901232	-1.51489756	-2.75326440
O	1.04277918	-0.85649368	-3.37373905
C	1.39513486	-0.27822200	-4.65835612
H	2.20195714	0.45457144	-4.53753289
N	3.22595028	-0.20717002	1.84701061
C	4.17331072	0.67168669	4.11005598
H	3.35541496	0.67442271	4.84545152
H	4.55827115	1.69150298	3.97814411
H	4.98128409	0.01999392	4.46742312
C	3.66502017	0.17624301	2.85149440

[4.6a] - $[Pd\{(C(Ph)=C(Ph))_2C_6H_4CH_2NMe_2\text{-}kC,N\}(NCMe)]PF_6$ –
ZORA-GGAPBE-D3(BJ)/TZP_PhCl (COSMO) phase

C	-0.72455542	0.26356669	4.02613253
C	-1.89825148	0.83836184	4.34626003
C	-1.58186999	1.93640913	5.33383046
C	-0.74349727	3.01162232	4.91908913
C	-0.49585725	4.20554102	5.79846510
C	-0.95170699	5.43544422	5.28048996
H	-1.39687870	5.45372761	4.28489490
C	-0.88345213	6.61514207	6.01732498
H	-1.27201474	7.54494099	5.60212247
C	-0.30574626	6.60167054	7.28799309
H	-0.23555957	7.52120930	7.86779179
C	0.18968709	5.40102388	7.79410083
H	0.66095401	5.38628265	8.77861586
C	0.09549562	4.19527178	7.08198187
C	0.60713389	2.96377510	7.77770786
H	1.08678986	3.27500109	8.72084044
H	-0.22362880	2.29075979	8.03685658
C	2.75881638	2.95987346	6.59728176
H	2.43094611	3.80593439	5.98176158
H	3.44602184	2.33134469	6.01893362
H	3.28149230	3.34954667	7.48808156
C	2.03451458	1.03742185	7.87633474
H	2.49326187	1.44000836	8.79513803
H	2.76837576	0.42588980	7.34370178
H	1.17381054	0.41415859	8.14846097
C	-0.28594379	-0.81506449	3.14705048
C	-0.36343194	-2.16268648	3.54821658
H	-0.81733028	-2.40895970	4.50982235
C	0.13918187	-3.17556334	2.72881384
H	0.06969808	-4.21531279	3.05165706
C	0.72964043	-2.85941136	1.49938553
H	1.12526704	-3.65096590	0.86123660
C	0.81258304	-1.52132096	1.09393826
H	1.27136002	-1.26739933	0.13699564
C	0.31746019	-0.50510632	1.91260431
H	0.39657070	0.54145205	1.61011586
C	-3.26819679	0.58382217	3.87907705
C	-3.61851375	-0.60782576	3.21472201
H	-2.86872484	-1.38620761	3.07398427
C	-4.91413265	-0.80162546	2.73582531
H	-5.16357219	-1.73149793	2.22246831
C	-5.89144337	0.18619483	2.91316778

H	-6.90430295	0.03145783	2.53828900
C	-5.55904812	1.37177940	3.57688592
H	-6.30975934	2.14978812	3.72184878
C	-4.26239758	1.56676631	4.05510461
H	-4.01909667	2.50042094	4.56569669
C	-2.27811574	1.88307794	6.64816046
C	-2.31743905	0.66646583	7.35489384
H	-1.81877622	-0.20976435	6.93528155
C	-2.96267317	0.57987522	8.58839865
H	-2.96811466	-0.36585297	9.13160173
C	-3.60322763	1.70399925	9.12316825
H	-4.11052970	1.63959187	10.08698281
C	-3.59927517	2.90816659	8.41113990
H	-4.11167351	3.78351659	8.81190818
C	-2.93939116	2.99997995	7.18418910
H	-2.94581895	3.94384012	6.63867795
C	-0.44697856	3.26667914	3.46535915
C	-1.45150470	3.21463927	2.48867916
H	-2.47347644	2.96327844	2.77175818
C	-1.15768754	3.48829686	1.15040612
H	-1.95455517	3.44407376	0.40699173
C	0.14491040	3.82298021	0.76656189
H	0.37371020	4.03124349	-0.27962103
C	1.14921618	3.90515101	1.73887190
H	2.16657885	4.17963619	1.45709221
C	0.85095981	3.64161021	3.07571576
H	1.63847984	3.71441356	3.82802422
C	2.86227616	-0.79949845	4.46337332
C	3.80560534	-1.72443439	3.87734866
H	3.31752470	-2.24917819	3.04358642
H	4.13032725	-2.45526964	4.62956257
H	4.67993452	-1.17588671	3.50330973
N	1.58476595	2.14824578	6.99943945
N	2.09188117	-0.05982661	4.91904988
Pd	0.52566705	1.21439566	5.30097104
F	-2.22299075	11.09641871	9.18311188
F	-0.43689865	11.83158668	7.88168190
F	-0.68951620	9.98259662	6.48860838
F	-2.47459026	9.24865352	7.78895545
F	-2.49911100	11.39675101	6.88761355
F	-0.41345049	9.68395645	8.78376542
P	-1.45919950	10.54277704	7.83455001

A.5. Supplementary information to Chapter 8.

A.5.1. ITC data.

Table SI 5.1 Results of ITC experiments obtained by applying dimer dissociation model on integrated heat peaks and transformed to association thermodynamic parameters.

System	ITC dimer dissociation model							
	ΔH_d ± error		ΔG_d ± error		ΔS_d ± error		K_d ± error	
	kcal/mol	kcal/mol	kcal/mol	kcal/mol	cal/molK	cal/molK	M	M
5.3a	12.9	0.8	3.2	0.6	32.4	5.9	4.4E-03	8E-04
5.3b	10.1	0.6	2.9	0.5	24.3	4.5	7.8E-03	1E-03
5.3c	10.1	0.4	2.7	0.4	24.8	4.2	1.1E-02	2E-03
5.3d	4.6	0.5	2.2	1.3	8.3	5.1	2.7E-02	2E-03
5.3e	9.9	0.0						
5.3f	14.3	1.2	3.2	0.8	37.1	8.7	4.6E-03	1E-03
5.3g	11.8	0.3	1.9	0.4	33.0	6.4	3.7E-02	7E-03
5.3h	12.3	0.8	1.4	0.3	36.5	8.1	9.0E-02	2E-02
5.3i	9.3	0.3	1.4	0.2	26.6	3.4	1.0E-01	1E-02

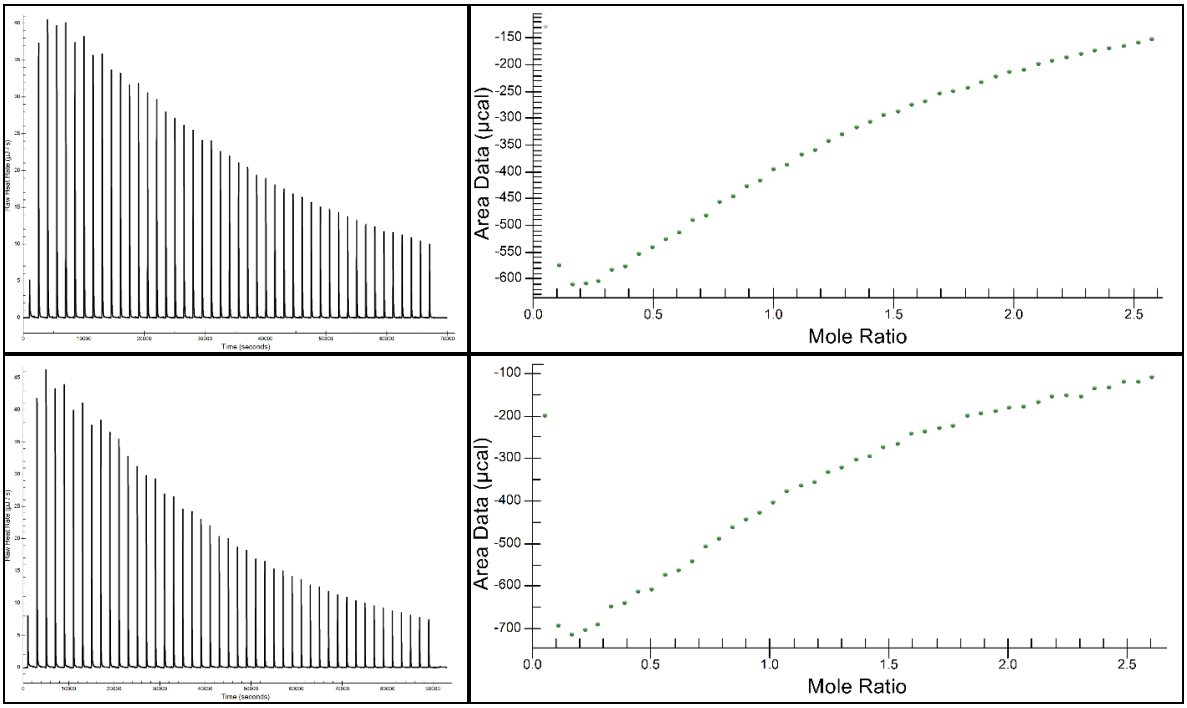

Figure SI 5.1. *up-left* – ITC thermogram of the reaction between **5.2a** (sample call, c=4.09 mM) and **5.1** (syringe, c=108.43 mM) in chlorobenzene. The titration was performed at 25ºC through 45 sequential additions (of 2.06 µL each). Time between two consecutive injections was 1500 s. Heat released is expressed in µJ/s versus time in s. *up-right* – ITC integrated heat peaks of the thermogram shown on the left side. Integrated heats are expressed in µcal versus number of injections and fitted by dimer dissociation model implemented in NanoAnalyze software. *up-left* – ITC thermogram of the reaction between **5.1** (sample call, c=4.09 mM) and **5.2a** (syringe, c=106.85 mM) in chlorobenzene. The titration was performed at 25ºC through 45 sequential additions (of 2.06 µL each). Time between two consecutive injections was 2000 s. Heat released is expressed in µJ/s versus time in s. *up-right* – ITC

integrated heat peaks of the thermogram shown on the left side. Integrated heats are expressed in µcal versus number of injections and fitted by dimer dissociation model implemented in NanoAnalyze software.

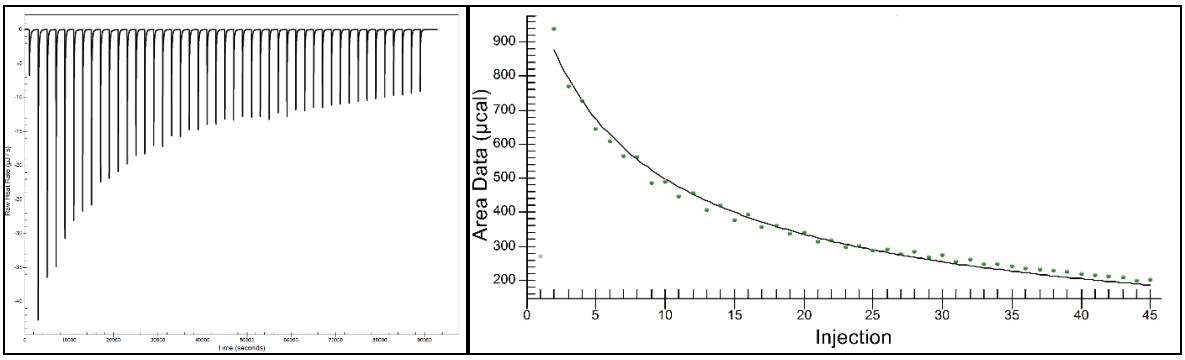

Figure SI 5.2. *left side* – ITC thermogram of the dissociation of the complex **5.1/5.2b** (syringe, c=129.99 mM) in chlorobenzene. The titration was performed at 25ºC through 45 sequential additions (of 2.06 µL each). Time between two consecutive injections was 2000 s. Heat released is expressed in µJ/s versus time in s. *right side* – ITC integrated heat peaks of the thermogram shown on the left side. Integrated heats are expressed in µcal versus number of injections and fitted by dimer dissociation model implemented in NanoAnalyze software.

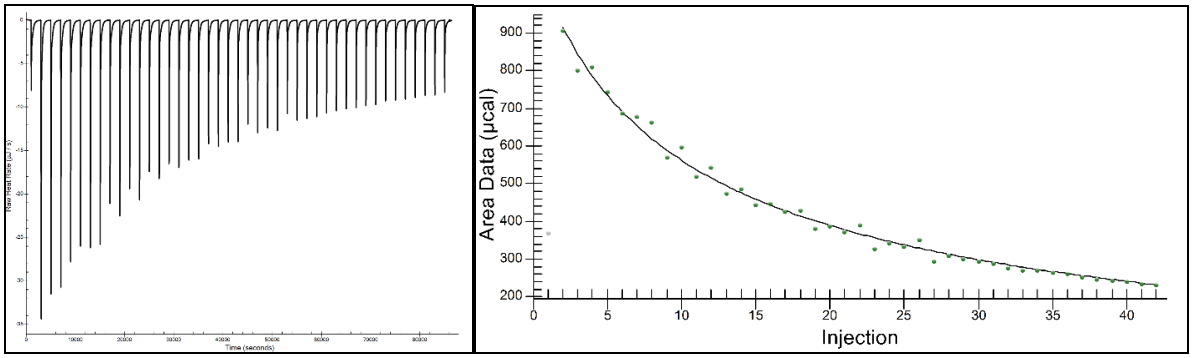

Figure SI 5.3. *left side* – ITC thermogram of the dissociation of the complex **5.1/5.2c** (syringe, c=131.36 mM) in chlorobenzene. The titration was performed at 25°C through 43 sequential additions (of 2.06 µL each). Time between two consecutive injections was 2000 s. Heat released is expressed in µJ/s versus time in s. *right side* – ITC integrated heat peaks of the thermogram shown on the left side. Integrated heats are expressed in µcal versus number of injections and fitted by the dimer dissociation model implemented in NanoAnalyze software.

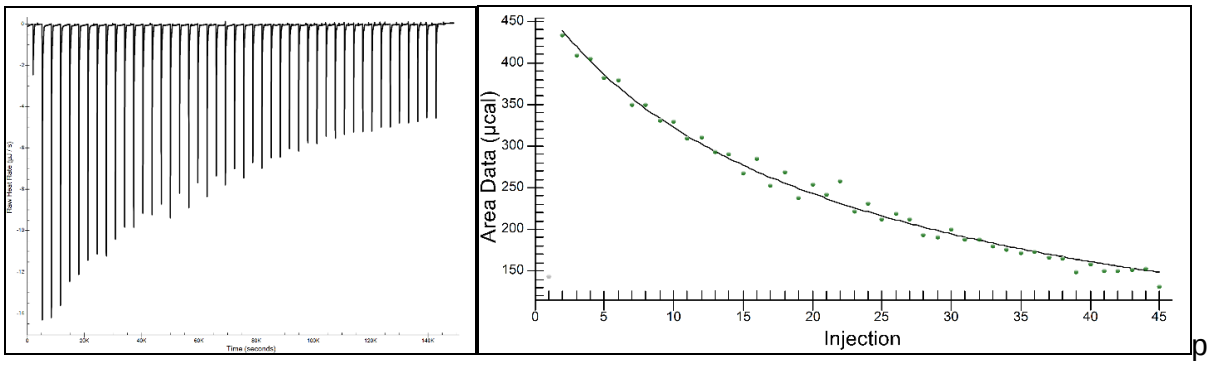

Figure SI 5.4.*left side* – ITC thermogram of the dissociation of the complex **5.1/5.2d** (syringe, c=130.45 mM) in chlorobenzene. The titration was performed at 25ºC through 45 sequential additions (of 2.06 µL each). Time between two consecutive injections was 3200 s. Heat released is expressed in µJ/s versus time in s. *right side* – ITC integrated heat peaks of the thermogram shown on the left side. Integrated heats are expressed in µcal versus number of injections and fitted by dimer dissociation model implemented in NanoAnalyze software.

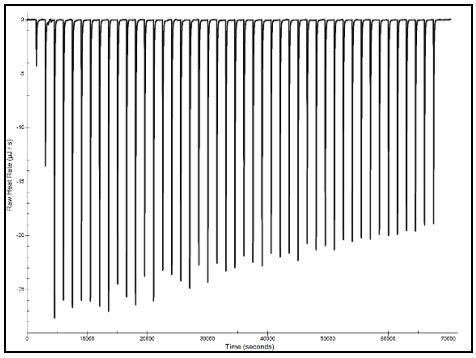

Figure SI 5.5. *left side* – ITC thermogram of the dissociation of the complex **5.1/5.2e** (syringe, c=132.07 mM) in chlorobenzene. The titration was performed at 25ºC through 45 sequential additions (of 2.06 µL each). Time between two consecutive injections was 1500 s. Heat released is expressed in µJ/s versus time in s. *right side* – ITC integrated heat peaks of the thermogram shown on the left side. Integrated heats are expressed in µcal versus number of injections and fitted by dimer dissociation model implemented in NanoAnalyze software.

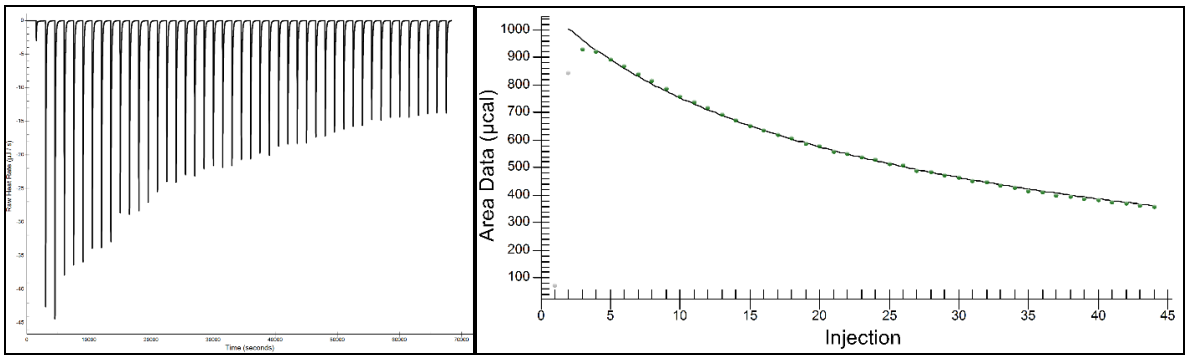

Figure SI 5.6. *left side* – ITC thermogram of the dissociation of the complex **5.1/5.2f** (syringe, c=132.11 mM) in chlorobenzene. The titration was performed at 25ºC through 44 sequential additions (of 2.06 µL each). Time between two consecutive injections was 1500 s. Heat released is expressed in µJ/s versus time in s. *right side* – ITC integrated heat peaks of the thermogram shown on the left side. Integrated heats are expressed in µcal versus number of injections and fitted by dimer dissociation model implemented in NanoAnalyze software.

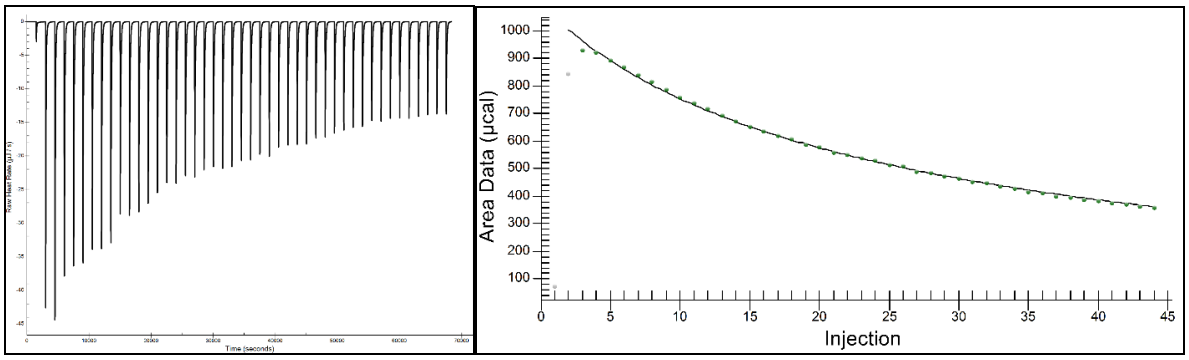

Figure SI 5.7. *left side* – ITC thermogram of the dissociation of the complex **5.1/5.2g** (syringe, c=129.14 mM) in chlorobenzene. The titration was performed at 25ºC through 44 sequential additions (of 2.06 µL each). Time between two consecutive injections was 1500 s. Heat released is expressed in µJ/s versus time in s. *right side* – ITC integrated heat peaks of the thermogram shown on the left side. Integrated heats are expressed in µcal versus number of injections and fitted by dimer dissociation model implemented in NanoAnalyze software.

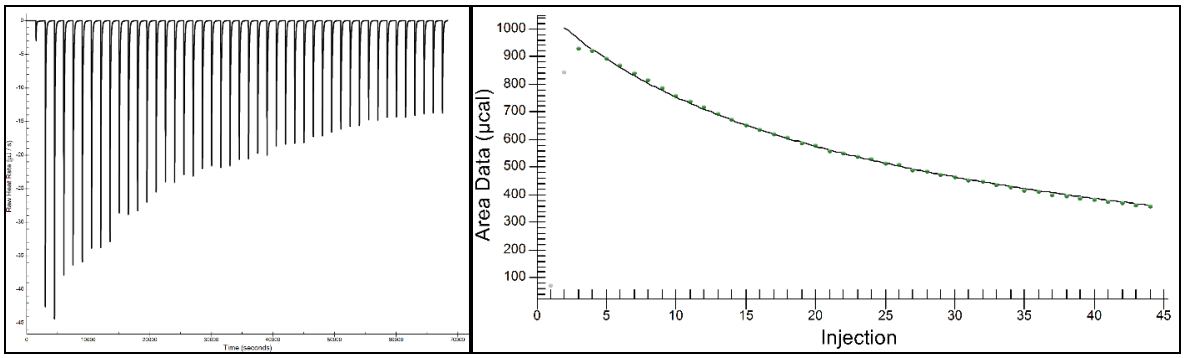

Figure SI 5.8. *left side* – ITC thermogram of the dissociation of the complex **5.1/5.2h** (syringe, c=129.14 mM) in chlorobenzene. The titration was performed at 25ºC through 44 sequential additions (of 2.06 µL each). Time between two consecutive injections was 1500 s. Heat released is expressed in µJ/s versus time in s. *right side* – ITC integrated heat peaks of the thermogram shown on the left side. Integrated heats are expressed in µcal versus number of injections and fitted by dimer dissociation model implemented in NanoAnalyze software.

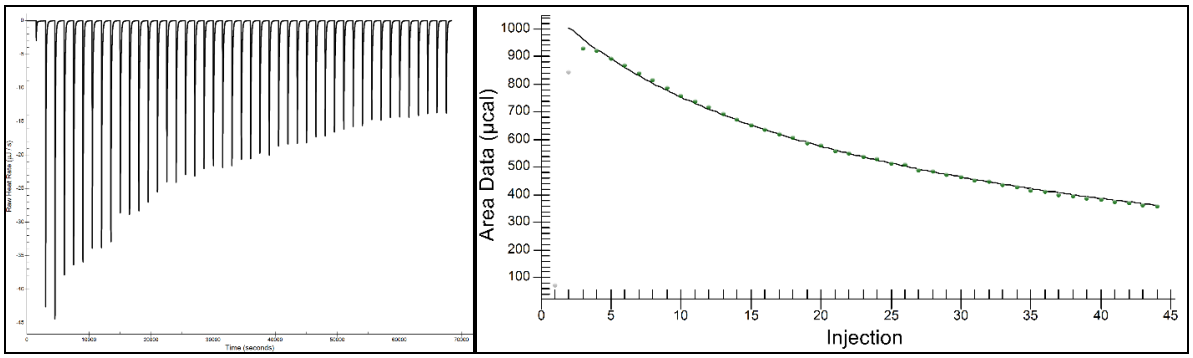

Figure SI 5.9. *left side* – ITC thermogram of the dissociation of the complex **5.1/5.2i** (syringe, c=124.84 mM) in chlorobenzene. The titration was performed at 25ºC through 44 sequential additions (of 2.06 µL each). Time between two consecutive injections was 1500 s. Heat released is expressed in µJ/s versus time in s. *right side* – ITC integrated heat peaks of the thermogram shown on the left side. Integrated heats are expressed in µcal versus number of injections and fitted by dimer dissociation model implemented in NanoAnalyze software.

A.5.2. DFT-D calculation data.

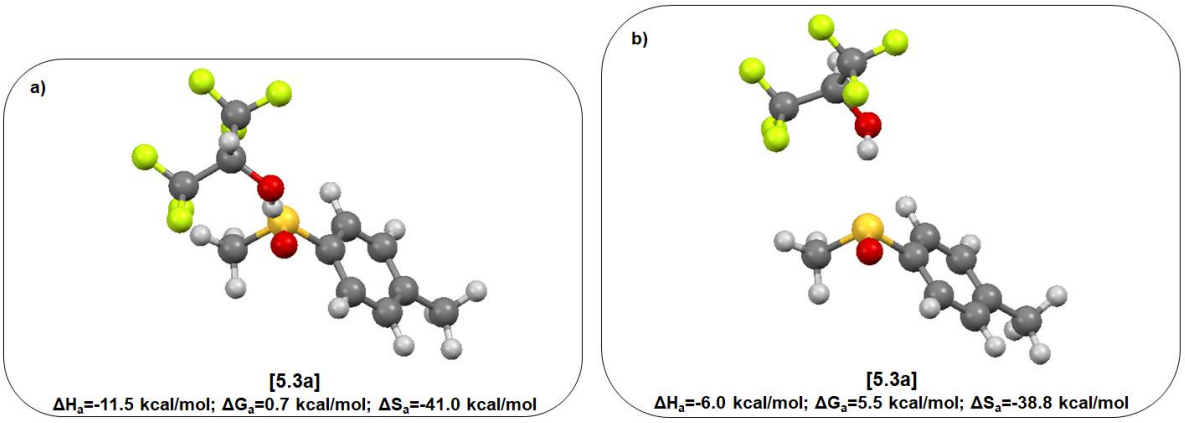

Figure SI 5.10 Graphic representations accompanied with the results of static DFT-D calculations of the **5.1/5.21** complex show the difference in thermochemical parameters of the two approaches of HFIP: *a)* oxygen atom and *b)* to sulfur atom. The calculations were performed at ZORA-GGAPBE-D3-BJ/TZP level of theory in gas phase. S: orange; O: red; F: yellowish; C: grey; H: white.

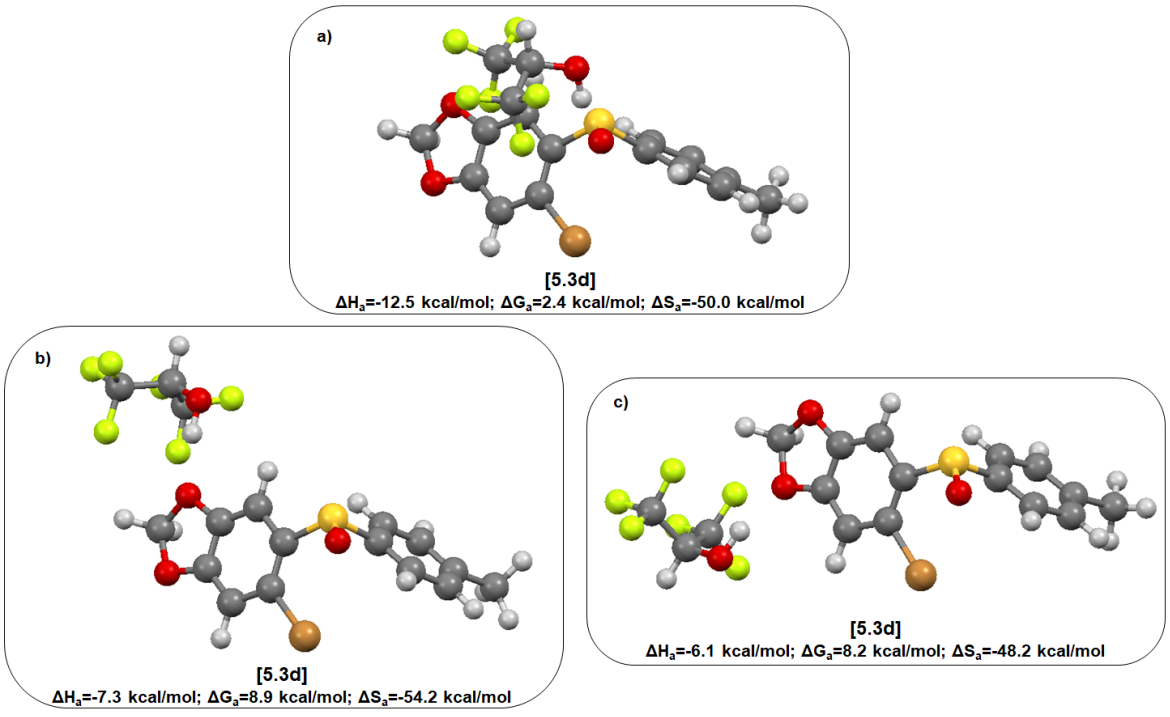

Figure SI 5.11 Graphic representations accompanied with the results of static DFT-D calculations of the **5.1/5.2d** complex show the difference in thermochemical parameters of the two approaches of HFIP: *a)* to oxygen atom doubly bonded to sulfur atom and *b)&c)* to oxygen atom that is part of *exo*-heterocyclic ring. The calculations were performed at ZORA-GGAPBE-D3-BJ/TZP level of theory in gas phase. S: orange; O: red; F: yellowish; Br: brown; C: grey; H: white.

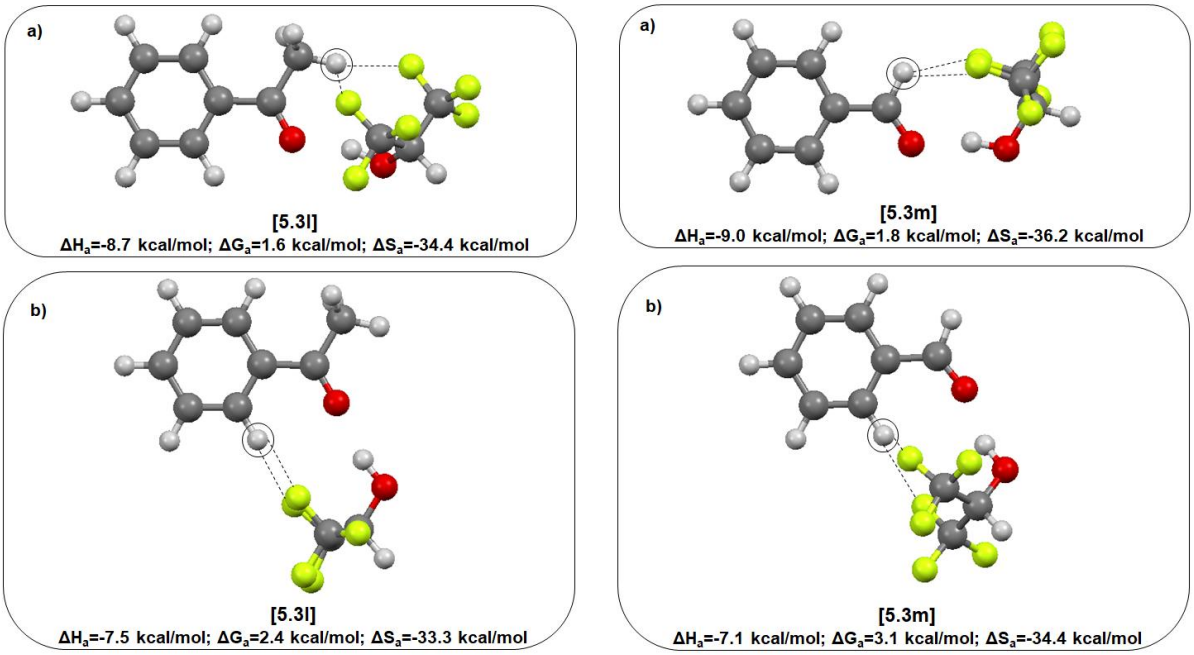

Figure SI 5.12 Graphic representations accompanied with the results of static DFT-D calculations of the **5.1/5.2l** (left hand side) and **5.1/5.2m** (right hand side) complexes show the difference in thermochemical parameters of the two approaches of HFIP: *a)* to aliphatic hydrogen and *b)* to aromatic hydrogen. The calculations were performed at ZORA-GGAPBE-D3-BJ/TZP level of theory in gas phase. O: red; F: yellowish; C: grey; H: white.

A.5.3. Synthesis and characterization.

For the sake on the authority of the group of Françoise Colobert (ECPM-Strasbourg), who has been synthesised the sulfoxides, the details of the sulfoxides' synthesises is not given.

[5.2.a]

^{1}H NMR (500 MHz, $CDCl_3$, δ ppm) 7.57 – 7.51 (m, 2H), 7.33 (dt, *J* = 8, 1 Hz, 2H), 2.70 (s, 3H), 2.41 (s, 3H).

^{13}C NMR (126 MHz, $CDCl_3$, δ ppm) 142.65, 141.65, 130.17, 123.68, 44.16, 21.54.

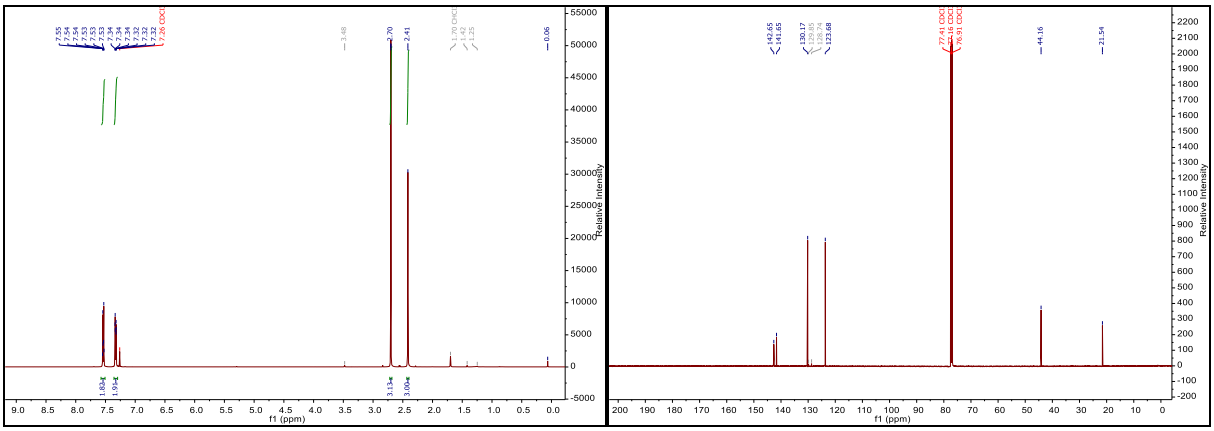

[5.2.b]

^{1}H NMR (500 MHz, $CDCl_3$, δ ppm) 7.58 – 7.52 (m, 2H), 7.34 – 7.29 (m, 2H), 2.85 (dd, *J* = 13, 7 Hz, 1H), 2.64 (dd, *J* = 13, 7 Hz, 1H), 2.41 (s, 3H), 1.03 – 0.89 (m, 1H), 0.67 – 0.56 (m, 2H), 0.34 – 0.18 (m, 2H).

^{13}C NMR (126 MHz, $CDCl_3$, δ ppm) 141.60, 140.70, 129.91, 124.39, 63.37, 21.52, 5.24, 4.96, 4.82.

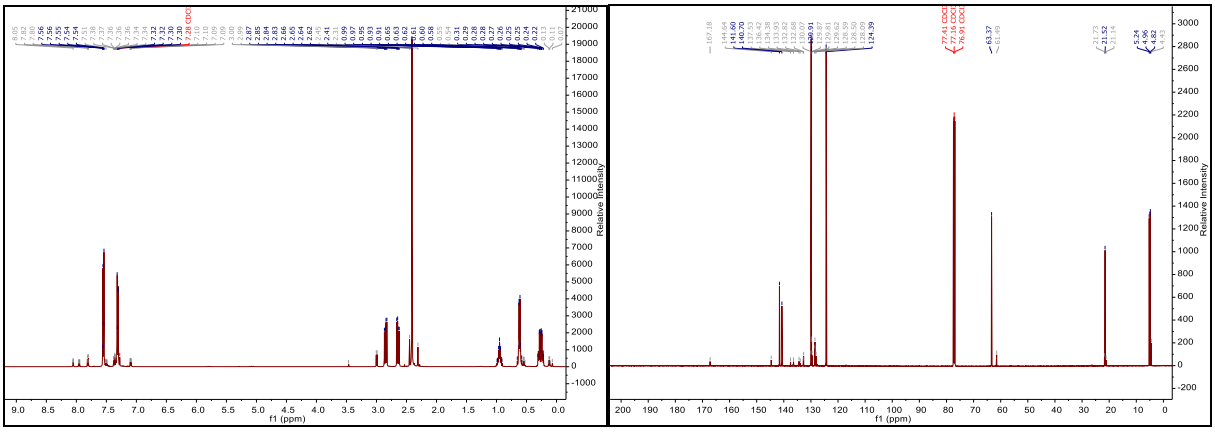

[5.2.c]

^{1}H NMR (500 MHz, $CDCl_3$, δ ppm) 8.22 (ddd, *J* = 36, 8, 1 Hz, 1H), 7.61 (tdd, *J* = 8, 5, 1 Hz, 1H), 7.48 (dtd, *J* = 19, 8, 1 Hz, 1H), 7.35 – 7.28 (m, 2H), 7.13 (dd, *J* = 8, 1 Hz, 1H), 7.09 – 7.02 (m, 2H), 7.00 (d, *J* = 8 Hz, 2H), 6.87 (d, *J* = 8 Hz, 1H), 6.50 (d, *J* = 7 Hz, 1H), 2.30 (d, *J* = 9 Hz, 3H), 1.78 (d, *J* = 467 Hz, 3H).

^{13}C NMR (126 MHz, $CDCl_3$, δ ppm) 143.95, 141.96, 141.77, 141.64, 141.07, 139.50, 137.55, 136.94, 136.86, 136.15, 131.03, 130.78, 130.54, 130.47, 130.45, 130.22, 130.21, 130.06, 129.62, 129.54, 128.68, 128.49, 128.46, 126.47, 126.07, 125.72, 125.68, 123.71, 123.65, 21.55, 21.53, 20.30, 19.45.

^{13}C NMR (126 MHz, $CDCl_3$, δ ppm) 144.01 (d, *J* = 15 Hz), 141.96, 141.70 (d, *J* = 16 Hz), 141.07, 139.84, 139.50, 137.55, 136.90 (d, *J* = 10 Hz), 136.15, 131.03, 130.78, 130.54, 130.46 (d, *J* = 3 Hz), 130.21 (d, *J* = 1 Hz), 130.06, 129.58 (d, *J* = 10 Hz), 128.68, 128.48 (d, *J* = 3 Hz), 126.47, 126.07, 125.70 (d, *J* = 4 Hz), 123.68 (d, *J* = 8 Hz), 21.54 (d, *J* = 3 Hz), 19.87 (d, *J* = 107 Hz).

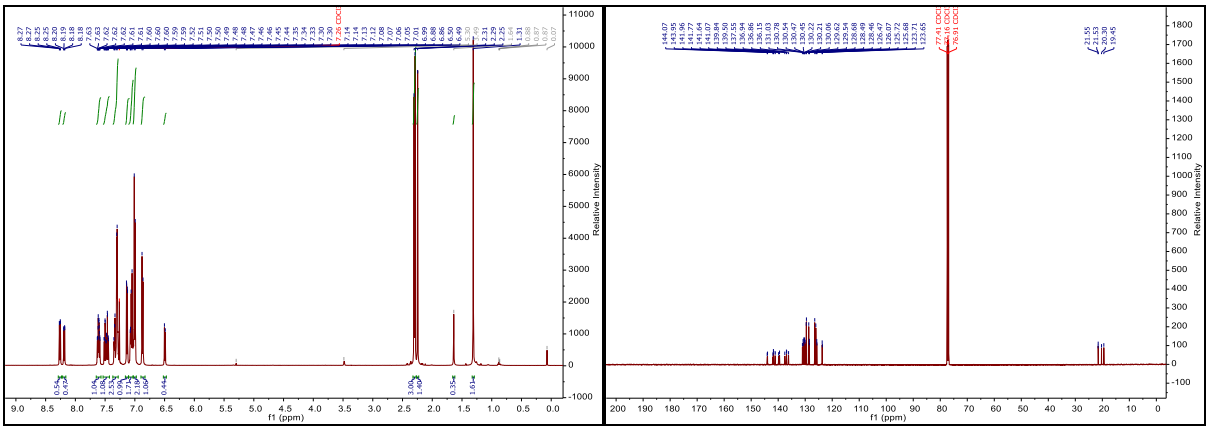

[5.2.d]

^{1}H NMR (500 MHz, $CDCl_3$, δ ppm) 7.64 – 7.58 (m, 2H), 7.42 (s, 1H), 7.26 – 7.20 (m, 2H), 6.92 (s, 1H), 6.04 (d, *J* = 1.3 Hz, 1H), 5.99 (d, *J* = 1.4 Hz, 1H), 2.35 (s, 3H).

^{13}C NMR (126 MHz, $CDCl_3$, δ ppm) 150.84, 148.73, 141.98, 141.85, 138.27, 130.01, 125.66, 112.92, 111.64, 106.01, 102.64, 21.53.

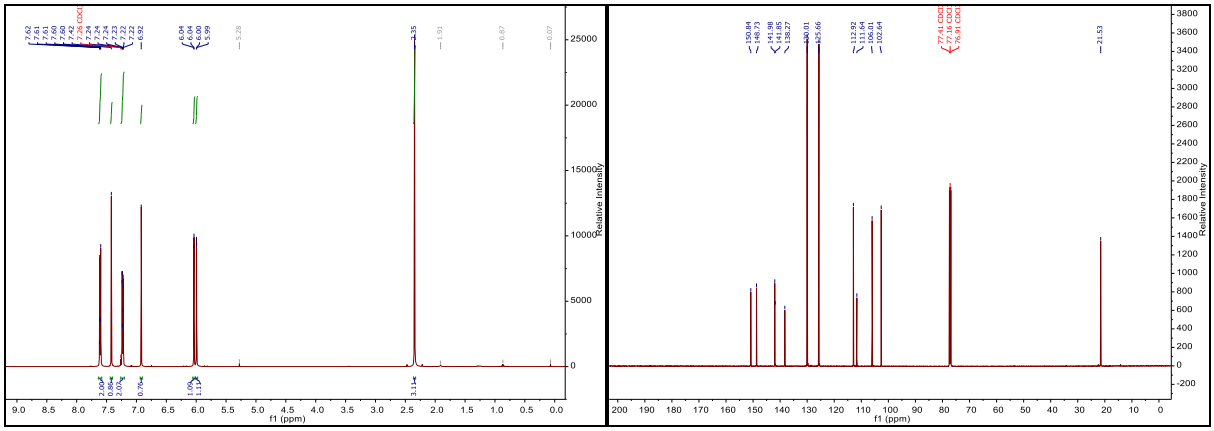

A.5.4. Purity checking by NMR

[5.2e] Aniline

^{1}H NMR (500 MHz, $CDCl_3$, δ ppm) 7.26 – 7.18 (m, 2H), 6.82 (tt, *J* = 7, 1 Hz, 1H), 6.73 – 6.67 (m, 2H), 3.64 (s, 2H).

^{13}C NMR (126 MHz, $CDCl_3$, δ ppm) 146.45, 129.26, 118.42, 115.06, 77.41, 77.16, 76.90.

[5.2f] Pyridine

^{1}H NMR (500 MHz, $CDCl_3$, δ ppm) 8.61 (dt, *J* = 4, 2 Hz, 2H), 7.66 (tt, *J* = 8, 2 Hz, 1H), 7.27 (ddd, *J* = 8, 4, 2 Hz, 2H).

^{13}C NMR (126 MHz, $CDCl_3$, δ ppm) 149.94, 135.99, 123.78.

[5.2g] 2-Phenylpyridine

^{1}H NMR (500 MHz, $CDCl_3$, δ ppm) 8.70 (dt, *J* = 5, 1 Hz, 1H), 8.03 – 7.97 (m, 2H), 7.78 – 7.69 (m, 2H), 7.52 – 7.46 (m, 2H), 7.46 – 7.38 (m, 1H), 7.22 (ddd, *J* = 6, 5, 3 Hz, 1H).
^{13}C NMR (126 MHz, $CDCl_3$, δ ppm) 157.55, 149.77, 139.50, 136.83, 129.04, 128.84, 127.00, 122.19, 120.65.

[5.2g] Benzo[*h*]quinoline

^{1}H NMR (500 MHz, $CDCl_3$, δ ppm) 9.33 – 9.27 (m, 1H), 9.01 (dd, *J* = 4, 2 Hz, 1H), 8.18 (dd, *J* = 8, 2 Hz, 1H), 7.95 – 7.89 (m, 1H), 7.82 (d, *J* = 9 Hz, 1H), 7.76 (dd, *J* = 7, 1 Hz, 1H), 7.74 – 7.65 (m, 2H), 7.53 (dd, *J* = 8, 4 Hz, 1H).
^{13}C NMR (126 MHz, $CDCl_3$, δ ppm) 148.98, 146.73, 135.98, 133.75, 131.65, 128.35, 127.97, 127.92, 127.23, 126.56, 125.50, 124.49, 121.95.

[5.2g] Dioxane

^{1}H NMR (300 MHz, $CDCl_3$, δ ppm) 7.26, 3.68, 3.68, 3.67, 1.75, 1.23, 0.05.
^{1}H NMR (300 MHz, $CDCl_3$, δ ppm) 3.71 – 3.64 (m, 8H).

A.5.5. Cartesian's coordinates of the optimized geometries of the investigated systems within the study of the affinity of Lewis donors to HFIP

[**5.1**] - 1,1,1,3,3,3-hexafluoropropan-2-ol (HFIP) - ZORA-GGAPBE-D3(BJ)/TZP_gas phase

F	2.01995651	-0.53014840	1.82099656
C	2.10411324	1.47238207	0.46671908
H	0.73191914	2.84740238	0.46671908
C	1.64284449	0.77070712	-0.83193742
F	2.18727593	1.40718430	-1.90089345
F	0.28715338	0.82536048	-0.96904070
F	2.01995651	-0.53014840	-0.88755841
C	1.64284449	0.77070712	1.76537558
F	2.18727593	1.40718430	2.83433160
F	0.28715338	0.82536048	1.90247885
O	1.71013347	2.82170938	0.46671908
H	3.20295017	1.44827383	0.46671908

[**5.1**] - 1,1,1,3,3,3-hexafluoropropan-2-ol (HFIP) - ZORA-GGAPBE-D3(BJ)/TZP_PhCl (COSMO) phase

F	2.51417032	-0.03246949	1.81376403
C	2.59852419	1.97948163	0.46671908
H	1.19832738	3.33946101	0.46671908
C	2.14619504	1.27220777	-0.83047661
F	2.70320865	1.89899596	-1.90069149
F	0.79124519	1.33238912	-0.98434064
F	2.51417032	-0.03246949	-0.88032588
C	2.14619504	1.27220777	1.76391476
F	2.70320865	1.89899596	2.83412964

F	0.79124519	1.33238912	1.91777879
O	2.17795382	3.32127218	0.46671908
H	3.69720420	1.97411659	0.46671908

[**5.2a**] - 1-methyl-4-(methylsulfinyl)benzene - ZORA-GGAPBE-D3(BJ)/TZP_gas phase

H	-2.92338426	0.23053206	-0.97605922
O	-0.14434520	-0.08047777	0.04612153
S	-1.14553789	0.98035083	0.43993878
H	-2.01761383	3.77902486	0.93555768
H	-2.96139424	2.02490771	-0.78546471
C	-2.32257283	1.14859844	-0.95929514
H	-1.74185400	1.25912739	-1.88324135
C	-0.34523623	2.59980567	0.20539156
C	0.96811892	2.60684837	-0.25128651
C	1.62891008	3.82897746	-0.40425232
C	0.99391888	5.04093195	-0.10090860
C	-0.32783353	5.00103462	0.37964051
C	-0.99778135	3.79024734	0.54393231
H	1.44961188	1.65357252	-0.47423236
H	2.66053361	3.83944113	-0.76355207
H	2.75903004	6.20942834	-0.54162237
H	-0.83581055	5.93440751	0.63486899
C	1.70310400	6.35877258	-0.28432310
H	1.23961906	6.94550429	-1.09175051
H	1.65612815	6.96858221	0.62902455

[**5.2b**] - 1-(cyclopropylsulfinyl)-4-methylbenzene - ZORA-GGAPBE-D3(BJ)/TZP_gas phase

H	-4.09770745	0.26932389	-1.96468351
O	-0.28106711	0.00217705	-0.19743065
S	-1.21836357	1.08068948	0.30312745
H	-1.94338229	3.83542285	1.05841556
H	-2.72292487	-0.78492703	-1.32472108
H	-1.02914326	0.54267705	-2.53182582
H	-2.32849800	1.64765375	-3.25685367
C	-0.34806321	2.67149672	0.16039712
C	0.94464112	2.67331235	-0.35811275
C	1.64382920	3.87834475	-0.43296182
C	1.06809696	5.08209494	0.00646600
C	-0.23164100	5.04639719	0.53510062
C	-0.94064875	3.84724627	0.62483799
H	1.37978458	1.72719010	-0.68308790
H	2.66012473	3.88475977	-0.83489803
H	2.82623968	6.28682614	0.37574424
H	-0.69157520	5.97079491	0.89206205
C	1.83433833	6.37758809	-0.08908758
H	1.99281481	6.66428686	-1.13955321
H	1.29920519	7.19737684	0.40619548
C	-2.41271519	1.39927575	-1.04722576
C	-3.04770644	0.19343653	-1.68214022
C	-2.01374012	1.00365913	-2.43619476
H	-3.00146735	2.30212638	-0.87317681

[**5.2c**] - 2-methyl-2'-(p-tolylsulfinyl)-1,1'-biphenyl - ZORA-GGAPBE-D3(BJ)/TZP_gas phase

C	2.89452492	4.76935727	-0.74654157

O	-1.41486720	-0.05159465	1.12678197
S	-1.93554404	1.30479070	0.70749961
H	-1.72081342	3.98555051	-0.48292288
H	2.92586410	4.99242740	-1.82370871
H	2.85436485	5.73265105	-0.21729608
H	-0.90224579	2.17445119	-4.81937027
C	-0.51519972	2.31113708	0.18821751
C	0.76322211	1.81932418	0.42829411
C	1.86593436	2.62097345	0.12130277
C	1.70370983	3.90885224	-0.40630813
C	0.39732951	4.38756678	-0.61432671
C	-0.71225850	3.60205463	-0.31480346
H	0.87488279	0.81331611	0.83335871
H	2.87330135	2.23435185	0.29293225
H	3.83503953	4.27279770	-0.47751889
H	0.24914396	5.39258945	-1.01746222
C	-2.81392851	1.24159261	-0.89919306
C	-4.15465181	1.63057288	-0.78489919
C	-4.97542615	1.68858110	-1.91123352
C	-4.44370280	1.34790191	-3.15597279
C	-3.10909036	0.95334593	-3.26482608
C	-2.26010373	0.88616814	-2.14799737
H	-4.54535183	1.89812206	0.19922124
H	-6.01839529	1.99255199	-1.81537993
H	-5.07177647	1.38007239	-4.04767914
H	-2.70633700	0.66978864	-4.23820554
C	-0.85374024	0.43051191	-2.32207630
C	-0.42824448	-0.72995999	-1.65716909
C	0.87022986	-1.21173612	-1.81527055
C	1.76352495	-0.52831598	-2.64117937
C	1.34709960	0.62818900	-3.30233699
C	0.04354315	1.12498668	-3.16756563
H	-1.12332927	-1.24268079	-0.99473442
H	1.18053413	-2.11419099	-1.28729404
H	2.78518176	-0.89037411	-2.76881095
H	2.05175865	1.17185348	-3.93629390
C	-0.34544591	2.38956096	-3.89439049
H	-0.98318317	3.03113240	-3.27161513
H	0.55018343	2.95942073	-4.17366440

[**5.2c**] - 2-methyl-2'-(p-tolylsulfinyl)-1,1'-biphenyl - ZORA-GGAPBE-D3(BJ)/TZP_PhCl (COSMO) phase

C	3.208644	4.301499	-2.619153
O	0.278675	-0.545487	1.048819
S	-0.296982	0.862032	1.026459
H	-0.570508	3.609157	0.070102
H	2.785828	4.344935	-3.635102
H	3.271951	5.334529	-2.251125
H	-2.357815	2.139916	-4.047431
C	0.690771	1.852010	-0.127262
C	1.864466	1.313176	-0.646767
C	2.681910	2.116655	-1.447218
C	2.344598	3.450559	-1.723794
C	1.164969	3.973250	-1.162075
C	0.339640	3.187026	-0.360647
H	2.117705	0.274869	-0.432571
H	3.598883	1.696310	-1.866359
H	4.224309	3.894241	-2.699822
H	0.889741	5.012654	-1.354869

C	-1.903129	0.929854	0.162247
C	-2.940020	1.344867	1.009775
C	-4.234573	1.509024	0.514781
C	-4.483279	1.253349	-0.835780
C	-3.447153	0.835051	-1.674676
C	-2.135126	0.658034	-1.204006
H	-2.721378	1.550683	2.059481
H	-5.037337	1.833268	1.177585
H	-5.489142	1.373132	-1.240666
H	-3.656438	0.624421	-2.724384
C	-1.080583	0.175169	-2.138460
C	-0.455135	-1.055398	-1.882010
C	0.511796	-1.566347	-2.748404
C	0.868742	-0.839492	-3.886240
C	0.252026	0.386929	-4.145633
C	-0.730413	0.913846	-3.294421
H	-0.725944	-1.606818	-0.982982
H	0.985730	-2.523983	-2.529434
H	1.628611	-1.222121	-4.569706
H	0.543117	0.962017	-5.027721
C	-1.351539	2.250757	-3.616149
H	-1.449646	2.871398	-2.714854
H	-0.734983	2.791845	-4.344900

[**5.2d**] - 5-bromo-6-(p-tolylsulfinyl)benzo[d][1,3]dioxole - ZORA-GGAPBE-D3(BJ)/TZP_gas phase

C	2.64315691	5.08648614	-0.48551498
O	-1.23322863	-0.24541127	0.77743130
S	-1.86578058	1.11406023	0.67183932
H	-1.88096718	4.00882431	0.13732351
H	2.96377602	5.02840690	-1.53708208
H	2.33093668	6.12015842	-0.28988776
H	-3.11059276	0.64429537	-4.21721562
C	-0.55415886	2.29667541	0.23291592
C	0.75721225	1.83330173	0.18449833
C	1.78842889	2.74518380	-0.04521473
C	1.52411366	4.11342757	-0.21475595
C	0.19154168	4.55141815	-0.14217117
C	-0.84988144	3.65335259	0.08506703
H	0.94359268	0.76865294	0.32720336
H	2.81986143	2.38716672	-0.08887508
H	3.52162730	4.86769048	0.13643961
H	-0.03261726	5.61375581	-0.26258477
C	-2.85120454	1.29000806	-0.85406743
C	-4.06836899	1.97212341	-0.63305127
C	-4.88224446	2.18894326	-1.72447288
C	-4.53897978	1.71738497	-2.99230767
C	-3.36831419	1.01931949	-3.22878573
C	-2.51658011	0.82200309	-2.12735501
H	-4.34361950	2.30309850	0.36874770
O	-6.12103110	2.79580757	-1.76779543
O	-5.54252824	2.00901445	-3.88797392
Br	-0.87312234	-0.10333978	-2.47149630
C	-6.44318853	2.87907207	-3.16958452
H	-6.29684145	3.91611307	-3.51695337
H	-7.47319427	2.53549380	-3.32358843

[**5.2e**] - aniline - ZORA-GGAPBE-D3(BJ)/TZP_gas phase

C	-1.62491834	4.74867777	-2.66494609
C	-0.20614227	6.71307808	-2.86473032
C	-1.47859494	6.13493986	-2.70739983
C	-0.51167833	3.90895984	-2.77374897
H	-0.63101795	2.82559588	-2.74389861
H	-2.35485316	6.78256650	-2.61908314
N	-0.04815047	8.10941661	-2.85843623
C	0.91182122	5.86595904	-2.96803193
C	0.75584163	4.48073580	-2.92323682
H	-2.62216382	4.32100673	-2.54843568
H	1.90718010	6.30309137	-3.08298868
H	1.63661753	3.84226709	-3.01031777
H	-0.87082480	8.61544994	-3.17691774
H	0.77989983	8.42854325	-3.35520350

[**5.2f**] - pyridine - ZORA-GGAPBE-D3(BJ)/TZP_gas phase

H	4.21883950	6.19990337	-3.25043786
H	1.79731598	2.63691421	-2.97811735
H	4.06870875	3.70861120	-3.20274976
C	1.90486582	3.72294726	-3.00280041
C	3.16350997	4.31395990	-3.12723709
C	3.24603813	5.70905847	-3.15379918
N	2.18230886	6.52437640	-3.06647215
C	0.97977872	5.93818733	-2.94729116
C	0.78707961	4.55422462	-2.91068994
H	0.12251593	6.61405419	-2.87716910
H	-0.21889106	4.14212056	-2.81205163

[**5.2g**] - quinoline - ZORA-GGAPBE-D3(BJ)/TZP_gas phase

C	-1.62503530	4.80173548	-2.69094065
C	-0.20165181	6.76392046	-2.84921885
C	-1.45822888	6.20841162	-2.72545512
C	-0.52955106	3.96893872	-2.78096764
C	3.16966807	4.31941900	-3.12788074
C	3.22696492	5.73516381	-3.15238921
N	2.17299593	6.52967354	-3.06568268
C	0.94647248	5.93476647	-2.94416419
C	0.77647571	4.50991794	-2.90910806
C	1.94132618	3.70846053	-3.00597627
H	1.84896507	2.62036726	-2.98267012
H	4.08901107	3.73792328	-3.20502527
H	4.19701400	6.23146544	-3.24884733
H	-2.62554451	4.37953913	-2.59267059
H	-0.65113904	2.88401300	-2.75500114
H	-2.33385721	6.85447815	-2.65323006
H	-0.04959439	7.84326276	-2.87792785

[**5.2h**] - benzo[h]quinoline - ZORA-GGAPBE-D3(BJ)/TZP_gas phase

C	-1.62028727	4.76373837	-2.69086427
C	-0.20867257	6.78607277	-2.84887003
C	-1.49778113	6.19113926	-2.72156240

C	-0.52388915	3.95700254	-2.78132939
C	3.18233217	4.31316881	-3.12896730
C	3.24196829	5.71957702	-3.15356546
N	2.17969653	6.51237411	-3.06606773
C	0.95867119	5.93084767	-2.94523933
C	0.78844002	4.51469742	-2.91027955
C	1.94434969	3.71108288	-3.00629151
C	-2.63411382	7.02843758	-2.62781822
H	4.09682287	3.72459151	-3.20556693
H	4.20912662	6.22025791	-3.24981561
H	-3.38766554	9.03911929	-2.58539968
C	-0.09888636	8.19260954	-2.87810854
H	1.84467411	2.62376851	-2.98231938
C	-1.22729931	8.98981525	-2.78455293
C	-2.50350725	8.40515327	-2.65857790
H	-0.62831092	2.87103991	-2.75693660
H	-3.61913712	6.56849997	-2.53046846
H	-2.61707062	4.33111532	-2.59279737
H	-1.12955436	10.07579442	-2.80832837
H	0.89583338	8.62443191	-2.97597371

[**5.2i**] - 1,4-dioxane - ZORA-GGAPBE-D3(BJ)/TZP_gas phase

O	1.90388380	6.91626347	-0.02209398
C	3.20638416	8.82214943	0.75160702
C	1.94404471	8.34800231	0.04676032
C	3.07598990	6.43800434	-0.69564087
C	4.33832935	6.91215146	0.00920584
O	4.37849026	8.34389030	0.07806013
H	4.37384628	6.48744917	1.03135334
H	3.20367484	8.46194854	1.79882572
H	3.26910014	9.91951236	0.74885768
H	1.90852778	8.77270460	-0.97538719
H	1.04570317	8.66063974	0.59756570
H	3.07869921	6.79820523	-1.74285956
H	3.01327392	5.34064141	-0.69289153
H	5.23667088	6.59951403	-0.54159955

[**5.2j**] - 2-phenylpyridine - ZORA-GGAPBE-D3(BJ)/TZP_gas phase

H	-3.66339718	6.65340959	-2.52752669
C	-0.25851507	6.74844430	-2.84374932
C	-1.55957537	6.23000528	-2.71637410
H	0.90895995	8.54315326	-2.97608506
C	3.23464380	4.34628635	-3.13425518
C	3.23573470	5.74249323	-3.15329981
N	2.13352560	6.49421238	-3.06155075
C	0.93904346	5.87308161	-2.94264010
C	0.84690742	4.46916706	-2.91506971
C	2.00302300	3.70139293	-3.01158700
C	-2.66307152	7.07775686	-2.62580895
H	4.16830842	3.78803487	-3.21303976
H	4.17836147	6.28936828	-3.24790769
H	-3.35452507	9.12713396	-2.58965918
C	-0.09995279	8.14503803	-2.87736446
H	1.94280331	2.61187313	-2.99123440
C	-1.20244217	8.99254615	-2.78688913
C	-2.49067098	8.46422055	-2.66056661

H	-1.05579226	10.07367244	-2.81512217
H	-1.72609212	5.15366538	-2.68636842
H	-0.11921227	3.97641713	-2.81902323

[**5.2k**] - 1,10-phenanthroline - ZORA-GGAPBE-D3(BJ)/TZP_gas phase

C	-1.63228428	4.75803447	-2.68967722
C	-0.23184236	6.80230660	-2.84694721
C	-1.51360326	6.18463217	-2.72001065
C	-0.52839456	3.96334199	-2.78099867
C	3.17095873	4.33484286	-3.12820939
C	3.22588449	5.74333530	-3.15240014
N	2.16525035	6.53532284	-3.06504290
C	0.94840068	5.95264721	-2.94458514
C	0.77816738	4.53478177	-2.90960189
C	1.93554355	3.73115432	-3.00574932
C	-2.64310676	7.02733410	-2.62697145
H	4.08696697	3.74838103	-3.20497809
H	4.19266033	6.24636029	-3.24864672
H	-3.31838273	9.07950752	-2.59235595
N	-0.07373500	8.14717300	-2.87981842
H	1.83603575	2.64415286	-2.98179695
C	-1.16117177	8.90158613	-2.78947227
C	-2.47116003	8.39661576	-2.66145400
H	-0.62140236	2.87633034	-2.75764739
H	-3.63572855	6.58328724	-2.52913447
H	-2.62700490	4.32016774	-2.59172997
H	-0.99776385	9.98295734	-2.81925866

[**5.2l**] - acetophenone - ZORA-GGAPBE-D3(BJ)/TZP_gas phase

C	1.44697711	0.54725396	-0.10583032
C	0.19873312	-0.06067047	-0.31933770
C	0.06338215	-1.44328662	-0.22904529
C	1.17493886	-2.23776661	0.07725722
C	2.42155511	-1.64371991	0.29143621
C	2.55782546	-0.25784505	0.19930348
H	-0.64931966	0.58210306	-0.55624922
H	-0.90953820	-1.90851773	-0.39608325
H	1.06861979	-3.32160218	0.14860800
H	3.28849643	-2.26138159	0.53015723
H	3.53496342	0.19609481	0.36886673
H	3.26628905	2.47422886	1.02301031
C	1.54099121	2.03865595	-0.21414222
H	2.77264461	3.78188215	-0.10064742
O	0.55092649	2.71625042	-0.48329077
C	2.88725929	2.69987426	0.01579154
H	3.63103715	2.32807886	-0.70399584

[**5.2m**] - benzaldehyde - ZORA-GGAPBE-D3(BJ)/TZP_gas phase

C	1.42622393	0.54345612	-0.19444134
C	0.16108987	-0.06474330	-0.25212754
C	0.04757213	-1.44079058	-0.07552656
C	1.19277491	-2.21522528	0.15980831
C	2.45411740	-1.61450644	0.21831711
C	2.56955487	-0.23616530	0.04059975

H	-0.71087468	0.56445404	-0.43589431
H	-0.93205253	-1.91942522	-0.11996068
H	1.09917411	-3.29369085	0.29800225
H	3.34180502	-2.22105381	0.40170323
H	3.54801230	0.24913871	0.08263141
O	0.65994426	2.78654454	-0.58626702
C	1.57568800	2.00225333	-0.37827950
H	2.63313199	2.36667466	-0.31343920

[**5.2n**] - chlorobenzene - ZORA-GGAPBE-D3(BJ)/TZP_gas phase

C	1.29293144	0.37357249	-0.00021049
C	0.06156586	-0.28362868	-0.00183604
C	0.04179423	-1.68091129	-0.00314421
C	1.23611189	-2.40710887	-0.00282827
C	2.45909797	-1.73030754	-0.00119153
C	2.49642226	-0.33338361	0.00013081
H	-0.86279840	0.29326348	-0.00206685
H	-0.91722040	-2.20090446	-0.00441776
H	1.21382861	-3.49762590	-0.00385490
H	3.39607018	-2.28904414	-0.00093352
H	3.44358113	0.20526503	0.00141181
Cl	1.32887670	2.13269066	0.00144557

[**5.3a**] - HFIP/1-methyl-4-(methylsulfinyl)benzene_OH-S - ZORA-GGAPBE-D3(BJ)/TZP_gas phase

F	-2.50760123	0.02552363	3.58573274
C	-2.14720777	2.38448406	3.95844489
H	-1.69066537	3.74335809	2.61208676
C	-0.72775357	2.25994768	4.56196358
F	-0.57340510	3.19763818	5.53350652
F	0.23354792	2.47493771	3.62515384
F	-0.50622149	1.04349723	5.12430235
C	-2.51433427	1.24068361	2.98345528
F	-3.76952957	1.45107027	2.49922636
F	-1.67086475	1.18581554	1.91428136
O	-2.32917488	3.64165373	3.36567855
H	-2.85102228	2.30431576	4.79992589
H	-2.06410728	2.50322427	-0.61651923
O	0.15004524	4.43318707	-0.33722285
S	-1.13868672	4.42651318	0.44133682
H	-3.41504248	5.68910405	1.82355837
H	-3.35994841	3.63462674	-0.07355568
C	-2.38344658	3.55151333	-0.56868910
H	-2.39815927	4.01146293	-1.56426215
C	-1.87773765	6.07938844	0.33880099
C	-1.27868372	7.01259025	-0.50121193
C	-1.81121468	8.30295304	-0.56719826
C	-2.92491029	8.66882740	0.20213935
C	-3.49555034	7.70672276	1.05529461
C	-2.97537268	6.41691751	1.13777026
H	-0.40241153	6.71764854	-1.07995492
H	-1.34847298	9.04122471	-1.22616195
H	-3.01329669	10.65432313	-0.65235484
H	-4.35533859	7.97724770	1.67269434
C	-3.48787063	10.06607969	0.14259194
H	-4.57129057	10.05022708	-0.04227158
H	-3.32807151	10.59436718	1.09446988

[**5.3a**] - HFIP/1-methyl-4-(methylsulfinyl)benzene_OH-O - ZORA-GGAPBE-D3(BJ)/TZP_gas phase

F	1.73342064	-0.13877913	2.02611217
C	2.53346354	1.67731784	0.63982344
H	1.75347928	3.47224335	0.22439150
C	2.18101915	1.02514950	-0.71938865
F	3.10752806	1.38105735	-1.64548017
F	0.96334794	1.42466822	-1.19069387
F	2.16650660	-0.33519165	-0.65661375
C	1.61820417	1.19910759	1.79753375
F	1.96822805	1.83743827	2.94270391
F	0.29783218	1.46301199	1.57151126
O	2.61070519	3.06163610	0.55832165
H	3.53527515	1.29409461	0.89391262
H	-1.51173188	2.48821013	-1.27787824
O	0.49910128	4.42713255	-0.36212159
S	-0.85881288	4.15989016	0.28571512
H	-3.10790864	4.99126022	1.90202700
H	-2.93829648	3.42851798	-0.68797150
C	-1.90329317	3.48714745	-1.04991647
H	-1.82250592	4.15448974	-1.91668812
C	-1.69176360	5.75436628	0.44953667
C	-1.22184037	6.85984507	-0.25392369
C	-1.87339036	8.08508480	-0.09644939
C	-2.97790694	8.21807094	0.75889816
C	-3.41556473	7.08684967	1.46921220
C	-2.77387578	5.85831633	1.32826927
H	-0.34881360	6.75154836	-0.89853226
H	-1.51394959	8.95757653	-0.64655851
H	-3.34020921	10.27352343	0.18863153
H	-4.26351206	7.17399767	2.15237496
C	-3.66506657	9.54673079	0.94324661
H	-4.75672812	9.44259062	0.87463912
H	-3.43976825	9.96822907	1.93459100

[**5.3a**] - 2xHFIP/1-methyl-4-(methylsulfinyl)benzene_OH-S + OH-O - ZORA-GGAPBE-D3(BJ)/TZP_gas phase

F	1.78341053	-0.26756521	1.25996672
C	2.73492478	1.74787322	0.29732667
H	1.89354018	3.54668033	0.18850508
C	2.40911189	1.30823980	-1.15197675
F	3.23666034	1.94839710	-2.01555401
F	1.12788502	1.60575903	-1.51621377
F	2.58615378	-0.03047502	-1.33201588
C	1.81591478	1.08813576	1.35355387
F	2.25743564	1.40272247	2.59724570
F	0.52541703	1.53407594	1.25754119
O	2.77020338	3.12980740	0.44571532
H	3.74435635	1.35559681	0.50071346
H	-1.39506376	2.28387587	-0.50011173
O	0.55504153	4.47813629	-0.26563536
S	-0.75273331	4.34050148	0.50496441
H	-3.13034397	5.42999909	1.80372841
H	-2.83499052	3.28180057	-0.05848601
C	-1.83529185	3.28832435	-0.51276592
H	-1.85759711	3.70444918	-1.52717481

C	-1.63978668	5.89981642	0.29674407
C	-1.14394654	6.83790865	-0.60401449
C	-1.81759747	8.05330235	-0.74833704
C	-2.96978505	8.33959935	-0.00145899
C	-3.43415372	7.37477357	0.91008444
C	-2.77334851	6.15936337	1.07416321
H	-0.23800987	6.61148819	-1.16657789
H	-1.43710259	8.79519559	-1.45402297
H	-3.32339358	10.21590714	-1.01957368
H	-4.32330817	7.58398423	1.50928618
C	-3.68135468	9.66080481	-0.14379898
H	-4.76633779	9.51947721	-0.24486344
H	-3.51615823	10.29037919	0.74363055
F	-3.34827873	0.40577080	4.13173603
C	-2.40650570	2.62312306	4.27862547
H	-1.39536419	3.60939762	2.91328687
C	-1.16563979	2.25202847	5.12426844
F	-0.91817065	3.25105978	6.01212075
F	-0.06131676	2.10965545	4.34568330
F	-1.33962005	1.10582344	5.82903273
C	-2.94352940	1.47070280	3.39768977
F	-4.02288317	1.91804379	2.69381602
F	-2.02080783	1.04208330	2.49632493
O	-2.15964620	3.77490018	3.51228909
H	-3.20944824	2.86415657	4.99019871

[**5.3b**] - HFIP/1-(cyclopropylsulfinyl)-4-methylbenzene_OH-S - ZORA-GGAPBE-D3(BJ)/TZP_gas phase

F	-3.68856436	1.22032569	3.89788043
C	-1.67435824	2.53326775	4.16320269
H	-0.99814173	3.97943877	3.00496783
C	-0.69075134	1.44681112	3.66564514
F	0.47164599	1.54478250	4.35933943
F	-0.39553402	1.59926876	2.34468605
F	-1.17326053	0.18839622	3.84301572
C	-3.10076362	2.39893734	3.57765901
F	-3.88396129	3.39663698	4.06875366
F	-3.11274209	2.51605469	2.21484574
O	-1.15858071	3.81857000	3.97160053
H	-1.78111552	2.37408437	5.24699934
C	-5.06004483	8.89416029	-0.47939141
O	0.62745031	5.37292842	0.35544284
S	-0.69294406	4.82482534	0.83714967
H	-3.41631156	5.16316496	1.84228153
H	-6.06168322	8.44597155	-0.43996984
H	0.02499204	4.46965871	-1.95021905
H	-5.03975366	9.71707489	0.25184353
C	-1.99157755	6.02355658	0.45107733
C	-1.72602059	7.02797833	-0.47691729
C	-2.73071866	7.94684344	-0.78318057
C	-3.99070209	7.87829965	-0.16696386
C	-4.22106729	6.86273270	0.77642250
C	-3.22720381	5.93833800	1.09719106
H	-0.73725712	7.08198793	-0.93368175
H	-2.53394801	8.73418655	-1.51476650
H	-4.91588711	9.33342021	-1.47475380
H	-5.19160118	6.79964280	1.27385049
C	-1.19779462	3.54819427	-0.35695632

C	-0.13419770	2.58301159	-0.79875322
C	-0.65328946	3.63878477	-1.75118924
H	-2.21587365	3.19916050	-0.17883719
H	-0.42983639	1.54268075	-0.93146685
H	0.87233959	2.74492555	-0.41047407
H	-1.31647202	3.35148426	-2.56639223

[**5.3b**] - HFIP/1-(cyclopropylsulfinyl)-4-methylbenzene_OH-O - ZORA-GGAPBE-D3(BJ)/TZP_gas phase

F	2.42539316	0.53933829	2.44196163
C	2.40637403	1.46188864	0.20847293
H	1.69979844	3.27376992	-0.26511728
C	1.29486961	0.51431797	-0.31090784
F	1.47041084	0.31260527	-1.64678923
F	0.04413807	1.02751815	-0.14225716
F	1.32445376	-0.70592824	0.28890796
C	2.34284127	1.70151742	1.73575583
F	3.39079925	2.48051010	2.11155590
F	1.20215384	2.33660486	2.11651814
O	2.45163936	2.65007284	-0.51467621
H	3.34943493	0.91866905	0.03544496
C	-4.24244254	8.88703112	1.54646966
O	0.59012019	4.52697246	-0.16042745
S	-0.86929081	4.06777226	-0.09279939
H	-3.57128500	4.29540396	0.86894667
H	-5.27819380	8.79019501	1.19399715
H	0.11135845	5.40273830	-2.50283460
H	-4.27652707	8.96217033	2.64426939
C	-1.84627433	5.50978645	0.37476034
C	-1.28994342	6.78508835	0.32799260
C	-2.07744199	7.87660722	0.69973686
C	-3.40630122	7.70784506	1.11912690
C	-3.93373617	6.40625381	1.16690342
C	-3.15906920	5.30490962	0.80786750
H	-0.25176726	6.90379380	0.01705456
H	-1.65091524	8.88170879	0.66475047
H	-3.83272998	9.82916204	1.16157255
H	-4.96250573	6.25325165	1.50090505
C	-1.42150924	3.96277953	-1.82401121
C	-0.49709637	3.29345976	-2.80353942
C	-0.71794929	4.78985342	-2.85857872
H	-2.49872327	3.79541067	-1.88743714
H	-0.95486382	2.65390794	-3.55777585
H	0.47523884	2.96160812	-2.43717254
H	-1.32557530	5.21864146	-3.65481636

[5.3b] - 2xHFIP/1-(cyclopropylsulfinyl)-4-methylbenzene_OH-S + OH-O - ZORA-GGAPBE-D3(BJ)/TZP_gas phase

F	2.26854321	0.64358357	2.05781687
C	2.68705136	2.13087181	0.20169678
H	1.57656456	3.64546496	-0.46891927
C	2.44985009	1.12527318	-0.95317301
F	3.39352642	1.31432000	-1.91293531
F	1.23395903	1.29322267	-1.54201234
F	2.53523115	-0.17161262	-0.54449041
C	1.85823434	1.79582614	1.46757117

F	1.98776141	2.79273529	2.38021576
F	0.51943541	1.66526143	1.20203349
O	2.53223774	3.44506102	-0.21850668
H	3.73735805	1.98920159	0.50338817
H	-3.07352136	2.75389115	4.79189657
O	0.07351187	4.23644751	-0.88672717
S	-0.91998152	4.34331288	0.27181570
H	-2.48872957	5.81477794	2.20590696
F	-2.13528099	0.77229992	2.31474524
H	-1.87347212	3.71269139	-2.41345581
O	-1.85522194	3.46384028	3.33429804
C	-1.59114633	6.01691313	0.24425170
C	-1.34743274	6.83815304	-0.85375864
C	-1.87933584	8.12840837	-0.85887303
C	-2.64437115	8.60478303	0.21811462
C	-2.86035433	7.75365040	1.31485159
C	-2.33070571	6.46386191	1.34219472
H	-0.73996996	6.46249650	-1.67733762
H	-1.69674868	8.77960976	-1.71693542
H	-3.39461751	10.35769545	-0.80508841
H	-3.44599276	8.11047039	2.16510053
C	-3.18782019	10.01094909	0.21563545
H	-4.11356450	10.08397556	0.80097754
H	-2.46106984	10.70884397	0.65963361
F	-3.52135713	0.30041830	3.95602561
C	-2.30024327	2.37728394	4.10704803
H	-1.13319194	3.16502094	2.73829971
C	-1.16211098	1.82510699	4.99782429
F	-0.71821762	2.81543518	5.81491769
F	-0.10672959	1.39790039	4.25578015
F	-1.57389484	0.79625097	5.78092935
C	-2.98776987	1.30942059	3.22391197
F	-4.00781925	1.89662556	2.53358843
C	-2.40941231	3.46905727	-0.28274070
C	-2.22098070	2.11807293	-0.91352733
C	-2.64118870	3.30390879	-1.75518812
H	-3.24304068	3.64128685	0.40035460
H	-2.95168018	1.35139448	-0.65818531
H	-1.19824132	1.76765257	-1.05220257
H	-3.66869444	3.37924290	-2.10936147

[**5.3c**] - HFIP/2-methyl-2'-(p-tolylsulfinyl)-1,1'-biphenyl_OH-S - ZORA-GGAPBE-D3(BJ)/TZP_gas phase

C	3.27137763	4.47606054	-2.72835609
O	-0.56664646	0.95793128	1.52289532
S	-1.08783867	2.23736658	0.92637284
H	-1.04368516	4.54943917	-0.89417923
H	2.89492664	4.68353323	-3.74021051
H	3.65491031	5.42511323	-2.32399991
H	-1.65086106	1.49724407	-4.62166391
C	0.16661391	2.88284051	-0.21074146
C	1.39866554	2.24028788	-0.25577418
C	2.39934449	2.75806413	-1.08218616
C	2.18580185	3.91334568	-1.84617430
C	0.93489931	4.55153444	-1.76126485
C	-0.07492316	4.04884496	-0.94517481
H	1.54745859	1.33711599	0.33595747
H	3.36365180	2.24797577	-1.13767723

H	4.11662205	3.78181158	-2.81267775
H	0.74950885	5.45473681	-2.34756210
C	-2.43533322	1.97479646	-0.27590611
C	-3.61018504	2.66245289	0.05336231
C	-4.71430671	2.61372219	-0.79767361
C	-4.63587355	1.86653910	-1.97371014
C	-3.46483790	1.17491703	-2.29051845
C	-2.33638969	1.20585047	-1.45585042
H	-3.65695948	3.24537356	0.97436212
H	-5.62703996	3.15031112	-0.53722878
H	-5.49379770	1.81146305	-2.64573966
H	-3.41753951	0.57603474	-3.20105245
C	-1.12416962	0.42426026	-1.82752405
C	-0.70113117	-0.61526549	-0.98471378
C	0.41157069	-1.39119301	-1.30510605
C	1.11935843	-1.12903925	-2.47872757
C	0.70168360	-0.09895041	-3.32270076
C	-0.41994686	0.68768095	-3.02589854
H	-1.24708045	-0.80184346	-0.06212098
H	0.72430491	-2.19169937	-0.63389572
H	1.99635820	-1.72431418	-2.73869722
H	1.26300054	0.11309871	-4.23572387
C	-0.81769228	1.79763458	-3.96790767
H	-1.13920236	2.69381049	-3.42045718
H	0.02665374	2.07099671	-4.61370913
F	-4.16706123	2.00146906	5.37628139
C	-2.76200107	3.68053926	4.35216877
H	-1.94016993	3.64280494	2.56263449
C	-1.46761978	3.30784005	5.11278140
F	-0.75193830	4.44021456	5.35208737
F	-0.68399480	2.46959645	4.38854253
F	-1.72094823	2.72190726	6.31276894
C	-3.75176286	2.50229710	4.18454450
F	-4.85974100	2.94900158	3.52386376
F	-3.22378124	1.48682261	3.45591232
O	-2.46720742	4.27715813	3.11712166
H	-3.28162000	4.42711242	4.97053566

[**5.3c**] - HFIP/2-methyl-2'-(p-tolylsulfinyl)-1,1'-biphenyl_OH-O - ZORA-GGAPBE-D3(BJ)/TZP_gas phase

C	3.23383459	4.35798062	-2.54551103
O	0.30179651	-0.55054529	0.92518649
S	-0.29495961	0.85445547	0.99816730
H	-0.53573247	3.63249250	0.15178897
H	2.66958573	5.16749296	-3.02707925
H	4.01136755	4.82549419	-1.92137768
H	-2.29003782	2.17113110	-4.02964575
C	0.69286823	1.86679544	-0.12626743
C	1.83779136	1.31844508	-0.69717940
C	2.64688825	2.13059452	-1.49376460
C	2.33506499	3.48111484	-1.71113222
C	1.18052787	4.00699114	-1.10703313
C	0.35985449	3.21211579	-0.30973102
H	2.06620403	0.26659777	-0.52744935
H	3.53636697	1.70176003	-1.96106904
H	3.74420718	3.77882920	-3.32604638
H	0.91970072	5.05598775	-1.26480209
C	-1.90274629	0.94237208	0.15310108

C	-2.92659266	1.38056989	1.00255347
C	-4.22120879	1.54748545	0.51386744
C	-4.48209488	1.26718966	-0.82840342
C	-3.45783365	0.82436955	-1.66775956
C	-2.14484732	0.64614056	-1.20469605
H	-2.69845215	1.58693590	2.04946951
H	-5.01759660	1.88296981	1.17861171
H	-5.49196870	1.38276671	-1.22478252
H	-3.67378956	0.58906103	-2.71095690
C	-1.09655225	0.14246124	-2.13503645
C	-0.51835037	-1.11368288	-1.89750745
C	0.45082463	-1.62915640	-2.75700817
C	0.85379421	-0.88525203	-3.86699610
C	0.27656001	0.36205139	-4.11177774
C	-0.70666385	0.89556693	-3.26721173
H	-0.83119425	-1.68372774	-1.02529081
H	0.88904721	-2.60672472	-2.55320654
H	1.61643201	-1.27418233	-4.54386411
H	0.59907351	0.94759481	-4.97602983
C	-1.29373033	2.25257576	-3.56866513
H	-1.40634334	2.85267906	-2.65542635
H	-0.64917369	2.80260248	-4.26610321
F	-3.20585550	-2.33578046	4.19252249
C	-1.17988202	-2.94630692	2.99776472
H	0.08362493	-1.70127017	2.09953905
C	-2.01167406	-3.28434745	1.73244073
F	-1.24915522	-3.99737713	0.86101437
F	-2.45689213	-2.17954108	1.07459690
F	-3.09840621	-4.04755947	2.03871771
C	-1.91500318	-1.97403024	3.95422738
F	-1.27082882	-1.94991610	5.15190499
F	-1.92741157	-0.69516971	3.47928355
O	0.10461669	-2.49769636	2.71602194
H	-1.09944082	-3.89604565	3.55072458

[**5.3c**] - HFIP/2-methyl-2'-(p-tolylsulfinyl)-1,1'-biphenyl_OH-S - ZORA-GGAPBE-D3(BJ)/TZP_PhCl (COSMO) phase

C	3.135887	4.758669	-2.924782
O	-0.388269	1.067933	1.455590
S	-0.982180	2.330995	0.883905
H	-1.015156	4.769605	-0.735947
H	2.674050	5.438122	-3.652075
H	3.866453	5.343596	-2.344423
H	-1.662770	1.502708	-4.283248
C	0.205064	3.028145	-0.292512
C	1.410008	2.362253	-0.499693
C	2.349779	2.924810	-1.366412
C	2.103079	4.146569	-2.013889
C	0.880532	4.799293	-1.772214
C	-0.069979	4.251962	-0.910707
H	1.589212	1.411235	0.002234
H	3.290753	2.400104	-1.546896
H	3.696040	3.986049	-3.467437
H	0.667858	5.748460	-2.268332
C	-2.356418	2.009615	-0.265655
C	-3.496010	2.777220	0.007646
C	-4.617049	2.687350	-0.818081
C	-4.591341	1.815525	-1.908777

C	-3.452053	1.048724	-2.169910
C	-2.306394	1.124252	-1.361805
H	-3.502629	3.456678	0.861309
H	-5.501648	3.287772	-0.605020
H	-5.462892	1.724692	-2.558301
H	-3.444410	0.363087	-3.018869
C	-1.126131	0.269243	-1.683108
C	-0.789460	-0.785600	-0.822149
C	0.284371	-1.631193	-1.105272
C	1.038148	-1.421106	-2.262453
C	0.705475	-0.373705	-3.125422
C	-0.374734	0.482160	-2.862729
H	-1.376234	-0.936309	0.083125
H	0.529967	-2.445683	-0.422565
H	1.883865	-2.070479	-2.494402
H	1.300896	-0.205026	-4.025603
C	-0.679385	1.618439	-3.805560
H	-0.692221	2.577965	-3.266277
H	0.078658	1.677088	-4.596363
F	-4.404661	2.146176	5.153042
C	-2.707026	3.675527	4.367289
H	-1.818411	3.675843	2.600960
C	-1.530340	3.037968	5.139784
F	-0.658255	4.012897	5.516145
F	-0.844083	2.151492	4.369298
F	-1.935426	2.392057	6.265021
C	-3.845308	2.681969	4.038172
F	-4.828360	3.336660	3.360211
F	-3.420964	1.657776	3.247346
O	-2.252597	4.329502	3.209643
H	-3.143008	4.433498	5.032846

[**5.3c**] - HFIP/2-methyl-2'-(p-tolylsulfinyl)-1,1'-biphenyl_OH-O - ZORA-GGAPBE-D3(BJ)/TZP_PhCl (COSMO) phase

C	3.263810	4.374726	-2.486815
O	0.273989	-0.583431	0.884179
S	-0.314120	0.832192	0.966192
H	-0.513588	3.622847	0.193117
H	3.705480	3.824817	-3.328140
H	2.721806	5.244531	-2.879252
H	-2.265755	2.197962	-3.976709
C	0.696405	1.848978	-0.130543
C	1.837639	1.303410	-0.713742
C	2.657607	2.128309	-1.486785
C	2.358531	3.488331	-1.670464
C	1.207232	4.009889	-1.054495
C	0.376420	3.202365	-0.278840
H	2.059923	0.245995	-0.573996
H	3.543947	1.702931	-1.962827
H	4.095251	4.753752	-1.872054
H	0.954584	5.063990	-1.186685
C	-1.912931	0.931562	0.115848
C	-2.936012	1.385108	0.959321
C	-4.226177	1.565884	0.461126
C	-4.481698	1.285872	-0.883220
C	-3.456154	0.829717	-1.716029
C	-2.148475	0.636477	-1.243503
H	-2.712943	1.602342	2.005019

H	-5.021478	1.917527	1.118693
H	-5.486257	1.415863	-1.288084
H	-3.670131	0.603543	-2.761683
C	-1.099683	0.120304	-2.168015
C	-0.546657	-1.148921	-1.937976
C	0.417902	-1.678589	-2.796104
C	0.842783	-0.932476	-3.897881
C	0.292302	0.329757	-4.134176
C	-0.685909	0.876195	-3.290533
H	-0.874054	-1.717488	-1.069346
H	0.837862	-2.665911	-2.599510
H	1.603164	-1.329738	-4.572437
H	0.634078	0.917368	-4.989309
C	-1.241163	2.248878	-3.578782
H	-1.277008	2.860714	-2.666318
H	-0.618562	2.766584	-4.319115
F	-3.176717	-2.322006	4.264368
C	-1.178101	-2.920096	3.022982
H	0.049607	-1.670775	2.059554
C	-2.028124	-3.274542	1.777346
F	-1.276831	-3.993409	0.899550
F	-2.491231	-2.180027	1.115012
F	-3.107011	-4.039910	2.108818
C	-1.900114	-1.941985	3.980580
F	-1.220518	-1.885572	5.160097
F	-1.948135	-0.673328	3.486591
O	0.095091	-2.453302	2.703475
H	-1.073593	-3.862623	3.582321

[**5.3c**] - 2xHFIP/2-methyl-2'-(p-tolylsulfinyl)-1,1'-biphenyl_OH-S + OH-O - ZORA-GGAPBE-D3(BJ)/TZP_gas phase

C	2.759059	5.264597	-0.974009
O	-0.379594	-0.431869	0.631592
S	-1.169406	0.868965	0.591131
H	-1.474377	3.735927	0.343475
H	2.394288	5.841562	-1.836369
H	2.890198	5.972696	-0.142610
H	-1.192313	2.483016	-4.515178
C	-0.015159	2.152309	0.072809
C	1.298187	1.810603	-0.228300
C	2.192197	2.828016	-0.571477
C	1.790346	4.170263	-0.604541
C	0.458902	4.481831	-0.271551
C	-0.446842	3.483582	0.074752
H	1.599667	0.763594	-0.201699
H	3.223091	2.568523	-0.821896
H	3.744437	4.855860	-1.229357
H	0.130447	5.523631	-0.276563
C	-2.325290	0.895337	-0.809853
C	-3.639645	1.198830	-0.431055
C	-4.637663	1.305082	-1.399037
C	-4.313190	1.095344	-2.740250
C	-3.002793	0.780980	-3.106569
C	-1.974509	0.670990	-2.157784
H	-3.876998	1.359229	0.621805
H	-5.660283	1.540433	-1.103317
H	-5.085761	1.164577	-3.507636
H	-2.759255	0.596939	-4.154301

C	-0.601663	0.301490	-2.607957
C	-0.080371	-0.951046	-2.253094
C	1.186043	-1.347877	-2.681060
C	1.945004	-0.487234	-3.475081
C	1.427614	0.757662	-3.837772
C	0.155801	1.174873	-3.422084
H	-0.676254	-1.614340	-1.628362
H	1.574070	-2.324579	-2.390600
H	2.938881	-0.783753	-3.814380
H	2.025567	1.434126	-4.452904
C	-0.350611	2.541576	-3.809465
H	-0.706707	3.094729	-2.927850
H	0.446502	3.126419	-4.285429
F	-3.589556	2.260362	6.423652
C	-2.913487	2.864726	4.198682
H	-2.378499	1.810097	2.628139
C	-1.466641	3.323440	4.491717
F	-1.209536	4.469330	3.802350
F	-0.562866	2.391731	4.088367
F	-1.254699	3.577314	5.807521
C	-3.419408	1.764552	5.167153
F	-4.626008	1.309721	4.740924
F	-2.575951	0.706117	5.243034
O	-3.049412	2.496431	2.850803
H	-3.562357	3.735566	4.370127
F	-1.091579	-2.218527	5.271257
C	-1.679221	-2.728929	2.980604
H	-0.950237	-1.812131	1.379277
C	-3.092185	-2.096672	3.040057
F	-3.931574	-2.803396	2.238570
F	-3.100978	-0.805266	2.586995
F	-3.624732	-2.096759	4.289474
C	-0.673434	-2.107198	3.980278
F	0.514610	-2.760463	3.881139
F	-0.437677	-0.790729	3.730649
O	-1.186238	-2.742247	1.679862
H	-1.813782	-3.771532	3.311073

[**5.3d**] - HFIP/5-bromo-6-(p-tolylsulfinyl)benzo[d][1,3]dioxole_OH-S - ZORA-GGAPBE-D3(BJ)/TZP_gas phase

C	3.04499394	4.92575917	-2.09213171
O	-1.06259957	0.61263397	1.02636198
S	-1.59985371	1.91258214	0.50672911
H	-1.44866877	4.52876896	-0.81959897
H	2.90242571	4.99690866	-3.18103599
H	3.11990126	5.95222774	-1.70629912
H	-3.18538930	0.00769910	-3.89555102
C	-0.24178063	2.79903226	-0.30872543
C	1.01954851	2.21509378	-0.31085033
C	2.08423514	2.91207822	-0.88898443
C	1.90094291	4.18338230	-1.45024484
C	0.61585141	4.75514191	-1.41003796
C	-0.45619065	4.07446242	-0.84003271
H	1.14603078	1.22809345	0.13357693
H	3.07714540	2.45710110	-0.90332706
H	4.00160713	4.42062125	-1.91072909
H	0.45503622	5.75005751	-1.83192267
C	-2.66511150	1.69676717	-0.95137569

C	-3.79846411	2.54109604	-0.93698099
C	-4.65783301	2.46159858	-2.01095597
C	-4.43971964	1.56206423	-3.05616472
C	-3.34845407	0.71205356	-3.08237709
C	-2.44905873	0.80374918	-2.00531927
H	-3.98850161	3.21852706	-0.10513343
O	-5.84207094	3.13949933	-2.21262075
O	-5.47132326	1.63736378	-3.96272192
Br	-0.91273812	-0.34150393	-2.07654110
C	-6.24330167	2.78772282	-3.55034810
H	-6.02493662	3.62876507	-4.23024430
H	-7.30740602	2.52383874	-3.54981381
F	-6.48047945	2.15978446	3.45572209
C	-4.42973170	3.41519931	3.23404463
H	-2.94638465	3.22017864	1.95136552
C	-3.65385510	2.71315476	4.37180399
F	-2.87988468	3.62745507	5.01580294
F	-2.83057074	1.74690189	3.88654355
F	-4.47603275	2.14802178	5.29225496
C	-5.51442049	2.52756998	2.57585171
F	-6.11996269	3.23563421	1.58051730
F	-4.99262891	1.40372036	2.02086375
O	-3.54694194	3.93968090	2.27622863
H	-4.96628521	4.25864954	3.69268909

[**5.3d**] - HFIP/5-bromo-6-(p-tolylsulfinyl)benzo[d][1,3]dioxole_OH-O - ZORA-GGAPBE-D3(BJ)/TZP_gas phase

C	0.86869791	7.02053872	0.35810834
O	0.46726264	0.34437604	-0.30201577
S	-0.77401248	1.14686314	0.07025256
H	-2.33970743	3.60700766	0.20155327
H	0.78324587	7.51469892	-0.62211233
H	0.22269744	7.56836228	1.05719506
H	-2.55786998	1.38430992	-4.64281594
C	-0.29975533	2.89123282	0.02706753
C	1.05271118	3.21701292	0.00911660
C	1.42482683	4.55897737	0.11964877
C	0.46498209	5.57171838	0.26012854
C	-0.89206649	5.20656696	0.28861792
C	-1.28181182	3.87467730	0.17836091
H	1.79010749	2.42278779	-0.09860201
H	2.48465349	4.82250262	0.10184529
H	1.90816337	7.12539735	0.69319915
H	-1.65583803	5.97916451	0.40280950
C	-1.98587838	1.12600824	-1.26748847
C	-3.27818058	0.77324656	-0.81523176
C	-4.27495413	0.67916300	-1.76101838
C	-4.01497268	0.89785384	-3.11526616
C	-2.75498358	1.22822902	-3.58431892
C	-1.73322025	1.34426020	-2.62620768
H	-3.45590883	0.55520973	0.23743198
O	-5.59164113	0.31105004	-1.58595774
O	-5.15437800	0.68636763	-3.85222349
Br	0.01069970	1.80291281	-3.26749066
C	-6.20446498	0.48205841	-2.87884234
H	-6.85416428	1.37252893	-2.86052064
H	-6.76000423	-0.42775505	-3.13737749
F	-2.40802513	-3.93368128	0.25556284

C	-0.24184789	-2.99063722	0.76452325
H	0.41792035	-1.12003312	0.55871790
C	0.57762416	-3.63534414	-0.38045732
F	1.77435818	-4.06335008	0.10930590
F	0.83488171	-2.75434790	-1.37905507
F	-0.04917090	-4.71817273	-0.92321506
C	-1.72653105	-2.76115702	0.37989393
F	-2.34351220	-2.04134871	1.36062225
F	-1.87707058	-2.07294954	-0.78248967
O	0.38085020	-1.84725632	1.25284777
H	-0.26749033	-3.73671358	1.57433401

[**5.3d**] - HFIP/5-bromo-6-(p-tolylsulfinyl)benzo[d][1,3]dioxole_mO - ZORA-GGAPBE-D3(BJ)/TZP_gas phase

C	1.50575808	6.21452349	-1.52570262
O	-0.34450803	0.27234710	0.98237321
S	-1.38218641	1.34276715	0.78590010
H	-2.36480139	3.96094097	-0.13969951
H	0.89070499	6.77097345	-2.24537370
H	1.74813926	6.90187002	-0.70024241
H	-2.86077667	-0.38883013	-3.73978374
C	-0.56221546	2.76159922	-0.00241312
C	0.81507926	2.70240653	-0.18611055
C	1.47773703	3.82074869	-0.69709142
C	0.78133148	4.99748098	-1.00992747
C	-0.60874653	5.02838948	-0.80183396
C	-1.28465632	3.92163875	-0.29433727
H	1.34086379	1.78205183	0.06888806
H	2.55768365	3.77740505	-0.85629062
H	2.44901118	5.94086216	-2.01525046
H	-1.16923065	5.93508120	-1.04139680
C	-2.51857387	0.93065425	-0.58614274
C	-3.86959475	1.21278574	-0.28207349
C	-4.80611579	0.94171901	-1.25670480
C	-4.44716805	0.37337357	-2.47835267
C	-3.13530496	0.06277564	-2.78869864
C	-2.16756356	0.36396584	-1.81514452
H	-4.14415954	1.61873795	0.69241498
O	-6.18972758	1.07628882	-1.20146960
O	-5.56956942	0.13306048	-3.23847149
Br	-0.34878814	-0.03278136	-2.27003123
C	-6.63215252	0.82302295	-2.56127654
H	-6.82321924	1.78707940	-3.05902111
H	-7.52073528	0.18459793	-2.53197493
F	-10.18918691	4.47944930	-0.91808362
C	-8.94182061	2.93869052	0.46915182
H	-7.24475851	2.04675118	0.01741096
C	-9.86283267	1.72636009	0.19302505
F	-9.87700961	0.91455555	1.27821368
F	-9.41521749	0.98306692	-0.86596178
F	-11.14229924	2.09030945	-0.07087750
C	-8.94843960	3.99515547	-0.66190736
F	-8.16181448	5.04084802	-0.30462581
F	-8.44776714	3.48953752	-1.83047829
O	-7.64092235	2.53095276	0.78128407
H	-9.35901312	3.44098569	1.35515984

[**5.3d**] - HFIP/5-bromo-6-(p-tolylsulfinyl)benzo[d][1,3]dioxole_pO - ZORA-GGAPBE-D3(BJ)/TZP_gas phase

C	1.29818944	6.46822995	0.07709640
O	0.07818342	-0.12475145	0.39227538
S	-1.06187129	0.84260561	0.54948682
H	-2.33382288	3.50433785	0.25750604
H	1.59657351	6.69823603	-0.95740346
H	0.57962987	7.23520387	0.39303162
H	-2.57127414	0.49865983	-4.27937418
C	-0.40193944	2.51721326	0.27752243
C	0.98227908	2.66613652	0.27238510
C	1.52546299	3.95058247	0.21247231
C	0.70227843	5.08634691	0.16518245
C	-0.69032472	4.90300241	0.18272775
C	-1.24918748	3.62759680	0.24472177
H	1.60781661	1.77427981	0.31499557
H	2.61121533	4.07269422	0.20831062
H	2.19580007	6.55671547	0.70360946
H	-1.34767102	5.77493970	0.15045782
C	-2.20547001	0.79540272	-0.87602546
C	-3.55859242	0.85380378	-0.47881276
C	-4.51440445	0.82546048	-1.47278435
C	-4.15832215	0.69539507	-2.81508108
C	-2.84261778	0.60751576	-3.23083834
C	-1.86001233	0.67537991	-2.22507400
H	-3.82530432	0.90959377	0.57691321
O	-5.88931204	0.83007965	-1.34346910
O	-5.30803319	0.61584660	-3.58580675
Br	-0.03226104	0.62043079	-2.79425166
C	-6.38044921	0.99566906	-2.68059575
H	-6.63069293	2.05434824	-2.85983411
H	-7.23378095	0.33111149	-2.84324907
F	-9.14776562	-0.60183814	-6.92868217
C	-6.84549028	0.14419736	-6.92488136
H	-5.61463661	0.15392914	-5.38922680
C	-7.21092285	1.64662633	-6.86774138
F	-6.22225293	2.37338746	-7.44453341
F	-7.34167526	2.08748447	-5.57883187
F	-8.36646050	1.92804054	-7.52002043
C	-7.93849030	-0.78432990	-6.34183864
F	-7.57700979	-2.07693067	-6.52723844
F	-8.09909601	-0.59650431	-4.99528071
O	-5.59929715	-0.10443910	-6.34128983
H	-6.77270670	-0.11031887	-7.99315415

[**5.3e**] - HFIP/aniline_OH-N - ZORA-GGAPBE-D3(BJ)/TZP_gas phase

C	-1.03557412	4.20355175	-2.74399522
C	-0.44238086	6.55218299	-2.69318076
C	-1.36013211	5.52550530	-2.43501256
C	0.20361418	3.89190321	-3.31053195
H	0.45285767	2.85904359	-3.55573408
H	-2.33096469	5.76525101	-1.99376773
N	-0.74952236	7.89984676	-2.33861742
C	0.80522687	6.24150288	-3.25120647
C	1.12063532	4.91768518	-3.55909769
H	-1.76107637	3.41377447	-2.54389602
H	1.52763814	7.03894672	-3.43875218

H	2.09277201	4.68843272	-3.99791911
H	-1.75627243	8.06418186	-2.31339447
H	-0.33449165	8.56780447	-2.98922870
F	2.73587020	11.22770740	-0.92252165
C	0.82838027	10.03819020	-0.02381150
H	-0.09524837	8.46506067	-0.81330861
C	-0.21893728	11.11351163	-0.40817734
F	-1.21228582	11.12388245	0.51748687
F	-0.80292774	10.85930027	-1.62068127
F	0.30469682	12.36566261	-0.46375989
C	2.07441471	10.04114029	-0.94549468
F	2.93952289	9.08000139	-0.54059888
F	1.75934074	9.77562285	-2.25416997
O	0.25701474	8.77593509	0.08633413
H	1.20240866	10.33705617	0.96889789

[**5.3f**] - HFIP/pyridine_OH-N - ZORA-GGAPBE-D3(BJ)/TZP_gas phase

F	2.22012600	-0.49904821	1.85789511
C	2.09436020	1.44925415	0.42139791
H	0.61025570	2.79453636	0.37668586
C	1.72335769	0.65442769	-0.85567848
F	2.21860810	1.29714416	-1.94506377
F	0.37240858	0.54767538	-1.02799967
F	2.23684158	-0.60660438	-0.85876345
C	1.66568730	0.73806962	1.72907254
F	2.06915552	1.47541627	2.79643099
F	0.31190277	0.59339449	1.82397684
O	1.63392647	2.75799137	0.36498812
H	3.19646800	1.46318402	0.44600818
H	-1.79495232	1.30423886	0.23070504
H	-4.67757683	4.49597781	0.63667878
H	-4.18525303	2.04123780	0.35724438
C	-3.64890443	4.13547287	0.57723733
C	-3.38007980	2.77415036	0.42212785
C	-2.05072030	2.35803268	0.35061896
N	-1.01547087	3.21109428	0.42354903
C	-1.28047000	4.52011658	0.57250484
C	-2.57716798	5.02745818	0.65383963
H	-0.41188036	5.17997613	0.62751798
H	-2.73789508	6.09964636	0.77424648

[**5.3g**] - HFIP/quinoline_OH-N - ZORA-GGAPBE-D3(BJ)/TZP_gas phase

C	-1.66483024	5.46744067	-2.81141929
C	0.23021417	6.96628108	-3.08956541
C	-1.13042402	6.76901303	-2.97606297
C	-0.82840396	4.37271518	-2.76146652
C	2.84008396	3.69905205	-2.94866383
C	3.27956385	5.03173776	-3.10957005
N	2.46211347	6.07272179	-3.15512542
C	1.11344818	5.85714051	-3.04122653
C	0.57671068	4.53806775	-2.87462637
C	1.48914747	3.45516696	-2.83095757
H	1.10870428	2.43908212	-2.70399426
H	3.57072614	2.89082738	-2.91932828
H	4.34389023	5.25159933	-3.20464017
H	-2.74362099	5.33480805	-2.72418827

H	-1.23179698	3.36623133	-2.63438789
H	-1.80530771	7.62485877	-3.01458736
H	0.65188462	7.96402677	-3.21669439
F	6.46665429	9.17408521	-2.22416053
C	4.40227714	9.06007985	-3.49201409
H	2.97644730	7.64358155	-3.31704425
C	5.09899680	8.51487238	-4.76400690
F	4.36098777	8.83886444	-5.85623104
F	5.22650133	7.15492597	-4.74838242
F	6.34230226	9.04002757	-4.94146109
C	5.17606869	8.74211380	-2.18816473
F	4.56765254	9.36225606	-1.14354523
F	5.19781310	7.40666531	-1.90956902
O	3.07476317	8.66333141	-3.41205256
H	4.43832485	10.15738584	-3.59147233

[**5.3h**] - HFIP/benzo[h]quinoline_OH-N - ZORA-GGAPBE-D3(BJ)/TZP_gas phase

C	-1.85638909	4.88030391	-2.87656505
C	-0.18011764	6.54368451	-2.12584535
C	-1.46674619	5.93776542	-1.99224379
C	-1.01416796	4.42153688	-3.84466864
C	2.41854360	5.12971262	-5.14224678
C	2.73643759	6.20212380	-4.29541936
N	1.91392928	6.67116333	-3.35873440
C	0.70023174	6.08012155	-3.18082406
C	0.28281578	5.00162962	-4.01860359
C	1.17654094	4.53938321	-5.00720861
C	-2.33868485	6.38462094	-0.97231724
H	3.13543958	4.79291579	-5.89057111
H	3.69665446	6.71417060	-4.38565598
H	-2.63965429	7.72860517	0.67637554
C	0.19156827	7.55819135	-1.21598847
H	0.87246070	3.71431822	-5.65514086
C	-0.68218195	7.97682368	-0.22726597
C	-1.95737573	7.39199135	-0.10520533
H	-1.31290984	3.60816026	-4.50785488
H	-3.32054602	5.91641781	-0.88058039
H	-2.84663653	4.43938346	-2.75142767
H	-0.37675753	8.76532370	0.46144562
H	1.17619785	8.01385128	-1.29053036
F	3.89844703	11.13730422	-5.06456208
C	3.05979128	10.03677241	-3.08393873
H	2.55923081	8.09391353	-2.78872091
C	1.62766405	10.62616163	-3.11049866
F	1.22713477	10.87320027	-1.82964411
F	0.72901345	9.77559412	-3.66336786
F	1.56199620	11.80525825	-3.78858650
C	3.68726530	9.91947245	-4.49668013
F	4.89989411	9.30235953	-4.40098948
F	2.93055866	9.18609479	-5.35816532
O	3.11806262	8.84633820	-2.36802921
H	3.67655411	10.78468699	-2.55982545

[**5.3i**] - HFIP/1,4-dioxane_OH-O - ZORA-GGAPBE-D3(BJ)/TZP_gas phase

O	1.73439502	6.57729874	-0.36464407
C	2.61400277	8.20827820	1.22134076

C	1.50442946	7.87032167	0.24077526
C	3.03375222	6.54905141	-0.99921709
C	4.12540664	6.90480735	-0.00408343
O	3.89144632	8.19694323	0.57031146
H	4.16977298	6.13797341	0.79326503
H	2.60842958	7.48220160	2.05713752
H	2.47405158	9.22039342	1.62576570
H	1.45514148	8.62968153	-0.55916705
H	0.53003793	7.80451213	0.74363285
H	3.03098281	7.26615337	-1.83866402
H	3.16292895	5.53010823	-1.38881237
H	5.10101801	6.95439003	-0.50767951
F	-1.91823522	3.63477409	1.47613650
C	0.49526800	3.76216328	1.34269232
H	1.55423679	5.32446805	0.74268585
C	0.61419528	2.93366453	0.04045395
F	1.78967364	2.24585061	0.05885014
F	0.62160508	3.71817997	-1.07120987
F	-0.38699515	2.02459422	-0.09616730
C	-0.86217436	4.48985676	1.49662362
F	-0.88578990	5.13773723	2.69441417
F	-1.06258899	5.42471003	0.52744616
O	1.56700961	4.64323837	1.48363577
H	0.53586236	3.03197651	2.16586795

[**5.3j**] - HFIP/2-phenylpyridine_OH-N - ZORA-GGAPBE-D3(BJ)/TZP_gas phase

F	3.40283940	8.82751678	-1.39892876
C	-0.06182464	6.83532844	-2.78709510
C	-0.84720534	6.68367272	-1.63101962
F	4.54788587	7.12985647	-2.18778902
C	2.64580298	3.81551718	-4.04013967
C	2.86818699	5.17466035	-4.24188719
N	2.02119588	6.13378335	-3.83463467
C	0.88226873	5.77214322	-3.19888322
C	0.58763717	4.41780314	-2.96258730
C	1.47574099	3.43340901	-3.38141542
C	-1.76171151	7.66754005	-1.25832367
H	3.37145041	3.08189416	-4.39145749
H	3.77080749	5.52443879	-4.74341511
H	-2.62656545	9.58751354	-1.75004760
C	-0.21096075	7.99884818	-3.55913493
H	1.25221633	2.37956370	-3.20769473
C	-1.12987358	8.97938667	-3.18797132
C	-1.90904969	8.81792410	-2.03907320
O	2.88474588	8.68685818	-4.12448854
H	-2.35413410	7.54112388	-0.35108020
H	4.20297209	10.12160770	-3.55672796
H	-1.23933971	9.87394870	-3.80264102
H	0.38852564	8.12703499	-4.45937677
F	5.56645950	9.01487807	-1.69813592
C	4.14474128	9.02398150	-3.64757446
H	2.64136853	7.70607350	-3.96716861
C	5.25157809	8.65083618	-4.66771675
F	5.00244498	9.28320891	-5.84543460
F	5.29499450	7.31147287	-4.93414018
F	6.49437867	9.02449347	-4.25994854
C	4.42475702	8.48622308	-2.22307079
H	-0.71992044	5.80107067	-1.00247488

H -0.35090146 4.14908206 -2.47919573

[**5.3k**] - HFIP/1,10-phenanthroline_OH-N - ZORA-GGAPBE-D3(BJ)/TZP_gas phase

C -1.98441727 4.50197135 -2.96666826
C -0.61468125 6.55602765 -2.77539375
C -1.89191581 5.92341166 -2.81586963
C -0.86166022 3.73467158 -3.07275862
C 2.84794967 4.20415470 -3.09423589
C 2.87073373 5.60633624 -2.94607567
N 1.78262387 6.35922767 -2.84866491
C 0.58104849 5.74081523 -2.88989639
C 0.44060548 4.32927218 -3.03702297
C 1.62430140 3.56551832 -3.14118278
C -3.03530626 6.74422335 -2.70185383
H 3.78249832 3.64711217 -3.16862910
H 3.82569952 6.13716175 -2.90525099
H -3.74200355 8.77229739 -2.46296421
N -0.47936737 7.89711824 -2.63078905
H 1.55560689 2.48144165 -3.25421265
C -1.57797226 8.63820695 -2.52357842
C -2.88184217 8.10893781 -2.55441552
H -0.93765284 2.65190315 -3.18579778
H -4.02690758 6.28779326 -2.73122416
H -2.97509554 4.04553339 -2.99493117
H -1.41460156 9.71227007 -2.40718541
F 3.96762889 10.23642537 -0.29151557
C 2.51711554 10.26882260 -2.21317311
H 0.97274963 9.02195557 -2.62035988
C 3.56573129 9.94728249 -3.30889178
F 3.32415596 10.73339015 -4.39502660
F 3.52305946 8.65836952 -3.72442274
F 4.84048872 10.20883031 -2.89530461
C 2.86111893 9.64948244 -0.83481461
F 1.83003854 9.86128974 0.02640720
F 3.08781209 8.31245315 -0.88415350
O 1.22390825 9.99800517 -2.64329503
H 2.59782566 11.35720189 -2.05879139

[**5.3k**] - 2xHFIP/1,10-phenanthroline_2xOH-N - ZORA-GGAPBE-D3(BJ)/TZP_gas phase

C -0.63063805 4.98206720 -1.55672576
C -0.07282612 7.12393755 -2.66714357
C -0.82821809 6.39341311 -1.70337112
C 0.26362146 4.31604502 -2.34272984
C 2.63643325 5.07336213 -5.13072249
C 2.39240512 6.45903403 -5.22819526
N 1.54284979 7.11831931 -4.45280758
C 0.86410533 6.41380436 -3.51774969
C 1.02221287 5.00787368 -3.34075678
C 1.94592798 4.34785601 -4.18117375
C -1.76071289 7.10773787 -0.91973469
H 3.36136375 4.59897943 -5.79250170
H 2.92389328 7.05642485 -5.97373759
H -2.62248792 9.05122353 -0.52367672
N -0.21027570 8.46515236 -2.81730623
H 2.10390290 3.27406983 -4.06482859
C -1.09976863 9.10461050 -2.06495470

C	-1.90829260	8.46866415	-1.10554937
H	0.41083894	3.24081510	-2.22684751
H	-2.35486715	6.57199959	-0.17638058
H	-1.21117284	4.45116662	-0.80064733
H	-1.17278819	10.18247279	-2.22675414
F	2.76135516	12.54515786	-2.10505209
C	2.01744013	11.08581073	-3.89072944
H	0.69839237	9.56310428	-3.81111610
C	3.33937872	10.27856211	-3.94803886
F	3.50535226	9.75723310	-5.18704435
F	3.36142740	9.23485886	-3.05720535
F	4.42921734	11.05089573	-3.68101095
C	1.76025252	11.70750852	-2.49290756
F	0.61209923	12.44393051	-2.53935269
F	1.60000065	10.77594286	-1.51637318
O	0.92786953	10.38169425	-4.37294229
H	2.18991973	11.94840306	-4.55629399
F	5.43771717	4.67956370	-1.90679551
C	6.25975198	6.91245472	-2.33497885
H	5.14348502	8.51146351	-2.43592285
C	6.48104814	6.70273835	-3.85286903
F	7.58479602	7.39549676	-4.24054551
F	5.42948233	7.16865037	-4.58186641
F	6.67767152	5.39963282	-4.19007282
C	5.17391896	6.00146686	-1.71643687
F	5.12373786	6.21562783	-0.37542449
F	3.94436592	6.26698497	-2.22297755
O	6.01366005	8.26359392	-2.05670409
H	7.20556495	6.64104999	-1.84510546

[**5.3l**] - HFIP/acetophenone_OH-O; Me side - ZORA-GGAPBE-D3(BJ)/TZP_gas phase

C	1.13291247	-0.00254927	-0.00680303
C	0.22810974	-0.39890219	-1.00736277
C	0.08573859	-1.74487301	-1.33237968
C	0.84988807	-2.71170872	-0.66705168
C	1.75736806	-2.32805040	0.32445129
C	1.89593162	-0.98086180	0.65682452
H	-0.35208463	0.37186461	-1.51417582
H	-0.62051882	-2.04657703	-2.10716470
H	0.74026938	-3.76630485	-0.92530602
H	2.35680406	-3.07998272	0.83914640
H	2.60637517	-0.69207737	1.43174850
H	2.01106684	1.28582118	2.33831989
C	1.26276553	1.44548022	0.31159743
H	2.04020024	2.93669685	1.63508057
O	0.62812831	2.28331079	-0.34515342
C	2.18267234	1.87376219	1.42733833
H	3.22725642	1.71058119	1.12179472
F	3.41145609	7.02046854	0.38023233
C	1.65406668	5.73430174	-0.68260635
H	0.72206319	4.00332521	-0.30232598
C	2.61313955	5.04551279	-1.68055803
F	1.92364500	4.67094395	-2.78840515
F	3.19070705	3.92527914	-1.15871915
F	3.61430647	5.87468482	-2.08262790
C	2.35723905	6.19445188	0.62129580
F	1.46785821	6.87927902	1.38689066
F	2.81706880	5.15238667	1.37256683

O	0.51785266	4.97863127	-0.40788422
H	1.33739247	6.66766481	-1.17705625

[**5.3l**] - HFIP/acetophenone_OH-O; Ph side - ZORA-GGAPBE-D3(BJ)/TZP_gas phase

C	1.75088672	0.41171166	-0.03079143
C	0.54974294	-0.27908543	-0.26537416
C	0.51979314	-1.66977522	-0.23144705
C	1.68994864	-2.38943327	0.03757217
C	2.89095235	-1.71316593	0.27138131
C	2.92271979	-0.31950338	0.23755063
H	-0.34915911	0.29745985	-0.47223479
H	-0.41729252	-2.19751330	-0.41410858
H	1.66540588	-3.48013549	0.06501782
H	3.80272504	-2.27377747	0.48095470
H	3.86445758	0.19812142	0.42275410
H	3.41760950	2.43276296	1.18064920
C	1.74232675	1.90076696	-0.07157499
H	2.84540870	3.72431145	0.07832682
O	0.70310478	2.52924762	-0.29564688
C	3.03382962	2.65091220	0.17340057
H	3.80745357	2.34403995	-0.54430187
F	-3.96558822	1.60813929	-2.36625096
C	-2.82169970	3.19287250	-0.93338905
H	-0.87170781	3.29122838	-0.64163071
C	-3.19178712	2.41926759	0.35613057
F	-3.15934053	3.26733459	1.41496131
F	-2.32267983	1.40144828	0.62010567
F	-4.44348892	1.88810184	0.29539768
C	-2.80965535	2.30757968	-2.20365236
F	-2.65074042	3.09675603	-3.29791590
F	-1.78197113	1.41204727	-2.19497988
O	-1.63212132	3.90628739	-0.79690246
H	-3.63530800	3.91922266	-1.08436552

[**5.3m**] - HFIP/benzaldehyde_OH-O; H side - ZORA-GGAPBE-D3(BJ)/TZP_gas phase

C	1.00544393	-0.24548392	0.01111489
C	-0.32722904	-0.62762755	-0.22576021
C	-0.73700270	-1.92065017	0.08223052
C	0.17682024	-2.83594119	0.62508160
C	1.50292837	-2.46090994	0.86287239
C	1.91710411	-1.16640328	0.55566498
H	-1.01509100	0.10507826	-0.64924068
H	-1.76853233	-2.22579684	-0.09949464
H	-0.14949221	-3.84983114	0.86275922
H	2.20852911	-3.17767594	1.28389424
H	2.94948985	-0.85630672	0.73356376
O	0.77314131	1.99938910	-0.78118379
C	1.47677245	1.10579182	-0.30371512
H	2.54949340	1.29532507	-0.08265657
F	4.64570008	5.23449178	0.28188237
C	2.86420138	4.86232561	-1.31958579
H	1.36960125	3.56263052	-1.14923530
C	3.76010238	4.03153100	-2.27109108
F	3.27367369	4.11182418	-3.53444521
F	3.79324885	2.70822088	-1.93047397
F	5.04461801	4.47917814	-2.29729494

C	3.34933200	4.84416940	0.15044082
F	2.58882670	5.69394970	0.88579991
F	3.23457719	3.60512463	0.71671206
O	1.52175128	4.51519609	-1.42364914
H	2.97475866	5.90669469	-1.65272073

[**5.3m**] - HFIP/benzaldehyde_OH-O; Ph side - ZORA-GGAPBE-D3(BJ)/TZP_gas phase

C	1.78888669	0.39974095	-0.28127045
C	0.63325008	-0.25860043	0.17413560
C	0.68049081	-1.62038916	0.45251962
C	1.87620558	-2.33167518	0.27886347
C	3.03106290	-1.68134829	-0.16837649
C	2.98772675	-0.31662488	-0.44619380
H	-0.28366209	0.31376010	0.30162075
H	-0.21440847	-2.13604751	0.80380115
H	1.90671860	-3.40073450	0.49628106
H	3.95834475	-2.23993145	-0.29988574
H	3.88029368	0.20642046	-0.79829212
O	0.80718515	2.58334582	-0.54799222
C	1.78022684	1.83348305	-0.59751860
H	2.77072051	2.24498111	-0.90795184
F	-3.76376688	1.01246019	-2.53620681
C	-2.83129142	2.75334413	-1.14420539
H	-0.91715468	3.07056637	-0.76959652
C	-3.26404710	2.14739277	0.21348111
F	-3.61626654	3.14881775	1.05933846
F	-2.25181402	1.45146235	0.81133319
F	-4.32856902	1.30850331	0.10349992
C	-2.62160407	1.69792327	-2.25733864
F	-2.22966431	2.31898809	-3.39842620
F	-1.65977321	0.78787152	-1.93407461
O	-1.72858318	3.59237640	-0.99554775
H	-3.68091780	3.36930831	-1.47765976

[**5.3n**] - HFIP/chlorobenzene_out of ring_pH - ZORA-GGAPBE-D3(BJ)/TZP_gas phase

C	1.27901353	-0.09341226	0.24748881
C	0.04284086	-0.74247197	0.23044110
C	-0.01458849	-2.07792519	-0.17619051
C	1.15042892	-2.75232861	-0.55968922
C	2.38134055	-2.08672402	-0.52704023
C	2.45364071	-0.75154802	-0.12302510
H	-0.85697749	-0.20607852	0.52962753
H	-0.97613074	-2.59190335	-0.19456627
H	1.09940143	-3.78682019	-0.89830933
H	3.29259514	-2.60846573	-0.82156370
H	3.40530508	-0.22193005	-0.09600223
Cl	1.35873155	1.58634687	0.74997704
F	-0.21640733	-7.09094541	2.17406940
C	1.39366420	-5.32381484	2.53623919
H	1.40322079	-3.57080870	1.64785943
C	2.51010111	-6.00410348	1.70677658
F	3.72081429	-5.60558342	2.17210589
F	2.44999126	-5.66513648	0.38544726
F	2.46107046	-7.35842291	1.78933847
C	-0.03646068	-5.74651006	2.12327076
F	-0.93450576	-5.17727259	2.96685654

F	-0.34678558	-5.33214789	0.85952243
O	1.53550805	-3.93273593	2.55494422
H	1.52820232	-5.68198705	3.56802846

[**5.3n**] - HFIP/chlorobenzene_out of ring_Cl - ZORA-GGAPBE-D3(BJ)/TZP_gas phase

C	1.37167804	0.31929450	-0.13485938
C	0.52881407	0.13509482	0.96034491
C	0.33760246	-1.16280435	1.44230977
C	0.97793359	-2.24761553	0.83710878
C	1.81827870	-2.03603332	-0.25955299
C	2.02238875	-0.74581141	-0.75583904
H	0.03440723	0.98523785	1.43040152
H	-0.31828581	-1.31976843	2.29949041
H	0.82327561	-3.25694957	1.22040981
H	2.32220753	-2.87708294	-0.73746806
H	2.67631029	-0.56577064	-1.60848049
Cl	1.63443171	1.95048164	-0.76280978
F	2.50190664	6.69006443	2.08779536
C	0.91791556	4.86282583	2.07948851
H	1.19596791	3.16001221	1.15249720
C	0.00011191	5.51642554	1.01875428
F	-1.26943597	5.06198564	1.18974007
F	0.38367774	5.19659626	-0.24780609
F	-0.03172383	6.86977435	1.12139329
C	2.38830841	5.33865752	2.01702970
F	3.07236579	4.81191036	3.06613972
F	3.00366918	4.92395285	0.87540336
O	0.84045139	3.46413516	2.02206590
H	0.53116423	5.18002978	3.05887121

[**5.3n**] - HFIP/chlorobenzene_in ring_pH - ZORA-GGAPBE-D3(BJ)/TZP_gas phase

C	1.06100435	0.20371053	-0.71073437
C	0.12778125	-0.75978043	-0.32513645
C	0.55282408	-2.08039053	-0.14686332
C	1.89444145	-2.42719220	-0.34681553
C	2.81323283	-1.44626094	-0.73311783
C	2.40181442	-0.12480430	-0.92012511
H	-0.91166808	-0.47724438	-0.16402742
H	-0.17274204	-2.83967105	0.14770387
H	2.21976036	-3.45813926	-0.20450609
H	3.86032869	-1.70737711	-0.88912616
H	3.10943425	0.64744573	-1.21968773
Cl	0.53955257	1.86478640	-0.92767391
F	3.24823225	0.59424446	4.44232578
C	1.58194695	-1.06861959	3.88184561
H	1.36868872	-1.81088095	2.08185361
C	0.43397347	-0.03105600	3.84779023
F	-0.75106440	-0.66979973	4.04413829
F	0.35779088	0.61831175	2.65675593
F	0.56251380	0.90072692	4.82912447
C	2.98153062	-0.46076535	3.62989156
F	3.92904158	-1.40984804	3.86460799
F	3.12475397	-0.05025118	2.34225279
O	1.33907971	-2.13880407	3.00991754
H	1.59705856	-1.47115845	4.90518657

[**5.3n**] - HFIP/chlorobenzene_in ring_Cl - ZORA-GGAPBE-D3(BJ)/TZP_gas phase

C	1.15441427	0.45162491	-0.40881515
C	-0.02483960	-0.29046966	-0.42446049
C	-0.03040178	-1.52224148	-1.08410050
C	1.12438252	-1.99258946	-1.71555130
C	2.29288434	-1.22627559	-1.69142442
C	2.31732415	0.00732245	-1.03505560
H	-0.91504505	0.08553416	0.07820447
H	-0.94532455	-2.11572649	-1.09776523
H	1.11434869	-2.95692777	-2.22506701
H	3.19783845	-1.58788294	-2.18121826
H	3.22359494	0.61069331	-1.00022578
Cl	1.17957924	1.99825479	0.44636219
F	0.38231517	-1.77151604	4.64386777
C	1.92115516	0.01394977	4.10550775
H	1.73992243	1.28444828	2.62323625
C	2.98333357	-0.89807472	3.44647045
F	4.21835083	-0.37225157	3.66988641
F	2.81247276	-0.98420154	2.10166293
F	2.97745835	-2.15805183	3.95488725
C	0.48283901	-0.55205196	4.05401751
F	-0.35269544	0.29270734	4.71537548
F	0.02400401	-0.66319680	2.77725585
O	1.97605422	1.31121215	3.58010178
H	2.18684596	0.07485379	5.17121108

[**5.3.1**] - 2xHFIP - ZORA-GGAPBE-D3(BJ)/TZP_gas phase

F	1.36771749	-1.21863618	1.18364580
C	1.65921002	0.94381411	0.15827621
H	1.12042565	2.64752365	0.96161765
C	0.43101989	0.83838820	-0.77402991
F	0.68089536	1.52522094	-1.91728174
F	-0.67215916	1.39319334	-0.19423273
F	0.13815513	-0.43942756	-1.10713791
C	1.56714582	0.09429481	1.44705320
F	2.72337812	0.21198298	2.14339621
F	0.55411160	0.52854841	2.25023222
O	1.90128673	2.29514345	0.48864274
H	2.52921665	0.58183606	-0.40584347
F	6.53750387	4.19086520	1.63658910
C	5.14392296	3.80149491	-0.30261293
H	3.23023785	3.36159369	-0.25040731
C	5.67437465	2.36582189	-0.52903395
F	5.55102575	2.04341658	-1.84368127
F	4.96058348	1.44104584	0.18215807
F	6.98031811	2.23012806	-0.19236734
C	5.26931313	4.29106949	1.16037408
F	4.90813718	5.60017941	1.22389579
F	4.44918059	3.59900374	1.99774074
O	3.83440490	3.94046234	-0.77430663
H	5.78911544	4.46090512	-0.90241507

[**5.3.1**] - 3xHFIP - ZORA-GGAPBE-D3(BJ)/TZP_gas phase

F	1.06128313	-0.96181866	0.45453093

C	1.62972543	1.18316257	-0.48418480
H	1.36688525	2.94260006	0.40394456
C	0.38298451	1.25425478	-1.39682186
F	0.66796183	1.99834020	-2.49390028
F	-0.66728180	1.85902851	-0.75782404
F	-0.03061405	0.03620081	-1.81456930
C	1.44128851	0.30101797	0.77415023
F	2.61307098	0.22469127	1.44967283
F	0.51130369	0.82405457	1.61852419
O	2.05304656	2.47722208	-0.13998344
H	2.42699557	0.71406087	-1.07852538
F	6.31977824	3.34548258	2.63716824
C	5.51828546	3.52622905	0.36371871
H	3.66760420	3.30459202	-0.26516778
C	6.04867192	2.15404276	-0.11645500
F	6.44291302	2.25648076	-1.41324416
F	5.08315047	1.19068351	-0.06211041
F	7.11210282	1.71744464	0.60455771
C	5.21786711	3.58724971	1.88120147
F	4.77131958	4.83490193	2.19665365
F	4.25006801	2.70533886	2.25268559
O	4.42022348	3.93385914	-0.39746097
H	6.33496334	4.24374733	0.19119766
F	-3.05210259	4.34990903	2.42207168
C	-0.95409779	4.48221554	1.24511619
H	0.81496450	4.60218734	2.09118230
C	-1.04861155	5.98951734	0.91546974
F	-0.44330718	6.22263186	-0.27594097
F	-0.40600339	6.73619221	1.85772498
F	-2.32750401	6.42113130	0.82883089
C	-1.73641074	4.04514895	2.50543047
F	-1.62280979	2.70302814	2.65582784
F	-1.22926999	4.63089323	3.62693090
O	0.40211828	4.10000392	1.35923062
H	-1.37948661	3.93434157	0.39437500

[**5.3.1**] - 4xHFIP - ZORA-GGAPBE-D3(BJ)/TZP_gas phase

F	2.57170902	1.60668881	4.37673380
C	2.47072193	2.13811330	2.02104284
H	2.12403475	3.96049632	1.28050308
C	1.02405834	1.60240474	1.89528528
F	0.74973894	1.33780599	0.59726666
F	0.10081254	2.50786158	2.33548739
F	0.85277794	0.45747989	2.60245108
C	2.85818094	2.55929775	3.45839624
F	4.18345095	2.81873059	3.51585587
F	2.20852713	3.71035274	3.84006402
O	2.72372873	3.17847235	1.11651171
H	3.12977203	1.29786846	1.75953769
F	7.04801987	0.77814407	-0.41636776
C	5.29956398	2.21130223	-1.28198873
H	3.93951668	3.16262885	-0.21642591
C	4.40437175	1.03515370	-1.74221165
F	3.63993798	1.43521616	-2.78950066
F	3.55629500	0.61985849	-0.75403992
F	5.12654230	-0.04138494	-2.14610292
C	6.25961204	1.84421718	-0.12391641
F	7.07131089	2.89901416	0.13860505

F	5.58246774	1.55581207	1.02834119
O	4.54475213	3.34653027	-0.97953212
H	5.94376034	2.45261681	-2.14139066
F	-1.13392558	6.19086011	-1.23624444
C	0.65997634	6.16370853	0.36725849
H	0.58276988	5.44441128	2.22025243
C	0.61566991	7.66396654	0.74613400
F	1.87742164	8.10713279	0.96845016
F	-0.09915505	7.86709031	1.89009288
F	0.06912164	8.42636747	-0.23158974
C	-0.70007022	5.59341295	-0.10098797
F	-0.56883875	4.26714349	-0.34864104
F	-1.66882536	5.74235555	0.84970036
O	1.19261560	5.41510101	1.43271366
H	1.34544608	6.07242040	-0.48767589
F	-3.53967296	4.46325661	4.91731905
C	-1.50084476	5.56670310	4.24717313
H	0.18722951	4.55611194	4.31279364
C	-1.41478428	6.36749070	5.56843011
F	-0.64692116	7.46805591	5.36991925
F	-0.84352706	5.63518297	6.56244893
F	-2.63581359	6.78021291	5.98655134
C	-2.33355827	4.26715181	4.33951839
F	-2.53796685	3.77098023	3.09444153
F	-1.66336566	3.31856128	5.05625395
O	-0.20203130	5.27652914	3.77421162
H	-1.98541703	6.21803764	3.50759465

A6. Scientific production

List of publications

1) - *full paper*

Is the R3Si Moiety in Metal-Silyl Complexes a Z ligand? An Answer from the Interaction Energy.

Dang Ho Binh[a], Milan R. Milovanović[a,b], Julia Puertes-Mico[a], Mustapha Hamdaoui[a], Snežana D. Zarić[b,c] and Jean-Pierre Djukic[a]

[a]*LCSOM, Institut de Chimie de Strasbourg (UMR 7177), Université de Strasbourg, Strasbourg, France*
[b]*Faculty of Chemistry, University of Belgrade, Belgrade, Serbia*
[c]*Faculty of Chemistry, Texas A&M University at Qatar, Doha, Qatar*

Chem. Eur. J. **2017**, *23*, 17058.
DOI: 10.1002/chem.201703373

2) - *full paper*

Investigation of interactions in Lewis pairs between phosphines and boranes by analyzing crystal structures from the Cambridge Structural Database

Milan R. Milovanović[a,b], Jelena M. Andrić[c], Vesna B. Medaković[b], Jean-Pierre Djukic[a] and Snežana D. Zarić[b,d]

[a]*LCSOM, Institut de Chimie de Strasbourg (UMR 7177), Université de Strasbourg, Strasbourg, France*
[b]*Faculty of Chemistry, University of Belgrade, Belgrade, Serbia*
[c]*Innovation center, Faculty of Chemistry, Studentski trg 12-16, Belgrade, Serbia*
[d]*Department of Chemistry, Texas A&M University at Qatar, Doha, Qatar*

Acta Cryst. **2018**, *B74*, 255.
DOI: 10.1107/S2052520618003736

3) - *full paper*

Isotherm Calorimetric Titration and DOSY NMR Analysis of so-Called Frustrated Lewis "Pairs" Rather Suggest Large Molecular Aggregate Formation

Milan R. Milovanović[a,b], Bruno Vincent[a], Anaëlle Bolley[a], Snežana D. Zarić[b,c] and Jean-Pierre Djukic[a]

[a]*LCSOM, Institut de Chimie de Strasbourg (UMR 7177), Université de Strasbourg, Strasbourg, France*
[b]*Faculty of Chemistry, University of Belgrade, Belgrade, Serbia*
[c]*Department of Chemistry, Texas A&M University at Qatar, Doha, Qatar*

being written

List of presentations

1) - *poster presentation*

BENCHMARKING TO DFT-D CALCULATIONS BY ITC EXPERIMENTAL DATA

Milan R. Milovanović[a,b], Sebastian Dohm[c], Andreas Hansen[c], Stefan Grimme[c], Snežana D. Zarić[b,d], Jean-Pierre Djukic[a]

[a]*LCSOM, Institut de Chimie de Strasbourg (UMR 7177), Université de Strasbourg, Strasbourg, France*
[b]*Faculty of Chemistry, University of Belgrade, Belgrade, Serbia*
[c]*Mulliken Center for Theoretical Chemistry, University of Bonn, Bonn, Germany*
[d]*Department of Chemistry, Texas A&M University at Qatar, Doha, Qatar*

1st Journal of Thermal Analysis and Calorimetry Conference and 6th V4 (Joint Czech-Hungarian-Polish-Slovakian) Thermoanalytical Conference (JTACC+V4) / Budapest, Hungary / 6-9 June 2017

2) - *poster presentation*

CRYSTALLOGRAPHIC INVESTIGATON OF INTERACTIONS BETWEEN PHOSPHINES AND BORANES

Milan R. Milovanović[a,b], Jelena M. Andrić[c], Snežana D. Zarić[b,d]

[a]*LCSOM, Institut de Chimie de Strasbourg (UMR 7177), Université de Strasbourg, Strasbourg, France*
[b]*Faculty of Chemistry, University of Belgrade, Belgrade, Serbia*
[c]*Innovation center, Faculty of Chemistry, Studentski trg 12-16, Belgrade, Serbia*
[d]*Department of Chemistry, Texas A&M University at Qatar, Doha, Qatar*

24th Conference of the Serbian Crystallographic Society / Vršac, Serbia / 22-24 June 2017

3) - *oral communication*

ARE PHOSPINE-BORANE PAIRS CLASSICAL OR FRUSTRATED? ANALYSIS OF CAMBRIDGE STRUCTURAL DATABASE

Milan R. Milovanović[a,b], Jelena M. Andrić[c], Vesna B. Medaković[b], Jean-Pierre Djukic[a], Snežana D. Zarić[b,d]

[a]*LCSOM, Institut de Chimie de Strasbourg (UMR 7177), Université de Strasbourg, Strasbourg, France*
[b]*Faculty of Chemistry, University of Belgrade, Belgrade, Serbia*
[c]*Innovation center, Faculty of Chemistry, Studentski trg 12-16, Belgrade, Serbia*
[d]*Department of Chemistry, Texas A&M University at Qatar, Doha, Qatar*

25th Conference of the Serbian Crystallographic Society / Bajina Bašta, Serbia / 22-24 June 2018

Chapter 11

References

List of used references

[N^0 1] P. Hobza, *Acc. Chem. Res*. **2012**, *45*, 663.
[N^0 2] R. Huenerbein, B. Schirmer, J. Moellmann, S. Grimme, *Phys. Chem. Chem. Phys.* **2010**, *12*, 6940.
[N^0 3] see section *1.4.2.1.3. Solvation treatment* for the details.
[N^0 4] F. London, *Z. Physik* **1930**, *63*, 245.
[N^0 5] A. J. Stone, *The Theory of Intermolecular Forces*; Oxford University Press. Oxford, **2002**. P.
[N^0 6] Hobza, K. Müller-Dethlefs, In *Non-Covalent Interactions: Theory and Experiment*; The Royal Society of Chemistry, **2009**
[N^0 7] see section *1.4.1. Experimental tools* for the details.
[N^0 8] see section *1.4.2. Theoretical tools* for the details.
[N^0 9] see section *1.3. Thermochemistry and Thermodynamics*. for the details.
[N^0 10] I. Müller, *A History of Thermodynamics – the Doctrine of Energy and Entropy*; Springer. **2007**.
[N^0 11] K. Müller-Dethlefs, P. Hobza, *Chem. Rev*. **2000**, *100*, 143.
[N^0 12] G. N. Lewis, *J. Am. Chem. Soc*. **1916**, *38*, 762.
[N^0 13] L. M. Brown, A. Pais, B. Pippard, *Twentieth Century Phisics*; Institute of Physics Pub.; American Institute of Phisics Press, Bristol; Philadelphia; New York, **1995**.
[N^0 14] J. D. van der Waals, In *Nobel Lecture: The Equation of State for Gases and Liquids*; NobelPrize.org. Nobel Media AB 2018. Wed. 22 Aug 2018.
https://www.nobelprize.org/prizes/physics/1910/waals/lecture/
[N^0 15] H. Kamerlingh Onnes, *Proc. R. Netherlands Acad. Arts Sci. (KNAW) 11* **1909**, 168.
[N^0 16] F. London, *Trans. Faraday Soc*. **1937**, *33*, 8.
[N^0 17] R. Eisenschitz, F. London, *Z. Physik* **1930**, *60*, 491.
[N^0 18] H. Hellmann, *Acta Physicochim*. **1935**, 273.
[N^0 19] L. Pauling, *J. Am. Chem. Soc*. **1931**, *53*, 1367.
[N^0 20] P. Hobza, R. Zahradnik, K. Müller-Dethlefs, *Collect Czech Chem. C* **2006**, *71*, 443.
[N^0 21] I. G. Kaplan, *Intermolecular Interactions; Physical Picture, Computational Methods and Model Potentials*; Wiley, Chichester, **2006**.
[N^0 22] J. O. Hirschfelder, C. F. Curtiss, R. B. Bird, *Molecular Theory of Gases and Liquids*; Wiley, New York, **1954**.
[N^0 23] P. Debye, *Phys. Z*. **1921**, *22*, 302.
[N^0 24] I. E. Dzyaloshinskii, E. M. Lifshitz, P. P. Lev, *Sov. Phys. Usp*. **1961**, *4*, 153.
[N^0 25] D. Lanfbein, *Phys. Rev. B* **1970**, *2*, 3371.
[N^0 26] H. C. Hamaker, *Physica* **1937**, *4*, 1058.
[N^0 27] Y. Zheng, A. Narayanaswamy, *Phys. Rev. A* **2011**, *83*, 042504.
[N^0 28] C. A. Coulomb, *Premier mémoire sur l'électicité et le magnétisme*; Histoire de l'Académie Royale des Sciences, Imprimerie Royale, **1785**, 569-577.
[N^0 29] C. A. Coulomb, *Second mémoire sur l'électicité et le magnétisme*; Histoire de l'Académie Royale des Sciences, Imprimerie Royale, **1785**, 578-611.
[N^0 30] J. D. Jackson, *Classical Electrodynamics*; John Wiley & Sons Ltd, **1962**.
[N^0 31] P. Atkins, J. de Paula, *Physical Chemistry for the Life Science*; Oxford University Press, Oxford. **2006**.
[N^0 32] F. London, *Z. Physik Chem*. **1930**, *11*, 222.
[N^0 33] J. W. Leachman, R. T. Jacobsen, S. G. Penoncello, E. W. Lemmon, *J. Phys. Chem. Ref. Data* **2009**, 38, 721.
[N^0 34] H. Kamerlingh Onnes, In *Nobel Lecture: Investigation into the Properties of Substances at Low Temperatures, which Have Led, amongst Other Things, to the Preparation of Liquid Helium*; NobelPrize.org. Nobel Media AB 2018. Wed. 22 Aug 2018. https://www.nobelprize.org/prizes/physics/1913/onnes/lecture/
[N^0 35] C. J. Benmore, B. Tomberli, P. A. Egelstaff, J. Neuefeind, *Mol. Phys*. **2001**, *99*, 787.
[N^0 36] E. Pavarini, E. Koch, F, Anders, In *Correlated electrons: From Models to Materials* 2012.
[N^0 37] V. F. Weisskopf, *Science* **1975**, *187*, 605.
[N^0 38] H. C. Andersen, D. Chandler, J. D. Weeks, *J. Chem. Phys*. **1972**, *56*, 3812.
[N^0 39] P. A. M. Dirac, *Proc. Royal. Soc. Lond. S. A* **1926**, *112*, 661.

[N^0 40] In IUPAC. Compendium of Chemical Terminology, Version 2.3.3. – 2014-02-24 – the “Gold Book” ed. XML version: Web.
[N^0 41] D. Chandler, *Nature* **2005**, *437*, 640.
[N^0 42] C. Tanford *Prot. Sci*. **1997**, *6*, 1358.
[N^0 43] H. J. Dyson, P. E. Wright, H. A. Scheraga, *Proc. Natl. Acad. Sci. USA* **2006**, *103*, 13057.
[N^0 44] M. Rapacioli, F. Calvo, F. Spiegelman, C. Joblin, D. J. Wales, *J. Phys. Chem. A* 2005, *109*, 2487.
[N^0 45] J. Grant hill, J. A. Platts, H.-J. Werner, *Phys. Chem. Chem. Phys*. **2006**, *8*, 4072.
[N^0 46] R. Podeszwa, R. Bukowski, K. Szalewicz, *J. Phys. Chem. A* **2006**, *110*, 10345.
[N^0 47] F. Cozzi, M. Cinquini, R. Annunziata, T. Dwyer, J. S. Siegel, *J. Am. Chem. Soc*. **1992**, *114*, 5729.
[N^0 48] C. A. Hunter, J. K. M. Snaders, *J. Am. Chem. Soc*. **1990**, *112*, 5525.
[N^0 49] E.-I. Kim. S. Paliwal, C. S. Wilcox, *J. Am. Chem. Soc*. **1998**, *120*, 11192.
[N^0 50] S. Grimme, *Angew. Chem. Int. Ed.* **2008**, *47*, 3430.
[N^0 51] M. O. Sinnokrot, C. D. Sherrill, *J. Phys. Chem. A* **2003**, *107*, 8377.
[N^0 52] M. O. Sinnokrot, C. D. Sherrill, *J. Am. Chem. Soc.* **2004**, *12*, 7690.
[N^0 53] S. E. Weeler. K. N. Houk, *J. Am. Chem. Soc*. **2008**, *130*, 10854.
[N^0 54] F. Cozzi, R. Annunziata, M. Banaglia, K. K. Baldridge, G. Aguirre, J. Estrada, Y. Sritana-Anant, J. S. Siegel, *Phys. Chem. Chem. Phys.* **2008**, *10*, 2686.
[N^0 55] S. L. Cockroft, C. A. Hunter, *Chem. Soc. Rev*. **2007**, *36*, 172.
[N^0 56] D. B. Ninković, J. M. Andrić, S. D. Zarić, *ChemPhysChem* **2013**, *14*, 237.
[N^0 57] D. B. Ninković, G. V. Janjić, D. Ž. Veljković, D. N. Sredojević, S. D. Zarić, *ChemPhysChem* **2011**, *12*, 3511.
[N^0 58] J. P. Gallivan, D. A. Dougherty, *J. Am. Chem. Soc*. **2000**, *122*, 870.
[N^0 59] S. Tsuzuki, M. Yoshida, T. Uchimaru, M. Mikami, *J. Phys. Chem. A* **2001**, *105*, 769.
[N^0 60] C. D. Sherrill, T. Takatani, E. G. Hohestein, *J. Phys. Chem. A* **2009**, *113*, 10146.
[N^0 61] S. Mecozzi, A. P. West. Jr., D. A. Dougherty, *Proc. Nat. Acad. Sci. USA*, **1996**, *93*, 10566.
[N^0 62] S. Mecozzi, A. P. West. Jr., D. A. Dougherty, *J. Am. Chem. Soc*. **1996**, *118*, 2307.
[N^0 63] S. E. Weeler. K. N. Houk, *J. Am. Chem. Soc*. **2009**, *131*, 3126.
[N^0 64] S. D. Zarić, *Eur. J. Inorg. Chem.* **2003**, 2197.
[N^0 65] C. Rapp, E. Goldberger, N. Tishbi, R. Kirshenbaum, *Proteins: Struct., Funct., Bioinf*. **2014**, *82*, 1494.
[N^0 66] K. K. Bania, A. K. Guha, P. K. Bhattacharyya, S. Sinha, *Dalton Trans*. **2014**, *43*, 1769.
[N^0 67] D. A. Dougherty, *Science*, **1996**, 271, 163.
[N^0 68] D. A. Dougherty, *J. Nutr*. **2007**, *137*, 1504.
[N^0 69] S. A. Pless, A. P. Hanek, K. L. Price, J. W. Lynch, H. A. Lester, D. A. Dougherty, S. C. Lummis, *Mol. Pharmaco*l. **2011**, *79*, 742.
[N^0 70] T. J. Anderson, G. D. Jones, D. A. Vicic, *J. Am. Chem. Soc*. **2004**, *126*, 8100.
[N^0 71] B. C. De Petar, H.-W. Fruehauf, K. Vrieze, R. De Gelder, E. J. Baerends, D. McCormack, M. Lutz, [N^0 70] L. Spek, F. Hartl, *Eur. J. Inorg, Chem*. **2004**, 1675.
[N^0 72] G. V. Janjić, J. M. Andrić, A. Kapor, Z. D. Bugarčić, S. D. Zarić, *CrystEngComm* **2010**, *12*, 3773.
[N^0 73] G. V. Janjić, P. V. Petrović, D. B. Ninković, S. D. Zarić, *J. Mol. Mod*. **2011**, *17*, 2083.
[N^0 74] D. N. Sredojević, Z. D. Tomić, S. D. Zarić, *Ctyst. Growth Des*. **2010**, *10*, 3901.
[N^0 75] D. N. Sredojević, D. Z. Vojislavljević, Z. D. Tomić, S. D. Zarić, *Acta Crystallogr.* **2012**, *B68*, 261.
[N^0 76] G. A. Bogdanović, A. Spasojević-de Biré, S. D. Zarić, *Eur. J. Inorg. Chem*. **2002**, 1599.
[N^0 77] G. A. Bogdanović V. B. Medaković, M. K. Milčić, S. D. Zarić, *Int. J. Mol. Sci*. **2004**, *5*, 174.
[N^0 78] V. B. Medaković, M. K. Milčić, G. A. Bogdanović, S. D. Zarić, *J. Inorg. Biochem*. **2004**, *98*, 1867.
[N^0 79] M. K. Milčić, V. B. Medaković, D. N. Sredojević, N. O. Juranić, S. D. Zarić, *Inorg. Chem*. **2006**, *45*, 4755.
[N^0 80] S. Đ. Stojanović, V. B. Medaković, G. Predović, M. Beljanski, S. D. Zarić, J. Biol. *Inorg. Chem*. **2007**, *12*, 1063.
[N^0 81] M. K. Milčić, V. B. Medaković, S. D. Zarić, *Inorg. Chim. Acta* **2006**, *359*, 4427.
[N^0 82] D. P. Malenov, D. B. Ninković, D. N. Sredojević, S. D. Zarić, *ChemPhysChem* **2014**, *15*, 2458.

[N⁰ 83] D. P. Malenov, D. B. Ninković, S. D. Zarić, *ChemPhysChem* **2015**, *16*, 761.
[N⁰ 84] D. N. Sredojević, D. B. Ninković, G. V. Janjić, J. Zhou, M. B. Hall, S. D. Zarić, *ChemPhysChem* **2013**, *14*, 1797.
[N⁰ 85] Z. D. Tomić, S. B. Novaković, S. D. Zarić, *Eur. J. Inorg. Chem*. **2004**, 2215.
[N⁰ 86] Z. D. Tomić, D. N. Sredojević, S. D. Zarić, *Cryst. Growth Des*. **2006**, *6*, 29.
[N⁰ 87] D. P. Malenov, S. D. Zarić, *Phys. Chem. Chem. Phys.* **2018**, *20*, 14053.
[N⁰ 88] D. P. Malenov, M. B. Hall, S. D. Zarić, *Int. J. Quantum Chem*. **2018**; e25629.
[N⁰ 89] D. P. Malenov, G. V. Janjić, V. B. Medaković, M. B. Hall, S. D. Zarić, *Coord. Chem. Rev*. **2017**, *345*, 318.
[N⁰ 90] J. P. Blagojević, D. Ž. Veljković, S. D. Zarić, *CrystEngComm* **2017**, *19*, 40.
[N⁰ 91] J. P. Blagojević, S. D. Zarić, *Chem. Commun.* **2015**, *51*, 12989.
[N⁰ 92] S. A. Arnstein, C. D. Sherrill, *Phys. Chem. Chem. Phys*. **2008**, *10*, 2646.
[N⁰ 93] S. T. Mutter, J. A: Platts, *Chemistry*, **2010**, *16*, 5391.
[N⁰ 94] P. Forbes, *The gecko's foot: How scientists are taking a leaf form nature's book*; Harper Perennial. **2006**.
[N⁰ 95] A. P. Russell, *J. Zool*. **1975**, *176*, 437.
[N⁰ 96] P. F. A. Maderson, *Nature* **1964**, *203*, 780.
[N⁰ 97] S. Hu, S. Lopez, P. H. Niewiarowski, Z. Xia, *J. Royal Soc. Inter*. **2012**.
[N⁰ 98] B. N. J. Persson, *MRS Bulletin* **2007**, *32*, 486.
[N⁰ 99] K. Autumn, A. M. Peattie, *Intergr. Comp. Biol*. **2002**, *42*, 1081.
[N⁰ 100] K. Autumn, Y. A. Liang, S. T. Hsieh, W. Zesch, W. P. Chan, T. W. Kenny, R. Fearilng, R. J. Full, *Nature* **2000**, *405*, 681.
[N⁰ 101] E. E. Williams, J. A. Peterson, *Science*, **1982**, *215*, 1509.
[N⁰ 102] C. Bissantz, B. Kuhn, M. Stahl*, J. Med. Chem*. **2010**, *53*, 5061.
[N⁰ 103] M. Ma, Y. Kuang, Y. Gao, Y. Zhang, P. Gao, B. Xu, *J. Am. Chem. Soc*. **2010**, *132*, 2719.
[N⁰ 104] L. M. Salonen, M. Ellermann, F. Diederich, *Angew. Chem. Int. Ed*. **2011**, *50*, 4808.
[N⁰ 105] H.-J. Schneider, *Angew. Chem. Int. Ed*. **2009**, 48, 3924.
[N⁰ 106] M. O. Sinnokrot, E. F. Valeev, C. D. Sherrill, *J. Am. Chem. Soc*. **2002**, *124*, 10887.
[N⁰ 107] R. Chelli, F. L. Gervasio, P. Procacci, V. Schettino, *J. Am. Chem. Soc*. **2002**, *124*, 6133.
[N⁰ 108] U. Samanta, P. Chakrabarti, *Protein Eng*. **2001**, *14*, 7.
[N⁰ 109] S. K. Burley, G. A. Petsko, *Science* **1985**, *229*, 23.
[N⁰ 110] V. L. Malinovskii, F. Samain, R. Haner*, Angew. Chem. Int. Ed*. **2007**, *46*, 4464.
[N⁰ 111] C. A. Eckert, D. L. Bergmann, D. L. Tomasko, M. P. Ekart, *Acc. Chem. Res*. **1993**, *26*, 621.
[N⁰ 112] O. Schuster, U. Monkowius, H. Schmidbaur, R. S. Ray, S. Krueger, N. Roesch, *Organometallics* **2006**, *25*, 1004.
[N⁰ 113] T. R. Ward, J. Collot, J. Gradinaru, A. Loosli, M. Skander, C. Letondor, E. Joseph, G. Klein, *Chimia* **2003**, *57*, 586.
[N⁰ 114] S. Li, Y. Xu, Q. Shen, X. Liu, J. Lu, Y. Chen, T. Lu, C. Luo, X. Luo, M. Zheng, H. Jiang, *Curr. Pharm. Des*. **2013**, *19*, 6522.
[N⁰ 115] A. K. Patri, J. F. Kukowska-Latallo, J. R. Baker Jr., *Adv. Drug Delivery Rev*. **2005**, *57*, 2203.
[N⁰ 116] P. Zhou, J. Huang, F. Tian. *Curr. Med. Chem*. **2012**, *19*, 226.
[N⁰ 117] D. B. Amabilino, J. Veciana, *Top. Curr. Chem*. **2006**, *265*, 253.
[N⁰ 118] C. G. Claessens, J. F. Stoddart, *J. Phys. Org. Chem*. **1997**, *10*, 254.
[N⁰ 119] J. A. A. W. Elemans, A. E. Rowan, R. J. M. Nolte, *J. Mater. Chem*. **2003**, *13*, 2661.
[N⁰ 120] A. S. Borovik, *Comments Inorg. Chem.* **2002**, *23*, 45.
[N⁰ 121] L. H. Doerrer, *Comments Inorg. Chem.* **2008***, 29, 93.*
[N⁰ 122] C. A. Hunter, *Chem. Soc. Rev*. **1994**, *23*, 101.
[N⁰ 123] J. K. Klosterman, Y. Yamauchi, M. Fujita, *Chem Soc. Rev*. **2009**, *38*, 1714.
[N⁰ 124] J. M. Pollino, M. Weck, *Chem. Soc. Rev*. **2005**, *34*, 193.
[N⁰ 125] S. Zhang, D. M. Marini, W. Hwang, S. Santoso, *Curr. Opin. Chem. Biol*. **2002**, *6*, 865.
[N⁰ 126] T. L. Brown, *Chemistry: the central science*; Prentice Hall, Boston, **2012**.
[N⁰ 127] D. H. Guston, *Encyclopedia of nanoscience and society*; Sage, Thousand Oaks, Calif, **2010**.
[N⁰ 128] A. Rajput, R. Mukherjee, *Coord. Chem. Rev*. **2013**, *257*, 350.
[N⁰ 129] C. Janiak, *Dalton Trans*. **2000**, 3885.

[N^0 130] J. A. Martinho Simoes, M. E. Minas da Piedade, *Molecular Energetics: condensed phase thermochemical techniques*; Oxford University Press, Inc, New York, **2008**. and related references therein.
[N^0 131] P. Hobza, H. L. Selzle, E. W. Schlag, *Chem. Rev.* **1994**, 94, 1767.
[N^0 132] P. Hobza, R. Zahradnik, *Chem. Rev*. **1988**, *88*, 871.
[N^0 133] B. C. Garrett, D. A. Dixon, D. M. Camaioni, D. M. Chipman, M. A. Johnson, C. D. Jonah, G. A. Kimmel, J. H. Miller, T. N. Rescigno, P.J. Rossky, S. S. Xantheas, S. D. Colson, A. H. Laufer, D. Ray, P. F. Barbara, D. M. Bartels, K. H. Becker, K. H. Bowen, Jr., S. E. Bradforth, I. Carmichael, J. V. Coe, L. R. Corrales, J. P. Cowin, M. Dupuis, K. B. Eisenthal, J. A. Franz, M. S. Gutowski, K. D. Jordan, B. D. Kay, J. A. LaVerne, S. V. Lymar, T. E. Madey, C. W. McCurdy, D. Meisel, S. Mukamel, A. R. Nilsson, T. M. Orlando, N. G. Petrik, S. M. Pimblott, J. R. Rustad, G. K. Schenter, S. J. Singer, A. Tokmakoff, L.-S. Wang, C. Wittig, T. S. Zwier, *Chem. Rev*. **2005**, *105*, 355.
[N^0 134] A. B. E. H. Abou El-Nasr, A. Fujii, T. Ebata, N. Mikami, *Mol. Phys*. **2005**, *103*, 1561.
[N^0 135] P. Imhof, D. Krugler, R. Brause, K. Kleinermanns, *J. Chem. Phys.* **2004**, *121*, 2598.
[N^0 136] R. H. Wu, B. Brutschy, *J. Phys. Chem. A* **2004**, *108*, 9715.
[N^0 137] E. A. El-Hakam, A. El-Nasr, A. Fujii, T. Yahagi, T. Ebata, N. Mikami, *J. Phys. Chem. A* **2005**, *109*, 2498.
[N^0 138] B. M. Giuliano, P. Ottaviani, W. Caminati, M. Schnell, D. Banser, J. U. Grabow, *Chem. Phys*. **2005**, *312*, 111.
[N^0 139] R. Sanchez, S. Blanco, A. Lesarri, J. C. Lopez, J. L. Alonso, *Chem. Phys. Lett*. **2005**, *401*, 259.
[N^0 140] S. Blanco, J. C. Lopez, A. Lesarri, W. Caminati, J. L. Alonso, *Mol. Phys.* **2005**, *103*, 1473.
[N^0 141] B. M. Giuliano, W. Caminati, *Angew. Chem. Int. Ed. Engl*. **2005**, *44*, 603.
[N^0 142] W. Caminati, J. C. Lopez, J. L. Alonso, J. U. Grabow, Angew. *Chem. Int. Ed. Engl*. **2005**, *44*, 3840.
[N^0 143] A. Lesarri, E. J. Cocinero, J. C. Lopez, J. L. Alonso, Angew. *Chem. Int. Ed. Engl*. **2004**, *43*, 605.
[N^0 144] J. L. Alonso, S. Antolinez, S. Blanco, A. Lesarri, J. C. Lopez, *J. Am. Chem. Soc*. **2004**, *126*, 3244.
[N^0 145] G. C. Cole, A. C. Legon, *J. Chem. Phys*. **2004**, *121*, 10467.
[N^0 146] P. W. Fowler, A. C. Legon, J. M. A. Thumwood, E. R. Waclawik, *Coord. Chem. Rev*. **2000**, *197*, 231.
[N^0 147] N. Goldman, C. Leforestier, R. J. Saykally, *Philos. Trans. Roy. Soc. A* **2005**, *363*, 493.
[N^0 148] F. N. Keutsch, J. D. Cruzan. R. J. Saykally, *Chem. Rev*. **2003**, *103*, 2533.
[N^0 149] J. D. Cruzan. L. B. Braly, K. Liu, M. G. Brown, J. G. Loeser, R. J. Saykally, *Science*, **1996**, *271*, 59.
[N^0 150] S. Chervenkov, P. Q. Wang, J. E. Braun, S. Georgiev, H. J. Neusser, C. K. Nandi, T. Chakraborty, *J. Chem. Phys*. **2005**, 122.
[N^0 151] T. V. Nguyen, T. M. Korter, D. W. Pratt, *Mol. Phys.* **2005**, *103*, 2453.
[N^0 151] S. Georgiev, H. J. Neusser, *J. Electron Spect*. **2005**, *142*, 207.
[N^0 153] C. Kang, D. W. Pratt, *Int. Rev. Phys. Chem*. **2005**, *24*, 1.
[N^0 154] D. W. Pratt, *Science* **2002**, *296*, 2347.
[N^0 155] M. S. Ford, K. Müler-Dethlefs, *Phys. Chem. Chem. Phys*. **2004**, *6*, 23.
[N^0 156] Y. H. Lee, J. W. Jung, B. Kim, P. Butz, L. C. Snoek, R. T. Kroemer, J. P. Simons, *J. Phys. Chem. A* **2004**, *108*, 69.
[N^0 157] X. Tong, M. S. Ford, C. E. H. Dessent, K. Müler-Dethlefs, *J. Chem. Phys*. **2003**, *119*, 12908.
[N^0 158] M. S. Ford, X. Tong, C. E. H. Dessent, K. Müler-Dethlefs, *J. Chem. Phys*. **2003**, *119*, 12914.
[N^0 159] D. A. Beattie, R. J. Donovan, *Prog. React. Kinet. Mec*. **1998**, *23*, 281.
[N^0 160] S. Leutwyler, J. Bosiger, *Chem. Rev*. **1990**, *90*, 489.
[N^0 161] R. B. Bernstein, *J. Phys. Chem*. **1982**, *86*, 1178.
[N^0 162] C. E. H. Dessent, K. Müler-Dethlefs, *Chem. Rev*. **2000**, *100*, 3999.
[N^0 163] K. Müler-Dethlefs, *J. Chem. Phys*, **1991**, *95*, 4821.
[N^0 164] K. Müler-Dethlefs, M. Sadner, E. W. Z. Schlag, *Z. Naturforsch. A* **1984**, *39*, 1089.
[N^0 165] K. Müler-Dethlefs, M. Sadner, E. W. Z. Schlag, *Chem. Phys. Lett*. **1984**, *112*, 291.
[N^0 166] W. Hebanicht, G. Reiser, K. Müler-Dethlefs, *J. Chem. Phys*. **1991**, *95*, 4809.
[N^0 167] H. Krause, H. J. Neusser, *J. Chem. Phys*. **1993**, *99*, 6278.
[N^0 168] L. Zhu, P. Johnson, *J. Chem. Phys*. **1991**, *94*, 5769.

[N^0 169] D. M. Chapman, K. Müler-Dethlefs, J. B. Peel, *J. Chem. Phys*. **1999**, *111*, 1955.
[N^0 170] M. Schmitt, C. Ratzer, W. L. Meerts, *J. Chem. Phys*. **2004**, *120*, 2752.
[N^0 171] A. Westphal, C. Jacoby, C. Ratzer, A. Reichelt, M. Schmitt, *Phys*. *Chem. Chem. Phys.* **2003**, *5*, 4114.
[N^0 172] M. Schmitt, C. Jacoby, M. Gerhards, C. Unterberg, W. Roth, K. Kleinermanns, *J. Chem. Phys*. **2000**, *113*, 2995.
[N^0 173] C. Jacoby, W. Roth, M. Schmitt, C. Janzen, D. Spangenberg, K. Kleinermanns, *J. Phys. Chem. A* **1998**, *102*, 4471.
[N^0 174] W. Roth, C. Jacoby, M. Schmitt, D. Spangenberg, C. Janzen, K. Kleinermanns, *Chem. Phys*. **1998**, *239*, 1.
[N^0 175] E. Condon, *Phys. Rev*. **1926**, *28*, 1182.
[N^0 176] M. Kleibeer, in *The fire of life: an introduction to animal energetics*; ed. E. R. Krieger, Pub. Co, Huntington, New York, **1987**.
[N^0 177] A. C. Buchholz, D. A. Schoeller, *Am. J. Clin. Nutr*. **2004**, *79*, 899.
[N^0 178] J. J. Christensen, R. M. Izatt, L. D. Hansen, J. A. Partridge, *J. Phys. Chem*. **1966**, *70*, 2003.
[N^0 179] L. D. Hansen, J. J. Christensen, R. M. Izatt, *Chem. Commun*. **1965**, 36.
[N^0 180] N. V. Beaudette, N. Langerman, *Anal. Biochem*. **1978**, *90*, 693.
[N^0 181] T. Wiseman, S. Williston, J. F. Brandts, L. N. Lin, *Anal. Biochem*. **1989**, *179*, 131.
[N^0 182] E. Freire, O. L. Mayorga, M. Straume, *Anal. Chem*. **1990**, *62*, 950A.
[N^0 183] M. W. Freyer, E. A. Lewis, in *Methods in Cell Biology*; eds. J. C. John, H. William Detrich, III, Academic Press, **2008**, vol. 87, 79-113.
[N^0 184] C. Spink, I. Wadso, *Methods Biochem. Anal*. **1976**, *23*, 1.
[N^0 185] M. J. Todd, J. Gomez, *Anal. Biochem*. **2001**, *296*, 179.
[N^0 186] B. A. Williams, E. J. Toone, *J. Org. Chem*. **1993**, *58*, 3507.
[N^0 187] N. A. Demarse, M. C. Killian, L. D. Hansen, C. F. Quinn, *Methods Mol. Biol*. **2013**, *978*, 21.
[N^0 188] T. Ehtezazi, U. Rungsardthong, S. Stolnik, *Langmuir* **2003**, *19*, 9387.
[N^0 189] M. Keller, M. R. Jorgensen, E. Perouzel, A. D. Miller, *Biochemistry* **2003**, *42*, 6067.
[N^0 190] D. Matulis, I. Rouzina, V. A. Bloomfield, *J. Am. Chem. Soc*. **2002**, *124*, 7331.
[N^0 191] C. K. Nisha, S. V. Manorama, M. Ganguli, S Maiti, J. N. Kizahakkedathu, *Langmuir* **2004**, *20*, 2386.
[N^0 192] E. Pozharski, R. C. MacDonald, *Biophys. J*. **2002**, *83*, 556.
[N^0 193] U. Rungsardthong, T. Ehtezazi, L. Bailey, S. P. Armes, M. C. Garnett, S. Stolnik, *Biomacromolecules* **2003**, *4*, 683.
[N^0 194] M. Keller, T. Tagawa, M. Preuss, A. D. Miller, *Biochemistry* **2002**, *41*, 652.
[N^0 195] A. Velazquez Campoy, E. Freire, *Biophys. Chem*. **2005**, *115*, 115.
[N^0 196] G. A. Holdgate, *BioTechniques* **2001**, *31*, 164.
[N^0 197] I. Jelesarov, H. R. Bosshard, *J Mol. Recognit*. **1999**, *12*, 3.
[N^0 198] J. E. Ladbury, *Thermochim. Acta*. **2001**, *380*, 209.
[N^0 199] E. A. Lewis, K. P. Murphy, *Methods Mol. Biol*. **2005**, *305*, 1.
[N^0 200] F. P. Schmidtchen, in *Macrocyclic Chemistry*; ed. K. Gloe, Springer Netherlands, **2005**, ch. 19, pp. 291-302.
[N^0 201] P. C. Weber, F. R. Salemme, *Curr. Opin. Chem. Biol*. **2003**, *13*, 115.
[N^0 202] A. Ababou, J. E. Ladbury, *J. Mol. Recognit*. **2007**, *20*, 4.
[N^0 203] M. J. Cliff, A. Gutierrez, J. E. Ladbury, *J. Mol. Recognit*. **2004**, *17*, 513.
[N^0 204] J. E. Ladbury, *Biochem. Soc. Trans*. **2010**, *38*, 888.
[N^0 205] E. A. Lewis, K. P. Murphy, *Methods Mol. Biol*. **2005**, *305*, 1.
[N^0 206] D. R. Bundle, B. W. Sigurskjold, *Methods Enzymol*. **1994**, *247*, 288.
[N^0 207] P. Puja, K. S. Gopinatha, *Photochem. Photobiol. Sci*. **2014**, *13*, 1192.
[N^0 208] E. Freire, *Drug Discovery Today: Technol*. **2014**, *1*, 295.
[N^0 209] L. Indyk, H. F. Fisher, *Methods Enzymol*. **1998**, *295*, 350.
[N^0 210] M. Hamdaoui, M. Ney, V. Sarda, L. Karmazin, C. Bailly, N. Sieffert, S. Dohm, A. Hansen, S. Grimme, and J.-P. Djukic, *Organometallics* **2016**, *35*, 2207.
[N^0 211] A. Hansen, C. Bannwarth, S. Grimme, P. Petrović, C. Werlé, J.-P. Djukic, *ChemistryOpen* **2014**, *3*, 177.
[N^0 212] P. V. Petrović, S. Grimme, S. D. Zarić, M. Pfeffer, J.-P. Djukic, *Phys. Chem. Chem. Phys*. **2014**, *16*, 14688.

[N^0 213] H. Fischer, P. Hofmann, *Organometallics* **1999**, *18,* 2590.
[N^0 214] E. Schrödinger, *Annalen der Physik* **1926**, *79*, 361.
[N^0 215] C. Froese Fischer, *Comp. Phis. Comm*. **1987**, *43*, 355.
[N^0 216] W. Koch, M. C. Holthausen, *A Chemist's Guide to Density Functional Theory*; Wiley-VCH, Weinheim, **2001**, and related references therein.
[N^0 217] C. Møller, M. S. Plesset *Phys. Rev*. **1934**, *46*, 618.
[N^0 218] J. Čižek, *J. Chem. Phys*. **1966**, *45*, 4256.
[N^0 219] J. Čižek, J. Paldus, *Int. J. Quantum Chem*. **1971**, *5*, 359.
[N^0 220] J. Paldus, J. Čižek, I. Shavitt, *Phys. Rev. A*, **1972**, *5*, 50.
[N^0 221] R. J. Bartlett, M. Musial, *Rev. Mod. Pys*, **2007**, 79, 291.
[N^0 222] K. Raghavachari, G. W. Trucks, J. A. Pople, M. Head-Gordon, *Chem. Phys. Lett*. **1989**, *157*, 479.
[N^0 223] R. J. Bartlett, *An. Rev. Phys. Chem*. **1981**, *32*, 359.
[N^0 224] B. Jeziorski, R, Moszinsky, K. Szalewicz, *Chem. Rev.* **1994**, *94*, 1887.
[N^0 225] R, J. Barllet, J. F. Stanton, *Rev. Comput. Chem*. **1995**, *5*, 65.
[N^0 226] A. Szabo, N. S. Ostlund, *Modern Quantum Chemistry: Introduction to Advanced Electronic Structure Theory*; MacMillan Publishing Co., New York, **1982**.
[N^0 227] R. Mc Wenny, *Methods of Molecular Quantum Mechanics*; 2nd Edition, Academic Press, London, **1992**.
[N^0 228] P. W. Atkins, R. S. Friedman, *Molecular Quantum Mechanics*; 3rd Edition, Oxford University Press, Oxford, **1997**.
[N^0 229] F. Jansen, *Introduction to Computational Chemistry*; Wiley, Chichester, **1999**.
[N^0 230] P. Hohenberg, W. Kohn, *Phys. Rev.* **1964**, *136*, B864.
[N^0 231] W. Kohn, L. J. Sham, *Phys. Rev.* **1965**, *140,* A1133.
[N^0 232] V. G. Rousseau, *Phys. Rev. E* **2008**, *77,* 056705.
[N^0 233] M. Mella, J. B. Anderson, *J. Chem. Phys*. **2003**, *119*, 8225.
[N^0 234] W. M. C. Foulkes, L. Mitas, R. J. Needs, G. Rajagopal, *Rev. Mod. Phys*. **2001**, *73*, 33.
[N^0 235] C. Diedrich, A. Luchow, S. Grimme, *J. Chem. Phys. Chem*. **2005**, *123*, 184106.
[N^0 236] E. Fermi*, Rend. Accad. Lincei* **1927**, *6*, 602.
[N^0 237] L. H. Tomas, *Proc. Camb. Phil. Soc*. **1927**, *23*, 542.
[N^0 238] J. C. Slater, *Phys. Rev.* **1951**, *81*, 385.
[N^0 239] S. Sirois, E. I. Proynov, D. T. Nguyen, D.R. Salahub, *J. Chem. Phys*. **1997**, *107*, 6770.
[N^0 240] F. Sim, A. St. Amant, I. Papai, D. R. Salahub, *J. Am. Chem. Soc*. **1992**, *114*, 4391.
[N^0 241] M. S. Liao, Y. Lu, V. D. Parker, S. Scheiner, *J. Chem. Phys*. **2003**, *107*, 8939.
[N^0 242] C. Desplanches, E. Ruiz, A. Rodríguez-Fortea, S. Alvarez, *J. Am. Chem. Soc*, **2002**, *124*, 5197.
[N^0 243] A. D. Becke, *J. Chem. Phys*, **1993**, *98*, 1372.
[N^0 244] P. M. W. Gill, R. D. Adamson, J. A. Pople, *Mol. Phys.* **1996**, *88*, 1005.
[N^0 245] P. Hobza, J. Sponer, T. Reschel, *J. Comput. Chem*. **1995**, *16*, 1315.
[N^0 246] S. Kristyan, P. Pulay, *Chem. Phys. Lett*. **1994**, *229*, 175.
[N^0 247] Y. K. Zhang. W. Pan, W. T. Yang, *J. Chem. Phys*, **1997**, *107*, 7921.
[N^0 248] R. M. Balabin, *J. Chem. Phys*. **2008**, *129*, 164101.
[N^0 249] B. Paizs, S. Suhai, *J. Comput. Chem.* **1998**, *19*, 575.
[N^0 250] G. A. DiLabio, A. Otero-de-la-Roza, *arXiv:1405.1771 [physics.chem-ph]* **2014**.
[N^0 251] J. Tomasi, B. Mennucci, R. Cammi, *Chem. Rev*. **2005**, *150*, 2999.
[N^0 252] W. J. Hehre, L. Radom, P. v. R. Schleyer, J. A. Pople, *Ab Initio Molecular Orbital Theory*, Wiley, New York, **1986**.
[N^0 253] S. Grimme, *J. Comput. Chem*. **2004**, *25*, 1463.
[N^0 254] S. Grimme, *J. Comput. Chem*. **2006**, *27*, 1787.
[N^0 255] S. Grimme, J. Antony, S. Ehrlich, H. Krieg, *J. Chem. Phys*. **2010**, *132*, 154104.
[N^0 256] E. Caldeweyher, C. Bannwarth, S. Grimme, *J. Chem. Phys*. **2017**, *147*, 034112.
[N^0 257] P. Jurecka, J. Cerny, P. Hobza, D. R. Salahub, *J. Comput. Chem*. **2007**, *28*, 555.
[N^0 258] J. Tao, J. P. Perdew, A. Ruzsinszky, *Proc. Nat. Acad. Sc*i. **2012**, *109*, 18.
[N^0 259] A. Tkatchenko, M. Scheffer, *Phys. Rev. Lett*. **2009**, *102*, 073005.
[N^0 260] A. Tkatchenko, A. Ambrosetti, R. A. DiStasio, *J. Chem. Phys.* **2013***, 138,* 074106*.*
[N^0 261] A. Otero-de-la-Roza, R. R. Johnson, *J. Chem. Phys*. **2013**, *138*, 054103.

[N^0 262] J. Luder, B. Sanyal, O. Eriksson, C. Puglia, B. Brena, *Phys. Rev. B* **2014**, *89*, 045416.
[N^0 263] G. A. DiLabio, E. R. Johnson, A. Otero-de-la-Roza, *Phys. Chem. Chem. Phys*. **2013**, *15*, 12821.
[N^0 264] N. Marom, A. Tkatchenko, M. Rossi, V. V. Gobre, O. Hod, M. Scheffer, L. Kronik, *J. Chem. Theory Comput.* **2011**, *7*, 3944.
[N^0 265] G. DiLibio, M. Koleini, E. Torres, *Theor. Chem. Acc*. **2013**, *132*,1.
[N^0 266] S. Grimme, *WIREs: Comput. Mol. Sci*. **2011**, *1*, 211.
[N^0 267] W. Hujo, S. Grimme, *Phys. Chem. Chem. Phys.* **2011**, *13*, 13942.
[N^0 268] S. Grimme, S. Ehrlich, L. Goerigk, *J. Comput. Chem*. **2011**, *32*, 1456.
[N^0 269] S. Grimme, M. Steinmetz, *Phys. Chem. Chem. Phys.* **2013**, *15*, 16031.
[N^0 270] S. Grimme, R. Huenerbein, S. Ehrlich, *ChemPhysChem* **2011**, *12*, 1258
[N^0 271] H. B. G. Casimir, D. Polder, *Phys. Rev*. **1948**, *73*, 360.
[N^0 272] Q. Wu, W. Yang, *J. Chem. Phys*. **2002**, *116*, 515.
[N^0 273] T. A. Halgren, *J. Am. Chem. Soc*. **1992**, *114*, 7827.
[N^0 274] M. Born, *Z. Phys*. **1920**, *1*, 45.
[N^0 275] J. G. Krikwood, *J. Chem. Phys*. **1934**, *2* 351.
[N^0 276] L. Onsager, *J. Am. Chem. Soc*. **1936**, *58*, 1486.
[N^0 277] A. Klamt, G. Schueuermann, *J. Chem. Soc. Perkin Trans. 2* **1993**, 799.
[N^0 278] A. Klamt, *Phys. Chem*. **1955**, *99*, 2224.
[N^0 279] J. G. Krikwood, *J. Chem. Phys*. **1939**, *7*, 911.
[N^0 280] K. V. Mikkelsen, H. Aagren, H. J. A. Jensen, T. Helgaker, *J. Chem. Phys*. **1988**, *89*, 3086.
[N^0 281] J. L. Rivail. D. Rinaldi, *Chem. Phys*. 1976, *18*, 233.
[N^0 282] M. W. Wong, M. J. Frisch, K. B. Wiberg, *J. Am. Chem. Soc*. **1991**, *113*, 4776.
[N^0 283] M. W. Wong, K. B. Wiberg, M. J. Frisch, *J. Am. Chem. Soc*. **1992**, *114*, 523.
[N^0 284] B. Mennucci, E. Cances, J. Tomasi, *J. Phys. Chem. B* **1997**, *101*, 10506.
[N^0 285] E. Cances, B. Mennucci, J. Tomasi, *J. Chem. Phys*. **1997**, *107*, 3032.
[N^0 286] D. M. Chipman, *J. Chem. Phys*. **1999**, *110*, 8012.
[N^0 287] D. M. Chipman, *J. Chem. Phys.* **2000**, *112*, 5558.
[N^0 288] D. M. Chipman, *J. Chem. Phys*. **2002**, *116*, 10129.
[N^0 289] D. Bashford, D. A. Case, *Annu. Rev. Phys. Chem*. **2000**, *51*, 129.
[N^0 290] A. Onufriev, D. Bashford, D. A. Case, *J. Phys. Chem. B*, **2000**, *104*, 3712.
[N^0 291] A. Klamt, V. Jonas, T. Burger, J. C. W. Lohrenz, *J. Phys. Chem. A*, **1998**, *102*, 5074.
[N^0 292] R. Putnam, R. Taylor, A. Klamt, F. Eckert, M. Schiller, *Ind. Eng. Chem. Res*. **2003**, *42*, 3635.
[N^0 293] www.tainstruments.com
[N^0 294] K. H. Ebrahimi, P.-L. Hagedoorn, D. Jacobs, W. R. Hagen, *Scientific Reports*, 5:16380.
[N^0 295] J. H. Espenson, *Chemical Kinetics and Reaction Mechanisms*; McGraw-Hill series in advanced chemistry, eds. J. Ricci, J.W. Bradley, McGraw-Hill, Inc, **1981**.
[N^0 296] G. te Velde, F.M. Bickelhaupt, S. J. A. van Gisbergen, C. Fonseca Guerra, E. J. Baerends, J. G. Snijders, T. Ziegler, *J. Comput. Chem.* **2001**, *22*, 931.
[N^0 297] C. Fonseca Guerra, J. G. Snijders, G. te Velde, E. J. Baerends, *Theor. Chem. Acc.* **1998**, *99*, 391.
[N^0 298] ADF2013, SCM, Theorical Chemistry, Vrije Universiteit, Amsterdam, The Netherlands, http://www.scm.com
The following list of authors and contributors:
E.J. Baerends, T. Ziegler, J. Autschbach, D. Bashford, A. Bérces, F. M. Bickelhaupt, C. Bo, P. M. Boerrigter, L. Cavallo, D. P. Chong, L. Deng, R. M. Dickson, D. E. Ellis, M. van Faassen, L. Fan, T. H. Fischer, C. Fonseca Guerra, M. Franchini, A. Ghysels, A. Giammona, S. J. A. van Gisbergen, A. W. Götz, J.A. Groeneveld, O. V. Gritsenko, M. Grüning, S. Gusarov, F. E. Harris, P. van den Hoek, C. R. Jacob, H. Jacobsen, L. Jensen, J. W. Kaminski, G. van Kessel, F. Kootstra, A. Kovalenko, M. V. Krykunov, E. van Lenthe, D. A. McCormack, A. Michalak, M. Mitoraj, S.M. Morton, J. Neugebauer, V. P. Nicu, L. Noodleman, V. P. Osinga, S. Patchkovskii, M. Pavanello, P. H. T. Philipsen, D. Post, C.C. Pye, W. Ravenek, J. I. Rodríguez, P. Ros, P. R. T. Schipper, G. Schreckenbach, J. S. Seldenthuis, M. Seth, J. G. Snijders, M. Solà, M. Swart, D. Swerhone, G. te Velde, P. Vernooijs, L. Versluis, L. Visscher, O. Visser, F. Wang, T. A. Wesolowski, E. M. van Wezenbeek, G. Wiesenekker, S. K. Wolff, T. K. Woo, A. L. Yakovlev

[N⁰ 299] M. J. Frisch, G. W. Trucks, H. B. Schlegel, G. E. Scuseria, M. A. Robb, J. R. Cheeseman, G. Scalmani, V. Barone, B. Mennucci, G. A. Petersson, H. Nakatsuji, M. Caricato, X. Li, H. P. Hratchian, A. F. Izmaylov, J. Bloino, G. Zheng, J. L. Sonnenberg, M. Hada, M. Ehara, K. Toyota, R. Fukuda, J. Hasegawa, M. Ishida, T. Nakajima, Y. Honda, O. Kitao, H. Nakai, T. Vreven, J. A. Montgomery, Jr., J. E. Peralta, F. Ogliaro, M. Bearpark, J. J. Heyd, E. Brothers, K. N. Kudin, V. N. Staroverov, R. Kobayashi, J. Normand, K. Raghavachari, A. Rendell, J. C. Burant, S. S. Iyengar, J. Tomasi, M. Cossi, N. Rega, J. M. Millam, M. Klene, J. E. Knox, J. B. Cross, V. Bakken, C. Adamo, J. Jaramillo, R. Gomperts, R. E. Stratmann, O. Yazyev, A. J. Austin, R. Cammi, C. Pomelli, J. W. Ochterski, R. L. Martin, K. Morokuma, V. G. Zakrzewski, G. A. Voth, P. Salvador, J. J. Dannenberg, S. Dapprich, A. D. Daniels, Ö. Farkas, J. B. Foresman, J. V. Ortiz, J. Cioslowski, and D. J. Fox, *Gaussian 09* (Gaussian, Inc., Wallingford CT, **2009**).
[N⁰ 300] C. R. Groom, I. J. Bruno, M. P. Lightfoot, S. C. Ward, *Acta Cryst*. **2016**, *B72*, 171.
[N⁰ 301] S. D. Zarić, *Chem. Phys. Lett.* **1999**, *311*, 77.
[N⁰ 302] S. D. Zarić, *Chem. Phys*. **2000**, *256*, 213.
[N⁰ 303] S. D. Zarić, D. Popović, E. W. Knapp, *Chem. Eur. J.* **2000**, *6*, 3935.
[N⁰ 304] C. I. Yeo, S. N. A. Halim, S. W. Ng, S. L. Tan, J. Zukerman-Schpector, M. A. B. Ferreira, E. R. T. Tiekink, *Chem. Commun.* **2014**, *50*, 5984.
[N⁰ 305] D. P. Malenov, J. Lj. Dragelj, G. V. Janjić, S. D. Zarić, *Cryst. Growth Des.* **2016**, *16*, 4169.
[N⁰ 306] T. Steiner, G. R. Desiraju, *Chem. Commun.* **1998**, *8*, 891.
[N⁰ 307] A. Nangia, *Cryst. Eng.* **2001**, *4*, 49.
[N⁰ 308] T. Steiner, *Chem. Commun.* **1997**, *8*, 727.
[N⁰ 309] T. Steiner, *Angew. Chem. Int. Ed.* **2002**, *41*, 48.
[N⁰ 310] A. Bauzá, R. Ramis, A. Frontera, *J. Phys. Chem. A* **2014**, *118*, 2827.
[N⁰ 311] J. Huang, S. Kingsbury, M. Kertesz, *Phys. Chem. Chem. Phys.* **2008**, *10*, 2625.
[N⁰ 312] T. J. Mooibroek, P. Gamez, J. Reedijk, *CrystEngComm* **2008**, *10*, 1500.
[N⁰ 313] E. R. T. Tiekink, *Coord. Chem. Rev.* **2017**, 345, 209.
[N⁰ 314] A. Bauzá, T. J. Mooibroek, A. Frontera, *ChemPhysChem* **2015**, *16*, 2496.
[N⁰ 315] R. Taylor, *CrystEngComm* **2014**, 16, 6852.
[N⁰ 316] Santiago Alvarez, *Dalton Trans.* **2013**, 42, 8617.
[N⁰ 317] G. Kuppuraj, M. Dudev, C. Lim, *J. Phys. Chem. B* **2009**, *113*, 2952.
[N⁰ 318] A. Nimmermark, L. Öhrström, J. Reedijk, *Z. Kristallogr.* **2013**, *228*, 3113.
[N⁰ 319] R. K. Hocking, T. W. Hambley, *Inorg. Chem.* **2003**, *42*, 2833.
[N⁰ 320] www.rcsb.org; H. M. Berman, J. Westbrook, Z. Feng, G. Gilliland, T. N. Bhat, H. Weissig, I. N. Shindyalov, P. E. Bourne, The Protein Data Bank *Nucleic Acids Research* **2000**, *28*, 235.
[N⁰ 321] I. M. Stanković, D. M. Božinovski, E. N. Brothers, M. R. Belić, M. B. Hall, S. D. Zarić, *Cryst. Growth Des*. **2017**, *17*, 6353.
[N⁰ 322] J. Lj. Dragelj, I. M. Stanković, D. M. Božinovski, T. Meyer, D. Ž. Veljković, V. B. Medaković, E.-W. Knapp, S. D. Zarić, *Cryst. Growth Des*. **2016**, *16*, 1948.
[N⁰ 323] D. B. Ninković, D. P. Malenov, P. V. Petrović, E. N. Brothers, S. Niu, M. B. Hall, M. R. Belić, S. D. Zarić, *Chem. Eur. J*. **2017**, *23*, 11046 – 11053.
[N⁰ 324] I. J. Bruno, J. C. Cole, P. R. Edgington, M. Kessler, C. F. Macrae, P. McCabe, J. Pearson, R. Taylor, *Acta Cryst*. **2002**, *B58*, 389.
[N⁰ 325] J. P. Perdew, K. Burke, M. Ernzerhof, *Phys. Rev. Lett.* **1996**, *77*, 3865.
[N⁰ 326] J. P. Perdew, K. Burke, M. Ernzerhof, *Phys. Rev. Lett.* **1997**,*78*, 1396.
[N⁰ 327] E. van Lenthe, E. J. Baerends, J. G. Snijders, *J. Chem. Phys.* **1993**, *99*, 4597.
[N⁰ 328] E. van Lenthe, E. J. Baerends, J. G. Snijders, *J. Chem. Phys.* **1994**,*101*, 9783.
[N⁰ 329] E. van Lenthe, A. E. Ehlers, E. J. Baerends, *J. Chem. Phys.* **1999**,*110*, 8943.
[N⁰ 330] E. van Lenthe and E. J. Baerends, *J. Comput. Chem.* **2003**, *24*, 1142.
[N⁰ 331] F. Weigend, R. Ahlrichs, *Phys. Chem. Chem. Phys.* **2005**, *7*, 3297.
[N⁰ 332] F. Weigend, *Phys. Chem. Chem. Phys.* **2006**, *8*, 1057.
[N⁰ 333] C. C. Pye, T. Ziegler, *Theor. Chem. Acc.* **1999**, *101*, 396-408.
[N⁰ 334] S. Miertuš, E. Scrocco, J. Tomasi, *Chem. Phys.* **1981**, *55*, 117-129.
[N⁰ 335] A. Bérces, R. M. Dickson, L. Fan, H. Jacobsen, D. Swerhone, T. Ziegler, *Comput. Phys. Commun.* **1997**, *100*, 247.
[N⁰ 336] H. Jacobsen, A. Bérces, D. Swerhone, T. Ziegler, *Comput. Phys. Commun.* **1997**, *100*, 263.
[N⁰ 337] S. K. Wolff, *Int. J. Quantum Chem.* **2005**, *104*, 645.

[N⁰ 338] C. F. Macrae, P. R. Edgington, P. McCabe, E. Pidcock, G. P. Shields, R. Taylor, M. Towler, J. van de Streek, *J. Appl. Cryst.* **2006**, *39*, 453.
[N⁰ 339] E. Gamble, P. Gilmont, *J. Am. Chem. Soc.* **1940**, *62*, 717.
[N⁰ 340] A. Cowley, M. Damasco, *J. Am. Chem. Soc.* **1971**, *93*, 6815.
[N⁰ 341] R. Foester, K. Cohn, *Inorg. Chem.* **1972**, 11, 2590.
[N⁰ 342] G. C. Welch, L. Cabrera, P. A. Chase, E. Hollink, J. D. Masuda, P. Wei, D. W. Stephan, *Dalton Trans.* **2007**, 3407.
[N⁰ 343] P. Spies, R. Fröhlich, G. Kehr, G. Erker, S. Grimme, *Chem. Eur. J.* **2008**, *14*, 333.
[N⁰ 344] D. W. Stephan, *Dalton Trans*. **2009**, 3129.
[N⁰ 345] G. Erker, *Dalton Trans*. **2011**, *40*, 7475.
[N⁰ 346] D. W. Stephan, *Dalton Trans*. **2012**, *41*, 9015.
[N⁰ 347] T. H. Warren, G. Erker, *Top. Curr. Chem*. **2013**, *334*, 219.
[N⁰ 348] D. W. Stephan, G. Erker, *Chem. Sci*. **2014**, *5*, 2625.
[N⁰ 349] J. S. J. McCahill, G. C. Welch, D. W. Stephan, *Angew. Chem. Int. Ed*. **2007**, *46*, 4968.
[N⁰ 350] M. A. Dureen, A. Lough, T. M. Gilbert, D. W. Stephan, *Chem. Commun.* **2008**, 4303.
[N⁰ 351] D. W. Stephan, *Org. Biomol. Chem*. **2008**, *6*, 1535.
[N⁰ 352] M. A. Dureen, D. W. Stephan, *J. Am. Chem. Soc*. **2009**, 131, 8396.
[N⁰ 353] M. A. Dureen, G. C. Welch, T. M. Gilbert, D. W. Stephan, *Inorg. Chem*. **2009**, 9910.
[N⁰ 354] J. S. J. McCahill, G. C. Welch, D. W. Stephan, *Dalton Trans*. **2009**, 8555
[N⁰ 355] C. M. Momming, E. Otten, G. Kehr, R. Frohlich, S. Grimme, D. W. Stephan, G. Erker, *Angew. Chem. Int. Ed. Engl*. **2009**, *48*, 6643.
[N⁰ 356] E. Otten, R. C. Neu, D. W. Stephan, *J. Am. Chem. Soc.* **2009**, *131*, 9918.
[N⁰ 357] M. Ullrich, K. S. H. Seto, A. J. Lough, D. W. Stephan, *Chem. Commun*. **2009**, 2335.
[N⁰ 358] B. Birkmann, T. Voss, S. J. Geier, M. Ullrich, G. Kehr, G. Erker, D. W. Stephan, *Organometallics* **2010**, *29*, 5310.
[N⁰ 359] C. Chen, R. Froehlich, G. Kehr, G. Erker, *Chem. Commun.* **2010**, *46*, 3580.
[N⁰ 360] T. Voss, C. Chen, G. Kehr, E. Nauha, G. Erker, D. W. Stephan, *Chem. - Eur. J*. **2010**, *16*, 3005.
[N⁰ 361] T. Holtrichter-Roessmann, C. Roesener, J. Hellmann, W. Uhl, E.-U. Wuerthwein, R. Froehlich, B. Wibbeling, *Organometallics* **2012**, *31*, 3272.
[N⁰ 362] E. Y. X. Chen, *Top. Curr. Chem.* **2013**, *334*, 239.
[N⁰ 363] M. Sajid, A. Klose, B. Birkmann, L. Liang, B. Schirmer, T. Wiegand, H. Eckert, A. J. Lough, R. Froehlich, C. G. Daniliuc, S. Grimme, D. W. Stephan, G. Kehr, G. Erker, *Chem. Sci*. **2013**, *4*, 213.
[N⁰ 364] A. L. Travis, S. C. Binding, H. Zaher, T. A. Q. Arnold, J.-C. Buffet, D. O'Hare, *Dalton Trans*. **2013**, *42*, 2431.
[N⁰ 365] T. H. Warren, A. J. P. Cardenas, *American Chemical Society*, **2013**, pp. CATL.
[N⁰ 366] D. P. Huber, G. Kehr, K. Bergander, R. Froehlich, G. Erker, S. Tanino, Y. Ohki, K. Tatsumi, *Organometallics* **2008**, *27*, 5279.
[N⁰ 367] T. A. Rokob, A. Hamza, A. Stirling, T. Soos, I. Papai, *Angew. Chem. Int. Ed*. **2008**, *47*, 2435.
[N⁰ 368] V. Sumerin, F. Schulz, M. Nieger, M. Leskela, T. Repo, B. Rieger, *Angew. Chem. Int. Ed*. **2008**, *47*, 6001.
[N⁰ 369] C. Jiang, O. Blacque, H. Berke, *Organometallics* **2009**, *28*, 5233.
[N⁰ 370] A. Ramos, A. J. Lough, D. W. Stephan, *Chem. Commun*. **2009**, 1118.
[N⁰ 371] M. Ullrich, A. J. Lough, D. W. Stephan, *Organometallics* **2010**, *29*, 3647.
[N⁰ 372] S. Kronig, E. Theuergarten, D. Holschumacher, T. Bannenberg, C. G. Daniliuc, P. G. Jones, M. Tamm, *Inorg. Chem*. **2011**, *50*, 7344.
[N⁰ 373] A. Schaefer, M. Reissmann, A. Schaefer, W. Saak, D. Haase, T. Mueller, *Angew. Chem. Int. Ed*. **2011**, *50*, 12636.
[N⁰ 374] T. J. Herrington, A. J. W. Thom, A. J. P. White, A. E. Ashley, *Dalton Trans.* **2012**, *41*, 9019.
[N⁰ 375] G. Menard, D. W. Stephan, *Angew. Chem. Int. Ed*. **2012**, *51*, 8272.
[N⁰ 376] S. Schwendemann, S. Oishi, S. Saito, R. Froehlich, G. Kehr, G. Erker, *Chem. - Asian J*. **2013**, *8*, 212.
[N⁰ 377] D. J. Scott, M. J. Fuchter, A. E. Ashley, *Chem. Soc. Rev*. 2017, *46*, 5689.
[N⁰ 378] C. Jiang, O. Blacque, T. Fox, H. Berke, *Organometallics* **2011**, *30*, 2117.
[N⁰ 379] B. Schirmer, S. Grimme, *Chem. Commun*. **2010**, *46*, 7942.

[N⁰ 380] Z. Lu, Z. Cheng, Z. Chen, L. Weng, Z. H. Li, H. Wang, *Angew. Chem. Int. Ed.* **2011**, *50*, 12227.
[N⁰ 381] D. W. Stephan, S. Greenberg, T. W. Graham, P. Chase, J. J. Hastie, S. J. Geier, J. M. Farrell, C. C. Brown, Z. M. Heiden, G. C. Welch, M. Ullrich, *Inorg. Chem.* **2011**, *50*, 12338.
[N⁰ 382] D. W. Stephan, G. Erker, *Angew. Chem. Int. Ed.* **2015**, *54*, 6400.
[N⁰ 383] D. W. Stephan, *Science* **2016**, *354*, aaf7229.
[N⁰ 384] B. Schirmer, S. Grimme, *Top. Curr. Chem*. **2013**, *332*, 213.
[N⁰ 385] T. A. Rokob, I. Bako, A. Stirling, A. Hamza, I. Papai, *J. Am. Chem. Soc*. **2013**, *135*, 4425.
[N⁰ 386] T. A. Rokob, I. Papai, *Top. Curr. Chem*. **2013**, *332*, 157.
[N⁰ 387] R. Ponec, P. Beran, *J. Phys. Chem. A* **2013**, *117*, 2656.
[N⁰ 388] M. Pu, T. Privalov, *J. Chem. Phys*. **2013**, *138*, 154305/1.
[N⁰ 389] T. Imamoto, *Pure Appl. Chem.* **1993**, *65*, 655.
[N⁰ 390] T. Imamoto, T. Oshiki, T. Onozawa, M. Matsuo, T. Hikosaka, M. Yanagawa, *Heteroat. Chem.* **1992**, *3*, 563.
[N⁰ 391] D. Mimeau, O. Delacroix, B. Join, A.-C. Gaumont, *C. R. Chimie*, **2004**, *7*, 845.
[N⁰ 392] J.-M. Denis, H. Forintos, H. Szelke, L. Toupet, T.-N. Pham, P.-J. Madec, A.-C. Gaumont, *Chem. Commun.* **2003**, 54.
[N⁰ 393] Z. M. Heiden, M. Schedler, D. W. Stephan, *Inorg. Chem.* **2011**, *50*, 1470.
[N⁰ 394] K. Izod, C. M. Dixon, E. McMeekin, L. Rodgers, R. W. Harrington, U. Baisch, *Organometallics* **2014**, *33*, 378.
[N⁰ 395] T. Özgön, G.-Q. Chen, C. G. Daniliuc, A. C. McQuilken, T. H. Warren, R. Knitsch, H. Eckert, G. Kehr, G. Erker, *Organometallics* **2016**, *35*, 3667.
[N⁰ 396] C.-H. Lim, A. M. Holder, J. T. Hynes, C. B. Musgrave, *Inorg. Chem.* **2013**, *52*, 10062.
[N⁰ 397] C. M. Thomas, J. C. Peters, *Inorg. Chem.* **2004**, *43*, 80.
[N⁰ 398] S. J. Geier, M. A. Dureen, E. Y. Ouyang, D. W. Stephan, *Chem. Eur. J.* **2010**, *16*, 988.
[N⁰ 399] T. Agou, J. Kobayashi, T. Kawashima, *Inorg. Chem.* **2006**, *45*, 9137.
[N⁰ 400] A. J. Lough, D. W. Stephan, *J. Am. Chem. Soc.* **2009**, *131*, 523.
[N⁰ 401] D. Chen, Y. Wang, J. Klankermayer, *Angew. Chem. Int. Ed*. **2010**, *49*, 9475;
[N⁰ 402] S. Schwendemann, T. A. Tumay, K. V. Axenov, I. Peuser, G. Kehr, R. Frohlich, G. Erker, *Organometallics* **2010**, *29*, 1067.
[N⁰ 403] D. W. Stephan, G. Erker, *Angew. Chem. Int. Ed*. **2010**, *49*, 46.
[N⁰ 404] G. Erker, *C. R. Chim*. **2011**, 14, 831.
[N⁰ 405] T. Mahdi, D. W. Stephan, *J. Am. Chem. Soc*. **2014**, *136*, 15809.
[N⁰ 406] J. Paradies, *Angew. Chem. Int. Ed*. **2014**, *53*, 3552.
[N⁰ 407] A. E. Ashley, A. L. Thompson, D. O'Hare, *Angew. Chem. Int. Ed*. **2009**, *48*, 9839.
[N⁰ 408] K. V. Axenov, G. Kehr, R. Frohlich, G. Erker, *Organometallics* **2009**, *28*, 5148.
[N⁰ 409] P. A. Chase, A. L. Gille, T. M. Gilbert, D. W. Stephan, *Dalton Trans*. **2009**, 7179.
[N⁰ 410] S. J. Geier, A. L. Gille, T. M. Gilbert, D. W. Stephan, *Inorg. Chem*. **2009**, *48*, 10466.
[N⁰ 411] S. J. Geier, D. W. Stephan, *J. Am. Chem. Soc*. **2009**, *131*, 3476.
[N⁰ 412] M. Alcarazo, C. Gomez, S. Holle, R. Goddard, *Angew. Chem. Int. Ed*. **2010**, *49*, 5788.
[N⁰ 413] R. S. Chellappa, T. Autrey, M. Somayazulu, V. V. Struzhkin, R. J. Hemley, *ChemPhysChem* **2010**, *11*, 93.
[N⁰ 414] F. Schulz, V. Sumerin, M. Leskelae, T. Repo, B. Rieger, *Dalton Trans*. **2010**, *39*, 1920.
[N⁰ 415] D. P. Curran, A. Solovyev, M. M. Brahmi, L. Fensterbank, M. Malacria, E. Lacote*, Angew. Chem. Int. Ed.* **2011**, *50*, 10294.
[N⁰ 416] F. Schulz, V. Sumerin, S. Heikkinen, B. Pedersen, C. Wang, M. Atsumi, M. Leskelae, T. Repo, P. Pyykkoe, W. Petry, B. Rieger, *J. Am. Chem. Soc*. **2011**, *133*, 20245.
[N⁰ 417] J. Iglesias-Siguenza, M. Alcarazo, *Angew. Chem. Int. Ed*. **2012**, *51*, 1523.
[N⁰ 418] S. Khan, M. Alcarazo, *Top. Curr. Chem.* **2013**, *334*, 157.
[N⁰ 419] E. L. Kolychev, E. Theuergarten, M. Tamm, *Top. Curr. Chem.* **2013**, *334*, 121.
[N⁰ 420] Z. Lu, H. Ye, H. Wang, *Top. Curr. Chem*. **2013**, *334*, 59.
[N⁰ 421] S. Froemel, R. Froehlich, C. G. Daniliuc, G. Kehr, G. Erker, *Eur. J. Inorg. Chem*. **2012**, 3774;
[N⁰ 422] M. Sajid, G. Kehr, T. Wiegand, H. Eckert, C. Schwickert, R. Poettgen, A. J. P. Cardenas, T. H. Warren, R. Froehlich, C. G. Daniliuc, G. Erker, *J. Am. Chem. Soc*. **2013**, *135*, 8882.
[N⁰ 423] T. Özgön, K.-Y. Ye, C. G. Daniliuc, B. Wibbeling, L. Liu, S. Grimme, G. Kehr, G. Erker, *Chem. Eur. J*. **2016**, *22*, 5988.

[N^0 424] A. Skancke, P. N. Skancke, *J. Phys. Chem.* **1996**, *100*, 15079.
[N^0 425] C. Bannwarth, A. Hansen, S. Grimme, *Isr. J. Chem.* **2015**, *55*, 235.
[N^0 426] V. Horváth, A. Kovács, I. Hargittai, *J. Phys. Chem. A* **2003**, *107*, 1197.
[N^0 427] T. A. Rokob, A. Hamza, I. Pápai, *J. Am. Chem. Soc*. **2009**, *131*, 10701.
[N^0 428] Z. X. Lu, G. Wang, H. X. Li, L. L. Zhao, *Chinese Sci. Bull.* **2010**, *55*, 239.
[N^0 429] S. Gao, W. Wu, Y. Mo, *Int. J. Quantum Chem.* **2011**, *111*, 3761.
[N^0 430] D. Wu, D. Jia, A. Liu, L. Liu, J. Guo, *Chem. Phys. Lett.* **2012**, *541*, 1.
[N^0 431] S. Tamke, Z.-W. Qu, N. A. Sitte, U. Flörke, S. Grimme, J. Paradies, *Angew. Chem. Int. Ed.* **2016**, *55*, 4336.
[N^0 432] G. E. Arnott, P. Moquist, C. G. Daniliuc, G. Kehr, G. Erker, *Eur. J. Inorg. Chem.* **2014**, 1394.
[N^0 433] G.-Q. Chen, G. Kehr, C. Mück-Lichtenfeld, C. G. Daniliuc, G. Erker, *J. Am. Chem. Soc.* **2016**, *138*, 8554.
[N^0 434] M. Sajid, L.-M. Elmer, C. Rosorius, C. G. Daniliuc, S. Grimme, G. Kehr, G. Erker, *Angew. Chem. Int. Ed.* **2013**, *52*, 2243.
[N^0 435] A. Tlili, A. Voituriez, A. Marinetti, P. Thuérya, T. Cantat, *Chem. Commun.* **2016**, 52, 7553.
[N^0 436] L. Liu, L. L. Cao, Y. Shao, G. Ménard, D. W. Stephan, *Chem.* **2017**, *3*, 259.
[N^0 437] R. T. Paine, H. Nöth, *Chem. Rev.* **1995**, *95*, 343.
[N^0 438] B. Carboni, L. Monnier, *Tetrahedron* **1999**, *95*, 1197.
[N^0 439] J. M. Brune, B. Faure, M. Maffei, *Coord. Chem. Rev.* **1998**, *178-180*, 665.
[N^0 440] Y. Zhu, N. S. Hosmane, *Coord. Chem. Rev.* **2015**, *293–294*, 357.
[N^0 441] G. Duret, R. Quinlan, P. Bisseret, N. Blanchard, *Chem. Sci.* **2015**, *6*, 5366.
[N^0 442] H. DeFrancesco, J. Dudley, A. Coca, *Boron Chemistry: An Overview*; ACS Symposium Series, American Chemical Society, Washington, DC, **2016**, vol. 1236, ch. 1, pp 1–25.
[N^0 443] A. Staubitz, A. P. M. Robertson, M. E. Sloan, I. Manners, *Chem. Rev.* **2010**, *110*, 4023.
[N^0 444] S. J. Grabowski, *ChemPhysChem* **2014**. *15*, 2985.
[N^0 445] S. J. Grabowski, *J. Comp. Chem.* **2018**, *39*, 472.
[N^0 446] F. Bertini, V. Lyaskovskyy, B. J. J. Timmer, F. J. J. de Kanter, M. Lutz, A. W. Ehlers, J. C. Slootweg, K. Lammertsma, *J. Am. Chem. Soc.* **2012**, *134*, 201.
[N^0 447] R. C. Neu, E. Y. Ouyang, S. J. Geier, X. Zhao, A. Ramos, D. W. Stephan, *Dalton Trans.* **2010**, 39, 4285.
[N^0 448] S. Kronig, E. Theuergarten, D. Holschumacher, T. Bannenberg, C. G. Daniliuc, P. G. Jones, M. Tamm, *Inorg. Chem.* **2011**, *50*, 7344;
[N^0 449] A. Hamza, A. Stirling, T. A. Rokob, I. Papai*, Int. J. Quantum Chem.* **2009**, *109*, 2416;
[N^0 450] S. M. Kathmann, H. Cho, T.-M. Chang, G. K. Schenter, K. Parab, T. Autrey, *J. Phys. Chem. B* **2014**, *118*, 4883.
[N^0 451] S. M. Whittemore, G. Edvenson, D. M. Camaioni, A. Karkamkar, D. Neiner, K. Parab, T. Autrey, *Catal. Today* **2015**, 251, 28;
[N^0 452] A. Y. Houghton, T. Autrey, *J. Phys. Chem. A* **2017**, *121*, 8785.
[N^0 453] L. Rocchigiani, G. Ciancaleoni, C. Zuccaccia, A. Macchioni, *J. Am. Chem. Soc*. **2014**, *136*, 112.
[N^0 453] L. Rocchigiani, G. Ciancaleoni, C. Zuccaccia, A. Macchioni, *J. Am. Chem. Soc*. **2014**, *136*, 112.
[N^0 453] L. Rocchigiani, G. Ciancaleoni, C. Zuccaccia, A. Macchioni, *J. Am. Chem. Soc*. **2014**, *136*, 112.
[N^0 454] G. C. Welch, R. Prieto, M. A. Dureen, A. J. Lough, O. A. Labeodan, T. Holtrichter-Rössmann, D. W. Stephan, *Dalton Trans*. **2009**, 1559.
[N^0 455] Mestrelab Reasearch S.L. www.mestrelab.caom
[N^0 456] G. Skara, B. Pinter, J. Top, P. Geerlings, F. De Proft, F. De Vleeschouwer, *Chem. Eur. J.* **2015**, *21*, 5510.
[N^0 457] H. J. Kwon, H. W. Kim, Y. M. Rhee*, Chem. Eur. J.* **2011**, *17*, 6501.
[N^0 458] M. R. Milovanović, J. M. Andrić, V. B. Medaković, J.-P. Djukic, S. D. Zarić, *Acta Cryst.* **2018**, *B74*, 255.
[N^0 459] H. Jacobsen, H. S. Berke, Döring, G. Kehr, G. Erker, R. Fröhlich, O. Meyer, *Organometallics* **1999**, *18*, 1724.
[N^0 460] A. G. Massey, A. J. Park, *J. Organomet. Chem.* **1964**, *.2*, 245.
[N^0 461] A. G. Massey, A. J. Park, F. G. A. Stone, *Proc. Chem. Soc*. **1963**, 212.

[N⁰ 462] W. Van Doorne, A. W. Cordes, G. W. Hunt, *Inorg. Chem.* **1973**, *12*, 1686.
[N⁰ 463] J. C. Huffman, W. A. Skupinski, K. G. Caulton, *Cryst. Struct. Commun.* **1982**, *11*, 1435.
[N⁰ 464] M. Lutz, A. L. Spek, A. Azghay, J. C. Slootweg, *CSD Commun*. **2009**.
[N⁰ 465] S. R. Ghanta, M. H. Raoa, K. Muralidharan. *Dalton Trans.* **2013**, *42*, 8420.
[N⁰ 466] A. C. McQuilken, Q. M. Dao, A. J. P. Cardenas, J. A. Bertke, S. Grimme, T.H. Warren, *Angew. Chem. Int. Ed.* **2016**, *55*, 14335.
[N⁰ 467] O. Ekkert, G. G. Miera, T. Wiegand, H. Eckert, B. Schirmer, J. L. Petersen, C. G. Daniliuc, R. Fröhlich, S. Grimme, G. Kehra, G. Erker, *Chem. Sci*. **2013**, *4*, 2657.
[N⁰ 468] R. Liedtke, F. Scheidt, J. Ren, B. Schirmer, A. J. P. Cardenas, C. G. Daniliuc, H. Eckert, T. H. Warren, S. Grimme, G. Kehr, G. Erker, *J. Am. Chem. Soc.* **2014**, *136*, 9014.
[N⁰ 469] K. Takeuchi, L. J. Hounjet, D. W. Stephan, *Organometallics* **2013**, *32*, 4469.
[N⁰ 470] C. B. Caputo, S. J. Geier, E. Y. Ouyang, C. Kreitner, D. W. Stephan, *Dalton Trans.* **2012**, *41*, 237.
[N⁰ 471] Z. M. Heiden, M. Schedler, D. W. Stephan, *Inorg. Chem.* **2011**, *50*, 1470.
[N⁰ 472] B. M. Barry, D. A. Dickie, L. J. Murphy, J. A. C. Clyburne, R. A. Kemp, *Inorg. Chem*. **2013**, *52*, 8312.
[N⁰ 473] J. Yu, G. Kehr, C. G. Daniliuc, G. Erker, *Inorg. Chem.* **2013**, *52*, 11661.
[N⁰ 474] S. J. Geier, D. W. Stephan, *Chem. Commun.* **2010**, *46*, 1026.
[N⁰ 475] O. Ekkert, G. Kehr, R. Fröhlich, G. Erker, *J. Am. Chem. Soc*. **2011**, *133*, 4610.
[N⁰ 476] P. Moquist, G.-Q. Chen, C. Mück-Lichtenfeld, K. Bussmann, C. G. Daniliuc, G. Kehr, G. Erker, *Chem. Sci.* **2015**, *6*, 816.
[N⁰ 477] P. Spies, G. Kehr, K. Bergander, B. Wibbeling, R. Fröhlich, G. Erker, *Dalton Trans.* **2009**, *9*, 1534.
[N⁰ 478] A. M. Chapman, M. F. Orton, J. P. H. Haddow, D. F. Wass, *Dalton Trans.* **2010**, *39*, 6184.
[N⁰ 479] J. Beckmann, E. Hupf, E. Lork, S. Mebs, *Inorg. Chem.* **2013**, *52*, 11881.
[N⁰ 480] R. Fröhlich, S. Grimme, G. Kehra, G. Erker, *Chem. Sci*. **2013**, *4*, 2657.
[N⁰ 481] T. Wiegand, H. Eckert, O. Ekkert, R. Fröhlich, G. Kehr, G. Erker, S. Grimme, *J. Am. Chem. Soc.* **2012**, *134*, 4236.
[N⁰ 482] R. D. Closson, J. Kozikowski, T. H. Coffield, J*. Org. Chem.* **1957**, *22*, 598.
[N⁰ 483] P. M. Treichel, F. G. A. Stone, *Advan. Ovganometal. Chem.* **1964**, *1*, 143.
[N⁰ 484] F. A. Cotton, R. M. Wing, *J. Ovganometal. Chem.* **1967**, *9*, 511.
[N⁰ 485] M. B. Hall, M. F. Guset, I. H. Hillier, *Chem. Phys. Lett*. **1972**, *15*, 592.
[N⁰ 486] S. Evans, J. C. Green, M. L. H. Green, A. F. Orchard, D. W. Turner, *Discuss. Faraday Soc*. **1969**, *41,* 112.
[N⁰ 487] D. L. Lichtenberger, R. F. Fenske *Inorg. Chem.* **1974**, *13*, 486.
[N⁰ 488] Z. Mahmood, M. Azam, A. Mushtaq, R. Kausar, S. Kausar, S. R. Gilani, *Spectrochim. Acta A* **2006**, *65*, 445.
[N⁰ 489] L. González, C. Daniel, *J Comput Chem*. **2006**, *27*, 1781.
[N⁰ 490] T. Leyssens, D. Peeters, A. Guy Orpen, J. N. Harvey, *Organometallics* **2007**, *26,* 2637.
[N⁰ 491] K. W. Feindel, K. J. Ooms, R. E. Wasylishen, *Phys. Chem. Chem. Phys*. **2007**, *9*, 1226.
[N⁰ 492] A.G. Algarra, V. V. Grushin, S. A. Macgregor, *Organometallics* **2012**, *31*, 1467.
[N⁰ 493] F. Calderazzo, F. A. Cotton, *Inorg. Chem*. **1962**, *1*, 30.
[N⁰ 494] K. A. Keblys, A. H. Filbey, *J. Am. Chem. Soc.* **1960**, *82*, 4202*.*
[N⁰ 495] R. J. Mawby, F. Basolo, R. G. Pearson, *J. Am. Chem. Soc.* **1964**, *86*, 3994.
[N⁰ 496] F. Calderazzo, F. A. Cotton, *Chim. Ind. (Milano)* **1964**, *46*, 1165*.*
[N⁰ 497] F. Calderazzo, K. Noack, *Coordin. Chem. Rev.* **1966**, *1*, 118.
[N⁰ 498] L.S. Reich, A. Schindler, *Polymerization by Organometallic Compounds*; Wiley–Interscience, New York, **1966**.
[N⁰ 499] C. Masters, *Adv. Organomet. Chem*. **1969**, *17*, 61.
[N⁰ 500] R. C. Brady, R. Pettit, *J. Am. Chem. Soc*. **1980**, *102*, 6181.
[N⁰ 501] J. R. Blackborow, R. J. Daroda, G. Wilkinson, *Coord. Chem. Re*v. **1982**, *43*, 17.
[N⁰ 502] E. J. Kuhlmann, J. J. Alexander, *Coord. Chem. Re*v. **1980**, *33*, 195.
[N⁰ 503] A*.* Wojciki, *Adv. Organomet. Chem*. **1973**, *11*, 87.
[N⁰ 504] F. Calderazzo, *Angew. Chem. Int. Ed. Engl*. **1977**, *16*, 299.
[N⁰ 505] J. J. Wax, R. G. Bergman, *J. Am. Chem. Soc.* **1981**, *103*, 7028.
[N⁰ 506] K. Noack, F. Calderazzo, *J. Organomet. Chem.* **1967**, *10*, 101.

[N⁰ 507] T. C. Flood, J. E. Jensen, J. A. Statler, *J. Am. Chem. Soc.* **1981**, *103*, 4410.
[N⁰ 508] T. H. Cotfield, J. Kozikowske, R. N. Closson, *J. Org. Chem.* **1957**, *22*, 598.
[N⁰ 509] T. H. Cotfield, J. Kozikowske, R. N. Closson, *Spec. Publ. Chem. Soc*. **1959**, *13*, 126.
[N⁰ 510] T. M. McHugh, A. J. Rest, *J. Chem. Soc., Dalton Trans.* **1980**, 2323.
[N⁰ 511] K. Nickolas, S. Raghu, M. Rosenblum, *J. Organomet. Chem.* **1974**, *78*, 133.
[N⁰ 512] K. Mashima. A. Nakamura, *J. Organomet. Chem.* **1992**, *428*, 49.
[N⁰ 513] M. Brookhart, M. L. H. Green, L. L. Wong, *Prog. Inorg. Chem.* **1988**, *36*, 1.
[N⁰ 514] H. Berke, R. Hoffmann, *J. Am. Chem. Soc.* **1978**, *100*, 7224.
[N⁰ 515] T. Ziegler, L. Versluis, V. Tschinke, *J. Am. Chem. Soc.* **1986**, *108*, 612.
[N⁰ 516] D. Saddei, H. J. Freund, G. G. Holnecher, *J. Organomet. Chem.***1980**, *186*, 63.
[N⁰ 517] M. E. Ruiz, A. Flores-Riveros, O. Novaro, *J. Catal.* ***1980***, *64*, 1.
[N⁰ 518] F. U. Axe, D. S. Marynick, *Organometallics* **1987**, *6*, 572.
[N⁰ 519] F. U. Axe, D. S. Marynick, *J. Am. Chem. Soc.* **1988**, *110*, 3728.
[N⁰ 520] R. J. Ruszczyk, B.-L. Huang, J. D. Atwood, *J. Organomet.Chem*. **1986**, *299*, 205.
[N⁰ 521]. M. Andersen, J. R. Moss, *Organometallics* **1994**, *13*, 5013.
[N⁰ 522] A. Derecskei-Kovacs, D. S. Marynick, J*. Am. Chem. Soc*. **2000**, *122*, 2078.
[N⁰ 523] X. H. Wang, E. Weitz, *J. Phys. Chem. A*. **2002**, *106*, 11782.
[N⁰ 524] X. Wang, E. Weitz, *J. Organomet. Chem*. **2004**, *689*, 2354.
[N⁰ 525] S. L. Webb, C. M. Giandomenico, J. Halpern, *J. Am. Chem. Soc.* **1986**, *108*, 34.
[N⁰ 526] W. T. Boese, B. Lee, D. W. Ryba, S. T. Belt, P. C. Ford, *Organometallics* **1993***, 12*, 4739.
[N⁰ 527] W. T. Boese, P. C. Ford, *J. Am. Chem. Soc.* **1995**, *117*, 8381.
[N⁰ 528] T. L Bent, J. D. Cotton, *Organometallics* **1991**, *10*, 3156.
[N⁰ 529] J. N. Cawse, R. A. Fiato, R. L. Pruett, *J. Organomet. Chem*. **1979**, *172*, 405. and related references therein.
[N⁰ 530] T. G. Richmond, F. Basolo, D. F. Shriver, *Inorg. Chem.* **1982**, *21*, 1272.
[N⁰ 531] R. L. Pruett, *Adv. Organomet. Chem*. **1979**, *17*, 1.
[N⁰ 532] D. Forster, *Adv. Organomet. Chem*. **1979**, *17*, 255.
[N⁰ 533] G. W. Parshall, *Homogeneous Catalysis*; John Wiley, New York, **1980**.
[N⁰ 534] C. Masters, *Homogeneous Transition-Metal Catalysis*; Chapman and Hall, **1981**.
[N⁰ 535] T. G. Richmond, F. Basolo, D.F. Shriver, *Inorg. Chem*. **1982**, *21*, 1272.
[N⁰ 536] J. P. Collman, R. G. Finke, J. N. Cawse, J. I. Brauman, *J. Am. Chem. Soc*. **1978**, *100*, 4766.
[N⁰ 537] J. R. Moss, *J. Molecular Catal. A: Chemical* **1996**, *107*, 169.
[N⁰ 538] P. L. Motz, D. J. Sheeran, M. Orchin, *J. Organomet. Chem.* **1990**, *383*, 201.
[N⁰ 539] M. A. Gonzalez, S. J. Carrington, N. L. Fry, J. L. Martinez, P. K. Mascharak, *Inorg. Chem.* **2012**, *51*, 11930.
[N⁰ 540] H. J. Haupt, G. Lohmann, U. Floerke, *Z. Anorg. Allg. Chem.* **1985**, *526*, 103.
[N⁰ 541] W. Ping, J. D. Atwood, *Organometallics* **1993**, *12*, 4247.
[N⁰ 542] I. J. Hart, J. C. Jeffery, R. M. Lowry, F. G. A. Stone, *Angew. Chem. Int. Ed. Engl.* **1988**, *27*, 1703.
[N⁰ 543] K. E. Warner, J. R. Norton, *Organometallics* **1985**, *4*, 2150.
[N⁰ 544] R. M. Bullock, B. J. Rappoli, *J. Am. Chem. Soc.* **1991**, *113*, 1659.
[N⁰ 545] G. D. Vaughn, K. A. Krein, J. A. Gladysz, *Organometallics* **1986**, *5*, 936.
[N⁰ 546] F. Carré, G. Cerveau, E. Colomer, R. J. P. Corriu, *J. Organomet. Chem.* **1982**, *229*, 257.
[N⁰ 547] P. DeShong, G. A. Slough, A. Rheingold, *Tetrahedron Lett.* **1987**, *28*, 2229.
[N⁰ 548] P. DeShong, D. R. Sidler, *J. Org. Chem.* **1988**, *53*, 4892.
[N⁰ 549] R. M. Ceder, J. Sales, X. Solans, M. Font-Altaba, *J. Chem. Soc., Dalton Trans.* **1986**, 1351.
[N⁰ 550] M. E. Dowler, T. X. Le, P. DeShong, W. von Philipsborn, M. Vöhler, D. Rentsch, *Tetrahedron* **1993**, *49*, 5673.
[N⁰ 551] B. Zhou, Y. Hu, C. Wang, *Angew. Chem. Int. Ed.* **2015**, 54, 13659.
[N⁰ 552] S. A. Llewellyn, M. L. H. Green, A. R. Cowley, *Dalton Trans.* **2006**, 1776.
[N⁰ 553] A. Fernández 1, J. M. Vila, *J. Organomet. Chem.* **2005**, *690*, 3638.
[N⁰ 554] J. Albert, J. Cadena, J. Granell, X. Solans, M. Font-Bardia, *J. Organomet. Chem.* **2004**, 689, 4889.
[N⁰ 555] E. Folga, T. Ziegler, *J. Am. Chem. Soc.* **1993**, *115*, 5169.
[N⁰ 556] R. S. Drago, N. M. Wong, D. C. Ferris, *J. Am. Chem. Soc.* **1992**, *114*, 91.

[N^0 557] J. A. Connor, M. T. Zefarani-Moattar, J. Bickerton, N. I. El Saied, S. Suradi, R. Carson, G. Al Takhin, H. A. Skinner, *Organometallics* **1982**, *1*, 1166.
[N^0 558] G. P. Smith, *Polyhedron* **1988**, *7*, 1605.
[N^0 559] C. S. Krainhanzel, P. K. Maples, *J. Chem. Soc.* **1965**, *87*, 5267.
[N^0 560] R. N. Haszeldine, *J. Chem. Soc.* (*A*), **1969**, 698.
[N^0 561] C. S. Krainhanzel, P. K. Maples, K. Peter, *Inorg. Chem.,* **1968**, *7*, 1806.
[N^0 562] E. O. Fischer, A. Maasböl, Angew. *Chem. Int. Ed. Engl*. **1964**, *3*, 580.
[N^0 563] K. H. Dötz, H. Fischer, P. Hofmann, F.R. Kreissl, U. Schubert, K. Weiss, *Transition Metal Carbene Complexes*; VCH, Weinheim, **1983**.
[N^0 564] C.-C. Wang, Y. Wang, H.-J. Liu, K.-J. Lin, L.-K. Chou, K.-S. Chan, *J. Phys. Chem*. *A* **1997**, *101*, 8887.
[N^0 565] T. F. Block, R. F. Fenske, *J. Am. Chem. Soc*. **1977**, *99*, 4321.
[N^0 566] J. Poater, M. Cases, X. Fradera, M. Duran, M. Solà, *Chem. Phys*. **2003**, *294*, 129.
[N^0 567] R. R. Schrock, *Chem. Rev.* ***2002***, *102*, 145.
[N^0 568] C. P. Casey, *J. Chem. Educ*. **2006**, *83*, 192.
[N^0 569] C. D. Montgomery, *J. Chem. Educ*. **2015**, *92*, 1653.
[N^0 570] U. Klabunde, *Thesis,* Northwestern University **1967**.
[N^0 571] H. Werner, H. Rascher, *Helv. Chim. Acta,* **1968**, *51*, 1765.
[N^0 572] E. Lindner, H. Behrens, *Spectrochim. Acta* **1967**, *23*, 3025.
[N^0 573] U. Klabunde, E. O. Fischer. *J. Am. Chem. Soc.* **1967**, *89*, 7141.
[N^0 574] B. Heckl, H. Werner, E. O. Fischer, *Angew. Chem. Int. Ed.* **1968**, *7,* 817.
[N^0 575] E. O. Fischer, V. Kiener, *Angew. Chem. Int. Ed.* **1967**, *6*, 961.
[N^0 576] C. G. Kreiter, *Angew. Chem. Int. Ed.* **1968**, *7,* 390.
[N^0 577] L. M. Toomey, J. D. Atwood, *Organometallics* **1997**, *16,* 490.
[N^0 578] K. H. Dötz, *Angew. Chem. Int. Ed. Engl*. **1984**, *23*, 587.
[N^0 579] W. D. Wulff, in *Comprehensive Organic Synthesis*, Pergamon Press, Oxford, **1991**. vol. 5.
[N^0 580] W. D. Wulff, *Comprehensive Organometallic Chemistry II*; Pergamon Press, Oxford, **1995**.
[N^0 581] A. de Meijere, *Pure Appl. Chem.* **1996**, *68*, 61.
[N^0 582] J. Barluenga, *J. Pure Appl. Chem*. **1996**, *68*, 543.
[N^0 583] D. F. Harvey, D.M. Sigano, *Chem. Rev*. **1996**, *96*, 271.
[N^0 584] R. Aumann, *Eur. J. Org. Chem.* **2000**, 17.
[N^0 585] M. A. Sierra, *Chem. Rev.* **2000**, *100*, 3591.
[N^0 586] A.de Meijere, H. Schirmer, M. Duetsch, *Angew. Chem. Int. Ed*. **2000**, 39, 3964.
[N^0 587] M. W. Davies, C. N. Johnson, J. P. A. Harrity, *J. Org. Chem.* **2001**, *66*, 3525.
[N^0 588] J. Barluenga, J. Santamaría, M. Tomás, *Chem. Rev*. **2004**, *104*, 2259.
[N^0 589] Y.-T. Wu, T. Kurahashi, A. de Meijere, *J. Organomet. Chem.* **2005**, *690*, 5900.
[N^0 590] H. K. Dötz, *Stendel. Chem. Rev.* **2009**, *109*, 3227.
[N^0 591] S. Lafollée-Bezzenine, A. Parlier, H. Rudler, J. Vaissermann, J.-C. Daran, *J. Organomet. Chem.* **1998**, 567, 83.
[N^0 592] K. H. Dötz, I. Pruskil, J. Mühlemeier*, Chem. Ber.* **1982**, *115*, 1278.
[N^0 593] M. P. López-Alberca, Israel Fernández, M. J. Mancheño, M. Gómez-Gallego, L. Casarrubios, M. A. Sierra, *Eur. J. Org. Chem.* **2011**, 3293.
[N^0 594] G. M. Chu, A. Guerrero-Martínez, I. Fernández, M. A. Sierra, *Chem. Eur. J.* **2014**, *20*, 1367.
[N^0 595] P. Dutta, S. Sawoo, N. Ray, O. Bouloussa, A. Sarkar, *Bioconjugate Chem.* **2011**, *22*, 1202.
[N^0 596] K. H. Dötz, C. Jäkel, W.-C. Haase, *J. Organomet. Chem.* **2001**, *617–618*, 119.
[N^0 597] E. O. Fischer, B. Heckl, H. Werner, *J. Organomet. Chem.* **1971**, *28*, 359.
[N^0 598] J. A. Connor, P. D. Rose, *J. Organomet. Chem*. **1972**,*46*, 329.
[N^0 599] H. Werner, E. O. Fischer, B. Heckl, C. G. Kreiter, *J. Orgonomet. Chem.* **1971**, *28,* 367.
[N^0 600] D. M. Andrada, J. O. C. Jimenez-Halla, M. Solà, *J. Org. Chem*. **2010**, *75*, 5821.
[N^0 601] D. M. Andrada, M. E. Zoloff Michoff, R. H. de Rossib, A. M. Granados, *Dalton Trans*., **2015**, *44*, 5520.
[N^0 602] C. F. Bernasconi, M. W. Stronach, *J. Am. Chem. Soc*. **1993**, *115*, 1341.
[N^0 603] D. M. Andrada, M. E. Zoloff Michoff, R. H. de Rossi, A. M. Granados, *Phys. Chem. Chem. Phys*. **2010**, *12*, 6616.
[N^0 604] C. F. Bernasconi, S. Bhattacharya, *Organometallics* **2003**, *22,* 1310.
[N^0 605] C. F. Bernasconi, C. Whitesell, R. A. Johnson, *Tetrahedron* **2000**, *56*, 4917.

[N⁰ 606] K. Gu, G. Yang, W. Zhang, X. Liu, Z. Yu, X. Han, X. Bao, *J. Organomet. Chem.* **2006**, *691*, 1984.
[N⁰ 607] G. M. Chu, I. Fernández, M. A. Sierra, *J. Org. Chem.* **2013**, *78*, 865.
[N⁰ 608] M. A. Sierra, J. C. del Amo, M. J. Mancheño, M. Gómez-Gallego, *Tetrahedron Lett.* **2001**, *42*, 5435.
[N⁰ 609] W. W. Schoeller, D. Eisner, S. Grigoleit, A. B. Rozhenko, A. Alijah, *J. Am. Chem. Soc.* **2000**, *122,* 10115.
[N⁰ 610] B. Karatas, I. Hyla-Kryspin, R. Aumann, *Organometallics* **2007**, *26,* 4983.
[N⁰ 611] M. L. Lage, I. Fernández, M. J. Mancheño, M. A. Sierra, *Inorg. Chem*. **2008**, *47*, 5253.
[N⁰ 612] N. Fey, M. F. Haddow, J. N. Harvey, C. L. McMullin, A. G. Orpen, *Dalton Trans.* **2009**, 8183.
[N⁰ 613] J. O. C. Jimenez-Halla, M. Solà, *Chem. Eur. J.* **2009**, *15*, 12503.
[N⁰ 614] I. Hoskovcová, J. Roháčová, D. Dvořák, T. Tobrman, S. Záliš, R. Zvěřinová, J. Ludvík, *Electrochimica Acta* **2010**, *55*, 8341.
[N⁰ 615] M. Landman, R. Pretorius, B. E. Buitendach, P. H. van Rooyen, J. Conradie, *Organometallics* **2013**, *32*, 5491.
[N⁰ 616] H. Kvapilová, I. Hoskovcová, M. Kayanuma, C. Daniel, S. Záliš, *J. Phys. Chem. A* **2013**, *117*, 11456.
[N⁰ 617] K. Yamamoto, C. P. Gordon, W.-C. Liao, C. Copéret, C. Raynaud, O. Eisenstein, *Angew. Chem. Int. Ed.* **2017**, *56*, 10127.
[N⁰ 618] D. Munz, *Organometallics* **2018**, *37*, 275.
[N⁰ 619] D. B. Grotjahn, F. E. K. Kroll, T. Schäfer, K. Harms, K. H. Dötz, *Organometallics* **1992**, *11*, 298.
[N⁰ 620] A. C. Cope, R. W. J. Siekman, *Am. Chem. Soc.* 1965, *87*, 3272.
[N⁰ 621] J. Spencer, M. Pfeffer, *Adv. Met-Org. Chem.* **1998**, *6*, 103.
[N⁰ 622] M. Pfeffer, *Recl. Trav. Chim. Pays-Bas* **1990**, *109*, 567.
[N⁰ 623] *Palladacycles: Synthesis, Characterization and Applications*; Eds. J. Dupont, M. Pfeffer, Wiley-VCH: Weinheim, Germany, **2008**.
[N⁰ 624] W. A. Herrmann, V. P. W. Bohm, C. P. J. Reisinger, *J. Organomet. Chem.* **1999**, 576, 23.
[N⁰ 625] J.-P. Djukic, A. Hijazi, H. D. Flack, G. Bernardinelli, *Chem. Soc. Rev.* **2008**, *37*, 406.
[N⁰ 626] R. F. Heck, *Palladium Reagents in Organic Syntheses*; Academic Press: New York, **1985**.
[N⁰ 627] *Comprehensive Organometallic Chemistry II*; Eds. G. Wilkinson, F. G. Stone, E. W. Abel, Pergamon Press: New York, **1995**; vol. 12.
[N⁰ 628] M. Ohff, A. Ohff, D. Milstein, *Chem. Commun.* **1999**, 357.
[N⁰ 629] Y. J. Wu, J. J. Hou, H. Y. Yun, X. L. Cui, R. J. Yuan, *J. Organomet. Chem.* **2001**, *637*, 793.
[N⁰ 630] J. Dupont, M. Pfeffer, J. Spencer, *Eur. J. Inorg. Chem.* **2001**, 1917.
[N⁰ 631] R. B. Bedford, *Chem. Commun.* **2003**, 1787.
[N⁰ 632] W. A. Herrmann, C. Brossmer, K. K. Öfele. C.-P. Reisinger, T. Priermeier. M. Beller, H. Fischer, *Angew. Chem. Int. Ed.* **1995**, *34*, 1844.
[N⁰ 633] T. Rosner, J. Le Bars, A. Pfaltz, D. G. Blackmond, *J. Am. Chem. Soc.* **2001**, *123,* 1848.
[N⁰ 634] A. V. Cheprakov, I. P. Beletskaya, *J. Organomet. Chem.* **2004**, *689*, 4055.
[N⁰ 635] J. Dupont, C. S. Consorti, Spencer, *J. Chem. Rev.* **2005**, 105,2527.
[N⁰ 636] D. M. Fan, C. T. Yang, J. D. Ranford, J. J. Vittal, P. F. Lee, *Dalton Trans.* **2003**, 3376.
[N⁰ 637] A. Gómez Quiroga, C. Navarro Ranninger, *Coord. Chem. Rev.* **2004**, *248*, 119.
[N⁰ 638] M. Albrecht, M. Lutz, A. L. Spek, G. van Koten, *Nature* **2000**, *406*, 970.
[N⁰ 639] M. Ghedini, D. Pucci, G. Barberio, *Liq. Cryst.* **2000**, *27*, 1277.
[N⁰ 640] L. Diez, P. Espinet, J. A. Miguel, M. B. Ros, *J. Mater. Chem.* **2002**, *12*, 3694.
[N⁰ 641] A. D. Ryabov, *Chem. Rev.* **1990**, *90*, 403.
[N⁰ 642] D. L. Davies, S. M. A. Donald, S. A. Macgregor, *J. Am. Chem. Soc*. **2005**, 127, 13754.
[N⁰ 643] Y. Boutadla, D. L. Davies, S. A. Macgregor, A. I. Poblador-Bahamonde*, Dalton Trans.* **2009**, 5820.
[N⁰ 644] A. Bahsoun, J. Dehand, M. Pfeffer, M. Zinsius, *J. Chem. Soc*. *Dalton Trans*. **1979**, 547.
[N⁰ 645] A. D. Ryabov, *Synthesis* **1985**, 233.
[N⁰ 646] M.-J. Oliva-Madrid, J.-A. García-López, I. Saura-Llamas, D. Bautista, José Vicente, *Organometallics* **2014**, *33*, 33.
[N⁰ 647] R. B. Bedford, Chem. Commun. **2003**, 1787.
[N⁰ 648] R. Ratti, *Can. Chem. Trans.* **2014**, *2*, 467.

[N^0 649] C. López, R. Bosque, X. Solans, M. Font-Bardía, J. Silver, G. Fern, *J. Chem. Soc.*, *Dalton Trans*. **1995**, 1835.
[N^0 650] R. C. Larock, E. K. Yum, M. J. Doty, K. K. C. J. Sham, *Org. Chem.* **1995**, *60*, 3270.
[N^0 651] A.-E. Gies, M. Pfeffer, C. Sirlin, J. Spencer, *Eur. J. Org. Chem*. **1999**, 1957.
[N^0 652] J. Vicente, J. A. Abad, R. Fernández-de-Bobadilla, P. G. M. Jones, C. Ramírez de Arellano, *Organometallics* **1996**, *15*, 24.
[N^0 653] J. Vicente, J. A. Abad, R. Bergs, P. G. Jones, M. C. Ramírez de Arellano*, Organometallics* **1996**, *15*, 1422.
[N^0 654] J. Vicente, J. A. Abad, J. Gil-Rubio, *Organometallics* **1996**, *15*, 3509.
[N^0 655] J. A. Abad, *Gazz. Chim. Ital.* **1997**, *127*, 119.
[N^0 656] R. C. Larock, E. K. Yum, M. D. Refvik, *J. Org. Chem.* **1998**, *63*, 7652.
[N^0 657] S. Cacchi, *J. Organomet. Chem.* **1999**, *576*, 42.
[N^0 658] J. Vicente, J. A. Abad, R. Bergs, M. C. Ramírez de Arellano, E. Martínez-Viviente, P. G. Jones*, Organometallics* **2000**, *19*, 5597.
[N^0 659] J. Vicente, J. A. Abad, B. López-Peláez, E. Martínez-Viviente, *Organometallics* **2002**, *21*, 58.
[N^0 660] J. Vicente, J. A. Abad, W. Förtsch, M.-J. López-Sáez, P. G. Jones, *Organometallics* **2004**, *23*, 4414.
[N^0 661] J. Vicente, J. A. Abad, J. López-Serrano, P. G. Jones, C. Nájera, L. Botella-Segura, *Organometallics* **2005**, *24*, 5044.
[N^0 662] J. Albert, J. Granell, A. Luque, M. Font-Bardia, X. Solans, *Polyhedron* **2006**, *25*, 793.
[N^0 663] G. Z. Wu, S. J. Geib, A. L. Rheingold, R. F. Heck, *J. Org. Chem*. **1988**, *53*, 3238.
[N^0 664] Y. Zhang, E. Negishi, *J. Am. Chem. Soc*. **1989**, *111*, 3454.
[N^0 665] L. S. Liebeskind, J. R. Gasdaska, J. S. McCallum, S. J. Tremont, *J. Org. Chem.* **1989**, *53*, 669.
[N^0 666] R. C. Larock, E. K. Yum, *J. Am. Chem. Soc.* **1991**, *113*, 6689.
[N^0 667] J. Vicente, J. A. Abad, J. Gil-Rubio, *J. Organomet. Chem*. **1992**, *436*, C9.
[N^0 668] J. Vicente, J. A. Abad, J. Gil-Rubio, P. G. Jones, *Organometallics* **1995**, *14*, 2677.
[N^0 669] J. Vicente, J. A. Abad, K. F. Shaw, J. Gil-Rubio, M. C. Ramírez de Arellano, P. G. Jones, *Organometallics* **1997**, *16*, 4557.
[N^0 670] K. R. Roesch, R. C. Larock, *J. Org. Chem*. **1998**, *63*, 5306.
[N^0 671] R. C. Larock, *J. Organomet. Chem*. **1999**, *576*, 111.
[N^0 672] J. Vicente, J. A. Abad, E. Martínez-Viviente, M. C. Ramírez de Arellano, P. G. Jones, *Organometallics* **2000**, *19*, 752.
[N^0 673] C. Arlen, M. Pfeffer, O. Bars, D. Grandjean, *J. Chem. Soc., Dalton Trans*. **1983**,1535.
[N^0 674] G. Z. Wu, A. L. Rheingold, S. J. Geib, R. F. Heck, *Organometallics* **1987**, *6*, 1941.
[N^0 675] F. Maassarani, M. Pfeffer, G. Le Borgne, *Organometallics* **1987**, *6*, 2029.
[N^0 676] W. Tao, L. J. Silverberg, A. L. Rheingold, R. F. Heck, *Organometallics* **1989**, *8*, 2550.
[N^0 677] M. Pfeffer, *Pure Appl. Chem.* **1992**, *64*, 335.
[N^0 678] J. Spencer, M. Pfeffer, *Tetrahedron*: *Asymmetry* **1995**, *6*, 419.
[N^0 679] E. G. Samsel, J. R. Norton, *J. Am. Chem. Soc*. **1984**, *106*, 5505.
[N^0 680] P. de Vaal, A. Dedieu, *J. Organomet. Chem*. **1994**, *478*, 121.
[N^0 681] F. Maassarani, M. Pfeffer, G. J. Le Borgne, *Chem. Soc. Chem. Commun*. **1986**, 488.
[N^0 682] G. Z. Wu, A. L. Rheingold, R. F Heck, *Organometallics* **1986**, *5*, 1922.
[N^0 683] A. D. Ryabov, R. van Eldik, G. Le Borgne, M. Pfeffer, *Organometallics* **1993**, *12*, 1386.
[N^0 684] Pfeffer, M, Goel, A. B. *Cyclopalladated Compounds in Inorganic Syntheses*; ed H. D. Kaesz, John Wiley & Sons, Inc., Hoboken, New York, **1989**, vol. 26, ch. 38, and related references therein.
[N^0 685] E. L. Eliel, T. N. Ferdinand, M. C. Herrmann, *J. Org. Chem.* 1954,*19*, 1693.
[N^0 686] I. Colomer, A. E. R. Chamberlain, M. B. Haughey, T. J. Donohoe, *Nat. Rev. Chem.* **2017**, *1*, 0088.
[N^0 687] H. Li, H. Yin, X. Liu, Y. Shi, M. Jin, D. Ding *Spectrochim. Acta* A: Molecular and Biomolecular Spectroscopy **2017**, *184*, 270.
[N^0 688] P. G. Seybold W. C. Kreye *Int. J. Quantum Chem.* **2012**, *112*, 3769.
[N^0 689] A. Berkessel, J. A. Adrio, D. Hüttenhain, J. M. Neudörfl, *J. Am. Chem. Soc.* **2006**, *128*, 8421.
[N^0 690] K. S. Ravikumar, F. Barbier, J.-P. Bégué, D. Bonnet-Delpon, *J. Fluorine Chem*. **1999**, *95*, 123.

[N⁰ 691] D. Vuluga, J. Legros, B. Crousse, A. M. Z. Slawin, C. Laurence, P. Nicolet, D. Bonnet-Delpon, *J. Org. Chem.* **2011**, *76*, 1126.
[N⁰ 692] R. Cabot, C. A. Hunter, L. M. Varley, *Org. Biomol. Chem.* **2010**, *8*, 1455.
[N⁰ 693] J. Graton, F. Besseau, A.-M. Brossard, E. Charpentier, A. Deroche, J.-Y. Le Questel, *J. Phys. Chem. A* **2013**, *117*, 13184.
[N⁰ 694] C. Zhang, Y. Rao, *Org. Lett.* **2015**, *17*, 4456.
[N⁰ 695] D. Leow, G. Li, T.-S. Mei, J.-Q. Yu, *Nature* **2012**, *486*, 518.
[N⁰ 696] G. Li, D. Leow, L. Wan, J.-Q. Yu, *Angew. Chem. Int. Ed*. **2013**, *52*, 1245.
[N⁰ 697] L. Wan, N. Dastbaravardeh, G. Li, J.-Q. Yu, *J. Am. Chem. Soc.* **2013**, *135*, 18056.
[N⁰ 698] W. Gong, G. Zhang, T. Liu, R. Giri, J.-Q. Yu, J*. Am. Chem. Soc.* **2014**, *136*, 16940.
[N⁰ 699] G. Chen, T. Shigenari, P. Jain, Z. Zhang, Z. Jin, J. He, S. Li, C. Mapelli, M. M. Miller, M. A. Poss, P. M. Scola, K.-S. Yeung, J.-Q. Yu, *J. Am. Chem. Soc.* **2015**, *137*, 3338.
[N⁰ 700] Q. Dherbassy, G. Schwertz, M. Chessé, C. K. Hazra, J. Wencel-Delord, F. Colobert, *Chem. Eur.J.* **2016**, 22, 1735.
[N⁰ 701] L. Eberson, M. P. Hartshorn, O. Persson, F. Radner, *Chem. Commun*. **1996**, 2105.
[N⁰ 702] A. Berkessel, J. A. Adrio, *J. Am. Chem. Soc*. **2006**, *128*, 13412.
[N⁰ 703] B. Elsler, A. Wiebe, D. Schollmeyer, K. M. Dyballa, R. Franke, S. R. Waldvogel, *Chem. - Eur. J.* **2015**, *21*, 12321.
[N⁰ 704] H. F. Motiwala, R. H. Vekariya, J. Aubé, *Org. Lett.* **2015**, *17*, 5484.
[N⁰ 705] S. J. Khaksar, *Fluorine Chem*. **2015**, *172*, 51.
[N⁰ 706] H. F. Motiwala, M. Charaschanya, V. W. Day, J. Aubé, *J. Org. Chem*. **2016**, *81*, 1593.
[N⁰ 707] R. H. Vekariya, J. Aubé, *J. Org. Lett*. **2016**, *18*, 3534.
[N⁰ 708] K. Kushwaha, B. Pinter, S. A. Shehzadi, C. C. Malakar, C. M. L. Vande Velde, F. de Proft, K. A. Tehrani, *Adv.Synth. Catal*. **2016**, *358*, 41.
[N⁰ 709] S. Možina, S. Stavber, J. Iskra, *Eur. J. Org*. *Chem*. 2017, **2017**, 448.
[N⁰ 710] V. D. Vuković, E. Richmond, E. Wolf, J. Moran, *Angew. Chem., Int. Ed*. **2017**, *56*, 3085.
[N⁰ 711] M. Ochiai, K. Miyamoto, T. Kaneaki, S. Hayashi, W. Nakanishi, *Science* **2011**, *332*, 448.
[N⁰ 712] L. Lu, H. Liu, R. Hua, *Org. Lett.* **2018**, *20*, 3197.
[N⁰ 713] D. Hong, M. Hoshino, R. Kuboi, Y. Goto, *J. Am. Chem. Soc*. **1999**, *121*, 8427.
[N⁰ 714] T. Fujinaga, S. Nakamura, S. Krishtal, K. Yoshida, S. Lee, K. Kanazawa, T. Nemoto, T. Yamaguchi, *Fukuoka Univ. Sci. Rep*. **2007**, *37*, 23.
[N⁰ 715] K. Yoshida, J. Kawaguchi, S. Lee, T. Yamaguchi, *Pure Appl. Chem*. **2008**, *80*, 1337.
[N⁰ 716] M. Buck, H. Schwalbe, C. M. Dobson, *Biochem.* **1995**, *34*, 13219.
[N⁰ 717] J. W. Nelson, N.R. Kallenbach, *Biochem.* **1989**, 28, 5256.
[N⁰ 718] T. Banerjee, N. Kishore, *J. Phys. Chem*. *B* **2005**, *109*, 22655.
[N⁰ 719] S. M. M. Reddy, G. Shanmugam, A. B. Mandal, *Org. Biomol. Chem*., **2014**, *12*, 6181.
[N⁰ 720] Y. Mengerink, S. van der Wal, H. A. Claessens, C. A. Cramers, *J. Chromatogr*. *A* **2000**, *871*, 259.
[N⁰ 721] J. Aussenac, D. Chassagne, C. Claparols, M. Charpentier, B. Duteurtre, M. Feuillat and C. Charpentier, *J. Chromatogr*. *A*, **2001**, *907*, 155.
[N⁰ 722] M. R. Nilsson, L. L. Nguyen, D. P. Raleigh, *Anal. Biochem*. **2001**, *288*, 76.
[N⁰ 723] A. Abedini, G. Singh, D. P. Raleigh, *Anal. Biochem*. **2006**, *351*, 181.
[N⁰ 724] A. Kundu, N. Kishore, *Biopolymers* **2004**, *73*, 405.
[N⁰ 725] S. W. Snyder, U. S. Ladror, W. S. Wade, G. T. Wang, L. W. Barrett, E. D. Matayoshi, H. J. Huffaker, G. Krafft, T. F. Holzman, *Biophys. J.* **1994**, *67*, 1216.
[N⁰ 726] H. Zhang, K. Kaneko, J. T. Nguyen, T. L. Livshits, M. A. Baldwin, F. E. Cohen, T. L. James, S. B. Prusiner*, J. Mol. Biol*. **1995**, *250*, 514.
[N⁰ 727] J. R. Cort, N. H. Andersen, *Biochem. Biophys. Res. Commun*. **1997**, *233*, 687.
[N⁰ 728] H. S. Mchaourab, J. S. Hyde, J. B. Feix, *Biochem.* **1993**, *32*, 11895.
[N⁰ 729] A. Galat, J. P. Degelaen, C. C. Yang, E. R. Blout, *Biochem.* **1981**, *20*, 7415.
[N⁰ 730] I. Sirangelo, F. D. Piaz, C. Malmo, M. Cassilo, L. Birolo, P. Pucci, G. Marino, G. Irace, *Biochem*. **2003**, *42*, 312.
[N⁰ 731] N. Hirota, K. Mizuno, Y. Goto, *Protein Sci.* **1997**, *6*, 416.
[N⁰ 732] M. Fioroni, K. Burger, A. E. Mark, D. Roccatano, *J. Phys. Chem*. *B* **2001**,*105*, 10967.
[N⁰ 733] K. Yoshida, T. Yamaguchi, T. Adachi, T. Otomo, D. Matsuo, T. Takamuku, N. Nishi, *J. Chem. Phys*. **2003**, *119*, 6132.

[N^0 734] K. Kinugawa, K. Nakanishi, *J. Chem. Phys*. **1988**, 89, 5834.
[N^0 735] Y. Mizutani, K. Kamogawa, T. Kitagawa, A. Shimizu, Y. Taniguchi, K. Nakanishi, *J. Phys. Chem*. **1991**, *95*, 1790.
[N^0 736] T. Takamuku, H. Wada, C. Kawatoko, T. Shimomura, R. Kanzakib, M. Takeuchic, *Phys. Chem. Chem. Phys.* **2012**, *14*, 8335.
[N^0 737] T. Takamuku, M. Tobiishi, H. Saito, *J. Solution Chem*. **2011**, *40*, 2046.
[N^0 738] A. Shahi, E. Arunan, *Phys. Chem. Chem. Phys.* **2015**, *17*, 24774.
[N^0 739] T. Yamaguchi, S. Imura, T. Kai, K. Yoshida, *Z. Naturforsch*. **2013**, *68a*, 145.
[N^0 740] N. C. Maiti, R. Carey, V. E. Anderson, *J. Phys. Chem. A* **2003**, *107,* 9910.

Milan MILOVANOVIĆ

Les approches Expérimentales et Théoriques combinées à la Thermochimie des réactions "in solutio" et le Rôle des interactions Non-covalentes

Résumé

Ce manuscrit aborde plusieurs interactions / réactions chimiques importantes se produisant dans la soluton en utilisant la calorimétrie par titrage isothermique (ITC) et la théorie de la densité fonctionnelle statique (DFT). Cette thèse porte son attention notamment sur: l'association de paires de Lewis (frustrées) ((F)LPs), la migration cis du groupe méthyle au sein du pentaméthylmanganèse induit par les phosphines, l'aminolyse de carbènes de Fischer, l'insertion d'alcynes dans des palladacycles, l'affinité de divers donneurs de Lewis à l'hexafluoroisopropanol. L'ITC s'est révélé être une technique expérimentale puissante pour obtenir des données thermochimiques fiables sur les systèmes étudiés. Les calculs statiques DFT-D ont montré une capacité d'estimation correcte des paramètres de réaction thermodynamique lorsque l'influence de la solvatation n'est pas significative. Autrement, lorsque l'influence du solvant est apparente, les calculs ne permettent pas de reproduire les résultats expérimentaux. En plus, les résultats expérimentaux et théoriques révèlent l'existence d'ensembles moléculaires plus grandes dans la solution de FLP, soulignant le rôle des interactions non covalentes.

Mots-clés: Paires de Lewis frustrées, Pentaméthylmanganèse, Carbènes de Fischer, Palladacycles, Hexafluoroisopropanol, Réactions organométalliques, Solution, Calorimétrie de titrage isothémal, Théorie statique de la fonctionnelle de la densité, Interactions non-covalentes, Dispersion, Solvation, Benchamark.

Résumé en anglais

This manuscript adressed several important chemical interactions/reactions taking place in solutuon by using Isothermal Titration Calorimetry (ITC) and static Density Functional Theory (DFT). Namely, this thesis dealt with: association of (frustrated) Lewis pairs ((F)LPs), *cis*-migration of methyl group within pentamethylmanganese induced by phosphines, aminolysis of Fischer carbenes, insertion of alkynes into palladacycles, affinity of various Lewis donors to hexafluoroisopropanol. The ITC proved to be powerful experimental technique for obteining reliable thermochemical data of sutudied systems. The static DFT-D calculations showed capability for proper estiamtion of thermodynamic reaction parameters when an influence of solvation is not sighnificant. Otherwise, when the influence of solvent is not innocent, the calculations moslty failed to reproduce the experimantal results. In addition, Both the experimantal and therortical results revield existance of larger molecular clusters in solution of FLPs emphasising a role of non-covalent interactions.

Keywords: Frustrated Lewis pairs, Pentamethylmanganese, Fischer carbenes, Palladacycles, Hexafluoroisopropanol, Organometallic reactions, Solution, Isothemal Titration Calorimentry, static Density Functional Theory, Non-covalent interactions, Dispersion, Solvation, Benchamark.